An Introduction to the Finite Element Method

Third Edition

J. N. REDDY

Department of Mechanical Engineering
Texas A&M University
College Station, Texas, USA 77843

Mc Graw Hill

Boston Burr Ridge, IL Dubuque, IA Madison, WI New York San Francisco St. Louis
Bangkok Bogotá Caracas Kuala Lumpur Lisbon London Madrid Mexico City
Milan Montreal New Delhi Santiago Seoul Singapore Sydney Taipei Toronto

The McGraw-Hill Companies

Mc Graw Hill

AN INTRODUCTION TO THE FINITE ELEMENT METHOD, THIRD EDITION
International Edition 2006

10 09 08 07 06 05 04 03 02 01
20 09 08 07 06 05
CTF BJE

Connecting Rod image courtesy of MSC.Software® Corporation. www.mscsoftware.com

Library of Congress Control Number: 2004058177

When ordering this title, use ISBN 007-124473-5

Printed in Singapore

www.mhhe.com

ABOUT THE AUTHOR

J. N. Reddy is a Distinguished Professor and the inaugural holder of the *Oscar S. Wyatt Endowed Chair* in the Department of Mechanical Engineering at Texas A&M University, College Station, Texas. Prior to his current position, he worked as a postdoctoral fellow at the University of Texas at Austin, as a research scientist for Lockheed Missiles and Space Company, and taught at the University of Oklahoma and Virginia Polytechnic Institute and State University, where he was the inaugural holder of the Clifton C. Garvin Endowed Professorship.

Professor Reddy is the author of over 320 journal papers and 14 text books on theoretical formulations and finite element analysis of problems in solid and structural mechanics (plates and shells), composite materials, computational fluid dynamics and heat transfer, and applied mathematics.

Professor Reddy is the recipient of numerous awards including the 1984 *Walter L. Huber Civil Engineering Research Prize* of the American Society of Civil Engineers, the 1985 Alumni Research Award at Virginia Polytechnic Institute, the 1992 *Worcester Reed Warner Medal* and the 1995 *Charles Russ Richards Memorial Award* of the American Society of Mechanical Engineers, the 1997 *Melvin R. Lohmann Medal* from Oklahoma State University, the 1997 *Archie Higdon Distinguished Educator Award* from the Mechanics Division of the American Society of Engineering Education, the 1998 *Nathan M. Newmark Medal* from the American Society of Civil Engineers, the 2000 *Excellence in the Field of Composites Award* and the 2004 *ASC Outstanding Research Award* from the American Society of Composite Materials, the 2000 *Faculty Distinguished Achievement Award for Research,* and the 2003 *Bush Excellence Award for Faculty in International Research* Award from Texas A&M University, and the 2003 *Computational Structural Mechanics Award* from the U.S. Association for Computational Mechanics. He is a fellow of the American Academy of Mechanics, the American Society of Civil Engineers, the American Society of Mechanical Engineers, the American Society of Composites, the International Association of Computational Mechanics, the U.S. Association of Computational Mechanics, and the Aeronautical Society of India. Dr. Reddy is the Editor-in-Chief of the journals *Mechanics of Advanced Materials and Structures, International Journal of Computational Methods in Engineering Science and Mechanics* and *International Journal of Structural Stability and Dynamics;* he also serves on the editorial boards of over two dozen other journals.

CONTENTS

Preface xiv

1 Introduction 1

1.1 General Comments 1
1.2 Mathematical Models 2
1.3 Numerical Simulations 9
1.4 The Finite Element Method 13
1.4.1 The Basic Idea 13
1.4.2 The Basic Features 13
1.4.3 Some Remarks 21
1.4.4 A Brief Review of History and Recent Developments 23
1.5 The Present Study 24
1.6 Summary 24
Problems 25
References for Additional Reading 26

2 Mathematical Preliminaries, Integral Formulations, and Variational Methods 27

2.1 General Introduction 27
2.1.1 Variational Principles and Methods 27
2.1.2 Variational Formulations 28
2.1.3 Need for Weighted-Integral Statements 28
2.2 Some Mathematical Concepts and Formulae 31
2.2.1 Coordinate Systems and the Del Operator 31
2.2.2 Boundary Value, Initial Value, and Eigenvalue Problems 33
2.2.3 Integral Identities 36
2.2.4 Linear and Bilinear Functionals 39
2.3 Elements of Calculus of Variations 41
2.3.1 Introduction 41
2.3.2 Variational Operator and First Variation 41
2.3.3 Fundamental Lemma of Variational Calculus 44
2.3.4 The Euler Equations 44
2.3.5 Natural and Essential Boundary Conditions 47
2.3.6 Hamilton's Principle 54

2.4 Integral Formulations 58
2.4.1 Introduction 58
2.4.2 Weighted-Integral and Weak Formulations 58
2.4.3 Linear and Bilinear Forms and Quadratic Functionals 64
2.4.4 Examples 66
2.5 Variational Methods 74
2.5.1 Introduction 74
2.5.2 The Ritz Method 74
2.5.3 Approximation Functions 76
2.5.4 Examples 77
2.5.5 The Method of Weighted Residuals 91
2.6 Summary 97
Problems 98
References for Additional Reading 102

3 Second-Order Differential Equations in One Dimension: Finite Element Models 103

3.1 Background 103
3.2 Basic Steps of Finite Element Analysis 105
3.2.1 Model Boundary Value Problem 105
3.2.2 Discretization of the Domain 106
3.2.3 Derivation of Element Equations 108
3.2.4 Connectivity of Elements 125
3.2.5 Imposition of Boundary Conditions 132
3.2.6 Solution of Equations 132
3.2.7 Postcomputation of the Solution 134
3.3 Some Remarks 141
3.4 Axisymmetric Problems 146
3.4.1 Model Equation 146
3.4.2 Weak Form 147
3.4.3 Finite Element Model 148
3.5 Summary 150
Problems 151
References for Additional Reading 154

4 Second-Order Differential Equations in One Dimension: Applications 155

4.1 Preliminary Comments 155
4.2 Discrete Systems 156
4.2.1 Linear Elastic Spring 156
4.2.2 Torsion of Circular Shafts 158
4.2.3 Electrical Resistor Circuits 159
4.2.4 Fluid Flow through Pipes 161
4.3 Heat Transfer 162
4.3.1 Governing Equations 162
4.3.2 Finite Element Models 166
4.3.3 Numerical Examples 166

4.4 Fluid Mechanics 181
4.4.1 Governing Equations 181
4.4.2 Finite Element Model 181
4.5 Solid and Structural Mechanics 183
4.5.1 Preliminary Comments 183
4.5.2 Finite Element Model of Bars and Cables 184
4.5.3 Numerical Examples 185
4.6 Plane Trusses 194
4.6.1 Introduction 194
4.6.2 Basic Truss Element 194
4.6.3 General Truss Element 195
4.6.4 Constraint Equations: Penalty Approach 202
4.6.5 Constraint Equations: A Direct Approach 211
4.7 Summary 214
Problems 215
References for Additional Reading 231

5 Beams and Frames 233

5.1 Introduction 233
5.2 Euler–Bernoulli Beam Element 233
5.2.1 Governing Equation 233
5.2.2 Discretization of the Domain 234
5.2.3 Derivation of Element Equations 234
5.2.4 Assembly of Element Equations 243
5.2.5 Imposition of Boundary Conditions 245
5.2.6 Postprocessing of the Solution 247
5.2.7 Numerical Examples 248
5.3 Timoshenko Beam Elements 261
5.3.1 Governing Equations 261
5.3.2 Weak Form 262
5.3.3 General Finite Element Model 264
5.3.4 Consistent Interpolation Elements 266
5.3.5 Reduced Integration Element 270
5.3.6 Numerical Examples 271
5.4 Plane Frame Elements 274
5.4.1 Introductory Comments 274
5.4.2 Frame Element 274
5.5 Summary 281
Problems 282
References for Additional Reading 290

6 Eigenvalue and Time-Dependent Problems 291

6.1 Eigenvalue Problems 291
6.1.1 Introduction 291
6.1.2 Formulation of Eigenvalue Problems 292
6.1.3 Finite Element Formulation 295
6.2 Time-Dependent Problems 314
6.2.1 Introduction 314
6.2.2 Semidiscrete Finite Element Models 316

6.2.3 Parabolic Equations 318
6.2.4 Hyperbolic Equations 324
6.2.5 Mass Lumping 326
6.2.6 Applications 328
6.3 Summary 337
Problems 337
References for Additional Reading 342

7 Computer Implementation 343

7.1 Numerical Integration 343
7.1.1 Background 343
7.1.2 Natural Coordinates 345
7.1.3 Approximation of Geometry 346
7.1.4 Isoparametric Formulations 347
7.1.5 Numerical Integration 348
7.2 Computer Implementation 356
7.2.1 Introductory Comments 356
7.2.2 General Outline 357
7.2.3 Preprocessor 359
7.2.4 Calculation of Element Matrices (Processor) 360
7.2.5 Assembly of Element Equations (Processor) 363
7.2.6 Imposition of Boundary Conditions (Processor) 365
7.2.7 Solving Equations and Postprocessing 367
7.3 Applications of Program FEM1D 370
7.3.1 General Comments 370
7.3.2 Illustrative Examples 370
7.4 Summary 401
Problems 401
References for Additional Reading 406

8 Single-Variable Problems in Two Dimensions 409

8.1 Introduction 409
8.2 Boundary Value Problems 410
8.2.1 The Model Equation 410
8.2.2 Finite Element Discretization 411
8.2.3 Weak Form 412
8.2.4 Finite Element Model 415
8.2.5 Derivation of Interpolation Functions 417
8.2.6 Evaluation of Element Matrices and Vectors 425
8.2.7 Assembly of Element Equations 436
8.2.8 Postcomputations 440
8.2.9 Axisymmetric Problems 441
8.3 A Numerical Example 442
8.4 Some Comments on Mesh Generation and Imposition of Boundary Conditions 453
8.4.1 Discretization of a Domain 453
8.4.2 Generation of Finite Element Data 455
8.4.3 Imposition of Boundary Conditions 456

8.5 Applications 458
8.5.1 Conduction and Convection Heat Transfer 458
8.5.2 Fluid Mechanics 472
8.5.3 Solid Mechanics 485
8.6 Eigenvalue and Time-Dependent Problems 490
8.6.1 Introduction 490
8.6.2 Parabolic Equations 491
8.6.3 Hyperbolic Equations 499
8.7 Summary 504
Problems 504
References for Additional Reading 522

9 Interpolation Functions, Numerical Integration, and Modeling Considerations 525

9.1 Introduction 525
9.2 Element Library 525
9.2.1 Triangular Elements 525
9.2.2 Rectangular Elements 532
9.2.3 The Serendipity Elements 537
9.2.4 Hermite Cubic Interpolation Functions 539
9.3 Numerical Integration 540
9.3.1 Preliminary Comments 540
9.3.2 Coordinate Transformations 543
9.3.3 Integration over a Master Rectangular Element 549
9.3.4 Integration over a Master Triangular Element 557
9.4 Modeling Considerations 561
9.4.1 Preliminary Comments 561
9.4.2 Element Geometries 562
9.4.3 Mesh Generation 563
9.4.4 Load Representation 567
9.5 Summary 569
Problems 570
References for Additional Reading 575

10 Flows of Viscous Incompressible Fluids 577

10.1 Preliminary Comments 577
10.2 Governing Equations 577
10.3 Velocity-Pressure Formulation 579
10.3.1 Weak Formulation 579
10.3.2 Finite Element Model 581
10.4 Penalty Function Formulation 583
10.4.1 Preliminary Comments 583
10.4.2 Formulation of the Flow Problem as a Constrained Problem 583
10.4.3 Lagrange Multiplier Model 584
10.4.4 Penalty Model 585
10.4.5 Time Approximation 588

10.5 Computational Aspects 588
10.5.1 Properties of the Matrix Equations 588
10.5.2 Choice of Elements 589
10.5.3 Evaluation of Element Matrices in the Penalty Model 590
10.5.4 Postcomputation of Stresses 591
10.6 Numerical Examples 591
10.7 Summary 602
Problems 603
References for Additional Reading 605

11 Plane Elasticity 607
11.1 Introduction 607
11.2 Governing Equations 607
11.2.1 Plane Strain 607
11.2.2 Plane Stress 608
11.2.3 Summary of Equations 610
11.3 Weak Formulations 612
11.3.1 Preliminary Comments 612
11.3.2 Principle of Virtual Displacements in Vector Form 612
11.3.3 Weak Form of the Governing Differential Equations 613
11.4 Finite Element Model 614
11.4.1 General Model 614
11.4.2 Eigenvalue and Transient Problems 617
11.5 Evaluation of Integrals 617
11.6 Assembly of Finite Element Equations 620
11.7 Examples 622
11.8 Summary 629
Problems 629
References for Additional Reading 633

12 Bending of Elastic Plates 635
12.1 Introduction 635
12.2 Classical Plate Theory 637
12.2.1 Displacement Field 637
12.2.2 Virtual Work Statement 638
12.2.3 Finite Element Model 642
12.2.4 Plate Bending Elements 643
12.3 Shear Deformation Plate Theory 646
12.3.1 Displacement Field 646
12.3.2 Virtual Work Statement 648
12.3.3 Finite Element Model 650
12.3.4 Shear Locking and Reduced Integration 652
12.4 Eigenvalue and Time-Dependent Problems 653
12.5 Examples 655
12.6 Summary 663
Problems 663
References for Additional Reading 665

13 Computer Implementation of Two-Dimensional Problems 667

13.1 Introduction 667
13.2 Preprocessor 669
13.3 Element Computations (Processor) 669
13.4 Applications of the Computer Program FEM2D 675
13.4.1 Introduction 675
13.4.2 Description of Mesh Generators 681
13.4.3 Applications (Illustrative Examples) 686
13.5 Summary 703
Problems 705
References for Additional Reading 709

14 Prelude to Advanced Topics 711

14.1 Introduction 711
14.2 Alternative Finite Element Models 711
14.2.1 Introductory Comments 711
14.2.2 Weighted Residual Finite Element Models 712
14.2.3 Mixed Formulations 722
14.3 Three-Dimensional Problems 725
14.3.1 Heat Transfer 726
14.3.2 Flows of Viscous Incompressible Fluids 727
14.3.3 Elasticity 728
14.3.4 Three-Dimensional Finite Elements 731
14.3.5 A Numerical Example 735
14.4 Nonlinear Problems 736
14.4.1 General Comments 736
14.4.2 Bending of Euler–Bernoulli Beams 736
14.4.3 The Navier–Stokes Equations in Two Dimensions 738
14.4.4 Solution Methods for Nonlinear Algebraic Equations 739
14.4.5 Numerical Examples 740
14.5 Errors in Finite Element Analysis 743
14.5.1 Types of Errors 743
14.5.2 Measures of Errors 744
14.5.3 Convergence and Accuracy of Solutions 745
14.6 Summary 750
Problems 751
References for Additional Reading 753

Index 757

PREFACE

The third edition of the book, like the previous two editions, represents an effort to select and present certain aspects of the finite element method that are most useful in developing and analyzing linear problems of engineering and science. In revising the book, students taking courses that might use this book as their textbook have been kept in mind. This edition is prepared to bring more clarity to the concepts being discussed while maintaining the necessary mathematical rigor and providing physical interpretations and engineering applications at every step.

This edition of the book is a revision of the second edition, which was well received by engineers as well as researchers in the fields of engineering and science. Most of the revisions in the current edition took place in Chapters 1 through 6 and 14. Chapter 5 on error analysis from the second edition is eliminated and a section on the same subject is added to Chapter 14. Chapter 3 from the second edition is now divided into two chapters, Chapter 3 on theoretical formulation and Chapter 4 on applications. Chapter 4 on beams from the second edition now became Chapter 5 in the current edition, making the total number of chapters in both editions the same. Another change is the interchanging of Chapters 10 and 11 to facilitate the natural transition from plane elasticity to plate bending (Chapter 12). New material on three-dimensional finite element formulations and nonlinear formulations is added in Chapter 14. In all the chapters, material is added and reorganized to aid the reader in understanding the concepts.

Another change in this edition is the removal of appendices containing the program listing of **FEM1D** and **FEM2D**, which would have taken up over 80 pages. The program listings, executables, and instructor resources are available on the text's website at www.mhhe.com/reddy3e. The source files of these programs may be obtained from the author for a small fee.

Most people who have used the earlier editions of the book liked the "differential equations approach" adopted here. This is natural because everyone, engineer or scientist, is looking for a way to solve differential equations arising in the study of physical phenomena. It is hoped that the third edition of the book serves the student even better than the previous editions in understanding the finite element method as applied to linear problems of engineering and science.

The author has benefited by teaching an introductory course from this book for many years. While it is not possible to name hundreds of students and colleagues who have contributed to the author's ability to explain concepts in a clear manner, the author

expresses his sincere appreciation to the following people for their helpful comments on this edition:

Ronald C. Averill, Michigan State University
Mahesh Gupta, Michigan Technological University
H.N. Hashemi, Northeastern University
Stephen M. Heinrich, Marquette University
Paul R. Heyliger, Colorado State University
John Jackson, University of Memphis
Mehdi Pourazady, University of Toledo
Robert L. Rankin, Arizona State University
N. Sukumar, University of California, Davis
Kumar Tamma, University of Minnesota
Chi-Tay Tsai, Florida Atlantic University

J. N. Reddy
jnreddy@tamu.edu

Tejashwina vadheetamasthu
(*May what we study be well studied*)

Chapter 1
INTRODUCTION

1.1 GENERAL COMMENTS

One of the most important things engineers and scientists do is to model physical phenomena. Virtually every phenomenon in nature, whether aerospace, biological, chemical, geological, or mechanical can be described, with the aid of the laws of physics or other fields in terms of algebraic, differential, and/or integral equations relating various quantities of interest. Determining the stress distribution in a pressure vessel with oddly shaped holes and numerous stiffeners and subjected to mechanical, thermal, and/or aerodynamic loads, finding the concentration of pollutants in lakes and seawater or in the atmosphere, and simulating weather in an attempt to understand and predict the formation of thunderstorms and tornadoes are a few examples of many important practical problems that engineers deal with.

Analytical descriptions of physical phenomena and processes are called *mathematical models*. Mathematical models of a process are developed using assumptions concerning how the process works and using appropriate axioms or laws governing the process, and they are often characterized by very complex differential and/or integral equations posed on geometrically complicated domains. Consequently, the processes to be studied, until the advent of electronic computation, were drastically simplified so that the governing equations can be solved analytically. Over the last three decades, however, computers have made it possible, with the help of suitable mathematical models and numerical methods, to solve many practical problems of engineering. The use of a numerical method and a computer to evaluate the mathematical model of a process and estimate its characteristics is called a *numerical simulation*. There now exists a new and growing body of knowledge connected with the development of mathematical models and use of numerical simulations of physical systems, and it is known as *computational mechanics* [1].

Any numerical simulation, such as the one by the finite element method, is not an end in itself but rather an aid to design and manufacturing. There are several reasons why an engineer or a scientist should study a numerical method, especially the finite element method:

1. Most practical problems involve complicated domains (both geometry and material constitution), loads, and nonlinearities that forbid the development of analytical solutions. Therefore, the only alternative is to find approximate solutions using numerical methods.

2. A numerical method, with the advent of a computer, can be used to investigate the effects of various parameters (e.g., geometry, material parameters, or loads) of the system on its response to gain a better understanding of the process/system being analyzed. It is cost-effective and saves time and material resources compared to the multitude of physical experiments needed to gain the same level of understanding.
3. Because of the power of numerical methods and electronic computation, it is possible to include all relevant features in a mathematical model of a physical process without worrying about its solution by exact means.
4. Those who are quick to use a computer program rather than *think* about the problem to be analyzed may find it difficult to interpret or explain the computer-generated results. Even to develop proper input data to the computer program, a good understanding of the underlying theory of the problem as well as the numerical method (on which the computer program is based) is required.
5. The finite element method and its generalizations are the most powerful computer-oriented methods ever devised to analyze practical engineering problems. Today, finite element analysis is an integral and major component in many fields of engineering design and manufacturing. Major established industries such as the automobile, aerospace, chemical, pharmaceutical, petroleum, electronics, and communications, as well as emerging technologies such as nanotechnology and biotechnology rely on the finite element method to simulate complex phenomenon at different scales for design and manufacture of high-technology products.

1.2 MATHEMATICAL MODELS

A *mathematical model* can be broadly defined as a set of equations that expresses the essential features of a physical system in terms of variables that describe the system. The mathematical models of physical phenomena are often based on fundamental scientific laws of physics such as the principle of conservation of mass, conservation of linear momentum, and conservation of energy. Below we consider three simple examples drawn from dynamics, heat transfer, and solid mechanics to illustrate how mathematical models of physical problems are formulated.

Example 1.2.1 (A Dynamics Problem)

A simple pendulum (such as the one used in a clock) consists of a bob of mass m (kg) attached to one end of a rod of length ℓ (m) and the other end is pivoted to a fixed point O, as shown in Fig. 1.2.1. In order to derive the governing equation of the problem, we must make certain assumptions concerning the system (the bob and rod) consistent with the goal of the analysis. If the goal is to study the simplest linear motion of the pendulum, we assume that the bob as well as the rod are rigid (i.e., not deformable) and the rod is massless (i.e., compared to that of the bob). In addition, we assume that there is no friction at the pivot point O and the resistance offered by the surrounding medium to the pendulum is also negligible.

Under these assumptions, the equation governing the motion of the system can be formulated using the *principle of conservation of linear momentum* (or simply Newton's second law),

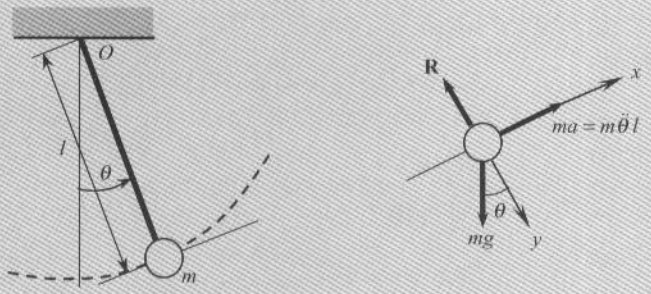

Figure 1.2.1 Simple pendulum.

which states, in the present case, that the vector sum of externally applied forces on a system is equal to the time rate of change of the linear momentum (mass times velocity) of the system:

$$\mathbf{F} = \frac{d}{dt}(m\mathbf{v}) = m\mathbf{a} \tag{1.2.1}$$

where $\mathbf{F}$ is the vector sum of all forces acting on the system, m is the mass of the system, $\mathbf{v}$ is the velocity vector, and $\mathbf{a}$ is the acceleration vector of the system. To write the equation governing the angular motion, we set up a coordinate system, as shown in Fig. 1.2.1. Applying Newton's second law to the x-direction (note that the dynamic equilibrium of forces in the y-direction gives the reaction force $R(N)$ in terms of the weight mg of the bob), we obtain

$$F_x = m\frac{dv_x}{dt} \tag{1.2.2}$$

where $F_x = -mg \sin\theta$, $v_x = \ell\frac{d\theta}{dt}$, θ is the angular displacement (radians), v_x is the component of velocity (m/s) along the x coordinate, and t denotes time (s). Thus, the equation for angular motion becomes

$$-mg \sin\theta = m\ell\frac{d^2\theta}{dt^2} \quad \text{or} \quad \frac{d^2\theta}{dt^2} + \frac{g}{\ell}\sin\theta = 0 \tag{1.2.3}$$

Equation (1.2.3) is nonlinear on account of the term $\sin\theta$. For small angular motions (consistent with the goal of the study), $\sin\theta$ is approximated as θ. Thus, the angular motion is described by the linear differential equation

$$\frac{d^2\theta}{dt^2} + \frac{g}{\ell}\theta = 0 \tag{1.2.4}$$

Equations (1.2.3) and (1.2.4) represent mathematical models of nonlinear and linear motions, respectively, of a rigid pendulum. Their solution requires knowledge of conditions at time $t = 0$ on θ and its time derivative $\dot{\theta}$ (angular velocity). These conditions are known as the *initial conditions*. Thus, the linear problem involves solving the differential equation (1.2.4) subjected to the initial conditions

$$\theta(0) = \theta_0, \qquad \frac{d\theta}{dt}(0) = v_0 \tag{1.2.5}$$

The problem described by Eqs. (1.2.4) and (1.2.5) is called an *initial-value problem*.

The linear problem described by Eqs. (1.2.4) and (1.2.5) can be solved analytically. The general analytical solution of the linear equation (1.2.4) ($\ddot{\theta} + \lambda^2\theta = 0$) is given by

$$\theta(t) = A \sin\lambda t + B \cos\lambda t \tag{1.2.6}$$

where $\lambda = \sqrt{\frac{g}{l}}$ and A and B are constants to be determined using the initial conditions in (1.2.5). We obtain

$$A = \frac{v_0}{\lambda}, \quad B = \theta_0 \tag{1.2.7}$$

and the solution to the linear problem is

$$\theta(t) = \frac{v_0}{\lambda} \sin \lambda t + \theta_0 \cos \lambda t \tag{1.2.8}$$

For zero initial velocity and nonzero initial position θ_0, we have

$$\theta(t) = \theta_0 \cos \lambda t \tag{1.2.9}$$

which represents a simple harmonic motion.

If we were to solve the nonlinear equation (1.2.3) subject to the conditions in (1.2.5), we may consider using a numerical method because it is not possible to solve it exactly for large values of θ. We will revisit this issue in the sequel.

Example 1.2.2 (A Heat Transfer Problem)

Here we wish to derive the governing equations (i.e., develop the mathematical model) of steady-state heat transfer through a cylindrical bar of nonuniform cross section. The bar is subject to a known temperature T_0 (°C) at the left end and exposed, both on the surface and at the right end, to a medium (such as cooling fluid or air) at temperature T_∞. We assume that temperature is uniform at any section of the bar, $T = T(x)$. Due to the difference between the temperatures of the bar and the surrounding medium, there is convective heat transfer across the surface of the body and at the right end. The principle of conservation of energy (or the *second law of thermodynamics*) can be used to derive the governing equations of the problem. The principle of conservation of energy requires that the rate of change (increase) of internal energy is equal to the sum of heat gained by conduction, convection, and internal heat generation (radiation not included). For a steady process, the time rate of internal energy is zero.

Consider a volume element of length Δx and having an area of cross section $A(x)$ (m^2) normal to the x axis (see Fig. 1.2.2). If q denotes the heat flux (heat flow per unit area, W/m^2), then $[Aq]_x$ is the net heat flow into the volume element at x, $[Aq]_{x+\Delta x}$ is the net heat flow out of the volume element at $x + \Delta x$, and $\beta P \Delta x(T_\infty - T)$ is the heat flow through the surface of the rod into the body. Here β denotes the film (that is formed between the body and the medium around) conductance [$W/(m^2 \cdot °C)$], T_∞ is the temperature of the surrounding medium, and P is the perimeter (m). We also assume that there is a heat source within the rod generating energy at a rate of g (W/m^3). In practice, such energy source can be due to nuclear fission or chemical reactions taking place within the rod, or due to the passage of electric current through the medium (i.e., volume heating) . Then the energy balance gives

$$[Aq]_x - [Aq]_{x+\Delta x} + \beta P \Delta x(T_\infty - T) + gA \Delta x = 0 \tag{1.2.10}$$

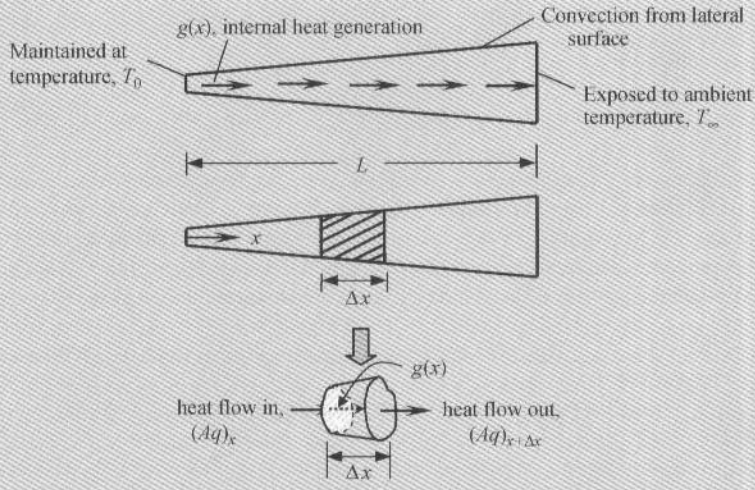

Figure 1.2.2 Heat transfer in a bar.

or, dividing throughout by Δx,

$$-\frac{[Aq]_{x+\Delta x}-[Aq]_x}{\Delta x}+\beta P(T_\infty - T)+Ag=0$$

and taking the limit $\Delta x \to 0$, we obtain

$$-\frac{d}{dx}(Aq)+\beta P(T_\infty - T)+Ag=0 \tag{1.2.11}$$

We can relate the heat flux q (W/m^2) to the temperature gradient. Such a relation is provided by the *Fourier law*

$$q(x)=-k\frac{dT}{dx} \tag{1.2.12}$$

where k denotes the thermal conductivity [W/(m·°C)] of the material. The minus sign on the right side of the equality in the above equation indicates that heat flows from high temperature to low temperature. Equation (1.2.12) is known as a *constitutive relation* because it contains a material property.

Now using the Fourier law (1.2.12) in (1.2.11), we arrive at the heat *conduction equation*

$$\frac{d}{dx}\left(kA\frac{dT}{dx}\right)+\beta P(T_\infty - T)+Ag=0 \tag{1.2.13}$$

which can also be written as

$$-\frac{d}{dx}\left(kA\frac{dT}{dx}\right)+\beta P(T-T_\infty)=Ag \tag{1.2.14}$$

Equation (1.2.14) is a linear, (nonhomogeneous) second-order differential equation, which can be solved with known conditions on temperature T or heat Aq (not both) at a boundary

point (e.g., ends of the bar). The known end conditions for the present case (recall the problem description at the start of this example) can be expressed as

$$T(0) = T_0, \quad \left[kA\frac{dT}{dx} + \beta A(T - T_\infty) \right]_{x=L} = 0 \tag{1.2.15}$$

These conditions are called *boundary conditions* because they represent conditions at the boundary points of the bar. The first condition in (1.2.15) is obvious. The second condition represents the balance of heat due to conduction $[kA(dT/dx)]$ and convection $[\beta A(T - T_\infty)]$. The problem described by Eqs. (1.2.14) and (1.2.15) is called, for obvious reasons, a *boundary-value problem*. This completes the mathematical model development of the problem.

Equations (1.2.14) and (1.2.15) can be simplified for various special cases. First let

$$\theta \equiv T - T_\infty, \quad a \equiv kA \text{ (W·m/°C)}, \quad c \equiv \beta P \text{ [W/(m·°C)]}, \quad f \equiv Ag \text{ (W/m)} \tag{1.2.16}$$

so that Eqs. (1.2.14) and (1.2.15) can be written as (note that a and c are always positive in heat transfer problems)

$$-\frac{d}{dx}\left(a\frac{d\theta}{dx}\right) + c\theta = f \tag{1.2.17}$$

$$\theta(0) = T_0 - T_\infty, \quad \left[a\frac{d\theta}{dx} + \beta A\theta \right]_{x=L} = 0 \tag{1.2.18}$$

Now if a and c are constant (e.g., homogeneous bar of constant cross section) and $g = 0$ (no internal heat generation), Eqs. (1.2.17) and (1.2.18) become

$$-\frac{d^2\theta}{dx^2} + \frac{c}{a}\theta = 0, \text{ where } 0 < x < L \tag{1.2.19}$$

$$\theta(0) = T_0 - T_\infty \equiv \theta_0, \quad \left[\frac{d\theta}{dx} + \frac{\beta}{k}\theta \right]_{x=L} = 0 \tag{1.2.20}$$

The general solution of (1.2.19) ($\theta'' - m^2\theta = 0$) is

$$\theta(x) = C_1 \cosh mx + C_2 \sinh mx, \quad m \equiv \sqrt{\frac{c}{a}} = \sqrt{\frac{\beta P}{kA}} \tag{1.2.21a}$$

where C_1 and C_2 are constants that can be determined using the boundary conditions (1.2.20). Using $\sinh x = (e^x - e^{-x})/2$ and $\cosh x = (e^x + e^{-x})/2$, we have

$$C_1 = \theta_0, \quad C_2 = -\theta_0 \left[\frac{\sinh mL + (\beta/mk)\cosh mL}{\cosh mL + (\beta/mk)\sinh mL} \right] \tag{1.2.21b}$$

Hence, the solution of Eqs. (1.2.19) and (1.2.20) becomes

$$\theta(x) = \theta(0) \left[\frac{\cosh m(L - x) + (\beta/mk)\sinh m(L - x)}{\cosh mL + (\beta/mk)\sinh mL} \right] \tag{1.2.22}$$

Example 1.2.3 (A Solid Mechanics Problem)

The last example is concerned with the mathematical formulation of the axial deformation of a bar of variable cross section. The term *bar* is used in solid and structural mechanics to mean a structural element that carries only axial loads (tensile as well as compressive). Practical examples of the problem are provided by the deformation of a slender body under its own weight and by a concrete pier supporting a bridge.

In the case of the concrete pier, it may be treated as a three-dimensional problem. The weight of the bridge as well as the weight of vehicles on the bridge is carried by the piers. The piers at the ends of a bridge take slightly different load than the ones in the interior. In a preliminary design of structures, we often try to obtain the orders-of-magnitude of the significant deformation and stress components in a typical pier rather than determine the detailed three-dimensional deformation and stress fields. With the former in mind, we make several simplifying assumptions to reduce the problem to a one-dimensional problem that allows us to determine the compression and associated stress in a typical pier. First, we know that the significant load taken by a pier is vertical (along the height of the pier). So the axial deformation (compression) and stress will be the significant quantities, and the lateral deformation due to the Poisson effect may be neglected. Second, we wish to consider the static case (as if all of the traffic on the bridge is standing still—like during heavy rush hour) with a magnitude of the axial load to represent the worst case scenario of heaviest traffic as well as snow fall (a quasi-static case may be included by magnifying the static loads). We may also take into account the weight (which is a volume force, called body force) of the pier itself. The governing equations of this simplified problem can be obtained using Newton's second law and a uniaxial stress-strain (constitutive) relation (note the similarity in the derivation of the equations of this solid mechanics problem with the heat transfer problem discussed earlier).

Figure 1.2.3 shows an element of length Δx with axial forces acting at both ends of the element, where σ_x denotes stress (i.e., force per unit area; N/m^2) in the x direction, which is taken positive downward, and $g(x)$ denotes the body force measured per unit volume (N/m^3). Hence, $[A\sigma_x]_x$ is the net tensile force on the volume element at x and $[A\sigma]_{x+\Delta x}$ is the net

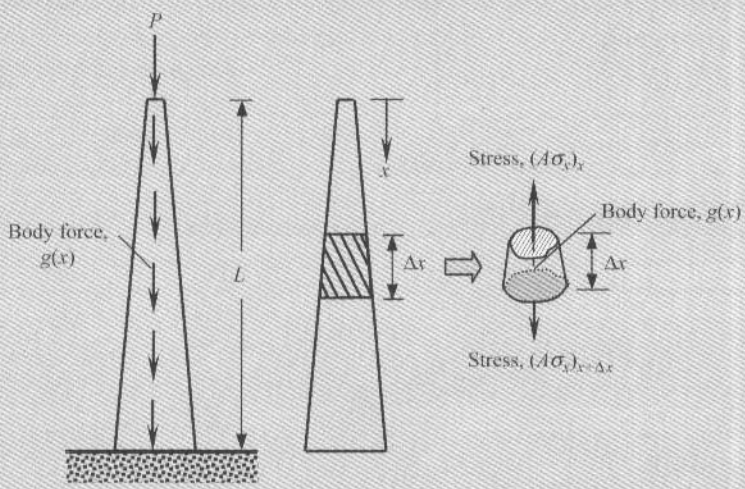

Figure 1.2.3 Axial deformation of a bar.

tensile force at $x + \Delta x$. Then setting the sum of the forces to zero (i.e., applying Newton's second law in the x-direction) yields

$$-[A\sigma_x]_x + [A\sigma_x]_{x+\Delta x} + gA\Delta x = 0$$

where $g(x)$ is the body force (i.e., weight of the body). Dividing throughout by Δx and taking the limit $\Delta x \to 0$, we obtain

$$\frac{d}{dx}(A\sigma_x) + Ag(x) = 0 \tag{1.2.23}$$

which represents the equilibrium of forces in the x-direction.

The stress σ_x can be related to the axial displacement using *Hooke's law*

$$\sigma_x = E\varepsilon_x, \quad \varepsilon_x = \frac{du}{dx} \tag{1.2.24}$$

where E is Young's modulus (N/m^2), u denotes the axial displacement (m), and ε_x is the axial strain (m/m). Again, we see that Eq. (1.2.24) is a constitutive equation. Note that a system can have several constitutive relations, each depending on the phenomenon being studied. The study of heat transfer in a bar (with nonuniform temperature) required us to employ Fourier's law to relate temperature gradient to heat flow, and the study of deformation of the same bar (subjected to axial forces) requires us to use Hooke's law to connect stress to displacement gradient.

Now using Eq. (1.2.24) in Eq. (1.2.23), we arrive at the equilibrium equation in terms of the displacement

$$\frac{d}{dx}\left(EA\frac{du}{dx}\right) + gA = 0, \quad 0 < x < L \tag{1.2.25}$$

This second-order equation can be solved using known boundary conditions at $x = 0$ and $x = L$. The boundary conditions of a bar involve specifying either the displacement u or the force $A\sigma_x$ at a boundary point.

The known boundary conditions of the problem at hand are (see Fig. 1.2.3)

$$u(L) = 0, \quad \left[EA\frac{du}{dx}\right]_{x=0} = -P \tag{1.2.26}$$

where P is the load carried by the pier (i.e., weight of the bridge and the load it carries divided by the number of piers supporting the bridge). The second boundary condition in (1.2.26) represents the force equilibrium at $x = L$. Equations (1.2.25) and (1.2.26) may not admit an analytical solution when $a = a(x)$, requiring us to seek approximate solutions using numerical methods.

The analytical solution of Eq. (1.2.25) subject to the boundary conditions in (1.2.26) may be found for the simple case in which $a \equiv EA$ and $f \equiv Ag$ are constant (homogeneous and uniform cross-sectional, pier). The general solution of (1.2.25) in this case is given by

$$u(x) = \frac{1}{a}\left(-\frac{f}{2}x^2 + C_1 x + C_2\right) \tag{1.2.27}$$

Use of the boundary conditions (1.2.26) give $C_1 = -P$ and $C_2 = fL^2/2 - PL$, and the solution becomes

$$u(x) = \frac{1}{E}\left[\frac{g}{2}(L^2 - x^2) + \frac{P}{A}(L - x)\right] \tag{1.2.28}$$

1.3 NUMERICAL SIMULATIONS

While the derivation of the governing equations for most problems is not unduly difficult, their solution by exact methods of analysis is often difficult due to geometric and material complexities. In such cases, numerical methods of analysis provide alternative means of finding solutions. By a *numerical simulation* of a process, we mean the solution of the governing equations (or mathematical model) of the process using a numerical method and a computer. Numerical methods typically transform differential equations governing a continuum to a set of algebraic equations of a discrete model of the continuum that are to be solved using computers.

There exist a number of numerical methods, many of which are developed to solve differential equations. In the finite difference approximation of a differential equation, the derivatives in the latter are replaced by difference quotients (or the function is expanded in a Taylor series) that involve the values of the solution at discrete mesh points of the domain. The resulting algebraic equations are solved for the values of the solution at the mesh points after imposing the boundary conditions. These ideas are illustrated with the help of two examples, one for an initial-value problem and another for a boundary-value problem.

In the solution of a differential equation by a classical variational method, the equation is put into an equivalent weighted-integral form and then the approximate solution over the domain is assumed to be a linear combination ($\sum_j c_j \phi_j$) of appropriately chosen approximation functions ϕ_j and undetermined coefficients c_j. The coefficients c_j are determined such that the integral statement equivalent to the original differential equation is satisfied. Various variational methods, e.g., the Ritz, Galerkin, collocation, and least-squares methods, differ from each other in the choice of the integral form, weight functions, and/or approximation functions. A more detailed discussion of variational methods will be given in Chapter 2. The classical variational methods, which are truly meshless methods, are powerful methods that provide globally continuous solutions but suffer from the disadvantage that the approximation functions for problems with arbitrary domains are difficult to construct (the modern meshless methods seem to provide a way to construct approximation functions for arbitrary domains).

Here we consider two examples of numerical simulations using the finite difference method to give the reader a taste of numerical methods and, in the process, introduce the finite difference method. The examples discussed here are based on the problems introduced in Examples 1.2.1 and 1.2.2. The bar problem of Example 1.2.3 is mathematically the same as the heat transfer problem in Example 1.2.2; therefore, its numerical solution is not discussed here.

Example 1.3.1 (Pendulum Problem)

Here we consider the numerical solution of Eq. (1.2.4) governing a simple pendulum. To introduce the finite difference method, we consider the first-order differential equation

$$\frac{du}{dt} = f(t, u) \tag{1.3.1}$$

where f is a known function of the unknown. Equation (1.3.1) must be solved for $t > 0$ subject to the (initial) condition $u(0) = u_0$. We approximate the derivative at t_i by

$$\left(\frac{du}{dt}\right)\bigg|_{t=t_i} \approx \frac{u(t_{i+1}) - u(t_i)}{t_{i+1} - t_i} \tag{1.3.2}$$

Note that we replaced the derivative at $t = t_i$ by its definition except that we did not take the limit $\Delta t \equiv t_{i+1} - t_i \to 0$; that is why it is an approximation. For increasingly small values of Δt, we expect the approximation to have decreasingly small error. Substituting (1.3.2) into (1.3.1) at $t = t_i$, we obtain

$$u_{i+1} = u_i + \Delta t\ f(u_i, t_i), \quad u_i = u(t_i), \quad \Delta t = t_{i+1} - t_i \tag{1.3.3}$$

Equation (1.3.3) can be solved, starting from the known value u_0 of $u(t)$ at $t = 0$, for $u_1 = u(t_1) = u(\Delta t)$. This process can be repeated to determine the values of u at times $t = \Delta t, 2\Delta t, \ldots, n\Delta t$. This is known as *Euler's explicit scheme* (or first-order Runga–Kutta method), also known as the *forward difference scheme*. Of course there are higher-order finite difference schemes that are more accurate than Euler's scheme, and we will not discuss them as they are outside the scope of this study. Note that we are able to convert the ordinary differential equation (1.3.1) to an algebraic equation (1.3.3) that needs to be evaluated at different times to construct the time history of $u(t)$.

We now apply Euler's explicit scheme to the second-order equation (1.2.4) subjected to the initial conditions (1.2.5). To apply the procedure described above to the equation at hand, we rewrite Eq. (1.2.4) as a pair of coupled (i.e., one cannot be solved without the other) first-order equations

$$\frac{d\theta}{dt} = v, \quad \frac{dv}{dt} = -\lambda^2\theta \tag{1.3.4}$$

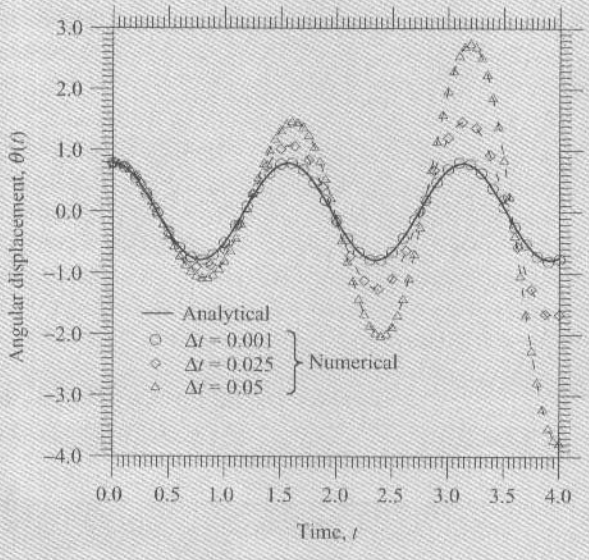

Figure 1.3.1 Analytical and numerical solutions $\theta(t)$ of the simple pendulum.

where $\lambda^2 = g/\ell$. Applying the scheme of Eq. (1.3.3) to the equations at hand, we obtain

$$\theta_{i+1} = \theta_i + \Delta t\, v_i; \quad v_{i+1} = v_i - \Delta t\, \lambda^2 \theta_i \tag{1.3.5}$$

The expressions for θ_{i+1} and v_{i+1} in Eq. (1.3.5) are repeatedly computed using the known solution (θ_i, v_i) from the previous time step. At time $t = 0$, we use the known initial values (θ_0, v_0). Thus, one needs a computer and a computer language like Fortran or C++ to implement the logic of repeatedly computing θ_{i+1} and v_{i+1} with the help of Eq. (1.3.5).

The numerical solutions of equation (1.3.5) for three different time steps, $\Delta t = 0.05, 0.025$, and 0.001, along with the exact linear solution (1.2.9) (with $\ell = 2.0$, $g = 32.2$, $\theta_0 = \pi/4$, and $v_0 = 0$) are presented in Fig. 1.3.1. The accuracy of the numerical solutions is dependent on the size of the time step; the solution is more accurate with smaller time steps. For large time steps, the solution even diverges from the true solution.

Example 1.3.2 (Heat Transfer Problem)

Here we consider the boundary-value problem of Example 1.2.2. The finite difference approximation of a boundary-value problem differs from that of an initial value problem. First we divide the domain $(0, L)$ into a finite set of N intervals of equal length Δx, as shown in Fig. 1.3.2. The ends of each interval is called a mesh point. Thus, there are $N + 1$ mesh points in the domain. Then we approximate the second-derivative directly using the centered difference scheme where the error is of order $O(\Delta x)^2$

$$\left(\frac{d^2\theta}{dx^2}\right)_{x=x_i} \approx \left(\frac{\theta_{i-1} - 2\theta_i + \theta_{i+1}}{(\Delta x)^2}\right) \tag{1.3.6}$$

Using the above approximation in Eq. (1.2.19), we obtain

$$-(\theta_{i-1} - 2\theta_i + \theta_{i+1}) + (m\Delta x)^2 \theta_i = 0 \quad \text{or} \quad -\theta_{i-1} + [2 + (m\Delta x)^2]\theta_i - \theta_{i+1} = 0 \tag{1.3.7}$$

Equation (1.3.7) is valid for any mesh point $x = x_i$, $i = 1, 2, \ldots, N$, and it contains values of θ both at $x = x_{i-1}$ and $x = x_{i+1}$. Note that Eq. (1.3.7) is not used at mesh point $x = x_0 = 0$ because the temperature is known there [see Eq. (1.2.20)]. However, use of Eq. (1.3.7) at mesh point $x = x_N = L$ requires the knowledge of the fictitious value θ_{N+1} (as we see in the sequel,

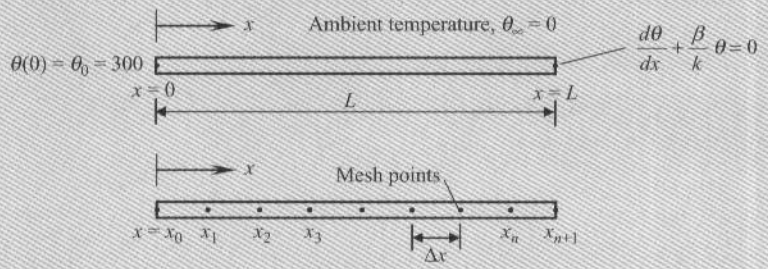

Figure 1.3.2 Heat transfer in a bar and a typical finite difference mesh.

we never have to deal with such fictitious values in the finite element method). The forward finite difference approximation of the second boundary condition in (1.2.20) at mesh point $x = L$ gives

$$\frac{\theta_{N+1} - \theta_N}{\Delta x} + \frac{\beta}{k}\theta_N = 0$$

from which we have

$$\theta_{N+1} = \left(1 - \frac{\beta \Delta x}{k}\right)\theta_N \tag{1.3.8}$$

Application of the formula (1.3.7) to mesh points at $x_1, x_2, \ldots, x_N$ yields

$$\begin{aligned} -\theta_0 + D\theta_1 - \theta_2 &= 0 \\ -\theta_1 + D\theta_2 - \theta_3 &= 0 \\ -\theta_2 + D\theta_3 - \theta_4 &= 0 \\ \cdots \quad &\cdots \quad \cdots \\ -\theta_{N-1} + D\theta_N - \theta_{N+1} &= 0 \end{aligned} \tag{1.3.9}$$

where $D = [2 + (m\Delta x)^2]$; Eq. (1.3.9) consists of N equations in N unknowns, θ_1, $\theta_2, \ldots, \theta_N$.

As a specific example, consider a steel rod of diameter $d = 0.02$ m, length $L = 0.05$ m, and thermal conductivity $k = 50$ W/(m·°C). Suppose that the temperature at the left end is $T_0 = 320$°C, ambient temperature is $T_\infty = 20$°C and film conductance (or heat transfer coefficient) $\beta = 100$ W/(m²·°C). For this data, we have

$$\frac{\beta}{k} = 2, \quad m^2 = \frac{\beta P}{kA} = \frac{\beta(\pi d)}{k(\pi d^2/4)} = 400, \quad \theta_0 = \theta(0) = 300^\circ\text{C}$$

For a subdivision of four intervals ($N = 4$), we have $\Delta x = 0.0125$ m and $D = 2 + (20 \times 0.0125)^2 = 2.0625$. For this case, there are four equations in four unknowns:

$$\begin{array}{rrrrcr} 2.0625\theta_1 & -\theta_2 & & & = & 300 \\ -\theta_1 & +2.0625\theta_2 & -\theta_3 & & = & 0 \\ & -\theta_2 & +2.0625\theta_3 & -\theta_4 & = & 0 \\ & & -\theta_3 & +1.0875\theta_4 & = & 0 \end{array} \tag{1.3.10}$$

The above *tridiagonal* system of algebraic equations can be solved using the Gauss elimination method (this is where we need a computer!). The solution is given by

$$\{\theta\} = \{245.81,\ 206.98,\ 181.10,\ 166.52\}^T$$

The analytical solution at the same points is

$$\{\theta\} = \{248.75,\ 213.13,\ 190.90,\ 180.66\}^T$$

The maximum error is about 7.8 percent. When the number of mesh points is doubled, the maximum error goes down to 4.2 percent, and it is 1 percent when the number of mesh points is increased to 32.

1.4 THE FINITE ELEMENT METHOD

1.4.1 The Basic Idea

The finite element method is a numerical method like the finite difference method but is more general and powerful in its application to real-world problems that involve complicated physics, geometry, and/or boundary conditions. In the finite element method, a given domain is viewed as a collection of subdomains, and over each subdomain the governing equation is approximated by any of the traditional variational methods. The main reason behind seeking approximate solution on a collection of subdomains is the fact that it is easier to represent a complicated function as a collection of simple polynomials, as can be seen from Fig. 1.4.1. Of course, each individual segment of the solution should fit with its neighbors in the sense that the function and possibly derivatives up to a chosen order are continuous at the connecting points. These ideas will be more clear in the sequel.

1.4.2 The Basic Features

The method is endowed with three distinct features that account for its superiority over other competing methods. First, a geometrically complex domain Ω of the problem, such as the one in Fig. 1.4.2(a), is represented as a collection of geometrically simple subdomains, called *finite elements* [see Fig. 1.4.2(b)]. Each finite element Ω_e [Fig. 1.4.2(c)] is viewed as an independent domain by itself. Here the word "domain" refers to the geometric region over which the equations are solved. Second, over each finite element, algebraic equations among the quantities of interest are developed using the governing equations of the problem. Third, the relationships from all elements are assembled (i.e., elements are put back into their original positions of the total domain) as indicated in Fig. 1.4.2(d), using certain interelement relationships. These statements may not make complete sense to the reader until some specific examples to illustrate the features are discussed in the coming pages.

Approximations enter engineering analyses at several stages. The division of the whole domain into finite elements may not be exact (i.e., the assemblage of elements, Ω_h, does not match the original domain Ω), introducing error in the domain being modeled. The second stage is when element equations are derived. Typically, the dependent unknowns (u) of the problem are approximated using the basic idea that any continuous function can be

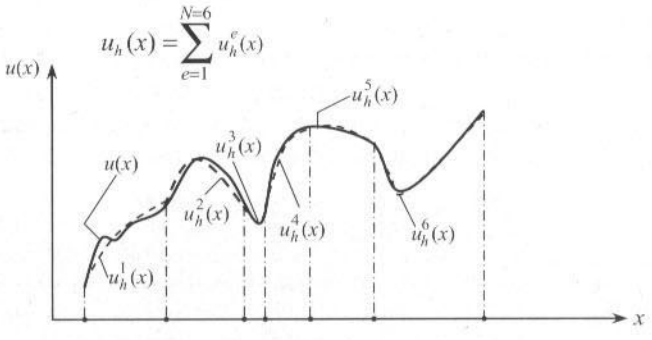

Figure 1.4.1 Piecewise approximation of a function.

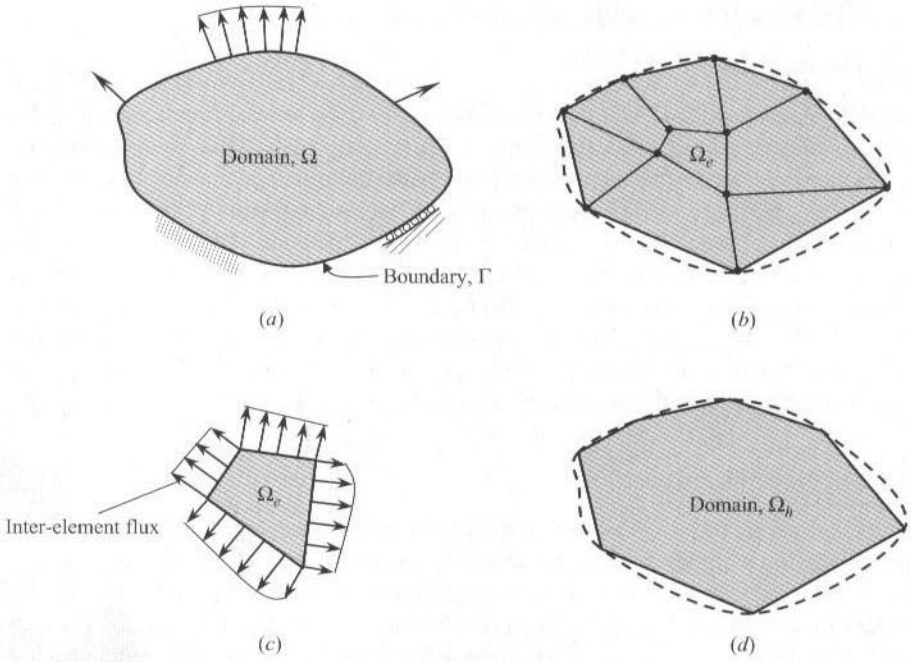

Figure 1.4.2 Representation of a two-dimensional domain by a collection of triangles and quadrilaterals.

represented by a linear combination of known functions ϕ_i and undetermined coefficients c_i ($u \approx u_h = \sum c_i \phi_i$). Algebraic relations among the undetermined coefficients c_j are obtained by satisfying the governing equations, in a weighted-integral sense, over each element. The approximation functions ϕ_i are often taken to be polynomials, and they are derived using concepts from interpolation theory. Therefore, they are termed *interpolation functions*. Thus, approximation errors in the second stage are introduced both in representing the solution u as well as in evaluating the integrals. Finally, errors are introduced in solving the assembled system of equations. Obviously, some of the errors discussed above can be zero. When all the errors are zero, we obtain the exact solution of the problem (which is not the case in most problems).

Next, the basic ideas and some terminology of the finite element method are introduced via several simple examples. The reader should try to understand the basic features rather than to question the use of an approximation method to solve such a simple problem (which can possibly be solved exactly without using the finite element method).

Example 1.4.1 (Approximation of the Perimeter of a Circle)

This discussion is an expansion of an article written by the author in 1978 for a student magazine at the University of Oklahoma (Reddy, 1978). Consider the problem of determining the perimeter (quantity of interest) of a circle of radius R [see Fig. 1.4.3(*a*)]. We *pretend*

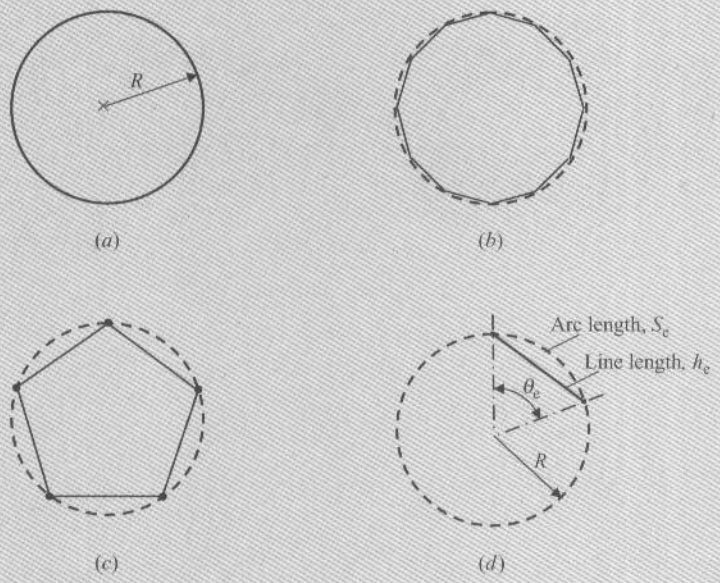

Figure 1.4.3 Determination of the perimeter of a circle.

that we do not know the formula ($P = 2\pi R$) for the perimeter (circumference) of a circle. Ancient mathematicians estimated the value of the perimeter of a circle by approximating it by (straight) line segments, whose lengths they were able to measure. The approximate value of the circumference is obtained by summing the lengths of the line segments used to represent it.

The three basic features of the finite element method in the present case take the following form. First, the division of the perimeter of a circle into a collection of line segments. In theory, we need an infinite number of such line elements to represent the perimeter; otherwise, the value computed will have some error. Second, writing an equation for the quantity of interest (perimeter) over an element (line segment) in this case is exact, as we shall see. Third, assembly of elements amounts to simply adding the element lengths to obtain the total value.

Although this is a trivial example, it illustrates several (but not all) ideas and steps involved in the finite element analysis of a problem. We outline the steps involved in computing an approximate value of the perimeter of the circle. In doing so, we introduce certain terms that are used in the finite element analysis of any problem.

1. *Finite element discretization.* First, the domain (i.e., the perimeter of the circle) is represented as a collection of a finite number n of subdomains, namely, line segments [Fig. 1.4.3(*b*)]. This is called *discretization of the domain*. Each subdomain (i.e., line segment) is called an *element*. The collection of elements is called the *finite element mesh*. The elements are connected to each other at points called *nodes*. In the present case, we discretize the perimeter into a mesh of five ($n = 5$) line segments [Fig. 1.4.3(*c*)]. The line segments can be of different lengths. When all the elements are of the same length, the mesh is said to be *uniform*; otherwise, it is called a *nonuniform* mesh.
2. *Element equations.* A typical element (i.e., line segment, Ω_e) is isolated and its required properties, i.e., length, are computed by some appropriate means. Let h_e be the length of element

Ω_e in the mesh. For a typical element Ω_e, h_e is given by [see Fig. 1.4.3(*d*)]

$$h_e = 2R \sin \frac{1}{2}\theta_e \tag{1.4.1}$$

where R is the radius of the circle and $\theta_e < \pi$ is the angle subtended by the line segment. The above equations are called *element equations*. Ancient mathematicians most likely made measurements, rather than using Eq. (1.4.1), to find h_e (they did not know π).

3. *Assembly of element equations and solution.* The approximate value of the perimeter of the circle is obtained by putting together the element properties in a meaningful way; this process is called the *assembly* of the element equations. It is based, in the present case, on the simple idea that the total perimeter of the polygon Ω_h (assembly of elements) is equal to the sum of the lengths of individual elements:

$$P_n = \sum_{e=1}^{n} h_e \tag{1.4.2}$$

Then P_n represents an approximation to the actual perimeter, P. If the mesh is uniform, or h_e is the same for each of the elements in the mesh, then $\theta_e = 2\pi/n$, and we have

$$P_n = n\left(2R \sin \frac{\pi}{n}\right) \tag{1.4.3}$$

4. *Convergence and error estimate.* For this simple problem, we know the exact solution: $P = 2\pi R$. We can estimate the error in the approximation and show that the approximate solution P_n converges to the exact value P in the limit as $n \to \infty$. Consider a typical element Ω_e. The error in the approximation is equal to the difference between the length of the sector and that of the line segment [see Fig. 1.4.3(*d*)]

$$E_e = |S_e - h_e| \tag{1.4.4}$$

where $S_e = R\theta_e$ is the length of the sector. Thus, the error estimate for an element in the mesh is given by

$$E_e = R\left(\frac{2\pi}{n} - 2 \sin \frac{\pi}{n}\right) \tag{1.4.5}$$

The total error (called *global* error) is given by multiplying E_e by n:

$$E = nE_e = 2R\left(\pi - n \sin \frac{\pi}{n}\right) = 2\pi R - P_n = P - P_n \tag{1.4.6}$$

We now show that E goes to zero as $n \to \infty$. Letting $x = 1/n$, we have

$$P_n = 2Rn \sin \frac{\pi}{n} = 2R \frac{\sin \pi x}{x}$$

and

$$\lim_{n\to\infty} P_n = \lim_{x\to 0}\left(2R \frac{\sin \pi x}{x}\right) = \lim_{x\to 0}\left(2\pi R \frac{\cos \pi x}{1}\right) = 2\pi R \tag{1.4.7}$$

Hence, E_n goes to zero as $n \to \infty$. This completes the proof of convergence.

Example 1.4.2 (Geometric Centroid of an Irregular Body)

It should be recalled, from a first course on statics of rigid bodies, that the calculation of the mass center or the geometric centroid (quantity of interest) of an irregular volume makes use of the so-called method of composite bodies, in which a body is conveniently divided (mesh discretization) into several parts (elements) of simple shape for which the mass and the center of mass (element properties) can be computed readily. The center of mass of the whole body is then obtained using the moment *principle of Varignon* (a basis for the assembly of element equations):

$$(m_1 + m_2 + \cdots + m_n)\bar{X} = m_1\bar{x}_1 + m_2\bar{x}_2 + \cdots + m_n\bar{x}_n \tag{1.4.8}$$

where $\bar{X}$ is the x-coordinate of the center of mass of the whole body, m_e is the mass of the eth part, and $\bar{x}_e$ is the x-coordinate of the center of mass of the eth part. Similar expressions hold for the y and z coordinates of the center of mass of the whole body. Analogous relations hold for composite lines, areas, and volumes, wherein the masses are replaced by lengths, areas, and volumes, respectively.

When a given body is not expressible in terms of simple geometric shapes (elements) for which the mass and the center of the mass can be represented mathematically, it is necessary to use a method of approximation to represent the "properties" of an element. As an example, consider the problem of finding the centroid $(\bar{X}, \bar{Y})$ of the irregular region shown in Fig. 1.4.4(*a*). The region can be divided into a finite number of trapezoidal strips (elements), a typical element

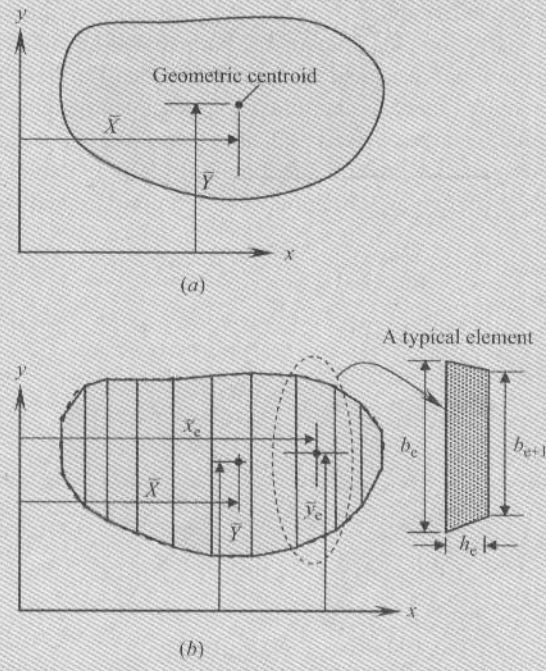

Figure 1.4.4 Determination of the centroid of an irregular region.

having width h_e and heights b_e and b_{e+1} [see Fig. 1.4.4(*b*)]. The area of the eth strip is given by

$$A_e = \frac{1}{2} h_e (b_e + b_{e+1}) \tag{1.4.9}$$

The area A_e is an approximation of the true area of the element because $(b_e + b_{e+1})/2$ is an estimated average height of the element. The coordinates of the centroid of the region are obtained by applying the moment principle:

$$\bar{X} = \frac{\sum_e A_e \bar{x}_e}{\sum_e A_e}, \quad \bar{Y} = \frac{\sum_e A_e \bar{y}_e}{\sum_e A_e} \tag{1.4.10}$$

where $\bar{x}_e$ and $\bar{y}_e$ are the coordinates of the centroid of the eth element with respect to the coordinate system used for the whole body. It should be noted that the accuracy of the approximation will be improved by increasing the number of strips (i.e., decreasing their width, h_e).

When the center of mass is required, A_e in the above equations is replaced by the mass $m_e = \rho_e A_e$, ρ_e being the mass density of the eth element. For a homogeneous body, ρ_e is the same for all elements, and therefore Eq. (1.4.10) also gives the coordinates of the center of mass of a homogeneous body.

The two examples considered above illustrates how the idea of piecewise approximation is used to approximate irregular geometry and calculate required quantities. Thus, subdividing a geometrically complex domain into parts that allow the evaluation of desired quantities is a very natural and practical approach. The idea can be extended to approximate functions representing physical quantities. For example, the temperature variation in a two-dimensional domain can be viewed as a curved surface, and it can be approximated over any part of the domain, i.e., over a subdomain, by a polynomial of desired degree. A curved surface over a triangular subregion may be approximated by a planar surface,

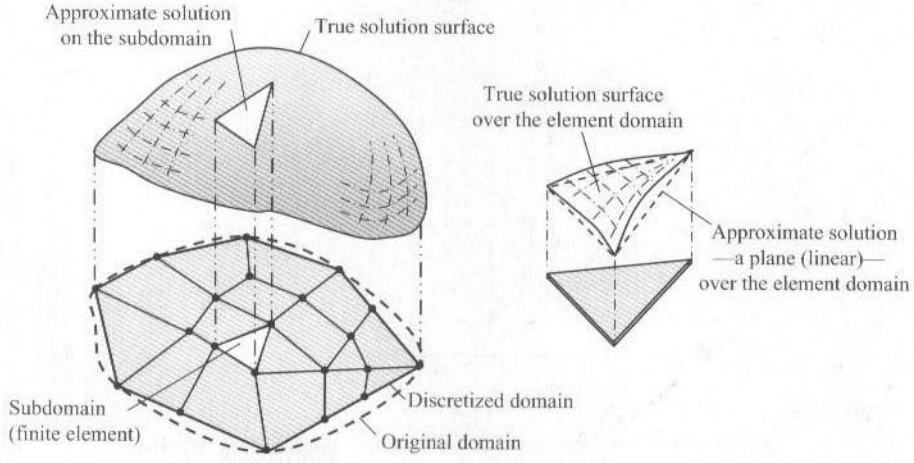

Figure 1.4.5 Approximation of a curved surface by a planar surface.

as shown in Fig. 1.4.5. Such ideas form the basis of finite element approximations. The next example illustrates this idea for a one-dimensional continuous system described by a differential equation.

Example 1.4.3 (Solution of a Differential Equation)

Consider the temperature variation in a composite cylinder consisting of two coaxial layers in perfect thermal contact, as shown in Fig. 1.4.6(*a*). Heat dissipation from a wire (with two insulations) carrying an electric current and heat flow across a thick-walled composite circular cylindrical tube are typical examples. Because of the axisymmetric geometry, boundary conditions, material and loading, the temperature T is independent of the angular coordinate θ, i.e., every radial line has the same temperature T at any radial distance r, $T = T(r)$. Therefore, it is sufficient to consider an arbitrary radial line and determine temperature along it. We wish to determine an approximation $T_e(r)$ to $T(r)$ over the radius of the cylinder. The equation governing the axisymmetric heat transfer can be formulated using the principle of conservation of energy (as was done in Example 1.2.2):

$$-\frac{1}{r}\frac{d}{dr}\left(rk\frac{dT}{dr}\right) = g(r) \tag{1.4.11}$$

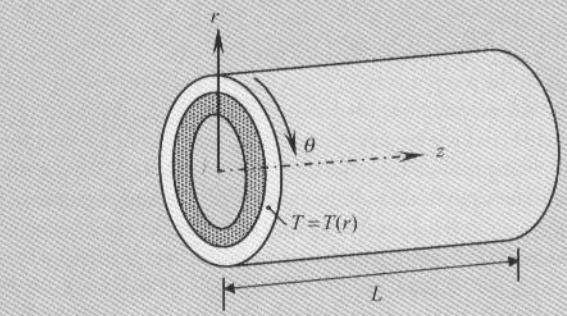

(*a*)

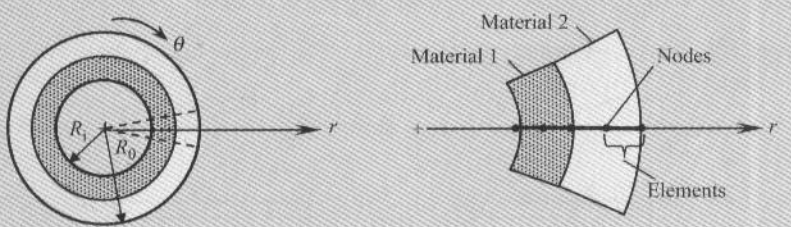

(*b*) (*c*)

Figure 1.4.6 (*a*) Coaxial cylinder made of two different materials. (*b*) Typical cross section of the composite cylinder. (*c*) Finite element discretization by line segments (linear elements).

Equation (1.4.11) is subject to appropriate boundary conditions, for example, insulated at $r = R_i$ and subjected to a temperature T_0 at $r = R_0$:

$$kr\frac{dT}{dr} = 0 \quad \text{at} \quad r = R_i; \quad T(r) = T_0 \quad \text{at} \quad r = R_0 \tag{1.4.12}$$

Here k denotes the thermal conductivity, which varies from layer to layer, R_i and R_0 are the inner and outer radii of the cylinder [Fig. 1.4.6(*b*)], and g is the rate of energy generation in the medium. When it is difficult to obtain an exact solution of Eqs. (1.4.11) and (1.4.12), either because of complex geometry and material properties or because $g(r)$ is a complicated function that does not allow exact evaluation of its integral, we seek an approximate one. In the finite element method, the domain (R_i, R_0) is divided into N subintervals [Fig. 1.4.6(*c*)], and the approximate solution is sought in the form

$$\begin{aligned}
T_1(r) &= \sum_{j=1}^{n} T_j^{(1)} \psi_j^{(1)}(r), \quad R_i \le r \le R_i + h_1 \text{ (first interval)} \\
T_2(r) &= \sum_{j=1}^{n} T_j^{(2)} \psi_j^{(2)}(r), \quad R_i + h_1 \le r \le R_i + h_1 + h_2 \text{ (second interval)} \\
&\vdots \\
T_N(r) &= \sum_{j=1}^{n} T_j^{(N)} \psi_j^{(N)}(r), \quad R_i + h_1 + \cdots + h_{N-1} \le r \le R_0 \ (N\text{th interval})
\end{aligned} \tag{1.4.13}$$

where h_e denotes the length of the eth interval, T_j (the element label "e" is omitted in the interest of brevity) is the value of the temperature $T_e(r)$ at the jth geometric point (called the node) of the eth interval, ψ_j are the interpolation polynomials on the eth interval (finite element), and T_j are termed the nodes values (which are unknown). Thus, the continuous function $T(r)$ is approximated in each finite element by a desired degree of interpolation polynomials, and the polynomial is expressed in terms of the values of the function at a selected number of points in the interval. The number of points is equal to the number of parameters in the polynomial. For example, a linear polynomial approximation of the temperature over the interval requires two values, and hence two points, are identified in the interval. The endpoints of the interval are selected for this purpose because the two points, called nodes, also define the length of the interval (see Fig. 1.4.7). For higher-order polynomial approximations, additional nodes are

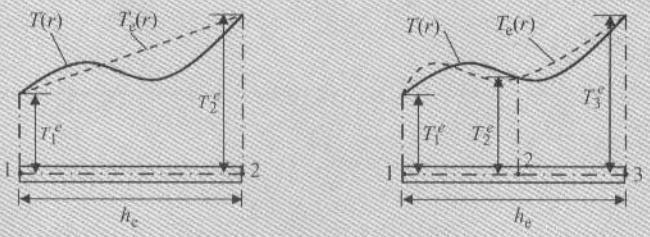

Figure 1.4.7 (*a*) Linear approximation $T_e(r)$ of a function $T(r)$ over an element. (*b*) Quadratic approximation $T_e(r)$ of $T(r)$.

identified inside the element domain. The importance of these geometric points (i.e., nodes) is that they are the base points required to define the interpolation polynomials. The nodal values T_j are determined such that $T_e(r)$ satisfies the differential equation (1.4.11) and boundary conditions (1.4.12) in some sense, often, in integral sense over each element:

$$0 = \int_{r_a}^{r_b} w(r) \left[-\frac{1}{r}\frac{d}{dr}\left(rk\frac{dT}{dr} \right) - g(r) \right] r\,dr \tag{1.4.14}$$

for all independent choices of the weight function, w. Often we select $w = \psi_i$ $(i = 1, 2, \cdots)$ to obtain n relations among the n unknowns. These ideas will be discussed in more detail in Chapter 3.

The piecewise (i.e., elementwise) approximation of the solution allows us to include any discontinuous data, such as the material properties, and to use meshes of many lower-order elements or a mesh of few higher-order elements to represent large gradients of the solution. Polynomial approximations of the form (1.4.13) can be derived systematically for any assumed degree of variation. The satisfaction of the differential equation in a weighted-integral sense leads, for steady-state problems, to algebraic relations among nodal temperatures T_j and heats Q_j of the element. The algebraic equations of all elements are assembled (i.e., related to each other) such that the temperature is continuous and the heats are balanced at nodes common to elements. Then the assembled equations are solved for the nodal values of temperatures and heats after imposing the boundary conditions of the problem. More details of this example will be presented in Chapter 3.

1.4.3 Some Remarks

In summary, in the finite element method a given domain is divided into subdomains, called finite elements, and an approximate solution to the problem is developed over each element. The subdivision of a whole domain into parts has two advantages:

1. Allows accurate representation of complex geometry and inclusion of dissimilar material properties.
2. Enables easy representation of the total solution by functions defined within each element that capture local effects (e.g., large gradients of the solution).

The three fundamental steps of the finite element method that are illustrated via the examples are:

1. Divide the whole domain into parts (both to represent the geometry and solution of the problem).
2. Over each part, seek an approximation to the solution as a linear combination of nodal values and approximation functions, and derive the algebraic relations among the nodal values of the solution over each part.
3. Assemble the parts and obtain the solution to the whole.

Although the above examples illustrate the basic idea of the finite element method, there are several other features that are either not present or not apparent from the examples. Some remarks are in order.

1. We can discretize the geometry of the domain, depending on its shape, into a mesh of more than one type of element (by shape or order). For example, in the approximation of an irregular domain, we can use a combination of rectangles and triangles. However, the element interfaces must be compatible in the sense that the solution is continuous.
2. If more than one type of element is used in the representation of the domain, one of each kind should be isolated and its equations developed.
3. The governing equations of problems considered in this book are differential equations. In most cases, the equations cannot be solved over an element for two reasons. First, they do not permit the exact solution. It is here that the variational methods come into play. Second, the discrete equations obtained in the variational methods cannot be solved independent of the remaining elements because the assemblage of the elements is subjected to certain continuity, boundary, and/or initial conditions.
4. There are two main differences in the form of the approximate solution used in the finite element method and in the classical variational methods (i.e., variational methods applied to the whole domain). First, instead of representing the solution u as a linear combination ($u_h = \sum_j c_j \phi_j$) in terms of arbitrary parameters c_j as in the variational methods, in the finite element method the solution is often represented as a linear combination ($u_h = \sum_j c_j \phi_j$) in terms of the values u_j of u_h (and possibly its derivatives as well) at the nodal points. Second, the approximate functions in the finite element method are often polynomials that are derived using interpolation theory. However, the finite element method is not restricted to the use of approximations that are linear combinations of nodal values u_j and interpolation functions ψ_j that are algebraic polynomials. One may use nodeless variables and nonpolynomial functions to approximate a function (like in meshless or element-free methods).
5. The number and the location of the nodes in an element depend on (a) the geometry of the element, (b) the degree of the polynomial approximation, and (c) the weighted-integral form of the equations. By representing the required solution in terms of its values at the nodes, we directly obtain the approximate solution at the nodes.
6. The assembly of elements, in a general case, is based on the idea that the solution (and possibly its derivatives for higher-order equations) is continuous at the interelement boundaries.
7. In general, the assemblage of finite elements is subjected to boundary and/or initial conditions. The discrete equations associated with the finite element mesh are solved only after the boundary and/or initial conditions have been imposed.
8. There are three sources of error in a finite element solution: (a) those due to the approximation of the domain (this was the only error present in the first two examples); (b) those due to the approximation of the solution; and (c) those due to numerical computation (e.g., numerical integration and round-off errors in a computer). The estimation of these errors, in general, is not simple. However, under certain conditions, they can be estimated for an element and problem.
9. The accuracy and convergence of the finite element solution depends on the differential equation, its integral form, and the element used. "Accuracy" refers to the difference between the exact solution and the finite element solution, while "convergence" refers to the accuracy as the number of elements in the mesh is increased.

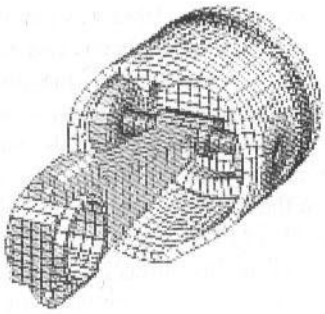

Figure 1.4.8 Finite element discretization of a connecting rod and piston.

10. For time-dependent problems, a two-stage formulation is usually followed. In the first stage, the differential equations are approximated by the finite element method to obtain a set of ordinary differential equations in time. In the second, the differential equations in time are solved exactly or further approximated by either variational methods or finite difference methods to obtain algebraic equations, which are then solved for the nodal values (see Chapter 6).
11. The desktop computers of today are more powerful than the supercomputers that existed when the finite element method was first implemented. Consequently, the analysis time is considerably reduced, provided the mesh used to model the problem is adequate (a finite element mesh of a connecting rod and piston is shown in Fig. 1.4.8). Even the automatic mesh generation programs cannot guarantee meshes that are free of irregularly shaped elements or have sufficient number of elements in a region containing high gradients in the solution, both of which result in loss of accuracy or, in the case of nonlinear problems, nonconvergence of solutions.
12. Element-free methods that require no assembly (because there are no elements) are being developed. Such methods have applications in fracture mechanics and wave propagation problems where re-meshing is necessary.

1.4.4 A Brief Review of History and Recent Developments

The idea of representing a given domain as a collection of discrete parts is not unique to the finite element method. It was recorded that ancient mathematicians estimated the value of π by noting that the perimeter of a polygon inscribed in a circle approximates the circumference of the latter. They predicted the value of π to accuracy of almost 40 significant digits by representing the circle as a polygon of a finitely large number of sides (Reddy, 1978, 1993). In modern times, the idea found a home in aircraft structural analysis, where, for example, wings and fuselages are treated as assemblages of stringers, skins, and shear panels. In 1941, Hrenikoff [1941] introduced the so-called framework method in which a plane elastic medium was represented as a collection of bars and beams. The use of piecewise-continuous functions defined over a subdomain to approximate an unknown function can be found in the work of Courant (1943), who used an assemblage of triangular elements and the principle of minimum total potential energy to study the St. Venant torsion problem. Although certain key features of the finite element method can be found in

the works of Hrenikoff (1941) and Courant (1943), its formal presentation is attributed to Turner, Clough, Martin, and Topp (1956) and Argyris and Kelsey (1960). The term "finite element" was first used by Clough (1960). Since its inception, the literature on finite element applications has grown exponentially, and today there are numerous journals that are primarily devoted to the theory and application of the method. Additional information on the history of the finite element method can be found in the review article by Babuska (1994) and in the early books on the finite element method [e.g., Zienkiewicz and Cheung (1967), Oden (1972), Strang and Fix (1973), and Oden and Reddy (1976)].

In recent years, extensions and modifications of the finite element method have been proposed. These include the *partition of unity method* (PUM) of Melenk and Babuska (1996), the *h-p Cloud method* of Duarte and Oden (1996) and *meshless methods* advanced by Belytschko and his colleagues (1996). All of these methods and numerous other methods not named here are very closely related.

1.5 THE PRESENT STUDY

This is a book on the finite element method and its application to linear problems in engineering and applied sciences. Most introductory finite element textbooks written for use in engineering schools are intended for students of solid and structural mechanics, and these introduce the method as an offspring of matrix methods of structural analysis. A few texts that treat the method as a variationally based technique leave the variational formulations and the associated methods of approximation to an appendix. The approach taken in this book is one in which the finite element method is introduced as a numerical technique of solving classes of problems, each class having a common mathematical structure in the form of governing differential equations. This approach makes the student understand the generality of the finite element method, irrespective of the student's subject background. It also enables the student to see the mathematical structure common to various physical problems, and thereby to gain additional insight into various engineering problems.

1.6 SUMMARY

Scientists and engineers develop conceptual and mathematical models of phenomena and systems that they wish to understand. The understanding may be used to develop and improve systems that contribute to human convenience and comfort. Mathematical models are developed using axioms or laws of nature that govern the phenomena. Mathematical models consist of algebraic, differential, and/or integral equations, which are often difficult to solve for the desired variables of the system for a variety of input parameters (called data), necessitating the use of numerical simulations of the phenomena.

In a numerical simulation of physical processes, we employ a numerical method and computer to evaluate the mathematical model of the process. The finite element method is a powerful numerical method of solving algebraic, differential, and integral equations, and it is devised to study complex physical processes. The method is characterized by three features:

1. The domain of the problem is represented by a collection of simple subdomains, called finite elements. The collection of finite elements is called the finite element mesh.

2. Over each finite element, the physical process is approximated by functions of the desired type (polynomials or otherwise), and algebraic equations relating physical quantities at selective points, called nodes, of the element are developed.
3. The element equations are assembled using continuity and/or "balance" of physical quantities.

In the finite element method, we seek an approximation u_h of u in the form

$$u \approx u_h = \sum_{j=1}^{n} u_j \psi_j + \sum_{j=1}^{m} c_j \phi_j$$

where u_j are the values of u_h at the element nodes, ψ_j are the interpolation functions, c_j are coefficients that are *not* associated with nodes, and ϕ_j are the associated approximation functions. Direct substitution of such approximations into the governing differential equations does not always result, for an arbitrary choice of the data of the problem, in a necessary and sufficient number of equations for the undetermined coefficients u_j and c_j. Therefore, a procedure whereby a necessary and sufficient number of equations can be obtained is needed. One such procedure is provided by a weighted-integral form of the governing differential equation. Chapter 2 is devoted to the study of weighted-integral formulations of differential equations and their solution by variational methods of approximation.

There is only one method of finite elements that is characterized by the three features stated above. Of course, there can be more than one *finite element model* of the same problem (i.e., governing equations). The type of model depends on the differential equations, methods used to derive the algebraic equations (i.e., the weighted-integral form used) for the undetermined coefficients over an element, and nature of the approximation functions used. Although the Ritz-Galerkin methods and polynomial approximations are used frequently to generate the finite element equations, any appropriate method and approximations can be used, in principle, to generate the algebraic equations. In this spirit, the collocation method, subdomain method, boundary integral methods, etc., can be used to generate the algebraic equations among discrete values of the primary and secondary variables (see Chapter 14).

The basic theory of the finite element method can be found in more than three dozen textbooks. For the beginner, it is not necessary to consult any of the other books on the finite element method as the present book provides complete details of the method as applied to linear field problems, with examples drawn from fluid mechanics, heat transfer, and solid and structural mechanics.

PROBLEMS

1.1 Newton's second law can be expressed as

$$\mathbf{F} = m\mathbf{a} \tag{1}$$

where $\mathbf{F}$ is the net force acting on the body, m mass of the body, and $\mathbf{a}$ is the acceleration of the body in the direction of the net force. Use Eq. (1) to determine the mathematical model, i.e., governing equation, of a free-falling body. Consider only the forces due to gravity and the air resistance. Assume that the air resistance is linearly proportional to the velocity of the falling body.

1.2 A cylindrical storage tank of diameter D contains a liquid at depth (or head) $h(x, t)$. Liquid is supplied to the tank at a rate of q_i (m^3/day) and drained at a rate of q_0 (m^3/day). Use the principle of conservation of mass to arrive at the governing equation of the flow problem.

1.3 Consider the simple pendulum of Example 1.3.1. Write a computer program to numerically solve the nonlinear equation (1.2.3) using the Euler method. Tabulate the numerical results for two different time steps $\Delta t = 0.05$ and $\Delta t = 0.025$ along with the exact linear solution.

1.4 An improvement of Euler's method is provided by Heun's method, which uses the average of the derivatives at the two ends of the interval to estimate the slope. Applied to the equation

$$\frac{du}{dt} = f(t, u) \tag{1}$$

Heun's scheme has the form

$$u_{i+1} = u_i + \frac{\Delta t}{2}\left[f(t_i, u_i) + f(t_{i+1}, u^0_{i+1})\right], \; u^0_{i+1} = u_i + \Delta t \; f(t_i, u_i) \tag{2}$$

Equation (2) is called the *predictor* equation, and Eq. (1) is called the *corrector* equation. Apply Heun's method to Eqs. (1.3.4) and obtain the numerical solution for $\Delta t = 0.05$.

REFERENCES FOR ADDITIONAL READING

1. *Research Directions in Computational Mechanics*, National Academy Press, Washington, DC, 1991.
2. Argyris, J. H. and Kelsey, S., *Energy Theorems and Structural Analysis*, Butterworth, London, 1960; first appeared in *Aircraft Engineering*, **26**, 1954 and **27**, 1955.
3. Babuska, I., "Courant Element: Before and After," Krizek, M. and Neittaanmäki, P. (eds.), *In Finite Element Methods: Fifty Years of the Courant Element*, Marcel Dekker, 1994.
4. Belytschko, T., Krongauz, Y., Organ, D., Fleming, M., and Krysl, P., "Meshless Methods: An Overview and Recent Developments," *Computer Methods in Applied Mechanics and Engineering*, **139**, 3–47, 1996.
5. Clough, R. W., "The Finite Element Method in Plane Stress Analysis," *Journal of Structures Division, ASCE, Proceedings of 2nd Conference on Electronic Computation*, 345–378, 1960.
6. Courant, R., "Variational Methods for the Solution of Problems of Equilibrium and Vibrations," *Bulletin of the American Mathematical Society*, **49**, 1–23, 1943.
7. Duarte, C. A. and Oden, J. T., "An h-p Adaptive Method Using Clouds," *Computer Methods in Applied Mechanics and Engineering*, **139**, 237–262, 1996.
8. Hrenikoff, A., "Solution of Problems in Elasticity by the Frame Work Method," *Journal of Applied Mechanics, Transactions of the ASME*, **8**, 169–175, 1941.
9. Melenk, J. M. and Babuska, I., "The Partition of Unity Finite Element Method: Basic Theory and Applications," *Computer Methods in Applied Mechanics and Engineering*, **139**, 289–314, 1996.
10. Oden, J. T., *Finite Elements of Nonlinear Continua*, McGraw-Hill, New York, 1972.
11. Oden, J. T. and Reddy, J. N., *An Introduction to the Mathematical Theory of Finite Elements*, John Wiley, New York, 1976.
12. Reddy, J. N., "The Finite Element Method: A Child of the Computer Age," *Sooner Shamrock* (engineering student magazine at the University of Oklahoma), 23–26, Fall 1978.
13. Reddy, J. N., *An Introduction to the Finite Element Method*, 2nd ed., McGraw-Hill, New York, 1993 (see Chapter 1).
14. Strang, G. and Fix, G., *An Analysis of the Finite Element Method*, Prentice Hall, Englewood Cliffs, NJ, 1973.
15. Turner, M. J., Clough, R. W., Martin, H. C., and Topp, L. J., "Stiffness and Deflection Analysis of Complex Structures," *Journal of Aeronautical Science*, **23**, 805–823, 1956.
16. Zienkiewicz, O. C. and Cheung, Y. K., *The Finite Element Method in Structural and Continuum Mechanics*, McGraw-Hill, London, 1967.

Chapter 2

MATHEMATICAL PRELIMINARIES, INTEGRAL FORMULATIONS, AND VARIATIONAL METHODS

2.1 GENERAL INTRODUCTION

2.1.1 Variational Principles and Methods

This chapter is devoted to a review of some mathematical preliminaries that prove to be useful in the sequel and to a study of integral formulations and more commonly used variational methods such as the Ritz, Galerkin, collocation, and least-squares methods. Since the finite element method can be viewed as an elementwise application of a variational method (see Section 1.4), it is useful to learn how variational methods work. We begin with a discussion of the general meaning of the phrases "variational methods" and "variational formulations" used in the context of finite element formulations.

The phrase "direct variational methods" refers to methods that make use of variational principles, such as the principles of virtual work and the principle of minimum total potential energy in solid and structural mechanics, to determine approximate solutions of problems [see Oden and Reddy (1983) and Reddy (2002)]. In the classical sense, a *variational principle* has to do with finding the extremum (i.e., minimum or maximum) or stationary values of a functional with respect to the variables of the problem. The functional includes all the intrinsic features of the problem, such as the governing equations, boundary and/or initial conditions, and constraint conditions, if any. In solid and structural mechanics problems, the functional represents the total energy of the system, and in other problems, it is simply an integral representation of the governing equations.

Variational principles have always played an important role in mechanics (see the references at the end of the chapter). First, many problems of mechanics are posed in terms of finding the extremum (i.e., minima or maxima) and thus, by their nature, can be formulated in terms of variational statements. Second, there are problems that can be formulated by other means, such as the conservation laws (as illustrated in Chapter 1), but these can also be formulated by means of variational principles. Third, variational formulations form a powerful basis for obtaining approximate solutions to practical problems, many of which

are intractable otherwise. The principle of minimum total potential energy, for example, can be regarded as a substitute to the equations of equilibrium of an elastic body as well as a basis for the development of displacement finite element models that can be used to determine approximate displacement and stress fields in the body [Reddy (2002)]. Variational formulations can also serve to unify diverse fields, suggest new theories, and provide a powerful means to study the existence and uniqueness of solutions to problems. Similarly, Hamilton's principle [see Reddy (2002)] can be used in lieu of the equations governing dynamical systems, and the variational forms presented by Biot (1972) replace certain equations in linear continuum thermodynamics.

2.1.2 Variational Formulations

The classical use of the phrase "variational formulations" refers to the construction of a functional (whose meaning will be made clear shortly) or a variational principle that is equivalent to the governing equations of the problem. The modern use of the phrase refers to the formulation in which the governing equations are translated into equivalent weighted-integral statements that are not necessarily equivalent to a variational principle. Even those problems that do not admit variational principles in the classical sense (e.g., the Navier–Stokes equations governing the flow of viscous or inviscid fluids) can now be formulated using weighted-integral statements.

The importance of variational formulations of physical laws, in the modern or general sense of the phrase, goes far beyond its use as simply an alternate to other formulations [Oden and Reddy (1983)]. In fact, variational forms of the laws of continuum physics may be the only natural and rigorously correct way to think of them. While all sufficiently smooth fields lead to meaningful variational forms, the converse is not true: There exist physical phenomena which can be adequately modeled mathematically only in a variational setting; they are nonsensical when viewed locally.

The starting point for the discussion of the finite element method is differential equations governing the physical phenomena under study. As such, we shall first discuss why integral statements of the differential equations are needed.

2.1.3 Need for Weighted-Integral Statements

In almost all approximate methods used to determine the solution of differential and/or integral equations, we seek a solution in the form

$$u(\mathbf{x}) \approx U_N(\mathbf{x}) = \sum_{j=1}^{N} c_j \phi_j(\mathbf{x}) \tag{2.1.1}$$

where u represents the solution of a particular differential equation and associated boundary conditions, and U_N is its approximation that is represented as a linear combination of unknown parameters c_j and known functions ϕ_j of position $\mathbf{x}$ in the domain Ω on which the problem is posed. We shall shortly discuss the conditions on ϕ_j. The approximate solution U_N is completely known only when c_j are known. Thus, we must find a means to determine c_j such that U_N satisfies the equations governing u. If somehow we can find U_N that satisfies the differential equation at every point $\mathbf{x}$ of the domain Ω

and conditions on the boundary Γ of Ω, then $U_N(\mathbf{x}) = u(\mathbf{x})$, which is the exact solution of the problem. Of course, approximate methods are not about problems for which exact solutions can be determined by some methods of mathematical analysis; the role of approximate methods is to find an approximate solution of problems that do not admit analytical solutions. When the exact solution cannot be determined, the alternative is to find a solution U_N that satisfies the governing equations in an approximate way. In the process of satisfying the governing equations approximately, we obtain (not accidentally but by planning) N algebraic relations among the N parameters $c_1, c_2, \cdots, c_N$. A detailed discussion of these ideas is given in the next few paragraphs in connection with a specific problem.

Consider the problem of solving the differential equation

$$-\frac{d}{dx}\left[a(x)\frac{du}{dx}\right] + c(x)u = f(x) \quad \text{for } 0 < x < L \tag{2.1.2a}$$

subjected to the boundary conditions

$$u(0) = u_0, \qquad \left[a(x)\frac{du}{dx}\right]_{x=1} = Q_0 \tag{2.1.2b}$$

where $a(x)$, $c(x)$, and $f(x)$ are known functions, u_0 and Q_0 are known parameters, and $u(x)$ is the function to be determined. The set $a(x)$, $c(x)$, $f(x)$, u_0, and Q_0 is called the problem *data*. An example of the above problem is given by the heat transfer in an uninsulated rod (see Example 1.2.2): here u denotes the temperature (θ), $f(x)$ is the internal heat generation per unit length (Ag), $a(x)$ is the thermal resistance (kA), $c = \beta P$, u_0 is the specified temperature (θ_0), and Q_0 is the specified heat.

We seek an approximate solution over the entire domain $\Omega = (0, L)$ in the form

$$U_N \equiv \sum_{j=1}^{N} c_j \phi_j(x) + \phi_0(x) \tag{2.1.3}$$

where the c_j are coefficients to be determined and $\phi_j(x)$ and $\phi_0(x)$ are functions chosen such that the specified boundary conditions of the problem are satisfied by the N-parameter approximate solution U_N. Note that the particular form in (2.1.3) has two parts: one containing the unknowns ($\sum c_j \phi_j$) that is termed the homogeneous part and the other is the nonhomogeneous part (ϕ_0) that has the sole purpose of satisfying the specified boundary conditions of the problem. Since ϕ_0 satisfies the boundary conditions, the sum $\sum c_j \phi_j$ must satisfy, for arbitrary c_j, the homogeneous form of the boundary conditions ($Bu = \hat{u}$ is said to be a nonhomogeneous boundary condition when $\hat{u} \neq 0$, and it is termed a homogeneous boundary condition when $\hat{u} = 0$; here B denotes some operator). Thus, in the present case, the actual boundary conditions are both nonhomogeneous ($B = 1$ and $\hat{u} = u_0$ at $x = 0$, and $B = a(x)(d/dx)$ and $\hat{u} = Q_0$ at $x = L$). The particular form (2.1.3) is convenient in selecting ϕ_0 and ϕ_j. Thus, ϕ_0 and ϕ_j satisfy the conditions

$$B\phi_0 = \hat{u}, \qquad B\phi_j = 0 \text{ for all } j = 1, 2, \cdots, n \tag{2.1.4}$$

To be more specific, let $L = 1$, $u_0 = 1$, $Q_0 = 0$, $a(x) = x$, $c(x) = 1$, $f(x) = 0$, and $N = 2$. Then we choose the approximate solution in the form

$$U_2 = c_1\phi_1 + c_2\phi_2 + \phi_0 \text{ with } \phi_0 = 1,\ \phi_1(x) = x^2 - 2x,\ \phi_2 = x^3 - 3x$$

that satisfies the boundary conditions (2.1.2*b*) of the problem for any values of c_1 and c_2 because

$$\phi_0(0)=1, \quad \left(x\frac{d\phi_0}{dx}\right)_{x=1}=0; \quad \phi_j(0)=0, \quad \left(\frac{d\phi_j}{dx}\right)_{x=1}=0 \text{ for } j=1,2 \tag{2.1.5}$$

To make U_2 satisfy the differential equation (2.1.2*a*), we must have

$$\begin{aligned} -\frac{dU_2}{dx}-x\frac{d^2U_2}{dx^2}+U_2 &= -2c_1(x-1)-3c_2(x^2-1)-2c_1x-6c_2x^2 \\ &\quad +c_1(x^2-2x)+c_2(x^3-3x)+1=0 \end{aligned} \tag{2.1.6}$$

Since this expression must be zero for any value of x, the coefficients of the various powers of x must be zero:

$$\begin{aligned} 1+2c_1+3c_2&=0 \\ -(6c_1+3c_2)&=0 \\ c_1-9c_2&=0 \\ c_2&=0 \end{aligned}$$

The above relations are inconsistent; hence, there is *no solution* to the equations. On the other hand, we can require the approximate solution U_N to satisfy the differential equation (2.1.2*a*) in the weighted-integral sense,

$$\int_0^1 w(x)R\,dx=0 \tag{2.1.7}$$

where R denotes the left side of the equality in (2.1.6) and is called the *residual,*

$$R\equiv -\frac{dU_N}{dx}-x\frac{d^2U_N}{dx^2}+U_N$$

and $w(x)$ is called a *weight function.* From (2.1.7), we obtain as many linearly independent equations as there are linearly independent functions for $w(x)$. The number of linearly independent choices of w must be restricted to $N=2$ so that we have exactly the same number of equations as the number of unknown coefficients, c_j. For example, in the present example, if we take $w=1$ and $w=x$, we obtain

$$\begin{aligned} 0&=\int_0^1 1\cdot R\,dx=(1+2c_1+3c_2)+\frac{1}{2}(-6c_1-3c_2)+\frac{1}{3}(c_1-9c_2)+\frac{1}{4}c_2 \\ 0&=\int_0^1 x\cdot R\,dx=\frac{1}{2}(1+2c_1+3c_2)+\frac{1}{3}(-6c_1-3c_2)+\frac{1}{4}(c_1-9c_2)+\frac{1}{5}c_2 \end{aligned}$$

or

$$\frac{2}{3}c_1+\frac{5}{4}c_2=1, \quad \frac{3}{4}c_1+\frac{31}{20}c_2=\frac{1}{2} \tag{2.1.8}$$

which provides two linearly independent equations for c_1 and c_2 (whose solution is $c_1=\frac{222}{23}$ and $c_2=-\frac{100}{23}$).

The above discussion clearly demonstrates the need for weighted-integral statements of the type in (2.1.7); they provide the means for obtaining as many algebraic equations

as there are unknown coefficients in the approximate solution. This chapter deals with the construction of different types of integral statements used in different variational methods. The variational methods differ from each other in the choice of the weight function w and/or the integral statement used, which in turn dictates the choice of the approximation functions ϕ_j. In the finite element method, a given domain is viewed as an assemblage of subdomains (i.e., finite elements), and an approximate solution is sought over each subdomain in the same way as in variational methods. Therefore, it is informative to study variational methods before we study the finite element method.

Our goal in this chapter is to illustrate the basic steps in the weighted-integral formulations and associated approximations of boundary value, eigenvalue, and initial value problems. Toward this goal, we first introduce the necessary terminology and notation.

2.2 SOME MATHEMATICAL CONCEPTS AND FORMULAE

2.2.1 Coordinate Systems and the Del Operator

In the analytical description of physical phenomena, a coordinate system in the chosen frame of reference is introduced, and various physical quantities involved in the description are expressed in terms of measurements made in that system. The vector and tensor quantities are expressed in terms of their components in that coordinate system. For example, a vector $\mathbf{A}$ in a three-dimensional space may be expressed in terms of its components (a_1, a_2, a_3) and *basis vectors* $(\mathbf{e}_1, \mathbf{e}_2, \mathbf{e}_3)$ ($\mathbf{e}_i$ are not necessarily unit vectors) as*

$$\mathbf{A} = a_1\mathbf{e}_1 + a_2\mathbf{e}_2 + a_3\mathbf{e}_3 \tag{2.2.1}$$

When the basis vectors of a coordinate system are constants, i.e., with fixed lengths and directions, the coordinate system is called a *Cartesian coordinate system*. The general Cartesian system is oblique. When the Cartesian system is orthogonal, it is called *rectangular Cartesian*. The rectangular Cartesian coordinates are denoted by

$$(x_1, x_2, x_3) \text{ or } (x, y, z) \tag{2.2.2}$$

The familiar rectangular Cartesian coordinate system is shown in Fig. 2.2.1. We shall always use a right-hand coordinate system. When the basis vectors are of unit lengths and mutually orthogonal, they are called *orthonormal*. In many situations an *orthonormal basis* simplifies calculations. We denote an orthonormal Cartesian basis by

$$(\hat{\mathbf{e}}_1, \hat{\mathbf{e}}_2, \hat{\mathbf{e}}_3) \text{ or } (\hat{\mathbf{e}}_x, \hat{\mathbf{e}}_y, \hat{\mathbf{e}}_z) \tag{2.2.3}$$

For an orthonormal basis, the vector $\mathbf{A}$ can be written as

$$\mathbf{A} = A_1\hat{\mathbf{e}}_1 + A_2\hat{\mathbf{e}}_2 + A_3\hat{\mathbf{e}}_3$$

where $\hat{\mathbf{e}}_i$ $(i = 1, 2, 3)$ is the orthonormal basis and A_i are the corresponding *physical components* (i.e., the components have the same physical dimensions as the vector). Although the analytical description depends upon the chosen coordinate system and may appear different

*Vectors and matrices in this book are written with boldface letters.

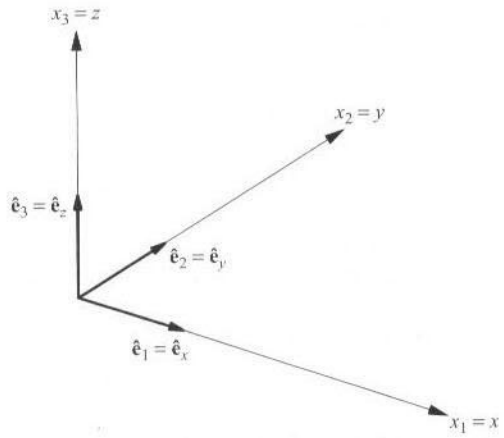

Figure 2.2.1 A rectangular Cartesian coordinate system, $(x_1, x_2, x_3) = (x, y, z)$; $(\hat{\mathbf{e}}_1, \hat{\mathbf{e}}_2, \hat{\mathbf{e}}_3) = (\hat{\mathbf{e}}_x, \hat{\mathbf{e}}_y, \hat{\mathbf{e}}_z)$ are the unit basis vectors.

in another type of coordinate system, one must keep in mind that *the laws of nature are independent of the choice of coordinate system.*

It is useful to abbreviate a summation of terms by understanding that a repeated index means summation over all values of that index. Thus, the summation

$$\mathbf{A} = \sum_{i=1}^{3} A_i \mathbf{e}_i$$

can be shortened to

$$\mathbf{A} = A_i \mathbf{e}_i \tag{2.2.4}$$

The repeated index is a *dummy index* and thus can be replaced by *any other symbol that has not already been used.* Thus, we can also write

$$\mathbf{A} = A_i \mathbf{e}_i = A_m \mathbf{e}_m$$

and so on.

The "dot product" $\hat{\mathbf{e}}_i \cdot \hat{\mathbf{e}}_j$ and "cross product" $\hat{\mathbf{e}}_i \times \hat{\mathbf{e}}_j$ of base vectors in a right-handed system are defined by

$$\hat{\mathbf{e}}_i \cdot \hat{\mathbf{e}}_j \equiv \delta_{ij} = \begin{cases} 0, & \text{if } i \neq j \\ 1, & \text{if } i = j \end{cases} \tag{2.2.5}$$

$$\hat{\mathbf{e}}_i \times \hat{\mathbf{e}}_j \equiv \varepsilon_{ijk} \hat{\mathbf{e}}_k \tag{2.2.6}$$

where δ_{ij} is the *Kronecker delta* and ε_{ijk} is the *alternating symbol* or *permutation symbol*

$$\varepsilon_{ijk} = \begin{cases} 1, & \text{if } i, j, k \text{ are in cyclic order} \\ & \text{and not repeated } (i \neq j \neq k) \\ -1, & \text{if } i, j, k \text{ are not in cyclic order} \\ & \text{and not repeated } (i \neq j \neq k) \\ 0, & \text{if any of } i, j, k \text{ are repeated} \end{cases} \tag{2.2.7}$$

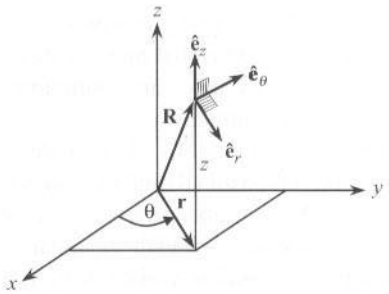

Figure 2.2.2 Cylindrical coordinate system.

Differentiation of vector functions with respect to the coordinates is common in science and engineering. Most of the operations involve the "del operator," denoted by ∇. In a rectangular Cartesian system, it has the form

$$\nabla \equiv \hat{\mathbf{e}}_x \frac{\partial}{\partial x} + \hat{\mathbf{e}}_y \frac{\partial}{\partial y} + \hat{\mathbf{e}}_z \frac{\partial}{\partial z} \tag{2.2.8}$$

It is important to note that the del operator has some of the properties of a vector, but it does not have them all because it is an operator. The operation $\nabla\phi(\mathbf{x})$ is called the *gradient* of a scalar function ϕ whereas $\nabla \times \mathbf{A}(\mathbf{x})$ is called the *curl* of a vector function $\mathbf{A}$. The operator $\nabla^2 \equiv \nabla \cdot \nabla$ is called the Laplace operator. In a 3-D rectangular Cartesian coordinate system, it has the form

$$\nabla^2 = \frac{\partial^2}{\partial x^2} + \frac{\partial^2}{\partial y^2} + \frac{\partial^2}{\partial z^2} \tag{2.2.9}$$

We have the following relations between the rectangular Cartesian coordinates (x, y, z) and cylindrical coordinates (r, θ, z) (see Fig. 2.2.2):

$$x = r\cos\theta, \quad y = r\sin\theta, \quad z = z \tag{2.2.10}$$

$$\hat{\mathbf{e}}_r = \cos\theta\, \hat{\mathbf{e}}_x + \sin\theta\, \hat{\mathbf{e}}_y, \quad \hat{\mathbf{e}}_\theta = -\sin\theta\, \hat{\mathbf{e}}_x + \cos\theta\, \hat{\mathbf{e}}_y, \quad \hat{\mathbf{e}}_z = \hat{\mathbf{e}}_z \tag{2.2.11}$$

$$\frac{\partial \hat{\mathbf{e}}_r}{\partial \theta} = -\sin\theta\, \hat{\mathbf{e}}_x + \cos\theta\, \hat{\mathbf{e}}_y = \hat{\mathbf{e}}_\theta, \quad \frac{\partial \hat{\mathbf{e}}_\theta}{\partial \theta} = -\cos\theta\, \hat{\mathbf{e}}_x - \sin\theta \hat{\mathbf{e}}_y = -\hat{\mathbf{e}}_r \tag{2.2.12}$$

and all other derivatives of the base vectors are zero. For more on vector calculus, see Reddy and Rasmussen (1982) and Reddy (2002), among other references.

2.2.2 Boundary Value, Initial Value, and Eigenvalue Problems

The objective of most analyses is to determine unknown functions, called *dependent variables,* that are governed by a set of differential equations posed in a given domain Ω and some conditions on the boundary Γ of the domain. Often, a domain not including its boundary is called an open domain. A domain Ω with its boundary Γ is called a closed domain and is denoted by $\bar{\Omega} = \Omega \cup \Gamma$.

A function u of several variables $(x, y, \cdots)$ is said to be of class $C^m(\Omega)$ in a domain Ω if all its partial derivatives with respect to $(x, y, \cdots)$ of order up to and including m exist

and are *continuous* in Ω. Thus, if u is of class C^0 in a two-dimensional domain Ω, then u is continuous in Ω (i.e., $\partial u/\partial x$ and $\partial u/\partial y$ exist but may not be continuous). Similarly, if u is of class C^1, then u, $\partial u/\partial x$, and $\partial u/\partial y$ exist and are continuous (hence, $\partial^2 u/\partial x^2$, $\partial^2 u/\partial y^2$, and $\partial^2 u/\partial y \partial x$ exist but may not be continuous).

When the dependent variables are functions of one independent variable (say, x), the domain is a line segment (i.e., one-dimensional) and the end points of the domain are called boundary points. When the dependent variables are functions of two independent variables (say, x and y), the domain is two-dimensional and the boundary is the closed curve enclosing it. In a three-dimensional domain, dependent variables are functions of three coordinates (say x, y, and z) and the boundary is a two-dimensional surface.

As discussed in Section 1.2, a differential equation is said to describe a *boundary value problem* over the domain Ω if the dependent variable and possibly its derivatives are required to take specified values on the boundary Γ of Ω. An *initial value problem* is one in which the dependent variable and possibly its derivatives are specified initially (i.e., at time $t = 0$). Initial value problems are generally time-dependent problems. Examples of boundary and initial value problems were discussed in Section 1.2. A problem can be both a boundary value and initial value problem if the dependent variable is subject to both boundary and initial conditions. Another type of problem we encounter is one in which a differential equation governing the dependent unknown also contains an unknown parameter and we are required to find both the dependent variable and the parameter such that the differential equation and associated boundary conditions are satisfied. Such problems are called *eigenvalue problems*. Examples of various types of problems we encounter in science and engineering are given below (the mathematical classification of differential equations into elliptic, parabolic, and hyperbolic is of no interest at the moment).

Boundary Value Problems. *Steady State Heat Transfer in a Fin and Axial Deformation of a Bar* [Fig. 2.2.3(*a*)]: Find $u(x)$ that satisfies the second-order differential equation and *boundary conditions*:

$$-\frac{d}{dx}\left(a\frac{du}{dx}\right) + cu = f \quad \text{for} \quad 0 < x < L \tag{2.2.13a}$$

$$u(0) = u_0, \qquad \left(a\frac{du}{dx}\right)_{x=L} = q_0 \tag{2.2.13b}$$

Bending of Elastic Beams under Transverse Load: Find $u(x)$ that satisfies the fourth-order differential equation and *boundary conditions*:

$$\frac{d^2}{dx^2}\left(b\frac{d^2u}{dx^2}\right) + cu = f \quad \text{for} \quad 0 < x < L \tag{2.2.14a}$$

$$u(0) = u_0, \qquad \left(\frac{du}{dx}\right)_{x=0} = d_0$$

$$\left[\frac{d}{dx}\left(b\frac{d^2u}{dx^2}\right)\right]_{x=L} = m_0, \qquad \left(b\frac{d^2u}{dx^2}\right)_{x=L} = v_0 \tag{2.2.14b}$$

Steady Heat Conduction in a Two-Dimensional Region and *Transverse Deflections of a Membrane* [Fig. 2.2.3(*b*)]: Find $u(x, y)$ that satisfies the second-order partial differential

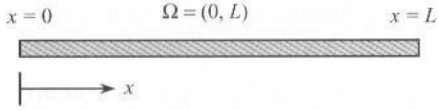

(*a*) A one-dimensional domain

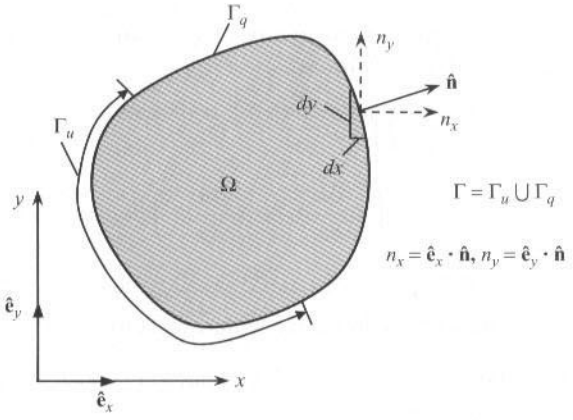

(*b*) A two-dimensional domain

Figure 2.2.3 (*a*) One-dimensional domain. (*b*) Two-dimensional domain.

equation and *boundary conditions*:

$$-\left[\frac{\partial}{\partial x}\left(a_1\frac{\partial u}{\partial x}\right)+\frac{\partial}{\partial y}\left(a_2\frac{\partial u}{\partial y}\right)\right]+cu=f \quad \text{in } \Omega \tag{2.2.15a}$$

$$u=u_0 \text{ on } \Gamma_u, \quad \left(a_1\frac{\partial u}{\partial x}n_x+a_2\frac{\partial u}{\partial x}n_y\right)=q_0 \text{ on } \Gamma_q \tag{2.2.15b}$$

where (n_x, n_y) are the direction cosines of the unit normal vector $\hat{\mathbf{n}}$ to the boundary Γ_q.

Initial Value Problems. *A General First-Order Equation:* Find $u(t)$ that satisfies the first-order differential equation and *initial conditions*:

$$a\frac{du}{dt}+cu=f \quad \text{for} \quad 0<t\le T \tag{2.2.16a}$$

$$u(0)=u_0 \tag{2.2.16b}$$

A General Second-Order Equation: Find $u(t)$ that satisfies the second-order differential equation and *initial conditions*:

$$a\frac{du}{dt}+b\frac{d^2u}{dt^2}+cu=f \quad \text{for} \quad 0<t\le T \tag{2.2.17a}$$

$$u(0)=u_0, \left(b\frac{du}{dt}\right)_{t=0}=v_0 \tag{2.2.17b}$$

Boundary and Initial Value Problems. *Unsteady Heat Transfer in a Rod:* Find $u(x, t)$ that satisfies the partial differential equation and *initial* and *boundary conditions*:

$$-\frac{\partial}{\partial x}\left(a\frac{\partial u}{\partial x}\right)+\rho\frac{\partial u}{\partial t}=f(x,t) \quad \text{for} \quad 0<x<L,\ 0<t\le T \tag{2.2.18a}$$

$$u(0,t)=d_0(t), \quad \left(a\frac{du}{dx}\right)_{x=L}=q_0(t), \quad u(x,0)=u_0(x) \tag{2.2.18b}$$

Unsteady Motion of a Membrane: Find $u(x, y, t)$ that satisfies the partial differential equation and *initial* and *boundary conditions*:

$$-\left[\frac{\partial}{\partial x}\left(a_1\frac{\partial u}{\partial x}\right)+\frac{\partial}{\partial y}\left(a_2\frac{\partial u}{\partial y}\right)\right]+\rho\frac{\partial^2 u}{\partial t^2}=f(x,y,t) \quad \text{in } \Omega,\ 0<t\le T \tag{2.2.19a}$$

$$u=u_0(t) \text{ on } \Gamma_u, \quad \left(a_1\frac{\partial u}{\partial x}n_x+a_2\frac{\partial u}{\partial y}n_y\right)=q_0(t) \text{ on } \Gamma_q \tag{2.2.19b}$$

$$u(x,y,0)=d_0, \quad \dot{u}(x,y,0)=v_0 \tag{2.2.19c}$$

where the superposed dot indicates a derivative with respect to time t.

Eigenvalue Problems. *Axial Vibrations of a Bar:* Find $u(x)$ and λ that satisfy the differential equation and *boundary conditions*:

$$-\frac{d}{dx}\left(a\frac{du}{dx}\right)-\lambda u=0 \quad \text{for} \quad 0<x<L \tag{2.2.20a}$$

$$u(0)=0, \quad \left(a\frac{du}{dx}\right)_{x=L}=0 \tag{2.2.20b}$$

Transverse Vibrations of a Membrane: Find $u(x, y)$ and λ that satisfy the partial differential equation and *boundary conditions*:

$$-\left[\frac{\partial}{\partial x}\left(a_1\frac{\partial u}{\partial x}\right)+\frac{\partial}{\partial y}\left(a_2\frac{\partial u}{\partial y}\right)\right]-\lambda u=0 \quad \text{in } \Omega \tag{2.2.21a}$$

$$u=0 \text{ on } \Gamma_u, \quad \left(a_1\frac{\partial u}{\partial x}n_x+a_2\frac{\partial u}{\partial y}n_y\right)=0 \text{ on } \Gamma_q \tag{2.2.21b}$$

The values of λ are called *eigenvalues,* and the associated functions u are called *eigenfunctions*.

The set of specified functions and parameters (e.g., a, b, c, ρ, f, u_0, d_0, q_0, v_0, and so on) are called the *data* of the problem. Differential equations in which the right-hand side f is zero are called *homogeneous differential equations,* and boundary (initial) conditions in which the specified data is zero are called homogeneous boundary (initial) conditions. The *exact solution* of a differential equation is the function that identically satisfies the differential equation at every point of the domain and for all times $t > 0$, and satisfies the specified boundary and/or initial conditions.

2.2.3 Integral Identities

Integration by parts is frequently used in the integral formulation of differential equations. In two- and three-dimensional cases, integration by parts is carried out with the help of

the gradient and divergence theorems. In this section, we derive some useful identities for future use.

Integration-by-Parts Formulae. Let u, v, and w be sufficiently differentiable functions of the coordinate x. Then the following integration-by-parts formula holds:

$$\int_a^b w\,\frac{dv}{dx}\,dx = \int_a^b w\,dv = -\int_a^b v\,dw + [wv]_a^b$$

$$= -\int_a^b v\,\frac{dw}{dx}\,dx + w(b)\,v(b) - w(a)\,v(a) \tag{2.2.22}$$

This identity can easily be established. First, note the following identity from the product rule of differentiation:

$$\frac{d}{dx}(wv) = \frac{dw}{dx}\,v + w\,\frac{dv}{dx}$$

Therefore,

$$w\frac{dv}{dx} = \frac{d}{dx}(wv) - \frac{dw}{dx}\,v$$

Integrating both sides over the interval (a, b), we obtain the identity in (2.2.22)

$$\int_a^b w\frac{dv}{dx}\,dx = \int_a^b \left[\frac{d}{dx}(wv) - \frac{dw}{dx}\,v\right]dx$$

$$= \int_a^b \frac{d}{dx}(wv)\,dx - \int_a^b \frac{dw}{dx}\,v\,dx$$

$$= [wv]_a^b - \int_a^b \frac{dw}{dx}\,v\,dx$$

Next, consider the expression

$$\int_a^b w\,\frac{d^2u}{dx^2}\,dx = \int_a^b w\,\frac{d}{dx}\left(\frac{du}{dx}\right)dx = \int_a^b w\,\frac{dv}{dx}\,dx$$

where $v \equiv \frac{du}{dx}$. Using (2.2.22), we obtain

$$\int_a^b w\,\frac{d^2u}{dx^2}\,dx = -\int_a^b v\,\frac{dw}{dx}\,dx + w(b)\,v(b) - w(a)\,v(a)$$

$$= -\int_a^b \frac{du}{dx}\,\frac{dw}{dx}dx + w(b)\frac{du}{dx}\bigg|_b - w(a)\frac{du}{dx}\bigg|_a \tag{2.2.23a}$$

or

$$-\int_a^b \frac{du}{dx}\,\frac{dw}{dx}\,dx = \int_a^b w\,\frac{d^2u}{dx^2}\,dx + w(a)\frac{du}{dx}\bigg|_a - w(b)\frac{du}{dx}\bigg|_b \tag{2.2.23b}$$

Similarly,

$$\int_a^b v\,\frac{d^4w}{dx^4}\,dx = \int_a^b v\,\frac{d^2}{dx^2}\,\frac{d^2w}{dx^2}\,dx$$

$$= \int_a^b v\,\frac{d^2u}{dx^2}\,dx$$

where $u \equiv \frac{d^2w}{dx^2}$. Using (2.2.23$a$) with $w = v$, we can write the right-hand side as

$$-\int_a^b \frac{du}{dx}\frac{dv}{dx}\,dx + v(b)\frac{du}{dx}\bigg|_b - v(a)\frac{du}{dx}\bigg|_a \tag{2.2.24a}$$

We use (2.2.23b) with $w = u$ and $u = v$ to write (2.2.24a) as

$$\int_a^b u\frac{d^2v}{dx^2}\,dx + u(a)\frac{dv}{dx}\bigg|_a - u(b)\frac{dv}{dx}\bigg|_b + v(b)\frac{du}{dx}\bigg|_b - v(a)\frac{du}{dx}\bigg|_a \tag{2.2.24b}$$

and, finally, replacing u by its actual value $u = d^2w/dx^2$, we arrive at

$$\int_a^b v\frac{d^4w}{dx^4}\,dx = \int_a^b \frac{d^2w}{dx^2}\frac{d^2v}{dx^2}\,dx + \frac{d^2w}{dx^2}\bigg|_a\frac{dv}{dx}\bigg|_a - \frac{d^2w}{dx^2}\bigg|_b\frac{dv}{dx}\bigg|_b + v(b)\frac{d^3w}{dx^3}\bigg|_b - v(a)\frac{d^3w}{dx^3}\bigg|_a \tag{2.2.25}$$

Gradient and Divergence Theorems. Let ∇ and ∇^2 denote, respectively, the gradient operator and the Laplace operator in the two-dimensional Cartesian rectangular coordinate system (x, y):

$$\nabla = \hat{\mathbf{e}}_x\frac{\partial}{\partial x} + \hat{\mathbf{e}}_y\frac{\partial}{\partial y}, \quad \nabla^2 = \nabla\cdot\nabla = \frac{\partial^2}{\partial x^2} + \frac{\partial^2}{\partial y^2} \tag{2.2.26}$$

where $\hat{\mathbf{e}}_x$ and $\hat{\mathbf{e}}_y$ denote the unit basis vectors along the x and y coordinates, respectively. If $F(x, y)$ and $G(x, y)$ are scalar functions of class $C^0(\Omega)$ in the two-dimensional domain Ω shown in Fig. 2.2.3(b), the following gradient and divergence theorems hold.

Gradient Theorem

$$\int_\Omega \text{grad}F\,dxdy \equiv \int_\Omega \nabla F\,dxdy = \oint_\Gamma \hat{\mathbf{n}}\,F\,ds$$
$$\int_\Omega \left(\hat{\mathbf{e}}_x\frac{\partial F}{\partial x} + \hat{\mathbf{e}}_y\frac{\partial F}{\partial y}\right)dxdy = \oint_\Gamma \left(n_x\hat{\mathbf{e}}_x + n_y\hat{\mathbf{e}}_y\right)F\,ds \tag{2.2.27a}$$

The second equation implies, because two vectors are equal if and only if their components are equal, that the following relations hold:

$$\int_\Omega \frac{\partial F}{\partial x}\,dxdy = \oint_\Gamma n_x F\,ds, \quad \int_\Omega \frac{\partial F}{\partial y}\,dxdy = \oint_\Gamma n_y F\,ds \tag{2.2.27b}$$

Divergence Theorem

$$\int_\Omega \text{div}\mathbf{G}\,dxdy \equiv \int_\Omega \nabla\cdot\mathbf{G}\,dxdy = \oint_\Gamma \hat{\mathbf{n}}\cdot\mathbf{G}\,ds \tag{2.2.28a}$$

$$\int_\Omega \left(\frac{\partial G_x}{\partial x} + \frac{\partial G_y}{\partial y}\right)dxdy = \oint_\Gamma (n_x G_x + n_y G_y)ds \tag{2.2.28b}$$

Here the dot denotes the scalar product of vectors, $\hat{\mathbf{n}}$ denotes the unit vector normal to the surface Γ of the domain Ω; n_x and n_y (G_x and G_y) are the rectangular components of $\hat{\mathbf{n}}(\mathbf{G})$; and the circle on the boundary integral indicates that the integration is taken over the entire

boundary [see Fig. 2.2.3(*b*)]. The direction cosines n_x and n_y of the unit vector $\hat{\mathbf{n}}$ can be written as

$$n_x = \cos(x, \hat{\mathbf{n}}) = \hat{\mathbf{e}}_x \cdot \hat{\mathbf{n}}, \quad n_y = \cos(y, \hat{\mathbf{n}}) = \hat{\mathbf{e}}_y \cdot \hat{\mathbf{n}} \tag{2.2.29}$$

where $\cos(x, \hat{\mathbf{n}})$, for example, is the cosine of the angle between the positive x direction and the unit vector $\hat{\mathbf{n}}$.

The following identities, which can be derived using the gradient and divergence theorems, will be useful in the sequel. Let w and G be scalar functions defined in a two-dimensional domain Ω. Then

$$\int_\Omega (\nabla G)\, w \, dxdy = -\int_\Omega (\nabla w)\, G \, dxdy + \int_\Gamma \hat{\mathbf{n}}\, w\, G \, ds \tag{2.2.30a}$$

and

$$-\int_\Omega \left(\nabla^2 G\right) w \, dxdy = \int_\Omega \nabla w \cdot \nabla G \, dxdy - \oint_\Gamma \frac{\partial G}{\partial n} w \, ds \tag{2.2.30b}$$

where $\partial/\partial n$ denotes the normal derivative operator,

$$\frac{\partial}{\partial n} = \hat{\mathbf{n}} \cdot \nabla = n_x \frac{\partial}{\partial x} + n_y \frac{\partial}{\partial y} \tag{2.2.31}$$

The following component form of (2.2.30a), with an appropriate change of variables, is useful in the sequel:

$$\int_\Omega w \frac{\partial G}{\partial x} \, dxdy = -\int_\Omega \frac{\partial w}{\partial x} G \, dxdy + \oint_\Gamma n_x\, w\, G \, ds \tag{2.2.32a}$$

$$\int_\Omega w \frac{\partial G}{\partial y} \, dxdy = -\int_\Omega \frac{\partial w}{\partial y} G \, dxdy + \oint_\Gamma n_y\, w\, G \, ds \tag{2.2.32b}$$

Equations (2.2.32*a*) and (2.2.32*b*) can easily be established by means of (2.2.27*b*).

2.2.4 Linear and Bilinear Functionals

Consider the integral expression of the form

$$I(u) = \int_a^b F(x, u, u')\, dx, \quad u = u(x), \quad u' = \frac{du}{dx} \tag{2.2.33}$$

where the integrand $F(x, u, u')$ is a given function of the coordinate x (independent variable), dependent variable u, and its derivative du/dx. For a given real function $u = u(x)$, $I(u)$ is a real number. Therefore, I can be viewed as an operator that transforms functions $u(x)$ into real numbers, and such operators are called *functionals*. We shall use the term "functional" to describe functions defined by integrals whose arguments themselves are functions. Thus, loosely speaking, a functional is a "function of functions." A formal definition from functional analysis is that a functional is an operator I mapping functions u from a linear vector space into real number field. The following integrals qualify as functionals:

$$I(u) = \int_a^b \left(p(x)\frac{du}{dx} + q(x)u^2\right) dx + Pu(a)$$

$$I(u, v) = \int_\Omega \left(p(x, y)\frac{du}{dx}\frac{dv}{dx} + q(x, y)v\right) dxdy + \int_\Gamma Q\, u \, ds \tag{2.2.34}$$

where u and v are the dependent variables and all other parameters are either constants or functions of position.

A functional $I(u)$ is said to be *linear* in u if and only if it satisfies the relation

$$I(\alpha u + \beta v) = \alpha I(u) + \beta I(v) \tag{2.2.35}$$

for any real numbers α and β and dependent variables u and v. Examples of linear functionals are provided by

$$I(u) = \int_a^b f(x)\, u\, dx + q\, u(b), \quad I(u, v) = \int_\Omega (f(x, y)\, u + q(x, y) v)\, dx dy$$

Note that the functionals

$$I_1(u) = \int_a^b u \frac{du}{dx}\, dx, \quad I_2(u) = \int_a^b f(x)\, u\, dx + c, \quad c \text{ is a constant}$$

do not qualify as linear functionals (why?).

A functional $B(u, v)$ is said to be *bilinear* if it is linear in each of its arguments u and v:

$$B(\alpha u_1 + \beta u_2, v) = \alpha B(u_1, v) + \beta B(u_2, v) \text{ linear in the first argument} \tag{2.2.36a}$$

$$B(u, \alpha v_1 + \beta v_2) = \alpha B(u, v_1) + \beta B(u, v_2) \text{ linear in the second argument} \tag{2.2.36b}$$

where u, u_1, u_2, v, v_1, and v_2 are dependent variables and α and β are real numbers. Note that a bilinear functional necessarily contains two arguments (dependent variables), and it must be linear with respect to each argument. Examples of bilinear forms are

$$\begin{aligned} B_1(u, v) &= \int_a^b \left(p(x) u v + q(x) \frac{du}{dx} \frac{dv}{dx} \right) dx + k u(a) v(a) \\ B_2(\mathbf{u}, \mathbf{v}) &= \int_a^b \left(p(x) \mathbf{u} \cdot \mathbf{v} + q(x) \frac{d\mathbf{u}}{dx} \cdot \mathbf{v} \right) dx \\ B_3(\mathbf{u}, \mathbf{v}) &= \int_\Omega (p(\mathbf{x}) \mathbf{u} \cdot \mathbf{v} + q(\mathbf{x})\, \nabla \mathbf{u} \cdot \nabla \mathbf{v})\, d\mathbf{x} \end{aligned} \tag{2.2.37}$$

The functionals

$$\begin{aligned} I_1(u, v) &= \int_a^b \left[p(x) u^2 + q(x) \left(\frac{dv}{dx} \right)^2 \right] dx \\ I_2(\mathbf{u}, \mathbf{v}) &= \int_a^b \left(p(x) \mathbf{u} \cdot \mathbf{u} + q(x) \frac{d\mathbf{v}}{dx} \cdot \frac{d\mathbf{v}}{dx} \right) dx \\ I_3(u, v) &= \int_\Omega \left[p(x, y) \left(\frac{\partial u}{\partial x} \right)^2 v + q(x, y) u \right] dx dy \end{aligned} \tag{2.2.38}$$

are not linear in their arguments.

A bilinear form $B(u, v)$ is said to be *symmetric* in its arguments u and v if

$$B(u, v) = B(v, u) \tag{2.2.39}$$

for all u and v. Examples of symmetric bilinear forms are provided by $B_1(u, v)$ and $B_3(\mathbf{u}, \mathbf{v})$ listed above. Note that $B_2(\mathbf{u}, \mathbf{v})$ is not symmetric.

A *quadratic* functional $Q(u)$ is one that satisfies the relation

$$Q(\alpha u) = \alpha^2 Q(u) \tag{2.2.40}$$

for all real numbers α.

2.3 ELEMENTS OF CALCULUS OF VARIATIONS

2.3.1 Introduction

Calculus of variations is a branch of mathematics that deals with extrema and stationary behavior of functionals. As discussed in the introduction to this chapter, there are many problems that can be posed only as finding the extremum of functionals [see, for example, the *Brachistochrone problem, geodesic problem,* and *isoperimetric problem* discussed on pages 129 and 130 of Reddy (2002)]. The field of solid and structural mechanics heavily depends on the use of energy principles that are stated in terms of finding the extrema or stationary values of functionals to construct finite element models (e.g., the principle of minimum total potential energy, the principle of maximum total complementary energy, and the Hu–Washizu and Hellinger–Reissner mixed variational principles). The direct variational methods like the Ritz method use variational principles to obtain approximate solutions directly, bypassing the derivation of the governing equations.

In this section we study the concept of variational operator and its properties, first variation of functionals, and Euler equations resulting from the condition of vanishing of the first variation of a functional. In the interest of keeping the scope of the study within reasonable limits, only necessary concepts are covered.

Although the material covered in this section is not absolutely necessary for an understanding of the finite element method, it is deemed useful, at least for those readers who have solid and structural mechanics background, to understand the concepts from calculus of variations. Other readers may skip the section and go directly to Section 2.4.

2.3.2 Variational Operator and First Variation

Consider the function $F(x, u, u')$. For an arbitrarily fixed value of the independent variable x, F depends on u and u'. The change ϵv in u, where ϵ is a constant and v is a function, is called the *variation* of u and is denoted by δu (see Fig. 2.3.1):

$$\delta u \equiv \epsilon v \tag{2.3.1}$$

The operator δ is called the *variational operator*. The variation δu of a function u represents an admissible change in the function $u(x)$ at a *fixed* value of the independent variable x. If u is specified at a point (usually on the boundary), the variation of u is zero there because the specified value cannot be varied. Thus, the variation of a function u should satisfy the homogeneous form of the boundary conditions for u. The variation δu represents a *virtual* but admissible change in u. Associated with this change in u (i.e., when u is changed to $u + \epsilon v$), there is a change in F,

$$\Delta F = F(x, u + \epsilon v, u' + \epsilon v') - F(x, u, u')$$

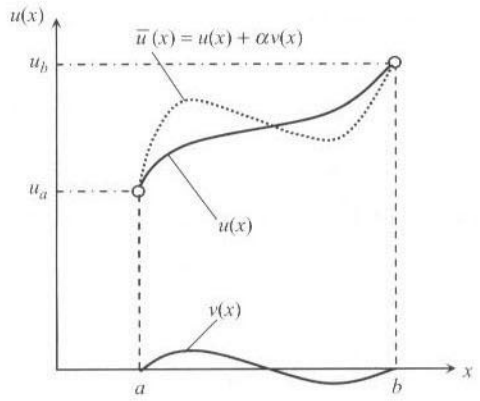

Figure 2.3.1 The variations of $u(x)$.

Expanding in powers of ϵ gives (treating $u + \epsilon v$ and $u' + \epsilon v'$ as dependent functions)

$$\begin{aligned}\Delta F &= F(x, u, u') + \epsilon v \frac{\partial F}{\partial u} + \epsilon v' \frac{\partial F}{\partial u'} + \frac{(\epsilon v)^2}{2!} \frac{\partial^2 F}{\partial u^2} \\ &\quad + \frac{(\epsilon v)(\epsilon v')}{2!} \frac{\partial^2 F}{\partial u \partial u'} + \frac{(\epsilon v')^2}{2!} \frac{\partial^2 F}{\partial u'^2} + \cdots - F(x, u, u') \\ &= \epsilon v \frac{\partial F}{\partial u} + \epsilon v' \frac{\partial F}{\partial u'} + \epsilon R_1(\epsilon) \end{aligned} \tag{2.3.2}$$

where $lim_{\epsilon \to 0} R_1(\epsilon) = 0$. The *first variation* of F is defined by

$$\begin{aligned}\delta F &= \epsilon \left[\lim_{\epsilon \to 0} \frac{F(x, u + \epsilon v, u' + \epsilon v') - F(x, u, u')}{\epsilon} \right] = \epsilon \left[\lim_{\epsilon \to 0} \frac{\Delta F}{\epsilon} \right] \\ &\equiv \epsilon \left[\frac{d}{d\epsilon} (F(u + \epsilon v)) \right]_{\epsilon = 0} \\ &= \epsilon \left(v \frac{\partial F}{\partial u} + v' \frac{\partial F}{\partial u'} \right) = \frac{\partial F}{\partial u} \delta u + \frac{\partial F}{\partial u'} \delta u' \end{aligned} \tag{2.3.3}$$

Thus, the first variation of F can be written in terms of the variations of the dependent variable u and its derivatives. Note that in the special case when $F = u$, Eq. (2.3.3) gives the result in Eq. (2.3.1). Further, note the analogy between the first variation, (2.3.3), and the total differential of F,

$$dF = \frac{\partial F}{\partial x} dx + \frac{\partial F}{\partial u} du + \frac{\partial F}{\partial u'} du' \tag{2.3.4}$$

Since x is *not varied* during the variation of u to $u + \delta u$, $dx = 0$ and the analogy between δF and dF becomes apparent, i.e., *δ acts as a differential operator with respect to dependent variables.*

The above discussion can be extended to two dimensions and to functions F that depend on more than one dependent variable in two or more dimensions. Let $F = F(x, y, u, v, u_x, v_x, u_y, v_y)$, where $u = u(x, y)$ and $v = v(x, y)$ are dependent variables,

and $u_x = \partial u/\partial x$, $u_y = \partial u/\partial y$, and so on. The first variation of F is given by

$$\delta F = \frac{\partial F}{\partial u}\delta u + \frac{\partial F}{\partial v}\delta v + \frac{\partial F}{\partial u_x}\delta u_x + \frac{\partial F}{\partial v_x}\delta v_x + \frac{\partial F}{\partial u_y}\delta u_y + \frac{\partial F}{\partial v_y}\delta v_y$$

It can easily be verified that the laws of variation of sums, products, ratios, powers, and so forth are completely analogous to the corresponding laws of differentiation. For example, if $F_1 = F_1(u)$ and $F_2 = F_2(u)$, then

$$\begin{aligned} \delta(F_1 \pm F_2) &= \delta F_1 \pm \delta F_2 \\ \delta(F_1\, F_2) &= \delta F_1\, F_2 + F_1 \delta F_2 \\ \delta\left(\frac{F_1}{F_2}\right) &= \frac{\delta F_1\, F_2 - F_1\, \delta F_2}{F_2^2} \\ \delta(F_1)^n &= n(F_1)^{n-1}\delta F_1 \end{aligned} \tag{2.3.5}$$

If $G = G(u, v, w)$ is function of several dependent variables u, v, and w (and possibly their derivatives), the total variation is the sum of the partial variations:

$$\delta G = \delta_u G + \delta_v G + \delta_w G \tag{2.3.6}$$

Furthermore, the variational operator can commute with differential and integral operators (as long as the coordinates x and y are the fixed coordinates):

$$\frac{d}{dx}(\delta u) = \frac{d}{dx}(\epsilon v) = \epsilon\frac{dv}{dx} = \epsilon v' = \delta u' = \delta\left(\frac{du}{dx}\right) \tag{2.3.7a}$$

$$\delta\int_a^b u(x)\,dx = \int_a^b \delta u(x)\,dx \tag{2.3.7b}$$

The first variation of a functional can now be computed readily. Consider the functional in Eq. (2.2.33). The first variation of $I(u)$ is

$$\begin{aligned} \delta I(u) &= \delta\int_a^b F(x, u, u')\,dx = \int_a^b \delta F(x, u, u')\,dx \\ &= \int_a^b \left(\frac{\partial F}{\partial u}\delta u + \frac{\partial F}{\partial u'}\delta u'\right)dx \end{aligned} \tag{2.3.8}$$

More specific functionals are considered in the next example.

Example 2.3.1

Consider the functionals in (2.2.34). We wish to find their first variations. We have

$$\begin{aligned} \delta I(u) &= \int_a^b \left(p(x)\frac{d\delta u}{dx} + 2q(x)u\delta u\right)dx + P\delta u(a) \\ \delta I(u, v) &= \int_\Omega \left[p(x, y)\left(\frac{d\delta u}{dx}\frac{dv}{dx} + \frac{du}{dx}\frac{d\delta v}{dx}\right) + q(x, y)\delta v\right]dxdy \\ &\quad + \int_\Gamma Q\,\delta u\,ds \end{aligned} \tag{2.3.9}$$

Note that functions of position, p and q, do not undergo variation because they are not functions of the dependent variables.

2.3.3 Fundamental Lemma of Variational Calculus

The *fundamental lemma of calculus of variations* can be stated as follows: *for any integrable function $G(x)$, if the statement*

$$\int_a^b G(x)\,\eta(x)\,dx = 0 \tag{2.3.10}$$

holds for any arbitrary continuous function $\eta(x)$, for all x in (a, b), then it follows that $G(x) = 0$ in (a, b). A simple proof of the lemma follows from setting $\eta(x)$, which is arbitrary, equal to G. We have

$$\int_a^b [G(x)]^2\,dx = 0$$

Since an integral of a positive function, G^2, is positive, the above statement implies that $G(x) = 0$ in the domain $\Omega = (a, b)$.

A more general statement of the fundamental lemma is as follows: If $\eta(x)$ is arbitrary in $a < x < b$ and $\eta(a)$ is arbitrary, then the statement

$$\int_a^b G\eta\,dx + B(a)\eta(a) = 0 \tag{2.3.11a}$$

implies that

$$G = 0 \text{ in } a < x < b \text{ and } B(a) = 0 \tag{2.3.11b}$$

because $\eta(x)$ is independent of $\eta(a)$.

2.3.4 The Euler Equations

As stated in the introduction, certain problems are formulated as one of seeking the extremum of functionals (i.e., functions of dependent unknowns of the problem). For example, problems of solid mechanics can be formulated as one of minimizing the total potential energy of the system (Reddy, 2002). Typically, the total potential energy (functional) is written in terms of the displacement field and applied loads. Then it is useful to derive the differential equations that govern the displacement field from this minimum principle. Here we outline the steps in obtaining such equations.

Consider, for example, the problem of finding a function $u = u(x)$ such that

$$u(a) = u_a, \quad u(b) = u_b \tag{2.3.12a}$$

and

$$I(u) = \int_a^b F(x, u(x), u'(x))\,dx \tag{2.3.12b}$$

is a minimum. In analyzing the problem, we are not interested in all functions u but only in those functions that satisfy the stated boundary (or end) conditions. The set of all such functions is called, for obvious reasons, the *set of competing functions* (or set of admissible functions). We shall denote the set by $\mathcal{C}$. The problem is to seek an element u from $\mathcal{C}$ that renders I a minimum. If $u \in \mathcal{C}$ (the symbol $\in$ means 'an element of'), then $(u + \epsilon v) \in \mathcal{C}$ for every v satisfying the conditions $v(a) = v(b) = 0$. The space of all such elements is called the space of admissible variations, as already mentioned. Figure 2.3.1 shows a typical competing function $\bar{u}(x) = u(x) + \epsilon v(x)$ and a typical admissible variation $v(x)$.

Let $I(u)$ be a differentiable functional in the sense that

$$\frac{dI(u+\epsilon v, u'+\epsilon v')}{d\epsilon}$$

exists, and let $\mathcal{C}$ denote the space of competing functions. Then, an element u in $\mathcal{C}$ is said to yield a *relative minimum (maximum)* for $I(\bar{u})$ in $\mathcal{C}$ if

$$I(\bar{u}) - I(u) \geq 0 \qquad (\leq 0) \tag{2.3.13}$$

If $I(\bar{u})$ assumes a relative minimum (maximum) at $u \in \mathcal{C}$ relative to elements $\bar{u} \in \mathcal{C}$, then it follows from the definition of the space of admissible variations $\mathcal{H}$ and Eq. (2.3.13) that

$$I(u+\epsilon v) - I(u) \geq 0 \qquad (\leq 0) \tag{2.3.14}$$

for all $v \in \mathcal{H}$, $||v|| < \varepsilon$, and ϵ a real number. Since u is the minimizer, any other function $u \in \mathcal{C}$ is of the form $\bar{u} = u + \epsilon v$, and the actual minimizer is determined by setting $\epsilon = 0$. Once $u(x)$ and $v(x)$ are assigned, $I(\bar{u})$ is a function of ϵ alone, say $\bar{I}(\epsilon)$. Now a necessary condition for $I(\bar{u}) = \bar{I}(\epsilon)$ to attain a minimum is that

$$\frac{d\bar{I}(\epsilon)}{d\epsilon} = \frac{d}{d\epsilon}[I(u+\epsilon v)] = 0 \tag{2.3.15}$$

On the other hand, $I(\bar{u})$ attains its minimum at u, i.e., $\epsilon = 0$. These two conditions together imply $(d\bar{I}(\epsilon)/d\epsilon)|_{\epsilon=0} = 0$, which is nothing but

$$\delta I(u) = 0 \tag{2.3.16}$$

Analogous to the sufficient condition for ordinary functions, the sufficient condition for a functional to assume a relative minimum (maximum) is that the second variation $\delta^2 I(u)$ is greater (less) than zero. The second variation $\delta^2 I(u)$ of a functional $I(u)$ is given by

$$\delta^2 I(u) \equiv \frac{\epsilon^2}{2}\left[\frac{d^2}{d\epsilon^2} I(u+\epsilon v)\right]_{\epsilon=0} \tag{2.3.17}$$

for all $v \in \mathcal{C}$ and real number ϵ.

It is clear that any candidate for the minimizing functional should satisfy the end conditions in Eq. (2.3.12*a*) and be sufficiently differentiable (twice in the present case, as we shall see shortly). The set of all such functions is the set of admissible functions or competing functions for the present case. Functions from the admissible set can be viewed as smooth (i.e., differentiable twice) functions passing through points (a, u_a) and (b, u_b), as shown in Fig. 2.3.1. Clearly, any element $\bar{u}$ in $\mathcal{C}$ (the set of competing functions) has the form

$$\bar{u} = u + \epsilon v \tag{2.3.18}$$

where ϵ is a small number and v is a sufficiently differentiable function that satisfies the homogeneous form of the end conditions (because $\bar{u}$ must satisfy the specified end conditions) in Eq. (2.3.12*a*)

$$v(a) = v(b) = 0 \tag{2.3.19}$$

and u is the function that minimizes the functional in Eq. (2.3.12*b*). The set of all functions v is the set of admissible variations, $\mathcal{H}$. Now assuming that, for each admissible function $\bar{u}$, $F(x, \bar{u}, \bar{u}')$ exists and is continuously differentiable with respect to its arguments, and $I(\bar{u})$ takes one and only one real value, we seek the particular function $u(x)$ that makes the integral a minimum.

The necessary condition (2.3.15) for I to attain a minimum gives

$$0 = \frac{dI(u+\epsilon v)}{d\epsilon}\bigg|_{\epsilon=0} = \left[\frac{d}{d\epsilon}\int_a^b F(x, \bar{u}, \bar{u}')dx\right]_{\epsilon=0}$$

$$= \int_a^b \left(\frac{\partial F}{\partial \bar{u}}\frac{\partial \bar{u}}{\partial \epsilon} + \frac{\partial F}{\partial \bar{u}'}\frac{\partial \bar{u}'}{\partial \epsilon}\right)\bigg|_{\epsilon=0} dx = \int_a^b \left(\frac{\partial F}{\partial u}v + \frac{\partial F}{\partial u'}v'\right)dx \qquad (2.3.20)$$

where $\bar{u} = u + \epsilon v$. Integrating the second term in the last equation by parts to transfer differentiation from v to u, we obtain

$$0 = \int_a^b v\left[\frac{\partial F}{\partial u} - \frac{d}{dx}\left(\frac{\partial F}{\partial u'}\right)\right]dx + \left(\frac{\partial F}{\partial u'}v\right)\bigg|_a^b \qquad (2.3.21)$$

The boundary term vanishes because v is zero at $x = a$ and $x = b$ [see Eq. (2.3.19)]. The fact that v is arbitrary inside the interval (a, b) and yet the equation should hold implies, by the fundamental lemma of the calculus of variations, that the expression in the square brackets is zero identically:

$$\frac{\partial F}{\partial u} - \frac{d}{dx}\left(\frac{\partial F}{\partial u'}\right) = 0 \text{ in } a < x < b \qquad (2.3.22)$$

Equation (2.3.22) is called the *Euler equation* of the functional in Eq. (2.3.12*b*). Of all the admissible functions, the one that satisfies (i.e., the solution of) Eq. (2.3.22) is the true minimizer of the functional I.

Next consider the problem of finding (u, v), defined on a two-dimensional region Ω, such that the following functional is to be minimized:

$$I(u, v) = \int_\Omega F(x, y, u, v, u_x, v_x, u_y, v_y)dxdy \qquad (2.3.23)$$

where $u_x = \partial u/\partial x$, $u_y = \partial u/\partial y$, and so on. For the moment we assume that u and v are specified on the boundary Γ of Ω. The vanishing of the first variation of $I(u, v)$ is written as

$$\delta I(u, v) = \delta_u I(u, v) + \delta_v I(u, v) = 0$$

Here δ_u and δ_v denote (partial) variations with respect to u and v, respectively. We have

$$\delta I = \int_\Omega \left(\frac{\partial F}{\partial u}\delta u + \frac{\partial F}{\partial u_x}\delta u_x + \frac{\partial F}{\partial u_y}\delta u_y + \frac{\partial F}{\partial v}\delta v + \frac{\partial F}{\partial v_x}\delta v_x + \frac{\partial F}{\partial v_y}\delta v_y\right)dxdy \qquad (2.3.24)$$

The next step in the development involves the use of integration by parts, or the gradient theorem on the second, third, fifth, and sixth terms in Eq. (2.3.24). Consider the second term. We have

$$\int_\Omega \frac{\partial F}{\partial u_x}\frac{\partial \delta u}{\partial x}\,dxdy = \int_\Omega \left[\frac{\partial}{\partial x}\left(\frac{\partial F}{\partial u_x}\delta u\right) - \frac{\partial}{\partial x}\left(\frac{\partial F}{\partial u_x}\right)\delta u\right]dxdy$$

$$= \oint_\Gamma \frac{\partial F}{\partial u_x}\delta u\, n_x\, ds - \int_\Omega \frac{\partial}{\partial x}\left(\frac{\partial F}{\partial u_x}\right)\delta u\, dxdy \qquad (2.3.25)$$

Using a similar procedure on the other terms and collecting the coefficients of δu and δv separately, we obtain

$$0 = \int_\Omega \left\{\left[\frac{\partial F}{\partial u} - \frac{\partial}{\partial x}\left(\frac{\partial F}{\partial u_x}\right) - \frac{\partial}{\partial y}\left(\frac{\partial F}{\partial u_y}\right)\right]\delta u\right.$$

$$+\left[\frac{\partial F}{\partial v}-\frac{\partial}{\partial x}\left(\frac{\partial F}{\partial v_x}\right)-\frac{\partial}{\partial y}\left(\frac{\partial F}{\partial v_y}\right)\right]\delta v\Bigg\}\,dxdy$$

$$+\oint_\Gamma\left[\left(\frac{\partial F}{\partial u_x}n_x+\frac{\partial F}{\partial u_y}n_y\right)\delta u+\left(\frac{\partial F}{\partial v_x}n_x+\frac{\partial F}{\partial v_y}n_y\right)\delta v\right]ds \tag{2.3.26}$$

Since (u, v) are specified on Γ, $\delta u=\delta v=0$ and the boundary expressions vanish. Then, since δu and δv are arbitrary and independent of each other in Ω, the fundamental lemma yields the Euler equations

$$\delta u\text{:}\quad \frac{\partial F}{\partial u}-\frac{\partial}{\partial x}\left(\frac{\partial F}{\partial u_x}\right)-\frac{\partial}{\partial y}\left(\frac{\partial F}{\partial u_y}\right)=0 \tag{2.3.27a}$$

$$\delta v\text{:}\quad \frac{\partial F}{\partial v}-\frac{\partial}{\partial x}\left(\frac{\partial F}{\partial v_x}\right)-\frac{\partial}{\partial y}\left(\frac{\partial F}{\partial v_y}\right)=0 \tag{2.3.27b}$$

2.3.5 Natural and Essential Boundary Conditions

First, consider the problem of minimizing the functional in Eq. (2.3.12*b*) subject to *no* end conditions [hence, an element v of the set of admissible variation is arbitrary even at the end points, i.e., $v(a)\neq 0$ and $v(b)\neq 0$]. Then the functional $I(u)$ has the form

$$I(u)=\int_a^b F(x, u(x), u'(x))\,dx-Q_a\,u(a)-Q_b\,u(b) \tag{2.3.28}$$

where Q_a and Q_b are known values. The necessary condition for I to attain a minimum yields [cf. Eq. (2.3.21)]

$$0=\int_a^b v\left[\frac{\partial F}{\partial u}-\frac{d}{dx}\left(\frac{\partial F}{\partial u'}\right)\right]dx+\left(\frac{\partial F}{\partial u'}v\right)\Big|_a^b-Q_a\,v(a)-Q_b\,v(b) \tag{2.3.29}$$

Now suppose that $\frac{\partial F}{\partial u'}$ and v are selected such that

$$\left(-\frac{\partial F}{\partial u'}-Q_a\right)v=0 \text{ for } x=a,\quad \left(\frac{\partial F}{\partial u'}-Q_b\right)v=0 \text{ for } x=b \tag{2.3.30}$$

Then using the fundamental lemma of the calculus of variations, we obtain the same Euler equation as in Eq. (2.3.22).

Equations in (2.3.30) are satisfied identically for any of the following combinations:

$$\begin{aligned}
&(1)\quad v(a)=0,\quad v(b)=0\\
&(2)\quad v(a)=0,\quad \frac{\partial F}{\partial u'}\bigg|_b-Q_b=0\\
&(3)\quad -\frac{\partial F}{\partial u'}\bigg|_a-Q_a=0,\quad v(b)=0\\
&(4)\quad -\frac{\partial F}{\partial u'}\bigg|_a-Q_a=0,\quad \frac{\partial F}{\partial u'}\bigg|_b-Q_b=0
\end{aligned} \tag{2.3.31}$$

The requirement that $v=0$ at an end point is equivalent to the requirement that u is specified (to be some value) at that point. The end conditions in (2.3.31) are classified into two types:

essential boundary conditions, which require v (and possibly its derivatives) to vanish at the boundary, and *natural boundary conditions*, which require the specification of *the coefficient of* v (and possibly its derivatives). Thus, we have

Essential Boundary Conditions:

$$\text{specify } v = 0 \text{ or } u = \hat{u} \text{ on the boundary} \tag{2.3.32a}$$

Natural Boundary Conditions:

$$\text{specify } \frac{\partial F}{\partial u'} = Q \text{ on the boundary} \tag{2.3.32b}$$

where $Q = -Q_a$ at $x = a$ and $Q = Q_b$ at $x = b$. In a given problem, only one of the four combinations given in Eq. (2.3.31) can be specified. Problems in which all of the boundary conditions are of the essential type are called *Dirichlet boundary-value problems*, and those in which all of the boundary conditions are of the natural type are called *Neumann boundary-value problems*. *Mixed boundary-value problems* are those in which both essential and natural boundary conditions are specified. Essential boundary conditions are also known as *Dirichlet* or *geometric* boundary conditions, and natural boundary conditions are known as *Neumann* or *dynamic* boundary conditions.

As a general rule, the vanishing of the variation v (or δu) at a point implies that u is specified there (in general, to be nonzero). The specification of u on the boundary constitutes the essential boundary condition. Vanishing of the coefficient of the variation v in the boundary expression constitutes the natural boundary condition. This rule applies to any functional in one, two, and three dimensions, and to integrands that are functions of one or more dependent variables and their derivatives of any order.

Next consider the functional in Eq. (2.3.23), and suppose that (u, v) are arbitrary on Γ for the moment. It is easy to identify the natural and essential boundary conditions of the problem from Eq. (2.3.26): In each of the pairings on boundary Γ, specifying the first element (which contains no variations of the dependent variables) constitutes the natural boundary condition, and vanishing of the second element (or, equivalently, specifying the quantity in front of the variational operator) constitutes the essential boundary condition. Thus, we have either

$$u = \hat{u} \text{ (specified) so that } \delta u = 0 \quad \text{on} \quad \Gamma \tag{2.3.33a}$$

$$v = \hat{v} \text{ (specified) so that } \delta v = 0 \quad \text{on} \quad \Gamma \tag{2.3.33b}$$

or

$$\frac{\partial F}{\partial u_x} n_x + \frac{\partial F}{\partial u_y} n_y = 0 \quad \text{on} \quad \Gamma \tag{2.3.34a}$$

$$\frac{\partial F}{\partial v_x} n_x + \frac{\partial F}{\partial v_y} n_y = 0 \quad \text{on} \quad \Gamma \tag{2.3.34b}$$

Equations (2.3.33a) and (2.3.33b) represent the essential boundary conditions and Eqs. (2.3.34a) and (2.3.34b) the natural boundary conditions. The pair of elements (u, v) are called the *primary variables* and

$$Q_x \equiv \frac{\partial F}{\partial u_x} n_x + \frac{\partial F}{\partial u_y} n_y \text{ and } Q_y \equiv \frac{\partial F}{\partial v_x} n_x + \frac{\partial F}{\partial v_y} n_y$$

are called the *secondary variables*. Thus, specification of the primary variables constitute essential boundary conditions and specification of the secondary variables constitute natural boundary conditions. In general, one element of each pair (u, Q_x) and (v, Q_y) (but not both elements of the same pair) may be specified at any point of the boundary. Thus, there are four possible combinations of natural and essential boundary conditions for the problem under discussion.

Example 2.3.2

Consider an elastic bar of length L, modulus of elasticity E, and area of cross section A. Assume that it is fixed at the left end, spring supported at the right end, and subjected to distributed axial load $f(x)$ (see Fig. 2.3.2). The total potential energy functional $\Pi = U + V$ of the bar is (here we assumed that one knows how to write the total potential energy of the bar)

$$\Pi(u) = \int_0^L \left[\frac{EA}{2} \left(\frac{du}{dx} \right)^2 - fu \right] dx + \frac{k}{2}[u(L)]^2 \tag{2.3.35}$$

where u denotes the axial displacement of the bar. The first term in $\Pi(u)$ represents the strain energy U stored in the bar, the second term denotes the work done V on the bar by the distributed load f, and the last term denotes the strain energy stored in the linear elastic spring. We wish to determine the Euler equation of the bar by requiring that $\Pi(u)$ be a minimum subject to the geometric boundary condition $u(0) = 0$. The statement $\delta\Pi = 0$ is known as *the principle of minimum total potential energy*.

The first variation of Π is given by

$$\delta\Pi(u) = \int_0^L \left(EA \frac{du}{dx} \frac{d\delta u}{dx} - f\delta u \right) dx + ku(L)\,\delta u(L)$$

where δu is arbitrary in $0 < x < L$ and at $x = L$ but satisfies the condition $\delta u(0) = 0$. To use the fundamental lemma of variational calculus, we must relieve δu of any differentiation.

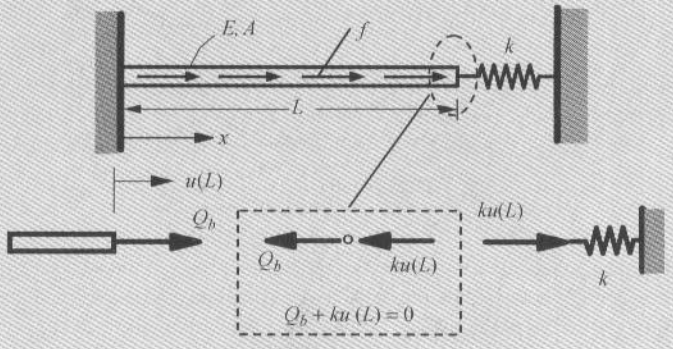

Figure 2.3.2 Elastic bar problem discussed in Example 2.3.2.

Integrating the first term by parts, we get

$$\delta\Pi(u) = \int_0^L \left[-\frac{d}{dx}\left(EA\frac{du}{dx}\right) - f \right] \delta u \, dx + \left[EA\frac{du}{dx}\,\delta u \right]_0^L + ku(L)\,\delta u(L)$$

$$= \int_0^L \delta u \left[-\frac{d}{dx}\left(EA\frac{du}{dx}\right) - f \right] dx + \delta u(L)\left[EA\frac{du}{dx} + ku(L) \right]_{x=L}$$

$$- \delta u(0)\left[EA\frac{du}{dx} \right]_{x=0}$$

The last term is zero because $\delta u(0) = 0$. Setting the coefficients of δu in $(0, L)$ and δu at $x = L$ to zero separately, we obtain the Euler equation and the natural (or force) boundary condition of the problem:

Euler Equation:

$$-\frac{d}{dx}\left(EA\frac{du}{dx}\right) - f = 0, \quad 0 < x < L \tag{2.3.36a}$$

Natural Boundary Condition:

$$EA\frac{du}{dx} + ku(L) = 0 \text{ at } x = L \tag{2.3.36b}$$

Thus, the solution u of Eqs. (2.3.36a) and (2.3.36b) that satisfies $u(0) = 0$ is the minimizer of the energy functional $\Pi(u)$ in Eq. (2.3.35).

Equations (2.3.36a) and (2.3.36b) can be obtained directly from Eq. (2.3.22) and (2) of Eq. (2.3.31) (with $Q_b = -ku(L)$ as shown in Fig. 2.3.2) by substituting

$$F(x, u, u') = \frac{EA}{2}\left(\frac{du}{dx}\right)^2 - f(x)u(x), \quad \frac{\partial F}{\partial u} = -f, \quad \frac{\partial F}{\partial u'} = EA\frac{du}{dx} \tag{2.3.37}$$

Example 2.3.3

The total potential energy of a linear elastic body in three dimensions, subjected to body force $\mathbf{f}$ (measured per unit volume) and surface traction $\hat{\mathbf{t}}$ (measured per unit area) on portion S_2 of the surface [see Fig. 2.3.3(a)] is given by (summation on repeated indices is implied)

$$\Pi(\mathbf{u}) = \int_V \left(\frac{1}{2}\sigma_{ij}\varepsilon_{ij} - f_i u_i \right) dV - \int_{S_2} \hat{t}_i u_i \, dS \tag{2.3.38}$$

where u_i denote the displacement components, σ_{ij} are the stress components [see Fig. 2.3.3(b)], and ε_{ij} are strain components. It is assumed that the body is subjected to specified displacements on the remaining portion S_1 of the surface, and therefore the virtual displacements vanish there:

$$u_i = \hat{u}_i \quad \text{and} \quad \delta u_i = 0 \quad \text{on} \quad S_1 \tag{2.3.39}$$

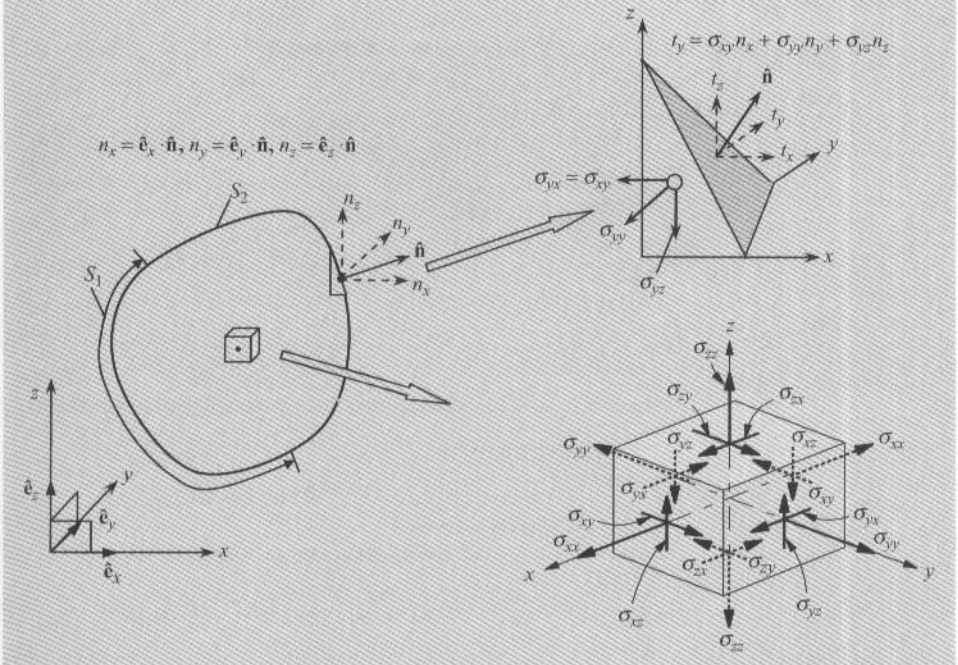

(*a*) A 3-D domain (*b*) Stress components

Figure 2.3.3 (*a*) An elastic body with specified displacements and tractions. (*b*) The stress components at a typical point inside the body and on the boundary.

In Eq. (2.3.38), and in the following discussion, summation on repeated indices is assumed. Use of the index notation and the summation convention in the 3-D case saves considerable space (i.e., the explicit form of Eq. (2.3.38) and subsequent manipulations would take considerably more space). The first term under the volume integral represents the strain energy density of the elastic body and the second term represents the work done by the body force $\mathbf{f}$; and the surface integral denotes the work done by the specified traction $\hat{\mathbf{t}}$.

For an isotropic body the stress-strain relations are given by (the generalized Hooke's law)

$$\sigma_{ij} = 2\mu\varepsilon_{ij} + \lambda\delta_{ij}\varepsilon_{kk} \tag{2.3.40}$$

where μ and λ are the Lamé (material) constants. Hence,

$$\sigma_{ij}\varepsilon_{ij} = 2\mu\varepsilon_{ij}\varepsilon_{ij} + \lambda\varepsilon_{ii}\varepsilon_{kk} \tag{2.3.41}$$

The linear strain-displacement relations of the linear theory are given by

$$\varepsilon_{ij} = \frac{1}{2}(u_{i,j} + u_{j,i}) \tag{2.3.42}$$

where $u_{i,j} = (\partial u_i / \partial x_j)$.

Substituting Eqs. (2.3.41) and (2.3.42) into Eq. (2.3.38), we obtain

$$\Pi(\mathbf{u}) = \int_V \left[\frac{\mu}{4}\left(u_{i,j}+u_{j,i}\right)\left(u_{i,j}+u_{j,i}\right) + \frac{\lambda}{2}u_{i,i}u_{k,k} - f_i\,u_i\right] dV - \int_{S_2} \hat{t}_i\,u_i\,dS \tag{2.3.43}$$

Now we wish to derive the Euler equations associated with the functional in Eq. (2.3.43) using the principle of minimum total potential energy, $\delta\Pi = 0$ (i.e., minimize Π) and $\delta u_i = 0$ on S_1.

Setting the first variation of Π to zero, we obtain

$$0 = \int_V \left[\frac{\mu}{2}\left(\delta u_{i,j}+\delta u_{j,i}\right)\left(u_{i,j}+u_{j,i}\right) + \lambda\delta u_{i,i}u_{k,k} - f_i\,\delta u_i\right] dV - \int_{S_2} \hat{t}_i\,\delta u_i\,dS \tag{2.3.44}$$

wherein the product rule of variation is used and similar terms are combined. Using integration by parts

$$\int_V \delta u_{i,j}(u_{i,j}+u_{j,i})dV = -\int_V \delta u_i(u_{i,j}+u_{j,i})_{,j}\,dV + \oint_S \delta u_i(u_{i,j}+u_{j,i})n_j\,dS$$

where n_j denotes the jth direction cosine of the unit normal to the surface, we obtain

$$\begin{aligned}
0 &= \int_V \left[-\frac{\mu}{2}(u_{i,j}+u_{j,i})_{,j}\delta u_i - \frac{\mu}{2}(u_{i,j}+u_{j,i})_{,i}\delta u_j - \lambda u_{k,ki}\delta u_i - f_i\,\delta u_i\right] dV \\
&\quad + \oint_S \left[\frac{\mu}{2}(u_{i,j}+u_{j,i})(n_j\delta u_i + n_i\delta u_j) + \lambda u_{k,k}\,n_i\,\delta u_i\right] dS - \int_{S_2} \delta u_i\,\hat{t}_i\,dS \\
&= \int_V \left[-\mu(u_{i,j}+u_{j,i})_{,j} - \lambda u_{k,ki} - f_i\right]\delta u_i\,dV \\
&\quad + \oint_S \left[\mu(u_{i,j}+u_{j,i}) + \lambda u_{k,k}\delta_{ij}\right] n_j\delta u_i\,dS - \int_{S_2} \delta u_i\hat{t}_i\,dS
\end{aligned} \tag{2.3.45}$$

In arriving at the last step, a change of dummy indices is made to combine terms. Recognizing that the expression inside the square brackets of the closed surface integral is nothing but σ_{ij}, and $\sigma_{ij}n_j = t_i$ by Cauchy's formula [which is nothing but a statement of the equilibrium of forces on the tetrahedral element; see Fig. 2.3.3(b)], we can write

$$\oint_S t_i\,\delta u_i\,dS = \int_{S_1} t_i\,\delta u_i\,dS + \int_{S_2} t_i\,\delta u_i\,dS = \int_{S_2} t_i\,\delta u_i\,dS$$

The integral over S_1 is zero by virtue of Eq. (2.3.39). Hence, we have

$$0 = \int_V \left[-\mu\left(u_{i,j}+u_{j,i}\right)_{,j} - \lambda u_{k,ki} - f_i\right]\delta u_i dV + \int_{S_2} \delta u_i\left(t_i - \hat{t}_i\right) dS$$

Using the fundamental lemma of calculus of variations, we set the coefficients of δu_i in V and δu_i on S_2 to zero separately and obtain

$$\mu(u_{i,jj}+u_{j,ij}) + \lambda u_{k,ki} + f_i = 0 \text{ in } V \tag{2.3.46}$$

$$\sigma_{ij}n_j - \hat{t}_i = 0 \text{ on } S_2 \tag{2.3.47}$$

for $i = 1, 2, 3$.

Equations (2.3.46) are the well-known Navier's equations of equilibrium of three-dimensional elasticity, and (2.3.47) are the traction boundary conditions. The explicit forms of Eqs. (2.3.40), (2.3.42), (2.3.46), and (2.3.47) in a rectangular Cartesian coordinate system (x, y, z) are given below ($x_1 = x$, $x_2 = y$, $x_3 = z$, $f_1 = f_x$, $f_2 = f_y$, $f_3 = f_z$, $\sigma_{11} = \sigma_{xx}$, $\sigma_{13} = \sigma_{xz} = \sigma_{zx}$, and so on).

Stress-Strain Relations (Hooke's Law for an Orthotropic Material):

$$\begin{Bmatrix} \sigma_{xx} \\ \sigma_{yy} \\ \sigma_{zz} \\ \sigma_{yz} \\ \sigma_{xz} \\ \sigma_{xy} \end{Bmatrix} = \begin{bmatrix} C_{11} & C_{12} & C_{13} & 0 & 0 & 0 \\ C_{12} & C_{22} & C_{23} & 0 & 0 & 0 \\ C_{13} & C_{23} & C_{33} & 0 & 0 & 0 \\ 0 & 0 & 0 & C_{44} & 0 & 0 \\ 0 & 0 & 0 & 0 & C_{55} & 0 \\ 0 & 0 & 0 & 0 & 0 & C_{66} \end{bmatrix} \begin{Bmatrix} \varepsilon_{xx} \\ \varepsilon_{yy} \\ \varepsilon_{zz} \\ \gamma_{yz} \\ \gamma_{xz} \\ \gamma_{xy} \end{Bmatrix} \tag{2.3.48a}$$

where $\gamma_{xy} = 2\varepsilon_{xy}$, $\gamma_{xz} = 2\varepsilon_{xz}$ and $\gamma_{yz} = 2\varepsilon_{yz}$ are the engineering shear strains. The elastic material stiffness coefficients C_{ij} are known in terms of the engineering material constants by

$$\begin{aligned} C_{11} &= \frac{1 - \nu_{23}\nu_{32}}{E_2 E_3 \Delta}, \quad C_{12} = \frac{\nu_{21} + \nu_{31}\nu_{23}}{E_2 E_3 \Delta} = \frac{\nu_{12} + \nu_{32}\nu_{13}}{E_1 E_3 \Delta} \\ C_{13} &= \frac{\nu_{31} + \nu_{21}\nu_{32}}{E_2 E_3 \Delta} = \frac{\nu_{13} + \nu_{12}\nu_{23}}{E_1 E_2 \Delta} \\ C_{22} &= \frac{1 - \nu_{13}\nu_{31}}{E_1 E_3 \Delta}, \quad C_{23} = \frac{\nu_{32} + \nu_{12}\nu_{31}}{E_1 E_3 \Delta} = \frac{\nu_{23} + \nu_{21}\nu_{13}}{E_1 E_3 \Delta} \\ C_{33} &= \frac{1 - \nu_{12}\nu_{21}}{E_1 E_2 \Delta}, \quad C_{44} = G_{23} \quad C_{55} = G_{31} \quad C_{66} = G_{12} \\ \Delta &= \frac{1 - \nu_{12}\nu_{21} - \nu_{23}\nu_{32} - \nu_{31}\nu_{13} - 2\nu_{21}\nu_{32}\nu_{13}}{E_1 E_2 E_3} \end{aligned} \tag{2.3.48b}$$

Here E_1, E_2, and E_3 are Young's moduli in 1, 2, and 3 material directions, respectively; ν_{ij} are Poisson's ratios, defined as the ratio of transverse strain in the jth direction to the axial strain in the ith direction when stressed in the ith direction; and G_{23}, G_{13}, and G_{12} are shear moduli in the 2-3, 1-3, and 1-2 planes, respectively. In addition, the following reciprocity relations among the engineering constants hold:

$$\frac{\nu_{21}}{E_2} = \frac{\nu_{12}}{E_1}; \quad \frac{\nu_{31}}{E_3} = \frac{\nu_{13}}{E_1}; \quad \frac{\nu_{32}}{E_3} = \frac{\nu_{23}}{E_2} \tag{2.3.49}$$

For the isotropic case, we have $E_1 = E_2 = E_3 = E$, $G_{12} = G_{13} = G_{23} = G$, and $\nu_{12} = \nu_{13} = \nu_{23} = \nu$ with $G = 0.5E/(1 + \nu)$. The Lamé constants are related to the engineering constants by

$$\lambda = K - \frac{2}{3}G, \quad \mu = G \tag{2.3.50}$$

where K is the bulk modulus.

Strain-Displacement Relations:

$$\varepsilon_{xx} = \frac{\partial u}{\partial x}; \qquad \varepsilon_{yy} = \frac{\partial v}{\partial y}; \qquad \varepsilon_{zz} = \frac{\partial w}{\partial z}$$
$$\varepsilon_{xy} = \frac{1}{2}\left(\frac{\partial u}{\partial y} + \frac{\partial v}{\partial x}\right); \ \varepsilon_{xz} = \frac{1}{2}\left(\frac{\partial u}{\partial z} + \frac{\partial w}{\partial x}\right); \ \varepsilon_{yz} = \frac{1}{2}\left(\frac{\partial v}{\partial z} + \frac{\partial w}{\partial y}\right) \tag{2.3.51}$$

where (u, v, w) are the displacements of a point along the (x, y, z) coordinates, respectively.

Stress Equilibrium Equations:

$$\begin{aligned} \frac{\partial \sigma_{xx}}{\partial x} + \frac{\partial \sigma_{xy}}{\partial y} + \frac{\partial \sigma_{xz}}{\partial z} + f_x &= 0 \\ \frac{\partial \sigma_{xy}}{\partial x} + \frac{\partial \sigma_{yy}}{\partial y} + \frac{\partial \sigma_{yz}}{\partial z} + f_y &= 0 \\ \frac{\partial \sigma_{xz}}{\partial x} + \frac{\partial \sigma_{yz}}{\partial y} + \frac{\partial \sigma_{zz}}{\partial z} + f_z &= 0 \end{aligned} \tag{2.3.52}$$

Stress-Traction Relations (Cauchy's formula; see Fig. 2.3.3):

$$\begin{aligned} \sigma_{xx} n_x + \sigma_{xy} n_y + \sigma_{xz} n_z &= t_x \\ \sigma_{xy} n_x + \sigma_{yy} n_y + \sigma_{yz} n_z &= t_y \\ \sigma_{xz} n_x + \sigma_{yz} n_y + \sigma_{zz} n_z &= t_z \end{aligned} \tag{2.3.53}$$

2.3.6 Hamilton's Principle

The principle of minimum total potential energy is limited to static equilibrium of solids. Hamilton's principle is a generalization of the principle of virtual displacements (see Reddy, 2002) to dynamics (i.e., time-dependent response) of solids. The principle assumes that the system under consideration is characterized by two energy functions: *kinetic energy* K and *potential energy* Π. For *continuous* systems (i.e., systems that cannot be described by a finite number of generalized coordinates), the energies can be expressed in terms of the dependent variables (which are functions of position) of the problem.

Newton's second law of motion for a continuous body can be written in general terms as

$$\mathbf{F} - m\mathbf{a} = \mathbf{0} \tag{2.3.54}$$

where m is the mass, $\mathbf{a}$ the acceleration vector, and $\mathbf{F}$ is the resultant of *all* forces acting on the body. The actual path $\mathbf{u} = \mathbf{u}(\mathbf{x}, t)$ followed by a material particle in position $\mathbf{x}$ in the body is varied, consistent with kinematic (essential) boundary conditions, to $\mathbf{u} + \delta\mathbf{u}$, where $\delta\mathbf{u}$ is the admissible variation (or virtual displacement) of the path. We suppose that the varied path differs from the actual path except at initial and final times, t_1 and t_2, respectively. Thus, an admissible variation $\delta\mathbf{u}$ satisfies the conditions,

$$\delta\mathbf{u} = \mathbf{0} \text{ on } \Gamma_u \text{ for all } t \tag{2.3.55a}$$

$$\delta\mathbf{u}(\mathbf{x}, t_1) = \delta\mathbf{u}(\mathbf{x}, t_2) = \mathbf{0} \text{ for all } \mathbf{x} \tag{2.3.55b}$$

where Γ_u denotes the portion of the boundary of the body where the displacement vector $\mathbf{u}$ is specified. Note that the scalar product of Eq. (2.3.54) with $\delta\mathbf{u}$ gives work done at point $\mathbf{x}$, because $\mathbf{F}$, $\mathbf{a}$, and $\mathbf{u}$ are vector functions of position (whereas the work is a scalar). Integration of the product over the volume (and surface) of the body gives the total work done by all points in moving through their respective displacements.

The *work done on the body* at time t by the resultant force in moving through the virtual displacement $\delta\mathbf{u}$ is given by

$$\int_V \mathbf{f}\cdot\delta\mathbf{u}\,dV + \int_{\Gamma_\sigma} \hat{\mathbf{t}}\cdot\delta\mathbf{u}\,dS - \int_V \overleftrightarrow{\sigma} : \delta\overleftrightarrow{\varepsilon}\,dV \tag{2.3.56}$$

where $\mathbf{f}$ is the body force vector, $\hat{\mathbf{t}}$ the specified surface traction vector, and $\overleftrightarrow{\sigma}$ and $\overleftrightarrow{\varepsilon}$ are the stress and strain tensors. The "double-dot product" has the meaning $\overleftrightarrow{\sigma} : \delta\overleftrightarrow{\varepsilon} = \sigma_{ij}\varepsilon_{ji}$. The last term in Eq. (2.3.56) represents the *virtual work* of internal forces *stored in the body*. The strains $\delta\overleftrightarrow{\varepsilon}$ are assumed to be compatible in the sense that the strain-displacement relations (2.3.42) are satisfied. The work done by the inertia force $m\mathbf{a}$ in moving through the virtual displacement $\delta\mathbf{u}$ is given by

$$\int_V \rho\frac{\partial^2\mathbf{u}}{\partial t^2}\cdot\delta\mathbf{u}\,dV \tag{2.3.57}$$

where ρ is the mass density (can be a function of position) of the medium. We have the result

$$\int_{t_1}^{t_2}\left\{\int_V \rho\frac{\partial^2\mathbf{u}}{\partial t^2}\cdot\delta\mathbf{u}\,dV - \left[\int_V\left(\mathbf{f}\cdot\delta\mathbf{u} - \overleftrightarrow{\sigma} : \delta\overleftrightarrow{\varepsilon}\right)dV + \int_{\Gamma_\sigma}\hat{\mathbf{t}}\cdot\delta\mathbf{u}\,dS\right]\right\}dt = 0$$

or

$$\int_{t_1}^{t_2}\left[\int_V \rho\frac{\partial\mathbf{u}}{\partial t}\cdot\frac{\partial\delta\mathbf{u}}{\partial t}\,dV + \int_V\left(\mathbf{f}\cdot\delta\mathbf{u} - \overleftrightarrow{\sigma} : \delta\overleftrightarrow{\varepsilon}\right)dV + \int_{\Gamma_\sigma}\hat{\mathbf{t}}\cdot\delta\mathbf{u}\,dS\right]dt = 0 \tag{2.3.58}$$

In arriving at the expression in Eq. (2.3.58), integration by parts is used on the first term; the integrated terms vanish because of the initial and final conditions in Eq. (2.3.55*b*). Equation (2.3.58) is known as the general form of Hamilton's principle for a continuous medium (conservative or not, and elastic or not).

For an ideal elastic body, we recall from the previous discussions that the forces $\mathbf{f}$ and $\mathbf{t}$ are conservative,

$$\delta V = -\left(\int_V \mathbf{f}\cdot\delta\mathbf{u}\,dV + \int_{\Gamma_\sigma}\hat{\mathbf{t}}\cdot\delta\mathbf{u}\,dS\right) \tag{2.3.59a}$$

and that there exists a strain energy density function $U_0 = U_0(\varepsilon_{ij})$ such that

$$\delta U_0(\varepsilon_{ij}) = \frac{\partial U_0}{\partial\varepsilon_{ij}}\delta\varepsilon_{ij} = \sigma_{ij}\delta\varepsilon_{ij} \tag{2.3.59b}$$

Substituting Eqs. (2.3.59*a*) and (2.3.59*b*) into Eq. (2.3.58), we obtain

$$\delta\int_{t_1}^{t_2}[K - (V+U)]dt = 0 \tag{2.3.60}$$

where K and U are the kinetic and strain energies:

$$K = \int_V \frac{\rho}{2}\frac{\partial\mathbf{u}}{\partial t}\cdot\frac{\partial\mathbf{u}}{\partial t}\,dV, \quad U = \int_V U_0\,dV \tag{2.3.61}$$

Equation (2.3.60) represents Hamilton's principle for an elastic body. Recall that the sum of the strain energy and potential energy of external forces, $U + V$, is called the total potential energy, Π, of the body. For bodies involving no motion (i.e., forces are applied sufficiently slowly such that the motion is independent of time and the inertia forces are negligible), Hamilton's principle (2.3.60) reduces to the principle of minimum total potential energy:

$$\delta(U + V) \equiv \delta\Pi = 0 \tag{2.3.62}$$

The Euler equations, known as the *Euler–Lagrange equations*, associated with the Lagrangian $L = K - \Pi$, can be obtained from Eq. (2.3.60):

$$\begin{aligned} 0 &= \delta \int_{t_1}^{t_2} L(\mathbf{u}, \nabla\mathbf{u}, \dot{\mathbf{u}})\, dt \\ &= \int_{t_1}^{t_2} \left[\int_V \left(\rho \frac{\partial^2 \mathbf{u}}{\partial t^2} - \operatorname{div} \overleftrightarrow{\sigma} - \mathbf{f} \right) \cdot \delta\mathbf{u}\, dV + \int_{\Gamma_\sigma} (\mathbf{t} - \hat{\mathbf{t}}) \cdot \delta\mathbf{u}\, dS \right] dt \end{aligned} \tag{2.3.63}$$

where integration by parts, gradient theorems, and Eqs. (2.3.55*a*) and (2.3.55*b*) were used in arriving at Eq. (2.3.63) from Eq. (2.3.60). Because $\delta\mathbf{u}$ is arbitrary for t, $t_1 < t < t_2$, for $\mathbf{x}$ in V, and also on Γ_σ, it follows that

$$\begin{aligned} \rho \frac{\partial^2 \mathbf{u}}{\partial t^2} - \operatorname{div} \overleftrightarrow{\sigma} - \mathbf{f} = \mathbf{0} \quad &\text{in } V \\ \mathbf{t} - \hat{\mathbf{t}} = \mathbf{0} \quad &\text{on } \Gamma_\sigma \end{aligned} \tag{2.3.64}$$

Equations (2.3.64) are the Euler-Lagrange equations for an elastic body [cf. Eq. (2.3.46)]. Next, we consider a specific example of application of Hamilton's principle [see Reddy (2002)].

Example 2.3.4

Consider the axial motion of an elastic bar of length L, area of cross section A, modulus of elasticity E, and mass density ρ, and subjected to distributed force f per unit length and an end load P. We wish to determine the equations of motion for the bar. The kinetic and total potential energies of the system are

$$K = \int_V \frac{\rho}{2} \left(\frac{\partial u}{\partial t} \right)^2 dV = \int_0^L \frac{\rho A}{2} \left(\frac{\partial u}{\partial t} \right)^2 dx \tag{2.3.65a}$$

$$\begin{aligned} \Pi &= \int_V \frac{1}{2} \sigma_{ij} \varepsilon_{ij} dV - \int_0^L f u\, dx - P u(L) \\ &= \int_0^L \frac{A}{2} \sigma_{xx} \varepsilon_{xx}\, dx - \int_0^L f u\, dx - P u(L) \end{aligned} \tag{2.3.65b}$$

wherein u, σ_{xx}, and ε_{xx} are assumed to be functions of x only, and

$$\begin{aligned} u(0, t) &= 0 \quad \text{(bar is fixed at } x = 0) \\ \varepsilon_{xx} &= \frac{\partial u}{\partial x} \quad \text{(strain-displacement relation)} \end{aligned} \tag{2.3.65c}$$

Substituting for K and Π from Eqs. (2.3.65a) and (2.3.65b) into Eq. (2.3.60), we obtain

$$
\begin{aligned}
0 &= \int_{t_1}^{t_2} \left\{ \int_0^L \left[A\rho \frac{\partial u}{\partial t} \frac{\partial \delta u}{\partial t} - A\sigma_{xx} \delta \left(\frac{\partial u}{\partial x} \right) + f \delta u \right] dx + P \delta u(L) \right\} dt \\
&= \int_0^L \left[\int_{t_1}^{t_2} -\frac{\partial}{\partial t} \left(\rho A \frac{\partial u}{\partial t} \right) \delta u \, dt + \rho A \frac{\partial u}{\partial t} \delta u \Big|_{t_1}^{t_2} \right] dx \\
&\quad + \int_{t_1}^{t_2} \left\{ \int_0^L \left[\frac{\partial}{\partial x} (A\sigma_{xx}) + f \right] \delta u \, dx - (A\sigma_{xx} \delta u) \Big|_0^L + P \delta u(L) \right\} dt \\
&= -\int_{t_1}^{t_2} \left\{ \int_0^L \left[\frac{\partial}{\partial t} \left(\rho A \frac{\partial u}{\partial t} \right) - \frac{\partial}{\partial x} (A\sigma_{xx}) - f \right] \delta u \, dx \right. \\
&\quad \left. - (A\sigma_{xx} - P)\big|_{x=L} \delta u(L) \right\} dt
\end{aligned}
\tag{2.3.66}
$$

where $\delta u(0, t) = 0$ and $\delta u(x, t_1) = \delta u(x, t_2) = 0$ are used to simplify the expression. The Euler-Lagrange equations are obtained by setting the coefficients of δu in $(0, L)$ and at $x = L$ to zero separately:

$$
\frac{\partial}{\partial t} \left(\rho A \frac{\partial u}{\partial t} \right) - \frac{\partial}{\partial x} (A\sigma_{xx}) - f = 0, \quad 0 < x < L \tag{2.3.67a}
$$

$$
(A\sigma_{xx})\big|_{x=L} - P = 0 \tag{2.3.67b}
$$

for all $t, t_1 < t < t_2$. For linear elastic materials, we have $\sigma_{xx} = E\varepsilon_{xx} = E(\partial u/\partial x)$, and Eqs. (2.3.67$a$) and (2.3.67$b$) become

$$
\frac{\partial}{\partial t} \left(\rho A \frac{\partial u}{\partial t} \right) - \frac{\partial}{\partial x} \left(EA \frac{\partial u}{\partial x} \right) - f = 0, \quad 0 < x < L \tag{2.3.68a}
$$

$$
\left(AE \frac{\partial u}{\partial x} \right)\Big|_{x=L} - P = 0 \tag{2.3.68b}
$$

Now suppose that the bar also experiences a nonconservative (viscous damping) force proportional to the velocity,

$$
F^* = -\mu \frac{\partial u}{\partial t} \tag{2.3.69}
$$

where μ is the damping coefficient (a constant). Then the Euler-Lagrange equations from Eq. (2.3.58) are given by

$$
\frac{\partial}{\partial t} \left(\rho A \frac{\partial u}{\partial t} \right) - \frac{\partial}{\partial x} \left(EA \frac{\partial}{\partial x} \right) - f + \mu \frac{\partial u}{\partial t} = 0, \quad 0 < x < L \tag{2.3.70a}
$$

$$
\left(AE \frac{\partial u}{\partial x} \right)_{x=L} - P = 0 \tag{2.3.70b}
$$

2.4 INTEGRAL FORMULATIONS

2.4.1 Introduction

Recall from Section 2.1.3 that the motivation for the use of weighted-integral statements of differential equations comes from the fact that we wish to have a means to determine the unknown parameters c_j in the approximate solution $U_N = \sum_j c_j \phi_j$. The variational methods of approximation, e.g., the Ritz, Galerkin, least-squares, collocation, or, in general, weighted-residual methods to be discussed in Section 2.5 are based on weighted-integral statements of the governing equations. Since the finite element method is a technique for constructing approximation functions required in an elementwise application of a variational method, it is necessary to study the weighted-integral formulation and the so-called weak formulation of differential equations. The weak formulations also facilitate, in a natural way, the classification of boundary conditions into natural and essential types. As we shall see shortly, this classification plays a crucial role in the derivation of the approximation functions and the selection of the nodal degrees of freedom of the finite element model.

In this section, our primary objective will be to construct the weak form of a given differential equation and to classify the boundary conditions associated with the equation. A *weak form* is defined to be a weighted-integral statement of a differential equation in which the differentiation is transferred from the dependent variable to the weight function such that all natural boundary conditions of the problem are also included in the integral statement. These ideas will be more clear in the sequel.

2.4.2 Weighted-Integral and Weak Formulations

Consider the problem of solving the differential equation

$$-\frac{d}{dx}\left[a(x)\frac{du}{dx}\right] = f(x) \quad \text{for} \quad 0 < x < L \tag{2.4.1a}$$

for $u(x)$, subject to the boundary conditions

$$u(0) = u_0, \qquad \left(a\frac{du}{dx}\right)\bigg|_{x=L} = Q_L \tag{2.4.1b}$$

Here $a(x)$ and $f(x)$ are known functions of the coordinate x; u_0 and Q_L are known values; and L is the size of the one-dimensional domain. When the specified values are nonzero ($u_0 \neq 0$ or $Q_L \neq 0$), the boundary conditions are said to be nonhomogeneous; when the specified values are zero, the boundary conditions are said to be homogeneous. The homogeneous form of the boundary condition $u(0) = u_0$ is $u(0) = 0$, and the homogeneous form of the boundary condition $(adu/dx)|_{x=L} = Q_L$ is $(adu/dx)|_{x=L} = 0$.

Equations of the type (2.4.1a) arise, for example, in the study of axial heat conduction in a rod (e.g., heat exchanger fin) or radial heat conduction in a long axisymmetric cylinder. In the former case, $a = kA$, with k being the thermal conductivity and the A the cross-sectional area, the L being the length of the rod. For the axisymmetric case, $a = 2\pi Lkx$, x being the radial coordinate r and L the length of the cylinder. In both cases, f denotes the heat generation term, u_0 is the specified temperature, and Q_L is the specified heat. Other physical problems are also described by the same equation but with different meanings for the variables. Typical examples of field problems with a description of the variables are presented in Table 2.4.1.

Table 2.4.1 Some examples of engineering problems in which the second-order equation (2.4.1*a*) and its boundary conditions (2.4.1*b*) arise.

$$-\frac{d}{dx}\left(a\frac{du}{dx}\right)=f \quad \text{for } 0<x<L; \quad u(0)=u_0; \quad \left(a\frac{du}{dx}\right)_{x=L}=Q_L$$

Field	Primary variable u	Coefficient* a	Source term f	Secondary variable Q_0
1. Cables	Transverse deflection	T	Distributed vertical force	Axial force
2. Bars	Longitudinal displacement	EA	Distributed axial force	Axial load
3. Heat transfer	Temperature	k	Internal heat generation	Heat flux
4. Pipe flow	Hydrostatic pressure	$\frac{\pi D^4}{128\mu}$	Flow source	Flow rate
5. Viscous flows	Velocity	μ	Pressure gradient	Stress
6. Seepage	Fluid head	ε	Fluid flux	Flow
7. Electrostatics	Electrical potential	ϵ	Charge density	Electric flux

*E = Young's modulus; A = area of cross section; D = diameter of the pipe; k = thermal conductivity; μ = viscosity; T = tension; ε = permeability; and ϵ = dielectric constant.

Residual Function. Suppose that we seek an approximation of $u(x)$ in the form

$$u(x)\approx U_N(x)=\sum_{j=1}^{N}c_j\phi_j(x)+\phi_0(x) \tag{2.4.2}$$

and determine c_j such that $U_N(x)$ satisfies the differential equation (2.4.1*a*). Substitution of U_N into Eq. (2.4.1*a*) yields

$$-\frac{d}{dx}\left[a(x)\frac{dU_N}{dx}\right]=f(x) \quad \text{for} \quad 0<x<L \tag{2.4.3a}$$

Since the left side of the equality is now an approximate value, we cannot expect it to be equal, in general, to the right side of the equality. The difference

$$R(x,c_j)\equiv-\frac{d}{dx}\left[a(x)\frac{dU_N}{dx}\right]-f(x)\neq 0 \quad \text{for} \quad 0<x<L \tag{2.4.3b}$$

is called the *residual* of approximation in the differential equation. It is a function of x and c_j. Any approximate method (especially a variational method) seeks a set of N equations among c_j by making R equal to zero. Since it cannot be made zero identically at every point of the domain (as explained in Section 2.1.3), we must find an alternate way to find the necessary relations among c_j such that R is zero. If we require R to be zero at N selected points of the domain, we have

$$R(x,c_j)=0 \text{ for } x=x_i,\ i=1,2,\cdots,N \tag{2.4.4}$$

which is known as the *collocation method.* Another way to make R zero is to minimize the integral of the square of the residual (R is squared to make it positive) with respect to c_j:

$$\delta I \equiv \delta \int_0^L R^2 \, dx = 0 \quad \text{or} \quad \frac{\partial}{\partial c_j} \int_0^L R^2 \, dx = 0 \tag{2.4.5}$$

The method based on (2.4.5) is called the *least-squares method.* Equations (2.4.4) and (2.4.5), each, give N equations that can be solved for parameters c_j.

Weighted-Residual Method. Yet another way to determine the c_j is to require R to vanish in a "weighted-residual" sense:

$$\int_0^L w_i(x) \, R(x, c_j) \, dx = 0 \quad (i = 1, 2, \cdots, N) \tag{2.4.6}$$

where $w_i(x)$ are a set of linearly independent functions, called *weight functions,* which in general can be different from the approximation functions $\phi_i(x)$. This method is known as the *weighted-residual method.* Indeed, the statement in (2.4.6) includes (2.4.4) as well as (2.4.5) as special cases. When $w_i = \phi_i$, Eq. (2.4.6) is known as the *Galerkin method.* Thus, we have the following special cases of (2.4.6):

$$\begin{aligned}
&\textit{Petrov–Galerkin method:} && w_i = \psi_i \neq \phi_i \\
&\textit{Galerkin's method:} && w_i = \phi_i \\
&\textit{Least squares method:} && w_i = \frac{d}{dx}\left(a(x)\frac{d\phi_i}{dx}\right) \\
&\textit{Collocation method:} && w_i = \delta(x - x_i)
\end{aligned} \tag{2.4.7}$$

Here x_i is the ith collocation point of the domain of the problem and $\delta(\cdot)$ is the Dirac delta function defined such that its value is zero for all nonzero values of its arguments:

$$\delta(x - x_0) = 0 \text{ when } x \neq x_0, \qquad \int_{-\infty}^{\infty} f(x)\delta(x - x_0) \, dx = f(x_0) \tag{2.4.8}$$

Due to the different choices of w_i—even when the ϕ_i used in (2.4.4), (2.4.5) and (2.4.6) are the same—the system of algebraic equations will have different characteristics in different method. For linear differential equations of any order, only the least-squares method yields a system of matrix equations whose coefficient matrix is symmetric. One other method that has the symmetry property is the *Ritz method,* which uses the weak form of even-order (second, fourth, and so on; called self-adjoint) differential equations with $w_i = \phi_i$; the Ritz method is *not* a special case of the weighted-residual method. As we shall see shortly, the weak form of a self-adjoint differential equation always contains the same order derivatives of both the weight function w and the dependent unknown u, and the order is equal to half that of the original differential equation. In the following paragraphs, we discuss the weak form development.

Development of Weak Forms. There are three steps in the development of the weak form of any differential equation. These steps are illustrated by means of the model differential equation (2.4.1a) and boundary conditions (2.4.1b).

Step 1. (Weighted-integral statement.) This step is the same as in a weighted-residual method. Move all terms of the differential equation to one side (so that it reads $\ldots = 0$), multiply the entire equation with a function $w(x)$, and integrate over the domain $\Omega = (0, L)$

of the problem:

$$0 = \int_0^L w \left[-\frac{d}{dx}\left(a\frac{du}{dx}\right) - f \right] dx \tag{2.4.9}$$

Recall that the expression in the square brackets is not identically zero since u is replaced by its approximation, U_N. Mathematically, in (2.4.9) the error in the differential equation (due to the approximation of the solution) is made zero in the weighted-integral sense. The integral statement (2.4.9) allows us to choose N linearly independent functions for w and obtain N equations for $c_1, c_2, \cdots, c_N$ of (2.4.2).

Note that the weighted-integral statement of any differential equation can be readily written. The weighted-integral statement is equivalent only to the differential equation and does not include any boundary conditions. The weight function w in (2.4.9) can be any nonzero integrable function and has no differentiability requirements.

Step 2. While the weighted-integral statement (2.4.9) allows us to obtain the necessary number (N) of algebraic relations among c_j for N different choices of the weight function w, it requires that the approximation functions ϕ_j be such that U_N [see (2.4.2)] is differentiable as many times as called for in the original differential equation (2.4.1a) and satisfies the specified boundary conditions. If this is not a concern, one can proceed with the integral statement (2.4.9) and obtain the necessary algebraic equations for c_j (using any one of the choices listed in Eq. (2.4.7) for $w \sim w_i$).

If we plan to use the approximation functions ϕ_i for $w \sim w_i$, it makes sense to shift half of the derivatives from u to w so that both are differentiated equally, and we have fewer (or weaker) continuity requirements on ϕ_j. The resulting integral form is known as the weak form. Of course, weakening the differentiability of u (and hence ϕ_i) is purely a mathematical (and perhaps computational) consideration. As will be seen shortly, the weak formulation has two desirable characteristics. First, it requires weaker, as already indicated, continuity of the dependent variable, and for self-adjoint equations (as is the case with problems studied in this book) it always results in a symmetric coefficient matrix. Second, the natural boundary conditions of the problem are included in the weak form, and therefore the approximate solution U_N is required to satisfy only the essential boundary conditions of the problem. These two features of a weak form play an important role in the development of finite element models of a problem.

A word of caution is in order. Differentiating the weight function instead of the dependent variable (in addition to the weakening the continuity requirements on ϕ_i) is also dictated by the need to include physically meaningful boundary terms into the weak form, regardless of the effect on the continuity requirements. Therefore, this trade-off should not be performed if it results in boundary terms that are not physically meaningful.

Returning to the integral statement (2.4.9), we integrate the first term of the expression by parts to obtain

$$\begin{aligned} 0 &= \int_0^L \left\{ w \left[-\frac{d}{dx}\left(a\frac{du}{dx}\right) \right] - w f \right\} dx \\ &= \int_0^L \left(a\frac{dw}{dx}\frac{du}{dx} - w f \right) dx - \left[w\, a\frac{du}{dx} \right]_0^L \end{aligned} \tag{2.4.10}$$

where the integration-by-parts formula [see Eq. (2.2.22)]

$$\int_0^L w\, dv = -\int_0^L v\, dw + [wv]_0^L$$

is used with $v = -a du/dx$ on the first term to arrive at the second line of (2.4.10). Note that now the weight function w is required to be differentiable at least once.

An important part of Step 2 is to identify the two types of boundary conditions associated with *any* differential equation: *natural* and *essential*. The classification is important for both the variational methods of approximation considered in this chapter and the finite element formulations presented in the subsequent chapters. The following rule is used to identify the natural boundary conditions and their form. After trading between differentiating the weight function w and the variable u of the problem, examine all boundary terms of the integral statement. The boundary terms will involve both the weight function and the dependent variable. Coefficients of the weight function (and possibly its derivatives for higher-order equations) in the boundary expression(s) are termed the *secondary variables* (SV). For example, for the problem at hand the coefficient of w in the boundary term is $a(du/dx)$, which is the secondary variable. Specification of a secondary variable on the boundary constitutes the *natural boundary condition* (NBC).

The dependent variable of the problem (u), expressed in the *same form* as the weight function (w) appearing in the boundary term, is called the *primary variable* (PV), and its specification on the boundary constitutes the *essential boundary condition* (EBC). For the case under consideration, the weight function appears in the boundary expression [see (2.4.10)] as w (in higher-order equations, it may appear as w in one boundary term and as dw/dx in other). Therefore, the primary variable is u (for higher-order equations, the primary variables may include u as well as du/dx), and the essential boundary condition involves specifying u at the boundary points.

The secondary variables always have physical meaning and are often quantities of interest. In the case of heat transfer problems, the secondary variable represents heat, Q. We shall denote the secondary variable by

$$Q \equiv \left(a\frac{du}{dx}\right) n_x \tag{2.4.11}$$

where n_x denotes the direction cosine, i.e., n_x = cosine of the angle between the positive x axis and the normal to the boundary. For one-dimensional problems, the normal at the boundary points is always along the length of the domain. Thus, we have $n_x = -1$ at the left end and $n_x = 1$ at the right end of the domain.

It should be noted that the number and form of the primary and secondary variables depend on the order of the differential equation. The number of primary and secondary variables is always the same, and with each primary variable there is an associated secondary variable, i.e., they always appear in pairs (e.g., displacement and force, temperature and heat, and so on). Only one of the pair, either the primary or the secondary variable, may be specified at a point of the boundary. Thus, a given problem can have its specified boundary conditions in one of three categories: (1) all specified boundary conditions are EBC; (2) some of the specified boundary conditions are EBC and the remaining are NBC; or (3) all specified boundary conditions are NBC. For a single second-order equation, as in the present case, there is one primary variable u and one secondary variable Q. At a boundary

point, only one of the pair (u, Q) can be specified. For a fourth-order equation, such as that for the classical (i.e., Euler-Bernoulli) theory of beams, there are two of each kind (i.e., two PVs and two SVs), as will be illustrated later (see Example 2.4.2). In general, a $2m$th-order differential equation require m integration by parts to transfer m derivatives from u to w and therefore there will be m boundary terms involving m primary variables and m secondary variables, i.e., m pairs of primary and secondary variables.

Returning to Eq. (2.4.10), we rewrite it using the notation of (2.4.11):

$$\begin{aligned} 0 &= \int_0^L \left(a \frac{dw}{dx} \frac{du}{dx} - w f \right) dx - \left[w a \frac{du}{dx} \right]_0^L \\ &= \int_0^L \left(a \frac{dw}{dx} \frac{du}{dx} - w f \right) dx - \left(w a \frac{du}{dx} n_x \right) \Big|_{x=0} - \left(w a \frac{du}{dx} n_x \right) \Big|_{x=L} \\ &= \int_0^L \left(a \frac{dw}{dx} \frac{du}{dx} - w f \right) dx - (w Q)_0 - (w Q)_L \end{aligned} \tag{2.4.12}$$

Equation (2.4.12) is called the *weak form* of the differential equation (2.4.1a). The word "weak" refers to the reduced (i.e., weakened) continuity of u, which is required to be twice-differentiable in the weighted-integral statement (2.4.9) but only once-differentiable in (2.4.12).

Step 3. The third and last step of the weak formulation is to impose the actual boundary conditions of the problem under consideration. It is here that we require the weight function w to vanish at boundary points where the essential boundary conditions are specified, i.e., w is required to satisfy the *homogeneous form* of the specified essential boundary conditions of the problem (recall Section 2.3). In weak formulations, the weight function has the meaning of a *virtual* change (or variation) of the primary variable $w \sim \delta u$. If a primary variable is specified at a point, the virtual change there must be zero. For the problem at hand, the boundary conditions are given in (2.4.1b). By the rules of classification of the boundary conditions, $u = u_0$ is the essential boundary condition and $(adu/dx)|_{x=L} = Q_L$ is the natural boundary condition. Thus, the weight function w is required to satisfy $w(0) = 0$ because $u(0) = u_0$. Since $w(0) = 0$ and

$$Q(L) = \left(a \frac{du}{dx} n_x \right) \Big|_{x=L} = \left(a \frac{du}{dx} \right) \Big|_{x=L} = Q_L$$

Eq. (2.4.12) reduces to the expression

$$0 = \int_0^L \left(a \frac{dw}{dx} \frac{du}{dx} - w f \right) dx - w(L) Q_L \tag{2.4.13}$$

which is the weak form equivalent to the original differential equation (2.4.1a) and the natural boundary condition (2.4.1b). This completes the steps involved in the development of the weak form of a differential equation.

The terms "variational form" and "weak form" will be used interchangeably. The weak form of a differential equation is a weighted-integral statement equivalent to the differential equation *and* the specified natural boundary condition of the problem. Note that the weak form exists for all problems—linear or nonlinear—that are described by second- and higher-order differential equations. When the differential equation is linear and of even order, the

resulting weak form will have a *symmetric* bilinear form in the dependent variable u and weight function w, as we shall see shortly.

In summary, there are three steps in the development of a weak form. In the first step, we put all expressions of the differential equation on one side (so that the other side is equal to zero), then multiply the entire equation by a weight function and integrate over the domain of the problem. The resulting expression is called the weighted-integral form of the equation. In the second step, we use integration by parts to distribute differentiation evenly between the dependent variable and the weight function, and use the boundary terms to identify the form of the primary and secondary variables. In the third step, we modify the boundary terms by restricting the weight function to satisfy the homogeneous form of the specified essential boundary conditions and replacing the secondary variables by their specified values.

It should be recalled that a weighted-integral statement or the weak form of a differential equation is needed to obtain as many algebraic equations as there are unknown coefficients in the approximation of the dependent variables of the equation. For different choices of the weight function, different algebraic equations can be obtained. Because of the restrictions placed on the weight function in Step 3 ($w \sim \delta u$) of the variational formulation, it must belong to the same space of functions as the approximation functions (i.e., $w \sim \phi_i$).

2.4.3 Linear and Bilinear Forms and Quadratic Functionals

It is informative, although not necessary for the use of variational methods or the finite element method, to see the relation between the weak form and the minimum of a quadratic functional associated with the differential equation. The weak form (2.4.13) contains two types of expressions: those involving both the dependent variable u and the weight function w, and those involving only the latter. We shall denote these two types of expressions by $B(w, u)$ and $l(w)$, respectively:

$$B(w,u) = \int_0^L a \frac{dw}{dx}\frac{du}{dx}\,dx, \quad l(w) = \int_0^L w\, f\, dx + w(L)\, Q_L \tag{2.4.14}$$

Hence, the weak form (2.4.13) can be expressed in the form

$$0 = B(w,u) - l(w) \quad \text{or} \quad B(w,u) = l(w) \tag{2.4.15}$$

which is termed the *variational problem* associated with Eqs. (2.4.1a) and (2.4.1b). Using the definitions of linear and bilinear forms from Section 2.2.4, it can be verified that $B(w, u)$ is bilinear and symmetric in w and u and that $l(w)$ is linear. The variational problem associated with (2.4.1a) and (2.4.1b) can be stated as one of finding the solution u (from a suitable vector space, H) such that

$$B(w,u) = l(w) \tag{2.4.16}$$

holds for any w (in H) that satisfies the homogeneous form of the specified essential boundary conditions and continuity conditions implied by the weak form. The function w can be viewed as a variation of the actual solution $w = \delta u$, and Eq. (2.4.15) can be written as

$$0 = B(\delta u, u) - l(\delta u) \tag{2.4.17}$$

If $B(\cdot, \cdot)$ is bilinear and symmetric and $l(\cdot)$ is linear, we have

$$B(\delta u, u) = \frac{1}{2}\delta[B(u,u)], \quad l(\delta u) = \delta[l(u)] \tag{2.4.18a}$$

so that (2.4.17) can be expressed as

$$0 = B(\delta u, u) - l(\delta u) = \frac{1}{2}\delta[B(u,u)] - \delta[l(u)] \equiv \delta I(u) \tag{2.4.18b}$$

where

$$I(u) = \frac{1}{2}B(u,u) - l(u) \tag{2.4.19}$$

The result in (2.4.18a) can be verified for the problem at hand:

$$\begin{aligned} B(\delta u, u) &= \int_0^L a\frac{d\delta u}{dx}\frac{du}{dx}\,dx = \delta\int_0^L \frac{a}{2}\left(\frac{du}{dx}\right)^2 dx \\ &= \frac{1}{2}\delta\int_0^L a\frac{du}{dx}\frac{du}{dx}\,dx = \frac{1}{2}\delta[B(u,u)] \\ l(\delta u) &= \int_0^L \delta u\, f\, dx + \delta u(L)Q_L \\ &= \delta\left[\int_0^L u\, f\, dx + u(L)Q_L\right] = \delta[l(u)] \end{aligned}$$

Now we can restate the variational problem (2.4.16) as one of minimizing the functional $I(u)$:

$$\delta I = 0 = B(\delta u, u) - l(\delta u), \quad \delta^2 I = B(\delta u, \delta u) > 0 \text{ for } \delta u \neq 0 \tag{2.4.20}$$

Thus, the function u that minimizes $I(u)$ is the solution of (2.4.16); conversely, the solution of (2.4.16) minimizes the functional. Mathematical proof of these assertions can be found in Reddy (1986, 2002).

Note that the key step in the derivation of the functional $I(u)$ from the weak form is the bilinearity and symmetry of the bilinear form $B(w,u)$. Thus, whenever $B(w,u)$ is bilinear and symmetric, and $l(w)$ is linear, the functional associated with the variational problem (2.4.16) is given by (2.4.19). When $B(w,u)$ is not linear in w and u, but is symmetric, the functional $I(u)$ can be derived, but not from (2.4.19). The interested reader may consult the books by Oden and Reddy (1983) and Reddy (1986).

For solid mechanics problems, $I(u)$ represents the total potential energy functional, and $\delta I = 0$ is the statement of the principle of the minimum total potential energy: Of all admissible functions u, the one that makes the total potential energy $I(u)$ a minimum also satisfies the differential equation(s) and natural boundary condition(s). In other words, the weak form of a differential equation is the same as the statement of the principle of minimum total potential energy. For problems outside solid mechanics, the functional $I(u)$, if it exists, may not have any physical meaning, but it is still useful for mathematical analysis (e.g., in proving the existence and uniqueness of solutions).

As noted earlier, every differential equation admits a weighted-integral statement, and a weak form exists provided the equation is of order two or higher. When the bilinear form is symmetric, we will also have a functional whose first variation set equal to zero is equivalent to the governing equations. Recall that we can always construct the least-squares functional associated with any set of governing equations. However, the traditional variational methods and the finite element method use only an integral statement or a weak form of the equation(s) to be solved.

2.4.4 Examples

Here, we consider some representative examples of differential equations in one and two dimensions, and develop their weak forms. These examples are of primary interest in the study of the finite element method in the coming chapters. All problems considered here correspond to one or more physical problems of science and engineering.

Example 2.4.1 (Model Second-Order Equation in One Dimension)

Consider the differential equation

$$-\frac{d}{dx}\left(a\frac{du}{dx}\right)+cu=f \quad \text{for} \quad 0<x<L \tag{2.4.21a}$$

subject to the boundary conditions

$$u(0)=u_0, \quad \left(a\frac{du}{dx}\right)+\beta\,(u-u_\infty)=Q_0 \ \text{ at } x=L \tag{2.4.21b}$$

The data of the problem consists of specifying $a(x)$, $c(x)$, $f(x)$, u_0, β, u_∞, and Q_0.

Following the three steps outlined above for the construction of variational statements, we obtain

$$\textit{Step 1:} \qquad 0=\int_0^L w\left[-\frac{d}{dx}\left(a\frac{du}{dx}\right)+cu-f\right]dx$$

$$\textit{Step 2:} \qquad 0=\int_0^L\left(a\frac{dw}{dx}\frac{du}{dx}+cwu-wf\right)-\left[w\,a\frac{du}{dx}\right]_0^L \tag{2.4.22}$$

From the boundary term, it is clear that the specification of u is an essential boundary condition, and the specification of $a\,du/dx$ is a natural boundary condition. Since $w=0$ at $x=0$ (because u is specified there) and

$$a\frac{du}{dx}=Q_0-\beta\,(u-u_\infty) \ \text{ at } x=L$$

we obtain

$$\textit{Step 3:} \qquad 0=\int_0^L\left(a\frac{dw}{dx}\frac{du}{dx}+cwu\right)dx-\int_0^L wf\,dx+w(L)\beta(u(L)-u_\infty)-w(L)Q_0 \tag{2.4.23a}$$

Variational Problem and Quadratic Functional: Equation (2.4.23*a*) can be expressed in the form

$$B(w,u)=l(w) \tag{2.4.23b}$$

where

$$\begin{aligned} B(w,u)&=\int_0^L\left(a\frac{dw}{dx}\frac{du}{dx}+cwu\right)dx+\beta w(L)u(L)\\ l(w)&=\int_0^L wf\,dx+\beta w(L)u_\infty+Q_0u(L)\end{aligned} \tag{2.4.23c}$$

It is clear that since $B(w, u)$ is linear and symmetric in w and u, and $l(w)$ is linear in w, we can compute the quadratic functional from (2.4.19):

$$I(u) = \frac{1}{2}\int_0^L \left[a\left(\frac{du}{dx}\right)^2 + cu^2 \right] dx + \frac{1}{2}\beta[u(L)]^2 - \int_0^L fu\,dx - \beta u(L)u_\infty - Q_0 u(L) \tag{2.4.24}$$

Equations of the type of (2.4.21a) arise, for example, in the study of the axial deformation of a bar or flow of heat in a bar. In the former case, u denotes the axial displacement, a the product of modulus of elasticity (E) and area of cross section (A), and c the resistance offered by an external medium to the axial deformation (often, $c = 0$). In the case of heat flow, u denotes the temperature (T), a the product of thermal conductivity (k) times the area of cross section (A) of the bar, and c is the product of film conductance (β) times the perimeter (P).

The next example illustrates the variational formulation of a fourth-order differential equation governing bending of elastic beams according to the Euler-Bernoulli beam theory [see Reddy (2002)].

Example 2.4.2 (Euler-Bernoulli Beam)

Consider the problem of finding the function $w(x)$ that satisfies the differential equation

$$\frac{d^2}{dx^2}\left[b(x)\frac{d^2w}{dx^2} \right] + c_f w - q(x) = 0 \quad \text{for} \quad 0 < x < L \tag{2.4.25}$$

This equation arises in the study of the elastic bending of beams (under the Euler-Bernoulli hypothesis that plane sections perpendicular to the axis of the beam before deformation remain plane after deformation), where w denotes the transverse deflection of the beam, L is the length of the beam, $b(x) > 0$ is the flexural rigidity of the beam (i.e., the product of modulus of elasticity E and second moment of inertia I), c_f is the foundation modulus, and $q(x)$ is the transverse distributed load, as shown in Fig. 2.4.1. At the moment, we do not have to consider any specific boundary conditions of the problem.

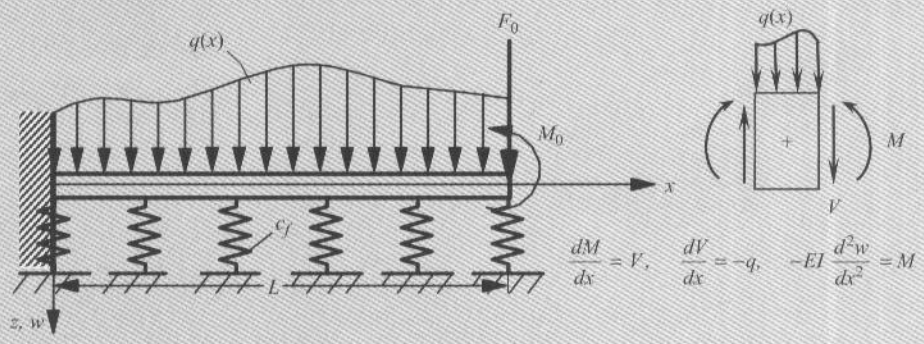

Figure 2.4.1 Cantilever beam with a set of loads.

Since the equation contains a fourth-order derivative, we should integrate it twice by parts to distribute the derivatives equally between the dependent variable w and the weight function v. In this case, v must be twice differentiable and satisfy the homogeneous form of an EBC. Multiplying (2.4.25) by v, and integrating the first term by parts twice with respect to x, we obtain

$$\textit{Step 1:}\quad 0=\int_0^L v\left[\frac{d^2}{dx^2}\left(b\frac{d^2w}{dx^2}\right)+c_f w-q\right]dx \tag{2.4.26}$$

$$\begin{aligned}\textit{Step 2:}\quad 0&=\int_0^L\left[\left(-\frac{dv}{dx}\right)\frac{d}{dx}\left(b\frac{d^2w}{dx^2}\right)+c_f vw-vq\right]dx+\left[v\frac{d}{dx}\left(b\frac{d^2w}{dx^2}\right)\right]_0^L\\&=\int_0^L\left(\frac{d^2v}{dx^2}b\frac{d^2w}{dx^2}+c_f vw-vq\right)dx+\left[v\frac{d}{dx}\left(b\frac{d^2w}{dx^2}\right)-\frac{dv}{dx}b\frac{d^2w}{dx^2}\right]_0^L\end{aligned} \tag{2.4.27}$$

From the last line, it follows that the specification of w and dw/dx constitutes the essential (geometric or static) boundary conditions, and the specification of

$$\frac{d}{dx}\left(b\frac{d^2w}{dx^2}\right)\ \text{(shear force)}\quad\text{and}\quad b\left(\frac{d^2w}{dx^2}\right)\ \text{(bending moment)} \tag{2.4.28a}$$

constitutes the natural boundary conditions for the Euler-Bernoulli beam theory.

Now consider a specific beam problem. Let us consider a beam fixed at the left end and subjected to transverse force and bending moment at $x=L$, as shown in Fig. 2.4.1:

$$w(0)=0,\quad \left(\frac{dw}{dx}\right)\bigg|_{x=0}=0,\quad \left(b\frac{d^2w}{dx^2}\right)\bigg|_{x=L}=-M_0,\quad \left[\frac{d}{dx}\left(b\frac{d^2w}{dx^2}\right)\right]_{x=L}=-F_0 \tag{2.4.28b}$$

where M_0 is the bending moment and F_0 is the transverse load. Since w and dw/dx (both are primary variables) are specified at $x=0$, we require the weight function v and its derivative dv/dx to be zero there

$$v(0)=\left(\frac{dv}{dx}\right)\bigg|_{x=0}=0$$

The remaining two boundary conditions in (2.4.28*b*) are natural boundary conditions, which place no restrictions on v and its derivatives. Thus, Eq. (2.4.27) becomes

$$\textit{Step 3:}\quad 0=\int_0^L\left(b\frac{d^2v}{dx^2}\frac{d^2w}{dx^2}+c_f vw-vq\right)dx-v(L)F_0+\left(\frac{dv}{dx}\right)\bigg|_{x=L}M_0 \tag{2.4.29}$$

Variational Problem and Quadratic Functional: Equation (2.4.30*a*) can be written in the form

$$B(v,w)=l(v) \tag{2.4.30a}$$

where

$$\begin{aligned}B(v,w)&=\int_0^L\left(b\frac{d^2v}{dx^2}\frac{d^2w}{dx^2}+c_f vw\right)dx\\ l(v)&=\int_0^L vq\,dx+v(L)F_0-\left(\frac{dv}{dx}\right)\bigg|_{x=L}M_0\end{aligned} \tag{2.4.30b}$$

The functional, known as the total potential energy of the beam, is obtained using (2.4.19):

$$I(w) = \int_0^L \left[\frac{b}{2}\left(\frac{d^2w}{dx^2}\right)^2 + \frac{c_f}{2}w^2 - wq \right] dx - w(L)F_0 + \left(\frac{dw}{dx}\right)\Big|_{x=L} M_0 \tag{2.4.31}$$

Note that for the fourth-order equation, the essential boundary conditions involve not only the dependent variable but also its first derivative. As pointed out earlier, at any boundary point, only one of the two boundary conditions (essential or natural) can be specified. For example, if the transverse deflection is specified at a boundary point, then one cannot specify the shear force V at the same point, and vice versa. Similar comments apply to the slope dw/dx and the bending moment M. Note that in the present case, w and dw/dx are the primary variables, and V and M are the secondary variables.

The next example is concerned with the weak-form development of a pair of second-order differential equations in one dimension. The approach used for a single equation is followed for each equation of the pair. However, writing the variational problem and the associated functional is a bit tricky.

Example 2.4.3 (Timoshenko Beam)

Consider the following pair of coupled differential equations governing bending of the Timoshenko beam:

$$-\frac{d}{dx}\left[S\left(\frac{dw}{dx}+\phi_x\right)\right] + c_f w = q \tag{2.4.32a}$$

$$-\frac{d}{dx}\left(D\frac{d\phi_x}{dx}\right) + S\left(\frac{dw}{dx}+\phi_x\right) = 0 \tag{2.4.32b}$$

where S is the shear stiffness ($S = K_s GA$; K_s is the shear correction coefficient, G is the shear modulus, and A is the area of the cross section), $D = EI$ is the bending stiffness, w is the transverse deflection, ϕ_x is the rotation, k is the foundation modulus, and q is the distributed transverse load. We shall develop the weak form of the above equations using the three-step procedure.

Steps 1 and 2: Multiply the first equation with weight function v_1 and the second one with weight function v_2 and integrate over the length of the beam:

$$\textit{Step 1a:}\quad 0 = \int_0^L v_1 \left\{ -\frac{d}{dx}\left[S\left(\frac{dw}{dx}+\phi_x\right)\right] + c_f w - q \right\} dx$$

$$\begin{aligned}\textit{Step 2a:}\quad 0 &= \int_0^L \left[\frac{dv_1}{dx} S\left(\frac{dw}{dx}+\phi_x\right) + c_f v_1 w - v_1 q\right] dx - \left[v_1 S\left(\frac{dw}{dx}+\phi_x\right)\right]_0^L \\ &= \int_0^L \left[\frac{dv_1}{dx} S\left(\frac{dw}{dx}+\phi_x\right) + c_f v_1 w - v_1 q\right] dx - v_1(L)\left[S\left(\frac{dw}{dx}+\phi_x\right)\right]_{x=L} \\ &\quad + v_1(0)\left[S\left(\frac{dw}{dx}+\phi_x\right)\right]_{x=0}\end{aligned} \tag{2.4.33a}$$

$$\textit{Step 1}b\text{:}\quad 0=\int_0^L v_2\left[-\frac{d}{dx}\left(D\frac{d\phi_x}{dx}\right)+S\left(\frac{dw}{dx}+\phi_x\right)\right]dx$$

$$\textit{Step 2}b\text{:}\quad 0=\int_0^L\left[D\frac{dv_2}{dx}\frac{d\phi_x}{dx}+v_2\,S\left(\frac{dw}{dx}+\phi_x\right)\right]dx-\left[v_2\,D\frac{d\phi_x}{dx}\right]_0^L$$

$$=\int_0^L\left[D\frac{dv_2}{dx}\frac{d\phi_x}{dx}+v_2\,S\left(\frac{dw}{dx}+\phi_x\right)\right]dx$$

$$-v_2(L)\left[D\frac{d\phi_x}{dx}\right]_{x=L}+v_2(0)\left[D\frac{d\phi_x}{dx}\right]_{x=0}\qquad(2.4.33b)$$

Note that integration-by-parts was used such that the expression $w_{,x}+\phi_x$ is preserved, as it enters the boundary term representing the shear force. Such considerations can only be used by knowing the mechanics of the problem at hand. Also, note that the pair of weight functions (v_1, v_2) satisfy the homogeneous form of specified essential boundary conditions on the pair (w, ϕ_x) (with the correspondence $v_1 \sim w$ and $v_2 \sim \phi_x$).

Steps 3: An examination of the boundary terms shows that $w \sim v_1$ and $\phi_x \sim v_2$ are the primary variables, and the secondary variables are given by [cf. Eq. (2.4.28*a*)]

$$S\left(\frac{dw}{dx}+\phi_x\right)\quad\text{(shear force)}\qquad(2.4.34a)$$

$$D\frac{d\phi_x}{dx}\quad\text{(bending moment)}\qquad(2.4.34b)$$

To finalize the weak forms, we must take care of the boundary terms by considering a specific beam problem. Using the beam of Fig. 2.4.1, we see that

$$w(0)=0,\quad \phi_x(0)=0,\quad \left[S\left(\frac{dw}{dx}+\phi_x\right)\right]_{x=L}=F_0,\quad \left[D\frac{d\phi_x}{dx}\right]_{x=L}=M_0\qquad(2.4.35)$$

and hence, $v_1(0)=0$ and $v_2(0)=0$. Consequently, the weak forms (2.4.33*a*) and (2.4.33*b*) become

$$0=\int_0^L\left[\frac{dv_1}{dx}\,S\left(\frac{dw}{dx}+\phi_x\right)+c_f v_1 w-v_1 q\right]dx-v_1(L)\,F_0\qquad(2.4.36a)$$

$$0=\int_0^L\left[\frac{dv_2}{dx}\,D\frac{d\phi_x}{dx}+v_2\,S\left(\frac{dw}{dx}+\phi_x\right)\right]dx-v_2(L)\,M_0\qquad(2.4.36b)$$

Variational Problem and Quadratic Functional: To write the variational problem of finding (w, ϕ_x) such that

$$B((v_1, v_2), (w, \phi_x)) = l((v_1, v_2))\qquad(2.4.37)$$

holds for all (v_1, v_2), we must combine the two weak forms into a single expression

$$0=\int_0^L\left[\left(\frac{dv_1}{dx}+v_2\right)S\left(\frac{dw}{dx}+\phi_x\right)+\frac{dv_2}{dx}\,D\frac{d\phi_x}{dx}+c_f v_1 w-v_1 q\right]dx-v_1(L)\,F_0-v_2(L)\,M_0$$

$$(2.4.38)$$

Thus, the bilinear and linear forms of the problem are given by

$$B((v_1, v_2), (w, \phi_x)) = \int_0^L \left[S\left(\frac{dv_1}{dx} + v_2\right)\left(\frac{dw}{dx} + \phi_x\right) + D\frac{dv_2}{dx}\frac{d\phi_x}{dx} + c_f v_1 w \right] dx \quad (2.4.39a)$$

$$l((v_1, v_2)) = \int_0^L v_1 q \, dx + v_1(L) F_0 + v_2(L) M_0 \quad (2.4.39b)$$

Clearly, $B((v_1, v_2), (w, \phi_x))$ is symmetric in its arguments (i.e. interchange of v_1 with w *and* v_2 with ϕ_x yields the same expression). Hence the functional is given by

$$I((w, \phi_x)) = \frac{1}{2}\int_0^L \left[S\left(\frac{dw}{dx} + \phi_x\right)^2 + D\left(\frac{d\phi_x}{dx}\right)^2 + \frac{c_f}{2} w^2 \right] dx - \left(\int_0^L w q \, dx + w(L) F_0 + \phi_x(L) M_0 \right) \quad (2.4.40)$$

The last example of this section is concerned with a second-order differential equation in two dimensions. The equation arises in a number of fields, including heat transfer, stream function or velocity potential formulation of inviscid flows, transverse deflections of a membrane, torsion of a cylindrical member, and others.

Example 2.4.4 (Poisson's Equation in Two Dimensions)

Consider the problem of determining the solution $u(x, y)$ to the partial differential equation,

$$-\frac{\partial}{\partial x}\left(a_1 \frac{\partial u}{\partial x}\right) - \frac{\partial}{\partial y}\left(a_2 \frac{\partial u}{\partial y}\right) + a_0 u = f \quad \text{in } \Omega \quad (2.4.41)$$

in a closed two-dimensional domain Ω with boundary Γ, as shown in Fig. 2.4.2. Here a_0, a_1, a_2, and f are known functions of position (x, y) in Ω. The function u is required to satisfy, in addition to the differential equation (2.4.41), certain boundary conditions on the boundary Γ of Ω. The weak formulation to be discussed next will reveal the precise form of the essential and natural boundary conditions of the equation.

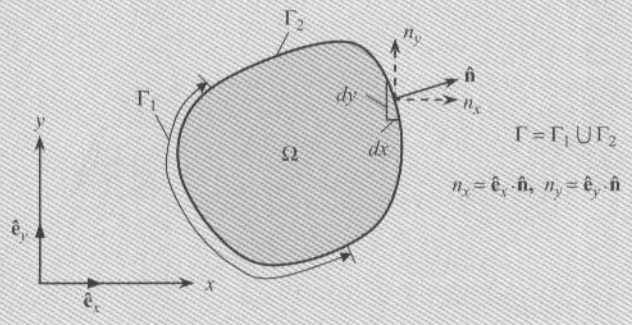

Figure 2.4.2 A two-dimensional domain Ω with boundary Γ.

The three step procedure applied to Eq. (2.4.41) results in the following equations:

$$\textit{Step 1:} \qquad 0 = \int_\Omega w \left[-\frac{\partial}{\partial x}\left(a_1 \frac{\partial u}{\partial x}\right) - \frac{\partial}{\partial y}\left(a_2 \frac{\partial u}{\partial y}\right) + a_0 u - f \right] dxdy \tag{2.4.42}$$

$$\textit{Step 2:} \qquad 0 = \int_\Omega \left(a_1 \frac{\partial w}{\partial x}\frac{\partial u}{\partial x} + a_2 \frac{\partial w}{\partial y}\frac{\partial u}{\partial y} + a_0 wu - wf \right) dxdy - \oint_\Gamma w \left(a_1 \frac{\partial u}{\partial x} n_x + a_2 \frac{\partial u}{\partial y} n_y \right) ds \tag{2.4.43}$$

where we used integration by parts [or the gradient and divergence theorems, Eqs. (2.2.27*b*) and (2.2.28*b*)] to transfer differentiation from u to w so that both u and w have the same order derivatives in Ω. The boundary term shows that u is the primary variable while

$$a_1 \frac{\partial u}{\partial x} n_x + a_2 \frac{\partial u}{\partial y} n_y$$

is the secondary variable.

Step 3: The last step in the procedure is to impose the specified boundary conditions. Suppose that u is specified on portion Γ_1 and the natural boundary condition is specified on the remaining portion Γ_2 of the boundary as (see Fig. 2.4.2):

$$u = \hat{u} \text{ on } \Gamma_1, \quad a_1 \frac{\partial u}{\partial x} n_x + a_2 \frac{\partial u}{\partial y} n_y = \hat{g} \text{ on } \Gamma_2 \tag{2.4.44}$$

Then w is arbitrary on Γ_2 and equal to zero on Γ_1. Consequently, Eq. (2.4.43) simplifies to

$$0 = \int_\Omega \left(a_1 \frac{\partial w}{\partial x}\frac{\partial u}{\partial x} + a_2 \frac{\partial w}{\partial y}\frac{\partial u}{\partial y} + a_0 wu - wf \right) dxdy - \int_{\Gamma_2} w\hat{g}\, ds \tag{2.4.45}$$

Variational Problem and Quadratic Functional: The weak statement (2.4.45) can be expressed as $B(w, u) = \ell(w)$, where the bilinear form and linear form are

$$B(w,u) = \int_\Omega \left(a_1 \frac{\partial w}{\partial x}\frac{\partial u}{\partial x} + a_2 \frac{\partial w}{\partial y}\frac{\partial u}{\partial y} + a_0 wu \right) dxdy, \tag{2.4.46a}$$

$$\ell(w) = \int_\Omega wf\, dxdy + \int_{\Gamma_2} w\hat{g}\, ds, \tag{2.4.46b}$$

The associated quadratic functional is

$$I(u) = \frac{1}{2}\int_\Omega \left[a_1 \left(\frac{\partial u}{\partial x}\right)^2 + a_2 \left(\frac{\partial u}{\partial y}\right)^2 + a_0 u^2 \right] dxdy - \int_\Omega uf\, dxdy - \int_{\Gamma_2} \hat{g}u\, ds. \tag{2.4.46c}$$

In the case of transverse deflections of a membrane, $I(u)$ represents the total potential energy.

As a specific example of the Poisson equation, consider steady heat conduction in a two-dimensional domain Ω, enclosed by lines AB, BC, CD, DE, EF, FG, GH, and HA, as indicated

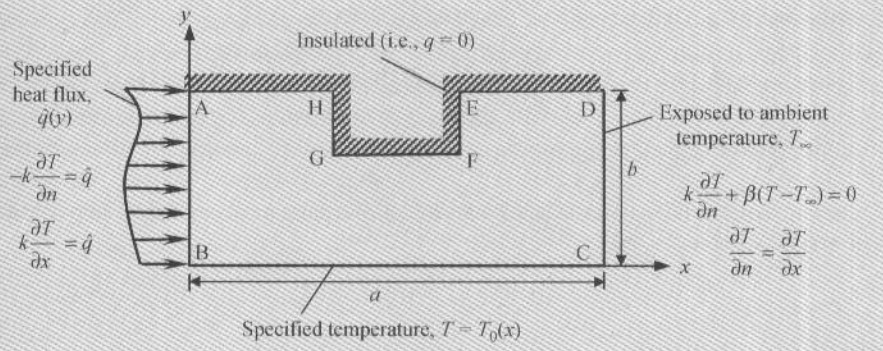

Figure 2.4.3 A two-dimensional heat transfer problem with a variety of boundary conditions.

in Fig. 2.4.3. The governing equation is

$$-k\left(\frac{\partial^2 T}{\partial x^2} + \frac{\partial^2 T}{\partial y^2}\right) = g_0 \quad \text{in} \quad \Omega \tag{2.4.47}$$

where g_0 is the uniform heat generation, k is the conductivity of the isotropic material of the domain, and T is the temperature. At the second step of the weak-form development, we have

$$0 = \int_\Omega \left[k\left(\frac{\partial w}{\partial x}\frac{\partial T}{\partial x} + \frac{\partial w}{\partial y}\frac{\partial T}{\partial y}\right) - w g_0\right] dx\, dy - \oint_\Gamma wk\left(\frac{\partial T}{\partial x}n_x + \frac{\partial T}{\partial y}n_y\right) ds \tag{2.4.48}$$

In order to simplify the boundary expression, we first recognize the fact that the boundary Γ of the domain consists of several line segments, and they are subject to different types of boundary conditions as shown in Fig. 2.4.3:

$$\begin{aligned}
&\Gamma_1 = \text{AB}: n_x = -1,\ n_y = 0; && \text{heat flux is specified } q = \hat{q}(y)\\
&\Gamma_2 = \text{BC}: n_x = 0,\ \ n_y = -1; && \text{temperature is specified } T = T_0(x)\\
&\Gamma_3 = \text{CD}: n_x = 1,\ \ n_y = 0; && \text{boundary exposed to ambient temperature } T_\infty\\
& && \text{(convection) } k\frac{\partial T}{\partial n} + \beta\,(T - T_\infty) = 0 \qquad (2.4.49)\\
&\Gamma_4 = \text{DEFGHA}: && \text{insulated boundary } \frac{\partial T}{\partial n} = 0
\end{aligned}$$

Using the boundary information, the boundary integral in (2.4.48) can be simplified as follows (note that $w = 0$ on portion of the boundary wherever T is specified, Γ_2):

$$\begin{aligned}
\oint_\Gamma w\left(k\frac{\partial T}{\partial n}\right) ds &= \int_{\Gamma_1} w q_n\, ds + \int_{\Gamma_2} 0\left(k\frac{\partial T}{\partial n}\right) ds\\
&\quad - \int_{\Gamma_3} w[\beta(T - T_\infty)]\, ds + \int_{\Gamma_4} w\, 0\, ds\\
&= -\int_0^b w(0, y)\hat{q}(y)\, dy - \beta\int_0^b w(a, y)[T(a, y) - T_\infty]\, dy
\end{aligned} \tag{2.4.50}$$

Substituting (2.4.50) into (2.4.48), we obtain the weak form

$$0 = \int_\Omega \left[k\left(\frac{\partial w}{\partial x}\frac{\partial T}{\partial x} + \frac{\partial w}{\partial y}\frac{\partial T}{\partial y} \right) - wg_0 \right] dx\, dy + \int_0^b w(0, y)\hat{q}(y)dy + \beta \int_0^b w(a, y)[T(a, y) - T_\infty]\, dy \tag{2.4.51}$$

Collecting terms involving both w and T into $B(\cdot, \cdot)$, and those involving only w into $l(\cdot)$, we can write (2.4.51) as

$$B(w, T) = l(w) \tag{2.4.52a}$$

where

$$B(w, T) = \int_\Omega k\left(\frac{\partial w}{\partial x}\frac{\partial T}{\partial x} + \frac{\partial w}{\partial y}\frac{\partial T}{\partial y} \right) dx\, dy + \beta \int_0^b w(a, y)T(a, y)dy$$

$$l(w) = \int_\Omega wg_0\, dx\, dy - \int_0^b w(0, y)\hat{q}(y)\, dy + \beta \int_0^b w(a, y)T_\infty\, dy \tag{2.4.52b}$$

The quadratic functional is given by

$$I(T) = \frac{k}{2}\int_\Omega \left[\left(\frac{\partial T}{\partial x} \right)^2 + \left(\frac{\partial T}{\partial y} \right)^2 \right] dx\, dy + \frac{\beta}{2}\int_0^b T^2(a, y)\, dy - \int_\Omega Tg_0\, dx\, dy + \int_0^b T(0, y)\hat{q}(y)\, dy - \beta \int_0^b T(a, y)T_\infty\, dy \tag{2.4.53}$$

Note that the boundary integrals in this example are defined along the y or x axes, because the boundaries are parallel to either the x- or y-axis.

2.5 VARIATIONAL METHODS

2.5.1 Introduction

Our objective in this section is to study the variational methods of approximation because they provide a background for the development of finite element models. The methods to be discussed include the Ritz and weighted-residual (e.g., Galerkin, Petrov–Galerkin, least-squares, and collocation) methods. In all these methods, we seek an approximate solution in the form of a linear combination of suitable approximation functions ϕ_j and undetermined parameters c_j: $\sum_j c_j\phi_j$. The Ritz method uses the weak form, whereas the weighted-residual methods use the weighted-integral form (Step 1 of the weak-form development) to determine the parameters c_j. Various methods differ from each other in the choice of weight function w and approximation functions ϕ_j. As we shall see in the coming chapters, the finite element method is a elementwise application of the classical variational methods.

2.5.2 The Ritz Method

In the Ritz method, the coefficients c_j of the approximation are determined using the weak form of the problem, and hence, the choice of weight functions is restricted to the

approximation functions, $w = \phi_j$ ($w \sim u$). Recall that the weak form contains both the governing differential equation and the natural boundary conditions of the problem, and hence it places weaker continuity requirements on the approximate solution than the original differential equation or its weighted-integral form. The method is described here for a linear variational problem (which is the same as the weak form).

Consider the variational problem resulting from the weak form: Find the solution u such that

$$B(w, u) = l(w) \tag{2.5.1}$$

for all sufficiently differentiable functions w that satisfy the homogeneous form of specified essential boundary conditions on u. In general, $B(\cdot, \cdot)$ can be unsymmetric in w and u, and it can be even nonlinear in u [$B(\cdot, \cdot)$ is always linear in w]. When $B(\cdot, \cdot)$ is bilinear and symmetric in w and u and l is linear, the problem in (2.5.1) is equivalent to minimization of the quadratic functional [see Eq. (2.4.19)]

$$I(u) = \frac{1}{2} B(u, u) - l(u) \tag{2.5.2}$$

In the Ritz method, we seek an approximate solution to (2.5.1) in the form of a finite series [see Eq. (2.4.2)]

$$U_N(x) = \sum_{j=1}^{N} c_j \phi_j(x) + \phi_0(x) \tag{2.5.3}$$

where the constants c_j, called the *Ritz coefficients*, are determined such that (2.5.1) holds for each $w = \phi_i$ ($i = 1, 2, \ldots, N$), i.e., (2.5.1) holds for N different choices of w, so that N independent algebraic relations among c_j are obtained. The functions ϕ_j and ϕ_0, called *approximation functions*, are chosen such that U_N satisfies the specified essential boundary conditions [recall that the specified natural boundary conditions are already included in the variational problem (2.5.1) and hence in the functional $I(u)$]. More details on this will be discussed shortly. The ith algebraic equation is obtained from Eq. (2.5.1) by substituting $w = \phi_i$ and U_N from (2.5.2) for u:

$$B\left(\phi_i, \sum_{j=1}^{N} c_j \phi_j + \phi_0\right) = l(\phi_i) \quad (i = 1, 2, \cdots, N)$$

Since $B(\cdot, \cdot)$ is linear in u, we have

$$\sum_{j=1}^{N} B(\phi_i, \phi_j) c_j = l(\phi_i) - B(\phi_i, \phi_0)$$

or

$$\sum_{j=1}^{N} K_{ij} c_j = F_i, \quad i = 1, 2, \ldots, N \tag{2.5.4a}$$

$$K_{ij} = B(\phi_i, \phi_j), \quad F_i = l(\phi_i) - B(\phi_i, \phi_0) \tag{2.5.4b}$$

The algebraic equations in (2.5.4a) can be expressed in matrix form as

$$[K]\{c\} = \{F\} \quad \text{or} \quad \mathbf{Kc} = \mathbf{F} \tag{2.5.5}$$

As stated earlier, for symmetric bilinear forms the Ritz method can also be viewed as seeking a solution of the form in (2.5.3) in which the parameters c_j are determined by minimizing the quadratic functional $I(u)$ in (2.5.2). After substituting U_N from (2.5.3) for u into (2.5.2) and integrating, the functional $I(u)$ becomes an ordinary function of the parameters $c_1, c_2, \ldots c_N$. Then the necessary condition for the minimization of $I(c_1, c_2, \ldots, c_N)$ is that its partial derivatives with respect to each of the parameters be zero:

$$\frac{\partial I}{\partial c_1} = 0, \quad \frac{\partial I}{\partial c_2} = 0, \quad \cdots, \quad \frac{\partial I}{\partial c_N} = 0 \tag{2.5.6}$$

Thus, there are N linear algebraic equations in N unknowns, c_j $(j = 1, 2, \cdots, N)$. These equations are exactly the same as those in (2.5.4) for all problems for which the variational problem (2.5.1) is equivalent to $\delta I = 0$. Of course, when $B(\cdot, \cdot)$ is not symmetric, we do not have a quadratic functional. In other words, (2.5.4a) is more general than (2.5.6), and they are the same when $B(\cdot, \cdot)$ is bilinear and symmetric. In all problems of interest in the present study, we shall have a symmetric bilinear form.

2.5.3 Approximation Functions

Returning to the approximation U_N in (2.5.3), we wish to discuss the selection of the approximation functions ϕ_j and ϕ_0 for the Ritz method. First, we note that U_N must satisfy only the specified essential boundary conditions of the problem, since the specified natural boundary conditions are included in the variational problem (2.5.1). The particular form of U_N in (2.5.3) facilitates satisfaction of specified boundary conditions. To see this, suppose that the approximate solution is sought in the form

$$U_N(x) = \sum_{j=1}^{N} c_j \phi_j(x)$$

and suppose that the specified essential boundary condition is $u(x_0) = u_0$. Then U_N must also satisfy the condition $U_N(x_0) = u_0$ at a boundary point $x = x_0$:

$$\sum_{j=1}^{N} c_j \phi_j(x_0) = u_0$$

Since c_j are unknown parameters to be determined, it is not easy to choose $\phi_j(x)$ such that the above relation holds. If $u_0 = 0$, then we can select all ϕ_j such that $\phi_j(x_0) = 0$ and satisfy the condition $U_N(x_0) = 0$. By writing the approximate solution U_N in the form (2.5.3), a sum of a homogeneous part $\sum c_j \phi_j(x)$ and a nonhomogeneous part $\phi_0(x)$, we require $\phi_0(x)$ to satisfy the specified essential boundary conditions while the homogeneous part vanishes at the same boundary point where the essential boundary condition is specified. This follows from

$$U_N(x_0) = \sum_{j=1}^{N} c_j \phi_j(x_0) + \phi_0(x_0)$$

$$u_0 = \sum_{j=1}^{N} c_j \phi_j(x_0) + u_0 \rightarrow \sum_{j=1}^{N} c_j \phi_j(x_0) = 0$$

which is satisfied, for arbitrary c_j, by choosing $\phi_j(x_0) = 0$.

If all specified essential boundary conditions are homogeneous (i.e., the specified value u_0 is zero), then ϕ_0 is taken to be zero and ϕ_j must still satisfy the same conditions, $\phi_j(x_0) = 0$, $j = 1, 2, \ldots, N$. Note that the requirement that w be zero at the boundary points where the essential boundary conditions are specified is satisfied by the choice $w = \phi_j(x)$.

In summary, the approximation functions $\phi_i(x)$ and $\phi_0(x)$ are required to satisfy the following conditions:

1. (a) ϕ_i must be such that $B(\phi_i, \phi_j)$ is defined and nonzero, i.e., ϕ_i are sufficiently differentiable and integrable as required in the evaluation of $B(\phi_i, \phi_j)$.
   (b) ϕ_i must satisfy the homogeneous form of the specified essential boundary conditions of the problem.
2. For any N, the set $\{\phi_i\}_{i=1}^N$ along with the columns (and rows) of $B(\phi_i, \phi_j)$ must be *linearly independent*.
3. The set $\{\phi_i\}$ must be *complete*. For example, when ϕ_i are algebraic polynomials, completeness requires that the set $\{\phi_i\}$ contains all terms of the lowest order admissible, up to the highest order desired.
4. The only requirement on ϕ_0 is that it satisfy the specified essential boundary conditions. When the specified essential boundary conditions are zero, then ϕ_0 is identically zero. Also, for completeness reasons, ϕ_0 must be the lowest-order function that satisfies the specified essential boundary conditions.

2.5.4 Examples

Here, we consider a few examples of the application of the Ritz method to equilibrium, eigenvalue, and time-dependent problems.

Example 2.5.1

Consider the differential equation (see Example 2.4.1; set $a = 1$, $c = -1$, $L = 1$, and $f = -x^2$)

$$-\frac{d^2u}{dx^2} - u + x^2 = 0 \quad \text{for} \quad 0 < x < 1 \tag{2.5.7}$$

We consider two sets of boundary conditions:

$$\textit{Set } 1\text{:} \quad u(0) = 0, \quad u(1) = 0 \tag{2.5.8}$$

$$\textit{Set } 2\text{:} \quad u(0) = 0, \quad \left.\frac{du}{dx}\right|_{x=1} = 1 \tag{2.5.9}$$

Boundary Conditions Set 1. The bilinear form and the linear functional associated with Eqs. (2.5.7) and (2.5.8) are [see (2.4.23c)]

$$B(w, u) = \int_0^1 \left(\frac{dw}{dx}\frac{du}{dx} - wu\right) dx, \quad l(w) = -\int_0^1 w x^2 \, dx \tag{2.5.10}$$

and K_{ij} and F_i are given by

$$K_{ij} = B(\phi_i, \phi_j) = \int_0^1 \left(\frac{d\phi_i}{dx} \frac{d\phi_j}{dx} - \phi_i \phi_j \right) dx, \quad l(\phi_i) = -\int_0^1 \phi_i \, x^2 \, dx \tag{2.5.11}$$

The same result as in (2.5.11) can be obtained by minimizing the quadratic functional [set $a = 1$, $c = -1$, $f = -x^2$, $L = 1$, and $u(1) = 0$ in Eq. (2.4.24)]

$$I(u) = \frac{1}{2} \int_0^1 \left[\left(\frac{du}{dx} \right)^2 - u^2 + 2x^2 u \right] dx$$

Substituting for $u \approx U_N$ from (2.5.3), with $\phi_0 = 0$, into the above functional, we obtain

$$I(c_1, c_2, \ldots, c_N) = \frac{1}{2} \int_0^1 \left[\left(\sum_{j=1}^N c_j \frac{d\phi_j}{dx} \right)^2 - \left(\sum_{j=1}^N c_j \phi_j \right)^2 + 2x^2 \left(\sum_{j=1}^N c_j \phi_j \right) \right] dx$$

The necessary condition for the minimum of I is that

$$\begin{aligned} \frac{\partial I}{\partial c_i} = 0 &= \int_0^1 \left[\frac{d\phi_i}{dx} \left(\sum_{j=1}^N c_j \frac{d\phi_j}{dx} \right) - \phi_i \left(\sum_{j=1}^N c_j \phi_j \right) + \phi_i x^2 \right] dx \\ &= \sum_{j=1}^N \left[\int_0^1 \left(\frac{d\phi_i}{dx} \frac{d\phi_j}{dx} - \phi_i \phi_j \right) dx \right] c_j + \int_0^1 \phi_i \, x^2 \, dx \\ &= \sum_{j=1}^N K_{ij} c_j - F_i \quad \text{for } i = 1, 2, \ldots, N \end{aligned} \tag{2.5.12}$$

Clearly, K_{ij} and F_i are the same as those defined in Eq. (2.5.11). Equations (2.5.12) hold for any choice of admissible approximation functions ϕ_i.

Next, we discuss the choice of ϕ_i and ϕ_0. Since both boundary conditions $u(0) = u(1) = 0$ are homogeneous and of the essential type, we take $\phi_0 = 0$ and select ϕ_i in the N-parameter Ritz approximation to satisfy the conditions $\phi_i(0) = \phi_i(1) = 0$. Clearly, the function $(0 - x)(1 - x)$ vanishes at $x = 0$ and $x = 1$, and its first derivative is nonzero. Hence, we take $\phi_1 = x(1 - x)$. The next function in the sequence is obviously $\phi_2 = x^2(1 - x)$(or $\phi_2 = x(1 - x)^2$). Thus, the following set of functions are admissible:

$$\phi_1 = x(1 - x), \; \phi_2 = x^2(1 - x), \ldots, \; \phi_i = x^i(1 - x), \ldots, \; \phi_N = x^N(1 - x) \tag{2.5.13}$$

The approximation

$$U_N = c_1 x(1 - x) + c_2 x^2(1 - x) + \ldots + c_N x^N(1 - x) \tag{2.5.14a}$$

is equivalent to

$$U_N = \hat{c}_1 x(1 - x) + \hat{c}_2 x(1 - x)^2 + \ldots + \hat{c}_N x(1 - x)^N \tag{2.5.14b}$$

It should be noted that if we select, for example, the functions $\phi_1 = x^2(1 - x)$, $\phi_2 = x^3(1 - x)$, and so on [not including $x(1 - x)$], the completeness requirement is violated, because the set cannot be used to generate the linear term x of the exact solution, if the solution has such a term. As a rule, we must start with the lowest-order admissible function and include all admissible, higher-order functions up to the desired degree.

For the choice of approximation functions in (2.5.13), the matrix coefficients $K_{ij} = B(\phi_i, \phi_j)$ and vector coefficients $F_i = l(\phi_i)$ can be computed as follows:

$$K_{ij} = \int_0^1 \left\{ [ix^{i-1} - (i+1)x^i][jx^{j-1} - (j+1)x^j] - (x^i - x^{i+1})(x^j - x^{j-1}) \right\} dx$$

$$= \frac{2ij}{(i+j)[(i+j)^2 - 1]} - \frac{2}{(i+j+1)(i+j+2)(i+j+3)} \tag{2.5.15a}$$

$$F_i = -\int_0^1 x^2(x^i - x^{i+1})dx = -\frac{1}{(i+3)(i+4)} \tag{2.5.15b}$$

for $i, j = 1, 2, \ldots, N$. We consider the one-, two- and three-parameter approximations to illustrate how the Ritz solution converges to the exact solution of the problem

$$u(x) = \frac{\sin x + 2\sin(1-x)}{\sin 1} + x^2 - 2 \tag{2.5.16}$$

For $N = 1$, we have

$$K_{11} = \frac{3}{10}, \quad F_1 = -\frac{1}{20} \quad \rightarrow \quad c_1 = -\frac{1}{6} = -0.1667$$

The one-parameter Ritz solution is given by

$$U_1 = c_1\phi_1 = -\frac{1}{6}(x - x^2)$$

For $N = 2$, we have

$$\frac{1}{420}\begin{bmatrix} 126 & 63 \\ 63 & 52 \end{bmatrix}\begin{Bmatrix} c_1 \\ c_2 \end{Bmatrix} = -\frac{1}{60}\begin{Bmatrix} 3 \\ 2 \end{Bmatrix}$$

Solving the linear equations using Cramer's rule, we obtain

$$c_1 = -\frac{10}{123} = -0.0813, \quad c_2 = -\frac{21}{123} = -0.1707$$

The two-parameter Ritz solution is given by

$$U_2 = c_1\phi_1 + c_2\phi_2 = -\frac{10}{123}(x - x^2) - \frac{21}{123}(x^2 - x^3)$$
$$= -0.0813x - 0.0894x^2 + 0.1707x^3$$

For $N = 3$, we have

$$\frac{1}{2520}\begin{bmatrix} 756 & 378 & 228 \\ 378 & 312 & 237 \\ 228 & 237 & 206 \end{bmatrix}\begin{Bmatrix} c_1 \\ c_2 \\ c_3 \end{Bmatrix} = -\frac{1}{420}\begin{Bmatrix} 21 \\ 14 \\ 10 \end{Bmatrix}$$

Note that the previously computed coefficients K_{ij} and F_i for $i, j = 1, 2$ remain unchanged and we only need to compute K_{3i}, $i = 1, 2, 3$, and F_3. The solution of the above equations is

$$c_1 = -0.0952, \quad c_2 = -0.1005, \quad c_3 = -0.0702$$

Table 2.5.1 Comparison of the Ritz and exact solutions of the equation

$$-\frac{d^2u}{dx^2} - u + x^2 = 0 \text{ for } 0 < x < 1; \quad u(0) = u(1) = 0$$

Ritz coefficients†		x	Ritz solution, $-10u$			Exact solution
			$N=1$	$N=2$	$N=3$	
$N=1$:	$c_1=-0.1667$	0.0	0.0	0.0	0.0	0.0
		0.1	0.1500	0.0885	0.0954	0.0955
		0.2	0.2667	0.1847	0.1890	0.1890
$N=2$:	$c_1=-0.0813$	0.3	0.3500	0.2783	0.2766	0.2764
	$c_2=-0.1707$	0.4	0.4000	0.3590	0.3520	0.3518
		0.5	0.4167	0.4167	0.4076	0.4076
$N=3$:	$c_1=-0.0952$	0.6	0.4000	0.4410	0.4340	0.4342
	$c_2=-0.1005$	0.7	0.3500	0.4217	0.4200	0.4203
	$c_3=-0.0702$	0.8	0.2667	0.3486	0.3529	0.3530
		0.9	0.1500	0.2115	0.2183	0.2182
		1.0	0.0	0.0	0.0	0.0

†The four-parameter Ritz solution coincides with the exact solution up to four decimal places.

The three-parameter Ritz solution is given by

$$\begin{aligned} U_3 &= c_1\phi_1 + c_2\phi_2 + c_3\phi_3 = -0.0952(x - x^2) - 0.1005(x^2 - x^3) - 0.0702(x^3 - x^4) \\ &= -0.0952x - 0.0053x^2 + 0.0303x^3 + 0.0702x^4 \end{aligned}$$

The values of the Ritz coefficients c_i, $i = 1, 2, \ldots, N$ for various values of N can be obtained by solving the matrix equation $[K]\{c\} = \{F\}$ with the coefficients of K_{ij} and F_i given by (2.5.15*a*) and (2.5.15*b*). The Ritz coefficients and a comparison of the Ritz solution with the exact solution (2.5.16) is presented in Table 2.5.1 and Fig. 2.5.1. If the exact solution (2.5.16) is expanded in a series in terms of powers of x, we note that it is an infinite series. However, the three-parameter Ritz solution is already a good approximation of the exact solution, as can be seen from Fig. 2.5.1 and Table 2.5.1.

Boundary Conditions Set 2. For the second set of boundary conditions (2.5.9), the bilinear form is the same as that given in (2.5.10). The linear form is given by

$$l(w) = -\int_0^1 w\, x^2\, dx + w(1) \tag{2.5.17}$$

Therefore, we have

$$F_i = -\int_0^1 x^2 \phi_i\, dx + \phi_i(1) \tag{2.5.18}$$

As for the approximation functions, ϕ_0 is still zero and the ϕ_i must be selected to satisfy the condition $\phi_i(0) = 0$. Clearly, $\phi_1(x) = x$, $\phi_2 = x^2$, and so on meet the requirement. Thus, we have

$$U_N = c_1 x + c_2 x^2 + \ldots + c_i x^i + \ldots + c_N x^N \tag{2.5.19}$$

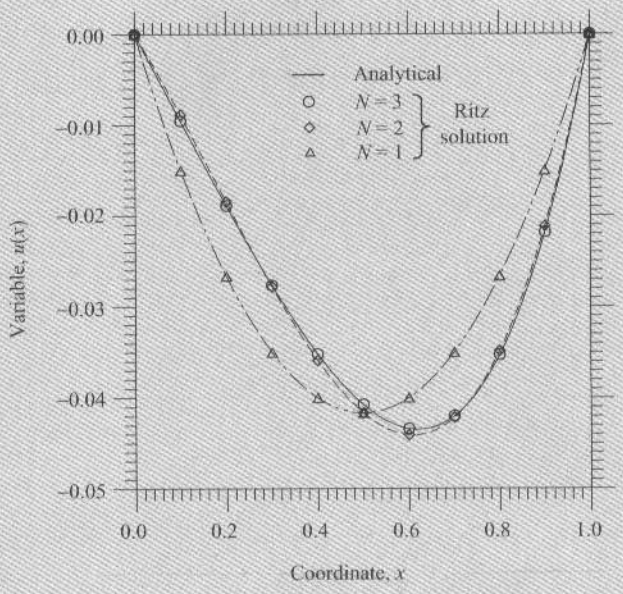

Figure 2.5.1 Comparison of the Ritz solution with the exact solution of Eqs. (2.5.7) and (2.5.8). The three-parameter Ritz solution and the exact solution do not differ on the scale of the plot.

The coefficients K_{ij} and F_i can be computed using

$$K_{ij} = \int_0^1 (ijx^{i+j-2} - x^{(i+j)})\, dx = \frac{ij}{i+j-1} - \frac{1}{i+j+1}$$

$$F_i = -\int_0^1 x^{i+2}\, dx + 1 = -\frac{1}{i+3} + 1 \tag{2.5.20}$$

For example, for $N = 2$ we have

$$\frac{1}{60}\begin{bmatrix} 40 & 45 \\ 45 & 68 \end{bmatrix}\begin{Bmatrix} c_1 \\ c_2 \end{Bmatrix} = \frac{1}{20}\begin{Bmatrix} 15 \\ 16 \end{Bmatrix}$$

Solving the linear equations using Cramer's rule, we obtain

$$c_1 = \frac{180}{139} = 1.2950, \quad c_2 = -\frac{21}{139} = -0.1511$$

The two-parameter Ritz solution is given by

$$U_2 = c_1\phi_1 + c_2\phi_2 = 1.2950x - 0.1511x^2$$

The exact solution for this case is

$$u(x) = \frac{2\cos(1-x) - \sin x}{\cos 1} + x^2 - 2 \tag{2.5.21}$$

A comparison of the Ritz solutions with the exact solution is presented in Table 2.5.2.

Table 2.5.2 Comparison of the Ritz and exact solutions of the equation

$$-\frac{d^2u}{dx^2} - u + x^2 = 0 \text{ for } 0 < x < 1; \quad u(0) = 0, \quad \left(\frac{du}{dx}\right)\Big|_{x=1} = 1$$

Ritz coefficients†		x	Ritz solution, u			Exact solution
			$N=1$	$N=2$	$N=3$	
$N=1$	$c_1 = 1.1250$	0.0	0.0	0.0	0.0	0.0
		0.1	0.1125	0.1280	0.1271	0.1262
		0.2	0.2250	0.2530	0.2519	0.2513
$N=2$	$c_1 = 1.2950$	0.3	0.3375	0.3749	0.3740	0.3742
	$c_2 = -0.1511$	0.4	0.4500	0.4938	0.4934	0.4944
		0.5	0.5625	0.6097	0.6099	0.6112
$N=3$	$c_1 = 1.2831$	0.6	0.6750	0.7226	0.7234	0.7244
	$c_2 = -0.1142$	0.7	0.7875	0.8325	0.8337	0.8340
	$c_3 = -0.0246$	0.8	0.9000	0.9393	0.9407	0.9402
		0.9	1.0125	1.0431	1.0443	1.0433
		1.0	1.1250	1.1439	1.1442	1.1442

†The four-parameter Ritz solution coincides with the exact solution up to four decimal places.

Example 2.5.2

Consider the problem of finding the transverse deflection of a cantilever beam under a uniform transverse load of intensity q_0 per unit length and subjected to point load F_0 and bending moment M_0 at the free end (see Example 2.4.2). The governing equations according to the Euler-Bernoulli beam theory are

$$\frac{d^2}{dx^2}\left(EI\frac{d^2w}{dx^2}\right) - q_0 = 0 \quad \text{for} \quad \begin{cases} 0 < x < L \\ EI > 0 \end{cases} \tag{2.5.22}$$

$$w(0) = \left(\frac{dw}{dx}\right)\Big|_{x=0} = 0, \quad \left(EI\frac{d^2w}{dx^2}\right)\Big|_{x=L} = -M_0, \quad \left[\frac{d}{dx}\left(EI\frac{d^2w}{dx^2}\right)\right]\Big|_{x=L} = F_0 \tag{2.5.23}$$

The weak form of (2.5.22) and (2.5.23) (which includes the specified NBC) was derived in Example 2.4.2, and is given by (2.4.30*a*).

We now construct an N-parameter Ritz solution using the variational form, (2.4.30*b*). Since the specified EBCs $w(0) = 0$ and $(dw/dx)|_{x=0}$ are homogeneous, we set $\phi_0 = 0$. Next, we select algebraic approximation functions ϕ_i that satisfy the continuity conditions and homogeneous form of the specified EBCs. The lowest-order algebraic function that meets these conditions is $\phi_1 = x^2$. The next function in the sequence is $\phi_2 = x^3$. Thus, we have

$$\phi_1 = x^2, \ \phi_2 = x^3, \ \ldots, \ \phi_i = x^{i+1}, \ \ldots, \ \phi_N = x^{N+1} \tag{2.5.24}$$

The N-parameter Ritz approximation is

$$W_N(x) = \sum_{j=1}^{N} c_j \phi_j, \quad \phi_j = x^{j+1} \tag{2.5.25}$$

Substituting (2.5.25) for w and $v = \phi_i$ into (2.4.30a) with $c_f = 0$, we obtain

$$[K]\{c\} = \{F\} \tag{2.5.26a}$$

$$K_{ij} = B(\phi_i, \phi_j) = \int_0^L EI(i+1)ix^{i-1}(j+1)jx^{j-1}\,dx$$

$$= EI(L)^{i+j-1}\frac{ij(i+1)(j+1)}{(i+j-1)} \tag{2.5.26b}$$

$$F_i = l(\phi_i) = \int_0^L q_0 x^{i+1}\,dx + (L)^{i+1}F_0 - (i+1)(L)^i M_0$$

$$= q_0(L)^{i+2}\frac{1}{i+2} + (L)^{i+1}F_0 - (i+1)(L)^i M_0 \tag{2.5.26c}$$

For $N = 1$, Eq. (2.5.26a) gives

$$c_1 = \left(\frac{q_0 L^4}{12EI} + \frac{F_0 L^3}{4EI} - \frac{M_0 L}{2EI}\right)$$

and the one-parameter Ritz solution is

$$W_1(x) = \left(\frac{q_0 L^4}{12EI} + \frac{F_0 L^3}{4EI} - \frac{M_0 L}{2EI}\right)\frac{x^2}{L^2}$$

For $N = 2$, we have

$$EI\begin{bmatrix} 4L & 6L^2 \\ 6L^2 & 12L^3 \end{bmatrix}\begin{Bmatrix} c_1 \\ c_2 \end{Bmatrix} = \frac{q_0 L^3}{12}\begin{Bmatrix} 4 \\ 3L \end{Bmatrix} + F_0 L^2\begin{Bmatrix} 1 \\ L \end{Bmatrix} - M_0 L\begin{Bmatrix} 2 \\ 3L \end{Bmatrix} \tag{2.5.27}$$

Solving for c_1 and c_2, we obtain

$$c_1 = \frac{1}{24EI}\left(5q_0 L^2 + 12F_0 L - 12M_0\right), \quad c_2 = -\frac{1}{12EI}\left(q_0 L + 2F_0\right)$$

and solution (2.5.25) becomes

$$W_2(x) = \frac{q_0 L^4}{24EI}\left(5\frac{x^2}{L^2} - 2\frac{x^3}{L^3}\right) + \frac{F_0 L^3}{6EI}\left(3\frac{x^2}{L^2} - \frac{x^3}{L^3}\right) - \frac{M_0 L^2}{2EI}\frac{x^2}{L^2} \tag{2.5.28}$$

For $N = 3$, we obtain the matrix equation

$$EI\begin{bmatrix} 4 & 6L & 8L^2 \\ 6L & 12L^2 & 18L^3 \\ 8L^2 & 18L^2 & \frac{144}{5}L^4 \end{bmatrix}\begin{Bmatrix} c_1 \\ c_2 \\ c_3 \end{Bmatrix} = \frac{q_0 L^3}{60}\begin{Bmatrix} 20 \\ 15L \\ 12L^2 \end{Bmatrix} + F_0 L^2\begin{Bmatrix} 1 \\ L \\ L^2 \end{Bmatrix} - M_0 L\begin{Bmatrix} 2 \\ 3L \\ 4L^2 \end{Bmatrix} \tag{2.5.29}$$

The solution of these equations when substituted into (2.5.25) for $N = 3$, gives

$$W_3(x) = \frac{q_0 L^4}{24EI}\frac{x^2}{L^2}\left(6 - 4\frac{x}{L} + \frac{x^2}{L^2}\right) + \frac{FL^3}{6EI}\left(3\frac{x^2}{L^2} - \frac{x^3}{L^3}\right) - \frac{M_0 L^2}{2EI}\frac{x^2}{L^2} \tag{2.5.30}$$

which coincides with the exact solution of Eqs. (2.5.22) and (2.5.23). Note that the one-parameter solution is exact when the beam is subjected to end moment M_0 only; the two-parameter solution is exact when the beam is subjected to both F_0 and M_0. If we try to compute the four-parameter solution without knowing that the three-parameter solution is exact for a beam subjected to distributed load q_0, point load F_0, and bending moment M_0, the parameters c_j $(j > 3)$ will be zero.

The next example deals with two-dimensional heat conduction in a square region. Note that the dependent variable, namely the temperature, is denoted by T, consistent with the standard notation used in heat transfer books.

Example 2.5.3

Consider the Poisson equation governing two-dimensional heat transfer in a square region

$$-k\left(\frac{\partial^2 T}{\partial x^2}+\frac{\partial^2 T}{\partial y^2}\right)=g_0 \quad \text{in} \quad \Omega=\{(x, y): 0<(x, y)<1\} \tag{2.5.31}$$

with the following boundary conditions:

$$T=0 \quad \text{on sides } x=1 \quad \text{and} \quad y=1 \tag{2.5.32a}$$

$$\frac{\partial T}{\partial n}=0 \quad \text{on sides } x=0 \quad \text{and} \quad y=0 \tag{2.5.32b}$$

where g_0 is the rate of uniform heat generation in the region. Equation (2.5.31) is called Poisson's equation $(-k\nabla^2 T=g_0)$.

The variational problem is of the form (see Example 2.4.4; set $u=T$, $a_1=a_2=k$, $a_0=0$, and $f=g_0$)

$$B(w, T)=l(w) \tag{2.5.33a}$$

where the bilinear and linear functionals are

$$\begin{aligned} B(w, T) &= \int_0^1 \int_0^1 k\left(\frac{\partial w}{\partial x}\frac{\partial T}{\partial x}+\frac{\partial w}{\partial y}\frac{\partial T}{\partial y}\right) dx\, dy \\ l(w) &= \int_0^1 \int_0^1 w g_0\, dx\, dy \end{aligned} \tag{2.5.33b}$$

We consider an N-parameter approximation of the form

$$T_N=\sum_{i,j=1}^{N} c_{ij} \cos\alpha_i x \cos\alpha_j y, \quad \alpha_i=\frac{1}{2}(2i-1)\pi \tag{2.5.34}$$

Note that (2.5.34) involves a double summation. Since the boundary conditions are homogeneous, we have $\phi_0=0$. Incidentally, ϕ_i also satisfies the natural boundary conditions of the

problem but that is not necessary to be admissible. While the choice $\hat{\phi}_{ij} = \sin i\pi x \sin j\pi y$ meets the essential boundary conditions, $\hat{\phi}_{ij}$ is not complete because it cannot be used to generate the solution that *does not* vanish on the sides $x = 0$ and $y = 0$. Hence, $\hat{\phi}_{ij}$ are not admissible.

The coefficients K_{ij} and F_i can be computed by substituting (2.5.34) into (2.5.33*b*). Since the double Fourier series has two summations, we introduce the notation

$$\begin{aligned} K_{(ij)(kl)} &= k\int_0^1\int_0^1 [(\alpha_i \sin\alpha_i x \cos\alpha_j y)(\alpha_k \sin\alpha_k x \cos\alpha_l y) \\ &\quad +(\alpha_j \cos\alpha_i x \sin\alpha_j y)(\alpha_l \cos\alpha_k x \sin\alpha_l y)]\, dx\, dy \\ &= \begin{cases} 0 & \text{if } i \neq k \text{ or } j \neq l \\ \frac{1}{4}k(\alpha_i^2 + \alpha_j^2) & \text{if } i = k \text{ and } j = l \end{cases} \end{aligned} \tag{2.5.35a}$$

$$F_{ij} = g_0 \int_0^1\int_0^1 \cos\alpha_i x \cos\alpha_j y\, dx\, dy = \frac{g_0}{\alpha_i\alpha_j} \sin\alpha_i \sin\alpha_j \tag{2.5.35b}$$

In evaluating the integrals, the following orthogonality conditions were used

$$\int_0^1 \sin\alpha_i x \sin\alpha_j x\, dx = \begin{cases} 0 & \text{if } i \neq j \\ \frac{1}{2} & \text{if } i = j \end{cases}$$

$$\int_0^1 \cos\alpha_i x \cos\alpha_j x\, dx = \begin{cases} 0 & \text{if } i \neq j \\ \frac{1}{2} & \text{if } i = j \end{cases}$$

Owing to the diagonal form of the coefficient matrix (2.5.35*a*), we can readily solve for the coefficients c_{ij}:

$$c_{ij} = \frac{F_{ij}}{K_{(ij)(ij)}} = \frac{4g_0}{k} \frac{\sin\alpha_i \sin\alpha_j}{(\alpha_i^2 + \alpha_j^2)\alpha_i\alpha_j} \tag{2.5.36}$$

The one- and two-parameter Ritz solutions are (the one-parameter solution has one term but the two-parameter solution has four terms)

$$T_1 = \frac{32g_0}{k\pi^4} \cos\frac{1}{2}\pi x \cos\frac{1}{2}\pi y \tag{2.5.37}$$

$$\begin{aligned} T_2 = \frac{g_0}{k}[&0.3285 \cos\frac{1}{2}\pi x \cos\frac{1}{2}\pi y - 0.0219(\cos\frac{1}{2}\pi x \cos\frac{3}{2}\pi y \\ &+ \cos\frac{3}{2}\pi x \cos\frac{1}{2}\pi y) + 0.0041 \cos\frac{3}{2}\pi x \cos\frac{3}{2}\pi y] \end{aligned} \tag{2.5.38}$$

If algebraic polynomials are to be used in the approximation of T, we can choose $\phi_1 = (1 - x)(1 - y)$ or $\phi_1 = (1 - x^2)(1 - y^2)$, both of which satisfy the (homogeneous) essential boundary conditions. However, the choice $\phi_1 = (1 - x^2)(1 - y^2)$ also meets the natural boundary conditions of the problem. The one-parameter Ritz solution for the choice $\phi_1 = (1 - x^2)(1 - y^2)$ is

$$T_1(x, y) = \frac{5g_0}{16k}(1 - x^2)(1 - y^2) \tag{2.5.39}$$

The exact solution of Eqs. (2.5.31), (2.5.32*a*), and (2.5.32*b*) is

$$T(x, y) = \frac{g_0}{2k}\left[(1 - y^2) + 4\sum_{n=1}^{\infty} \frac{(-1)^n \cos \alpha_n y \cosh \alpha_n x}{\alpha_n^3 \cosh \alpha_n}\right] \tag{2.5.40}$$

where $\alpha_n = \frac{1}{2}(2n - 1)\pi$. The Ritz solutions (2.5.37), (2.5.38), and (2.5.39) are compared with the exact solution (2.5.40) in Fig. 2.5.2. The analytical solution is evaluated using 50 terms of the series in Eq. (2.5.40).

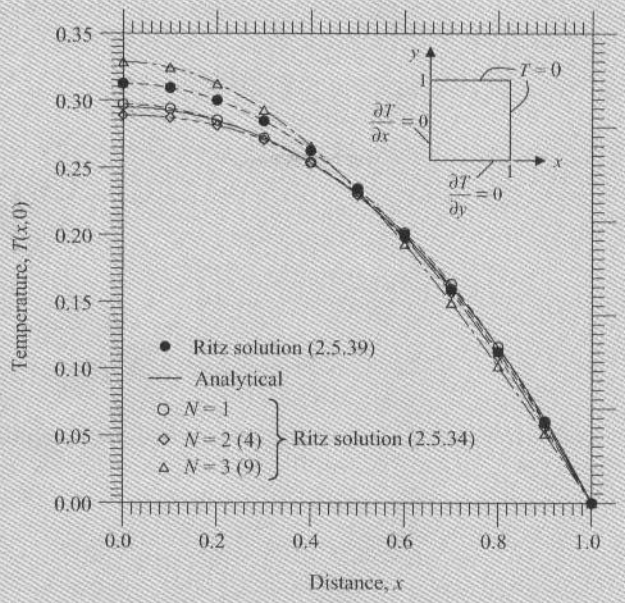

Figure 2.5.2 Comparison of the Ritz solutions with the analytical solution of the Poisson equations (2.5.31), (2.5.32*a*) and (2.5.32*b*) in two dimensions.

The next example deals with an eigenvalue problem, namely axial vibration of a bar [see Example 2.3.4 and Reddy (2002)].

Example 2.5.4

Consider a uniform cross-section bar of length L, with the left end fixed and the right end connected to a rigid support via a linear elastic spring (with spring constant k), as shown in Fig. 2.5.3. We wish to determine the first two natural axial frequencies of the bar using the Ritz method.

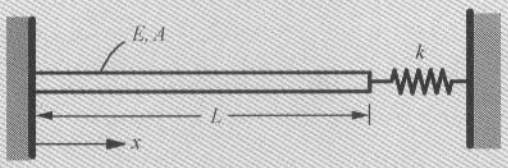

Figure 2.5.3 A uniform bar with an end spring.

The starting point is to construct the Lagrangian function $L = K - (U + V)$ (see Section 2.3.6). The kinetic energy K and the strain energy U associated with the axial motion of a bar are

$$K = \int_0^L \frac{\rho A}{2}\left(\frac{\partial u}{\partial t}\right)^2 dx, \quad U = \int_0^L \frac{EA}{2}\left(\frac{\partial u}{\partial x}\right)^2 dx + \frac{k}{2}[u(L,t)]^2 \tag{2.5.41}$$

For potential energy due to applied loads, $V = 0$.

Substituting for K and U from Eq. (2.5.41) and $V = 0$ in Hamilton's principle (2.3.60), we obtain [$\delta u(x, t_1) = \delta u(x, t_2) = 0$ and $\delta u(0, t) = 0$]

$$\begin{aligned}
0 &= \int_{t_1}^{t_2} \delta(K - U)dt \\
&= \int_{t_1}^{t_2} \delta\left\{\frac{1}{2}\int_0^L \left[\rho A\left(\frac{\partial u}{\partial t}\right)^2 - EA\left(\frac{\partial u}{\partial x}\right)^2\right]dx - \frac{k}{2}[u(L,t)]^2\right\}dt \\
&= \int_{t_1}^{t_2}\left[\int_0^L \left(\rho A\frac{\partial u}{\partial t}\frac{\partial \delta u}{\partial t} - EA\frac{\partial u}{\partial x}\frac{\partial \delta u}{\partial x}\right)dx - ku(L,t)\delta u(L,t)\right]dt \\
&= \int_{t_1}^{t_2}\left[\int_0^L \left(-\rho A\frac{\partial^2 u}{\partial t^2}\delta u - EA\frac{\partial u}{\partial x}\frac{\partial \delta u}{\partial x}\right)dx - ku(L,t)\delta u(L,t)\right]dt
\end{aligned} \tag{2.5.42}$$

The Euler–Lagrange equations associated with (2.5.42) are given by

$$\begin{aligned}
&-\rho A\frac{\partial^2 u}{\partial t^2} + \frac{\partial}{\partial x}\left(EA\frac{\partial u}{\partial x}\right) = 0, \quad 0 < x < L \\
&\left[\left(EA\frac{\partial u}{\partial x}\right) + ku(x,t)\right]_{x=L} = 0
\end{aligned} \tag{2.5.43}$$

Natural vibration is nothing but the periodic motion of the form

$$u(x,t) = u_0(x)e^{i\omega t}, \quad i = \sqrt{-1} \tag{2.5.44}$$

where ω is the frequency of natural vibration and $u_0(x)$ is the amplitude. Substituting Eq. (2.5.44) into Eq. (2.5.42), we obtain

$$0 = \int_0^L \left(\rho A\omega^2 u_0 \delta u_0 - EA\frac{du_0}{dx}\frac{d\delta u_0}{dx}\right)dx - ku_0(L)\delta u_0(L) \tag{2.5.45}$$

where $(i\omega)^2 = -\omega^2$, and $\int_{t_1}^{t_2} e^{2i\omega t}\,dt$, being nonzero, is factored out. Equation (2.5.45) is the weak form of the equations governing natural vibration of a bar with left end fixed and the right end spring supported. The Euler equation and natural boundary condition associated with Eq. (2.5.45) are

$$-\frac{d}{dx}\left(EA\frac{du_0}{dx}\right) - \rho A\omega^2 u_0 = 0, \quad 0 < x < L \tag{2.5.46a}$$

$$EA\frac{du_0}{dx} + ku_0 = 0 \quad \text{at } x = L \tag{2.5.46b}$$

The essential boundary condition is $u_0(0) = 0$. Conversely, we can use the three step procedure to obtain the weak form (2.5.45) from Eqs. (2.5.46*a*) and (2.5.46*b*).

Next, we seek a $N-$parameter Ritz approximation (obviously, $\phi_0 = 0$)

$$u_0(x) \approx U_N(x) = \sum_{i=1}^{N} c_i\phi_i(x)$$

Substituting into Eq. (2.5.45), we obtain

$$0 = \sum_{i=1}^{N}\left\{\sum_{j=1}^{N}\left[\lambda\int_0^L \rho A\phi_i\phi_j\,dx - \left(\int_0^L EA\frac{d\phi_i}{dx}\frac{d\phi_j}{dx}\,dx + k\phi_i(L)\phi_j(L)\right)\right]c_j\right\}\delta c_i$$

where $\lambda = \omega^2$. Because of the independent nature of δc_i, we obtain

$$0 = \sum_{j=1}^{N}\left[\lambda\int_0^L \rho A\phi_i\phi_j\,dx - \left(\int_0^L EA\frac{d\phi_i}{dx}\frac{d\phi_j}{dx}\,dx + k\phi_i(L)\phi_j(L)\right)\right]c_j \tag{2.5.47a}$$

and in matrix form

$$([A] - \lambda[M])\{c\} = \{0\} \quad \text{or} \quad (\mathbf{A} - \lambda\mathbf{M})\mathbf{c} = 0 \tag{2.5.47b}$$

where

$$a_{ij} = \int_0^L EA\frac{d\phi_i}{dx}\frac{d\phi_j}{dx}\,dx + k\phi_i(L)\phi_j(L), \quad m_{ij} = \int_0^L \rho A\phi_i\phi_j\,dx \tag{2.5.47c}$$

Equation (2.5.47*b*) represents a matrix eigenvalue problem, and we obtain N eigenvalues, λ_i, $i = 1, 2, \cdots, N$.

For the problem at hand, the approximation functions $\phi_i(x)$ are required to be differentiable once with respect to x and vanish at $x = 0$. Hence, we choose

$$\phi_i(x) = \left(\frac{x}{L}\right)^i \tag{2.5.48a}$$

Substituting ϕ_i from (2.5.48*a*) into (2.5.47*c*), we obtain

$$m_{ij} = \int_0^L \rho A\phi_i\phi_j\,dx = \rho AL\frac{1}{i+j+1}$$

$$a_{ij} = \int_0^L EA\frac{d\phi_i}{dx}\frac{d\phi_j}{dx}\,dx + k\phi_i(L)\phi_j(L) = \frac{EA}{L}\frac{ij}{i+j-1} + k \tag{2.5.48b}$$

Since we wish to determine two eigenvalues, we take $N=2$ and obtain

$$m_{11}=\frac{\rho AL}{3},\quad m_{12}=\frac{\rho AL}{4},\quad m_{22}=\frac{\rho AL}{5},\quad a_{11}=\frac{EA}{L}+k,\quad a_{12}=\frac{EA}{L}+k,\quad a_{22}=\frac{4EA}{3L}+k$$

and the matrix eigenvalue problem (2.5.47*b*) becomes

$$\left(\frac{EA}{3L}\begin{bmatrix}3+3\alpha & 3+3\alpha\\ 3+3\alpha & 4+3\alpha\end{bmatrix}-\lambda\frac{\rho AL}{60}\begin{bmatrix}20 & 15\\ 15 & 12\end{bmatrix}\right)\begin{Bmatrix}c_1\\ c_2\end{Bmatrix}=\begin{Bmatrix}0\\ 0\end{Bmatrix} \tag{2.5.49}$$

where $\alpha=kL/EA$. The algebraic eigenvalue problem (2.5.49) must be solved for $\lambda=\omega^2$ and c_i [hence, for the mode shape $u_0(x)$].

To carry out the remaining steps to obtain the numerical values for the natural frequencies, we take $\alpha=kL/EA=1$. Then, for a nontrivial solution (i.e., $c_1\neq 0,\quad c_2\neq 0$), we set the determinant of the coefficient matrix in Eq. (2.5.49) to zero:

$$\begin{vmatrix}2-\dfrac{\bar\lambda}{3} & 2-\dfrac{\bar\lambda}{4}\\ 2-\dfrac{\bar\lambda}{4} & \dfrac{7}{3}-\dfrac{\bar\lambda}{5}\end{vmatrix}=0,\quad \bar\lambda=\frac{\lambda\rho L^2}{E}=\frac{\omega^2\rho L^2}{E} \tag{2.5.50a}$$

or

$$15\bar\lambda^2-640\bar\lambda+2400=0$$

The quadratic equation has two roots

$$\bar\lambda_1=4.1545,\quad \bar\lambda_2=38.512\ \rightarrow\ \omega_1=\frac{2.038}{L}\sqrt{\frac{E}{\rho}},\ \omega_2=\frac{6.206}{L}\sqrt{\frac{E}{\rho}} \tag{2.5.50b}$$

The eigenvectors (or mode shapes) are given by

$$U_2^{(i)}=c_1^{(i)}\frac{x}{L}+c_2^{(i)}\frac{x^2}{L^2}$$

where $c_1^{(i)}$ and $c_2^{(i)}$ are calculated from the equations [see Eq. (2.5.49)]

$$\begin{bmatrix}2-\dfrac{\bar\lambda_i}{3} & 2-\dfrac{\bar\lambda_i}{4}\\ 2-\dfrac{\bar\lambda_i}{4} & \dfrac{7}{3}-\dfrac{\bar\lambda_i}{5}\end{bmatrix}\begin{Bmatrix}c_1^{(i)}\\ c_2^{(i)}\end{Bmatrix}=\begin{Bmatrix}0\\ 0\end{Bmatrix}$$

The above pair of equations is linearly dependent. Hence, one of the two equations can be used to determine c_2 in terms of c_1 (or vice versa) for each value of λ. We obtain

$$\bar\lambda_1=4.1545:\quad c_1^{(1)}=1.0000,\ c_2^{(1)}=-0.6399\ \rightarrow\ U_2^{(1)}(x)=\frac{x}{L}-0.6399\frac{x^2}{L^2}$$

$$\bar\lambda_2=38.512:\quad c_1^{(2)}=1.0000,\ c_2^{(2)}=-1.4207\ \rightarrow\ U_2^{(2)}(x)=\frac{x}{L}-1.4207\frac{x^2}{L^2}$$

Plots of the two mode shapes are shown in Fig. 2.5.4.

The exact values of λ are the roots of the transcendental equation (the reader may verify this)

$$\lambda+\tan\lambda=0 \tag{2.5.51a}$$

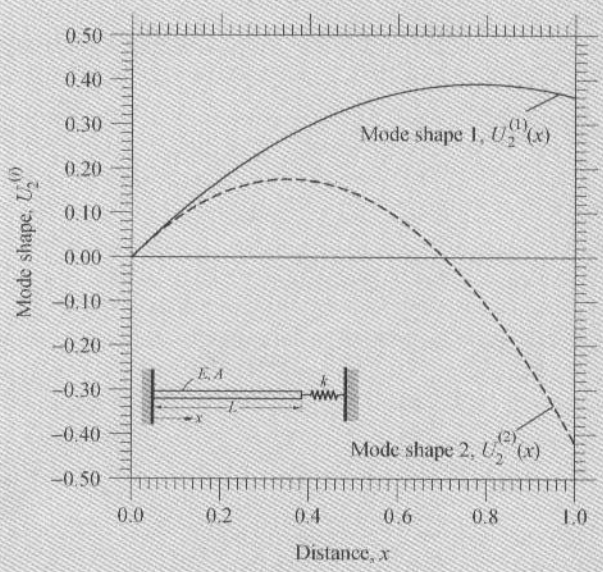

Figure 2.5.4 First two mode shapes obtained by the Ritz method for the natural longitudinal vibrations of a spring-supported bar.

whose first two roots are ($\omega^2 = \lambda$)

$$\omega_1 = \frac{2.02875}{L}\sqrt{\frac{E}{\rho}}, \quad \omega_2 = \frac{4.91318}{L}\sqrt{\frac{E}{\rho}} \tag{2.5.51b}$$

Note that the first approximate frequency is closer to the exact than the second.

If we select ϕ_0 and ϕ_i to satisfy the natural boundary condition also, the degree of polynomials will inevitably go up. For example, the lowest-order function that satisfies the homogeneous form (we still have $\phi_0 = 0$) of the natural boundary condition $u'(1) + u(1) = 0$ is

$$\hat{\phi}_1 = 3x - 2x^2$$

The one-parameter solution with the choice of $\hat{\phi}_1 = 3x - 2x^2$ gives $\lambda_1 = 50/12 = 4.1667$, which is no better than the two-parameter solution computed using $\phi_1 = x$ and $\phi_2 = x^2$. Of course, solution $c_1\hat{\phi}_1$ would yield a more accurate value for λ_1 than the solution $c_1\phi_1$. Although $c_1\hat{\phi}_1$ and $c_1\phi_1 + c_2\phi_2$ are of the same degree (polynomials), the latter gives better accuracy for λ_1 because of the number of parameters is greater, which provides greater freedom to adjust the parameters c_i in satisfying the weak form.

The eigenvalues and mode shapes determined through eigenvalue analysis are also useful in determining the transient response. The general homogeneous solution to the transient problem is [see Eq. (2.5.44)]

$$U_2(x, t) = (c_{11}\cos\omega_1 t + c_{12}\sin\omega_1 t)\,x + (c_{21}\cos\omega_2 t + c_{22}\sin\omega_2 t)\,x^2$$

where c_{1j} and c_{2j} are constants to be determined using the initial conditions.

2.5.5 The Method of Weighted Residuals

As noted in Section 2.4.2, one can always write the weighted-integral form of a differential equation, whether the equation is linear or nonlinear (in the dependent variables). The weak form can be developed if the equations are second-order or higher, even if they are nonlinear. However, it is not always possible to construct a functional $I(u)$ whose first variation is equal to the variational form, $\delta I = B(\delta u, u) - l(\delta u) = 0$. The Ritz method can be applied to all problems, including nonlinear problems, that have weak forms.

The weighted-residual method is a generalization of the Ritz method in that the weight functions can be chosen from an independent set of functions, and it requires only the weighted-integral form to determine the parameters. Since the latter form does not include any of the specified boundary conditions of the problem, the approximation functions must be selected such that the approximate solution satisfies both the natural and essential boundary conditions. In addition, the weight functions can be selected independently of the approximation functions, but are required to be linearly independent (so that the resulting algebraic equations are linearly independent).

We discuss the general method of weighted residuals first, and then consider certain special cases that are known by specific names (e.g., the Galerkin method, the collocation method, the least-squares method, and so on). Although a limited use of the weighted-residual method is made in this book (see Chapter 14), it is informative to have a knowledge of this class of methods for use in the formulation of certain nonlinear problems and non-self-adjoint problems (i.e., which do not admit a functional formulation).

The method of weighted residuals can be described in its generality by considering the operator equation

$$A(u) = f \quad \text{in} \quad \Omega \tag{2.5.52}$$

where A is an operator (linear or nonlinear), often a differential operator, acting on the dependent variable u, and f is a known function of the independent variables. Some examples of such operators are given below.

$$\begin{aligned}
&(1)\quad A(u) = -\frac{d}{dx}\left(a\frac{du}{dx}\right) + cu \\
&(2)\quad A(u) = \frac{d^2}{dx^2}\left(b\frac{d^2u}{dx^2}\right) \\
&(3)\quad A(u) = -\left[\frac{\partial}{\partial x}\left(k_x\frac{\partial u}{\partial x}\right) + \frac{\partial}{\partial y}\left(k_y\frac{\partial u}{\partial y}\right)\right] \\
&(4)\quad A(u) = -\frac{d}{dx}\left(u\frac{du}{dx}\right) \\
&(5)\quad A(u,v) = u\frac{\partial u}{\partial x} + v\frac{\partial u}{\partial y} + \frac{\partial^2 u}{\partial x^2} + \frac{\partial}{\partial y}\left(\frac{\partial u}{\partial y} + \frac{\partial v}{\partial x}\right)
\end{aligned} \tag{2.5.53}$$

For an operator A to be *linear* in its arguments, it must satisfy the relation

$$A(\alpha u + \beta v) = \alpha A(u) + \beta A(v) \tag{2.5.54}$$

for any scalars α and β and dependent variables u and v. It can be easily verified that all operators in (2.5.53), except for 4 and 5, are linear. When an operator does not satisfy the condition (2.5.54), it is said to be *nonlinear*.

The function u is not only required to satisfy the operator equation (2.5.52), it is also required to satisfy the boundary conditions associated with the operator equation. From the examples considered so far, the boundary conditions associated with the operators defined in 1, 2, and 3 of (2.5.53) are obvious (see Examples 2.4.1–2.4.3).

In the weighted-residual method, the solution u is approximated, in much the same way as in the Ritz method, by the expression

$$U_N(\mathbf{x}) = \sum_{j=1}^{N} c_j \phi_j(\mathbf{x}) + \phi_0(\mathbf{x}) \tag{2.5.55}$$

except that the requirements on ϕ_0 and ϕ_j for the weighted-residual method are more stringent than those for the Ritz method. Substitution of the approximate solution U_N into the left-hand side of (2.5.52) gives a function $A(U_N)$ that, in general, is not equal to the specified function f. The difference $A(U_N) - f$, called the *residual* of the approximation, is nonzero:

$$R \equiv A(U_N) - f = A\left(\sum_{j=1}^{N} c_j \phi_j + \phi_0\right) - f \neq 0 \tag{2.5.56a}$$

Note that the residual R is a function of position as well as of the parameters c_j. In the weighted-residual method, as the name suggests, the parameters c_j are determined by requiring the residual R to vanish in the weighted-integral sense:

$$\int_{\Omega} \psi_i(\mathbf{x}) R(\mathbf{x}, c_j)\, dx\, dy = 0 \quad (i = 1, 2, \cdots, N) \tag{2.5.56b}$$

where Ω is a two-dimensional domain and ψ_i are *weight functions,* which, in general, are not the same as the approximation functions ϕ_i. The set $\{\psi_i\}$ must be a linearly independent set; otherwise, the equations provided by (2.5.56*b*) will not be linearly independent and hence will not be solvable.

The requirements on ϕ_0 and ϕ_j for the weighted-residual method are different from those for the Ritz method, which is based on the weak (integral) form of the differential equation. The differentiability requirement on ϕ_j in the weighted-residual method is dictated by the integral statement (2.5.56*b*), as opposed to the weak form in the Ritz method. Thus, ϕ_j must have nonzero derivatives up to the order appearing in the operator equation (2.5.52). Since the weighted-integral form (2.5.56*b*) does not include any of the specified (either essential or natural) boundary conditions, we must also require U_N in (2.5.55) to satisfy all specified boundary conditions of the problem. Consequently, ϕ_0 is required to satisfy the homogeneous form of all specified boundary conditions of the problem. These requirements on ϕ_0 and ϕ_j will increase the order of the polynomial expressions used for the weighted-residual method. In general, the ϕ_j used in this method are higher-order functions than those used in the Ritz method, and the functions used in the latter may not satisfy the continuity (i.e., differentiability) requirements of the weighted-residual method. Various special cases of the weighted-residual method are discussed in the following paragraphs.

The Petrov–Galerkin Method. The weighted-residual method is referred to as the *Petrov–Galerkin method* when $\psi_i \neq \phi_i$. When the operator A is linear, (2.5.56*b*) can be simplified to the form

$$\sum_{j=1}^{N} \left[\int_\Omega \psi_i A(\phi_j)\, d\mathbf{x} \right] c_j = \int_\Omega \psi_i [f - A(\phi_0)]\, d\mathbf{x}$$

or

$$\sum_{j=1}^{N} A_{ij} c_j = F_i \quad (\mathbf{Ac} = \mathbf{F}) \tag{2.5.57}$$

Note that the coefficient matrix $[A]$ is not symmetric:

$$A_{ij} = \int_\Omega \psi_i A(\phi_j)\, d\mathbf{x} \neq A_{ji} \tag{2.5.58}$$

The Galerkin Method. If the weight function ψ_i is chosen to be equal to the approximation function ϕ_i, the weighted-residual method is better known as the Galerkin method. The algebraic equations of the Galerkin approximation are

$$\mathbf{Ac} = \mathbf{F} \tag{2.5.59a}$$

where

$$A_{ij} = \int_\Omega \phi_i A(\phi_j)\, d\mathbf{x} \quad F_i = \int_\Omega \phi_i [f - A(\phi_0)]\, d\mathbf{x} \tag{2.5.59b}$$

Once again, we note that A_{ij} is not symmetric.

In general, the Galerkin method is *not* the same as the Ritz method. This should be clear from the fact that the former uses the weighted-integral form whereas the latter uses the weak (or variational) form to determine the coefficients c_j. Consequently, the approximation functions used in the Galerkin method are required to be of higher order than those in the Ritz method.

If the equation permits, and one wishes, differentiation from the dependent variable(s) can be transferred to the weight function $w = \phi_i$, thereby obtaining the weak form. Then there is no difference between the Galerkin method and the Ritz method. Thus, Ritz and Galerkin methods yield the same solutions in two cases: (*a*) when the specified boundary conditions of the problem are all of the essential type, and therefore the requirements on ϕ_i in the two methods become the same and the weighted-integral form reduces to the weak form; and (*b*) when the approximation functions of the Galerkin method are used in the Ritz method.

The Least-Squares Method. In least-squares method, we determine the parameters c_j by minimizing the integral of the square of the residual (2.5.56*a*):

$$\frac{\partial}{\partial c_i} \int_\Omega R^2(\mathbf{x}, c_j)\, d\mathbf{x} = 0$$

or

$$\int_\Omega \frac{\partial R}{\partial c_i} R\, d\mathbf{x} = 0 \tag{2.5.60a}$$

Comparison of (2.5.60*a*) with (2.5.56*b*) shows that $\psi_i = \partial R/\partial c_i$. If A is a linear operator, $\psi_i = A(\phi_i)$, and (2.5.60*a*) becomes

$$\sum_{j=1}^{N} \left[\int_\Omega A(\phi_i) A(\phi_j)\, d\mathbf{x} \right] c_j = \int_\Omega A(\phi_i)[f - A(\phi_0)]\, d\mathbf{x}$$

or

$$\mathbf{Ac} = \mathbf{F} \tag{2.5.60b}$$

where

$$A_{ij} = \int_\Omega A(\phi_i) A(\phi_j)\, d\mathbf{x}, \quad F_i = A(\phi_i)[f - A(\phi_0)]\, d\mathbf{x} \tag{2.5.60c}$$

Note that the coefficient matrix A_{ij} is symmetric, but it involves the same order of differentiation as in the governing differential equation $A(u) - f = 0$.

The Collocation Method. In the collocation method, we seek an approximate solution U_N to (2.5.52) in the form of (2.5.55) by requiring the residual to vanish identically at N selected points $\mathbf{x}^i \equiv (x^i, y^i, z^i)$ $(i = 1, 2, \ldots, N)$ in the domain Ω

$$R(\mathbf{x}^i, c_j) = 0 \quad (i = 1, 2, \ldots, N) \tag{2.5.61}$$

The selection of the points $\mathbf{x}^i$ is crucial in obtaining a well-conditioned system of equations and ultimately in obtaining an accurate solution. The collocation method can be shown to be a special case of (2.5.56*b*) with $\psi_i = \delta(\mathbf{x} - \mathbf{x}^i)$, where $\delta(\mathbf{x})$ is the Dirac delta function, which is defined by

$$\int_\Omega f(\mathbf{x}) \delta(\mathbf{x} - \xi)\, d\mathbf{x} = f(\xi) \tag{2.5.62}$$

With this choice of weight functions, the weighted-residual statement (2.5.56*b*) becomes

$$\int_\Omega \delta(\mathbf{x} - \mathbf{x}^i) R(\mathbf{x}, c_j)\, d\mathbf{x} = 0$$

or

$$R(\mathbf{x}^i, c_j) = 0 \tag{2.5.63}$$

We consider an example to illustrate the use of various types of weighted-residual methods.

Example 2.5.5

Consider the differential equation (see Example 2.5.1 with Set 2 boundary conditions):

$$-\frac{d^2u}{dx^2} - u + x^2 = 0, \quad u(0) = 0, \quad u'(1) = 1 \tag{2.5.64}$$

For a weighted-residual method, ϕ_0 and ϕ_i should satisfy the following conditions:

$\phi_0(0) = 0$, $\phi_0'(1) = 1$ (satisfy actual boundary conditions)
$\phi_i(0) = 0$, $\phi_i'(1) = 0$ (satisfy homogeneous form of the specified boundary conditions)

For a choice of algebraic polynomials, we assume $\phi_0(x) = a + bx$ and use the two conditions on ϕ_0 to determine the constants a and b. We obtain

$$\phi_0(x) = x$$

Since there are two homogeneous conditions, we must assume at least a three-parameter polynomial to obtain a nonzero function, $\phi_1 = a + bx + cx^2$. Using the conditions on ϕ_i, we obtain

$$\phi_1 = cx(2 - x)$$

The constant c can be set equal to unity because it will be absorbed into the parameter c_1. For ϕ_2, we can assume one of the forms

$$\phi_2 = a + bx + dx^3 \quad \text{or} \quad \phi_2 = a + cx^2 + dx^3$$

with $d \neq 0$; ϕ_2 does not contain all-order terms in either case, but the approximate solution is complete because $\{\phi_1, \phi_2\}$ contains all terms up to degree three. For the second choice of ϕ_2, we obtain

$$\phi_2 = x^2\left(1 - \frac{2}{3}x\right)$$

The residual in the approximation of the equation is

$$\begin{aligned} R &= -\left(0 + \sum_{i=1}^{N} c_i \frac{d^2\phi_i}{dx^2}\right) - \left(\phi_0 + \sum_{i=1}^{N} c_i\phi_i\right) + x^2 \\ &= c_1(2 - 2x + x^2) + c_2\left(-2 + 4x - x^2 + \frac{2}{3}x^3\right) - x + x^2 \end{aligned} \tag{2.5.65}$$

We next consider various methods.

The Petrov–Galerkin Method. Let the weight functions be

$$\psi_1 = x, \quad \psi_2 = x^2 \tag{2.5.66}$$

Then

$$\int_0^1 xR\,dx = 0, \quad \int_0^1 x^2R\,dx = 0$$

or

$$\frac{7}{12}c_1 + \frac{13}{60}c_2 - \frac{1}{12} = 0, \quad \frac{11}{30}c_1 + \frac{11}{45}c_2 - \frac{1}{20} = 0 \tag{2.5.67}$$

Solving for c_i, we obtain $c_1 = \frac{103}{682}$ and $c_2 = -\frac{15}{682}$; the solution becomes

$$U_{PG} = 1.302053x - 0.173021x^2 - 0.014663x^3 \tag{2.5.68}$$

The Galerkin Method. Taking $\psi_i = \phi_i$, we have

$$\int_0^1 x(2 - x)R\,dx = 0, \quad \int_0^1 x^2\left(1 - \frac{2}{3}x\right)R\,dx = 0$$

or

$$\frac{4}{5}c_1 + \frac{28}{45}c_2 - \frac{7}{60} = 0, \quad \frac{17}{90}c_1 + \frac{29}{315}c_2 - \frac{1}{36} = 0 \tag{2.5.69}$$

Hence, the solution becomes (with $c_1 = \frac{623}{4306}$, $c_2 = \frac{21}{4306}$),

$$U_G = 1.2894x - 0.1398x^2 - 0.00325x^3 \tag{2.5.70}$$

The Least-Squares Method. Taking $\psi_i = \frac{\partial R}{\partial c_i}$, we have

$$\int_0^1 (2 - 2x + x^2) R\, dx = 0, \quad \int_0^1 \left(-2 + 4x - x^2 + \frac{2}{3}x^3 \right) R\, dx = 0$$

or

$$\frac{28}{15}c_1 - \frac{47}{90}c_2 - \frac{13}{60} = 0, \quad -\frac{47}{90}c_1 + \frac{253}{315}c_2 - \frac{1}{36} = 0 \tag{2.5.71}$$

The least-squares solution is given by (with $c_1 = \frac{1292}{9935}$, $c_2 = \frac{991}{19870}$),

$$U_{LS} = 1.2601x - 0.08017x^2 - 0.03325x^3 \tag{2.5.72}$$

The Collocation Method. Choosing the points $x = \frac{1}{3}$ and $x = \frac{2}{3}$ as the collocation points, we evaluate the residuals at these points and set them equal to zero:

$$\begin{aligned} R\left(\frac{1}{3}\right) = 0: &\quad 117c_1 - 61c_2 = 18 \\ R\left(\frac{2}{3}\right) = 0: &\quad 90c_1 - 34c_2 = 18 \end{aligned} \tag{2.5.73}$$

The solution is given by ($c_1 = 1710/9468$, $c_2 = 486/9468$)

$$U_C = 1.3612x - 0.12927x^2 - 0.03422x^3 \tag{2.5.74}$$

The four approximate solutions are compared in Table 2.5.3 with the exact solution (2.5.21). For this problem, the Petrov–Galerkin method gives the most accurate solution.

Table 2.5.3 Comparison of the Ritz, weighted-residual, and exact solutions[1] of the boundary value problem in Example 2.5.5.

x	u_{exact}	U_R	U_{PG}	U_G	U_{LS}	U_C
0.0	0.0000	0.0000	0.0000	0.0000	0.0000	0.0000
0.1	0.1262	0.1280	0.1285	0.1275	0.1252	0.1348
0.2	0.2513	0.2529	0.2536	0.2523	0.2485	0.2668
0.3	0.3742	0.3749	0.3754	0.3741	0.3699	0.3958
0.4	0.4943	0.4938	0.4941	0.4932	0.4891	0.5216
0.5	0.6112	0.6097	0.6096	0.6093	0.6058	0.6440
0.6	0.7244	0.7226	0.7221	0.7226	0.7200	0.7628
0.7	0.8340	0.8324	0.8317	0.8329	0.8314	0.8778
0.8	0.9402	0.9393	0.9384	0.9404	0.9397	0.9887
0.9	1.0433	1.0431	1.0424	1.0448	1.0449	1.0954
1.0	1.1442	1.1439	1.1437	1.1463	1.1467	1.1977

[1] Subscripts are as follows: R, Ritz; PG, Petrov–Galerkin; G, Galerkin; LS, least-squares; C, collocation.

2.6 SUMMARY

In this chapter, we have studied two major topics that are of immediate interest in the study of finite element method in the forthcoming chapters:

1. Weighted-integral and weak formulations of differential equations
2. Solution of boundary value problems by the Ritz and weighted-residual (e.g., the Galerkin, least-squares, and collocation) methods

The weighted-integral statements are required in order to generate the necessary and sufficient number of algebraic equations to solve for the parameters c_i in the approximate solution. Thus, the algebraic equations are equivalent to minimizing, in a weighted-integral sense, the error introduced in the approximation of the differential equation.

In studying the two topics, a three-step procedure for developing the weak form of differential equations is presented, and methods for obtaining algebraic equations in terms of the unknown parameters in the approximate solution are developed. These topics are immediately applicable in the finite element method, which is an elementwise application of a variational method. Thus, the material covered in this chapter forms the core of the finite element method. A few remarks are in order on the classical variational methods studied here.

- The traditional variational methods (e.g., Ritz, Galerkin, and least-squares) presented in Section 2.5 provide a simple means of finding spatially continuous approximate solutions to physical problems. The approximate solutions obtained via these methods are continuous functions of position in the domain.
- The main limitation of classical variational methods that prevents them from being competitive with traditional finite difference methods is the difficulty encountered in constructing the approximation functions. The construction process becomes more difficult when the domain is geometrically complex. The so-called "meshless methods" are a return to the classical variational methods but with a procedure to construct the approximation functions.
- From the preceding discussion, it is apparent that the variational methods can provide a powerful means of finding approximate solutions, provided one can find a way to systematically construct approximation functions, for almost any geometry, that depend only on the differential equation being solved and not on the boundary conditions of the problem. This property enables one to develop a computer program for a particular class of problem (each problem in the class differs from the others only in the data), i.e., a *general-purpose* computer program. Since the functions must be constructed for a geometrically complex domain, it seems that (recall the discussion of the method of composites for the determination of the center of mass of an irregular shape from Chapter 1) the region must be represented (or approximated if required) as an assemblage of simple geometric shapes for which the construction of approximation functions becomes simpler. The finite element method to be discussed in the forthcoming chapters is based on these ideas.
- In the finite element method, a given domain is represented (discretized) by a collection of geometrically simple shapes (elements), and on each element of the collection, the governing equation is *formulated* using any one of the variational methods. The approximation functions are systematically generated for each (typical) element using the

essential boundary conditions. The elements are *connected* together by imposing the continuity of the dependent variables across the interelement boundaries.

The remaining chapters of this book are devoted to the introduction of the finite element method and its use in the analysis of several model differential equations representing mathematical models for many physical processes.

PROBLEMS

In Problems 2.1–2.5, construct the weak forms and, whenever possible, quadratic functionals.

2.1 A nonlinear equation:

$$-\frac{d}{dx}\left(u\frac{du}{dx}\right)+f=0 \quad \text{for} \quad 0<x<L$$

$$\left(u\frac{du}{dx}\right)\Big|_{x=0}=0 \quad u(1)=\sqrt{2}$$

2.2 The Euler-Bernoulli-von Kármán nonlinear theory of beams:

$$-\frac{d}{dx}\left\{EA\left[\frac{du}{dx}+\frac{1}{2}\left(\frac{dw}{dx}\right)^2\right]\right\}=f \quad \text{for} \quad 0<x<L$$

$$\frac{d^2}{dx^2}\left(EI\frac{d^2w}{dx^2}\right)-\frac{d}{dx}\left\{a\frac{dw}{dx}\left[\frac{du}{dx}+\frac{1}{2}\left(\frac{dw}{dx}\right)^2\right]\right\}=q$$

$$u=w=0 \quad \text{at} \quad x=0,\ L; \quad \left(\frac{dw}{dx}\right)\Big|_{x=0}=0; \quad \left(EI\frac{d^2w}{dx^2}\right)\Big|_{x=L}=M_0$$

where EA, EI, f, and q are functions of x, and M_0 is a constant. Here u denotes the axial displacement and w the transverse deflection of the beam.

2.3 A second-order equation:

$$-\frac{\partial}{\partial x}\left(a_{11}\frac{\partial u}{\partial x}+a_{12}\frac{\partial u}{\partial y}\right)-\frac{\partial}{\partial y}\left(a_{21}\frac{\partial u}{\partial x}+a_{22}\frac{\partial u}{\partial y}\right)+f=0 \quad \text{in} \quad \Omega$$

$$u=u_0 \ \text{ on } \Gamma_1, \quad \left(a_{11}\frac{\partial u}{\partial x}+a_{12}\frac{\partial u}{\partial y}\right)n_x+\left(a_{21}\frac{\partial u}{\partial x}+a_{22}\frac{\partial u}{\partial y}\right)n_y=t_0 \ \text{ on } \Gamma_2$$

where $a_{ij}=a_{ji}$ $(i,j=1,2)$ and f are given functions of position (x, y) in a two-dimensional domain Ω, and u_0 and t_0 are known functions on portions Γ_1 and Γ_2 of the boundary Γ: $\Gamma_1+\Gamma_2=\Gamma$.

2.4 Navier-Stokes equations for two-dimensional flow of viscous, incompressible fluids:

$$\left.\begin{aligned} u\frac{\partial u}{\partial x}+v\frac{\partial u}{\partial y}&=-\frac{1}{\rho}\frac{\partial P}{\partial x}+\nu\left(\frac{\partial^2 u}{\partial x^2}+\frac{\partial^2 u}{\partial y^2}\right)\\ u\frac{\partial v}{\partial x}+v\frac{\partial v}{\partial y}&=-\frac{1}{\rho}\frac{\partial P}{\partial y}+\nu\left(\frac{\partial^2 v}{\partial x^2}+\frac{\partial^2 v}{\partial y^2}\right)\\ \frac{\partial u}{\partial x}+\frac{\partial v}{\partial y}&=0 \end{aligned}\right\} \quad \text{in} \quad \Omega \qquad (1)$$

$$u = u_0, \quad v = v_0 \quad \text{on} \quad \Gamma_1 \tag{2}$$

$$\left.\begin{aligned} \nu\left(\frac{\partial u}{\partial x}n_x + \frac{\partial u}{\partial y}n_y\right) - \frac{1}{\rho}Pn_x = \hat{t}_x \\ \nu\left(\frac{\partial v}{\partial x}n_x + \frac{\partial v}{\partial y}n_y\right) - \frac{1}{\rho}Pn_y = \hat{t}_y \end{aligned}\right\} \quad \text{on} \quad \Gamma_2 \tag{3}$$

2.5 Two-dimensional flow of viscous, incompressible fluids (stream function–vorticity formulation):

$$\left.\begin{aligned} -\nabla^2\psi - \zeta = 0 \\ -\nabla^2\zeta + \frac{\partial\psi}{\partial x}\frac{\partial\zeta}{\partial y} - \frac{\partial\psi}{\partial y}\frac{\partial\zeta}{\partial x} = 0 \end{aligned}\right\} \quad \text{in} \quad \Omega$$

Assume that all essential boundary conditions are specified to be zero.

2.6 Compute the coefficient matrix and the right-hand side of the N-parameter Ritz approximation of the equation

$$-\frac{d}{dx}\left[(1+x)\frac{du}{dx}\right] = 0 \quad \text{for} \quad 0 < x < 1$$
$$u(0) = 0, \quad u(1) = 1$$

Use algebraic polynomials for the approximation functions. Specialize your result for $N = 2$ and compute the Ritz coefficients. *Answer:* $c_1 = \frac{55}{131}$ and $c_2 = -\frac{20}{131}$.

2.7 Use trigonometric functions for the two-parameter approximation of the equation in Problem 2.6 and obtain the Ritz coefficients.

2.8 A steel rod of diameter $d = 2$ cm, length $L = 25$ cm, and thermal conductivity $k = 50$ W/(m · °C) is exposed to ambient air $T_\infty = 20$°C with a heat-transfer coefficient $\beta = 64$ W/(m^2 · °C). Given that the left end of the rod is maintained at a temperature of $T_0 = 120$°C and the other end is exposed to the ambient temperature, determine the temperature distribution in the rod using a two-parameter Ritz approximation with polynomial approximation functions. The equation governing the problem is given by

$$-\frac{d^2\theta}{dx^2} + c\theta = 0 \quad \text{for} \quad 0 < x < 25 \text{ cm}$$

where $\theta = T - T_\infty$, T is the temperature, and c is given by

$$c = \frac{\beta P}{Ak} = \frac{\beta\pi D}{\frac{1}{4}\pi D^2 k} = \frac{4\beta}{kD} = 256/\text{m}^2$$

P being the perimeter and A the cross-sectional area of the rod. The boundary conditions are

$$\theta(0) = T(0) - T_\infty = 100°\text{C}, \quad \left(k\frac{d\theta}{dx} + \beta\theta\right)\Big|_{x=L} = 0$$

Answer: For $L = 0.25$ m, $\phi_0 = 100$, $\phi_i = x^i$, the Ritz coefficients are $c_1 = -1,033.385$ and $c_2 = 2,667.261$.

2.9 Set up the equations for the N-parameter Ritz approximation of the following equations associated with a simply supported beam and subjected to a uniform transverse load $q = q_0$:

$$\frac{d^2}{dx^2}\left(EI\frac{d^2w}{dx^2}\right) = q_0 \quad \text{for} \quad 0 < x < L$$

$$w = EI\frac{d^2w}{dx^2} = 0 \quad \text{at} \quad x = 0,\ L$$

(a) Use algebraic polynomials.

(b) Use trigonometric functions.

Compare the two-parameter Ritz solutions with the exact solution. *Answer:* (a) $c_1 = q_0L^2/(24EI)$ and $c_2 = 0$.

2.10 Repeat Problem 2.9 for $q = q_0 \sin(\pi x/L)$. *Answer:* $N = 2$: $c_1 = c_2L = 2q_0L^2/(3EI\pi^3)$.

2.11 Repeat Problem 2.9 for $q = Q_0\delta(x - \frac{1}{2}L)$, where $\delta(x)$ is the Dirac delta function (i.e., a point load Q_0 is applied at the center of the beam).

2.12 Develop the N-parameter Ritz solution for a simply supported beam under uniform transverse load using Timoshenko beam theory. The governing equations are given in Eqs. (2.4.32a) and (2.4.32b). Use Trigonometric functions to approximate w and Ψ.

2.13 Solve the Poisson equation governing heat conduction in a square region:

$$-k\nabla^2 T = g_0$$

$$T = 0 \quad \text{on sides} \quad x = 1 \quad \text{and} \quad y = 1$$

$$\frac{\partial T}{\partial n} = 0 \quad \text{(insulated) on sides} \quad x = 0 \quad \text{and} \quad y = 0$$

using a one-parameter Ritz approximation of the form

$$T_1(x, y) = c_1(1 - x^2)(1 - y^2)$$

Answer: $c_1 = \frac{5g_0}{16k}$.

2.14 Determine ϕ_i for a two-parameter Galerkin approximation with algebraic approximation functions for Problem 2.8.

2.15 Consider the (Neumann) boundary value problem

$$-\frac{d^2u}{dx^2} = f \quad \text{for} \quad 0 < x < L$$

$$\left(\frac{du}{dx}\right)\Big|_{x=0} = \left(\frac{du}{dx}\right)\Big|_{x=L} = 0$$

Find a two-parameter Galerkin approximation of the problem using trigonometric approximation functions, when (a) $f = f_0 \cos(\pi x/L)$ and (b) $f = f_0$. *Answer:* (a) $\phi_i = \cos(i\pi x/L)$, $c_1 = f_0L^2/\pi^2$, $c_i = 0$ for $i \neq 1$.

2.16 Find a one-parameter approximate solution of the nonlinear equation

$$-2u\frac{d^2u}{dx^2} + \left(\frac{du}{dx}\right)^2 = 4 \quad \text{for} \quad 0 < x < 1$$

subject to the boundary conditions $u(0) = 1$ and $u(1) = 0$, and compare it with the exact solution $u_0 = 1 - x^2$. Use (a) the Galerkin method, (b) the least-squares method, and (c) the Petrov–Galerkin method with weight function $w = 1$. *Answer:* (a) $(c_1)_1 = 1$, and $(c_1)_2 = -3$.

2.17 Give a one-parameter Galerkin solution of the equation

$$-\nabla^2 u = 1 \quad \text{in} \quad \Omega \quad (= \text{unit square})$$
$$u = 0 \quad \text{on} \quad \Gamma$$

Use (*a*) algebraic and (*b*) trigonometric approximation functions.
Answer: (*b*) $c_{ij} = \frac{16}{\pi^4} \frac{1}{ij(i^2+j^2)}$ $(i, j \quad \text{odd})$, $\phi_{ij} = \sin i\pi x \sin j\pi y$

2.18 Repeat Problem 2.17(*a*) for an equilateral triangular domain. *Hint:* Use the product of equations of the lines representing the sides of the triangle for the approximation function.
Answer: $c_1 = -\frac{1}{2}$.

2.19 Consider the differential equation

$$-\frac{d^2u}{dx^2} = \cos \pi x \quad \text{for} \quad 0 < x < 1$$

subject to the following three sets of boundary conditions:

(1) $u(0) = 0, \quad u(1) = 0$

(2) $u(0) = 0, \quad \left(\frac{du}{dx}\right)\Big|_{x=1} = 0$

(3) $\left(\frac{du}{dx}\right)\Big|_{x=0} = 0, \quad \left(\frac{du}{dx}\right)\Big|_{x=1} = 0$

Determine a three-parameter solution, with trigonometric functions, using (*a*) the Ritz method, (*b*) the least-squares method, and (*c*) collocation at $x = \frac{1}{4}, \frac{1}{2}$, and $\frac{3}{4}$, and compare with the exact solutions:

(1) $u_0 = \pi^{-2}(\cos \pi x + 2x - 1)$

(2) $u_0 = \pi^{-2}(\cos \pi x - 1)$

(3) $u_0 = \pi^{-2} \cos \pi x$

Answer: (1*a*) $c_i = \frac{4}{\pi^5 i(i^2-1)}$.

2.20 Consider a cantilever beam of variable flexural rigidity, $EI = a_0[2 - (x/L)^2]$ and carrying a distributed load, $q = q_0[1 - (x/L)]$. Find a three-parameter solution using $\phi_i = X^{(i+1)}$ and the collocation method. *Answer:* $c_1 = -\frac{q_0 L^2}{4a_0}$, $c_2 = \frac{q_0 L}{12a_0}$, and $c_3 = 0$.

2.21 Consider the problem of finding the fundamental frequency of a circular membrane of radius a, fixed at its edge. The governing equation for axisymmetric vibration is

$$-\frac{1}{r}\frac{d}{dr}\left(r\frac{du}{dr}\right) - \lambda u = 0, \quad 0 < r < a$$

where λ is the frequency parameter and u is the deflection of the membrane. (*a*) Determine the trigonometric approximation functions for the Galerkin method, (*b*) use one-parameter Galerkin approximation to determine λ, and (*c*) use two-parameter Galerkin approximation to determine λ. *Answer:* $\lambda = 5.832/a^2$.

2.22 Find the first two eigenvalues associated with the differential equation

$$-\frac{d^2u}{dx^2} = \lambda u, \; 0 < x < 1$$
$$u(0) = 0, \; u(1) + u'(1) = 0$$

Use the least-squares method with algebraic polynomials. Use the operator definition to be $A = -(d^2/dx^2)$ to avoid increasing the degree of the characteristic polynomial for λ. *Answer:* $\lambda_1 = 4.212$ and $\lambda_2 = 34.188$.

2.23 Repeat Problem 2.22 using the Ritz method with algebraic polynomials. *Answer:* $\lambda_1 = 4.1545$ and $\lambda_2 = 38.512$.

2.24 Consider the Poisson equation

$$-\nabla^2 u = 0, \quad 0 < x < 1, \quad 0 < y < \infty$$
$$u(0, y) = u(1, y) = 0 \quad \text{for} \quad y > 0$$
$$u(x, 0) = x(1 - x), \quad u(x, \infty) = 0, \quad 0 \le x \le 1$$

Assuming an approximation of the form

$$u(x, y) = c_1(y)x(1 - x)$$

find the differential equation for $c_1(y)$ and solve it exactly. *Answer:* $U_1(x, y) = (x - x^2)e^{-\sqrt{10}y}$.

REFERENCES FOR ADDITIONAL READING

1. Aris, R., *Vectors, Tensors, and the Basic Equations of Fluid Mechanics*, Dover Publications, New York, 1989.
2. Becker, M., *The Principles and Applications of Variational Methods*, MIT Press, Cambridge, MA, 1964.
3. Biot, M. A., *Variational Principles in Heat Transfer*, Clarendon, London, 1972.
4. Forray, M. J., *Variational Calculus in Science and Engineering*, McGraw-Hill, New York, 1968.
5. Gantmacher, F. R., *The Theory of Matrices*, Chelsea, New York, 1959.
6. Graham, A., *Matrix Theory and Applications for Engineers and Mathematicians*, Halsted Press, New York, 1979.
7. Hildebrand, F. B., *Methods of Applied Mathematics*, 2nd ed., Prentice-Hall, New York, 1965.
8. Jeffreys, H., *Cartesian Tensors*, Cambridge University Press, London, 1965.
9. Lanczos, C., *The Variational Principles of Mechanics*, 4th ed., The University of Toronto Press, Toronto, 1970; reproduced by Dover Publications, New York, 1986.
10. Langhaar, H. L., *Energy Methods in Applied Mechanics*, John Wiley, New York, 1962.
11. Leipholz, H., *Direct Variational Methods and Eigenvalue Problems in Engineering*, Noordhoff, Leyden, 1977.
12. Lippmann, H., *Extremum and Variational Principles in Mechanics*, Springer-Verlag, New York, 1972.
13. Mikhlin, S. G., *Variational Methods in Mathematical Physics*, Pergamon Press, New York, 1964.
14. Mikhlin, S. G., *The Numerical Performance of Variational Methods*, Wolters-Noordhoff, Groningen, 1971.
15. Oden, J. T. and Reddy, J. N., *Variational Methods in Theoretical Mechanics*, 2nd ed., Springer-Verlag, New York, 1983.
16. Reddy, J. N., *Applied Functional Analysis and Variational Methods in Engineering*, McGraw-Hill, New York, 1986; Krieger, Melbourne, FL, 1991.
17. Reddy, J. N., *Energy Principles and Variational Methods in Applied Mechanics*, 2nd ed., John Wiley, New York, 2002.
18. Reddy, J. N. and Rasmussen, M. L., *Advanced Engineering Analysis*, John Wiley, New York, 1982; Krieger, Melbourne, FL, 1990.
19. Rektorys, K., *Variational Methods in Mathematics, Science and Engineering*, Reidel, Boston, 1977.
20. Washizu, K., *Variational Methods in Elasticity and Plasticity*, 3rd ed., Pergamon Press, New York, 1982.
21. Weinstock, R., *Calculus of Variations with Applications to Physics and Engineering*, McGraw-Hill, New York, 1952.
22. Wrede, R. C., *Introduction to Vector and Tensor Analysis*, Dover Publications, New York, 1972.

Chapter 3

SECOND-ORDER DIFFERENTIAL EQUATIONS IN ONE DIMENSION: FINITE ELEMENT MODELS

3.1 BACKGROUND

The traditional variational methods (e.g., the Ritz, Galerkin, and least-squares) described in Chapter 2 cease to be effective because of a serious shortcoming, namely, the difficulty in constructing the approximation functions. The approximation functions, apart from satisfying continuity, linear independence, completeness, and essential boundary conditions, are arbitrary; the selection becomes even more difficult when the given domain is geometrically complex. Since the quality of the approximation is directly affected by the choice of the approximation functions, it is discomforting to know that there exists no systematic procedure to construct them. Because of this shortcoming, despite the simplicity in obtaining approximate solutions, the traditional variational methods of approximation were never regarded as competitive computationally when compared with traditional finite difference schemes. The finite element method overcomes the shortcomings of the traditional variational methods by providing a systematic way of constructing the approximation functions.

Ideally speaking, an effective computational method should have the following features:

1. It should have a sound mathematical as well as physical basis (i.e., yield convergent solutions and be applicable to practical problems).
2. It should not have limitations with regard to the geometry, the physical composition of the domain, or the nature of the "loading."
3. The formulative procedure should be independent of the shape of the domain and the specific form of the boundary conditions.
4. It should be flexible enough to allow different degrees of approximation without reformulating the entire problem.
5. It should involve a systematic procedure that can be automated for use on digital computers.

The finite element method is a technique in which a given domain is represented as a collection of simple domains, called *finite elements*, so that it is possible to systematically construct the approximation functions needed in a variational or weighted-residual approximation of the solution of a problem over each element. Thus, the finite element method differs from the traditional Ritz, Galerkin, least-squares, collocation, and other weighted-residual methods in the manner in which the approximation functions are constructed. But this difference is responsible for the following three basic features of the finite element method:

1. *Division of whole domain into subdomains* that enable a systematic derivation of the approximation functions as well as representation of complex domains.
2. *Derivation of approximation functions* over each element. The approximation functions are often algebraic polynomials that are derived using interpolation theory. However, approximation functions need not be polynomials (like in meshless form of the finite element method).
3. *Assembly of elements* is based on continuity of the solution and balance of internal fluxes; the assemblage of elements results in a numerical analog of the mathematical model of the problem being analyzed.

These three features, which constitute three major steps of the finite element formulation, are closely related. The geometry of the elements used to represent the domain of a problem should be such that the approximation functions can be uniquely derived. The approximation functions depend not only on the geometry but also on the number and location of points, called nodes, in the element and the quantities to be interpolated (e.g., solution, or solution and its derivatives). Once the approximation functions have been derived, the procedure to obtain algebraic relations among the unknown coefficients (which give the values of the dependent variable at the nodes) is exactly the same as that used in the Ritz and weighted-residual methods. Hence, a study of Chapter 2, especially the weak-form development and the Ritz method, makes the present study easier.

The finite element method not only overcomes the shortcomings of the traditional variational methods, but it is also endowed with the features of an effective computational technique. The basic steps involved in the finite element analysis of a problem are given in Table 3.1.1.

In the sections that follow, our objective is to introduce many fundamental ideas that form the basis of the finite element method. In doing so, we postpone some issues of practical and theoretical complexity to later sections of this chapter and to Chapters 4–14. The basic steps of a finite element analysis are introduced via a model second-order differential equation.

3.2 BASIC STEPS OF FINITE ELEMENT ANALYSIS

3.2.1 Model Boundary Value Problem

Consider the problem of finding the function $u(x)$ that satisfies the differential equation

$$-\frac{d}{dx}\left(a\frac{du}{dx}\right)+cu-f=0 \quad \text{for} \quad 0<x<L \tag{3.2.1}$$

Table 3.1.1 Steps involved in the finite element analysis of a typical problem.

1. Discretization (or representation) of the given domain into a collection of preselected finite elements. (This step can be postponed until the finite element formulation of the equation is completed.)
   (*a*) Construct the finite element mesh of preselected elements.
   (*b*) Number the nodes and the elements.
   (*c*) Generate the geometric properties (e.g., coordinates and cross-sectional areas) needed for the problem.
2. Derivation of element equations for all typical elements in the mesh.
   (*a*) Construct the variational formulation of the given differential equation over the typical element.
   (*b*) Assume that a typical dependent variable u is of the form

$$u = \sum_{i=1}^{n} u_i \psi_i$$

   and substitute it into Step 2*a* to obtain element equations in the form

$$[K^e]\{u^e\} = \{F^e\}$$

   (*c*) Select, if already available in the literature, or derive element interpolation functions ψ_i and compute the element matrices.
3. Assembly of element equations to obtain the equations of the whole problem.
   (*a*) Identify the interelement continuity conditions among the primary variables (relationship between the local degrees of freedom and the global degrees of freedom—connectivity of elements) by relating element nodes to global nodes.
   (*b*) Identify the "equilibrium" conditions among the secondary variables (relationship between the local source or force components and the globally specified source components).
   (*c*) Assemble element equations using Steps 3*a* and 3*b*.
4. Imposition of the boundary conditions of the problem.
   (*a*) Identify the specified global primary degrees of freedom.
   (*b*) Identify the specified global secondary degrees of freedom (if not already done in Step 3*b*).
5. Solution of the assembled equations.
6. Postprocessing of the results.
   (*a*) Compute the gradient of the solution or other desired quantities from the primary degrees of freedom computed in Step 5.
   (*b*) Represent the results in tabular and/or graphical form.

and the boundary conditions

$$u(0) = u_0, \quad \left(a\frac{du}{dx}\right)\bigg|_{x=L} = Q_0 \tag{3.2.2}$$

where $a = a(x)$, $c = c(x)$, $f = f(x)$, and u_0, and Q_0 are the *data* (i.e., known quantities) of the problem. Equation (3.2.1) arises in connection with the analytical description of many physical processes. For example, conduction and convection heat transfer in a plane wall or fin [see Fig. 3.2.1(*a*)], flow through channels and pipes, transverse deflection of cables, axial deformation of bars [see Fig. 3.2.1(*b*)], and many other physical processes are described by Eq. (3.2.1). A list of field problems described by Eq. (3.2.1) when $c(x) = 0$ are presented in Table 3.2.1 [see Reddy (2004)]. Thus, if we can develop a numerical procedure by which Eq. (3.2.1) can be solved for all possible boundary conditions, the procedure can be used to solve all field problems listed in Table 3.2.1, as well as many others. This fact provides us with the motivation to use (3.2.1) as the model second-order equation in one dimension. A step-by-step procedure for the formulation and solution of (3.2.1) by the

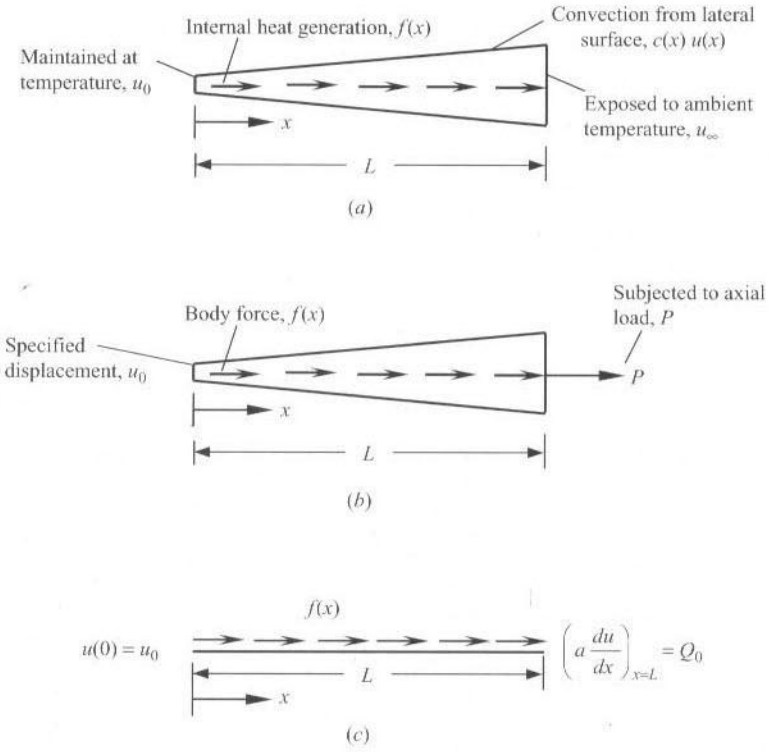

Figure 3.2.1 (a) Heat transfer in a fin. (b) Axial deformation of a bar. (c) Mathematical idealization of the problem in (a) or (b).

finite element method is summarized in Table 3.1.1. The mathematical problem consists of solving the differential equation (3.2.1) in one-dimensional domain $\Omega = (0, L)$ subject to a suitable set of specified boundary conditions at the boundary points $x = 0$ and $x = L$, as shown in Fig. 3.2.1(c). As already shown in Chapter 2, the type of boundary conditions associated with a differential equation emerges in a natural way during the weak-form development of the differential equation. A detailed discussion of these ideas is presented next.

3.2.2 Discretization of the Domain

In the finite element method, the domain Ω of the problem [Fig. 3.2.2(a)] is divided into a set of subintervals, i.e., line elements, called *finite elements*. A typical element is denoted Ω_e and it is located between points A and B with coordinates x_a and x_b (i.e., of length $h_e = x_b - x_a$). The collection of finite elements in a domain is called the *finite element mesh* of the domain [see Fig. 3.2.2(b)].

The reason for dividing a domain into a set of subdomains, i.e., finite elements, is two-fold. First, domains of most systems, by design, are a composite of geometrically and/or

Table 3.2.1 Some examples of engineering problems governed by the second-order equation (3.2.1) (see the footnote for the meaning of some parameters*).

Field of study	Primary variable u	Problem data a	Problem data c	Problem data f	Secondary variable Q
Heat transfer	Temperature $T - T_\infty$	Thermal conductance kA	Surface convection $AP\beta$	Heat generation f	Heat Q
Flow through porous medium	Fluid head ϕ	Permeability μ	0	Infiltraction f	Point source Q
Flow through pipes	Pressure P	Pipe resistance $1/R$	0	0	Point source Q
Flow of viscous fluids	Velocity v_x	Viscosity μ	0	Pressure gradient $-dP/dx$	Shear stress σ_{xz}
Elastic cables	Displacement u	Tension T	0	Transverse force f	Point force P
Elastic bars	Displacement u	Axial stiffness EA	0	Axial force f	Point force P
Torsion of bars	Angle of twist θ	Shear stiffness GJ	0	0	Torque T
Electrostatics	Electrical potential ϕ	Dielectric constant ϵ	0	Charge density ρ	Electric flux E

*k = thermal conductance; β = convective film conductance; p = perimeter; P = pressure or force; T_∞ = ambient temperature of the surrounding fluid medium; $R = 128\mu h/(\pi d^4)$ with μ being the viscosity, h the length, and d the diameter of the pipe; E = Young's modulus; A = area of cross section; J = polar moment of inertia.

materially different parts, and the solution on these subdomains is represented by different functions that are continuous at the interfaces of these subdomains. Therefore, it is appropriate to seek approximation of the solution over each subdomain. Second, approximation of the solution over each element of the mesh is simpler than its approximation over the entire domain. Approximation of the geometry of the domain in the present case is not a

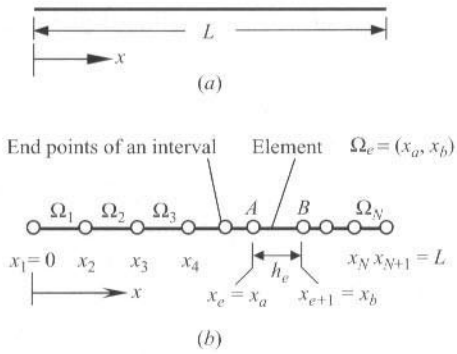

Figure 3.2.2 (*a*) Whole domain. (*b*) Finite element discretization (mesh).

concern, since it is a straight line. We must, however, seek a suitable approximation of the solution over each subdomain (i.e., finite element).

The number of elements into which the total domain is divided in a problem depends mainly on the geometry of the domain and on the desired accuracy of the solution. In the one-dimensional problem at hand, geometry is simple enough to represent it exactly. Since the exact solution is not known *a priori*, we may begin with a number of elements that are considered to be reasonable. Most often, the analyst has knowledge of the qualitative behavior of the solution, and this helps to choose a starting mesh. Whenever a problem is solved by the finite element method for the first time, we are required to investigate the convergence of the finite element solution by gradually *refining the mesh* (i.e., increasing the number of elements) and comparing the solution with those obtained by *higher-order* elements. The *order* of an element refers to the degree of polynomial used to represent the solution over the element. This is made clearer in the sequel.

3.2.3 Derivation of Element Equations

Next, we develop the algebraic equations among the unknown parameters, much the same way as we did in the Ritz and Galerkin methods discussed in Chapter 2 [see Eq. (2.5.5)]. The main difference here is that we work with a finite element (i.e., subdomain) as opposed to the total domain. This step results in a matrix equation of the form $[K^e]\{c^e\} = \{F^e\}$, which is called *the finite element model* of the original equation. Since the element is physically connected to its neighbors, the resulting algebraic equations will contain more unknowns (c^es as well as F^es are unknown in the element equations) than the number of algebraic equations. Then it becomes necessary to put the elements together (i.e., assembly) to eliminate the extra unknowns. This process is discussed in Section 3.2.5.

The derivation of finite element equations, i.e., algebraic equations among the unknown parameters of the finite element approximation, involves the following three steps:

1. Construct the weighted-residual or weak form of the differential equation.
2. Assume the form of the approximate solution over a typical finite element.
3. Derive the finite element equations by substituting the approximate solution into the weighted-residual or weak form.

A typical element $\Omega_e = (x_a, x_b)$ [see Fig. 3.2.3(*a*)], whose endpoints have the coordinates $x = x_a$ and $x = x_b$, is isolated from the mesh. We seek an approximate solution to the governing differential equation over the element. In principle, any method that allows the derivation of necessary algebraic relations among the nodal values of the dependent variable can be used. In this book we develop the algebraic equations using the Ritz method, which is based on the weak form of the differential equation. Other methods, such as the least-squares method, may also be used to construct the finite element equations. Apart from the method used to derive the algebraic equations, the steps presented in this book for the Ritz (or weak-form Galerkin) finite element models are the same for other methods. The three steps in the derivation of finite element equations associated with the model differential equation over a *typical element* of the mesh are discussed next.

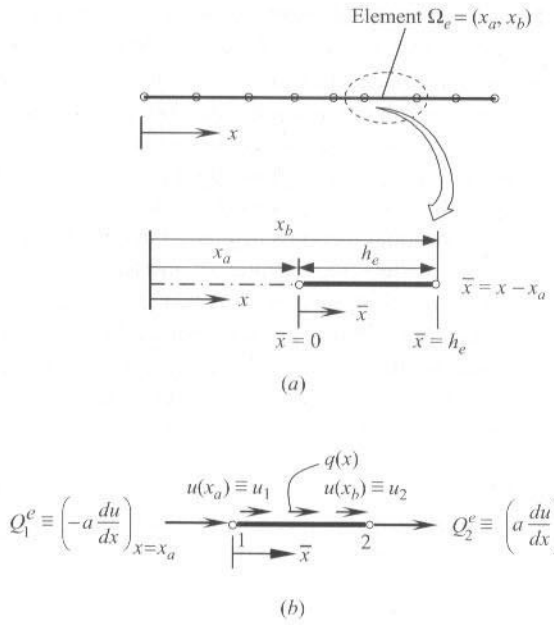

Figure 3.2.3 Finite element discretization of a one-dimensional domain for the model problem in (3.2.1). (*a*) A typical finite element from the finite element mesh. (*b*) A typical element, with the definition of the primary (u) and secondary (Q) variables at the element nodes.

Step 1. Weak Form and Minimum of a Quadratic Functional

In the finite element method, we seek an approximate solution to (3.2.1) over each finite element. The polynomial approximation of the solution within a typical finite element Ω_e is assumed to be of the form

$$u_h^e = \sum_{j=1}^{n} u_j^e \psi_j^e(x) \tag{3.2.3}$$

where u_j^e are the values of the solution $u(x)$ at the nodes of the finite element Ω_e, and ψ_j^e are the approximation functions over the element. The particular form in (3.2.3) will be derived in the next section. Note that the approximation in (3.2.3) differs from the one used in the Ritz method in that $c_j \phi_j(x)$ is now replaced with $u_j^e \psi_j^e$ (and $\phi_0 = 0$), and u_j^e plays the role of undetermined parameters and ψ_j^e the role of approximation functions. As we shall see later, writing the approximation in terms of the nodal values of the solution is necessitated by the fact that the continuity of $u(x)$ between elements can be readily imposed. The coefficients u_j^e are determined such that (3.2.1) is satisfied in a weighted-integral sense. As discussed in Chapter 2, the necessary and sufficient number of algebraic relations among the u_j^e can be obtained by recasting the differential equation (3.2.1) in a weighted-integral form:

$$0 = \int_{x_a}^{x_b} w \left[-\frac{d}{dx}\left(a\frac{du}{dx}\right) + cu - f \right] dx \tag{3.2.4}$$

where $w(x)$ denotes the weight function and $\Omega_e = (x_a, x_b)$ is the domain of a typical element [see Fig. 3.2.3(*a*)]. For $u \approx u_h^e$ and each independent choice of w, we obtain an independent

algebraic equation relating all u_j^e of the element. A total of n independent equations are required to solve for the parameters u_j^e, $j = 1, 2, \ldots, n$. When w is selected to be ψ_i^e and (3.2.4) is used to obtain the ith equation of the required n equations, the resulting finite element model (i.e., system of algebraic equations among the nodal values) is termed the *Galerkin finite element model*. Since (3.2.4) contains the second derivative of u, the approximation functions ψ_j^e must be twice differentiable. In addition, if the secondary variables are to be included in the model, ψ_i^e must be at least cubic. Similar arguments apply for cases of the weighted-residual methods discussed in Chapter 2. For details of the weighted-residual finite element models, see Chapter 14 and Reddy (1986).

To weaken the continuity required of the functions $\psi_j^e(x)$, we trade the differentiation in (3.2.4) from u to w such that both u and w are differentiated equally—once each in the present case. The resulting integral form is termed the *weak form* of (3.2.1). This form is not only equivalent to (3.2.1) but it also contains the natural boundary conditions of the problem. The three-step procedure of constructing the weak form of (3.2.1) was presented in Chapter 2 and is revisited in the next few paragraphs.

The first step is to multiply the governing differential equation with a weight function w and integrate over a *typical element,* as given in (3.2.4). The second step is to trade differentiation from u to w using integration by parts:

$$0 = \int_{x_a}^{x_b} \left(a \frac{dw}{dx} \frac{du}{dx} + cwu - wf \right) dx - \left[wa \frac{du}{dx} \right]_{x_a}^{x_b} \tag{3.2.5}$$

The third and last step is to identify the primary and secondary variables of the weak form. This requires us to classify the boundary conditions of each differential equation into *essential* (or geometric) and *natural* (or force) boundary conditions. The classification is made uniquely by examining the boundary term appearing in the weak form (3.2.5),

$$\left[wa \frac{du}{dx} \right]_{x_a}^{x_b}$$

As a rule, the coefficient of the weight function w in the boundary expression is called a *secondary variable,* and its specification constitutes the *natural* or Neumann boundary condition. The dependent unknown u *in the same form as the weight function* w appearing in the boundary expression is termed a *primary variable,* and its specification constitutes the *essential* or Dirichlet boundary condition. For the model equation at hand, the primary and secondary variables are

$$u \quad \text{and} \quad a \frac{du}{dx} \equiv Q$$

The primary and secondary variables at the nodes are shown on the typical element in Fig. 3.2.3(*b*).

In writing the final form of the weighted-integral statement (i.e., weak form) we wish to use, we must address the fate of the boundary terms. For a typical line element, the end points (nodes 1 and 2) are the boundary points. At these points we have the following four conditions (none of them specified at the moment)

$$u_h^e(x_a) = u_1^e, \left(-a \frac{du}{dx} \right)_{x=x_a} = Q_1^e, u_h^e(x_b) = u_2^e, \left(a \frac{du}{dx} \right)_{x=x_b} = Q_2^e$$

If we select $u_h^e(x)$ in (3.2.3) such that it automatically satisfies the end conditions $u_h^e(x_a) = u_1^e$ and $u_h^e(x_b) = u_2^e$, then it remains that we include the remaining conditions

$$Q_1 = \left(-a\frac{du}{dx}\right)\bigg|_{x_a}, \quad Q_2 = \left(a\frac{du}{dx}\right)\bigg|_{x_b} \tag{3.2.6}$$

in the weak form (3.2.5). With the notation in (3.2.6), the weak form becomes

$$0 = \int_{x_a}^{x_b} \left(a\frac{dw}{dx}\frac{du}{dx} + cwu - wf\right) dx - w(x_a)Q_1 - w(x_b)Q_2 \tag{3.2.7}$$

This completes the three-step procedure of constructing the weak form of the model equation (3.2.1). The finite element model based on the weak form (3.2.7) is called the *weak form Galerkin finite element model.* It is clear that the weak form (3.2.7) admits approximation functions that are lower order than the weighted-residual statement (3.2.4).

Students of engineering recognize that Fig. 3.2.3(*b*) is the *free-body diagram* of a typical element. For axial deformation of bars, u denotes displacement, du/dx is the strain ε, $E\varepsilon$ is the stress σ, and $A\sigma$ denotes the force, where E is Young's modulus and A is the area of cross section of the bar; hence, $Q = EA(du/dx) = a(du/dx)$ has the meaning of force. The quantities Q_1^e and Q_2^e are the reaction forces at the left and right ends of the member; Q_1^e is a compressive force while Q_2^e is a tensile force [algebraically, both are positive, as shown in Fig. 3.2.3(*b*)]. For heat conduction problems, u denotes temperature, du/dx is the temperature gradient, $-k(du/dx)$ is the heat flux q, and Aq denotes the heat, where k is the thermal conductivity and A is the area of cross section of the bar; hence, $Q = kA(du/dx) = a(du/dx)$ has the meaning of heat; $Q_1^e = -kA(du/dx)_a$ is the heat *input* at node 1, while $Q_2^e = kA(du/dx)_b$ denote the heat *input* at node 2. Thus, the arrow on the second node should be reversed for heat transfer problems. For additional details on heat transfer, see Section 3.3.1.

The weak form in (3.2.7) contains two types of expressions: those containing both w and u (bilinear form) and those containing only w (linear form):

$$\begin{aligned} B^e(w,u) &= \int_{x_a}^{x_b} \left(a\frac{dw}{dx}\frac{du}{dx} + cwu\right) dx \\ l^e(w) &= \int_{x_a}^{x_b} w\, f\, dx + w(x_a)Q_1 + w(x_b)Q_2 \end{aligned} \tag{3.2.8}$$

The weak form can be expressed as

$$B^e(w,u) = l^e(w) \tag{3.2.9}$$

which is called the *variational problem* associated with (3.2.1). As will be seen later, the bilinear form results directly in the element coefficient matrix, and the linear form leads to the right-hand-side column vector of the finite element equations. Derivation of the variational problem of the type in (3.2.9) is possible for all problems described by differential equations. However, the bilinear form $B^e(w,u)$ may not be linear in u, and it may not be symmetric in its arguments w and u.

Those who have a background in applied mathematics or solid and structural mechanics will appreciate the fact that the variational problem (3.2.9), when $B^e(w,u)$ is symmetric $B^e(w,u) = B^e(u,w)$ and $l^e(w)$ is linear in w, is the same as the statement of the minimum

of the quadratic functional $I^e(u)$, $\delta I^e = 0$, where

$$I^e(u) = \frac{1}{2}B^e(u,u) - l^e(u)$$
$$= \frac{1}{2}\int_{x_a}^{x_b}\left[a\left(\frac{du}{dx}\right)^2 + cu^2\right]dx$$
$$- \int_{x_a}^{x_b} u\,f\,dx - u(x_a)Q_1 - u(x_b)Q_2 \tag{3.2.10}$$

Thus, the relationship between the weak form and the minimum of quadratic functional I^e is obvious [cf. (3.2.9)]:

$$0 = \delta I^e = B^e(w,u) - l^e(w), \quad w = \delta u$$

The statement $\delta I^e = 0$ in solid and structural mechanics is also known as the *principle of minimum total potential energy*. When (3.2.1) describes the axial deformation of a bar, $\frac{1}{2}B^e(u,u)$ represents the elastic strain energy stored in the bar element, $l^e(u)$ represents the work done by applied forces, and $I^e(u)$ is the total potential energy (Π^e) of the bar element. Thus, the finite element model can be developed using either the statement of the principle of minimum total potential energy of an element or the weak form of the governing equations of an element. However, this choice is restricted to those problems where the minimum of a quadratic finctional $I^e(u)$ corresponds to the governing equations. On the other hand, we can always construct a weak form of any set of differential equations, linear or not, of order 2 and higher. Finite element formulations do not require the existence of the functional $I^e(u)$; they only need weighted-integral statements or weak forms. However, when the functional $I^e(u)$ exists with an extremum (i.e., minimum or maximum principle), existence and uniqueness of solution to the variational problem and its discrete analog can be established. In all problems discussed in this book, the variational problem is derivable from a quadratic functional.

Step 2. Approximate Solution

Recall that in the traditional variational methods, approximate solutions are sought over the total domain $\Omega = (0, L)$ at once. Consequently, the approximate solution $[u(x) \approx U_N(x) = \sum c_j\phi_j(x) + \phi_0(x)]$ is required to satisfy the boundary conditions of the problem. This places severe restrictions on the derivation of the approximation functions $\phi_j(x)$ and $\phi_0(x)$, especially when discontinuities exist in the geometry, material properties, and/or loading of the problem (see Chapter 2 for details). The finite element method overcomes this shortcoming by seeking approximate solution (3.2.3) over each element. Obviously, geometry of the element should be simpler than that of the whole domain, and the geometry should allow a systematic derivation of the approximation functions, as we shall see shortly.

To put the elements back together into their original positions, i.e., connect the approximate solution from each element to form a continuous solution over the whole domain, we require the solution to be the same at points common to the elements. Therefore, we identify the end points of each line element as the *element nodes*, which play the role of interpolation points (or base points) in constructing the approximation functions over an element. Depending on the degree of polynomial approximation used to represent the solution, additional nodes may be identified inside the element.

Since the weak form over an element is equivalent to the differential equation and the natural boundary conditions (3.2.6), i.e., conditions on Q_i^e of the element, the approximate solution u_h^e of (3.2.3) is required to satisfy only the end conditions $u_h^e(x_a) = u_1^e$ and $u_h^e(x_b) = u_2^e$. We seek the approximate solution in the form of algebraic polynomials, although this is not always the case. The reason for this choice is two-fold: First, the interpolation theory of numerical analysis can be used to develop the approximation functions systematically over an element; second, numerical evaluation of integrals of algebraic polynomials is easy.

As in classical variational methods, the approximation solution u_h^e must fulfill certain conditions in order that it be convergent to the actual solution u as the number of elements is increased. These are:

1. It should be continuous over the element and differentiable, as required by the weak form.
2. It should be a *complete* polynomial, i.e., include all lower-order terms up to the highest order used.
3. It should be an interpolant of the primary variables at the nodes of the finite element (at least the nodes on the boundary of the element so that the continuity of the solution can be imposed across the interelement boundary).

The reason for the first condition is obvious; it ensures a nonzero coefficient matrix. The second condition is necessary in order to capture all possible states, i.e., constant, linear, and so on, of the actual solution. For example, if a linear polynomial without the constant term is used to represent the temperature distribution in a one-dimensional system, the approximate solution can never be able to represent a uniform state of temperature in the element should such a state occur. The third condition is necessary in order to enforce continuity of the primary variables at points common to the elements.

For the weak form in (3.2.7), the minimum polynomial order of u_h^e is linear. A complete linear polynomial is of the form

$$u_h^e(x) = c_1^e + c_2^e x \tag{3.2.11}$$

where c_1^e and c_2^e are constants. The phrase "complete polynomial" refers to the inclusion of all terms up to the order desired; omission of c_1^e would make it an incomplete linear polynomial. Similarly, $c_1^e + c_3^e x^2$ is an incomplete quadratic polynomial because the linear term is missing. The expression in (3.2.11) meets the first two conditions of an approximation. The third condition is satisfied if c_1^e and c_2^e meet the conditions

$$u_h^e(x_a) = c_1^e + c_2^e x_a \equiv u_1^e, \quad u_h^e(x_b) = c_1^e + c_2^e x_b \equiv u_2^e \tag{3.2.12}$$

Equation (3.2.12) provides two relations between (c_1^e, c_2^e) and (u_1^e, u_2^e), which can be expressed in matrix form as

$$\begin{Bmatrix} u_1^e \\ u_2^e \end{Bmatrix} = \begin{bmatrix} 1 & x_a \\ 1 & x_b \end{bmatrix} \begin{Bmatrix} c_1^e \\ c_2^e \end{Bmatrix} \tag{3.2.13}$$

Inverting (3.2.13), we obtain

$$\begin{aligned} c_1^e &= \frac{1}{h_e}(u_1^e x_b - u_2^e x_a) \equiv \frac{1}{h_e}(\alpha_1^e u_1^e + \alpha_2^e u_2^e) \\ c_2^e &= \frac{1}{h_e}(u_2^e - u_1^e) \equiv \frac{1}{h_e}(\beta_1^e u_1^e + \beta_2^e u_2^e) \end{aligned} \tag{3.2.14}$$

where $h_e = x_b - x_a$ and ($\alpha_1^e = x_b$, $\alpha_2^e = -x_a$, $\beta_1^e = 1$, and $\beta_2^e = -1$)

$$\alpha_i^e = (-1)^j x_j^e, \quad \beta_i^e = (-1)^j; \quad x_1^e = x_a, \quad x_2^e = x_b \tag{3.2.15}$$

In (3.2.15), i and j permute in a natural order:

$$\text{if } i = 1 \quad \text{then } j = 2; \quad \text{if } i = 2 \quad \text{then } j = 1$$

The α_i^e and β_i^e are introduced to show the typical form of the interpolation functions. Substituting c_1^e and c_2^e from (3.2.15) into (3.2.11), we obtain

$$\begin{aligned} u_h^e(x) &= \frac{1}{h_e}[(\alpha_1^e u_1^e + \alpha_2^e u_2^e) + (\beta_1^e u_1^e + \beta_2^e u_2^e)x] \\ &= \frac{1}{h_e}(\alpha_1^e + \beta_1^e x)u_1^e + \frac{1}{h_e}(\alpha_2^e + \beta_2^e x)u_2^e \\ &= \psi_1^e(x)u_1^e + \psi_2^e(x)u_2^e = \sum_{j=1}^{2} \psi_j^e(x)u_j^e \end{aligned} \tag{3.2.16}$$

where

$$\psi_1^e(x) = \frac{1}{h_e}(\alpha_1^e + \beta_1^e x) = \frac{x_b - x}{x_b - x_a}, \quad \psi_2^e(x) = \frac{1}{h_e}(\alpha_2^e + \beta_2^e x) = \frac{x - x_a}{x_b - x_a} \tag{3.2.17}$$

which are called the linear *finite element approximation functions.*

The approximation functions $\psi_i^e(x)$ have some interesting properties. First, note that

$$u_1^e \equiv u_h^e(x_a) = \psi_1^e(x_a)u_1^e + \psi_2^e(x_a)u_2^e$$

implies $\psi_1^e(x_a) = 1$ and $\psi_2^e(x_a) = 0$. Similarly,

$$u_2^e \equiv u_h^e(x_b) = \psi_1^e(x_b)u_1^e + \psi_2^e(x_b)u_2^e$$

gives $\psi_1^e(x_b) = 0$ and $\psi_2^e(x_b) = 1$. In other words, ψ_i^e is unity at the ith node and zero at the other node. This property is known as the interpolation property (i.e., u_h^e is an interpolant of $u(x)$ through nodes 1 and 2) of $\psi_i^e(x)$ and they are also called *interpolation functions.* When they are derived to interpolate function values only and not the derivatives of the function, they are known as the *Lagrange interpolation functions.* When the function and its derivatives are interpolated, the resulting interpolation functions are known as the *Hermite family of interpolation functions.* These will be discussed in connection with beam finite elements in Chapter 5.

Another property of $\psi_i^e(x)$ is that their sum is unity. To see this, consider a constant state of $u_h^e = c_0$. Then the nodal values u_1^e and u_2^e should be equal to each other and both equal to the constant c_0. Hence, we have

$$u_h^e(x) = \psi_1^e(x)u_1^e + \psi_2^e(x)u_2^e = c_0 \;\rightarrow\; 1 = \psi_1^e(x) + \psi_2^e(x)$$

This property of $\psi_i^e(x)$ is known as the *partition of unity.* In summary, we have

$$\psi_i^e(x_j^e) = \begin{cases} 0 \text{ if } i \neq j \\ 1 \text{ if } i = j \end{cases} \tag{3.2.18a}$$

$$\sum_{i=1}^{n} \psi_i^e(x) = 1 \tag{3.2.18b}$$

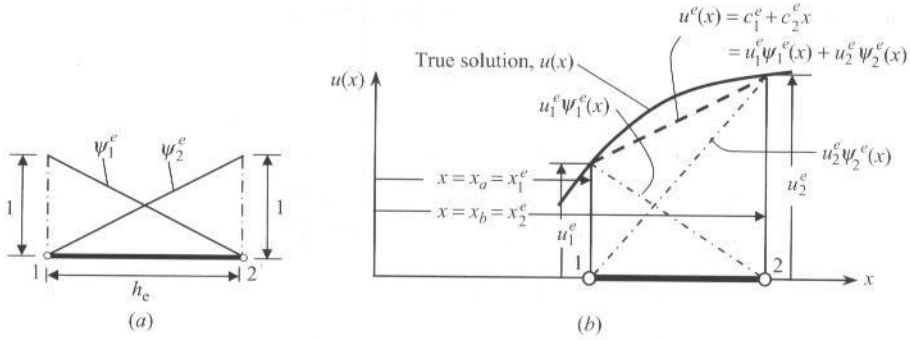

Figure 3.2.4 (*a*) Linear interpolation functions. (*b*) Linear finite element approximation.

where $x_1^e = x_a$ and $x_2^e = x_b$ [see Eq. (3.2.15)]. The functions ψ_i^e are shown in Fig. 3.2.4(*a*) and $u_h^e(x)$ is shown in Fig. 3.2.4(*b*). Although properties (3.2.18*a*) and (3.2.18*b*) are verified for the linear Lagrange interpolation functions, they hold for Lagrange interpolation functions of all degrees.

The element interpolation functions ψ_i^e in (3.2.17) were derived in terms of the *global coordinate* x [i.e., the coordinate appearing in the governing differential equation (3.2.1)], but they are defined only on the element domain $\Omega_e = (x_a, x_b)$. If we choose to express them in terms of a coordinate $\bar{x}$ (convenient in evaluating integrals of ψ_i^e), with the origin fixed at node 1 of the element Ω_e, the functions ψ_i^e of (3.2.17) in terms of $\bar{x}$ are

$$\psi_1^e(\bar{x}) = 1 - \frac{\bar{x}}{h_e}, \quad \psi_2^e(\bar{x}) = \frac{\bar{x}}{h_e} \tag{3.2.19}$$

The coordinate $\bar{x}$ is termed the *local* or *element coordinate* [see Fig. 3.2.3(*a*)].

The interpolation functions ψ_i^e are derived systematically: Starting with an assumed degree of a complete algebraic polynomial for the primary variable u and determining the coefficients c_i^e of the polynomial in terms of the values u_i^e of the primary variable u at the element nodes, the primary variable is finally expressed as a linear combination of approximation functions $\psi_i^e(x)$ and the nodal values u_i^e, which are called the element *nodal degrees of freedom*. The key point in this procedure is the selection of the number and the location of nodes in the element so that the geometry of the element is uniquely defined and interelement continuity may be easily imposed. The number of nodes must be sufficient to allow the rewriting of the coefficients in the assumed polynomial in terms of the primary variables. For a linear polynomial approximation, two nodes with one primary variable per node are sufficient to rewrite the polynomial in terms of the values of the primary variable at the two nodes and also define the geometry of the element, provided the two nodes are the end points of the element.

The degree (or order) of the polynomial approximation can be increased to improve the accuracy (see Fig. 3.2.5). To illustrate the derivation of the interpolation functions of higher order, we consider the quadratic approximation of $u(x)$

$$u_h^e(x) = c_1^e + c_2^e x + c_3^e x^2 \tag{3.2.20}$$

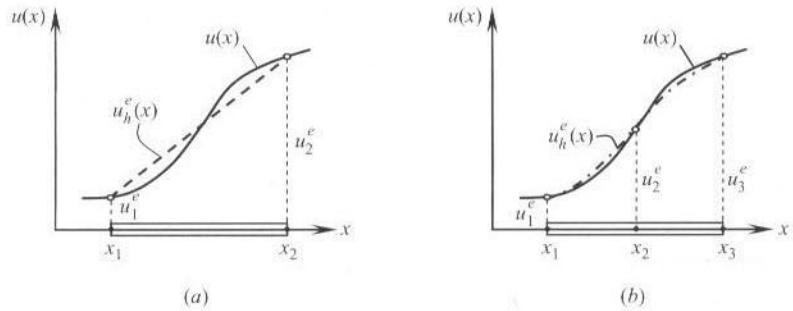

Figure 3.2.5 (*a*) Linear approximation. (*b*) Quadratic approximation.

Since there are three parameters c_i^e $(i = 1, 2, 3)$, we must identify three nodes in the element so that the three parameters can be expressed in terms of the three nodal values u_i^e. Two of the nodes are identified as the endpoints of the element to define its geometry, and the third node is taken interior to the element. In theory, the third node can be placed at any interior point. However, the midpoint of the element, being equidistant from the end nodes, is the best choice. Other choices are dictated by special considerations (e.g., to have a certain degree of singularity in the derivative of the solution), and we will not discuss such special cases here. Thus, we identify three nodes, two at the ends and one in the middle, of the element of length h_e [see Fig. 3.2.5(*b*)]. Following the procedure outlined for the linear polynomial, we eliminate c_i^e by rewriting $u_h^e(x)$ in terms of the three nodal values, (u_1^e, u_2^e, u_3^e). The three relations among c_i^e and u_i^e are

$$\begin{aligned} u_1^e &\equiv u_h^e(x_1^e) = c_1^e + c_2^e x_1^e + c_3^e (x_1^e)^2 \\ u_2^e &\equiv u_h^e(x_2^e) = c_1^e + c_2^e x_2^e + c_3^e (x_2^e)^2 \\ u_3^e &\equiv u_h^e(x_3^e) = c_1^e + c_2^e x_3^e + c_3^e (x_3^e)^2 \end{aligned} \tag{3.2.21a}$$

or, in matrix form,

$$\begin{Bmatrix} u_1^e \\ u_2^e \\ u_3^e \end{Bmatrix} = \begin{bmatrix} 1 & x_1^e & (x_1^e)^2 \\ 1 & x_2^e & (x_2^e)^2 \\ 1 & x_3^e & (x_3^e)^2 \end{bmatrix} \begin{Bmatrix} c_1^e \\ c_2^e \\ c_3^e \end{Bmatrix} \tag{3.2.21b}$$

where x_i^e $(i = 1, 2, 3)$ is the global coordinate of the ith node of the element Ω_e $(x_1^e = x_a$, $x_2^e = x_a + 0.5h_e$, and $x_3^e = x_b)$. Inverting (3.2.21*b*), we obtain

$$\begin{aligned} c_1^e &= \frac{1}{D^e} \sum_{i=1}^{3} \alpha_i^e u_i^e, \quad \alpha_i^e = x_j^e (x_k^e)^2 - x_k^e (x_j^e)^2 \\ c_2^e &= \frac{1}{D^e} \sum_{i=1}^{3} \beta_i^e u_i^e, \quad \beta_i^e = (x_j^e)^2 - (x_k^e)^2 \\ c_3^e &= \frac{1}{D^e} \sum_{i=1}^{3} \gamma_i^e u_i^e, \quad \gamma_i^e = -(x_j^e - x_k^e), \quad D^e = \sum_{i=1}^{3} \alpha_i^e \end{aligned} \tag{3.2.22}$$

where D^e denotes the determinant of the matrix in (3.2.21*b*), and α_i^e, β_i^e, and γ_i^e are defined in (3.2.22) in terms of the nodal coordinates. The subscripts used in (3.2.22) permute in a natural order:

$$\begin{array}{llllll} \text{if} & i=1, & \text{then} & j=2 & \text{and} & k=3 \\ \text{if} & i=2, & \text{then} & j=3 & \text{and} & k=1 \\ \text{if} & i=3, & \text{then} & j=1 & \text{and} & k=2 \end{array} \tag{3.2.23}$$

For example, α_2^e, β_3^e, and γ_1^e are given by

$$\alpha_2^e = x_3^e (x_1^e)^2 - x_1^e (x_3^e)^2, \quad \beta_3^e = (x_1^e)^2 - (x_2^e)^2, \quad \gamma_1^e = x_3^e - x_2^e$$

Note that if x_2^e is very close to either x_1^e or x_3^e (i.e., node 2 is placed close to node 1 or node 3), making the rows of the coefficient matrix in (3.2.21) nearly the same, which makes the matrix nearly singular and not invertable.

Substituting for c_i^e from (3.2.22) into (3.2.20) and collecting the coefficients of u_1^e, u_2^e, and u_3^e separately, we obtain

$$u_h^e(x) = \psi_1^e(x) u_1^e + \psi_2^e(x) u_2^e + \psi_3^e(x) u_3^e = \sum_{j=1}^{3} \psi_j^e(x) u_j^e \tag{3.2.24}$$

where ψ_j^e are the *quadratic Lagrange interpolation functions,*

$$\psi_i^e(x) = \frac{1}{D^e}(\alpha_i^e + \beta_i^e x + \gamma_i^e x^2) \quad (i = 1, 2, 3) \tag{3.2.25}$$

Once again, the quadratic interpolation functions can be expressed in terms of the *local coordinate* $\bar{x}$. When the interior node, node 2, is placed at a distance $\bar{x} = \alpha h_e$, $0 < \alpha < 1$, the quadratic interpolation functions are given by

$$\begin{aligned} \psi_1^e(\bar{x}) &= \left(1 - \frac{\bar{x}}{h}\right)\left(1 - \frac{1}{\alpha}\frac{\bar{x}}{h}\right) \\ \psi_2^e(\bar{x}) &= \frac{1}{\alpha(1-\alpha)}\frac{\bar{x}}{h}\left(1 - \frac{\bar{x}}{h}\right) \\ \psi_3^e(\bar{x}) &= -\frac{\alpha}{(1-\alpha)}\frac{\bar{x}}{h}\left(1 - \frac{1}{\alpha}\frac{\bar{x}}{h}\right) \end{aligned} \tag{3.2.26}$$

For $\alpha = \frac{1}{2}$, i.e., when node 2 is placed at the midpoint of the element, the interpolation functions in (3.2.26) become

$$\begin{aligned} \psi_1^e(\bar{x}) &= \left(1 - \frac{\bar{x}}{h}\right)\left(1 - \frac{2\bar{x}}{h}\right) \\ \psi_2^e(\bar{x}) &= 4\frac{\bar{x}}{h}\left(1 - \frac{\bar{x}}{h}\right) \\ \psi_3^e(\bar{x}) &= -\frac{\bar{x}}{h}\left(1 - \frac{2\bar{x}}{h}\right) \end{aligned} \tag{3.2.27}$$

Plots of the quadratic interpolation functions are given in Fig. 3.2.6. The function ψ_i^e is equal to 1 at node i and zero at the other two nodes, but varies quadratically between the nodes.

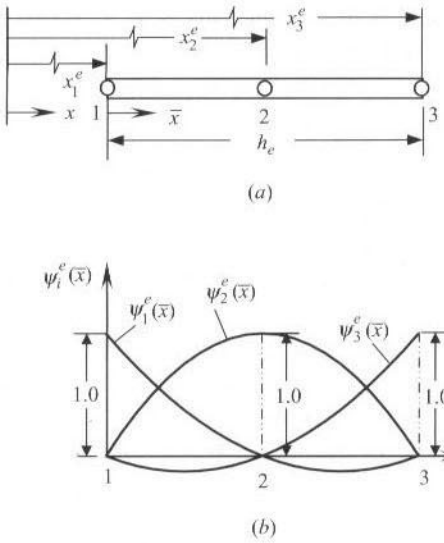

Figure 3.2.6 One-dimensional Lagrange quadratic element and its interpolation functions: (*a*) geometry of the element; (*b*) interpolation functions.

The interpolation properties (3.2.18*a*) and (3.2.18*b*) can be used to construct the Lagrange interpolation functions of any degree. For example, the quadratic interpolation functions (3.2.27) can be derived using the interpolation property (3.2.18*a*). Since $\psi_1^e(\bar{x})$ must vanish at nodes 2 and 3, i.e., at $\bar{x} = \frac{1}{2}h_e$ and $x = h_e$, respectively, $\psi_1^e(\bar{x})$ is of the form

$$\psi_1^e(\bar{x}) = C_1(\bar{x} - \frac{1}{2}h_e)(\bar{x} - h_e)$$

The constant C_1 is determined such that ψ_1^e is equal to 1 at $\bar{x} = 0$:

$$1 = C_1(0 - \frac{1}{2}h_e)(0 - h_e) \quad \text{or} \quad C_1 = 2/h_e^2$$

This gives

$$\psi_1^e(\bar{x}) = \frac{2}{h_e^2}(\bar{x} - \frac{1}{2}h_e)(\bar{x} - h_e) = \left(1 - \frac{\bar{x}}{h_e}\right)\left(1 - \frac{2\bar{x}}{h_e}\right)$$

which is identical to that in (3.2.27). The other two interpolations functions can be derived in a similar manner.

Although a detailed discussion is presented here on how to construct the Lagrange interpolation functions for one-dimensional elements, they are readily available in books on numerical analysis, and their derivation is independent of the physics of the problem to be solved. Their derivation depends only on the geometry of the element and the number and location of the nodes. The number of nodes must be equal to the number of terms in the polynomial. Thus, the interpolation functions derived above are useful not only in the finite element approximation of the problem at hand but also in all problems that admit

Lagrange interpolation of the variables, i.e., all problems for which the primary variables are the dependent unknowns—not their derivatives.

Step 3. Finite Element Model

The weak form (3.2.7) or (3.2.9) is equivalent to the differential equation (3.2.1) over the element Ω_e, and it also contains the natural boundary conditions (3.2.6). Further, the finite element approximations (3.2.16) and (3.2.24) are the interpolants of the solution. The substitution of (3.2.16) or (3.2.24) into (3.2.7) will give the necessary algebraic equations among the nodal values u_i^e and Q_i^e of the element Ω_e. In order to develop the finite element model based on the weak form (3.2.7), it is *not* necessary to decide *a priori* the degree of approximation of u_h^e. The finite element model can be developed for an arbitrary degree of interpolation:

$$u \approx u_h^e = \sum_{j=1}^{n} u_j^e \psi_j^e(x) \tag{3.2.28}$$

where ψ_j^e are the Lagrange interpolation functions of degree $n-1$. For $n > 2$, the weak form in (3.2.7) must be modified to include nonzero secondary variables, if any, at interior nodes. This modification is discussed next.

The integration by parts in Step 2 [see Eq. (3.2.5)] of the weak-form development for an element with interior nodes is carried out by intervals $(x_1^e, x_2^e), (x_2^e, x_3^e), \ldots, (x_{n-1}^e, x_n^e)$:

$$\begin{aligned}
0 &= \sum_{i=1}^{n-1} \left\{ \int_{x_i^e}^{x_{i+1}^e} \left(a\frac{dw}{dx}\frac{du}{dx} + cwu - wf \right) dx - \left[w(x) a \frac{du}{dx} \right]_{x_i^e}^{x_{i+1}^e} \right\} \\
&= \int_{x_1^e}^{x_n^e} \left(a\frac{dw}{dx}\frac{du}{dx} + cwu - wf \right) dx - w(x_1^e) \left(-a\frac{du}{dx} \right)_{x_1^e} - w(x_2^e) \left(a\frac{du}{dx} \right)_{x_2^e} \\
&\quad - w(x_2^e) \left(-a\frac{du}{dx} \right)_{x_2^e} - w(x_3^e) \left(a\frac{du}{dx} \right)_{x_3^e} - \cdots \\
&\quad - w(x_{n-1}^e) \left(-a\frac{du}{dx} \right)_{x_{n-1}^e} - w(x_n^e) \left(a\frac{du}{dx} \right)_{x_n^e} \\
&= \int_{x_1^e}^{x_n^e} \left(a\frac{dw}{dx}\frac{du}{dx} + cwu - wf \right) dx - w(x_1^e) \left(-a\frac{du}{dx} \right)_{x_1^e} \\
&\quad - w(x_2^e) \left[\left(a\frac{du}{dx} \right)_{x_2^{e-}} + \left(-a\frac{du}{dx} \right)_{x_2^{e+}} \right] - w(x_3^e) \left[\left(a\frac{du}{dx} \right)_{x_3^{e-}} + \left(-a\frac{du}{dx} \right)_{x_3^{e+}} \right] \\
&\quad \cdots - w(x_{n-1}^e) \left[\left(a\frac{du}{dx} \right)_{x_{n-1}^{e-}} + \left(-a\frac{du}{dx} \right)_{x_{n-1}^{e+}} \right] - w(x_n^e) \left(a\frac{du}{dx} \right)_{x_n^e} \\
&= \int_{x_1^e}^{x_n^e} \left(a\frac{dw}{dx}\frac{du}{dx} + cwu - wf \right) dx - w(x_1^e) Q_1^e - w(x_2^e) Q_2^e - w(x_3^e) Q_3^e \\
&\quad - \cdots - w(x_{n-1}^e) Q_{n-1}^e - w(x_n^e) Q_n^e
\end{aligned} \tag{3.2.29a}$$

where x_i^{e-} and x_i^{e+} denote the left and right sides, respectively, of node i, and

$$Q_1^e = \left(-a\frac{du}{dx}\right)_{x_1^e}, \quad Q_2^e = \left[\left(a\frac{du}{dx}\right)_{x_2^{e-}} + \left(-a\frac{du}{dx}\right)_{x_2^{e-}}\right]$$

$$\vdots \tag{3.2.29b}$$

$$Q_{n-1}^e = \left[\left(a\frac{du}{dx}\right)_{x_{n-1}^{e-}} + \left(-a\frac{du}{dx}\right)_{x_{n-1}^{e-}}\right], \quad Q_n^e = \left(a\frac{du}{dx}\right)_{x_n^e}$$

Thus, Q_i^e, $i = 2, 3, \ldots, n-1$, denotes the jump in the value of the secondary variable in going from the left to the right of the ith node. This value is zero if no external source is applied at the node. Thus, for an element with n nodes, the weak form becomes

$$0 = \int_{x_a}^{x_b} \left(a\frac{dw}{dx}\frac{du}{dx} + cwu\right) dx - \int_{x_a}^{x_b} wq\, dx - \sum_{j=1}^{n} w(x_j^e) Q_j^e \tag{3.2.30}$$

Note that $Q_1^e = Q_a^e$ and $Q_n^e = Q_b^e$ represent the unknown point sources at the end nodes, and all other Q_i^e ($i = 2, 3, \ldots, n-1$) are the specified point sources, if any, at the interior nodes.

Next, we develop the finite element model of Eq. (3.2.1) when the $(n-1)$st-degree Lagrange polynomials are used to approximate $u(x)$. Following the Ritz procedure developed in Section 2.5.2, we substitute (3.2.28) for u and $w = \psi_1^e$, $w = \psi_2^e$, $\ldots$, $w = \psi_n^e$ into the weak form (3.2.30) to obtain n algebraic equations:

$$0 = \int_{x_a}^{x_b} \left[a\frac{d\psi_1^e}{dx}\left(\sum_{j=1}^{n} u_j^e \frac{d\psi_j^e}{dx}\right) + c\psi_1^e\left(\sum_{j=1}^{n} u_j^e \psi_j^e(x)\right) - \psi_1^e f\right] dx - \sum_{j=1}^{n} \psi_1^e(x_j^e) Q_j^e$$

(1st equation)

$$0 = \int_{x_a}^{x_b} \left[a\frac{d\psi_2^e}{dx}\left(\sum_{j=1}^{n} u_j^e \frac{d\psi_j^e}{dx}\right) + c\psi_2^e\left(\sum_{j=1}^{n} u_j^e \psi_j^e(x)\right) - \psi_2^e f\right] dx - \sum_{j=1}^{n} \psi_2^e(x_j^e) Q_j^e$$

(2nd equation)

$$\vdots$$

$$0 = \int_{x_a}^{x_b} \left[a\frac{d\psi_i^e}{dx}\left(\sum_{j=1}^{n} u_j^e \frac{d\psi_j^e}{dx}\right) + c\psi_i^e\left(\sum_{j=1}^{n} u_j^e \psi_j^e(x)\right) - \psi_i^e f\right] dx - \sum_{j=1}^{n} \psi_i^e(x_j^e) Q_j^e$$

(ith equation)

$$\vdots$$

$$0 = \int_{x_a}^{x_b} \left[a\frac{d\psi_n^e}{dx}\left(\sum_{j=1}^{n} u_j^e \frac{d\psi_j^e}{dx}\right) + c\psi_n^e\left(\sum_{j=1}^{n} u_j^e \psi_j^e(x)\right) - \psi_n^e f\right] dx - \sum_{j=1}^{n} \psi_n^e(x_j^e) Q_j^e$$

(nth equation)

The ith algebraic equation of the system of n equations can be written as

$$0 = \sum_{j=1}^{n} K_{ij}^e u_j^e - f_i^e - Q_i^e \quad (i = 1, 2, \ldots, n) \tag{3.2.31a}$$

where

$$K_{ij}^e = B^e(\psi_i^e, \psi_j^e) = \int_{x_a}^{x_b} \left(a \frac{d\psi_i^e}{dx} \frac{d\psi_j^e}{dx} + c\psi_i^e \psi_j^e \right) dx$$

$$f_i^e = \int_{x_a}^{x_b} f \psi_i^e \, dx \tag{3.2.31b}$$

Note that the interpolation property (3.2.18a) is used to write

$$\sum_{j=1}^{n} \psi_i^e(x_j^e) Q_j^e = Q_i^e \tag{3.2.32}$$

Equations (3.2.31a) can be expressed in terms of the coefficients K_{ij}^e, f_i^e, and Q_i^e as

$$\begin{aligned} K_{11}^e u_1^e + K_{12}^e u_2^e + \cdots + K_{1n}^e u_n^e &= f_1^e + Q_1^e \\ K_{21}^e u_1^e + K_{22}^e u_2^e + \cdots + K_{2n}^e u_n^e &= f_2^e + Q_2^e \\ &\vdots \\ K_{n1}^e u_1^e + K_{n2}^e u_2^e + \cdots + K_{nn}^e u_n^e &= f_n^e + Q_n^e \end{aligned} \tag{3.2.33a}$$

In matrix notation, the linear algebraic equations (3.2.33a) can be written as

$$[K^e]\{u^e\} = \{f^e\} + \{Q^e\} \quad \text{or} \quad \mathbf{K}^e \mathbf{u}^e = \mathbf{f}^e + \mathbf{Q}^e \tag{3.2.33b}$$

The matrix $\mathbf{K}^e$ is called the *coefficient matrix,* or *stiffness matrix* in structural mechanics applications. The column vector $\mathbf{f}^e$ is the *source vector,* or *force vector* in structural mechanics problems. Note that Eq. (3.2.33) contains $2n$ unknowns: $(u_1^e, u_2^e, \ldots, u_n^e)$ and $(Q_1^e, Q_2^e, \ldots, Q_n^e)$, called primary and secondary element *nodal degrees of freedom*; hence, it cannot be solved without having an additional n conditions. Some of these are provided by the boundary conditions and the remainder by "balance" or equilibrium of the secondary variables Q_i^e at nodes common to several elements. This balance can be implemented by putting the elements together (i.e., assembling the element equations). Upon assembly and imposition of boundary conditions, we shall obtain exactly the same number of algebraic equations as the number of unknown primary and secondary degrees of freedom. The ideas underlying the assembly procedure are discussed in the next section.

The coefficient matrix $[K^e]$, which is symmetric, and source vector $\{f^e\}$ can be evaluated for a given element and data (a, c, and f). For elementwise-constant values of a, c, and f (say, a_e, c_e, and f_e) the coefficients K_{ij}^e and f_i^e can easily be evaluated for a typical element, as discussed next.

Linear Element. For a mesh of linear elements, the element Ω_e is located between the global nodes $x_a = x_e$ and $x_b = x_{e+1}$ [see Fig. 3.2.2(b)]. Hence,

$$K_{ij}^e = \int_{x_e}^{x_{e+1}} \left(a_e \frac{d\psi_i^e}{dx} \frac{d\psi_j^e}{dx} + c_e \psi_i^e \psi_j^e \right) dx, \quad f_i^e = \int_{x_e}^{x_{e+1}} f_e \psi_i^e \, dx$$

or, in the local coordinate system $\bar{x}$,

$$K_{ij}^e = \int_0^{h_e} \left(a_e \frac{d\psi_i^e}{d\bar{x}} \frac{d\psi_j^e}{d\bar{x}} + c_e \psi_i^e \psi_j^e \right) d\bar{x}, \quad f_i^e = \int_0^{h_e} f_e \psi_i^e \, d\bar{x}$$

where $x = x_1^e + \bar{x}$ and

$$dx = d\bar{x}, \quad \frac{d\psi_i^e}{dx} = \frac{d\psi_i^e}{d\bar{x}}$$

The ψ_i^e can be expressed in terms of $\bar{x}$ as [see (3.2.19)]

$$\psi_1^e(\bar{x}) = 1 - \bar{x}/h_e, \quad \psi_2^e(\bar{x}) = \bar{x}/h_e$$

We can compute K_{ij}^e and f_i^e by evaluating the integrals. We have

$$\begin{aligned} K_{11}^e &= \int_0^{h_e} \left[a_e \left(-\frac{1}{h_e} \right) \left(-\frac{1}{h_e} \right) + c_e \left(1 - \frac{\bar{x}}{h_e} \right) \left(1 - \frac{\bar{x}}{h_e} \right) \right] d\bar{x} \\ &= \frac{a_e}{h_e} + \frac{1}{3} c_e h_e \\ K_{12}^e &= \int_0^{h_e} \left[a_e \left(-\frac{1}{h_e} \right) \frac{1}{h_e} + c_e \left(1 - \frac{\bar{x}}{h_e} \right) \frac{\bar{x}}{h_e} \right] d\bar{x} \\ &= -\frac{a_e}{h_e} + \frac{1}{6} c_e h_e = K_{21}^e \quad \text{(by symmetry)} \\ K_{22}^e &= \int_0^{h_e} \left(a_e \frac{1}{h_e} \frac{1}{h_e} + c_e \frac{\bar{x}}{h_e} \frac{\bar{x}}{h_e} \right) d\bar{x} = \frac{a_e}{h_e} + \frac{1}{3} c_e h_e \end{aligned}$$

Similarly,

$$f_1^e = \int_0^{h_e} f_e \left(1 - \frac{\bar{x}}{h_e} \right) d\bar{x} = \frac{1}{2} f_e h_e, \quad f_2^e = \int_0^{h_e} f_e \frac{\bar{x}}{h_e} \, d\bar{x} = \frac{1}{2} f_e h_e$$

Thus, for constant f_e, the total source $f_e h_e$ is equally distributed to the two nodes. The coefficient matrix and column vector are

$$[K^e] = \frac{a_e}{h_e} \begin{bmatrix} 1 & -1 \\ -1 & 1 \end{bmatrix} + \frac{c_e h_e}{6} \begin{bmatrix} 2 & 1 \\ 1 & 2 \end{bmatrix}, \quad \{f^e\} = \frac{f_e h_e}{2} \begin{Bmatrix} 1 \\ 1 \end{Bmatrix} \tag{3.2.34}$$

If $a = a_e x$ and $c = c_e$, the coefficient matrix $[K^e]$ can be evaluated as

$$[K^e] = \frac{a_e}{h_e} \left(\frac{x_e + x_{e+1}}{2} \right) \begin{bmatrix} 1 & -1 \\ -1 & 1 \end{bmatrix} + \frac{c_e h_e}{6} \begin{bmatrix} 2 & 1 \\ 1 & 2 \end{bmatrix} \tag{3.2.35}$$

The reader should verify this. Note that when a is a linear function of x, this is equivalent to replacing a in the coefficient matrix with its average value [compare (3.2.34) with (3.2.35)]:

$$a_{\text{avg}} = \frac{1}{2}(x_e + x_{e+1}) a_e$$

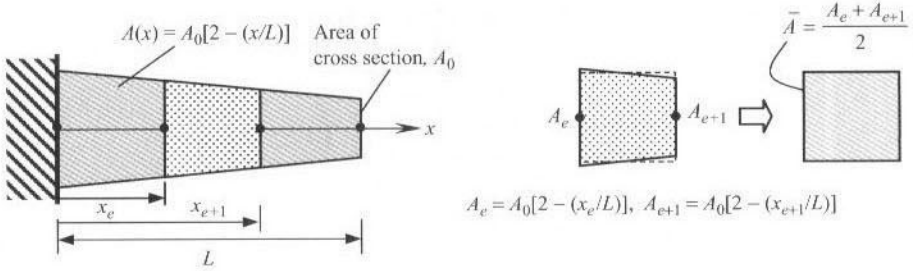

Figure 3.2.7 Approximation of an element with linearly varying cross section by an equivalent element of constant cross section.

For example, in the study of bars with linearly varying cross section (see Fig. 3.2.7)

$$a = EA(x) = E\left(A_e + \frac{A_{e+1} - A_e}{h_e}\bar{x}\right)$$

this amounts to replacing the linearly varying cross section with a constant cross section within each element, the cross-sectional area of the constant section being the average area of the linearly varying element. Here A_e denotes the cross-sectional area at x_e and A_{e+1} is the area at $x = x_{e+1}$.

Quadratic Element. For a mesh of quadratic elements, element Ω_e is located between global nodes $x_a = x_{2e-1}$ and $x_b = x_{2e+1}$. Hence,

$$K_{ij}^e = \int_{x_{2e-1}}^{x_{2e+1}} \left(a_e \frac{d\psi_i^e}{dx}\frac{d\psi_j^e}{dx} + c_e \psi_i^e \psi_j^e\right) dx$$

$$= \int_0^{h_e} \left(a_e \frac{d\psi_i^e}{d\bar{x}}\frac{d\psi_j^e}{d\bar{x}} + c_e \psi_i^e \psi_j^e\right) d\bar{x} \tag{3.2.36a}$$

$$f_i^e = \int_{x_{2e-1}}^{x_{2e-1}} \psi_i^e f_e \, dx = \int_0^{h_e} \psi_i^e f_e \, d\bar{x} \tag{3.2.36b}$$

where $\psi_i^e(\bar{x})$ $(i = 1,2,3)$ are the Lagrange quadratic interpolation functions in (3.2.27). Evaluating the integrals in (3.2.36*a*) and (3.2.36*b*), we obtain

$$K_{11}^e = \int_0^{h_e} \left\{a_e \left(-\frac{3}{h_e} + \frac{4\bar{x}}{h_e^2}\right)\left(-\frac{3}{h_e} + \frac{4\bar{x}}{h_e^2}\right) + c_e\left[1 - \frac{3\bar{x}}{h_e} + 2\left(\frac{\bar{x}}{h_e}\right)^2\right]\left[1 - \frac{3\bar{x}}{h_e} + 2\left(\frac{\bar{x}}{h_e}\right)^2\right]\right\} d\bar{x}$$

$$= \frac{7}{3}\frac{a_e}{h_e} + \frac{2}{15}c_e h_e$$

$$K_{12}^e = \int_0^{h_e} \left\{ a_e \left(-\frac{3}{h_e} + \frac{4\bar{x}}{h_e^2} \right) \left(\frac{4}{h_e} - \frac{8\bar{x}}{h_e} \right) + c_e \left[1 - \frac{3\bar{x}}{h_e} + 2\left(\frac{\bar{x}}{h_e} \right)^2 \right] \left[4\frac{\bar{x}}{h_e} \left(1 - \frac{\bar{x}}{h_e} \right) \right] \right\} d\bar{x}$$

$$= -\frac{8}{3}\frac{a_e}{h_e} + \frac{2}{30} c_e h_e = K_{21}^e$$

$$K_{22}^e = \int_0^{h_e} \left\{ a_e \left(\frac{4}{h_e} - \frac{8\bar{x}}{h_e} \right) \left(\frac{4}{h_e} - \frac{8\bar{x}}{h_e} \right) + c_e \left[4\frac{\bar{x}}{h_e} \left(1 - \frac{\bar{x}}{h_e} \right) \right] \left[4\frac{\bar{x}}{h_e} \left(1 - \frac{\bar{x}}{h_e} \right) \right] \right\} d\bar{x}$$

$$= \frac{7}{3}\frac{a_e}{h_e} + \frac{2}{15} c_e h_e$$

and so on. Similarly,

$$f_1^e = \int_0^{h_e} f_e \left[1 - \frac{3\bar{x}}{h_e} + 2\left(\frac{\bar{x}}{h_e} \right)^2 \right] d\bar{x} = \frac{1}{6} f_e h_e$$

$$f_2^e = \int_0^{h_e} f_e \left[4\frac{\bar{x}}{h_e} \left(1 - \frac{\bar{x}}{h_e} \right) \right] d\bar{x} = \frac{4}{6} f_e h_e$$

$$f_3^e = f_1^e \quad \text{(by symmetry)}$$

Thus, the element coefficient matrix and source vector for a quadratic element are

$$[K^e] = \frac{a_e}{3h_e} \begin{bmatrix} 7 & -8 & 1 \\ -8 & 16 & -8 \\ 1 & -8 & 7 \end{bmatrix} + \frac{c_e h_e}{30} \begin{bmatrix} 4 & 2 & -1 \\ 2 & 16 & 2 \\ -1 & 2 & 4 \end{bmatrix} \tag{3.2.37a}$$

$$\{f^e\} = \frac{f_e h_e}{6} \begin{Bmatrix} 1 \\ 4 \\ 1 \end{Bmatrix} \tag{3.2.37b}$$

Note that, for quadratic elements, the total value of the source $f_e h_e$ is not distributed equally between the three nodes. The distribution is *not* equivalent to that of two linear elements of length $\frac{1}{2}h_e$. The computation of f_i^e should be based on the interpolation functions of that element. The sum of f_i^e for *any element* should always be equal to the integral of $f(x)$ over the element:

$$\sum_{i=1}^{n} f_i^e = \int_{x_a}^{x_b} f(x)\, dx \tag{3.2.38}$$

In summary, for elementwise-constant values of the data a, c, and f, the element matrices of a linear and quadratic elements are

Linear Element

$$\left(\frac{a_e}{h_e}\begin{bmatrix} 1 & -1 \\ -1 & 1 \end{bmatrix} + \frac{c_e h_e}{6}\begin{bmatrix} 2 & 1 \\ 1 & 2 \end{bmatrix}\right)\begin{Bmatrix} u_1^e \\ u_2^e \end{Bmatrix} = \frac{f_e h_e}{2}\begin{Bmatrix} 1 \\ 1 \end{Bmatrix} + \begin{Bmatrix} Q_1^e \\ Q_2^e \end{Bmatrix} \tag{3.2.39}$$

Quadratic Element

$$\left(\frac{a_e}{3h_e}\begin{bmatrix} 7 & -8 & 1 \\ -8 & 16 & -8 \\ 1 & -8 & 7 \end{bmatrix} + \frac{c_e h_e}{30}\begin{bmatrix} 4 & 2 & -1 \\ 2 & 16 & 2 \\ -1 & 2 & 4 \end{bmatrix}\right)\begin{Bmatrix} u_1^e \\ u_2^e \\ u_3^e \end{Bmatrix} = \frac{f_e h_e}{6}\begin{Bmatrix} 1 \\ 4 \\ 1 \end{Bmatrix} + \begin{Bmatrix} Q_1^e \\ Q_2^e \\ Q_3^e \end{Bmatrix} \tag{3.2.40}$$

When the coefficient $c_e = 0$, the corresponding contribution to the above equations should be omitted.

When a, c, and f are algebraic polynomials in x, the evaluation of K_{ij}^e and f_j^e is straightforward. When they are complicated functions of x, the integrals in $[K^e]$ and $\{f^e\}$ are evaluated using numerical integration. A complete discussion of numerical integration will be presented in Chapter 7.

3.2.4 Connectivity of Elements

In deriving the element equations, we isolated a typical element (the eth element) from the mesh and formulated the variational problem (or weak form) and developed its finite element model. The finite element model of a typical element contains n equations among $2n$ unknowns, $(u_1^e, u_2^e, \ldots, u_n^e)$ and $(Q_1^e, Q_2^e, \ldots, Q_n^e)$. Hence, they cannot be solved without using the equations from other elements to get rid of extra unknowns. From a physical point of view, this makes sense because we should not be able to solve the element equations without considering the complete set of elements and the boundary conditions of the total problem.

To obtain the finite element equations of the total problem, we must put the elements back into their original positions (undoing of what was done before formulating the discrete problem). In putting the elements with their nodal degrees of freedom back into their original positions, we must require that the solution $u(x)$ is uniquely defined (i.e., u is continuous) and their source terms Q_i^e are "balanced" at the points where elements are connected to each other. Of course, if the variable u is not continuous, we do not impose its continuity; but in all problems studied in this book, unless otherwise stated explicitly (like in the case of an internal hinge in the case of beam bending), the primary variables are assumed to be continuous. The continuity of the primary variables refers to the single-valued nature of the

solution; balance of secondary variables refers to the equilibrium of point sources. Thus, the assembly of elements is carried out by imposing the following two conditions:

1. If the node i of element Ω^e is connected to the node j of element Ω^f and node k of element Ω^g, the continuity of the primary variable u requires

$$u_i^{(e)} = u_j^{(f)} = u_k^{(g)} \tag{3.2.41}$$

When elements are connected in series, as shown in Fig. 3.2.8, the continuity of u requires

$$u_n^e = u_1^{e+1} \tag{3.2.42}$$

2. For the same three elements, the balance of secondary variables at connecting nodes requires

$$Q_i^{(e)} + Q_j^{(f)} + Q_k^{(g)} = Q_I \tag{3.2.43}$$

where I is the global node number assigned to the nodal point that is common to the three elements, and Q_I is the value of externally applied source, if any (otherwise zero), at this node [the sign of Q_I must be consistent with the sign of Q_i^e in Fig. 3.2.3(*b*)]. For the case shown in Fig. 3.2.8, we have

$$Q_n^e + Q_1^{e+1} = \begin{cases} 0 & \text{if no external point source is applied} \\ Q_I & \text{if an external point source of magnitude } Q_I \text{ is applied} \end{cases} \tag{3.2.44}$$

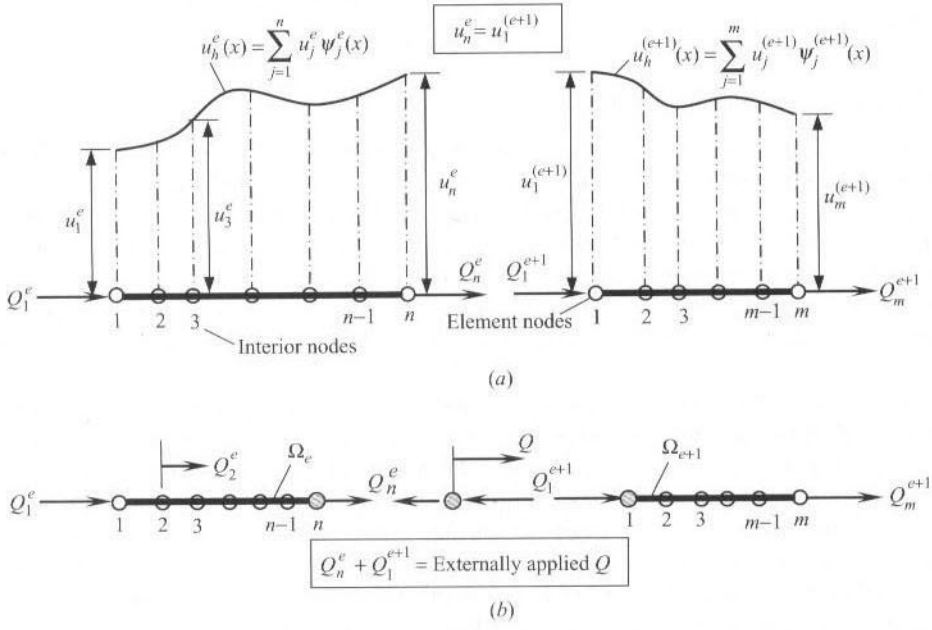

Figure 3.2.8 Assembly of two Lagrange elements: (*a*) continuity of the primary variable; (*b*) balance of the secondary variables.

The balance of secondary variables can be interpreted as the continuity of $a(du/dx)$ [not $a(du_h^e/dx)$] at the node (say, global node I) common to elements Ω_e and Ω_{e+1} when no change in adu/dx is imposed externally:

$$\left(a\frac{du}{dx}\right)_I^e = \left(a\frac{du}{dx}\right)_I^{e+1}$$

or

$$\left(a\frac{du}{dx}\right)_I^e + \left(-a\frac{du}{dx}\right)_I^{e+1} = 0 \rightarrow Q_n^e + Q_1^{e+1} = 0 \tag{3.3.45a}$$

If there is a discontinuity of magnitude Q_I in $a\frac{du}{dx}$ in going from one side of the node to the other side (in the positive x direction), we impose

$$\left(a\frac{du}{dx}\right)_I^e + \left(-a\frac{du}{dx}\right)_I^{e+1} = Q_I \rightarrow Q_n^e + Q_1^{e+1} = Q_I \tag{3.3.45b}$$

The interelement continuity of the primary variables can be imposed by simply renaming the variables of all elements connected to the common node. For the connection in Eq. (3.2.41), we simply use the name

$$u_i^{(e)} = u_j^{(f)} = u_k^{(g)} \equiv U_I \tag{3.2.46}$$

where I is the global node number at which the three elements are connected. For example, for a mesh of N linear finite elements ($n = 2$) connected in series [see Fig. 3.2.2(*b*)], we have

$$u_1^1 = U_1,\ u_2^1 = u_1^2 = U_2,\ u_2^2 = u_1^3 = U_3, \ldots, u_2^{N-1} = u_1^N = U_N,\ u_2^N = U_{N+1}$$

Figure 3.2.9 shows the connected finite element solution, u_h, composed of the element solutions u_h^e. From the connected solution, we can identify the *global interpolation functions* Φ_I, which can be defined in terms of the element interpolation functions ψ_i^e corresponding to the global node I, as shown in Fig. 3.2.9.

To enforce balance of the secondary variables, it is clear that we can set [see Eq. (3.2.44)] $Q_i^{(e)} + Q_j^{(f)} + Q_k^{(g)}$ equal to zero or to a specified value Q_I only if we have such an expression in the finite element equations. To obtain such expressions, it is clear that we must add the ith equation of the element Ω_e, the jth equation of element Ω_f, and the kth equation of element Ω_e. For the case shown in Fig. 3.2.8, the nth equation of element Ω_e must be added to the first equation of the element Ω_{e+1}, i.e., we add

$$\sum_{j=1}^{n} K_{nj}^e u_j^e = f_n^e + Q_n^e$$

and

$$\sum_{j=1}^{n} K_{1j}^{e+1} u_j^{e+1} = f_1^{e+1} + Q_1^{e+1}$$

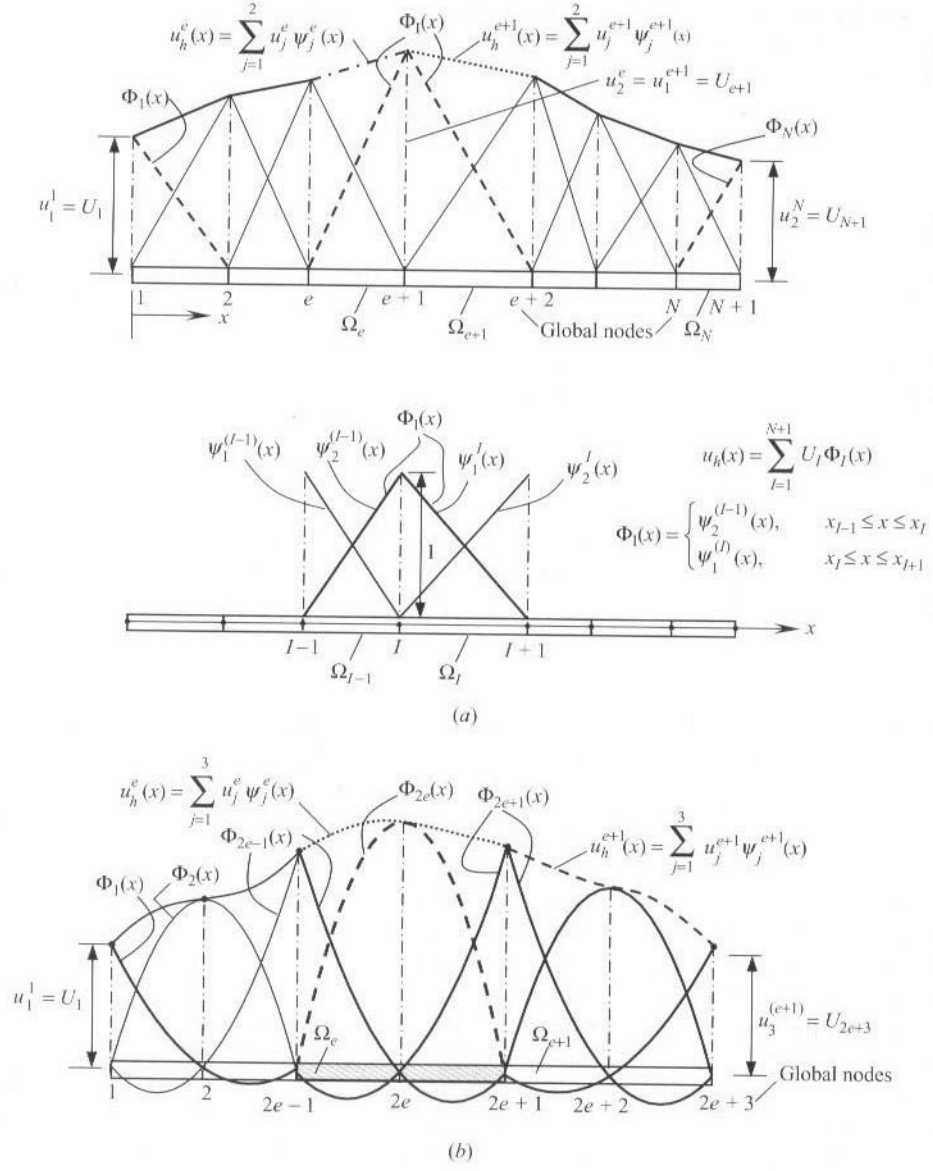

Figure 3.2.9 Global interpolation functions for the (*a*) linear elements and (*b*) quadratic elements.

to obtain

$$\sum_{j=1}^{n} \left(K_{nj}^e u_j^e + K_{1j}^{e+1} u_j^{e+1} \right) = f_n^e + f_1^{e+1} + \left(Q_n^e + Q_1^{e+1} \right)$$
$$= f_n^e + f_1^{e+1} + Q_I \tag{3.2.47}$$

This process reduces the number of equations from $2N$ to $N + 1$ in a mesh of N linear elements. The first equation of the first element and the last equation of the last element

will remain unchanged, except for renaming of the primary variables. The left-hand side of (3.2.47) can be written in terms of the global nodal values as

$$\begin{aligned}
&\left(K^e_{n1}\, u^e_1 + K^e_{n2}u^e_2 + \cdots + K^e_{nn}u^e_n\right) + \left(K^{e+1}_{11}u^{e+1}_1 + K^{e+1}_{12}u^{e+1}_2 + \cdots + K^{e+1}_{1n}u^{e+1}_n\right) \\
&\quad = \left(K^e_{n1}U_N + K^e_{n2}U_{N+1} + \cdots + K^e_{nn}U_{N+n-1}\right) \\
&\qquad + \left(K^{e+1}_{11}U_{N+n-1} + K^{e+1}_{12}U_{N+n} + \ldots + K^{e+1}_{1n}U_{N+2n-2}\right) \\
&\quad = K^e_{n1}U_N + K^e_{n2}U_{N+1} + \cdots + K^e_{n(n-1)}U_{N+n-2} + \left(K^e_{nn} + K^{e+1}_{11}\right)U_{N+n-1} \\
&\qquad + K^{e+1}_{12}U_{N+n} + \ldots + K^{e+1}_{1n}U_{N+2n-2}
\end{aligned} \tag{3.2.48}$$

where $N = (n-1)e + 1$. For a mesh of N linear elements ($n = 2$), we have

$$\begin{aligned}
K^1_{11}U_1 + K^1_{12}U_2 &= f^1_1 + Q^1_1 \quad \text{(unchanged)} \\
K^1_{21}U_1 + \left(K^1_{22} + K^2_{11}\right)U_2 + K^2_{12}U_3 &= f^1_2 + f^2_1 + Q^1_2 + Q^2_1 \\
K^2_{21}U_2 + \left(K^2_{22} + K^3_{11}\right)U_3 + K^3_{12}U_4 &= f^2_2 + f^3_1 + Q^2_2 + Q^3_1 \\
&\vdots \\
K^{N-1}_{21}U_{N-1} + \left(K^{N-1}_{22} + K^N_{11}\right)U_N + K^N_{12}U_{N+1} &= f^{N-1}_2 + f^N_1 + Q^{N-1}_2 + Q^N_1 \\
K^N_{21}U_N + K^N_{22}U_{N+1} &= f^N_2 + Q^N_2 \quad \text{(unchanged)}
\end{aligned} \tag{3.2.49}$$

These are called the *assembled equations*. They contain the sum of coefficients and source terms at nodes common to two elements. Note that the numbering of the global equations corresponds to the numbering of the global primary degrees of freedom, U_I. This correspondence carries the symmetry of element matrices to the global matrix. Equations (3.2.49) can be expressed in matrix form as

$$\begin{bmatrix}
K^1_{11} & K^1_{12} & & & \\
K^1_{21} & K^1_{22} + K^2_{11} & K^2_{12} & \mathbf{0} & \\
 & K^2_{21} & K^2_{22} + K^3_{11} & & \\
\cdots & \cdots & \cdots & \cdots & \cdots \\
 & \mathbf{0} & & K^{N-1}_{22} + K^N_{11} & K^N_{12} \\
 & & & K^N_{21} & K^N_{22}
\end{bmatrix}
\begin{Bmatrix} U_1 \\ U_2 \\ U_3 \\ \vdots \\ U_N \\ U_{N+1} \end{Bmatrix}$$

$$= \begin{Bmatrix} f^1_1 \\ f^1_2 + f^2_1 \\ f^2_2 + f^3_1 \\ \vdots \\ f^{N-1}_2 + f^N_1 \\ f^N_2 \end{Bmatrix} + \begin{Bmatrix} Q^1_1 \\ Q^1_2 + Q^2_1 \\ Q^2_2 + Q^3_1 \\ \vdots \\ Q^{N-1}_2 + Q^N_1 \\ Q^N_2 \end{Bmatrix} \tag{3.2.50}$$

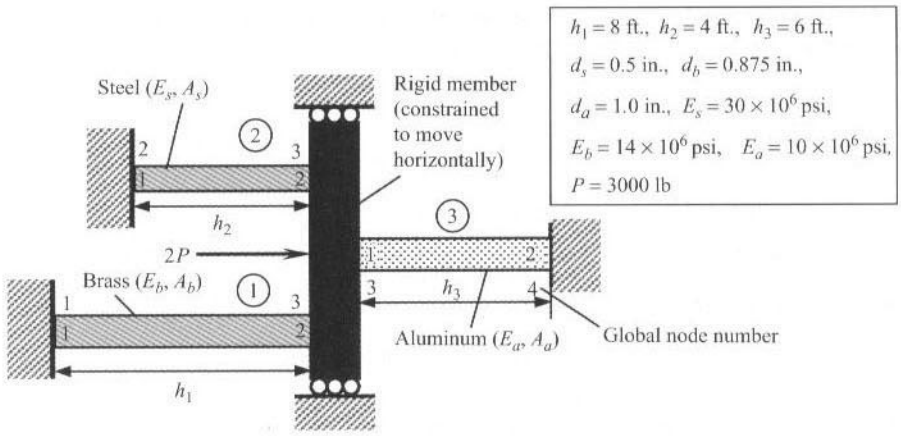

Figure 3.2.10 The geometry and finite element mesh of a three-bar structure.

Note that the discussion of assembly in Eqs. (3.2.49) and (3.2.50) is based on the assumption that elements are connected in series. In general, several elements can be connected at a global node, and the elements do not have to be consecutively numbered. In that case, the coefficients coming from all elements connected at that global node will add up. For example, consider the structure consisting of three bar elements shown in Fig. 3.2.10. Suppose that the connecting bar is rigid (i.e., not deformable) and is constrained to remain horizontal at all times. Then the continuity and force balance conditions for the structure are

$$u_2^1 = u_1^3 = u_2^2 \equiv U_3, \quad Q_2^1 + Q_1^3 + Q_2^2 = 2P \tag{3.2.51}$$

To enforce these conditions, we must add the second equation of element 1, the first equation of element 3, and the second equation of element 2:

$$\begin{aligned}\left(K_{21}^1 u_1^1 + K_{22}^1 u_2^1\right) + \left(K_{11}^3 u_1^3 + K_{12}^3 u_2^3\right) + \left(K_{21}^2 u_1^2 + K_{22}^2 u_2^2\right) \\ = f_2^1 + f_1^3 + f_2^2 + Q_2^1 + Q_1^3 + Q_2^2\end{aligned} \tag{3.2.52}$$

We note the following correspondence of local and global nodal values (see Fig. 3.2.10):

$$u_1^1 = U_1, \quad u_1^2 = U_2, \quad u_2^1 = u_1^3 = u_2^2 = U_3, \quad u_2^3 = U_4$$

Hence, (3.2.52) becomes

$$\begin{aligned}K_{21}^1 U_1 + K_{21}^2 U_2 + (K_{22}^1 + K_{11}^3 + K_{22}^2) U_3 + K_{12}^3 U_4 \\ = f_2^1 + f_1^3 + f_2^2 + Q_2^1 + Q_1^3 + Q_2^2 \\ = f_2^1 + f_1^3 + f_2^2 + 2P\end{aligned}$$

The other equations remain unchanged, except for renaming of the primary variables. The assembled equations are

$$\begin{bmatrix} K_{11}^1 & 0 & K_{12}^1 & 0 \\ 0 & K_{11}^2 & K_{12}^2 & 0 \\ K_{21}^1 & K_{21}^2 & \hat{K} & K_{12}^3 \\ 0 & 0 & K_{21}^3 & K_{22}^3 \end{bmatrix} \begin{Bmatrix} U_1 \\ U_2 \\ U_3 \\ U_4 \end{Bmatrix} = \begin{Bmatrix} f_1^1 \\ f_1^2 \\ f_2^1 + f_1^3 + f_2^2 \\ f_2^3 \end{Bmatrix} + \begin{Bmatrix} Q_1^1 \\ Q_1^2 \\ Q_2^1 + Q_1^3 + Q_2^2 \\ Q_2^3 \end{Bmatrix} \tag{3.2.53}$$

where $\hat{K} = K_{22}^1 + K_{11}^3 + K_{22}^2$. Note that all f_i^e are zero for the problem in Fig. 3.2.10 because there is no distributed axial force ($f = 0$ for all elements).

The coefficients of the assembled matrix can be obtained directly. We note that the global coefficient K_{IJ} is a physical property of the system, relating global node I to global node J. For axial deformation of bars, K_{IJ} denotes the force required at node I to induce a unit displacement at node J, while the displacements at all other nodes are zero. Therefore, K_{IJ} is equal to the sum of all K_{ij}^e for which i corresponds to I and j corresponds to J, and i and j are the local nodes of the element Ω_e. Thus, if we have a correspondence between element node numbers and global node numbers, then the assembled global coefficients can readily be written in terms of the element coefficients. The correspondence can be expressed through a matrix $[B]$, called the *connectivity matrix,* whose coefficient b_{ij} has the following meaning: b_{ij} is the global node number corresponding to the jth node of element i. For example, for the structure shown in Fig. 3.2.10, the matrix $[B]$ is of order 3×2 (3 elements and 2 nodes per element):

$$[B] = \begin{bmatrix} 1 & 3 \\ 2 & 3 \\ 3 & 4 \end{bmatrix}$$

This array can be used in a variety of ways—not only for assembly, but also in the computer implementation of finite element computations. The matrix $[B]$ is used to assemble coefficient matrices as follows:

$K_{11}^1 = K_{11}$ because local node 1 of element 1 corresponds to global node 1.
$K_{12}^1 = K_{13}$ because local nodes 1 and 2 of element 1 correspond to global nodes 1 and 3, respectively

and so on. When more than one element is connected at a global node, the element coefficients are to be added. For example, global node 3 appears in all three rows (i.e., elements) of the matrix $[B]$, implying that all three elements are connected to a global node 3. More specifically, it indicates that node 2 of element 1, node 2 of element 2, and node 1 of element 3 are the same as global node 3. Hence,

$$K_{22}^1 + K_{22}^2 + K_{11}^3 = K_{33}$$

Assembly by hand can be carried out by examining the finite element mesh of the problem. For the mesh shown in Fig. 3.2.10, we have

$K_{23} = K_{12}^2$ because global node 2 is the same as node 1 and global node 3 is the same as node 2 of element 2.

$K_{24} = 0$ because global nodes 2 and 4 do not belong to the same element
$K_{33} = K_{22}^1 + K_{22}^2 + K_{11}^3$

and so on. The problem can also be solved by numbering global nodes 1 and 2 to be the same node. This leads to a 3×3 global system of equations.

In summary, assembly of finite elements is carried out by imposing interelement continuity of primary variables and balance of secondary variables. Renaming the primary variables of an element in terms of the global primary variables and using the correspondence between the local and global nodes allows the assembly. When certain primary nodal values are not required to be continuous across elements (as dictated by physics or the variational formulation of the problem), such variables may be *condensed* out at the element level before assembling the elements.

3.2.5 Imposition of Boundary Conditions

The discussion in Section 3.2.1–3.2.4 is valid for any differential equation that is a special case of the model equation (3.2.1). Each problem differs from the other in the specification of the data (a, c, f) and boundary conditions on the primary and secondary variables (u, Q). Here we discuss how to impose the boundary conditions of a problem on the assembled set of finite element (algebraic) equations. To this end, we use the problem in Fig. 3.2.10. The boundary conditions of the problem are evident, at least for an engineering student, from the structure shown. The known primary degrees of freedom (i.e., displacements) are

$$u_1^1 = U_1 = 0, \quad u_1^2 = U_2 = 0, \quad u_2^3 = U_4 = 0 \tag{3.3.54a}$$

The known secondary degrees of freedom (i.e., forces) are

$$Q_2^1 + Q_2^2 + Q_1^3 = 2P \tag{3.3.54b}$$

The forces Q_1^1, Q_1^2, and Q_2^3 are unknown (reaction forces), and they can be determined after the primary degrees of freedom are determined.

Imposing the boundary conditions (3.2.54*a*) and (3.2.54*b*) on the assembled system of equations (3.2.53) with $f_i^e = 0$, we obtain

$$\begin{bmatrix} K_{11}^1 & 0 & K_{12}^1 & 0 \\ 0 & K_{11}^2 & K_{12}^2 & 0 \\ K_{21}^1 & K_{21}^2 & K_{22}^1 + K_{22}^2 + K_{11}^3 & K_{12}^3 \\ 0 & 0 & K_{21}^3 & K_{22}^3 \end{bmatrix} \begin{Bmatrix} U_1 = 0 \\ U_2 = 0 \\ U_3 \\ U_4 = 0 \end{Bmatrix} = \begin{Bmatrix} Q_1^1 \\ Q_1^2 \\ 2P \\ Q_2^3 \end{Bmatrix} \tag{3.2.55}$$

This contains four equations in four unknowns: U_3, Q_1^1, Q_1^2, and Q_2^3.

3.2.6 Solution of Equations

As a standard procedure in finite element analysis, the unknown primary degrees of freedom are determined first by *considering the algebraic equations corresponding to the unknown primary variables*. Thus, in the present case, we consider the third equation in (3.2.55) to solve for U_3:

$$K_{21}^1 U_1 + K_{21}^2 U_2 + (K_{22}^1 + K_{22}^2 + K_{11}^3) U_3 + K_{12}^3 U_4 = 2P$$

or

$$(K_{22}^1 + K_{22}^2 + K_{11}^3)U_3 = 2P - (K_{21}^1 U_1 + K_{21}^2 U_2 + K_{12}^3 U_4) \tag{3.2.56}$$

Equation (3.2.56) is called the *condensed equation* for the unknown U_3. The term in parentheses on the right-hand side is zero because all specified displacements are zero in the present problem. Hence, the solution is given by

$$U_3 = \frac{2P}{K_{22}^1 + K_{22}^2 + K_{11}^3} \tag{3.2.57}$$

The unknown secondary variables are determined by considering the remaining equations of (3.2.55), i.e., those that contain the unknown secondary variables:

$$\begin{Bmatrix} Q_1^1 \\ Q_1^2 \\ Q_2^3 \end{Bmatrix} = \begin{bmatrix} K_{11}^1 & 0 & K_{12}^1 & 0 \\ 0 & K_{11}^2 & K_{12}^2 & 0 \\ 0 & 0 & K_{21}^3 & K_{22}^3 \end{bmatrix} \begin{Bmatrix} U_1 \\ U_2 \\ U_3 \\ U_4 \end{Bmatrix} = \begin{Bmatrix} K_{12}^1 U_3 \\ K_{12}^2 U_3 \\ K_{21}^3 U_3 \end{Bmatrix} \tag{3.2.58}$$

because U_1, U_2, and U_4 are zero.

It is possible, although not common with commercial finite element programs, to move all the unknowns to the left-hand side of (3.2.53) and solve for them all at once. But this process destroys the symmetry of the coefficient matrix and requires more computational time in practical problems.

To obtain numerical values, we use the geometric and material data shown in Fig. 3.2.10. We obtain

$$K_{11}^1 = \frac{E_b A_b}{h_1} = \frac{(14 \times 10^6)(\pi d_b^2/4)}{8 \times 12} = 87,693 \text{ lb-in.}$$

$$K_{11}^2 = \frac{E_s A_s}{h_2} = \frac{(30 \times 10^6)(\pi d_s^2/4)}{4 \times 12} = 122,718 \text{ lb-in.}$$

$$K_{11}^3 = \frac{E_a A_a}{h_3} = \frac{(10 \times 10^6)(\pi d_a^2/4)}{6 \times 12} = 109,083 \text{ lb-in.}$$

The displacement of node 3 is $U_3 = 0.01878$ in., reaction at node 1 is $Q_1^1 = -1,647$ lbs, $Q_1^2 = -2,305$ lbs and reaction at node 4 is $Q_2^3 = -2,049$ lbs. Hence, the stresses in elements 1, 2, and 3 are $\sigma^1 = 2,739$ psi, $\sigma^2 = 11,739$ psi, and $\sigma^3 = -2,609$ psi, respectively.

In general, the assembled finite element equations can be partitioned according to the sets of specified and unspecified displacements into the following form:

$$\begin{bmatrix} \mathbf{K}^{11} & \mathbf{K}^{12} \\ \mathbf{K}^{21} & \mathbf{K}^{22} \end{bmatrix} \begin{Bmatrix} \mathbf{U}^1 \\ \mathbf{U}^2 \end{Bmatrix} = \begin{Bmatrix} \mathbf{F}^1 \\ \mathbf{F}^2 \end{Bmatrix} \tag{3.2.59}$$

where $\mathbf{U}^1$ is the column of known (i.e., specified) primary variables, $\mathbf{U}^2$ is the column of unknown primary variables, $\mathbf{F}^1$ is the column of unknown secondary variables, and $\mathbf{F}^2$ is the column of known secondary variables. Writing (3.2.59) as two matrix equations, we obtain

$$\mathbf{K}^{11}\mathbf{U}^1 + \mathbf{K}^{12}\mathbf{U}^2 = \mathbf{F}^1 \tag{3.2.60a}$$

$$\mathbf{K}^{21}\mathbf{U}^1 + \mathbf{K}^{22}\mathbf{U}^2 = \mathbf{F}^2 \tag{3.2.60b}$$

From (3.2.60*b*), we have

$$\mathbf{U}^2 = \left(\mathbf{K}^{22}\right)^{-1}\left(\mathbf{F}^2 - \mathbf{K}^{21}\mathbf{U}^1\right) \tag{3.2.60c}$$

Once $\mathbf{U}^2$ is known from (3.2.60*c*), the vector of unknown secondary variables, $\mathbf{F}^1$, can be computed using Eq. (3.2.60*a*).

In most finite element computer programs, element matrices are assembled as soon as they are generated and they are not stored in the memory of the computer. Thus, element equations are not available for postcomputation of the secondary variables. Also, due to the fact that the assembled coefficient matrix is modified (when operations are performed to invert a matrix) during the solution of equations, Eq. (3.2.60*a*) cannot be used. Therefore, secondary variables can only be computed using their definitions, as discussed next.

3.2.7 Postcomputation of the Solution

The solution of the finite element equations gives the nodal values U_I of the primary unknowns (e.g., displacement, velocity, or temperature). Once the nodal values of the primary variables are known, we can use the finite element approximation $u_h^e(x)$ to compute the desired quantities. The process of computing desired quantities in numerical form or graphical form from the known finite element solution is termed *postcomputation* or *postprocessing;* these phrases are meant to indicate that further computations are made after obtaining the solution of the finite element equations for the nodal values of the primary variables.

Postprocessing of the solution includes one or more of the following tasks:

1. Computation of the primary and secondary variables at points of interest; primary variables are known at nodal points.
2. Interpretation of the results to check whether the solution makes sense (an understanding of the physical process and experience are the guides when other solutions are not available for comparison).
3. Tabular and/or graphical presentation of the results.

To determine the solution u as a continuous function of position x, we return to the approximation (3.2.28) over each element:

$$u(x) \approx \begin{cases} u_h^1(x) = \displaystyle\sum_{j=1}^{n} u_j^1 \psi_j^1(x) \\ u_h^2(x) = \displaystyle\sum_{j=1}^{n} u_j^2 \psi_j^2(x) \\ \vdots \\ u_h^N(x) = \displaystyle\sum_{j=1}^{n} u_j^N \psi_j^N(x) \end{cases} \tag{3.2.61}$$

where N is the number of elements in the mesh. Depending on the value of x, the corresponding element equation from (3.2.61) is used. The derivative of the solution is obtained by differentiating (3.2.61):

$$\frac{du}{dx} \approx \begin{cases} \dfrac{du_h^1}{dx} = \displaystyle\sum_{j=1}^{n} u_j^1 \frac{d\psi_j^1}{dx} \\ \dfrac{du_h^2}{dx} = \displaystyle\sum_{j=1}^{n} u_j^2 \frac{d\psi_j^2}{dx} \\ \vdots \\ \dfrac{du_h^N}{dx} = \displaystyle\sum_{j=1}^{n} u_j^N \frac{d\psi_j^N}{dx} \end{cases} \tag{3.2.62}$$

Note that the derivative du_h^e/dx of the finite element approximation u_h^e based on Lagrange interpolation is discontinuous, for any order element, at the nodes connecting different elements because the continuity of the derivative of the finite element solution at the connecting nodes is not imposed. In the case of linear elements, the derivative of the solution is constant within each element (see Fig. 3.2.11).

The secondary variables Q_j^e can be computed in two different ways. In Eq. (3.2.58), we determined the unknown secondary variables Q_1^1, Q_1^2, and Q_2^3 from the assembled equations of the problem in Fig. 3.2.10. Since the assembled equations often represent the equilibrium relations of a system, the Q_I^e computed from them will be denoted by $(Q_I^e)_{\text{equil}}$. The Q_I^e can also be determined using the definitions in (3.2.6), replacing u with U. We shall denote Q_I^e computed in this way by $(Q_I^e)_{\text{def}}$. Since $(Q_I^e)_{\text{def}}$ are calculated using the approximate solution u_h^e, they are not as accurate as $(Q_I^e)_{\text{equil}}$. However, in finite element computer codes, $(Q_I^e)_{\text{def}}$ are calculated instead of $(Q_I^e)_{\text{equil}}$. This is primarily due to computational reasons. Recall that, in arriving at the results in (3.2.58), we used part of the assembled coefficient matrix. In the numerical solution of simultaneous algebraic equations in a computer, the original assembled coefficient matrix is often modified, and therefore the coefficients needed for the determination of the secondary variables are not available, unless they are saved in an additional array. For the problem in Fig. 3.2.10, we

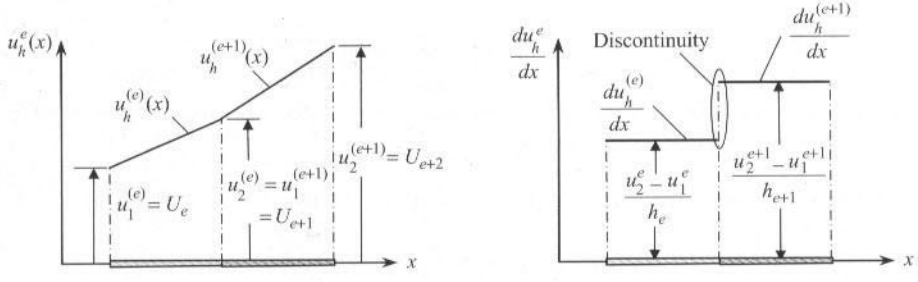

Figure 3.2.11 Gradient of the finite element solution.

have

$$(Q_1^1)_{\text{def}} = -\left(EA\frac{du_h^1}{dx}\right)\bigg|_{x=0} = -EA\frac{U_3 - U_1}{h_1} = -\frac{EA}{h_1}U_3 = K_{12}^1 U_3$$

$$(Q_1^2)_{\text{def}} = -\left(EA\frac{du_h^2}{dx}\right)\bigg|_{x=0} = K_{12}^2 U_3 \tag{3.2.63}$$

$$(Q_2^3)_{\text{def}} = \left(EA\frac{du_h^3}{dx}\right)\bigg|_{x=h_1+h_3} = EA\frac{U_4 - U_3}{h_3} = -\frac{EA}{h_3}U_3 = K_{21}^3 U_3$$

where h_1 and h_3 are the lengths of elements 1 and 3, respectively.

The secondary variables computed using the definitions (3.2.63) are the same as those derived from the assembled equations for the problem in Fig. 3.2.10. This equality is *not to be expected in general*. In fact, when the source vector f is not zero, the secondary variables computed from the definitions (3.2.6) will be in error compared with those computed from the assembled equations. The error decreases as the number of elements or the degree of interpolation is increased.

This completes the basic steps involved in the finite element analysis of the model equation (3.2.1). Next, we consider an example of application of the finite element method. Additional applications of the method to one-dimensional problems of heat transfer, fluid mechanics, and solid mechanics, are presented in Chapter 4.

Example 3.2.1

We wish to use the finite element method to solve the problem described by the following differential equation and boundary conditions (see Example 2.5.1):

$$-\frac{d^2u}{dx^2} - u + x^2 = 0 \quad \text{for} \quad 0 < x < 1 \tag{3.2.64}$$

$$u(0) = 0, \quad u(1) = 0 \tag{3.2.65}$$

The differential equation in (3.2.64) is a special case of the model equation (3.2.1) for the following data: $a = 1$, $c = -1$, and $f(x) = -x^2$. Hence, the coefficient matrix is given by

$$K_{ij}^e = \int_{x_b}^{x_a} \left(\frac{d\psi_i^e}{dx}\frac{d\psi_j^e}{dx} - \psi_i^e\psi_j^e\right) dx$$

$$f_i^e = \int_{x_b}^{x_a} (-x^2)\psi_i^e \, dx$$

First we consider a mesh of four linear elements and next a mesh of two quadratic elements to solve the problem.

Linear Elements. The element coefficient matrix is given by [see Eq. (3.2.34), with $a_e = 1$, $c_e = -1$, $h_e = \frac{1}{4}$]

$$[K^e] = \frac{1}{24}\begin{bmatrix} 94 & -97 \\ -97 & 94 \end{bmatrix} = \begin{bmatrix} 3.9167 & -4.0417 \\ -4.0417 & 3.9167 \end{bmatrix}$$

The coefficients f_i^e are evaluated as

$$f_1^e = -\frac{1}{h_e}\left[\frac{x_b}{3}\left(x_b^3 - x_a^3\right) - \frac{1}{4}\left(x_b^4 - x_a^4\right)\right]$$

$$f_2^e = -\frac{1}{h_e}\left[\frac{1}{4}\left(x_b^4 - x_a^4\right) - \frac{x_a}{3}\left(x_b^3 - x_a^3\right)\right]$$

Element 1. $(h_1 = \frac{1}{4}, x_a = 0, x_b = h_1 = \frac{1}{4})$:

$$f_1^1 = -0.001302, \quad f_2^1 = -0.003906$$

Element 2. $(h_2 = \frac{1}{4}, x_a = h_1 = \frac{1}{4}, x_b = h_1 + h_2 = \frac{1}{2})$:

$$f_1^2 = -0.014323, \quad f_2^2 = -0.022135$$

Element 3. $(h_3 = \frac{1}{4}, x_a = h_1 + h_2 = \frac{1}{2}, x_b = h_1 + h_2 + h_3 = \frac{3}{4})$:

$$f_1^3 = -0.042969, \quad f_2^3 = -0.05599$$

Element 4. $(h_4 = \frac{1}{4}, x_a = h_1 + h_2 + h_3 = \frac{3}{4}, x_b = h_1 + h_2 + h_3 + h_4 = 1)$:

$$f_1^4 = -0.08724, \quad f_2^4 = -0.10547$$

The assembled set of equations is

$$\begin{bmatrix} 3.9167 & -4.0417 & 0 & 0 & 0 \\ -4.0417 & 7.8333 & -4.0417 & 0 & 0 \\ 0 & -4.0417 & 7.8333 & -4.0417 & 0 \\ 0 & 0 & -4.0417 & 7.8333 & -4.0417 \\ 0 & 0 & 0 & -4.0417 & 3.9167 \end{bmatrix} \begin{Bmatrix} U_1 \\ U_2 \\ U_3 \\ U_4 \\ U_5 \end{Bmatrix}$$

$$= -\begin{Bmatrix} 0.00130 \\ 0.01823 \\ 0.06510 \\ 0.14323 \\ 0.10547 \end{Bmatrix} + \begin{Bmatrix} Q_1^1 \\ Q_2^1 + Q_1^2 \\ Q_2^2 + Q_1^3 \\ Q_2^3 + Q_1^4 \\ Q_2^4 \end{Bmatrix}$$

Since $U_1 = 0$ and $U_5 = 0$, the condensed equations are obtained by omitting the first and fifth rows and columns of the assembled equations. The condensed equations are

$$\begin{bmatrix} 7.8333 & -4.0417 & 0 \\ -4.0417 & 7.8333 & -4.0417 \\ 0 & -4.0417 & 7.8333 \end{bmatrix} \begin{Bmatrix} U_2 \\ U_3 \\ U_4 \end{Bmatrix} = -\begin{Bmatrix} 0.01823 \\ 0.06510 \\ 0.14323 \end{Bmatrix}$$

The solution is (obtained using a computer)

$$U_1 = 0.0, \quad U_2 = -0.02323, \quad U_3 = -0.04052, \quad U_4 = -0.03919, \quad U_5 = 0.0$$

The secondary variables can be computed using either the definition or from the element equations. We have

$$(Q_1^1)_{def} \equiv \left(-a\frac{du_h^1}{dx}\right)\bigg|_{x=0} = \frac{U_1 - U_2}{h} = 0.09293$$

$$(Q_2^4)_{def} \equiv \left(a\frac{du_h^4}{dx}\right)\bigg|_{x=1} = \frac{U_5 - U_4}{h} = 0.15676$$

$$(Q_1^1)_{equil} = K_{11}^1 U_1 + K_{12}^1 U_2 - f_1^1 = 0.09520$$

$$(Q_2^4)_{equil} = K_{21}^4 U_4 + K_{22}^4 U_5 - f_2^4 = 0.26386$$

Quadratic Elements. The element coefficient matrix is given by [see Eq. (3.2.37a), with $a_e = 1$, $c_e = -1$, $h_e = \frac{1}{2}$]

$$[K^e] = \frac{1}{60}\begin{bmatrix} 276 & -322 & 41 \\ -322 & 624 & -322 \\ 41 & -322 & 276 \end{bmatrix} = \begin{bmatrix} 4.6000 & -5.3667 & 0.6833 \\ -5.3667 & 10.4000 & -5.3667 \\ 0.6833 & -5.3667 & 4.6000 \end{bmatrix}$$

The coefficients f_i^e are evaluated as

$$f_1^e = -\frac{h_e}{60}\left(-h_e^2 + 10x_a^2\right)$$

$$f_2^e = -\frac{h_e}{15}\left(3h_e^2 + 10x_a^2 + 10x_a^2 h_e\right)$$

$$f_3^e = -\frac{h_e}{60}\left(9h_e^2 + 20x_a^2 + 20x_a h_e\right)$$

Element 1. ($h_1 = \frac{1}{2}$, $x_a = 0$, $x_b = h_1 = \frac{1}{2}$):

$$f_1^1 = 0.00208,\quad f_2^1 = -0.02500,\quad f_3^1 = -0.01875$$

Element 2. ($h_2 = \frac{1}{2}$, $x_a = h_1 = \frac{1}{2}$, $x_b = h_1 + h_2 = 1$):

$$f_1^2 = -0.01875,\quad f_2^2 = -0.19167,\quad f_3^2 = -0.08125$$

The assembled set of equations are

$$\begin{bmatrix} 4.6000 & -5.3667 & 0.6833 & 0 & 0 \\ -5.3667 & 10.4000 & -5.3667 & 0 & 0 \\ 0.6833 & -5.3667 & 9.2000 & -5.3667 & 0.6833 \\ 0 & 0 & -5.3667 & 10.4000 & -5.3667 \\ 0 & 0 & 0.6833 & -5.3667 & 4.6000 \end{bmatrix} \begin{Bmatrix} U_1 \\ U_2 \\ U_3 \\ U_4 \\ U_5 \end{Bmatrix}$$

$$= -\begin{Bmatrix} -0.00208 \\ 0.02500 \\ 0.03750 \\ 0.19167 \\ 0.08125 \end{Bmatrix} + \begin{Bmatrix} Q_1^1 \\ Q_2^1 \\ Q_3^1 + Q_1^2 \\ Q_2^2 \\ Q_3^2 \end{Bmatrix}$$

Again, using $U_1 = 0$ and $U_5 = 0$, the condensed equations are obtained as

$$\begin{bmatrix} 10.4000 & -5.3667 & 0 \\ -5.3667 & 9.2000 & -5.3667 \\ 0 & -5.3667 & 10.4000 \end{bmatrix} \begin{Bmatrix} U_2 \\ U_3 \\ U_4 \end{Bmatrix} = - \begin{Bmatrix} 0.02500 \\ 0.03750 \\ 0.19167 \end{Bmatrix}$$

The solution is

$$U_1 = 0.0,\ U_2 = -0.02345,\ U_3 = -0.04078,\ U_4 = -0.03947,\ U_5 = 0.0$$

The secondary variables can be computed using either the definition or from the element equations. We have

$$(Q_1^1)_{def} \equiv \left(-a \frac{du_h^1}{dx} \right)\bigg|_{x=0} = -\left[\frac{U_1}{h}\left(-3 + 4\frac{x}{h}\right) + \frac{U_2}{h}\left(4 - 8\frac{x}{h}\right) + \frac{U_3}{h}\left(-1 + 4\frac{x}{h}\right) \right]_{x=0}$$

$$= \left(\frac{1}{h} U_1 - \frac{4}{h} U_2 + \frac{1}{h} U_3 \right) = 0.10602$$

Table 3.2.1 Comparison of the finite element results with the exact solution $(-10u)$ of eqs. (3.2.64) and (3.2.65).

	FEM* solution			Ritz† Solution	Exact Solution
x	4L	2Q	4Q		
0.0000	**0.0000**‡	**0.0000**	**0.0000**	0.0000	0.0000
0.0625	0.0581	0.0644	0.0602	0.0596	0.0598
0.1250	0.1162	0.1249	**0.1193**	0.1191	0.1192
0.1875	0.1743	0.1816	0.1771	0.1776	0.1775
0.2500	**0.2323**	**0.2345**	**0.2337**	0.2339	0.2337
0.3125	0.2756	0.2835	0.2876	0.2868	0.2866
0.3750	0.3188	0.3288	**0.3345**	0.3347	0.3345
0.4375	0.3620	0.3702	0.3745	0.3757	0.3755
0.5000	**0.4052**	**0.4078**	**0.4076**	0.4076	0.4076
0.5625	0.4019	0.4403	0.4298	0.4282	0.4283
0.6250	0.3986	0.4490	**0.4350**	0.4347	0.4350
0.6875	0.3952	0.4338	0.4231	0.4244	0.4246
0.7500	**0.3919**	**0.3947**	**0.3942**	0.3940	0.3942
0.8125	0.2939	0.3318	0.3421	0.3401	0.3402
0.8750	0.1960	0.2451	**0.2591**	0.2592	0.2590
0.9375	0.0980	0.1345	0.1450	0.1472	0.1470
1.0000	**0.0000**	**0.0000**	**0.0000**	0.0000	0.0000

* FEM, finite element method

† Three-parameter Ritz solution from Example 2.5.1.

‡ Numbers in bold are the nodal values; others are the interpolated values (4L = 4 linear elements; 2Q = 2 quadratic elements; 4Q = 4 quadratic elements).

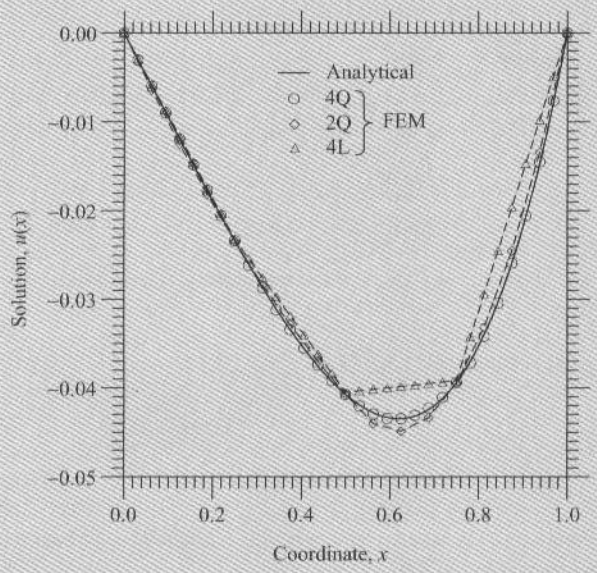

Figure 3.2.12 Comparison of the finite element solutions u_h with the exact and Ritz solutions.

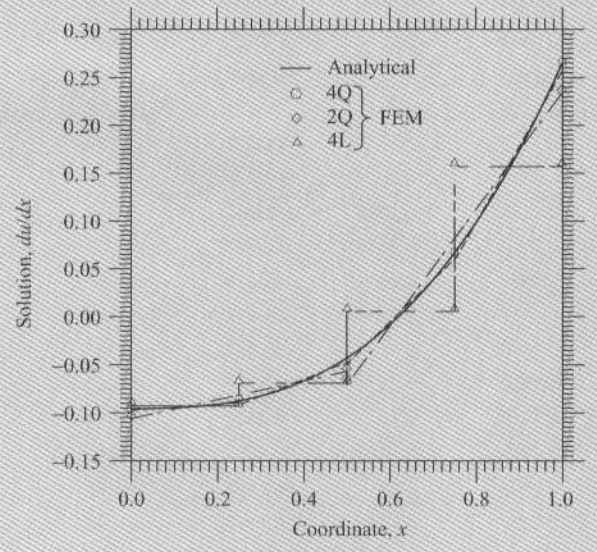

Figure 3.2.13 Comparison of the finite element solutions du_h/dx with the exact and Ritz solutions.

$$(Q_3^2)_{def} \equiv \left(a\frac{du_h^2}{dx}\right)\Big|_{x=1} = \left[\frac{U_3}{h}\left(-3+4\frac{\bar{x}}{h}\right)+\frac{U_4}{h}\left(4-8\frac{\bar{x}}{h}\right)+\frac{U_5}{h}\left(-1+4\frac{\bar{x}}{h}\right)\right]_{\bar{x}=h}$$

$$= \left(\frac{1}{h}U_3 - \frac{4}{h}U_4 + \frac{3}{h}U_5\right) = 0.23442$$

$$(Q_1^1)_{equil} = K_{11}^1 U_1 + K_{12}^1 U_2 + K_{13}^1 U_3 - f_1^1 = 0.10006$$

$$(Q_3^2)_{equil} = K_{13}^2 U_3 + K_{23}^2 U_4 + K_{33}^2 U_5 - f_3^2 = 0.26521$$

Table 3.2.1 contains a comparison of the finite element results against the three-parameter Ritz solution and the exact solution (see Example 2.5.1 and Table 2.5.1). The four linear-element and two quadratic-element solutions are not as accurate as the three-parameter Ritz solution. However, the four quadratic-element solution at the nodes (details are not given here) is virtually the same as the exact solution. Plots of u_h and du_h/dx are shown in Figs. 3.2.12 and 3.2.13, respectively. Note that the finite element solutions for the derivative [postcomputed from $u_h(x)$] are discontinuous between the elements; the value of the difference in du_h/dx between elements reduces as we move from linear to quadratic elements and from coarse to refined meshes.

3.3 SOME REMARKS

A few remarks are in order on the steps described for the model equation.

Remark 1. Although the Ritz method was used to set up the element equations, any other method, such as a weighted-residual (i.e., the least-squares or Galerkin) method could be used.

Remark 2. Steps 1–6 (see Table 3.1.1) are common for any problem. The derivation of interpolation functions depends only on the element geometry and on the number and position of nodes in the element. The number of nodes in the element and the degree of approximation used are related.

Remark 3. The finite element equations (3.2.33*b*) are derived for the linear operator equation

$$A(u) = f, \quad \text{where} \quad A = -\frac{d}{dx}\left(a\frac{d}{dx}\right) + c \tag{3.3.1}$$

Hence, they are valid for any physical problem that is described by the operator equation $A(u) = f$ or its special cases. One need only interpret the quantities appropriately. Examples of problems described by this operator are listed in Table 3.2.1. Thus, a computer program written for the finite element analysis of (3.2.1) can be used to analyze any of the problems in Table 3.2.1. Also, note that the data $a = a(x)$, $c = c(x)$, and $f = f(x)$ can be different in different elements.

Remark 4. Integration of the element matrices in (3.2.31*b*) can be implemented on a computer using numerical integration. When these integrals are algebraically complicated, we have no other choice but numerical integration (see Chapter 7).

Remark 5. As discussed in (3.2.45*a*) and (3.2.45*b*) the point sources at the nodes are included in the finite element model via the balance of sources at the nodes. Thus, in constructing finite element meshes, we should include nodes at the locations of point sources. If a point source does not occur at a node, it is possible to "distribute" it to the element nodes, consistent with the finite element approximation. Let Q_0 denote a point source at a point $\bar{x} = \bar{x}_0$, $\bar{x}_1^e \le \bar{x}_0 \le \bar{x}_n^e$, where $\bar{x}$ is the local coordinate. The point source Q_0 can be represented as a "function" with the help of the Dirac delta function

$$f(\bar{x}) = Q_0 \delta(\bar{x} - \bar{x}_0) \tag{3.3.2}$$

where the Dirac delta function $\delta(\cdot)$ is defined by

$$\int_{-\infty}^{\infty} F(\bar{x}) \delta(\bar{x} - \bar{x}_0)\, d\bar{x} = F(\bar{x}_0) \tag{3.3.3}$$

The contribution of the function $f(\bar{x})$ to the nodes of the element $\Omega_e = (\bar{x}_1, \bar{x}_n)$ is computed from [see Eq. (3.2.31*b*)]

$$f_i^e = \int_0^{h_e} f(\bar{x}) \psi_i^e(\bar{x})\, d\bar{x} = \int_0^{h_e} Q_0 \delta(\bar{x} - \bar{x}_0) \psi_i^e(\bar{x})\, d\bar{x} = Q_0 \psi_i^e(\bar{x}_0) \tag{3.3.4}$$

where ψ_i^e are the interpolation functions of the element Ω_e. Thus, the point source Q_0 is distributed to the element node i by the value $Q_0 \psi_i^e(\bar{x}_0)$. Equation (3.3.4) holds for any element, irrespective of the degree of the interpolation, the nature of the interpolation (i.e., Lagrange or Hermite polynomials), or the dimension (i.e., one-dimensional, two-dimensional, or three-dimensional) of the elements. For one-dimensional linear Lagrange interpolation functions, Eq. (3.3.4) yields

$$f_1^e = Q_0 \left(1 - \frac{\bar{x}_0}{h_e}\right), \quad f_2^e = Q_0 \left(\frac{\bar{x}_0}{h_e}\right)$$

Note that $f_1^e + f_2^e = Q_0$. When $\bar{x}_0 = h_e/2$, we have $f_1^e = f_2^e = Q_0/2$, as expected.

Remark 6. There are three sources of error that may contribute to the inaccuracy of the finite element solution of a problem:

1. *Domain approximation error,* which is due to the approximation of the domain.
2. *Computational errors,* which are due to inexact evaluation of the coefficients K_{ij}^e and f_i^e, or are introduced owing to the finite arithmetic in a computer.
3. *Approximation error,* which is due to approximation of the solution by piecewise polynomials.

For the structure shown in Fig. 3.2.10, the geometry of the problem is exactly represented and the linear approximation is able to represent the exact solution at the nodes when a is a constant, $c = 0$, and f is arbitrary [see Reddy (1986), p. 403; also, see Sec. 14.5]. Therefore, the first and third type of errors are zero. The only error that can be introduced into the final numerical results is possibly due to the computer evaluation of the coefficients K_{ij}^e and f_i^e and the solution of algebraic equations. However, in general, computational as well

as approximation errors exist even in one-dimensional problems. Additional discussion of the errors in the finite element approximation can be found in Oden and Carey (1983) and Reddy (1986); also, see Sec. 14.5.

Remark 7. The approach used in matrix methods of structural analysis to solve the problem in Fig. 3.2.10 is not much different than that presented here. The difference lies only in the derivation of the element equations (3.2.39) for the case $c_e = 0$. In matrix methods of structural analysis, the element equations are obtained directly from the definitions of stress and strain and their relationship. For example, consider the free-body diagram of a bar element [see Fig. 3.2.3(b)]. From a course on mechanics of deformable solids, we have

$$\begin{aligned} \text{strain, } \varepsilon &= \text{elongation/original length} \\ \text{stress, } \sigma &= \text{Young's modulus} \times \text{strain} \\ \text{load, } P &= \text{stress} \times \text{area of cross section} \end{aligned}$$

The strain defined above is the average (or engineering) strain. Mathematically, strain for one-dimensional problems is defined as $\varepsilon = du/dx$, u being displacement, which includes rigid body motion as well as elongation of the bar. Hence, the compressive force at the left end of the bar element is

$$P_1^e = A_e \sigma_1^e = A_e E_e \varepsilon_1^e = A_e E_e \frac{u_1^e - u_2^e}{h_e} = \frac{A_e E_e}{h_e}(u_1^e - u_2^e)$$

where E_e is Young's modulus of the bar element. Similarly, the force at the right end is

$$P_2^e = \frac{A_e E_e}{h_e}(u_2^e - u_1^e)$$

In matrix form, these relations can be expressed as

$$\frac{A_e E_e}{h_e}\begin{bmatrix} 1 & -1 \\ -1 & 1 \end{bmatrix}\begin{Bmatrix} u_1^e \\ u_2^e \end{Bmatrix} = \begin{Bmatrix} P_1^e \\ P_2^e \end{Bmatrix} \tag{3.3.5a}$$

which is the same as (3.2.39) obtained for a linear finite element with $a_e = A_e E_e$, $c_e = 0$, and $P_i^e = Q_i^e + f_i^e$. Note that in deriving the element equations, we have used knowledge of the mechanics of materials and the assumption that the strain is constant (or the displacement is linear) over the length of the element. If a higher-order representation of the displacement is required, we cannot write the force-displacement relations (3.3.5a) directly, i.e., the element equations of a quadratic finite elements cannot be derived using the arguments presented above.

A similar approach can be used to develop the relations between the temperatures and heats at the ends of an insulated fin. From a course on basic heat transfer, we have

$$\begin{aligned} \text{temperature gradient} &= \text{difference in temperature/length} \\ \text{heat flux, } q &= \text{conductivity} \times (-\text{temperature gradient}) \\ \text{heat, } Q &= \text{heat flux} \times \text{area of cross section} \end{aligned}$$

Then, if the temperature is assumed to vary linearly between the ends of the fin and there is no internal heat generation, the heat input at the left end of the fin is

$$Q_1^e = A_e q_1^e = A_e k_e \frac{T_1^e - T_2^e}{h_e} = \frac{A_e k_e}{h_e}(T_1^e - T_2^e)$$

where k_e is thermal conductivity of the fin. Similarly, the heat *input* at the right end is

$$Q_2^e = A_e q_2^e = A_e k_e \frac{T_2^e - T_1^e}{h_e} = \frac{A_e k_e}{h_e}(T_2^e - T_1^e)$$

In matrix form, we have

$$\frac{A_e k_e}{h_e}\begin{bmatrix} 1 & -1 \\ -1 & 1 \end{bmatrix}\begin{Bmatrix} T_1^e \\ T_2^e \end{Bmatrix} = \begin{Bmatrix} Q_1^e \\ Q_2^e \end{Bmatrix} \tag{3.3.5b}$$

which are the same as those in (3.3.5*a*) with E_e replaced by k_e, T_i^e by u_i^e, and P_i^e by Q_i^e [and reverse the arrow at node 2 in Fig. 3.2.3(*b*)].

Equations of the type (3.3.5*a*) can also be derived for discrete systems (as opposed to a continuum) consisting of spring elements, pipe-flow elements, electrical resistor elements, and so on. These elements will be discussed in Chapter 4 using physical principles. However, such a direct approach cannot be used when the element data is not constant or when higher-order approximation of the dependent unknowns is used.

Remark 8. Another interpretation of (3.2.39) for $c_e = 0$ can be given in terms of the finite difference approximation. The axial force at any point x is given by $P(x) = EA\, du/dx$. Using the forward difference approximation, we approximate the derivative du/dx and write

$$-P_1^e \equiv P(x)|_{x_e} = E_e A_e [u(x_{e+1}) - u(x_e)]/h_e \tag{3.3.6a}$$

$$P_2^e \equiv P(x)|_{x_{e+1}} = E_e A_e [u(x_{e+1}) - u(x_e)]/h_e \tag{3.3.6b}$$

which are the same as (3.3.5*a*), with $u_1^e = u(x_e)$ and $u_2^e = u(x_{e+1})$. Note that no explicit approximation of $u(x)$ itself is assumed in writing (3.3.6*a*) and (3.3.6*b*), but the fact that we used values of the function from two consecutive points to define its slope implies that we assumed a linear approximation of the function. Thus, to compute the value of u at a point other than the nodes (or mesh points), linear interpolation must be used.

Remark 9. For the model problem considered, the element matrices $[K^e]$ in (3.2.31*b*) are symmetric: $K_{ij}^e = K_{ji}^e$. This enables one to compute K_{ij}^e $(I = 1, 2, \ldots, n)$ for $j \le i$ only. In other words, we need compute only the diagonal terms and the upper or lower diagonal terms. Because of the symmetry of the element matrices, the assembled global matrix will also be symmetric. Thus, we need to store only the upper triangle, including the diagonal, of the assembled matrix in a finite element computer program. Another property characteristic of the finite element method is the *sparseness* of the assembled matrix. Since $K_{IJ} = 0$, if global nodes I and J do not belong to the same finite element, the global coefficient matrix is *banded,* i.e., all coefficients beyond a certain distance from the diagonal are zero. The maximum of the distances between the diagonal element, including the latter, of a row and the last nonzero coefficient in that row is called the *half-bandwidth*. When a matrix is banded and symmetric, we need to store only entries in the upper or lower band of the matrix. Equation solvers written for the solution of banded symmetric equations are available for use in such cases (see Chapter 7 for additional discussion). The symmetry of the coefficient matrix depends on the type of the differential equation, its variational form, and the numbering of the finite element equations. The sparseness of the matrix is a result of the finite element interpolation functions, which have nonzero values only over an element of the domain (i.e., so-called "compactness" property of the approximation functions).

Remark 10. The balance (or "equilibrium") of the secondary variables Q_I^e at the interelement boundaries is expressed by (3.2.43). This amounts to imposing the condition that the secondary variable adu/dx at the node, where u is the actual solution, be continuous. However, this does not imply continuity of adu_h^e/dx, where u_h^e is the finite element solution. Thus, we have

$$Q_2^e + Q_1^{e+1} = 0 \quad \text{or} \quad Q_0 \tag{3.3.7}$$

but

$$\left(a\frac{du_h^e}{dx}\right)\Big|_{x_e} + \left(-a\frac{du_h^{e+1}}{dx}\right)\Big|_{x_e} \neq 0 \quad \text{or} \quad Q_0 \tag{3.3.8}$$

In most books on the finite element method, this point is not made clear to the reader. These books consider the quadratic form or weak form of the total problem and omit the sum of the interelement contributions (for linear elements),

$$\sum_{e=1}^{N}\left(\sum_{i=1}^{2} Q_i^e u_i^e\right) \tag{3.3.9}$$

in the quadratic form (or functional) of the problem. However, this amounts to imposing equilibrium conditions of the form (3.3.8). When the secondary variable is specified to be nonzero (say, Q_0) at an interelement boundary (say, at global node 2), we have

$$Q_2^1 + Q_1^2 = Q_0$$

In other books, Q_0 is included in the functional as $Q_0 U_2$, where U_2 is the value of u at global node 2.

To fully understand the difference between the direct use of the global statement versus using the assembly of element equations, consider the model problem described by Eqs. (3.2.1) and (3.2.2) with $c = 0$. The variational form of these equations over the entire domain is given by

$$0 = \int_0^L \left(a\frac{dv}{dx}\frac{du}{dx} - vq\right) dx - v(L)Q_0 \tag{3.3.10}$$

When u is approximated by functions that are defined only on a local interval (which is the case in the finite element method), use of the above variational form implies the omission of the sum of the interelement contributions of (3.3.9).

Consider a mesh of three linear elements. Since $\psi_i^e (e = 1, 2, 3)$ is zero in any element Ω_f for $e \neq f$, the (global) finite element solution for the entire domain is given by

$$u_h(x) = \sum_{e=1}^{3}\left(\sum_{i=1}^{2} u_i^e \psi_i^e\right) \equiv \sum_{I=1}^{4} U_I \Phi_I(x) \tag{3.3.11}$$

where $\Phi_I(x)$ $(I = 1, 2, 3, 4)$ are the piecewise-continuous *global interpolation functions* (see Fig. 3.2.9),

$$\Phi_I(x) = \begin{cases} \psi_2^{(I-1)}(x) & \text{for } x_{I-1} \le x \le x_I \\ \psi_1^{(I)}(x) & \text{for } x_I \le x \le x_{I+1} \end{cases} \tag{3.3.12}$$

Substituting (3.3.11) for u and $v = \Phi_I$ into (3.3.10), we obtain

$$0 = \int_0^L \left[a \frac{d\Phi_I}{dx} \left(\sum_{J=1}^{4} U_J \frac{d\Phi_j}{dx} \right) - \Phi_I q \right] dx - \Phi_I(L) Q_0 \tag{3.3.13}$$

Since Φ_I is nonzero only between x_{I-1} and x_{I+1}, the integral becomes

$$0 = \int_{x_{I-1}}^{x_{I+1}} \left[a \frac{d\Phi_I}{dx} \left(U_{I-1} \frac{d\Phi_{I-1}}{dx} + U_I \frac{d\Phi_I}{dx} + U_{I+1} \frac{d\Phi_{I+1}}{dx} \right) - \Phi_I q \right] dx - \Phi_I(L) Q_0 \tag{3.3.14}$$

and we have

$$\begin{aligned}
I = 1 : 0 &= \int_{x_1=0}^{x_2} \left[a \frac{d\Phi_1}{dx} \left(U_1 \frac{d\Phi_1}{dx} + U_2 \frac{d\Phi_2}{dx} \right) - \Phi_1 q \right] dx - \Phi_1(L) Q_0 \\
I = 2 : 0 &= \int_{x_1=0}^{x_3} \left[a \frac{d\Phi_2}{dx} \left(U_1 \frac{d\Phi_1}{dx} + U_2 \frac{d\Phi_2}{dx} + U_3 \frac{d\Phi_3}{dx} \right) - \Phi_2 q \right] dx \\
&\quad - \Phi_2(L) Q_0 \\
I = 3 : 0 &= \int_{x_2}^{x_4=L} \left[a \frac{d\Phi_3}{dx} \left(U_2 \frac{d\Phi_2}{dx} + U_3 \frac{d\Phi_3}{dx} + U_4 \frac{d\Phi_4}{dx} \right) - \Phi_3 q \right] dx \\
&\quad - \Phi_3(L) Q_0 \\
I = 4 : 0 &= \int_{x_3}^{x_4=L} \left[a \frac{d\Phi_4}{dx} \left(U_3 \frac{d\Phi_3}{dx} + U_4 \frac{d\Phi_4}{dx} \right) - \Phi_4 q \right] dx - \Phi_4(L) Q_0
\end{aligned} \tag{3.3.15}$$

These equations, upon performing the integration, yield (3.2.50), with the last column (containing Qs) in the latter replaced by

$$\begin{Bmatrix} 0 \\ Q_0 \\ 0 \\ 0 \end{Bmatrix} \tag{3.3.16}$$

Although this procedure, known as the *direct stiffness method* in structural mechanics, gives the assembled equations directly, it is algebraically complicated (especially for two-dimensional problems) and not amenable to simple computer implementation.

3.4 AXISYMMETRIC PROBLEMS

3.4.1 Model Equation

The equations governing physical processes in a cylindrical geometry are described analytically in terms of cylindrical coordinates (see Fig. 3.4.1; also see Fig. 1.4.5). When the geometry, loading, and boundary conditions are independent of the circumferential direction (i.e., θ-coordinate in Fig. 3.4.1), the problem is said to be axisymmetric and the governing equations become two-dimensional in terms of r and z. The equations are functions of only

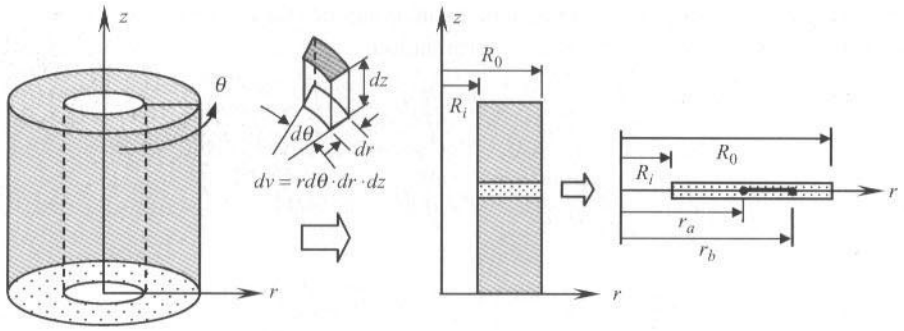

Figure 3.4.1 Volume element and computational domain of an axisymmetric problem.

the radial coordinate r if the problem geometry and data are independent of z. Here, we consider a model second-order equation in a single variable and formulate its finite element model.

Consider the differential equation [an analogue of (3.2.1)]

$$-\frac{1}{r}\frac{d}{dr}\left[a(r)\frac{du}{dr}\right] = f(r) \quad \text{for} \quad R_i < r < R_0 \tag{3.4.1}$$

where r is the radial coordinate, a and f are known functions of r, and u is the dependent variable. Such equations arise, for example, in connection with radial heat flow in a long circular cylinder of inner radius R_i and outer radius R_0. The radially symmetric conditions require that both $a = kr$ (k is the conductivity) and f (internal heat generation) be functions of only r. Since the cylinder is long, the temperature distribution at any section along its length (except perhaps at the ends) is the same, and it is sufficient to consider any cross section away from the ends, i.e., the problem is reduced from a three-dimensional problem to a two-dimensional one. Since a and f are independent of the circumferential direction θ, the temperature distribution along any radial line is the same, reducing the two-dimensional problem to a one-dimensional one, as described by (3.4.1).

3.4.2 Weak Form

In developing the weak form of (3.4.1), we multiply it with a weight function $w(r)$ and integrate over the volume of the cylinder of unit length (see Fig. 3.4.1)

$$\begin{aligned} 0 &= \int_V w\left[-\frac{1}{r}\frac{d}{dr}\left(a\frac{du}{dr}\right) - f\right] dv \\ &= \int_0^1 \int_0^{2\pi} \int_{r_a}^{r_b} w\left[-\frac{1}{r}\frac{d}{dr}\left(a\frac{du}{dr}\right) - f\right] r\, dr\, d\theta\, dz \\ &= 2\pi \int_{r_a}^{r_b} w\left[-\frac{1}{r}\frac{d}{dr}\left(a\frac{du}{dr}\right) - f\right] r\, dr \end{aligned} \tag{3.4.2}$$

where (r_a, r_b) is the domain of a typical element along the radial direction. Next, we carry out the remaining two steps of the weak formulation:

$$0 = 2\pi \int_{r_a}^{r_b} \left(a \frac{dw}{dr} \frac{du}{dr} - rwf \right) dr - 2\pi \left[wa \frac{du}{dr} \right]_{r_a}^{r_b}$$

$$0 = 2\pi \int_{r_a}^{r_b} \left(a \frac{dw}{dr} \frac{du}{dr} - rwf \right) dr - w(r_a) Q_1^e - w(r_b) Q_2^e \tag{3.4.3a}$$

where

$$Q_1^e \equiv -2\pi \left(a \frac{du}{dr} \right) \Big|_{r_a}, \quad Q_2^e \equiv 2\pi \left(a \frac{du}{dr} \right) \Big|_{r_b} \tag{3.4.3b}$$

3.4.3 Finite Element Model

The finite element model is obtained by substituting the approximation

$$u(r) \approx \sum_{j=1}^{n} u_j^e \psi_j^e(r) \tag{3.4.4}$$

and $w = \psi_1, \psi_2, \ldots, \psi_n$ into (3.4.3a). The finite-element model is given by

$$[K^e]\{u^e\} = \{f^e\} + \{Q^e\} \tag{3.4.5a}$$

where

$$K_{ij}^e = 2\pi \int_{r_a}^{r_b} a \frac{d\psi_i^e}{dr} \frac{d\psi_j^e}{dr} dr, \quad f_i^e = 2\pi \int_{r_a}^{r_b} \psi_i^e f r \, dr \tag{3.4.5b}$$

and ψ_i^e are the interpolation functions expressed in terms of the radial coordinate r. For example, the linear interpolation functions are of the form $(h_e = r_b - r_a)$ [see Eq. (3.2.17)]

$$\psi_1^e(r) = \frac{r_b - r}{h_e}, \quad \psi_2^e(r) = \frac{r - r_a}{h_e} \tag{3.4.6}$$

The explicit forms of the coefficients K_{ij}^e and f_i^e for $a = a_e r$ and $f = f_e$ are given below (r_a denotes the global coordinate of node 1 of the element).

Linear Element

$$[K^e] = \frac{2\pi a_e}{h_e} (r_a + \frac{1}{2} h_e) \begin{bmatrix} 1 & -1 \\ -1 & 1 \end{bmatrix}, \quad \{f^e\} = \frac{2\pi f_e h_e}{6} \begin{Bmatrix} 3r_a + h_e \\ 3r_a + 2h_e \end{Bmatrix} \tag{3.4.7}$$

Quadratic Element

$$[K^e] = \frac{2\pi a_e}{6h_e} \begin{bmatrix} 3h_e + 14r_a & -(4h_e + 16r_a) & h_e + 2r_a \\ -(4h_e + 16r_a) & 16h_e + 32r_a & -(12h_e + 16r_a) \\ h_e + 2r_a & -(12h_e + 16r_a) & 11h_e + 14r_a \end{bmatrix}$$

$$\{f^e\} = \frac{2\pi f_e h_e}{6} \begin{Bmatrix} r_a \\ 4r_a + 2h_e \\ r_a + h_e \end{Bmatrix} \tag{3.4.8}$$

Example 3.4.1

Equation (3.4.1) governs, for example, temperature distribution $u(r)$ in a *long* solid cylindrical bar of radius R and thermal conductivity k (i.e., $a(r) = rk$) that is heated by the passage of an electric current, which generates heat energy f_0. Heat is dissipated from the surface of the bar by convection into the surrounding medium at an ambient temperature of u_∞. We wish to determine the temperature distribution as a function of the radial distance. The boundary conditions for this case are

$$\frac{du}{dr} = 0 \text{ at } r = 0 \text{ (symmetry)}, \quad k\frac{du}{dr} + \beta(u - u_\infty) = 0 \text{ at } r = R_0 \text{ (convection)} \tag{3.4.9}$$

Let us consider the following data for numerical computations:

$$R = 0.05 \text{ m}, \quad k = 40 \text{ W/(m} \cdot {}^\circ\text{C)}, \quad f_0 = 4 \times 10^6 \text{ W/m}^3, \quad \beta = 400 \text{ W/(m}^2 \cdot {}^\circ\text{C)}, \quad u_\infty = 20^\circ\text{C} \tag{3.4.10}$$

For the uniform mesh of four linear elements ($h = 0.0125$ m), we have (omitting the common factor 2π) the following coefficient matrices.

Element 1. ($r_a = 0$ and $r_b = h$):

$$[K^1] = \frac{40}{2}\begin{bmatrix} 1 & -1 \\ -1 & 1 \end{bmatrix}, \quad \{f^1\} = \frac{4 \times 10^6 (0.0125)^2}{6}\begin{Bmatrix} 1 \\ 2 \end{Bmatrix}$$

Element 2. ($r_a = h$ and $r_b = 2h$):

$$[K^2] = \frac{40}{2}\begin{bmatrix} 3 & -3 \\ -3 & 3 \end{bmatrix}, \quad \{f^2\} = \frac{4 \times 10^6 (0.0125)^2}{6}\begin{Bmatrix} 4 \\ 5 \end{Bmatrix}$$

Element 3. ($r_a = 2h$ and $r_b = 3h$):

$$[K^3] = \frac{40}{2}\begin{bmatrix} 5 & -5 \\ -5 & 5 \end{bmatrix}, \quad \{f^3\} = \frac{4 \times 10^6 (0.0125)^2}{6}\begin{Bmatrix} 7 \\ 8 \end{Bmatrix}$$

Element 4. ($r_a = 3h$ and $r_b = 4h$):

$$[K^2] = \frac{40}{2}\begin{bmatrix} 7 & -7 \\ -7 & 7 \end{bmatrix}, \quad \{f^4\} = \frac{4 \times 10^6 (0.0125)^2}{6}\begin{Bmatrix} 10 \\ 11 \end{Bmatrix}$$

The assembled equations are

$$\begin{bmatrix} 20 & -20 & 0 & 0 & 0 \\ -20 & 80 & -60 & 0 & 0 \\ 0 & -60 & 160 & -100 & 0 \\ 0 & 0 & -100 & 240 & -140 \\ 0 & 0 & 0 & -140 & 140 \end{bmatrix}\begin{Bmatrix} U_1 \\ U_2 \\ U_3 \\ U_4 \\ U_5 \end{Bmatrix} = 104.166\begin{Bmatrix} 1 \\ 6 \\ 12 \\ 18 \\ 11 \end{Bmatrix} + \begin{Bmatrix} Q_1^1 \\ Q_2^1 + Q_1^2 \\ Q_2^2 + Q_1^3 \\ Q_2^3 + Q_1^4 \\ Q_2^4 \end{Bmatrix}$$

The boundary and balance conditions require

$$Q_1^1 = 0,\quad Q_2^1 + Q_1^2 = 0,\quad Q_2^2 + Q_1^3 = 0,\quad Q_2^3 + Q_1^4 = 0,\quad Q_2^4 = -R_0\beta(U_5 - u_\infty) = -20(U_5 - 20)$$

The condensed equations are (here, no equations are eliminated)

$$\begin{bmatrix} 20 & -20 & 0 & 0 & 0 \\ -20 & 80 & -60 & 0 & 0 \\ 0 & -60 & 160 & -100 & 0 \\ 0 & 0 & -100 & 240 & -140 \\ 0 & 0 & 0 & -140 & 160 \end{bmatrix} \begin{Bmatrix} U_1 \\ U_2 \\ U_3 \\ U_4 \\ U_5 \end{Bmatrix} = 104.166 \begin{Bmatrix} 1 \\ 6 \\ 12 \\ 18 \\ 11 \end{Bmatrix} + \begin{Bmatrix} 0 \\ 0 \\ 0 \\ 0 \\ 400 \end{Bmatrix}$$

The solution of these equations (with the help of a computer) is

$$U_1 = 334.68,\ U_2 = 329.47,\ U_3 = 317.32,\ U_4 = 297.53,\ U_5 = 270.00$$

The uniform mesh of two quadratic elements yields the nodal values

$$U_1 = 332.50,\ U_2 = 328.59,\ U_3 = 316.87,\ U_4 = 297.34,\ U_5 = 270.00$$

which coincide with the exact solution at the nodes

$$u(r) = u_\infty + \frac{f_0 R_0}{2\beta} + \frac{f_0 R_0^2}{4k}\left(1 - \frac{r^2}{R_0^2}\right) \tag{3.4.11}$$

3.5 SUMMARY

A systematic study of the steps involved in the finite element formulation of a model second-order differential equation in single variable is presented. The basic steps of the formulation and analysis of a typical equation are outlined in Table 3.1.1. The model equation is representative of the equations arising in various fields of engineering (see Table 3.2.1). Couple of numerical examples are presented to illustrate the steps in the finite element analysis of second-order differential equations. Additional examples, especially those arising in heat transfer, fluid mechanics, and solid mechanics will be presented in Chapter 4.

The finite element model is developed following three steps:

1. Weak (or variational) formulation of the differential equation over an element.
2. Finite element interpolation of the primary variables of the weak formulation.
3. Finite element model (i.e., a set of algebraic equations relating the "primary" and "secondary" variables) development over a typical element.

The weak formulation itself involves a three-step procedure, which enables identification of primary and secondary variables. The primary variables are required to be continuous throughout the domain, including the nodes at which elements are connected. The secondary variables are included in the weak form. The finite element interpolation functions have been developed systematically on the basis of continuity, completeness, and linear independence. The finite element model has been developed by substituting appropriate interpolation of the primary variable into the weak form of the differential equation.

PROBLEMS

For Problems 3.1–3.4, carry out the following tasks:

(a) Develop the *weak forms* of the given differential equation(s) over a typical finite element, which is a geometric subdomain located between $x = x_a$ and $x = x_b$. Note that there are no "specified" boundary conditions at the element level. Therefore, in going from Step 2 to Step 3 of the weak-form development, one must identify the secondary variable(s) at the two ends of the domain by some symbols (like Q_1^e and Q_2^e for the first problem) and complete the weak form.

(b) Assume an approximation(s) of the form

$$u(x) = \sum_{j=1}^{n} u_j^e \psi_j^e(x) \tag{1}$$

where u is a primary variable of the formulation, $\psi_j^e(x)$ are the interpolation functions, and u_j^e are the values of the primary variable(s) at the jth node of the element. Substitute the expression in (1) for the primary variable and ψ_j^e for the weight function into the weak form(s) and derive the finite element model. Be sure to define all coefficients of the model in terms of the problem data and ψ_i^e.

3.1 Develop the weak form and the finite element model of the following differential equation over an element:

$$-\frac{d}{dx}\left(a\frac{du}{dx}\right) + \frac{d^2}{dx^2}\left(b\frac{d^2u}{dx^2}\right) + cu = f \quad \text{for} \quad x_a < x < x_b$$

where a, b, c, and f are known functions of position x. Ensure that the element coefficient matrix $[K^e]$ is symmetric. What is the nature of the interpolation functions for the problem?

3.2 Construct the weak form and the finite element model of the differential equation

$$-\frac{d}{dx}\left(a\frac{du}{dx}\right) - b\frac{du}{dx} = f \quad \text{for} \quad 0 < x < L$$

over a typical element $\Omega_e = (x_a, x_b)$. Here a, b, and f are known functions of x, and u is the dependent variable. The natural boundary condition should *not* involve the function $b(x)$. What type of interpolation functions may be used for u?

3.3 Develop the weak forms of the following pair of coupled second-order differential equations over a typical element (x_a, x_b):

$$-\frac{d}{dx}\left[a(x)\left(u + \frac{dv}{dx}\right)\right] = f(x) \tag{1a}$$

$$-\frac{d}{dx}\left(b(x)\frac{du}{dx}\right) + a(x)\left(u + \frac{dv}{dx}\right) = q(x) \tag{1b}$$

where u and v are the dependent variables, and a, b, f, and q are known functions of x. Also identify the primary and secondary variables of the formulation.

3.4 Consider the following weak forms of a pair of coupled differential equations:

$$0 = \int_{x_a}^{x_b} \left(\frac{dw_1}{dx}\frac{dv}{dx} - w_1 f\right) dx - P_a w_1(x_a) - P_b w_1(x_b) \tag{1a}$$

$$0 = \int_{x_a}^{x_b} \left(\frac{dw_2}{dx}\frac{du}{dx} + c\, w_2 v - w_2 q\right) dx - Q_a w_2(x_a) - Q_b w_2(x_b) \tag{1b}$$

where $c(x)$ is a known function, w_1 and w_2 are weight functions, u and v are dependent variables (primary variables), and P_a, P_b, Q_a, and Q_b are the secondary variables of the formulation. Use the finite element approximations of the form

$$u(x) = \sum_{j=1}^{m} u_j^e \psi_j^e(x), \quad v(x) = \sum_{j=1}^{n} v_j^e \varphi_j^e(x) \tag{2}$$

and $w_1 = \psi_i$ and $w_2 = \varphi_i$ and derive the finite element equations from the weak forms. The finite element equations should be in the form

$$0 = \sum_{j=1}^{m} K_{ij}^{11} u_j^e + \sum_{j=1}^{n} K_{ij}^{12} v_j^e - F_i^1 \tag{3a}$$

$$0 = \sum_{j=1}^{m} K_{ij}^{21} u_j^e + \sum_{j=1}^{n} K_{ij}^{22} v_j^e - F_i^2 \tag{3b}$$

Define the coefficients K_{ij}^{11}, K_{ij}^{12}, K_{ij}^{21}, K_{ij}^{22}, F_i^1, and F_i^2 in terms of the interpolation functions, known data, and secondary variables.

3.5 Derive the Lagrange cubic interpolation functions for a four-node (one-dimensional) element (with equally spaced nodes) using the alternative procedure based on interpolation properties (3.2.18*a*) and (3.2.18*b*). Use the local coordinate $\bar{x}$ for simplicity.

3.6 Evaluate the element matrices $[K^{11}]$, $[K^{12}]$, and $[K^{22}]$ for the linear interpolation of $u(x)$ and $v(x)$ in Problem 3.4.

3.7 Evaluate the following coefficient matrices and source vector using the linear Lagrange interpolation functions:

$$K_{ij}^e = \int_{x_a}^{x_b} (a_0^e + a_1^e x) \frac{d\psi_i^e}{dx} \frac{d\psi_j^e}{dx} dx, \quad M_{ij}^e = \int_{x_a}^{x_b} (c_0^e + c_1^e x) \psi_i^e \psi_j^e dx$$

$$f_i^e = \int_{x_a}^{x_b} (f_0^e + f_1^e x) \psi_i^e dx$$

where a_0^e, a_1^e, c_0^e, c_1^e, f_0^e, and f_1^e are constants.

3.8 (*Heat transfer in a rod*) The governing differential equation and convection boundary condition are of the form:

$$-\frac{d^2\theta}{dx^2} + c\theta = 0, \quad 0 < x < L \tag{1}$$

$$\theta(0) = T_0 - T_\infty, \quad \left[k\frac{d\theta}{dx} + \beta\theta \right]_{x=L} = 0 \tag{2}$$

where $\theta = T - T_\infty$, $c = \beta P/(Ak)$, β is the heat transfer coefficient, P is the perimeter, A is the area of cross section, and k is the conductivity. For a mesh of two linear elements (of equal length), give (*a*) the boundary conditions on the nodal variables (primary as well as secondary variables) and (*b*) the final condensed finite element equations for the unknowns (both primary and secondary nodal variables). Use the following data: $T_0 = 120°\text{C}$, $T_\infty = 20°\text{C}$, $L = 0.25$ m, $c = 256$, $\beta = 64$, and $k = 50$ (with proper units).

3.9 (*Axial deformation of a bar*) The governing differential equation is of the form (E and A are constant):

$$-\frac{d}{dx}\left[EA\frac{du}{dx} \right] = 0, \quad 0 < x < L \tag{1}$$

For the minimum number of linear elements, give (*a*) the boundary conditions on the nodal variables (primary as well as secondary variables) and (*b*) the final condensed finite element equations for the unknowns.

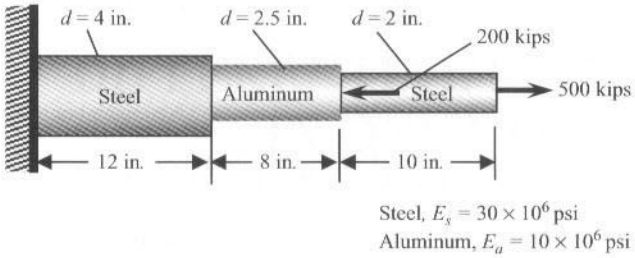

Figure P3.9

3.10 Resolve the problem in Example 3.2.1 using the uniform mesh of three linear finite elements. *Answer:* $U_2 = -0.02999$, $U_3 = -0.04257$, $(Q_1^1)_{def} = 0.08998$, $(Q_2^3)_{def} = 0.12771$.

3.11 Solve the differential equation in Example 3.2.1 for the mixed boundary conditions

$$u(0) = 0, \quad \left(\frac{du}{dx}\right)\bigg|_{x=1} = 1$$

Use the uniform mesh of three linear elements. The exact solution is

$$u(x) = \frac{2\cos(1-x) - \sin x}{\cos(1)} + x^2 - 2$$

Answer: $U_2 = 0.4134$, $U_3 = 0.7958$, $U_4 = 1.1420$, $(Q_1^1)_{\text{def}} = -1.2402$.

3.12 Solve the differential equation in Example 3.2.1 for the *natural* (or Neumann) boundary conditions

$$\left(\frac{du}{dx}\right)\bigg|_{x=0} = 1, \quad \left(\frac{du}{dx}\right)\bigg|_{x=1} = 0$$

Use the uniform mesh of three linear finite elements to solve the problem. Verify your solution with the analytical solution

$$u(x) = \frac{\cos(1-x) + 2\cos x}{\sin(1)} + x^2 - 2$$

Answer: $U_1 = 1.0280$, $U_2 = 1.3002$, $U_4 = 1.4447$, $U_5 = 1.4821$.

3.13 Solve the problem described by the following equations

$$-\frac{d^2u}{dx^2} = \cos \pi x, \quad 0 < x < 1; \quad u(0) = 0, \quad u(1) = 0$$

Use the uniform mesh of three linear elements to solve the problem and compare against the exact solution

$$u(x) = \frac{1}{\pi^2}(\cos \pi x + 2x - 1)$$

3.14 Solve the differential equation in Problem 3.13 using the mixed boundary conditions

$$u(0) = 0, \quad \left(\frac{du}{dx}\right)\bigg|_{x=1} = 0$$

Use the uniform mesh of three linear elements to solve the problem and compare against the exact solution

$$u(x) = \frac{1}{\pi^2}(\cos \pi x - 1)$$

3.15 Solve the differential equation in Problem 3.13 using the Neumann boundary conditions

$$\left(\frac{du}{dx}\right)\bigg|_{x=0} = 0, \quad \left(\frac{du}{dx}\right)\bigg|_{x=1} = 0$$

Use the uniform mesh of three linear elements to solve the problem and compare against the exact solution

$$u(x) = \frac{\cos \pi x}{\pi^2}$$

Note: For Neumann boundary conditions, none of the primary dependent variables are specified, and therefore the solution can be determined within an arbitrary constant for this equation (i.e., when the *cu* term is not present, the coefficient matrix is singular and cannot be inverted). In such cases, one of the U_i should be set equal to a constant to remove the "rigid-body" mode (i.e., to determine the arbitrary constant in the solution).

REFERENCES FOR ADDITIONAL READING

1. Crandall, S. H., *Engineering Analysis*, McGraw-Hill, New York, 1956.
2. Holman, J. P., *Heat Transfer*, 7th ed., McGraw-Hill, New York, 1990.
3. Kreith, F. and Bohn, M. S., *Principles of Heat Transfer*, 5th ed., West Publishing Company, St. Paul, MN, 1993.
4. Mikhlin, S. G., *Variational Methods in Mathematical Physics*, Pergamon Press, New York, 1964.
5. Mikhlin, S. G., *The Numerical Performance of Variational Methods*, Wolters-Noordhoff, Groningen, 1971.
6. Oden, J. T. and Carey, G. F., *Finite Elements. Mathematical Aspects, Volume IV*, Prentice–Hall, Englewood Cliffs, NJ, 1983.
7. Oden, J. T. and Reddy, J. N., *Variational Methods in Theoretical Mechanics*, Springer-Verlag, New York, 1976; 2d ed., 1983.
8. Özisik, M. N., *Heat Conduction*, 2nd ed., John Wiley, New York, 1993.
9. Reddy, J. N., *Energy Principles and Variational Methods in Applied Mechanics*, 2nd ed., John Wiley, New York, 2002.
10. Reddy, J. N., *Applied Functional Analysis and Variational Methods in Engineering*, McGraw-Hill, New York, 1986; Krieger, Melbourne, FL, 1991.
11. Reddy, J. N. and Rasmussen, M. L., *Advanced Engineering Analysis*, John Wiley, New York, 1982; Krieger, Melbourne, FL, 1990.
12. Reddy, J. N., *An Introduction to Nonlinear Finite Element Analysis*, Oxford University Press, Oxford, UK, 2004.
13. Rektorys, K., *Variational Methods in Mathematics, Science and Engineering*, Reidel, Boston, 1977.

Chapter 4

SECOND-ORDER DIFFERENTIAL EQUATIONS IN ONE DIMENSION: APPLICATIONS

4.1 PRELIMINARY COMMENTS

In Chapter 3 we developed weak forms and finite element models of continuum problems described by a fairly general second-order differential equation. For discrete systems, such as a network of springs or electrical circuits, no differential equations exist and the weak form concept is not applicable. Therefore, an alternate approach based on the laws of physics must be used to develop finite element models (i.e., relations between the cause and effect) of such systems. Physical principles can also be used to develop finite element models of continuum problems (as discussed in Remark 7 of Chapter 3) but the approach cannot be used to derive finite element models with higher-order approximation of the field variable.

The objective of this chapter is two-fold. First, we derive finite element models of some typical discrete systems. Finite element models of discrete systems are developed using physical laws familiar to most engineering and applied science majors, and the approach requires no concept of weak form. Second, we present numerical examples of application of finite element models developed for both discrete systems and continuum systems. We will consider several examples to illustrate the steps involved in the finite element analysis of one-dimensional second-order differential equations arising in heat transfer, fluid mechanics, and solid mechanics. The examples presented here make use of the element equations already developed in Chapter 3. While the notation used for the dependent variables, independent coordinates, and data of problems from field to field is different, the reader should keep the common mathematical structure in mind and not get confused with the change of notation from problem to problem and field to field.

4.2 DISCRETE SYSTEMS

4.2.1 Linear Elastic Spring

A linear elastic spring is a discrete element (i.e., not a continuum) whose load-displacement relationship can be expressed as

$$F = k\delta \tag{4.2.1}$$

where F is the force (N) at the right end, δ is the displacement (m) of the right end of the spring relative to the left end in the direction of the force, and k is the constant known as the *spring constant* (N/m). The spring constant depends on the elastic modulus, area of cross section, and number of turns in the coil of the spring. Often a spring is used to characterize the elastic behavior of complex physical systems.

A relationship between the end forces (F_1^e, F_2^e) and end displacements (δ_1^e, δ_2^e) of a typical spring element [see Fig. 4.2.1(a)] can be developed as discussed in Remark 7 for a bar element. The force F_1^e at node 1 is equal to the spring constant multiplied by the relative displacement of node 1 with respect to node 2, $\delta_1^e - \delta_2^e$:

$$F_1^e = k_e(\delta_1^e - \delta_2^e) = k_e\delta_1^e - k_e\delta_2^e$$

Similarly, the force at node 2 is equal to

$$F_2^e = k_e(\delta_2^e - \delta_1^e) = -k_e\delta_1^e + k_e\delta_2^e$$

Note that the force equilibrium, $F_1^e + F_2^e = 0$, is automatically satisfied. The above equations can be written in matrix form as

$$k_e \begin{bmatrix} 1 & -1 \\ -1 & 1 \end{bmatrix} \begin{Bmatrix} \delta_1^e \\ \delta_2^e \end{Bmatrix} = \begin{Bmatrix} F_1^e \\ F_2^e \end{Bmatrix} \tag{4.2.2}$$

Equation (4.2.2) is applicable to any spring element whose force-displacement relation is linear. Thus a typical spring in a network of springs of different spring constants obey Eq. (4.2.2).

Example 4.2.1

Consider the spring assemblage shown in Fig. 4.2.1(b). We wish to determine the displacement of the rigid block and forces in the springs. Assume that the rigid block is required to remain vertical (i.e., no tilting from its vertical position). Since the rigid block must remain vertical, all points on it will move horizontally by the same amount; hence, all global nodes on the block must have the same node number, say 2. Each spring in the assemblage has the same force-displacement relationship as in Eq. (4.2.2), except that element number will be different for different elements.

The three elements are connected at node 2 through the rigid block. Hence, the continuity and equilibrium conditions at node 2 require

$$\delta_2^{(1)} = \delta_1^{(2)} = \delta_1^{(3)} = U_2 \tag{4.2.3a}$$

$$F_2^{(1)} + F_1^{(2)} + F_1^{(3)} = F_2 \tag{4.2.3b}$$

The equilibrium condition (4.2.3*b*) suggests that we must add the second equation of element 1, the first equation of element 2, and the first equation of element 3 together to replace the sum of three unknowns forces $F_2^{(1)} + F_1^{(2)} + F_1^{(3)}$ with the known force F_2. Thus, we have four equations: the first equation of element 1, the sum of the three equations stated above, the second equation of element 2, and the second equation of element 3:

$$\begin{aligned} k_1U_1 - k_1U_2 &= F_1 \\ -k_1U_1 + (k_1 + k_2 + k_3)U_2 - k_2U_3 - k_3U_4 &= F_2 \\ -k_2U_2 + k_2U_3 &= F_3 \\ -k_3U_2 + k_3U_4 &= F_4 \end{aligned} \tag{4.2.4a}$$

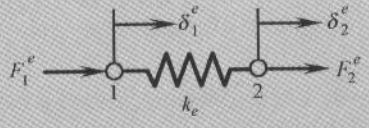

(*a*)

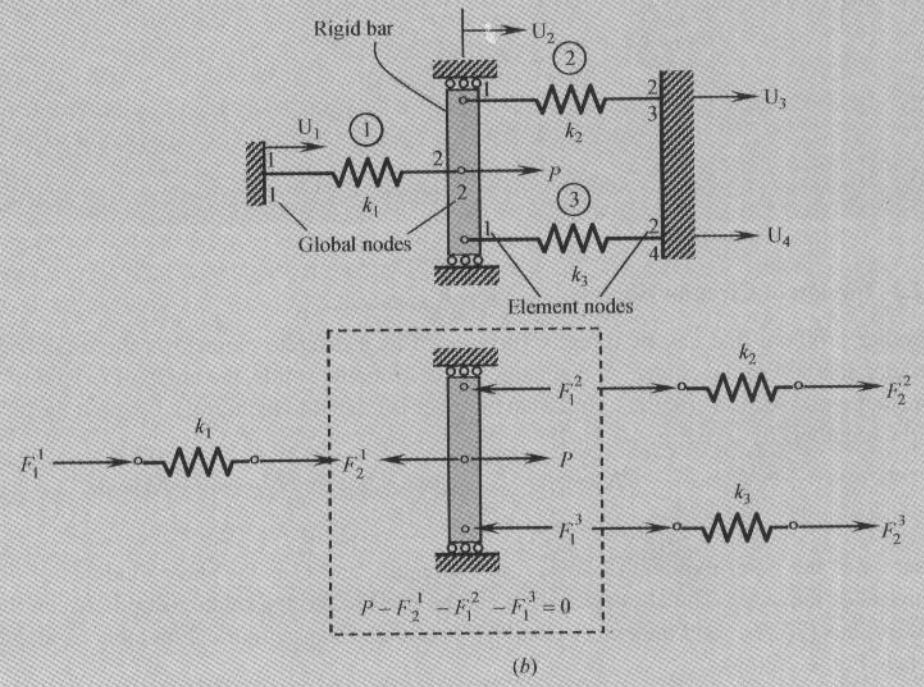

(*b*)

Figure 4.2.1 (*a*) A spring finite element. (*b*) Three-spring assemblage.

In matrix form, the above equations can be expressed as

$$\begin{bmatrix} k_1 & -k_1 & 0 & 0 \\ -k_1 & k_1+k_2+k_3 & -k_2 & -k_3 \\ 0 & -k_2 & k_2 & 0 \\ 0 & -k_3 & 0 & k_3 \end{bmatrix} \begin{Bmatrix} U_1 \\ U_2 \\ U_3 \\ U_4 \end{Bmatrix} = \begin{Bmatrix} F_1 \\ F_2 \\ F_3 \\ F_4 \end{Bmatrix} \tag{4.2.4b}$$

Next, we identify the boundary conditions and impose them on Eq. (4.2.4*b*). From Fig. 4.2.1, it is clear that the displacements of nodes 1, 3, and 4 are zero, and the force at node 2 is specified to be P:

$$U_1 = U_3 = U_4 = 0, \qquad F_2 = P \tag{4.2.5}$$

Thus, there are four unknowns ($F_1 = F_1^{(1)}$, U_2, $F_3 = F_2^{(2)}$, $F_4 = F_2^{(3)}$) and four equations. Using the second equation in (4.2.4*a*), we determine U_2 (condensed equation for the displacement)

$$(k_1+k_2+k_3)\,U_2 = P \text{ or } U_2 = \frac{P}{k_1+k_2+k_3} \tag{4.2.6}$$

The forces F_1, F_3, and F_4 can be calculated using equations 1, 3, and 4 of (4.2.4*a*). The condensed equations for forces are

$$\begin{aligned} F_1 = F_1^{(1)} &= -k_1 U_2 = -\frac{Pk_1}{k_1+k_2+k_3} \\ F_3 = F_2^{(2)} &= -k_2 U_2 = -\frac{Pk_2}{k_1+k_2+k_3} \\ F_4 = F_2^{(3)} &= -k_3 U_2 = -\frac{Pk_3}{k_1+k_2+k_3} \end{aligned} \tag{4.2.7}$$

4.2.2 Torsion of Circular Shafts

Another problem that can be directly formulated as a discrete element is the torsion of circular shafts. From a course on mechanics of deformable solids, the angle of twist θ of a constant cross-section circular cylindrical member is related to the torque T (about the axis of the member) by [see Fig. 4.2.2(*a*)]

$$T = \frac{GJ}{L}\theta \tag{4.2.8}$$

where J is the polar moment of area, L is the length, and G is the shear modulus of the material of the shaft. The above equation can be used to write a relationship between the end torques (T_1^e, T_2^e) and the end twists (θ_1^e, θ_2^e) of a circular cylindrical member of length h_e [see Fig. 4.2.2(*b*)]:

$$T_1^e = \frac{G_e J_e}{h_e}\left(\theta_1^e - \theta_2^e\right), \; T_2^e = \frac{G_e J_e}{h_e}\left(\theta_2^e - \theta_1^e\right)$$

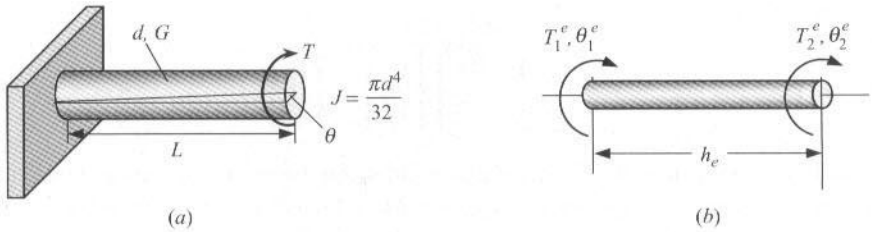

Figure 4.2.2 Torsion of a circular shaft.

or

$$\frac{G_e J_e}{h_e}\begin{bmatrix} 1 & -1 \\ -1 & 1 \end{bmatrix}\begin{Bmatrix} \theta_1^e \\ \theta_2^e \end{Bmatrix} = \begin{Bmatrix} T_1^e \\ T_2^e \end{Bmatrix} \tag{4.2.9}$$

4.2.3 Electrical Resistor Circuits

There is a direct analogy between a network of mechanical springs and a direct current electric resistor network. Ohm's law provides the relationship between flow of electric current I (amperes) through an ideal resistor and voltage drop V (volts) between the ends of the resistor

$$V = IR \tag{4.2.10}$$

where R denotes the electric resistance (ohms) of the wire.

Kirchhoff's voltage rule states that the algebraic sum of the voltage changes in any loop must be equal to zero. Applied to a single resistor, the rule gives [see Fig. 4.2.3(*a*)]

$$I_1^e R_e + V_2^e - V_1^e = 0, \quad I_2^e R_e + V_1^e - V_2^e = 0$$

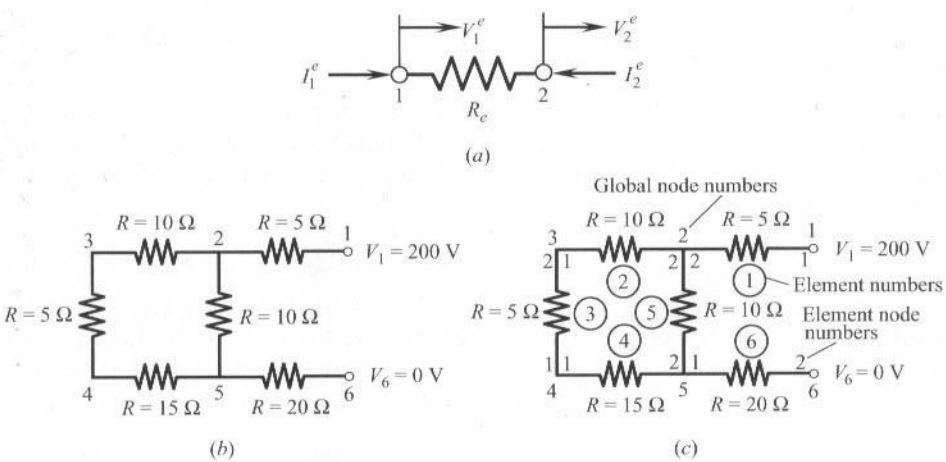

Figure 4.2.3 (*a*) Direct current electric element (current flows from high to low voltage). (*b*) A resistor circuit. (*c*) Finite element mesh of the resistor circuit.

or in matrix form

$$\frac{1}{R_e}\begin{bmatrix} 1 & -1 \\ -1 & 1 \end{bmatrix}\begin{Bmatrix} V_1^e \\ V_2^e \end{Bmatrix} = \begin{Bmatrix} I_1^e \\ I_2^e \end{Bmatrix} \tag{4.2.11}$$

Thus, once again we have the same form of relationship between voltages and currents as in the case of springs. The quantity $1/R_e$ is known as the *electrical conductance.*

The assembly of resistor equations is based on the following rules:

1. Voltage is single-valued.
2. *Kirchhoff current rule:* The sum of all currents entering a node is equal to zero.

Example 4.2.2

Consider the resistor circuit shown in Fig. 4.2.3(*b*). We wish to determine the currents in the loops and voltage at the nodes. The element numbering, element node numbering, and global node numbering are indicated in Fig. 4.2.3(*c*). The element node numbering is important in assembling the element equations. From the element notation indicated in Fig. 4.2.3(*a*), it is clear that current flows from node 1 to node 2 of the element. The element node numbering in Fig. 4.2.3(*c*) indicates the assumed direction of the currents.

The assembled coefficient matrix is given by

$$[K] = \begin{array}{c} \begin{matrix} 1 & 2 & 3 & 4 & 5 & 6 \end{matrix} \\ \begin{bmatrix} K_{11}^1 & K_{12}^1 & 0 & 0 & 0 & 0 \\ & K_{22}^1 + K_{22}^2 + K_{22}^5 & K_{21}^2 & 0 & K_{21}^5 & 0 \\ & & K_{11}^2 + K_{22}^3 & K_{21}^3 & 0 & 0 \\ & & & K_{11}^3 + K_{11}^4 & K_{12}^4 & 0 \\ \text{symm.} & & & & K_{22}^4 + K_{11}^5 + K_{11}^6 & K_{12}^6 \\ & & & & & K_{22}^6 \end{bmatrix} \begin{matrix} 1 \\ 2 \\ 3 \\ 4 \\ 5 \\ 6 \end{matrix} \end{array}$$

$$= \begin{bmatrix} 0.2 & -0.2 & 0 & 0 & 0 & 0 \\ & 0.2+0.1+0.1 & -0.1 & 0 & -0.1 & 0 \\ & & 0.1+0.2 & -0.2 & 0 & 0 \\ & & & 0.2+0.0667 & -0.0667 & 0 \\ \text{symm.} & & & & 0.0667+0.1+0.05 & -0.05 \\ & & & & & 0.05 \end{bmatrix} \tag{4.2.12}$$

The boundary conditions are $V_1 = 200$ V and $V_6 = 0$ V. The condensed equations for the nodal voltages are obtained by omitting the first row and last row of the system, and then moving

the terms involving V_1 and V_6 to the right. We obtain

$$\begin{bmatrix} 0.4 & -0.1 & 0.0 & -0.1 \\ -0.1 & 0.3 & -0.2 & 0.0 \\ 0.0 & -0.2 & 0.2667 & -0.0667 \\ -0.1 & 0.0 & -0.0667 & 0.2167 \end{bmatrix} \begin{Bmatrix} V_2 \\ V_3 \\ V_4 \\ V_5 \end{Bmatrix} = \begin{Bmatrix} 0.2V_1 \\ 0 \\ 0 \\ 0.05V_6 \end{Bmatrix}$$

The solution of these equations is given by (obtained with the aid of a computer)

$$V_2 = 169.23 \text{ V}, \; V_3 = 153.85 \text{ V}, \; V_4 = 146.15 \text{ V}, \; V_5 = 123.08 \text{ V}$$

The condensed equations for the unknown currents at nodes 1 and 6 can be calculated from equations 1 and 6 of the system. We have

$$I_1^{(1)} = 0.2V_1 - 0.2V_2 = 40 - 33.846 = 6.154 \text{ A}$$

$$I_2^{(6)} = -0.05V_5 + 0.05V_6 = -6.154 \text{ A}$$

The negative sign on $I_2^{(6)}$ indicates that the current is flowing out of global node 6.

The currents through each element can be calculated using the element equations (4.2.11). For example, the nodal currents in resistor 5 are given by

$$\begin{Bmatrix} I_1^{(5)} \\ I_2^{(5)} \end{Bmatrix} = \begin{bmatrix} 0.1 & -0.1 \\ -0.1 & 0.1 \end{bmatrix} \begin{Bmatrix} 123.08 \\ 169.23 \end{Bmatrix} = \begin{Bmatrix} -4.615 \\ 4.615 \end{Bmatrix}$$

which indicates that the net current flow in resistor 5 is from its node 2 to node 1 (or global node 2 to global node 5), and its value is 4.615 amps (which is the same as 6.154 – 1.539). The finite element solutions for the voltages and currents are shown in Figure 4.2.4.

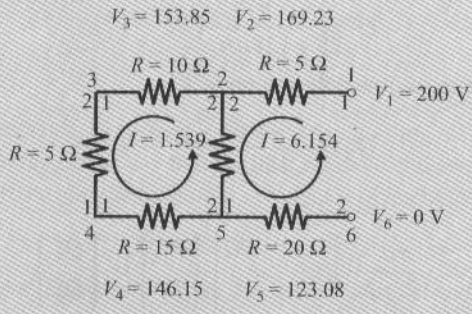

Figure 4.2.4 The solution for currents and voltages obtained with the finite element method.

4.2.4 Fluid Flow through Pipes

Another example of a discrete element is provided by steady, fully developed, flows of viscous incompressible fluids through circular pipes. The velocity of fully developed laminar

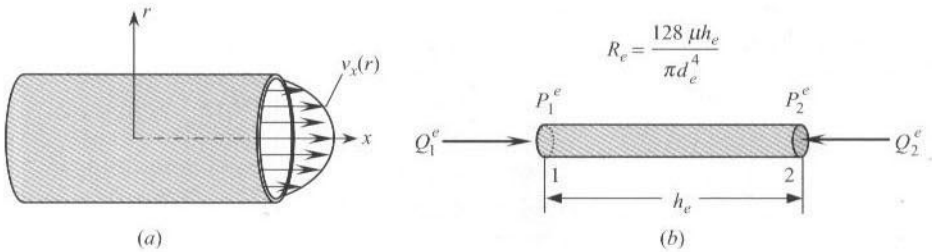

Figure 4.2.5 Flow of viscous fluids through pipes.

flow of viscous fluids through circular pipes is given by

$$v_x = -\frac{1}{4\mu}\frac{dP}{dx}\left[1 - \left(\frac{2r}{d}\right)^2\right] \tag{4.2.13a}$$

where dP/dx is the pressure gradient, d is the diameter of the pipe, and μ is the viscosity of the fluid [see Fig. 4.2.5(*a*)]. The volume rate of flow, Q, is obtained by integrating v_x over the pipe cross section. Thus, the relationship between Q and the pressure gradient dP/dx is given by the equation

$$Q = -\frac{\pi d^4}{128\mu}\frac{dP}{dx} \tag{4.2.13b}$$

The negative sign indicates that the flow is in the direction of negative pressure gradient.

Equation (4.2.13*b*) can be used to develop a relationship between the nodal values of the volume rate of flow, (Q_1^e, Q_2^e) and the pressure, (P_1^e, P_2^e), of a pipe element of length h_e and diameter d_e. The volume rate of flow entering node 1 is given by [see Fig. 4.2.5(*b*)]

$$Q_1^e = -\frac{\pi d_e^4}{128\mu h_e}\left(P_2^e - P_1^e\right)$$

Similarly, the volume rate of flow entering node 2 is

$$Q_2^e = -\frac{\pi d^4}{128\mu h_e}\left(P_1^e - P_2^e\right)$$

Thus, we have

$$\frac{\pi d^4}{128\mu h_e}\begin{bmatrix} 1 & -1 \\ -1 & 1 \end{bmatrix}\begin{Bmatrix} P_1^e \\ P_2^e \end{Bmatrix} = \begin{Bmatrix} Q_1^e \\ Q_2^e \end{Bmatrix} \tag{4.2.14}$$

The constant, $R_e = 128\mu h_e/\pi d_e^4$ is called the *pipe resistance*, in analogy with the electrical resistance [see Eq. (4.2.11)].

4.3 HEAT TRANSFER

4.3.1 Governing Equations

The equations governing conduction heat transfer were discussed in Example 1.2.2. Here we briefly-review the pertinent equations for our use.

The Fourier heat conduction law for one-dimensional systems states that the heat flow $q(x)$ is relate the temperature gradient $\partial T/\partial x$ by the relation (with heat flow in the positive direction of x)

$$q = -kA\frac{\partial T}{\partial x} \tag{4.3.1}$$

where k is the thermal conductivity of the material, A the cross-sectional area, and T the temperature. The negative sign in (4.3.1) indicates that heat flows downhill on the temperature scale. The balance of energy requires that

$$\frac{\partial}{\partial x}\left(kA\frac{\partial T}{\partial x}\right) + Ag = \rho cA\frac{\partial T}{\partial t} \tag{4.3.2}$$

where g is the heat energy generated per unit volume, ρ is the density, c is the specific heat of the material, and t is time. Equation (4.3.2) governs the transient heat conduction in a slab or fin (i.e., a one-dimensional system) when the heat flow in the normal to the x-direction is zero. For a plane wall, we take $A = 1$.

In the case of radially symmetric problems with cylindrical geometries, (4.3.2) takes a different form. Consider a long cylinder of inner radius R_i, outer radius R_o, and length L. When L is very large compared with the diameter, it is assumed that heat flows in the radial direction r. The transient radially symmetric heat flow in a cylinder is governed by

$$\frac{1}{r}\frac{\partial}{\partial r}\left(kr\frac{\partial T}{\partial r}\right) + g = \rho c\frac{\partial T}{\partial t} \tag{4.3.3}$$

A cylindrical fuel element of a nuclear reactor, a current-carrying electrical wire, and a thick-walled circular tube provide examples of one-dimensional radial systems.

The boundary conditions for heat conduction involve specifying either the temperature T or the heat flow Q at a point:

$$T = T_0 \quad \text{or} \quad Q \equiv -kA\frac{\partial T}{\partial x} = Q_0 \tag{4.3.4}$$

It is known that when a heated surface is exposed to a cooling medium, such as air or liquid, the surface will cool faster. We say that the heat is convected away. The *convection heat transfer* between the surface and the medium in contact is given by *Newton's law of cooling*:

$$Q = \beta A(T_s - T_\infty) \tag{4.3.5}$$

where T_s is the surface temperature, T_∞ is the temperature of the surrounding medium, called the *ambient temperature*; and β is the *convection heat transfer coefficient* or *film conductance* (or film coefficient). The heat flow due to conduction and convection at a boundary point must be in balance with the applied flow Q_0:

$$\pm kA\frac{\partial T}{\partial x} + \beta A(T - T_\infty) + Q_0 = 0 \tag{4.3.6}$$

The sign of the first term in (4.3.6) is negative when the heat flow is from the fluid at T_∞ to the surface at the left end of the element, and it is positive when the heat flow is from the fluid at T_∞ to the surface at the right end.

Convection of heat from a surface to the surrounding fluid can be increased by attaching thin strips of conducting metal to the surface. The metal strips are called *fins*. For a fin with heat flow along its length, heat can convect across the lateral surface of the fin [see Fig. 4.3.1(*a*)]. To account for the convection of heat through the surface, we must add the rate of heat loss by convection to the right-hand side of (4.3.2):

$$\frac{\partial}{\partial x}\left(Ak\frac{\partial T}{\partial x}\right) + Aq = \rho cA\frac{\partial T}{\partial t} + P\beta(T - T_\infty) \tag{4.3.7a}$$

where P is the perimeter and β is the film coefficient. Equation (4.3.7*a*) can be expressed in the alternative form

$$\rho cA\frac{\partial T}{\partial t} - \frac{\partial}{\partial x}\left(kA\frac{\partial T}{\partial x}\right) + P\beta T = Ag + P\beta T_\infty \tag{4.3.7b}$$

The units of various quantities (in metric system) are as follows:

T	°C (celsius)	k	$W/(m \cdot °C)$
g	W/m^3	ρ	kg/m^3
c	$J/(kg \cdot °C)$	β	$W/(m^2 \cdot °C)$

For a steady state, we set the time derivatives in (4.3.2), (4.3.3), (4.3.7*a*), and (4.3.7*b*) equal to zero. The steady-state equations for various one-dimensional systems are summarized below [see Fig. 4.3.1(*b*) and (*c*); see Eqs. (1.2.14) and (1.2.17)].

Plane Wall $[Q = k(dT/dx)]$

$$-\frac{d}{dx}\left(k\frac{dT}{dx}\right) = Ag \tag{4.3.8}$$

Fin $[Q = kA(dT/dx)]$

$$-\frac{d}{dx}\left(kA\frac{dT}{dx}\right) + cT = Ag + cT_\infty, \quad c = P\beta \tag{4.3.9}$$

Cylindrical System $[Q = k(dT/dr)]$

$$-\frac{1}{r}\frac{d}{dr}\left(kr\frac{dT}{dr}\right) = g(r) \tag{4.3.10}$$

The essential and natural boundary conditions associated with these equations are of the form

$$T = T_0, \quad Q + \beta A(T - T_\infty) + Q_0 = 0$$

Equations (4.3.8)–(4.3.10) are a special case of the model equation (3.2.1) discussed in Section 3.2, with $a = kA$, $c = P\beta$, and $f \to Ag + P\beta T_\infty$. We immediately have the finite element model of Eqs. (4.3.8) and (4.3.9) from (3.2.31*a*) and (3.2.31*b*):

$$[K^e]\{T^e\} = \{f^e\} + \{Q^e\} \tag{4.3.11a}$$

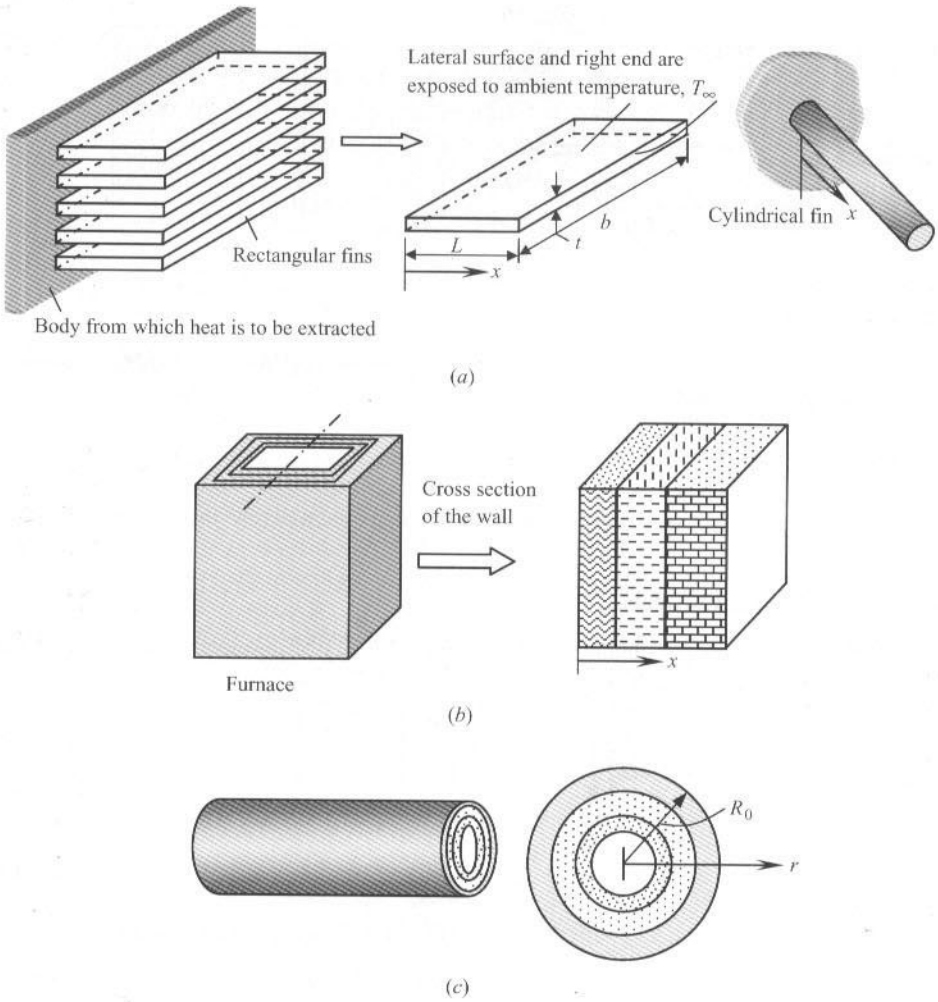

Figure 4.3.1 Heat transfer in (*a*) fins, (*b*) plane wall, and (*c*) radially symmetric system.

Here

$$K_{ij}^e = \int_{x_a}^{x_b} \left(kA \frac{d\psi_i^e}{dx} \frac{d\psi_j^e}{dx} + P\beta \psi_i^e \psi_j^e \right) dx, \quad f_i^e = \int_{x_a}^{x_b} \psi_i^e (Ag + P\beta T_\infty)\, dx$$

$$Q_1^e = \left(-kA \frac{dT}{dx} \right) \Big|_{x_a}, \quad Q_2^e = \left(kA \frac{dT}{dx} \right) \Big|_{x_b} \tag{4.3.11b}$$

where Q_1^e and Q_2^e denote heat flow *into* the element at the nodes.

Equation (4.3.10) is also a special case of the model boundary value problem. However, in developing the weak forms of (4.3.10), integration must be carried over a typical volume element of each system, as discussed in Section 3.4 [see Eq. (3.4.2)].

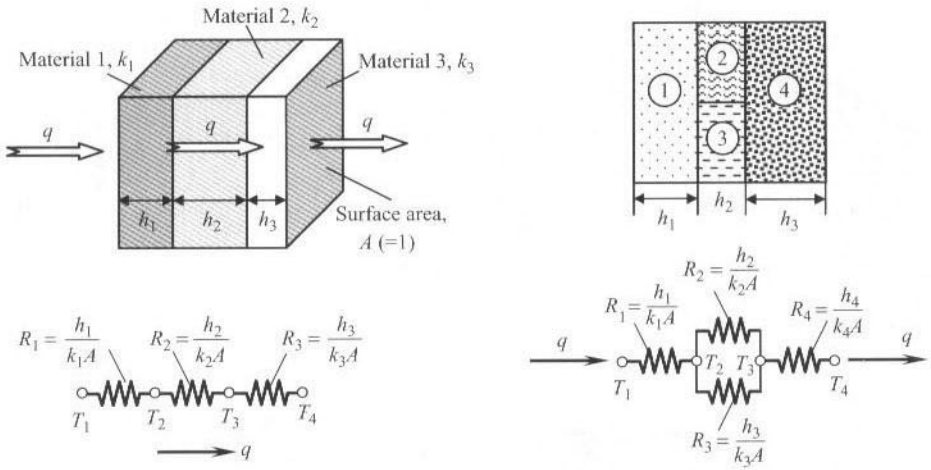

Figure 4.3.2 One-dimensional heat transfer through composite walls and their thermal circuits.

4.3.2 Finite Element Models

It is interesting to note the analogy between Eq. (4.2.11) of an electric resistor and Eq. (3.3.5*b*) of one-dimensional heat transfer (see Remark 7 of Section 3.3):

$$\frac{A_e k_e}{h_e}\begin{bmatrix} 1 & -1 \\ -1 & 1 \end{bmatrix}\begin{Bmatrix} T_1^e \\ T_2^e \end{Bmatrix} = \begin{Bmatrix} Q_1^e \\ Q_2^e \end{Bmatrix} \tag{4.3.12}$$

If we identify *thermal resistance* R_{th}^e by

$$R_{th}^e = \frac{h_e}{k_e A_e} \tag{4.3.13}$$

Equations (4.2.11) and (4.3.12) are the same with the following correspondence:

$$R_e \sim R_{th}^e, \quad I_i^e \sim Q_i^e, \quad V_i^e \sim T_i^e \tag{4.3.14}$$

This allows us to model complicated problems involving both series and parallel thermal resistances. Typical problems and their electrical analogies are shown in Figure 4.3.2.

4.3.3 Numerical Examples

Example 4.3.1

A composite wall consists of three materials, as shown in Fig. 4.3.3. The inside wall temperature is 200°C and the outside air temperature is 50°C with a convection coefficient of $\beta =$ 10 W (m^2·K). We wish to determine the temperature along the composite wall.

First, we note that the problem is governed by the equation

$$-kA\frac{d^2T}{dx^2} = 0, \quad 0 < x < L \tag{4.3.15}$$

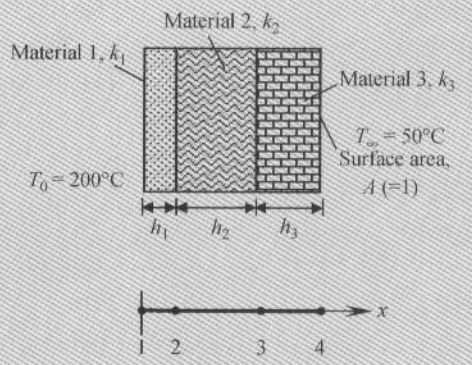

$k_1 = 70$ W/(m·K)
$k_2 = 40$ W/(m·K)
$k_3 = 20$ W/(m·K)
$h_1 = 2$ cm
$h_2 = 2.5$ cm
$h_3 = 4$ cm
$T_\infty = 50°C$
$\beta = 10$ W/(m^2·K)

Figure 4.3.3 Heat transfer problem discussed in Example 4.3.1.

and is subjected to the boundary conditions

$$T(0) = T_0, \quad \left[kA\frac{dT}{dx} + \beta A\,(T - T_\infty) \right]_{x=L} = 0 \tag{4.3.16}$$

where A is the area of cross section (can be taken to be equal to 1) and k is the conductivity.

The data is discontinuous (i.e., different values of $a_e = k_e A_e$ and h_e for different elements). The source term $f = 0$ and therefore $\{f\}^{(e)} = \{0\}$ for $e = 1, 2, 3$. For a mesh of three linear elements (minimum needed), we have

$$[\mathbf{K}]^{(1)} = \frac{k_1 A}{h_1}\begin{bmatrix} 1 & -1 \\ -1 & 1 \end{bmatrix} = \frac{70 \times 1}{0.02}\begin{bmatrix} 1 & -1 \\ -1 & 1 \end{bmatrix} = \begin{bmatrix} 3500 & -3500 \\ -3500 & 3500 \end{bmatrix}$$

$$[\mathbf{K}]^{(2)} = \frac{k_2 A}{h_2}\begin{bmatrix} 1 & -1 \\ -1 & 1 \end{bmatrix} = \frac{40 \times 1}{0.025}\begin{bmatrix} 1 & -1 \\ -1 & 1 \end{bmatrix} = \begin{bmatrix} 1600 & -1600 \\ -1600 & 1600 \end{bmatrix}$$

$$[\mathbf{K}]^{(3)} = \frac{k_3 A}{h_3}\begin{bmatrix} 1 & -1 \\ -1 & 1 \end{bmatrix} = \frac{20 \times 1}{0.04}\begin{bmatrix} 1 & -1 \\ -1 & 1 \end{bmatrix} = \begin{bmatrix} 500 & -500 \\ -500 & 500 \end{bmatrix}$$

The assembled equations are

$$\begin{bmatrix} 3500 & -3500 & 0 & 0 \\ -3500 & 3500+1600 & -1600 & 0 \\ 0 & -1600 & 1600+500 & -500 \\ 0 & 0 & -500 & 500 \end{bmatrix}\begin{Bmatrix} U_1 \\ U_2 \\ U_3 \\ U_4 \end{Bmatrix} = \begin{Bmatrix} Q_1^1 \\ Q_2^1 + Q_1^2 \\ Q_2^2 + Q_1^3 \\ Q_2^3 \end{Bmatrix}$$

The boundary and balance conditions are

$$U_1 = 200,\ Q_2^1 + Q_1^2 = 0,\ Q_2^2 + Q_1^3 = 0,\ Q_2^3 = -\beta A\,(U_4 - T_\infty) = -10 \times 1(U_4 - 50)$$

Hence, the condensed equations (obtained by omitting first row and column and modifying the right-hand side) for the unknown temperatures are

$$\begin{bmatrix} 3500+1600 & -1600 & 0 \\ -1600 & 1600+500 & -500 \\ 0 & -500 & 500 \end{bmatrix}\begin{Bmatrix} U_2 \\ U_3 \\ U_4 \end{Bmatrix} = \begin{Bmatrix} 3500 \times 200 \\ 0 \\ -10U_4 + 500 \end{Bmatrix}$$

or

$$\begin{bmatrix} 5100 & -1600 & 0 \\ -1600 & 2100 & -500 \\ 0 & -500 & 510 \end{bmatrix} \begin{Bmatrix} U_2 \\ U_3 \\ U_4 \end{Bmatrix} = \begin{Bmatrix} 7 \times 10^5 \\ 0 \\ 500 \end{Bmatrix}$$

The solution is given by

$$U_1 = 200\,^\circ\text{C}, U_2 = 199.58\,^\circ\text{C}, U_3 = 198.67\,^\circ\text{C}, \; U_4 = 195.76\,^\circ\text{C}$$

The condensed equations for the unknown heats (per unit area) are

$$Q_1^{(1)} = 3500U_1 - 3500U_2 = 3500 \times 200 - 3500 \times 199.58354 = 1457.6 \text{ W/m}^2 \text{(heat in)}$$

$$Q_2^{(3)} = -10 \times 1\,(U_4 - 50) = -10(195.76 - 50) = -1457.6 \text{ W/m}^2 \text{ (heat out)}$$

It can be shown that for this problem the finite element solution for the nodal temperatures and heats coincides with the exact solution (see Remark 6 of Chapter 3), which is given by

$$T_{\text{exact}}(x) = \begin{cases} A_1 + A_2 x, & 0 < x < h_1 \\ B_1 + B_2 x, & h_1 < x < h_1 + h_2 \\ C_1 + C_2 x, & h_1 + h_2 < x < h_1 + h_2 + h_3 = L \end{cases} \tag{4.3.17a}$$

where

$$A_1 = T_0, \; A_2 = \frac{T_\infty - T_0}{\Delta}, \; B_1 = T_0 + h_1 \left(1 - \frac{k_1}{k_2}\right) A_2$$

$$B_2 = \frac{k_1}{k_2} A_2, \; C_1 = T_\infty - k_1 \left(\frac{1}{\beta} + \frac{L}{k_3}\right) A_2, \; C_2 = \frac{k_2}{k_3} B_2$$

$$\Delta = k_1 \left(\frac{h_1}{k_1} + \frac{h_2}{k_2} + \frac{h_3}{k_3} + \frac{1}{\beta}\right) \tag{4.3.17b}$$

Example 4.3.2

Rectangular fins are used to remove heat from a heated surface [see Fig. 4.3.1(*a*)]. The fins are exposed to ambient air at T_∞. The heat transfer coefficient associated with fin material and the air is β. Assuming that heat is conducted along the length of the fin and uniform along the width and thickness directions, we wish to determine the temperature distribution along the fin and heat loss per fin for two different sets of boundary conditions.

The governing differential equation and boundary conditions of the problem are

$$-kA \frac{d^2T}{dx^2} + \beta P\,(T - T_\infty) = 0, \quad 0 < x < L \tag{4.3.18}$$

Set 1: $T(0) = T_0, \quad \left[kA \dfrac{dT}{dx} + \beta A\,(T - T_\infty)\right]_{x=L} = 0$ (4.3.19*a*)

Set 2: $T(0) = T_0, \quad T(L) = T_L$ (4.3.19*b*)

where T is the temperature, k the conductivity, β is the heat transfer coefficient, P is the perimeter, and A is the area of cross section. Compared to the model equation (3.2.1), we have the following data:

$$a = kA,\ c = P\beta,\ f = P\beta T_\infty$$

For this case, $c \neq 0$, and the finite element solution at the nodes does not coincide with the exact solution.

We consider a uniform mesh (i.e., $h_1 = h_2 = h_3 = h_4 = L/4$) of four linear elements (see Fig. 4.3.4). The element matrices are

$$[K]^{(e)} = \frac{kA}{h_e}\begin{bmatrix} 1 & -1 \\ -1 & 1 \end{bmatrix} + \frac{P\beta h_e}{6}\begin{bmatrix} 2 & 1 \\ 1 & 2 \end{bmatrix},\ \{f\}^{(e)} = \frac{P\beta T_\infty}{2}\begin{Bmatrix} 1 \\ 1 \end{Bmatrix}$$

The assembled system of equations is given by ($h_1 = h_2 = h_3 = h_4 = h = L/4$)

$$\left(\frac{kA}{h}\begin{bmatrix} 1 & -1 & 0 & 0 & 0 \\ -1 & 2 & -1 & 0 & 0 \\ 0 & -1 & 2 & -1 & 0 \\ 0 & 0 & -1 & 2 & -1 \\ 0 & 0 & 0 & -1 & 1 \end{bmatrix} + \frac{\beta P h}{6}\begin{bmatrix} 2 & 1 & 0 & 0 & 0 \\ 1 & 4 & 1 & 0 & 0 \\ 0 & 1 & 4 & 1 & 0 \\ 0 & 0 & 1 & 4 & 1 \\ 0 & 0 & 0 & 1 & 2 \end{bmatrix}\right)\begin{Bmatrix} U_1 \\ U_2 \\ U_3 \\ U_4 \\ U_5 \end{Bmatrix} = \begin{Bmatrix} Q_1^1 \\ Q_2^1 + Q_1^2 \\ Q_2^2 + Q_1^3 \\ Q_2^3 + Q_1^4 \\ Q_2^4 \end{Bmatrix} + \begin{Bmatrix} f_1^1 \\ f_2^1 + f_1^2 \\ f_2^2 + f_1^3 \\ f_2^3 + f_1^4 \\ f_2^4 \end{Bmatrix}$$

Set 1 Boundary Conditions

The boundary and balance conditions are

$$U_1 = T_0,\ Q_2^1 + Q_1^2 = 0,\ Q_2^2 + Q_1^3 = 0,\ Q_2^3 + Q_1^4 = 0,\ Q_2^4 = -\beta A U_5 + \beta A T_\infty$$

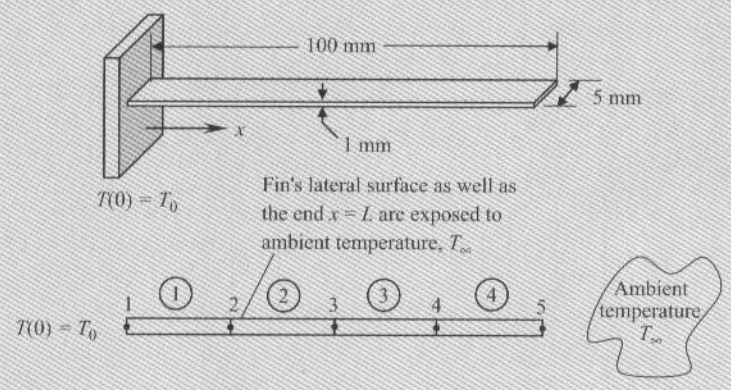

Figure 4.3.4 Finite element mesh of a rectangular fin.

Hence, the condensed equations are

$$\left(\frac{kA}{h}\begin{bmatrix}2 & -1 & 0 & 0\\ -1 & 2 & -1 & 0\\ 0 & -1 & 2 & -1\\ 0 & 0 & -1 & 1\end{bmatrix}+\frac{\beta Ph}{6}\begin{bmatrix}4 & 1 & 0 & 0\\ 1 & 4 & 1 & 0\\ 0 & 1 & 4 & 1\\ 0 & 0 & 1 & 2+\alpha\end{bmatrix}\right)\begin{Bmatrix}U_2\\ U_3\\ U_4\\ U_5\end{Bmatrix}$$

$$=\begin{Bmatrix}\left(\frac{kA}{h}-\frac{\beta Ph}{6}\right)T_0\\ 0\\ 0\\ \beta AT_\infty\end{Bmatrix}+\frac{P\beta T_\infty h}{2}\begin{Bmatrix}1+1\\ 1+1\\ 1+1\\ 1\end{Bmatrix}$$

$$Q_1^1=-f_1^1+\left(\frac{kA}{h}+\frac{\beta Ph}{3}\right)T_0+\left(-\frac{kA}{h}+\frac{\beta Ph}{6}\right)U_2$$

$$Q_2^4=-\beta AU_5+\beta AT_\infty$$

where $\alpha=\beta A/(\beta Ph/6)=6A/Ph$.

For the choice of the following data (material of the fin is copper),

$$k=385\ \text{W(m}\cdot{}^\circ\text{C)},\ \beta=25\ \text{W(m}^2\cdot{}^\circ\text{C)},\ T_0=100^\circ\text{C},\ T_\infty=20^\circ\text{C}$$

$$L=100\ \text{mm},\ t=1\ \text{mm},\ b=5\ \text{mm}$$

we have

$$\frac{kA}{h}=\frac{385\times5\times10^{-6}}{25\times10^{-3}}=0.077,\quad \frac{\beta Ph}{6}=\frac{25\times12\times10^{-3}\times25\times10^{-3}}{6}=0.00125$$

$$\beta PT_\infty h=25\times12\times10^{-3}\times20\times25\times10^{-3}=0.15,\ \beta AT_\infty=25\times5\times10^{-6}\times20=0.0025$$

$$\alpha=6\frac{A}{Ph}=\frac{6\times5}{12\times25}=0.1$$

The condensed equations for the unknown nodal temperatures become

$$\left(\begin{bmatrix}0.154 & -0.077 & 0 & 0\\ -0.077 & 0.154 & -0.077 & 0\\ 0 & -0.077 & 0.154 & -0.077\\ 0 & 0 & -0.077 & 0.077\end{bmatrix}+\begin{bmatrix}0.005 & 0.00125 & 0 & 0\\ 0.00125 & 0.005 & 0.00125 & 0\\ 0 & 0.00125 & 0.005 & 0.00125\\ 0 & 0 & 0.00125 & 0.002625\end{bmatrix}\right)$$

$$\times\begin{Bmatrix}U_2\\ U_3\\ U_4\\ U_5\end{Bmatrix}=\begin{Bmatrix}(0.077-0.0025)\,100\\ 0\\ 0\\ 25\times5\times10^{-6}\times20\end{Bmatrix}+\begin{Bmatrix}0.15\\ 0.15\\ 0.15\\ 0.075\end{Bmatrix}$$

The solution of these equations is

$$U_1=100.0^\circ\text{C},\ U_2=82.283^\circ\text{C},\ U_3=70.732^\circ\text{C},\ U_4=64.204^\circ\text{C},\ U_5=62.053^\circ\text{C}$$

The heat input at node 1 is

$$Q_1^1 = -0.075 + (0.077 + 0.0025)\,100 + (-0.077 + 0.00125)\,82.283 = 1.642 \text{ W}$$

The total heat loss from the surface of the fin can be calculated using

$$\begin{aligned} Q &= \sum_{e=1}^{4} Q^e + \beta A(T(L) - T_\infty) = \sum_{e=1}^{4} \int_{x_a}^{x_b} P\beta(T - T_\infty)dx + kA(T(L) - T_\infty) \\ &= \sum_{e=1}^{4} \int_{x_a}^{x_b} P\beta\left(T_1^e\psi_1^e + T_2^e\psi_2^e - T_\infty\right)dx + \beta A(U_5 - T_\infty) \\ &= \sum_{e=1}^{4} \beta P h_e \left(\frac{T_1^e + T_2^e}{2} - T_\infty\right) + \beta A(U_5 - T_\infty) \\ &= 0.0075\,(0.5U_1 + U_2 + U_3 + U_4 + 0.5U_5 - 4T_\infty) + 25 \times 5 \times 10^{-6}(62.053 - 20) \\ &= 1.6368 + 0.00526 = 1.642 \text{ W} \end{aligned}$$

The exact solution of Eqs. (4.3.18) and (4.3.19*a*) is

$$\frac{T(x) - T_\infty}{T_0 - T_\infty} = \left[\frac{\cosh m(L - x) + (\beta/mk)\sinh m(L - x)}{\cosh mL + (\beta/mk)\sinh mL}\right], \; m^2 = \frac{\beta P}{Ak} \tag{4.3.20a}$$

$$Q(0) = -kA\frac{dT}{dx} = (T_0 - T_\infty)M\left[\frac{\sinh mL + (\beta/mk)\cosh mL}{\cosh mL + (\beta/mk)\sinh mL}\right], \; M^2 = \beta PAk \tag{4.3.20b}$$

Evaluating the exact solution at the nodes, we obtain

$$T(0.025) = 82.414^\circ\text{C}, \; T(0.05) = 70.958^\circ\text{C}, \; T(0.075) = 64.505^\circ\text{C}, \; T(0.1) = 62.422^\circ\text{C}$$

and $Q_1^1 = 1.62995$ W.

Next, we consider a mesh of two quadratic elements to analyze the problem described by Eqs. (4.3.18) and (4.3.19*a*). The assembled equations of two quadratic elements ($h_1 = h_2 = L/2$) is

$$\left(\frac{kA}{3h}\begin{bmatrix} 7 & -8 & 1 & 0 & 0 \\ -8 & 16 & -8 & 0 & 0 \\ 1 & -8 & 7+7 & -8 & 1 \\ 0 & 0 & -8 & 16 & -8 \\ 0 & 0 & 1 & -8 & 7 \end{bmatrix} + \frac{\beta Ph}{30}\begin{bmatrix} 4 & 2 & -1 & 0 & 0 \\ 2 & 16 & 2 & 0 & 0 \\ -1 & 2 & 4+4 & 2 & -1 \\ 0 & 0 & 2 & 16 & 2 \\ 0 & 0 & -1 & 2 & 4 \end{bmatrix}\right)\begin{Bmatrix} U_1 \\ U_2 \\ U_3 \\ U_4 \\ U_5 \end{Bmatrix}$$

$$= \begin{Bmatrix} Q_1^1 \\ Q_2^1 \\ Q_3^1 + Q_1^2 \\ Q_2^2 \\ Q_3^2 \end{Bmatrix} + \frac{\beta PT_\infty h}{6}\begin{Bmatrix} 1 \\ 4 \\ 1+1 \\ 4 \\ 1 \end{Bmatrix}$$

The boundary and balance conditions are [for boundary conditions in Eq. (4.3.19*a*)]

$$U_1 = T_0,\ Q_2^1 = 0,\ Q_3^1 + Q_1^2 = 0,\ Q_2^2 = 0,\ Q_3^2 = -\beta A U_5 + \beta A T_\infty$$

Hence, the condensed equations are

$$\left(\frac{kA}{3h} \begin{bmatrix} 16 & -8 & 0 & 0 \\ -8 & 14 & -8 & 1 \\ 0 & -8 & 16 & -8 \\ 0 & 1 & -8 & 7 \end{bmatrix} + \frac{\beta P h}{30} \begin{bmatrix} 16 & 2 & 0 & 0 \\ 2 & 8 & 2 & -1 \\ 0 & 2 & 16 & 2 \\ 0 & -1 & 2 & 4+\alpha \end{bmatrix} \right) \begin{Bmatrix} U_2 \\ U_3 \\ U_4 \\ U_5 \end{Bmatrix}$$

$$= \begin{Bmatrix} \left(\frac{7kA}{3h} - \frac{4\beta P h}{30}\right) T_0 \\ 0 \\ 0 \\ \beta A T_\infty \end{Bmatrix} + \frac{\beta P T_\infty h}{6} \begin{Bmatrix} 4 \\ 2 \\ 4 \\ 1 \end{Bmatrix}$$

where $\alpha = \beta A/(\beta P h/30) = 30A/Ph$.

The solution of the condensed equations for the unknown temperatures is

$$U_1 = 100.0^\circ\text{C},\ U_2 = 82.374^\circ\text{C},\ U_3 = 70.884^\circ\text{C},\ U_4 = 64.380^\circ\text{C},\ U_5 = 62.240^\circ\text{C}$$

The heat input at node 1 is

$$Q_1^1 = -0.05 + 0.091833 \times 100 - 0.10167 \times 82.374 + 0.012333 \times 70.884 = 1.633\ \text{W}$$

The total heat loss from the surface of the fin can be calculated using

$$Q = \sum_{e=1}^{4} \int_{x_a}^{x_b} P\beta \left(T_1^e \psi_1^e + T_2^e \psi_2^e + T_3^e \psi_3^e - T_\infty\right) dx + \beta A (U_5 - T_\infty)$$

$$= \sum_{e=1}^{4} \beta P h_e \left(\frac{T_1^e + 4T_2^e + T_3^e}{6} - T_\infty \right) + \beta A (U_5 - T_\infty)$$

$$= \frac{\beta P h}{6} (U_1 + 4U_2 + 2U_3 + 4U_4 + U_5 - 12T_\infty) = 1.62756 + 0.00528 = 1.633\ \text{W}$$

Set 2 Boundary Conditions

For Set 2 boundary conditions (4.3.19*b*), the finite element boundary and balance conditions for the mesh of four linear elements are

$$U_1 = T_0,\ Q_2^1 + Q_1^2 = 0,\ Q_2^2 + Q_1^3 = 0,\ Q_2^3 + Q_1^4 = 0,\ U_5 = T_L = 20^\circ\text{C}$$

and the finite element solution is

$$U_1 = 100.0^\circ\text{C},\ U_2 = 73.955^\circ\text{C},\ U_3 = 53.252^\circ\text{C},\ U_4 = 35.842^\circ\text{C},\ U_5 = 20^\circ\text{C}$$

The heats at nodes 1 and 5 are

$$Q_1^1 = -0.075 + (0.077 + 0.0025)\,100 + (-0.077 + 0.00125)\,73.955 = 2.273\ \text{W}$$

$$Q_2^4 = -0.075 + (-0.077 + 0.00125)\,35.842 + (0.077 + 0.0025)\,20 = -1.2\ \text{W}$$

Thus, the heat loss from the end of the fin is overestimated by assuming that the end $x = L$ is at the ambient temperature. The total heat loss from the lateral surface of the fin is given by

$$Q = \sum_{e=1}^{4} Q^e = 0.0075\,(0.5U_1 + U_2 + U_3 + U_4 + 0.5U_5 - 4T_\infty) = 1.073 \text{ W}$$

The exact solution of Eqs. (4.3.18) and (4.3.19*b*) is ($\theta_L = T_L - T_\infty$ and $\theta_0 = T_0 - T_\infty$)

$$T(x) - T_\infty = \left[\frac{\theta_L \sinh mx + \theta_0 \sinh m(L-x)}{\sinh mL}\right], \quad m^2 = \frac{\beta P}{Ak} \tag{4.3.21a}$$

$$Q(0) = -kA\frac{dT}{dx} = M\left[\frac{\theta_0 \cosh mL - \theta_L}{\sinh mL}\right], \quad M^2 = \beta PAk \tag{4.3.21b}$$

Evaluating the exact solution at the nodes, we obtain

$$T(0.025) = 74^\circ\text{C}, \quad T(0.05) = 53.3^\circ\text{C}, \quad T(0.075) = 35.87^\circ\text{C}, \quad T(0.1) = 20^\circ\text{C}$$

and $Q_1^1 = 2.268$ W.

The next example is concerned with heat transfer in a rod and comparison of finite difference and finite element analysis steps.

Example 4.3.3

A steel rod of diameter $D = 0.02$ m, length $L = 0.05$m, and thermal conductivity $k = 50$ W/(m $\cdot$°C) is exposed to ambient air at $T_\infty = 20$°C with a heat transfer coefficient $\beta = 100$ W/(m^2 $\cdot$°C). The left end of the rod is maintained at temperature $T_0 = 320$°C and the other end is insulated. We wish to determine the temperature distribution and the heat input at the left end of the rod [see Fig. 4.3.5(*a*)].

The governing equation of the problem is the same as in Eq. (4.3.18). We rewrite Eq. (4.3.18) in the nondimensional form

$$-\frac{d^2\theta}{dx^2} + m^2\theta = 0 \quad \text{for} \quad 0 < x < L \tag{4.3.22}$$

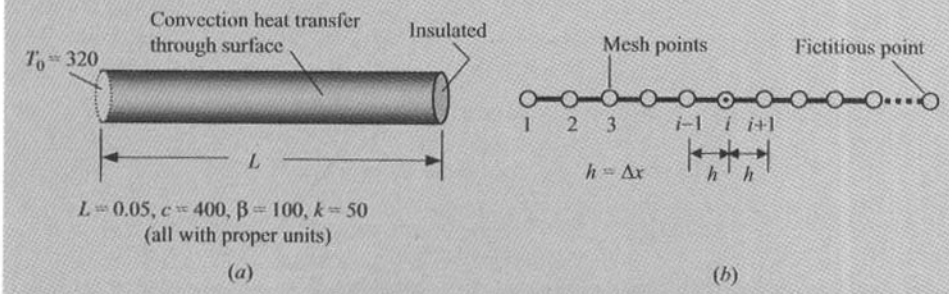

Figure 4.3.5 (*a*) Heat transfer in a rod. (*b*) Finite difference mesh.

where $\theta = T - T_\infty$, T being the temperature, and m^2 is given by

$$m^2 = \frac{\beta P}{Ak} = \frac{\beta \pi D}{\frac{1}{4}\pi D^2 k} = \frac{4\beta}{kD} \tag{4.3.23}$$

The boundary conditions of the problem become

$$\theta(0) = T(0) - T_\infty = 300^\circ\text{C}, \quad \left(\frac{d\theta}{dx}\right)\bigg|_{x=L} = 0 \tag{4.3.24}$$

The exact solution is given by [see Eqs. (4.3.20*a*) and (4.3.20*b*)]

$$\theta(x) = \theta(0)\frac{\cosh m(L-x)}{\cosh mL}, \quad Q(0) = \theta(0)\sqrt{\beta PAk}\frac{\sinh mL}{\cosh mL} \tag{4.3.25}$$

For the sake of comparison, we will consider both finite difference and finite element solutions of the problem.

Finite Difference Solutions

The second-derivative may be approximated with the centered finite difference formula (see Example 1.3.2)

$$\frac{d^2\theta}{dx^2} \approx \frac{1}{h^2}(\theta_{i+1} - 2\theta_i + \theta_{i-1}) \tag{4.3.26}$$

Substituting the above formula for the second derivative into Eq. (4.3.22), we arrive at

$$-\theta_{i+1} + (2 + m^2h^2)\theta_i - \theta_{i-1} = 0 \tag{4.3.27}$$

which is valid for any point where θ is not specified.

We choose a mesh of three points ($h = 0.025$), two end points and one in the middle [note that there is no concept of elements in the finite difference method; instead, we identify the number of mesh points (or nodes) in the domain at which we apply the formula (4.3.27), i.e., we arrive at the global equations directly]. Applying the formula (4.3.27) at nodes 2 and 3, we obtain ($m^2 = 400$)

$$(2 + 400h^2)\theta_2 - \theta_3 = \theta_1, \quad -\theta_2 + (2 + 400h^2)\theta_3 - \theta_4 = 0 \tag{4.3.28}$$

where $\theta_1 = \theta(0) = 300^\circ\text{C}$. Note that θ_4 is the value of θ at the fictitious node 4, which is considered to be a mirror image because of the boundary condition $d\theta/dx = 0$ [see Fig. 4.3.5(*b*)]. To eliminate θ_4, we can use one of the following formulas:

$$\left(\frac{d\theta}{dx}\right)_{x=0} = \frac{\theta_4 - \theta_3}{h} = 0 \quad \text{(forward)} \tag{4.3.29a}$$

$$\left(\frac{d\theta}{dx}\right)_{x=0} = \frac{\theta_4 - \theta_2}{2h} = 0 \quad \text{(centered)} \tag{4.3.29b}$$

The latter is of order $O(h^2)$, consistent with the centered difference formula (4.3.26). Using (4.3.29*b*), we set $\theta_4 = \theta_2$ in Eq. (4.3.28). Equations (4.3.28) can be written in matrix form as

(the coefficient matrix is not symmetric)

$$\begin{bmatrix} 2.25 & -1 \\ -2 & 2.25 \end{bmatrix} \begin{Bmatrix} \theta_2 \\ \theta_3 \end{Bmatrix} = \begin{Bmatrix} 300 \\ 0 \end{Bmatrix}$$

The solution of these equations is

$$\theta_2 = 220.41^\circ\text{C}, \quad \theta_3 = 195.92^\circ\text{C}$$

The heat at node 1 ($x = 0$) can be computed using the definition

$$Q(0) = kA\left(-\frac{d\theta}{dx}\right)_{x=0} = kA\frac{\theta_1 - \theta_2}{h} = 50.01 \text{ W}$$

Next, we use a mesh of five points. Applying Eq. (4.3.27) at nodes 2, 3, 4, and 5, and using $\theta_6 = \theta_4$, we obtain ($h = 0.0125$)

$$\begin{bmatrix} 2.0625 & -1 & 0 & 0 \\ -1 & 2.0625 & -1 & 0 \\ 0 & -1 & 2.0625 & -1 \\ 0 & 0 & -2 & 2.0625 \end{bmatrix} \begin{Bmatrix} \theta_2 \\ \theta_3 \\ \theta_4 \\ \theta_5 \end{Bmatrix} = \begin{Bmatrix} 300 \\ 0 \\ 0 \\ 0 \end{Bmatrix}$$

The solution of these equations is

$$\theta_2 = 251.89^\circ\text{C}, \quad \theta_3 = 219.53^\circ\text{C}, \quad \theta_4 = 200.89^\circ\text{C}, \quad \theta_5 = 194.80^\circ\text{C}$$

The heat at node 1 ($x = 0$) is

$$Q(0) = kA\left(-\frac{d\theta}{dx}\right)_{x=0} = kA\frac{\theta_1 - \theta_2}{h} = 60.46 \text{ W}$$

Finite Element Solutions

For the choice of two linear elements, the assembled system of equations is (U_I denotes the temperature $\theta(x)$ at the Ith global node)

$$\begin{bmatrix} 43.333 & -38.333 & 0 \\ -38.333 & 86.667 & -38.333 \\ 0 & -38.333 & 43.333 \end{bmatrix} \begin{Bmatrix} U_1 \\ U_2 \\ U_3 \end{Bmatrix} = \begin{Bmatrix} Q_1^{(1)} \\ Q_2^{(1)} + Q_1^{(2)} \\ Q_2^{(2)} \end{Bmatrix} \tag{4.3.30}$$

The boundary conditions are

$$U_1 = 300^\circ\text{C}, \quad Q_2^{(1)} + Q_1^{(2)} = 0, \quad Q_2^{(2)} = 0$$

Hence, we have

$$\begin{bmatrix} 86.667 & -38.333 \\ -38.333 & 43.333 \end{bmatrix} \begin{Bmatrix} U_2 \\ U_3 \end{Bmatrix} = \begin{Bmatrix} 38.333 \times 300 \\ 0 \end{Bmatrix}$$

The solution of these equations is

$$U_2 = 217.98^\circ\text{C}, \quad U_3 = 192.83^\circ\text{C}$$

The heat at node 1 ($x = 0$) can be computed using the first equation of the first element

$$Q(0) = kAQ_1^{(1)} = kA(43.333U_1 - 38.333U_2) = 72.95 \text{ W}$$

Once we have the nodal values U_1, U_2, and U_3, values at other points (intermediate to the nodes) can be computed using the interpolation

$$\theta^e(\bar{x}) = \sum_{j=1}^{2} \theta_j^e \psi_j^e(\bar{x}), \quad 0 \le \bar{x} \le h_e$$

where $\theta_1^1 = U_1$, $\theta_2^1 = U_2 = \theta_1^2$, and $\theta_2^2 = U_3$.

For the choice of four linear elements, the assembled system of equations is

$$\begin{bmatrix} 81.667 & -79.167 & 0 & 0 & 0 \\ -79.167 & 163.333 & -79.167 & 0 & 0 \\ 0 & -79.167 & 163.333 & -79.167 & 0 \\ 0 & 0 & -79.167 & 163.333 & -79.167 \\ 0 & 0 & 0 & -79.167 & 81.667 \end{bmatrix} \begin{Bmatrix} U_1 \\ U_2 \\ U_3 \\ U_4 \\ U_5 \end{Bmatrix} = \begin{Bmatrix} Q_1^{(1)} \\ Q_2^{(1)} + Q_1^{(2)} \\ Q_2^{(2)} + Q_1^{(3)} \\ Q_2^{(3)} + Q_1^{(4)} \\ Q_2^{(4)} \end{Bmatrix} \tag{4.3.31}$$

The boundary conditions are ($e = 1, 2, 3$):

$$U_1 = 300^\circ\text{C}, \quad Q_2^{(e)} + Q_1^{(e+1)} = 0, \quad Q_2^{(4)} = 0$$

Hence, we have

$$\begin{bmatrix} 163.333 & -79.167 & 0 & 0 \\ -79.167 & 81.667 & -79.167 & 0 \\ 0 & -79.167 & 81.667 & -79.167 \\ 0 & 0 & -79.167 & 81.667 \end{bmatrix} \begin{Bmatrix} U_2 \\ U_3 \\ U_4 \\ U_5 \end{Bmatrix} = \begin{Bmatrix} 79.167 \times 300 \\ 0 \\ 0 \\ 0 \end{Bmatrix}$$

The solution of these equations is

$$U_2 = 251.52^\circ\text{C}, \quad U_3 = 218.92^\circ\text{C}, \quad U_4 = 200.16^\circ\text{C}, \quad U_5 = 194.03^\circ\text{C}$$

The heat at node 1 ($x = 0$) is

$$Q(0) = kAQ_1^{(1)} = kA(81.667U_1 - 79.167U_2) = 72.07 \text{ W}$$

A comparison of the numerical results with the exact solution is presented in Table 4.3.1. The finite element solution is the best solution in the sence that it gives the minimum value of the integral of the square of $|u - u_n|$ over the domain. The exact value of $Q(0)$ is 71.78 W.

Table 4.3.1 Comparison of finite difference and finite element solutions with the exact solution of $-\dfrac{d^2\theta}{dx^2} + 400\theta = 0, \theta(0) = 300, \dfrac{d\theta}{dx}(0.05) = 0.$

x	Exact solution	FEM† solution		FDM solution	
		$N=2$	$N=4$	$N=2$	$N=4$
0.0000	300.00	300.00	300.00	300.00	300.00
0.0125	251.71	258.99*	251.52	260.21*	251.89
0.0250	219.23	217.98	218.92	220.41	219.53
0.0375	200.52	205.41*	200.16	208.17*	200.89
0.0500	194.42	192.83	194.03	195.92	194.80

*Values computed by interpolation.
† FEM, finite element method; FDM, finite difference method.

The last example of heat transfer deals with radially symmetric heat transfer in a cylinder.

Example 4.3.4

Consider a *long*, homogeneous, solid cylinder of radius R_0 [see Fig. 4.3.1(*c*)] in which energy is generated at a constant rate g_0 (W/m^3). The boundary surface at $r = R_0$ is maintained at a constant temperature T_0. We wish to calculate the temperature distribution $T(r)$ and heat flux $q(r) = -kdT/dr$ (or heat $Q = AkdT/dr$).

The governing equation for this problem is given by (4.3.10) with $g = g_0$. The boundary conditions are

$$T(R_0) = T_0, \quad \left(2\pi kr\frac{dT}{dr}\right)\bigg|_{r=0} = 0 \tag{4.3.32}$$

The zero-flux boundary condition at $r = 0$ is a result of the radial symmetry at $r = 0$. If the cylinder is hollow with inner radius R_i then the boundary condition at $r = R_i$ can be a specified temperature, specified heat flux, or convection boundary condition, depending on the situation. The finite element solution will not be exact at nodes because a is not constant.

The finite element model of the governing equation is [see Eqs. (3.4.5*a*) and (3.4.5*b*)]

$$[K^e]\{T^e\} = \{f^e\} + \{Q^e\} \tag{4.3.33}$$

where

$$K_{ij}^e = 2\pi\int_{r_a}^{r_b} kr\frac{d\psi_i^e}{dr}\frac{d\psi_j^e}{dr}\,dr, \quad f_i^e = 2\pi\int_{r_a}^{r_b}\psi_i^e g_0 r\,dr \tag{4.3.34a}$$

$$Q_1^e = -2\pi k\left(r\frac{dT}{dr}\right)\bigg|_{r_a}, \quad Q_2^e = 2\pi k\left(r\frac{dT}{dr}\right)\bigg|_{r_b} \tag{4.3.34b}$$

and (r_a, r_b) are the global coordinates of typical element $\Omega_e = (r_a, r_b)$.

For linear interpolation of $T(r)$, the element equations for a typical element are given by Eq. (3.4.7). The element equations for individual elements are obtained from these by giving the element length h_e and the global coordinates of the element nodes, $r_e = r_a$ and $r_{e+1} = r_b$.

For the mesh of one linear element, we have $r_a = r_1 = 0$ and $r_2 = h_e = R_0$, and

$$\pi k \begin{bmatrix} 1 & -1 \\ -1 & 1 \end{bmatrix} \begin{Bmatrix} U_1 \\ U_2 \end{Bmatrix} = \frac{\pi g_0 R_0}{3} \begin{Bmatrix} R_0 \\ 2R_0 \end{Bmatrix} + \begin{Bmatrix} Q_1^1 \\ Q_2^1 \end{Bmatrix}$$

The boundary conditions imply $U_2 = T_0$ and $Q_1^1 = 0$. Hence the temperature at node 1 is

$$U_1 = \frac{g_0 R_0^2}{3k} + T_0$$

and the heat at $r = R_0$ is

$$Q_2^1 = \pi k(U_2 - U_1) - \frac{2}{3}\pi g_0 R_0^2 = -\pi g_0 R_0^2$$

The negative sign indicates that heat is removed from the body (because $dT/dr < 0$). The one-element solution as a function of the radial coordinate r is

$$T_h(r) = U_1 \psi_1^1(r) + U_2 \psi_2^1(r) = \frac{g_0 R_0^2}{3k}\left(1 - \frac{r}{R_0}\right) + T_0$$

and the heat flux is

$$q(r) \equiv -k\frac{dT_h}{dr} = \frac{1}{3} g_0 R_0$$

For a mesh of two linear elements, we take $h_1 = h_2 = \frac{1}{2}R_0$, $r_1 = 0$, $r_2 = h_1 = \frac{1}{2}R_0$, and $r_3 = h_1 + h_2 = R_0$. The two-element assembly gives

$$\pi k \begin{bmatrix} 1 & -1 & 0 \\ -1 & 1+3 & -3 \\ 0 & -3 & 3 \end{bmatrix} \begin{Bmatrix} U_1 \\ U_2 \\ U_3 \end{Bmatrix} = \frac{\pi g_0 R_0^2}{6} \begin{Bmatrix} \frac{1}{2} \\ 1+2 \\ \frac{1}{2}+2 \end{Bmatrix} \begin{Bmatrix} Q_1^1 \\ Q_2^1 + Q_1^2 \\ Q_2^2 \end{Bmatrix}$$

Imposing the boundary conditions $U_3 = T_0$, $Q_2^1 + Q_1^2 = 0$, and $Q_1^1 = 0$, the condensed equations for the unknown temperatures are

$$\pi k \begin{bmatrix} 1 & -1 \\ -1 & 4 \end{bmatrix} \begin{Bmatrix} U_1 \\ U_2 \end{Bmatrix} = \frac{\pi g_0 R_0^2}{12} \begin{Bmatrix} 1 \\ 6 \end{Bmatrix} + \pi k \begin{Bmatrix} 0 \\ 3T_0 \end{Bmatrix}$$

The nodal values are

$$U_1 = \frac{5}{18}\frac{g_0 R_0^2}{k} + T_0, \quad U_2 = \frac{7}{36}\frac{g_0 R_0^2}{k} + T_0$$

From equilibrium, Q_2^2 is computed as

$$Q_2^2 = -\frac{5}{12}\pi g_0 R_0^2 + 3\pi k(U_3 - U_2) = -\pi g_0 R_0^2$$

The finite element solution becomes

$$T_h(r) = \begin{cases} U_1\psi_1^1(r) + U_2\psi_2^1(r) = \left(\frac{5}{18}\frac{g_0R_0^2}{k} + T_0\right)\left(1 - 2\frac{r}{R_0}\right) + 2\left(\frac{7}{36}\frac{g_0R_0^2}{k} + T_0\right)\frac{r}{R_0} \\ U_2\psi_1^2 + U_3\psi_2^2 = 2\left(\frac{7}{36}\frac{g_0R_0^2}{k} + T_0\right)\left(1 - \frac{r}{R_0}\right) + T_0\left(2\frac{r}{R_0} - 1\right) \end{cases}$$

$$= \begin{cases} \frac{1}{18}\frac{g_0R_0^2}{k}\left(5 - 3\frac{r}{R_0}\right) + T_0, & \text{for } 0 \le r \le \frac{1}{2}R_0 \\ \frac{7}{18}\frac{g_0R_0^2}{k}\left(1 - \frac{r}{R_0}\right) + T_0, & \text{for } \frac{1}{2}R_0 \le r \le R_0 \end{cases}$$

The exact solution of the problem is

$$T(r) = \frac{g_0R_0^2}{4k}\left[1 - \left(\frac{r}{R_0}\right)^2\right] + T_0(^\circ\text{C}) \tag{4.3.35}$$

$$q(r) = \frac{1}{2}g_0r \ (\text{W/m}^2), \quad Q(R_0) = \left(2\pi kr\frac{dT}{dr}\right)\Big|_{R_0} = -\pi g_0R_0^2 \ (\text{W}) \tag{4.3.36}$$

The temperature at the center of the cylinder according to the exact solution is $T(0) = g_0R_0^2/4k + T_0$, whereas it is $g_0R_0^2/3k + T_0$ and $5g_0R_0^2/18k + T_0$ according to the one- and two-element models, respectively.

The finite element solutions obtained using one-, two-, four-, and eight-element meshes of linear elements are compared with the exact solution in Table 4.3.2. Convergence of the finite element solutions, $\bar{T} = (T - T_0)k/g_0R_0^2$, to the exact solution with an increasing number of elements is clear (see Fig. 4.3.6). Figure 4.3.7 shows plots of $\bar{Q}(r) = Q(r)/2\pi R_0g_0$ and $Q(r) = 2\pi krdT/dr$, versus $\bar{r} = r/R_0$, as computed in the finite element analysis and the exact solution.

Table 4.3.2 Comparison of the finite element and exact solutions for heat transfer in a radially symmetric cylinder $R_0 = 0.01$ m, $g_0 = 2 \times 10^8$ W/m^3, $k = 20$ W/(m·°C), $T_0 = 100$°C.

	Temperature $T(r)$[†]				
r/R_0	One element	Two elements	Four elements	Eight elements	Exact
0.000	433.33	377.78	358.73	352.63	350.00
0.125	391.67	356.24	348.31	347.42	346.09
0.250	350.00	335.11	337.90	335.27	334.38
0.375	308.33	315.28	313.59	315.48	314.84
0.500	266.67	294.44	289.29	287.95	287.50
0.625	225.00	245.83	249.70	252.65	252.34
0.750	183.33	197.22	210.12	209.56	209.38
0.875	141.67	148.61	155.06	158.68	158.59
1.000	100.00	100.00	100.00	100.00	100.00

[†] The underlined terms are nodal values and others are interpolated values.

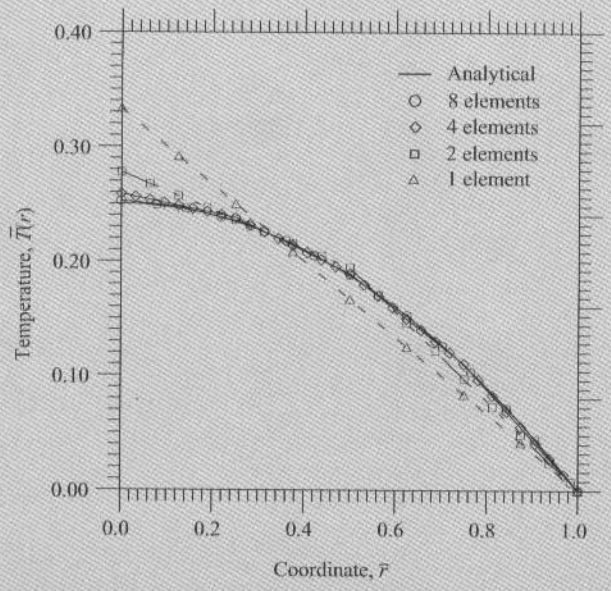

Figure 4.3.6 Comparison of the finite element solutions with the exact solution for heat transfer in a radially symmetric problem with cylindrical geometry.

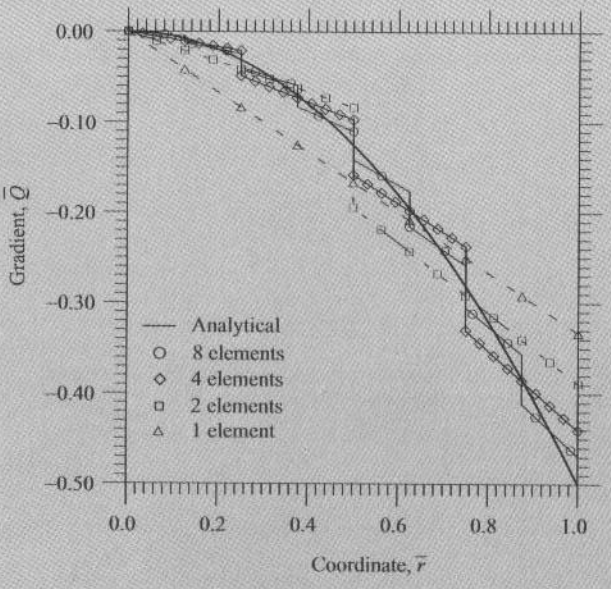

Figure 4.3.7 Comparison of the finite element solution with the exact solution for the temperature gradient in a radially symmetric problem with cylindrical geometry.

4.4 FLUID MECHANICS

4.4.1 Governing Equations

All bulk matter in nature exists in one of two forms: solid or fluid. A solid body is characterized by the relative immobility of its molecules whereas a fluid state is characterized by relative mobility of its molecules. Fluids can exist either as gases or liquids. The field of fluid mechanics is concerned with the motion of fluids and the conditions affecting the motion (see Reddy and Gartling, 2001).

The basic equations of fluid mechanics are derived from the global laws of conservation of mass, momentum, and energy. Conservation of mass gives the continuity equation, while the conservation of momentum results in the equations of motion. The conservation of energy, considered in the last section, is the first law of thermodynamics, and it results in Eqs. (4.3.8)–(4.3.10) for one-dimensional systems when thermal-fluid coupling is omitted. For additional details, see Schlichting (1979), Bird et al. (1960), and Reddy and Gartling (2001). More details are provided in Chapter 10, which is dedicated to finite element models of two-dimensional flows of viscous incompressible fluids.

Here, we consider so-called parallel flow, where only one velocity component is different from zero resulting in all the fluid particles moving in one direction, i.e., $u = u(x, y, z)$, where u is the velocity component along the x coordinate. We assume that there are no body forces. The z-momentum equation requires that $u = u(x, y)$. The conservation of mass in this case reduces to

$$\frac{\partial u}{\partial x} = 0$$

which implies that $u = u(y)$. The y-momentum equation simplifies to

$$\frac{\partial P}{\partial y} = 0$$

which implies that $P = P(x)$, where P is the pressure. The x-momentum equation simplifies to

$$\mu \frac{d^2 u}{dy^2} = \frac{dP}{dx} \tag{4.4.1}$$

The energy equation for this problem reduces to

$$\rho c u \frac{\partial T}{\partial x} = k\left(\frac{\partial^2 T}{\partial x^2} + \frac{\partial^2 T}{\partial y^2}\right) + \mu\left(\frac{du}{dy}\right)^2 \tag{4.4.2}$$

Here we are primarily interested in the finite element analysis of Eq. (4.4.1).

4.4.2 Finite Element Model

Equation (4.4.1) is a special case of the model equation (3.2.1) with the following correspondence:

$$f = -\frac{dP}{dx}, \quad a = \mu = \text{constant}, \quad c = 0, \quad x = y \tag{4.4.3}$$

Therefore, the finite element model in (3.2.31*a*) and (3.2.31*b*) is valid for this problem:

$$[K^e]\{u^e\} = \{f^e\} + \{Q^e\} \quad \text{or} \quad \boldsymbol{K}^e\boldsymbol{u}^e = \boldsymbol{f}^e + \boldsymbol{Q}^e \tag{4.4.4a}$$

where

$$K_{ij}^e = \int_{y_a}^{y_b} \mu \frac{d\psi_i^e}{dy}\frac{d\psi_j^e}{dy}\,dy, \quad f_i^e = \int_{y_a}^{y_b} \left(-\frac{dP}{dx}\right)\psi_i^e\,dy$$

$$Q_1^e = -\left(\mu\frac{du}{dy}\right)\bigg|_a, \quad Q_2^e = -\left(\mu\frac{du}{dy}\right)\bigg|_b \tag{4.4.4b}$$

Next, we consider an example.

Example 4.4.1

Consider parallel flow between two long flat walls separated by a distance $2L$ [see Fig. 4.4.1(*a*)]. We wish to determine the velocity distribution $u(y)$, $-L < y < L$, for a given pressure gradient $-dP/dx$, using the finite element method.

For a two-element mesh of linear elements ($h = L$), we have

$$\frac{\mu}{h}\begin{bmatrix} 1 & -1 & 0 \\ -1 & 2 & -1 \\ 0 & -1 & 1 \end{bmatrix}\begin{Bmatrix} U_1 \\ U_2 \\ U_3 \end{Bmatrix} = \frac{f_0 h}{2}\begin{Bmatrix} 1 \\ 2 \\ 1 \end{Bmatrix} + \begin{Bmatrix} Q_1^1 \\ Q_2^1 + Q_1^2 \\ Q_2^2 \end{Bmatrix}$$

We consider two sets of boundary conditions [see Fig. 4.4.1(*b*)]

Set 1: $u(-L) = 0,\ u(L) = 0$ (two stationary walls)

Set 2: $u(-L) = 0,\ u(L) = U_0$ (bottom wall stationary and top wall moving) (4.4.5)

For the first case, we may use symmetry and model domain $0 < x < L$. Here we consider the full domain for the two sets of boundary conditions.

For Set 1, we have $U_1 = U_3 = 0$. The finite element solution is given by

$$U_2 = \frac{f_0 L^2}{2\mu}, \quad u_h(y) = \frac{f_0 L^2}{2\mu}\frac{y}{L} \tag{4.4.6}$$

For set 2, we have $U_1 = 0$ and $U_3 = U_0$. The finite element solution is

$$U_2 = \frac{f_0 L^2}{2\mu} + \frac{1}{2}U_0, \quad u_h(y) = \left(\frac{f_0 L^2}{2\mu} + \frac{1}{2}U_0\right)\frac{y}{L} \tag{4.4.7}$$

For a one-element mesh of the quadratic element ($h = 2L$), we have

$$\frac{\mu}{6L}\begin{bmatrix} 7 & -8 & 1 \\ -8 & 16 & -8 \\ 1 & -8 & 7 \end{bmatrix}\begin{Bmatrix} U_1 \\ U_2 \\ U_3 \end{Bmatrix} = \frac{f_0 L}{3}\begin{Bmatrix} 1 \\ 4 \\ 1 \end{Bmatrix} + \begin{Bmatrix} Q_1^1 \\ 0 \\ Q_3^1 \end{Bmatrix} \tag{4.4.8}$$

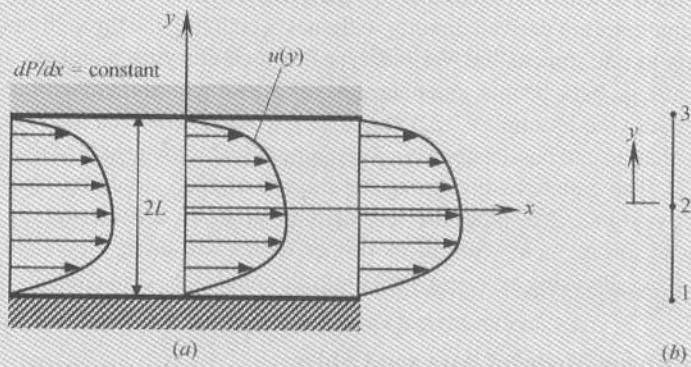

Figure 4.4.1 (*a*) Flow between parallel plates. (*b*) Finite element mesh; $u(L) = 0$ for set 1 and $u(L) = U_0$ for set 2.

and the finite element solutions for the two sets of boundary conditions are

$$\begin{aligned} U_2 &= \frac{f_0 L^2}{2\mu} \qquad \text{for Set 1} \\ U_2 &= \frac{f_0 L^2}{2\mu} + \frac{1}{2} U_0 \quad \text{for Set 2} \end{aligned} \tag{4.4.9}$$

Although the nodal values predicted in the linear- and quadratic-element meshes are the same, they vary linearly and quadratically between nodes of linear and quadratic elements, respectively.

The exact solutions for the two sets of boundary conditions in (4.4.5) are ($-L \le y \le L$)

$$\begin{aligned} u(y) &= \frac{f_0 L^2}{2\mu}\left(1 - \frac{y^2}{L^2}\right) \qquad \text{for Set 1} \\ u(y) &= U_0 \frac{1}{2}\left(1 + \frac{y}{L}\right) + \frac{f_0 L^2}{2\mu}\left(1 - \frac{y^2}{L^2}\right) \qquad \text{for Set 2} \end{aligned} \tag{4.4.10}$$

Note that the finite element solutions at the nodes are exact, as expected. The quadratic-element solution agrees with the exact solutions (4.4.10) for every value of y.

4.5 SOLID AND STRUCTURAL MECHANICS

4.5.1 Preliminary Comments

Solid mechanics is that branch of mechanics dealing with the motion and deformation of solids. The Lagrangian description of motion is used to express the global conservation laws. The conservation of mass for solid bodies is trivially satisfied because of the fixed material viewpoint used in the Lagrangian description. The conservation of momentum is nothing but Newton's second law of motion. Under isothermal conditions, the energy equation uncouples from the momentum equations, and we need only consider the equations of motion or equilibrium (see Example 2.3.3).

Unlike in fluid mechanics, the equations governing solid bodies undergoing different forms of deformations are derived directly without specializing the three-dimensional elasticity equations to one dimension. Various types of load-carrying members are called by different names, e.g., bars, beams, and plates. A *bar* is a structural member that is subjected to only axial loads (see Examples 1.2.3 and 2.3.2), while a *beam* is a member that is subjected to loads that tend to bend it about an axis perpendicular to the axis of the member (see Example 2.4.2). The equations governing the motion of such structural elements are not deduced directly from (2.3.52), but they are derived either by considering the equilibrium of an element of the member with all its proper forces and using Newton's second law (Example 1.2.3), or by using an energy principle (Examples 2.3.2 and 2.4.2).

4.5.2 Finite Element Model of Bars and Cables

The equation of motion governing axial deformation of a bar is (see Example 1.2.3)

$$\rho A \frac{\partial^2 u}{\partial t^2} - \frac{\partial}{\partial x}\left(EA\frac{\partial u}{\partial x}\right) = f(x,t) \tag{4.5.1}$$

For static problems, Eq. (4.5.1) reduces to

$$-\frac{d}{dx}\left(EA\frac{du}{dx}\right) = f(x) \tag{4.5.2}$$

It should be recalled that Eq. (4.5.2) is derived under the assumption that all material points on the line x = constant (i.e., all points on any cross section) move by the same amount $u(x)$. This is equivalent to the assumption that the stress on any cross section is uniform. Equation (4.5.2) is the same as the model equation (3.2.1), with $a = EA$ and $c = 0$. Hence, the finite element model in (3.2.31*a*) and (3.2.31*b*) is valid for bars.

The average transverse deflection $u(x)$ of a cable made of elastic material is also governed by an equation of the form:

$$-\frac{d}{dx}\left(T\frac{du}{dx}\right) = f(x) \tag{4.5.3}$$

where T is the uniform tension in the cable and f is the distributed transverse force. Again, Eq. (4.5.3) is a special case of Eq. (3.2.1), with $a = T$ and $c = 0$.

In structural mechanics problems, the quadratic functional of (3.2.10) takes the special meaning of total potential energy, Π^e, which can be expressed in the form

$$\Pi^e = \frac{1}{2}\int_{x_a}^{x_b} \boldsymbol{\varepsilon}^{\mathrm{T}}\boldsymbol{\sigma} A_e \; dx - \int_{x_a}^{x_b} uf\, dx - \sum_i u_i^e Q_i^e$$

where u is the displacement, $\boldsymbol{\varepsilon}$ the strain and $\boldsymbol{\sigma}$ the stress. The finite element approximation (3.2.24) of u can be written as

$$u_h = \left\{\psi_1^e \;\; \psi_2^e \;\; \ldots \;\; \psi_n^e\right\} \begin{Bmatrix} u_1^e \\ u_2^e \\ \vdots \\ u_n^e \end{Bmatrix} = \mathbf{N}^e \mathbf{u}^e$$

and the strains and stresses take the form

$$\varepsilon = \frac{du}{dx} = \frac{d}{dx}\left(\mathbf{N}^e\mathbf{u}^e\right) \equiv \mathbf{B}^e\mathbf{u}^e$$
$$\sigma = E\varepsilon = E_e\mathbf{B}^e\mathbf{u}^e$$

and the expression for the total potential energy becomes

$$\Pi^e = \frac{1}{2}\int_{x_a}^{x_b} A_e E_e \mathbf{u}^{\mathrm{T}}\mathbf{B}^{\mathrm{T}}\mathbf{B}\mathbf{u}\, dx - \int_{x_a}^{x_b} \mathbf{u}^{\mathrm{T}}\mathbf{B}^{\mathrm{T}} f\, dx - \mathbf{u}^{\mathrm{T}}\mathbf{Q}$$

where the element label on $\mathbf{B}$ and $\mathbf{u}$ is omitted for brevity. Then the principle of minimum total potential energy, $\delta\Pi^e = 0$, yields the finite element model

$$\delta\Pi^e = \delta\mathbf{u}^{\mathrm{T}}\left[\left(\int_{x_a}^{x_b} A_e E_e \mathbf{B}^{\mathrm{T}}\mathbf{B}\, dx\right)\mathbf{u} - \int_{x_a}^{x_b} \mathbf{B}^{\mathrm{T}} f\, dx - \mathbf{Q}\right] = 0$$

or

$$\mathbf{K}^e\mathbf{u}^e = \mathbf{f}^e + \mathbf{Q}^e \tag{4.5.4a}$$

where

$$\mathbf{K}^e = \int_{x_a}^{x_b} A_e E_e \mathbf{B}^{\mathrm{T}}\mathbf{B}\, dx, \quad \mathbf{f}^e = \int_{x_a}^{x_b} \mathbf{B}^{\mathrm{T}} f\, dx, \quad \mathbf{B} = \frac{d\mathbf{N}}{dx} \tag{4.5.4b}$$

These are just matrix form of the equations already presented in (3.2.31*a*) and (3.2.31*b*).

4.5.3 Numerical Examples

In this section we consider a number of examples of finite element analysis of bars.

Example 4.5.1

A bridge is supported by several concrete piers, and the geometry and loads of a typical pier are shown in Fig. 4.5.1. The load 20 kN/m^2 represents the weight of the bridge and an assumed distribution of the traffic on the bridge. The concrete weighs approximately 25 kN/m^3 and its modulus is $E = 28 \times 10^6$ kN/m^2. We wish to analyze the pier for displacements and stresses using the finite element method. The pier is indeed a three-dimensional structure. However, we wish to approximate the deformation and stress fields in the pier as one-dimensional.

We represent the distributed force at the top of the pier as a point force

$$F = (0.5 \times 0.5)20 = 5 \text{ kN}$$

The weight of the concrete is represented as the body force per unit length. The total force at any distance x is equal to the weight of the concrete above that point. The weight at a distance x is equal to the product of the volume of the body above x and the specific weight of the concrete:

$$W(x) = 0.5\frac{0.5 + (0.5 + 0.5x)}{2}x \times 25.0 = 6.25(1 + 0.5x)x$$

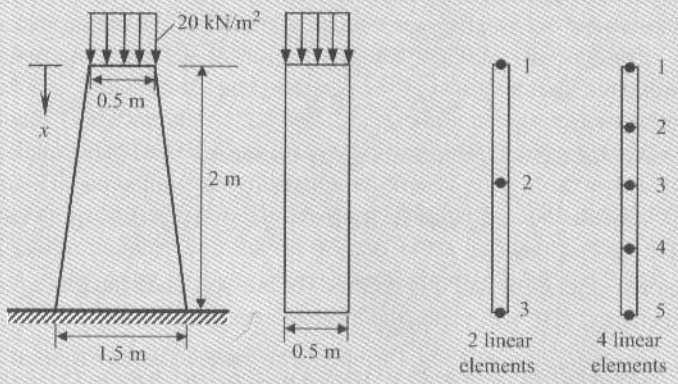

Figure 4.5.1 The geometry and loading in the concrete pier problem of Example 4.5.1.

The body force per unit length is computed from

$$f = \frac{dW}{dx} = 6.25(1 + x)$$

This completes the load representation of the problem.

The governing differential equation for the problem is given by (4.5.2), with $E = 28 \times 10^6$ kN/m^2 and cross-sectional area $A(x)$:

$$A(x) = (0.5 + 0.5x)0.5 = \frac{1}{4}(1 + x)$$

Thus, the concrete pier problem is idealized as a one-dimensional problem whose axial displacement u is governed by the equation

$$-\frac{d}{dx}\left[\frac{1}{4}E(1+x)\frac{du}{dx}\right] = 6.25(1 + x) \tag{4.5.5a}$$

subject to the boundary conditions

$$\left[\frac{1}{4}E(1+x)\frac{du}{dx}\right]\Bigg|_{x=0} = -5, \quad u(2) = 0 \tag{4.5.5b}$$

Equation (4.5.5a) is a special case of the model equation (3.2.1) with the following correspondance:

$$a(x) = 0.25E(1 + x), \quad f(x) = 6.25(1 + x) \tag{4.5.6}$$

For a typical linear element, the stiffness matrix and force vector can be computed using Eq. (3.2.31b). We have

$$\begin{aligned} [K^e] &= \frac{E}{4h_e}\left[1 + \frac{1}{2}(x_e + x_{e+1})\right]\begin{bmatrix} 1 & -1 \\ -1 & 1 \end{bmatrix} \\ \{f^e\} &= 6.25\frac{h_e}{2}\left(\begin{Bmatrix} 1 \\ 1 \end{Bmatrix} + \frac{1}{3}\begin{Bmatrix} x_{e+1} + 2x_e \\ 2x_{e+1} + x_e \end{Bmatrix}\right) \end{aligned} \tag{4.5.7}$$

Let us consider a two-element mesh with $h_1 = h_2 = 1$ m. We have

$$[K^1] = \frac{E}{4}\begin{bmatrix} 1.5 & -1.5 \\ -1.5 & 1.5 \end{bmatrix}, \quad \{f^1\} = \frac{6.25}{6}\begin{Bmatrix} 3+1 \\ 3+2 \end{Bmatrix} = \begin{Bmatrix} 4.167 \\ 5.208 \end{Bmatrix}$$

$$[K^2] = \frac{E}{4}\begin{bmatrix} 2.5 & -2.5 \\ -2.5 & 2.5 \end{bmatrix}, \quad \{f^2\} = \frac{6.25}{6}\begin{Bmatrix} 3+4 \\ 3+5 \end{Bmatrix} = \begin{Bmatrix} 7.292 \\ 8.333 \end{Bmatrix}$$

The assembled equations are

$$E\begin{bmatrix} 0.375 & -0.375 & 0.000 \\ -0.375 & 1.000 & -0.625 \\ 0.000 & -0.625 & 0.625 \end{bmatrix}\begin{Bmatrix} U_1 \\ U_2 \\ U_3 \end{Bmatrix} \begin{Bmatrix} 4.167 \\ 12.500 \\ 8.333 \end{Bmatrix} + \begin{Bmatrix} Q_1^1 \\ Q_2^1 + Q_1^2 \\ Q_2^2 \end{Bmatrix}$$

The boundary and equilibrium conditions require

$$U_3 = 0, \quad Q_2^1 + Q_1^2 = 0, \quad Q_1^1 = 5 \text{ kN}$$

The condensed equations for the unknown displacements and forces are

$$E\begin{bmatrix} 0.375 & -0.375 \\ -0.375 & 1.000 \end{bmatrix}\begin{Bmatrix} U_1 \\ U_2 \end{Bmatrix} = \begin{Bmatrix} 9.167 \\ 12.500 \end{Bmatrix}, \quad Q_2^2 = -0.6255U_2 - 8.333$$

The solution is given by (positive displacements, because of the coordinate system used, indicate that the pier is in compression)

$$U_1 = 2.111 \times 10^{-6}\text{m}, \quad U_2 = 1.238 \times 10^{-6}\text{m}, \quad Q_2^2 = -30 \text{ kN}$$

Hence, the stress at the fixed end is (compressive)

$$\sigma_x = Q_2^2/A = -30/0.75 = -40 \text{ kN/m}^2$$

The four-element model gives 2.008×10^{-6} m and 1.228×10^{-6}m, respectively.

The exact solution of Eqs. (4.5.5*a*) and (4.5.5*b*) is

$$u(x) = \frac{1}{E}\left[56.25 - 6.25(1+x)^2 - 7.5 \ln\left(\frac{1+x}{3}\right)\right] \tag{4.5.8}$$

The exact values of u at nodes 1 and 2 are

$$u(0) = 2.08 \times 10^{-6}\text{m}, \quad u(1) = 1.225 \times 10^{-6}\text{m}$$

The finite element solution at the nodes is not exact because $a = EA$ is not a constant in this problem.

Example 4.5.2

Consider the composite bar consisting of a tapered steel bar fastened to an aluminum rod of uniform cross section and subjected to loads as shown in Figure 4.5.2. We wish to determine the displacement field in the bar using the finite element method.

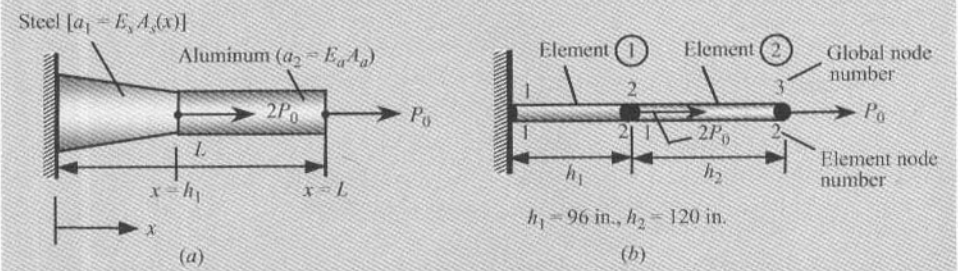

Figure 4.5.2 Axial deformation of a composite member (*a*) Geometry and loading. (*b*) Finite element representation.

The governing equations are given by

$$\begin{aligned} -\frac{d}{dx}\left(E_s A_s \frac{du}{dx}\right) &= 0, \quad 0 < x < h_1 \\ -\frac{d}{dx}\left(E_a A_a \frac{du}{dx}\right) &= 0, \quad h_1 < x < h_1 + h_2 = L \end{aligned} \tag{4.5.9}$$

where the subscript "s" refers to steel and "a" to aluminum. The boundary conditions are obvious. We consider the following data:

$$\begin{aligned} &E_s = 30 \times 10^6 \text{ psi}, \; A_s = (c_1 + c_2 x)^2, \; E_a = 10^7 \text{ psi} \\ &A_a = 1 \text{ in.}^2, \; h_1 = 96 \text{ in.}, \; L = 216 \text{ in.}, \; P_0 = 10,000 \text{ lb} \end{aligned} \tag{4.5.10}$$

The finite element equations for a uniform bar element with constant $E_e A_e$ and $f(x) = 0$ are given by [see Eq. (3.3.5*a*)]

$$\frac{E_e A_e}{h_e}\begin{bmatrix} 1 & -1 \\ -1 & 1 \end{bmatrix}\begin{Bmatrix} u_1^e \\ u_2^e \end{Bmatrix} = \begin{Bmatrix} Q_1^e \\ Q_2^e \end{Bmatrix} \tag{4.5.11a}$$

where Q_i^e are the end forces

$$Q_1^e = \left[-EA\frac{du}{dx}\right]_{x_a}, \quad Q_2^e = \left[EA\frac{du}{dx}\right]_{x_b} \tag{4.5.11b}$$

For the present problem, A_e is not constant, but Eq. (4.6.11a) is still valid with

$$A_e = (c_1^e)^2 + \frac{1}{3}(c_2^e)^2(x_b^2 + x_a^2 + x_a x_b) + c_1^e c_2^e (x_b + x_a)$$

To see this, we calculate K_{ij}^e for the problem using the local coordinate $\bar{x}$ ($x = \bar{x} + x_a$). We have

$$K_{ij}^e = \int_{x_a}^{x_b} E_e (c_1^e + c_2^e x)^2 \frac{d\psi_i^e}{dx}\frac{d\psi_j^e}{dx}dx = \int_0^{h_e} E_e \left[c_1^e + c_2^e(\bar{x} + x_a)\right]^2 \frac{d\psi_i^e}{dx}\frac{d\psi_j^e}{dx}d\bar{x}$$

$$K_{11}^e = \frac{E_e}{h_e^2}\int_{x_e}^{x_b} (c_1^e + c_2^e x)^2 dx$$

$$= \frac{E_e}{h_e^2}\left[(c_1^e)^2 h_e + \frac{1}{3}(c_2^e)^2(x_b^3 - x_a^3) + c_1^e c_2^e (x_b^2 - x_a^2)\right]$$

$$= \frac{E_e}{h_e}\left[(c_1^e)^2 + \frac{1}{3}(c_2^e)^2(x_b^2 + x_a^2 + x_a x_b) + c_1^e c_2^e (x_b + x_a)\right] = \frac{E_e A_e}{h_e}$$

$K_{12}^e = K_{21}^e = -K_{11}^e$ and $K_{22}^e = K_{11}^e$, where we have used the algebraic equalities, $a^2 - b^2 = (a-b)(a+b)$ and $a^3 - b^3 = (a-b)(a^2 + b^2 + ab)$ to simplify the expressions.

For two linear elements of lengths $h_1 = 96$ in. and $h_2 = 120$ in., we have $c_1^1 = 1.5$, $c_2^1 = -0.5/96$, $c_1^2 = 1$, $c_2^2 = 0$, and the element stiffness matrices become

$$[K^1] = \frac{4.75}{96} \times 10^7 \begin{bmatrix} 1 & -1 \\ -1 & 1 \end{bmatrix} = 10^4 \begin{bmatrix} 49.479 & -49.479 \\ -49.479 & 49.479 \end{bmatrix}$$

$$[K^2] = \frac{1}{120} \times 10^7 \begin{bmatrix} 1 & -1 \\ -1 & 1 \end{bmatrix} = 10^4 \begin{bmatrix} 8.333 & -8.333 \\ -8.333 & 8.333 \end{bmatrix}$$

The assembled equations are

$$10^4 \begin{bmatrix} 49.479 & -49.479 & 0.000 \\ -49.479 & 57.812 & -8.333 \\ 0.000 & -8.333 & 8.333 \end{bmatrix} \begin{Bmatrix} U_1 \\ U_2 \\ U_3 \end{Bmatrix} = \begin{Bmatrix} Q_1^1 \\ Q_2^1 + Q_1^2 \\ Q_2^2 \end{Bmatrix}$$

The boundary conditions imply

$$U_1 = 0, \quad Q_2^1 + Q_1^2 = 2P_0, \quad Q_2^2 = P_0$$

Hence, the condensed equations are

$$10^4 \begin{bmatrix} 57.812 & -8.333 \\ -8.333 & 8.333 \end{bmatrix} \begin{Bmatrix} U_2 \\ U_3 \end{Bmatrix} = \begin{Bmatrix} 2P_0 \\ P_0 \end{Bmatrix}, \quad Q_1^1 = -10^4 \times 49.479\, U_2$$

whose solution is

$$U_2 = 0.06063 \text{ in.}, \quad U_3 = 0.18063 \text{ in.}, \quad Q_1^1 = -30,000 \text{ lb}$$

The negative sign indicates that the reaction is acting away from the end (i.e., tensile force). The magnitude of Q_1^1 is consistent with the static equilibrium of the forces:

$$Q_1^1 + 2P_0 + P_0 = 0 \text{ or } Q_1^1 = -3P_0 = -30,000 \text{ lb}$$

The axial displacement at any point x along the bar is given by

$$u_h(x) = \begin{cases} u_1^{(1)}\psi_1^{(1)} + u_2^{(1)}\psi_2^{(1)} = 0.06063x/96, & 0 \le x \le 96 \\ u_1^{(2)}\psi_1^{(2)} + u_2^{(2)}\psi_2^{(2)} = -0.03537 + 0.001x, & 96 \le x \le 216 \end{cases}$$

and its first derivative is given by

$$\frac{du_h}{dx} = \begin{cases} \dfrac{0.06063}{96}, & 0 \le x \le 96 \\ 0.0001, & 96 \le x \le 216 \end{cases}$$

The exact solution of Eqs. (4.5.9) subject to the boundary conditions

$$u(0) = 0, \quad \left[\left(a\frac{du}{dx}\right)_{x=96^+} - \left(a\frac{du}{dx}\right)_{x=96^-}\right] = 2P_0, \quad \left(a\frac{du}{dx}\right)_{x=216} = P_0$$

is given by

$$u(x) = \begin{cases} 0.128[x/(288-x)], & 0 \le x \le 96 \\ 0.001(x-32), & 96 \le x \le 216 \end{cases}$$

$$\frac{du}{dx} = \begin{cases} 36.864/(288-x)^2, & 0 \le x \le 96 \\ 0.001, & 96 \le x \le 216 \end{cases}$$

In particular, the exact solution at nodes 2 and 3 is given by

$$u(96) = 0.064 \text{ in.}, \quad u(216) = 0.1840 \text{ in.}$$

Thus, the two-element solution is about 1.8 percent off from the maximum displacement.

Next consider a two-element mesh of quadratic elements. The element matrix and force vector for element 1 are

$$[K^1] = 10^4 \begin{bmatrix} 142.19 & -159.37 & 17.18 \\ -159.37 & 266.67 & -107.29 \\ 17.18 & -107.29 & 90.10 \end{bmatrix}, \quad \{F^1\} = \begin{Bmatrix} Q_1^1 \\ 0 \\ Q_3^1 \end{Bmatrix}$$

The assembled stiffness matrix is of order 5×5, and it is of the form

$$[K] = \begin{bmatrix} K_{11}^1 & K_{12}^1 & K_{13}^1 & 0 & 0 \\ K_{21}^1 & K_{22}^1 & K_{23}^1 & 0 & 0 \\ K_{31}^1 & K_{32}^1 & K_{33}^1 + K_{11}^2 & K_{12}^2 & K_{13}^2 \\ 0 & 0 & K_{21}^2 & K_{22}^2 & K_{23}^2 \\ 0 & 0 & K_{31}^2 & K_{32}^2 & K_{33}^2 \end{bmatrix}$$

After imposing boundary conditions ($U_1 = 0$, $Q_3^1 + Q_1^2 = 20,000$, $Q_3^2 = 10,000$), and solving the resulting 4×4 equations, we obtain

$$U_2 = 0.02572 \text{ in.}, \; U_3 = 0.06392 \text{ in.}, \; U_4 = 0.12392 \text{ in.}, \; U_5 = 0.18392 \text{ in.}$$

The two-element solution obtained using the quadratic element is very accurate, as can be seen from a comparison of the finite element solution with the exact solution presented in Table 4.5.1.

Table 4.5.1 Comparison of the finite element solutions with the exact solution of the bar problem in Example 4.5.2.

		Linear					Quadratic	
x (in.)	Exact	$(1, 1)^\dagger$	$(2, 1)$	$(3, 2)$	$(4, 2)$	$(6, 2)$	$(1, 1)$	$(2, 1)$
16	0.00753	—	—	—	—	0.00752	—	—
24	0.01600	—	—	—	0.01161	—	—	0.01164
32	0.01600	—	—	0.01593	—	0.01598	—	—
48	0.02560	—	0.02532	—	0.02553	0.02557	0.02572	0.02560
64	0.03657	—	—	0.03638	—	0.03652	—	—
72	0.04267	—	—	—	0.04253	—	—	0.04268
80	0.04923	—	—	—	—	0.04916	—	—
96	0.06400	0.06063	0.06309	0.06359	0.06377	0.06390	0.06392	0.06399
156	0.12392	—	—	—	0.12377	0.12390	0.12392	0.12399
216	0.18400	0.18063	0.18309	0.18359	0.18377	0.18390	0.18392	0.18399

$^\dagger(m, n)$ means m elements in the interval (0,96) and n elements in the interval (96,216); all elements in each interval are of the same size.

Example 4.5.3

Consider a hollow circular cylinder with inner radius a, outer radius b, and length L. The outer surface of the hollow cylinder is assumed to be fixed and its inner surface ideally bonded to a rigid circular cylindrical core of radius a and length L, as shown in Fig. 4.5.3. Suppose that an axial force P is applied to the rigid core along its centroidal axis. We wish to find the axial displacement δ of the rigid core by assuming that the displacement field in the hollow cylinder is of the form

$$u_r = u_\theta = 0, \quad u_z = U(r) \tag{4.5.12}$$

where (u_r, u_θ, u_z) are the displacements along (r, θ, z) coordinates.

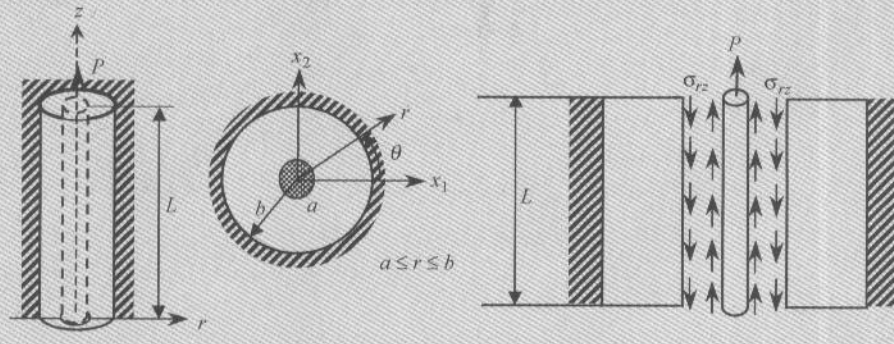

Figure 4.5.3 Axisymmetric deformation of a hollow cylinder fixed at the outer surface and pulled by a rigid core at the inner surface.

The equation governing $U(r)$ can be determined as follows. First, we note that

$$\varepsilon_{rr} = \varepsilon_{\theta\theta} = \varepsilon_{zz} = \varepsilon_{r\theta} = \varepsilon_{\theta z} = 0, \quad 2\varepsilon_{rz} = \frac{dU}{dr} \tag{4.5.13a}$$

$$\sigma_{rr} = \sigma_{\theta\theta} = \sigma_{zz} = \sigma_{\theta r} = \sigma_{\theta z} = 0; \quad \sigma_{rz} = G\frac{dU}{dr} \tag{4.5.13b}$$

where G is the shear modulus. Of the three stress-equilibrium equations in the cylindrical coordinates, the two equilibrium equations associated with r and θ directions are trivially satisfield (in the absence of body forces) by the stress field. The third equilibrium equation

$$\frac{1}{r}\left[\frac{\partial}{\partial r}(r\sigma_{rz}) + \frac{\partial \sigma_{\theta z}}{\partial \theta} + r\frac{\partial \sigma_{zz}}{\partial z}\right] = 0$$

yields the equation

$$\frac{1}{r}\frac{d}{dr}\left(rG\frac{dU}{dr}\right) = 0 \tag{4.5.14}$$

The boundary conditions on $U(r)$ are

$$u_z(b) = 0 \rightarrow U(b) = 0, \quad -2\pi L(r\sigma_{rz})|_{r=a} = P \rightarrow -\left(rG\frac{dU}{dr}\right)_{r=a} = \frac{P}{2\pi L} \tag{4.5.15}$$

This completes the theoretical formulation of the problem. We wish to analyze the problem using the finite element method.

The finite element model of Eq. (4.5.14) [cf. Eq. (3.4.1)] is given by Eqs. (3.4.5a) and (3.4.5b) with $a(r) = rG$ and $f = 0$. One linear element in the domain yields ($r_a = a$ and $h = b - a$)

$$\frac{2\pi G}{h}\left(r_a + \frac{1}{2}h\right)\begin{bmatrix} 1 & -1 \\ -1 & 1 \end{bmatrix}\begin{Bmatrix} U_1 \\ U_2 \end{Bmatrix} = \begin{Bmatrix} Q_1^1 \\ Q_2^1 \end{Bmatrix}$$

and with $U_2 = 0$ and $Q_1^1 = P/L$, we obtain

$$U_1 = \frac{P}{\pi LG}\frac{(b-a)}{(b+a)} \tag{4.5.16}$$

The exact solution of Eqs. (4.5.14) and (4.5.15) is given by

$$U(r) = -\frac{P}{2\pi LG}\log(r/b), \quad U(a) \equiv \delta = \frac{P}{2\pi LG}\log(b/a) \tag{4.5.17}$$

The one element solution in Eq. (4.5.16) corresponds to the first term in the logarithmic series of δ [i.e., $\log(a/b)$].

Use of one quadratic element gives ($h = b - a$)

$$\frac{2\pi G}{6h}\begin{bmatrix} 3h+14a & -(4h+16a) & h+2a \\ -(4h+16a) & 16h+32a & -(12h+16a) \\ h+2a & -(12h+16a) & 11h+14a \end{bmatrix}\begin{Bmatrix} U_1 \\ U_2 \\ U_3 \end{Bmatrix} = \begin{Bmatrix} Q_1^1 \\ 0 \\ Q_3^1 \end{Bmatrix} \tag{4.5.18}$$

Using the boundary conditions $U_3 = 0$ and $Q_1^1 = P/L$, we obtain the following condensed equations in U_1 and U_2:

$$\frac{2\pi G}{6h}\begin{bmatrix} 3h+14a & -(4h+16a) \\ -(4h+16a) & 16h+32a \end{bmatrix}\begin{Bmatrix} U_1 \\ U_2 \end{Bmatrix} = \begin{Bmatrix} P/L \\ 0 \end{Bmatrix} \tag{4.5.19}$$

whose solution is

$$\begin{aligned} U_1 &= \frac{3hP}{\pi GL}\frac{h+2a}{3h^2+20ah+28a^2} \\ U_2 &= \frac{3hP}{\pi GL}\frac{h+4a}{12h^2+80ah+112a^2} \end{aligned} \tag{4.5.20}$$

The finite element solution becomes

$$U_h(r) = U_1(1-r/h)(1-2r/h) + 4U_2(r/h)(1-r/h)$$

A comparison of the finite element solutions obtained with linear and quadratic elements with the analytical solution is shown in Fig. 4.5.4. The four-element mesh of quadratic elements virtually gives the exact solution.

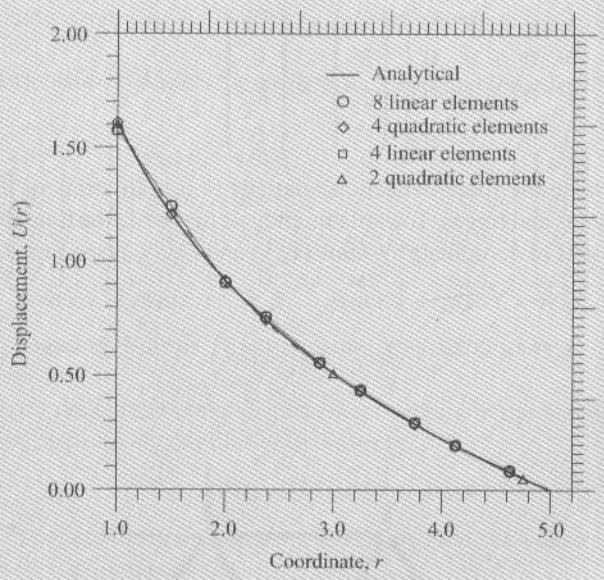

Figure 4.5.4 Comparison of finite element solutions with the analytical solution for axisymmetric deformation of a hollow cylinder fixed at the outer surface and pulled by a rigid core at the inner surface.

4.6 PLANE TRUSSES

4.6.1 Introduction

Consider a structure consisting of several bar elements connected to each other by pins, as shown in Figure 4.6.1. The members may rotate freely about the axis of the pin. Consequently, each member carries only axial forces. The planar structure with pin-connected members (i.e., all members lie in the same plane) is called a *plane truss*. Since each member is oriented differently with respect to a global coordinate system (x, y), it is necessary to transform the force displacement relations that were derived in element coordinate system $(\bar{x}, \bar{y})$ to the global coordinate system (x, y) so that the structure stiffness can be assembled from the element stiffness referred to the same global coordinate system.

4.6.2 Basic Truss Element

First, we consider a uniform bar element with constant EA and oriented at an angle θ_e, measured counterclockwise, from the positive x-axis. If the member coordinate system $(\bar{x}_e, \bar{y}_e)$ is taken as shown in Figure 4.6.2(a), and $(\bar{u}_i^e, \bar{v}_i^e)$ and $(\bar{F}_i^e, 0)$ denote the displacements and forces at node i with respect to the member coordinate system $(\bar{x}_e, \bar{y}_e)$, respectively, the element equations (4.5.11a) can be expressed as (we now use the notation $\bar{Q}_i^e + \bar{f}_i^e = \bar{F}_i^e$)

$$\frac{E_e A_e}{h_e}\begin{bmatrix} 1 & 0 & -1 & 0 \\ 0 & 0 & 0 & 0 \\ -1 & 0 & 1 & 0 \\ 0 & 0 & 0 & 0 \end{bmatrix}\begin{Bmatrix} \bar{u}_1^e \\ \bar{v}_1^e \\ \bar{u}_2^e \\ \bar{v}_2^e \end{Bmatrix} = \begin{Bmatrix} \bar{F}_1^e \\ 0 \\ \bar{F}_2^e \\ 0 \end{Bmatrix} \quad \text{or} \quad [\bar{K}^e]\{\bar{\Delta}^e\} = \{\bar{F}^e\} \tag{4.6.1}$$

We wish to write the force-deflection relations (4.6.1) in terms of the corresponding global displacements and forces. Toward this end, we first write the transformation relations between the two sets of coordinate systems (x, y) and $(\bar{x}_e, \bar{y}_e)$ (see Fig. 4.6.2)

$$\bar{x}_e = x\cos\theta_e + y\sin\theta_e, \quad \bar{y}_e = -x\sin\theta_e + y\cos\theta_e$$
$$x = \bar{x}_e\cos\theta_e - \bar{y}_e\sin\theta_e, \quad y = \bar{x}_e\sin\theta_e + \bar{y}_e\cos\theta_e$$

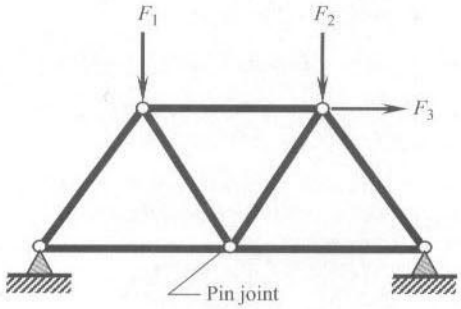

Figure 4.6.1 A plane truss structure.

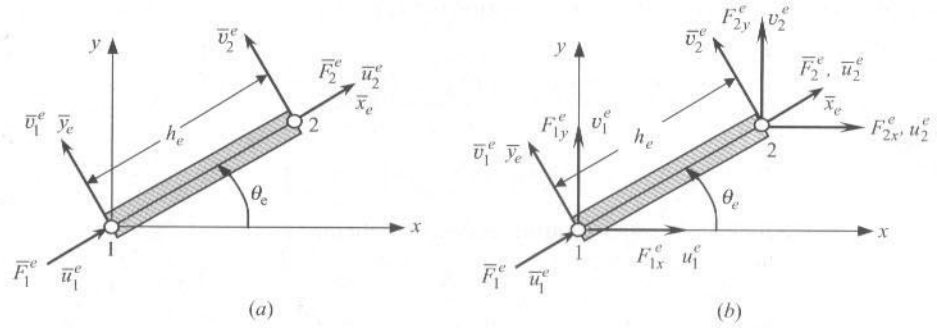

Figure 4.6.2 A bar element oriented at an angle with respect to the global coordinate system (x, y). (a) Forces and displacements in the element coordinates. (b) Forces and displacements in the global coordinates.

or, in matrix form, we have

$$\begin{Bmatrix} \bar{x}_e \\ \bar{y}_e \end{Bmatrix} = \begin{bmatrix} \cos\theta_e & \sin\theta_e \\ -\sin\theta_e & \cos\theta_e \end{bmatrix} \begin{Bmatrix} x \\ y \end{Bmatrix}, \quad \begin{Bmatrix} x \\ y \end{Bmatrix} = \begin{bmatrix} \cos\theta_e & -\sin\theta_e \\ \sin\theta_e & \cos\theta_e \end{bmatrix} \begin{Bmatrix} \bar{x}_e \\ \bar{y}_e \end{Bmatrix} \tag{4.6.2}$$

where θ_e is the angle between the positive x-axis and positive $\bar{x}_e$-axis, measured in the counterclockwise direction. Note that all quantities with a bar over them refer to the member (or local) coordinate system $(\bar{x}_e, \bar{y}_e)$, while the quantities without a bar refer to the global coordinate system (x, y).

The above relationship also holds for the displacements and forces of the two coordinate systems. We have

$$\begin{Bmatrix} \bar{u}_1^e \\ \bar{v}_1^e \\ \bar{u}_2^e \\ \bar{v}_2^e \end{Bmatrix} = \begin{bmatrix} \cos\theta_e & \sin\theta_e & 0 & 0 \\ -\sin\theta_e & \cos\theta_e & 0 & 0 \\ 0 & 0 & \cos\theta_e & \sin\theta_e \\ 0 & 0 & -\sin\theta_e & \cos\theta_e \end{bmatrix} \begin{Bmatrix} u_1^e \\ v_1^e \\ u_2^e \\ v_2^e \end{Bmatrix} \tag{4.6.3a}$$

or

$$\{\bar{\Delta}^e\} = [T^e]\{\Delta^e\} \tag{4.6.3b}$$

where $\{\bar{\Delta}^e\}$ and $\{\Delta^e\}$ denote the nodal displacement vectors in the member and structure coordinate systems, respectively. Similarly, we have

$$\{\bar{F}^e\} = [T^e]\{F^e\} \tag{4.6.4}$$

Here $\{\bar{F}^e\}$ and $\{F^e\}$ denote the nodal force vectors in the member and structure coordinate systems, respectively (see Figures 4.6.2).

4.6.3 General Truss Element

Next, we derive the relationship between the global displacements and global forces. Using Eqs. (4.6.3b) and (4.6.4) in Eq. (4.6.1), we obtain

$$[\bar{K}^e][T^e]\{\Delta^e\} = [T^e]\{F^e\} \tag{4.6.5}$$

Premultiplying both sides of the above equation with $[T^e]^{\mathrm{T}}$ and noting that $[T^e]^{-1} = [T^e]^{\mathrm{T}}$, we obtain

$$[T^e]^{\mathrm{T}}[\bar{K}^e][T^e]\{\Delta^e\} = \{F^e\} \quad \text{or} \quad [K^e]\{\Delta^e\} = \{F^e\} \tag{4.6.6}$$

where

$$[K^e] = [T^e]^{\mathrm{T}}[\bar{K}^e][T^e], \quad \{F^e\} = [T^e]^{\mathrm{T}}\{\bar{F}^e\} \tag{4.6.7}$$

Carrying out the indicated matrix multiplications, we obtain

$$[K^e] = \frac{E_e A_e}{h_e}\begin{bmatrix} \cos^2\theta_e & \frac{1}{2}\sin 2\theta_e & -\cos^2\theta_e & -\frac{1}{2}\sin 2\theta_e \\ \frac{1}{2}\sin 2\theta_e & \sin^2\theta_e & -\frac{1}{2}\sin 2\theta_e & -\sin^2\theta_e \\ -\cos^2\theta_e & -\frac{1}{2}\sin 2\theta_e & \cos^2\theta_e & \frac{1}{2}\sin 2\theta_e \\ -\frac{1}{2}\sin 2\theta_e & -\sin^2\theta_e & \frac{1}{2}\sin 2\theta_e & \sin^2\theta_e \end{bmatrix} \tag{4.6.8}$$

$$\{F^e\} = \begin{Bmatrix} F_1^e \\ F_2^e \\ F_3^e \\ F_4^e \end{Bmatrix} = \begin{Bmatrix} \bar{F}_1^e \cos\theta_e \\ \bar{F}_1^e \sin\theta_e \\ \bar{F}_2^e \cos\theta_e \\ \bar{F}_2^e \sin\theta_e \end{Bmatrix} + \begin{Bmatrix} \bar{f}_1^e \cos\theta_e \\ \bar{f}_1^e \sin\theta_e \\ \bar{f}_2^e \cos\theta_e \\ \bar{f}_2^e \sin\theta_e \end{Bmatrix} \tag{4.6.9}$$

where $\bar{f}_i^e$ are computed using Eq. (3.2.31*b*) [also see Eq. (3.2.34)]

$$\bar{f}_i^e = \int_0^{h_e} f(\bar{x})\psi_i^e(\bar{x})\, d\bar{x} \tag{4.6.10}$$

Equations (4.6.8) and (4.6.9) provide the means to compute the element stiffness matrix $[K^e]$ and force vector $\{F^e\}$, respectively, both referred to the global coordinate system, of a bar element oriented at an angle θ_e. The assembly of elements with their stiffness matrix and force vector in the global coordinates follows the same ideas as discussed before except that we must note that each node now has two displacement degrees of freedom. These ideas are illustrated in the following example.

Example 4.6.1

Consider a three-member truss shown in Figure 4.6.3(*a*). All members of the truss have identical areas of cross section A and modulus E. The hinged supports at joints A, B, and C allow free rotation of the members about the z-axis (taken positive out of the plane of the paper). We wish to determine the horizontal and vertical displacements at the joint C and forces in each member of the structure.

Finite Element Mesh

We use three finite elements to model the structure. Any further subdivision of the members does not add to the accuracy because the finite element solutions for displacements and forces at the nodes are exact for all truss problems. The global node numbers and element numbers are shown in Figure 4.6.3(*b*). There are two displacement degrees of freedom, horizontal and

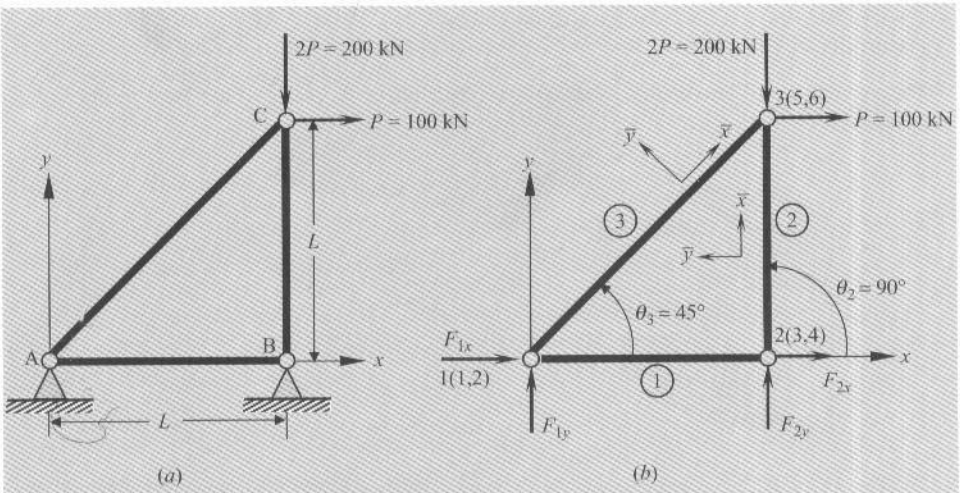

Figure 4.6.3 Geometry and finite element representation of a plane truss. (*a*) Geometry and applied loads. (*b*) Element numbering and reaction forces.

vertical displacements, at each node of the element. The element stiffness matrix in the local coordinate system is given by Eq. (4.6.1) while the stiffness matrix and force vector (with $\bar{f}_i^e = 0$) in the global coordinate system is given by Eqs. (4.6.8) and (4.6.9), respectively. The element data and connectivity is given in the following table.

Element number	Global nodes	Geometric properties	Material property	Orientation
1	1 2	$A,\ h_1 = L$	E	$\theta_1 = 0°$
2	2 3	$A,\ h_2 = L$	E	$\theta_2 = 90°$
3	1 3	$A,\ h_3 = \sqrt{2}L$	E	$\theta_3 = 45°$

Element Matrices

The element stiffness matrices are given by $[1/(2\sqrt{2}) = 0.3536]$

$$[K^1] = \frac{EA}{L}\begin{bmatrix} 1 & 0 & -1 & 0 \\ 0 & 0 & 0 & 0 \\ -1 & 0 & 1 & 0 \\ 0 & 0 & 0 & 0 \end{bmatrix}, \quad [K^2] = \frac{EA}{L}\begin{bmatrix} 0 & 0 & 0 & 0 \\ 0 & 1 & 0 & -1 \\ 0 & 0 & 0 & 0 \\ 0 & -1 & 0 & 1 \end{bmatrix}$$

$$[K^3] = \frac{EA}{L}\begin{bmatrix} 0.3536 & 0.3536 & -0.3536 & -0.3536 \\ 0.3536 & 0.3536 & -0.3536 & -0.3536 \\ -0.3536 & -0.3536 & 0.3536 & 0.3536 \\ -0.3536 & -0.3536 & 0.3536 & 0.3536 \end{bmatrix} \tag{4.6.11}$$

Assembly of Elements

The assembled stiffness matrix is given by (subscripts of K_{ij} refer to the local degrees of freedom)

$$[K]=\begin{array}{c} \begin{matrix} 1 & 2 & 3 & 4 & 5 & 6 \end{matrix} \\ \begin{bmatrix} K_{11}^1+K_{11}^3 & K_{12}^1+K_{12}^3 & K_{13}^1 & K_{14}^1 & K_{13}^3 & K_{14}^3 \\ & K_{22}^1+K_{22}^3 & K_{23}^1 & K_{24}^1 & K_{23}^3 & K_{24}^3 \\ & & K_{33}^1+K_{11}^2 & K_{34}^1+K_{12}^2 & K_{13}^2 & K_{14}^2 \\ & \text{symm.} & & K_{44}^1+K_{22}^2 & K_{23}^2 & K_{24}^2 \\ & & & & K_{33}^2+K_{33}^3 & K_{34}^2+K_{34}^3 \\ & & & & & K_{44}^2+K_{44}^3 \end{bmatrix} \begin{matrix} 1 \\ 2 \\ 3 \\ 4 \\ 5 \\ 6 \end{matrix} \end{array} \tag{4.6.12}$$

The element stiffness matrices of (4.6.11) can be used in Eq. (4.6.12) to obtain the assembled global stiffness matrix

$$[K]=\frac{EA}{L}\begin{bmatrix} 1.3536 & 0.3536 & -1.0 & 0.0 & -0.3536 & -0.3536 \\ & 0.3536 & 0.0 & 0.0 & -0.3536 & -0.3536 \\ & & 1.0 & 0.0 & 0.0 & 0.0 \\ & & & 1.0 & 0.0 & -1.0 \\ \text{symm.} & & & & 0.3536 & 0.3536 \\ & & & & & 1.3536 \end{bmatrix} \tag{4.6.13}$$

The displacement continuity conditions are

$$\begin{aligned} u_1^1=u_1^3=U_1,\quad & v_1^1=v_1^3=V_1 \\ u_2^1=u_1^2=U_2,\quad & v_2^1=v_1^2=V_2 \\ u_2^2=u_2^3=U_3,\quad & v_2^2=v_2^3=V_3 \end{aligned} \tag{4.6.14}$$

and the force equilibrium conditions are

$$\begin{aligned} F_1^1+F_1^3=F_{1x},\quad & F_2^1+F_2^3=F_{1y} \\ F_3^1+F_1^2=F_{2x},\quad & F_4^1+F_2^2=F_{2y} \\ F_3^2+F_3^3=F_{3x},\quad & F_4^2+F_4^3=F_{3y} \end{aligned} \tag{4.6.15}$$

which can be used to write the global displacement and force vectors as

$$\{\Delta\}=\begin{Bmatrix} U_1 \\ V_1 \\ U_2 \\ V_2 \\ U_3 \\ V_3 \end{Bmatrix},\quad \{F\}=\begin{Bmatrix} F_1^1+F_1^3 \\ F_2^1+F_2^3 \\ F_3^1+F_1^2 \\ F_4^1+F_2^2 \\ F_3^2+F_3^3 \\ F_4^2+F_4^3 \end{Bmatrix}=\begin{Bmatrix} F_{1x} \\ F_{1y} \\ F_{2x} \\ F_{2y} \\ F_{3x} \\ F_{3y} \end{Bmatrix} \tag{4.6.16}$$

where (U_I, V_I) and (F_{Ix}, F_{Iy}) denote the x and y components of the displacement and external forces, respectively, at the global node I.

Boundary Conditions

The specified displacement and force degrees of freedom are

$$U_1 = V_1 = U_2 = V_2 = 0, \quad F_{3x} = P, \quad F_{3y} = -2P \tag{4.6.17}$$

The first two boundary conditions correspond to the horizontal and vertical displacements at node 1, the next two correspond to the horizontal and vertical displacements at node 2, and the last correspond to the force boundary conditions at node 3. The unknowns are: the displacements (U_3, V_3) of node 3 and forces (F_{1x}, F_{1y}) at node 1 and forces (F_{2x}, F_{2y}) at node 2.

Condensed Equations

The condensed equations for the unknown displacements (U_3, V_3) are obtained from the last two equations of the system, as indicated by the dotted lines in (4.6.13)

$$\frac{EA}{L}\begin{bmatrix} 0.3536 & 0.3536 \\ 0.3536 & 1.3536 \end{bmatrix}\begin{Bmatrix} U_3 \\ V_3 \end{Bmatrix} = \begin{Bmatrix} P \\ -2P \end{Bmatrix} \tag{4.6.18}$$

and the condensed equations for the unknown reactions are (from the first four equations of the system)

$$\begin{Bmatrix} F_{1x} \\ F_{1y} \\ F_{2x} \\ F_{2y} \end{Bmatrix} = \frac{EA}{L}\begin{bmatrix} -0.3536 & -0.3536 \\ -0.3536 & -0.3536 \\ 0.0 & 0.0 \\ 0.0 & -1.0 \end{bmatrix}\begin{Bmatrix} U_3 \\ V_3 \end{Bmatrix} \tag{4.6.19}$$

Solution of the Finite Element Equations

Solving Eqs. (4.6.18) for U_5 and U_6, we obtain

$$U_3 = (3 + 2\sqrt{2})\frac{PL}{EA} = 5.828\,\frac{PL}{EA}, \quad V_3 = -\frac{3PL}{EA} \tag{4.6.20}$$

and the reaction forces are computed using Eq. (4.6.19)

$$F_{1x} = -P, \quad F_{1y} = -P, \quad F_{2x} = 0.0, \quad F_{2y} = 3P \tag{4.6.21}$$

Postcomputation

The stress in each member can be computed from the relation

$$\sigma^e = -\frac{\bar{P}_1^e}{A_e} = \frac{\bar{P}_2^e}{A_e} \tag{4.6.22}$$

where $\bar{P}_1^e$ and $\bar{P}_2^e$ can be determined from the element equations

$$\begin{Bmatrix} \bar{P}_1^e \\ \bar{P}_2^e \end{Bmatrix} = \frac{A_e E_e}{h_e}\begin{bmatrix} 1 & -1 \\ -1 & 1 \end{bmatrix}\begin{Bmatrix} \bar{u}_1^e \\ \bar{u}_2^e \end{Bmatrix} \tag{4.6.23}$$

and the element displacements $(\bar{u}_1^e, \bar{u}_2^e)$ are determined from the transformation relation (4.6.3*a*)

$$\begin{Bmatrix} \bar{u}_1^e \\ \bar{v}_1^e \\ \bar{u}_2^e \\ \bar{v}_2^e \end{Bmatrix} = \begin{bmatrix} \cos\theta_e & \sin\theta_e & 0 & 0 \\ -\sin\theta_e & \cos\theta_e & 0 & 0 \\ 0 & 0 & \cos\theta_e & \sin\theta_e \\ 0 & 0 & -\sin\theta_e & \cos\theta_e \end{bmatrix} \begin{Bmatrix} u_1^e \\ v_1^e \\ u_2^e \\ v_2^e \end{Bmatrix} \tag{4.6.24}$$

By definition [see Eqs. (4.6.14)], we have

$$u_1^1 = v_1^1 = u_2^1 = v_2^1 = 0, \quad u_1^2 = v_1^2 = u_1^3 = v_1^3 = 0$$
$$u_2^2 = u_2^3 = U_3 = (3 + 2\sqrt{2})\frac{PL}{EA}, \; v_2^2 = v_2^3 = V_3 = -\frac{3PL}{EA} \tag{4.6.25}$$

Hence, Eqs. (4.6.22)–(4.6.25) give

$$\sigma^e = \frac{E_e}{h_e}(\bar{u}_2^e - \bar{u}_1^e) \tag{4.6.26}$$

$$\begin{aligned} \bar{u}_1^1 &= u_1^1 \cos\theta_1 + v_1^1 \sin\theta_1 = 0 \\ \bar{u}_2^1 &= u_2^1 \cos\theta_1 + v_2^1 \sin\theta_1 = 0 \\ \bar{u}_1^2 &= u_1^2 \cos\theta_2 + v_1^2 \sin\theta_2 = 0 \\ \bar{u}_2^2 &= U_3 \cos\theta_2 + V_3 \sin\theta_2 = V_3 = -\frac{3PL}{EA} \\ \bar{u}_1^3 &= u_1^3 \cos\theta_3 + v_1^3 \sin\theta_3 = 0 \\ \bar{u}_2^3 &= U_3 \cos\theta_3 + V_3 \sin\theta_3 = \frac{1}{\sqrt{2}}(U_3 + V_3) = \frac{2PL}{EA} \end{aligned} \tag{4.6.27}$$

Thus, the member forces are

$$\bar{P}_1^1 = -\bar{P}_2^1 = 0, \quad \bar{P}_1^2 = -\bar{P}_2^2 = 3P, \quad \bar{P}_1^3 = -\bar{P}_2^3 = -\sqrt{2}P \tag{4.6.28}$$

The axial stresses in the members are

$$\sigma^{(1)} = 0, \quad \sigma^{(2)} = -\frac{3P}{A}, \quad \sigma^{(3)} = \sqrt{2}\,\frac{P}{A} \tag{4.6.29}$$

Interpretation and Verification of the Results

An examination of the structure and the sense of loads applied indicate that the displacements (U_3, V_3) are qualitatively correct (positive U_3 and negative V_3). Also, the geometry of the structure indicates that it has relatively more stiffness in the vertical direction (member 2 takes much of the load directly) compared to the horizontal direction, which explains the relatively large displacement in the horizontal direction.

The forces in Eq. (4.6.21) can be verified by applying the method of sections to the free-body-diagram in Figure 4.6.3(*b*). Sections AA, BB, and CC (see Figure 4.6.4) yield

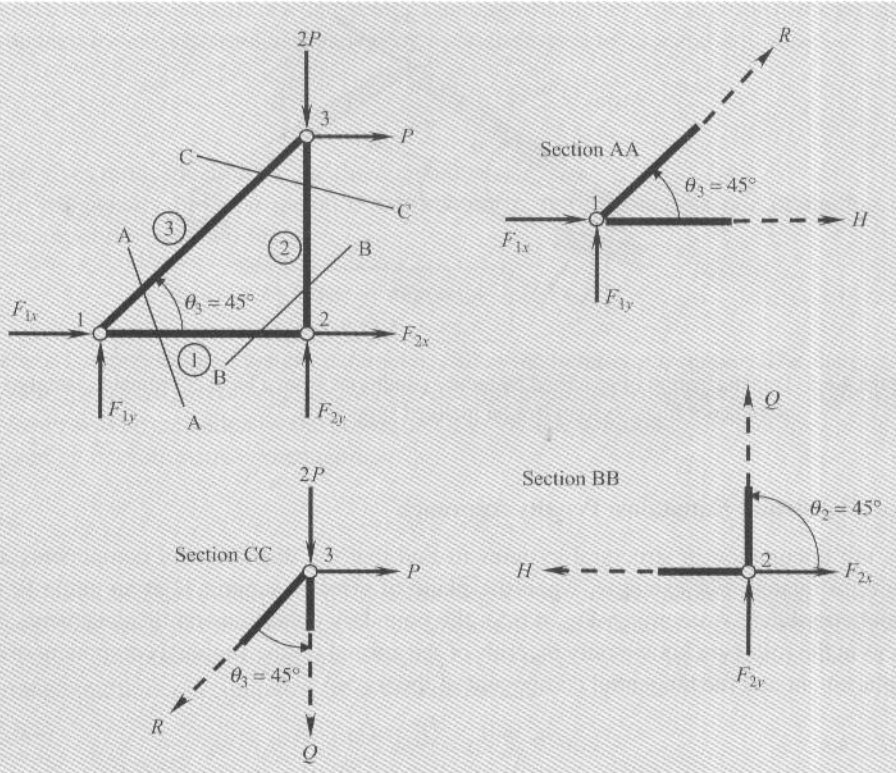

Figure 4.6.4 Method of sections to determine the member forces.

the relations ($H = 0$)

$$\frac{1}{\sqrt{2}}R + F_y^1 = 0, \quad F_x^1 + H + \frac{1}{\sqrt{2}}R = 0 \tag{4.6.30a}$$

$$F_x^2 - H = 0, \quad F_y^2 + Q = 0 \tag{4.6.30b}$$

$$-\frac{1}{\sqrt{2}}R + P = 0, \quad \frac{1}{\sqrt{2}}R + Q + 2P = 0 \tag{4.6.30c}$$

which yield

$$Q = -3P, \quad R = \sqrt{2}P, \quad F_y^2 = 3P, \quad F_y^1 = -P, \quad F_x^1 = -P, \quad H = F_x^2 = 0 \tag{4.6.30d}$$

Note that the member forces computed using the method of sections agree with those computed in the finite element method ($\bar{P}_1^1 = H$, $\bar{P}_1^2 = -Q$, and $\bar{P}_1^3 = -R$). It should be noted that this exercise is only for checking purposes, and the finite element method can be used to determine the member forces Q, R, and H, as discussed in the postcomputation. This completes the example.

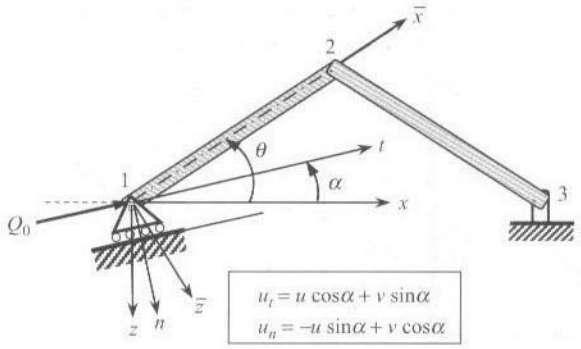

Figure 4.6.5 Transformation of specified boundary conditions from a local coordinate system to the global coordinate system (for an inclined support).

4.6.4 Constraint Equations: Penalty Approach

It is not uncommon in structural systems to find that the displacement components at a point are related. For example, when the plane of a roller support is at an angle to the global coordinate system (see Fig. 4.6.5), the boundary conditions on displacements and forces at the roller are known only in terms of the normal (to the support) component of the displacement and the tangential component of the force

$$u_n^e = 0, \quad Q_t^e = Q_0 \tag{4.6.31}$$

where u_n^e is the normal component of displacement and Q_t^e is the tangential component of the force at node 1 of the element Ω^e; Q_0 is any specified tangential force. These conditions, when expressed in terms of the global components of displacements and forces by means of the transformation of the form (4.6.3*b*) and (4.6.4), become

$$u_n^e = -u_1^e \sin\alpha + u_2^e \cos\alpha = 0 \tag{4.6.32a}$$

$$Q_t^e = Q_1^e \cos\alpha + Q_2^e \sin\alpha = Q_0 \tag{4.6.32b}$$

where (u_1^e, u_2^e) and (Q_1^e, Q_2^e) are the x and y components of the displacements and forces, respectively, at the support. Equations (4.6.32*a*) can be viewed as constraint equations among the global displacements, which have a companion relation among the associated forces, namely Eq. (4.6.32*b*). Here, we present the penalty function method through which constraint equations of the type in (4.6.32*a*) and (4.6.32*b*) can be included in the finite element equations.

The penalty function method allows us to reformulate a problem with constraints as one without constraints. The basic idea of the method can be described by considering an algebraic constrained problem:

minimize the function $f(x, y)$ *subject to the constraint* $G(x, y) = 0$

In the Lagrange multiplier method the problem is reformulated as one of determining the stationary (or critical) points of the modified function $F_L(x, y)$,

$$F_L(x, y) = f(x, y) + \lambda G(x, y) \tag{4.6.33}$$

subject to no constraints. Here λ denotes the Lagrange multiplier. The solution to the problem is obtained by setting partial derivatives of F_L with respect to x, y and λ to zero:

$$\frac{\partial F_L}{\partial x} = 0, \quad \frac{\partial F_L}{\partial y} = 0, \quad \frac{\partial F_L}{\partial \lambda} = 0 \tag{4.6.34}$$

which gives three equations in the three unknowns (x, y, λ).

In the penalty function method, the problem is reformulated as one of finding the minimum of the modified function F_P,

$$F_P(x, y) = f(x, y) + \frac{\gamma}{2}[G(x, y)]^2 \tag{4.6.35}$$

where γ is a preassigned weight parameter, called the *penalty parameter*. The factor $\frac{1}{2}$ in Eq. (4.6.35) is used for convenience: When F_p is differentiated with respect to its arguments, the factor will be cancelled by the power on $G(x, y)$. The solution to the modified problem is given by the following two equations:

$$\frac{\partial F_P}{\partial x} = 0, \quad \frac{\partial F_P}{\partial y} = 0 \tag{4.6.36a}$$

The solution of Eqs. (4.6.36*a*) will be a function of the penalty parameter, (x_γ, y_γ). The larger the value of γ, the more exactly the constraint is satisfied (in a least-squares sense), and (x_γ, y_γ) approaches the actual solution (x, y) as $\gamma \to \infty$. An approximation to the Lagrange multiplier is computed from the equation,

$$\lambda_\gamma = \gamma G(x_\gamma, y_\gamma) \tag{4.6.36b}$$

We consider a specific example to illustrate the ideas presented above.

Example 4.6.2

Minimize the quadratic function

$$f(x, y) = 4x^2 - 3y^2 + 2xy + 6x - 3y + 5$$

subject to the constraint

$$G(x, y) \equiv 2x + 3y = 0$$

Geometrically, we seek the inflection point of the surface $f(x, y)$ that is on the line $2x + 3y = 0$. We solve the problem using the Lagrange multiplier method and the penalty function method.

Lagrange Multiplier Method. The modified functional is

$$F_L(x, y) = f(x, y) + \lambda(2x + 3y)$$

where λ is the Lagrange multiplier to be determined. We have

$$\frac{\partial F_L}{\partial x} = 8x + 2y + 6 + 2\lambda = 0$$

$$\frac{\partial F_L}{\partial y} = -6y + 2x - 3 + 3\lambda = 0$$

$$\frac{\partial F_L}{\partial \lambda} = 2x + 3y = 0$$

Solving the three algebraic equations, we obtain

$$x = -3,\ y = 2,\ \lambda = 7$$

Penalty Function Method. The modified functional is

$$F_P(x, y) = f(x, y) + \frac{\gamma}{2}(2x + 3y)^2$$

and we have

$$\frac{\partial F_P}{\partial x} = 8x + 2y + 6 + 2\gamma(2x + 3y) = 0$$

$$\frac{\partial F_P}{\partial y} = -6y + 2x - 3 + 3\gamma(2x + 3y) = 0$$

The solution of these equations is

$$x_\gamma = \frac{15 - 36\gamma}{-26 + 12\gamma},\ y_\gamma = \frac{18 + 24\gamma}{-26 + 12\gamma}$$

The Lagrange multiplier is given by

$$\lambda_\gamma = \gamma G(x_\gamma, y_\gamma) = \frac{84\gamma}{-26 + 12\gamma}$$

Clearly, in the limit $\gamma \to \infty$, the penalty function solution approaches the exact solution:

$$\lim_{\gamma\to\infty} x_\gamma = -3,\ \lim_{\gamma\to\infty} y_\gamma = 2,\ \lim_{\gamma\to\infty} \lambda_\gamma = 7$$

An approximate solution to the problem can be obtained, within a desired accuracy, by selecting a finite value of the penalty parameter (see Table 4.6.1). This completes the example.

Table 4.6.1 Convergence of penalty function solution with increasing penalty parameter.

γ	x_γ	y_γ	λ_γ	$E_\gamma = 2x_\gamma + 3y_\gamma$
0	−0.5769	−0.6923	0.0000	−3.2308
1	1.5000	−3.0000	−6.0000	−6.0000
10	−3.6702	2.7447	8.9362	0.8936
100	−3.0537	2.0596	7.1550	0.0716
1,000	−3.0053	2.0058	7.0152	0.0068
10,000	−3.0005	2.0006	7.0015	0.0008
∞	−3.0000	2.0000	7.0000	0.0000

Now we turn our attention to constraint equations of the form used with bar elements

$$\beta_m u_m + \beta_n u_n = \beta_{mn} \tag{4.6.37}$$

where β_m, β_n and β_{mn} are known constants, and u_m and u_n are the mth and nth displacement degrees of freedom in the mesh, respectively. The functional that must be minimized subject to the constraint in (4.6.37) in this case is the total potential energy of the system (see Section 4.5.2)

$$\Pi = \frac{1}{2}\int_\Omega AE\mathbf{u}^{\mathrm{T}}\mathbf{B}^{\mathrm{T}}\mathbf{B}\mathbf{u}\,dx - \int_\Omega \mathbf{u}^{\mathrm{T}}\mathbf{B}^{\mathrm{T}} f\,dx - \mathbf{u}^{\mathrm{T}}\mathbf{Q} \tag{4.6.38}$$

The penalty functional is given by

$$\Pi_p = \frac{1}{2}\int_\Omega AE\mathbf{u}^{\mathrm{T}}\mathbf{B}^{\mathrm{T}}\mathbf{B}\mathbf{u}\,dx - \int_\Omega \mathbf{u}^{\mathrm{T}}\mathbf{B}^{\mathrm{T}} f\,dx - \mathbf{u}^{\mathrm{T}}\mathbf{Q} + \frac{\gamma}{2}(\beta_m u_m + \beta_n u_n - \beta_{mn})^2 \tag{4.6.39}$$

The functional Π_p attains a minimum only when $\beta_m u_m + \beta_n u_n - \beta_{mn}$ is very small, i.e., approximately satisfying the constraint (4.6.37). Setting $\delta\Pi_p = 0$ yields

$$(\mathbf{K} + \mathbf{K}_p)\,\mathbf{u} = \mathbf{f} + \mathbf{Q} + \mathbf{Q}_p \tag{4.6.40a}$$

where [see Eq. (4.5.4a)]

$$\mathbf{K} = \int_\Omega AE\mathbf{B}^{\mathrm{T}}\mathbf{B}\,dx, \quad \mathbf{K}_p = \begin{bmatrix} \cdots & \cdots & \cdots & \cdots & \cdots \\ \cdots & \gamma\beta_m^2 & \cdots & \gamma\beta_m\beta_n & \cdots \\ \cdots & \cdots & \cdots & \cdots & \cdots \\ \cdots & \gamma\beta_m\beta_n & \cdots & \gamma\beta_n^2 & \cdots \\ \cdots & \cdots & \cdots & \cdots & \cdots \end{bmatrix}$$

$$\mathbf{f} = \int_\Omega \mathbf{B}^{\mathrm{T}} f\,dx, \quad \mathbf{Q}_p = \begin{Bmatrix} \cdots \\ \gamma\beta_{mn}\beta_m \\ \cdots \\ \gamma\beta_{mn}\beta_n \\ \cdots \end{Bmatrix} \tag{4.6.40b}$$

Thus, a modification of the stiffness and force coefficients associated with the constrained degrees of freedom will provide the desired solution to the constrained problem. As illustrated in Example 4.6.2, the value of the penalty parameter γ dictates the degree to which the constraint condition (4.6.37) is met. An analysis of the discrete problem shows that the following value of γ may be used:

$$\gamma = \max|K_{ij}| \times 10^4, \quad 1 \le i, j \le N \tag{4.6.41}$$

where N is the order of the global coefficient matrix. The reaction forces associated with the constrained displacement degrees of freedom are obtained from

$$F_{mp} = -\gamma\beta_m(\beta_m u_m + \beta_n u_n - \beta_{mn}), \quad F_{np} = -\gamma\beta_n(\beta_m u_m + \beta_n u_n - \beta_{mn}) \tag{4.6.42}$$

Because of the large magnitudes of the penalty terms, it is necessary to carry out computations in double precision (hand calculations do not give accurate results).

Example 4.6.3

Consider the structure shown in Fig. 4.6.6(*a*). The rigid bar ABE is supported by deformable bars AC and BD. Bar AC is made of aluminum ($E_a = 70$ GPa) and has cross-sectional area of $A_a = 500$ mm^2; bar BD is made of steel ($E_s = 200$ GPa) and has a cross-sectional area of $A_s = 600$ mm^2. The rigid bar carries loads of $F_1 = 10$ kN and $F_2 = 30$ kN at points O and E, respectively. We wish to determine the displacements of points A, B, and E, and the stresses in the aluminum and steel bars.

One may note that this is a statically determinate problem, i.e., the forces at points A and B can be readily determined from statics. Using the free-body diagram of the rigid bar ABE [see Fig. 4.6.6(*b*)], we obtain

$$F_{AC} + F_{BD} = F_1 + F_2, \quad 0.3F_{AC} + 0.5F_{BD} - 0.9F_2 = 0$$

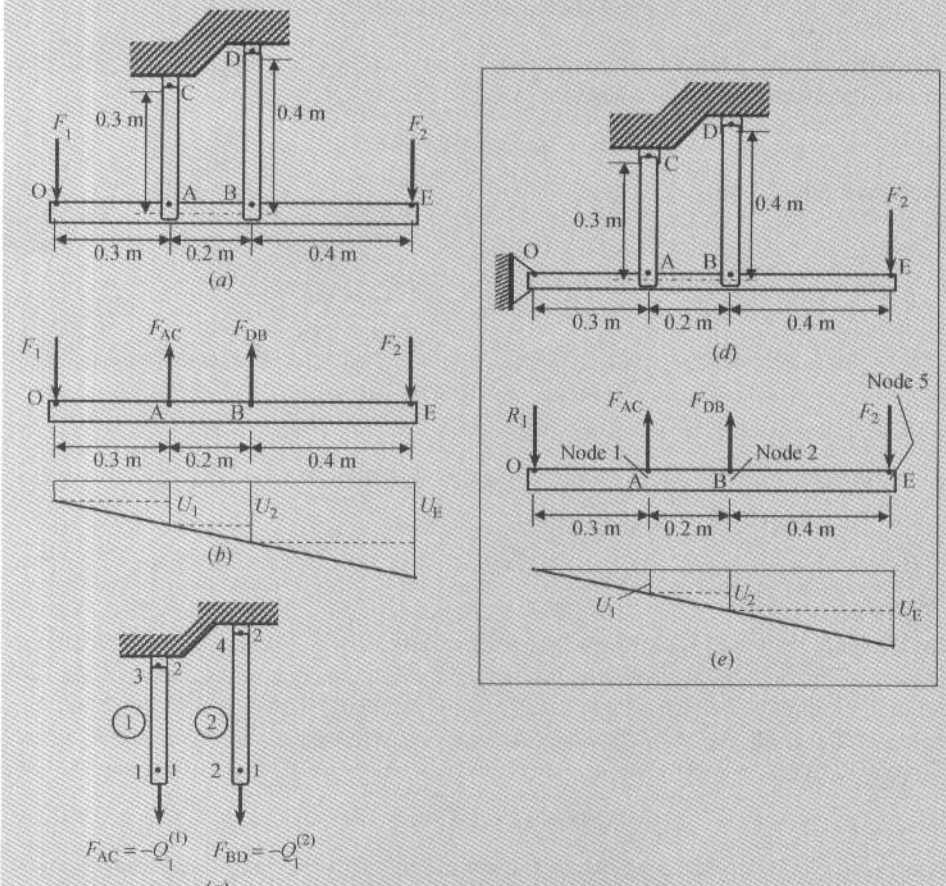

Figure 4.6.6 (*a*) Given structure. (*b*) Free-body diagram. (*c*) Finite element mesh. (*d*) Modified structure. (*e*) Free-body diagram of the modified structure.

which yield the values

$$F_{AC} = 2.5F_1 - 2F_2 = -35\text{kN}, \quad F_{BD} = -1.5F_1 + 3F_2 = 75\text{kN}$$

If we use two linear finite elements to represent the bars AC and BD, the assembled matrix of the structure is given by [see Fig. 4.6.6(*c*)]

$$\begin{matrix} & 1 & 2 & 3 & 4 \\ 1 \\ 2 \\ 3 \\ 4 \end{matrix} \begin{bmatrix} k_1 & 0 & -k_1 & 0 \\ 0 & k_2 & 0 & -k_2 \\ -k_1 & 0 & k_1 & 0 \\ 0 & -k_2 & 0 & k_2 \end{bmatrix} \begin{Bmatrix} U_1 \\ U_2 \\ U_3 \\ U_4 \end{Bmatrix} = \begin{Bmatrix} Q_1^1 \\ Q_1^2 \\ Q_2^1 \\ Q_2^2 \end{Bmatrix} \tag{4.6.43}$$

where

$$k_1 = \frac{E_a A_a}{h_1} = 116.6667 \times 10^6 \text{ N/m}, \quad k_2 = \frac{E_s A_s}{h_2} = 300 \times 10^6 \text{ N/m}$$

The boundary conditions of the problem are

$$U_3 = U_4 = 0; \quad Q_1^1 = -F_{AC} = 35 \text{ kN}, \quad Q_1^2 = -F_{BD} = -75 \text{ kN}$$

Hence, the condensed equations are given by

$$10^6 \begin{bmatrix} 116.6667 & 0 \\ 0 & 300 \end{bmatrix} \begin{Bmatrix} U_1 \\ U_2 \end{Bmatrix} = 10^3 \begin{Bmatrix} 35 \\ -75 \end{Bmatrix}$$

whose solution is

$$U_1 = 0.30 \times 10^{-3} \text{ m} = 0.30 \text{ mm}, \quad U_2 = -0.25 \times 10^{-3} \text{ m} = -0.25 \text{ mm}$$

Using the principle of similar triangles, we can determine the displacement of point E. We have

$$\frac{U_E - U_1}{0.6} = \frac{U_2 - U_1}{0.2} \quad \rightarrow \quad U_E = 3U_2 - 2U_1 = -1.35 \text{ mm}$$

Thus, end A of the bar AC moves up by 0.3 mm, end B of BD moves down by 0.25 mm, and point E moves down by 1.35 mm. The stresses in bars AC and BD are

$$\sigma_{AC} = \frac{F_{AC}}{A_a} = -\frac{35}{500 \times 10^{-6}} = -70 \text{ MPa}, \quad \sigma_{BD} = \frac{F_{BD}}{A_s} = \frac{75}{600 \times 10^{-6}} = 125 \text{ MPa}$$

Next, consider the case in which point O is pin connected to a fixed, immovable part, as shown in Fig. 4.6.6(*d*). Then the problem becomes a statically indeterminate one. Of course, the finite element method can still be used to solve the problem. The assembled equations (4.6.43) are still valid for this case. However, forces Q_1^1 and Q_1^2 are not known (because we cannot solve for F_{AC} and F_{BD}). In addition, points A and B are constrained to move as the rigid member ABE is rotated about point O. This geometric constraint is equivalent to the following conditions among the displacements U_1, U_2, and U_5:

$$\frac{U_1}{0.3} = \frac{U_5}{0.9} \rightarrow 3U_1 - U_5 = 0, \quad \frac{U_2}{0.5} = \frac{U_5}{0.9} \rightarrow 1.8U_2 - U_5 = 0 \tag{4.6.44}$$

These constraints bring in an additional degree of freedom, namely U_5, into the equations. Hence, the assembled equations before including the constraint conditions are

$$10^6\begin{bmatrix} 116.67 & 0 & -116.67 & 0 & 0 \\ 0 & 300 & 0 & -300 & 0 \\ -116.67 & 0 & 116.67 & 0 & 0 \\ 0 & -300 & 0 & 300 & 0 \\ 0 & 0 & 0 & 0 & 0 \end{bmatrix}\begin{Bmatrix} U_1 \\ U_2 \\ U_3 \\ U_4 \\ U_5 \end{Bmatrix} = \begin{Bmatrix} Q_1^1 \\ Q_1^2 \\ Q_2^1 \\ Q_2^2 \\ F_2 \end{Bmatrix} \tag{4.6.45}$$

The last row and column of the above equation are added to facilitate the addition of penalty terms. Without the addition of the penalty contributions the last equation is nonsensical.

Using the procedure developed in this section, we can include the constraints, $3U_1 - U_5 = 0$ and $1.8U_2 - U_5 = 0$ into assembled equations (4.6.43). The value of the penalty parameter is selected to be $\gamma = (300 \times 10^6)10^4$. The stiffness additions due to the two constraints are ($\beta_1 = 3$, $\beta_2 = 1.8$, $\beta_5 = -1$, and $\beta_{15} = \beta_{25} = 0$)

$$\begin{array}{c} \\ 1 \\ 5 \end{array}\begin{array}{c} \begin{array}{cc} 1 & 5 \end{array} \\ \begin{bmatrix} (3)^2\gamma & 3(-1)\gamma \\ (-1)3\gamma & (-1)^2\gamma \end{bmatrix} \end{array} = 10^{10}\begin{bmatrix} 2700.00 & -900.00 \\ -900.00 & 300.00 \end{bmatrix}$$

$$\begin{array}{c} \\ 2 \\ 5 \end{array}\begin{array}{c} \begin{array}{cc} 2 & 5 \end{array} \\ \begin{bmatrix} (1.8)^2\gamma & (-1)1.8\gamma \\ (-1)1.8\gamma & (-1)^2\gamma \end{bmatrix} \end{array} = 10^{10}\begin{bmatrix} 972.00 & -540.00 \\ -540.00 & 300.00 \end{bmatrix} \tag{4.6.46}$$

The force additions are zero on account of $\beta_{15} = \beta_{25} = 0$. Hence, the modified finite element equations become

$$10^6\begin{bmatrix} 27{,}000{,}117 & 0 & -117 & 0 & -9{,}000{,}000 \\ 0 & 9{,}720{,}300 & 0 & -300 & -5{,}400{,}000 \\ -116.67 & 0 & 117 & 0 & 0 \\ 0 & -300 & 0 & 300 & 0 \\ -9{,}000{,}000 & -5{,}400{,}000 & 0 & 0 & 6{,}000{,}000 \end{bmatrix}\begin{Bmatrix} U_1 \\ U_2 \\ U_3 \\ U_4 \\ U_5 \end{Bmatrix} = \begin{Bmatrix} Q_1^1 \\ Q_1^2 \\ Q_2^1 \\ Q_2^2 \\ F_2 \end{Bmatrix} \tag{4.6.47}$$

The condensed equations are

$$10^6\begin{bmatrix} 27{,}000{,}117 & 0 & -9{,}000{,}000 \\ 0 & 9{,}720{,}300 & -5{,}400{,}000 \\ -9{,}000{,}000 & -5{,}400{,}000 & 6{,}000{,}000 \end{bmatrix}\begin{Bmatrix} U_1 \\ U_2 \\ U_5 \end{Bmatrix} = \begin{Bmatrix} 0 \\ 0 \\ 30 \times 10^3 \end{Bmatrix} \tag{4.6.48}$$

whose solution (using an equation solver) is (deflections are in the direction of the force)

$$U_1 = 0.09474\ (\text{mm}),\quad U_2 = 0.15789\ (\text{mm}),\quad U_5 = 0.28422\ (\text{mm}) \tag{4.6.49a}$$

The forces in the bars AC and BD can be calculated using Eq. (4.6.45)

$$\begin{Bmatrix} Q_1^1 \\ Q_1^2 \end{Bmatrix} = 10^6 \begin{bmatrix} 116.6667 & 0 \\ 0 & 300 \end{bmatrix} \begin{Bmatrix} U_1 \\ U_2 \end{Bmatrix} = 10^3 \begin{Bmatrix} 11.053 \\ 47.367 \end{Bmatrix} \text{N}$$

The stresses are $\sigma_{AC} = 22.11$ MPa and $\sigma_{BD} = 79$ MPa. Alternatively, from Eq. (4.6.42) we have (one must include significant number of decimal points in the computation)

$$\begin{aligned} (Q_1^1)_p &= -900 \times 10^7 \left(3 \times 0.094739 \times 10^{-3} - 0.28422 \times 10^{-3}\right) = 11.053 \text{ kN} \\ (Q_1^2)_p &= -540 \times 10^7 \left(1.8 \times 0.15789 \times 10^{-3} - 0.28422 \times 10^{-3}\right) = 47.368 \text{ kN} \end{aligned} \tag{4.6.49b}$$

Next, we consider a plane truss with an inclined support. The penalty approach is used to include the constraint condition among the displacement components at the support.

Example 4.6.4

Consider the truss shown in Fig. 4.6.7(*a*). We wish to determine the unknown displacements of nodes 2 and 3 and the reactions associated with these displacements.

The element stiffness matrices are

$$[K^1] = 10^9 \begin{bmatrix} 0.000 & 0.000 & 0.000 & 0.000 \\ 0.000 & 0.126 & 0.000 & -0.126 \\ 0.000 & 0.000 & 0.000 & 0.000 \\ 0.000 & -0.126 & 0.000 & 0.126 \end{bmatrix}$$

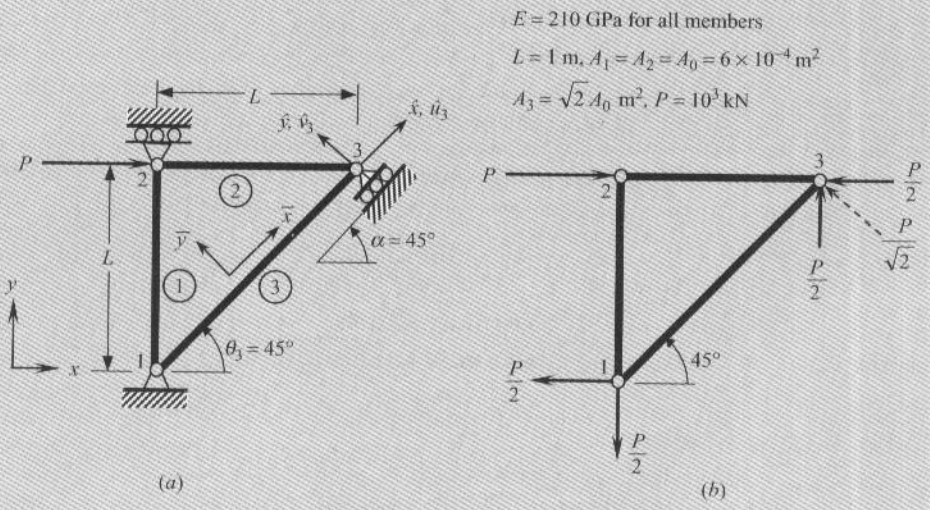

Figure 4.6.7 (*a*) Given structure. (*b*) Reaction forces.

$$[K^2] = 10^9 \begin{bmatrix} 0.126 & 0.000 & -0.126 & 0.000 \\ 0.000 & 0.000 & 0.000 & 0.000 \\ -0.126 & 0.000 & 0.126 & 0.000 \\ 0.000 & 0.000 & 0.000 & 0.000 \end{bmatrix}$$

$$[K^3] = 0.63 \times 10^8 \begin{bmatrix} 1.0 & 1.0 & -1.0 & -1.0 \\ 1.0 & 1.0 & -1.0 & -1.0 \\ -1.0 & -1.0 & 1.0 & 1.0 \\ -1.0 & -1.0 & 1.0 & 1.0 \end{bmatrix}$$

The assembled equations before including the constraint conditions are

$$10^8 \begin{bmatrix} 0.63 & 0.63 & 0.00 & 0.00 & -0.63 & -0.63 \\ 0.63 & 1.89 & 0.00 & -1.26 & -0.63 & -0.63 \\ 0.00 & 0.00 & 1.26 & 0.00 & -1.26 & 0.00 \\ 0.00 & -1.26 & 0.00 & 1.26 & 0.00 & 0.00 \\ 0.00 & -0.63 & -1.26 & 0.00 & 1.89 & 0.63 \\ -0.63 & -0.63 & 0.00 & 0.00 & 0.63 & 0.63 \end{bmatrix} \begin{Bmatrix} U_1 \\ U_2 \\ U_3 \\ U_4 \\ U_5 \\ U_6 \end{Bmatrix} = \begin{Bmatrix} Q_1^1 + Q_1^3 \\ Q_2^1 + Q_2^3 \\ Q_3^1 + Q_1^2 \\ Q_4^1 + Q_2^2 \\ Q_3^2 + Q_3^3 \\ Q_4^2 + Q_4^3 \end{Bmatrix} \tag{4.6.50}$$

The constraint condition at node 3 is

$$u_n \equiv -u \sin\alpha + v \cos\alpha = 0 \rightarrow -0.7071u + 0.7071v = 0$$

Comparing this constraint equation to the general constraint equation (4.6.37), we find that $\beta_1 = -0.7071$, $\beta_2 = 0.7071$, and $\beta_{12} = 0$.

The value of the penalty parameter is selected to be $\gamma = (1.89 \times 10^8)10^4$. The stiffness additions due to the constraint are

$$\begin{array}{c} \\ 5 \\ 6 \end{array} \begin{array}{c} \begin{array}{cc} \quad 5 & \quad 6 \end{array} \\ \gamma \begin{bmatrix} (-0.7071)^2 & -(0.7071)^2 \\ -(0.7071)^2 & (0.7071)^2 \end{bmatrix} \end{array} = 1.89 \times 10^{12} \begin{bmatrix} 0.5 & -0.5 \\ -0.5 & 0.5 \end{bmatrix}$$

The assembled equations after including the constraint conditions are (the numbers shown are truncated but more accurate numbers are used in actual computation in a computer)

$$10^8 \begin{bmatrix} 0.63 & 0.63 & 0.00 & 0.00 & -0.63 & -0.63 \\ 0.63 & 1.89 & 0.00 & -1.26 & -0.63 & -0.63 \\ 0.00 & 0.00 & 1.26 & 0.00 & -1.26 & 0.00 \\ 0.00 & -1.26 & 0.00 & 1.26 & 0.00 & 0.00 \\ 0.00 & -0.63 & -1.26 & 0.00 & 6301.8 & 6299.2 \\ -0.63 & -0.63 & 0.00 & 0.00 & 6299.2 & 6300.5 \end{bmatrix} \begin{Bmatrix} U_1 \\ U_2 \\ U_3 \\ U_4 \\ U_5 \\ U_6 \end{Bmatrix} = \begin{Bmatrix} Q_1^1 + Q_1^3 \\ Q_2^1 + Q_2^3 \\ Q_3^1 + Q_1^2 \\ Q_4^1 + Q_2^2 \\ Q_3^2 + Q_3^3 \\ Q_4^2 + Q_4^3 \end{Bmatrix}$$

Imposing the boundary and force equilibrium conditions $U_1 = U_2 = U_4 = 0$ and $Q_3^1 + Q_1^2 = P$, we obtain the condensed equations

$$10^8 \begin{bmatrix} 1.26 & -1.26 & 0.00 \\ -1.26 & 6301.8 & 6299.2 \\ 0.00 & 6299.2 & 6300.5 \end{bmatrix} \begin{Bmatrix} U_3 \\ U_5 \\ U_6 \end{Bmatrix} = \begin{Bmatrix} P \\ 0 \\ 0 \end{Bmatrix}$$

The solution to these equations (as computed in double precision in a computer) is

$$U_3 = 11.905 \times 10^{-3}\ \text{m}, \quad U_5 = 3.9688 \times 10^{-3}\ \text{m}, \quad U_6 = 3.9680 \times 10^{-3}\ \text{m}$$

and the reactions at node 3, as computed using (4.6.50) are

$$F_{3x} = -500\ \text{kN}, \quad F_{3y} = 500\ \text{kN}$$

The reactions of the whole structure are shown in Fig. 4.6.7(*b*).

4.6.5 Constraint Equations: A Direct Approach

Here, we present an exact method by which constraint equations of the type in (4.6.32*a*) and (4.6.32*b*) can be included in the assembled equations for the unknowns. The method involves expressing the global displacement degrees of freedom at the node with a constraint in terms of the local displacement degrees of freedom so that the boundary conditions can be readily imposed.

Recall from Eqs. (4.6.2) and (4.6.3*a*) that the displacements $(\hat{u}, \hat{v})$, referred to the local coordinate system $(\hat{x}, \hat{y})$ at a point, are related to the displacements (u, v), referred to the global coordinates system (x, y), by

$$\begin{Bmatrix} \hat{u} \\ \hat{v} \end{Bmatrix}_c = \begin{bmatrix} \cos\beta & \sin\beta \\ -\sin\beta & \cos\beta \end{bmatrix} \begin{Bmatrix} u \\ v \end{Bmatrix}_c \quad \rightarrow \quad \hat{\mathbf{u}}_c = \mathbf{A}\mathbf{u}_c \tag{4.6.51a}$$

and the inverse relation is given by

$$\mathbf{u}_c = \mathbf{A}^{\mathrm{T}}\hat{\mathbf{u}}_c, \quad \text{where} \quad \mathbf{A} = \begin{bmatrix} \cos\beta & \sin\beta \\ -\sin\beta & \cos\beta \end{bmatrix} \tag{4.6.51b}$$

where the subscript "c" refers to the constrained degrees of freedom. Since we wish to express the global displacements at a given node in terms of the local displacements at a specific node, we construct the transformation of the whole (global) system as

$$[T] = \begin{bmatrix} [I] & [0] & [0] \\ [0] & [A] & [0] \\ [0] & [0] & [I] \end{bmatrix} \tag{4.6.52}$$

Thus, all displacement degrees of freedom that are not constrained are unaffected and only global displacements that are constrained are transformed to the local displacements. Further, note that the transformation matrix $[A]$ is placed in $[T]$ in such a way that only the constrained degrees of freedom are transformed. We have

$$\begin{Bmatrix} \Delta^1 \\ \mathbf{u}_c \\ \Delta^2 \end{Bmatrix} = \begin{bmatrix} \mathbf{I} & \mathbf{0} & \mathbf{0} \\ \mathbf{0} & \mathbf{A}^{\mathrm{T}} & \mathbf{0} \\ \mathbf{0} & \mathbf{0} & \mathbf{I} \end{bmatrix} \begin{Bmatrix} \Delta^1 \\ \hat{\mathbf{u}} \\ \Delta^2 \end{Bmatrix} \quad \text{or} \quad \boldsymbol{\Delta} = \mathbf{T}^{\mathrm{T}}\hat{\boldsymbol{\Delta}} \tag{4.6.53}$$

where $\boldsymbol{\Delta}^1$ and $\boldsymbol{\Delta}^2$ denote vectors of the global displacement components ahead and behind (in terms of numbering) the constrained displacement degrees of freedom $\mathbf{u}_c$ in the mesh. We also note that the transformed displacement vector $\hat{\boldsymbol{\Delta}}$ contains the global displacement vectors $\boldsymbol{\Delta}^1$ and $\boldsymbol{\Delta}^2$ and the local (constrained) displacement vector $\hat{\mathbf{u}}_c$.

The remaining steps of the procedure are the same as that described in Sections 4.6.2 and 4.6.3. Thus, we obtain

$$\hat{\mathbf{K}}\hat{\boldsymbol{\Delta}} = \hat{\mathbf{F}} \tag{4.6.54}$$

where the transformed global stiffness matrix $\hat{\mathbf{K}}$ and global force vector $\hat{\mathbf{F}}$ are known in terms of the assembled global stiffness matrix $\mathbf{K}$ and force vector $\mathbf{F}$ as [see Eq. (4.6.7)]

$$\hat{\mathbf{K}} = \mathbf{T}^{\mathrm{T}}\mathbf{K}\mathbf{T}, \quad \hat{\mathbf{F}} = \mathbf{T}^{\mathrm{T}}\mathbf{F} \tag{4.6.55}$$

Since the constrained displacements are a part of the global system of equations, we may impose the boundary conditions on them directly (such as $\hat{u}_n = 0$ at an inclined roller support, where n denotes the coordinate normal to the roller).

In summary, we may introduce a transformation of the displacements that facilitates the imposition of boundary conditions or inclusion of constraints on the displacements. Once the transformation $\mathbf{T}$ is identified, we may use Eq. (4.6.7) or (4.6.55) to obatin the modified equations that have the desired effect. We revisit the problems of Examples 4.6.3 and 4.6.4 to illustrate the ideas described here.

Example 4.6.5

As an example to illustrate the direct approach, consider the structure shown in Fig. 4.6.6(*d*). The assembled equations are

$$10^3\begin{bmatrix} 116.67 & 0 & -116.67 & 0 \\ 0 & 300.00 & 0 & -300.00 \\ -116.67 & 0 & 116.67 & 0 \\ 0 & -300.00 & 0 & 300.00 \end{bmatrix}\begin{Bmatrix} U_1 \\ U_2 \\ U_3 \\ U_4 \end{Bmatrix} = \begin{Bmatrix} Q_1^1 \\ Q_1^2 \\ Q_2^1 \\ Q_2^2 \end{Bmatrix} \tag{4.6.56}$$

The geometric constraint between the displacements U_1 and U_2 is

$$\frac{U_1}{0.3} = \frac{U_2}{0.5} \rightarrow U_1 = 0.6U_2 \tag{4.6.57}$$

In this case, we can introduce a transformation $\mathbf{T}$ between (U_1, U_2, U_3, U_4) and (U_2, U_3, U_4) (i.e., eliminate U_1 by means of the constraint equation $U_1 = 0.6U_2$) as

$$\begin{Bmatrix} U_1 \\ U_2 \\ U_3 \\ U_4 \end{Bmatrix} = \begin{bmatrix} 0.6 & 0.0 & 0.0 \\ 1.0 & 0.0 & 0.0 \\ 0.0 & 1.0 & 0.0 \\ 0.0 & 0.0 & 1.0 \end{bmatrix}\begin{Bmatrix} U_2 \\ U_3 \\ U_4 \end{Bmatrix} \text{ or } \boldsymbol{\Delta} = \mathbf{T}\hat{\boldsymbol{\Delta}}$$

Hence, the transformed equations are

$$\hat{\mathbf{K}}\hat{\boldsymbol{\Delta}} = \hat{\mathbf{F}}, \quad \boldsymbol{\Delta} = \begin{Bmatrix} U_1 \\ U_2 \\ U_3 \\ U_4 \end{Bmatrix}, \quad \hat{\boldsymbol{\Delta}} = \begin{Bmatrix} U_2 \\ U_3 \\ U_4 \end{Bmatrix}$$

or, in explicit form,

$$10^3 \begin{bmatrix} 342.0 & -70.0 & -300.0 \\ -70.0 & 116.67 & 0 \\ -300.0 & 0 & 300.0 \end{bmatrix} \begin{Bmatrix} U_2 \\ U_3 \\ U_4 \end{Bmatrix} = \begin{Bmatrix} 0.6Q_1^1 + Q_1^2 \\ Q_2^1 \\ Q_2^2 \end{Bmatrix}$$

From the free-body diagram of the bar OABE, we find that $0.6F_{AC} + F_{BD} = 1.8F_2$; therefore, we have $0.6Q_1^1 + Q_1^2 = 1.8F_2 = 54$ kN and the condensed equation for the unknown U_2 is ($U_3 = U_4 = 0.0$)

$$342U_2 = 54, \quad U_2 = 0.15789 \text{ (mm)}, \quad U_1 = 0.6U_2 = 0.09474 \text{ (mm)}$$

The forces in the bars AC and BD are calculated using Eq. (4.6.56) ($U_3 = U_4 = 0.0$)

$$\begin{Bmatrix} Q_1^1 \\ Q_1^2 \end{Bmatrix} = 10^3 \begin{bmatrix} 116.6667 & 0 \\ 0 & 300 \end{bmatrix} \begin{Bmatrix} U_1 \\ U_2 \end{Bmatrix} = 10^3 \begin{Bmatrix} 11.053 \\ 47.368 \end{Bmatrix}$$

The stresses are $\sigma_{AC} = 22.11$ MPa and $\sigma_{BD} = 79$ MPa.

Example 4.6.6

Here we consider the truss in Figure 4.6.7(a). The assembled global equations are given by Eq. (4.6.50). The transformation between the global degrees of freedom ($U_1 = u_1$, $U_2 = v_1$, $U_3 = u_2$, $U_4 = v_2$, $U_5 = u_3$, $U_6 = v_3$) and ($U_1 = u_1$, $U_2 = v_1$, $U_3 = u_2$, $U_4 = v_2$, $\hat{u}_3 = u_t$, $\hat{v}_3 = u_n$) is given by [i.e., Eq. (4.6.53) for the problem at hand takes the form]

$$\begin{Bmatrix} U_1 \\ U_2 \\ U_3 \\ U_4 \\ U_5 \\ U_6 \end{Bmatrix} = \begin{bmatrix} 1 & 0 & 0 & 0 & 0 & 0 \\ 0 & 1 & 0 & 0 & 0 & 0 \\ 0 & 0 & 1 & 0 & 0 & 0 \\ 0 & 0 & 0 & 1 & 0 & 0 \\ 0 & 0 & 0 & 0 & \cos\alpha & -\sin\alpha \\ 0 & 0 & 0 & 0 & \sin\alpha & \cos\alpha \end{bmatrix} \begin{Bmatrix} U_1 \\ U_2 \\ U_3 \\ U_4 \\ \hat{u}_3 \\ \hat{v}_3 \end{Bmatrix} \tag{4.6.58a}$$

where $\alpha = 45°$. Using Eq. (4.6.55), we obtain the transformed equations

$$10^8 \begin{bmatrix} 0.630 & 0.630 & 0.000 & 0.00 & -0.891 & 0.000 \\ 0.630 & 1.890 & 0.000 & -1.26 & -0.891 & 0.000 \\ 0.000 & 0.000 & 1.260 & 0.00 & -0.891 & 0.891 \\ 0.000 & -1.260 & 0.000 & 1.26 & 0.000 & 0.000 \\ -0.891 & -0.891 & -0.891 & 0.00 & 1.890 & -0.630 \\ 0.000 & 0.000 & 0.891 & 0.00 & -0.630 & 0.630 \end{bmatrix} \begin{Bmatrix} U_1 \\ U_2 \\ U_3 \\ U_4 \\ \hat{u}_3 \\ \hat{v}_3 \end{Bmatrix} = \begin{Bmatrix} Q_1^1 + Q_1^3 \\ Q_2^1 + Q_2^3 \\ Q_3^1 + Q_1^2 \\ Q_4^1 + Q_2^2 \\ \hat{F}_{3t} \\ \hat{F}_{3n} \end{Bmatrix} \tag{4.6.58b}$$

where $\hat{F}_{3t}$ and $\hat{F}_{3n}$ are the reaction forces at node 3 in the tangential and normal directions, respectively.

Now applying the boundary conditions

$$U_1 = U_2 = U_4 = \hat{v}_3 = 0, \quad Q_3^1 + Q_1^2 = P = 10^6, \quad \hat{F}_{3t} = 0$$

we obtain the following condensed equations:

$$10^8 \begin{bmatrix} 1.26000 & -0.89095 \\ -0.89095 & 1.88990 \end{bmatrix} \begin{Bmatrix} U_3 \\ \hat{u}_3 \end{Bmatrix} = \begin{Bmatrix} 10^6 \\ 0 \end{Bmatrix} \tag{4.6.59}$$

The x component of displacement at node 2 and the tangential displacement $\hat{u}_3$ of node 3 are

$$U_3 = 11.905 \times 10^{-3} \text{ m}, \quad \hat{u}_3 = 5.6122 \times 10^{-3} \text{ m} \tag{4.6.60a}$$

The unknown reactions can be calculated from Eq. (4.6.58b) as

$$F_{1x} = -500 \text{ kN}, \quad F_{1y} = -500 \text{ kN}, \quad F_{2y} = 0 \text{ kN}, \quad \hat{F}_{3n} = 707.1 \text{ kN} \tag{4.6.60b}$$

These results are the same as those obtained by the penalty method in Example 4.6.4.

4.7 SUMMARY

In this chapter, finite element models of discrete systems have been developed and applications of finite element models to the solution of problems of heat transfer, fluid mechanics, and solid mechanics have been presented. To aid the reader, a brief review of the basic terminology and governing equations of each of the three fields has also been given. Analysis of plane trusses and inclusion of constraint relations between primary variables by two different methods is also discussed.

It has been shown that the secondary variables of a problem can be computed using either the global algebraic equations of the finite element mesh (i.e., condensed equations for the secondary variables) or by their original definition through finite element interpolation.

The former method gives more accurate results, which will satisfy the equilibrium at inter-element nodes, whereas the latter gives less accurate results that are discontinuous at the nodes. The secondary variables computed using the linear elements are elementwise constant, while they are elementwise linear for the Lagrange quadratic elements. The magnitude of discontinuity can be reduced by refining the mesh (h or p refinement). The discontinuity of the secondary variables at nodes is due to the fact that the secondary variables are not made continuous across the elements.

In closing this chapter, the reader is reminded that the finite element method is a powerful tool for engineering analysis. The power of the method lies in transforming the traditional variational methods (e.g., Ritz, Galerkin, least-squares, and other weighted-residual methods) into a powerful computer-based technique by developing suitable approximation functions for complex problems. Without a good understanding of the method as well as the engineering background behind each problem, one is ill-equipped to analyze the problem.

PROBLEMS

Many of the following problems are designed for hand calculation while some are intended specifically for computer calculations using the program FEM1D (see Chapter 7 for details on how to use the program). The problem set should give the student deeper understanding of what is involved in the setting up of the finite element equations, imposition of boundary conditions, and identifying the condensed equations for the unknown primary and secondary variables of a given problem. When the number of equations to be solved is greater than three, the student should opt for a computer solution of the equations. The calculations can be verified, in most cases, by solving the same problem using FEM1D.

Discrete Elements

4.1 Consider the system of linear elastic springs shown in Fig. P4.1. Assemble the element equations to obtain the force-displacement relations for the entire system. Use the boundary conditions to write the condensed equations for the unknown displacements and forces.

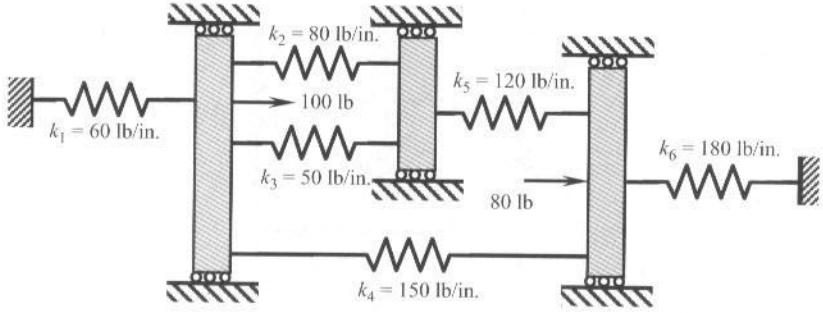

Figure P4.1

4.2 Repeat Problem 4.1 for the system of linear springs shown in Fig. P4.2.

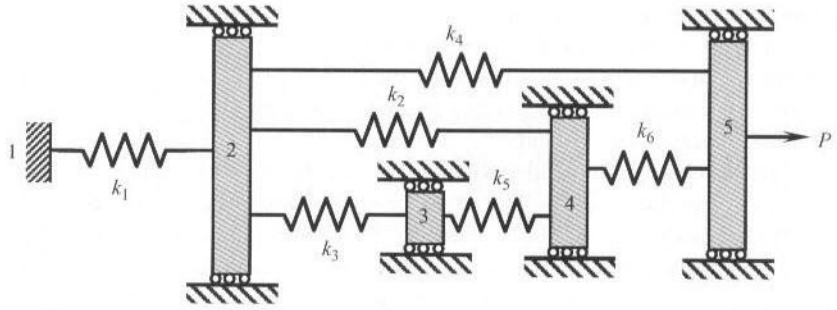

Figure P4.2

4.3 Consider the direct current electric network shown in Fig. P4.3. We wish to determine the voltages V and currents I in the network using the finite element method. Set up the algebraic equations (i.e., condensed equations) for the unknown voltages and currents.

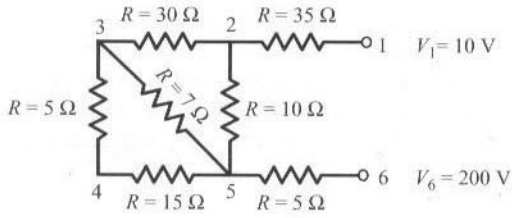

Figure P4.3

4.4 Repeat Problem 4.3 for the direct current electric network shown in Fig. P4.4.

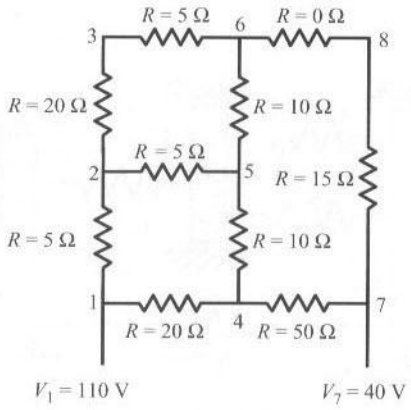

Figure P4.4

4.5 Write the condensed equations for the unknown pressures and flows (use the minimum number of elements) for the hydraulic pipe network shown in Fig. P4.5. *Answer:* $P_1 = \frac{39}{14}Qa$, $P_2 = \frac{12}{7}Qa$, and $P_3 = \frac{15}{14}Qa$.

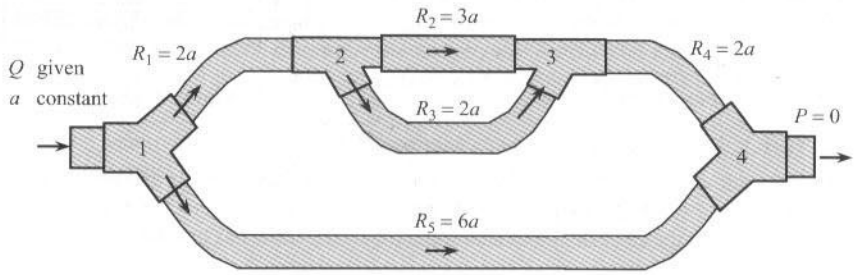

Figure P4.5

4.6 Consider the hydraulic pipe network (the flow is assumed to be laminar) shown in Fig. P4.6. Write the condensed equations for the unknown pressures and flows (use minimum number of elements.)

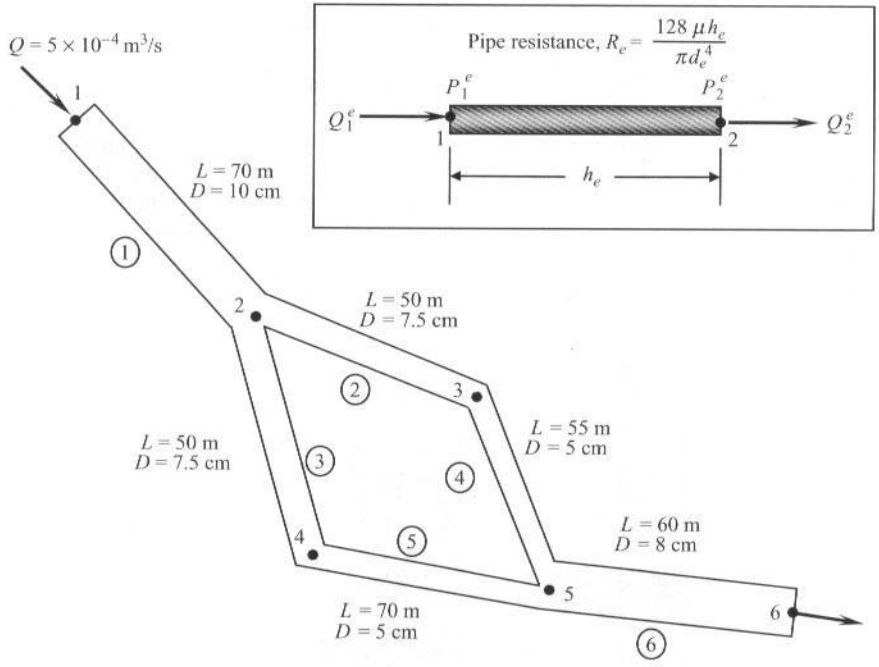

Figure P4.6

4.7 Determine the maximum shear stresses in the solid steel ($G_s = 12$ Msi) and aluminum ($G_a = 4$ Msi) shafts shown in Fig. P4.7.

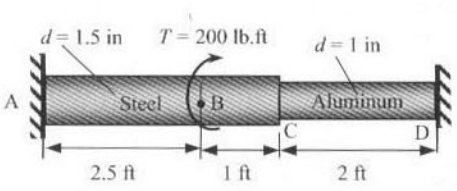

Figure P4.7

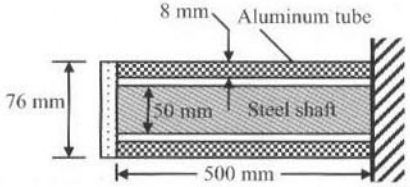

Figure P4.8

4.8 A steel shaft and an aluminum tube are connected to a fixed support and to a rigid disk, as shown in Fig. P4.8. If the torque applied at the end is equal to $T = 6,325$ N·m, determine the shear stresses in the steel shaft and aluminum tube. Use $G_s = 77$ GPa and $G_a = 27$ GPa.

Heat Transfer

4.9 Consider heat transfer in a plane wall of total thickness L. The left surface is maintained at temperature T_0 and the right surface is exposed to ambient temperature T_∞ with heat transfer coefficient β. Determine the temperature distribution in the wall and heat input at the left surface of the wall for the following data: $L = 0.1$ m, $k = 0.01$ W/(m · °C), $\beta = 25$ W/(m^2 · °C), $T_0 = 50$°C, and $T_\infty = 5$°C. Solve for nodal temperatures and the heat at the left wall using (*a*) two linear finite elements and (*b*) one quadratic element. *Answer:* (*a*) $U_2 = 27.59$°C, $U_3 = 5.179$°C, $Q_1^1 = 4.482$ W/m$^2 = -Q_2^2$.

4.10 An insulating wall is constructed of three homogeneous layers with conductivities k_1, k_2, and k_3 in intimate contact (see Fig. P4.10). Under steady-state conditions, the temperatures of the media in contact at the left and right surfaces of the wall are at ambient temperatures of T_∞^L and T_∞^R, respectively, and film coefficients β_L and β_R, respectively. Determine the temperatures on the left and right surfaces as well as at the interfaces. Assume that there is no internal heat generation and that the heat flow is one-dimensional ($\partial T/\partial y = 0$). *Answer:* $U_1 = 61.582$°C, $U_2 = 61.198$°C, $U_3 = 60.749$°C, $U_4 = 60.612$°C.

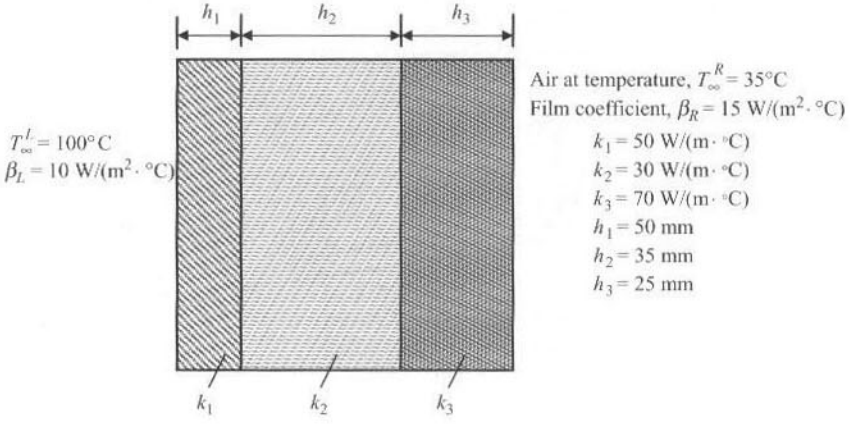

Figure P4.10

4.11 Rectangular fins are used to remove heat from the surface of a body by conduction along the fins and convection from the surface of the fins into the surroundings. The fins are 100 mm long, 5 mm wide, and 1 mm thick, and made of aluminum with thermal conductivity $k = 170$ W/(m · °C). The natural convection heat transfer coefficient associated with the surrounding air is $\beta = 35$ W/(m^2 · °C) and the ambient temperature is $T_\infty = 20$°C. Assuming that the heat transfer is one dimensional along the length of the fins and that the heat transfer in each fin is independent of the others, determine the temperature distribution along the fins and the heat removed from each fin by convection. Use (*a*) four linear elements, and (*b*) two quadratic elements.

4.12 Find the heat transfer per unit area through the composite wall shown in Fig. P4.12. Assume one-dimensional heat flow.

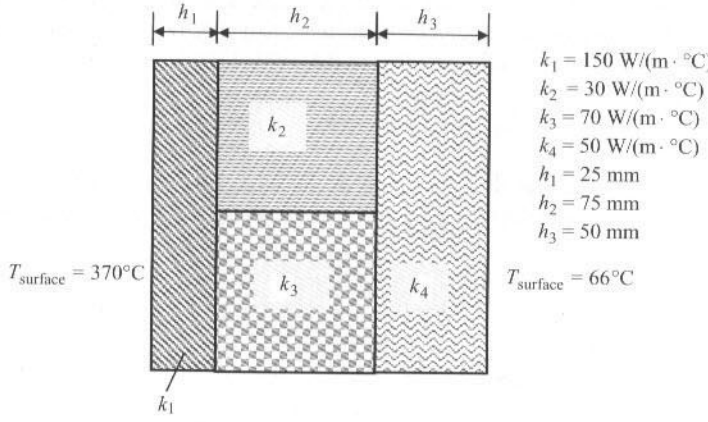

Figure P4.12

4.13 A steel rod of diameter $D = 2$ cm, length $L = 5$ cm, and thermal conductivity $k = 50$ W/(m·°C) is exposed to ambient air at $T_\infty = 20$°C with a heat transfer coefficient $\beta = 100$ W/(m^2·°C). If the left end of the rod is maintained at temperature $T_0 = 320$°C, determine the temperatures at distances 25 mm and 50 mm from the left end, and the heat at the left end. The governing equation of the problem is

$$-\frac{d^2\theta}{dx^2} + m^2\theta = 0 \quad \text{for} \quad 0 < x < L$$

where $\theta = T - T_\infty$, T is the temperature, and $m^2 = \beta P/Ak$. The boundary conditions are

$$\theta(0) = T(0) - T_\infty = 300\text{°C}, \qquad \left(\frac{d\theta}{dx} + \frac{\beta}{k}\theta\right)\bigg|_{x=L} = 0$$

Use (*a*) two linear elements and (*b*) one quadratic element to solve the problem by the finite element method. Compare the finite element nodal temperatures against the exact values. *Answer:* (*a*) $U_1 = 300$°C, $U_2 = 211.97$°C, $U_3 = 179.24$°C, $Q_1^1 = 3{,}521.1$ W/m^2. (*b*) $U_1 = 300$°C, $U_2 = 213.07$°C, $U_3 = 180.77$°C, $Q_1^1 = 4{,}569.9$ W/m^2.

4.14 Find the temperature distribution in the tapered fin shown in Fig. P4.14. Assume that the temperature at the root of the fin is 250°F, the conductivity $k = 120$ Btu/(h·ft·°F), and the film coefficient $\beta = 15$ Btu/(h·ft^2·°F); use three linear elements. The ambient temperature at the top and bottom of the fin is $T_\infty = 75$°F. *Answer:* T_1(tip) = 166.23°F, $T_2 = 191.1$°F, $T_3 = 218.89$°F.

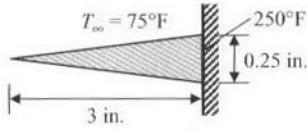

Figure P4.14

4.15 Consider steady heat conduction in a wire of circular cross section with an electrical heat source. Suppose that the radius of the wire is R_0, its electrical conductivity is K_e (Ω^{-1}/cm), and it is carrying an electric current density of I (A/cm^2). During the transmission of an electric current, some of the electrical energy is converted into thermal energy. The rate of heat production per unit volume is given by $q_e = I^2/K_e$. Assume that the temperature rise in the wire is sufficiently small that the dependence of the thermal or electric conductivity on temperature can be neglected. The governing equations of the problem are

$$-\frac{1}{r}\frac{d}{dr}\left(rk\frac{dT}{dr}\right) = q_e \quad \text{for} \quad 0 \le r \le R_0, \qquad \left(rk\frac{dT}{dr}\right)\bigg|_{r=0} = 0, \qquad T(R_0) = T_0$$

Determine the distribution of temperature in the wire using (*a*) two linear elements and (*b*) one quadratic element, and compare the finite element solution at eight equal intervals with the exact solution

$$T(r) = T_0 + \frac{q_e R_0^2}{4k}\left[1 - \left(\frac{r}{R_0}\right)\right]$$

Also, determine the heat flow, $Q = -2\pi R_0 k(dT/dr)|_{R_0}$, at the surface using (i) the temperature field and (ii) the balance equations.

4.16 Consider a nuclear fuel element of spherical form, consisting of a sphere of "fissionable" material surrounded by a spherical shell of aluminum "cladding" as shown in Fig. P4.16. Nuclear fission is a source of thermal energy, which varies nonuniformly from the center of the sphere to the interface of the fuel element and the cladding. We wish to determine the temperature distribution in the nuclear fuel element and the aluminum cladding.

The governing equations for the two regions are the same, with the exception that there is no heat source term for the aluminum cladding. We have

$$-\frac{1}{r^2}\frac{d}{dr}\left(r^2 k_1 \frac{dT_1}{dr}\right) = q \quad \text{for} \quad 0 \le r \le R_F$$

$$-\frac{1}{r^2}\frac{d}{dr}\left(r^2 k_2 \frac{dT_2}{dr}\right) = 0 \quad \text{for} \quad R_F \le r \le R_C$$

where subscripts 1 and 2 refer to the nuclear fuel element and cladding, respectively. The heat generation in the nuclear fuel element is assumed to be of the form

$$q_1 = q_0\left[1 + c\left(\frac{r}{R_F}\right)^2\right]$$

where q_0 and c are constants depending on the nuclear material. The boundary conditions are

$$kr^2\frac{dT_1}{dr} = 0 \quad \text{at} \quad r = 0$$

$$T_1 = T_2 \quad \text{at} \quad r = R_F, \quad \text{and} \quad T_2 = T_0 \quad \text{at} \quad r = R_C$$

Use two linear elements to determine the finite element solution for the temperature distribution, and compare the nodal temperatures with the exact solution

$$T_1 - T_0 = \frac{q_0 R_F^2}{6k_1}\left\{\left[1-\left(\frac{r}{R_F}\right)^2\right]+\frac{3}{10}c\left[1-\left(\frac{r}{R_F}\right)^4\right]\right\}+\frac{q_0 R_F^2}{3k_2}\left(1+\frac{3}{5}c\right)\left(1-\frac{R_F}{R_C}\right)$$

$$T_2 - T_0 = \frac{q_0 R_F^2}{3k_2}\left(1+\frac{3}{5}c\right)\left(\frac{R_F}{r}-\frac{R_F}{R_C}\right)$$

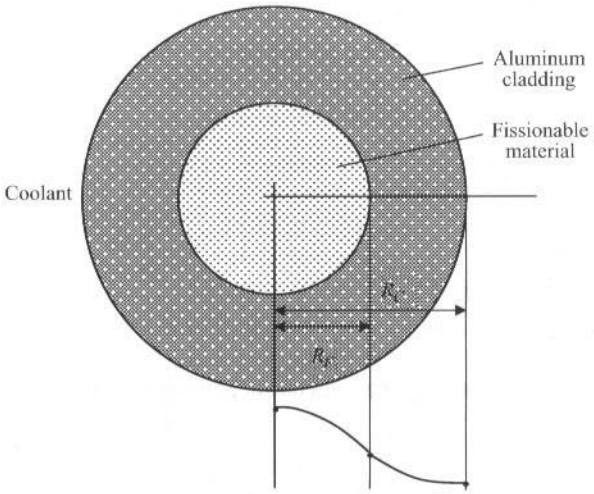

Figure P4.16

Fluid Mechanics

4.17 Consider the flow of a Newtonian viscous fluid on an inclined flat surface, as shown in Fig. P4.17. Examples of such flow can be found in wetted-wall towers and the application of coatings to wallpaper rolls. The momentum equation, for a fully developed steady laminar flow along the z coordinate, is given by

$$-\mu\frac{d^2w}{dx^2} = \rho g\cos\beta$$

where w is the z component of the velocity, μ is the viscosity of the fluid, ρ is the density, g is the acceleration due to gravity, and β is the angle between the inclined surface and the vertical.

The boundary conditions associated with the problem are that the shear stress is zero at $x = 0$ and the velocity is zero at $x = L$:

$$\left(\frac{dw}{dx}\right)\Big|_{x=0} = 0, \quad w(L) = 0$$

Use (a) two linear finite elements of equal length and (b) one quadratic finite element in the domain (0, L) to solve the problem and compare the two finite element solutions at four points

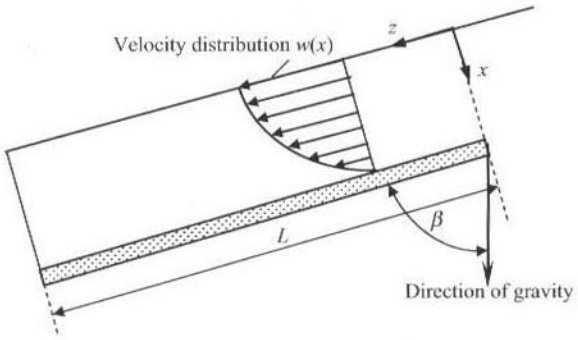

Figure P4.17

$x = 0$, $\frac{1}{4}L$, $\frac{1}{2}L$, and $\frac{3}{4}L$ of the domain with the exact solution

$$w_e = \frac{\rho g L^2 \cos\beta}{2\mu}\left[1 - \left(\frac{x}{L}\right)^2\right]$$

Evaluate the shear stress ($\tau_{xz} = -\mu\, dw/dx$) at the wall using (i) the velocity fields and (ii) the equilibrium equations, and compare with the exact value. *Answer:* (*a*) $U_1 = \frac{1}{2}f_0$, $U_2 = \frac{3}{8}f_0$, $f_0 = (\rho g \cos\beta)L^2/\mu$.

4.18 Consider the steady laminar flow of a viscous fluid through a long circular cylindrical tube. The governing equation is

$$-\frac{1}{r}\frac{d}{dr}\left(r\mu\frac{dw}{dr}\right) = \frac{P_0 - P_L}{L} \equiv f_0$$

where w is the axial (i.e., z) component of velocity, μ is the viscosity, and f_0 is the gradient of pressure (which includes the combined effect of static pressure and gravitational force). The boundary conditions are

$$\left(r\frac{dw}{dr}\right)\bigg|_{r=0} = 0, \quad w(R_0) = 0$$

Using the symmetry and (*a*) two linear elements and (*b*) one quadratic element, determine the velocity field and compare with the exact solution at the nodes:

$$w_e(r) = \frac{f_0 R_0^2}{4\mu}\left[1 - \left(\frac{r}{R_0}\right)^2\right]$$

4.19 In the problem of the flow of a viscous fluid through a circular cylinder (Problem 4.18), assume that the fluid slips at the cylinder wall; i.e., instead of assuming that $w = 0$ at $r = R_0$, use the boundary condition that

$$kw = -\mu\frac{dw}{dr} \quad \text{at} \quad r = R_0$$

in which k is the "coefficient of sliding friction." Solve the problem with two linear elements.

4.20 Consider the steady laminar flow of a Newtonian fluid with constant density in a long annular region between two coaxial cylinders of radii R_i and R_0 (see Fig. P4.20). The differential

equation for this case is given by

$$-\frac{1}{r}\frac{d}{dr}\left(r\mu\frac{dw}{dr}\right)=\frac{P_1-P_2}{L}\equiv f_0$$

where w is the velocity along the cylinders (i.e., the z component of velocity), μ is the viscosity, L is the length of the region along the cylinders in which the flow is fully developed, and P_1 and P_2 are the pressures at $z=0$ and $z=L$, respectively (P_1 and P_2 represent the combined effect of static pressure and gravitational force).

The boundary conditions are

$$w=0 \quad \text{at} \quad r=R_0 \quad \text{and} \quad R_i$$

Solve the problem using (*a*) two linear elements and (*b*) one quadratic element, and compare the finite element solutions with the exact solution at the nodes:

$$w_e(r)=\frac{f_0R_0^2}{4\mu}\left[1-\left(\frac{r}{R_0}\right)^2+\frac{1-k^2}{\ln(1/k)}\ln\left(\frac{r}{R_0}\right)\right]$$

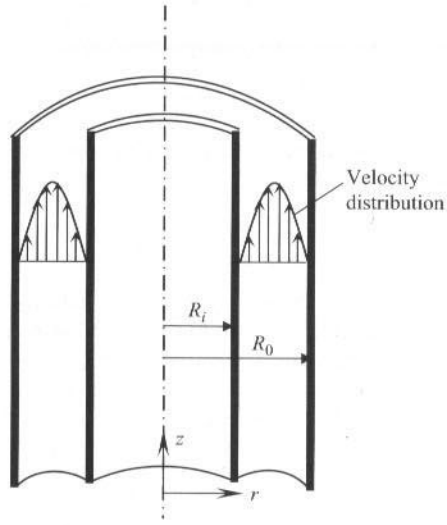

Figure P4.20

where $k=R_i/R_0$. Determine the shear stress $\tau_{rz}=-\mu\,dw/dr$ at the walls using (i) the velocity field and (ii) the equilibrium equations, and compare with the exact values. (Note that the steady laminar flow of a viscous fluid through a long cylinder or a circular tube can be obtained as a limiting case of $k\to 0$.)

4.21 Consider the steady laminar flow of two immiscible incompressible fluids in a region between two parallel stationary plates under the influence of a pressure gradient. The fluid rates are adjusted such that the lower half of the region is filled with fluid I (the denser and more viscous fluid) and the upper half is filled with fluid II (the less dense and less viscous fluid), as shown in Fig. P4.21. We wish to determine the velocity distributions in each region using the finite element method.

The governing equations for the two fluids are

$$-\mu_1 \frac{d^2u_1}{dx^2} = f_0, \quad -\mu_2 \frac{d^2u_2}{dx^2} = f_0$$

where $f_0 = (P_0 - P_L)/L$ is the pressure gradient. The boundary conditions are

$$u_1(-b) = 0 \quad u_2(b) = 0, \quad u_1(0) = u_2(0)$$

Solve the problem using four linear elements, and compare the finite element solutions with the exact solution at the nodes

$$u_i = \frac{f_0 b^2}{2\mu_i}\left[\frac{2\mu_i}{\mu_1 + \mu_2} + \frac{\mu_1 - \mu_2}{\mu_1 + \mu_2}\frac{y}{b} - \left(\frac{y}{b}\right)^2\right] \quad (i = 1, 2)$$

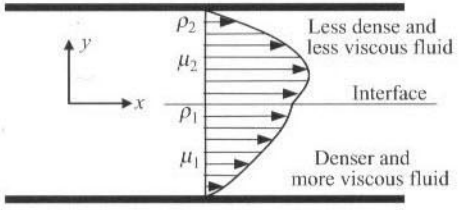

Figure P4.21

4.22 The governing equation for an unconfined aquifer with flow in the radial direction is given by the differential equation

$$-\frac{1}{r}\frac{d}{dr}\left(rk\frac{du}{dr}\right) = f$$

where k is the coefficient of permeability, f the recharge, and u the piezometric head. Pumping is considered to be a negative recharge. Consider the following problem. A well penetrates an aquifer and pumping is performed at $r = 0$ at a rate $Q = 150$ m^3/h. The permeability of the aquifer is $k = 25$ m^3/h. A constant head $u_0 = 50$ m exists at a radial distance $L = 200$ m. Determine the piezometric head at radial distances of 0, 10, 20, 40, 80, and 140 m (see Fig. P4.22). You are required to set up the finite element equations for the unknowns using a nonuniform mesh of six linear elements.

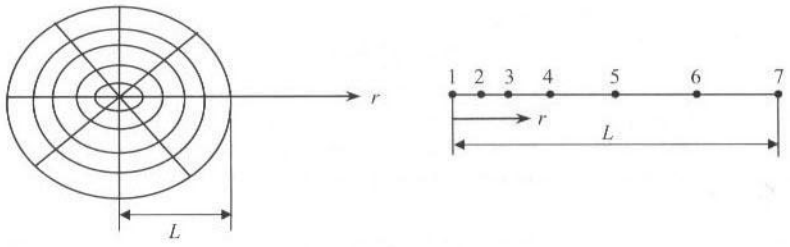

Figure P4.22

4.23 Consider a slow, laminar flow of a viscous substance (for example, glycerin solution) through a narrow channel under controlled pressure drop of 150 Pa/m. The channel is 5 m long (flow

direction), 10 cm high, and 50 cm wide. The upper wall of the channel is maintained at 50°C while the lower wall is maintained at 25°C. The viscosity and density of the substance are temperature dependent, as given in Table P4.23. Assuming that the flow is essentially one dimensional (justified by the dimensions of the channel), determine the velocity field and mass flow rate of the fluid through the channel.

Table P4.23: Properties of the viscous substance of Problem 4.23.

y (m)	Temp. (°C)	Viscosity [kg/(m· s)]	Density (kg/m^3)
0.00	50	0.10	1233
0.02	45	0.12	1238
0.04	40	0.20	1243
0.06	35	0.28	1247
0.08	30	0.40	1250
0.10	25	0.65	1253

Solid and Structural Mechanics

4.24 The equation governing the axial deformation of an elastic bar in the presence of applied mechanical loads f and P and a temperature change T is

$$-\frac{d}{dx}\left[EA\left(\frac{du}{dx}-\alpha T\right)\right]=f \quad \text{for} \quad 0<x<L$$

where α is the thermal expansion coefficient, E the modulus of elasticity, and A the cross-sectional area. Using three linear finite elements, determine the axial displacements in a nonuniform rod of length 30 in., fixed at the left end and subjected to an axial force P = 400 lb and a temperature change of 60°F. Take $A(x)=6-\frac{1}{10}x$ in.^{2} $E=30\times10^6$ lb/in.^{2}, and $\alpha=12\times10^{-6}$/(in. ·°F).

4.25 Find the stresses and compressions in each section of the composite member shown in Fig. P4.25. Use $E_s=30\times10^6$ psi, $E_a=10^7$ psi, $E_b=15\times10^6$ psi, and the minimum number of linear elements.

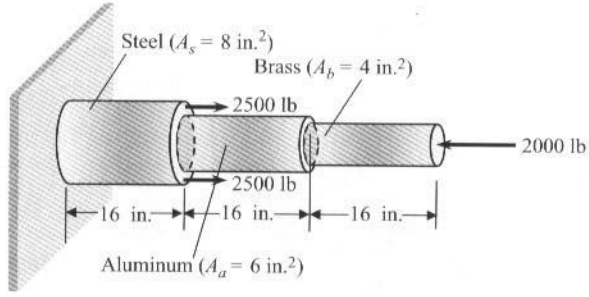

Figure P4.25

4.26 Find the three-element finite element solution to the stepped-bar problem. See Fig. P4.26 for the geometry and data. *Hint:* Solve the problem to see if the end displacement exceeds the gap. If it does, resolve the problem with modified boundary condition at $x=24$ in.

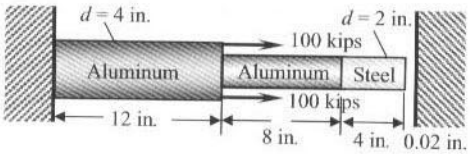

Steel, $E_s = 30 \times 10^6$ psi, Aluminum, $E_a = 10 \times 10^6$ psi

Figure P4.26

4.27 Analyze the stepped bar with its right end supported by a linear axial spring (see Fig. P4.27). The boundary condition at $x = 24$ in. is

$$EA\frac{du}{dx} + ku = 0$$

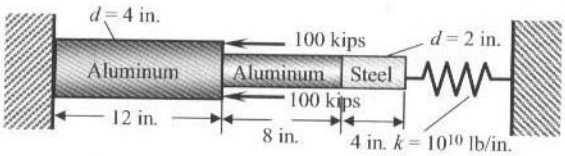

Steel, $E_s = 30 \times 10^6$ psi, Aluminum, $E_a = 10 \times 10^6$ psi

Figure P4.27

4.28 A solid circular brass cylinder ($E_b = 15 \times 10^6$ psi, $d_b = 0.25$ in.) is encased in a hollow circular steel ($E_s = 30 \times 10^6$ psi, $d_s = 0.21$ in). A load of $P = 1330$ lb compresses the assembly, as shown in Fig. P4.28. Determine (a) the compression, and (b) compressive forces and stresses in the steel shell and brass cylinder. Use the minimum number of linear finite elements. Assume that the Poisson effect is negligible.

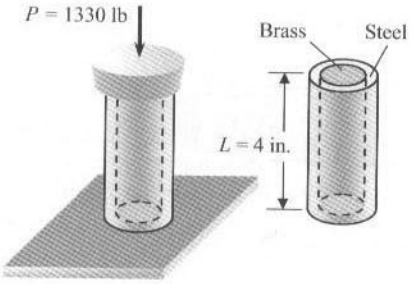

Figure P4.28

4.29 A rectangular steel bar ($E_s = 30 \times 10^6$ psi) of length 24 in. has a slot in the middle half of its length, as shown in Fig. 4.29. Determine the displacement of the ends due to the axial loads $P = 2000$ lb. Use the minimum number of linear elements.

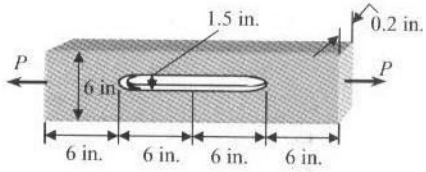

Figure P4.29

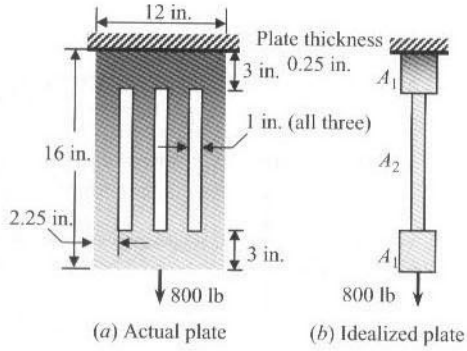

Figure P4.30

4.30 Repeat Problem 4.29 for the steel bar shown in Fig. P4.30.

4.31 The aluminum and steel pipes shown in Fig. P4.31 are fastened to rigid supports at ends A and B and to a rigid plate C at their junction. Determine the displacement of point C and stresses in the aluminum and steel pipes. Use the minimum number of linear finite elements.

4.32 A steel bar ABC is pin-supported at its upper end A to an immovable wall and loaded by a force F_1 at its lower end C, as shown in Fig. P4.32. A rigid horizontal beam BDE is pinned to the vertical bar at B, supported at point D, and carries a load F_2 at end E. Determine the displacements u_B and u_C at points B and C.

4.33 Repeat Problem 4.32 when point C is supported vertically by a spring ($k = 1000$ lb/in.).

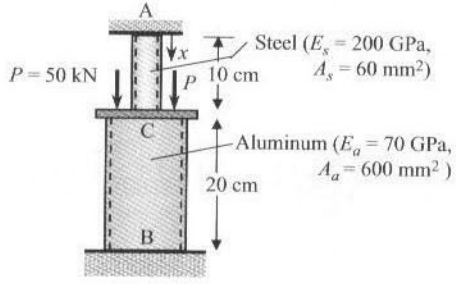

Figure P4.31

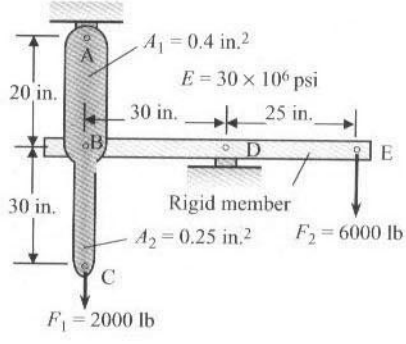

Figure P4.32

4.34 Consider the steel column (a typical column in a multi-storey building structure) shown in Fig. P4.34. The loads shown are due to the loads of different floors. The modulus of elasticity is $E = 30 \times 10^6$ psi and cross-sectional area of the column is $A = 40$ in^2. Determine the vertical displacements and axial stresses in the column at various floor-column connection points.

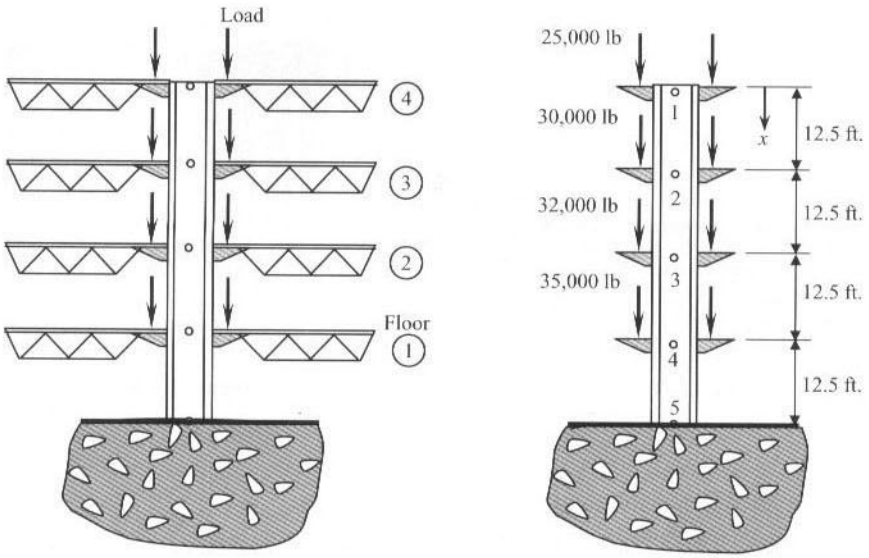

Figure P4.34

4.35 The bending moment (M) and transverse deflection (w) in a beam according to the Euler-Bernoulli beam theory are related by

$$-EI\frac{d^2w}{dx^2} = M(x)$$

For statically determinate beams, we can readily obtain the expression for the bending moment in terms of the applied loads. Thus, $M(x)$ is a known function of x. Determine the maximum deflection of the simply supported beam under uniform load (see Fig. P4.35) using the finite element method.

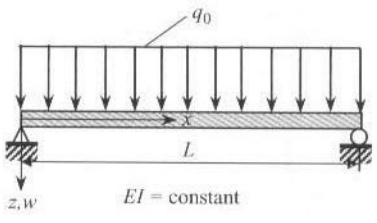

Figure P4.35

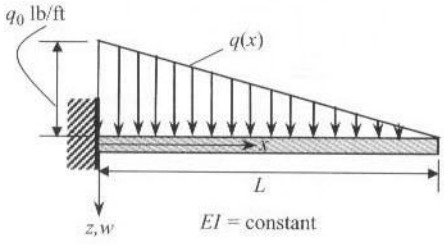

Figure P4.36

4.36 Repeat Problem 4.35 for the cantilever beam shown in Fig. P4.36.

4.37 Turbine disks are often thick near their hub and taper down to a smaller thickness at the periphery. The equation governing a variable-thickness $t = t(r)$ disk is

$$\frac{d}{dr}(rt\sigma_r) - t\sigma_\theta + t\rho\omega^2 r^2 = 0$$

where ω^2 is the angular speed of the disk and

$$\sigma_r = c\left(\frac{du}{dr} + \nu\frac{u}{r}\right), \quad \sigma_\theta = c\left(\frac{u}{r} + \nu\frac{du}{dr}\right), \quad c = \frac{E}{1-\nu^2}$$

(*a*) Construct the weak integral form of the governing equation such that the bilinear form is symmetric and the natural boundary condition involves specifying the quantity $tr\sigma_r$.

(*b*) Develop the finite element model associated with the weak form derived in part (*a*).

4.38–4.44 For the plane truss structures shown in Figs. P4.38–P4.44, give (*a*) the transformed element matrices, (*b*) the assembled element matrices, and (*c*) the condensed matrix equations for the unknown displacements and forces.

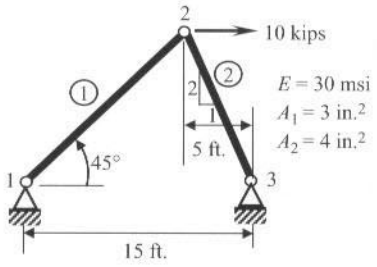

Figure P4.38

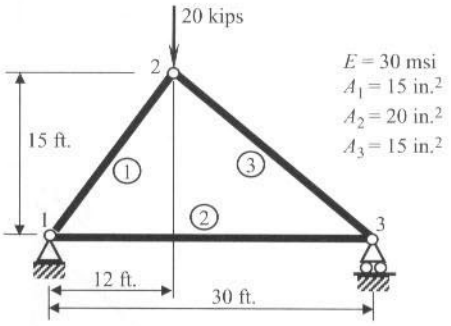

Figure P4.39

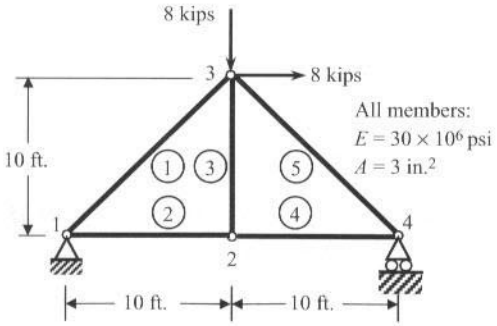

Figure P4.40

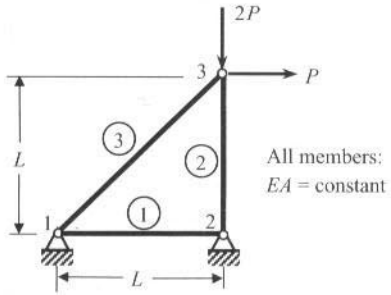

Figure P4.41

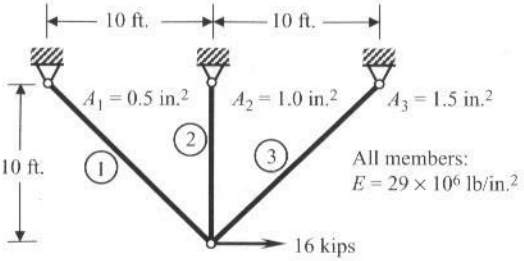

Figure P4.42

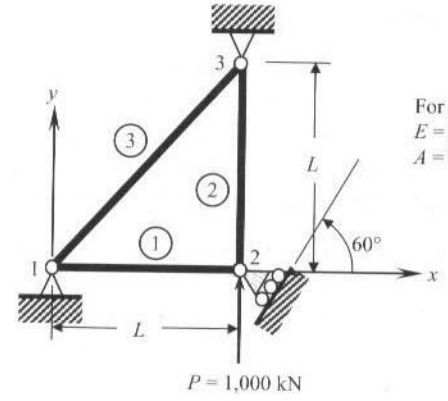

Figure P4.43

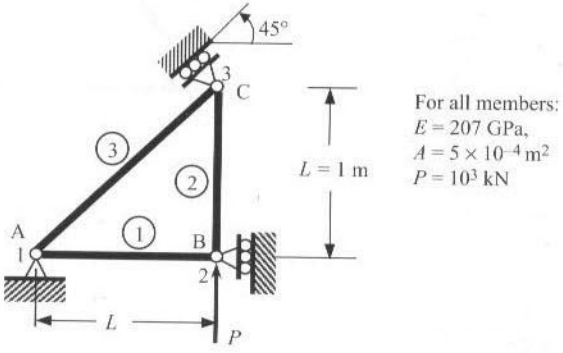

Figure P4.44

4.45 Determine the forces and elongations of each bar in the structure shown in Fig. P4.45. Also, determine the vertical displacements of points A and D.

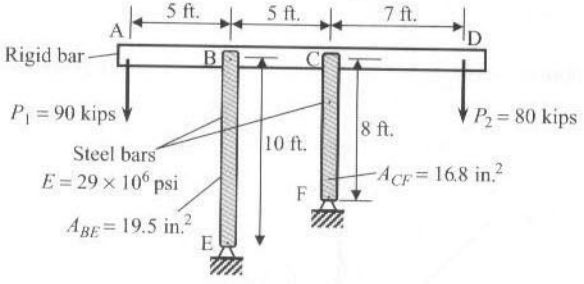

Figure P4.45

4.46 Determine the forces and elongations of each bar in the structure shown in Fig. P4.45 when end A is pinned to a rigid wall (and P_1 is removed).

REFERENCES FOR ADDITIONAL READING

1. Bird, R. B., Stewart, W. E. and Lightfoot, E. N., *Transport Phenomena*, John Wiley, New York, 1960.
2. Holman, J. P., *Heat Transfer*, 7th ed., McGraw-Hill, New York, 1990.
3. Kreith, F. and Bohn, M. S., *Principles of Heat Transfer*, 5th ed., West Publishing Company, St. Paul, MN, 1993.
4. Özisik, M. N., *Heat Conduction*, 2nd Ed., John Wiley, New York, 1993.
5. Reddy, J. N., *Energy Principles and Variational Methods in Applied Mechanics*, 2nd ed., John Wiley, New York, 2002.
6. Reddy, J. N. and Gartling, D. K., *The Finite Element Method in Heat Transfer and Fluid Dynamics*, 2nd ed, CRC Press, Boca Raton, FL, 2001.
7. Slaughter, W. S., *The Linearized Theory of Elasticity*, Birkhäuser, Boston, 2002.
8. Schlichting, H., *Boundary Layer Theory* (translated by J. Kestin), 7th ed., McGraw-Hill, New York (1979).
9. Timenshenko, S. P. and Goodier, J. N., *Theory of Elasticity*, McGraw-Hill, New York, 1970.

Chapter 5
BEAMS AND FRAMES

5.1 INTRODUCTION

Here we consider the finite element formulation of the one-dimensional fourth-order differential equation that arises in the Euler–Bernoulli beam theory and the pair of one-dimensional second-order equations associated with the Timoshenko beam theory. The superposition of the beam and bar elements give rise to frame elements that can be used to analyze plane frame structures. The formulations of a fourth-order equation as well as coupled second-order equations (see Problems 3.1 and 3.3) involve the same steps as described in Section 3.2 for a second-order equation, but the mathematical details are somewhat different, especially in the finite element formulation of the equations.

5.2 EULER–BERNOULLI BEAM ELEMENT

5.2.1 Governing Equation

In the Euler-Bernoulli beam theory, it is assumed that plane cross sections perpendicular to the axis of the beam remain plane and perpendicular to the axis after deformation. In this theory, the transverse deflection w of the beam is governed by the fourth-order differential equation

$$\frac{d^2}{dx^2}\left(EI\frac{d^2w}{dx^2}\right)+c_f w=q(x) \quad \text{for} \quad 0<x<L \tag{5.2.1}$$

where $EI=E(x)I(x)$, $c_f=c_f(x)$, $q=q(x)$ are given functions of x (i.e., data), and w is the dependent variable; E denotes the modulus of elasticity, I the second moment of area about the y axis of the beam, q is the distributed transverse load, c_f the elastic foundation modulus (if any), and w is the transverse deflection of the beam. The sign convention used in the derivation of (5.2.1) is shown in Fig. 5.2.1. In addition to satisfying the differential equation (5.2.1), w must also satisfy appropriate boundary conditions; since the equation is of fourth order, four boundary conditions are needed to solve it. The weak formulation of the equation will provide the form of these four boundary conditions. A step-by-step procedure for the finite element analysis of (5.2.1) is presented next (see Example 2.4.2).

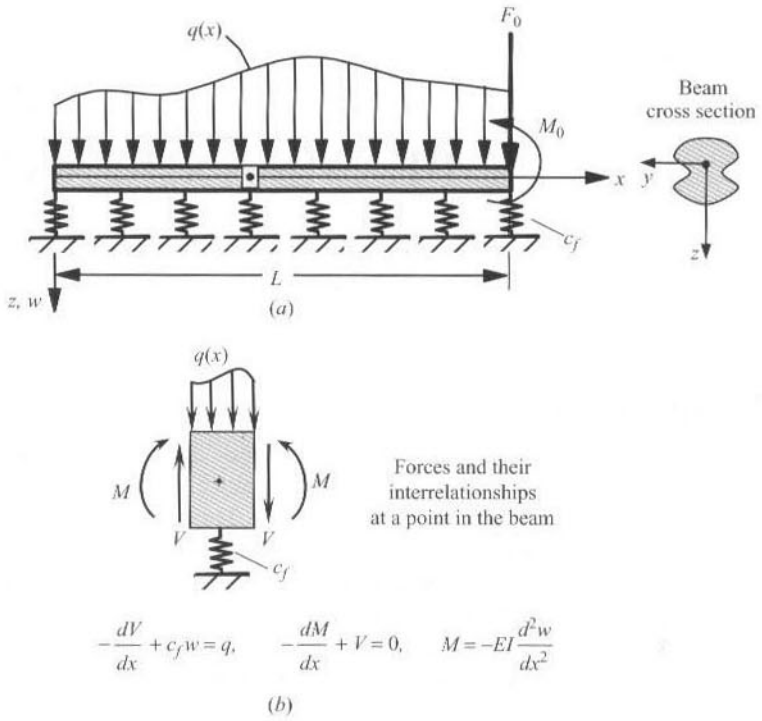

Figure 5.2.1 (*a*) Typical beam with distributed load $q(x)$ and point force F_0 and moment M_0. (*b*) The shear force-bending moment-deflection relations and the sign convention.

5.2.2 Discretization of the Domain

The domain $\Omega_e = (x_a, x_b) = (x_e, x_{e+1})$ of the straight beam [see Fig. 5.2.2(*a*)] is divided into a set of N line elements, each element having at least the two end nodes [see Fig. 5.2.2(*b*)]. Although the element is geometrically the same as that used for bars, the number and form of the primary and secondary unknowns at each node are dictated by the variational formulation of the differential equation (5.2.1). In most practical problems, the discretization of a given structure into a minimum number of elements is often dictated by the geometry, loading, and material properties.

5.2.3 Derivation of Element Equations

We isolate a typical element $\Omega_e = (x_e, x_{e+1})$ [see Fig. 5.2.2(*b*)] and construct the weak form of (5.2.1) over the element. The variational formulation provides the primary and secondary variables of the problem. Then suitable approximations for the primary variables are selected, interpolation functions are developed, and the element equations are derived.

Weak Form. The weak forms of problems in solid mechanics can be developed either from the principle of virtual work (i.e., the principle of virtual displacements or virtual forces) or from the governing differential equations. Here we start with a given differential equation and use the three-step procedure to obtain the weak form. Following the three-step procedure

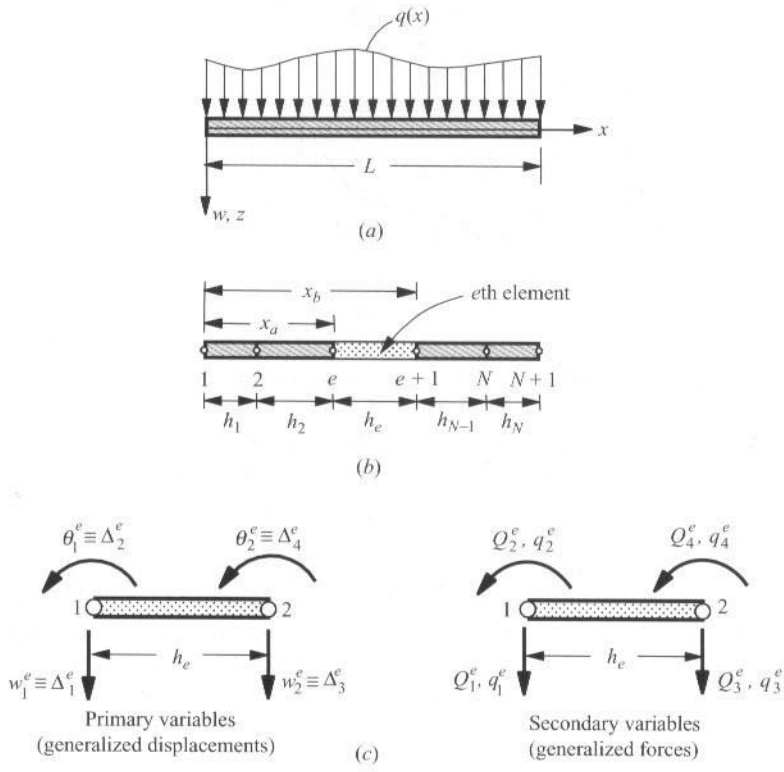

Figure 5.2.2 (*a*) Geometry and loads on a beam. (*b*) Finite element discretization. (*c*) Generalized displacements and generalized forces on a typical element.

illustrated in Chapter 2 (see Example 2.4.2) and revisited in Section 3.2.3, we write

$$
\begin{aligned}
0 &= \int_{x_e}^{x_{e+1}} v\left[\frac{d^2}{dx^2}\left(EI\frac{d^2w}{dx^2}\right) + c_f w - q\right] dx \\
&= \int_{x_e}^{x_{e+1}} \left[-\frac{dv}{dx}\frac{d}{dx}\left(EI\frac{d^2w}{dx^2}\right) + c_f vw - vq\right] dx + \left[v\frac{d}{dx}\left(EI\frac{d^2w}{dx^2}\right)\right]_{x_e}^{x_{e+1}} \\
&= \int_{x_e}^{x_{e+1}} \left(EI\frac{d^2v}{dx^2}\frac{d^2w}{dx^2} + c_f vw - vq\right) dx + \left[v\frac{d}{dx}\left(EI\frac{d^2w}{dx^2}\right) - \frac{dv}{dx}EI\frac{d^2w}{dx^2}\right]_{x_e}^{x_{e+1}}
\end{aligned}
\tag{5.2.2}
$$

where $v(x)$ is a weight function that is twice differentiable with respect to x. Note that, in the present case, the first term of the equation is integrated twice by parts, to yield two differentiations to the weight function v while retaining two derivatives of the dependent variable, w; the result is that the differentiation is distributed equally between the weight function v and the dependent variable w. Because of the two integration by parts, there appear two boundary expressions (see Example 2.4.2), which are to be evaluated at the two boundary points

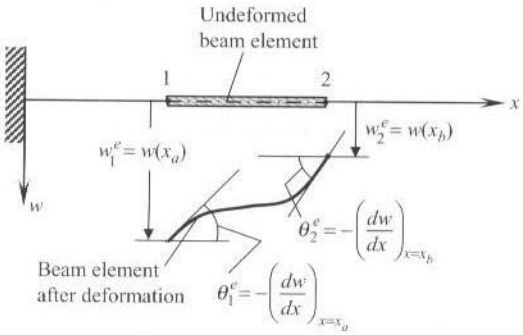

Figure 5.2.3 Deformation of a beam element.

$x = x_a = x_e$ and $x = x_b = x_{e+1}$. Examination of the boundary terms indicates that the essential boundary conditions involve the specification of the deflection w and slope dw/dx, and the natural boundary conditions involve the specification of the bending moment $EI\,d^2w/dx^2$ and shear force $(d/dx)(EI\,d^2w/dx^2)$ at the endpoints of the element. Thus, there are two essential boundary conditions and two natural boundary conditions; therefore, we must identify w and dw/dx as the primary variables at each node (so that the essential boundary conditions are included in the interpolation). The natural boundary conditions always remain in the weak form and end up on the right-hand side, $\{F^e\}$, of the matrix equation.

We introduce the following notation for the secondary variables that is consistent with the sign convention in Fig. 5.2.1(b) ($\theta = -dw/dx$; see Fig. 5.2.3):

$$\begin{aligned}
Q_1^e &\equiv \left[\frac{d}{dx}\left(EI\frac{d^2w}{dx^2}\right)\right]\Bigg|_{x_e} = -V(x_e)\\
Q_2^e &\equiv \left(EI\frac{d^2w}{dx^2}\right)\Bigg|_{x_e} = -M(x_e)\\
Q_3^e &\equiv -\left[\frac{d}{dx}\left(EI\frac{d^2w}{dx^2}\right)\right]\Bigg|_{x_{e+1}} = V(x_{e+1})\\
Q_4^e &\equiv -\left(EI\frac{d^2w}{dx^2}\right)\Bigg|_{x_{e+1}} = M(x_{e+1})
\end{aligned} \tag{5.2.3}$$

where Q_1^e and Q_3^e denote the shear forces, and Q_2^e and Q_4^e denote the bending moments [see Fig. 5.2.2c]. The set $\{Q_1^e, Q_2^e, Q_3^e, Q_4^e\}$ is often referred to as the *generalized forces*. The corresponding displacements and rotations are called the *generalized displacements*.

With the notation in (5.2.3), the weak form (5.2.2) can be expressed as

$$\begin{aligned}
0 &= \int_{x_e}^{x_{e+1}} \left(EI\frac{d^2v}{dx^2}\frac{d^2w}{dx^2} + c_f vw - vq\right) dx\\
&\quad - v(x_e)Q_1^e - \left(-\frac{dv}{dx}\right)\Bigg|_{x_e} Q_2^e - v(x_{e+1})Q_3^e - \left(-\frac{dv}{dx}\right)\Bigg|_{x_{e+1}} Q_4^e\\
&\equiv B(v, w) - l(v)
\end{aligned} \tag{5.2.4}$$

We can identify the bilinear and linear forms of the problem as

$$B(v,w)=\int_{x_e}^{x_{e+1}}\left(EI\frac{d^2v}{dx^2}\frac{d^2w}{dx^2}+c_f vw\right)dx$$

$$l(v)=\int_{x_e}^{x_{e+1}} vq\,dx+v(x_e)Q_1^e+\left(-\frac{dv}{dx}\right)\Big|_{x_e}Q_2^e \tag{5.2.5}$$

$$+v(x_{e+1})Q_3^e+\left(-\frac{dv}{dx}\right)\Big|_{x_{e+1}}Q_4^e$$

Equation (5.2.4) is a statement of the principle of virtual displacements (where v denotes virtual displacement δw) for the Euler–Bernoulli beam theory. The quadratic functional, known as the *total potential energy* of the isolated beam element, is given by [see Eq. (2.4.31)]

$$\Pi_e(w)=\int_{x_e}^{x_{e+1}}\left[\frac{EI}{2}\left(\frac{d^2w}{dx^2}\right)^2+\frac{1}{2}c_f w^2-wq\right]dx-w(x_e)Q_1^e-w(x_{e+1})Q_3^e$$

$$-\left(-\frac{dw}{dx}\right)\Big|_{x_e}Q_2^e-\left(-\frac{dw}{dx}\right)\Big|_{x_{e+1}}Q_4^e \tag{5.2.6}$$

The first term in the square brackets represents the elastic strain energy due to bending, the second is the strain energy stored in the elastic foundation, and the third is the work done by the distributed load; the remaining terms account for the work done by the generalized forces Q_i^e in moving through the respective generalized displacements of the element. Conversely, we may go from the total potential energy functional (5.2.6) to the weak form (5.2.4) by using the principle of minimum potential energy, $\delta\Pi^e=0$.

Interpolation Functions. The variational form (5.2.4) requires that the interpolation functions of an element be continuous with nonzero derivatives up to order two. The approximation $w_h^e(x)$ of $w(x)$ over a finite element should be such that it is twice differentiable and satisfies the interpolation properties, i.e., satisfies the following essential "boundary conditions" of the element [see Fig. 5.2.2(*c*)]:

$$w_h^e(x_e)=w_1^e,\quad w_h^e(x_{e+1})=w_2^e,\quad \theta_h^e(x_e)=\theta_1^e,\quad \theta_h^e(x_{e+1})=\theta_2^e \tag{5.2.7}$$

In satisfying the essential boundary conditions (5.2.7), the approximation automatically satisfies the continuity conditions. Hence, we pay attention to the satisfaction of (5.2.7), which forms the basis for the derivation of the interpolation functions of the Euler–Bernoulli beam element.

Since there are a total of four conditions in an element (two per node), a four-parameter polynomial must be selected for w_h^e:

$$w(x)\approx w_h^e(x)=c_1^e+c_2^e x+c_3^e x^2+c_4^e x^3 \tag{5.2.8}$$

Note that the continuity conditions (i.e., the existence of a nonzero second derivative of w_h^e in the element) are automatically met. The next step involves expressing c_i^e in terms of the primary nodal variables (i.e., generalized displacements)

$$\Delta_1^e\equiv w_h^e(x_e),\quad \Delta_2^e\equiv-\frac{dw_h^e}{dx}\Big|_{x=x_e},\quad \Delta_3^e\equiv w_h^e(x_{e+1}),\quad \Delta_4^e\equiv-\frac{dw_h^e}{dx}\Big|_{x=x_{e+1}}$$

such that the conditions (5.2.7) are satisfied:

$$\begin{aligned}
\Delta_1^e &= w_h^e(x_e) && = c_1^e + c_2^e x_e + c_3^e x_e^2 + c_4^e x_e^3 \\
\Delta_2^e &= -\left.\frac{dw_h^e}{dx}\right|_{x=x_e} && = -c_2^e - 2c_3^e x_e - 3c_4^e x_e \\
\Delta_3^e &= w_h^e(x_{e+1}) && = c_1^e + c_2^e x_{e+1} + c_3^e x_{e+1}^2 + c_4^e x_{e+1}^3 \\
\Delta_4^e &= -\left.\frac{dw_h^e}{dx}\right|_{x=x_{e+1}} && = -c_2^e - 2c_3^e x_{e+1} - 3c_4^e x_{e+1}
\end{aligned}$$

or

$$\begin{Bmatrix} \Delta_1^e \\ \Delta_2^e \\ \Delta_3^e \\ \Delta_4^e \end{Bmatrix} = \begin{bmatrix} 1 & x_e & x_e^2 & x_e^3 \\ 0 & -1 & -2x_e & -3x_e^2 \\ 1 & x_{e+1} & x_{e+1}^2 & x_{e+1}^3 \\ 0 & -1 & -2x_{e+1} & -3x_{e+1}^2 \end{bmatrix} \begin{Bmatrix} c_1^e \\ c_2^e \\ c_3^e \\ c_4^e \end{Bmatrix} \tag{5.2.9}$$

Inverting this matrix equation to express c_i^e in terms of Δ_1^e, Δ_2^e, Δ_3^e, and Δ_4^e, and substituting the result into (5.2.8), we obtain

$$w_h^e(x) = \Delta_1^e \phi_1^e + \Delta_2^e \phi_2^e + \Delta_3^e \phi_3^e + \Delta_4^e \phi_4^e = \sum_{j=1}^{4} \Delta_j^e \phi_j^e \tag{5.2.10}$$

where (with $x_{e+1} = x_e + h_e$)

$$\begin{aligned}
\phi_1^e &= 1 - 3\left(\frac{x - x_e}{h_e}\right)^2 + 2\left(\frac{x - x_e}{h_e}\right)^3 \\
\phi_2^e &= -(x - x_e)\left(1 - \frac{x - x_e}{h_e}\right)^2 \\
\phi_3^e &= 3\left(\frac{x - x_e}{h_e}\right)^2 - 2\left(\frac{x - x_e}{h_e}\right)^3 \\
\phi_4^e &= -(x - x_e)\left[\left(\frac{x - x_e}{h_e}\right)^2 - \frac{x - x_e}{h_e}\right]
\end{aligned} \tag{5.2.11}$$

Note that the cubic interpolation functions in (5.2.11) are derived by interpolating w as well as its derivative dw/dx at the nodes. Such polynomials are known as the *Hermite family of interpolation functions*, and ϕ_i^e in (5.2.11) are called the *Hermite cubic interpolation* (or *cubic spline*) *functions*. Plots of the Hermite cubic interpolation functions are shown in Fig. 5.2.4.

Recall that the Lagrange cubic interpolation functions are derived to interpolate a function, but not its derivatives, at the nodes. Hence, a Lagrange cubic element will have four nodes, with the dependent variable, not its derivative, as the nodal degree of freedom. Since the slope (or derivative) of the dependent variable is also required by the weak form to be continuous at the nodes for the Euler–Bernoulli beam theory, the Lagrange cubic

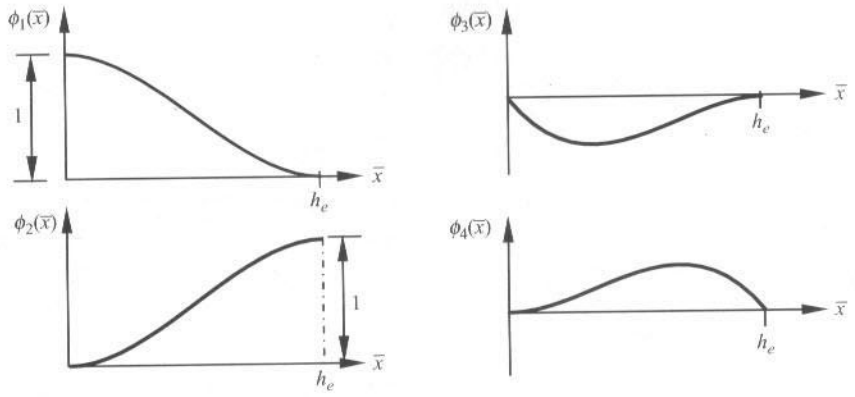

Figure 5.2.4 Hermite cubic interpolations functions used in the Euler–Bernoulli beam element.

interpolation of w, although it meets the continuity requirement for w, is *not admissible* in the finite element approximation of the Euler–Bernoulli beam theory.

The interpolation functions ϕ_i^e can be expressed in terms of the local coordinate $\bar{x} = x - x_e$:

$$\begin{aligned} \phi_1^e &= 1 - 3\left(\frac{\bar{x}}{h_e}\right)^2 + 2\left(\frac{\bar{x}}{h_e}\right)^3, \quad \phi_2^e = -\bar{x}\left(1 - \frac{\bar{x}}{h_e}\right)^2 \\ \phi_3^e &= 3\left(\frac{\bar{x}}{h_e}\right)^2 - 2\left(\frac{\bar{x}}{h_e}\right)^3, \quad \phi_4^e = -\bar{x}\left[\left(\frac{\bar{x}}{h_e}\right)^2 - \frac{\bar{x}}{h_e}\right] \end{aligned} \tag{5.2.12}$$

The first, second, and third derivatives of ϕ_i^e with respect to $\bar{x}$ are

$$\frac{d\phi_1^e}{d\bar{x}} = -\frac{6}{h_e}\frac{\bar{x}}{h_e}\left(1 - \frac{\bar{x}}{h_e}\right), \quad \frac{d\phi_2^e}{d\bar{x}} = -\left[1 + 3\left(\frac{\bar{x}}{h_e}\right)^2 - 4\frac{\bar{x}}{h_e}\right] \tag{5.2.13a}$$

$$\frac{d\phi_3^e}{d\bar{x}} = -\frac{d\phi_1^e}{d\bar{x}} = \frac{6}{h_e}\frac{\bar{x}}{h_e}\left(1 - \frac{\bar{x}}{h_e}\right), \quad \frac{d\phi_4^e}{d\bar{x}} = -\frac{\bar{x}}{h_e}\left(3\frac{\bar{x}}{h_e} - 2\right)$$

$$\frac{d^2\phi_1^e}{d\bar{x}^2} = -\frac{6}{h_e^2}\left(1 - 2\frac{\bar{x}}{h_e}\right), \quad \frac{d^2\phi_2^e}{d\bar{x}^2} = -\frac{2}{h_e}\left(3\frac{\bar{x}}{h_e} - 2\right) \tag{5.2.13b}$$

$$\frac{d^2\phi_3^e}{d\bar{x}^2} = -\frac{d^2\phi_1^e}{d\bar{x}^2} = \frac{6}{h_e^2}\left(1 - 2\frac{\bar{x}}{h_e}\right), \quad \frac{d^2\phi_4^e}{d\bar{x}^2} = -\frac{2}{h_e}\left(3\frac{\bar{x}}{h_e} - 1\right)$$

$$\begin{aligned} \frac{d^3\phi_1^e}{d\bar{x}^3} &= \frac{12}{h_e^3}, \quad \frac{d^3\phi_2^e}{d\bar{x}^3} = -\frac{6}{h_e^2} \\ \frac{d^3\phi_3^e}{d\bar{x}^3} &= -\frac{12}{h_e^3}, \quad \frac{d^3\phi_4^e}{d\bar{x}^3} = -\frac{6}{h_e^2} \end{aligned} \tag{5.2.13c}$$

Plots of $d\phi_i^e/dx$ are shown in Fig. 5.2.5.

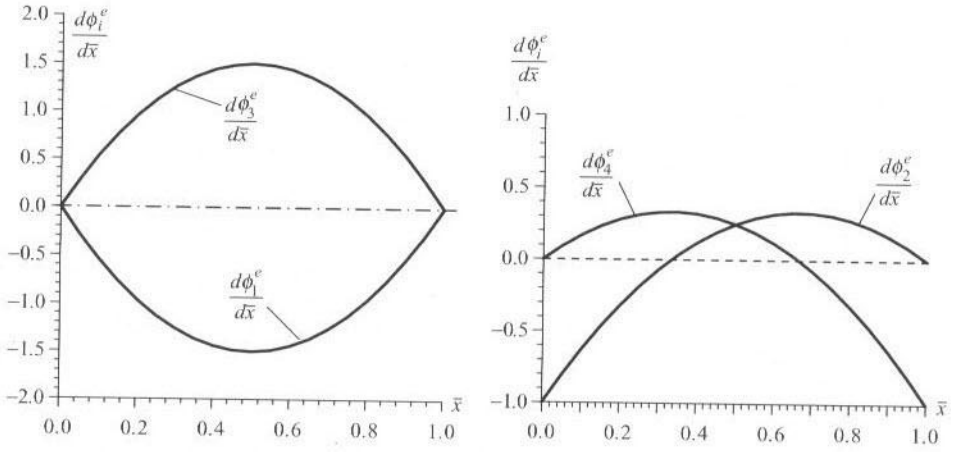

Figure 5.2.5 Plots of the first derivatives, $d\phi_i^e/d\bar{x}$, of the Hermite cubic interpolations functions.

The Hermite cubic interpolation functions (5.2.11) or (5.2.12) satisfy the following interpolations properties (see Figs. 5.2.4 and 5.2.5):

$$\begin{aligned}
&\phi_1^e(x_e) = 1, && \phi_i^e(x_e) = 0 \quad (i \neq 1)\\
&\phi_3^e(x_{e+1}) = 1, && \phi_i^e(x_{e+1}) = 0 \quad (i \neq 3)\\
&\left(-\frac{d\phi_2^e}{dx}\right)\Big|_{x_e} = 1, && \left(-\frac{d\phi_i^e}{dx}\right)\Big|_{x_e} = 0 \quad (i \neq 2)\\
&\left(-\frac{d\phi_4^e}{dx}\right)\Big|_{x_{e-1}} = 1, && \left(-\frac{d\phi_i^e}{dx}\right)\Big|_{x_{e+1}} = 0 \quad (i \neq 4)
\end{aligned} \tag{5.2.14a}$$

These can be stated in compact form as $(i, j = 1, 2)$

$$\begin{aligned}
&\phi_{2i-1}^e(\bar{x}_j) = \delta_{ij}, \quad \phi_{2i}^e(\bar{x}_j) = 0, \quad \sum_{i=1}^{2} \phi_{2i-1}^e = 1\\
&\left(\frac{d\phi_{2i-1}^e}{dx}\right)\Big|_{\bar{x}_j} = 0, \quad \left(-\frac{d\phi_{2i}^e}{dx}\right)\Big|_{\bar{x}_j} = \delta_{ij}
\end{aligned} \tag{5.2.14b}$$

where $\bar{x}_1 = 0$ and $\bar{x}_2 = h_e$ are the local coordinates of nodes 1 and 2 of the element $\Omega^e = (x_e, x_{e+1})$. The finite element solution

$$w_h^e(x) = \Delta_1^e \phi_1^e(x) + \Delta_2^e \phi_2^e(x) + \Delta_3^e \phi_3^e(x) + \Delta_4^e \phi_4^e(x)$$

is a linear combination of four terms, which is shown in Fig. 5.2.6 along with the actual function.

It should be noted that the order of the interpolation functions derived above is the minimum required for the variational formulation (5.2.4). If a higher-order (i.e., higher than cubic) approximation of w is desired, we must either identify additional primary

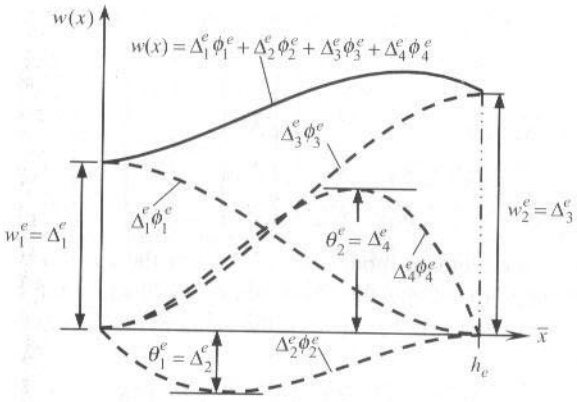

Figure 5.2.6 Finite element solution over an element.

unknowns at each of the two nodes or add additional nodes with the two degrees of freedom $(w, -dw/dx)$. For example, if we add d^2w/dx^2 as the primary unknown at each of the two nodes or add a third node with $(w, -dw/dx)$ at each node, there will be a total of six conditions, and a fifth-order polynomial is required to interpolate the end conditions (see Problems 5.4 and 5.5). However, interelement continuity of d^2w/dx^2 (curvature) is not required by the weak form (5.2.4).

Finite Element Model. The finite element model of the Euler–Bernoulli beam is obtained by substituting the finite element interpolation (5.2.10) for w and the ϕ_j^e for the weight function v into the weak form (5.2.4). Since there are four nodal variables Δ_i^e, four different choices are used for v: $v = \phi_1^e$, ϕ_2^e, ϕ_3^e, and ϕ_4^e, allowing us to obtain a set of four algebraic equations. The ith algebraic equation of the finite element model is (for $v = \phi_i^e$)

$$0 = \sum_{j=1}^{4} \left[\int_{x_e}^{x_{e+1}} \left(EI \frac{d^2\phi_i^e}{dx^2} \frac{d^2\phi_j^e}{dx^2} + c_f \phi_i^e \phi_j^e \right) dx \right] u_j^e - \int_{x_e}^{x_{e+1}} \phi_i^e q \, dx - Q_i^e \tag{5.2.15a}$$

or

$$\sum_{j=1}^{4} K_{ij}^e \Delta_j^e - F_i^e = 0 \quad \text{or} \quad [K^e]\{\Delta^e\} = \{F^e\} \tag{5.2.15b}$$

where

$$K_{ij}^e = \int_{x_e}^{x_{e+1}} \left(EI \frac{d^2\phi_i^e}{dx^2} \frac{d^2\phi_j^e}{dx^2} + c_f \phi_i^e \phi_j^e \right) dx \tag{5.2.16a}$$

$$F_i^e = \int_{x_e}^{x_{e+1}} \phi_i^e q \, dx + Q_i^e \tag{5.2.16b}$$

Note that the coefficients K_{ij}^e are symmetric: $K_{ij}^e = K_{ji}^e$. In matrix notation, (5.2.15*b*) can be written as

$$\begin{bmatrix} K_{11}^e & K_{12}^e & K_{13}^e & K_{14}^e \\ K_{21}^e & K_{22}^e & K_{23}^e & K_{24}^e \\ K_{31}^e & K_{32}^e & K_{33}^e & K_{34}^e \\ K_{41}^e & K_{42}^e & K_{43}^e & K_{44}^e \end{bmatrix} \begin{Bmatrix} \Delta_1^e \\ \Delta_2^e \\ \Delta_3^e \\ \Delta_4^e \end{Bmatrix} = \begin{Bmatrix} q_1^e \\ q_2^e \\ q_3^e \\ q_4^e \end{Bmatrix} + \begin{Bmatrix} Q_1^e \\ Q_2^e \\ Q_3^e \\ Q_4^e \end{Bmatrix} \tag{5.2.17}$$

This represents the finite element model of (5.2.1). For the case in which EI and q are constant over an element, the element stiffness matrix $[K^e]$ and force vector $\{F^e\}$ have the following specific forms [see Fig. 5.2.2(*c*) for the element displacement and force degrees of freedom]

$$[K^e] = \frac{2E_eI_e}{h_e^3} \begin{bmatrix} 6 & -3h_e & -6 & -3h_e \\ -3h_e & 2h_e^2 & 3h_e & h_e^2 \\ -6 & 3h_e & 6 & 3h_e \\ -3h_e & h_e^2 & 3h_e & 2h_e^2 \end{bmatrix} + \frac{c_f^e h_e}{420} \begin{bmatrix} 156 & -22h_e & 54 & 13h_e \\ -22h_e & 4h_e^2 & -13h_e & -3h_e^2 \\ 54 & -13h_e & 156 & 22h_e \\ 13h & -3h_e^2 & 22h_e & 4h_e^2 \end{bmatrix}$$

$$\{F^e\} = \frac{q_e h_e}{12} \begin{Bmatrix} 6 \\ -h_e \\ 6 \\ h_e \end{Bmatrix} + \begin{Bmatrix} Q_1 \\ Q_2 \\ Q_3 \\ Q_4 \end{Bmatrix} \tag{5.2.18}$$

It can be verified that the generalized force vector in (5.2.18) represents the "statically equivalent" forces and moments at nodes 1 and 2 due to the uniformly distributed load of intensity q_e over the element (see Fig. 5.2.7). For any given function $q(x)$, (5.2.16*b*) provides a straightforward way of computing the components of the generalized force vector $\{q^e\}$

$$q_i^e = \int_{x_e}^{x_{e+1}} \phi_i^e q \, dx \tag{5.2.19}$$

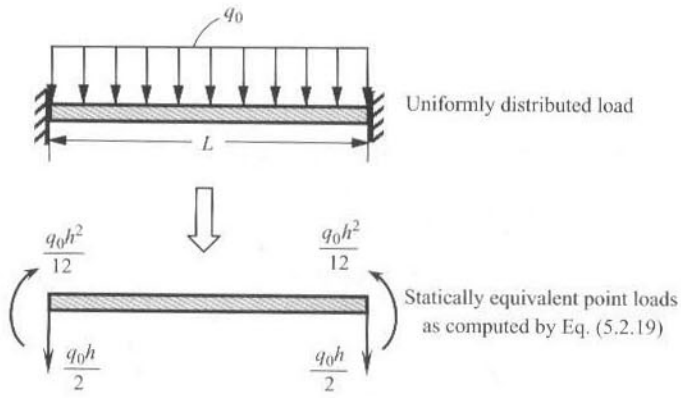

Figure 5.2.7 Generalized nodal forces due to uniformly distributed load.

When a transverse point force F_0^e is applied at a point x_0 inside the element, it is distributed to the element nodes by the relation [see Remark 5 in Chapter 3; Eq. (3.3.4)]:

$$q_i^e = \int_{x_e}^{x_{e+1}} \phi_i^e(x) F_0^e \delta(x - x_0)\, dx = F_0^e \phi_i^e(x_0), \quad x_e \le x_0 \le x_{e+1} \tag{5.2.20}$$

which contains both transverse forces (q_1^e and q_3^e) and bending moments (q_2^e and q_4^e).

5.2.4 Assembly of Element Equations

The assembly procedure for beam elements is the same as that used for bar elements except that we must take into account the two degrees of freedom at each node. Recall that the assembly of elements is based on: (a) interelement continuity of the primary variables (deflection and slope) and (b) interelement equilibrium of the secondary variable (shear force and bending moment) at the nodes common to elements. To demonstrate the assembly procedure, we select a two-element model (see Fig. 5.2.8). There are three global nodes and a total of six global generalized displacements and six generalized forces in the problem. The continuity of the primary variables implies the following relation between the element degrees of freedom Δ_i^e and the global degrees of freedom U_i (see Fig. 5.2.8):

$$\begin{aligned} &\Delta_1^1 = U_1, \quad \Delta_2^1 = U_2, \quad \Delta_3^1 = \Delta_1^2 = U_3 \\ &\Delta_4^1 = \Delta_2^2 = U_4, \quad \Delta_3^2 = U_5, \quad \Delta_4^2 = U_6 \end{aligned} \tag{5.2.21}$$

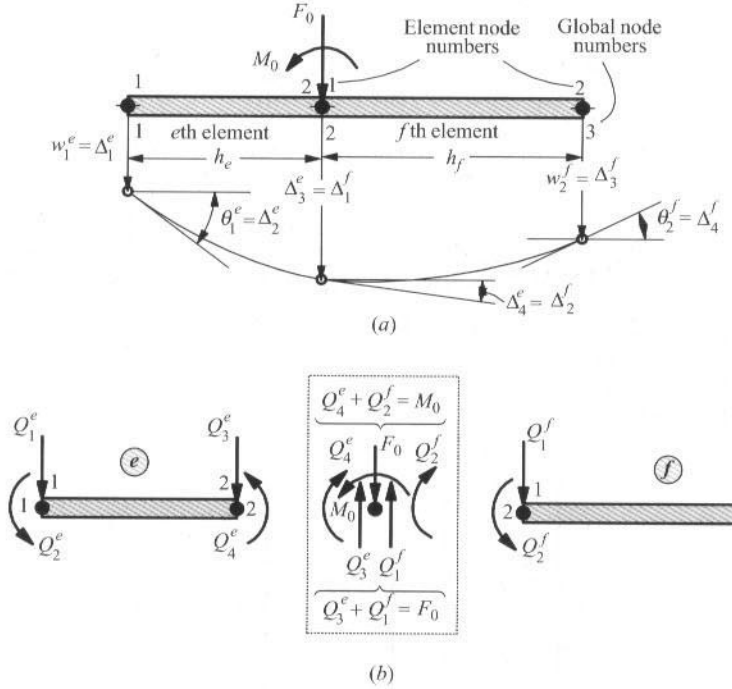

Figure 5.2.8 Assembly of two Euler–Bernoulli beam finite elements. (*a*) Continuity of generalized displacements. (*b*) Balance of the generalized forces.

In general, the equilibrium of the generalized forces at a node between two connecting elements Ω_e and Ω_f requires that

$$\begin{aligned} Q_3^e + Q_1^f &= \text{applied external point force} \\ Q_4^e + Q_2^f &= \text{applied external bending moment} \end{aligned} \tag{5.2.22}$$

If no external applied forces are given, the sum should be equated to zero. In equating the sums to the applied generalized forces (i.e., force or moment), the sign convention for the element force degrees of freedom [see Fig. 5.2.2(*c*)] should be followed. Forces are taken as positive when they act in the direction of positive z-axis, and moments are taken as positive when they follow the right-hand screw rule (i.e., when the thumb is along the positive y-axis, the four fingers show the direction of the moment). With respect to the coordinate system used in Figs. 5.2.1 and 5.2.2, *forces acting downward are positive and counterclockwise moments are positive.*

To impose the equilibrium of forces in (5.2.22), it is necessary to add the third and fourth equations (corresponding to the second node) of element Ω^e to the first and second equations (corresponding to the first node) of element Ω^f. Consequently, the global stiffness parameters K_{33}, K_{34}, K_{43}, and K_{44} associated with global node 2 are the superposition of the element stiffnesses:

$$K_{33} = K_{33}^1 + K_{11}^2, \quad K_{34} = K_{34}^1 + K_{12}^2, \quad K_{43} = K_{43}^1 + K_{21}^2, \quad K_{44} = K_{44}^1 + K_{22}^2 \tag{5.2.23}$$

In general, the assembled stiffness matrix and force vector for beam elements connected in series have the forms given in Eqs. (5.2.24*a*) and (5.2.24*b*):

$$[K] = \begin{array}{c} \overbrace{}^{\text{Global node 1}} \quad \overbrace{}^{\text{Global node 2}} \quad \overbrace{}^{\text{Global node 3}} \\ \left[\begin{array}{cccccc} K_{11}^1 & K_{12}^1 & K_{13}^1 & K_{14}^1 & & \\ K_{21}^1 & K_{22}^1 & K_{23}^1 & K_{24}^1 & & \\ K_{31}^1 & K_{32}^1 & K_{33}^1 + K_{11}^2 & K_{34}^1 + K_{12}^2 & K_{13}^2 & K_{14}^2 \\ K_{41}^1 & K_{42}^1 & K_{43}^1 + K_{21}^2 & K_{44}^1 + K_{22}^2 & K_{23}^2 & K_{24}^2 \\ & & K_{31}^2 & K_{32}^2 & K_{33}^2 & K_{34}^2 \\ & & K_{41}^2 & K_{42}^2 & K_{43}^2 & K_{44}^2 \end{array}\right] \begin{array}{l} \} \ 1 \\ \\ \} \ 2 \\ \\ \} \ 3 \end{array} \end{array} \tag{5.2.24a}$$

$$\{F\} = \begin{Bmatrix} q_1^1 \\ q_2^1 \\ q_3^1 + q_1^2 \\ q_4^1 + q_2^2 \\ q_3^2 \\ q_4^2 \end{Bmatrix} + \begin{Bmatrix} Q_1^1 \\ Q_2^2 \\ Q_3^1 + Q_1^2 \\ Q_4^1 + Q_2^2 \\ Q_3^2 \\ Q_4^2 \end{Bmatrix} \tag{5.2.24b}$$

5.2.5 Imposition of Boundary Conditions

At this step of the analysis, we must impose the particular boundary conditions of the problem being analyzed. The type of essential (also know as *geometric*) boundary conditions for a specific beam problem depend on the nature of the geometric support. Table 5.2.1 contains a list of commonly used geometric supports for beams. The natural (also called *force*) boundary conditions involve the specification of generalized forces when the corresponding primary variables are not constrained. One must bear in mind that one and only one element of each of the following pairs must be specified at every node of the finite element mesh:

$$\left(w,\ \frac{d}{dx}\left[EI\frac{d^2w}{dx^2}\right]\right),\quad \left(\frac{dw}{dx},\ EI\frac{d^2w}{dx^2}\right) \tag{5.2.25}$$

At an interior node, we impose the continuity of generalized displacements and balance of generalized forces as discussed in Eqs. (5.2.21) and (5.2.22).

Table 5.2.1 Types of commonly used support conditions for beams and frames.

Type of support	Displacement boundary conditions	Force boundary conditions
Free 	None	All, as specified
Pinned 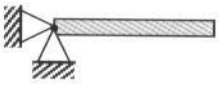	$u=0$ $w=0$	Moment is specified
Roller (vertical) 	$u=0$	Transverse force and moment are specified
Roller (horizontal) 	$w=0$	Horizontal force and bending moment are specified
Fixed (or clamped) 	$u=0$ $w=0$ $dw/dx=0$	None specified
Elastically restrained 	$EI(d^2w/dx^2)+\mu\theta=M_0$, M_0 specified $EI(d^3w/dx^3)+kw=Q_0$, Q_0 specified	

There are two alternative ways to include the effect of a linear elastic spring (extensional as well as torsional). (1) Include the spring through the boundary condition for the appropriate degree of freedom (see Table 5.2.1). (2) Include the spring as another finite element, whose element equations are given by Eq. (4.2.2). In the former case, after assembly of the element equations, the secondary variable in the direction of the spring action is replaced by the negative of the spring constant times the associated primary variable. Let Q^v, and Q^θ denote the secondary variables associated with the transverse and rotational degrees of freedom at a node. Then, we have, respectively

$$Q^v + kw = 0 \text{ or } Q^v = -kw \text{ for vertical spring with spring constant } k$$

$$Q^\theta + \mu\theta = 0 \text{ or } Q^\theta = -\mu\theta \text{ for torsional spring with spring constant } \mu$$

Note that Q^v is the shear force and Q^θ the bending moment. In the second case, the spring element may be assembled along with beam elements by noting that the axial displacement of the spring is the same as the transverse displacement of the beam.

For example, consider the case of a beam clamped at the left end and supported by a spring at the right end, as shown in Fig. 5.2.9(a). Using one-element model of the beam, we obtain [set $c_f = 0$ in Eq. (5.2.18)]

$$\frac{2EI}{L^3}\begin{bmatrix} 6 & -3L & -6 & -3L \\ -3L & 2L^2 & 3L & L^2 \\ -6 & 3L & 6 & 3L \\ -3L & L^2 & 3L & 2L^2 \end{bmatrix}\begin{Bmatrix} U_1 \\ U_2 \\ U_3 \\ U_4 \end{Bmatrix} = \frac{q_0 L}{12}\begin{Bmatrix} 6 \\ -L \\ 6 \\ L \end{Bmatrix} + \begin{Bmatrix} Q_1 \\ Q_2 \\ Q_3 \\ Q_4 \end{Bmatrix}$$

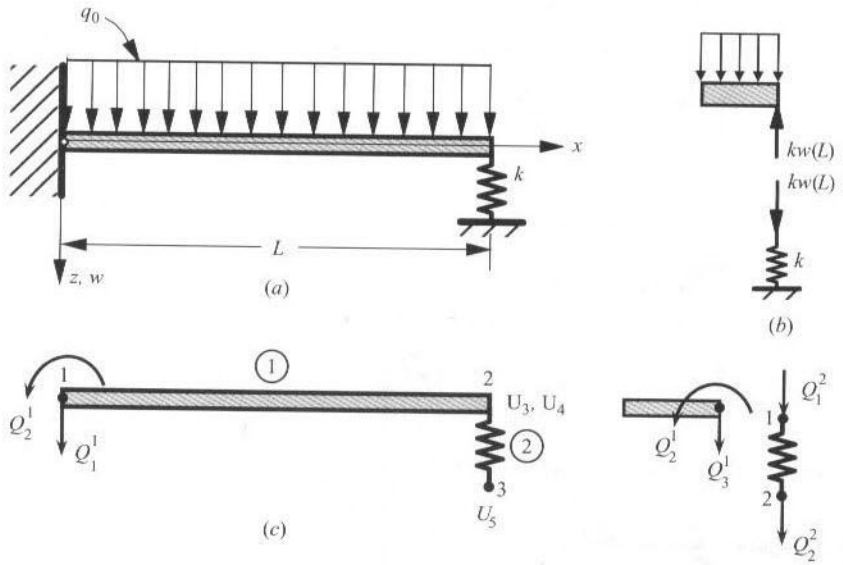

Figure 5.2.9 (a) A spring supported cantilever beam. (b) Spring action. (c) Finite element mesh of beam and spring elements.

The obvious boundary conditions are $U_1 = U_2 = Q_4 = 0$. The effect of the spring is that [see Fig. 5.2.9(*b*)] it exerts a force of kU_3 upward on the beam. Hence, $Q_3 = -kU_3$. Thus, we have

$$\frac{2EI}{L^3}\begin{bmatrix} 6 & -3L & -6 & -3L \\ -3L & 2L^2 & 3L & L^2 \\ -6 & 3L & 6 & 3L \\ -3L & L^2 & 3L & 2L^2 \end{bmatrix}\begin{Bmatrix} 0 \\ 0 \\ U_3 \\ U_4 \end{Bmatrix} = \frac{q_0 L}{12}\begin{Bmatrix} 6 \\ -L \\ 6 \\ L \end{Bmatrix} + \begin{Bmatrix} Q_1 \\ Q_2 \\ -kU_3 \\ 0 \end{Bmatrix}$$

and the condensed equations for the unknown displacements U_3 (deflection) and U_4 (rotation) become

$$\begin{bmatrix} \frac{12EI}{L^3} + k & \frac{6EI}{L^2} \\ \frac{6EI}{L^2} & \frac{4EI}{L} \end{bmatrix}\begin{Bmatrix} U_3 \\ U_4 \end{Bmatrix} = \frac{q_0 L}{12}\begin{Bmatrix} 6 \\ L \end{Bmatrix}$$

whose solution is

$$U_3 = w(L) = \frac{q_0 L^4}{8EI}\frac{1}{\left(1 + \frac{kL^3}{3EI}\right)}, \quad U_4 = \theta(L) = -\frac{q_0 L^3}{6EI}\frac{\left(EI - \frac{kL^3}{24}\right)}{\left(EI + \frac{kL^3}{3}\right)}$$

Note that when $k = 0$, we obtain the deflection $U_3 = q_0 L^4/8EI$ and rotation $U_4 = -q_0 L^3/6EI$ at the free end of a cantilever beam under uniformly distributed load of intensity q_0. When $k \to \infty$, we obtain the deflection $U_3 = 0$ and rotation $U_4 = -q_0 L^3/48EI$ at $x = L$ (where it is simply supported).

Alternatively, the assembly of the beam and spring elements [see Fig. 5.2.9(*c*)] yields the result

$$\begin{bmatrix} \frac{12EI}{L^3} & -\frac{6EI}{L^2} & -\frac{12EI}{L^3} & -\frac{6EI}{L^2} & 0 \\ -\frac{6EI}{L^2} & \frac{4EI}{L} & \frac{6EI}{L^2} & \frac{2EI}{L} & 0 \\ -\frac{12EI}{L^3} & \frac{6EI}{L^2} & \frac{12EI}{L^3} + k & \frac{6EI}{L^2} & -k \\ -\frac{6EI}{L^2} & \frac{2EI}{L} & \frac{6EI}{L} & \frac{4EI}{L} & 0 \\ 0 & 0 & -k & 0 & k \end{bmatrix}\begin{Bmatrix} U_1 \\ U_2 \\ U_3 \\ U_4 \\ U_5 \end{Bmatrix} = \frac{q_0 L}{12}\begin{Bmatrix} 6 \\ -L \\ 6 \\ L \\ 0 \end{Bmatrix} + \begin{Bmatrix} Q_1^1 \\ Q_2^1 \\ Q_3^1 + Q_1^2 \\ Q_4^1 \\ Q_2^2 \end{Bmatrix}$$

Using the boundary conditions, $U_1 = U_2 = U_5 = 0$ and $Q_4^1 = 0$, and the equilibrium condition $Q_3^1 + Q_1^2 = 0$, we obtain the condensed equations

$$\begin{bmatrix} \frac{12EI}{L^3} + k & \frac{6EI}{L^2} \\ \frac{6EI}{L^2} & \frac{4EI}{L} \end{bmatrix}\begin{Bmatrix} U_3 \\ U_4 \end{Bmatrix} = \frac{q_0 L}{12}\begin{Bmatrix} 6 \\ L \end{Bmatrix}$$

which are identical to those obtained earlier.

5.2.6 Postprocessing of the Solution

Once the boundary conditions are imposed, the resulting equations are solved for the unknown nodal displacements and forces. The solution is then given by Eq. (5.2.10) in each

element. The slope of the deflection at an interior point is

$$-\frac{dw_h^e}{dx} = -\sum_{j=1}^{4} \Delta_j^e \frac{d\phi_j^e}{dx} \tag{5.2.26}$$

Similarly, the bending moment at any point in the element Ω^e of the beam can be computed from the formula

$$M(x) = \int_A \sigma_x \, z \, dA = B \int_{-H/2}^{H/2} \sigma_x \, z \, dz = -BE \int_{-H/2}^{H/2} z^2 \frac{d^2 w}{dx^2} \, dz = -EI \frac{d^2 w}{dx^2}$$
$$= -EI \sum_{j=1}^{4} \Delta_j^e \frac{d^2 \phi_j^e}{dx^2} \tag{5.2.27}$$

where B is the width and H is the height of the beam (for a rectangular cross-section beam). The bending stress is given by

$$\sigma_x(x, z) = -\frac{M(x)z}{I} = Ez\frac{d^2 w}{dx^2} = Ez \sum_{j=1}^{4} \Delta_j^e \frac{d^2 \phi_j^e(x)}{dx^2} \tag{5.2.28}$$

The maximum tensile stress occurs at the bottom ($z = H/2$) and the maximum compressive stress at the top ($z = -H/2$) of the beam.

We close this section with a note that whenever the flexural rigidity EI is a constant in each element, the finite element solution for the generalized displacements at the nodes is exact for any applied transverse load q. Further, the solution is exact at all points if the distributed load is such that the exact solution is a cubic.

5.2.7 Numerical Examples

Example 5.2.1

Consider a cantilever beam of length L and subjected to linearly varying distributed load $q(x)$, point load F_0, and moment M_0, as shown in Fig. 5.2.10. We wish to determine the displacement field and bending moment in the beam using two elements ($h = L/2$).

First we note that $q(x) = q_0(1 - x/L)$. There, we must evaluate its contribution to the element load vector by computing [see Eq. (5.2.19)]

$$q_i^e = \int_{x_e}^{x_{e+1}} q_0 \left(1 - \frac{x}{L}\right) \phi_i^e(x) \, dx = \int_0^{h_e} q_0 \left(1 - \frac{\bar{x} + x_e}{L}\right) \phi_i^e(\bar{x}) \, d\bar{x}$$

where $\phi_i^e(\bar{x})$ are given in Eq. (5.2.12). Evaluating the integrals,

$$\{q^e\} = \frac{q_0 h_e}{12} \begin{Bmatrix} 6 \\ -h_e \\ 6 \\ h_e \end{Bmatrix} + \frac{q_0 h_e}{60L} \begin{Bmatrix} -(9h_e + 30x_e) \\ h_e(2h_e + 5x_e) \\ -(21h_e + 30x_e) \\ -h_e(3h_e + 5x_e) \end{Bmatrix}$$

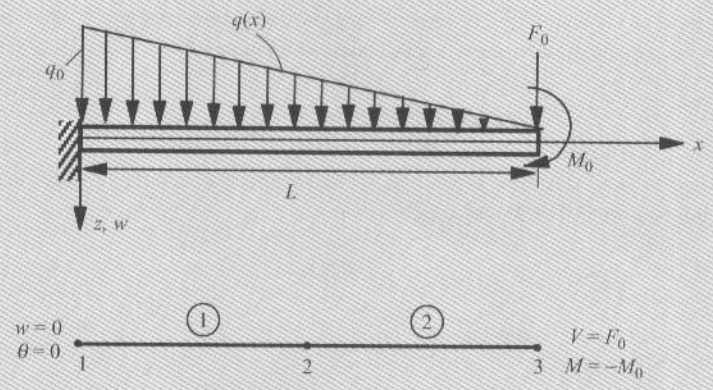

Figure 5.2.10 The cantilever beam problem considered in Example 5.2.1.

and specializing the above vectors to element 1 ($x_e = 0$) and element 2 ($x_e = h_e$), we obtain

$$\{q^1\} = \frac{q_0 L}{48}\begin{Bmatrix} 12 \\ -L \\ 12 \\ L \end{Bmatrix} + \frac{q_0 L^2}{480}\begin{Bmatrix} -18 \\ 2L \\ -42 \\ -3L \end{Bmatrix}; \{q^2\} = \frac{q_0 L}{48}\begin{Bmatrix} 12 \\ -L \\ 12 \\ L \end{Bmatrix} + \frac{q_0 L^2}{480}\begin{Bmatrix} -78 \\ 7L \\ -102 \\ -8L \end{Bmatrix}$$

The assembled system of equations for a mesh of two elements with constant EI (and foundation modulus $c_f = 0$) is

$$\frac{2EI}{h^3}\begin{bmatrix} 6 & -3h & -6 & -3h & 0 & 0 \\ -3h & 2h^2 & 3h & h^2 & 0 & 0 \\ -6 & 3h & 6+6 & 3h-3h & -6 & -3h \\ -3h & h^2 & 3h-3h & 2h^2+2h^2 & 3h & h^2 \\ 0 & 0 & -6 & 3h & 6 & 3h \\ 0 & 0 & -3h & h^2 & 3h & 2h^2 \end{bmatrix}\begin{Bmatrix} U_1 \\ U_2 \\ U_3 \\ U_4 \\ U_5 \\ U_6 \end{Bmatrix}$$

$$= \frac{q_0 L}{48}\begin{Bmatrix} 12 \\ -L \\ 24 \\ 0 \\ 12 \\ L \end{Bmatrix} + \frac{q_0 L}{480}\begin{Bmatrix} -18 \\ 2L \\ -120 \\ 4L \\ -102 \\ -8L \end{Bmatrix} + \begin{Bmatrix} Q_1^1 \\ Q_2^1 \\ Q_3^1 + Q_1^2 \\ Q_4^1 + Q_2^2 \\ Q_3^2 \\ Q_4^2 \end{Bmatrix}$$

At global node 1, Q_1^1 and Q_2^1 (the shear force and the bending moment, respectively), i.e., the reactions at the fixed end are not known. Hence, the corresponding generalized displacements,

U_1 and U_2 must be known. Since the end $x = 0$ is fixed, we have $U_1 = U_2 = 0$. At global node 2, there are no externally applied shear forces and bending moment, i.e.,

$$Q_3^1 + Q_1^2 = 0, \quad Q_4^1 + Q_2^2 = 0$$

At global node 3, the shear force is given as F_0, and the bending moment as M_0 [note the sign convention for F_0 and M_0 from Fig. 5.2.2(*c*)]:

$$Q_3^2 = F_0, \quad Q_4^2 = -M_0$$

Hence, the assembled equations take the form

$$\frac{4EI}{L^3}\begin{bmatrix} 24 & -6L & -24 & -6L & 0 & 0 \\ -6L & 2L^2 & 6L & L^2 & 0 & 0 \\ -24 & 6L & 48 & 0 & -24 & -6L \\ -6L & L^2 & 0 & 4L^2 & 6L & L^2 \\ 0 & 0 & -24 & 6L & 24 & 6L \\ 0 & 0 & -6L & L^2 & 6L & 2L^2 \end{bmatrix}\begin{Bmatrix} 0 \\ 0 \\ U_3 \\ U_4 \\ U_5 \\ U_6 \end{Bmatrix}$$

$$= \frac{q_0 L}{48}\begin{Bmatrix} 12 \\ -L \\ 24 \\ 0 \\ 12 \\ L \end{Bmatrix} + \frac{q_0 L}{480}\begin{Bmatrix} -18 \\ 2L \\ -120 \\ 4L \\ -102 \\ -8L \end{Bmatrix} + \begin{Bmatrix} Q_1^1 \\ Q_2^1 \\ 0 \\ 0 \\ F_0 \\ -M_0 \end{Bmatrix}$$

Thus, the condensed equations for the unknown generalized displacements and generalized forces are

$$\frac{4EI}{L^3}\begin{bmatrix} 48 & 0 & -24 & -6L \\ 0 & 4L^2 & 6L & L^2 \\ -24 & 6L & 24 & 6L \\ -6L & L^2 & 6L & 2L^2 \end{bmatrix}\begin{Bmatrix} U_3 \\ U_4 \\ U_5 \\ U_6 \end{Bmatrix} = \frac{q_0 L}{48}\begin{Bmatrix} 24 \\ 0 \\ 12 \\ L \end{Bmatrix} + \frac{q_0 L}{480}\begin{Bmatrix} -120 \\ 4L \\ -102 \\ -8L \end{Bmatrix} + \begin{Bmatrix} 0 \\ 0 \\ F_0 \\ -M_0 \end{Bmatrix}$$

$$\begin{Bmatrix} Q_1^1 \\ Q_2^1 \end{Bmatrix} = \frac{4EI}{L^3}\begin{bmatrix} -24 & -6L & 0 & 0 \\ 6L & L^2 & 0 & 0 \end{bmatrix}\begin{Bmatrix} U_3 \\ U_4 \\ U_5 \\ U_6 \end{Bmatrix} - \frac{q_0 L}{48}\begin{Bmatrix} 12 \\ -L \end{Bmatrix} - \frac{q_0 L}{480}\begin{Bmatrix} -18 \\ 2L \end{Bmatrix}$$

The solution of the condensed equations for the displacements yields

$$\begin{Bmatrix} U_3 \\ U_4 \\ U_5 \\ U_6 \end{Bmatrix} = \frac{L^3}{4EI}\begin{bmatrix} 48 & 0 & -24 & -6L \\ 0 & 4L^2 & 6L & L^2 \\ -24 & 6L & 24 & 6L \\ -6L & L^2 & 6L & 2L^2 \end{bmatrix}^{-1} \begin{Bmatrix} \frac{1}{4}q_0L \\ \frac{1}{120}q_0L^2 \\ F_0 + \frac{3}{80}q_0L \\ -M_0 + \frac{1}{240}q_0L^2 \end{Bmatrix}$$

$$= \frac{L}{48EI}\begin{bmatrix} 2L^2 & -6L & 5L^2 & -6L \\ -6L & 24 & -18L & 24 \\ 5L^2 & -18L & 16L^2 & -24L \\ -6L & 24 & -24L & 48 \end{bmatrix} \begin{Bmatrix} \frac{1}{4}q_0L \\ \frac{1}{120}q_0L^2 \\ F_0 + \frac{3}{80}q_0L \\ -M_0 + \frac{1}{240}q_0L^2 \end{Bmatrix}$$

$$= \frac{L}{48EI}\begin{Bmatrix} 5L^2F_0 + 6LM_0 + \frac{49}{80}q_0L^3 \\ -18LF_0 - 24M_0 - \frac{15}{8}q_0L^2 \\ 16L^2F_0 + 24LM_0 + \frac{16}{10}q_0L^3 \\ -24LF_0 - 48M_0 - 2q_0L^2 \end{Bmatrix} \tag{5.2.29}$$

The reactions Q_1^1 and Q_2^1 are

$$\begin{Bmatrix} Q_1^1 \\ Q_2^1 \end{Bmatrix} = \frac{4EI}{L^3}\begin{bmatrix} -24 & -6L \\ 6L & L^2 \end{bmatrix} \begin{Bmatrix} U_3 \\ U_4 \end{Bmatrix} - \frac{q_0L}{480}\begin{Bmatrix} 102 \\ -8L \end{Bmatrix} = \begin{Bmatrix} -\left(F_0 + \frac{1}{2}q_0L\right) \\ L\left(F_0 + \frac{1}{6}q_0L\right) + M_0 \end{Bmatrix} \tag{5.2.30}$$

It is clear that the reactions Q_1^1 and Q_2^1 computed above satisfy the static equilibrium equations of the beam:

$$Q_1^1 + F_0 + \frac{1}{2}q_0L = 0, \quad Q_2^1 - \left(F_0L + \frac{1}{6}q_0L^2 + M_0\right) = 0$$

The reactions Q_1^1 and Q_2^1 can also be computed using the definitions (5.2.3):

$$(Q_1^1)_{\text{def}} \equiv \frac{d}{dx}\left(EI\frac{d^2w}{dx^2}\right)\bigg|_{x=0}, \quad (Q_2^1)_{\text{def}} \equiv \left(EI\frac{d^2w}{dx^2}\right)\bigg|_{x=0}$$

From (5.2.13*b*) and (5.2.13*c*), we note that the second derivative of the Hermite cubic interpolation functions is linear over the element and the third derivative is constant over the element. Therefore, the bending moment and shear force computed using the definition (5.2.3) are elementwise linear and constant, respectively. Further, at nodes connecting two elements, they yield discontinuous values because the second and third derivatives of w are not made continuous across the interelement nodes. Thus, we have

$$(Q_1^1)_{\text{def}} = EI\left(U_3\frac{d^3\phi_3^1}{dx^3} + U_4\frac{d^3\phi_4^1}{dx^3}\right)\bigg|_{x=0} = EI\left[U_3\left(-\frac{96}{L^3}\right) + U_4\left(-\frac{24}{L^2}\right)\right]$$

$$= -\left(F_0 + \frac{23}{80}q_0L\right)$$

$$(Q_2^1)_{\text{def}} = EI\left(U_3\frac{24}{L^2} + U_4\frac{4}{L}\right) = \left(M_0 + F_0L + \frac{3}{20}q_0L^2\right)$$

which are in error by $q_1^e = -\frac{17}{80} q_0 L$ and $q_2^e = \frac{1}{60} q_0 L^2$ compared with those computed using the condensed (i.e., equilibrium) equations [see Eq. (5.2.30)].

The finite element solution as a function of position x is given by

$$w_h^e(x) = \begin{cases} U_3\phi_3^1 + U_4\phi_4^1 & \text{for } 0 \le x \le h \\ U_3\phi_1^2 + U_4\phi_2^2 + U_5\phi_3^2 + U_6\phi_4^2 & \text{for } h \le x \le 2h \end{cases} \tag{5.2.31a}$$

where

$$\begin{aligned} \phi_3^1 &= 3\left(\frac{x}{h}\right)^2 - 2\left(\frac{x}{h}\right)^3, & \phi_4^1 &= h\left[\left(\frac{x}{h}\right)^2 - \left(\frac{x}{h}\right)^3\right] \\ \phi_1^2 &= 1 - 3\left(1 - \frac{x}{h}\right)^2 - 2\left(1 - \frac{x}{h}\right)^3, & \phi_2^2 &= h\left(1 - \frac{x}{h}\right)\left(2 - \frac{x}{h}\right)^2 \\ \phi_3^2 &= 3\left(1 - \frac{x}{h}\right)^2 + 2\left(1 - \frac{x}{h}\right)^3, & \phi_4^2 &= h\left[\left(1 - \frac{x}{h}\right)^3 + \left(1 - \frac{x}{h}\right)^2\right] \end{aligned} \tag{5.2.31b}$$

The exact solution of the problem in Fig. 5.2.9 can be obtained by direct integration and is given by

$$\begin{aligned} w(x) &= \frac{q_0 L^4}{120EI}\left[10\left(\frac{x}{L}\right)^2 - 10\left(\frac{x}{L}\right)^3 + 5\left(\frac{x}{L}\right)^4 - \left(\frac{x}{L}\right)^5\right] \\ &\quad + \frac{F_0 L^3}{6EI}\left[-\left(\frac{x}{L}\right)^3 + 3\left(\frac{x}{L}\right)^2\right] + \frac{M_0 L^2}{2EI}\left(\frac{x}{L}\right)^2 \\ \theta(x) &= -\frac{q_0 L^3}{24EI}\left[4\left(\frac{x}{L}\right) - 6\left(\frac{x}{L}\right)^2 + 4\left(\frac{x}{L}\right)^3 - \left(\frac{x}{L}\right)^4\right] \\ &\quad + \frac{F_0 L^2}{2EI}\left[\left(\frac{x}{L}\right)^2 - 2\left(\frac{x}{L}\right)\right] - \frac{M_0}{EI}\left(\frac{x}{L}\right) \\ M(x) &= -\frac{q_0 L^2}{6}\left[1 - 3\left(\frac{x}{L}\right) + 3\left(\frac{x}{L}\right)^2 - \left(\frac{x}{L}\right)^3\right] + F_0 L\left[\left(\frac{x}{L}\right) - 1\right] - M_0 \end{aligned} \tag{5.2.32}$$

The finite element solution (5.2.31) and the exact solution (5.2.32) are compared in Table 5.2.2 for the data

$$\begin{aligned} &q_0 = 24 \text{ kN/m}, \quad F_0 = 60 \text{ kN}, \quad L = 3 \text{ m}, \quad M_0 = 0 \text{ kN-m} \\ &E = 200 \times 10^6 \text{ kN/m}^2, \quad I = 29 \times 10^6 \text{ mm}^4, \quad (EI = 5800 \text{ kN-m}^2) \end{aligned} \tag{5.2.33}$$

As expected, the finite element solution for w and θ coincides with the exact solution at the nodes. At points other than the nodes, the difference between the finite element and exact solutions is virtually negligible.

Table 5.2.2 Comparison of the finite element method (FEM) solution with the exact solution of the cantilever beam of Example 5.2.1 (2 elements).

	$w(m)$		$-\theta = dw/dx$		$-M \times 10^{-6}$ (kN m)	
x (m)	FEM	Exact	FEM	Exact	FEM	Exact
0.0000	0.0000†	0.0000	0.0000†	0.0000	0.2124†	0.2160
0.1875	0.0006	0.0006	0.0066	0.0067	0.1973	0.1984
0.3750	0.0025	0.0025	0.0128	0.0128	0.1821	0.1816
0.5625	0.0054	0.0054	0.0184	0.0185	0.1670	0.1656
0.7500	0.0093	0.0094	0.0235	0.0235	0.1519	0.1502
0.9375	0.0142	0.0142	0.0282	0.0282	0.1367	0.1354
1.1250	0.0199	0.0199	0.0324	0.0323	0.1216	0.1213
1.3125	0.0263	0.0263	0.0361	0.0360	0.1065	0.1077
1.5000	0.0333†	0.0334	0.0393†	0.0393	0.0913*	0.0945
1.6875	0.0410	0.0410	0.0421	0.0421	0.0814	0.0818
1.8750	0.0491	0.0491	0.0445	0.0446	0.0696	0.0694
2.0625	0.0577	0.0577	0.0466	0.0466	0.0579	0.0574
2.2500	0.0666	0.0666	0.0483	0.0483	0.0461	0.0456
2.4375	0.0758	0.0758	0.0496	0.0496	0.0344	0.0340
2.6250	0.0852	0.0852	0.0505	0.0505	0.0226	0.0226
2.8025	0.0947	0.0947	0.0510	0.0510	0.0109	0.0113
3.0000	0.1043†	0.1042	0.0512†	0.0512	−0.0009	0.0000

* 0.0932 from the second element.
† Nodal values; all others are computed by interpolation;

Example 5.2.2

Consider the indeterminate beam shown in Fig. 5.2.11(a). We assume the following discontinuous data ($c_f = 0$):

$$EI = \begin{cases} 2 \times 10^8 \text{ lb-ft.}^2 & \text{for } 0 \le x \le 10 \text{ ft.} \\ 10^8 \text{ lb-ft.}^2 & \text{for } 10 \le x \le 28 \text{ ft.} \end{cases} \tag{5.2.34a}$$

$$q(x) = \begin{cases} 2400 \text{ lb/ft.} & \text{for } 0 \le x \le 10 \text{ ft.} \\ 0 & \text{for } 10 \le x \le 28 \text{ ft.} \end{cases} \tag{5.2.34b}$$

The boundary conditions are

$$[EI(d^3w/dx^3) + kw]_{x=0} = 0, \quad [EI(d^2w/dx^2)]_{x=0} = 0, \quad w(28) = 0, \quad [dw/dx]_{x=28} = 0$$

We shall use three elements to analyze the problem. There are four nodes and eight global degrees of freedom in the nonuniform mesh of three elements.

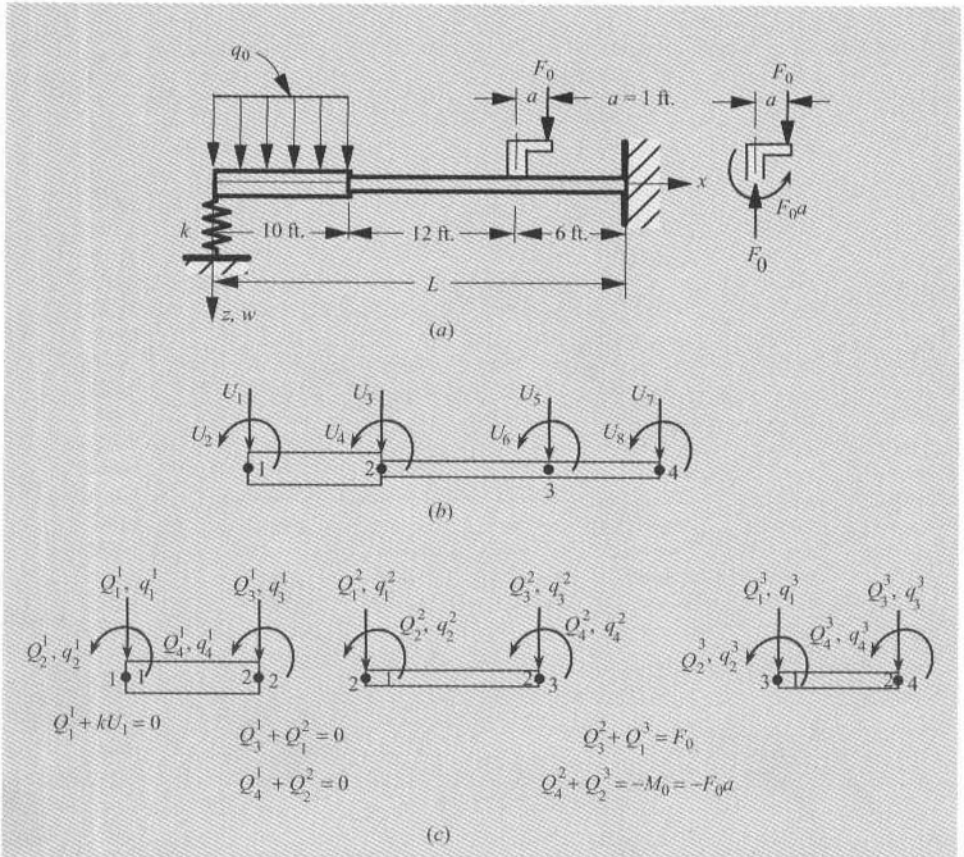

Figure 5.2.11 (*a*) Physical problem. (*b*) Finite element mesh of three elements. (*c*) Equilibrium of generalized forces.

Since EI and q are elementwise-constant, the element stiffness matrix and the force vector are given by (5.2.18), with $q_e = 2400$ lb/ft. in element 1 and $q_e = 0$ in elements 2 and 3. The assembled equations are

$$10^7 \begin{bmatrix} 0.2400 & -1.2000 & -0.2400 & -1.2000 & & & & \\ & 8.0000 & 1.2000 & 4.0000 & & & \mathbf{0} & \\ & & 0.3094 & 0.7833 & -0.0694 & -0.4167 & & \\ & & & 11.3333 & 0.4167 & 1.6667 & & \\ & & & & 0.6250 & -1.2500 & -0.5556 & -1.6667 \\ & & & & & 10.0000 & 1.6667 & 3.3333 \\ & \text{symmetric} & & & & & 0.5556 & 1.6667 \\ & & & & & & & 6.6667 \end{bmatrix}$$

$$\times \begin{Bmatrix} U_1 \\ U_2 \\ U_3 \\ U_4 \\ U_5 \\ U_6 \\ U_7 \\ U_8 \end{Bmatrix} = 10^3 \begin{Bmatrix} 12 \\ -20 \\ 12 \\ 20 \\ 0 \\ 0 \\ 0 \\ 0 \end{Bmatrix} + \begin{Bmatrix} Q_1^1 \\ Q_2^1 \\ Q_3^1 + Q_1^2 \\ Q_4^1 + Q_2^2 \\ Q_3^2 + Q_1^3 \\ Q_4^2 + Q_2^3 \\ Q_3^3 \\ Q_4^3 \end{Bmatrix}$$

The boundary conditions and equilibrium of internal forces and moments are given by

$$Q_2^1 = 0, \quad Q_3^1 + Q_1^2 = 0, \quad Q_4^1 + Q_2^2 = 0, \quad Q_3^2 + Q_1^3 = F_0, \quad Q_4^2 + Q_2^3 = -aF_0$$

Note that the forces Q_1^1 and Q_3^3 and the moment Q_4^3 (the reactions at the supports) are not known. The boundary conditions on the generalized displacements are

$$\left[EI\frac{d^3w}{dx^3} + kw\right]_{x=0} = 0 \Rightarrow Q_1^1 + kU_1 = 0; \; w(28) = 0 \Rightarrow U_7 = 0; \; \left(\frac{dw}{dx}\right)\Big|_{x=28} = 0 \Rightarrow U_8 = 0$$

Using the boundary and equilibrium conditions listed above, we can write the condensed equations for the unknown generalized displacements and forces. The condensed equations for the unknown generalized displacements can be obtained by deleting the last two rows and two columns, which correspond to the known U_i ($F_0 = 10^3$ lb):

$$10^7 \begin{bmatrix} 0.24+\alpha & -1.200 & -0.240 & -1.200 & 0.000 & 0.000 \\ & 8.000 & 1.200 & 4.000 & 0.000 & 0.000 \\ & & 0.309 & 0.783 & -0.069 & -0.417 \\ & & & 11.333 & 0.417 & 1.667 \\ & & \text{symmetric} & & 0.625 & -1.250 \\ & & & & & 10.000 \end{bmatrix} \begin{Bmatrix} U_1 \\ U_2 \\ U_3 \\ U_4 \\ U_5 \\ U_6 \end{Bmatrix} = 10^3 \begin{Bmatrix} 12 \\ -20 \\ 12 \\ 20 \\ 10 \\ -10 \end{Bmatrix}$$

where $\alpha = 10^{-7}k$. The unknown reactions can be computed from ($Q_1^1 = -kU_1$)

$$\begin{Bmatrix} Q_3^3 \\ Q_4^3 \end{Bmatrix} = 10^7 \begin{bmatrix} -0.5556 & 1.6667 \\ -1.6667 & 3.3333 \end{bmatrix} \begin{Bmatrix} U_5 \\ U_6 \end{Bmatrix}$$

This completes the finite element analysis of the problem.

The solution (with the help of a computer) of the condensed equations for the generalized displacements, when $k = 10^{11}$ lb/in. (a hard spring), gives $U_1 = 0.18356 \times 10^{-6} \approx 0$, and (rounded to six decimal points)

$$U_2 = -0.003686, \; U_3 = 0.026560 \text{ ft.}, \; U_4 = -0.001097, \; U_5 = 0.010215 \text{ ft.}, \; U_6 = 0.002466$$

The reaction forces, from the element equilibrium equations, are

$$(Q_1^1)_{\text{equil}} = -kU_1 = -18{,}356 \text{ lb}, \quad (Q_3^3)_{\text{equil}} = -15{,}644 \text{ lb}, \quad (Q_4^3)_{\text{equil}} = -88{,}040 \text{ ft-lb}$$

Based on the definitions, we have

$$(Q_3^3)_{\text{def}} = -15{,}644 \text{ lb}, \quad (Q_4^3)_{\text{def}} = -88{,}038 \text{ ft-lb}$$

For $k = 10^5$ lb/in. (a soft spring or no spring), we obtain

$$U_1 = 0.16104 \text{ ft.}, \quad U_2 = 0.004579, \quad U_3 = 0.10682 \text{ ft.}, \quad U_4 = 0.006605$$
$$U_5 = 0.020755 \text{ ft.}, \quad U_6 = 0.005844$$

Because of the discontinuity in the loading and the flexural rigidity, the exact solution $w(x)$ is also defined by three separate expressions for the three regions.

Example 5.2.3

This example deals with the indeterminate beam shown in Fig. 5.2.12. The beam is made of steel ($E = 30 \times 10^6$ psi) and the cross-sectional dimensions are 2×3 in. ($I = 4.5$ in.^{4}). We are interested in finding the transverse deflection w using the Euler–Bernoulli beam finite element.

Because of the discontinuity in loading, the beam should be divided into three elements: $\Omega_1 = (0, 16)$, $\Omega_2 = (16, 36)$, and $\Omega_3 = (36, 48)$; the element lengths are: $h_1 = 16$ in., $h_2 = 20$ in., and $h_3 = 12$ in. The load variation in each element is given by

$$q^{(1)}(x) = \left(30 - \frac{10}{16}x\right), \quad q^{(2)}(x) = 20, \quad q^{(3)}(x) = 0$$

Using Eq. (5.2.19), we obtain the following load vectors due to the distributed loads:

$$\{q^1\} = \begin{Bmatrix} 216.00 \\ -554.67 \\ 184.00 \\ 512.00 \end{Bmatrix}, \quad \{q^2\} = \begin{Bmatrix} 200.00 \\ -666.77 \\ 200.00 \\ 666.67 \end{Bmatrix}, \{q^3\} = \{0\}$$

The element stiffness matrices can be computed from Eq. (5.2.18) by substituting appropriate values of h, E, I, and $c_f = 0$. For Element 1, for example, we have ($h_1 = 16$ in., $EI = 135 \times 10^6$ lb-in.^{2}),

$$[K^1] = 10^6 \begin{bmatrix} 0.3955 & -3.1641 & -0.3955 & -3.1641 \\ -3.1641 & 33.7500 & 3.1641 & 16.8750 \\ -0.3955 & 3.1641 & 0.3955 & 3.1641 \\ -3.1641 & 16.8750 & 3.1641 & 33.750 \end{bmatrix}$$

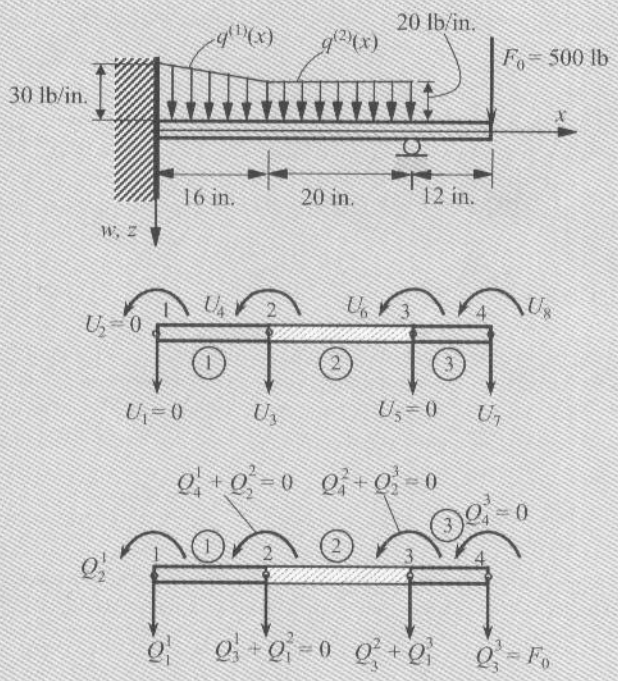

Figure 5.2.12 Finite element modeling of an indeterminate beam.

The assembled stiffness matrix and load vector for this mesh is of the same form as given in Eqs. (5.2.24*a*) and (5.2.24*b*). The boundary conditions for the problem are

$$w(0) = 0 \to U_1 = 0, \quad \frac{dw}{dx}(0) = 0 \to U_2 = 0, \quad w(36) = 0 \to U_5 = 0$$

$$Q_3^1 + Q_1^2 = 0, \quad Q_4^1 + Q_2^2 = 0, \quad Q_4^2 + Q_2^3 = 0, \quad Q_3^3 = 500, \quad Q_4^3 = 0$$

Note that Q_1^1, Q_2^1, and $Q_3^2 + Q_1^3$ are the reactions that are not known and are to be calculated in the postcomputation. Since the specified boundary conditions on the primary variables are homogeneous, we can delete the rows and columns corresponding to the specified displacements (i.e., delete rows and columns 1, 2, and 5) and solve the remaining five equations for U_3, U_4, U_6, U_7, and U_8:

$$U_3 = -0.000322 \text{ in.}, \quad U_4 = 0.0000593 \text{ rad.}, \quad U_6 = -0.0002513 \text{ rad.}$$
$$U_7 = 0.00515 \text{ in.}, \quad U_8 = -0.000518 \text{ rad.}$$

The exact deflection in the three intervals of the beam is given by (large numbers were rounded to whole numbers)

$$w(x) = \begin{cases} \dfrac{1}{EI}\left(268.543x^2 - \dfrac{691}{15}x^3 + \dfrac{5}{4}x^4 - \dfrac{1}{192}x^5\right) & 0 \le x \le 16 \\ \dfrac{1}{EI}\left(-\dfrac{16{,}384}{3} + \dfrac{5120}{3}x + 55.2097x^2 - \dfrac{491}{15}x^3 + \dfrac{5}{6}x^4\right) & 16 \le x \le 36 \\ \dfrac{1}{EI}\left(6{,}554{,}368 - 506.066x + 12{,}000x^2 - \dfrac{250}{3}x^3\right) & 36 \le x \le 48 \end{cases}$$

A comparison of the finite element solutions for deflections (w), slopes (θ), and bending moments (M) (calculated in the postcomputation) at points other than the nodes are compared with the exact values in Table 5.2.3 for three different meshes. The values of deflections, slopes, and bending moments were computed using the finite element solution and its derivatives.

Table 5.2.3 Comparison of the finite element solution with the exact solution (units of the quantities should be obvious) of the beam problem considered in Example 5.2.3.

		$w_0 \times 10^6$		$(-dw_0/dx) \times 10^6$		$-(d^2w_0/dx^2) \times 10^6$	
x	N†	FEM	Exact	FEM	Exact	FEM	Exact
	3	−0.8570		1.1553		−1.0250	
2.0	5	4.1405	5.3739	−3.3386	−4.1552	0.4663	0.3219
	6	5.2319		−4.1558		0.4638	
	3	−18.4510		8.8348		−2.8147	
6.0	5	8.3936	9.6048	4.4199	5.2328	−4.3456	−4.4727
	6	9.4751		5.2323		−4.3431	
	3	−138.2300		33.7760		−5.4992	
12.0	5	−122.5900	−120.8100	39.6630	39.6720	−5.4794	−5.9238
	6	−122.5900		39.6630		−5.4794	
	3	−674.3600		71.5620		3.5507	
21.0	5	−643.4900	−639.6300	62.3030	62.3020	3.5507	2.9335
	6	−643.4900		62.3030		3.5507	
	3	−812.9300		−83.7970		27.5210	
31.0	5	−782.0700	−778.1900	−74.5370	−74.5390	27.5210	26.9040
	6	−782.0700		−74.5370		27.5210	
	3	2174.9000		−451.3600		22.2220	
42.0	5	2174.9000	2174.8000	−451.3600	−451.3600	22.2220	22.2220
	6	2174.9000		−451.3600		22.2220	

†3-elements: $h_1 = 16, h_2 = 20, h_3 = 12$. 5-Elements: $h_1 = 8, h_2 = 8, h_3 = 10, h_4 = 10, h_5 = 12$. 6-Elements: $h_1 = 4, h_2 = 4, h_3 = 8, h_4 = 10, h_5 = 10, h_6 = 12$.

Example 5.2.4 (Beam Element with Nodal Hinge)

The last example of this section deals with a beam with an internal hinge (see Fig. 5.2.13). It is not uncommon to find beams with an internal hinge about which the beam is free to rotate. Thus, at the hinge there cannot be any moment and the rotation is *not* continuous across the hinge. To account for the discontinuity in the rotation at a hinge, we must eliminate the rotation associated with the hinge.

Consider a uniform beam element with a hinge at node 2. The element equation is given by Eq. (5.2.17) with the stiffness matrix given in (5.2.18) (with zero foundation modulus, $c_f = 0$)

$$\frac{2EI}{h^3}\left[\begin{array}{cccc:c} 6 & -3h & -6 & -3h & \\ -3h & 2h^2 & 3h & h^2 & \\ -6 & 3h & 6 & 3h & \\ \cdots & \cdots & \cdots & \cdots & \\ -3h & h^2 & 3h & 2h^2 & \end{array}\right]\left\{\begin{array}{c} w_1 \\ \theta_1 \\ w_2 \\ \cdots \\ \theta_2 \end{array}\right\} = \left\{\begin{array}{c} F_1 \\ F_2 \\ F_3 \\ \cdots \\ F_4 \end{array}\right\} \tag{5.2.35}$$

Since the moment at a hinge is zero, we have $Q_4 = 0$ and $F_4 = q_4 + Q_4 = q_4$, which is known. This allows us to eliminate θ_2 (rotation at node 2) using the method discussed in Eqs. (3.2.59)–(3.2.60). Comparing Eq. (5.2.35) with Eq. (3.2.59), we have the following definitions:

$$\mathbf{K}^{11} = \frac{2EI}{h^3}\begin{bmatrix} 6 & -3h & -6 \\ -3h & 2h^2 & 3h \\ -6 & 3h & 6 \end{bmatrix}, \quad \mathbf{K}^{12} = \frac{2EI}{h^3}\begin{Bmatrix} -3h \\ h^2 \\ 3h \end{Bmatrix}, \quad \mathbf{K}^{21} = (\mathbf{K}^{12})^{\mathrm{T}}$$

$$\mathbf{K}^{22} = \frac{4EI}{h}, \quad \mathbf{U}^1 = \begin{Bmatrix} w_1 \\ \theta_1 \\ w_2 \end{Bmatrix}, \quad \mathbf{U}^2 = \theta_2$$

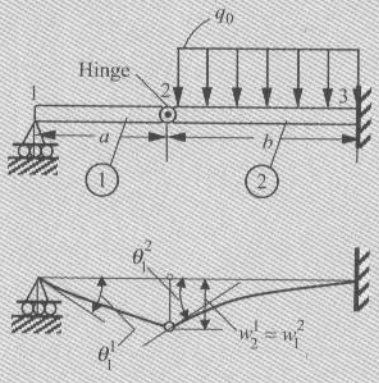

Figure 5.2.13 Compound beam with an internal hinge.

Substituting (3.2.60*c*) for $\mathbf{U}^2 = \theta_2$ into (3.2.60*a*), we obtain

$$\begin{aligned}\hat{\mathbf{K}} &= \mathbf{K}^{11} - \mathbf{K}^{12}\left(\mathbf{K}^{22}\right)^{-1}\mathbf{K}^{21} \\ &= \frac{EI}{h^3}\begin{bmatrix} 12 & -6h & -12 \\ -6h & 4h^2 & 6h \\ -12 & 6h & 12 \end{bmatrix} - \frac{2EI}{h^3}\begin{Bmatrix} -3h \\ h^2 \\ 3h \end{Bmatrix}\frac{h}{4EI}\frac{2EI}{h^3}\left\{-3h\ h^2\ 3h\right\} \\ &= \frac{3EI}{h^3}\begin{bmatrix} 1 & -h & -1 \\ -h & h^2 & h \\ -1 & h & 1 \end{bmatrix}\end{aligned}$$

Thus, the equations for a beam element with a hinge at node 2 can be written as

$$\frac{3EI}{h^3}\begin{bmatrix} 1 & -h & -1 & 0 \\ -h & h^2 & h & 0 \\ -1 & h & 1 & 0 \\ 0 & 0 & 0 & 0 \end{bmatrix}\begin{Bmatrix} w_1 \\ \theta_1 \\ w_2 \\ \theta_2 \end{Bmatrix} = \begin{Bmatrix} F_1 \\ F_2 \\ F_3 \\ 0 \end{Bmatrix} \tag{5.2.36}$$

Similarly, we can derive the element equations for a beam element with hinge at node 1

$$\frac{3EI}{h^3}\begin{bmatrix} 1 & 0 & -1 & -h \\ 0 & 0 & 0 & 0 \\ -1 & 0 & 1 & h \\ -h & 0 & h & h^2 \end{bmatrix}\begin{Bmatrix} w_1 \\ \theta_1 \\ w_2 \\ \theta_2 \end{Bmatrix} = \begin{Bmatrix} F_1 \\ 0 \\ F_3 \\ F_4 \end{Bmatrix} \tag{5.2.37}$$

As a specific example of application of the equations derived, consider the beam in Fig. 5.2.13. We use a two-element mesh, with element 1 having the hinge at its node 2, while element 2 is the usual beam element. The assembled system of equations is

$$EI\begin{bmatrix} \frac{3}{a^3} & -\frac{3}{a^2} & -\frac{3}{a^3} & 0 & 0 & 0 \\ -\frac{3}{a^2} & \frac{3}{a} & \frac{3}{a^2} & 0 & 0 & 0 \\ -\frac{3}{a^3} & \frac{3}{a^2} & \frac{3}{a^3}+\frac{12}{b^3} & -\frac{6}{b^2} & -\frac{12}{b^3} & -\frac{6}{b^2} \\ 0 & 0 & -\frac{6}{b^2} & \frac{4}{b} & \frac{6}{b^2} & \frac{2}{b} \\ 0 & 0 & -\frac{12}{b^3} & \frac{6}{b^2} & \frac{12}{b^3} & \frac{6}{b^2} \\ 0 & 0 & -\frac{6}{b^2} & \frac{2}{b} & \frac{6}{b^2} & \frac{4}{b} \end{bmatrix}\begin{Bmatrix} w_1^1 \\ \theta_1^1 \\ w_2^1 = w_1^2 \\ \theta_1^2 \\ w_2^2 \\ \theta_2^2 \end{Bmatrix} = \begin{Bmatrix} Q_1^1 \\ Q_2^1 \\ Q_3^1 + Q_1^2 \\ Q_4^1 + Q_2^2 \\ Q_3^2 \\ Q_4^2 \end{Bmatrix} + \frac{q_0 b}{12}\begin{Bmatrix} 0 \\ 0 \\ 6 \\ -b \\ 6 \\ b \end{Bmatrix} \tag{5.2.38}$$

Using the boundary conditions

$$w_1^1 = 0,\quad w_2^2 = 0,\quad \theta_2^2 = 0,\quad Q_2^1 = 0,\quad Q_3^1 + Q_1^2 = 0,\quad Q_4^1 + Q_2^2 = 0$$

we obtain the condensed equations

$$EI\begin{bmatrix} \frac{3}{a^3} & \frac{3}{a^2} & 0 \\ \frac{3}{a^2} & \frac{3}{a^3}+\frac{12}{b^3} & -\frac{6}{b^2} \\ 0 & -\frac{6}{b^2} & \frac{4}{b} \end{bmatrix}\begin{Bmatrix} \theta_1^1 \\ w_2^1 = w_1^2 \\ \theta_1^2 \end{Bmatrix} = \frac{q_0 b}{12}\begin{Bmatrix} 0 \\ 6 \\ -b \end{Bmatrix} \tag{5.2.39}$$

and the solution is given by

$$\theta_1^1 = -\frac{q_0 b^4}{8aEI}, \quad w_2^1 = w_1^2 = \frac{q_0 b^4}{8EI}, \quad \theta_2^2 = \frac{q_0 b^3}{2EI}$$

5.3 TIMOSHENKO BEAM ELEMENTS

5.3.1 Governing Equations

Recall that the Euler–Bernoulli beam theory is based on the assumption that plane cross sections remain plane and *normal* to the longitudinal axis after bending [see Fig. 5.3.1(*a*)]. This assumption results in zero transverse shear strain. When the normality assumption is not used, i.e., plane sections remain plane but not necessarily normal to the longitudinal axis after deformation, the transverse shear strain $\gamma_{xz} = 2\varepsilon_{xz}$ is not zero. Therefore, the rotation

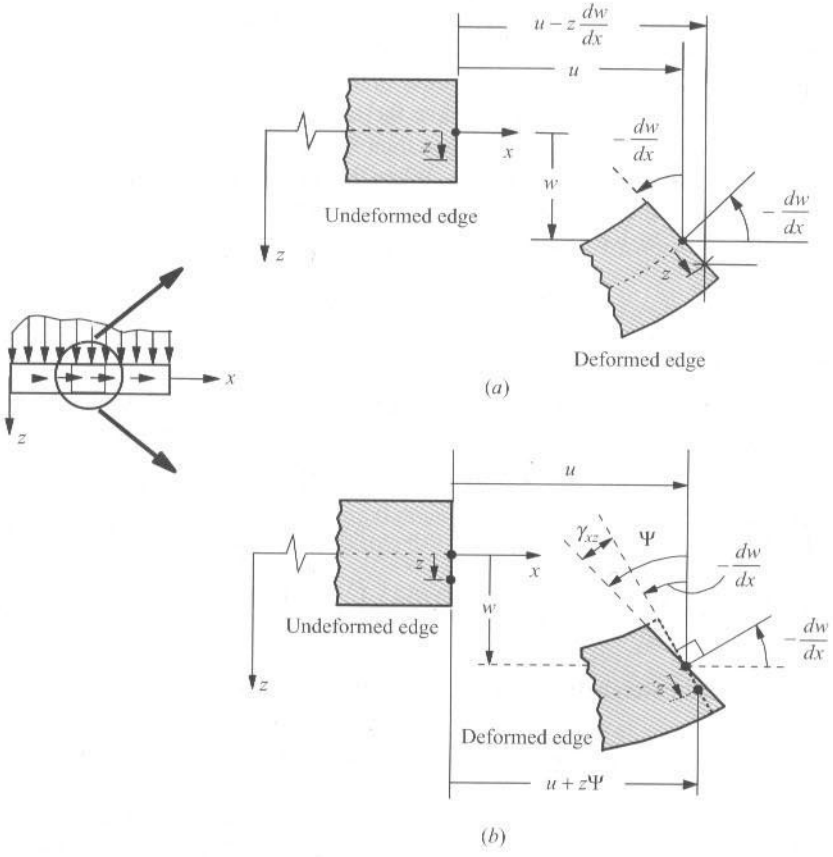

Figure 5.3.1 (*a*) Kinematics of the Euler–Bernoulli beam theory. (*b*) Kinematics of the Timoshenko beam theory where normals before deformation no longer remain normal after deformation.

of a transverse normal plane about the y-axis is not equal to $-dw/dx$ [see Fig. 5.3.1(b)]. Beam theory based on these relaxed assumptions is known as a *shear deformation beam theory*, most commonly known as the *Timoshenko beam theory*. We denote the rotation about the y-axis by an independent function $\Psi(x)$.

The equilibrium equations of the Timoshenko beam theory [see Example 2.4.3; also see Reddy (2002)] are the same as those of the Euler–Bernoulli beam theory (see Fig. 5.2.1), but the kinematic relations are different:

$$-\frac{dV}{dx}+c_f w=q,\quad -\frac{dM}{dx}+V=0,\quad M=EI\frac{d\Psi}{dx},\quad V=GAK_s\left(\frac{dw}{dx}+\Psi\right) \tag{5.3.1}$$

Thus, the governing equations in terms of the deflection w and rotation Ψ become

$$-\frac{d}{dx}\left[GAK_s\left(\Psi+\frac{dw}{dx}\right)\right]+c_f w=q \tag{5.3.2a}$$

$$-\frac{d}{dx}\left(EI\frac{d\Psi}{dx}\right)+GAK_s\left(\Psi+\frac{dw}{dx}\right)=0 \tag{5.3.2b}$$

where G is the shear modulus and K_s is the *shear correction coefficient*, which is introduced to account for the difference in the constant state of shear stress in this theory and the parabolic variation of the shear stress predicted by the elasticity theory through the beam thickness. All other quantities have the same meaning as before. For short and chubby beams (i.e., length-to-height ratio less than 20), $\Psi \neq -(dw/dx)$ and the difference, $\Psi+(dw/dx)$, is the transverse shear strain. When the shear strain is zero (i.e., for long slender beams), substituting the second equation into the first for $GAK_s(\Psi+dw/dx)$ and replacing Ψ with $-dw/dx$, we obtain governing equation (5.2.1) of the Euler–Bernoulli beam theory.

5.3.2 Weak Form

The weak form of Eqs. (5.3.2a) and (5.3.2b) over an element $\Omega^e=(x_a, x_b)$ can be developed using the usual three-step procedure, as already discussed in Example 2.4.3. At the end of the second step (i.e., after integration by parts), we obtain

$$0=\int_{x_a}^{x_b}\left[\frac{dv_1}{dx}GAK_s\left(\Psi+\frac{dw}{dx}\right)+c_f v_1 w-v_1 q\right]dx-\left[v_1 GAK_s\left(\Psi+\frac{dw}{dx}\right)\right]_{x_a}^{x_b}$$

$$0=\int_{x_a}^{x_b}\left[\frac{dv_2}{dx}EI\frac{d\Psi}{dx}+v_2 GAK_s\left(\Psi+\frac{dw}{dx}\right)\right]dx-\left[v_2 EI\frac{d\Psi}{dx}\right]_{x_a}^{x_b}$$

The coefficients of the weight functions v_1 and v_2 in the boundary integrals are, respectively,

$$GAK_s\left(\Psi+\frac{dw}{dx}\right)\equiv V\quad\text{and}\quad EI\frac{d\Psi}{dx}\equiv M \tag{5.3.3}$$

where V is the shear force and M is the bending moment; these coefficients constitute the secondary variables of the weak form. The weight functions v_1 and v_2 must have the physical interpretations such that the products $v_1 V$ and $v_2 M$ have the units of work. Clearly, v_1 must be equivalent to (the variation of) the transverse deflection w, and v_2 must be equivalent to

(the variation of) the rotation function Ψ:

$$v_1 \sim w, \quad v_2 \sim \Psi$$

Hence, the primary variable of the formulation are w and Ψ. Denoting the shear forces and bending moments at the endpoints of the element by the expressions [cf. Eq. (5.2.3)]

$$\begin{aligned} Q_1^e &\equiv -\left[GAK_s\left(\Psi + \frac{dw}{dx}\right)\right]\Big|_{x_a} = -V(x_a) \\ Q_2^e &\equiv -\left(EI\frac{d\Psi}{dx}\right)\Big|_{x_a} = -M(x_a) \\ Q_3^e &\equiv \left[GAK_s\left(\Psi + \frac{dw}{dx}\right)\right]\Big|_{x_b} = V(x_b) \\ Q_4^e &\equiv \left(EI\frac{d\Psi}{dx}\right)\Big|_{x_b} = M(x_b) \end{aligned} \tag{5.3.4}$$

we arrive at the final weak statements of Eqs. (5.3.2a) and (5.3.2b):

$$\begin{aligned} 0 &= \int_{x_a}^{x_b}\left[GAK_s\frac{dv_1}{dx}\left(\Psi + \frac{dw}{dx}\right) + c_f\, v_1 w - v_1 q\right]dx - v_1(x_a)Q_1^e - v_1(x_b)Q_3^e \\ 0 &= \int_{x_a}^{x_b}\left[EI\frac{dv_2}{dx}\frac{d\Psi}{dx} + GAK_s v_2\left(\Psi + \frac{dw}{dx}\right)\right]dx - v_2(x_a)Q_2^e - v_2(x_b)Q_4^e \end{aligned} \tag{5.3.5}$$

We note that Q_i^e have the same meaning as well as sense as in the Euler–Bernoulli beam theory.

We can identify the bilinear and linear forms from the weak forms as

$$\begin{aligned} B((v_1, v_2), (w, \Psi)) &= \int_{x_a}^{x_b}\left[GAK_s\left(\frac{dv_1}{dx} + v_2\right)\left(\Psi + \frac{dw}{dx}\right) + EI\frac{dv_2}{dx}\frac{d\Psi}{dx}\right]dx \\ l((v_1, v_2)) &= \int_{x_a}^{x_b} v_1 q\, dx + v_1(x_a)Q_1^e + v_2(x_a)Q_2^e + v_1(x_b)Q_3^e + v_2(x_b)Q_4^e \end{aligned} \tag{5.3.6}$$

Equations (5.3.5) are equivalent to the statement of the principle of virtual displacements for the Timoshenko beam theory. The total potential energy functional of the isolated beam finite element is given by [see Eq. (2.4.40)]

$$\begin{aligned} \Pi_e(w, \Psi) = \int_{x_e}^{x_{e+1}}&\left[\frac{EI}{2}\left(\frac{d\Psi}{dx}\right)^2 + \frac{GAK_s}{2}\left(\frac{dw}{dx} + \Psi\right)^2 + \frac{1}{2}c_f\, w^2 - wq\right]dx \\ &- w(x_a)Q_1^e - \Psi(x_a)Q_2^e - w(x_b)Q_3^e - \Psi(x_b)Q_4^e \end{aligned} \tag{5.3.7}$$

The first term in the square brackets represents the elastic strain energy due to bending, the second term represents the elastic energy due to the transverse shear deformation, the third is the strain energy stored in the elastic foundation, and the fourth is the work done by the distributed load; the remaining terms account for the work done by the generalized forces Q_i^e in moving through the respective generalized displacements (w, Ψ) at the ends of the element. Once again, the principle of minimum total potential energy, $\delta\Pi_e = 0$, gives the weak forms in Eq. (5.3.5).

5.3.3 General Finite Element Model

A close examination of the terms in (5.3.5) shows that both w and Ψ are differentiated only once with respect to x. Since the primary variables are the dependent unknowns themselves (and do not include their derivatives), the Lagrange interpolation of both w and Ψ is admissible here. The minimum admissible degree of interpolation is linear, so that $dw/dx \neq 0$ and $d\Psi/dx \neq 0$. The variables w and Ψ do not have the same physical units; they can be interpolated, in general, with different degrees of interpolation.

Let us consider Lagrange interpolation of w and Ψ in the form

$$w = \sum_{j=1}^{m} w_j \psi_j^{(1)}, \quad \Psi = \sum_{j=1}^{n} S_j \psi_j^{(2)} \tag{5.3.8}$$

where $\psi_j^{(1)}$ and $\psi_j^{(2)}$ are the Lagrange interpolation functions of degree $m-1$ and $n-1$, respectively. In general, m and n are independent of each other, although $m=n$ is most common. However, when $m=n=2$ (i.e., linear interpolation of both w and Ψ is used; see Fig. 5.3.2), the derivative of w is

$$\left(\frac{dw}{dx}\right)^e = \frac{w_2^e - w_1^e}{h_e}$$

which is elementwise-constant. The rotation Ψ, being linear, is not consistent with that predicted by $w(x)$. For thin beams, the transverse shear deformation is negligible, and we must have $\Psi = -dw/dx$, which requires

$$S_1^e \frac{x_b - x}{h_e} + S_2^e \frac{x - x_a}{h_e} = -\frac{w_2^e - w_1^e}{h_e}$$

or, equivalently (by equating like coefficients on both sides),

$$S_1^e x_b - S_2^e x_a = -(w_2^e - w_1^e), \quad S_2^e - S_1^e = 0$$

which in turn requires

$$S_1^e = S_2^e = -\frac{w_2^e - w_1^e}{h_e} \tag{5.3.9}$$

This implies that $\Psi(x)$ is a constant, i.e., $S_1^e = S_2^e = S^e$:

$$\Psi(x) = S_1^e \frac{x_b - x}{h_e} + S_2^e \frac{x - x_a}{h_e} = S^e \tag{5.3.10}$$

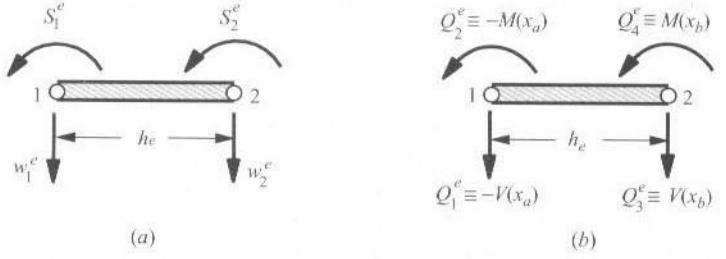

Figure 5.3.2 Linear Timoshenko beam finite element. (*a*) Generalized displacements. (*b*) Generalized forces.

However, a constant state of $\Psi(x)$ is not admissible because the bending energy of the element,

$$\int_{x_a}^{x_b} \frac{EI}{2}\left(\frac{d\Psi}{dx}\right)^2 dx \tag{5.3.11}$$

would be zero. This numerical problem is known in the finite element literature as *shear locking*.

To overcome shear locking, two alternative procedures have been used in the literature:

1. *Consistent interpolation.* Use an approximation of w and Ψ such that dw/dx and Ψ are polynomials of the same degree (i.e., $m = n + 1$).
2. *Reduced integration.* Use equal interpolation (i.e., $m = n$) for w and Ψ and evaluate the bending stiffness coefficients associated with (5.3.11) using a numerical integration rule (to be discussed in Chapter 7) consistent with the actual interpolation of Ψ. However, the stiffness coefficients associated with the shear energy

$$\int_{x_a}^{x_b} \frac{GAK_s}{2}\left(\frac{dw}{dx} + \Psi\right)^2 dx \tag{5.3.12}$$

must be evaluated using a numerical integration rule that treats Ψ as if it is the same order polynomial as dw/dx. Thus, if w and Ψ are approximated with linear polynomials, dw/dx is a constant and Ψ is linear. In evaluating the stiffness terms coming from the shear energy (5.3.12), we must use one-point integration, as dictated by dw/dx and not Ψ. Note that one-point integration in this case is sufficient to evaluate the bending energy exactly but not the shear energy because it is quadratic in Ψ. Thus, it amounts to underintegrating the term. This is known as the *reduced integration* technique.

For illustrative purposes, we take a detailed look at the expression

$$\frac{GAK_s}{2}\int_{x_a}^{x_b}\left(\frac{dw}{dx} + \Psi\right)^2 dx = \frac{GAK_s}{2}\left[\left(\frac{dw}{dx} + \Psi\right)^2\Big|_{x=x_a+h_e/2}\right]h_e$$

where $x = x_a + \frac{1}{2}h_e$ is the midpoint of the element and h_e is its length. Substituting (5.3.8) into this expression (with $m = n = 2$) and equating to zero for thin beams, we obtain

$$\frac{GAK_s h_e}{2}\left(\frac{w_2^e - w_1^e}{h_e} + S_1^e\frac{x_b - x}{h_e} + S_2^e\frac{x - x_a}{h_e}\right)^2\Big|_{x=x_a+h_e/2}$$

$$= \frac{GAK_s h_e}{2}\left(\frac{w_2^e - w_1^e}{h_e} + \frac{S_1^e + S_2^e}{2}\right)^2 = 0 \tag{5.3.13}$$

which is a weaker requirement than (5.3.9), i.e., if (5.3.9) holds, then (5.3.13) also holds, but (5.3.13) does not imply (5.3.9). We note that (5.3.9) must hold only for problems for which the transverse shear energy (5.3.12) is negligible.

In summary, we use either consistent interpolation ($m = n + 1$) or equal interpolation with reduced integration in the evaluation of the transverse shear stiffness coefficients in the Timoshenko beam element. We consider both forms of elements here. First, we complete the finite element model development using the general interpolations given in Eq. (5.3.8) and then discuss the specific choice of interpolations functions used for w and Ψ.

Substitution of (5.3.8) for w and Ψ, and $v_1 = \psi_i^{(1)}$ and $v_2 = \psi_i^{(2)}$ into the weak forms (5.3.5), we obtain the following finite element equations of the Timoshenko beam element:

$$\begin{aligned} 0 &= \sum_{j=1}^{m} K_{ij}^{11} w_j + \sum_{j=1}^{n} K_{ij}^{12} s_j - F_i^1 \quad (i = 1, 2, \ldots, m) \\ 0 &= \sum_{j=1}^{m} K_{ij}^{21} w_j + \sum_{j=1}^{n} K_{ij}^{22} s_j - F_i^2 \quad (i = 1, 2, \ldots, n) \end{aligned} \tag{5.3.14}$$

where

$$\begin{aligned} K_{ij}^{11} &= \int_{x_a}^{x_b} \left(GAK_s \frac{d\psi_i^{(1)}}{dx} \frac{d\psi_j^{(1)}}{dx} + c_f \psi_i^{(1)} \psi_j^{(1)} \right) dx \\ K_{ij}^{12} &= \int_{x_a}^{x_b} GAK_s \frac{d\psi_i^{(1)}}{dx} \psi_j^{(2)} \, dx = K_{ji}^{21} \quad \text{(i.e., } [K^{21}] = [K^{12}]^{\mathrm{T}}\text{)} \\ K_{ij}^{22} &= \int_{x_a}^{x_b} \left(EI \frac{d\psi_i^{(2)}}{dx} \frac{d\psi_j^{(2)}}{dx} + GAK_s \psi_i^{(2)} \psi_j^{(2)} \right) dx \\ F_i^1 &= \int_{x_a}^{x_b} q \psi_i^{(1)} \, dx + Q_{2i-1}, \qquad F_i^2 = Q_{2i} \end{aligned} \tag{5.3.15}$$

In the interest of clarity, the element label e on the quantities is omitted. Equations (5.3.14) can be written in matrix form as

$$\begin{bmatrix} [K^{11}] & [K^{12}] \\ [K^{21}] & [K^{22}] \end{bmatrix} \begin{Bmatrix} \{w\} \\ \{s\} \end{Bmatrix} = \begin{Bmatrix} \{F^1\} \\ \{F^2\} \end{Bmatrix} \tag{5.3.16}$$

The finite element model in (5.3.16) with the coefficients given in (5.3.15) is the most general displacement finite element model of the Timoshenko beam theory. It can be used to obtain a number of special finite element models, as discussed next.

5.3.4 Consistent Interpolation Elements

The first consistent interpolation element (CIE) that we will consider is the one in which quadratic interpolation is used for w and linear interpolation for Ψ so that dw/dx and Ψ are of the same order polynomial (and hence, no shear locking occurs). That is, we select $\psi_i^{(1)}$ to be quadratic polynomials and $\psi_i^{(2)}$ to be linear polynomials. For this choice of interpolation, $[K^{11}]$ is 3×3, $[K^{12}]$ is 3×2, and $[K^{22}]$ is 2×2. The explicit forms of the matrices, when EI and GAK_s are constant, are (note that some of the matrix coefficients are readily available from Chapter 3)

$$[K^{11}] = \frac{G_e A_e K_s}{3h_e} \begin{bmatrix} 7 & -8 & 1 \\ -8 & 16 & -8 \\ 1 & -8 & 7 \end{bmatrix} + \frac{c_f^e h_e}{30} \begin{bmatrix} 4 & 2 & -1 \\ 2 & 16 & 2 \\ -1 & 2 & 4 \end{bmatrix}$$

$$[K^{12}] = \frac{G_e A_e K_s}{6}\begin{bmatrix} -5 & -1 \\ 4 & -4 \\ 1 & 5 \end{bmatrix} = [K^{21}]^{\mathrm{T}}$$

$$[K^{22}] = \frac{EI}{h_e}\begin{bmatrix} 1 & -1 \\ -1 & 1 \end{bmatrix} + \frac{G_e A_e K_s h_e}{6}\begin{bmatrix} 2 & 1 \\ 1 & 2 \end{bmatrix} \tag{5.3.17}$$

When $c_f = 0$, the finite element equations for this choice of interpolation are given by (see Fig. 5.3.3)

$$\frac{GAK_s}{6h_e}\begin{bmatrix} 14 & -16 & 2 & -5h_e & -h_e \\ -16 & 32 & -16 & 4h_e & -4h_e \\ 2 & -16 & 14 & h_e & 5h_e \\ -5h_e & 4h_e & h_e & 2h_e^2\Sigma_e & h_e^2\Theta_e \\ -h_e & -4h_e & 5h_e & h_e^2\Theta_e & 2h_e^2\Sigma_e \end{bmatrix}\begin{Bmatrix} w_1^e \\ w_c^e \\ w_2^e \\ S_1^e \\ S_2^e \end{Bmatrix} = \begin{Bmatrix} q_1^e \\ q_c^e \\ q_2^e \\ 0 \\ 0 \end{Bmatrix} + \begin{Bmatrix} Q_1^e \\ \hat{Q}_c^e \\ Q_3^e \\ Q_2^e \\ Q_4^e \end{Bmatrix} \tag{5.3.18}$$

where

$$\Lambda_e = \frac{E_e I_e}{G_e A_e K_s h_e^2}, \quad \mu_0 = 12\Lambda_e, \quad \Theta_e = 1 - 6\Lambda_e, \quad \Sigma_e = 1 + 3\Lambda_e \tag{5.3.19}$$

$(Q_1^e, Q_2^e, Q_3^e, Q_4^e)$ are the generalized forces defined in Eq. (5.3.4), w_c^e and $\hat{Q}_c^e$ are the deflection and applied external load, respectively, at the center node of the quadratic element, and

$$q_i^e = \int_{x_a}^{x_b} \psi_i^{(1)} q \, dx, \quad (i = 1, 2, \mathrm{c}), \quad \psi_i^{(1)} = \text{quadratic} \tag{5.3.20}$$

This element is designated as CIE-1 (see Fig. 5.3.3).

Note that node c, which is the center node of the element, is not connected to other elements, and the only degree of freedom there is the transverse deflection. Thus, there are different number of degrees of freedom at different nodes of the element, and this therefore complicates the assembly of elements and its implementation on a computer. Hence, we eliminate the node c dependence in the system of element equations by condensing out w_c^e. The second equation of (5.3.18) can be used to express w_c^e in terms of w_1^e, w_2^e, S_1^e, S_2^e, q_c^e,

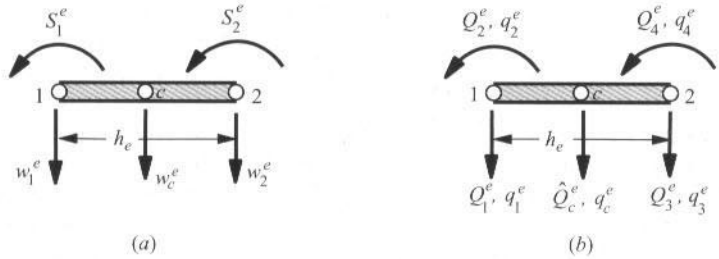

Figure 5.3.3 Consistent interpolation Timoshenko beam element, CIE-1. (*a*) Generalized displacements. (*b*) Generalized forces.

and $\hat{Q}_c^e$:

$$w_c^e = \frac{6h_e}{32G_eA_eK_s}\left(q_c^e + \hat{Q}_c^e\right) + \left(\frac{w_1^e + w_2^e}{2}\right) + h_e\left(\frac{S_2^e - S_1^e}{8}\right) \tag{5.3.21}$$

Substituting for w_c^e from Eq. (5.3.21) into the remaining equations of (5.3.18) [i.e., eliminate w_c^e from Eq. (5.3.18)] and rearranging the equations, we obtain

$$\left(\frac{2E_eI_e}{\mu_0 h_e^3}\right)\begin{bmatrix} 6 & -3h_e & -6 & -3h_e \\ -3h_e & h_e^2(1.5+6\Lambda_e) & 3h_e & h_e^2(1.5-6\Lambda_e) \\ -6 & 3h_e & 6 & 3h_e \\ -3h_e & h_e^2(1.5-6\Lambda_e) & 3h_e & h_e^2(1.5+6\Lambda_e) \end{bmatrix}\begin{Bmatrix} w_1^e \\ S_1^e \\ w_2^e \\ S_2^e \end{Bmatrix} = \begin{Bmatrix} q_1^e + \frac{1}{2}\hat{q}_c^e \\ -\frac{1}{8}\hat{q}_c^e h_e \\ q_2^e + \frac{1}{2}\hat{q}_c^e \\ \frac{1}{8}\hat{q}_c^e h_e \end{Bmatrix} + \begin{Bmatrix} Q_1^e \\ Q_2^e \\ Q_3^e \\ Q_4^e \end{Bmatrix} \tag{5.3.22}$$

where $\hat{q}_c^e = q_c^e + \hat{Q}_c^e$. For simplicity, but without loss of generality, we will assume that $\hat{Q}_c^e = 0$ (i.e., no external point force is placed at the center of the element) so that $\hat{q}_c^e = q_c^e$. Note that the load vector is equivalent to that of the Euler–Bernoulli beam element [see Eq. (5.2.18)]. In fact, for uniform load q, the load vector in Eq. (5.3.22) is identical to the one in (5.2.18). Thus, the CIE-1 element, for all analysis steps, is exactly the same as that shown in Fig. 5.3.2 with the element equations given by (5.3.22). However, one must keep in mind that w and q_i^e are determined by quadratic interpolations functions.

The second consistent interpolation element, denoted CIE-2, is based on Lagrange cubic interpolation of $w(x)$ and quadratic interpolation of $\Psi(x)$. However, this element leads to 7×7 element stiffness matrix with seven degrees of freedom $(w_1^e, w_e^2, w_3^e, w_4^e, S_1^e, S_2^e, S_3^e)$ per element. Elimination of the internal nodal degrees of freedom will result in a 4×4 matrix. Alternatively, the same element can be derived directly by assuming Hermite cubic interpolation of $w(x)$ and a *dependent* quadratic interpolation of $\Psi(x)$. This approach leads to an element that yields, as a special case, the Euler–Bernoulli beam element [see Reddy (1997, 2000)]. The derivation is presented here for the case $c_f^e = 0$.

The exact solution of Eqs. (5.3.2*a*) and (5.3.2*b*) for the homogeneous case (i.e., $q = 0$) and when $c_f = 0$ is

$$w(x) = -\frac{1}{EI}\left(c_1\frac{x^3}{6} + c_2\frac{x^2}{2} + c_3x + c_4\right) + \frac{1}{GAK_s}(c_1x) \tag{5.3.23a}$$

$$EI\Psi(x) = c_1\frac{x^2}{2} + c_2x + c_3 \tag{5.3.23b}$$

where c_1 through c_4 are the constants of integration. Note that the constants c_1, c_2, and c_3 appearing in (5.3.23*b*) are the same as those in Eq. (5.3.23*a*). This suggests that one may use cubic approximation of $w(x)$ and an *interdependent* quadratic approximation of $\Psi(x)$. The resulting finite element model is termed an *interdependent interpolation element* (IIE).

Since the solutions in (5.3.23*a*) and (5.3.23*b*) are valid also for a typical finite element (replace c_i with c_i^e), we proceed to express c_i^e in terms of the nodal values of w and Ψ.

The resulting four relations among $(w_1^e, w_2^e, S_1^e, S_2^e)$ and $(c_1^e, c_2^e, c_3^e, c_4^e)$, when inverted and substituted back into Eqs. (5.3.23*a*) and (5.3.24*b*), give

$$w(x) \approx w_h^e(x) = \sum_{j=1}^{m} \bar{\phi}_j^e \Delta_j^e, \quad \Psi(x) \approx \Psi_h^e(x) = \sum_{j=1}^{n} \varphi_j^e \Delta_j^e \tag{5.3.24a}$$

$$\Delta_1^e = w_1^e, \quad \Delta_2^e = S_1^e, \quad \Delta_3^e = w_2^e, \quad \Delta_4^e = S_2^e \tag{5.3.24b}$$

where $\bar{\phi}_i^e$ and φ_i^e are the approximation functions

$$\begin{aligned}
\bar{\phi}_1^e &= \frac{1}{\mu_e}\left[\mu_e - 12\Lambda_e\bar{x} - (3-2\bar{x})\bar{x}^2\right] \\
\bar{\phi}_2^e &= -\frac{h_e}{\mu_e}\left[(1-\bar{x})^2\bar{x} + 6\Lambda_e(1-\bar{x})\bar{x}\right] \\
\bar{\phi}_3^e &= \frac{1}{\mu_e}\left[(3-2\bar{x})\bar{x}^2 + 12\Lambda_e\bar{x}\right] \\
\bar{\phi}_4^e &= \frac{h_e}{\mu_e}\left[(1-\bar{x})\bar{x}^2 + 6\Lambda_e(1-\bar{x})\bar{x}\right]
\end{aligned} \tag{5.3.25a}$$

$$\begin{aligned}
\varphi_1^e &= \frac{6}{h_e\mu_e}(1-\bar{x})\bar{x} \\
\varphi_2^e &= \frac{1}{\mu_e}(\mu_e - 4\bar{x} + 3\bar{x}^2 - 12\Lambda_e\bar{x}) \\
\varphi_3^e &= -\frac{6}{h_e\mu_e}(1-\bar{x})\bar{x} \\
\varphi_4^e &= \frac{1}{\mu_e}(3\bar{x}^2 - 2\bar{x} + 12\Lambda_e\bar{x})
\end{aligned} \tag{5.3.25b}$$

Here, $\bar{x}$ is the nondimensional local coordinate

$$\bar{x} = \frac{x - x_a}{h_e}, \quad \mu_e = 1 + 12\Lambda_e, \quad \Lambda_e = \frac{E_e I_e}{G_e A_e K_s h_e^2} \tag{5.3.26}$$

Note that the Hermite cubic interpolation functions $\phi_i^e(x)$ of Eq. (5.2.11) are a special case of $\bar{\phi}_i^e$, i.e., ϕ_i^e can be obtained from $\bar{\phi}_i^e$ by setting $\Lambda_e = 0$ (hence, $\mu_e = 1$).

Substitution of Eq. (5.3.24*a*) into the total potential energy functional in (5.3.7) and differentiating it with respect to Δ_i^e yields the finite element model

$$[K^e]\{\Delta^e\} = \{q^e\} + \{Q^e\} \tag{5.3.27a}$$

where

$$\begin{aligned}
K_{ij}^e &= \int_{x_a}^{x_b} \left[E_e I_e \frac{d\varphi_i^e}{dx}\frac{d\varphi_j^e}{dx} + G_e A_e K_s \left(\varphi_i^e + \frac{d\bar{\phi}_i^e}{dx}\right)\left(\varphi_j^e + \frac{d\bar{\phi}_j^e}{dx}\right)\right] dx \\
q_i^e &= \int_{x_a}^{x_b} \bar{\phi}_i^e q(x)\, dx
\end{aligned} \tag{5.3.27b}$$

and Q_i^e have the same meaning as before [see Eq. (5.3.4)]. Equation (5.3.27*a*) has the explicit form

$$\left(\frac{2E_eI_e}{\mu_e h_e^3}\right)\begin{bmatrix} 6 & -3h_e & -6 & -3h_e \\ -3h_e & 2h_e^2\Sigma_e & 3h_e & h_e^2\Theta_e \\ -6 & 3h_e & 6 & 3h_e \\ -3h_e & h_e^2\Theta_e & 3h_e & 2h_e^2\Sigma_e \end{bmatrix}\begin{Bmatrix} w_1^e \\ S_1^e \\ w_2^e \\ S_2^e \end{Bmatrix} = \begin{Bmatrix} q_1^e \\ q_2^e \\ q_3^e \\ q_4^e \end{Bmatrix} + \begin{Bmatrix} Q_1^e \\ Q_2^e \\ Q_3^e \\ Q_4^e \end{Bmatrix} \tag{5.3.28a}$$

where

$$\Lambda_e = \frac{E_eI_e}{G_eA_eK_sh_e^2}, \quad \mu_e = 1 + 12\Lambda_e, \quad \Theta_e = 1 - 6\Lambda_e, \quad \Sigma_e = 1 + 3\Lambda_e \tag{5.3.28b}$$

For uniformly distributed load, $q(x) = q_0$, the load vector in (5.3.27*b*) yields

$$\{q^e\} = \frac{q_0h_e}{12}\begin{Bmatrix} 6 \\ -h_e \\ 12 \\ h_e \end{Bmatrix} \tag{5.3.28c}$$

which is exactly the same as that in the Euler–Bernoulli beam element (EBE). Of course, for nonuniform loads the load vectors of the two elements are different.

In the thin beam limit (i.e., $\Lambda_e \to 0$), Eq. (5.3.28*a*) reduces to the EBE equations (5.2.17) and (5.2.18) (with $c_f^e = 0$). The IIE element leads to the exact nodal values for any distribution of the transverse load $q(x)$ provided that the bending stiffness EI and shear stiffness K_sGA are elementwise constant (and $c_f = 0$). Such an element is said to be *superconvergent*. Note that the bar element and EBE are also superconvergent elements (i.e., bar element, IIE, and EBE yield exact nodal values of the respective theories).

5.3.5 Reduced Integration Element

When equal interpolation of $w(x)$ and $\Psi(x)$ is used ($m = n$), all submatrices in (5.3.16) are of the same order: $n \times n$, where n is the number of terms in the polynomial (or $n - 1$ is the degree of interpolation). The element coefficient matrices K_{ij}^{11}, K_{ij}^{12} as well as the first part of K_{ij}^{22} must be evaluated exactly. The second part of K_{ij}^{22} is to be evaluated using reduced integration. For the choice of linear interpolation functions, and for elementwise constant values of GAK_s and EI, the matrices have the following explicit values (when $c_f^e = 0$):

$$\begin{aligned} [K^{11}] &= \frac{G_eA_eK_s}{h_e}\begin{bmatrix} 1 & -1 \\ -1 & 1 \end{bmatrix}, \quad [K^{12}] = \frac{G_eA_eK_s}{2}\begin{bmatrix} -1 & -1 \\ 1 & 1 \end{bmatrix} \\ [K^{22}] &= \frac{E_eI_e}{h_e}\begin{bmatrix} 1 & -1 \\ -1 & 1 \end{bmatrix} + \frac{G_eA_eK_sh_e}{4}\begin{bmatrix} 1 & 1 \\ 1 & 1 \end{bmatrix} \end{aligned} \tag{5.3.29}$$

where one-point integration is used to evaluate the second part of $[K^{22}]$. Note that $[K^{11}]$, $[K^{12}]$, and the first part of $[K^{22}]$ can be evaluated exactly with one-point quadrature (i.e., numerical integration) when EI and GAK_s are constant because the integrands of these coefficients are constant. Hence, one-point integration for $[K^{\alpha\beta}]$ satisfies all the requirements. The resulting beam element is termed the reduced integration element (RIE).

The element equations of the RIE are ($\alpha_e = 4E_eI_e/G_eA_eK_s$)

$$\frac{G_eA_eK_s}{4h_e}\begin{bmatrix} 4 & -2h_e & -4 & -2h_e \\ -2h_e & h_e^2+\alpha_e & 2h_e & h_e^2-\alpha_e \\ -4 & 2h_e & 4 & 2h_e \\ -2h_e & h_e^2-\alpha_e & 2h_e & h_e^2+\alpha_e \end{bmatrix}\begin{Bmatrix} w_1^e \\ S_1^e \\ w_2^e \\ S_2^e \end{Bmatrix} = \begin{Bmatrix} Q_1^e \\ Q_2^e \\ Q_3^e \\ Q_4^e \end{Bmatrix} + \begin{Bmatrix} q_1^e \\ 0 \\ q_2^e \\ 0 \end{Bmatrix} \tag{5.3.30a}$$

or, in alternative form (to resemble those of the EBE)

$$\frac{2E_eI_e}{\mu_0 h_e^3}\begin{bmatrix} 6 & -3h_e & -6 & -3h_e \\ -3h_e & h_e^2(1.5+6\Lambda_e) & 3h_e & h_e^2(1.5-6\Lambda_e) \\ -6 & 3h_e & 6 & 3h_e \\ -3h_e & h_e^2(1.5-6\Lambda_e) & 3h_e & h_e^2(1.5+6\Lambda_e) \end{bmatrix}\begin{Bmatrix} w_1^e \\ S_1^e \\ w_2^e \\ S_2^e \end{Bmatrix} = \begin{Bmatrix} q_1^e \\ 0 \\ q_2^e \\ 0 \end{Bmatrix} + \begin{Bmatrix} Q_1^e \\ Q_2^e \\ Q_3^e \\ Q_4^e \end{Bmatrix} \tag{5.3.30b}$$

where

$$q_i^e = \int_{x_a}^{x_b} \psi_i^e q\, dx, \quad (i=1,2) \tag{5.3.31}$$

$$\Lambda_e = \frac{E_eI_e}{G_eA_eK_sh_e^2}, \quad \mu_0 = 12\Lambda_e \tag{5.3.32}$$

and ψ_i are the linear interpolation functions.

It is interesting to note that the element stiffness matrix (5.3.30*b*) of the linear RIE is the same as that of the CIE-1 in (5.3.22) obtained using quadratic approximation of w and linear approximation of Ψ. The only difference is the load representation. In CIE-1, the load vector is equivalent to that of the Euler–Bernoulli beam theory, whereas in RIE it is based on (5.3.31), which contributes only to the force degrees of freedom and not to the moment degrees of freedom.

The quadratic interpolation of both w and Ψ with full integration of the element coefficient matrices also suffers slightly from the shear-locking phenomenon. A uniform two-point quadrature rule has the desired effect on $[K^{11}]$, $K^{12}]$, and $[K^{22}]$, i.e., $[K^{11}]$, $[K^{12}]$, and the first term of $[K^{22}]$ will be evaluated exactly and the second term of $[K^{22}]$ approximately. As the degree of approximation and/or the number of elements in the mesh is increased, shear locking will disappear and reduced integration is not necessary.

5.3.6 Numerical Examples

Example 5.3.1

Consider a simply supported beam under distributed transverse load of intensity q_0. The following data is used in computing the numerical values:

$$E = 10^6,\ \nu = 0.25,\ K_s = \frac{5}{6},\ q_0 = 1,\ I = \frac{bH^3}{12},\ A = bH,\ b = 1$$

Table 5.3.1 Comparison of the finite element solutions with the exact maximum deflection and rotation of a simply supported isotropic beam of Example 5.3.1.

Element	$N^*=1$	$N=2$	$N=4$	$N=1$	$N=2$	$N=4$
	$w(L/2)\times(EH^3/q_0L^4)$			$-\Psi(0)\times 10^3$		
	Uniform load $(L/H=10)$					
RIE	0.09750	0.14438	0.15609	0.37500	0.46875	0.49219
CIE-1	0.12875	0.15219	0.15805	0.50000	0.50000	0.50000
IIE†	0.16000	0.16000	0.16000	0.50000	0.50000	0.50000
EBE†	0.15625	0.15625	0.15625	0.50000	0.50000	0.50000
	Uniform load $(L/H=100)$					
RIE	0.09379	0.14066	0.15238	0.37500	0.46875	0.49219
CIE-1	0.12504	0.14847	0.15433	0.50000	0.50000	0.50000
IIE†	0.15629	0.15629	0.15629	0.50000	0.50000	0.50000
EBE†	0.15625	0.15625	0.15625	0.50000	0.50000	0.50000
	Sinusoidal load $(L/H=100)$					
RIE	0.07639	0.11079	0.12007	0.30543	0.36702	0.38204
CIE-1	0.09679	0.11682	0.12163	0.38705	0.38702	0.38702
IIE†	0.12322	0.12322	0.12322	0.38702	0.38702	0.38702
EBE†	0.12319	0.12319	0.12319	0.38702	0.38702	0.38702

*N is the number of elements used in the half beam.
†Exact values compared to the respective beam theories.

Two different beam length-to-height ratios, $L/H=10$ and $L/H=100$, are considered. Table 5.3.1 shows a comparison of the finite element solutions obtained with one, two, and four elements in half beam with the exact beam solutions for two different types of loads, namely, uniform load and sinusoidal load. The exact solutions according to the two theories are given below [see Wang et al. (2000)].

Euler–Bernoulli Beam Theory

$$\begin{aligned} &\textit{Uniform Load} && w^E(x)=\frac{q_0L^4}{24EI}\left(\bar{x}-2\bar{x}^3+\bar{x}^4\right)\\ &\textit{Sinusoidal Load} && w^E(x)=\frac{16q_0L^4}{\pi EI}\sin\pi\bar{x},\ \bar{x}=\frac{x}{L}\end{aligned} \tag{5.3.33}$$

Timoshenko Beam Theory

Uniform Load

$$\begin{aligned} w^T(x)&=\left[w^E(x)+\frac{1}{GAK_s}M^E(x)\right]=\frac{q_0L^4}{24EI}\left(\bar{x}-2\bar{x}^3+\bar{x}^4\right)+\frac{q_0L^2}{2GAK_s}\left(\bar{x}-\bar{x}^3\right)\\ \Psi(x)&=-\frac{dw^E}{dx}=-\frac{q_0L^3}{24EI}\left(1-6\bar{x}^2+4\bar{x}^3\right),\quad \bar{x}=\frac{x}{L}\end{aligned} \tag{5.3.34}$$

Sinusoidal Load

$$\begin{aligned} w^T(x)&=\left[w^E(x)+\frac{1}{GAK_s}M^E(x)\right]=\left(\frac{16q_0L^4}{\pi EI}+\frac{16\pi q_0L^2}{GAK_s}\right)\sin\pi\bar{x}\\ \Psi(x)&=-\frac{dw^E}{dx}=-\frac{16q_0L^3}{EI}\cos\pi\bar{x},\quad \bar{x}=\frac{x}{L}\end{aligned} \tag{5.3.35}$$

where the superscripts E and T refer to the Euler–Bernoulli and Timoshenko beam theories, respectively. Clearly, more than two elements of CIE-1 and RIE are required to obtain acceptable solutions. On the other hand, IIE yields exact nodal values with one element (because it is a superconvergent element).

Example 5.3.2

Consider the cantilever beam of Example 5.2.1. We wish to analyze the problem using various Timoshenko beam finite elements. The problem data is given in (5.2.33); $\nu = 0.25$, $K_s = 5/6$. The exact solution of the problem according to the Timoshenko beam theory is given by [see Wang et al. (2000)]

$$w^T(x) = w^E(x) + GAK_s\left[M^E(x) - M^E(0)\right], \quad \Psi(x) = -\frac{dw^E}{dx}$$

where again the superscripts E and T refer to the Euler–Bernoulli and Timoshenko beam theories, respectively. Table 5.3.2 contains the end deflection $w(L)$ and end rotation $\Psi(L)$ for two, four, and eight elements in full beam.

To further understand the effect of shear locking, we consider Timoshenko beam elements with equal interpolation of w and Ψ. Linear as well as quadratic elements with and without reduced integration are tested and the results are included in Table 5.3.3. It is clear that the *full integration elements* (FIEs) produce erroneous results, implying that shear locking is present. Shear locking gradually vanishes as the mesh is refined with either linear elements or quadratic elements.

The following general observations can be made about various finite element models based on the Timoshenko beam theory:

1. The RIE exhibits less locking compared with the FIE.
2. As the number of elements in the mesh is increased or the degree of approximation is increased (i.e., higher-order elements are used), the finite element solutions obtained by both RIE and FIE improve; i.e., the effect of locking is reduced with mesh refinements and with the use of higher-order elements.

Table 5.3.2 Comparison of the finite element solutions obtained with various types of finite elements for the cantilever beam of Example 5.3.2.

	$w(L)$ (m)				$-\Psi(L)$			
N	EBE	RIE	CIE-1	IIE	EBE	RIE	CIE-1	IIE
Thin beam, $H = 0.0703$ (w and Ψ)								
2	0.1043	0.0995	0.0974	0.1043	0.0512	0.0524	0.0512	0.0512
4	0.1043	0.1031	0.1026	0.1043	0.0512	0.0515	0.0512	0.0512
8	0.1043	0.1040	0.1039	0.1043	0.0512	0.0513	0.0512	0.0512
Thick beam, $H = 0.3$ ($w \times 10^2$ and $\Psi \times 10^3$)								
2	0.1344	0.1293	0.1265	0.1355	0.6600	0.6750	0.6600	0.6600
4	0.1344	0.1340	0.1332	0.1355	0.6600	0.6638	0.6600	0.6600
8	0.1344	0.1351	0.1349	0.1355	0.6600	0.6609	0.6600	0.6600

† For EBE, $\Psi = \theta \equiv -dw/dx$.

Table 5.3.3 Effect of reduced integration of transverse shear coefficients on the deflections of the cantilever beam of Example 5.3.2.

	Linear			Quadratic		
Element	$N=2$	$N=4$	$N=8$	$N=1$	$N=2$	$N=4$
Thin beam, $H=0.0703$ (exact $w=0.1043$)						
RIE $(2\times 1)^{\dagger}$	0.0995	0.1031	0.1040	0.1048	0.1043	0.1043
FIE (2×2)	0.0007	0.0027	0.0100	0.0771	0.0976	0.1028
Thick beam, $H=0.3$ (exact $w\times 10^2=0.1355$)						
RIE (3×2)	0.1293	0.1340	0.1351	0.1361	0.1355	0.1355
FIE (3×3)	0.0148	0.0442	0.0892	0.1048	0.1299	0.1348

† Gauss integration rule used to evaluate bending and shear terms.

3. The IIE (i.e., Hermite cubic approximation of w and a dependent quadratic approximation of Ψ) with full integration yields exact nodal values.
4. The element with quadratic approximation of both w and Ψ and reduced integration of the coefficients yields more accurate results than the CIE with quadratic approximation of w and the linear approximation of Ψ and with full integration of the coefficients.
5. The IIE is the best element for the analysis of bending beams as it contains the EBE as a special case; IIE automatically takes into account the transverse shear deformation if it is significant.

5.4 PLANE FRAME ELEMENTS

5.4.1 Introductory Comments

Recall that a bar element oriented arbitrarily in a plane is called a truss element. A plane truss element contains two degrees of freedom per node (u, v), an axial (u) and transverse displacement (v). By definition, a bar element can carry only axial loads and deform axially, whereas beams can take transverse loads and bending moments about an axis perpendicular to the plane of the member. A superposition of bar and beam degrees of freedom gives a finite element that is known as a frame element (see Fig. 5.4.1). Members of a frame structure are connected by rigid connections (e.g., welded or riveted), and therefore axial and transverse forces and bending moments are developed in the members. The objective of this section is to formulate a frame finite element, with the help of the developments from Sections 4.6, 5.2, and 5.3.

5.4.2 Frame Element

In many truss and frame structures, the bar and beam structural elements are found in many different orientations (see, for example, Fig. 4.6.1). Analysis of such structures for displacements and stresses requires the setting up of a global coordinate system and referencing all quantities (i.e., displacements, forces, and stiffnesses) of individual elements to the common (global) coordinate system in order to assemble the elements and impose boundary conditions on the whole structure.

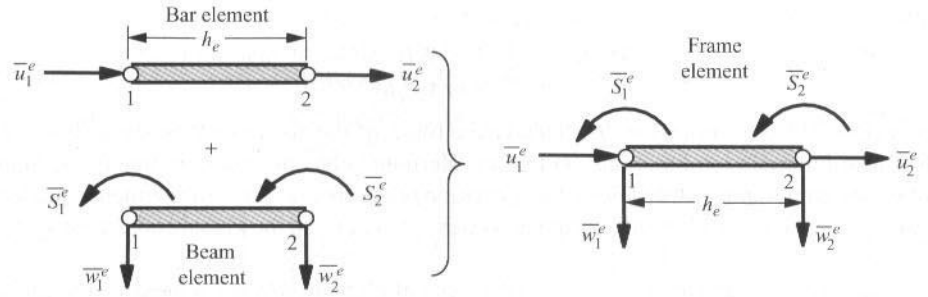

Figure 5.4.1 Superposition of bar and beam element to obtain a frame element [degrees of freedom are referred to the element coordinate system $(\bar{x}, \bar{y}, \bar{z})$].

A superposition of the bar element of Section 4.6 with the EBE of Section 5.2 or the Timoshenko beam element (RIE, CIE, or IIE) of Section 5.3 gives a frame element with three primary degrees of freedom (u, w, S) per node (note that the transverse displacement v of Section 4.6 is now denoted by w to be consistent with Sections 5.2 and 5.3). When the axial stiffness EA and bending stiffness EI are elementwise constant, the superposition of the linear bar element with the IIE gives the following element equations (see Fig. 5.4.1):

$$[\bar{K}]^e\{\bar{\Delta}\}^e = \{\bar{F}\}^e \tag{5.4.1a}$$

or, in explicit form,

$$\frac{2EI}{\mu_0 h^3}\begin{bmatrix} \mu & 0 & 0 & -\mu & 0 & 0 \\ 0 & 6 & -3h & 0 & -6 & -3h \\ 0 & -3h & h^2(1.5+6\Lambda) & 0 & 3h & h^2(1.5-6\Lambda) \\ -\mu & 0 & 0 & \mu & 0 & 0 \\ 0 & -6 & 3h & 0 & 6 & 3h \\ 0 & -3h & h^2(1.5-6\Lambda) & 0 & 3h & h^2(1.5+6\Lambda) \end{bmatrix}^e \begin{Bmatrix} \bar{u}_1 \\ \bar{w}_1 \\ \bar{S}_1 \\ \bar{u}_2 \\ \bar{w}_2 \\ \bar{S}_2 \end{Bmatrix}^e = \begin{Bmatrix} \bar{F}_1 \\ \bar{F}_2 \\ \bar{F}_3 \\ \bar{F}_4 \\ \bar{F}_5 \\ \bar{F}_6 \end{Bmatrix}^e \tag{5.4.1b}$$

where

$$\begin{Bmatrix} \bar{F}_1 \\ \bar{F}_2 \\ \bar{F}_3 \\ \bar{F}_4 \\ \bar{F}_5 \\ \bar{F}_6 \end{Bmatrix}^e = \begin{Bmatrix} \bar{f}_1 \\ \bar{q}_1 \\ \bar{q}_2 \\ \bar{f}_2 \\ \bar{q}_3 \\ \bar{q}_4 \end{Bmatrix}^e + \begin{Bmatrix} \bar{Q}_1 \\ \bar{Q}_2 \\ \bar{Q}_3 \\ \bar{Q}_4 \\ \bar{Q}_5 \\ \bar{Q}_6 \end{Bmatrix}^e \tag{5.4.2a}$$

$$\bar{f}_i = \int_0^{h_e} f^e(\bar{x})\psi_i^e(\bar{x})\,d\bar{x} \quad (i=1,2), \quad \bar{q}_i = \int_0^{h_e} q^e(\bar{x})\phi_i^e(\bar{x})\,d\bar{x} \quad (i=1,2,3,4) \tag{5.4.2b}$$

and

$$\mu = \frac{A\mu_0 h^2}{2I}, \quad \Lambda = \frac{EI}{GAK_s h^2}, \quad \mu_0 = 12\Lambda \tag{5.4.3}$$

In Eq. (5.4.2*b*), f^e denotes the distributed axial force, q^e the distributed transverse force, ψ_i^e the linear interpolation functions, and ϕ_i^e the Hermite cubic interpolation functions. In the following paragraphs, we develop transformation relations to express the element equations (5.4.1*b*)—valid in the element coordinate system $(\bar{x}, \bar{y}, \bar{z})$—to the global coordinate system (x, y, z).

The local coordinates $(\bar{x}_e, \bar{y}_e, \bar{z}_e)$ of a typical element Ω_e are related to the global coordinates (x, y, z) by [cf. Eq. (4.6.2)]

$$\begin{Bmatrix} \bar{x} \\ \bar{y} \\ \bar{z} \end{Bmatrix}^e = \begin{bmatrix} \cos\alpha & 0 & \sin\alpha \\ 0 & 1 & 0 \\ -\sin\alpha & 0 & \cos\alpha \end{bmatrix}^e \begin{Bmatrix} x \\ y \\ z \end{Bmatrix} \tag{5.4.4}$$

where the angle α_e is measured clockwise from the global x-axis to the element $\bar{x}_e$-axis. Note that the y and $\bar{y}_e$ coordinates are parallel to each other, and they are *out of* the plane of the paper (see Fig. 5.4.2). The same transformation relations hold for displacements (u, w) along the global coordinates (x, z) and displacements $(\bar{u}, \bar{w})$ in the local coordinates

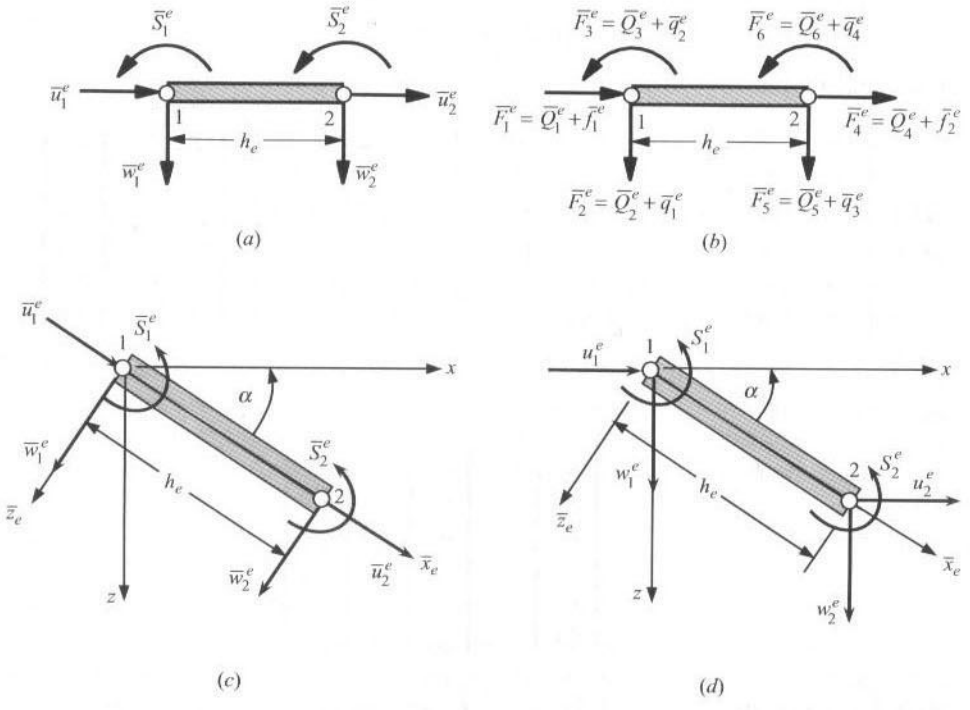

Figure 5.4.2 (*a*) Generalized displacements. (*b*) Generalized forces. (*c*) Generalized displacements in the element coordinates. (*d*) Generalized displacements in the global coordinates.

$(\bar{x}, \bar{z})$. Note that there is no displacement in the direction of the coordinate y (i.e., $v = 0$). However, there is a rotation about the y-axis, and it remains the same in both coordinate systems because $y = \bar{y}$. Note that rotation θ is equal to $-dw/dx$ in Euler–Bernoulli beam theory and it is equal to Ψ in Timoshenko beam theory. Hence, the relationship between (u, w, θ) and $(\bar{u}, \bar{w}, \bar{\theta})$ can be written as

$$\begin{Bmatrix} \bar{u} \\ \bar{w} \\ \bar{\theta} \end{Bmatrix}^e = \begin{bmatrix} \cos\alpha & \sin\alpha & 0 \\ -\sin\alpha & \cos\alpha & 0 \\ 0 & 0 & 1 \end{bmatrix}^e \begin{Bmatrix} u \\ w \\ \theta \end{Bmatrix}^e \tag{5.4.5}$$

Therefore, the three nodal degrees of freedom $(\bar{u}_i^e, \bar{w}_i^e, \bar{S}_i^e)$ at the ith node $(i = 1, 2)$ in the $(\bar{x}, \bar{y}, \bar{z})$ system are related to the three degrees of freedom (u_i^e, w_i^e, S_i^e) in the (x, y, z) system by

$$\begin{Bmatrix} \bar{u}_1 \\ \bar{w}_1 \\ \bar{S}_1 \\ \bar{u}_2 \\ \bar{w}_2 \\ \bar{S}_2 \end{Bmatrix}^e = \begin{bmatrix} \cos\alpha & \sin\alpha & 0 & & & \\ -\sin\alpha & \cos\alpha & 0 & & \mathbf{0} & \\ 0 & 0 & 1 & & & \\ & & & \cos\alpha & \sin\alpha & 0 \\ & \mathbf{0} & & -\sin\alpha & \cos\alpha & 0 \\ & & & 0 & 0 & 1 \end{bmatrix}^e \begin{Bmatrix} u_1 \\ w_1 \\ S_1 \\ u_2 \\ w_2 \\ S_2 \end{Bmatrix}^e \tag{5.4.6a}$$

or

$$\{\bar{\Delta}^e\} = [T^e]\{\Delta^e\} \tag{5.4.6b}$$

Analogously, the element force vectors in the local and global coordinate systems are related according to

$$\{\bar{F}\}^e = [T]^e\{F\}^e \tag{5.4.7}$$

Returning to Eq. (5.4.1a), we substitute the transformation equations (5.4.6b) and (5.4.7) into (5.4.1a) and obtain

$$[\bar{K}]^e[T]^e\{\Delta\}^e = [T]^e\{F\}^e$$

Premultiplying both sides with $[T]^{-1} = [T]^{\mathrm{T}}$, we obtain

$$[T]^{\mathrm{T}}[\bar{K}]^e[T]^e\{\Delta\}^e = \{F\}^e \quad \text{or} \quad [K]^e\{\Delta\}^e = \{F\}^e \tag{5.4.8}$$

where

$$[K^e] = [T]^{\mathrm{T}}[\bar{K}]^e[T]^e, \quad \{F\}^e = [T]^{\mathrm{T}}\{\bar{F}\}^e \tag{5.4.9}$$

Thus, if we know the element matrices $[\bar{K}]^e$ and $\{\bar{F}\}^e$ of an element Ω_e in the local coordinate system $(\bar{x}, \bar{y}, \bar{z})$, the element matrices in the global coordinate system are obtained by (5.4.9).

Using $[\bar{K}]^e$ and $\{\bar{F}\}^e$ from Eq. (5.4.1b) in (5.4.9) and carrying out the indicated matrix multiplications, we arrive at the following element stiffness matrix $[K^e]$ referred to the

global coordinates:

$$[K]^e = \frac{2EI}{\mu_0 h^3}\begin{bmatrix} \mu\cos^2\alpha + 6\sin^2\alpha & (\mu-6)\cos\alpha\sin\alpha & 3h\sin\alpha \\ (\mu-6)\cos\alpha\sin\alpha & \mu\sin^2\alpha + 6\cos^2\alpha & -3h\cos\alpha \\ 3h\sin\alpha & -3h\cos\alpha & h^2(1.5+6\Lambda) \\ -(\mu\cos^2\alpha + 6\sin^2\alpha) & -(\mu-6)\sin\alpha\cos\alpha & -3h\sin\alpha \\ -(\mu-6)\cos\alpha\sin\alpha & -(\mu\sin^2\alpha + 6\cos^2\alpha) & 3h\cos\alpha \\ 3h\sin\alpha & -3h\cos\alpha & h^2(1.5-6\Lambda) \end{bmatrix}$$

$$\begin{bmatrix} -(\mu\cos^2\alpha + 6\sin^2\alpha) & -(\mu-6)\cos\alpha\sin\alpha & 3h\sin\alpha \\ -(\mu-6)\sin\alpha\cos\alpha & -(\mu\sin^2\alpha + 6\cos^2\alpha) & -3h\cos\alpha \\ -3h\sin\alpha & 3h\cos\alpha & h^2(1.5-6\Lambda) \\ (\mu\cos^2\alpha + 6\sin^2\alpha) & (\mu-6)\cos\alpha\sin\alpha & -3h\sin\alpha \\ (\mu-6)\cos\alpha\sin\alpha & \mu\sin^2\alpha + 6\cos^2\alpha & 3h\cos\alpha \\ -3h\sin\alpha & 3h\cos\alpha & h^2(1.5+6\Lambda) \end{bmatrix} \tag{5.4.10a}$$

$$\{F\}^e = \begin{Bmatrix} F_1 \\ F_2 \\ F_3 \\ F_4 \\ F_5 \\ F_6 \end{Bmatrix}^e = \begin{Bmatrix} \bar{F}_1\cos\alpha - \bar{F}_2\sin\alpha \\ \bar{F}_1\sin\alpha + \bar{F}_2\cos\alpha \\ \bar{F}_3 \\ \bar{F}_4\cos\alpha - \bar{F}_5\sin\alpha \\ \bar{F}_4\sin\alpha + \bar{F}_5\cos\alpha \\ \bar{F}_6 \end{Bmatrix}^e \tag{5.4.10b}$$

which is the element force vector referred to the global coordinates.

Example 5.4.1

The frame structure shown in Fig. 5.4.3 is to be analyzed for displacements and forces. Both members of the structure are made of the same material (E) and have the same geometric properties (A, I). The element stiffness matrices and force vectors in the global coordinate system (x, y, z) can be computed from (5.4.10a) and (5.4.10b). The geometric and material properties of each element are as follows (f is the axial and q is the transverse distributed load).

Element 1.

$$L = 144 \text{ in.}, \quad A = 10 \text{ in.}^2, \quad I = 10 \text{ in.}^2, \quad \cos\alpha_1 = 0.0, \quad \sin\alpha_1 = -1.0$$
$$E = 10^6 \text{ psi}, \quad f^{(1)} = 0, \quad q^{(1)} = \frac{P}{72} \text{ lb/in.} \tag{5.4.11}$$

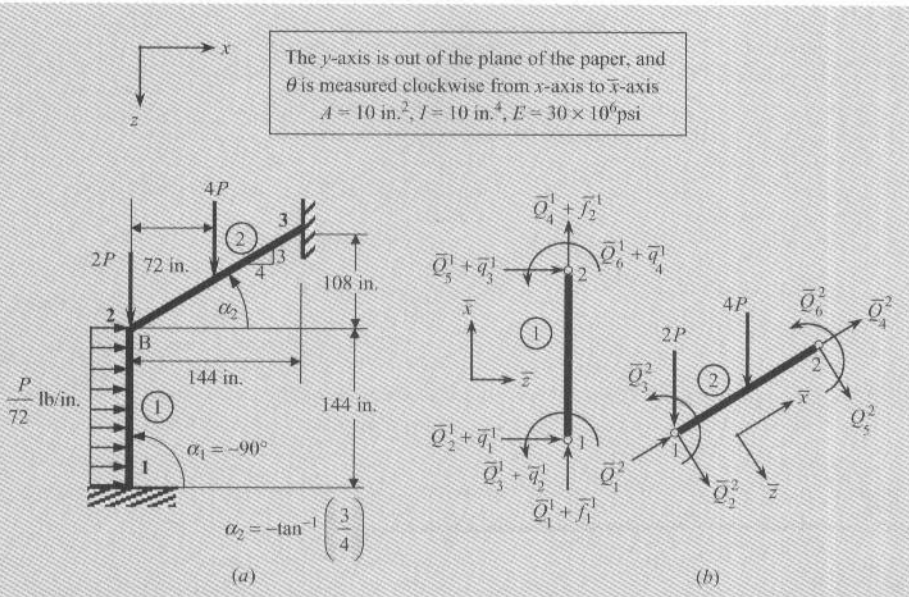

Figure 5.4.3 (*a*) Geometry and loading, and (*b*) member forces in the plane frame structure of Example 5.4.1.

$$[K^1] = 10^5 \begin{bmatrix} 0.0004 & 0.0000 & -0.0289 & -0.0004 & 0.0000 & -0.0289 \\ 0.0000 & 0.6944 & 0.0000 & 0.0000 & -0.6944 & 0.0000 \\ -0.0289 & 0.0000 & 2.7778 & 0.0289 & 0.0000 & 1.3889 \\ -0.0004 & 0.0000 & 0.0289 & 0.0004 & 0.0000 & 0.0289 \\ 0.0000 & -0.6944 & 0.0000 & 0.0000 & 0.6944 & 0.0000 \\ -0.0289 & 0.0000 & 1.3889 & 0.0289 & 0.0000 & 2.7778 \end{bmatrix}$$

$$\{f^1\} = P\{1.0 \quad 0.0 \quad -24.0 \quad 1.0 \quad 0.0 \quad 24.0\}^{\mathrm{T}}$$

Element 2.

$$L = 180 \text{ in.}, \quad A = 10 \text{ in.}^2, \quad I = 10 \text{ in.}^2, \quad \cos\alpha_2 = 0.8, \quad \sin\alpha_2 = -0.6$$
$$E = 10^6 \text{ psi}, \quad f^{(2)} = 0, \quad q^{(2)} = 0 \tag{5.4.12}$$

The load $F_0 = 4P$ at the center of the element ($\cos\alpha = -0.6$ and $\sin\alpha = 0.8$) is distributed to the nodes according to Eq. (5.2.20).

$$[K^2] = 10^5 \begin{bmatrix} 0.3556 & -0.2666 & -0.0111 & -0.3556 & 0.2666 & -0.0111 \\ -0.2666 & 0.2001 & -0.0148 & 0.2666 & -0.2001 & -0.0148 \\ -0.0111 & 0.0148 & 2.2222 & 0.0111 & 0.0148 & 1.1111 \\ -0.3556 & 0.2666 & 0.0111 & 0.3556 & -0.2666 & 0.0111 \\ 0.2666 & -0.2001 & 0.0148 & -0.2666 & 0.2001 & 0.0148 \\ -0.0111 & -0.0148 & 1.1111 & 0.0111 & 0.0148 & 2.2222 \end{bmatrix}$$

$$\{f^2\} = P\{0.0 \quad 2.0 \quad -72.0 \quad 0.0 \quad 2.0 \quad 72.0\}^{\mathrm{T}}$$

The assembled stiffness matrix and force vectors are obtained by superposing the last three rows and columns of element 1 to the first three rows and columns of element 2, i.e., the 3×3 submatrix associated with rows and columns 4, 5, and 6 of element 1, and the 3×3 submatrix associated with rows and columns 1, 2, and 3 of element 2 overlap in the global stiffness matrix.

The known geometric boundary conditions are

$$U_1 = 0, \quad U_2 = 0, \quad U_3 = 0, \quad U_7 = 0, \quad U_8 = 0, \quad U_9 = 0 \tag{5.4.13a}$$

The force boundary conditions are

$$Q_4^1 + Q_1^2 = 0, \quad Q_5^1 + Q_2^2 = 2P, \quad Q_6^1 + Q_3^2 = 0 \tag{5.4.13b}$$

Since all specified values of the known boundary conditions on the primary variables are zero, the condensed equations for the unknown generalized displacement degrees of freedom are

$$10^5 \begin{bmatrix} 0.3560 & -0.2666 & 0.0178 \\ -0.2666 & 0.8946 & -0.0148 \\ 0.0178 & -0.0148 & 5.0000 \end{bmatrix} \begin{Bmatrix} U_4 \\ U_5 \\ U_6 \end{Bmatrix} = P \begin{Bmatrix} 1.0 \\ 2.0 \\ -4.8 \end{Bmatrix} \tag{5.4.14}$$

The solution is

$$U_4 = 0.8390 \times 10^{-4} P \text{ (in.)}, \quad U_5 = 0.6812 \times 10^{-4} P \text{ (in.)}, \quad U_6 = -0.9610 \times 10^{-4} P \text{ (rad.)} \tag{5.4.15}$$

The reactions and forces in each member in the global coordinates can be computed from the element equations

$$\{Q^e\} = [K^e]\{u^e\} - \{f^e\} \tag{5.4.16a}$$

The forces $\{Q^e\}$ can be transformed to those in the element coordinate system by means of (5.4.7):

$$\{\bar{Q}^e\} = [T^e]\{Q^e\} \tag{5.4.16b}$$

We obtain

$$\{\bar{Q}^1\} = \begin{Bmatrix} 4.731 \\ -0.725 \\ 10.900 \\ -4.731 \\ -1.275 \\ -50.450 \end{Bmatrix} P, \quad \{\bar{Q}^2\} = \begin{Bmatrix} 2.658 \\ -1.420 \\ 50.45 \\ -0.258 \\ -1.780 \\ -82.87 \end{Bmatrix} P \tag{5.4.17}$$

Table 5.4.1 contains the displacements obtained by various types of elements at point B. As noted earlier, one EBE or IIE per member of a structure gives exact displacements, whereas at least two RIE or CIE per member are needed to obtain acceptable results. The forces in each element are included in Table 5.4.2. The forces calculated from the element equations are also exact for EBE and IIE.

Table 5.4.1 Comparison of the generalized displacements [$\bar{v} = (v/P) \times 10^4$ where v is a typical displacement] at point B of the frame structure shown in Fig. 5.4.3.

Displ.	RIE(1)*	RIE (2)	RIE (4)	CIE (1)	CIE (2)	CIE (4)	IIE†	EBE†
$\bar{u}_B$	0.27092	0.84765	0.84107	0.28435	0.84146	0.83959	0.83898	0.83904
$\bar{w}_B$	0.46609	0.68056	0.68108	0.44315	0.68083	0.68114	0.68123	0.68124
$-\bar{\phi}_B$	−0.0016	0.86647	0.94501	0.00036	0.77029	0.91640	0.96206	0.96098

*Number in the parenthesis denotes the number of elements per member.
†Values are independent of the number of elements (and coincide with the exact values predicated by the respective beam theories).

Table 5.4.2 Comparison of the generalized forces (divided by P) in each member of the frame structure.

Element*	$\bar{Q}_1$	$-\bar{Q}_2$	$\bar{Q}_3$	$-\bar{Q}_4$	$-\bar{Q}_5$	$-\bar{Q}_6$
RIE(1)	3.237	1.865	62.24	3.237	0.136	62.26
	0.850	0.908	62.26	1.550	2.292	62.28
RIE(2)	4.723	0.671	0.332	4.723	1.329	47.70
	2.699	1.384	47.70	0.299	1.816	86.67
RIE(4)	4.730	0.713	8.362	4.730	1.288	49.76
	2.668	1.411	49.76	0.268	1.789	83.74
CIE(1)	3.077	1.575	65.39	3.077	0.425	17.38
	0.987	0.607	17.38	1.413	2.593	161.4
CIE(2)	4.728	0.708	8.327	4.728	1.292	50.37
	2.670	1.407	50.37	0.270	1.793	85.07
CIE(4)	4.730	0.721	10.30	4.730	1.279	50.43
	2.661	1.417	50.43	0.261	1.783	83.39
IIE†	4.731	0.725	10.92	4.731	1.275	50.45
	2.658	1.420	50.45	0.258	1.780	82.87
EBE†	4.731	0.725	10.90	4.731	1.275	50.45
	2.658	1.420	50.45	0.258	1.780	82.87

*Number in the parenthesis denotes the number of elements per member, and the two rows correspond to the two members of the structure.
† Values are independent of the number of elements (and coincide with the exact values predicated by the respective beam theories).

5.5 SUMMARY

In this chapter, finite element models of the classical (i.e., Euler–Bernoulli) and Timoshenko beam theories have been developed. The classical beam theory is governed by a fourth-order differential equation and therefore results in a weak form whose primary variables contain the transverse deflection and its first derivative. Therefore, Hermite interpolation of the transverse deflection is required in order to impose the continuity of the deflection and its derivative at the nodes between elements. In the case of the Timoshenko beam theory, there

are two, coupled, second-order equations governing the transverse deflection and the rotation. The weak forms of these equations require Lagrange interpolation of the transverse deflection and rotation. Since the rotation function is like the (negative of) the derivative of the transverse deflection, the degree of the interpolation used for the rotation should be one less than that used for the transverse deflection. Such selective interpolation of the variables is called *consistent interpolation*. When the same interpolation functions are used to approximate the transverse deflection and the rotation, the resulting stiffness matrix is often too stiff to yield good solutions—especially when the number of elements used is small. This is due to the inconsistency of interpolation of the variables, and the phenomenon is known as *shear locking*. It is overcome by the use of reduced integration to evaluate the stiffness coefficients associated with transverse shear strains. The elements developed here are RIE, CIE-1, which has quadratic interpolation of the transverse deflection and linear interpolation of the rotation, and IIE.

The plane frame element based on the unified beam element (i.e., IIE) that contains the classical beam theory and Timoshenko beam theory have also been discussed. The frame element is a superposition of the beam and bar elements and has three degrees of freedom (axial displacement, transverse deflection, and rotation about an axis perpendicular to the plane of axial and transverse coordinates) per node. The general plane frame element is oriented at an angle from the horizontal position, and its equations are obtained by transforming the equations of the frame element in local coordinates.

PROBLEMS

5.1 The natural vibration of a beam under applied axial compressive load N_0 is governed by the differential equation

$$\frac{d^2}{dx^2}\left(EI\frac{d^2w}{dx^2}\right)+N_0\frac{d^2w}{dx^2}=\rho A\omega^2 w$$

where ω denotes nondimensional frequency of natural vibration, EI is the bending stiffness, and ρA is the mass (mass density times cross-sectional area) of the beam. Develop (*a*) the weak form and (*b*) finite element model of the equation.

5.2 The differential equation governing axisymmetric bending of circular plates on elastic foundation is given by

$$-\frac{1}{r}\frac{d}{dr}\left[\frac{d}{dr}(rM_{rr})-M_{\theta\theta}\right]+kw=q(r)$$

where k is the modulus of the elastic foundation, q is the transverse distributed load, and

$$M_{rr}=-D\left(\frac{d^2w}{dr^2}+\nu\frac{1}{r}\frac{dw}{dr}\right),\quad M_{\theta\theta}=-D\left(\nu\frac{d^2w}{dr^2}+\frac{1}{r}\frac{dw}{dr}\right)$$

Develop (*a*) the weak form and identify the primary and secondary variables, and (*b*) the finite element model. Note that the shear force is defined by

$$Q_r=\frac{1}{r}\left[\frac{d}{dr}(rM_{rr})-M_{\theta\theta}\right]$$

5.3 The differential equations governing axisymmetric bending of circular plates according to the shear deformation plate theory are

$$-\frac{1}{r}\frac{d}{dr}(rQ_r) - q = 0 \tag{1}$$

$$-\frac{1}{r}\left[\frac{d}{dr}(rM_{rr}) - M_{\theta\theta}\right] + Q_r = 0 \tag{2}$$

where

$$M_{rr} = D\left(\frac{d\Psi}{dr} + \upsilon\frac{\Psi}{r}\right), \; M_{\theta\theta} = D\left(\upsilon\frac{d\Psi}{dr} + \frac{\Psi}{r}\right)$$
$$Q_r = K_s G H\left(\Psi + \frac{dw}{dr}\right)$$

where $D = EH^3/[12(1-\upsilon^2)]$ and H is the plate thickness. Develop (a) the weak form of the equations over an element and (b) the finite element model of the equations.

5.4 Consider the fourth-order equation (5.2.1) and its weak form (5.2.4). Suppose that a two-node element is employed, with *three* primary variables at each node: w, θ, and κ, where $\theta = dw/dx$ and $\kappa = d^2w/dx^2$. Show that the associated Hermite interpolation functions are given by

$$\phi_1 = 1 - 10\frac{\bar{x}^3}{h^3} + 15\frac{\bar{x}^4}{h^4} - 6\frac{\bar{x}^5}{h^5}, \qquad \phi_2 = \bar{x}\left(1 - 6\frac{\bar{x}^2}{h^2} + 8\frac{\bar{x}^3}{h^3} - 3\frac{\bar{x}^4}{h^4}\right)$$

$$\phi_3 = \frac{\bar{x}^2}{2}\left(1 - 3\frac{\bar{x}}{h} + 3\frac{\bar{x}^2}{h^2} - \frac{\bar{x}^3}{h^3}\right), \quad \phi_4 = 10\frac{\bar{x}^3}{h^3} - 15\frac{\bar{x}^4}{h^4} + 6\frac{\bar{x}^5}{h^5}$$

$$\phi_5 = -\bar{x}\left(4\frac{\bar{x}^2}{h^2} - 7\frac{\bar{x}^3}{h^3} + 3\frac{\bar{x}^4}{h^4}\right), \qquad \phi_6 = \frac{\bar{x}^2}{2}\left(\frac{\bar{x}}{h} - 2\frac{\bar{x}^2}{h^2} + \frac{\bar{x}^3}{h^3}\right)$$

where $\bar{x}$ is the element coordinate with the origin at node 1.

5.5 Consider the weak form (5.2.4) of the EBE. Use a three-node element with two degrees of freedom (w, θ), where $\theta \equiv -dw/dx$. Derive the Hermite interpolation functions for the element. Compute the element stiffness matrix and force vector. *Partial answer:*

$$\phi_1 = 1 - 23\frac{\bar{x}^2}{h^2} + 66\frac{\bar{x}^3}{h^3} - 68\frac{\bar{x}^4}{h^4} + 24\frac{\bar{x}^5}{h^5}$$

5.6–5.20 Use the minimum number of Euler–Bernoulli beam finite elements to analyze the beam problems shown in Figs. P5.6–P5.20. In particular, give:

(a) The assembled stiffness matrix and force vector.

(b) The specified global displacements and forces, and the equilibrium conditions.

(c) The condensed matrix equations for the primary unknowns (i.e., generalized forces) separately. Exploit symmetries, if any, in analyzing the problems. The positive convention used for the generalized displacements and forces is the same as that given in Fig. 5.2.2.

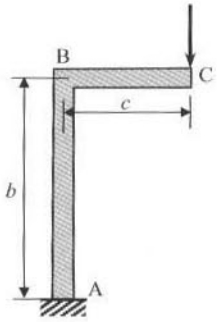

Figure P5.6

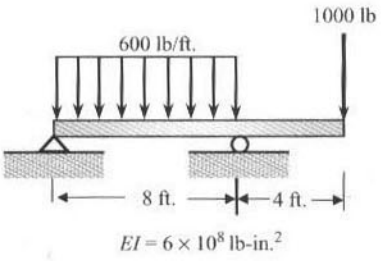

Figure P5.7

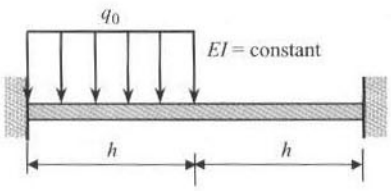

Figure P5.8

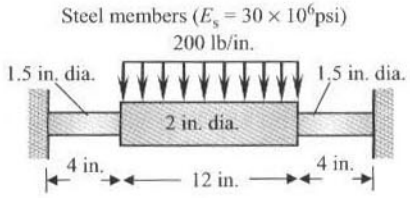

Figure P5.9

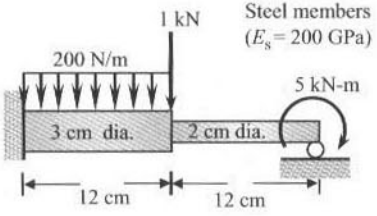

Figure P5.10

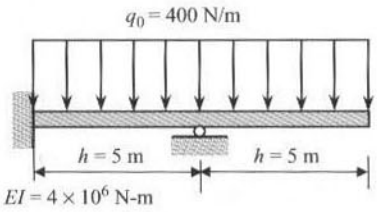

Figure P5.11

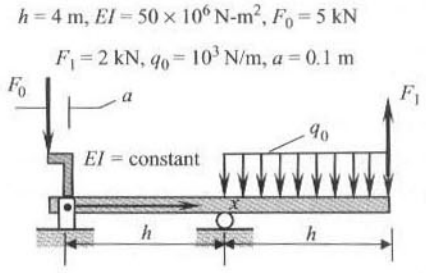

Figure P5.12

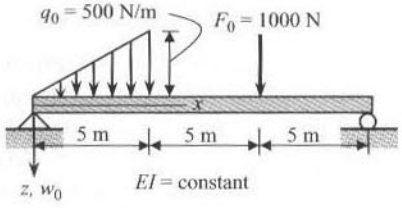

Figure P5.13

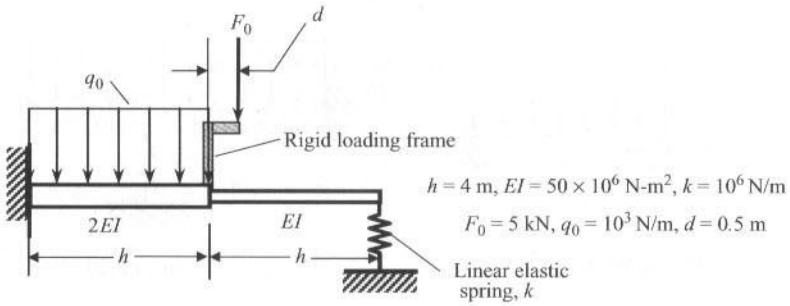

Figure P5.14

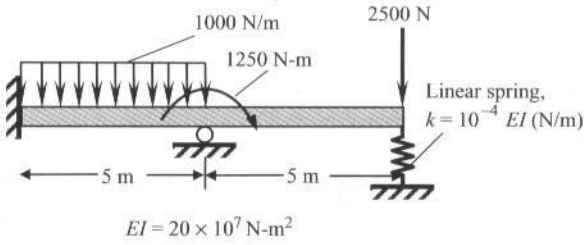

Figure P5.15

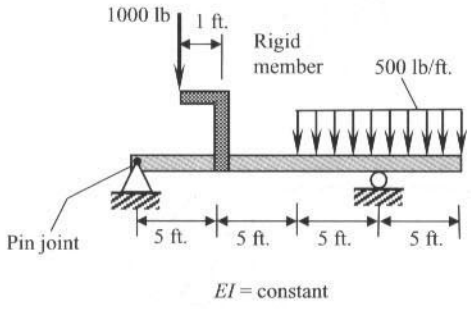

Figure P5.16

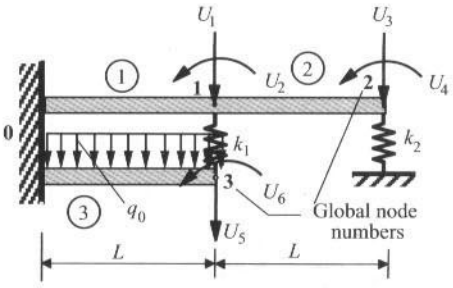

Figure P5.17

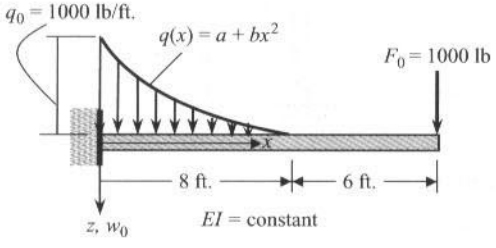

Figure P5.18

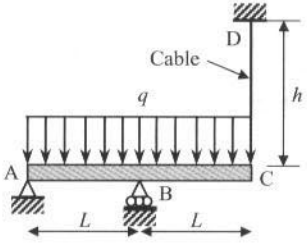

Figure P5.19

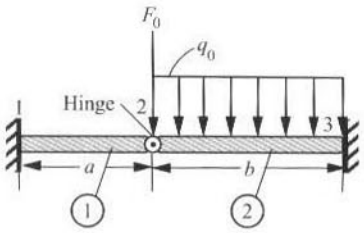

Figure P5.20

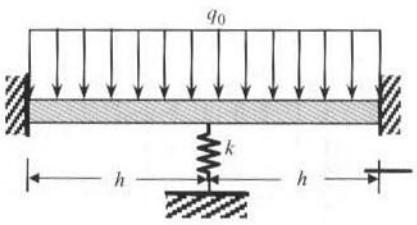

Figure P5.24

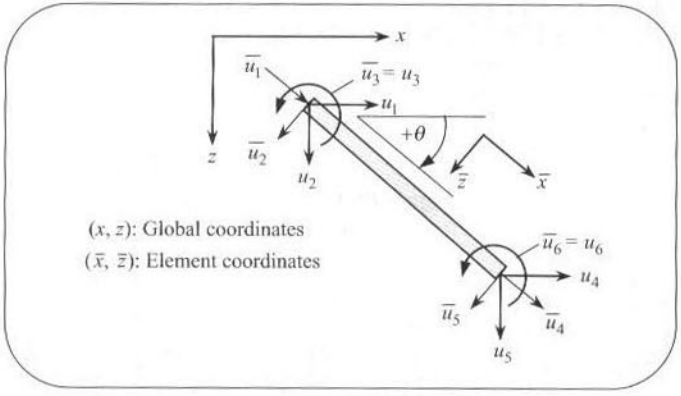

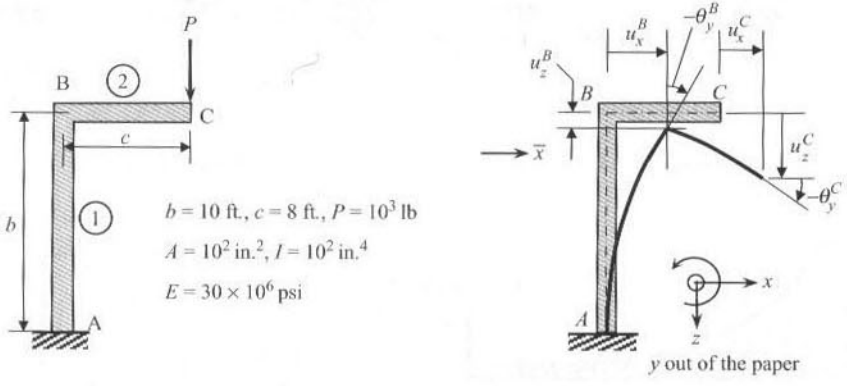

Figure P5.28

5.21 Analyze Problem 5.8 using the reduced-integration Timoshenko beam finite element (i.e., RIE). Use a value of $\frac{5}{6}$ for the shear correction factor and $\nu = 0.25$.

5.22 Analyze Problem 5.8 using the consistent interpolation (quadratic w and linear Ψ) Timoshenko beam element (i.e., CIE-1). Use a value of $\frac{5}{6}$ for the shear correction factor and $\nu = 0.25$.

5.23 Analyze Problem 5.8 using the consistent interpolation (cubic w and quadratic Ψ) Timoshenko beam element (i.e., CIE-2). Use a value of $\frac{5}{6}$ for the shear correction factor and $\nu = 0.25$.

5.24 Analyze the problem in Fig. P5.24 using the consistent interpolation (quadratic w and linear Ψ) Timoshenko beam element (i.e., CIE-1). Use a value of $\frac{5}{6}$ for the shear correction factor and $\nu = 0.25$.

5.25 Analyze the problem in Fig. P5.24 using the consistent interpolation (cubic w and quadratic Ψ) Timoshenko beam element (i.e., CIE-2). Use a value of $\frac{5}{6}$ for the shear correction factor and $\nu = 0.25$.

5.26 Consider a thin isotropic circular plate of radius R_0 and suppose that the plate is clamped at $r = R_0$. If two finite elements (see Problem 5.2) are used in the domain $(0 \le r \le R_0)$, give the boundary conditions on the primary and secondary variables of the mesh if the plate is subjected to (a) a uniformly distributed transverse load of intensity q_0 and (b) point load Q_0 at the center.

5.27 Repeat the circular plate problem of Problem 5.26 when a two-element mesh of Timoshenko elements is used.

5.28–5.35 For the frame problems shown in Figs. P5.28–P5.35, give (a) the transformed element matrices; (b) the assembled element matrices; and (c) the condensed matrix equations for the unknown generalized displacements and forces. Use the sign conventions shown in the figure below for global and element displacement (and force) degrees of freedom. The angle between the +ve x-axis and +ve $\bar{x}$-axis is measured in the clockwise sense.

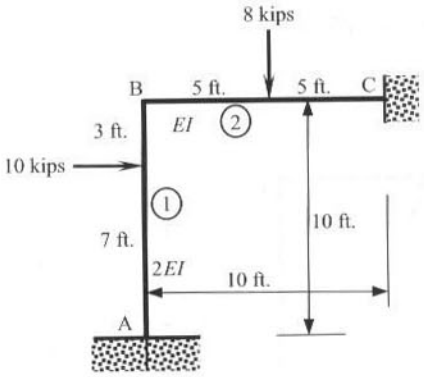

EI, *EA* are the same for the two members
$E = 30 \times 10^6$ lb/in.^{2}, $\nu = 0.3$
$A = 100$ in.^{2}, $I = 100$ in.^{4}

Figure P5.29

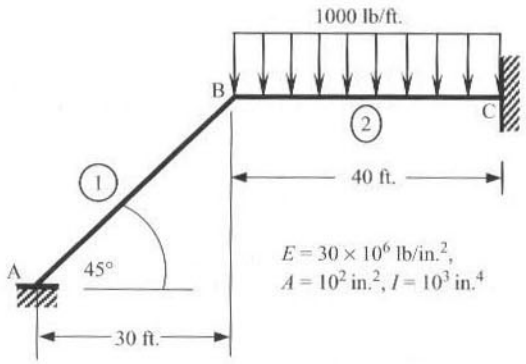

Figure P5.30

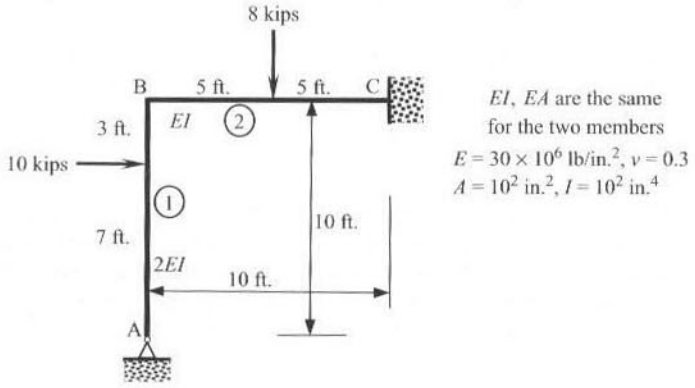

Figure P5.31

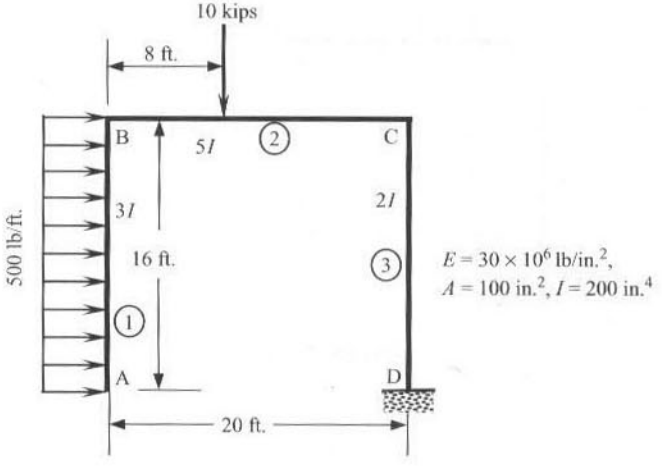

Figure P5.32

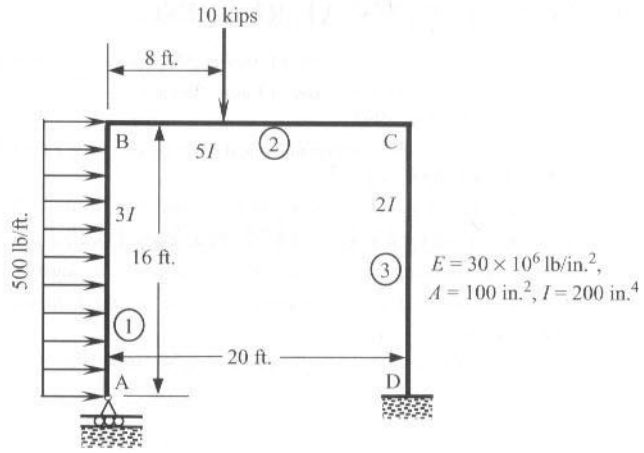

Figure P5.33

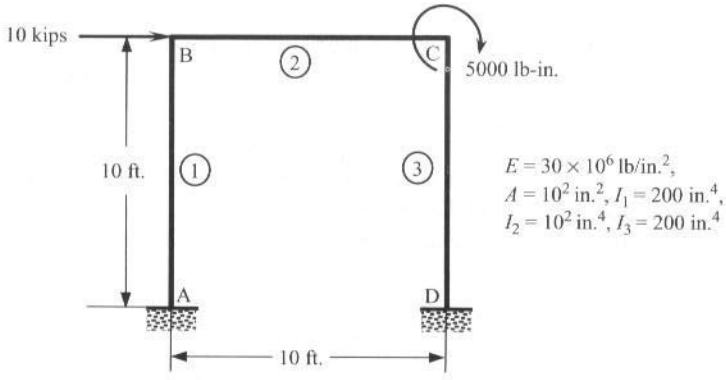

Figure P5.34

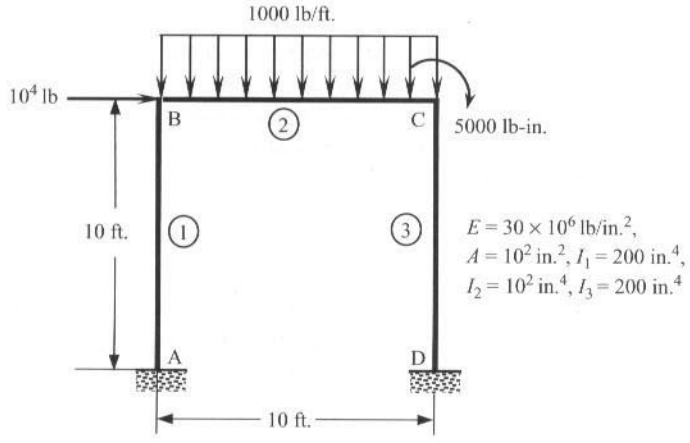

Figure P5.35

REFERENCES FOR ADDITIONAL READING

1. Reddy, J. N., *Energy Principles and Variational Methods in Applied Mechanics*, John Wiley, New York, 2002.
2. Reddy, J. N., "On Locking-Free Shear Deformable Beam Finite Elements," *Computer Methods in Applied Mechanics and Engineering*, **149**, 113–132, 1997.
3. Reddy, J. N., "On the Derivation of the Superconvergent Timoshenko Beam Finite Element," *Int. J. Comput. Civil and Struct. Engng.*, **1**(2), 71–84, 2000.
4. Timoshenko, S. P. and Goodier, J. N., *Theory of Elasticity*, McGraw-Hill, New York, 1970.
5. Ugural, A. C. and Fenster, S. K., *Advanced Strength and Applied Elasticity*, Elsevier, New York, 1975.
6. Wang, C.-K. and Salmon, C. G., *Introductory Structural Analysis*, Prentice-Hall, Englewood Cliffs, NJ, 1984.
7. Wang, C. M., Reddy, J. N., and Lee, K. H., *Shear Deformable Beams and Plates. Relationships with Classical Solutions*, Elsevier, Oxford, UK, 2000.
8. Willems, N. and Lucas, Jr., W. M., *Structural Analysis for Engineers*, McGraw-Hill, New York, 1978.

Chapter 6

EIGENVALUE AND TIME-DEPENDENT PROBLEMS

6.1 EIGENVALUE PROBLEMS

6.1.1 Introduction

An *eigenvalue problem* is defined to be one in which we seek the values of the parameter λ such that the equation

$$A(u) = \lambda B(u) \tag{6.1.1}$$

is satisfied for nontrivial values of u. Here A and B denote either matrix operators or differential operators, and values of λ for which Eq. (6.1.1) is satisfied are called *eigenvalues*. For each value of λ there is a vector u, called an *eigenvector* or *eigenfunction*. For example, the equation

$$-\frac{d^2u}{dx^2} = \lambda u(x), \quad \text{with } A = -\frac{d^2}{dx^2}, \quad B = 1$$

which arises in connection with natural axial vibrations of a bar or the transverse vibration of a cable, constitutes an eigenvalue problem. Here λ denotes the square of the frequency of vibration, ω.

In general, the determination of the eigenvalues is of engineering as well as mathematical importance. In structural problems, the eigenvalues denote either natural frequencies or buckling loads. In fluid mechanics and heat transfer, eigenvalue problems arise in connection with the determination of the homogeneous parts of the transient solution, as will be shown shortly. In these cases, eigenvalues often denote amplitudes of the Fourier components making up the solution. Eigenvalues are also useful in determining the stability characteristics of temporal schemes, as discussed in Section 6.2.

In this section, we develop finite element models of eigenvalue problems described by differential equations. In view of the close similarity between the differential equations governing eigenvalue and boundary value problems, the steps involved in the construction of their finite element models are entirely analogous. Differential eigenvalue problems are reduced to algebraic eigenvalue problems (i.e., $[A]\{X\} = \lambda[B]\{X\}$) by means of the finite element approximation. The methods of solution of algebraic eigenvalue problems are then used to solve for the eigenvalues and eigenvectors.

6.1.2 Formulation of Eigenvalue Problems

Parabolic Equation

Consider the partial differential equation

$$\rho cA\frac{\partial u}{\partial t} - \frac{\partial}{\partial x}\left(kA\frac{\partial u}{\partial x}\right) = q(x,t) \tag{6.1.2}$$

which arises in connection with transient heat transfer in one-dimensional systems (e.g., a plane wall or a fin). Here u denotes the temperature, k the thermal conductivity, ρ the density, A the cross-sectional area, c the specific heat, and q the heat generation per unit length. Equations involving the first-order time derivative are called *parabolic equations.*

The homogenous solution (i.e., the solution when $q = 0$) of Eq. (6.1.2) is often sought in the form of a product of a function of x and a function of t (i.e., through the *separation-of-variables* technique):

$$u^h(x,t) = U(x)T(t) \tag{6.1.3}$$

Substitution of this assumed form of solution into the homogeneous form of (6.1.2) gives

$$\rho cAU\frac{dT}{dt} - \frac{d}{dx}\left(kA\frac{dU}{dx}\right)T = 0$$

Separating variables of t and x (assuming that ρcA and kA are functions of x only), we arrive at

$$\frac{1}{T}\frac{dT}{dt} = \frac{1}{\rho cA}\frac{1}{U}\frac{d}{dx}\left(kA\frac{dU}{dx}\right) \tag{6.1.4}$$

Note that the left-hand side of this equation is a function of t only while the right-hand side is a function of x only. For two functions of two independent variables to be equal for all values of the independent variables, both functions must be equal to the same constant, say $-\lambda$ ($\lambda > 0$):

$$\frac{1}{T}\frac{dT}{dt} = \frac{1}{\rho cA}\frac{1}{U}\frac{d}{dx}\left(kA\frac{dU}{dx}\right) = -\lambda$$

or

$$\frac{dT}{dt} = -\lambda T \tag{6.1.5}$$

$$-\frac{d}{dx}\left(kA\frac{dU}{dx}\right) - \lambda\rho cAU = 0 \tag{6.1.6}$$

The negative sign of the constant λ is based on the physical requirement that the solution $U(x)$ be harmonic in x while $T(t)$ decay exponentially with increasing t.

The solution of (6.1.5) is

$$T(t) = Ke^{-\lambda t} \tag{6.1.7}$$

where K is a constant of integration. The values of λ are determined by solving (6.1.6), which also gives $U(x)$. With $T(t)$ and $U(x)$ known, we have the complete homogeneous solution (6.1.3) of Eq. (6.1.2). The problem of solving (6.1.6) for λ and $U(x)$ is termed an *eigenvalue problem,* and λ is called the eigenvalue and $U(x)$ the eigenfunction. When k,

A, ρ, and c are constants, the solution of Eq. (6.1.6) is

$$U(x) = C \sin \alpha x + D \cos \alpha x, \quad \alpha^2 = \frac{\rho c}{k} \lambda \tag{6.1.8}$$

where C and D are constants of integration. Boundary conditions of the problem are used to find algebraic relations among C and D. The algebraic relations can be expressed in matrix form as $([A] - \alpha[B])\{V\} = \{0\}$, where $[A]$ and $[B]$ depend, in general, on k, c, and ρ, and $\{V\}$ is the vector of integration constants C and D. Since C and D both cannot be zero (otherwise, we obtain the trivial solution), we require the determinant of the coefficient matrix $[A] - \alpha[B]$ to be zero. This results in an algebraic eigenvalue problem whose solution yields α (hence, λ) and $\{V\} = (C, D)$.

To fix the ideas, consider Eq. (6.1.6) subject to the boundary conditions (e.g., a fin with specified temperature at $x = 0$ and insulated at $x = L$)

$$U(0) = 0, \quad \left[kA \frac{dU}{dx} \right]_{x=L} = 0 \tag{6.1.9}$$

We note that nonhomogeneous boundary conditions can be converted to homogeneous boundary conditions by a change of variables. Using the above boundary conditions in (6.1.8), we obtain

$$0 = C \cdot 0 + D \cdot 1, \quad 0 = \alpha (C \cos \alpha L - D \sin \alpha L)$$

or

$$\left(\begin{bmatrix} 0 & 1 \\ 0 & 0 \end{bmatrix} - \alpha \begin{bmatrix} 0 & 0 \\ \cos \alpha L & -\sin \alpha L \end{bmatrix} \right) \begin{Bmatrix} C \\ D \end{Bmatrix} = \begin{Bmatrix} 0 \\ 0 \end{Bmatrix} \tag{6.1.10}$$

For nontrivial solution (i.e., not both C and D are equal to zero), we set the determinant of the coefficient matrix in (6.1.10) to zero and obtain (since α cannot be zero)

$$\cos \alpha L = 0 \quad \rightarrow \quad \alpha_n L = \frac{(2n-1)\pi}{2}$$

Hence, the homogeneous solution becomes [note that the constant K of Eq. (6.1.7) is absorbed into C_n]

$$u^h(x,t) = \sum_{n=1}^{\infty} C_n e^{-\lambda_n t} \sin \alpha_n x, \quad \lambda_n = \alpha_n^2 \left(\frac{k}{\rho c} \right), \quad \alpha_n = \frac{(2n-1)\pi}{2L} \tag{6.1.11}$$

The constants C_n are determined using the initial condition of the problem, $u(x, 0) = u_0(x)$:

$$u^h(x,0) = \sum_{n=1}^{\infty} C_n \sin \alpha_n x = u_0(x)$$

Multiplying both sides with $\sin \alpha_m x$, integrating over the interval $(0, L)$, and making use of the orthogonality condition

$$\int_0^L \sin \alpha_n x \, \sin \alpha_m x \, dx = \begin{cases} 0, & \text{if } m \neq n \\ \dfrac{L}{2}, & \text{if } m = n \end{cases} \tag{6.1.12}$$

we obtain

$$C_n = \frac{2}{L} \int_0^L u_0(x) \sin \alpha_n x \, dx \tag{6.1.13}$$

The complete solution of Eq. (6.1.2) is given by the sum of the homogeneous solution and the particular solution $u(x,t) = u^h(x,t) + u^p(x,t)$.

The example discussed above provides the need for determining eigenvalues (α_n) in the context of finding the transient response of a parabolic equation. Next, we consider the transient response of a second-order equation in time, known as a *hyperbolic equation*.

Hyperbolic Equation

The axial motion of a bar, for example, is described by the equation [see Reddy (2002), pp. 185–187]

$$\rho A \frac{\partial^2 u}{\partial t^2} - \frac{\partial}{\partial x}\left(EA\frac{\partial u}{\partial x}\right) = f(x,t) \tag{6.1.14}$$

where u denotes the axial displacement, E the modulus of elasticity, A the cross-sectional area, ρ the density, and f the axial force per unit length. The solution of (6.1.14) consists of two parts: homogeneous solution u^h (i.e., when $f = 0$) and particular solution u^p. The homogeneous part is determined by the separation-of-variables technique, as we discussed for the parabolic equation.

The homogenous solution of Eq. (6.1.14) is also assumed to be of the form in (6.1.3). Substitution of (6.1.3) into the homogeneous form of (6.1.14) gives

$$\rho A U \frac{d^2 T}{dt^2} - \frac{d}{dx}\left(EA\frac{dU}{dx}\right) T = 0$$

Assuming that ρA and EA are functions of x only, we arrive at

$$\frac{1}{T}\frac{d^2 T}{dt^2} = \frac{1}{\rho A}\frac{1}{U}\frac{d}{dx}\left(kA\frac{dU}{dx}\right) = -\alpha^2$$

or

$$\frac{d^2 T}{dt^2} + \alpha^2 T = 0 \tag{6.1.15}$$

$$-\frac{d}{dx}\left(EA\frac{dU}{dx}\right) - \alpha^2 \rho A U = 0 \tag{6.1.16}$$

The negative sign of the constant α is based on the physical requirement that the solution $u(x,t)$ be harmonic in x and t.

The solution of (6.1.15) is

$$T(t) = Ke^{-i\alpha t} = K_1 \cos \alpha t + K_2 \sin \alpha t \tag{6.1.17}$$

where K_1 and K_2 are constants of integration. The solution of (6.1.16), when E, A, and ρ, are constants, is

$$U(x) = C \sin \bar{\alpha} x + D \cos \bar{\alpha} x, \quad \bar{\alpha}^2 = \frac{\rho}{E}\alpha^2 \tag{6.1.18}$$

where again C and D are constants of integration. In the process of determining the constants C and D using the boundary conditions of the problem, once again we are required to solve an eigenvalue problem (the steps are analogous to those described for a parabolic equation). Unlike in the case of heat conduction problem, the quantities α_n in the case of bars have direct physical meaning, namely, they represent natural frequencies of the system. Thus, in

structural mechanics we may be interested in determining only the natural frequencies of the system but not the transient response.

When we are interested only in natural frequencies of the system, the eigenvalue problem may be formulated directly from the equation of motion (6.1.14) by assuming a solution form that is periodic in time t

$$u(x,t) = U(x)e^{-i\omega t} \tag{6.1.19}$$

where ω denotes the frequency of natural vibration, i equals $\sqrt{-1}$, and $U(x)$ denotes the configuration of the structure at that frequency, called the *mode shape* (i.e., for each value of ω, there is an associated mode shape). Substitution of (6.1.19) into the homogeneous form of (6.1.14) gives

$$\left[-\rho A\omega^2 U - \frac{d}{dx}\left(EA\frac{dU}{dx}\right)\right]e^{-i\omega t} = 0$$

or

$$-\frac{d}{dx}\left(EA\frac{dU}{dx}\right) - \omega^2 \rho A U = 0$$

which is identical to Eq. (6.1.16) with $\alpha = \omega$. Similar equations can be formulated for natural vibration of beams. Another eigenvalue problem that arises directly from the governing equilibrium equation is that of buckling of beam-columns. We shall return to this topic shortly.

In summary, eigenvalue problems associated with parabolic equations are obtained from the corresponding equations of motion by assuming solution of the form

$$u(x,t) = U(x)e^{-\alpha t}, \quad \lambda = \alpha \tag{6.1.20a}$$

whereas those associated with hyperbolic equations are obtained by assuming solution of the form

$$u(x,t) = U(x)e^{-i\omega t}, \quad \lambda = \omega^2 \tag{6.1.20b}$$

where λ denotes the eigenvalue. Finite element formulations of both problems are presented next.

6.1.3 Finite Element Formulation

Comparison of Eqs. (6.1.6) and (6.1.16) with the model equation (3.2.1) reveals that the equations governing eigenvalue problems are special cases of the model equations studied in Chapters 3 and 5. Here we summarize the steps in the finite element formulation of eigenvalue problems for the sake of completeness and ready reference. We will consider eigenvalue problems described by (*a*) a single equation in a single unknown (e.g., heat transfer, bar, and Euler–Bernoulli beam problems), and (*b*) a pair of equations in two variables (e.g., Timoshenko beam theory).

Heat Transfer and Bar-Like Problems

Consider the problem of solving the equation

$$-\frac{d}{dx}\left[a(x)\frac{dU}{dx}\right] + c(x)U(x) = \lambda c_0(x)U(x) \tag{6.1.21}$$

for λ and $U(x)$. Here a, c, and c_0 are known quantities that depend on the physical problem (i.e., data), λ is the eigenvalue, and U is the eigenfunction. Special cases of Eq. (6.1.21) are given below.

$$\text{Heat transfer:} \quad a = kA, \quad c = P\beta, \quad c_0 = \rho cA \tag{6.1.22}$$

$$\text{Bars:} \quad a = EA, \quad c = 0, \quad c_0 = \rho A \tag{6.1.23}$$

Over a typical element Ω_e, we seek a finite element approximation of U in the form

$$U_h^e(x) = \sum_{j=1}^{n} u_j^e \psi_j^e(x) \tag{6.1.24}$$

The weak form of (6.1.21) is

$$0 = \int_{x_a}^{x_b} \left(a \frac{dw}{dx}\frac{dU}{dx} + cwU(x) - \lambda c_0 wU \right) dx - Q_1^e w(x_a) - Q_n^e w(x_b) \tag{6.1.25}$$

where w is the weight function, and Q_1^e and Q_n^e are the secondary variables at node 1 and node n, respectively (assume that $Q_i^e = 0$ when $i \neq 1$ and $i \neq n$)

$$Q_1^e = -\left[a\frac{dU}{dx} \right]_{x_a}, \quad Q_n^e = \left[a\frac{dU}{dx} \right]_{x_b} \tag{6.1.26}$$

Substitution of the finite element approximation into the weak form gives the finite element model of the eigenvalue equation (6.1.21):

$$[K^e]\{u^e\} - \lambda[M^e]\{u^e\} = \{Q^e\} \tag{6.1.27a}$$

where

$$K_{ij}^e = \int_{x_a}^{x_b} \left[a(x)\frac{d\psi_i^e}{dx}\frac{d\psi_j^e}{dx} + c(x)\psi_i^e\psi_j^e \right] dx, \quad M_{ij}^e = \int_{x_a}^{x_b} c_0(x)\psi_i^e\psi_j^e \, dx \tag{6.1.27b}$$

Equation (6.1.27a) contains the finite element models of the eigenvalue equations (6.1.6) and (6.1.16) as special cases.

The assembly of element equations and imposition of boundary conditions on the assembled equations remain the same as in static problems of Chapter 3. However, the solution of the condensed equations for the unknown primary nodal variables is reduced to an algebraic eigenvalue problem in which the determinant of the coefficient matrix is set to zero to determine the values of λ and subsequently the nodal values of the eigenfunction $U(x)$. These ideas are illustrated through examples.

Example 6.1.1

Consider a plane wall, initially at a uniform temperature T_0, which has both surfaces suddenly exposed to a fluid at temperature T_∞. The governing differential equation is (for constant data)

$$k\frac{\partial^2 T}{\partial x^2} = \rho c_0 \frac{\partial T}{\partial t} \tag{6.1.28a}$$

and the initial condition is

$$T(x, 0) = T_0 \tag{6.1.28b}$$

where k is the thermal conductivity, ρ the density, and c_0 the specific heat at constant pressure. Equation (6.1.28*a*) is also known as the *diffusion equation* with diffusion coefficient $\alpha = k/\rho c_0$.

We consider two sets of boundary conditions, each being representative of a different scenario for $x = L$. It amounts to solving Eq. (6.1.28*a*) and (6.1.28*b*) for two different sets of boundary conditions.

Set 1. If the heat transfer coefficient at the surfaces of the wall is assumed to be infinite, the boundary conditions can be expressed as

$$T(0,t) = T_\infty, \quad T(L,t) = T_\infty \quad \text{for } t > 0 \tag{6.1.29a}$$

Set 2. If we assume that the wall at $x = L$ is subjected to ambient temperature, we have

$$T(0,t) = T_\infty, \quad \left[k\frac{\partial T}{\partial x} + \beta(T - T_\infty)\right]\Big|_{x=L} = 0 \tag{6.1.29b}$$

Equation (6.1.28*a*) can be normalized to make the boundary conditions homogeneous. Let

$$\alpha = \frac{k}{\rho c_0}, \quad \bar{x} = \frac{x}{L}, \quad \bar{t} = \frac{\alpha t}{L^2}, \quad u = \frac{T - T_\infty}{T_0 - T_\infty}$$

The differential equation (6.1.28*a*), initial condition (6.1.28*b*), and boundary conditions (6.1.29*a*) and (6.1.29*b*) become

$$-\frac{\partial^2 u}{\partial x^2} + \frac{\partial u}{\partial t} = 0 \tag{6.1.30a}$$

$$u(0,t) = 0, \quad u(1,t) = 0 \quad u(x,0) = 1 \tag{6.1.30b}$$

$$u(0,t) = 0, \quad \left(\frac{\partial u}{\partial x} + Hu\right)\Big|_{x=1} = 0, \quad H = \frac{\beta L}{k} \tag{6.1.30c}$$

where the bars over x and t are omitted in the interest of brevity.

Solution of (6.1.30*a*) and (6.1.30*b*) by separation-of-variables technique (or substitute $u = Ue^{-\lambda t}$) leads to the solution of the eigenvalue problem

$$-\frac{d^2U}{dx^2} - \lambda U = 0, \quad U(0) = 0, \quad U(1) = 0 \tag{6.1.31a}$$

whereas solution of (6.1.30*a*) and (6.1.30*c*) results in

$$-\frac{d^2U}{dx^2} - \lambda U = 0, \quad U(0) = 0, \quad \left(\frac{dU}{dx} + HU\right)\Big|_{x=1} = 0 \tag{6.1.31b}$$

This differential equation is a special case of Eq. (6.1.21) with $a = 1$, $c = 0$, and $c_0 = 1$.

For a linear element, the element equations (6.1.27*a*) have the explicit form [see Eq. (3.2.34) for element matrices]

$$\left(\frac{1}{h_e}\begin{bmatrix} 1 & -1 \\ -1 & 1 \end{bmatrix} - \lambda\frac{h_e}{6}\begin{bmatrix} 2 & 1 \\ 1 & 2 \end{bmatrix}\right)\begin{Bmatrix} u_1^e \\ u_2^e \end{Bmatrix} = \begin{Bmatrix} Q_1^e \\ Q_2^e \end{Bmatrix} \tag{6.1.32a}$$

For a quadratic element, we have [see Eq. (3.2.37*a*) for element matrices]

$$\left(\frac{1}{3h_e}\begin{bmatrix} 7 & -8 & 1 \\ -8 & 16 & -8 \\ 1 & -8 & 7 \end{bmatrix} - \lambda\frac{h_e}{30}\begin{bmatrix} 4 & 2 & -1 \\ 2 & 16 & 2 \\ -1 & 2 & 4 \end{bmatrix}\right)\begin{Bmatrix} u_1^e \\ u_2^e \\ u_3^e \end{Bmatrix} = \begin{Bmatrix} Q_1^e \\ 0 \\ Q_3^e \end{Bmatrix} \tag{6.1.32b}$$

Solution for Set 1. For a mesh of two linear elements (the minimum number needed for Set 1 boundary conditions), with $h_1 = h_2 = 0.5$, the assembled equations are

$$\left(2\begin{bmatrix} 1 & -1 & 0 \\ -1 & 2 & -1 \\ 0 & -1 & 1 \end{bmatrix} - \lambda \frac{1}{12}\begin{bmatrix} 2 & 1 & 0 \\ 1 & 4 & 1 \\ 0 & 1 & 2 \end{bmatrix}\right)\begin{Bmatrix} U_1 \\ U_2 \\ U_3 \end{Bmatrix} = \begin{Bmatrix} Q_1^1 \\ Q_2^1 + Q_1^2 \\ Q_2^2 \end{Bmatrix}$$

The boundary conditions $U(0) = 0$, $Q_2^1 + Q_1^2 = 0$, and $U(1) = 0$ require $U_1 = U_3 = 0$. Hence, the eigenvalue problem reduces to the single equation

$$\left(4 - \lambda \frac{4}{12}\right) U_2 = 0, \quad \text{or} \quad \lambda_1 = 12.0, \quad U_2 \neq 0$$

The mode shape is given (within an arbitrary constant; take $U_2 = 1$) by

$$U(x) = U_2 \Phi_2(x) = \begin{cases} U_2 \psi_2^1(x) = x/h = 2x & 0 \le x \le 0.5 \\ U_2 \psi_1^2(x) = (2h - x)/h = 2(1 - x) & 0.5 \le x \le 1.0 \end{cases}$$

For a mesh of one quadratic element, we have ($h = 1.0$)

$$\frac{16}{3} - \lambda \frac{16}{30} = 0, \quad \text{or} \quad \lambda_1 = 10.0, \quad U_2 \neq 0$$

The corresponding eigenfunction is

$$U(x) = U_2 \Phi_2(x) = U_2 \psi_2^1 = 4 \frac{x}{h}\left(1 - \frac{x}{h}\right), \quad 0 \le x \le 1.0$$

The exact eigenvalues are $\lambda_n = (n\pi)^2$ and $\lambda_1 = \pi^2 = 9.8696$. The exact eigenfunctions for Set 1 boundary conditions are $U_n(x) = \sin n\pi x$ and $U_1(x) = \sin \pi x$. Clearly, one quadratic element gives more accurate solution than two linear elements.

The eigenvalues and eigenfunctions can be used to construct the solution of the transient problem. For example, the solution of (6.1.30*a*) and (6.1.30*b*) is

$$u(x, t) = \sum_{n=1}^{\infty} C_n U_n(x) e^{-\lambda_n t} = \sum_{n=1}^{\infty} C_n \sin n\pi x \, e^{-(n\pi)^2 t} \tag{6.1.33}$$

where C_n are constants to be determined using the initial condition of the problem [see Eq. (6.1.13)]. The finite element solution of the same problem, when one quadratic element is used, is given by

$$u_h(x, t) = 4x(1 - x)e^{-10t} T_0$$

which is very close to the one-term solution in (6.1.33).

Solution for Set 2. For a mesh of two linear elements, the Set 2 boundary conditions translate into $U_1 = 0$ and $Q_2^2 + HU_3 = 0$. The condensed equations are

$$\left(\frac{1}{h}\begin{bmatrix} 2 & -1 \\ -1 & 1 \end{bmatrix} - \lambda \frac{h}{6}\begin{bmatrix} 4 & 1 \\ 1 & 2 \end{bmatrix}\right)\begin{Bmatrix} U_2 \\ U_3 \end{Bmatrix} = \begin{Bmatrix} 0 \\ -HU_3 \end{Bmatrix}$$

or

$$\left(\begin{bmatrix} 4 & -2 \\ -2 & 2 + H \end{bmatrix} - \frac{\lambda}{12}\begin{bmatrix} 4 & 1 \\ 1 & 2 \end{bmatrix}\right)\begin{Bmatrix} U_2 \\ U_3 \end{Bmatrix} = \begin{Bmatrix} 0 \\ 0 \end{Bmatrix} \tag{6.1.34}$$

For nontrivial solution (i.e., at least one of the U_i is nonzero), the determinant of the coefficient matrix should be zero:

$$\begin{vmatrix} 4-4\bar{\lambda} & -(2+\bar{\lambda}) \\ -(2+\bar{\lambda}) & 2+H-2\bar{\lambda} \end{vmatrix} = 0, \quad \bar{\lambda} = \frac{\lambda}{12}$$

or

$$7\bar{\lambda}^2 - 4(5+H)\bar{\lambda} + 4(1+H) = 0$$

The above equation is known as the *characteristic equation* of the eigenvalue problem. The two roots of this quadratic equation for $H = 1$ are

$$\bar{\lambda}_{1,2} = \frac{12 \pm \sqrt{(12)^2 - 7 \times 8}}{7} \rightarrow \bar{\lambda}_1 = 0.374167, \quad \bar{\lambda}_2 = 3.0544$$

and the eigenvalues are ($\lambda = 12\bar{\lambda}$)

$$\lambda_1 = 4.49, \quad \lambda_2 = 36.6529$$

The eigenvectors associated with each eigenvalue can be computed from equations (6.1.34)

$$\begin{bmatrix} 4-4\bar{\lambda}_i & -(2+\bar{\lambda}_i) \\ -(2+\bar{\lambda}_i) & 3-2\bar{\lambda}_i \end{bmatrix} \begin{Bmatrix} U_2 \\ U_3 \end{Bmatrix}^{(i)} = \begin{Bmatrix} 0 \\ 0 \end{Bmatrix}, \quad i = 1, 2$$

For example, for $\bar{\lambda}_1 = 0.374167$ ($\lambda_1 = 4.4900$), we have

$$2.5033U_2^{(1)} - 2.3742U_3^{(1)} = 0$$

Taking $U_2^{(1)} = 1$, we obtain

$$\{U^{(1)}\} = \begin{Bmatrix} U_2^{(1)} \\ U_3^{(1)} \end{Bmatrix} = \begin{Bmatrix} 1.0000 \\ 1.0544 \end{Bmatrix}$$

On the other hand, if we normalize the components, $(U_2^{(1)})^2 + (U_3^{(1)})^2 = 1$, we obtain

$$\{U^{(1)}\} = \begin{Bmatrix} U_2^{(1)} \\ U_3^{(1)} \end{Bmatrix} = \begin{Bmatrix} 0.6881 \\ 0.7256 \end{Bmatrix}$$

In other words, we obtain a mode shape whose amplitude is not unique. Hence, the eigenfunction corresponding to $\lambda_1 = 4.4900$ ($h = 0.5$) is

$$U^{(1)}(x) = \begin{cases} 0.6881\, x/h & \text{for } 0 \le x \le 0.5 \\ 0.6881\,(1-x)/h + 0.7256(2x-1)/2h & \text{for } 0.5 \le x \le 1.0 \end{cases}$$

Similarly, the eigenvector components corresponding to $\lambda_2 = 36.6529$ is (not normalized)

$$\{U^{(2)}\} = \begin{Bmatrix} U_2^{(2)} \\ U_3^{(2)} \end{Bmatrix} = \begin{Bmatrix} 1.0000 \\ -1.6258 \end{Bmatrix}$$

For a mesh of one quadratic element, the condensed equations are

$$\left(\frac{1}{3} \begin{bmatrix} 16 & -8 \\ -8 & 7+3H \end{bmatrix} - \lambda \frac{1}{30} \begin{bmatrix} 16 & 2 \\ 2 & 4 \end{bmatrix} \right) \begin{Bmatrix} U_2 \\ U_3 \end{Bmatrix} = \begin{Bmatrix} 0 \\ 0 \end{Bmatrix}$$

and the characteristic equation is

$$15\bar{\lambda}^2 - 4(13+3H)\bar{\lambda} + 12(1+H) = 0, \quad \bar{\lambda} = \frac{\lambda}{10}$$

The two roots of this quadratic equation for $H = 1$ are

$$\bar{\lambda}_{1,2} = \frac{32 \pm \sqrt{(32)^2 - 15 \times 24}}{15} \rightarrow \bar{\lambda}_1 = 0.41545, \quad \bar{\lambda}_2 = 3.85121$$

and the eigenvalues are ($\lambda = 12\bar{\lambda}$)

$$\lambda_1 = 4.1545, \quad \lambda_2 = 38.5121$$

The corresponding eigenvector components are (not normalized)

$$\{U^{(1)}\} = \begin{Bmatrix} U_2^{(1)} \\ U_3^{(1)} \end{Bmatrix} = \begin{Bmatrix} 1.0000 \\ 1.0591 \end{Bmatrix}$$

$$\{U^{(2)}\} = \begin{Bmatrix} U_2^{(2)} \\ U_3^{(2)} \end{Bmatrix} = \begin{Bmatrix} 1.0000 \\ -2.9052 \end{Bmatrix}$$

The exact eigenfunctions for Set 2 boundary conditions are

$$U_n(x) = \sin \sqrt{\lambda_n}\, x \tag{6.1.35a}$$

and the eigenvalues λ_n are computed from the equation

$$H \sin \sqrt{\lambda_n} + \sqrt{\lambda_n} \cos \sqrt{\lambda_n} = 0 \tag{6.1.35b}$$

The first two roots of the transcendental equation (6.1.35*b*) are (for $H = 1$)

$$\sqrt{\lambda_1} = 2.0288 \rightarrow \lambda_1 = 4.1160; \quad \sqrt{\lambda_2} = 4.9132 \rightarrow \lambda_2 = 24.1393$$

A comparison of the eigenvalues obtained using meshes of linear and quadratic elements with the exact values is presented in Table 6.1.1. Note that the number of eigenvalues obtained in

Table 6.1.1 Eigenvalues of the heat conduction equations (6.1.31*a*) and (6.1.31*b*) for two sets of boundary conditions.

Mesh	λ_1	λ_2	λ_3	λ_4	λ_5	λ_6	λ_7
2L	12.0000						
	(4.4900)*	(36.6529)					
4L	10.3866	48.0000	126.756				
	(4.2054)	(27.3318)	(85.7864)	(177.604)			
8L	9.9971	41.5466	99.4855	192.000	328.291	507.025	686.512
	(4.1380)	(24.9088)	(69.1036)	(143.530)	(257.580)	(417.701)	(607.022)
1Q	10.000						
	(4.1545)	(38.5121)					
2Q	9.9439	40.000	128.723				
	(4.1196)	(24.8995)	(81.4446)	(207.653)			
4Q	9.8747	39.7754	91.7847	160.000	308.253	514.891	794.794
	(4.1161)	(24.2040)	(64.7704)	(129.261)	(240.540)	(405.254)	(658.133)
Exact	9.8696	39.4784	88.8264	157.9137	246.740	355.306	483.611
	(4.1160)	(24.1393)	(63.6597)	(122.889)	(201.851)	(300.550)	(418.987)

* The second line for each mesh corresponds to set 2 boundary conditions.

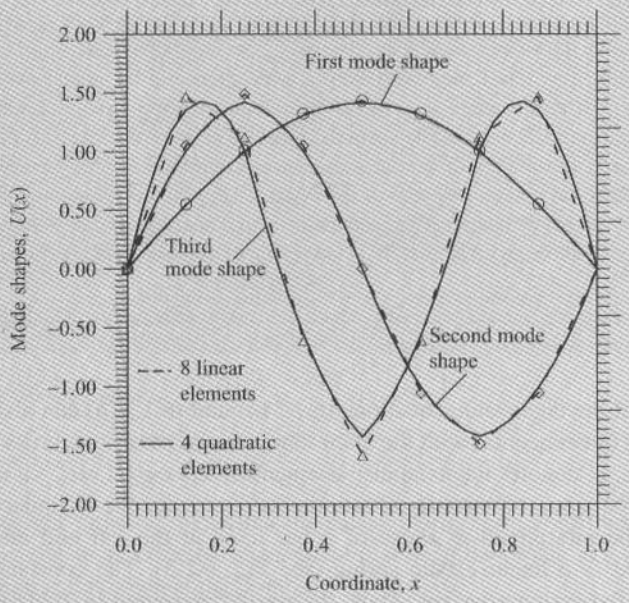

Figure 6.1.1 The first three mode shapes as predicted by a mesh of eight linear elements and a mesh of four quadratic elements for the heat transfer problem of Example 6.1.1 (Set 1 boundary conditions).

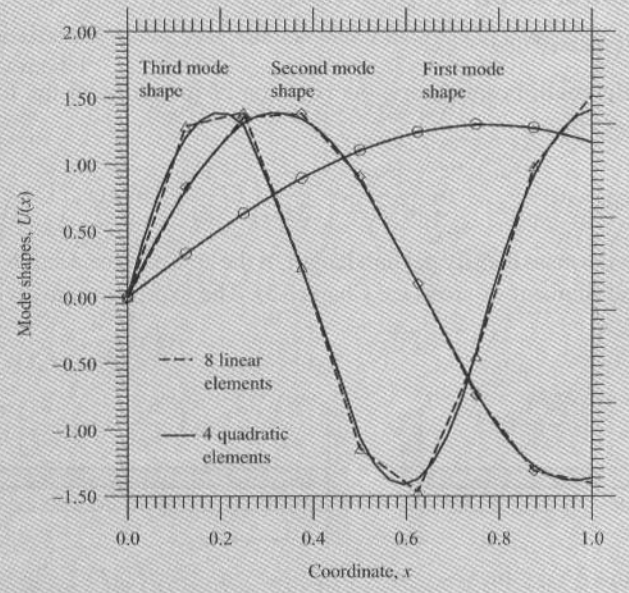

Figure 6.1.2 The first three mode shapes of the heat transfer problem of Example 6.1.1 (Set 2 boundary conditions).

the finite element method is always equal to the number of unknown nodal values. As the mesh is refined, not only do we increase the number of eigenvalues but we also improve the accuracy of the preceding eigenvalues. Note also that the convergence of the numerical eigenvalues to the exact ones is from the above, i.e., the finite element solution provides an upper bound to the exact eigenvalues. For structural systems, this can be interpreted as follows: According to the principle of minimum total potential energy, any approximate displacement field would overestimate the total potential energy of the system. This is equivalent to approximating the stiffness of the system with a larger value than the actual one. A stiffer system will have larger eigenvalues (or frequencies). The first three mode shapes of the system are shown in Figs. 6.1.1 and 6.1.2.

We note that the eigenvalue equations (6.1.31*a*) and (6.1.31*b*) can also be interpreted as those arising in connection with the axial vibrations of a constant cross sectional member. In that case, U denotes the axial displacement $[u(x,t) = U(x)e^{-i\omega t}]$ and $\lambda = \omega^2\rho/E$, ω being the frequency of natural vibration. For example, the boundary conditions in (6.1.31*b*) can be interpreted as those of a bar fixed at the left end and the right end being connected to a linear elastic spring (see Fig. 6.1.3). The constant H is equal to k/EA, k being the spring constant. Thus, the results presented in Table 6.1.1 can be interpreted as $\omega^2\rho/E$ of an uniform bar for the two different boundary conditions shown in Fig. 6.1.3.

Natural Vibration of Beams

Euler–Bernoulli Beam Theory

For the Euler–Bernoulli beam theory, the equation of motion is of the form [see Reddy (2002), pp. 193–196]

$$\rho A\frac{\partial^2 w}{\partial t^2} - \rho I\frac{\partial^4 w}{\partial t^2 \partial x^2} + \frac{\partial^2}{\partial x^2}\left(EI\frac{\partial^2 w}{\partial x^2}\right) = q(x,t) \tag{6.1.36}$$

where ρ denotes the mass density per unit length, A the area of cross section, E the modulus, and I the second moment of area (see Chapter 5). The expression involving ρI is called

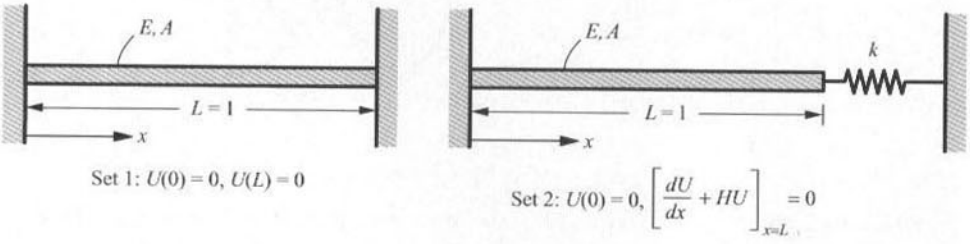

Figure 6.1.3 Uniform bar with two sets of boundary conditions.

rotary inertia term. Equation (6.1.36) can be formulated as an eigenvalue problem in the interest of finding the frequency of natural vibration by assuming periodic motion

$$w(x,t) = W(x)e^{-i\omega t} \tag{6.1.37}$$

where ω is the frequency of natural transverse motion and $W(x)$ is the mode shape of the transverse motion. Substitution of Eq. (6.1.37) into (6.1.36) yields

$$\frac{d^2}{dx^2}\left(EI\frac{d^2W}{dx^2}\right) - \lambda\left(\rho AW - \rho I\frac{d^2W}{dx^2}\right) = 0 \tag{6.1.38}$$

where $\lambda = \omega^2$.

The weak form of Eq. (6.1.38) is given by

$$\begin{aligned} 0 = &\int_{x_a}^{x_b}\left(EI\frac{d^2v}{dx^2}\frac{d^2W}{dx^2} - \lambda\rho Avw - \lambda\rho I\frac{dv}{dx}\frac{dW}{dx}\right)dx \\ &+ \left\{v\left[\frac{d}{dx}\left(EI\frac{d^2W}{dx^2}\right) + \lambda\rho I\frac{dW}{dx}\right]\right\}_{x_a}^{x_b} + \left[\left(-\frac{dv}{dx}\right)EI\frac{d^2W}{dx^2}\right]_{x_a}^{x_b} \end{aligned} \tag{6.1.39}$$

where v is the weight function. Note that the rotary inertia term contributes to the shear force term, giving rise to an effective shear force that must be known at a boundary point when the deflection is unknown at the point.

To obtain the finite element model of Eq. (6.1.39), assume finite element approximation of the form

$$W(x) = \sum_{j=1}^{4} \Delta_j^e \phi_j^e(x) \tag{6.1.40}$$

where ϕ_j^e are the Hermite cubic polynomials [see Eqs. (5.2.11) and (5.2.12)], and obtain the finite element model

$$\left([K^e] - \omega^2[M^e]\right)\{\Delta^e\} = \{Q^e\} \tag{6.1.41a}$$

where

$$K_{ij}^e = \int_{x_a}^{x_b} EI\frac{d^2\phi_i^e}{dx^2}\frac{d^2\phi_j^e}{dx^2}\,dx, \quad M_{ij}^e = \int_{x_a}^{x_b}\left(\rho A\,\phi_i^e\,\phi_j^e + \rho I\,\frac{d\phi_i^e}{dx}\frac{d\phi_j^e}{dx}\right)dx \tag{6.1.41b}$$

$$\begin{aligned} Q_1^e &\equiv \left[\frac{d}{dx}\left(EI\frac{d^2W}{dx^2}\right) + \lambda\rho I\frac{dW}{dx}\right]\Bigg|_{x_a}, \qquad Q_2^e \equiv \left(EI\frac{d^2W}{dx^2}\right)\Bigg|_{x_a} \\ Q_3^e &\equiv -\left[\frac{d}{dx}\left(EI\frac{d^2W}{dx^2}\right) + \lambda\rho I\frac{dW}{dx}\right]\Bigg|_{x_b}, \quad Q_4^e \equiv -\left(EI\frac{d^2W}{dx^2}\right)\Bigg|_{x_b} \end{aligned} \tag{6.1.41c}$$

For constant values of EI and ρA, the stiffness matrix $[K^e]$ and mass matrix $[M^e]$ are

$$[K^e] = \frac{2E_eI_e}{h_e^3}\begin{bmatrix} 6 & -3h_e & -6 & -3h_e \\ -3h_e & 2h_e^2 & 3h_e & h_e^2 \\ -6 & 3h_e & 6 & 3h_e \\ -3h_e & h_e^2 & 3h_e & 2h_e^2 \end{bmatrix}$$

$$[M^e] = \frac{\rho^e A_e h_e}{420}\begin{bmatrix} 156 & -22h_e & 54 & 13h_e \\ -22h_e & 4h_e^2 & -13h_e & -3h_e^2 \\ 54 & -13h_e & 156 & 22h_e \\ 13h & -3h_e^2 & 22h_e & 4h_e^2 \end{bmatrix} + \frac{\rho^e I_e}{30h_e}\begin{bmatrix} 36 & -3h_e & -36 & -3h_e \\ -3h & 4h_e^2 & 3h_e & -h_e^2 \\ -36 & 3h_e & 36 & 3h_e \\ -3h_e & -h_e^2 & 3h_e & 4h_e^2 \end{bmatrix} \tag{6.1.42}$$

When rotary inertia is neglected, we omit the second part of the mass matrix in (6.1.42).

Timoshenko Beam Theory

The equations of motion of the Timoshenko beam theory are [see Reddy (2002), pp. 193–196]

$$\rho A\frac{\partial^2 w}{\partial t^2} - \frac{\partial}{\partial x}\left[GAK_s\left(\frac{\partial w}{\partial x} + \Psi\right)\right] = 0 \tag{6.1.43a}$$

$$\rho I\frac{\partial^2 \Psi}{\partial t^2} - \frac{\partial}{\partial x}\left(EI\frac{\partial \Psi}{\partial x}\right) + GAK_s\left(\frac{\partial w}{\partial x} + \Psi\right) = 0 \tag{6.1.43b}$$

where G is the shear modulus ($G = E/[2(1+\nu)]$) and K_s is the shear correction factor ($K_s = 5/6$). Note that Eq. (6.1.43*b*) contains the rotary inertia term. Once again, we assume periodic motion and write

$$w(x,t) = W(x)e^{-i\omega t}, \quad \Psi(x,t) = S(x)e^{-i\omega t} \tag{6.1.44}$$

and obtain the eigenvalue problem from Eqs. (6.1.43*a*) and (6.1.43*b*)

$$-\frac{d}{dx}\left[GAK_s\left(\frac{dW}{dx} + S\right)\right] - \omega^2\rho A W = 0 \tag{6.1.45a}$$

$$-\frac{d}{dx}\left(EI\frac{dS}{dx}\right) + GAK_s\left(\frac{dW}{dx} + S\right) - \omega^2\rho I\, S = 0 \tag{6.1.45b}$$

For equal interpolation of $W(x)$ and $S(x)$

$$W(x) = \sum_{j=1}^{n} W_j^e \psi_j^e(x), \quad S(x) = \sum_{j=1}^{n} S_j^e \psi_j^e(x) \tag{6.1.46}$$

where ψ_j^e are the $(n-1)$ order Lagrange polynomials, the finite element model is given by

$$\left(\begin{bmatrix} [K^{11}] & [K^{12}] \\ [K^{21}] & [K^{22}] \end{bmatrix} - \omega^2\begin{bmatrix} [M^{11}] & [0] \\ [0] & [M^{22}] \end{bmatrix}\right)\begin{Bmatrix} \{W\} \\ \{S\} \end{Bmatrix} = \begin{Bmatrix} \{F^1\} \\ \{F^2\} \end{Bmatrix} \tag{6.1.47}$$

where $[K^e]$ is the stiffness matrix and $[M^e]$ is the mass matrix

$$K_{ij}^{11} = \int_{x_a}^{x_b} GAK_s \frac{d\psi_i^e}{dx}\frac{d\psi_j^e}{dx}dx$$

$$K_{ij}^{12} = \int_{x_a}^{x_b} GAK_s \frac{d\psi_i^e}{dx}\psi_j^e\, dx = K_{ji}^{21}$$

$$K_{ij}^{22} = \int_{x_a}^{x_b} \left(EI \frac{d\psi_i^e}{dx} \frac{d\psi_j^e}{dx} + GAK_s \psi_i^e \psi_j^e \right) dx$$

$$M_{ij}^{11} = \int_{x_a}^{x_b} \rho A \psi_i^e \psi_j^e \, dx, \quad M_{ij}^{22} = \int_{x_a}^{x_b} \rho I \psi_i^e \psi_j^e \, dx$$

$$F_j^1 = Q_{2i-1}, \quad F_i^2 = Q_{2i} \tag{6.1.48a}$$

$$Q_1^e \equiv -\left[GAK_s \left(S + \frac{dW}{dx} \right) \right] \Big|_{x_a}, \quad Q_2^e \equiv -\left(EI \frac{dS}{dx} \right) \Big|_{x_a}$$

$$Q_3^e \equiv \left[GAK_s \left(S + \frac{dW}{dx} \right) \right] \Big|_{x_b}, \quad Q_4^e \equiv \left(EI \frac{dS}{dx} \right) \Big|_{x_b} \tag{6.1.48b}$$

For the choice of linear interpolation functions, Eq. (6.1.47) has the explicit form (after rearranging the nodal variables)

$$[K^e] = \left(\frac{2E_e I_e}{\mu_0 h_e^3} \right) \begin{bmatrix} 6 & -3h_e & -6 & -3h_e \\ -3h_e & h_e^2(1.5 + 6\Lambda_e) & 3h_e & h_e^2(1.5 - 6\Lambda_e) \\ -6 & 3h_e & 6 & 3h_e \\ -3h_e & h_e^2(1.5 - 6\Lambda_e) & 3h_e & h_e^2(1.5 + 6\Lambda_e) \end{bmatrix}$$

$$[M^e] = \frac{\rho^e A_e}{6} \begin{bmatrix} 2 & 0 & 1 & 0 \\ 0 & 2r_e & 0 & r_e \\ 1 & 0 & 2 & 0 \\ 0 & r_e & 0 & 2r_e \end{bmatrix}, \quad r_e = \frac{I_e}{A_e} \tag{6.1.49a}$$

$$\Lambda_e = \frac{E_e I_e}{G_e A_e K_s h_e^2}, \quad \mu_0 = 12\Lambda_e \tag{6.1.49b}$$

For Hermite cubic interpolation of $W(x)$ and related quadratic approximation of $S(x)$ [i.e., *interdependent interpolation element* (IIE)], the resulting mass matrix is cumbersome and depends on the stiffness parameters (E and G). We will not consider it here [see Reddy (1999*b*, 2000)].

Example 6.1.2

Consider a uniform beam of rectangular cross section ($B \times H$), fixed at $x = 0$ and free at $x = L$ (i.e., a cantilever beam). We wish to determine the first four flexural frequencies of the beam.

The boundary conditions of the structure are

$$W(0) = 0, \quad \frac{dW}{dx} = 0, \quad \left[EI \frac{d^2W}{dx^2} \right]_{x=L} = 0, \quad \left[EI \frac{d^3W}{dx^3} \right]_{x=L} = 0 \tag{6.1.50a}$$

in the Euler–Bernoulli beam theory and

$$W(0) = 0, \quad S(0) = 0, \quad \left[EI \frac{dS}{dx} \right]_{x=L} = 0, \quad \left[GAK_s \left(\frac{dW}{dx} + S \right) \right]_{x=L} = 0 \tag{6.1.50b}$$

in the Timoshenko beam theory. The first two terms in each case are the essential (or geometric) boundary conditions and the last two are the natural (or force) boundary conditions.

The number of eigenvalues we wish to determine dictates the minimum number of elements to be used to analyze the structure. First, consider the Euler–Bernoulli beam element. Since two primary degrees of freedom are specified ($U_1 = U_2 = 0$), a one-element mesh will have only two unknown degrees of freedom (U_3 and U_4). Hence, we can determine only two natural frequencies. Thus, a minimum of two Euler–Bernoulli beam elements are needed to determine four natural frequencies. If we use the reduced integration Timoshenko beam element, a mesh of two linear elements can only represent the first two mode shapes of the cantilever beam (see Fig. 6.1.4) because there are only two independent deflection degrees of freedom that are unspecified. In order to represent the first four mode shapes using the *reduced integration element* (RIE), we must use at least four linear elements or two quadratic elements. However, the four computed frequencies may not be the lowest four.

For illustrative purpose, first we consider the one-element mesh of the Euler–Bernoulli beam element. We have

$$\left(\frac{2EI}{L^3} \begin{bmatrix} 6 & -3L & -6 & -3L \\ -3L & 2L^2 & 3L & L^2 \\ -6 & 3L & 6 & 3L \\ -3L & L^2 & 3L & 2L^2 \end{bmatrix} - \omega^2 \frac{\rho AL}{420} \begin{bmatrix} 156 & -22L & 54 & 13L \\ -22L & 4L^2 & -13L & -3L^2 \\ 54 & -13L & 156 & 22L \\ 13L & -3L^2 & 22L & 4L^2 \end{bmatrix} - \omega^2 \frac{\rho I}{30L} \begin{bmatrix} 36 & -3L & -36 & -3L \\ -3h & 4L^2 & 3L & -L^2 \\ -36 & 3L & 36 & 3L \\ -3L & -L^2 & 3L & 4L^2 \end{bmatrix} \right) \begin{Bmatrix} W_1 \\ \Theta_1 \\ W_2 \\ \Theta_2 \end{Bmatrix} = \begin{Bmatrix} Q_1 \\ Q_2 \\ Q_3 \\ Q_4 \end{Bmatrix}$$

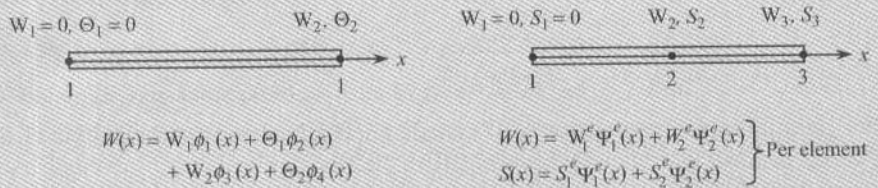

$$W(x) = W_1\phi_1(x) + \Theta_1\phi_2(x) + W_2\phi_3(x) + \Theta_2\phi_4(x)$$

$$\left.\begin{aligned} W(x) &= W_1^e\Psi_1^e(x) + W_2^e\Psi_2^e(x) \\ S(x) &= S_1^e\Psi_1^e(x) + S_2^e\Psi_2^e(x) \end{aligned}\right\} \text{Per element}$$

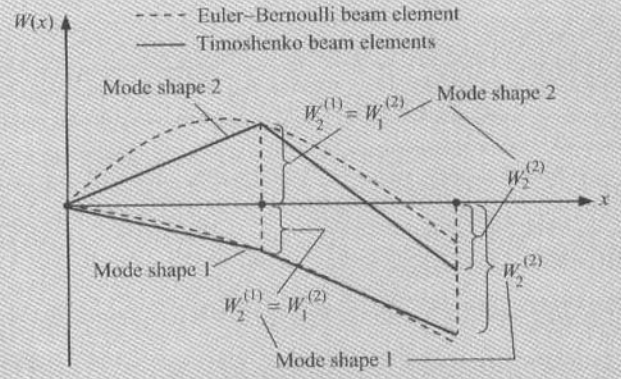

Figure 6.1.4 Two possible nonzero mode shapes of a cantilever beam that can be represented by a mesh of two linear Timoshenko beam elements (or one Euler–Bernoulli beam element).

The specified displacement and force degrees of freedom are $W_1 = 0$, $\Theta_1 = 0$, $Q_3 = 0$, and $Q_4 = 0$. Hence, the condensed equations are

$$\left(\frac{2EI}{L^3}\begin{bmatrix} 6 & 3L \\ 3L & 2L^2 \end{bmatrix} - \omega^2 \frac{\rho AL}{420}\begin{bmatrix} 156 & 22L \\ 22L & 4L^2 \end{bmatrix} - \omega^2 \frac{\rho I}{30L}\begin{bmatrix} 36 & 3L \\ 3L & 4L^2 \end{bmatrix}\right)\begin{Bmatrix} W_2 \\ \Theta_2 \end{Bmatrix} = \begin{Bmatrix} 0 \\ 0 \end{Bmatrix}$$

Setting the determinant of the coefficient matrix in the above equation to zero, we obtain a quadratic characteristic equation in ω^2.

First, consider the case in which the rotary inertia is neglected. The characteristic equation for this case is

$$15120 - 1224\lambda + \lambda^2 = 0, \quad \lambda = \frac{\rho AL^4}{EI}\omega^2$$

whose roots are

$$\lambda_1 = 12.48 \quad \lambda_2 = 1211.52, \quad \text{or} \quad \omega_1 = \frac{3.5327}{L^2}\sqrt{\frac{EI}{\rho A}}, \quad \omega_2 = \frac{34.8069}{L^2}\sqrt{\frac{EI}{\rho A}}$$

The exact frequencies are $\bar{\omega}_1 = 3.5160$ and $\bar{\omega}_2 = 22.0345$, where $\bar{\omega}_i = \omega_i(L^2\sqrt{\rho A/EI})$. The eigenvector components are computed from the first of the condensed equations

$$W_2^{(i)} = -L\left(\frac{1260 - 11\lambda_i}{420 - 13\lambda_i}\right)\Theta_2^{(i)}, \quad i = 1, 2$$

Hence, the eigenvectors are

$$\begin{Bmatrix} W_2 \\ \Theta_2 \end{Bmatrix}^{(1)} = \begin{Bmatrix} 0.7259L \\ -1.0000 \end{Bmatrix}, \quad \begin{Bmatrix} W_2 \\ \Theta_2 \end{Bmatrix}^{(2)} = \begin{Bmatrix} 0.1312L \\ -1.0000 \end{Bmatrix}$$

For the case in which rotary inertia is not neglected, we write $\rho I = \rho A\,(H^2/12)$ and take $H/L = 0.01$. The characteristic equation is

$$15112 - 1223.406\lambda + \lambda^2 = 0, \quad \lambda = \frac{\rho AL^4}{EI}\omega^2$$

whose roots are

$$\lambda_1 = 12.4797, \quad \lambda_2 = 1210.926 \quad \text{or} \quad \omega_1 = \frac{3.5327}{L^2}\sqrt{\frac{EI}{\rho A}}, \quad \omega_2 = \frac{34.7984}{L^2}\sqrt{\frac{EI}{\rho A}}$$

The exact frequencies are $\bar{\omega}_1 = 3.5158$ and $\bar{\omega}_2 = 22.0226$, where $\bar{\omega}_i = \omega_i(L^2\sqrt{\rho A/EI})$.

Next, we consider the one-element mesh of the Timoshenko beam element (RIE). We have

$$\left(\frac{2EI}{\mu_0 L^3}\begin{bmatrix} 6 & -3L & -6 & -3L \\ -3L & L^2\Xi_1 & 3L & L^2\Xi_2 \\ -6 & 3L & 6 & 3L \\ -3L & L^2\Xi_2 & 3L & L^2\Xi_1 \end{bmatrix} - \omega^2\frac{\rho AL}{6}\begin{bmatrix} 2 & 0 & 1 & 0 \\ 0 & 2r & 0 & r \\ 1 & 0 & 2 & 0 \\ 0 & r & 0 & 2r \end{bmatrix}\right)\begin{Bmatrix} W_1 \\ S_1 \\ W_2 \\ S_2 \end{Bmatrix} = \begin{Bmatrix} Q_1 \\ Q_2 \\ Q_3 \\ Q_4 \end{Bmatrix}$$

where $K_s = 5/6$, $r = I/A = H^2/12$, and

$$\Xi_1 = 1.5 + 6\Lambda, \quad \Xi_2 = 1.5 - 6\Lambda, \quad \Lambda = \frac{EI}{GAK_sL^2} = \frac{1+\nu}{5}\frac{H^2}{L^2}, \quad \mu_0 = 12\Lambda$$

The specified displacement and force degrees of freedom are $W_1 = 0$, $S_1 = 0$, $Q_3 = 0$, and $Q_4 = 0$; and the condensed equations are

$$\left(\frac{2EI}{\mu_0 L^3}\begin{bmatrix} 6 & 3L \\ 3L & L^2(1.5 + 6\Lambda) \end{bmatrix} - \omega^2\frac{\rho AL}{6}\begin{bmatrix} 2 & 0 \\ 0 & 2r \end{bmatrix}\right)\begin{Bmatrix} W_2 \\ S_2 \end{Bmatrix} = \begin{Bmatrix} 0 \\ 0 \end{Bmatrix}$$

Setting the determinant of the coefficient matrix to zero, we obtain the characteristic equation

$$\bar{\lambda}^2 - 3\left(1 + 3s^2 + 12s^2\Lambda\right)\bar{\lambda} + 108s^2 = 0, \quad \bar{\lambda} = \frac{\rho A L^4 \Lambda}{EI}\omega^2$$

where s is the length-to-height ratio, $s = L/H$.

When the rotary inertia is neglected, we have

$$\bar{\lambda} = \frac{12\Lambda}{1 + 4\Lambda}$$

To further simplify the expression, we assume $\nu = 0.25$ and obtain

$$\omega^2 = \frac{12}{(1 + H^2/L^2)} \frac{EI}{\rho A L^4}$$

and

$$\frac{L}{H} = 100: \quad \omega = \frac{3.4639}{L^2}\sqrt{\frac{EI}{\rho A}}; \qquad \frac{L}{H} = 10: \quad \omega = \frac{3.4469}{L^2}\sqrt{\frac{EI}{\rho A}}$$

The exact frequency is $\bar{\omega} = 3.5158$ for $L/H = 100$ and $\bar{\omega} = 3.5092$ for $L/H = 10$, where $\bar{\omega}_i = \omega_i(L^2\sqrt{\rho A/EI})$. If the rotary inertia is included, we obtain

$$\frac{L}{H} = 100: \quad \omega = \frac{3.4639}{L^2}\sqrt{\frac{EI}{\rho A}}; \qquad \frac{L}{H} = 10: \quad \omega = \frac{3.4413}{L^2}\sqrt{\frac{EI}{\rho A}}$$

The frequencies obtained by the Euler–Bernoulli beam elements and Timoshenko beam elements (RIE) are shown in Table 6.1.2 for two different values of the length-to-height ratio L/H. The value $L/H = 100$ makes the effect of shear deformation negligible, and we obtain essentially the same result as in the Euler–Bernoulli beam theory. Since the frequencies are normalized, $\bar{\omega} = \omega L^2\sqrt{(\rho A/EI)}$, it is necessary only to select the values of ν and L/H. For

Table 6.1.2 Natural frequencies of a cantilever beam according to Timoshenko beam theory (TBT) and Euler–Bernoulli beam theory (EBT) $[\bar{\omega} = \omega L^2(\rho A/EI)^{1/2}]$.

	$L/H = 100$				$L/H = 10$			
Mesh	$\bar{\omega}_1$	$\bar{\omega}_2$	$\bar{\omega}_3$	$\bar{\omega}_4$	$\bar{\omega}_1$	$\bar{\omega}_2$	$\bar{\omega}_3$	$\bar{\omega}_4$
4L	3.5406	25.6726	98.3953	417.1330	3.5137	24.1345	80.2244	189.9288
8L	3.5223	22.8851	68.8937	151.8431	3.4956	21.7004	60.6297	119.2798
16L	3.5174	22.2350	63.3413	127.5434	3.4908	21.1257	56.4714	104.6799
2Q	3.5214	23.3226	78.3115	328.3250	3.4947	22.0762	67.0884	181.0682
4Q	3.5161	22.1054	63.3271	133.9828	3.4895	21.0103	56.4572	108.6060
8Q	3.5158	22.0280	61.7325	121.4458	3.4892	20.4421	55.2405	100.7496
EBT†	3.5158	22.0226	61.6179	120.6152	3.4892	20.9374	55.1530	100.2116
TBT†	3.5158	22.0315	61.6774	120.8300	3.5092	21.7425	59.8013	114.2898
EBT‡	3.5160	22.0345	61.6972	120.9019	3.5160	22.0345	61.6972	120.9019

† Rotary inertia is included (Exact).

‡ Rotary inertia is neglected; the results are independent of the ratio L/H (Exact).

computational purposes, we take $\nu = 0.25$; also, note that

$$GAK = \frac{E}{2(1+\nu)} BH\frac{5}{6} = \frac{4EI}{H^2}, \quad \rho I = \frac{H^2 \rho A}{12}$$

where B and H are the width and height, respectively, of the beam.

We note from Table 6.1.2 that the finite element results converge with h-refinement (i.e., when more of the same kind of elements are used) and also with p-refinement (i.e., when higher-order elements are used). The p-refinement shows more rapid convergence of the fundamental (i.e., first) frequency. Note that the effect of shear deformation is to reduce the magnitude of natural frequency when compared to the EBT. In other words, the assumed infinite shear rigidity makes the EBT over-predict the magnitude of frequencies. The first four mode shapes of the cantilever beam, as obtained using the 16-element mesh of linear elements, are shown in Fig. 6.1.5.

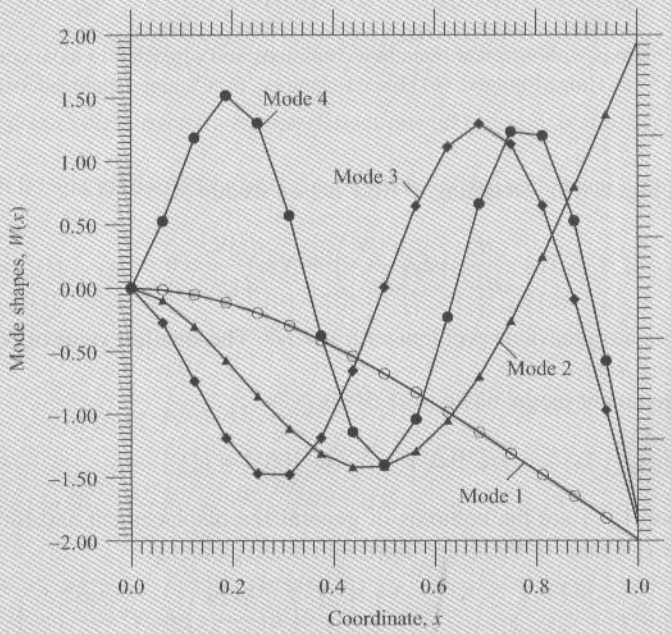

Figure 6.1.5 First four natural mode shapes of a cantilever beam, as predicted using a 16-element mesh of linear Timoshenko beam elements ($L/H = 10$).

In closing the discussion on natural vibration, it is noted that when the symmetry of the system is used to model the problem, only symmetric modes are predicted. It is necessary to model the whole system in order to obtain all the modes of vibration.

Stability (Buckling) of Beams

EBT

The study of buckling of beam-columns also leads to an eigenvalue problem. For example, the equation governing onset of buckling of a column subjected to an axial compressive

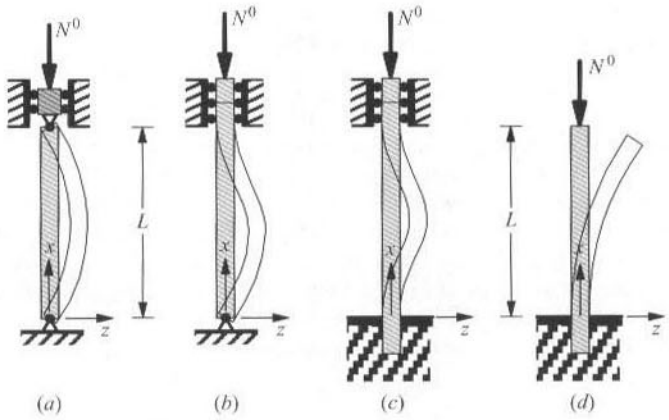

Figure 6.1.6 Columns with different boundary conditions and subjected to axial compressive load, N^0. (*a*) Hinged-hinged. (*b*) Hinged-clamped. (*c*) Clamped-clamped. (*d*) Clamped-free.

force N^0 (see Fig. 6.1.6), according to EBT is [see Reddy (1999*b*)]

$$\frac{d^2}{dx^2}\left(EI\frac{d^2W}{dx^2}\right)+N^0\frac{d^2W}{dx^2}=0 \tag{6.1.51}$$

which describes an eigenvalue problem with $\lambda = N^0$. The smallest value of N^0 is called the *critical buckling load*.

The finite element model of Eq. (6.1.51) is

$$[K^e]\{\Delta^e\}-N^0[G^e]\{\Delta^e\}=\{Q^e\} \tag{6.1.52a}$$

where $\{\Delta^e\}$ and $\{Q^e\}$ are the columns of generalized displacement and force degrees of freedom at the two ends of the Euler–Bernoulli beam element:

$$\{\Delta\}^e=\begin{Bmatrix} W_1 \\ \left(-\dfrac{dW}{dx}\right)_1 \\ W_2 \\ \left(-\dfrac{dW}{dx}\right)_2 \end{Bmatrix}^e, \quad \{Q\}^e=\begin{Bmatrix} \left[\dfrac{d}{dx}\left(EI\dfrac{d^2W}{dx^2}\right)+N^0\dfrac{dW}{dx}\right]_1 \\ \left(EI\dfrac{d^2W}{dx^2}\right)_1 \\ \left[-\dfrac{d}{dx}\left(EI\dfrac{d^2W}{dx^2}\right)-N^0\dfrac{dW}{dx}\right]_2 \\ \left(-EI\dfrac{d^2W}{dx^2}\right)_2 \end{Bmatrix}^e \tag{6.1.52b}$$

where the subscripts 1 and 2 refer to element nodes 1 and 2 (at $x = x_a$ and $x = x_b$, respectively). The coefficients of the stiffness matrix $[K^e]$ and the *stability matrix* $[G^e]$ are

$$K_{ij}^e=\int_{x_a}^{x_b} EI\frac{d^2\phi_i^e}{dx^2}\frac{d^2\phi_j^e}{dx^2}\,dx, \quad G_{ij}^e=\int_{x_a}^{x_b}\frac{d\phi_i^e}{dx}\frac{d\phi_j^e}{dx}\,dx \tag{6.1.52c}$$

where ϕ_i^e are the Hermite cubic interpolation functions. The explicit form of $[G^e]$ is [see the second part of the mass matrix in Eq. (6.1.42)]

$$[G^e] = \frac{1}{30h_e}\begin{bmatrix} 36 & -3h_e & -36 & -3h_e \\ -3h_e & 4h_e^2 & 3h_e & -h_e^2 \\ -36 & 3h_e & 36 & 3h_e \\ -3h_e & -h_e^2 & 3h_e & 4h_e^2 \end{bmatrix} \tag{6.1.52d}$$

TBT

For TBT, the equations governing buckling of beams are [see Reddy (1999*b*)]

$$-\frac{d}{dx}\left[GAK_s\left(\frac{dW}{dx}+S\right)\right] + N^0\frac{d^2W}{dx^2} = 0 \tag{6.1.53a}$$

$$-\frac{d}{dx}\left(EI\frac{dS}{dx}\right) + GAK_s\left(\frac{dW}{dx}+S\right) = 0 \tag{6.1.53b}$$

Here $W(x)$ and $S(x)$ denote the transverse deflection and rotation, respectively, at the onset of buckling.

The finite element model of Eqs. (6.1.53*a*) and (6.1.53*b*), with equal interpolation of W and S, is

$$\left(\begin{bmatrix} [K^{11}] & [K^{12}] \\ [K^{12}]^{\mathrm{T}} & [K^{22}] \end{bmatrix} - N^0\begin{bmatrix} [G] & [0] \\ [0] & [0] \end{bmatrix}\right)\begin{Bmatrix} \{W^e\} \\ \{S^e\} \end{Bmatrix} = \begin{Bmatrix} \{V^e\} \\ \{M^e\} \end{Bmatrix} \tag{6.1.54a}$$

where

$$\begin{aligned}
K_{ij}^{11} &= \int_{x_a}^{x_b} GAK_s\frac{d\psi_i^e}{dx}\frac{d\psi_j^e}{dx}\,dx \\
K_{ij}^{12} &= \int_{x_a}^{x_b} GAK_s\frac{d\psi_i^e}{dx}\psi_j^e\,dx \\
K_{ij}^{22} &= \int_{x_a}^{x_b}\left(GAK_s\psi_i^e\psi_j^e + EI\frac{d\psi_i^e}{dx}\frac{d\psi_j^e}{dx}\right)dx \\
G_{ij} &= \int_{x_a}^{x_b}\psi_i^e\psi_j^e\,dx \\
V_1^e \equiv Q_1^e &= \left[-GAK_s\left(\frac{dW}{dx}+S\right) + N^0\frac{dW}{dx}\right]_{x_a} \\
V_n^e \equiv Q_3^e &= \left[GAK_s\left(\frac{dW}{dx}+S\right) - N^0\frac{dW}{dx}\right]_{x_b} \\
M_1^e \equiv Q_2^e &= \left(-EI\frac{dS}{dx}\right)_{x_a} \\
M_n^e \equiv Q_4^e &= \left(-EI\frac{dS}{dx}\right)_{x_b}
\end{aligned} \tag{6.1.54b}$$

For the linear RIE, the stiffness matrix $[K^e]$ is given in Eq. (6.1.49*a*). The stability matrix is given by

$$[G^e] = \frac{1}{h_e}\begin{bmatrix} 1 & 0 & -1 & 0 \\ 0 & 0 & 0 & 0 \\ -1 & 0 & 1 & 0 \\ 0 & 0 & 0 & 0 \end{bmatrix} \tag{6.1.55}$$

Example 6.1.3

Consider a uniform column (L, A, I, E, and ν) fixed at one end and pinned at the other, as shown in Fig. 6.1.7. We wish to determine the critical buckling load.

Let us consider a mesh of two Euler–Bernoulli beam elements. The assembled system of finite element equations is ($h = L/2$)

$$\left(\frac{2EI}{h^3}\begin{bmatrix} 6 & -3h & -6 & -3h & 0 & 0 \\ -3h & 2h^2 & 3h & h^2 & 0 & 0 \\ -6 & 3h & 6+6 & 3h-3h & -6 & -3h \\ -3h & h^2 & 3h-3h & 2h^2+2h^2 & 3h & h^2 \\ 0 & 0 & -6 & 3h & 6 & 3h \\ 0 & 0 & -3h & h^2 & 3h & 2h^2 \end{bmatrix} - \frac{N^0}{30h}\begin{bmatrix} 36 & -3h & -36 & -3h & 0 & 0 \\ -3h & 4h^2 & 3h & -h^2 & 0 & 0 \\ -36 & 3h & 36+36 & 3h-3h & -36 & -3h \\ -3h & -h^2 & 3h-3h & 4h^2+4h^2 & 3h & -h^2 \\ 0 & 0 & -36 & 3h & 36 & 3h \\ 0 & 0 & -3h & -h^2 & 3h & 4h^2 \end{bmatrix} \right) \begin{Bmatrix} U_1 \\ U_2 \\ U_3 \\ U_4 \\ U_5 \\ U_6 \end{Bmatrix} = \begin{Bmatrix} Q_1^1 \\ Q_2^1 \\ Q_3^1 + Q_1^2 \\ Q_4^1 + Q_2^2 \\ Q_3^2 \\ Q_4^2 \end{Bmatrix}$$

where U_I denote the generalized displacements of the global nodes.

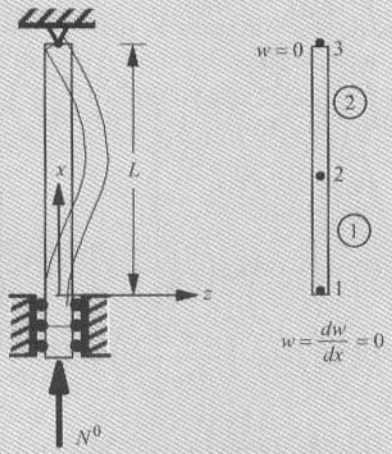

Figure 6.1.7 A column fixed at $x = 0$ and hinged at $x = L$, and subjected to axial compressive load N^0.

The geometric supports and equilibrium conditions of the column require that (note that the axial compressive force N^0 enters the equilibrium equation and the boundary condition through Q_3^2)

$$U_1 = U_2 = U_5 = 0, \quad Q_3^1 + Q_1^2 = 0, \quad Q_4^1 + Q_2^2 = 0, \quad Q_4^2 = 0$$

Hence, the condensed equations become

$$\left(\frac{2EI}{h^3} \begin{bmatrix} 12 & 0 & -3h \\ 0 & 4h^2 & h^2 \\ -3h & h^2 & 2h^2 \end{bmatrix} - \frac{N^0}{30h} \begin{bmatrix} 72 & 0 & -3h \\ 0 & 8h^2 & -h^2 \\ -3h & -h^2 & 4h^2 \end{bmatrix} \right) \begin{Bmatrix} U_3 \\ U_4 \\ U_6 \end{Bmatrix} = \begin{Bmatrix} 0 \\ 0 \\ 0 \end{Bmatrix}$$

which defines the eigenvalue problem for the determination of N^0 and U_I.

Setting the determinant of the coefficient matrix to zero, we obtain a cubic equation for N^0. The smallest value of N^0 is the critical buckling load, which is (obtained using FEM1D)

$$N_{\text{cri}}^0 = 20.7088 \frac{EI}{L^2}$$

whereas the "exact" solution is $20.187\, EI/L^2$ [see Reddy (1999*b*), pp. 155–166].

Next, consider a two-element mesh of the RIE. The assembled equations are

$$\left(\frac{2EI}{\mu_0 h^3} \begin{bmatrix} 6 & -3h & -6 & -3h & 0 & 0 \\ -3h & h^2\Xi_1 & 3h & h^2\Xi_2 & 0 & 0 \\ -6 & 3h & 12 & 0 & -6 & -3h \\ -3h & h^2\Xi_2 & 0 & 2h^2\Xi_1 & 3h & h^2\Xi_2 \\ 0 & 0 & -6 & 3h & 6 & 3h \\ 0 & 0 & -3h & h^2\Xi_2 & 3h & h^2\Xi_1 \end{bmatrix} - \frac{N^0}{h} \begin{bmatrix} 1 & 0 & -1 & 0 & 0 & 0 \\ 0 & 0 & 0 & 0 & 0 & 0 \\ -1 & 0 & 2 & 0 & -1 & 0 \\ 0 & 0 & 0 & 0 & 0 & 0 \\ 0 & 0 & -1 & 0 & 1 & 0 \\ 0 & 0 & 0 & 0 & 0 & 0 \end{bmatrix} \right) \begin{Bmatrix} U_1 \\ U_2 \\ U_3 \\ U_4 \\ U_5 \\ U_6 \end{Bmatrix} = \begin{Bmatrix} Q_1^1 \\ Q_2^1 \\ Q_3^1 + Q_1^2 \\ Q_4^1 + Q_2^2 \\ Q_3^2 \\ Q_4^2 \end{Bmatrix}$$

where $K_s = 5/6$, and

$$\Xi_1 = 1.5 + 6\Lambda, \quad \Xi_2 = 1.5 - 6\Lambda, \quad \mu_0 = 12\Lambda, \quad \Lambda = \frac{EI}{GAK_s h^2} = \frac{1+\nu}{5}\frac{H^2}{h^2}$$

The condensed equations are

$$\left(\frac{2EI}{\mu_0 h^3} \begin{bmatrix} 12 & 0 & -3h \\ 0 & 2h^2\Xi_1 & h^2\Xi_2 \\ -3h & h^2\Xi_2 & h^2\Xi_1 \end{bmatrix} - \frac{N^0}{h} \begin{bmatrix} 2 & 0 & 0 \\ 0 & 0 & 0 \\ 0 & 0 & 0 \end{bmatrix} \right) \begin{Bmatrix} U_3 \\ U_4 \\ U_6 \end{Bmatrix} = \begin{Bmatrix} 0 \\ 0 \\ 0 \end{Bmatrix}$$

Note that because of the zero diagonal element in the stability matrix, we obtain a linear algebraic equation for N^0 ($\nu = 0.25$ and $\Lambda = H^2/L^2$)

$$N^0 = \frac{180 + 144\Lambda}{2.25 + 54\Lambda + 36\Lambda^2} \frac{EI}{L^2}$$

which is almost four times the correct value! A mesh of eight linear RIEs yields $21.348\,EI/L^2$ and four quadratic elements yields $20.267\,EI/L^2$ for $L/H = 100$. Clearly, the RIE has slow convergence rate for buckling problems.

We close this section with a note that eigenvalue problems (for natural vibration and buckling analysis) of frame structures can be formulated using the ideas discussed in Section 5.4. The transformed element equations are of the form

$$[K^e]\{\Delta^e\} - \omega^2[M^e]\{\Delta^e\} = \{Q^e\}, \quad [K^e]\{\Delta^e\} - N^0[G^e]\{\Delta^e\} = \{Q^e\}$$
$$[K^e] = [T^e]^{\mathrm{T}}[\bar{K}^e][T^e], \quad [M^e] = [T^e]^{\mathrm{T}}[\bar{M}^e][T^e], \quad [G^e] = [T^e]^{\mathrm{T}}[\bar{G}^e][T^e] \tag{6.1.56}$$

6.2 TIME-DEPENDENT PROBLEMS

6.2.1 Introduction

In this section, we develop the finite element models of one-dimensional time-dependent problems and describe time approximation schemes to convert ordinary differential equations in time to algebraic equations. We consider finite element models of the time-dependent version of the differential equations studied in Chapters 3 and 5. These include the second-order (in space) parabolic (i.e., first time derivative) and hyperbolic (i.e., second time derivative) equations and fourth-order hyperbolic equations arising in connection with the bending of beams [see Eqs. (6.1.2), (6.1.14), (6.1.36), (6.1.43*a*), and (6.1.43*b*)].

Finite element models of time-dependent problems can be developed in two alternative ways: (*a*) coupled formulation in which the time t is treated as an additional coordinate along with the spatial coordinate x and (*b*) decoupled formulation where time and spatial variations are assumed to be separable. Thus, the approximation in the two formulations takes the form

$$u(x,t) \approx u_h^e(x,t) = \sum_{j=1}^{n} \hat{u}_j^e \hat{\psi}_j^e(x,t) \quad \text{(coupled formulation)} \tag{6.2.1a}$$

$$u(x,t) \approx u_h^e(x,t) = \sum_{j=1}^{n} u_j^e(t)\psi_j^e(x) \quad \text{(decoupled formulation)} \tag{6.2.1b}$$

where $\hat{\psi}_j^e(x,t)$ are time-space (two-dimensional) interpolation functions and $\hat{u}_j$ are the nodal values that are independent of x and t, where $\psi_j^e(x)$ are the usual one-dimensional interpolation functions in spatial coordinate x only and the nodal values $u_j^e(t)$ are functions of time t only. Derivation of the interpolation functions in two coordinates will be discussed in Chapters 8 and 9 in connection with the finite element analysis of two-dimensional problems. Space-time coupled finite element formulations are not common, and they have not been adequately studied. In this section, we consider the space-time decoupled formulation only.

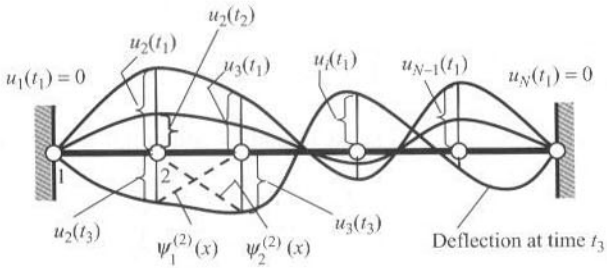

Figure 6.2.1 Deflections of a cable at different times.

The space-time decoupled finite element formulation of time-dependent problems involves two steps:

1. *Spatial approximation,* where the solution u of the equation under consideration is approximated by expressions of the form (6.2.1*b*), and the spatial finite element model of the equation is developed using the procedures of static or steady-state problems while carrying all time-dependent terms in the formulation. This step results in a set of ordinary differential equations (i.e., a semidiscrete system of equations) in time for the nodal variables $u_j^e(t)$ of the element. Equation (6.2.1*b*) represents the spatial approximation of u for any time t. When the solution is separable into functions of time only and space only, $u(x, t) = T(t)X(x)$, the approximation (6.2.1*b*) is clearly justified. Even when the solution is not separable, (6.2.1*b*) can represent a good approximation of the actual solution provided a sufficiently small time step is used.
2. *Temporal approximation,* where the system of ordinary differential equations are further approximated in time, often using finite difference formulae for the time derivatives. This step allows conversion of the system of ordinary differential equations into a set of algebraic equations among u_j^e at time $t_{s+1} = (s+1)\Delta t$, where Δt is the time increment and s is a nonnegative integer.

All time approximation schemes seek to find u_j at time t_{s+1} using the known values of u_j from previous times:

$$\text{compute} \quad \{u\}_{s+1} \quad \text{using} \quad \{u\}_s,\ \{u\}_{s-1},\ \ldots$$

Thus, at the end of the two-stage approximation, we have a continuous spatial solution at discrete intervals of time:

$$u(x, t_s) \approx u_h^e(x, t_s) = \sum_{j=1}^{n} u_j^e(t_s)\psi_j^e(x) \quad (s = 0, 1, \ldots) \tag{6.2.2}$$

Note that the approximate solution (6.2.2) has the same form as that in the separation-of-variables technique used to solve boundary value and initial value problems. By taking nodal values to be functions of time, we see that the spatial points in an element take on different values for different times (see Fig. 6.2.1).

We study the details of the two steps by considering a model differential equation that contains both second- and fourth-order spatial derivatives and first- and second-order time

derivatives:

$$-\frac{\partial}{\partial x}\left(a\frac{\partial u}{\partial x}\right)+\frac{\partial^2}{\partial x^2}\left(b\frac{\partial^2 u}{\partial x^2}\right)+c_0u+c_1\frac{\partial u}{\partial t}+c_2\frac{\partial^2 u}{\partial t^2}=f(x,t) \tag{6.2.3a}$$

The above equation is subject to appropriate boundary and initial conditions. The boundary conditions are of the form

$$\begin{aligned}&\text{specify} \quad u(x,t) \quad \text{or} \quad -a\frac{\partial u}{\partial x}+\frac{\partial}{\partial x}\left(b\frac{\partial^2 u}{\partial x^2}\right)\\ &\text{specify} \quad \frac{\partial u}{\partial x} \quad \text{or} \quad b\frac{\partial^2 u}{\partial x^2}\end{aligned} \tag{6.2.3b}$$

at $x=0$, L, and the initial conditions involve specifying

$$c_2u(x,0) \quad \text{and} \quad c_2\dot{u}(x,0)+c_1u(x,0) \tag{6.2.3c}$$

where $\dot{u}\equiv\partial u/\partial t$. Equation (6.2.3$a$) describes, for example, the following physical problems:

(a) Heat transfer and fluid flow: $c_2=0$ and $b=0$

(b) Transverse motion of a cable: $a=T$, $c_0=0$, $b=0$, $c_1=\rho$, $c_2=0$

(c) The longitudinal motion of a rod: $a=EA$, $b=0$; if damping is not considered, $c_1=0$, $c_2=\rho A$

(d) The transverse motion of an Euler–Bernoulli beam: $a=0$, $b=EI$, $c_0=k$, $c_1=0$, $c_2=\rho A$

We will consider these special cases through examples.

6.2.2 Semidiscrete Finite Element Models

The semidiscrete formulation involves approximation of the spatial variation of the dependent variable. The formulation follows essentially the same steps as described in Section 3.2. The first step involves the construction of the weak form of the equation over a typical element. In the second step, we develop the finite element model by seeking approximation of the form in (6.2.1b).

Following the three-step procedure of constructing the weak form of a differential equation, we can develop the weak form of (6.2.3a) over an element. Integration by parts is used once on the first term and twice on the second term to distribute the spatial derivatives equally between the weight function w and the dependent variable u:

$$\begin{aligned}0&=\int_{x_a}^{x_b} w\left[-\frac{\partial}{\partial x}\left(a\frac{\partial u}{\partial x}\right)+\frac{\partial^2}{\partial x^2}\left(b\frac{\partial^2 u}{\partial x^2}\right)+c_0u+c_1\frac{\partial u}{\partial t}+c_2\frac{\partial^2 u}{\partial t^2}-f\right]dx\\ &=\int_{x_a}^{x_b}\left[\frac{\partial w}{\partial x}a\frac{\partial u}{\partial x}+\frac{\partial^2 w}{\partial x^2}b\frac{\partial^2 u}{\partial x^2}+c_0wu+c_1w\frac{\partial u}{\partial t}+c_2w\frac{\partial^2 u}{\partial t^2}-wf\right]dx\\ &\quad+\left[w\left[\left(-a\frac{\partial u}{\partial x}\right)+\frac{\partial}{\partial x}\left(b\frac{\partial^2 u}{\partial x^2}\right)\right]+\frac{\partial w}{\partial x}\left(-b\frac{\partial^2 u}{\partial x^2}\right)\right]_{x_a}^{x_b}\end{aligned}$$

$$= \int_{x_a}^{x_b} \left(a\frac{\partial w}{\partial x}\frac{\partial u}{\partial x} + b\frac{\partial^2 w}{\partial x^2}\frac{\partial^2 u}{\partial x^2} + c_0 wu + c_1 w\frac{\partial u}{\partial t} + c_2 w\frac{\partial^2 u}{\partial t^2} - wf \right) dx$$

$$-\hat{Q}_1 w(x_a) - \hat{Q}_3 w(x_b) - \hat{Q}_2\left(-\frac{\partial w}{\partial x}\right)\Big|_{x_a} - \hat{Q}_4\left(-\frac{\partial w}{\partial x}\right)\Big|_{x_b} \tag{6.2.4a}$$

where

$$\hat{Q}_1 = \left[-a\frac{\partial u}{\partial x} + \frac{\partial}{\partial x}\left(b\frac{\partial^2 u}{\partial x^2}\right)\right]_{x_a}, \qquad \hat{Q}_2 = \left[b\frac{\partial^2 u}{\partial x^2}\right]_{x_a}$$
$$\hat{Q}_3 = -\left[-a\frac{\partial u}{\partial x} + \frac{\partial}{\partial x}\left(b\frac{\partial^2 u}{\partial x^2}\right)\right]_{x_b}, \qquad \hat{Q}_4 = -\left[b\frac{\partial^2 u}{\partial x^2}\right]_{x_b} \tag{6.2.4b}$$

Next, we assume that u is interpolated by an expression of the form (6.2.1b). Equation (6.2.1b) implies that, at any arbitrarily fixed time $t > 0$, the function u can be approximated by a linear combination of the ψ_j^e and $u_j^e(t)$, with $u_j^e(t)$ being the value of u at time t at the jth node of the element Ω_e. In other words, the time and spatial variations of u are separable. This assumption is not valid, in general, because it may not be possible to write the solution $u(x, t)$ as the product of a function of time only and a function of space only. However, with sufficiently small time steps, it is possible to obtain accurate solutions to even those problems for which the solution is not separable in time and space. The finite element solution that we obtain at the end of the analysis is continuous in space but not in time. We only obtain the finite element solution in the form

$$u(x, t_s) = \sum_{j=1}^{n} u_j^e(t_s)\psi_j^e(x) = \sum_{j=1}^{n} (u_j^s)^e \psi_j^e(x) \quad (s = 1, 2, \ldots) \tag{6.2.5}$$

where $(u_j^s)^e$ is the value of $u(x, t)$ at time $t = t_s$ and node j of the element Ω_e.

Substituting $w = \psi_i(x)$ (to obtain the ith equation of the system) and (6.2.1b) into (6.2.4a), we obtain

$$0 = \int_{x_a}^{x_b} \left[a\frac{d\psi_i}{dx}\left(\sum_{j=1}^{n} u_j\frac{d\psi_j}{dx}\right) + b\frac{d^2\psi_i}{dx^2}\left(\sum_{j=1}^{n} u_j\frac{d^2\psi_j}{dx^2}\right) + c_0\psi_i\left(\sum_{j=1}^{n} u_j\psi_j\right) \right.$$
$$\left. + c_1\psi_i\left(\sum_{j=1}^{n}\frac{du_j}{dt}\psi_j\right) + c_2\psi_i\left(\sum_{j=1}^{n}\frac{d^2u_j}{dt^2}\psi_j\right) - \psi_i f \right] dx$$
$$- \hat{Q}_1\psi_i(x_a) - \hat{Q}_3\psi_i(x_b) - \hat{Q}_2\left(-\frac{d\psi_i}{dx}\right)\Big|_{x_a} - \hat{Q}_4\left(-\frac{d\psi_i}{dx}\right)\Big|_{x_b}$$
$$= \sum_{j=1}^{n}\left[(K_{ij}^1 + K_{ij}^2)u_j + M_{ij}^1\frac{du_j}{dt} + M_{ij}^2\frac{d^2u_j}{dt^2} \right] - F_i \tag{6.2.6}$$

In matrix form, we have

$$[K]\{u\} + [M^1]\{\dot{u}\} + [M^2]\{\ddot{u}\} = \{F\} \tag{6.2.7a}$$

where

$$[K] = [K^1] + [K^2] + [M^0] \tag{6.2.7b}$$

$$\begin{aligned} M_{ij}^0 &= \int_{x_a}^{x_b} c_0\, \psi_i \psi_j \, dx, & M_{ij}^1 &= \int_{x_a}^{x_b} c_1\, \psi_i \psi_j \, dx \\ M_{ij}^2 &= \int_{x_a}^{x_b} c_2\, \psi_i \psi_j \, dx, & K_{ij}^1 &= \int_{x_a}^{x_b} a \frac{d\psi_i}{dx} \frac{d\psi_j}{dx} \, dx \\ K_{ij}^2 &= \int_{x_a}^{x_b} b \frac{d^2\psi_i}{dx^2} \frac{d^2\psi_j}{dx^2} \, dx, & F_i &= \int_{x_a}^{x_b} \psi_i f \, dx + \hat{Q}_i \end{aligned} \tag{6.2.7c}$$

Equation (6.2.7*a*) is a hyperbolic equation, and it contains the parabolic equation as a special case (set $[M^2] = [0]$). The time approximation of (6.2.7*a*) for these two cases will be considered separately. We begin with the parabolic equation.

6.2.3 Parabolic Equations

Time Approximation

The time approximation is discussed with the help of a single first-order differential equation. Suppose that we wish to determine $u(t)$ for $t > 0$ such that $u(t)$ satisfies

$$a\frac{du}{dt} + bu = f(t), \quad 0 < t < T \quad \text{and} \quad u(0) = u_0 \tag{6.2.8}$$

where $a \neq 0$, b, and u_0 are constants, and f is a function of time t. The exact solution of the problem consists of two parts: the homogeneous and particular solutions. The homogeneous solution is

$$u^h(t) = Ae^{-kt}, \quad k = \frac{b}{a}$$

The particular solution is given by

$$u^p(t) = \frac{1}{a} e^{-kt} \left(\int_0^t e^{k\tau} f(\tau)\, d\tau \right)$$

The complete solution is given by

$$u(t) = e^{-kt} \left(A + \frac{1}{a} \int_0^t e^{k\tau} f(\tau)\, d\tau \right) \tag{6.2.9}$$

In the finite difference solution of (6.2.8), we replace the derivatives with their finite difference approximation. The most commonly used scheme for solving (6.2.8) is the *α-family of approximation* in which a weighted average of the time derivatives at two consecutive time steps is approximated by linear interpolation of the values of the variable at the two steps (see Fig. 6.2.2):

$$(1 - \alpha)\dot{u}_s + \alpha\, \dot{u}_{s+1} = \frac{u_{s+1} - u_s}{\Delta t_{s+1}} \quad \text{for } 0 \leq \alpha \leq 1 \tag{6.2.10a}$$

where u_s denotes the value of $u(t)$ at time $t = t_s = \sum_{i=1}^{s} \Delta t_i$, and $\Delta t_s = t_s - t_{s-1}$ is the sth time step. If the total time $[0,\ T]$ is divided into equal time steps, then $t_s = s\Delta t$. Equation (6.2.10*a*) can be expressed as

$$\begin{aligned} u_{s+1} &= u_s + \Delta t\, \dot{u}_{s+\alpha} \\ \dot{u}_{s+\alpha} &= (1 - \alpha)\dot{u}_s + \alpha\, \dot{u}_{s+1} \quad \text{for } 0 \leq \alpha \leq 1 \end{aligned} \tag{6.2.10b}$$

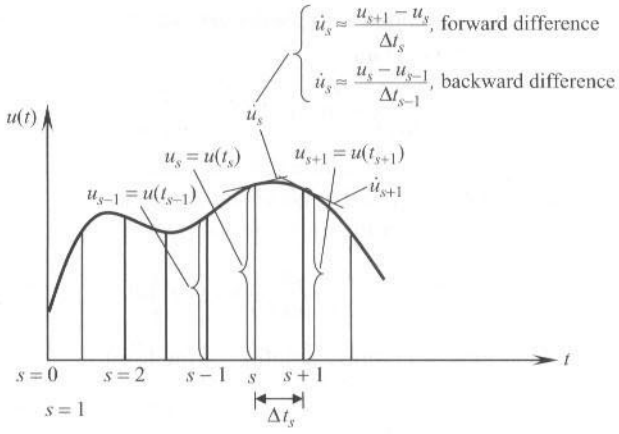

Figure 6.2.2 Approximation of the derivative of a function.

When $\alpha = 0$, Eq. (6.2.10a) gives

$$\dot{u}_s = \frac{u_{s+1} - u_s}{\Delta t_{s+1}}$$

which is nothing but the slope of the function $u(t)$ at time $t = t_s$ based on the values of the function at time t_s and t_{s+1}. Since the value of the function from a step in front is used, it is termed a *forward difference* approximation. When $\alpha = 1$, we obtain

$$\dot{u}_{s+1} = \frac{u_{s+1} - u_s}{\Delta t_{s+1}} \quad \rightarrow \quad \dot{u}_s = \frac{u_s - u_{s-1}}{\Delta t_s}$$

which is termed, for obvious reason, the *backward difference* approximation.

Returning to Eq. (6.2.8), we note that it is valid for all times $t > 0$. In particular, it is valid at times $t = t_s$ and $t = t_{s+1}$. Hence, from Eq. (6.2.8) we have

$$\dot{u}_s = \frac{1}{a}(f_s - bu_s), \quad \dot{u}_{s+1} = \frac{1}{a}(f_{s+1} - bu_{s+1})$$

Substituting the above expressions into Eq. (6.2.10a), we arrive at

$$(1-\alpha)(f_s - bu_s) + \alpha(f_{s+1} - bu_{s+1}) = a\left(\frac{u_{s+1} - u_s}{\Delta t_{s+1}}\right)$$

Solving for u_{s+1}, we obtain

$$[a + \alpha\,\Delta t_{s+1}\,b]\,u_{s+1} = [a - (1-\alpha)\,\Delta t_{s+1}\,b]\,u_s + \Delta t_{s+1}\,[\alpha\,f_{s+1} + (1-\alpha)f_s] \tag{6.2.11a}$$

or

$$u_{s+1} = \frac{a - (1-\alpha)\,\Delta t_{s+1}\,b}{a + \alpha\,\Delta t_{s+1}\,b}u_s + \Delta t_{s+1}\frac{[\alpha\,f_{s+1} + (1-\alpha)f_s]}{a + \alpha\,\Delta t_{s+1}\,b} \tag{6.2.11b}$$

Thus, Eq. (6.2.11) can be used repeatedly to march in time and obtain the solution at times $t = t_{s+1}, t_{s+2}, \ldots, t_N$, where Ntime is the number of time steps required to reach the final

time T (or the solution reaches a steady state). At the very beginning, i.e., $s = 0$, the solution u_1 is calculated using the initial value u_0:

$$u_1 = \frac{a - (1-\alpha)\,\Delta t_1\, b}{a + \alpha\,\Delta t_1\, b} u_0 + \Delta t_1 \frac{[\alpha\, f_1 + (1-\alpha) f_0]}{a + \alpha\,\Delta t_1\, b} \tag{6.2.12}$$

We may also develop a time approximation scheme using the finite element method. To this end, we consider the problem in (6.2.8). We wish to determine u_{s+1} in terms of u_s. The weighted-integral form of (6.2.8) over the time interval (t_s, t_{s+1}) is

$$0 = \int_{t_s}^{t_{s+1}} v(t) \left(a \frac{du}{dt} + bu - f \right) dt \tag{6.2.13}$$

where v is the weight function. Assuming a solution of the form

$$u(t) \approx \sum_{j=1}^{n} u_j \psi_j(t)$$

where $\psi_j(t)$ are interpolation functions of order $(n-1)$. The Galerkin finite element model is obtained by substituting the above approximation for u and $v = \psi_i$ into (6.2.13). We obtain

$$[A]\{u\} = \{F\} \tag{6.2.14}$$

where

$$A_{ij} = \int_{t_s}^{t_{s+1}} \psi_i(t) \left(a \frac{d\psi_j}{dt} + b\psi_j \right) dt, \quad F_i = \int_{t_s}^{t_{s+1}} \psi_i(t) f(t)\, dt \tag{6.2.15}$$

Equation (6.2.14) is valid with the time interval (t_s, t_{s+1}), and it represents a relationship between the values $u_1, u_2, \ldots, u_n$, which are the values of u at time $t_s, t_{s+\Delta t/(n-1)}, t_{s+2\Delta t/(n-1)}, \ldots, t_{s+1}$, respectively. This would yield a multistep approximation scheme.

To obtain a single-step approximation scheme, i.e., write u_{s+1} in terms of u_s only, we assume linear approximation (i.e., $n = 2$)

$$u(t) = u_s \psi_1(t) + u_{s+1} \psi_2(t)$$

where $\psi_1(t) = \frac{t_{s+1} - t}{\Delta t}$ and $\psi_2(t) = \frac{t - t_s}{\Delta t}$. In the same fashion, $f(t)$ can be represented in terms of its values at t_s and t_{s+1}:

$$f(t) = f_s \psi_1(t) + f_{s+1} \psi_2(t)$$

For this choice of approximation, Eq. (6.2.15) becomes

$$\left(\frac{a}{2} \begin{bmatrix} -1 & 1 \\ -1 & 1 \end{bmatrix} + \frac{b\Delta t}{6} \begin{bmatrix} 2 & 1 \\ 1 & 2 \end{bmatrix} \right) \begin{Bmatrix} u_s \\ u_{s+1} \end{Bmatrix} = \frac{\Delta t}{6} \begin{Bmatrix} f_s \\ 2f_{s+1} \end{Bmatrix} \tag{6.2.16}$$

Assuming that u_s is known, we solve for u_{s+1} from the second equation in (6.2.16)

$$\left(a + \frac{2b\Delta t}{3} \right) u_{s+1} = \left(a - \frac{b\Delta t}{3} \right) u_s + \Delta t \left(\frac{f_s}{3} + \frac{2f_{s+1}}{3} \right) \tag{6.2.17}$$

Comparing Eq. (6.2.17) with Eq. (6.2.11a), we find that the Galerkin scheme is a special case of the α-family of approximation, with $\alpha = 2/3$.

Stable and Conditionally Stable Schemes

Equation (6.2.11*b*) can be written in the form

$$u_{s+1} = A(u_s) + F_{s,s+1}, \quad A = \frac{a - (1-\alpha)\,\Delta t_{s+1}\, b}{a + \alpha\,\Delta t_{s+1}\, b}$$

$$F_{s,s+1} = \Delta t_{s+1} \frac{[\alpha\, f_{s+1} + (1-\alpha) f_s]}{a + \alpha\,\Delta t_{s+1}\, b} \tag{6.2.18}$$

The operator A is known as the *amplification operator*. Since u_s is an approximate solution, the error $E_s = u_a(t_s) - u_s$ at time t_s (where u_a is the exact solution) will influence the solution at t_{s+1}. The error will grow (i.e., E_s will be amplified) as we march in time if the magnitude of the operator is greater than 1, $|A| > 1$. When the error grows without bound, the computational scheme (6.2.11*b*) becomes unstable (i.e., solution u_{s+1} becomes unbounded with time). Therefore, in order for the scheme to be stable, it is necessary that $|A| \leq 1$:

$$\left| \frac{a - (1-\alpha)\,\Delta t_{s+1}\, b}{a + \alpha\,\Delta t_{s+1}\, b} \right| \leq 1 \tag{6.2.19}$$

The above equation places a restriction on the magnitude of the time step for certain values of α. When the error remains bounded for any time step [i.e., condition (6.2.19) is trivially satisfied for any value of Δt], the scheme is *stable*. If the error remains bounded only when the time step remains below certain value [in order to satisfy (6.2.19)], the scheme is said to be *conditionally stable*.

For different values of α, the time approximation scheme in (6.2.11*b*) yields a different scheme. The following well-known time-approximation schemes along with their order of accuracy and stability should be noted:

$$\alpha = \begin{cases} 0, & \text{the forward difference (or Euler) scheme (conditionally stable); order of accuracy } = O(\Delta t) \\ \frac{1}{2}, & \text{the Crank–Nicolson scheme (stable); } O(\Delta t)^2 \\ \frac{2}{3}, & \text{the Galerkin method (stable); } O(\Delta t)^2 \\ 1, & \text{the backward difference scheme (stable); } O(\Delta t) \end{cases} \tag{6.2.20}$$

Of these, the Crank–Nicolson method is the most commonly used scheme.

Fully Discretized Finite Element Equations

We now have the tools necessary to convert the set of ordinary differential equations (6.2.7*a*) to a set of algebraic equations in much the same way we converted a single differential equation (6.2.8) to an algebraic equation (6.2.11*b*). Here, we work with matrix equation [i.e., $[M^1] = [M]$ and $[M^2] = [0]$ in Eq. (6.2.7*a*)]

$$[M]\{\dot{u}\} + [K]\{u\} = \{F\} \tag{6.2.21a}$$

subject to the initial conditions

$$\{u\}_0 = \{u_0\} \tag{6.2.21b}$$

where $\{u\}_0$ denotes the vector of nodal values of u at time $t=0$, whereas $\{u_0\}$ denotes the column of nodal values u_{j0}. As applied to a vector of time derivatives of the nodal values, the α-family of approximation reads as

$$\Delta t_{s+1}\,[(1-\alpha)\{\dot{u}\}_s + \alpha\{\dot{u}\}_{s+1}] = \{u\}_{s+1} - \{u\}_s \quad \text{for } 0 \le \alpha \le 1 \tag{6.2.22a}$$

or

$$\begin{aligned} \{u\}_{s+1} &= \{u\}_s + \Delta t\{\dot{u}\}_{s+\alpha} \\ \{\dot{u}\}_{s+\alpha} &= (1-\alpha)\{\dot{u}\}_s + \alpha\{\dot{u}\}_{s+1} \end{aligned} \tag{6.2.22b}$$

for $0 \le \alpha \le 1$. Equation (6.2.22a) can be used to reduce the ordinary differential equations (6.2.21a) to algebraic equations among the u_j at time t_{s+1}. Since (6.2.21a) is valid for any $t > 0$, we can write it for times $t = t_s$ and $t = t_{s+1}$:

$$[M]\{\dot{u}\}_s + [K]_s\{u\}_s = \{F\}_s \tag{6.2.23a}$$

$$[M]\{\dot{u}\}_{s+1} + [K]_{s+1}\{u\}_{s+1} = \{F\}_{s+1} \tag{6.2.23b}$$

where it is assumed that the matrix $[M]$ is independent of time. Premultiplying both sides of (6.2.22a) with $[M]$ we obtain

$$\Delta t_{s+1}\alpha[M]\{\dot{u}\}_{s+1} + \Delta t_{s+1}(1-\alpha)[M]\{\dot{u}\}_s = [M](\{u\}_{s+1} - \{u\}_s)$$

Substituting for $[M]\{\dot{u}\}_{s+1}$ and $[M]\{\dot{u}\}_s$ from (6.2.23a) and (6.2.23b), respectively, we arrive at

$$\Delta t_{s+1}\alpha(\{F\}_{s+1} - [K]_{s+1}\{u\}_{s+1}) + \Delta t_{s+1}(1-\alpha)(\{F\}_s - [K]_s\{u\}_s) = [M](\{u\}_{s+1} - \{u\}_s)$$

Solving for the vector $\{u\}_{s+1}$, we obtain

$$[\hat{K}]_{s+1}\{u\}_{s+1} = [\bar{K}]_s\{u\}_s + \{\bar{F}\}_{s,s+1} \tag{6.2.24a}$$

where

$$\begin{aligned} [\hat{K}]_{s+1} &= [M] + a_1[K]_{s+1}, \quad [\bar{K}]_s = [M] - a_2[K]_s \\ \{\bar{F}\}_{s,s+1} &= \Delta t_{s+1}[\alpha\{F\}_{s+1} + (1-\alpha)\{F\}_s] \\ a_1 &= \alpha\Delta t_{s+1}, \quad a_2 = (1-\alpha)\Delta t_{s+1} \end{aligned} \tag{6.2.24b}$$

Note that, in deriving (6.2.24a) and (6.2.24b), it has been assumed that $[M]$ is independent of time and that the time step is nonuniform.

Equations (6.2.24a) and (6.2.24b) are valid for a typical finite element whose semidiscretized equations are of the form (6.2.21a). In other words, Eqs. (6.2.24a) and (6.2.24b) hold for any problem, independent of the dimension and method of spatial approximation, as long as the end result is Eq. (6.2.21a). The assembly, imposition of boundary conditions, and solution of the assembled equations are the same as described before for steady-state problems. Calculation of $[\hat{K}]$ and $\{\bar{F}\}$ at time $t=0$ requires knowledge of the initial conditions $\{u\}_0$ and the time variation of $\{F\}$. Note that for $\alpha = 0$ (the forward difference scheme), we obtain $[\hat{K}] = [M]$. If matrix $[M]$ is diagonal, (6.2.24a) becomes

$$u_i^{s+1} = \frac{1}{M_{(ii)}}\left(\sum_{j=1}^{n} \bar{K}_{ij}^s u_j^s + \hat{F}_i^{s,s+1}\right), \quad \text{(no sum on } i\text{)} \tag{6.2.25}$$

Thus, no inversion of the coefficient matrix is required in solving for $\{u\}^{s+1}$. Such a scheme is called *explicit*. A scheme is said to be *implicit* when it is not explicit (i.e., an implicit scheme requires the inversion of a coefficient matrix). Thus, explicit schemes are computationally less expensive compared to implicit schemes; implicit schemes are more accurate and have larger critical time steps. In real-world problems, the cost of computation precludes the use of implicit schemes.

In conventional finite element formulations, $[M]$ is seldom diagonal. Therefore, explicit schemes in finite element analysis can exist only if the time-approximation scheme is such that $[\hat{K}] = [M]$ and $[M]$ is *diagonal*. The matrix $[M]$ computed according to the definition (6.2.7*c*) is called the *consistent (mass) matrix*, and it is not diagonal unless ψ_i are orthogonal functions over the element domain. There are several ways to diagonalize mass matrices; these will be discussed in Section 6.2.5.

Consistency, Accuracy, and Stability

Since (6.2.22*a*) represents an approximation, which is used to derive (6.2.24*a*), error is introduced into the solution $\{u\}_{s+1}$ at each time step. In addition to the truncation error introduced in approximating the derivative, round-off errors can be introduced because of the finite arithmetic used in the computations. Since the solution at time t_{s+1} depends on the solution at time t_s, the error can grow with time. As discussed earlier, if the error is bounded, the solution scheme is said to be stable. The numerical scheme (6.2.24*a*) is said to be *consistent* with the continuous problem (6.2.7*a*) if the round-off and truncation errors go to zero as $\Delta t \to 0$. *Accuracy* of a numerical scheme is a measure of the closeness between the approximate solution and the exact solution whereas *stability* of a solution is a measure of the boundedness of the approximate solution with time. As we might expect, the size of the time step can influence both accuracy and stability. When we construct an approximate solution, we like it to converge to the true solution when the number of elements or the degree of approximation is increased and the time step Δt is decreased. A time-approximation scheme is said to be *convergent* if, for fixed t_s, the numerical value $\{u\}_s$ converges to its true value $\{u(t_s)\}$ as $\Delta t \to 0$. Accuracy is measured in terms of the rate at which the approximate solution converges. If a numerical scheme is stable and consistent, it is also convergent.

For all numerical schemes in which $\alpha < \frac{1}{2}$, the α-family of approximations is stable only if the time step satisfies the following (stability) condition [follows from Eq. (6.2.19)]:

$$\Delta t < \Delta t_{\text{cri}} \equiv \frac{2}{(1-2\alpha)\lambda} \tag{6.2.26}$$

where λ is the largest eigenvalue associated with the problem and Δt_{cri} is (see below)

$$([M] - \lambda[K])\{u\} = \{Q\} \tag{6.2.27}$$

Note that the same mesh as that used for the transient analysis must be used to calculate the eigenvalues.

6.2.4 Hyperbolic Equations

Time Approximation

Consider matrix equations of the form [set $[M^1] = [C]$ and $[M^2] = [M]$ in Eq. (6.2.7*a*)]

$$[K]\{u\} + [C]\{\dot{u}\} + [M]\{\ddot{u}\} = \{F\} \tag{6.2.28a}$$

subjected to initial conditions

$$\{u(0)\} = \{u_0\}, \quad \{\dot{u}(0)\} = \{v_0\} \tag{6.2.28b}$$

Such equations arise in structural dynamics, where $[M]$ denotes mass matrix, $[C]$ the damping matrix, and $[K]$ the stiffness matrix. The damping matrix $[C]$ is often taken to be a linear combination of the mass and stiffness matrices, $[C] = \beta_1[M] + \beta_2[K]$, where β_1 and β_2 are determined from physical experiments. In the present study, we will not consider damping (i.e., $[C] = [0]$) in the numerical examples, although the theoretical developments will account for it. Transient analysis of both bars and beams lead to equations of the type given in (6.2.28*a*) and (6.2.28*b*). The mass and stiffness matrices for these problems are discussed below.

Axial Motion of Bars

The equation of motion is given by Eq. (6.1.14). The semidiscretization results in Eq. (6.2.28*a*), with $[M^e]$ and $[K^e]$ given by Eq. (6.1.27*b*) and $[C] = [0]$.

Transverse Motion of Euler–Bernoulli Beams

The equation of motion is given by Eq. (6.1.36). The semidiscretized equation is the same as Eq. (6.2.28*a*), with $[M^e]$ and $[K^e]$ given by Eq. (6.1.41*b*) and $[C] = [0]$.

Transverse Motion of Timoshenko Beams

The equations of motion are given by Eqs. (6.1.43*a*) and (6.1.43*b*). The semidiscretization results in Eq. (6.2.28*a*), with $[M^e]$ and $[K^e]$ given by Eq. (6.1.48*a*). Note that $[M^e]$ and $[K^e]$ are the matrices given in Eq. (6.1.47).

There are several numerical methods available to approximate the second-order time derivatives and convert differential equations to algebraic equations. Among these, the Newmark family of time-approximation schemes is widely used in structural dynamics [Newmark (1959)]. Other methods, such as the Wilson method [Bathe and Wilson (1973)] and the Houbolt method [Houbolt (1950)], can also be used to develop the algebraic equations from the second-order differential equations (6.2.28*a*). Here we consider the Newmark family of approximation schemes.

Newmark's Scheme

In the Newmark method, the function and its first time derivative are approximated according to

$$\{u\}_{s+1} = \{u\}_s + \Delta t\{\dot{u}\}_s + \frac{1}{2}(\Delta t)^2\{\ddot{u}\}_{s+\gamma} \tag{6.2.29a}$$

$$\{\dot{u}\}_{s+1} = \{\dot{u}\}_s + \{\ddot{u}\}_{s+\alpha}\Delta t \tag{6.2.29b}$$

where

$$\{\ddot{u}\}_{s+\theta} = (1-\theta)\{\ddot{u}\}_s + \theta\{\ddot{u}\}_{s+1} \tag{6.2.29c}$$

and α and γ $(=2\beta)$ are parameters that determine the stability and accuracy of the scheme. Equations (6.2.29*a*) and (6.2.29*b*) can be viewed as Taylor's series expansions of u and $\dot{u}$. The following schemes are special cases of (6.2.29*a*) and (6.2.29*b*):

$$\begin{array}{lll}
\alpha = \frac{1}{2}, & \gamma = 2\beta = \frac{1}{2} & \text{Constant-average acceleration method (stable)} \\
\alpha = \frac{1}{2}, & \gamma = 2\beta = \frac{1}{3} & \text{Linear acceleration method (conditionally stable)} \\
\alpha = \frac{1}{2}, & \gamma = 2\beta = 0 & \text{Central difference method (conditionally stable)} \\
\alpha = \frac{3}{2}, & \gamma = 2\beta = \frac{8}{5} & \text{Galerkin method (stable)} \\
\alpha = \frac{3}{2}, & \gamma = 2\beta = 2 & \text{Backward difference method (stable)}
\end{array} \tag{6.2.30}$$

For all schemes in which $\gamma < \alpha$ and $\alpha \geq \frac{1}{2}$, the stability requirement is

$$\Delta t \leq \Delta t_{\text{cri}} = \left[\frac{1}{2}\omega_{\max}^2(\alpha - \gamma)\right]^{-1/2} \tag{6.2.31}$$

where $\omega_{\max}$ is the maximum natural frequency of the system (6.2.28*a*) without $[C]$:

$$\left([M] - \omega^2[K]\right)\{u\} = \{F\} \tag{6.2.32}$$

Fully Discretized Finite Element Equations

Eliminating $\{\ddot{u}\}_{s+1}$ from Eqs. (6.2.29*a*) and (6.2.29*b*) and writing the result for $\{\dot{u}\}_{s+1}$, we obtain

$$\{\dot{u}\}_{s+1} = a_6\left(\{u\}_{s+1} - \{u\}_s\right) - a_7\{\dot{u}\}_s - a_8\{\ddot{u}\}_s \tag{6.2.33}$$

where

$$a_6 = \frac{\alpha}{\beta\Delta t}, \quad a_7 = \frac{\alpha}{\beta} - 1, \quad a_8 = \left(\frac{\alpha}{\gamma} - 1\right)\Delta t \tag{6.2.34}$$

Now premultiplying Eq. (6.2.29*a*) with $[M]_{s+1}$ and substituting for $[M]_{s+1}\{\ddot{u}\}_{s+1}$ from Eq. (6.2.28*a*), we obtain

$$\begin{aligned}\left([M]_{s+1} + \beta(\Delta t)^2[K]_{s+1}\right)\{u\}_{s+1} = {} & [M]_{s+1}\{b\}_s + \beta(\Delta t)^2\{F\}_{s+1} \\ & -\beta(\Delta t)^2[C]_{s+1}\{\dot{u}\}_{s+1}\end{aligned} \tag{6.2.35}$$

where

$$\{b\}_s = \{u\}_s + \Delta t\{\dot{u}\}_s + \frac{1}{2}(1-\gamma)(\Delta t)^2\{\ddot{u}\}_s \tag{6.2.36}$$

Now, multiplying throughout with $a_3 = 1/[\beta(\Delta t)^2]$, we arrive at

$$\left(a_3[M]_{s+1} + [K]_{s+1}\right)\{u\}_{s+1} = a_3[M]_{s+1}\{b\}_s + \{F\}_{s+1} - [C]_{s+1}\{\dot{u}\}_{s+1} \tag{6.2.37}$$

Using Eq. (6.2.33) for $\{\dot{u}\}_{s+1}$ in Eq. (6.2.37) and collecting terms, we obtain the final result

$$[\hat{K}]_{s+1}\{u\}_{s+1} = \{\hat{F}\}_{s,s+1} \tag{6.2.38}$$

where

$$\begin{aligned} [\hat{K}]_{s+1} &= [K]_{s+1} + a_3[M]_{s+1} + a_6[C]_{s+1} \\ \{\hat{F}\}_{s,s+1} &= \{F\}_{s+1} + [M]_{s+1}\{A\}_s + [C]_{s+1}\{B\}_s \\ \{A\}_s &= a_3\{b\}_s = a_3\{u\}_s + a_4\{\dot{u}\}_s + a_5\{\ddot{u}\}_s \\ \{B\}_s &= a_6\{u\}_s + a_7\{\dot{u}\}_s + a_8\{\ddot{u}\}_s \end{aligned} \tag{6.2.39}$$

and

$$a_3 = \frac{1}{\beta(\Delta t)^2}, \quad a_4 = a_3\Delta t\ , \quad a_5 = \frac{1}{\gamma} - 1 \tag{6.2.40}$$

Note that the calculation of $[\hat{K}]$ and $\{\hat{F}\}$ requires knowledge of the initial conditions $\{u\}_0$, $\{\dot{u}\}_0$, and $\{\ddot{u}\}_0$. In practice, we do not know $\{\ddot{u}\}_0$. As an approximation, it can be calculated from (6.2.28*a*) (we often assume that the applied force is zero at $t = 0$):

$$\{\ddot{u}\}_0 = [M]^{-1}(\{F\}_0 - [K]\{u\}_0 - [C]\{\dot{u}\}_0) \tag{6.2.41}$$

At the end of each time step, the new velocity vector $\{\dot{u}\}_{s+1}$ and acceleration vector $\{\ddot{u}\}_{s+1}$ are computed using [from Eqs. (6.2.29*a*) and (6.2.29*b*)]

$$\begin{aligned} \{\ddot{u}\}_{s+1} &= a_3(\{u\}_{s+1} - \{u\}_s) - a_4\{\dot{u}\}_s - a_5\{\ddot{u}\}_s \\ \{\dot{u}\}_{s+1} &= \{\dot{u}\}_s + a_2\{\ddot{u}\}_s + a_1\{\ddot{u}\}_{s+1} \\ a_1 &= \alpha\Delta t, \quad a_2 = (1-\alpha)\Delta t \end{aligned} \tag{6.2.42}$$

The remaining procedure stays the same as in static problems.

The fully discretized model in (6.2.38) is based on the assumption that $\gamma \neq 0$. Obviously, for centered difference scheme ($\gamma = 0$), the formulation must be modified (see Problem 6.26).

6.2.5 Mass Lumping

Recall from the time approximation of parabolic equations that use of the forward difference scheme (i.e., $\alpha = 0$) results in the following time marching scheme [see (6.2.24*a*) and (6.2.24*b*)]:

$$[M^e]\{u\}_{s+1} = ([M^e] - \Delta t[K^e])\{u\}_s + \Delta t\{F^e\}_s \tag{6.2.43}$$

The mass matrix $[M^e]$ derived from the weighted-integral formulations of the governing equation is called the *consistent mass matrix*, and it is symmetric positive-definite and nondiagonal. Solution of the global equations associated with (6.2.43) requires inversion of the assembled mass matrix. If the mass matrix is diagonal, then the assembled equations can be solved directly (i.e., without inverting a matrix)

$$(U_I)_{s+1} = M_{II}^{-1}\left[M_{II}(U_I)_s - \Delta t\sum_{J=1}^{N} K_{IJ}(U_J)_s + \Delta t(F_I)_s\right] \tag{6.2.44}$$

and thus saving computational time. The explicit nature of (6.2.44) has motivated analysts to find rational ways of diagonalizing the mass matrix.

There are several ways of constructing diagonal mass matrices, also known as *lumped mass matrices*. The *row-sum* and *proportional lumping* techniques are discussed here.

Row-Sum Lumping

The sum of the elements of each row of the consistent mass matrix is used as the diagonal element:

$$M_{ii}^e = \sum_{j=1}^{n} \int_{x_a}^{x_b} \rho \psi_i^e \psi_j^e \, dx = \int_{x_a}^{x_b} \rho \psi_i^e \, dx \tag{6.2.45}$$

where the property $\sum_{j=1}^{n} \psi_j^e = 1$ of the interpolation functions is used. When ρ is constant, (6.2.45) gives

$$[M^e]_L = \frac{\rho h_e}{2} \begin{bmatrix} 1 & 0 \\ 0 & 1 \end{bmatrix} \quad \text{(linear element)}$$

$$[M^e]_L = \frac{\rho h_e}{6} \begin{bmatrix} 1 & 0 & 0 \\ 0 & 4 & 0 \\ 0 & 0 & 1 \end{bmatrix} \quad \text{(quadratic element)} \tag{6.2.46}$$

Compare these lumped mass matrices with the consistent mass matrices

$$[M^e]_C = \frac{\rho h_e}{6} \begin{bmatrix} 2 & 1 \\ 1 & 2 \end{bmatrix} \quad \text{(linear element)}$$

$$[M^e]_C = \frac{\rho h_e}{30} \begin{bmatrix} 4 & 2 & -1 \\ 2 & 16 & 2 \\ -1 & 2 & 4 \end{bmatrix} \quad \text{(quadratic element)} \tag{6.2.47}$$

Here subscripts L and C refer to lumped and consistent mass matrices, respectively.

Proportional Lumping

Here the diagonal elements of the lumped mass matrix are computed to be proportional to the diagonal elements of the consistent mass matrix while conserving the total mass of the element:

$$M_{ii}^e = \alpha \int_{x_a}^{x_b} \rho \psi_i^e \psi_i^e \, dx, \quad \alpha = \int_{x_a}^{x_b} \rho \, dx \Big/ \sum_{i=1}^{n} \int_{x_a}^{x_b} \rho \psi_i^e \psi_i^e \, dx \tag{6.2.48}$$

For constant ρ, proportional lumping gives the same lumped mass matrices as those obtained in the row-sum technique for the Lagrange linear and quadratic elements.

The use of a lumped mass matrix in transient analyses can save computational time in two ways. First, for forward difference schemes, lumped mass matrices result in explicit algebraic equations not requiring matrix inversions. Second, the critical time step required for conditionally stable schemes is larger, and hence less computational time is required when lumped mass matrices are used. To see this, consider the stability criterion in (6.2.31) for the case $\alpha = \frac{1}{2}$ and $\beta = 0$. For a one linear element model of a uniform bar of stiffness

EA and mass ρA, fixed at the left end, the eigenvalue problem with a consistent mass matrix is

$$\left(\frac{EA}{h}\begin{bmatrix}1 & -1\\ -1 & 1\end{bmatrix} - \omega^2\frac{\rho Ah}{6}\begin{bmatrix}2 & 1\\ 1 & 2\end{bmatrix}\right)\begin{Bmatrix}U_1\\ U_2\end{Bmatrix} = \begin{Bmatrix}Q_1^1\\ Q_2^1\end{Bmatrix} \tag{6.2.49}$$

Since $U_1 = 0$ and $Q_2^1 = 0$, we have

$$\omega^2 = \frac{EA}{h}\Big/\frac{\rho Ah}{3} = \frac{3E}{\rho h^2}$$

Substituting this into the critical time step relation (6.2.31), we have,

$$(\Delta t_{\text{cri}})_C = 2/\omega_{\max} = h(4\rho/3E)^{1/2}$$

If we use the lumped matrix, ω is given by

$$\omega = (2E/\rho)^{1/2}/h$$

and the critical time step is

$$(\Delta t_{\text{cri}})_L = h(2\rho/E)^{1/2} > (\Delta t_{\text{cri}})_C \tag{6.2.50}$$

Thus, explicit schemes require larger time steps than implicit schemes.

6.2.6 Applications

Here we consider two examples of applications of finite element models of one-dimensional problems. Example 6.2.1 is taken from transient heat transfer (parabolic equation), and Example 6.2.2 is taken from solid mechanics (hyperbolic equation).

Example 6.2.1

Consider the transient heat conduction problem described by the differential equation

$$\frac{\partial u}{\partial t} - \frac{\partial^2 u}{\partial x^2} = 0 \quad \text{for } 0 < x < 1 \tag{6.2.51a}$$

with boundary conditions

$$u(0, t) = 0, \quad \frac{\partial u}{\partial x}(1, t) = 0 \tag{6.2.51b}$$

and initial condition

$$u(x, 0) = 1.0 \tag{6.2.51c}$$

where u is the nondimensionalized temperature. The problem at hand is a special case of (6.2.3a) with $a = 1$, $b = 0$, $c_0 = 0$, $c_1 = 1$, $c_2 = 0$, and $f = 0$ [or Eq. (6.1.2) with $kA = 1$, $\rho cA = 1$, and $q = 0$]. The finite element model is

$$[M^e]\{\dot{u}\} + [K^e]\{u\} = \{Q^e\}$$

where

$$M_{ij}^e = \int_{x_a}^{x_b} \psi_i^e \psi_j^e \, dx, \quad K_{ij}^e = \int_{x_a}^{x_b} \frac{d\psi_i^e}{dx} \frac{d\psi_j^e}{dx} \, dx$$

For the choice of linear interpolation functions, the semidiscrete equations of a typical element are

$$\frac{h_e}{6}\begin{bmatrix} 2 & 1 \\ 1 & 2 \end{bmatrix}\begin{Bmatrix} \dot{u}_1^e \\ \dot{u}_2^e \end{Bmatrix} + \frac{1}{h_e}\begin{bmatrix} 1 & -1 \\ -1 & 1 \end{bmatrix}\begin{Bmatrix} u_1^e \\ u_2^e \end{Bmatrix} = \begin{Bmatrix} Q_1^e \\ Q_2^e \end{Bmatrix}$$

where h_e is the length of the element. Use of the α-family of approximation (6.2.10a) results in the equation [see (6.2.24a)]

$$([M^e] + \Delta t\, \alpha [K^e])\{u^e\}_{s+1} = ([M^e] - \Delta t(1-\alpha)[K^e])\{u^e\}_s + \Delta t(\alpha\{Q^e\}_{s+1} + (1-\alpha)\{Q^e\}_s)$$

where Δt is the time step.

First, consider a one-element mesh. We have ($h = 1$)

$$\begin{bmatrix} \frac{1}{3}h + \alpha\frac{\Delta t}{h} & \frac{1}{6}h - \alpha\frac{\Delta t}{h} \\ \frac{1}{6}h - \alpha\frac{\Delta t}{h} & \frac{1}{3}h + \alpha\frac{\Delta t}{h} \end{bmatrix}\begin{Bmatrix} U_1 \\ U_2 \end{Bmatrix}_{s+1} = \begin{bmatrix} \frac{1}{3}h - (1-\alpha)\frac{\Delta t}{h} & \frac{1}{6}h + (1-\alpha)\frac{\Delta t}{h} \\ \frac{1}{6}h + (1-\alpha)\frac{\Delta t}{h} & \frac{1}{3}h - (1-\alpha)\frac{\Delta t}{h} \end{bmatrix}\begin{Bmatrix} U_1 \\ U_2 \end{Bmatrix}_s + \Delta t\begin{Bmatrix} \bar{Q}_1 \\ \bar{Q}_2 \end{Bmatrix}$$

where $\bar{Q}_i = \alpha(Q_i^1)_{s+1} + (1-\alpha)(Q_i^1)_s$. The boundary conditions of the problem require

$$(U_1)_s = 0, \quad (Q_2^1)_s = 0 \quad \text{for all } s > 0 \text{ (i.e., } t > 0)$$

However, the initial condition (6.2.51c) requires

$$U_1(0)\psi_1(x) + U_2(0)\psi_2(x) = 1$$

Since the initial condition should be consistent with the boundary conditions, we take $(U_1)_0 = 0$. Then it follows that $(U_2)_0 = 1$.

Using the boundary conditions, we can write for the one-element model ($h = 1.0$)

$$\left(\frac{1}{3}h + \alpha\frac{\Delta t}{h}\right)(U_2)_{s+1} = \left[\frac{1}{3}h - (1-\alpha)\frac{\Delta t}{h}\right](U_2)_s \tag{6.2.52}$$

which can be solved repeatedly for U_2 at different times, $s = 0, 1, \ldots$.

Repeated use of (6.2.52) can cause the temporal approximation error to grow with time, depending on the value of α. As noted earlier, the forward difference scheme ($\alpha = 0$) is a conditionally stable scheme. To determine the critical time step for the one-element mesh, we first calculate the maximum eigenvalue of the associated system

$$\left(-\lambda\frac{h}{6}\begin{bmatrix} 2 & 1 \\ 1 & 2 \end{bmatrix} + \frac{1}{h}\begin{bmatrix} 1 & -1 \\ -1 & 1 \end{bmatrix}\right)\begin{Bmatrix} U_1 \\ U_2 \end{Bmatrix} = \begin{Bmatrix} Q_1^1 \\ Q_2^1 \end{Bmatrix}, \quad U_1 = 0, \quad Q_2^1 = 0$$

The eigenvalue is (there is only one)

$$-\frac{1}{3}\lambda h U_2 + h^{-1}U_2 = 0, \quad \text{or} \quad \lambda = 3/h^2 = 3$$

Hence, from Eq. (6.2.26) we have $\Delta t_{\text{cri}} = 2/\lambda = 0.66667$. Thus, in order for the forward difference scheme (6.2.52)

$$\frac{1}{3}h(U_2)_{s+1} = \left(\frac{1}{3}h - \frac{\Delta t}{h}\right)(U_2)_s$$

to be stable, the time step should be smaller than $\Delta t_{\text{cri}} = 0.6667$; otherwise, the solution will be unstable, as shown in Fig. 6.2.3.

For a two-element mesh, we have ($h_1 = h_2 = h = 0.5$); the condensed equations of the time-marching scheme are given by

$$\begin{bmatrix} \frac{2}{3}h + 2\alpha\frac{\Delta t}{h} & \frac{1}{6}h - \alpha\frac{\Delta t}{h} \\ \frac{1}{6}h - \alpha\frac{\Delta t}{h} & \frac{1}{3}h + \alpha\frac{\Delta t}{h} \end{bmatrix} \begin{Bmatrix} U_2 \\ U_3 \end{Bmatrix}_{s+1} = \begin{bmatrix} \frac{2}{3}h - 2(1-\alpha)\frac{\Delta t}{h} & \frac{1}{6}h + (1-\alpha)\frac{\Delta t}{h} \\ \frac{1}{6}h + (1-\alpha)\frac{\Delta t}{h} & \frac{1}{3}h - (1-\alpha)\frac{\Delta t}{h} \end{bmatrix} \begin{Bmatrix} U_2 \\ U_3 \end{Bmatrix}_s$$

with $(U_2)_0$ and $(U_3)_0$. The forward difference scheme yields

$$\frac{h}{6}\begin{bmatrix} 4 & 1 \\ 1 & 2 \end{bmatrix}\begin{Bmatrix} U_2 \\ U_3 \end{Bmatrix}_{s+1} = \frac{h}{6}\begin{bmatrix} 4-2\mu & 1+\mu \\ 1+\mu & 2-\mu \end{bmatrix}\begin{Bmatrix} U_2 \\ U_3 \end{Bmatrix}_s, \quad \mu = \frac{6\Delta t}{h^2}$$

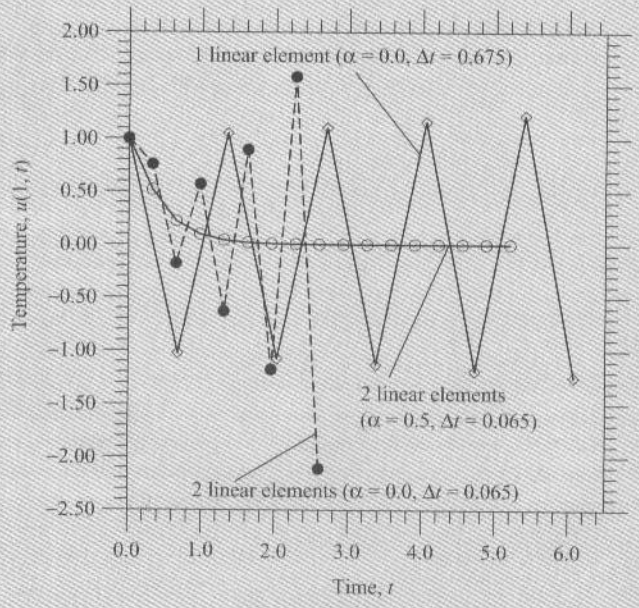

Figure 6.2.3 Stability of the forward difference ($\alpha = 0.0$) and Crank–Nicolson ($\alpha = 0.5$) schemes as applied to a parabolic equation.

The associated eigenvalue problem is

$$\left(-\lambda\frac{h}{6}\begin{bmatrix}4 & 1\\ 1 & 2\end{bmatrix}+\frac{1}{h}\begin{bmatrix}2 & -1\\ -1 & 1\end{bmatrix}\right)\begin{Bmatrix}U_2\\ U_3\end{Bmatrix}=\begin{Bmatrix}0\\ 0\end{Bmatrix}$$

The characteristic equation is

$$7\bar{\lambda}^2-10\bar{\lambda}+1=0,\quad \bar{\lambda}=\frac{\lambda h^2}{6}$$

whose roots are $\lambda_1=2.5967$ and $\lambda_2=31.6891$. Hence, the critical time step becomes $\Delta t_{\text{cri}}=2/31.6891=0.0631$. A time step of $\Delta t=0.065$ results in an unstable solution, as shown in Fig. 6.2.3.

For (unconditionally) stable schemes ($\alpha\geq\frac{1}{2}$), there is no restriction on the time step (e.g., Crank–Nicolson method with two linear elements and $\Delta t=0.065$ yield very smooth and stable solution, as shown in Fig. 6.2.3). However, to obtain a sufficiently accurate solution, the time step must be taken as a fraction of Δt_{cri}. Of course, the accuracy of the solution also depends on the mesh size h. As this is decreased (i.e., the number of elements is increased), Δt_{cri} decreases.

Plots of $u(1,t)$ versus time for $\alpha=0$ and $\alpha=0.5$ with $\Delta t=0.05$ are shown in Fig. 6.2.4. Solutions predicted by meshes of one, two, or four linear (L) or quadratic (Q) elements are compared. The convergence of the solution with increasing number of elements is clear. The finite element solutions obtained with different methods, time steps, and meshes are compared with the exact solution in Table 6.2.1.

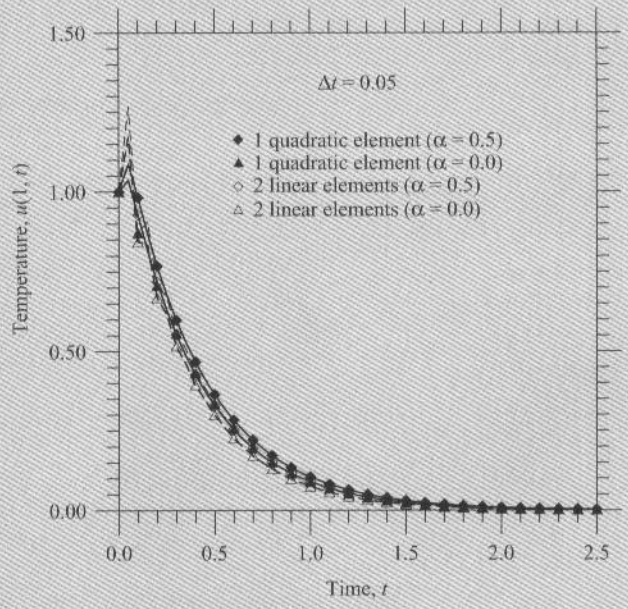

Figure 6.2.4 Transient solution of a parabolic equation according to linear and quadratic finite elements.

Table 6.2.1 A comparison of the finite element solutions obtained using various time approximation schemes and meshes with the analytical solution of a parabolic equation ($\Delta t = 0.05$).

	$\alpha = 0$	$\alpha = 1$	$\alpha = 0.5$							
t	1L	1L	1L	2L	4L	4L	1Q	2Q	4Q	Exact
0.00	1.0000	1.0000	1.0000	1.0000	1.0000	1.0000	1.0000	1.0000	1.0000	1.0000
0.05	0.8500	0.8696	0.8605	1.0359	0.9951	0.9933	1.0870	0.9942	0.9928	0.9969
0.10	0.7225	0.7561	0.7404	0.9279	0.9588	0.9554	0.9819	0.9550	0.9549	0.9493
0.15	0.6141	0.6575	0.6371	0.8169	0.8639	0.8707	0.8693	0.8831	0.8725	0.8642
0.20	0.5220	0.5718	0.5482	0.7176	0.7557	0.7694	0.7679	0.7633	0.7731	0.7723
0.25	0.4437	0.4972	0.4717	0.6300	0.6759	0.6824	0.6780	0.6933	0.6855	0.6854
0.30	0.3771	0.4323	0.4059	0.5533	0.5906	0.6037	0.5987	0.6006	0.6070	0.6068
0.35	0.3206	0.3759	0.3492	0.4858	0.5250	0.5325	0.5286	0.5394	0.5358	0.5367
0.40	0.2725	0.3269	0.3005	0.4266	0.4608	0.4713	0.4668	0.4710	0.4741	0.4745
0.45	0.2316	0.2843	0.2586	0.3746	0.4083	0.4158	0.4121	0.4201	0.4188	0.4194
0.50	0.1969	0.2472	0.2225	0.3289	0.3592	0.3676	0.3639	0.3687	0.3701	0.3708
0.55	0.1673	0.2149	0.1914	0.2888	0.3176	0.3247	0.3213	0.3275	0.3273	0.3277
0.60	0.1422	0.1869	0.1647	0.2536	0.2798	0.2868	0.2837	0.2883	0.2890	0.2897
0.65	0.1209	0.1625	0.1418	0.2227	0.2472	0.2535	0.2505	0.2556	0.2556	0.2561
0.70	0.1028	0.1413	0.1220	0.1955	0.2180	0.2238	0.2212	0.2253	0.2258	0.2264
0.75	0.0874	0.1229	0.1050	0.1717	0.1924	0.1979	0.1953	0.1995	0.1996	0.2001
0.80	0.0743	0.1069	0.0903	0.1508	0.1697	0.1747	0.1725	0.1761	0.1764	0.1769
0.85	0.0631	0.0929	0.0777	0.1324	0.1498	0.1544	0.1523	0.1557	0.1559	0.1563
0.90	0.0536	0.0808	0.0669	0.1162	0.1322	0.1363	0.1345	0.1375	0.1378	0.1382
0.95	0.0456	0.0703	0.0575	0.1020	0.1166	0.1205	0.1187	0.1216	0.1218	0.1222
1.00	0.0388	0.0611	0.0495	0.0896	0.1029	0.1065	0.1048	0.1074	0.1076	0.1080

Example 6.2.2

We wish to determine the transverse motion of a beam clamped at both ends and subjected to initial deflection using EBT and TBT. The governing equations are

$$\frac{\partial^2 w}{\partial t^2} + \frac{\partial^4 w}{\partial x^4} = 0 \quad \text{for } 0 < x < 1 \tag{6.2.53a}$$

$$w(0,t) = 0, \quad \frac{\partial w}{\partial x}(0,t) = 0, \quad w(1,t) = 0, \quad \frac{\partial w}{\partial x}(1,t) = 0 \tag{6.2.53b}$$

$$w(x,0) = \sin \pi x - \pi x(1-x), \quad \frac{\partial w}{\partial t}(x,0) = 0 \tag{6.2.53c}$$

Note that the initial deflection of the beam is consistent with the boundary conditions. The initial slope is given by

$$\theta(x,0) = -\left(\frac{\partial w}{\partial x}\right)_{t=0} = -\pi \cos \pi x + \pi(1-2x) \tag{6.2.53d}$$

Because of symmetry about $x = 0.5$ (center of the beam), we consider only a half span of the beam for finite element modeling. Here we use the first half of the beam, $0 \le x \le 0.5$, as the

computational domain. The boundary condition at $x = 0.5$ is $\theta(0.5, t) = -(\partial w/\partial x)(0.5, t) = 0$. The semidiscretized finite element model of a typical element is

$$\frac{h_e}{420}\begin{bmatrix} 156 & -22h_e & 54 & 13h_e \\ -22h_e & 4h_e^2 & -13h_e & -3h_e^2 \\ 54 & -13h_e & 156 & 22h_e \\ 13h_e & -3h_e^2 & 22h_e & 4h_e^2 \end{bmatrix}\begin{Bmatrix} \ddot{\Delta}_1^e \\ \ddot{\Delta}_2^e \\ \ddot{\Delta}_3^e \\ \ddot{\Delta}_4^e \end{Bmatrix} + \frac{2}{h_e^3}\begin{bmatrix} 6 & -3h_e & -6 & -3h_e \\ -3h_e & 2h_e^2 & 3h_e & h_e^2 \\ -6 & 3h_e & 6 & 3h_e \\ -3h_e & h_e^2 & 3h_e & 2h_e^2 \end{bmatrix}\begin{Bmatrix} \Delta_1^e \\ \Delta_2^e \\ \Delta_3^e \\ \Delta_4^e \end{Bmatrix} = \begin{Bmatrix} Q_1^e \\ Q_2^e \\ Q_3^e \\ Q_4^e \end{Bmatrix}$$

We begin with a one-element mesh with the Euler–Bernoulli beam element. The semidiscretized model is

$$\frac{h}{420}\begin{bmatrix} 156 & -22h & 54 & 13h \\ -22h & 4h^2 & -13h & -3h^2 \\ 54 & -13h & 156 & 22h \\ 13h & -3h^2 & 22h & 4h^2 \end{bmatrix}\begin{Bmatrix} \ddot{U}_1 \\ \ddot{U}_2 \\ \ddot{U}_3 \\ \ddot{U}_4 \end{Bmatrix} + \frac{2}{h^3}\begin{bmatrix} 6 & -3h & -6 & -3h \\ -3h & 2h^2 & 3h & h^2 \\ -6 & 3h & 6 & 3h \\ -3h & h^2 & 3h & 2h^2 \end{bmatrix}\begin{Bmatrix} U_1 \\ U_2 \\ U_3 \\ U_4 \end{Bmatrix} = \begin{Bmatrix} Q_1^1 \\ Q_2^1 \\ Q_3^1 \\ Q_4^1 \end{Bmatrix}$$

The boundary conditions for the one-element model translate into

$$U_1 = 0, \quad U_2 = 0, \quad U_4 = 0, \quad Q_3^1 = 0 \quad \text{for all } t > 0$$

The initial conditions can be computed from (6.2.53*c*) and (6.2.53*d*)

$$\left.\begin{array}{llll} U_1 = 0, & U_2 = 0, & U_3 = 0.2146, & U_4 = 0 \\ \dot{U}_1 = 0, & \dot{U}_2 = 0, & \dot{U}_3 = 0 & \dot{U}_4 = 0 \end{array}\right\} \quad \text{for } t = 0$$

The condensed equation of the time marching scheme for this case takes the form

$$(K_{33} + a_3 M_{33})(U_3)_{s+1} = (\hat{F}_3)_{s,s+1} \equiv M_{33}(a_3 U_3 + a_4 \dot{U}_3 + a_5 \ddot{U}_3)_s, \quad s = 0, 1, \ldots$$

where a_3, a_4, and a_5 are defined in (6.2.40). The second derivative $\ddot{U}_3$ for time $t = 0$ (i.e., when $s = 0$) is computed from the equation of motion:

$$(\ddot{U}_3)_0 = -\frac{K_{33}(U_3)_0}{M_{33}} = -\left(\frac{12}{h^3} \times 0.2146\right)\frac{420}{156h} = -110.932$$

For $\gamma < \frac{1}{2}$, we must compute the critical time step Δt_{cri}, which depends on the square of maximum natural frequency of the beam [see Eq. (6.2.31)]. For the present model, $\omega_{\max}$ is computed from the eigenvalue problem

$$(K_{33} - \omega^2 M_{33})U_3 = 0 \quad \text{or } \omega^2 = K_{33}/M_{33} = 516.923$$

Hence, the critical time step for $\alpha = 0.5$ and $\gamma = \frac{1}{3}$ (i.e., the linear acceleration scheme) is

$$\Delta t_{\text{cri}} = \sqrt{12}/\omega_{\max} = 0.15236$$

Although there is no restriction on time integration schemes with $\alpha = 0.5$ and $\gamma > 0.5$, the critical time step provides an estimate of the time step to be used to obtain transient solution.

Figure 6.2.5 shows plots of $w(0.5, t)$ versus time for the scheme with $\alpha = 0.5$ and $\gamma = \frac{1}{3}$. Three different time steps, $\Delta t = 0.175$, 0.150, and 0.05, are used to illustrate the accuracy. For $\Delta t = 0.175 > \Delta t_{\text{cri}}$, the solution is unstable, whereas for $\Delta t < \Delta t_{\text{cri}}$, it is stable but inaccurate. The period of the solution is given by

$$T = 2\pi/\omega = 0.27635$$

For two- and four-element meshes of Euler–Bernoulli elements, the critical time steps are (details are not presented here)

$$(\Delta t_{\text{cri}})_2 = 0.00897, \quad (\Delta t_{\text{cri}})_4 = 0.00135$$

where the subscripts refer to the number of elements in the mesh. The transverse deflection obtained with the one and two Euler–Bernoulli elements ($\Delta t = 0.005$) in half beam for a complete period (0, 0.28) are shown in Fig. 6.2.6.

The problem can also be analyzed using the Timoshenko beam element (RIE). In writing the governing equations [see (6.1.43*a*) and (6.1.43*b*)] of the TBT as they apply to the present problem, we first identify the coefficients GAK_s, EI, ρA, and ρI consistent with those in the differential equation (6.2.53*a*). We have $EI = 1.0$ and $\rho A = 1.0$. Then GAK_s can be computed as

$$GAK_s = \frac{E}{2(1+\nu)} BHK_s = \frac{EI}{2(1+\nu)} \frac{12}{H^2} \frac{5}{6} = \frac{4}{H^2} EI \tag{6.2.54}$$

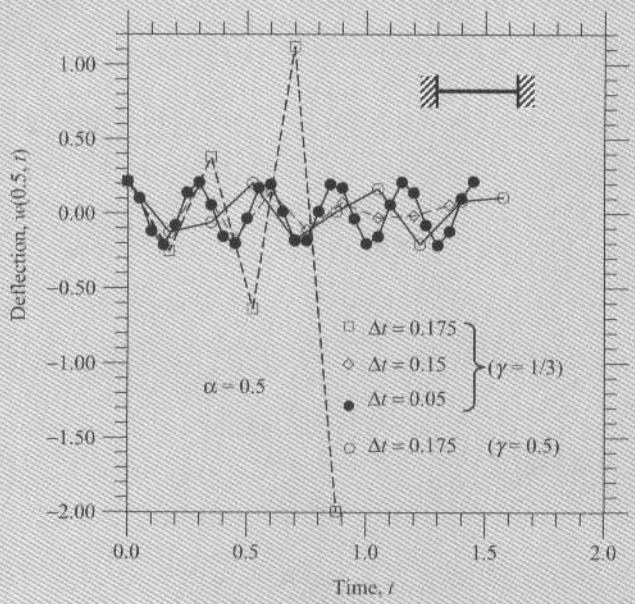

Figure 6.2.5 Center deflection $w(0.5, t)$ versus time t for a clamped beam.

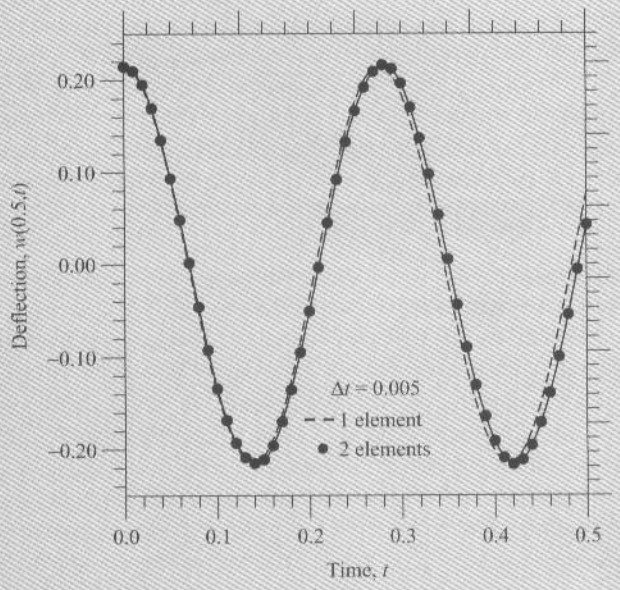

Figure 6.2.6 Center transverse deflection versus time for a clamped beam subjected to an initial transverse deflection ($\Delta t = 0.005$, $\alpha = 0.5$, and $\gamma = 0.5$).

where B is the width and H the height of the beam, and $I = \frac{1}{12}BH^3$, $\nu = 0.25$, and $K_s = \frac{5}{6}$ are used in arriving at the last expression. Similarly,

$$\rho I = \rho \frac{1}{12} BH^3 = \frac{1}{12} \rho A H^2 \tag{6.2.55}$$

Thus, the governing equations of the TBT for the problem at hand are

$$\frac{\partial^2 w}{\partial t^2} - \frac{4}{H^2} \frac{\partial}{\partial x} \left(\frac{\partial w}{\partial x} + \Psi \right) = 0 \tag{6.2.56a}$$

$$\frac{H^2}{12} \frac{\partial^2 \Psi}{\partial t^2} - \frac{\partial^2 \Psi}{\partial x^2} + \frac{4}{H^2} \left(\frac{\partial w}{\partial x} + \Psi \right) = 0 \tag{6.2.56b}$$

The values of $w(0.5, t)$ as obtained using the Euler–Bernoulli and Timoshenko elements (both elements include the rotary inertia) for various numbers of elements are presented in Table 6.2.2. The time step is taken to be $\Delta t = 0.005$, which is smaller than the critical time step of the two-element mesh of the Euler–Bernoulli beam element when $\gamma = \frac{1}{3}$. Plots of $w(0.5, t)$ obtained with two and four linear Timoshenko beam elements, two quadratic Timoshenko beam elements for $L/H = 100$ (since $L = 1.0$, we take $H = 0.01$; for $L/H = 100$ the shear deformation effect is negligible) along with the two-element solution of the Euler–Bernoulli beam element are shown in Fig. 6.2.7. The two linear element mesh of TBT beam elements predicts transient response that differs significantly from the EBT solution, and the TBT solution converges to the EBT solution as the number of elements or the degree of approximation is increased. Should we use conditionally stable schemes, it can be shown that the Timoshenko beam element requires larger Δt_{cri} than the Euler–Bernoulli beam element. This is because, as L/H is decreased, the $\omega_{\max}$ predicted by the TBT is smaller than that predicted by the EBT.

Table 6.2.2 Effect of mesh on the transient response of a beam clamped at both ends ($\Delta t = 0.005$).

	EBT elements					TBT elements*		
	$\alpha = 0.5, \gamma = 1/3$		$\alpha = 0.5, \gamma = 0.5$			$\alpha = 0.5, \gamma = 0.5$		
Time t	1	2	1	2	4	2L	4L	2Q
0.00	0.2146	0.2146	0.2146	0.2146	0.2146	0.2146	0.2146	0.2146
0.01	0.2091	0.2098	0.2091	0.2098	0.2098	0.2124	0.2099	0.2116
0.02	0.1928	0.1951	0.1928	0.1951	0.1951	0.1938	0.1936	0.1951
0.03	0.1666	0.1696	0.1667	0.1696	0.1698	0.1550	0.1686	0.1690
0.04	0.1319	0.1346	0.1320	0.1348	0.1350	0.1145	0.1374	0.1427
0.05	0.0904	0.0930	0.0905	0.0931	0.0935	0.0695	0.0980	0.1067
0.06	0.0442	0.0481	0.0443	0.0482	0.0483	0.0093	0.0073	0.0657
0.07	−0.0043	0.0014	−0.0041	0.0014	0.0018	−0.0467	−0.0403	0.0234
0.08	−0.0525	−0.0462	−0.0523	−0.0459	−0.0455	−0.0917	−0.0844	−0.0267
0.09	−0.0980	−0.0926	−0.0978	−0.0923	−0.0916	−0.1422	−0.1254	−0.0706
0.10	−0.1385	−0.1345	−0.1383	−0.1342	−0.1336	−0.1833	−0.1588	−0.1100
0.11	−0.1719	−0.1685	−0.1717	−0.1685	−0.1682	−0.2010	−0.1875	−0.1461
0.12	−0.1964	−0.1933	−0.1963	−0.1933	−0.1932	−0.2154	−0.2069	−0.1717
0.13	−0.2108	−0.2088	−0.2108	−0.2088	−0.2087	−0.2205	−0.2063	−0.1969
0.14	−0.2144	−0.2153	−0.2144	−0.2150	−0.2148	−0.1986	−0.2138	−0.2110
0.15	−0.2070	−0.2113	−0.2071	−0.2112	−0.2111	−0.1696	−0.2134	−0.2146

* 2L = two linear elements; 4L = four linear elements; 2Q = two quadratic elements.

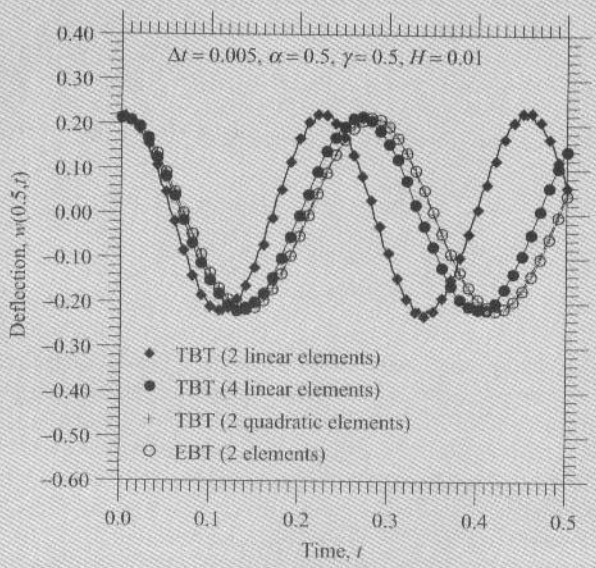

Figure 6.2.7 Transient response of a beam clamped at both ends, according to the TBT and EBT ($EI = 1$, $\rho A = 1$, $H = 0.01$, $\Delta t = 0.005$, $\alpha = 0.5$, and $\gamma = 0.5$).

6.3 SUMMARY

In this chapter, finite element formulations of eigenvalue problems and time-dependent problems are developed. One-dimensional, second- and fourth-order equations (beams) have been discussed. The eigenvalue problems studied include problems of heat transfer (and the like), bars, and beams. In the case of bars and beams, the eigenvalue problems arise in connection with natural vibrations and buckling of columns. Except for the solution procedure, the finite element formulation of eigenvalue problems is entirely analogous to boundary value problems.

Finite element models of time-dependent problems described by parabolic and hyperbolic equations have also been presented. A two-step procedure to derive finite element models from differential equations has been described. In the first step, we seek spatial approximations of the dependent variables of the problem as linear combinations of nodal values that are functions of time and interpolation functions that are functions of space. This procedure is entirely analogous to the finite element formulation presented for boundary value problems in Chapters 3–5. The end result of this step is a set of ordinary differential equations (in time) among the nodal values. In the second step, the ordinary differential equations are further approximated using the finite difference approximation of the time derivatives. The resulting algebraic equations can be solved for repeatedly, marching in time. Examples using both transient heat transfer and beam bending are presented.

PROBLEMS

Section 6.1

Most problems are formulative in nature. For eigenvalue problems, we need to write the final characteristic equations for the eigenvalues.

6.1 Determine the first two eigenvalues associated with the heat transfer problem whose governing equations and boundary conditions are given by (Fig. P6.1)

$$-\frac{\partial}{\partial x}\left(a\frac{\partial u}{\partial x}\right)+b\frac{\partial u}{\partial t}+cu=0 \quad \text{for } 0<x<L$$

$$u(0)=0, \quad \left(a\frac{\partial u}{\partial x}+\beta u\right)\Big|_{x=L}=0$$

where a, b, c, and β are constants. Use (a) two linear finite elements and (b) one quadratic element in the domain to solve the problem.

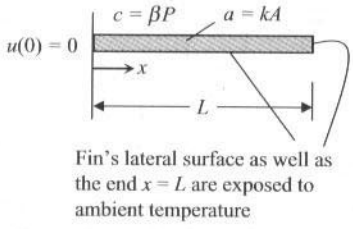

Figure P6.1

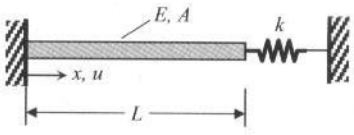

Figure P6.2

6.2 Determine the first two longitudinal frequencies of a rod (with Young's modulus E, area of cross section A, and length L) that is fixed at one end (say, at $x = 0$) and supported axially at the other end (at $x = L$) by a linear elastic spring (with spring constant k), as shown in Fig. P6.1:

$$-EA\frac{\partial^2 u}{\partial x^2} + \rho A\frac{\partial^2 u}{\partial t^2} = 0 \quad \text{for } 0 < x < L$$

$$u(0) = 0, \quad \left(EA\frac{du}{dx} + ku\right)\Big|_{x=L} = 0$$

Use (a) two linear finite elements and (b) one quadratic element in the domain to solve the problem. *Answer:* (a) The characteristic equation is $7\lambda^2 - (10 + 4c)\lambda + (1 + 2c) = 0$, $c = kL/2EA$, $\lambda = (\rho h^2/6E)\omega^2$.

6.3 Determine the smallest natural frequency of a beam with clamped ends and of constant cross-sectional area A, moment of inertia I, and length L. Use the symmetry and two Euler–Bernoulli beam elements in the half beam.

6.4 Resolve the above problem with two RIEs in the half-beam.

6.5 Consider a beam (of Young's modulus E, shear modulus G, area of cross section A, second moment area about the axis of bending I, and length L) with its left end ($x = 0$) clamped and its right end ($x = L$) supported vertically by a linear elastic spring (see Fig. P6.5). Determine the fundamental natural frequency using (a) one Euler–Bernoulli beam element and (b) one Timoshenko beam element (IIE) (use the same mass matrix in both elements).

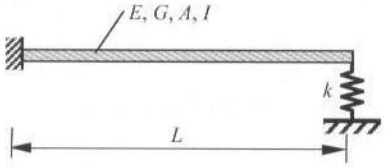

Figure P6.5

6.6 Consider a simply supported beam (of Young's modulus E, mass density ρ, area of cross section A, second moment of area about the axis of bending I, and length L) with an elastic support at the center of the beam (see Fig. P6.6). Determine the fundamental natural frequency using the minimum number of Euler–Bernoulli beam elements. *Answer:* The characteristic polynomial is $455\lambda^2 - 2(129 + c)\lambda + 3 + 2c = 0$.

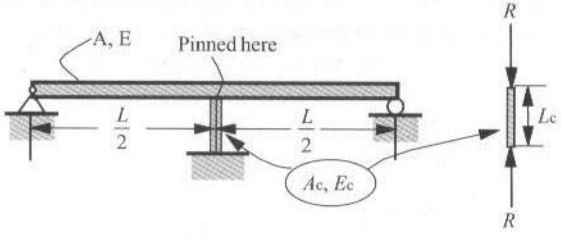

Figure P6.6

6.7 Determine the critical buckling load of a cantilever beam (A, I, L, E) using (a) one Euler–Bernoulli beam element and (b) one Timoshenko beam element.

6.8 The natural vibration of a beam under applied axial compressive load N^0 is governed by the differential equation

$$EI\frac{d^4w}{dx^4} + N^0\frac{d^2w}{dx^2} = \lambda w$$

where λ denotes nondimensional frequency of natural vibration and EI is the flexural stiffness of the beam. (*a*) Determine the fundamental (i.e., smallest) natural frequency ω of a cantilever beam (i.e., fixed at one end and free at the other end) of length L with axial compressive load N_0 using one beam element. (*b*) What is the buckling load of the beam? You are required to give the final characteristic equation in each case.

6.9 Determine the fundamental natural frequency of the truss shown in Fig. P6.9 (you are required only to formulate the problem).

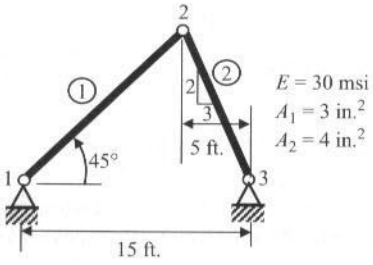

Figure P6.9

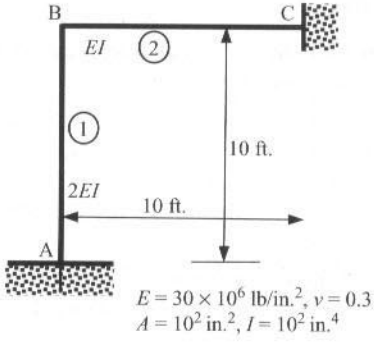

Figure P6.10

6.10 Determine the fundamental natural frequency of the truss shown in Fig. P6.10 (you are required only to formulate the problem).

6.11 Determine the first two longitudinal natural frequencies of a rod (A, E, L, m), fixed at one end and with an attached mass m_2 at the other. Use two linear elements. *Hint:* Note that the boundary conditions for the problem are $u(0) = 0$ and $(EA\,\partial u/\partial x + m_2\,\partial^2 u/\partial t^2)|_{x=L} = 0$.

6.12 The equation governing torsional vibration of a circular rod is

$$-GJ\frac{\partial^2\phi}{\partial x^2} + mJ\frac{\partial^2\phi}{\partial t^2} = 0$$

where ϕ is the angular displacement, J the moment of inertia, G the shear modulus, and m the density. Determine the fundamental torsional frequency of a rod with disk (J_1) attached at each end. Use the symmetry and (*a*) two linear elements and (*b*) one quadratic element.

6.13 The equations governing the motion of a beam according to TBT can be reduced to the single equation

$$a^2\frac{\partial^4 w}{\partial x^4} + \frac{\partial^2 w}{\partial t^2} - b^2\left(1 + \frac{E}{kG}\right)\frac{\partial^4 w}{\partial x^2 \partial t^2} + \frac{b^2 m}{kG}\frac{\partial^4 w}{\partial t^4} = 0$$

where $a^2 = EI/mA$ and $b^2 = I/A$. Here E is the Young's modulus, G is the shear modulus, m is the mass per unit length, A is the area of cross section, and I is the moment of inertia. Assuming that $(b^2 m/kG) << 1$ (i.e., neglect the last term in the governing equation), formulate the finite element model of the (*a*) eigenvalue problem for the determination of natural frequencies and (*b*) fully discretized problem for the determination of the transient response.

6.14 Use the finite element model of Problem 6.13 to determine the fundamental frequency of a simply supported beam.

6.15 Find the critical buckling load P_{cri} by determining the eigenvalues of the equation

$$EI\frac{d^4w}{dx^4} + P_{\text{cri}}\frac{d^2w}{dx^2} = 0 \quad \text{for } 0 < x < L$$

$$w(0) = w(L) = 0, \quad \left(EI\frac{d^2w}{dx^2}\right)\bigg|_{x=0} = \left(EI\frac{d^2w}{dx^2}\right)\bigg|_{x=L} = 0$$

Use one Euler–Bernoulli element in the half-beam. *Answer:* $P_{\text{cri}} = 9.9439EI/L^2$.

Section 6.2

6.16 Consider the partial differential equation arising in connection with unsteady heat transfer in an insulated rod:

$$\frac{\partial u}{\partial t} - \frac{\partial}{\partial x}\left(a\frac{\partial u}{\partial x}\right) = f \quad \text{for } 0 < x < L$$

$$u(0, t) = 0, \quad u(x, 0) = u_0, \quad \left[a\frac{\partial u}{\partial x} + \beta(u - u_\infty) + \hat{q}\right]\bigg|_{x=L} = 0$$

Following the procedure outlined in Section 6.2, derive the semidiscrete variational form, the semidiscrete finite element model, and the fully discretized finite element equations for a typical element.

6.17 Using a two-element (linear) model and the semidiscrete finite element equations derived in Problem 6.16, determine the nodal temperatures as functions of time for the case in which $a = 1$, $f = 0$, $u_0 = 1$, and $\hat{q} = 0$. Use the Laplace transform technique [see Reddy (2002)] to solve the ordinary differential equations in time.

6.18 Consider a uniform bar of cross-sectional area A, modulus of elasticity E, mass density m, and length L. The axial displacement under the action of time-dependent axial forces is governed by the wave equation

$$\frac{\partial^2 u}{\partial t^2} = a^2\frac{\partial^2 u}{\partial x^2}, \quad a = \left(\frac{E}{m}\right)^{1/2}$$

Determine the transient response [i.e., find $u(x, t)$] of the bar when the end $x = 0$ is fixed and the end $x = L$ is subjected to a force P_0. Assume zero initial conditions. Use one linear element to approximate the spatial variation of the solution, and solve the resulting ordinary differential equation in time exactly to obtain

$$u_2(x, t) = \frac{P_0 L}{AE}\frac{x}{L}(1 - \cos\alpha t), \quad \alpha = \sqrt{3}\frac{a}{L}$$

6.19 Resolve Problem 6.18 with a mesh of two linear elements. Use the Laplace transform method to solve the two ordinary differential equations in time.

6.20 Solve Problem 6.18 when the right end is subjected to an axial force F_0 and supported by an axial spring of stiffness k. *Answer:*

$$u_2(t) = c(1 - \cos\beta t), \quad c = \frac{3F_0}{mAL\beta^2}, \quad \beta = \sqrt{3}\frac{a}{L}\left(1 + \frac{kL}{EA}\right)^{1/2}$$

6.21 A bar of length L moving with velocity v_0 strikes a spring of stiffness k. Determine the motion $u(x, t)$ from the instant when the end $x = 0$ strikes the spring. Use one linear element.

6.22 A uniform rod of length L and mass m is fixed at $x = 0$ and loaded with a mass M at $x = L$. Determine the motion $u(x, t)$ of the system when the mass M is subjected to a force P_0. Use one linear element. *Answer:*

$$u_2(t) = c(1 - \cos \lambda t), \quad c = \frac{P_0 L}{AE}, \quad \lambda = \sqrt{3}\frac{a}{L}\left(\frac{3M}{AL} + m\right)^{-1}$$

6.23 The flow of liquid in a pipe, subjected to a surge-of-pressure wave (i.e., a water hammer), experiences a surge pressure p, which is governed by the equation

$$\frac{\partial^2 p}{\partial t^2} - c^2 \frac{\partial^2 p}{\partial x^2} = 0, \quad c^2 = \frac{1}{m}\left(\frac{1}{k} + \frac{D}{bE}\right)^{-1}$$

where m is the mass density and K the bulk modulus of the fluid, D is the diameter and b the thickness of the pipe, and E is the modulus of elasticity of the pipe material. Determine the pressure $p(x, t)$ using one linear finite element for the following boundary and initial conditions:

$$p(0, t) = 0, \quad \frac{\partial p}{\partial x}(L, t) = 0, \quad p(x, 0) = p_0, \quad \dot{p}(x, 0) = 0$$

6.24 Consider the problem of determining the temperature distribution of a solid cylinder, initially at a uniform temperature T_0 and cooled in a medium of zero temperature (i.e., $T_\infty = 0$). The governing equation of the problem is

$$\rho c \frac{\partial T}{\partial t} - \frac{1}{r}\frac{\partial}{\partial r}\left(rk\frac{\partial T}{\partial r}\right) = 0$$

The boundary conditions are

$$\frac{\partial T}{\partial r}(0, t) = 0, \quad \left(rk\frac{\partial T}{\partial r} + \beta T\right)\Big|_{r=R} = 0$$

The initial condition is $T(r, t) = T_0$. Determine the temperature distribution $T(r, t)$ using one linear element. Take $R = 2.5$ cm, $k = 215$ W/(m·°C), $\beta = 525$ W/(m·°C), $T_0 = 130$°C, $\rho = 2700$ kg/m^2, and $c = 0.9$ kJ/(kg·°C). What is the heat loss at the surface? Formulate the problem.

6.25 Determine the nondimensional temperature $\theta(r, t)$ in the region bounded by two long cylindrical surfaces of radii R_1 and R_2. The dimensionless heat conduction equation is

$$-\frac{1}{r}\frac{\partial}{\partial r}\left(r\frac{\partial \theta}{\partial r}\right) + \frac{\partial \theta}{\partial t} = 0$$

with boundary and initial conditions

$$\frac{\partial \theta}{\partial r}(R_1, t) = 0, \quad \theta(R_2, t) = 1, \quad \theta(r, 0) = 0$$

6.26 Show that (6.2.28*a*), (6.2.28*b*), (6.2.29*a*), and (6.2.29*b*) can be reworked to match the form in Eq. (6.2.38) as

$$[H]\{\ddot{u}\}_{s+1} = \{\tilde{F}\}_{s+1}$$

and define $[H]$ and $\{\tilde{F}\}_{s+1}$.

6.27 A uniform cantilever beam of length L, moment of inertia I, modulus of elasticity E, and mass m begins to vibrate with initial displacement

$$w(x, 0) = w_0 x^2 / L^2$$

and zero initial velocity. Find its displacement at the free end at any subsequent time. Use one Euler–Bernoulli beam element to determine the solution. Solve the resulting differential equations in time using the Laplace transform method.

6.28 Resolve Problem 6.27 using one Timoshenko beam element.

REFERENCES FOR ADDITIONAL READING

1. Argyris, J. H. and Scharpf, O. W., "Finite Elements in Time and Space," *Aeronautical Journal of the Royal Society,* **73**, 1041–1044, 1969.
2. Bathe, K. J., *Finite Element Procedures in Engineering Analysis,* Prentice-Hall, Englewood Cliffs, NJ, 1982.
3. Bathe, K. J. and Wilson, E. L., "Stability and Accuracy Analysis of Direct Integration Methods," *International Journal of Earthquake Engineering and Structural Dynamics,* **1**, 283–291, 1973.
4. Belytschko, T., "An Overview of Semidiscretization and Time Integration Procedures," in Belytschko T. and Hughes T. J. R. (eds.), *Computational Methods for Transient Analysis,* North-Holland, Amsterdam, pp. 1–65, 1983.
5. Goudreau, G. L., and Taylor, R. L., "Evaluation of Numerical Integration Methods in Elastodynamics," *Journal of Computer Methods in Applied Mechanics and Engineering,* **2**(1), 69–97, 1973.
6. Hilber, H. M., "Analysis and Design of Numerical Integration Methods in Structural Dynamics," EERC Report no. 77–29, Earthquake Engineering Research Center, University of California, Berkeley, CA, November 1976.
7. Houbolt, J. C., "A Recurrence Matrix Solution for the Dynamic Response of Elastic Aircraft," *Journal of Aeronautical Science,* **17**, 540–550, 1950.
8. Newmark, N. M., "A Method of Computation for Structural Dynamics," *Journal of Engineering Mechanics Division, ASCE,* **85**, 67–94, 1959.
9. Nickell, R. E., "On the Stability of Approximation Operators in Problems of Structural Dynamics," *International Journal of Solids and Structures,* **7**, 301–319, 1971.
10. Reddy, J. N., *Theory and Analysis of Elastic Plates,* Taylor and Francis, Philadelphia, PA, 1999*a*.
11. Reddy, J. N., "On the Dynamic Behavior of the Timoshenko Beam Finite Elements," *Sadhana* (Journal of the Indian Academy of Sciences), **24**, Part 3, 175–198, 1999*b*.
12. Reddy, J. N., "On the Derivation of the Superconvergent Timoshenko Beam Finite Element," *Int. J. Comput. Civil and Struct. Engng.,* **1**(2), 71–84, 2000.
13. Reddy, J. N., *Energy Principles and Variational Methods in Applied Mechanics,* John Wiley, New York, 2002.
14. Wood, W. L., "Control of Crank–Nicolson Noise in the Numerical Solution of the Heat Conduction Equation," *International Journal for Numerical Methods in Engineering,* **11**, 1059–1065, 1977.

Chapter 7

COMPUTER IMPLEMENTATION

7.1 NUMERICAL INTEGRATION

7.1.1 Background

The finite element method, like most numerical methods, converts a continuum problem to a discrete one (i.e., converting a system with an infinite number of degrees of freedom into one with a finite number of degrees of freedom). The finite element model of a system ultimately represents a set of algebraic equations among the values of the dependent variables of the system at the selected nodes of the domain. The coefficients of the algebraic equations are typically integrals of approximation functions multiplied by the data of the problem. Exact evaluation of these integrals is not always possible because of the algebraic complexity of the data $a(x), b(x), c(x)$, and $f(x)$ in the mathematical model. In such cases, it is natural to seek numerical evaluation of these integral expressions. Numerical evaluation of the coefficient matrices is also useful in problems with constraints, where reduced integration techniques are used (e.g., the reduced integration element of the Timoshenko beam theory in Section 5.3).

Numerical evaluation of integrals, called *numerical integration* or *numerical quadrature,* involves approximation of the integrand by a polynomial of sufficient degree, because the integral of a polynomial can be evaluated exactly. For example, consider the integral,

$$I = \int_{x_a}^{x_b} F(x)\, dx \tag{7.1.1}$$

We approximate the function $F(x)$ by a polynomial

$$F(x) \approx \sum_{I=1}^{N} F_I \psi_I(x) \tag{7.1.2}$$

where F_I denotes the value of $F(x)$ at the Ith point of the interval $[x_a, x_b]$ and $\psi_I(x)$ are polynomials of degree $N-1$. The representation (7.1.2) can be viewed as the finite element interpolation of $F(x)$, where F_I is the value of the function at the Ith node. The interpolation can be of the Lagrange type or the Hermite type.

Substitution of (7.1.2) into (7.1.1) and evaluation of the integral gives an approximate value of I. For example, suppose that we choose linear interpolation of $F(x)$. Then $N=2$, $\psi_1 = (x_b - x)/h$, $\psi_2 = (x - x_a)/h$, and

$$I = \frac{1}{2}h(F_1 + F_2), \quad F_1 = F(x_a), \quad F_2 = F(x_b) \tag{7.1.3}$$

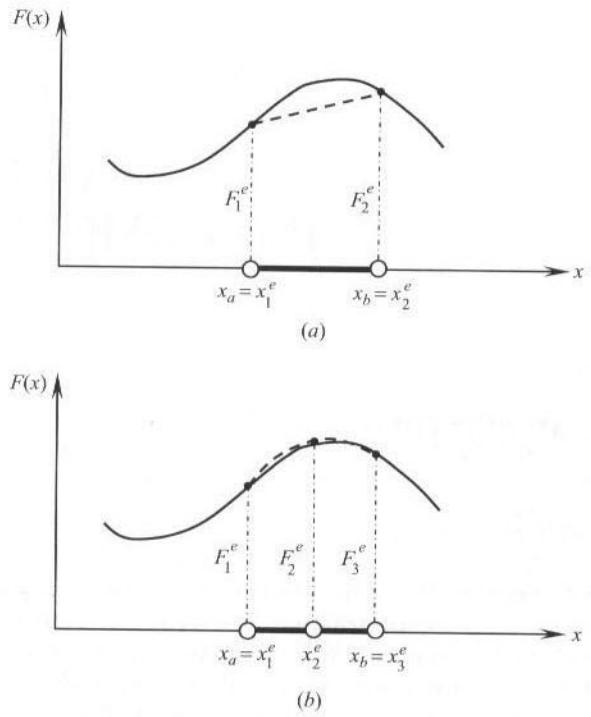

Figure 7.1.1 Approximate evaluation of an integral using the trapezoidal rule (*a*) two-point formula and (*b*) three-point formula.

Thus, the value of the integral is given by the area of a trapezoid used to approximate the area under the function $F(x)$ (see Fig. 7.1.1). Equation (7.1.3) is known as the *trapezoidal rule* of numerical integration. If we use the Lagrange quadratic interpolation of $F(x)$, we obtain

$$I = \frac{1}{6}h(F_1 + 4F_2 + F_3), \quad F_1 = F(x_a), \quad F_2 = F(x_a + 0.5h), \quad F_3 = F(x_b) \tag{7.1.4}$$

which is known as *Simpson's one-third rule*.

Equations (7.1.3) and (7.1.4) represent forms of numerical quadrature formulae. In general, a quadrature formula has the form

$$I = \int_{x_a}^{x_b} F(x)\, dx \approx \sum_{I=1}^{r} F(x_I) W_I \tag{7.1.5}$$

where x_I are called the *quadrature points* and W_I are the *quadrature weights*. These formulae require functional evaluations, multiplications, and additions to obtain the numerical value of the integral. They yield exact values of the integral whenever $F(x)$ is a polynomial of order $r - 1$.

In this section, we describe several numerical integration techniques and formulations in which the geometry as well as the dependent variables are approximated using different degrees of polynomials. We begin with the discussion of a local coordinate system.

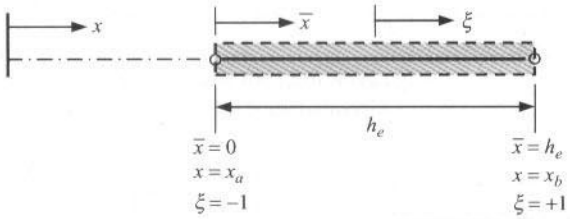

Figure 7.1.2 Global coordinate x, local coordinate $\bar{x}$, and normalized coordinate ξ.

7.1.2 Natural Coordinates

Of all the quadrature formulae, as will be discussed in the subsequent sections, the Gauss–Legendre one is the most commonly used. The details of the method itself will be discussed shortly. The formula requires the integral to be cast as one to be evaluated over the interval $[-1, 1]$. This requires the transformation of the problem coordinate x to a local coordinate ξ such that (see Fig. 7.1.2):

$$\text{when} \quad x = x_a, \quad \xi = -1; \quad \text{when} \quad x = x_b, \quad \xi = 1$$

The transformation between x and ξ can be represented by the linear "stretch" transformation

$$x = a + b\xi$$

where a and b are constants to be determined such that the above conditions hold:

$$x_a = a + b(-1), \quad x_b = a + b(1)$$

Solving for a and b, we obtain

$$b = \frac{1}{2}(x_b - x_a) = \frac{1}{2}h_e, \quad a = \frac{1}{2}(x_b + x_a) = x_a + \frac{1}{2}h_e$$

Hence, the transformation takes the form

$$x(\xi) = x_a + \frac{1}{2}h_e(1 + \xi) \tag{7.1.6}$$

where x_a denotes the global coordinate of the left-end node of the element Ω_e and h_e is the element length (see Fig. 7.1.2).

The local coordinate ξ is called the *normal coordinate* or *natural coordinate*, and its values always lie between -1 and 1, with its origin at the center of the element. The local coordinate ξ is useful in two ways: It is (a) convenient in constructing the interpolation functions and (b) required in numerical integration using Gauss–Legendre quadrature.

The derivation of the Lagrange family of interpolation functions in terms of the natural coordinate ξ is made easy by the following interpolation property of the approximation functions:

$$\psi_i(\xi_j) = \begin{cases} 1 & \text{if } i = j \\ 0 & \text{if } i \neq j \end{cases} \tag{7.1.7}$$

where ξ_j is the ξ coordinate of the jth node in the element. For an element with n nodes, ψ_i $(i = 1, 2, \ldots, n)$ are polynomials of degree $n - 1$. To construct ψ_i satisfying (7.1.7), we

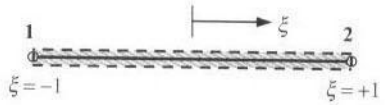

$$\psi_1(\xi) = \tfrac{1}{2}(1-\xi), \qquad \psi_2(\xi) = \tfrac{1}{2}(1+\xi)$$

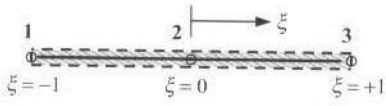

$$\psi_1(\xi) = -\tfrac{1}{2}\xi(1-\xi), \qquad \psi_2(\xi) = (1-\xi^2)$$
$$\psi_3(\xi) = \tfrac{1}{2}\xi(1+\xi)$$

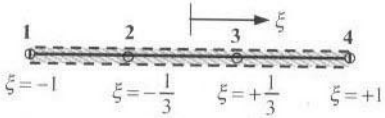

$$\psi_1(\xi) = -\tfrac{9}{16}(1-\xi)(\tfrac{1}{9}-\xi^2), \quad \psi_2(\xi) = \tfrac{27}{16}(1-\xi^2)(\tfrac{1}{3}-\xi)$$
$$\psi_3(\xi) = \tfrac{27}{16}(1-\xi^2)(\tfrac{1}{3}+\xi), \quad \psi_4(\xi) = -\tfrac{9}{16}(1+\xi)(\tfrac{1}{9}-\xi^2)$$

Figure 7.1.3 Lagrange family of one-dimensional interpolation functions in terms of the normalized coordinate.

proceed as follows: For each ψ_i, we form the product of $n-1$ linear functions $\xi - \xi_j$ ($j = 1, 2, \ldots, i-1, i+1, \ldots, n$; $j \neq i$):

$$\psi_i = c_i(\xi - \xi_1)(\xi - \xi_2)\cdots(\xi - \xi_{i-1})(\xi - \xi_{i+1})\cdots(\xi - \xi_n)$$

Note that ψ_i is zero at all nodes except the ith. Next, we determine the constant c_i such that $\psi_i = 1$ at $\xi = \xi_i$:

$$c_i = [(\xi_i - \xi_1)(\xi_i - \xi_2)\cdots(\xi_i - \xi_{i-1})(\xi_i - \xi_{i+1})\cdots(\xi_i - \xi_n)]^{-1}$$

Thus, the interpolation function associated with node i is

$$\psi_i(\xi) = \frac{(\xi - \xi_1)(\xi - \xi_2)\cdots(\xi - \xi_{i-1})(\xi - \xi_{i+1})\cdots(\xi - \xi_n)}{(\xi_i - \xi_1)(\xi_i - \xi_2)\cdots(\xi_i - \xi_{i-1})(\xi_i - \xi_{i+1})\cdots(\xi_i - \xi_n)} \tag{7.1.8}$$

The linear, quadratic, and cubic Lagrange interpolation functions in terms of the natural coordinate (for equally spaced nodes) are shown in Fig. 7.1.3.

7.1.3 Approximation of Geometry

We wish to use the Gauss–Legendre quadrature to numerically evaluate all integrals in the finite element method. The integrals are generally expressed in terms of the coordinate appearing in the problem description (like x or r). We shall call x and r as the *problem coordinates* or global coordinates. The Gauss–Legendre quadrature requires us to express the integral in terms of ξ over the interval -1 to $+1$. We assume a relation (or transformation) between the problem coordinate x and natural coordinate ξ in the form

$$x = f(\xi) \tag{7.1.9}$$

where f is assumed to be a one-to-one transformation. An example of $f(\xi)$ is provided by (7.1.6):

$$f(\xi) = x_a + \frac{1}{2}h_e(1+\xi)$$

In this case, $f(\xi)$ is a linear function of ξ. Hence, a straight line is transformed into a straight line.

It is natural to think of approximating the geometry in the same way as we approximated a dependent variable. In other words, the transformation $x = f(\xi)$ can be written as

$$x = \sum_{i=1}^{m} x_i^e \hat{\psi}_i^e(\xi) \tag{7.1.10}$$

where x_i^e is the global coordinate of the ith node of the element Ω_e and $\hat{\psi}_i^e$ are the Lagrange interpolation functions of degree $m-1$. When $m=2$, we have a linear transformation, and Eq. (7.1.10) is exactly the same as (7.1.6). When $m=3$, Eq.(7.1.10) expresses a quadratic relation between x and ξ. The functions $\hat{\psi}_i^e$ are called *shape functions* because they are used to express the geometry or shape of the element. When the element is a straight line, the mapping is linear (because two points, x_1^e and x_2^e, are sufficient to define a line).

The transformation (7.1.10) allows us to rewrite integrals involving x as those in terms of ξ:

$$\int_{x_a}^{x_b} F(x)\,dx = \int_{-1}^{1} \hat{F}(\xi)\,d\xi, \quad \hat{F}(\xi)\,d\xi = F(x(\xi))\,dx \tag{7.1.11}$$

so that the Gauss–Legendre quadrature can be used to evaluate the integral over $[-1, 1]$. The differential element dx in the global coordinate system x is related to the differential element $d\xi$ in the natural coordinate system ξ by

$$dx = \frac{dx}{d\xi} d\xi = J_e\,d\xi$$

where J_e is called the *Jacobian* of the transformation. We have

$$J_e = \frac{dx}{d\xi} = \frac{d}{d\xi}\left(\sum_{i=1}^{m} x_i^e \hat{\psi}_i^e\right) = \sum_{i=1}^{m} x_i^e \frac{d\hat{\psi}_i^e}{d\xi} \tag{7.1.12}$$

For a linear transformation [i.e., when $m=2$ in (7.1.10)], we have

$$\hat{\psi}_1^e = \frac{1}{2}(1-\xi), \quad \hat{\psi}_2^e = \frac{1}{2}(1+\xi)$$

$$J_e = x_1^e\left(-\frac{1}{2}\right) + x_2^e\left(\frac{1}{2}\right) = \frac{1}{2}(x_2^e - x_1^e) = \frac{1}{2}h_e \tag{7.1.13}$$

It can be shown that $J_e = \frac{1}{2}h_e$ whenever the element is a straight line, irrespective of the degree of interpolation used in the transformation (7.1.10).

7.1.4 Isoparametric Formulations

Recall that a dependent variable u is approximated in an element Ω_e by expressions of the form

$$u(x) = \sum_{j=1}^{n} u_j^e \psi_j^e(x) \tag{7.1.14}$$

In general, the degree of approximation used to describe the coordinate transformation (7.1.10) is not equal to the degree of approximation (7.1.14) used to represent a dependable

variable, i.e., $\hat{\psi}_i^e \neq \psi_i^e$. In other words, two independent meshes of elements may be used in the finite element formulation of a problem: one for the approximation of the geometry x and the other for the interpolation of the dependent variable u. Depending on the relationship between the degree of approximation used for the coordinate transformation and that used for the dependent variable, the finite element formulations are classified into three categories:

1. Subparametric formulations: $m < n$
2. Isoparametric formulations: $m = n$ (7.1.15)
3. Superparametric formulations: $m > n$

In subparametric formulations, the geometry is represented by lower-order elements than those used to approximate the dependent variable. An example of this category is provided by the Euler–Bernoulli beam element, where the Hermite cubic functions are used to approximate the deflection $w(x)$ and linear interpolation can be used, when straight beams are analyzed, to represent the geometry. In isoparametric formulations (which are the most common in practice), the same element is used to approximate the geometry as well as the dependent unknowns: $\psi_i(x) = \hat{\psi}_i(\xi)$. In the superparametric formulations, the geometry is represented with higher-order elements than those used to approximate the dependent variables. The superparametric formulation is seldom used in practice.

7.1.5 Numerical Integration

As discussed in the introduction, the evaluation of integrals of the form

$$\int_a^b F(x)\, dx \tag{7.1.16}$$

by exact means is either difficult or impossible owing to the complicated form of the integrand F. Numerical integration is also required when the integrand is to be evaluated inexactly (as in the Timoshenko beam element) or when the integrand is known only at discrete points (e.g., experimentally obtained data).

The basic idea behind all numerical integration techniques is to find a function $P(x)$, often a polynomial, that is both a suitable approximation of $F(x)$ and simple to integrate. The interpolating polynomials of degree n, denoted by P_n, which interpolate the integrand at $n + 1$ points of the interval $[a, b]$, often produce a suitable approximation and possess the desired property of simple integrability. An illustration of the approximation of the function $F(x)$ by the polynomial $P_4(x)$ that exactly matches the function $F(x)$ at the indicated base points is given in Fig. 7.1.4(*a*). The exact value of (7.1.16) is given by the area under the solid curve, while the approximate value

$$\int_a^b P_4(x)\, dx$$

is given by the area under the dashed curve. It should be noted that the difference (i.e., the error in the approximation) $E = F(x) - P_4(x)$ is not always of the same sign, and therefore the overall integration error may be small (because positive errors in one part cancel negative errors in other parts), even when P_4 is not a good approximation of F.

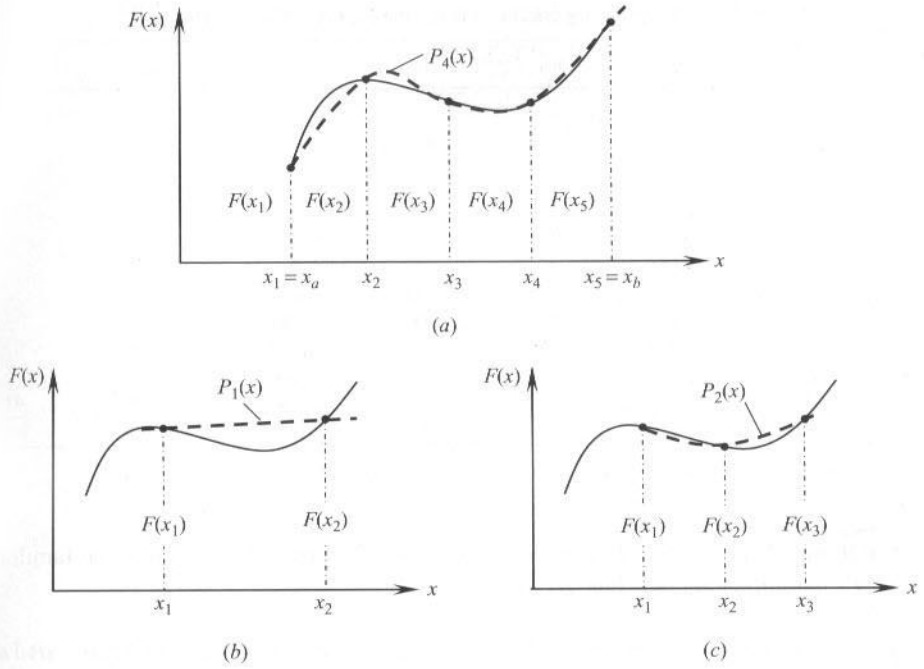

Figure 7.1.4 Numerical integration by the Newton–Cotes quadrature: (*a*) approximation of a function by $P_4(x)$; (*b*) the trapezoidal rule; and (*c*) Simpson's rule.

The commonly used numerical integration methods can be classified into two groups:

1. The Newton–Cotes formulae that employ values of the function at equally spaced points
2. The Gauss–Legendre quadrature formula that employs unequally spaced points

These two methods are described here.

The Newton–Cotes Quadrature. For r equally spaced base points, the *Newton–Cotes closed integration formula* is given by

$$\int_a^b F(x)\,dx = (b-a)\sum_{I=1}^{r} F(x_I)w_I \tag{7.1.17}$$

where w_I are the *weighting coefficients*, x_I are the *base points* that are equally spaced, and r is the number of base points (or $r-1$ is the number of intervals). Note that $r=1$ is a special case in which the number of base points as well as the number intervals is the same; in this case Eq. (7.1.17) gives the rectangle formula. For $r=2$, (7.1.17) gives the familiar *trapezoidal rule*, in which the required area under the solid curve in Fig. 7.1.4(*b*) is approximated by the area under the dotted straight line [i.e., $F(x)$ is approximated by $P_1(x)$]:

$$\int_{a=x_1}^{b=x_2} F(x)\,dx = \frac{b-a}{2}[F(x_1)+F(x_2)],\quad E=O(h^3),\quad h=b-a \tag{7.1.18}$$

where E denotes the error in the approximation and h is the uniform spacing between two base points. The notation $O(h)$, read as "order of h," is used to indicate the order of the

Table 7.1.1 Weighing coefficients for the Newton–Cotes formula.

r	w_1	w_2	w_3	w_4	w_5	w_6	w_7
1	1						
2	$\frac{1}{2}$	$\frac{1}{2}$					
3	$\frac{1}{6}$	$\frac{4}{6}$	$\frac{1}{6}$				
4	$\frac{1}{8}$	$\frac{3}{8}$	$\frac{3}{8}$	$\frac{1}{8}$			
5	$\frac{7}{90}$	$\frac{32}{90}$	$\frac{12}{90}$	$\frac{32}{90}$	$\frac{7}{90}$		
6	$\frac{19}{288}$	$\frac{75}{288}$	$\frac{50}{288}$	$\frac{50}{288}$	$\frac{75}{288}$	$\frac{19}{288}$	
7	$\frac{41}{840}$	$\frac{216}{840}$	$\frac{27}{840}$	$\frac{272}{840}$	$\frac{27}{840}$	$\frac{216}{840}$	$\frac{41}{840}$

error in terms of the spacing h. For $r = 3$ (i.e., two intervals), (7.1.17) gives the familiar *Simpson's one-third rule* [see Fig. 7.1.4(*c*)]:

$$\int_{a=x_1}^{b=x_3} F(x)\,dx = \frac{b-a}{6}[F(x_1) + 4F(x_2) + F(x_3)], \quad E = O(h^5), \quad h = 0.5(b-a) \tag{7.1.19}$$

The weighting coefficients for $r = 1, 2, \ldots, 7$ are given in Table 7.1.1. Note that $\sum_{I=1}^{r} w_I = 1$. The base point location for $r = 1$ is $x_1 = a + \frac{1}{2}(b-a) = \frac{1}{2}(a+b)$. For $r > 1$, the base point locations are

$$x_1 = a, \quad x_2 = a + \Delta x, \ldots, \; x_r = a + (r-1)\Delta x = b$$

and $\Delta x = (b-a)/(r-1)$. We note that when r is *odd* (i.e., when there is an even number of intervals or an odd number of base points), the formula is exact when $F(x)$ is a polynomial of degree r or less; when r is *even*, the formula is exact for a polynomial of degree $r-1$ or less. Odd-point formulas are frequently used because of their high order of accuracy [see Carnahan, Luther, and Wilkes (1969)].

The Gauss–Legendre Quadrature. In the Newton–Cotes quadrature, the base point locations have been specified. If the x_I are not specified, then there will be $2r+2$ undetermined parameters, $r+1$ weights w_I and $r+1$ base points x_I, which define a polynomial of degree $2r+1$. The Gauss–Legendre quadrature is based on the idea that the base points x_I and the weights w_I can be chosen so that the sum of the $r+1$ appropriately weighted values of the function yields the integral exactly when $F(x)$ is a polynomial of degree $2r+1$ or less. The Gauss–Legendre quadrature formula is given by

$$\int_a^b F(x)\,dx = \int_{-1}^{1} \hat{F}(\xi)\,d\xi \approx \sum_{I=1}^{r} \hat{F}(\xi_I) w_I \tag{7.1.20}$$

where w_I are the weight factors, ξ_I are the base points [roots of the Legendre polynomial $P_{r+1}(\xi)$], and $\hat{F}$ is the transformed integrand

$$\hat{F}(\xi) = F(x(\xi))J(\xi), \quad dx = J\,d\xi \tag{7.1.21}$$

Table 7.1.2 Weights and Gauss points for the Gauss–Legendre quadrature.

$$\int_{-1}^{1} F(\xi)d\xi = \sum_{i=1}^{r} F(\xi_i)w_i$$

Points, ξ_i†	r	Weights, w_i
0.0000000000	1	2.0000000000
±0.5773502692	2	1.0000000000
0.0000000000	3	0.8888888889
±0.7745966692		0.5555555555
±0.3399810435	4	0.6521451548
±0.8611363116		0.3478548451
0.0000000000	5	0.5688888889
±0.5384693101		0.4786286705
±0.9061798459		0.2369268850
±0.2386191861	6	0.4679139346
±0.6612093865		0.3607615730
±0.9324695142		0.1713244924

†Note that $0.57735\ldots = 1/\sqrt{3}$, $0.77459\ldots = \sqrt{3/5}$, and $0.888\ldots = 8/9$, and $0.555\ldots = 5/9$.

where J is the Jacobian of the transformation between x anbd ξ. The weight factors and Gauss points for the Gauss–Legendre quadrature (7.1.20) are given for $r = 1, \ldots, 6$ in Table 7.1.2.

The Gauss–Legendre quadrature is more frequently used than the Newton–Cotes quadrature because it requires fewer base points (hence, a saving in computation) to achieve the same accuracy. The error in the approximation is zero if the $(2r + 2)$th derivative of the integrand vanishes. In other words, a polynomial of degree p is integrated exactly by employing $r = \frac{1}{2}(p + 1)$ Gauss points. When $p + 1$ is odd, one should pick the nearest larger integer:

$$r = \left[\frac{1}{2}(p+1)\right] \tag{7.1.22}$$

In finite element formulations, we encounter integrals whose integrands F are functions of x, $\psi_i(x)$, and derivatives of $\psi_i(x)$ with respect to x. For the Gauss–Legendre quadrature, we must transform $F(x)dx$ to $\hat{F}(\xi)d\xi$ in order to use the formula (7.1.20). For example, consider the integral

$$K_{ij}^e = \int_{x_a}^{x_b} a(x)\frac{d\psi_i^e}{dx}\frac{d\psi_j^e}{dx}\,dx \tag{7.1.23}$$

Using the chain rule of differentiation, we have

$$\frac{d\psi_i^e(x)}{dx} = \frac{d\psi_i^e(\xi)}{d\xi}\frac{d\xi}{dx} = J^{-1}\frac{d\psi_i^e(\xi)}{d\xi} \tag{7.1.24}$$

Therefore, the integral in (7.1.23) can be written, with the help of (7.1.10), as

$$K_{ij}^e = \int_{-1}^{1} a(x(\xi))\frac{1}{J}\frac{d\psi_i^e}{d\xi}\frac{1}{J}\frac{d\psi_j^e}{d\xi}\,J\,d\xi \tag{7.1.25}$$

$$\approx \sum_{I=1}^{r} \hat{F}_{ij}^e(\xi_I)w_I \tag{7.1.26}$$

where

$$\hat{F}^e_{ij} = a\frac{1}{J}\frac{d\psi^e_i}{d\xi}\frac{d\psi^e_j}{d\xi}, \quad J = \sum_{i=1}^{m} x^e_i \frac{d\hat{\psi}^e_i}{d\xi} \tag{7.1.27}$$

For the isoparametric formulation, we take $\psi^e_i = \hat{\psi}^e_i$. As noted earlier, the Jacobian matrix will be the same ($J_e = \frac{1}{2}h_e$) when the element is a straight line, even if the coordinate transformation is quadratic or cubic. However, when the element is curved, the Jacobian is a function of ξ for transformations other than linear. The transformation from x to ξ is not required in the Newton–Cotes quadrature.

It is possible to determine the exact number of Gauss points required to evaluate the following element coefficients:

$$\begin{aligned}
K^e_{ij} &= \int_{x_a}^{x_b} \frac{d\psi^e_i}{dx}\frac{d\psi^e_j}{dx}\,dx = \int_{-1}^{+1} \frac{d\psi^e_i}{d\xi}\frac{d\psi^e_j}{d\xi}(J)^{-2}\,J\,d\xi \equiv \int_{-1}^{+1} G^K_{ij}(\xi)\,d\xi \\
&\approx \sum_{I=1}^{N^K} G^K_{ij}(\xi_I)\,W_I \\
M^e_{ij} &= \int_{x_a}^{x_b} \psi^e_i \psi^e_j\,dx = \int_{-1}^{+1} \psi^e_i(\xi)\,\psi^e_j(\xi)\,J\,d\xi \equiv \int_{-1}^{+1} G^M_{ij}(\xi)\,d\xi \\
&\approx \sum_{I=1}^{N^M} G^M_{ij}(\xi_I)\,W_I \\
f^e_i &= \int_{x_a}^{x_b} \psi^e_i\,dx = \int_{-1}^{+1} \psi^e_i(\xi)\,J\,d\xi \equiv \int_{-1}^{+1} G^F_{ij}(\xi)\,d\xi \\
&\approx \sum_{I=1}^{N^F} G^F_{ij}(\xi_I)\,W_I
\end{aligned} \tag{7.1.28}$$

when linear, quadratic, and cubic interpolation functions are used. For linear interpolation functions, the integrand of K^e_{ij} is constant, requiring only one-point Gauss–Legendre quadrature ($N^K = 1$). The integrand of the mass matrix M^e_{ij} is quadratic ($p = 2$), requiring [$r = \frac{1}{2}(p+1) = \frac{3}{2}$], the two-point quadrature ($N^M = 2$). The coefficients f^e_i are evaluated exactly by one-point quadrature ($N^F = 1$). Similarly, for quadratic and cubic elements, we can estimate the number of Gauss points needed to evaluate K^e_{ij}, M^e_{ij}, and f^e_i exactly. The results are summarized in Table 7.1.3. Note that, in estimating the quadrature points, it is assumed that the Jacobian J is a constant, which holds true when the element is a straight line.

If the matrices in (7.1.28) have variable coefficients or the elements are curved [and hence $J_e = J_e(\xi)$], the degree of the variation of the integrands changes and the number of Gauss points needed to exactly evaluate the integral changes. If the elements are straight and the coefficients $a = a(x)$ and $c = c(x)$ together with $f = f(x)$ are no more than linear in x, then the number of Gauss points for evaluating the coefficients

$$K^e_{ij} = \int_{x_a}^{x_b} a\frac{d\psi^e_i}{dx}\frac{d\psi^e_j}{dx}\,dx, \quad M^e_{ij} = \int_{x_a}^{x_b} c\psi^e_i\psi^e_j\,dx \tag{7.1.29}$$

Table 7.1.3 The number of Gauss–Legendre quadrature points required to evaluate K_{ij}^e, M_{ij}^e, and f_i^e of Eq. (7.1.28).

Element type	N^K	N^M	N^F
Linear	1	2	1
Quadratic	2	3	2
Cubic	3	4	2

remain the same as listed in the above table. However, the evaluation of f_i^e requires one point more than before. Conversely, the two-point quadrature for linear elements, three-point quadrature for quadratic elements, and four-point quadrature for cubic elements would exactly evaluate K_{ij}^e with a quadratic variation of $a(x)$, M_{ij}^e with linear variation of $c(x)$, and f_i^e with quadratic variation of $f(x)$.

The use of Gauss–Legendre quadrature in (7.1.28) yields the following values (exact up to the fifth decimal place) when the element is straight and the isoparametric formulation is used:

Quadratic Element (Three-Point Formula)

$$[K] = \frac{1}{h_e}\begin{bmatrix} 2.33333 & -2.66667 & 0.33333 \\ -2.66667 & 5.33333 & -2.66667 \\ 0.33333 & -2.66667 & 2.33333 \end{bmatrix}$$

$$[M] = \frac{h_e}{10}\begin{bmatrix} 1.33333 & 0.66667 & 0.33333 \\ 0.66667 & 5.33333 & 0.66667 \\ 0.33333 & 0.66667 & 1.333433 \end{bmatrix} \tag{7.1.30}$$

$$\{f\} = h_e\begin{Bmatrix} 0.166667 \\ 0.666667 \\ 0.166667 \end{Bmatrix}$$

Cubic Element (Four-Point Formula)

$$[K] = \frac{1}{h_e}\begin{bmatrix} 3.700 & -4.725 & 1.350 & -0.325 \\ -4.725 & 10.800 & -7.425 & 1.350 \\ 1.350 & -7.425 & 10.800 & -4.725 \\ -0.325 & 1.350 & -4.725 & 3.700 \end{bmatrix}$$

$$[M] = \frac{h_e}{10}\begin{bmatrix} 0.761905 & 0.589286 & -0.214286 & 0.113095 \\ 0.589286 & 3.857143 & -0.482143 & -0.214286 \\ -0.214286 & -0.482143 & 3.857143 & 0.589286 \\ 0.113095 & -0.214286 & 0.589286 & 0.761905 \end{bmatrix} \tag{7.1.31}$$

$$\{f\} = h_e\begin{Bmatrix} 0.125 \\ 0.375 \\ 0.375 \\ 0.125 \end{Bmatrix}$$

Example 7.1.1

We wish to evaluate the following integrals using the Newton–Cotes and Gauss–Legendre quadratures:

$$K_{12}=\int_{x_a}^{x_b}(x_0+x)\frac{d\psi_1}{dx}\frac{d\psi_2}{dx}\,dx, \quad G_{12}=\int_{x_a}^{x_b}(x_0+x)\psi_1\psi_2\,dx$$

where ψ_i are the linear interpolation functions

$$\psi_1=\frac{x-x_a}{x_b-x_a}=\frac{1}{2}(1-\xi), \quad \psi_2=\frac{x_b-x}{x_b-x_a}=\frac{1}{2}(1+\xi)$$

and x_0 is a constant.

Note that the integrand $F(x)$ in the integral of K_{12} is a linear polynomial (i.e., the degree is $r=1$). Hence, we expect the one-point Newton–Cotes or Gauss–Legendre quadrature to yield the exact value of K_{12}. On the other hand, the integrand of G_{12} is a cubic polynomial (i.e., the degree is $r=3$). Hence, we expect the three-point Newton–Cotes or two-point Gauss–Legendre quadrature to yield the exact value of G_{12}. The exact values are

$$K_{12}=-\frac{1}{x_b-x_a}\left[x_0+\frac{1}{2}(x_b+x_a)\right], \quad G_{12}=\frac{x_b-x_a}{6}\left[x_0+\frac{1}{2}(x_b+x_a)\right]$$

Newton–Cotes Quadrature: For various number of base points r, we have the following results:

$r=1$, $[x_1=0.5(x_a+x_b)]$:

$$\begin{aligned}
K_{12}&=\int_{x_a}^{x_b}(x_0+x)\frac{d\psi_1}{dx}\frac{d\psi_2}{dx}\,dx=\int_{x_a}^{x_b}(x_0+x)\left(-\frac{1}{x_b-x_a}\right)\left(\frac{1}{x_b-x_a}\right)dx\\
&=(x_b-x_a)\left[-\frac{1}{(x_b-x_a)^2}(x_0+x_1)\right]=-\frac{1}{x_b-x_a}\left[x_0+\frac{1}{2}(x_b+x_a)\right]\\
G_{12}&=\int_{x_a}^{x_b}(x_0+x)\psi_1\psi_2\,dx=\int_{x_a}^{x_b}(x_0+x)\left(\frac{x-x_a}{x_b-x_a}\right)\left(\frac{x_b-x}{x_b-x_a}\right)dx\\
&=(x_b-x_a)(x_0+x_1)\left(\frac{x_1-x_a}{x_b-x_a}\right)\left(\frac{x_b-x_1}{x_b-x_a}\right)\\
&=\frac{x_b-x_a}{4}\left[x_0+\frac{1}{2}(x_b+x_a)\right]
\end{aligned}$$

$r=2$, $(x_1=x_a, x_2=x_b)$:

$$\begin{aligned}
K_{12}&=-\frac{1}{2(x_b-x_a)}\left[(x_0+x_1)+(x_0+x_2)\right]\\
&=-\frac{1}{2(x_b-x_a)}(2x_0+x_a+x_b)=-\frac{1}{x_b-x_a}\left[x_0+\frac{1}{2}(x_b+x_a)\right]\\
G_{12}&=\frac{x_b-x_a}{2}\left[(x_0+x_1)\left(\frac{x_1-x_a}{x_b-x_a}\right)\left(\frac{x_b-x_1}{x_b-x_a}\right)\right.\\
&\quad\left.+(x_0+x_2)\left(\frac{x_2-x_a}{x_b-x_a}\right)\left(\frac{x_b-x_2}{x_b-x_a}\right)\right]=0
\end{aligned}$$

$r=3$, $[x_1=x_a, x_2=0.5(x_a+x_b), x_3=x_b]$:

$$K_{12} = -\frac{1}{6(x_b-x_a)}[(x_0+x_1)+4(x_0+x_2)+(x_0+x_3)]$$

$$= -\frac{1}{x_b-x_a}\left[x_0+\frac{1}{2}(x_b+x_a)\right]$$

$$G_{12} = \frac{x_b-x_a}{6}\left[(x_0+x_1)\left(\frac{x_1-x_a}{x_b-x_a}\right)\left(\frac{x_b-x_1}{x_b-x_a}\right)\right.$$

$$+4(x_0+x_2)\left(\frac{x_2-x_a}{x_b-x_a}\right)\left(\frac{x_b-x_2}{x_b-x_a}\right)$$

$$\left.+(x_0+x_3)\left(\frac{x_3-x_a}{x_b-x_a}\right)\left(\frac{x_b-x_3}{x_b-x_a}\right)\right]$$

$$= \frac{x_b-x_a}{6}\left[x_0+\frac{1}{2}(x_b+x_a)\right]$$

Gauss–Legendre Quadrature: The coefficient K_{12} for this case takes the form $[dx=0.5(x_b-x_a)d\xi$, $\psi_1=0.5(1-\xi)$, $\psi_2=0.5(1+\xi)$, and $d\psi_i/dx=(1/J)d\psi_i/d\xi$ with $J=0.5(x_b-x_a)]$

$$K_{12} = \int_{x_a}^{x_b}(x_0+x)\frac{d\psi_1}{dx}\frac{d\psi_2}{dx}\,dx$$

$$= -\frac{1}{2(x_b-x_a)}\int_{-1}^{1}\left[x_0+x_a+\frac{x_b-x_a}{2}(1+\xi)\right]d\xi$$

The polynomial order is $p=1$; hence, the one-point Gauss rule ($r=1$) would yield the exact value:

$$K_{12} = -\frac{1}{2(x_b-x_a)}\left[x_0+x_a+\frac{x_b-x_a}{2}(1+0.0)\right]\cdot 2$$

$$= -\frac{1}{x_b-x_a}\left[x_0+\frac{1}{2}(x_b+x_a)\right]$$

The coefficient G_{12} takes the form

$$G_{12} = \int_{x_a}^{x_b}(x_0+x)\psi_1\psi_2\,dx$$

$$= \frac{x_b-x_a}{8}\int_{-1}^{1}\left[x_0+x_a+\frac{x_b-x_a}{2}(1+\xi)\right](1-\xi^2)d\xi$$

The polynomial order is $p = 3$. Therefore, the two-point Gauss rule ($r = 2$) would yield the exact value

$$G_{12} = \frac{x_b - x_a}{8}\left\{\left[x_0 + x_a + \frac{x_b - x_a}{2}\left(1 - \frac{1}{\sqrt{3}}\right)\right]\left(1 - \frac{1}{3}\right) + \left[x_0 + x_a + \frac{x_b - x_a}{2}(1 + \frac{1}{\sqrt{3}})\right](1 - \frac{1}{3})\right\}$$
$$= \frac{x_b - x_a}{6}\left[x_0 + \frac{1}{2}(x_b + x_a)\right]$$

7.2 COMPUTER IMPLEMENTATION

7.2.1 Introductory Comments

Chapters 3–6 were devoted to the finite element formulations of two *classes* of boundary value, initial value, or eigenvalue problems in one dimension:

1. Second-order differential equations (e.g., heat transfer, fluid mechanics, one-dimensional elasticity, bars, and the Timoshenko beam theory)
2. Fourth-order differential equations governing the Euler–Bernoulli beam theory

The frame element, obtained by superposing the bar element and the beam element, was discussed in Chapter 5.

By now, it should be clear to the reader that the steps involved in the finite element analysis of a general class of problems (e.g., single second-order, single fourth-order, and a pair of second-order equations) are systematic, and once the finite element formulation is completed, the model can be implemented on a digital computer. Indeed, the success of the finite element method is largely due to the ease with which the analysis of a class of problems, without regard to the geometry and boundary conditions, can be implemented on a digital computer. A particular class of problems (say that described by the model equation of Chapter 3) can be solved by simply supplying the required input data to the program. For example, if we develop a general computer program to solve equations of the form

$$c_1\frac{\partial u}{\partial t} + c_2\frac{\partial^2 u}{\partial t^2} - \frac{\partial}{\partial x}\left(a\frac{\partial u}{\partial x}\right) + \frac{\partial^2}{\partial x^2}\left(b\frac{\partial^2 u}{\partial x^2}\right) + cu = f \tag{7.2.1}$$

then all physical problems described by Eqs. (3.1.1) and (5.1.1) and their time-dependent versions can be solved for any compatible boundary and initial conditions.

The purpose of this section is to discuss the basic steps involved in the development of a computer program for second- and fourth-order one-dimensional differential equations studied in the preceding chapters. The ideas presented here are used in the development of the model program **FEM1D,** and they are meant to be illustrative of the steps used in a typical finite element program development. One can make use of the ideas presented here and implement them using **FEM1D** to develop a program of one's own. The discussion here focuses on the finite element computations, and no attempt is made to discuss the Gauss elimination

procedure used to solve the resulting system of algebraic equations (a solver is provided with **FEM1D**; see Appendix 1 located on the book's website at www.mhhe.com/reddy3e).

7.2.2 General Outline

A typical finite element program consists of three basic units (see Fig. 7.2.1):

1. Preprocessor
2. Processor
3. Postprocessor

In the preprocessor part of the program, the input data of the problem are read in and/or generated. This includes the geometry (e.g., length of the domain and boundary conditions), the data of the problem (e.g., coefficients in the differential equation), finite element mesh information (e.g., element type, number of elements, element length, coordinates of the nodes, and connectivity matrix), and indicators for various options (e.g., print, no print, type of field problem analyzed, static analysis, eigenvalue analysis, transient analysis, and degree of interpolation).

In the processor part, all the steps in the finite element method discussed in the preceding chapter, except for postprocessing, are performed. The major steps of the processor are:

1. Generation of the element matrices using numerical integration
2. Assembly of element equations
3. Imposition of the boundary conditions
4. Solution of the algebraic equations for the nodal values of the primary variables

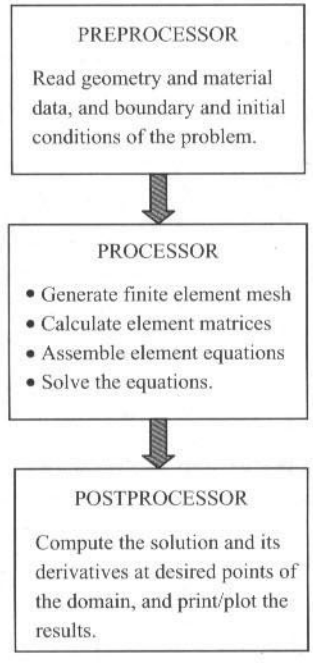

Figure 7.2.1 The three main functional units of a finite element program.

In the postprocessor part of the program, the solution is computed by interpolation at points other than nodes, secondary variables that are derivable from the solution are computed, and the output data are processed in a desired format for printout and/or plotting.

The preprocessor and postprocessors can be a few Fortran statements to read and print pertinent information, simple subroutines (e.g., subroutines to generate mesh and compute the gradient of the solution), or complex programs linked to other units via disk and tape files. The processor, where typically large amounts of computing time are spent, can consist of several subroutines, each having a special purpose (e.g., a subroutine for the calculation of element matrices, a subroutine for the imposition of boundary conditions, and a subroutine for the solution of equations). The degree of sophistication and the complexity of a finite element program depend on the general class of problems being programmed, the generality of the data in the equation, and the intended user of the program. It is always desirable to describe, through comment statements, all variables used in the computer program. A flow chart of the computer program **FEM1D** is presented in Fig. 7.2.2. The objective of each of the subroutines listed in the flow chart is described below.

ASSEMBLE: Subroutine for the assembly of element equations. The equations are assembled in upper-banded form for static and transient problems, and in full matrix form for eigenvalue problems.

EIGNSLVR: Subroutine for the solution of the eigenvalue problem $[A]\{X\} = \lambda[B]\{X\}$.

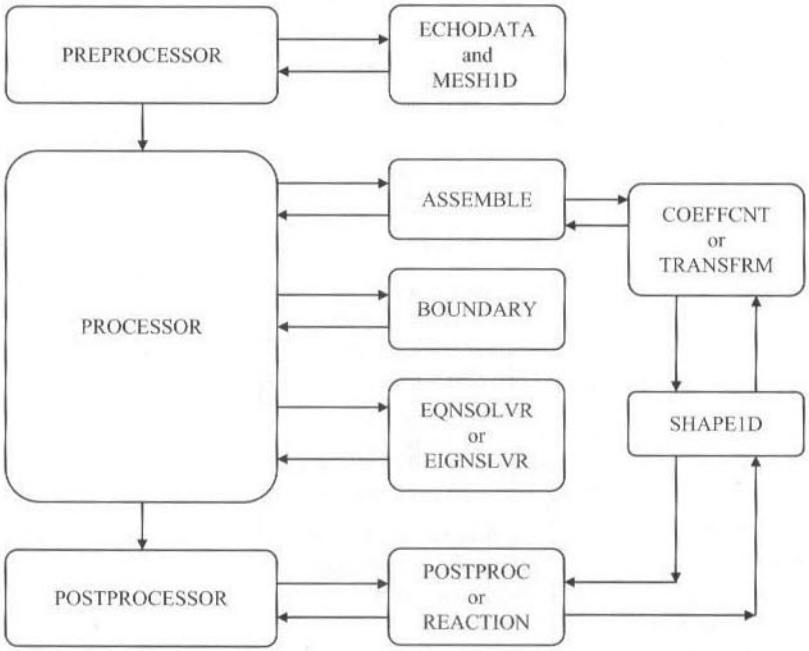

Figure 7.2.2 Flow chart of the computer program **FEM1D**.

BOUNDARY: Subroutine for imposition of specified boundary conditions (Dirichlet, Neumann, and Newton type).

COEFFCNT: Subroutine for computing element matrices $[K^e]$, $[M^e]$, and $\{f^e\}$ for all model problems except for truss and frame elements.

ECHODATA: Subroutine to echo the input to the program.

MESH1D: Subroutine to generate the mesh (coordinates of the global nodes and the connectivity array).

POSTPROC: Subroutine to postprocess the solution for all model problems except for truss and frame elements.

REACTION: Subroutine to calculate the reactions (i.e., generalized forces) for truss and frame elements.

SHAPE1D: Subroutine to compute the approximation functions and their derivatives.

EQNSOLVR: Subroutine for solving banded symmetric system of algebraic equations.

TRANSFRM: Subroutine to compute element stiffness matrix and force vector for truss and frame elements.

In the following sections, a discussion of the basic components of a typical finite element program is presented, and then the ideas are illustrated via FORTRAN statements.

7.2.3 Preprocessor

The preprocessor unit reads the input data, generates the finite element mesh, and prints the data and mesh information. The input data to a finite element program consist of element type IELEM (i.e., Lagrange element or Hermite element), number of elements used (NEM), specified boundary conditions on primary and secondary variables (number of boundary conditions, global node number and degree of freedom, and specified values of the degrees of freedom), the global coordinates of global nodes, and element properties (e.g., coefficients $a(x)$, $b(x)$, $c(x)$, $f(x)$, etc.). If a uniform mesh is used, the length of the domain should be read in, and global coordinates of the nodes can be generated in the program.

The preprocessor portion that deals with the generation of finite element mesh (when not supplied by the user) can be separated into a subroutine (**MESH1D**), depending on the convenience and complexity of the program. Mesh generation includes computation of the global coordinates X_I and the connectivity array $[B] = \text{NOD}$. Recall that the connectivity matrix describes the relationship between element nodes to global nodes as

$\text{NOD}(I, J) =$ *global node number* corresponding to the Jth (local) node of element I

This array is used in the assembly procedure as well as to transfer information from the element to the global system and vice versa. For example, to extract the vector ELX of global coordinates of element nodes from the vector GLX of global coordinates of global nodes, we can use the matrix NOD as follows: The global coordinate $x_i^{(n)}$ of the ith node of the nth element is the same as the global coordinate X_I of the global node I, where $I = \text{NOD}(n, i)$:

$$\{x_i^{(n)}\} = \{X_I\}, \quad I = \text{NOD}(n, i) \rightarrow \text{ELX}(i) = \text{GLX}(\text{NOD}(n, i))$$

The arrays ELX and GLX are used in **FEM1D** to denote $\{x^{(n)}\}$ and $\{X\}$, respectively.

7.2.4 Calculation of Element Matrices (Processor)

The most significant function of a processor is to generate element matrices. The element matrices are computed in various subroutines (**COEFFCNT** and **TRANSFRM**), depending on the type of problem being solved. These subroutines typically involve numerical evaluations of the element matrices $[K^e]$ and $[M^e]$ (program variables ELK and ELM) and the element vector $\{f^e\}$ (program variable ELF) for various field problems. The Gauss–Legendre quadrature described in Section 7.1.5 is used to evaluate element matrices and vectors, and the arrays are assembled as soon as they are computed. Thus, a loop on the number of elements in the mesh (NEM) is used to compute element matrices and assemble them (subroutine **ASSEMBLE**). It is here that the connectivity array NOD plays a crucial role. By putting one element matrix into global locations at a time, we avoid the computation of all element matrices at once.

Element matrices for different model equations (MODEL) and type of problem (NTYPE) are generated by assigning values as discussed next. Governing equations are listed for the static case. The variables used have the following meaning: $H =$ thickness of the beam/plate; $B =$ width of a beam; $E =$ Young's modulus; $G = E/[2(1+\nu)] =$ shear modulus; $\nu =$ Poisson's ratio; $D =$ bending stiffness ($D = EI = EBH^3/12$ for beams and $D = EH^3/[12(1-\nu^2)]$ for plates); $A =$ cross-sectional area; $K_s =$ shear correction factor; and $c_f =$ foundation modulus.

1. MODEL = 1, NTYPE = 0 All field problems described by the model equations (3.2.1) and (3.4.1), including radially symmetric heat-transfer-type problems:

$$-\frac{d}{dx}\left(a\frac{du}{dx}\right) + cu - f = 0; \quad AX = a(x), \quad CX = c(x), \quad FX = f(x)$$

$$-\frac{1}{r}\frac{d}{dr}\left(ra\frac{du}{dr}\right) + cu - f = 0; \quad AX = ra(r), \quad CX = rc(r), \quad FX = rf(r)$$

2. MODEL = 1, NTYPE = 1 Radially symmetric deformation of polar orthotropic disks (see Problem 4.37):

$$-\frac{d}{dr}\left[H\left(c_{11}r\frac{du}{dr} + c_{12}u\right)\right] + H\left(c_{22}\frac{u}{r} + c_{12}\frac{du}{dr}\right) = rf(r)$$

$$c_{11} = \frac{E_1}{1-\nu_{12}\nu_{21}}, \quad c_{12} = \frac{\nu_{12}E_2}{1-\nu_{12}\nu_{21}}, \quad c_{22} = \frac{E_2}{1-\nu_{12}\nu_{21}}$$

where $f(r)$ is the distributed force per unit volume (i.e., $Hf(r) = \hat{f}$ is the distributed force per unit area). For the isotropic case, $E_1 = E_2 = E$ and $\nu_{12} = \nu_{21} = \nu$.

3. MODEL = 1, NTYPE = 2 Radially symmetric deformation of cylinders:

$$-\frac{d}{dr}\left\{c\left[(1-\nu)r\frac{du}{dr} + \nu u\right]\right\} + c\left[(1-\nu)\frac{u}{r} + \nu\frac{du}{dr}\right] = rf(r)$$

$$c = \frac{E}{(1+\nu)(1-2\nu)}$$

4. MODEL = 2, NTYPE = 0 (reduced integration element; RIE) or MODEL = 2, NTYPE = 2 (consistent interpolation element; CIE) Bending of straight beams using

the Timoshenko beam theory:

$$-\frac{d}{dx}\left[GAK_s\left(\Psi+\frac{dw}{dx}\right)\right]+c_f w=q$$

$$-\frac{d}{dx}\left(EI\frac{d\Psi}{dx}\right)+GAK_s\left(\Psi+\frac{dw}{dx}\right)=0$$

$$AX=GAK_s,\quad CX=c_f(x),\quad FX=q(x),\quad BX=EI$$

5. MODEL = 2, NTYPE = 1 (RIE) or MODEL = 2, NTYPE = 3 (CIE) Axisymmetric bending of circular plates using the shear deformation plate theory:

$$-\frac{1}{r}\left[\frac{d}{dr}(rM_{rr})-M_{\theta\theta}\right]+Q_r=0,\quad -\frac{1}{r}\frac{d}{dr}(rQ_r)-q=0$$

$$M_{rr}=D\left(\frac{d\Psi}{dr}+\nu\frac{\Psi}{r}\right),\quad M_{\theta\theta}=D\left(\nu\frac{d\Psi}{dr}+\frac{\Psi}{r}\right),\quad Q_r=K_sGh\left(\Psi+\frac{dw}{dr}\right)$$

6. MODEL = 3, NTYPE = 0 Bending of straight beams using the Euler–Bernoulli beam theory:

$$\frac{d^2}{dx^2}\left(EI\frac{d^2w}{dx^2}\right)+c_f w=q(x),\quad BX=EI,\quad CX=c_f(x),\quad FX=q(x)$$

7. MODEL = 3, NTYPE = 1 Axisymmetric bending of circular plates using the classical plate theory:

$$D\frac{1}{r}\frac{d}{dr}\left\{r\frac{d}{dr}\left[\frac{1}{r}\frac{d}{dr}\left(r\frac{dw}{dr}\right)\right]\right\}+c_f w=q$$

8. MODEL = 4, NTYPE = 0 Two-node truss element.
9. MODEL = 4, NTYPE = 1 Two-node Euler–Bernoulli frame element.
10. MODEL = 4, NTYPE = 2 Two-node Timoshenko frame element.

The time-dependent option is exercised through variable ITEM:

ITEM = 0 static analysis
ITEM = 1 first-order time derivative (i.e., parabolic) problems
ITEM = 2 second-order time derivative (i.e., hyperbolic) problems

The element matrices are evaluated using the Gauss–Legendre quadrature except for MODEL = 4, where the explicit forms of element coefficients are programmed in the interest of computational efficiency.

The element shape functions SF and their derivatives GDSF are evaluated at the Gauss points in subroutine **SHAPE1D**. The gaussian weights and points associated with two-, three-, four-, and five-point integration are stored in arrays GAUSWT and GAUSPT, respectively. The nth column of GAUSWT, for example, contains the weights corresponding to the n-point Gauss–Legendre quadrature rule:

GAUSPT $(i, n) = i$th Gauss point corresponding to the n-point Gauss rule

The variable NGP is used to denote the number of Gauss points, which is selected to achieve good accuracy. As noted earlier, the linear, quadratic and cubic interpolation

functions require two, three, and four quadrature points, respectively, to evaluate the element coefficients exactly. Thus, if IELEM is the element type,

$$\text{IELEM} = \begin{cases} 1 & \text{linear} \\ 2 & \text{quadratic (Lagrange elements)} \\ 3 & \text{cubic} \end{cases}$$

then NGP = IELEM +1 would evaluate K_{ij}^e, M_{ij}^e, and f_i^e [see (7.1.29)] exactly when $c(x)$ is linear, and $a(x)$, $b(x)$, and $f(x)$ are quadratic functions. The Hermite cubic element is identified with IELEM = 0, in which case NGP is taken to be 4.

The coefficients $a(x) = \text{AX}$, $b(x) = \text{BX}$, and $c(x) = \text{CX}$, together with $f(x) = \text{FX}$ in the differential equation (7.2.1) are assumed to vary with x as follows:

AX=AX0+AX1*X	$(a = a_0 + a_1 x)$
BX=BX0+BX1*X	$(b = b_0 + b_1 x)$
CX=CX0+CX1*X	$(c = c_0 + c_1 x)$
FX=FX0+FX1*X+FX2*X*X	$(f = f_0 + f_1 x + f_2 x^2)$

(7.2.2)

For radially symmetric elasticity problems, (AX0, AX1) [or (BX0, BX1) for circular plates] are used to input Young's modulus E and Poisson's ratio ν.

The Gauss–Legendre quadrature formula (7.1.20) can be implemented in the computer as follows: Consider K_{ij}^e of the form

$$K_{ij}^e = \int_{x_a}^{x_b} \left[a(x) \frac{d\psi_i^e}{dx} \frac{d\psi_j^e}{dx} + c(x) \psi_i^e \psi_j^e \right] dx \tag{7.2.3}$$

We use the following program variables for the quantities in (7.2.3):

$$\text{ELK(I, J)} = K_{ij}^e, \quad \text{SF(I)} = \psi_i^e, \quad \text{GDSF(I)} = \frac{d\psi_i^e}{dx}$$

$$\text{AX} = a(x), \quad \text{CX} = c(x), \quad \text{ELX(I)} = x_i^e$$

$$\text{NPE} = n \quad \text{(the number of nodes in the element)}$$

After transforming x to ξ [or $x = x_a + 0.5 h_e (1 + \xi)$]

$$x = \sum_{i=1}^{n} x_i^e \psi_i^e \tag{7.2.4}$$

the coefficients K_{ij}^e in (7.2.3) can be written as

$$K_{ij}^e = \int_{-1}^{1} \left[a(\xi) \frac{1}{J} \frac{d\psi_i^e}{d\xi} \frac{1}{J} \frac{d\psi_j^e}{d\xi} + c(\xi) \psi_i^e \psi_j^e \right] J \, d\xi \equiv \int_{-1}^{1} G_{ij}^e(\xi) J \, d\xi \tag{7.2.5a}$$

$$= \sum_{I=1}^{\text{NGP}} G_{ij}^e(\xi_I) J W_I \tag{7.2.5b}$$

where G_{ij}^e denotes the expression in the square brackets in (7.2.5a), J is the Jacobian, and (ξ_I, W_I) are the Ith Gauss point and weight.

Examination of (7.2.5b) shows that there are three free indices: i, j, and I. We take the Gauss-point loop on I as the outermost one. Inside this loop, we evaluate G_{ij}^e at the Gauss point ξ_I for each i and j, multiply with the Jacobian $J = \frac{1}{2} h_e$ and the weights W_I, and sum

over the range of I:

$$\text{ELK}(i, j) = \text{ELK}(i, j) + G^e_{ij}(\xi_I) J W_I \tag{7.2.6}$$

Since $[K^e]$, $[M^e]$, $\{f^e\}$ are evaluated for $e = 1, 2, \ldots,$ NEM, where NEM denotes the number of elements in the mesh, we must initialize all arrays that are being evaluated using the Gauss–Legendre quadrature. The initialization must be made outside of the Gauss–Legendre quadrature loop.

The computation of coefficients K^e_{ij} in (7.2.5a) requires evaluation of a, c, ψ_i, and $d\psi_i/d\xi$ at the Gauss point ξ_I. Hence, inside the loop on I, we call subroutine **SHAPE1D** to evaluate ψ_i, $d\psi_i/dx = (d\psi_i/d\xi)/J$. Fortran statements to evaluate $[K^e]$ and $\{f^e\}$ are given below.

```
      DO 100 NI = 1,NGP
      XI = GAUSPT(NI,NGP)
C     Call subroutine SHP1D to evaluate the interpolation functions
C     (SF) and their global derivatives (GDSF) at the Gauss point XI
      CALL SHP1D(XI,NPE,SF,GDSF,GJ)
      CONST = GJ*GAUSWT(NI,NGP)
      DO 20 I = 1,NPE
20    X = X + SF(I)*ELX(I)
      AX = AX0 + AX1*X
      CX = CX0 + CX1*X
      DO 30 J = 1,NPE
      ELF(J) = ELF(J) + CONST*SF(J)*FX
      DO 30 I = 1,NPE
30    ELK(I,J) = ELK(I,J) + CONST*(AX*GDSF(I)*GDSF(J)
                 + CX*SF(I)*SF(J))
```

In the same way, all the other coefficients (e.g., M^e_{ij} and f^e_i) can be evaluated. Recall that the element properties (i.e., K^e_{ij}, M^e_{ij}, and f^e_i) are calculated by calling a suitable subroutine (**COEFFCNT** or **TRANSFRM**) for the field problem being analyzed within a loop with a counter based on the number of elements in the mesh (NEM).

7.2.5 Assembly of Element Equations (Processor)

The assembly of element equations should be carried out as soon as the element matrices are computed, rather than waiting till the element coefficients of all the elements are computed. The latter requires storage of the element coefficients of each element. In the former case, we can perform the assembly in the same loop in which a subroutine is called to calculate element matrices.

A feature of the finite element equations that enables us to save storage and computing time is the assembly of element matrices in upper-banded form. When element matrices are symmetric, the resulting global (or assembled) matrix is also symmetric, with many zeros away from the main diagonal. Therefore, it is sufficient to store only the upper *half-band* of

the assembled matrix. The half bandwidth of a matrix is defined as follows: Let N_i be the number of matrix elements between the diagonal element and the last nonzero element in the ith row, after which all elements in that row are zero; the half-bandwidth is the maximum of $(N_i + 1) \times$ NDF, where NDF is the number of degrees of freedom per node

$$b_I = \max_{1 \le i \le n} [(N_i + 1) \times \text{NDF}]$$

and n is the number of rows in the matrix (or equations in the problem). General-purpose equation solvers are available for such banded systems of equations.

The half-bandwidth NHBW of the assembled (i.e., global) finite element matrix can be determined in the finite element program itself. The local nature of the finite element interpolation functions (i.e., ψ_i^e are defined to be nonzero only over the element Ω_e) is responsible for the banded character of the assembled matrix. If two global nodes do not belong to the same element, then the corresponding entries in the global matrix are zeros:

$$K_{IJ} = 0 \quad \text{if global nodes } I \text{ and } J \text{ do not correspond to local nodes of the same element}$$

This property enables us to determine the half-bandwidth NHBW of the assembled matrix

$$\text{NHBW} = \max_{\substack{1 \le N \le \text{NEM} \\ 1 \le I,\ J \le \text{NPE}}} \{\text{abs}[\text{NOD}(N,\ I) - \text{NOD}(N,\ J)] + 1\} \times \text{NDF} \tag{7.2.7a}$$

where

$$\begin{aligned} \text{NEM} &= \text{number of elements in the mesh} \\ \text{NPE} &= \text{number of nodes per element} \\ \text{NDF} &= \text{number of degrees of freedom per element} \end{aligned} \tag{7.2.7b}$$

For example, for one-dimensional problems with elements connected in series, the maximum difference between the nodes of an element is equal to NPE − 1. Hence,

$$\text{NHBW} = [(\text{NPE} - 1) + 1] \times \text{NDF} = \text{NPE} \times \text{NDF} \tag{7.2.8}$$

Of course, NHBW is always less than or equal to the number of primary degrees of freedom in the mesh, i.e., the number of equations, NEQ.

The logic for assembling the element matrices K_{ij}^e into the upper-banded form of the global coefficients K_{ij} is that the assembly can be skipped whenever $J < I$ and $J >$ NHBW. The main diagonal, $I = J$, of the assembled square matrix (i.e., full storage form), becomes the first column of the assembled banded matrix (i.e., banded storage form), as shown in Fig. 7.2.3. The upper diagonals (parallel to the main diagonal) take the position of respective columns in the banded matrix. Thus, the banded matrix has dimension NEQ × NHBW, where NEQ denotes the total number of equations in the problem.

The element coefficients K_{ij}^n and f_i^n of a typical element Ω_n are to be assembled into the global coefficients matrix $[K]$ and source vector $\{F\}$, respectively. If the ith node of the element is equal to the Ith global node and the jth node of the element is equal to the Jth global node, we have

$$K_{IJ} = K_{ij}^n, \quad F_I = F_i^n \quad (\text{for NDF} = 1) \tag{7.2.9a}$$

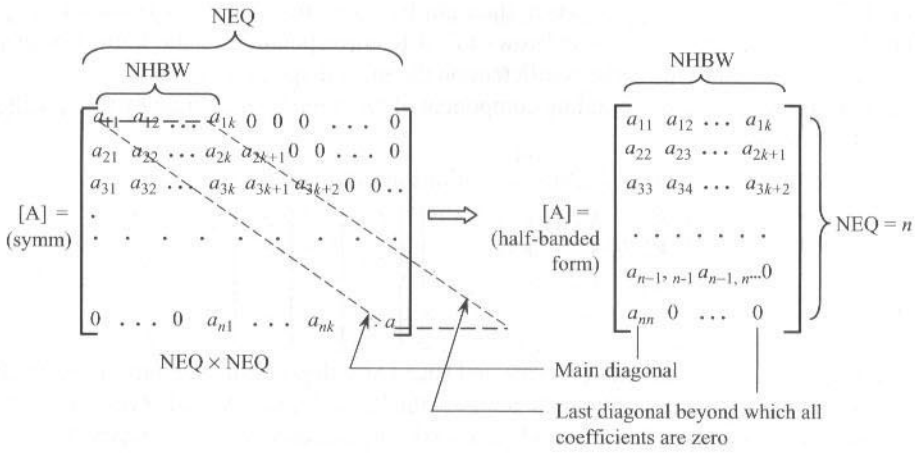

Figure 7.2.3 Finite element coefficient matrix storage in upper-half-banded form.

The values of I and J can be obtained with the help of array NOD:

$$I = \text{NOD}(n, i), \quad J = \text{NOD}(n, j) \tag{7.2.9b}$$

Recall that it is possible that the same I and J may correspond to a pair of i and j of some other element Ω^m. In that case, K_{ij}^m will be added to existing coefficients K_{IJ} during the assembly. For NDF > 1, the logic still holds, with the change

$$K_{(\text{NR})(\text{NC})} = K^n_{(i+p-1)(j+q-1)} \quad (p, q = 1, 2, \ldots, \text{NDF}) \tag{7.2.10a}$$

where

$$\text{NR} = (I - 1) \times \text{NDF} + p, \quad \text{NC} = (J - 1) \times \text{NDF} + q \tag{7.2.10b}$$

and I and J are related to i and j by (7.2.9*b*). These ideas are implemented in subroutine **ASSEMBLE**.

7.2.6 Imposition of Boundary Conditions (Processor)

Imposition of boundary conditions on the primary and secondary global degrees of freedom can be carried out through a subroutine **(BOUNDARY)**, which remains unchanged for two-dimensional or three-dimensional problems. There are three types of boundary conditions for any problem:

1. Essential boundary conditions, i.e., boundary conditions on primary variables (Dirichlet boundary conditions).
2. Natural boundary conditions, i.e., boundary conditions on secondary variables (Neumann boundary conditions).
3. Mixed boundary conditions (Newton boundary conditions).

The procedure for implementing the boundary conditions on the primary variables involves modifying the assembled coefficient matrix (GLK) and right-hand column vector (GLF) by three operations:

Step 1. Moving the known products to the right-hand column of the matrix equation.
Step 2. Replacing the columns and rows of GLK corresponding to the known primary variable by zeros, and setting the coefficient on the main diagonal to unity.
Step 3. Replacing the corresponding component of the right-hand column by the specified value of the variable.

Consider the following N algebraic equations in full matrix form:

$$\begin{bmatrix} K_{11} & K_{12} & K_{13} & \cdots \\ K_{21} & K_{22} & K_{23} & \cdots \\ K_{31} & K_{32} & K_{33} & \cdots \\ \vdots & \vdots & \vdots & \end{bmatrix} \begin{Bmatrix} U_1 \\ U_2 \\ U_3 \\ \vdots \end{Bmatrix} = \begin{Bmatrix} F_1 \\ F_2 \\ F_3 \\ \vdots \end{Bmatrix}$$

where U_I and F_I are the global primary and secondary degrees of freedom, respectively, and K_{IJ} are the assembled coefficients. Suppose that $U_S = \hat{U}_S$ is specified. Recall that when the primary degree of freedom at a node is known, the corresponding secondary degree of freedom is unknown, and vice versa. Set $K_{SS} = 1$ and $F_S = \hat{U}_S$; further, set $K_{SI} = K_{IS} = 0$ for $I = 1, 2, \ldots, N$ and $I \neq S$. For $S = 2$, the modified equations are

$$\begin{bmatrix} K_{11} & 0 & K_{13} & K_{14} & \cdots & K_{1n} \\ 0 & 1 & 0 & 0 & \cdots & 0 \\ K_{31} & 0 & K_{33} & K_{34} & \cdots & K_{3n} \\ \vdots & \vdots & \vdots & \vdots & & \vdots \\ K_{n1} & 0 & K_{n3} & K_{n4} & \cdots & K_{nn} \end{bmatrix} \begin{Bmatrix} U_1 \\ U_2 \\ U_3 \\ \vdots \\ U_n \end{Bmatrix} = \begin{Bmatrix} \hat{F}_1 \\ \hat{U}_2 \\ \hat{F}_3 \\ \vdots \\ \hat{F}_n \end{Bmatrix}$$

where

$$\hat{F}_i = F_i - K_{i2}\hat{U}_2 \quad (i = 1, 3, 4, 5, \ldots, n;\ i \neq 2)$$

Thus, in general, if $U_S = \hat{U}_S$ is known, we have

$$K_{SS} = 1, \quad F_S = \hat{U}_S; \quad \hat{F}_i = F_i - K_{iS}\hat{U}_S; \quad K_{Si} = K_{iS} = 0$$

where $i = 1, 2, \ldots, S-1, S+1, \ldots, n$ $(i \neq S)$. This procedure is repeated for every specified primary degree of freedom. It enables us to retain the original order of the matrix, and the specified boundary conditions on the primary degrees of freedom are printed as part of the solution. Of course, the logic should be implemented for a banded system of equations.

The specified secondary degrees of freedom (Q_i) are implemented directly by adding their specified values to the computed values. Suppose that the point source corresponding to the Rth secondary degree of freedom is specified to be $\hat{F}_R$. Then

$$F_R = f_R + \hat{F}_R$$

where f_R is the contribution due to the distributed source $f(x)$; f_R is computed as a part of the element computations and assembled.

Mixed-type boundary conditions are of the form

$$a\frac{du}{dx} + k(u - \bar{u}) = 0 \quad (\bar{u} \text{ and } k \text{ are known constants}) \tag{7.2.11}$$

which contains both the primary variable u and the secondary variable $a\ du/dx$. Thus, $a\ du/dx$ at the node p is replaced by $-k_p(u_p - \bar{u}_p)$:

$$Q_p = -k_p(U_p - \bar{U}_p)$$

This amounts to modifying K_{pp} by adding k_p to its existing value,

$$K_{pp} \leftarrow K_{pp} + k_p$$

and adding $k_p \bar{U}_p$ to F_p,

$$F_p \leftarrow F_p + k_p \bar{U}_p$$

All three types of boundary conditions are implemented in the subroutine **BOUNDARY** for boundary, initial, and eigenvalue problems. The following variable names are used in the subroutine **BOUNDARY:**

NSPV	Number of specified primary variables
NSSV	Number of specified secondary variables
NNBC	Number of Newton boundary conditions
VSPV	Column of the specified values $\bar{U}_S$ of primary variables
VSSV	Column of the specified values $\bar{F}_R$ of secondary variables
VNBC	Column of the specified values k_p
UREF	Column of the specified values $\bar{U}_p$
ISPV	Array of the global node and degree of freedom at the node that is specified [ISPV(I,1)=global node of the Ith boundary condition, ISPV(I,2)=degree of freedom specified at the global node, ISPV(I,1)]

Similar definitions are used for ISSV and INBC arrays.

7.2.7 Solving Equations and Postprocessing

Subroutine **EQNSOLVR** is used to solve a banded system of equations, and the solution is returned in array GLF. The program performs the gaussian elimination and back-substitution to compute the solution. For a discussion of the gaussian elimination used to solve a set of linear algebraic equations, the reader is referred to the book by Carnhan, Luther, and Wilkes (1969).

Postprocessing involves computation of the solution and its gradient at preselected points of the domain. The preselected points are the end points of the element, the midpoint, and three evenly spaced points between the end points and the midpoint. Subroutine **POSTPROC** is used to evaluate the solution and its derivatives at the preselected points of an element:

$$u^e(x) = \sum_{j=1}^{n} u_j^e \psi_j^e(x), \quad \left(\frac{du^e}{dx}\right)\bigg|_x = \sum_{j=1}^{n} u_j^e \left(\frac{d\psi_j^e}{dx}\right)\bigg|_x \tag{7.2.12}$$

for the Lagrange elements and

$$w^e(x) = \sum_{j=1}^{4} u_j^e \phi_j^e(x), \quad \frac{d^m w^e}{dx^m} = \sum_{j=1}^{4} u_j^e \left(\frac{d^m \phi_j^e}{dx^m}\right) \quad (m = 1, 2, 3) \tag{7.2.13}$$

for the Hermite cubic elements. The nodal values u_j^e of the element Ω_e are deduced from the global nodal values U_I as follows:

$$u_j^e = U_I, \quad I = \text{NOD}(e, j)$$

Table 7.3.1 Meaning of the program variables for various field problems. Subscripts 0, 1, and 2 on the variables denote the constant, linear, and quadratic coefficients of the variables, respectively, (e.g., f_0, f_1, f_2 denotes the coefficients in $f(x) = f_0 + f_1 \cdot x + f_2 \cdot x^2$).

	Field problem	MODEL	NTYPE	ITEM†	AX0	AX1	BX0	BX1	CX0	CX1	FX0	FX1	FX2	CT0‡	CT1†
1.	Plane wall	1	0	1	k_0	k_1	0.0	0.0	0.0	0.0	f_0	f_1	f_2	ρ_0	ρ_1
2.	Heat Exchanger fin	1	0	1	$(kA)_0$	$(kA)_1$	0.0	0.0	c_0	c_1	f_0	f_1	f_2	ρ_0	ρ_1
3.	Radially symmetric heat transfer	1	0	1	0.0	k_1	0.0	0.0	0.0	0.0	0.0	f_1	f_2	0.0	ρ_1
4.	Viscous flow through channels	1	0	1	μ_0	μ_1	0.0	0.0	0.0	0.0	f_0	f_1	f_2	ρ_0	ρ_1
5.	Viscous flow through pipes	1	0	1	0.0	μ_1	0.0	0.0	0.0	0.0	0.0	f_1	f_2	0.0	ρ_1
6.	Unidirectional seepage	1	0	1	μ_0	μ_1	0.0	0.0	0.0	0.0	f_0	f_1	f_2	ρ_0	ρ_1
7.	Radially symmetric seepage (ground water flow)	1	0	1	0.0	μ_1	0.0	0.0	0.0	0.0	0.0	f_1	f_2	0.0	ρ_1
8.	Axial deformation of a bar	1	0	2	$(AE)_0$	$(AE)_1$	0.0	0.0	c_0	c_1	f_0	f_1	f_2	$(\rho A)_0$	$(\rho A)_1$
9.	Radially symmetric deformation of a disk (plane stress)	1	1	2	E_1	E_2	v_{12}	H	c_0	c_1	f_0	f_1	f_2	$(\rho A)_0$	$(\rho A)_1$
10.	Radially symmetric deformation of a cylinder (plane strain)	1	2	2	E_1	E_2	v_{12}	H	c_0	c_2	f_0	f_1	f_2	$(\rho A)_0$	$(\rho A)_1$
11.	Euler–Bernoulli beam theory	3	0	2	0.0	0.0	$(EI)_0$	$(EI)_1$	c_0	c_1	f_0	f_1	f_2	ρA	ρ_I

Table 7.3.1 *Continued.*

	Field problem	MODEL	NTYPE	ITEM†	AX0	AX1	BX0	BX1	CX0	CX1	FX0	FX1	FX2	CT0‡	CT1†
12.	Euler–Bernoulli theory for circular plates	3	1	2	E_1	E_2	ν_{12}	H	c_0	c_2	f_0	f_1	f_2	ρ_A	ρ_I
13.	Timoshenko beam theory (RIE)*	2	0	2	$(SK)_0$	$(SK)_1$	$(EI)_0$	$(EI)_1$	c_0	c_1	f_0	f_1	f_2	ρ_A	ρ_I
14.	Timoshenko beam theory (CIE)*	2	2	2	$(SK)_0$	$(SK)_1$	$(EI)_0$	$(EI)_1$	c_0	c_1	f_0	f_1	f_2	ρ_A	ρ_I
15.	Timoshenko theory of circular plates (RIE)	2	1	2	E_1	E_2	ν_{12}	H	c_0	c_1	f_0	f_1	KG_{13}	ρ_A	ρ_I
16.	Timoshenko theory of circular plates (CIE)	2	3	2	E_1	E_2	ν_{12}	H	c_0	c_1	f_0	f_1	KG_{13}	ρ_A	ρ_I
17.	Plane truss	4	0	0											
18.	The Euler–Bernoulli frame element	4	1	0	For field problems 17–19, these parameters are not read; instead, E =SE, A =SA, L =SL, and so on are read for each member of the structure, where SE=modulus E, SA=cross-sectional area A, SI=moment of inertia I, SL=length L of the member, CN= $\cos\alpha$, SN= $\sin\alpha$, etc. (see Table 7.3.2).										
19.	The Timoshenko frame element	4	2	0											

* $S = GA$ and K is the shear correction factor ($K = 5/6$).

†For time-dependent problems only; when steady-state solution is required, set ITEM=0.

‡For transient analysis only; the transient analysis option is not available in **FEM1D** for truss and frame problems.

when NDF = 1. For NDF > 1, I is given by $I = [\text{NOD}(e, j) - 1] \times \text{NDF}$ and

$$u^e_{j+p} = U_{I+p} \quad (p = 1, 2, \ldots, \text{NDF})$$

The values computed using the derivatives of the solution are often inaccurate because the derivatives of the approximate solution become increasingly inaccurate with increasing order of differentiation. For example, the shear force computed in the Euler–Bernoulli beam theory (EBT)

$$V = -\frac{d}{dx}\left(b\frac{d^2w}{dx^2}\right) = \sum_{j=1}^{n} u^e_j \frac{d}{dx}\left(b\frac{d^2\phi^e_j}{dx^2}\right) \tag{7.2.14}$$

will be in considerable error in addition to being discontinuous across the elements. The accuracy increases, rather slowly, with mesh refinement and higher-order elements. The derivatives computed using (7.2.14) are more accurate if they are computed at the Gauss points. When accurate values of the secondary variables are desired at the nodes, it is recommended that they be computed from the element equations:

$$Q^e_i = \sum_{j=1}^{n} K^e_{ij} u^e_j - f^e_i \quad (i = 1, 2, \ldots, n) \tag{7.2.15}$$

However, this requires recomputation or saving of element coefficients K^e_{ij} and f^e_i. Recall that the nodal values of generalized forces are exact at the nodes when computed using (7.2.15) for certain problems as discussed before.

7.3 APPLICATIONS OF PROGRAM FEM1D

7.3.1 General Comments

The computer program **FEM1D**, which embodies the ideas presented in the previous section, is intended to illustrate the use of the finite element models developed in Chapters 3–6 to a variety of one-dimensional field problems, some of them are not discussed in this book. The program **FEM1D** is developed as a learning computational tool for students of a first course on the finite element method (see Appendix 1 for a listing of the program located on the book's website at www.mhhe.com/reddy3e). In the interest of simplicity and ease of understanding, only the model equations discussed in this book and their immediate extensions are included in the program.

Table 7.3.1 contains a summary of the definitions of coefficients of various model problems and their corresponding program variables. The table can be used as a ready reference to select proper values of AX0, AX1, and so on for different problems.

7.3.2 Illustrative Examples

Here we revisit some of the example problems considered earlier to illustrate the use of **FEM1D** in their solution. Only certain key observations concerning the input data are made, but complete listings of input files for each problem are given. In the interest of brevity, the complete output files for most problems are not included.

A description of the input variables to program **FEM1D** is presented in Table 7.3.2. In Table 7.3.2, "skip" means that the input data is omitted (i.e., no data is required). In the "free

Table 7.3.2 Description of the input variables to the program **FEM1D**

• **Data Card 1**	
TITLE	Title of the problem being solved (80 characters)
• **Data Card 2**	
MODEL	Model equation being solved (see below)
NTYPE	Type of problem solved (see below)
	MODEL = 1, NTYPE = 0: A problem of MODEL EQUATION (3.2.1)
	MODEL = 1, NTYPE = 1: A circular DISK (PLANE STRESS)
	MODEL = 1, NTYPE > 1: A circular DISK (PLANE STRAIN)
	MODEL = 2, NTYPE = 0: A Timoshenko BEAM (RIE) problem
	MODEL = 2, NTYPE = 1: A Timoshenko PLATE (RIE) problem
	MODEL = 2, NTYPE = 2: A Timoshenko BEAM ($CIE^{\dagger}$) problem
	MODEL = 2, NTYPE > 2: A Timoshenko PLATE (CIE) problem
	MODEL = 3, NTYPE = 0: A Euler–Bernoulli BEAM problem
	MODEL = 3, NTYPE > 0: A Euler–Bernoulli circular plate
	MODEL = 4, NTYPE = 0: A plane TRUSS problem
	MODEL = 4, NTYPE = 1: A Euler–Bernoulli FRAME problem
	MODEL = 4, NTYPE = 2: A Timoshenko (CIE) FRAME problem
ITEM	Indicator for transient analysis
	ITEM = 0, Steady-state solution
	ITEM = 1, Transient analysis of PARABOLIC equations
	ITEM = 2, Transient analysis of HYPERBOLIC equations
	ITEM = 3, Eigenvalue analysis
• **Data Card 3**	
IELEM	Type of finite element
	IELEM = 0, Hermite cubic finite element
	IELEM = 1, Linear Lagrange finite element
	IELEM = 2, Quadratic Lagrange finite element
NEM	Number of elements in the mesh
• **Data Card 4**	
ICONT	Indicator for continuity of data for the problem
	ICONT = 1, Data (AX,BX,CX,FX and mesh) is continuous
	ICONT = 0, Data is element dependent
NPRNT	Indicator for printing of element/global matrices
	NPRNT = 0, Not to print element or global matrices but postprocess the solution and print
	NPRNT = 1, Print Element 1 coefficient matrices only but postprocess the solution and print
	NPRNT = 2, Print Element 1 and global matrices but NOT postprocess the solution
	NPRNT > 2, Not to print element or global matrices and NOT postprocess the solution

Skip Cards 5–15 for TRUSS/FRAME problems (MODEL=4), and read Cards 5–15 only if MODEL $\neq$ 4. SKIP cards 5–9 if data is discontinuous (ICONT = 0).

• **Data Card 5**	
DX(I)	Array of element lengths. DX(1) denotes the global coordinate of Node 1 of the mesh; DX(I) (I = 2, NEM1) denotes the length of the (I - 1)st element, where NEM1 = NEM + 1, and NEM denotes the number of elements in the mesh.

Cards 6–9 define the coefficients in the model equations. All coefficients are expressed in terms of GLOBAL coordinate x. See Table 7.2.1 for the meaning of the coefficients.

(**Table 7.3.2** continued)

- **Data Card 6**

AX0	Constant term of the coefficient $[a(x) =]$ AX
AX1	Linear term of AX

- **Data Card 7**

BX0	Constant term of the coefficient $[b(x) =]$ BX
BX1	Linear term of the coefficient BX

- **Data Card 8**

CX0	Constant term of the coefficient $[c(x) =]$ CX
CX1	Linear term of the coefficient CX

SKIP Card 9 for eigenvalue problems (i.e., when ITEM = 3)

- **Data Card 9**

FX0	Constant term of the source $[f(x) =]$ FX
FX1	Linear term of FX
FX2	Quadratic term of FX

SKIP Cards 10–15 if data is continuous (ICONT $\neq 0$). Cards 10–15 are read for each element (i.e., NEM times). All coefficients are with respect to the LOCAL coordinate $\bar{x}$.

- **Data Card 10**

NNM	Number of global nodes in the mesh

- **Data Card 11**

NOD	Connectivity of the element: NOD(N,I) = Global node number corresponding to the Ith node of Element N (I=1, NPE) where NPE denotes the Number of nodes Per Element
GLX(I)	Length of the Ith element

- **Data Card 12**

DCAX	Constant and linear terms of the coefficient AX

- **Data Card 13**

DCBX	Constant and linear terms of the coefficient BX

- **Data Card 14**

DCCX	Constant and linear terms of the coefficient CX

- **Data Card 15**

DCFX	Constant, linear and quadratic terms of FX

READ Cards 16–23 only for TRUSS/FRAME problems (MODEL = 4); otherwise SKIP.

- **Data Card 16**

NNM	Number of nodes in the finite element mesh

SKIP Cards 17–19 for TRUSS problems (NTYPE = 0)

- **Data Card 17 (Read for each element)**

PR	Poisson's ratio of the material (not used in EBT)
SE	Young's modulus of the material
SL	Length of the element
SA	Cross-sectional area of the element
SI	Moment of inertia of the element
CS	Cosine of the angle of orientation of the element
SN	Sine of the angle of orientation of the element; the angle is measured clockwise from the global x axis

- **Data Card 18 (Read for each element)**

HF	Intensity of the horizontal distributed force
VF	Intensity of the transversely distributed force
PF	Point load on the element
XB	Distance from node 1, along the length of the element to the point of load application, PF
CNT	Cosine of the angle of orientation of the load PF
SNT	Sine of the angle of orientation of the load PF; the angle is measured clockwise from the element x axis.

(**Table 7.3.2** continued)

- **Data Card 19**

NOD	Connectivity of the element: NOD(N,I) = global node number corresponding to the Ith node of element N (I = 1,NPE)

READ Cards 20 and 21 only for TRUSS problems (NTYPE = 0).

- **Data Card 20 (Read for each element)**

SE	Young's modulus of the material
SL	Length of the element
SA	Cross-sectional area of the element
CS	Cosine of the angle of orientation of the element
SN	Sine of the angle of orientation of the element Angle is measured counterclockwise from x axis
HF	Intensity of the horizontal distributed force

- **Data Card 21**

NOD(N,I)	Connectivity of the element: NOD(N,I) = global node number corresponding to the Ith node of element N (I = 1,NPE)

- **Data Card 22**

NCON	Number of inclined support conditions

SKIP Card 23 if no inclined support conditions are specified (NCON=0).

- **Data Card 23 (I = 1 to NCON)**

ICON(I)	Global node number of the support
VCON(I)	Angle (in degrees) between the normal and the global x-axis

- **Data Card 24**

NSPV	Number of specified PRIMARY degrees of freedom

SKIP Card 25 if no primary variables is specified (NSPV=0).

- **Data Card 25 (I = 1 to NSPV)**

ISPV(I,1)	Node number at which the PV is specified
ISPV(I,2)	Specified local primary degree of freedom (DOF) at the node
VSPV(I)	Specified value of the primary variable (PV) (will not read for eigenvalue problems)

SKIP Card 26 for eigenvalue problems (i.e., when ITEM = 3).

- **Data Card 26**

NSSV	Number of specified (nonzero) SECONDARY variables

SKIP Card 27 if no secondary variables is specified (NSSV=0); repeat Card 27 NSSV times.

- **Data Card 27 (I = 1 to NSSV)**

ISSV(I,1)	Node number at which the SV is specified
ISSV(I,2)	Specified local secondary DOF at the node
VSSV(I)	Specified value of the secondary variable (SV)

- **Data Card 28**

NNBC	Number of the Newton (mixed) boundary conditions

SKIP Card 29 if no mixed boundary condition is specified (NNBC = 0). The mixed boundary condition is assumed to be of the form:

SV+VNBC *(PV − UREF) = 0. Repeat Card 29 NNBC times.

- **Data Card 29 (I = 1 to NNBC)**

INBC(I,1)	Node number at which the mixed B.C. is specified
INBC(I,2)	Local DOF of the PV and SV at the node
VNBC(I)	Value of the coefficient of the PV in the B.C.
UREF(I)	Reference value of the PV

(**Table 7.3.2** continued)

- **Data Card 30**

NMPC	Number of multipoint constraints (solid mechanics)

SKIP Card 31 if no multipoint conditions are specified (NMPC = 0). The multipoint condition is assumed to be of the form:
VMPC(.,1)*PV1+VMPC(.,2)*PV2=VMPC(.,3). Repeat Card 31 NMPC times.

- **Data Card 31 (I = 1 to NMPC)**

IMC1(I,1)	Node number associated with PV1
IMC1(I,2)	Local DOF of PV1
IMC2(I,1)	Node number associated with PV2
IMC2(I,2)	Local DOF of PV2
VMPC(I)	Values of the coefficients of the constraint equation
VMPC(4)	Value of the force applied at the node of PV1 or PV2

Skip Card 32 if ITEM = 0 (read only for time-dependent or eigenvalue problems).

- **Data Card 32**

CT0	Constant part of CT = CT0 + CT1*X
CT1	Linear part of CT = CT0 + CT1*X

Skip remaining cards if steady-state or eigenvalue analysis is to be performed (ITEM = 0 or ITEM = 3).

- **Data Card 33**

DT	Time increment (uniform)
ALFA	Parameter in the time approximation scheme
GAMA	Parameter in the time approximation scheme*
	GAMA (not used when ITEM = 1: parabolic equation).

Give GAMA= 10^{-6} when centered difference is used (formulation in Problem 6.23 is the correct way to implement the centered difference scheme).

- **Data Card 34**

INCOND	Indicator for initial conditions
	INCOND = 0, Homogeneous (zero) initial conditions
	INCOND > 0, Nonhomogeneous initial conditions
NTIME	Number of time steps for which solution is sought
INTVL	Time step intervals at which solution is to be printed

Skip Cards 35 and 36 if initial conditions are zero (INCOND = 0).

- **Data Card 35**

GUO	Array of initial values of the primary variables

Skip Card 36 for parabolic equations (ITEM = 1).

- **Data Card 36**

GUI	Array of initial values of the first time derivatives of the primary variables.

format" used here, variables of each "data card" (we shall use this terminology to imply an input sequence in a single instruction) are read from the same line; if the values are not found on the same line, the computer will look for them on the next line(s). However, data required by different data cards cannot be put on single line; each data card must start with a new line. The space available after typing required data on a given line may be used to include any comments. For example, we may list the variable names on that line for ready reference but only after all of the required data are listed. The text included thereafter is *not* read by the computer (except to echo the input file).

Example 7.3.1 (Steady Heat Transfer in a Rod)

Consider the heat transfer problem of Example 4.3.3. The problem is governed by

$$-\frac{d^2\theta}{dx^2} + m^2\theta = 0 \quad \text{for} \quad 0 < x < L$$

$$\theta(0) = \theta_0, \quad \left(\frac{d\theta}{dx}\right)\bigg|_{x=L} = 0$$

where θ is the nondimensional temperature, and L, m^2, θ_0, β, and k are

$$L = 0.05 \text{ m}, \quad m^2 = 400/\text{m}^2, \quad \theta_0 = 300^\circ\text{C},$$
$$\beta = 100 \text{ W/(m}^2\cdot{}^\circ\text{C)}, \quad k = 50 \text{ W/(m}\cdot{}^\circ\text{C)} \tag{7.3.1}$$

For this problem, we have MODEL = 1, NTYPE = 0, and ITEM = 0 (for a steady-state solution). Since $a = 1.0$ and $c = m^2 = P\beta/Ak = 400$ are the same for all elements, we set ICONT = 1, AX0 = 1.0, and CX0 = 400. All other coefficients are zero [$b = 0$ and $f = 0$] for this problem. For a uniform mesh of four linear elements (NEM = 4, IELEM = 1), the increments of the array DX(I) [where DX(1) is always the x coordinate of node 1 (see Figure 7.3.1) and $h = L/4 = 0.05/4 = 0.0125$] are: DX = {0.0, 0.0125, 0.0125, 0.0125, 0.0125}.

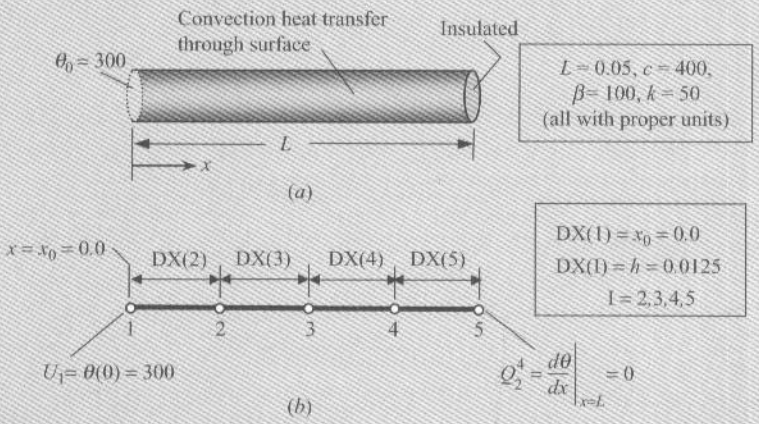

Figure 7.3.1 Finite element mesh of a rectangular fin.

The boundary conditions of the problem reduce to $U_1 = 0$ and $Q_2^4 = 0$. There is one specified boundary condition (BC) on the primary variable (NSPV = 1), and it is degree of freedom (DOF) (for heat transfer problems, there is only one DOF) at node 1 is: ISPV(1, 1) = 1 and ISPV(1, 2) = 1. The specified value is VSPV(1) = 300. Since the natural boundary condition ($Q_2^4 = 0$) is homogenous, there is no need to add a zero to the corresponding entry of the source vector (i.e., NSSV = 0). There are no mixed (i.e., convection) boundary conditions in this problem (NNBC = 0). The complete input data required to analyze the problem using **FEM1D** are presented in Box 7.3.1 and the output file is presented in Box 7.3.2. Input data and partial output for the same problem when a mesh of two quadratic elements are used are presented in Box 7.3.3.

Box 7.3.1 Input file from **FEM1D** for the problem in Example 7.3.1.

```
Example 7.3.1a: Heat transfer in a rod (4 linear elements)
  1 0 0                                        MODEL, NTYPE, ITEM
  1 4                                          IELEM, NEM
  1 1                                          ICONT, NPRNT
  0.0  0.0125   0.0125   0.0125   0.0125       DX(1)=X0; DX(2), etc. Element lengths
  1.0  0.0                                     AX0, AX1
  0.0  0.0                                     BX0, BX1
400.0  0.0                                     CX0, CX1
  0.0  0.0  0.0                                FX0, FX1,  FX2
  1                                            NSPV
  1  1   300.0                                 ISPV(1, 1), ISPV(1,2), VSPV(1)
  0                                            NSSV
  0                                            NNBC
  0                                            NMPC
```

Box 7.3.2 Edited output from FEM1D for the problem in Example 7.3.1.

```
        OUTPUT from program FEM1D by J. N. REDDY

Example 7.3.1a: Heat transfer in a rod (4 linear elements)

  *** ANALYSIS OF MODEL 1, AND TYPE 0 PROBLEM ***
          (see the code below)
  MODEL=1, NTYPE=0: A problem described by MODEL EQ. 1
  MODEL=1, NTYPE=1: A circular DISK (PLANE STRESS)
  MODEL=1, NTYPE>1: A circular DISK (PLANE STRAIN)
  MODEL=2, NTYPE=0: A Timoshenko BEAM (RIE) problem
  MODEL=2, NTYPE=1: A Timoshenko PLATE (RIE) problem
  MODEL=2, NTYPE=2: A Timoshenko BEAM (CIE) problem
  MODEL=2, NTYPE>2: A Timoshenko PLATE (CIE) problem
  MODEL=3, NTYPE=0: A Euler-Bernoulli BEAM problem
  MODEL=3, NTYPE>0: A Euler-Bernoulli Circular plate
  MODEL=4, NTYPE=0: A plane TRUSS problem
  MODEL=4, NTYPE=1: A Euler-Bernoulli FRAME problem
  MODEL=4, NTYPE=2: A Timoshenko (CIE) FRAME problem

      Element type (0, Hermit e,>0, Lagrange)  ..=  1
      No. of deg. of freedom per node, NDF  ...=  1
      No. of elements in the mesh, NEM .......=  4
      No. of total DOF in the model, NEQ  ..... =  5
      No. of specified primary DOF, NSPV  .....=  1
      No. of specified secondary DOF, NSSV....=  0
      No. of specified Newton B. C.: NNBC .....=  0
```

(**Box 7.3.2** is continued from the previous page)

```
Boundary information on primary variables:

   1   1   0.30000E+03

Global coordinates of the nodes, {GLX}:

 0.00000E+00 0.12500E-01  0.25000E-01  0.37500E-01  0.50000E-01

Coefficients of the differential equation:
     AX0 = 0.1000E+01    AX1 = 0.0000E+00
     BX0 = 0.0000E+00    BX1 = 0.0000E+00
     CX0 = 0.4000E+03    CX1 = 0.0000E+00
     FX0 = 0.6000E+01    FX1 = 0.0000E+00     FX2 =  0.0000E+00

Element coefficient matrix, [ELK]:
 0.81667E+02 -0.79167E+02
-0.79167E+02  0.81667E+02

Element source vector, {ELF}:
 0.00000E+00  0.00000E+00

SOLUTION (values of PVs) at the NODES:

 0.30000E+03  0.25152E+03  0.21892E+03  0.20016E+03  0.19403E+03
```

X	P. Variable	S. Variable
0.00000E+00	0.30000E+03	-0.38785E+04
0.12500E-01	0.25152E+03	-0.26076E+04
0.25000E-01	0.21893E+03	-0.15015E+04
0.37500E-01	0.20016E+03	-0.49018E+03

Box 7.3.3 Input and partial output using quadratic elements.

```
Example 7.3.1: Heat transfer in a rod (2 quadratic elements)

 1  0  0                    MODEL, NTYPE, ITEM
 2  2                       IELEM, NEM
 1  1                       ICONT, NPRNT
 0.0  0.025  0.025          DX(1)=X0; DX(2), etc. Ele. lengths
 1.0  0.0                   AX0,  AX1
 0.0  0.0                   BX0, BX1
400.0  0.0                  CX0,  CX1
 0.0  0.0  0.0              FX0,  FX1,  FX2
 1                          NSPV
 1  1  300.0                ISPV(1,1), ISPV(1,2), VSPV(1)
 0                          NSSV
 0                          NNBC
 0                          NMPC
```

(**Box 7.3.3** is continued from the previous page)

OUTPUT from program FEM1D by J. N. REDDY

Example 7.3.1: Heat transfer in a rod (2 quadratic elements)

Element type (0, Hermite, > 0, Lagrange) ..= 2
No. of deg. of freedom per node, NDF ....= 1
No. of elements in the mesh, NEM .....= 2
No. of total DOF in the model, NEQ .....= 5
No. of specified primary DOF, NSPV .....= 1
No. of specified secondary DOF, NSSV....= 0
No. of specified Newton B. C.: NNBC .....= 0

Global coordinates of the nodes, {GLX}:
0.00000 E+00 0.12500E-01 0.25000E-01 0.37500E-01 0.50000E-01

Element coefficient matrix, [ELK]:
0.94667E+02 -0.10600E+03 0.13000E + 02
-0.10600E+03 0.21867E+03 -0.10600E + 03
0.13000E+02 -0.10600E+03 0.94667E + 02

Element source vector, {ELF}:
0.25000E-01 0.10000E+00 0.25000E-01

SOLUTION (values of PVs) at the NODES:
0.30000E+03 0.25170E+03 0.21923E+03 0.20052E+03 0.19442E+03

X	P.Variable	S. Variable
0.00000E+00	0.30000E+03	-0.44971E+04
0.25000E-01	0.21924E+03	-0.19642E+04
0.25000E-01	0.21924E+03	-0.20014E+04
0.50000E-01	0.19443E+03	0.16471E+02

Example 7.3.2 (Steady Heat Transfer in a Composite Wall)

Here we consider the composite wall problem of Example 4.3.1. The governing equations of the problem are

$$-\frac{d}{dx}\left(kA\frac{dT}{dx}\right)=0, \quad 0<x<L \tag{7.3.2a}$$

$$T(0)=T_0, \qquad \left[kA\frac{dT}{dx}+\beta A(T-T_\infty)\right]_{x=L}=0 \tag{7.3.2b}$$

This is a problem with *discontinuous data* (ICONT = 0) because $a=kA$ is discontinuous (as well as $h_1 \neq h_2 \neq h_3$). For a three-element (nonuniform) mesh of linear elements (see Figure 7.3.2), the input data and edited output are given in Box 7.3.4.

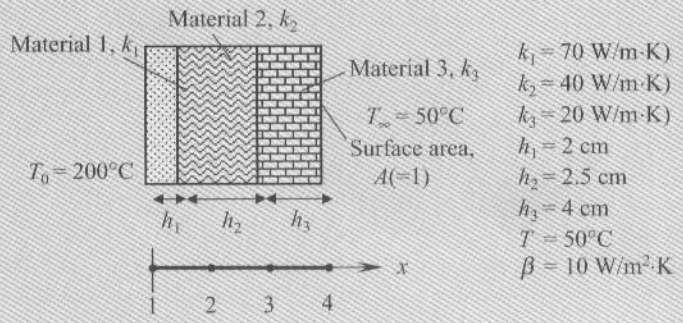

Figure 7.3.2 Heat transfer in a composite wall.

Box 7.3.4 Input for heat transfer in a composite wall (Example 7.3.2).

```
Example 7.3.2: Heat transfer in a composite wall
  1  0  0                          MODEL, NTYPE, ITEM
  1  3                             IELEM, NEM
  0  0                             ICONT, NPRNT
  4                                NNM
  1     2     0.02                 NOD(1,J), GLX(1)
 70.0  0.0                         AX0, AX1
  0.0   0.0                        BX0, BX1
  0.0   0.0                        CX0, CX1
  0.0   0.0   0.0                  FX0, FX1, FX2

  2     3     0.025                NOD(2,J) , GLX(2)
 40.0  0.0                         AX0, AX1
  0.0   0.0                        BX0, BX1
  0.0   0.0                        CX0, CX1
  0.0   0.0   0.0                  FX0, FX1, FX2

  3     4     0.04                 NOD(2,J), G LX(3)
 20.0  0.0                         AX0, AX1
  0.0   0.0                        BX0, BX1
  0.0   0.0                        CX0, CX1
  0.0   0.0   0.0                  FX0, FX1, FX2
  1                                NSPV
  1  1  200.0                      ISPV(1,1), ISPV(1,2), VSPV(1)
  0                                NSSV
  1                                NNBC
  4  1  10.0  50.0                 INBC(1,1), INBC(1, 2), VNBC(1), UREF(1)
  0                                NMPC

OUTPUT from program  FEM1D  by J. N. REDDY

SOLUTION (values of PVs) at the NODES:
0.20000E+03  0.19958E+03  0.19867E+03  0.19576E+03
```

Example 7.3.3 (Radially Symmetric Heat Transfer in a Solid Cylinder)

Consider radially symmetric heat transfer in a solid circular cylinder of radius R_0 of Example 4.3.4. The governing equations of the problem are given by

$$-\frac{d}{dr}\left(2\pi kr\frac{dT}{dr}\right) = 2\pi r g_0 \quad \text{for } 0 < r < R_0 \tag{7.3.3a}$$

$$\left(2\pi kr\frac{dT}{dr}\right)\Big|_{r=0} = 0, \quad T(R_0) = T_0 \tag{7.3.3b}$$

with $k = 20$ W/(m·°C), $g_0 = 2 \times 10^8$ W/m^3, $T_0 = 100$°C, and $R_0 = 0.01$ m. We have MODEL = 1, NTYPE = 0, and ITEM = 0 (for a steady-state solution), and the data is continuous (ICONT = 1) in the domain for a mesh of two quadratic elements (IELEM = 2, NEM = 2). The data are

$$a = 2\pi kr \to a_0 = 0, \quad a_1 = 2\pi k; \quad b = 0 \to b_0 = 0.0, \quad b_1 = 0.0$$

$$c = 0 \to c_0 = 0.0, \quad c_1 = 0.0; \quad f = 2\pi g_0 r \to f_0 = 0.0, \quad f_1 = 2\pi g_0, \quad f_2 = 0.0$$

Thus, we have [for values $k = 20$ W/(m·°C), $g_0 = 2 \times 10^8$ W/m^3]

$$\text{AX0} = 0.0, \quad \text{AX1} = 125.6637, \quad \text{BX0} = 0.0, \quad \text{BX1} = 0.0$$

$$\text{CX0} = 0.0, \quad \text{CX1} = 0.0, \quad \text{FX0} = 0.0, \quad \text{FX1} = 12.5664 \times 10^8, \quad \text{FX2} = 0.0$$

For two-element mesh of quadratic elements, the array {DX} and boundary information are given by

$$\text{DX} = \{0.0, 0.005, 0.005\}$$

$$\text{NSPV} = 1, \quad \text{ISPV}(1, 1) = 5, \quad \text{ISPV}(1, 2) = 1, \quad \text{VSPV}(1) = 100$$

The input file along with the modified output from FEM1D are presented in Boxes 7.3.5 and 7.3.6, respectively. Note that the finite element solution obtained with two quadratic elements is more accurate than the solution obtained with four linear elements, and it is essentially the same as the exact solution (see Table 4.3.2 for the results).

Box 7.3.5 Input data for radially symmetric problem of Example 7.3.3.

```
Example 7.3.3: Radially symmetric heat transfer in a cylinder (2 quadratic ele)

1 0 0                          MODEL, NTYPE, ITEM
2 2                            IELEM, NEM
1 1                            ICONT, NPRNT
0.0  0.005  0.005              DX(1) = X0; DX(2), etc. Ele. lengths
0.0  125.6637                  AX0, AX1
0.0  0.0                       BX0, BX1
0.0  0.0                       CX0, CX1
0.0  12.56637E08  0.0          FX0, FX1, FX2
1                              NSPV
5 1  100.0                     ISPV(1, 1), ISPV(1, 2), VSPV(1)
0                              NSS V
0                              NN BC
0                              NMPC
```

Box 7.3.6 Partial output for radially symmetric problem of Example 7.3.3.

```
OUTPUT from program FEM1D by J. N. REDDY

Example 7.3.3: Radially symmetric heat transfer in a cylinder (2 quadratic ele)

 Element type (0, Hermite, >0, Lagrange)..=  2
      No. of deg. of freedom per node, NDF ....=  1
      No. of elements in the mesh, NEM .......=  2
      No. of total DOF in the model, NEQ ......=  5
      No. of specified primary DOF, NSPV ......=  1
      No. of specified secondary DOF, NSSV....=  0
      No. of specified Newton B. C.: NNBC .....=  0

 Element coefficient matrix, [ELK]:
 0.62832E+02 -0.83776E+02  0.20944E+02
-0.83776E+02  0.33510E+03 -0.25133E+03
 0.20944E+02 -0.25133E+03  0.23038E+03

 Element source vector, {ELF}:
 0.00000E+00   0.10472E+05   0.52360E+04

 SOLUTION (values of PVs) at the NODES:
 0.35000E+03   0.33437E+03   0.28750E+03   0.20937E+03   0.10000E+03
```

X	P. Variable	S. Variable
0.00000E-00	0.35000E+03	0.00000E+00
0.62500E-03	0.34902E+03	-0.24544E+03
0.12500E-02	0.34609E+03	-0.98175E+03
0.18750E-02	0.34121E+03	-0.22089E+04
0.25000E-02	0.33437E+03	-0.39270E+04
0.31250E-02	0.32559E+03	-0.61359E+04
0.37500E-02	0.31484E+03	-0.88357E+04
0.43750E-02	0.30215E+03	-0.12026E+05
0.50000E-02	0.28750E+03	-0.15708E+05
0.50000E-02	0.28750E+03	-0.15708E+05
0.56250E-02	0.27090E+03	-0.19880E+05
0.62500E-02	0.25234E+03	-0.24544E+05
0.68750E-02	0.23184E+03	-0.29698E+05
0.75000E-02	0.20937E+03	-0.35343E+05
0.81250E-02	0.18496E+03	-0.41479E+05
0.87500E-02	0.15859E+03	-0.48106E+05
0.93750E-02	0.13027E+03	-0.55223E+05
0.10000E-01	0.10000E+03	-0.62832E+05

Next, we consider a couple of steady-state solid mechanics problems. The reader is asked to visit the corresponding examples from Chapter 4 to have a complete background of the problems discussed here.

Example 7.3.4 (Axial Deformation of a Pier)

Here we consider the axial deformation of a pier (Example 4.5.1). The problem is governed by the equations (see Fig. 7.3.3)

$$-\frac{d}{dx}\left[\frac{1}{4}E(1+x)\frac{du}{dx}\right]=6.25(1+x),\quad 0<x<2 \tag{7.3.4a}$$

$$\left[\frac{1}{4}E(1+x)\frac{du}{dx}\right]\Bigg|_{x=0}=-5,\quad u(2)=0 \tag{7.3.4b}$$

For this case, the data of the problem is MODEL = 1, NTYPE = 1, and ITEM = 0 with

$$a=\frac{1}{4}E(1+x)\rightarrow a_0=0.25E,\quad a_1=0.25E;\quad b=0\rightarrow b_0=0.0,\quad b_1=0.0$$

$$c=0\rightarrow c_0=0.0,\quad c_1=0.0;\quad f=6.25(1+x)\rightarrow f_0=6.25,\quad f_1=6.25,\quad f_2=0.0$$

For $E=28\times 10^9$ N/m^2, the input data becomes

$$\text{AX0}=7\times 10^9,\quad \text{AX1}=7\times 10^9,\quad \text{BX0}=0.0,\quad \text{BX1}=0.0$$

$$\text{CX0}=0.0,\quad \text{CX1}=0.0,\quad \text{FX0}=6.25\times 10^3,\quad \text{FX1}=6.25\times 10^3,\quad \text{FX2}=0.0$$

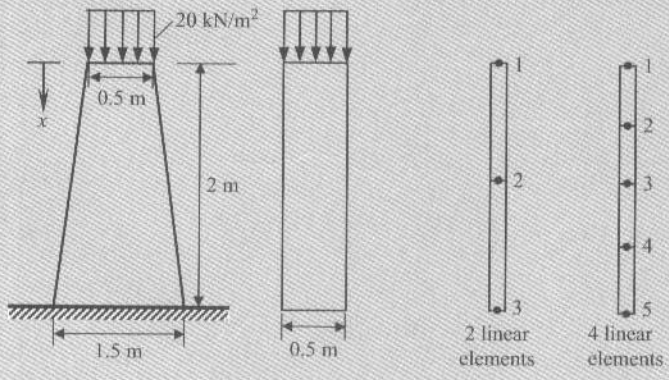

Figure 7.3.3 The concrete pier problem of Example 7.3.4.

For two-element mesh of linear elements, the array DX and boundary information are given by (NMPC = 0)

$$\text{DX} = \{0.0, 1.0, 1.0\}$$

$$\text{NSPV} = 1, \quad \text{ISPV}(1,1) = 3, \quad \text{ISPV}(1,2) = 1, \quad \text{VSPV}(1) = 0$$

$$\text{NSSV} = 1, \quad \text{ISSV}(1,1) = 1, \quad \text{ISSV}(1,2) = 1, \quad \text{VSSV}(1) = 5 \times 10^3$$

The input file and modified output of the problem are presented in Boxes 7.3.7 and 7.3.8, respectively.

Box 7.3.7 Input data for the pier problem of Example 7.3.4.

```
Example 7.3.4: Axial deformation of a pier
1 0 0                                  MODEL, NTYPE, ITEM
 1 2                                   IELEM, NEM
 1 1                                   ICONT, NPRNT
 0.0      1.0     1.0                  DX(1)=X0;  DX(2), etc. Ele. lengths
 7.0E9     7.0E9                       AX0,  AX1
 0.0      0.0                          BX0,  BX1
 0.0      0.0                          CX0,  CX1
 6.25E3    6.25E3     0.0              FX0,  FX1, FX2
1                                      NSPV
3 1    0.0                             ISPV(1,1), ISPV(1,2), VSPV(1)
1                                      NSSV
1 1    5.0E3                           ISSV(1,1), ISSV(1,2), VSSV(1)
0                                      NNBC
0                                      NMPC
```

Box 7.3.8 Modified output for the pier problem of Example 7.3.4.

```
OUTPUT from program FEM1D by J. N. REDDY

Example 7.3.4: Axial deformation of a pier (2 linear elements)

 Boundary information on primary variables:
    3   1   0.00000E+00

 Boundary information on secondary variables:
    1   1   0.50000E+04

 Global coordinates of the nodes, {GLX}:
 0.00000 E+00  0.10000E+01   0.20000E+01
```

(**Box 7.3.8** is continued from the previous page)

```
Coefficients of the differential equation:
    AX0=0.7000E+10      AX1=0.7000E+10
    BX0=0.0000E+00      BX1=0.0000E+00
    CX0=0.0000E+00      CX1=0.0000E+00
    FX0=0.6250E+04      FX1=0.6250E+04      FX2= 0.0000E+00

 Element coefficient matrix, [ELK]:
  0.10500E+11 -0.10500E+11
 -0.10500E+11  0.10500E+11

 Element source vector, {ELF}:
  0.41667E+04   0.52083E+04

SOLUTION (values of PVs) at the NODES:
   0.21111E-05  0.12381E-05   0.00000E+00
```

Example 7.3.5 (Deformation of a Rotating Disk)

We wish to determine the deformation and stresses in a rotating homogeneous (solid) disk of thickness H and made of isotropic material (E, ν). The governing equation of the problem is (see Problem 4.37)

$$-\frac{d}{dr}\left[c\left(r\frac{du}{dr}+\nu u\right)\right]+c\left(\frac{u}{r}+\nu\frac{du}{dr}\right)=\rho\omega^2 r, \quad 0<r<R_0 \tag{7.3.5a}$$

$$c=\frac{E}{1-\nu^2} \tag{7.3.5b}$$

For this case, we have MODEL = 1, NTYPE = 1, and ITEM = 0. For a mesh of two quadratic elements (see Figure 7.3.4) (i.e., IEL = 2 and NEM = 2), we use ICONT = 1 and

$$\mathrm{DX}=\{0.0,\ 0.5R_0,\ 0.5R_0\}$$

where R_0 is the radius of the disk. Since we are seeking results in nondimensional form, we take

$$R_0=1.0, \quad E_1=E_2=E=1.0, \quad \nu_{12}=\nu=0.3, \quad \rho\omega^2=1$$

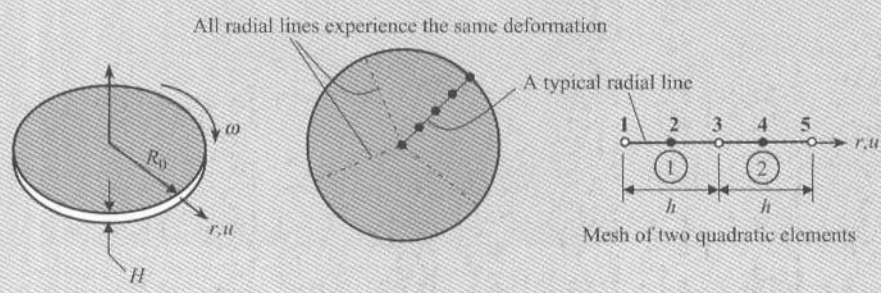

Figure 7.3.4 The rotating disk of Example 7.3.5.

where E_1 is the modulus along the radial direction and E_2 is the modulus in the circumferential direction. This information is supplied to the program through the following variables:

$$\text{AX0}(=E_1)=1.0,\ \text{AX1}(=E_2)=1.0,\ \text{BX0}(=\nu_{12})=0.3,\ \text{BX1}(=H)=1.0$$

$$\text{CX0}=0.0,\ \text{CX1}=0.0,\ \text{FX0}=0.0,\ \text{FX1}=1.0,\ \text{FX2}=0.0$$

The boundary conditions are

$$u(0)=0 \text{ (by symmetry)}, \quad Q_1^1=-(r\sigma_r)_0=0 \text{ at } r=R_0 \text{ (stress-free condition)}$$

Since the secondary variable is homogeneous, there is no need to include it in the data (NSSV=0). We have NSPV = 1, NNBC = 0, and NMPC = 0 with

$$\text{ISPV}(1,1)=1,\ \text{ISPV}(1,2)=1,\ \text{VSPV}(1)=0.0$$

The input data and modified output for this problem are presented in Boxes 7.3.9 and 7.3.10, respectively.

Box 7.3.9 Input data for the rotating disk problem of Example 7.3.5.

```
Example 7.3.5: Deformation of a circulardisk (2 quadratic elements)

 1  1  0                    MODEL, NTYPE, ITEM
 2  2                       IELEM, NEM
 1  1                       ICONT, NPRNT
  0.0  0.50  0.50           DX(I)
  1.0  1.0                  AX0, AX1
  0.3  1.0                  BX0, BX1
  0.0  0.0                  CX0, CX1
  0.0  1.0   0.0            FX0, FX1, FX2
 1                          NSPV
 1  1  0.0                  ISPV(1,1), ISPV(1, 2), VSPV(1)
 0                          NSSV
 0                          NNBC
 0                          NMPC
```

Box 7.3.10 Output for the rotating disk problem of Example 7.3.5.

```
OUTPUT from program FEM1D by J.N. REDDY

Example 7.3.5: Deformation of a circular disk (2 quadratic elements)

*** ANALYSIS OF MODEL 1, AND TYPE 1 PROBLEM ***

MODEL=1, NTYPE=0: A problem described by MODEL EQ. 1
MODEL=1, NTYPE=1: A circular DISK (PLANE STRESS)
MODEL=1, NTYPE>1: A circular DISK (PLANE STRAIN)
MODEL=2, NTYPE=0: A Timoshenko BEAM (RIE) problem
MODEL=2, NTYPE=1: A Timoshenko PLATE (RIE) problem
MODEL=2, NTYPE=2: A Timoshenko BEAM (CIE) problem
MODEL=2, NTYPE>2: A Timoshenko PLATE (CIE) problem
MODEL=3, NTYPE=0: A Euler-Bernoulli BEAM problem
MODEL=3, NTYPE>0: A Euler-Bernoulli Circular plate
```

(**Box 7.3.10** is continued from the previous page)

```
    Element type (0, Hermite,>0, Lagrange) ..=  2
    No. of deg. of freedom per node, NDF ....=  1
    No. of elements in the mesh, NEM ........=  2
    No. of total DOF in the model, NEQ ......=  5
    No. of specified primary DOF, NSPV ......=  1
    No. of specified secondary DOF, NSSV ...=  0
    No. of specified Newton B. C.: NNBC .....=  0

Boundary information on primary variables:
   1   1   0.00000E+00

Global coordinates of the nodes, {GLX}:
 0.00000E+00   0.25000E+00   0.50000E+00   0.75000E+00   0.10000E+01

  Element coefficient matrix, [ELK]:
   0.15018E+01    0.64565E-09     0.10761E-08
   0.64565E-09    0.43956E+01    -0.21978E+01
   0.10761E-08   -0.21978E+01     0.25275E+01

  Element source vector, {ELF}:
   -0.20833E-02    0.25000E-01     0.18750E-01

  SOLUTION (values of PVs) at the NODES:
   0.00000E+00  0.70706E-01  0.13004E+00  0.16875E+00  0.17500E+00
```

X	Displacemnt	Radial Strs	Hoop Stress
0.00000E+00	0.00000E+00	0.33580E+00	0.10074E+00
0.62500E-01	0.18743E-01	0.42216E+00	0.42654E+00
0.12500E+00	0.36775E-01	0.40779E+00	0.41654E+00
0.18750E+00	0.54096E-01	0.39341E+00	0.40654E+00
0.25000E+00	0.70706E-01	0.37904E+00	0.39654E+00
0.31250E+00	0.86606E-01	0.36466E+00	0.38654E+00
0.37500E+00	0.10179E+00	0.35029E+00	0.37654E+00
0.43750E+00	0.11627E+00	0.33591E+00	0.36654E+00
0.50000E+00	0.13004E+00	0.32154E+00	0.35654E+00
0.50000E+00	0.13004E+00	0.32727E+00	0.35826E+00
0.56250E+00	0.14276E+00	0.28952E+00	0.34065E+00
0.62500E+00	0.15345E+00	0.25111E+00	0.32086E+00
0.68750E+00	0.16212E+00	0.21223E+00	0.29948E+00
0.75000E+00	0.16875E+00	0.17299E+00	0.27690E+00
0.81250E+00	0.17336E+00	0.13348E+00	0.25341E+00
0.87500E+00	0.17593E+00	0.93750E-01	0.22919E+00
0.93750E+00	0.17648E+00	0.53846E-01	0.20440E+00
0.10000E+01	0.17500E+00	0.13802E-01	0.17914E+00

The exact displacement and stresses in the disc are given by

$$u(r) = \frac{(1-\nu)R_0^3}{8E}\left[(3+\nu)\frac{r}{R_0} - (1+\nu)\left(\frac{r}{R_0}\right)^3\right]\rho\omega^2$$

$$\sigma_{rr}(r) = \frac{(3+\nu)R_0^2}{8}\left[1 - \left(\frac{r}{R_0}\right)^3\right]\rho\omega^2 \tag{7.3.6}$$

$$\sigma_{\theta\theta}(r) = \frac{(3+\nu)R_0^2}{8}\left[1 - \frac{1+3\nu}{3+\nu}\left(\frac{r}{R_0}\right)^3\right]\rho\omega^2$$

The exact displacements at $x = 0.25$, $x = 0.5$, $x = 0.75$, and $x = 1.0$ are 0.0704, 0.1302, 0.1686, and 0.1750, respectively. The maximum values of stresses occur at $r = 0$, and they are $\sigma_{rr}(0) = \sigma_{\theta\theta}(0) = 0.4125$. The displacements obtained with two quadratic elements are in good agreement with the analytical solution. The postcomputed stresses at $r = 0$ are not accurate because of the singularity there:

$$\sigma_{rr} = \frac{E}{1-\nu^2}\left(\frac{du}{dr} + \nu\frac{u}{r}\right), \quad \sigma_{\theta\theta} = \frac{E}{1-\nu^2}\left(\nu\frac{du}{dr} + \frac{u}{r}\right) \tag{7.3.7}$$

The next example deals with a multipoint constraint problem of the type discussed in Example 4.6.3.

Example 7.3.6 (Multipoint Constraint Problem)

A rigid bar AB of length $L = 1.6$ m is hinged to a support at A and supported by two vertical bars attached at points C and D, as shown in Figure 7.3.5. Both bars have the same cross-sectional

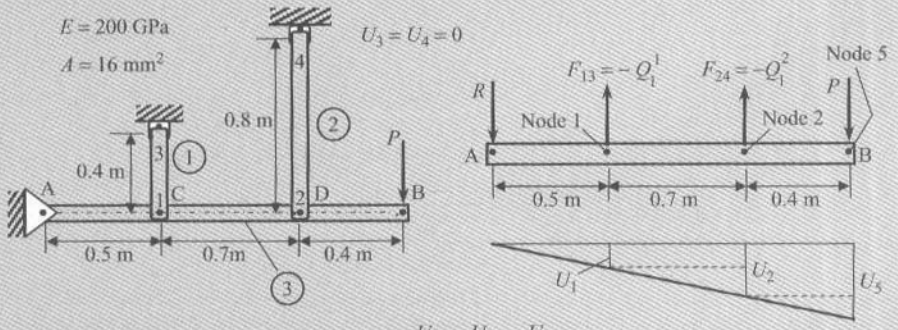

Figure 7.3.5 A rigid member supported by cables (Example 7.3.6).

area ($A = 16\ \text{mm}^2$) and are made of the same material with modulus $E = 200$ GPa. The lengths of the bars and the horizontal distances are shown in the figure. We wish to determine the elongations as well as tensile stresses in the bars.

The two geometric constraints are:

$$\frac{U_1}{0.5} = \frac{U_5}{1.6} \rightarrow 3.2U_1 - U_5 = 0, \quad \frac{U_2}{1.2} = \frac{U_5}{1.6} \rightarrow 1.333U_2 - U_5 = 0$$

Thus, we have [see Eq. (4.6.37)]

$$\beta_1^1 = 3.2,\ \beta_2^1 = -1.0,\ \beta_{12}^1 = 0.0; \quad \beta_1^2 = 1.333,\ \beta_2^2 = -1.0,\ \beta_{12}^2 = 0.0$$

In order to include the load P in the analysis, we introduce a node at B. Thus, we have NEM = 3 and NNM = 5 with $a = EA = 3.2 \times 10^6\ \text{m}^2$ for the bar elements and $a = 0$ for the third (rigid) element. It is sufficient to use linear finite elements to represent the bars. Thus, the data for the problem are MODEL = 1, NTYPE = 1, ITEM = 0, ICONT = 0. The boundary and constraint information are: NSPV = 2, ISPV(1,1) = 1, ISPV(1,2) = 1, VSPV(1) = 0, ISPV(2,1) = 2, ISPV(2, 2) = 1, VSPV(2) = 0, NSSV = 0, NNBC = 0, NMPC = 2, VMPC(1,1) = $\beta_1^1 = 3.2$, VMPC(1,2) = $\beta_2^1 = -1.0$, VMPC(1,3) = $\beta_{12}^1 = 0$, VMPC(1,4) = 0; VMPC(2,1) = $\beta_1^2 = 1.333$, VMPC(2,2) = $\beta_2^2 = -1.0$, VMPC(2,3) = $\beta_{12}^2 = 0$, and VMPC(2,4) = $P = 970$ N.

The input file and modified output of the problem are presented in Box 7.3.11. The displacements are $U_1 = 0.1$ mm, $U_2 = 0.24$ mm, and $U_5 = 0.32$ mm. The stresses are $\sigma_1 = 10^6(800/16) = 50$ MPa and $\sigma_2 = 10^6(960/16) = 60$ MPa.

Box 7.3.11 Input and edited output for the problem of Example 7.3.6.

```
Example 7.3.6: DEFORMATION OF A CONSTRAINED STRUCTURE
  1   0   0                    MODEL, NTYPE, ITEM
  1   3                        IELEM, NEM
  0   1                        ICONT, NPRNT
  5                            NNM

  1          3          0.4    NOD(1,J),GLX(1)
  3.2E6      0.0               AX0, AX1          Data for
  0.0        0.0               BX0, BX1          Element 1
  0.0        0.0               CX0, CX1
  0.0        0.0        0.0    FX0, FX1, FX2

  2          4          0.8    NOD(2,J),GLX(2)
  3.2E6      0.0               AX0, AX1          Data for
  0.0        0.0               BX0, BX1          Element 2
  0.0        0.0               CX0, CX1
  0.0        0.0        0.0    FX0, FX1, FX2

  1          5          1.6    NOD(3,J),GLX(3)
  0.0        0.0               AX0, AX1          Data for
  0.0        0.0               BX0, BX1          Element 3
  0.0        0.0               CX0, CX1
  0.0        0.0        0.0    FX0, FX1, FX2
```

(**Box 7.3.11** is continued from the previous page)

```
2                                   NS PV
3 1       0.0                       ISPV(1,1), ISPV(1,2), VSPV(1)
4 1       0.0                       ISpV(2,1), ISpV(2,2), VSpV(2)
0                                   NS SV
0                                   NN BC
2                                   NMPC
1 1       5 1       3.2             -1.0 0.0 0.0
2 1       5 1       1.33333         -1.0 0.0 970.0
                  IMC1(1,1),IMC1(1,2),IMC2(1,1),IMC2(1,2),
                                        (VMPC(1,I),I=1 to 4)
```

```
OUTPUT from program FEM1D by J. N. REDDY

Multipoint constraint information:

 1     1     5     1
 0.32000E+01        -0.10000E+01          0.00000E+00          0.00000E+00
 2     1     5     1
 0.13333E+01        -0.10000E+01          0.00000E+00          0.97000E+03
```

```
Properties of Element = 1

   Element length, H ..... = 0.4000E+00
   AX0 = 0.3200E+07    AX1 = 0.0000E+00
   BX0 = 0.0000E+00    BX1 = 0.0000E+00
   CX0 = 0.0000E+00    CX1 = 0.0000E+00
   FX0 = 0.0000E+00    FX1 = 0.0000E+00        FX2 = 0.0000E+00

Properties of Element = 2

   Element length, H ..... = 0.8000E+00
   AX0 = 0.3200E+07    AX1 = 0.0000E+00
   BX0 = 0.0000E+00    BX1 = 0.0000E+00
   CX0 = 0.0000E+00    CX1 = 0.0000E+00
   FX0 = 0.0000E+00    FX1 = 0.0000E+00        FX2 = 0.0000E+00

Properties of Element = 3

   Element length, H ..... = 0.1600E+01
   AX0 = 0.0000E+00    AX1 = 0.0000E+00
   BX0 = 0.0000E+00    BX1 = 0.0000E+00
   CX0 = 0.0000E+00    CX1 = 0.0000E+00
   FX0 = 0.0000E+00    FX1 = 0.0000E+00        FX2 = 0.0000E+00
```

(**Box 7.3.11** is continued from the previous page)

```
Element coefficient matrix, [ELK]:

 0.80000E+07 -0.80000E+07
-0.80000E+07  0.80000E+07

Element coefficient matrix, [ELK]:

 0.40000E+07 -0.40000E+07
-0.40000E+07  0.40000E+07

Element coefficient matrix, [ELK]:

 0.00000E+00  0.00000E+00
 0.00000E+00  0.00000E+00

SOLUTION (values of PVs) at the NODES:

 0.10000E-03   0.24000E-03   0.00000E+00   0.00000E+00   0.32001E-03

Forces at the constrained points:

 0.80001E+03   0.95999E+03
```

The next two examples deal with beams and frames of Chapter 5.

Example 7.3.7 (Clamped and Spring-Supported Beam)

Consider the spring-supported cantilever beam shown in Figure 7.3.6. We solve the problem first using the Euler–Bernoulli beam element (MODEL=3, NTYPE=0, IELEM=0) and then using the Timoshenko beam element (MODEL=2, NTYPE=0 or 2, IELEM=1,2,or 3). Since the loading is discontinuous, we set ICONT=0. A minimum of two elements are required to model the problem (i.e., NEM=2).

If we take $EI = 1.0E6$ (i.e., 10^6 lb-ft.^{2}), then

$$GAK = \frac{E}{2(1+\nu)} BH \frac{5}{6} = \frac{EI}{1+\nu} \frac{5}{H^2}$$

For $L/H = 10$, we have $H = 1.0$ because $L = 10$ ft. For the choice $\nu = 0.25$, we have

$$GAK = 4EI/H^2 = 4 \times 10^6 \text{ lb}$$

Thus, we use

$$\text{AX0} = 0.0, \quad \text{AX1} = 0.0, \quad \text{BX0}(= EI) = 1.0 \times 10^6$$
$$\text{BX1} = 0.0, \quad \text{CX0} = 0.0, \quad \text{CX1} = 0.0$$

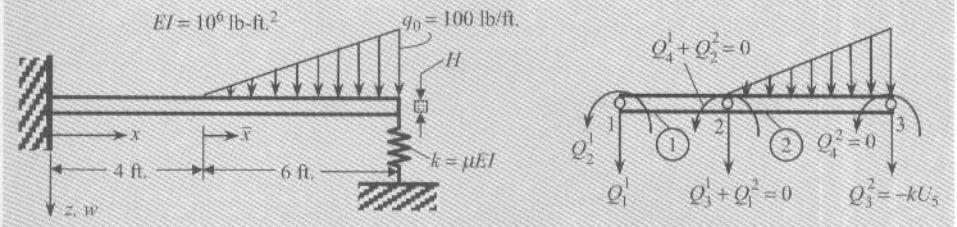

Figure 7.3.6 The spring-supported beam of Example 7.3.7.

for the Euler–Bernoulli beam and

$$\text{AX}(=GAK) = 4.0 \times 10^6, \quad \text{AX1} = 0.0, \quad \text{BX0}(=EI) = 1.0 \times 10^6$$
$$\text{BX1} = 0.0, \quad \text{CX0} = 0.0, \quad \text{CX1} = 0.0$$

for the Timoshenko beam.

The distributed transverse load is zero in element 1, and it is

$$q(\bar{x}) = \frac{100}{6}\bar{x}$$

in element 2. Hence,

$$\text{FX0} = 0.0, \quad \text{FX1} = 0.0, \quad \text{FX2} = 0.0 \text{ in element 1}$$
$$\text{FX0} = 0.0, \quad \text{FX1} = 16.666, \quad \text{FX2} = 0.0 \text{ in element 2}$$

The global coordinates of nodes and the connectivity matrix entries for each element are obvious from the geometry. For the Euler–Bernoulli beam element, the number of nodes is always equal to two (NPE = 2), whereas for the Timoshenko beam element, the number of nodes depends on the degree of interpolation (or element type) selected:

$$\text{NPE} = \text{IELEM} + 1$$

The boundary conditions for this problem are

$$w(0) = 0, \quad \left(\frac{dw}{dx}\right)\bigg|_{x=0} = 0, \quad (V + kw)\bigg|_{x=L} = 0$$

where V is the shear force. Therefore, we have (NSSV=0)

$$\text{NSPV} = 2, \quad \text{ISPV}(1,1) = 1, \quad \text{ISPV}(1,2) = 1, \quad \text{VSPV}(1) = 0.0$$
$$\text{ISPV}(2,1) = 1, \quad \text{ISPV}(2,2) = 2, \quad \text{VSPV}(2) = 0.0$$
$$\text{NNBC} = 1, \quad \text{INBC}(1,1) = 3, \quad \text{INBC}(1,2) = 1$$
$$\text{VNBC}(1)\ (=k) = 1.0 \times 10^6 \quad (\text{for } \mu = 1) \text{ and } 0.0 \ (\text{for } \mu = 0.0)$$
$$\text{UREF}(1) = 0.0$$

The inputs and modified outputs for the Euler–Bernoulli and Timoshenko elements are presented in Boxes 7.3.12 and 7.3.13, respectively. Note that the Euler–Bernoulli element is a Hermite cubic element, whereas the Timoshenko element is only a linear element (a quadratic element may be used if desired).

Box 7.3.12 Input and edited output files for the cantilever beam problem of Example 7.3.7 (Euler–Bernoulli beam element).

```
Example 7.3.7: CLAMPED AND SPRING-SUPPORTED BEAM (Euler-Bernoulli)
    3    0    0                                  MODEL, NTYPE, ITEM
    0    2                                       IELEM, NEM
    0    1                                       ICONT, NPRNT
         3                                       NNM
         1    2    4.0                           NOD(1,J),GLX(1)
         0.0       0.0                           AX0, AX1        |   Data for
         1.0E6     0.0                           BX0, BX1        |   Element 1
         0.0       0.0                           CX0, CX1        |
         0.0       0.0          0.0              FX0,FX1,FX2     |
         2    3    6.0                           NOD(2,J),GLX(2)
         0.0       0.0                           AX0, AX1        |   Data for
         1.0E6     0.0                           BX0, BX1        |   Element 2
         0.0       0.0                           CX0, CX1        |
         0.0       16.666667         0.0         FX0,FX1,FX2     |
    2                                            NSPV
    1    1    0.0                                ISPV(1,J), VSPV(1)
    1    2    0.0                                ISPV(2,J), VSPV(2)
    0                                            NSSV
    1                                            NNBC (with spring)
    3    1    1.0E4             0.0               INBC(1,1),INBC(1,2),VNBC(1),UREF
    0                                            NMPC
```

OUTPUT from program FEM1D by J. N. REDDY

```
Example 7.3.7: CLAMPED AND SPRING-SUPPORTED BEAM (Euler-Bernoulli)

    *** ANALYSIS OF MODEL 3, AND TYPE 0 PROBLEM ***
                (see the code below)

    MODEL=2, NTYPE=0: A Timoshenko BEAM (RIE) problem
    MODEL=2, NTYPE=1: A Timoshenko PLATE (RIE) problem
    MODEL=2, NTYPE=2: A Timoshenko BEAM (CIE) problem
    MODEL=2, NTYPE>2: A Timoshenko PLATE (CIE) problem
    MODEL=3, NTYPE=0: A Euler-Bernoulli BEAM problem

      Properties of Element = 1

          Element length, H . . . . . = 0.4000E+01
          AX0 =  0.0000E+00    AX1 = 0.0000E+00
          BX0 =  0.1000E+07    BX1 = 0.0000E+00
          CX0 =  0.0000E+00    CX1 = 0.0000E+00
          FX0 =  0.0000E+00    FX1 = 0.0000E+00    FX2 =  0.0000E+00
```

(**Box 7.3.12** is continued from the previous page)

Properties of Element = 2

Element length, H . . . . . = 0.6000E+01
AX0 = 0.0000E+00 AX1 = 0.0000E+00
BX0 = 0.1000E+07 BX1 = 0.0000E+00
CX0 = 0.0000E+00 CX1 = 0.0000E+00
FX0 = 0.0000E+00 FX1 = 0.1667E+02 FX2 = 0.0000E+00

Element coefficient matrix, [ELK]:

0.18750E+06 -0.37500E+06 -0.18750E+06 -0.37500E+06
-0.37500E+06 0.10000E+07 0.37500E+06 0.50000E+06
-0.18750E+06 0.37500E+06 0.18750E+06 0.37500E+06
-0.37500E+06 0.50000E+06 0.37500E+06 0.10000E+07

Element coefficient matrix, [ELK]:

0.55556E+05 -0.16667E+06 -0.55556E+05 -0.16667E+06
-0.16667E+06 0.66667E+06 0.16667E+06 0.33333E+06
-0.55556E+05 0.16667E+06 0.55556E+05 0.16667E+06
-0.16667E+06 0.33333E+06 0.16667E+06 0.66667E+06

Element source vector, {ELF}:

0.90000E+02 -0.12000E+03 0.21000E+03 0.18000E+03

SOLUTION (values of PVs) at the NODES:
0.00000E+00 0.00000E+00 0.46272E-02 -0.19510E-02 0.16403E-01
-0.16985E-02

x is the local coord. if ICONT=0

x	Deflect.	Rotation	B. Moment	Shear Force
0.00000E+00	0.00000E+00	0.00000E+00	0.75969E+03	-0.13597E+03
0.50000E+00	0.92129E-04	-0.36285E-03	0.69171E+03	-0.13597E+03
0.10000E+01	0.35718E-03	-0.69171E-03	0.62372E+03	-0.13597E+03
0.15000E+01	0.77817E-03	-0.98657E-03	0.55574E+03	-0.13597E+03
0.20000E+01	0.13381E-02	-0.12474E-02	0.48775E+03	-0.13597E+03
0.25000E+01	0.20200E-02	-0.14743E-02	0.41977E+03	-0.13597E+03
0.30000E+01	0.28068E-02	-0.16672E-02	0.35178E+03	-0.13597E+03
0.35000E+01	0.36815E-02	-0.18261E-02	0.28380E+03	-0.13597E+03
0.40000E+01	0.46272E-02	-0.19510E-02	0.21582E+03	-0.13597E+03
0.00000E+00	0.46272E-02	-0.19510E-02	0.95815E+02	-0.45969E+02
0.75000E+00	0.61142E-02	-0.20099E-02	0.61338E+02	-0.45969E+02
0.15000E+01	0.76357E-02	-0.20430E-02	0.26862E+02	-0.45969E+02
0.22500E+01	0.91722E-02	-0.20502E-02	-0.76154E+01	-0.45969E+02
0.30000E+01	0.10705E-01	-0.20316E-02	-0.42092E+02	-0.45969E+02
0.37500E+01	0.12213E-01	-0.19871E-02	-0.76569E+02	-0.45969E+02
0.45000E+01	0.13679E-01	-0.19167E-02	-0.11105E+03	-0.45969E+02
0.52500E+01	0.15082E-01	-0.18205E-02	-0.14552E+03	-0.45969E+02
0.60000E+01	0.16403E-01	-0.16985E-02	-0.18000E+03	-0.45969E+02

Box 7.3.13 Input and edited output files for the cantilever beam problem of Example 7.3.7 (Timoshenko beam element).

```
Example 7.3.7: CLAMPED AND SPRING-SUPPORTED BEAM (Timoshenko)
  2   0   0                              MODEL, NTYPE, ITEM
  1   2                                  IELEM, NEM
  0   1                                  ICONT, NPRNT
      3                                  NNM
      1   2     4.0                      NOD(1,J), GLX(1)
     4.0E6  0.0                          AX0, AX1        |  Data for
     1.0E6  0.0      (L/H = 10)          BX0, BX1        |  Element 1
     0.0    0.0                          CX0, CX1        |
     0.0    0.0      0.0                 FX0, FX1, FX2   |
      2   3     6.0                      NOD(2,J), GLX(2)
     4.0E6  0.0                          AX0, AX1        |  Data for
     1.0E6  0.0                          BX0, BX1        |  Element 2
     0.0    0.0                          CX0, CX1        |
     0.0    16.666667   0.0              FX0, FX1, FX2   |
  2                                      NSPV
  1   1     0.0                          ISPV(1,J), VSPV(1)
  1   2     0.0                          ISPV(2,J), VSPV(2)
  0                                      NSSV
  1                                      NNBC (with spring)
  3   1     1.0E4         0.0            INBC(1,1),INBC(1,2),VNBC(1),UREF
  0                                      NMPC
```

OUTPUT from program FEM1D by J. N. REDDY

```
 Example 7.3.7: CLAMPED AND SPRING-SUPPORTED BEAM (Timoshenko)

 Properties of Element = 2
                Element length, H . . . . . = 0.6000E+01
                AX0 = 0.4000E+07   AX1 = 0.0000E+00
                BX0 = 0.1000E+07   BX1 = 0.0000E+00
                CX0 = 0.0000E+00   CX1 = 0.0000E+00
                FX0 = 0.0000E+00   FX1 = 0.1667E+02  FX2 = 0.00

 Element coefficient matrix, [ELK]:
      0.66667E+06    -0.20000E+07    -0.66667E+06    -0.20000E+07
     -0.20000E+07     0.61667E+07     0.20000E+07     0.58333E+07
     -0.66667E+06     0.20000E+07     0.66667E+06     0.20000E+07
     -0.20000E+07     0.58333E+07     0.20000E+07     0.61667E+07

 Element source vector, {ELF}:
      0.10000E+03     0.00000E+00     0.20000E+03     0.00000E+00


  SOLUTION (values of PVs) at the NODES:

  0.00000E+00     0.00000E+00     0.38273E-02    -0.18473E-02     0.16727E-01
 -0.24364E-02
```

(**Box 7.3.13** is continued from the previous page)

x is the the local coord.if ICONT=0

x	Deflect.	Rotation	B. Moment	Shear Force
0.00000E+00	0.00000E+00	0.00000E+00	0.46182E+03	-0.38273E+04
0.50000E+00	0.47841E-03	-0.23091E-03	0.46182E+03	-0.29036E+04
0.10000E+01	0.95682E-03	-0.46182E-03	0.46182E+03	-0.19800E+04
0.15000E+01	0.14352E-02	-0.69273E-03	0.46182E+03	-0.10564E+04
0.20000E+01	0.19136E-02	-0.92364E-03	0.46182E+03	-0.13273E+03
0.25000E+01	0.23920E-02	-0.11545E-02	0.46182E+03	0.79091E+03
0.30000E+01	0.28705E-02	-0.13855E-02	0.46182E+03	0.17145E+04
0.35000E+01	0.33489E-02	-0.16164E-02	0.46182E+03	0.26382E+04
0.40000E+01	0.38273E-02	-0.18473E-02	0.46182E+03	0.35618E+04
0.00000E+00	0.38273E-02	-0.18473E-02	0.98182E+02	-0.12109E+04
0.75000E+00	0.54398E-02	-0.19209E-02	0.98182E+02	-0.91636E+03
0.15000E+01	0.70523E-02	-0.19945E-02	0.98182E+02	-0.62182E+03
0.22500E+01	0.86648E-02	-0.20682E-02	0.98182E+02	-0.32727E+03
0.30000E+01	0.10277E-01	-0.21418E-02	0.98182E+02	-0.32727E+02
0.37500E+01	0.11890E-01	-0.22155E-02	0.98182E+02	0.26182E+03
0.45000E+01	0.13502E-01	-0.22891E-02	0.98182E+02	0.55636E+03
0.52500E+01	0.15115E-01	-0.23627E-02	0.98182E+02	0.85091E+03
0.60000E+01	0.16727E-01	-0.24364E-02	0.98182E+02	0.11455E+04

Example 7.3.8 (Analysis of a Plane Truss)

Here, we consider the three-member plane truss shown in Figure 7.3.7 (see Example 4.6.1). A plane truss problem falls into MODEL = 4 and NTYPE = 0. To obtain the solution in nondimensional form, we take $E = 1$, $A = 1$, $P = 1$, and $L = 1$. The data are discontinuous (ICONT=0). The input and partial output are presented in Box 7.3.14.

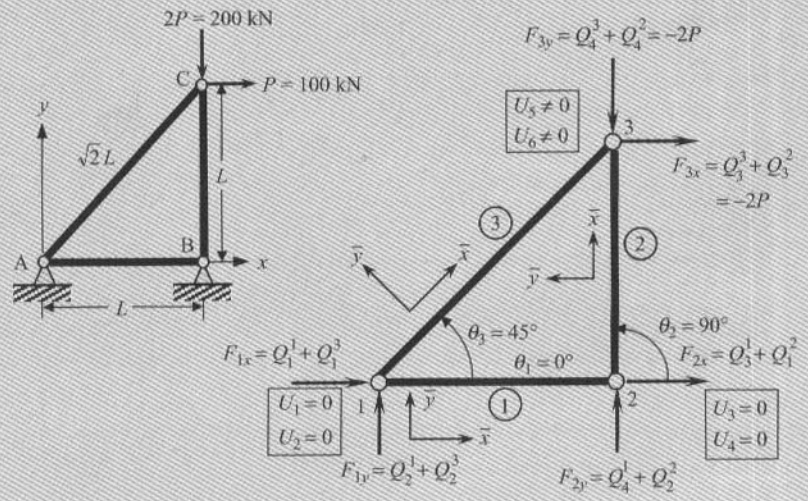

Figure 7.3.7 The plane truss problem of Example 7.3.8.

Box 7.3.14 Input and partial output for the plane truss problem of Example 7.3.8.

```
Example 7.3.8: ANALYSIS OF A PLANE TRUSS
 4 0 0                                  MODEL, NTYPE, ITEM
 0 3                                    IELEM, NEM
 0 1                                    ICONT, NPRNT
   3                                    NNM
 1.0   1.0   1.0   1.0   0.0  0.0      SE, SL, SA, CS, SN, HF
   2   3                                NOD(1, I)  (Element 1)
 1.0 1.414 1.0   0.707  0.707  0.0      same for Element 2
   1   3
 1.0 1.0   1.0   0.0  1.0
 0.0 0.0   0.0   0.0  0.0              Same for Element 3
   1   2                                0          NCON
   4                                    NSPV
   1   1   0.0
   1   2   0.0                          ISPV, VSPV
   2   1   0.0
   2   2   0.0
   2                                    NSSV
   3   1  -2.0                          ISSV, VSSV
   3   2   1.0
   0                                    NNBC
   0                                    NMPC
```

```
OUTPUT from program  FEM1D  by J. N. REDDY

SOLUTION (values of PVs) at the NODES:

 0.00000E+00  0.00000E+00  0.00000E+00  0.00000E+00  -0.30000E+01  -0.58289E+01

   Generalized forces in the element coordinates
  (second line gives the results in the global coordinates)

 Ele     Force, H1       Force, V1       Force, H2       Force, V2
  1    0.3000E+01     0.0000E+00    -0.3000E+01     0.0000E+00
       0.3000E+01     0.0000E+00    -0.3000E+01     0.0000E+00
  2   -0.1414E+01     0.0000E+00     0.1414E+01     0.0000E+00
      -0.1000E+01    -0.1000E+01     0.1000E+01     0.1000E+01
  3    0.0000E+00     0.0000E+00     0.0000E+00     0.0000E+00
       0.0000E+00     0.0000E+00     0.0000E+00     0.0000E+00
```

Example 7.3.9 (Analysis of a Plane Frame)

This example deals with the two-member frame structure shown in Figure 7.3.8 (see Example 5.4.1). We shall analyze the frame for displacements and member forces using first

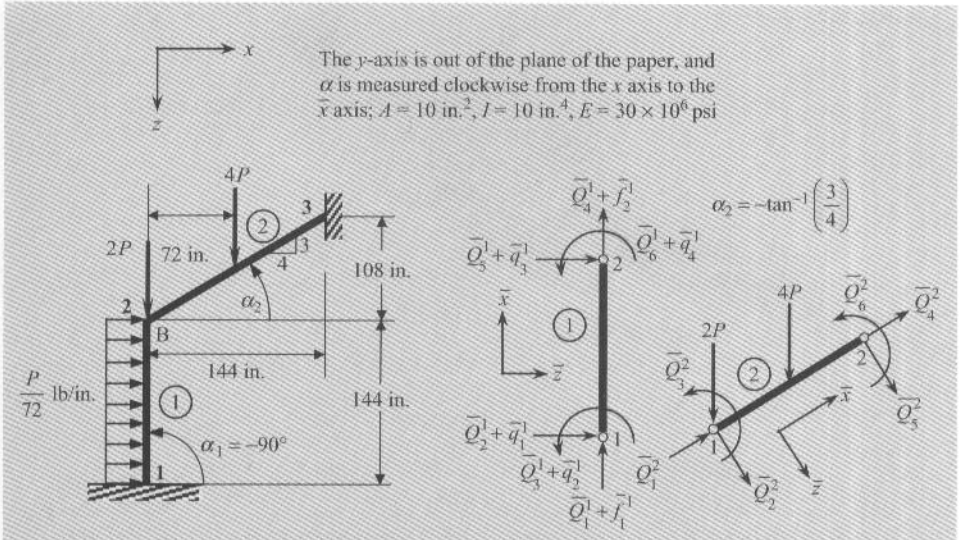

Figure 7.3.8 The plane frame problem of Example 7.3.9.

the Euler–Bernoulli frame element (MODEL = 4, NTYPE = 1) and then using the Timoshenko frame element (MODEL = 4, NTYPE = 2). The input files of the problem using two Euler–Bernoulli elements and 2 (linear) Timoshenko beam elements are presented in Box 7.3.15.

Box 7.3.15 Input data for the plane frame problem of Example 7.3.9.

```
Example 7.3.9(a): ANALYSIS OF A PLANE FRAME (2 Euler-Bernoulli elements)
 4  1  0                                  MODEL, NTYPE, ITEM
 0  2                                     IELEM, NEM
 0  1                                     ICONT, NPRNT
 3                                        NNM
 0.3  1.0E6  144.0  10.0  10.0  0.0  -1.0  PR, SE, SL, SA, SI, CS, SN
 0.0  0.0138888  0.0  0.0  0.0  0.0       HF, VF, PF, XB, CST, SNT
 1  2                                     NOD(1,J)
 0.3  1.0E6  180.0  10.0  10.0  0.8  -0.6  PR, SE, SL, SA, SI, CS, SN
 0.0  0.0    4.0  90.0  -0.6  0.8        HF, VF, PF, XB, CST, SNT
 2  3                                     NOD(2,J)
                                  0       NCON
 6                                        NSPV
 1  1   0.0
 1  2   0.0
 1  3   0.0
 3  1   0.0                               ISPV, VSPV
 3  2   0.0
 3  3   0.0
 1                                        NSSV
 2  2   2.0                               ISSV, VSSV
 0                                        NNBC
 0                                        NMPC
```

(**Box 7.3.15** is continued from the previous page)

```
Example 7.3.9(b): ANALYSIS OF A PLANE FRAME (2 TIMOSHENKO elements)
 4  2  0                          MODEL, NTYPE, ITEM
 0  2                             IELEM, NEM
 0  1                             ICONT, NPRNT
 3                                NNM
 0.3  1.0E6  144.0  10.0  10.0  0.0  -1.0   PR, SE, SL, SA, SI, CS, SN
 0.0  0.0138888  0.0  0.0  0.0  0.0         HF, VF, PF, XB, CST, SNT
 1  2                                      NOD(1,J)
 0.3  1.0E6  180.0  10.0  10.0  0.8  -0.6   PR, SE, SL, SA, SI, CS, SN
 0.0  0.0      4.0  90.0  -0.6  0.8         HF, VF, PF, XB, CST, SNT
 2  3                                      NOD(2,J)
                                0          NCON
 6                                         NSPV
 1  1  0.0
 1  2  0.0
 1  3  0.0
 3  1  0.0                                 ISPV, VSPV
 3  2  0.0
 3  3  0.0
 1                                         NSSV
 2  2  2.0                                 ISSV, VSSV
 0                                         NNBC
 0                                         NMPC
```

The next two examples deal with the use of **FEM1D** for eigenvalue and time-dependent problems (see Chapter 6).

Example 7.3.10 (Natural Vibration of a Cantilever Beam)

Here, we consider natural vibrations of a cantilever beam (see Example 6.1.2). The input data for all variables is the same as in the static analysis. In addition, we must input c_{t0} and c_{t1}. For the Timoshenko beam theory, c_{t0} denotes the inertia ρA, and c_{t1} denotes the rotatory inertia ρI. The eigenvalue solver used in **FEM1D** requires the matrix $[B]$ in $[A]\{x\} = \lambda[B]\{x\}$ to be positive-definite. Hence, c_{t0} and c_{t1} should be nonzero, otherwise, the mass matrix coefficients associated with Ψ will be zero. When rotary inertia is omitted in the Timoshenko beam theory, a small value for the inertia coefficient is used in order to ensure positive-definiteness of the mass matrix.

The input files for the natural vibrations of the cantilever beam by the two types of elements are given in Box 7.3.16. The reader can investigate the convergence characteristics of the elements in improving the accuracy of the fundamental frequency with the use of **FEM1D**.

Box 7.3.16 Input data files for beam vibration of Example 7.3.10.

```
Example 7.3.10(a): NATURAL VIBRATIONS OF A CANTILEVER BEAM (E-B; w/o RI)
 3 0 3                          MODEL, NTYPE, ITEM
 0 2                            IELEM, NEM
 1 1                            ICONT, NPRNT
  0.0   0.5   0.5               DX(I)
  0.0   0.0                     AX0, AX1
  1.0   0.0                     BX0, BX1
  0.0   0.0                     CX0, CX1
  2                             NSPV
 1 1                            ISPV(1, J)
 1 2                            ISPV(2, J)
 0                              NNBC
 0                              NMPC
 1.0  8.3333-06                 CT0, CT1
-----------------------------------------------------------------------
Example 7.3.10(b): NATURAL VIB. OF A CANTILEVER BEAM (TIM element w/o RI)
 2 0 3                          MODEL, NTYPE, ITEM
 1 2                            IELEM, NEM
 1 1                            ICONT, NPRNT
 0.0   0.5   0.5                DX(I)
 4.0E4 0.0                      AX0, AX1  (nu=0.25, H=0.01)
 1.0   0.0                      BX0, BX1
 0.0   0.0                      CX0, CX1
 2                              NSPV
 1 1                            ISPV(1,J)
 1 2                            ISPV(2,J)
 0                              NNBC
 0                              NMPC
 1.0  8.33333E-06               CT0, CT1  (L/H=100)
```

Example 7.3.11 (Transient Heat Transfer)

Consider the transient heat conduction in a plane wall. The governing equation is

$$\frac{\partial u}{\partial t} - \frac{\partial^2 u}{\partial x^2} = 0 \quad \text{for } 0 < x < 1 \tag{7.3.8}$$

The boundary conditions considered are

$$\textbf{Set 1:}\quad u(0,t) = 0 \quad \frac{\partial u}{\partial x}(1,t) = 0; \quad \textbf{Set 2:}\quad u(0,t) = 0, \quad \left(\frac{\partial u}{\partial x} + u\right)\bigg|_{x=1} = 0 \tag{7.3.9}$$

and the initial condition is taken to be

$$u(x,0) = 1 \tag{7.3.10}$$

We have MODEL = 1, NTYPE = 0, ICONT = 1, NSPV = 1, and NSSV = 0; NNBC = 0 for Set 1 and NNBC = 1 for Set 2. The coefficients of the differential equations are ($a = 1.0$, $b = 0.0$, $c = 0.0$, $c_t = 1.0$, and $f = 0$)

AX0 = 1.0, AX1 = 0.0, BX0 = 0.0, BX1 = 0.0, CX0 = 0.0, CX1 = 0.0

FX0 = 0.0, FX1 = 0.0, FX2 = 0.0, CT0 = 1.0, CT1 = 0.0

Box 7.3.17 Input files for the transient heat conduction problem of Example 7.3.11.

Example 7.3.11(a): Transient heat conduction in a plane wall (Set 1)

```
 1 0 1                    MODEL, NTYPE, ITEM
 1 2                      IELEM, NEM
 1 1                      ICONT, NPRNT
  0.0  0.5  0.5           DX(I)
  1.0  0.0                AX0, AX1
  0.0  0.0                BX0, BX1
  0.0  0.0                CX0, CX1
  0.0  0.0  0.0           FX0, FX1, FX2
  1                       NSPV
  1 1  0.0                ISPV(I, J), VSPV(I)
  0                       NSSV
  0                       NNBC
  0                       NMPC
  1.0  0.0                CT0, CT1
  0.05 0.5  0.0           DT, ALFA, GAMA
  1    20   1             INCOND, NTIME, INTVL
  0.0  1.0  1.0           GU0(I)
```

Example 7.3.11(b): Transient heat conduction in a plane wall (Set 2)

```
 1 0 1                    MODEL, NTYPE, ITEM
 1 2                      IELEM, NEM
 1 1                      ICONT, NPRNT
  0.0  0.5  0.5           DX(I)
  1.0  0.0                AX0, AX1
  0.0  0.0                BX0, BX1
  0.0  0.0                CX0, CX1
  0.0  0.0  0.0           FX0, FX1, FX2
  1                       NSPV
  1 1   0.0               ISPV(I, J), VSPV(I)
  0                       NSSV
  1                       NNBC
  0                       NMPC
  5 1  1.0  0.0           INBC, VNBC, UREF
  1.0  0.0                CT0, CT1
  0.05 0.5  0.0           DT, ALFA, GAMA
  1   20    1             INCOND, NTIME, INTVL
  0.0  1.0  1.0           GU0(I)
```

The boundary and initial conditions (since INCOND=1) are input as

$$\text{ISPV}(1,1)=1, \quad \text{ISPV}(1,2)=1, \quad \text{VSPV}(1)=0.0; \quad \text{GU0(I)}=\{0.0, 1.0, 1.0, \ldots\}$$

From the discussions of Example 6.2.1, we use $\Delta t = 0.05$ (DT=0.05) and print the solution for every time step (i.e., INTVL=1).

The input files of the problem for the two sets of boundary conditions are presented in Box 7.3.17 for a mesh of two linear elements.

7.4 SUMMARY

In this chapter three main items have been discussed: numerical integration of finite element coefficient matrices and vectors, numerical implementation of a typical finite element program and their contents, and applications of the finite element program **FEM1D.** The numerical evaluation of the coefficients is required because of (*a*) variable coefficients of the differential equations modeled and (*b*) special evaluation of the coefficients, as was required for the Timoshenko beam element with equal interpolation. The Newton–Cotes and Gauss–Legendre integration rules have been discussed. The integration rules require transformation of the integral expressions from the global coordinate system to a local coordinate system and interpolation of the global coordinate x. Depending on the relative degrees of interpolation of the geometry and the dependent variables, the formulations are classified as subparametric, isoparametric, and superparametric.

The three logical units—preprocessor, processor, and postprocessor—have been discussed. The contents of the processor, where most finite element calculations are carried out, have been considered in detail. Computer implementation for numerical evaluation of integral expressions, assembly of element coefficients, and imposition of boundary conditions have been discussed. A description of the input variables to the finite element computer program **FEM1D** has been presented, and application of **FEM1D** to problems of heat transfer and solid mechanics has been discussed. Fluid mechanics problems are similar in mathematical structure to heat transfer problems and hence not discussed in this chapter.

PROBLEMS

Section 7.1

In Problems 7.1–7.4, use the appropriate number of integration points, and verify the results with those obtained by the exact integration.

7.1 Evaluate the integrals in Example 7.1.1 using the Newton–Cotes formula and Gauss–Legendre quadrature when ψ_i are the quadratic interpolation functions

$$\psi_1 = \left(1 - \frac{x - x_a}{x_b - x_a}\right)\left(1 - 2\frac{x - x_a}{x_b - x_a}\right) = -\frac{1}{2}\xi(1 - \xi)$$
$$\psi_2 = 4\left(\frac{x - x_a}{x_b - x_a}\right)\left(1 - \frac{x - x_a}{x_b - x_a}\right) = (1 - \xi^2)$$
$$\psi_3 = -\frac{x - x_a}{x_b - x_a}\left(1 - 2\frac{x - x_a}{x_b - x_a}\right) = \frac{1}{2}\xi(1 + \xi)$$

7.2 Use Newton–Cotes integration formula to evaluate

$$K_{11} = \int_{x_a}^{x_b} \left(\frac{d^2\phi_1}{dx^2}\right)^2 dx, \quad G_{11} = \int_{x_a}^{x_b} (\phi_1)^2\, dx$$

where ϕ_i are the Hermite cubic interpolation functions [see Eqs. (5.2.12), (5.2.13*a*), and (5.2.13*b*)]. *Answer:* $r = 2$: $K_{11} = 12/h^3$ (exact), $G_{11} = 0.398148h$.

7.3 Use Gauss–Legendre quadrature to evaluate the integrals of Problem 7.2 for the case in which the interpolation functions ϕ_i are the fifth-order Hermite polynomials of Problem 5.4. *Answer:* $K_{11} = \frac{120}{7}h^3$, $G_{11} = \frac{181}{462}h$ (exact).

7.4 Repeat Problem 7.3 for the case in which the interpolation functions ϕ_i are the fifth-order Hermite polynomials of Problem 5.5. *Answer:* $K_{11} = \frac{5092}{35h_e^3}$, $G_{11} = \frac{523h_e}{3465}$ (exact).

Section 7.2

Computer Exercises (use FEM1D)

7.5 Solve the problem

$$-\frac{d}{dx}\left(k\frac{dT}{dx}\right) = g_0$$
$$\left(-k\frac{dT}{dx}\right)_{x=0} = Q_0, \quad \left[k\frac{dT}{dx} + \beta(T - T_\infty)\right]_{x=L} = 0$$

using two and four linear elements. Compare the results with the exact solution. Use the following data: $L = 0.02$ m, $k = 20$ W/(m $\cdot$°C), $g_0 = 10^6$ W/m^2, $Q_0 = 10^2$ W, $T_\infty = 50$°C, $\beta = 500$ W/(m $\cdot$°C).

7.6 Solve Problem 7.5 using two quadratic elements.

7.7 Solve the heat transfer problem in Example 4.3.3 (Set 1), using (*a*) four linear elements and (*b*) two quadratic elements (see Table 4.3.1).

7.8 Solve the axisymmetric problem in Example 4.3.4 using four quadratic elements and compare the solution with that obtained using eight linear elements and the exact solution of Table 4.3.2.

7.9 Solve the one-dimensional flow problem of Example 4.4.1 (Set 1), for $dP/dx = -24$, using eight linear elements (see Figure 4.4.1). Compare the finite element results with the exact solution $(4.4.20)_1$.

7.10 Solve the Couette flow problem in Example 4.4.1 (Set 2) using four quadratic elements. Compare the finite element solution with the exact solution.

7.11 Solve Problem 4.10 (heat flow in a composite wall) using the minimum number linear finite elements.

7.12 Solve Problem 4.22 (axisymmetric problem of unconfined aquifer) using the minimum number of linear finite elements.

7.13 Solve Problem 4.25.

7.14 Solve Problem 4.27.

7.15 Solve Problem 4.35 using two linear elements.

7.16 Determine the forces and elongations in the wires AB and CD shown in Figure P7.16. Each wire has a cross-sectional area of $A = 0.03$ in.^{2} and modulus of elasticity $E = 30 \times 10^6$ psi.

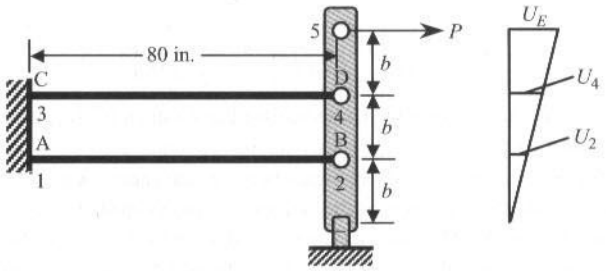

Figure P7.16

7.17 Solve the problem of axisymmetric deformation of a rotating circular disk using four linear elements (see Example 7.3.5).

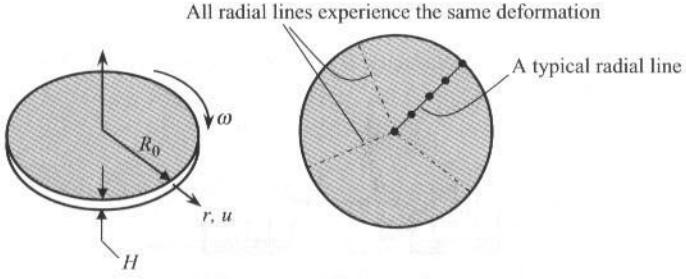

Figure P7.17

7.18–7.25 Solve Problems 5.7–5.14 using the minimum number of Euler–Bernoulli beam elements (*Note:* Numerous other beam problems can be found in books on mechanics of deformable solids).

7.26 Analyze Problem 7.22 (same as Problem 5.11) using the RIE Timoshenko element. Assume $\nu = 0.25$, $K_s = 5/6$, and $H = 0.1$ m (beam height). Use two, four and eight elements to see the convergence characteristics of the RIE (two-element model may yield results very far off from the Euler–Bernoulli beam solution).

7.27 Repeat Problem 7.26 using the CIE Timoshenko element.

7.28 Analyze a clamped circular plate under a uniformly distributed transverse load using the Euler–Bernoulli plate element. Investigate the convergence using two, four, and eight

elements by comparing with the exact solution [from Reddy (2002)]

$$w(r) = \frac{q_0 a^4}{64D}\left[1 - \left(\frac{r}{a}\right)^2\right]^2$$

where $D = EH^3/12(1-\nu^2)$, q_0 is the intensity of the distributed load, a is the radius of the plate, H is its thickness, and ν is Poisson's ratio ($\nu = 0.25$). Tabulate the center deflection.

7.29 Repeat Problem 7.28 with the RIE Timoshenko plate element for $a/H = 10$. Use four and eight linear elements and two and four quadratic elements and tabulate the center deflection. Take $E = 10^7$, $\nu = 0.25$, and $K_s = 5/6$. The exact solution is [see page 403 of Reddy (2002)]

$$w(r) = \frac{q_0 a^4}{64D}\left[1 - \left(\frac{r}{a}\right)^2\right]^2 + \frac{q_0 a^2}{4K_s G H}\left[1 - \left(\frac{r}{a}\right)^2\right]$$

7.30 Repeat Problem 7.29 with the Timoshenko plate element (CIE) (and linear elements) for $a/H = 10$.

7.31 Consider an annular plate of outer radius a, and an inner radius b, and thickness H. If the plate is simply supported at the outer edge and subjected to a uniformly distributed load q_0 (see Fig. P7.31), analyze the problem using the Euler–Bernoulli plate element. Compare the four-element solution with the analytical solution [from Reddy (2002)]

$$w = \frac{q_0 a^4}{64D}\left\{-1 + \left(\frac{r}{a}\right)^4 + \frac{2\alpha_1}{1+\nu}\left[1 - \left(\frac{r}{a}\right)^2\right] - \frac{4\alpha_2\beta^2}{1-\nu}\log\left(\frac{r}{a}\right)\right\}$$

$$\alpha_1 = (3+\nu)(1-\beta^2) - 4(1+\nu)\beta^2\kappa, \quad \alpha_2 = (3+\nu) + 4(1+\nu)\kappa$$

$$\kappa = \frac{\beta^2}{1-\beta^2}\log\beta, \quad \beta = \frac{b}{a}, \quad D = \frac{EH^3}{12(1-\nu^2)}$$

where E is the modulus of elasticity, H the thickness, and ν Poisson's ratio. Take $E = 10^7$, $\nu = 0.3$, and $b/a = 0.25$.

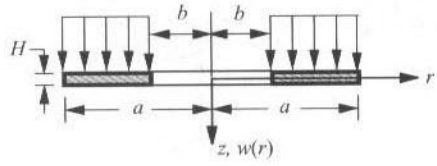

Figure P7.31

7.32 Repeat Problem 7.31 with (a) four linear elements and (b) two quadratic Timoshenko (RIE) elements for $a/H = 10$.

7.33–7.47 Analyze the truss problems in Figures P4.38–P4.44 and frame problems in Figures P5.28–P5.35.

7.48 Consider the axial motion of an elastic bar, governed by the second-order equation

$$EA\frac{\partial^2 u}{\partial x^2} = \rho A\frac{\partial^2 u}{\partial t^2} \quad \text{for } 0 < x < L$$

with the following data: length of bar $L = 500$ mm, cross-sectional area $A = 1$ mm^2, modulus of elasticity $E = 20,000$ N/mm^2, density $\rho = 0.008$ kg/mm^3, boundary conditions

$$u(0, t) = 0, \quad EA\frac{\partial u}{\partial x}(L, t) = 1$$

and zero initial conditions. Using 20 linear elements and $\Delta t = 0.002$ s, determine the axial displacement and plot the displacement as a function of position along the bar for $t = 0.8$ s.

7.49 Consider the following nondimensionalized differential equation governing the plane wall transient:

$$-\frac{\partial^2 T}{\partial x^2} + \frac{\partial T}{\partial t} = 0 \quad \text{for } 0 < x < 1$$

with boundary conditions $T(0, t) = 1$ and $T(1, t) = 0$, and initial condition $T(x, 0) = 0$. Solve the problem using eight linear elements. Determine the critical time step; solve the problem using the Crank–Nicholson method and $\Delta t = 0.002$ s.

Note: Modify program **FEM1D** to solve Problems 7.50–7.52 (solutions to these problems are not presented here for obvious reasons).

7.50 Consider a simply supported beam of length L subjected to a point load

$$P(t) = \begin{cases} P_0 \sin \frac{\pi t}{\tau} & \text{for } 0 \le t \le \tau \\ 0 & \text{for } t \ge \tau \end{cases}$$

at a distance c from the left end of the beam (assumed to be at rest at $t = 0$). The transverse deflection $w(x, t)$ is given by [see Harris and Crede (1961), pp. 8–53]

$$w(x, t) =$$

$$\begin{cases} \dfrac{2P_0L^3}{\pi^4 EI} \displaystyle\sum_{i=1}^{\infty} \frac{1}{i^4} \sin\frac{i\pi c}{L} \sin\frac{i\pi x}{L} \left[\frac{1}{1 - T_i^2/4\tau^2} \left(\sin\frac{\pi t}{\tau} - \frac{T_i}{2\tau} \sin\omega_i t \right) \right], & 0 \le t \le \omega\tau \\ \dfrac{2P_0L^3}{\pi^4 EI} \displaystyle\sum_{i=1}^{\infty} \frac{1}{i^4} \sin\frac{i\pi c}{L} \sin\frac{i\pi x}{L} \left[\frac{\frac{T_i}{\tau} \cos\frac{\pi\tau}{T_i}}{T_i^2/4\tau^2 - 1} \sin\omega_i (t - \frac{1}{2}\tau) \right], & t \ge \tau \end{cases}$$

where

$$T_i = \frac{2\pi}{\omega_i} = \frac{2L^2}{i^2\pi}\sqrt{\frac{A\rho}{EI}} = \frac{T_1}{i^2}$$

Use the data $P_0 = 1000$ lb, $\tau = 20 \times 10^{-6}$ s, $L = 30$ in., $E = 30 \times 10^6$ lb/in.^{2}, $\rho = 733 \times 10^{-6}$ lb/in.^{3}, $\Delta t = 10^{-6}$ s, and assume that the beam is of square cross section of 0.5 in by 0.5 in. Using five Euler–Bernoulli beam elements in the half-beam, obtain the finite element solution and compare with the series solution at midspan for the case $c = \frac{L}{2}$.

7.51 Repeat Problem 7.50 for $c = \frac{1}{4}L$ and eight elements in the full span.

7.52 Repeat Problem 7.50 for $P(t) = P_0$ at midspan and eight elements in the full span.

7.53 Consider a cantilevered beam with a point load P_0 at the free end (Fig. P7.53). Using the data of Problem 7.50, find the finite element solution for the transverse deflection using eight Euler–Bernoulli beam elements.

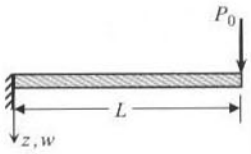

Figure P7.53

$E = 30 \times 10^6$ psi, $\nu = 0.3$,
$\rho = 733 \times 10^{-6}$ lb/in.^{3},
$L = 30$ in., $P_0 = 10^3$ lbs,
$A = 0.25$ in.^{2}, $\Delta t = 10^{-6}$ s

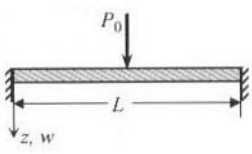

Figure P7.54

7.54 Repeat Problem 7.50 for a clamped beam with the load at the midspan (see Fig. P7.54).

7.55 Repeat Problem 7.54 using four linear Timoshenko beam elements. Use $\nu = 0.3$.

7.56 Repeat Problem 7.54 using two quadratic Timoshenko beam elements. Use $\nu = 0.3$.

REFERENCES FOR ADDITIONAL READING

Fluid mechanics

1. Bird, R. B., Stewart, W. E., and Lightfoot, E. N., *Transport Phenomena,* John Wiley, New York, 1960.
2. Duncan, W. J., Thom, A. S., and Young, A. D., *Mechanics of Fluids,* 2nd ed., Elsevier, New York, 1970.
3. Eskinazi, S., *Principles of Fluid Mechanics,* Allyn and Bacon, Boston, 1962.
4. Harr, M. E., *Groundwater and Seepage,* McGraw-Hill, New York, 1962.
5. Nadai, A., *Theory of Flow and Fracture of Solids,* vol. II, McGraw-Hill, New York, 1963.
6. Schlichting, H., *Boundary-Layer Theory* (translated by J. Kestin), 7th ed., McGraw-Hill, New York, 1979.
7. Shames, I. H., *Mechanics of Fluids,* 3rd ed., McGraw-Hill, New York, 1982.
8. Vallentine, H. R., *Applied Hydrodynamics,* Plenum Press, New York, 1967.
9. Verrujit, A., *Theory of Groundwater Flow,* Gordon and Breach, New York, 1970.

Heat transfer

10. Carslaw, H. S. and Jaeger, J. C., *Conduction of Heat in Solids,* 2nd ed., Oxford University Press, Oxford, 1986.
11. Holoman, J. P., *Heat Transfer,* 8th ed., McGraw-Hill, New York, 1996.
12. Kreith, F. and Bahn, M. S., *Principles of Heat Transfer,* 5th ed., Harper & Row, New York, 1993.
13. Myers, G. G., *Analytical Methods in Conduction Heat Transfer,* 2nd ed., AMCHT Publications, Madison, WI, 1998.
14. Ozisik, M. N., *Heat Transfer: A Basic Approach,* McGraw-Hill, New York, 1985.

Elasticity

15. Budynas, R. G., *Advanced Strength and Applied Stress Analysis,* McGraw-Hill, New York, 1977.
16. Harris, C. M. and Crede, C. E., *Shock and Vibration Handbook,* vol. 1, McGraw-Hill, New York, 1961.
17. Reddy, J. N., *Energy Principles and Variational Methods in Applied Mechanics,* John Wiley, New York, 2002.
18. Ugural, A. C. and Fenster, S. K., *Advanced Strength and Applied Elasticity,* 4th ed., Prentice Hall, Upper Saddle River, NJ, 2003.

Time approximations

19. Bathe, K. J., *Finite Element Procedures,* Prentice Hall, Englewood Cliffs, NJ, 1996.
20. Clough, R. W. and Penzien, J., *Dynamics of Structures,* 2nd ed., McGraw-Hill, New York, 1993.

21. Hughes, T. J. R., *The Finite Element Method,* Prentice Hall, Englewood Cliffs, NJ, 1987; Dover, New York, 2000.

Numerical integration

22. Carnahan, B., Luther, H. A., and Wilkes, J. O., *Applied Numerical Methods,* John Wiley, New York, 1969.
23. Loxan, A. N., Davids, N. and Levenson, A., "Table of the Zeros of the Legendre Polynomials of Order 1–16 and the Weight Coefficients for Gauss' Quadrature Formula," *Bulletin of the American Mathematical Society,* 48, pp. 739–743, 1942.
24. Stroud, A. H. and Secrest, D., *Gaussian Quadrature Formulas,* Prentice-Hall, Englewood Cliffs, NJ, 1966.
25. Zienkiewicz, O. C. and Taylor, R. L., *The Finite Element Method,* vols. 1 and 2, McGraw-Hill, 1989 and 1991.

Chapter 8

SINGLE-VARIABLE PROBLEMS IN TWO DIMENSIONS

8.1 INTRODUCTION

Finite element analysis of two-dimensional problems involves the same basic steps as those described for one-dimensional problems in Chapters 3–6. The analysis is somewhat complicated by the fact that two-dimensional problems are described by partial differential equations over geometrically complex regions. The boundary Γ of a two-dimensional domain Ω is, in general, a curve. Therefore, finite elements are simple two-dimensional geometric shapes that allow approximations of a given two-dimensional domain as well as the solution over it. Thus, in two-dimensional problems we not only seek an approximate solution to a given problem on a domain, but we also approximate the domain by a suitable finite element mesh. Consequently, we will have approximation errors due to the approximation of the solution as well as discretization errors due to the approximation of the domain in the finite element analysis of two-dimensional problems. The finite element mesh (discretization) consists of simple two-dimensional elements, such as triangles, rectangles, and/or quadrilaterals, that allow unique derivation of the interpolation functions. The elements are connected to each other at nodal points on the boundaries of the elements. The ability to represent domains with irregular geometries by a collection of finite elements makes the method a valuable practical tool for the solution of boundary, initial, and eigenvalue problems arising in various fields of engineering.

The objective of this chapter is to extend the basic steps discussed earlier for one-dimensional problems to two-dimensional boundary value problems involving a single dependent variable. Once again, we describe the basic steps of the finite element analysis with a model second-order partial differential equation governing a single variable. This equation arises in a number of fields including electrostatics, heat transfer, fluid mechanics, and solid mechanics (see Table 8.1.1).

Table 8.1.1 Some examples of the Poisson equation

$$-\nabla \cdot (k\nabla u) = f \text{ in } \Omega$$

Natural boundary condition: $k\dfrac{\partial u}{\partial n} + \beta(u - u_\infty) = q$ on Γ_q

Essential boundary condition: $u = \hat{u}$ on Γ_u

Field of application	Primary variable u	Material constant k	Source variable f	Secondary variables q, $\frac{\partial u}{\partial x}$, $\frac{\partial u}{\partial y}$
Heat transfer	Temperature T	Conductivity k	Heat source g	Heat flow due to conduction $k\frac{\partial T}{\partial n}$ convection $h(T - T_\infty)$
Irrotational flow of an ideal fluid	Stream function ψ	Density ρ	Mass production σ	Velocities $\frac{\partial \psi}{\partial x} = -v$ $\frac{\partial \psi}{\partial y} = u$
	Velocity potential ϕ	Density ρ	Mass production σ	$\frac{\partial \phi}{\partial x} = u$ $\frac{\partial \phi}{\partial y} = v$
Groundwater flow	Piezometric head ϕ	Permeability K	Recharge f (pumping, $-f$)	Seepage $q = k\frac{\partial \phi}{\partial n}$ Velocities $u = -k\frac{\partial \phi}{\partial x}$ $v = -k\frac{\partial \phi}{\partial y}$
Torsion of cylindrical members	Stress function Ψ	$k = 1$ G = shear modulus	$f = 2$ θ = angle of twist per unit length	$G\theta\frac{\partial \Psi}{\partial x} = -\sigma_{yz}$ $G\theta\frac{\partial \Psi}{\partial y} = \sigma_{xz}$
Electrostatics	Scalar potential ϕ	Dielectric constant ϵ	Charge density ρ	Displacement flux density D_n
Magnetostatics	Magnetic potential ϕ	Permeability μ	Charge density ρ	Magnetic flux density B_n
Membranes	Transverse deflection u	Tension in membrane T	Transversely distributed load	Normal force q

8.2 BOUNDARY VALUE PROBLEMS

8.2.1 The Model Equation

Consider the problem of finding the solution $u(x, y)$ of the second-order partial differential equation

$$-\frac{\partial}{\partial x}\left(a_{11}\frac{\partial u}{\partial x} + a_{12}\frac{\partial u}{\partial y}\right) - \frac{\partial}{\partial y}\left(a_{21}\frac{\partial u}{\partial x} + a_{22}\frac{\partial u}{\partial y}\right) + a_{00}u - f = 0 \qquad (8.2.1)$$

for given data a_{ij} $(i, j = 1, 2)$, a_{00} and f, and specified boundary conditions. The form of the boundary conditions will be apparent from the weak formulation. As a special case, we

can obtain the Poisson equation from (8.2.1) by setting $a_{11} = a_{22} = k(x, y)$ and $a_{12} = a_{21} = a_{00} = 0$:

$$-\nabla \cdot (k\nabla u) = f(x, y) \quad \text{in } \Omega \tag{8.2.2}$$

where ∇ is the gradient operator. If $\hat{\mathbf{i}}$ and $\hat{\mathbf{j}}$ denote the unit vectors directed along the x and y axes, respectively, the gradient operator can be expressed as (see Sec. 2.2.3)

$$\nabla = \hat{\mathbf{i}}\frac{\partial}{\partial x} + \hat{\mathbf{j}}\frac{\partial}{\partial y}$$

and (8.2.2) in the Cartesian coordinate system takes the form

$$-\frac{\partial}{\partial x}\left(k\frac{\partial u}{\partial x}\right) - \frac{\partial}{\partial y}\left(k\frac{\partial u}{\partial y}\right) = f(x, y) \tag{8.2.3}$$

In the following, we shall develop the finite element model of (8.2.1). The major steps are as follows:

1. Discretization of the domain into a set of finite elements.
2. Weak (or weighted-integral) formulation of the governing differential equation.
3. Derivation of finite element interpolation functions.
4. Development of the finite element model using the weak form.
5. Assembly of finite elements to obtain the global system of algebraic equations.
6. Imposition of boundary conditions.
7. Solution of equations.
8. Postcomputation of solution and quantities of interest.

Steps 6 and 7 remain unchanged from one-dimensional finite element analysis because at the end of Step 5 we have a set of algebraic equations whose form is independent of the dimension of the domain or nature of the problem. In the following sections, we discuss each step in detail.

8.2.2 Finite Element Discretization

In two dimensions there is more than one simple geometric shape that can be used as a finite element (see Fig. 8.2.1). As we shall see shortly, the interpolation functions depend not only on the number of nodes in the element and the number of unknowns per node, but also on the shape of the element. The shape of the element must be such that its geometry is uniquely defined by a set of points, which serve as the element nodes in the development of the interpolation functions. As will be discussed later in this section, a triangle is the simplest geometric shape, followed by a rectangle.

The representation of a given region by a set of elements (i.e., discretization or *mesh generation*) is an important step in finite element analysis. The choice of element type, number of elements, and density of elements depends on the geometry of the domain, the problem to be analyzed, and the degree of accuracy desired. Of course, there are no specific formulae to obtain this information. In general, the analyst is guided by his or her technical background, insight into the physics of the problem being modeled

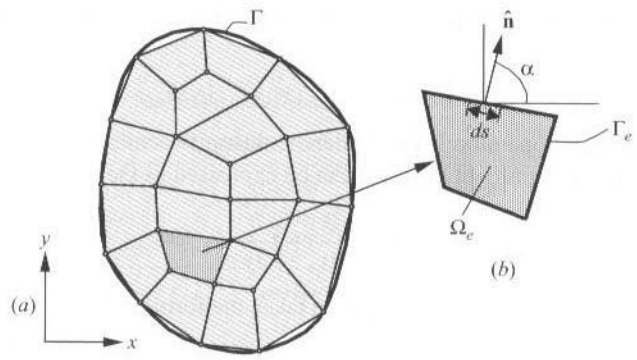

Figure 8.2.1 Finite element discretization of an irregular domain: (*a*) discretization of a domain by quadrilateral elements; and (*b*) a typical quadrilateral element Ω_e (with the unit normal $\hat{\mathbf{n}}$ on the boundary Γ_e of the element).

(e.g., a qualitative understanding of the solution), and experience with finite element modeling. The general rules of mesh generation for finite element formulations include:

1. The elements that are selected should characterize the governing equations of the problem.
2. The number, shape, and type (i.e., linear or quadratic) of elements should be such that the geometry of the domain is represented as accurately as desired.
3. The density of elements should be such that regions of large gradients of the solution are adequately modeled (i.e., use more elements or higher-order elements in regions of large gradients).
4. Mesh refinements should vary gradually from high-density regions to low-density regions. If *transition elements* are used, they should be used away from critical regions (i.e., regions of large gradients). Transition elements are those that connect lower-order elements to higher-order elements (e.g., linear to quadratic).

8.2.3 Weak Form

In the development of the weak form we need only consider a typical element. We assume that Ω_e is a typical element, whether triangular or quadrilateral, of the finite element mesh, and we develop the finite element model of (8.2.1) over Ω_e. Various two-dimensional elements will be discussed in the sequel.

Following the three-step procedure presented in Chapters 2 and 3, we develop the weak form of (8.2.1) over the typical element Ω_e. The first step is to multiply (8.2.1) with a weight function w, which is assumed to be differentiable once with respect to x and y, and then integrate the equation over the element domain Ω_e:

$$0 = \int_{\Omega_e} w\left[-\frac{\partial}{\partial x}(F_1) - \frac{\partial}{\partial y}(F_2) + a_{00}u - f\right] dx\, dy \tag{8.2.4a}$$

where

$$F_1 = a_{11}\frac{\partial u}{\partial x} + a_{12}\frac{\partial u}{\partial y}, \qquad F_2 = a_{21}\frac{\partial u}{\partial x} + a_{22}\frac{\partial u}{\partial y} \tag{8.2.4b}$$

In the second step we distribute the differentiation among u and w equally. To achieve this, we integrate the first two terms in (8.2.4a) by parts. First, we note the identities

$$\frac{\partial}{\partial x}(wF_1) = \frac{\partial w}{\partial x}F_1 + w\frac{\partial F_1}{\partial x} \quad \text{or} \quad -w\frac{\partial F_1}{\partial x} = \frac{\partial w}{\partial x}F_1 - \frac{\partial}{\partial x}(wF_1) \tag{8.2.5a}$$

$$\frac{\partial}{\partial y}(wF_2) = \frac{\partial w}{\partial y}F_2 + w\frac{\partial F_2}{\partial y} \quad \text{or} \quad -w\frac{\partial F_2}{\partial y} = \frac{\partial w}{\partial y}F_2 - \frac{\partial}{\partial y}(wF_2) \tag{8.2.5b}$$

Next, we use the component form of the gradient (or divergence) theorem

$$\int_{\Omega_e} \frac{\partial}{\partial x}(wF_1)\,dx\,dy = \oint_{\Gamma_e} wF_1 n_x\,ds \tag{8.2.6a}$$

$$\int_{\Omega_e} \frac{\partial}{\partial y}(wF_2)\,dx\,dy = \oint_{\Gamma_e} wF_2 n_y\,ds \tag{8.2.6b}$$

where n_x and n_y are the components (i.e., the direction cosines) of the unit normal vector

$$\hat{\mathbf{n}} = n_x\hat{\mathbf{i}} + n_y\hat{\mathbf{j}} = \cos\,\alpha\hat{\mathbf{i}} + \sin\,\alpha\hat{\mathbf{j}} \tag{8.2.7}$$

on the boundary Γ_e, and ds is the length of an infinitesimal line element along the boundary (see Fig. 8.2.1b). Using (8.2.5a), (8.2.5b), (8.2.6a), and (8.2.6b) in (8.2.4a), we obtain

$$\begin{aligned} 0 = \int_{\Omega_e} \left[\frac{\partial w}{\partial x}\left(a_{11}\frac{\partial u}{\partial x} + a_{12}\frac{\partial u}{\partial y}\right) + \frac{\partial w}{\partial y}\left(a_{21}\frac{\partial u}{\partial x} + a_{22}\frac{\partial u}{\partial y}\right) + a_{00}wu - wf \right] dx\,dy \\ - \oint_{\Gamma_e} w\left[n_x\left(a_{11}\frac{\partial u}{\partial x} + a_{12}\frac{\partial u}{\partial y}\right) + n_y\left(a_{21}\frac{\partial u}{\partial x} + a_{22}\frac{\partial u}{\partial y}\right)\right] ds \end{aligned} \tag{8.2.8}$$

From an inspection of the boundary integral in (8.2.8), we note that the specification of u constitutes the essential boundary condition, and hence u is the primary variable. The specification of the coefficient of the weight function in the boundary expression

$$q_n \equiv n_x\left(a_{11}\frac{\partial u}{\partial x} + a_{12}\frac{\partial u}{\partial y}\right) + n_y\left(a_{21}\frac{\partial u}{\partial x} + a_{22}\frac{\partial u}{\partial y}\right) \tag{8.2.9}$$

constitutes the natural boundary condition; thus, q_n is the secondary variable of the formulation. The function $q_n = q_n(s)$ denotes the projection of the vector $\mathbf{a}\cdot\nabla u$ along the unit normal $\hat{\mathbf{n}}$. By definition, q_n is taken positive outward from the surface as we move counterclockwise along the boundary Γ_e. In most problems, the secondary variable q_n is of physical interest. For example, in the case of heat transfer through an anisotropic medium, a_{ij} are the conductivities of the medium, and q_n is the negative of the heat flux (because of the Fourier heat conduction law) normal to the boundary of the element.

The third and last step of the formulation is to use the definition (8.2.9) in (8.2.8) and write the weak form of (8.2.1) as

$$\begin{aligned} 0 = \int_{\Omega_e} \left[\frac{\partial w}{\partial x}\left(a_{11}\frac{\partial u}{\partial x} + a_{12}\frac{\partial u}{\partial y}\right) + \frac{\partial w}{\partial y}\left(a_{21}\frac{\partial u}{\partial x} + a_{22}\frac{\partial u}{\partial y}\right) + a_{00}wu - wf \right] dx\,dy \\ - \oint_{\Gamma_e} wq_n\,ds \end{aligned} \tag{8.2.10}$$

or,

$$B^e(w, u) = l^e(w) \tag{8.2.11a}$$

where the bilinear form $B^e(\cdot, \cdot)$ and linear form $l^e(\cdot)$ are

$$B^e(w, u) = \int_{\Omega_e} \left[\frac{\partial w}{\partial x} \left(a_{11} \frac{\partial u}{\partial x} + a_{12} \frac{\partial u}{\partial y} \right) + \frac{\partial w}{\partial y} \left(a_{21} \frac{\partial u}{\partial x} + a_{22} \frac{\partial u}{\partial y} \right) + a_{00} w u \right] dx\, dy$$

$$l^e(w) = \int_{\Omega_e} w f \, dx\, dy + \oint_{\Gamma_e} w q_n \, ds \tag{8.2.11b}$$

The weak form (or *weighted integral statement*) in (8.2.10) or (8.2.11*a*) and (8.2.11*b*) is the basis of the finite element model of (8.2.1).

Whenever $B^e(w, u)$ is symmetric in its arguments w and u [i.e., $B^e(w, u) = B^e(u, w)$], the quadratic functional associated with the variational problem (8.2.11*a*) can be obtained from [see Eq. (2.4.19)]

$$I^e(w) = \frac{1}{2} B^e(w, w) - l^e(w) \tag{8.2.12a}$$

The bilinear form in (8.2.11*b*) is symmetric if and only if $a_{12} = a_{21}$. Then the functional is given by

$$I^e(w) = \frac{1}{2} \int_{\Omega_e} \left[a_{11} \left(\frac{\partial u}{\partial x} \right)^2 + 2a_{12} \frac{\partial u}{\partial x} \frac{\partial u}{\partial y} + a_{22} \left(\frac{\partial u}{\partial y} \right)^2 + a_{00} u^2 \right] dx\, dy$$

$$+ \int_{\Omega_e} u f \, dx\, dy + \oint_{\Gamma_e} u q_n \, ds \tag{8.2.12b}$$

Vector Form of the Variational Problem

It is common, especially in structural mechanics literature, to express finite element formulations in vector notation (i.e., in terms of matrices). While the vector/matrix notation is concise, it is not as transparent as the explicit form that has been used throughout the book. However, for the sake of completeness, the vector form of the variational (or weak) problem (8.2.11*a*) and (8.2.11*b*) is presented here. We shall use bold face letters for matrices of different order, including the 1×1 matrix and row and column matrices.

We begin with Eq. (8.2.11*a*), which can be written as

$$B^e(\mathbf{w}, \mathbf{u}) = l^e(\mathbf{w}) \tag{8.2.13}$$

where, in the present case, $\mathbf{w}$ is simply w and $\mathbf{u}$ is u. Next, we express $B^e(\cdot, \cdot)$ and $l^e(\cdot)$ in matrix form. Let

$$\mathbf{C} = \begin{bmatrix} a_{11} & a_{12} & 0 \\ a_{21} & a_{22} & 0 \\ 0 & 0 & a_{00} \end{bmatrix}, \quad \mathbf{D} = \begin{Bmatrix} \dfrac{\partial}{\partial x} \\ \dfrac{\partial}{\partial y} \\ 1 \end{Bmatrix} \tag{8.2.14}$$

Then B^e and l^e of (8.2.11b) can be expressed as

$$B^e(w,u)=\int_{\Omega_e}\begin{Bmatrix}\dfrac{\partial w}{\partial x}\\[2mm]\dfrac{\partial w}{\partial y}\\[2mm] w\end{Bmatrix}^{\mathrm{T}}\begin{bmatrix}a_{11}&a_{12}&0\\ a_{21}&a_{22}&0\\ 0&0&a_{00}\end{bmatrix}\begin{Bmatrix}\dfrac{\partial u}{\partial x}\\[2mm]\dfrac{\partial u}{\partial y}\\[2mm] u\end{Bmatrix}dx\,dy$$

$$l^e(w)=\int_{\Omega_e}\{w\}^{\mathrm{T}}\{f\}\,dx\,dy+\oint_{\Gamma_e}\{w\}^{\mathrm{T}}\{q_n\}\,ds \tag{8.2.15a}$$

or, simply

$$B^e(\mathbf{w},\mathbf{u})=\int_{\Omega_e}(\mathbf{Dw})^{\mathrm{T}}\mathbf{CDu}\,dx\,dy,\quad l^e(\mathbf{w})=\int_{\Omega_e}\mathbf{w}^{\mathrm{T}}\mathbf{f}\,dx\,dy+\int_{\Gamma_e}\mathbf{w}^{\mathrm{T}}\mathbf{q}\,ds \tag{8.2.15b}$$

8.2.4 Finite Element Model

The weak form in (8.2.10) requires that the approximation chosen for u should be at least linear in both x and y so that there are no terms in (8.2.10) that are identically zero. Since the primary variable is simply the function itself, the Lagrange family of interpolation functions is admissible.

Suppose that u is approximated over a typical finite element Ω_e by the expression

$$u(x,y)\approx u_h^e(x,y)=\sum_{j=1}^{n}u_j^e\psi_j^e(x,y)\ \text{ or }\ u_h^e(x,y)=(\Psi^e)^{\mathrm{T}}\mathbf{u}^e \tag{8.2.16a}$$

where $\mathbf{u}^e$ and Ψ^e are $n\times 1$ vectors

$$\mathbf{u}^e=\{u_1^e\ u_2^e\ u_3^e\ \ldots\ u_n^e\}^{\mathrm{T}},\quad \Psi^e=\{\psi_1^e\ \psi_2^e\ \psi_3^e\ \ldots\ \psi_n^e\}^{\mathrm{T}} \tag{8.2.16b}$$

and u_j^e is the value of u_h^e at the jth node (x_j, y_j) of the element and ψ_j^e are the Lagrange interpolation functions, with the property

$$\psi_i^e(x_j,y_j)=\delta_{ij}\quad (i,j=1,2,\ldots,n) \tag{8.2.17}$$

In deriving the finite element equations in algebraic terms, we need not know the shape of the element Ω_e or the form of ψ_i^e. The specific form of ψ_i^e will be developed for triangular and rectangular geometries of the element Ω_e in Section 8.2.5, and higher-order interpolation functions will be presented in Chapter 9.

Substituting the finite element approximation (8.2.16a) for u into the weak form (8.2.10) or (8.2.13), we obtain

$$0=\int_{\Omega_e}\left[\frac{\partial w}{\partial x}\left(a_{11}\sum_{j=1}^{n}u_j^e\frac{\partial\psi_j^e}{\partial x}+a_{12}\sum_{j=1}^{n}u_j^e\frac{\partial\psi_j^e}{\partial y}\right)+\frac{\partial w}{\partial y}\left(a_{21}\sum_{j=1}^{n}u_j^e\frac{\partial\psi_j^e}{\partial x}\right.\right.$$
$$\left.\left.+a_{22}\sum_{j=1}^{n}u_j^e\frac{\partial\psi_j^e}{\partial y}\right)+a_{00}w\sum_{j=1}^{n}u_j^e\psi_j^e-wf\right]dx\,dy-\oint_{\Gamma_e}wq_n\,ds \tag{8.2.18a}$$

or

$$0=\int_{\Omega_e}(\mathbf{Dw})^{\mathrm{T}}\mathbf{CD}\left(\Psi^{\mathrm{T}}\mathbf{u}^e\right)dx\,dy-\int_{\Omega_e}\mathbf{w}^{\mathrm{T}}\mathbf{f}\,dx\,dy-\oint_{\Gamma_e}\mathbf{w}^{\mathrm{T}}\mathbf{q}\,ds \tag{8.2.18b}$$

This equation must hold for every admissible choice of weight function w. Since we need n independent algebraic equations to solve for the n unknowns, $u_1^e, u_2^e, \ldots, u_n^e$, we choose n linearly independent functions for w: $w = \psi_1^e, \psi_2^e, \ldots, \psi_n^e$ (or, $\mathbf{w} = \{\psi_1^e \ \psi_2^e \ \ldots \ \psi_n^e\} = \Psi^{\mathrm{T}}$). This particular choice of weight function is a natural one when the weight function is viewed as a virtual variation of the dependent unknown (i.e., $w = \delta u \approx \sum_{i=1}^n \delta u_i \psi_i$), and the resulting finite element model is known as the *weak-form finite element model* or *Ritz finite element model*. For each choice of w we obtain an algebraic relation among $(u_1^e, u_2^e, \ldots, u_n^e)$. We label the algebraic equation resulting from substitution of ψ_1^e for w into (8.2.18a) as the first algebraic equation, that resulting from $w = \psi_2^e$ as the second equation, and so on. Thus, the ith algebraic equation is obtained by substituting $w = \psi_i^e$ into (8.2.18a):

$$0 = \sum_{j=1}^{n} \left\{ \int_{\Omega_e} \left[\frac{\partial \psi_i^e}{\partial x} \left(a_{11} \frac{\partial \psi_j^e}{\partial x} + a_{12} \frac{\partial \psi_j^e}{\partial y} \right) + \frac{\partial \psi_i^e}{\partial y} \left(a_{21} \frac{\partial \psi_j^e}{\partial x} + a_{22} \frac{\partial \psi_j^e}{\partial y} \right) + a_{00} \psi_i^e \psi_j^e \right] dx\, dy \right\} u_j - \int_{\Omega_e} f \psi_i^e \, dx\, dy - \oint_{\Gamma_e} \psi_i^e q_n \, ds$$

or

$$\sum_{j=1}^{n} K_{ij}^e u_j^e = f_i^e + Q_i^e \quad (i = 1, 2, \ldots, n) \tag{8.2.19a}$$

where

$$K_{ij}^e = \int_{\Omega_e} \left[\frac{\partial \psi_i^e}{\partial x} \left(a_{11} \frac{\partial \psi_j^e}{\partial x} + a_{12} \frac{\partial \psi_j^e}{\partial y} \right) + \frac{\partial \psi_i^e}{\partial y} \left(a_{21} \frac{\partial \psi_j^e}{\partial x} + a_{22} \frac{\partial \psi_j^e}{\partial y} \right) + a_{00} \psi_i^e \psi_j^e \right] dx\, dy \tag{8.2.19b}$$

$$f_i^e = \int_{\Omega_e} f \psi_i^e \, dx\, dy, \quad Q_i^e = \oint_{\Gamma_e} q_n \psi_i^e \, ds$$

In matrix notation, (8.2.19a) takes the form

$$[K^e]\{u^e\} = \{f^e\} + \{Q^e\} \quad \text{or} \quad \mathbf{K}^e \mathbf{u}^e = \mathbf{f}^e + \mathbf{Q}^e \tag{8.2.20a}$$

where [see Eq. (8.2.18b)]

$$\mathbf{K}^e = \int_{\Omega_e} \mathbf{B}^{\mathrm{T}} \mathbf{C} \mathbf{B} \, dx\, dy, \quad \mathbf{f}^e = \int_{\Omega_e} \Psi \mathbf{f} \, ds, \quad \mathbf{Q}^e = \int_{\Gamma_e} \Psi \mathbf{q} \, ds \tag{8.2.20b}$$

$$\mathbf{B} = \mathbf{D}\Psi^{\mathrm{T}} = \begin{bmatrix} \psi_{1,x}^e & \psi_{2,x}^e & \cdots & \psi_{n,x}^e \\ \psi_{1,y}^e & \psi_{2,y}^e & \cdots & \psi_{n,y}^e \\ \psi_1^e & \psi_2^e & \cdots & \psi_n^e \end{bmatrix}$$

Note that $K_{ij}^e = K_{ji}^e$ (i.e., $[K^e]$ is a symmetric matrix of order $n \times n$) only when $a_{12} = a_{21}$. Equations (8.2.20a) and (8.2.20b) represents the finite element model of (8.2.1). This completes the finite element model development. Before we discuss assembly of element equations, it is informative to consider the derivation of the interpolations ψ_i^e for certain basic elements and the evaluation of the element matrices in Eqs. (8.2.19b).

8.2.5 Derivation of Interpolation Functions

The finite element approximation $u_h^e(x, y)$ over an element Ω_e must satisfy the following conditions in order for the approximate solution to converge to the true solution:

1. u_h^e must be continuous as required in the weak form of the problem (i.e., all terms in the weak form are represented as nonzero values).
2. The polynomials used to represent u_h^e must be complete (i.e., all terms, beginning with a constant term up to the highest-order used in the polynomial, should be included in u_h^e).
3. All terms in the polynomial should be linearly independent.

The number of linearly independent terms in the representation of u_h^e dictates the shape and number of degrees of freedom of the element. Next, we discuss some of the basic polynomials and associated elements for the model problem with a single degree of freedom per node.

Triangular Element

An examination of the weak form (8.2.10) and the finite element matrices in (8.2.19*b*) shows that ψ_i^e should be at least linear functions of x and y. The complete linear polynomial in x and y in Ω_e is of the form

$$u_h^e(x, y) = c_1^e + c_2^e x + c_3^e y \tag{8.2.21}$$

where c_i^e are constants. The set $\{1, x, y\}$ is linearly independent and complete. Equation (8.2.21) defines a unique plane for fixed c_i^e. Thus, if $u(x, y)$ is a curved surface, $u_h^e(x, y)$ approximates the surface by a plane. In particular, $u_h^e(x, y)$ is uniquely defined on a triangle by the three values of $u_h^e(x, y)$ at the vertices of the triangle (see Fig. 8.2.2). Let us denote

$$u_h^e(x_1, y_1) = u_1^e, \quad u_h^e(x_2, y_2) = u_2^e, \quad u_h^e(x_3, y_3) = u_3^e \tag{8.2.22}$$

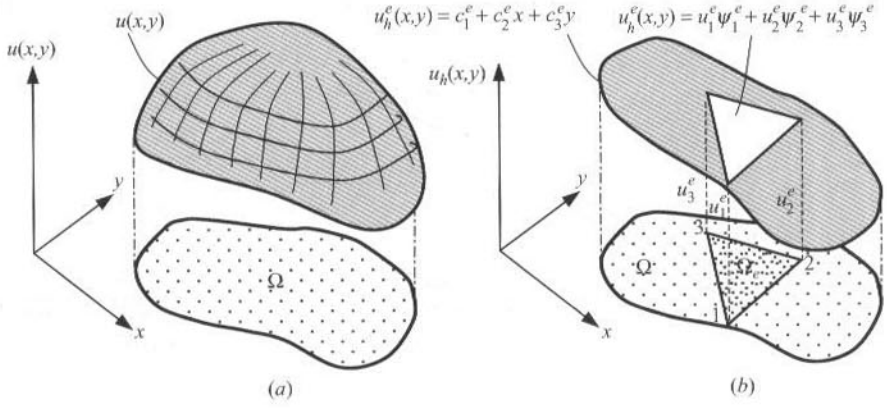

Figure 8.2.2 Approximation of a curved surface over a triangle by a plane.

where (x_i, y_i) denote the coordinates of the ith vertex of the triangle. Note that the triangle is uniquely defined by the three pairs of coordinates (x_i, y_i).

The three constants c_i^e $(i = 1, 2, 3)$ in (8.2.21) can be expressed in terms of three nodal values u_i^e $(i = 1, 2, 3)$. Thus, the polynomial (8.2.21) is associated with a triangular element and there are three nodes identified, namely, the vertices of the triangle. Equations in (8.2.22) have the explicit form

$$u_1 \equiv u_h(x_1, y_1) = c_1 + c_2 x_1 + c_3 y_1$$
$$u_2 \equiv u_h(x_2, y_2) = c_1 + c_2 x_2 + c_3 y_2$$
$$u_3 \equiv u_h(x_3, y_3) = c_1 + c_2 x_3 + c_3 y_3$$

where the element label e is omitted for simplicity. Throughout the following discussion, this format will be followed. In matrix form, we have

$$\begin{Bmatrix} u_1 \\ u_2 \\ u_3 \end{Bmatrix} = \begin{bmatrix} 1 & x_1 & y_1 \\ 1 & x_2 & y_2 \\ 1 & x_3 & y_3 \end{bmatrix} \begin{Bmatrix} c_1 \\ c_2 \\ c_3 \end{Bmatrix} \quad \text{or} \quad \mathbf{u} = \mathbf{A}\mathbf{c} \tag{8.2.23}$$

Solution of (8.2.23) for c_i $(i = 1, 2, 3)$ requires the inversion of the coefficient matrix $\mathbf{A}$ in (8.2.23). The inverse ceases to exist whenever any two rows or columns are the same. Two rows or columns of the coefficient matrix in (8.2.23) will be the same only when all three nodes lie on the same line. Thus, in theory, as long as the three vertices of the triangle are distinct and do not lie on a line, the coefficient matrix is invertible. However, in actual computations, if any two of the three nodes are *very close* to the third node or the three nodes are almost on the same line, the coefficient matrix can be *nearly singular* and numerically noninvertible. Hence, we should avoid elements with narrow geometries (see Fig. 8.2.3) in finite element meshes.

Inverting the coefficient matrix in (8.2.23), we obtain

$$[A]^{-1} = \frac{1}{2A} \begin{bmatrix} \alpha_1 & \alpha_2 & \alpha_3 \\ \beta_1 & \beta_2 & \beta_3 \\ \gamma_1 & \gamma_2 & \gamma_3 \end{bmatrix}, \quad 2A = \alpha_1 + \alpha_2 + \alpha_3$$

where $2A$ is the determinant of the matrix $\mathbf{A}$, A being the area of the triangle whose three vertices are at (x_i, y_i) $(i = 1, 2, 3)$. Solving for c_i in terms of u_i (i.e., $\{c\} = [A]^{-1}\{u\}$),

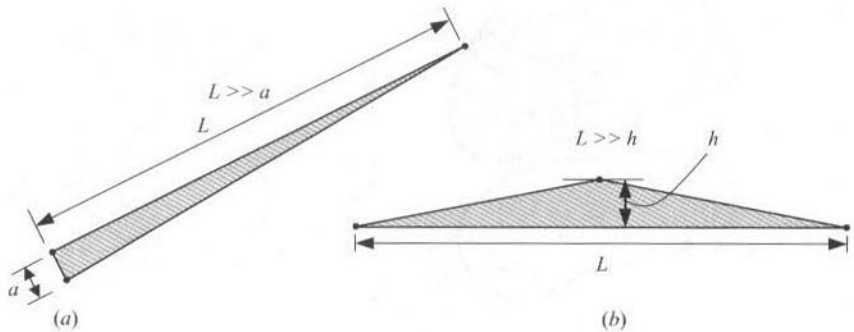

Figure 8.2.3 Triangular geometries that should be avoided in finite element meshes.

we obtain

$$c_1 = \frac{1}{2A}(\alpha_1 u_1 + \alpha_2 u_2 + \alpha_3 u_3)$$
$$c_2 = \frac{1}{2A}(\beta_1 u_1 + \beta_2 u_2 + \beta_3 u_3) \tag{8.2.24a}$$
$$c_3 = \frac{1}{2A}(\gamma_1 u_1 + \gamma_2 u_2 + \gamma_3 u_3)$$

where α_i, β_i, and γ_i are constants that depend only on the global coordinates of element nodes (x_i, y_i)

$$\left.\begin{aligned} \alpha_i &= x_j y_k - x_k y_j \\ \beta_i &= y_j - y_k \\ \gamma_i &= -(x_j - x_k) \end{aligned}\right\} \quad (i \neq j \neq k;\ i,\ j, \text{ and } k \text{ permute in a natural order}) \tag{8.2.24b}$$

Substituting for c_i from (8.2.24a) into (8.2.21), we obtain

$$\begin{aligned} u_h^e(x, y) &= \frac{1}{2A}[(u_1\alpha_1 + u_2\alpha_2 + u_3\alpha_3) + (u_1\beta_1 + u_2\beta_2 + u_3\beta_3)x \\ &\quad + (\gamma_1 u_1 + \gamma_2 u_2 + \gamma_3 u_3)y] \\ &= \sum_{i=1}^{3} u_i^e \psi_i^e(x, y) \end{aligned} \tag{8.2.25a}$$

where ψ_i^e are the linear interpolation functions for the triangular element

$$\psi_i^e = \frac{1}{2A_e}\left(\alpha_i^e + \beta_i^e x + \gamma_i^e y\right) \quad (i = 1, 2, 3) \tag{8.2.25b}$$

and α_i^e, β_i^e, and γ_i^e are the constants defined in (8.2.24b). The linear interpolation functions ψ_i^e are shown in Fig. 8.2.4.

The interpolation functions ψ_i^e have the properties

$$\psi_i^e\left(x_j^e, y_j^e\right) = \delta_{ij} \quad (i, j = 1, 2, 3) \tag{8.2.26a}$$

$$\sum_{i=1}^{3} \psi_i^e = 1, \quad \sum_{i=1}^{3} \frac{\partial \psi_i^e}{\partial x} = 0, \quad \sum_{i=1}^{3} \frac{\partial \psi_i^e}{\partial y} = 0 \tag{8.2.26b}$$

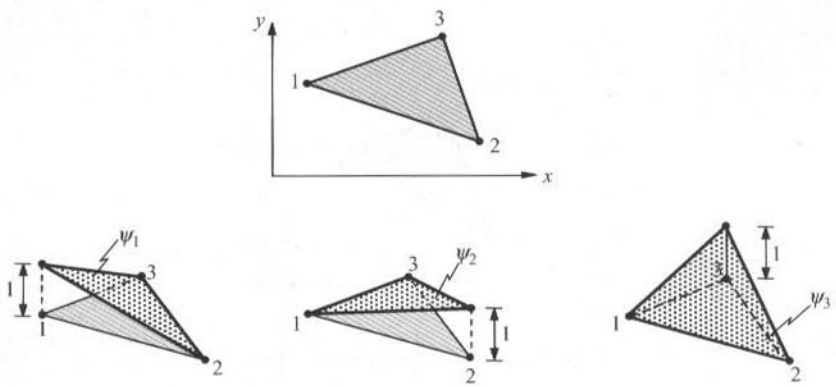

Figure 8.2.4 Interpolation functions for the three-node triangle.

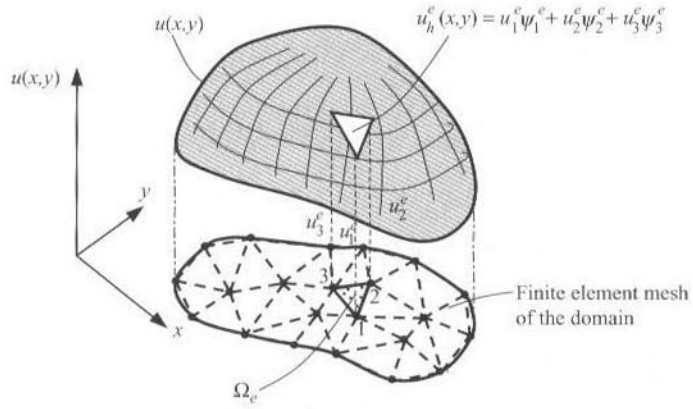

Figure 8.2.5 Representation of a continuous function $u(x, y)$ by linear interpolation functions of three-node triangular elements.

Note that (8.2.24*a*) determines a plane surface passing through u_1, u_2, and u_3. Hence, use of the linear interpolation functions ψ_i^e of a triangle will result in the approximation of the curved surface $u(x, y)$ by a planar function $u_h^e = \sum_{i=1}^{3} u_i^e \psi_i^e$ as shown in Fig. 8.2.5. We consider an example of computing ψ_i^e.

Example 8.2.1

Consider the triangular element shown in Fig. 8.2.6. Let

$$u_h(x, y) = c_1 + c_2 x + c_3 y = \{1 \; x \; y\} \begin{Bmatrix} c_1 \\ c_2 \\ c_3 \end{Bmatrix}$$

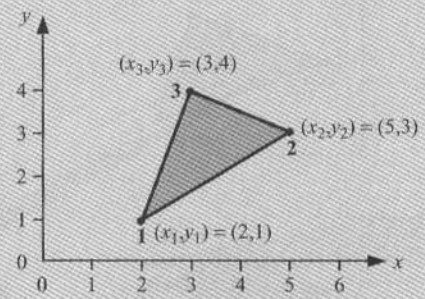

Figure 8.2.6 The triangular element of Example 8.2.1.

Evaluating this polynomial at nodes 1, 2, and 3, we obtain the equations

$$\begin{Bmatrix} u_1 \\ u_2 \\ u_3 \end{Bmatrix} = \begin{bmatrix} 1 & 2 & 1 \\ 1 & 5 & 3 \\ 1 & 3 & 4 \end{bmatrix} \begin{Bmatrix} c_1 \\ c_2 \\ c_3 \end{Bmatrix}, \quad \begin{Bmatrix} c_1 \\ c_2 \\ c_3 \end{Bmatrix} = [A]^{-1} \begin{Bmatrix} u_1 \\ u_2 \\ u_3 \end{Bmatrix}$$

where

$$[A]^{-1} = \begin{bmatrix} 1 & 2 & 1 \\ 1 & 5 & 3 \\ 1 & 3 & 4 \end{bmatrix}^{-1} = \frac{1}{7} \begin{bmatrix} 11 & -5 & 1 \\ -1 & 3 & -2 \\ -2 & -1 & 3 \end{bmatrix}$$

Substituting the last expression into u_h, we obtain

$$u_h(x, y) = \{1 \quad x \quad y\}[A]^{-1} \begin{Bmatrix} u_1 \\ u_2 \\ u_3 \end{Bmatrix} = \frac{1}{7}\{11 - x - 2y, \quad -5 + 3x - y, \quad 1 - 2x + 3y\} \begin{Bmatrix} u_1 \\ u_2 \\ u_3 \end{Bmatrix}$$

$$\equiv \{\psi_1^e \quad \psi_2^e \quad \psi_3^e\} \begin{Bmatrix} u_1 \\ u_2 \\ u_3 \end{Bmatrix} = \sum_{i=1}^{3} \psi_i^e u_i^e$$

where

$$\psi_1^e = \frac{1}{7}(11 - x - 2y), \quad \psi_2^e = \frac{1}{7}(-5 + 3x - y), \quad \psi_3^e = \frac{1}{7}(1 - 2x + 3y)$$

Alternatively, from definitions (8.2.24*b*), we have

$$\alpha_1 = 5 \times 4 - 3 \times 3 = 11, \quad \alpha_2 = 3 \times 1 - 2 \times 4 = -5, \quad \alpha_3 = 2 \times 3 - 5 \times 1 = 1$$

$$\beta_1 = 3 - 4 = -1, \quad \beta_2 = 4 - 1 = 3, \quad \beta_3 = 1 - 3 = -2$$

$$\gamma_1 = -(5 - 3) = -2, \quad \gamma_2 = -(3 - 2) = -1, \quad \gamma_3 = -(2 - 5) = 3$$

$$2A = \alpha_1 + \alpha_2 + \alpha_3 = 7$$

The interpolation functions are

$$\psi_1^e = \frac{1}{7}(11 - x - 2y), \quad \psi_2^e = \frac{1}{7}(-5 + 3x - y), \quad \psi_3^e = \frac{1}{7}(1 - 2x + 3y)$$

which are the same as those obtained earlier.

Linear Rectangular Element

Next, consider the complete polynomial

$$u_h^e(x, y) = c_1^e + c_2^e x + c_3^e y + c_4^e xy \tag{8.2.27}$$

which contains four linearly independent terms and is linear in x and y, with a bilinear term in x and y. This polynomial requires an element with four nodes. There are two possible geometric shapes: a triangle with the fourth node at the center (or centroid) of the triangle or

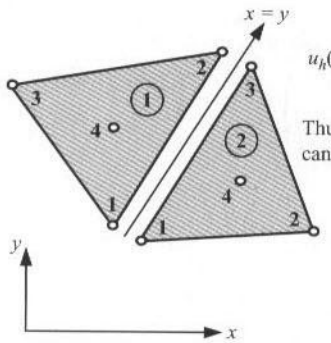

$$u_h(x,y) = c_1^{(e)} + c_2^{(e)}x + c_3^{(e)}y + c_4^{(e)}xy$$
$$= c_1^{(e)} + \left(c_2^{(e)} + c_3^{(e)}\right)x + c_4^{(e)}x^2 \quad (e = 1,2)$$

Thus, the quadratic variation of u_h along $x = y$ cannot be defined uniquely with only two nodal values.

Figure 8.2.7 Incompatible four-node triangular elements.

a rectangle with the nodes at the vertices. A triangle with a fourth node at the center does not provide a single-valued variation of u at interelement boundaries, resulting in *incompatible* variation of u at interelement boundaries and is therefore not admissible (see Fig. 8.2.7). The linear rectangular element is a compatible element because on any side u_h^e varies only linearly and there are two nodes to uniquely define it.

Here we consider an approximation of the form (8.2.27) and use a rectangular element with sides a and b [see Fig. 8.2.8(*a*)]. For the sake of convenience, we choose a local coordinate system $(\bar{x}, \bar{y})$ to derive the interpolation functions. We assume that (the element label is omitted)

$$u_h(\bar{x}, \bar{y}) = c_1 + c_2\bar{x} + c_3\bar{y} + c_4\bar{x}\bar{y} \tag{8.2.28}$$

and require

$$\begin{aligned} u_1 &= u_h(0,0) = c_1 \\ u_2 &= u_h(a,0) = c_1 + c_2 a \\ u_3 &= u_h(a,b) = c_1 + c_2 a + c_3 b + c_4 ab \\ u_4 &= u_h(0,b) = c_1 + c_3 b \end{aligned} \tag{8.2.29}$$

Solving for c_i $(i = 1, \ldots, 4)$, we obtain

$$\begin{aligned} c_1 &= u_1, & c_2 &= \frac{u_2 - u_1}{a} \\ c_3 &= \frac{u_4 - u_1}{b}, & c_4 &= \frac{u_3 - u_4 + u_1 - u_2}{ab} \end{aligned} \tag{8.2.30}$$

Substituting (8.2.30) into (8.2.28), we obtain

$$u_h(\bar{x}, \bar{y}) = u_1\left(1 - \frac{\bar{x}}{a} - \frac{\bar{y}}{b} + \frac{\bar{x}}{a}\frac{\bar{y}}{b}\right) + u_2\left(\frac{\bar{x}}{a} - \frac{\bar{x}}{a}\frac{\bar{y}}{b}\right) + u_3\frac{\bar{x}}{a}\frac{\bar{y}}{b} + u_4\left(\frac{\bar{y}}{b} - \frac{\bar{x}}{a}\frac{\bar{y}}{b}\right)$$

$$= u_1^e\psi_1^e + u_2^e\psi_2^e + u_3^e\psi_3^e + u_4^e\psi_4^e = \sum_{i=1}^{4} u_i^e\psi_i^e \tag{8.2.31}$$

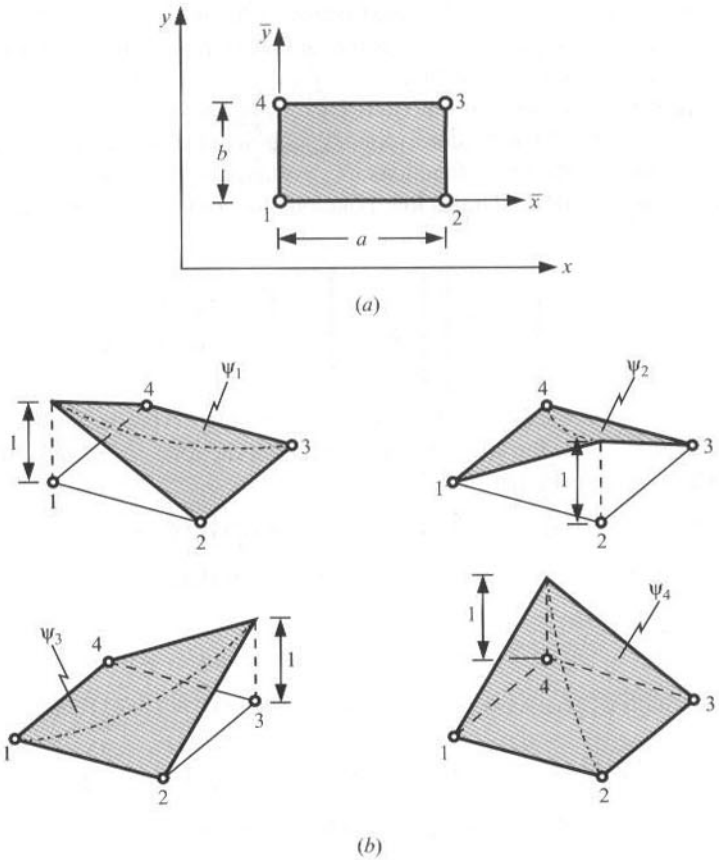

Figure 8.2.8 Linear rectangular element and its interpolation functions.

where

$$\psi_1^e = \left(1 - \frac{\bar{x}}{a}\right)\left(1 - \frac{\bar{y}}{b}\right), \quad \psi_2^e = \frac{\bar{x}}{a}\left(1 - \frac{\bar{y}}{b}\right)$$
$$\psi_3^e = \frac{\bar{x}}{a}\frac{\bar{y}}{b}, \quad \psi_4^e = \left(1 - \frac{\bar{x}}{a}\right)\frac{\bar{y}}{b} \tag{8.2.32a}$$

or, in concise form,

$$\psi_i^e(\bar{x}, \bar{y}) = (-1)^{i+1}\left(1 - \frac{\bar{x} + \bar{x}_i}{a}\right)\left(1 - \frac{\bar{y} + \bar{y}_i}{b}\right) \tag{8.2.32b}$$

where $(\bar{x}_i, \bar{y}_i)$ are the $(\bar{x}, \bar{y})$ coordinates of node i. The interpolation functions are shown in Fig. 8.2.8(b). Once again, we have

$$\psi_i^e(\bar{x}_j, \bar{y}_j) = \delta_{ij} \quad (i, j = 1, \ldots, 4), \quad \sum_{i=1}^{4} \psi_i^e = 1 \tag{8.2.33}$$

The procedure given above for the construction of the interpolation functions involves the inversion of an $n \times n$ matrix, where n is the number of nodes in the element. When n is large, the inversion becomes very tedious.

Alternatively, the interpolation functions for rectangular element can also be obtained by taking the tensor product of the corresponding one-dimensional interpolation functions. To obtain the linear interpolation functions of a rectangular element, we take the "tensor product" of the one-dimensional linear interpolation functions (3.2.19) associated with sides 1–2 and 1–3:

$$\begin{Bmatrix} 1 - \dfrac{\bar{x}}{a} \\ \dfrac{\bar{x}}{a} \end{Bmatrix} \begin{Bmatrix} 1 - \dfrac{\bar{y}}{b} \\ \dfrac{\bar{y}}{b} \end{Bmatrix}^{\mathrm{T}} = \begin{bmatrix} \psi_1 & \psi_4 \\ \psi_2 & \psi_3 \end{bmatrix} \tag{8.2.34}$$

The alternative procedure that makes use of the interpolation properties (8.2.33) can also be used. Here we illustrate the alternative procedure for the four-node rectangular element. Equation (8.2.26a) requires that

$$\psi_1^e(\bar{x}_i, \bar{y}_i) = 0 \quad (i = 2, 3, 4), \qquad \psi_1^e(\bar{x}_1, \bar{y}_1) = 1$$

That is, ψ_1^e is identically zero on lines $\bar{x} = a$ and $\bar{y} = b$. Hence, $\psi_1^e(\bar{x}, \bar{y})$ must be of the form

$$\psi_1^e(\bar{x}, \bar{y}) = c_1(a - \bar{x})(b - \bar{y}) \quad \text{for any } c_1 \neq 0$$

Using the condition $\psi_1^e(\bar{x}_1, \bar{y}_1) = \psi_1^e(0, 0) = 1$, we obtain $c_1 = 1/ab$. Hence,

$$\psi_1^e(\bar{x}, \bar{y}) = \frac{1}{ab}(a - \bar{x})(b - \bar{y}) = \left(1 - \frac{\bar{x}}{a}\right)\left(1 - \frac{\bar{y}}{b}\right)$$

Likewise, we can obtain the remaining three interpolation functions.

Quadratic Elements

A quadratic triangular element must have three nodes per side in order to define a unique quadratic variation along that side. Thus, there are a total of six nodes in a quadratic triangular element [see Fig. 8.2.9(a)]. A six-term complete polynomial that includes both x and y is

$$u_h^e(x, y) = c_1 + c_2 x + c_3 y + c_4 xy + c_5 x^2 + c_6 y^2 \tag{8.2.35}$$

The constants may be expressed in terms of the six nodal values by the procedure outlined for the three-node triangular element and four-node rectangular element. However, in practice the interpolation functions of higher-order elements are derived using the alternative procedure (i.e., use the interpolation properties).

Similarly, a quadratic rectangular element has three nodes per side, resulting in an eight-node rectangular element [see Fig. 8.2.9(b)]. The eight-term polynomial is

$$u_h^e(x, y) = c_1 + c_2 x + c_3 y + c_4 xy + c_5 x^2 + c_6 y^2 + c_7 xy^2 + c_8 yx^2 \tag{8.2.36}$$

The interpolation functions of this element cannot be generated by the tensor product of one-dimensional quadratic functions (3.2.27). Indeed, the two-dimensional interpolation functions associated with the tensor product of one-dimensional quadratic functions correspond to the nine-node rectangular element [see Fig. 8.2.9(c)]. The nine-term polynomial

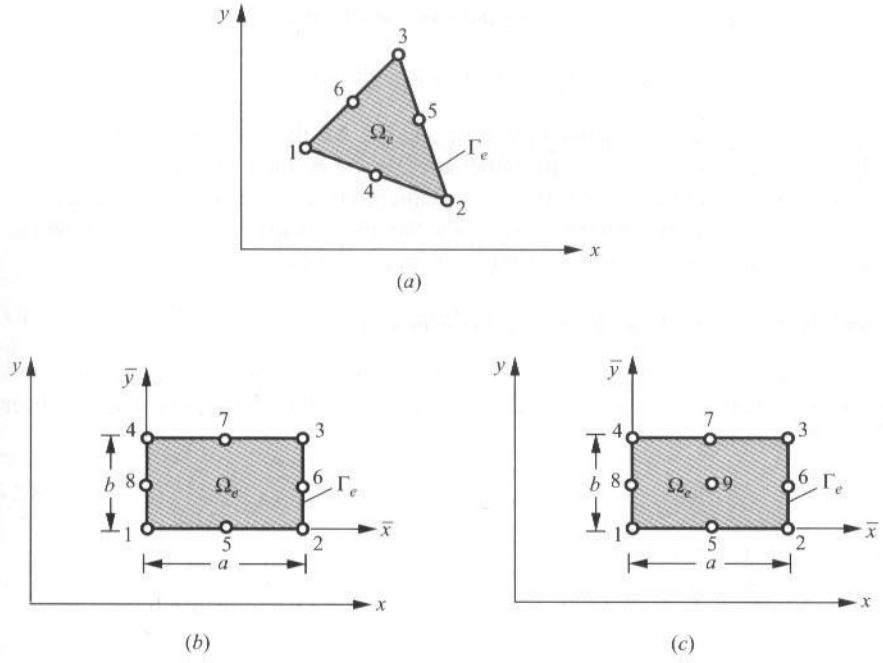

Figure 8.2.9 (*a*) Quadratic triangular element. (*b*) Eight-node quadratic rectangular element. (*c*) Nine-node quadratic rectangular element.

is given by

$$u_h^e(x, y) = c_1 + c_2x + c_3y + c_4xy + c_5x^2 + c_6y^2 + c_7xy^2 + c_8yx^2 + c_9x^2y^2 \quad (8.2.37)$$

Additional discussion on the derivation of element interpolation functions is presented in Chapter 9.

8.2.6 Evaluation of Element Matrices and Vectors

The exact evaluation of the element matrices $[K^e]$ and $\{f^e\}$ in (8.2.19*b*) is, in general, not easy. In general, they are evaluated using numerical integration techniques described in Section 9.3. However, when a_{ij}, a_{00}, and f are elementwise constant, it is possible to evaluate the integrals exactly over the linear triangular and rectangular elements discussed in the previous section. The boundary integral in $\{Q^e\}$ of (8.2.19*b*) can be evaluated whenever q_n is known. For an interior element (i.e., an element that does not have any of its sides on the boundary of the problem), the contribution from the boundary integral cancels with similar contributions from adjoining elements of the mesh (analogous to the Q_i^e in the one-dimensional problems). A more detailed discussion is given below.

For the sake of brevity, we rewrite $[K^e]$ in (8.2.19*b*) as the sum of five basic matrices $[S^{\alpha\beta}](\alpha, \beta = 0, 1, 2)$

$$[K^e] = a_{00}[S^{00}] + a_{11}[S^{11}] + a_{12}[S^{12}] + a_{21}[S^{12}]^T + a_{22}[S^{22}] \quad (8.2.38)$$

where $[\cdot]^{\mathrm{T}}$ denotes the transpose of the enclosed matrix, and

$$S_{ij}^{\alpha\beta} = \int_{\Omega_e} \psi_{i,\alpha} \psi_{j,\beta} \, dx \, dy \tag{8.2.39}$$

with $\psi_{i,\alpha} \equiv \partial \psi_i / \partial x_\alpha$, $x_1 = x$, and $x_2 = y$; $\psi_{i,0} = \psi_i$. All the matrices in (8.2.38) and interpolation functions in (8.2.39) are understood to be defined over an element, i.e., all expressions and quantities should have the element label e, but these are omitted in the interest of brevity. We now proceed to compute the matrices in (8.2.39) and (8.2.19*b*) using the linear interpolation functions derived in the previous section.

Element Matrices of a Linear Triangular Element

First, we note that integrals of polynomials over arbitrary shaped triangular domains can be evaluated exactly. To this end, let I_{mn} denote the integral of the expression $x^m y^n$ over an arbitrary triangle Δ

$$I_{mn} \equiv \int_\Delta x^m y^n \, dx \, dy \tag{8.2.40}$$

Then, it can be shown that

$$\begin{aligned}
I_{00} &= \int_\Delta x^0 y^0 \, dx \, dy = \int_\Delta 1 \cdot dx \, dy = A \quad \text{area of the triangle} \\
I_{10} &= \int_\Delta x^1 y^0 \, dx \, dy = \int_\Delta x \, dx \, dy = A\hat{x}, \quad \hat{x} = \frac{1}{3} \sum_{i=1}^{3} x_i \\
I_{01} &= \int_\Delta x^0 y^1 \, dx \, dy = \int_\Delta y \, dx \, dy = A\hat{y}, \quad \hat{y} = \frac{1}{3} \sum_{i=1}^{3} y_i \\
I_{11} &= \int_\Delta xy \, dx \, dy = \frac{A}{12} \left(\sum_{i=1}^{3} x_i y_i + 9\hat{x}\hat{y} \right) \\
I_{20} &= \int_\Delta x^2 \, dx \, dy = \frac{A}{12} \left(\sum_{i=1}^{3} x_i^2 + 9\hat{x}^2 \right) \\
I_{02} &= \int_\Delta y^2 \, dx \, dy = \frac{A}{12} \left(\sum_{i=1}^{3} y_i^2 + 9\hat{y}^2 \right)
\end{aligned} \tag{8.2.41}$$

where (x_i, y_i) are the coordinates of the vertices of the triangle. We can use the above results to evaluate integrals defined over triangular elements.

Next, we evaluate $[K^e]$ and $\{f^e\}$ for linear triangular element under the assumption that a_{ij} and f are elementwise constant. Also, note that (see Problem 8.1)

$$\sum_{i=1}^{3} \alpha_i^e = 2A_e, \quad \sum_{i=1}^{3} \beta_i^e = 0, \quad \sum_{i=1}^{3} \gamma_i^e = 0 \tag{8.2.42a}$$

$$\alpha_i^e + \beta_i^e \hat{x}_e + \gamma_i^e \hat{y}_e = \frac{2}{3} A_e \tag{8.2.42b}$$

$$\frac{\partial \psi_i}{\partial x} = \frac{\beta_i^e}{2A_e}, \quad \frac{\partial \psi_i}{\partial y} = \frac{\gamma_i^e}{2A_e} \tag{8.2.43}$$

we obtain

$$S_{ij}^{11} = \frac{1}{4A}\beta_i\beta_j, \quad S_{ij}^{12} = \frac{1}{4A}\beta_i\gamma_j, \quad S_{ij}^{22} = \frac{1}{4A}\gamma_i\gamma_j$$

$$S_{ij}^{00} = \frac{1}{4A}\left\{[\alpha_i\alpha_j + (\alpha_i\beta_j + \alpha_j\beta_i)\hat{x} + (\alpha_i\gamma_j + \alpha_j\gamma_i)\hat{y}]\right. \tag{8.2.44}$$

$$\left. + \frac{1}{A}[I_{20}\beta_i\beta_j + I_{11}(\gamma_i\beta_j + \gamma_j\beta_i) + I_{02}\gamma_i\gamma_j]\right\}$$

In view of the identity (8.2.42*b*) and for an elementwise constant value of $f = f_e$, we have

$$\begin{aligned} f_i^e &= \int_{\Delta_e} f_e\psi_i^e(x, y)\, dx\, dy = \frac{f_e}{2A_e}\int_{\Delta_e}\left(\alpha_i^e + \beta_i^e x + \gamma_i^e y\right) dx\, dy \\ &= \frac{f_e}{2A_e}\left(\alpha_i^e I_{00} + \beta_i^e I_{10} + \gamma_i^e I_{01}\right) \\ &= \frac{f_e}{2A_e}\left(\alpha_i^e A_e + \beta_i^e A_e\hat{x}_e + \gamma_i^e A_e\hat{y}_e\right) \\ &= \frac{1}{2}f_e\left(\alpha_i^e + \beta_i^e\hat{x}_e + \gamma_i^e\hat{y}_e\right) = \frac{1}{3}f_e A_e \end{aligned} \tag{8.2.45}$$

The result in (8.2.45) should be obvious because for a constant source f_e the total magnitude of the source (say, heat) on the element is equal to $f_e A_e$, which is then distributed equally among the three nodes, giving a nodal value of $f_e A_e/3$.

Once the coordinates of the element nodes are known, we can compute α_i^e, β_i^e, and γ_i^e from (8.2.24*b*) and substitute into (8.2.44) to obtain the element matrices, which in turn can be used in (8.2.38) to obtain the element matrix $[K^e]$. In particular, when a_{12}, a_{21}, and a_{00} are zero and a_{11} and a_{22} are elementwise constant, Eq. (8.2.1) becomes

$$-\left(a_{11}\frac{\partial^2 u}{\partial x^2} + a_{22}\frac{\partial^2 u}{\partial y^2}\right) - f = 0 \text{ in } \Omega_e \tag{8.2.46}$$

and the associated element coefficient matrix for a linear triangular element is

$$K_{ij}^e = \frac{1}{4A_e}\left(a_{11}^e\beta_i^e\beta_j^e + a_{22}^e\gamma_i^e\gamma_j^e\right) \tag{8.2.47}$$

Example 8.2.2

Consider the right-angle triangle shown in Fig. 8.2.10(*a*). We wish to determine the element coefficient matrix $[K^e]$ of (8.2.47) and source vector $\{f^e\}$ associated with the Poisson equation (8.2.46). We note that the element calculations do not depend on the global coordinate system (x, y). Therefore, we choose the local coordinate system $(\bar{x}, \bar{y})$ to compute A, α, β, and γ for

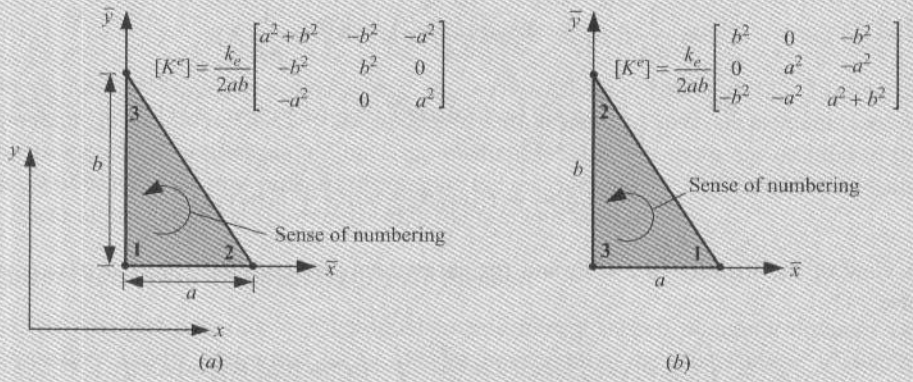

Figure 8.2.10 The right-angle linear triangular element of Example 8.2.2.

the element. We have

$$2A = ab, \quad \alpha_1 = ab, \quad \alpha_2 = 0, \quad \alpha_3 = 0, \quad \beta_1 = -b, \quad \beta_2 = b, \quad \beta_3 = 0, \quad \gamma_1 = -a, \quad \gamma_2 = 0, \quad \gamma_3 = a$$

$$\psi_1 = 1 - \frac{\bar{x}}{a} - \frac{\bar{y}}{b}, \quad \psi_2 = \frac{\bar{x}}{a}, \quad \psi_3 = \frac{\bar{y}}{b}$$

and

$$[K^e] = \frac{a_{11}^e}{2ab}\begin{bmatrix} b^2 & -b^2 & 0 \\ -b^2 & b^2 & 0 \\ 0 & 0 & 0 \end{bmatrix} + \frac{a_{22}^e}{2ab}\begin{bmatrix} a^2 & 0 & -a^2 \\ 0 & 0 & 0 \\ -a^2 & 0 & a^2 \end{bmatrix}, \quad \{f^e\} = \frac{f_e ab}{6}\begin{Bmatrix} 1 \\ 1 \\ 1 \end{Bmatrix} \tag{8.2.48}$$

If $a_{11}^e = a_{22}^e = k_e$, for the numbering system shown in Fig. 8.2.10(a), we have

$$[K^e] = \frac{k_e}{2ab}\begin{bmatrix} b^2+a^2 & -b^2 & -a^2 \\ -b^2 & b^2 & 0 \\ -a^2 & 0 & a^2 \end{bmatrix}, \quad \{f^e\} = \frac{f_e ab}{6}\begin{Bmatrix} 1 \\ 1 \\ 1 \end{Bmatrix} \tag{8.2.49}$$

In addition, if $a = b$, we have

$$[K^e] = \frac{k_e}{2}\begin{bmatrix} 2 & -1 & -1 \\ -1 & 1 & 0 \\ -1 & 0 & 1 \end{bmatrix}, \quad \{f^e\} = \frac{f_e a^2}{6}\begin{Bmatrix} 1 \\ 1 \\ 1 \end{Bmatrix} \tag{8.2.50}$$

We note that contents of $[K^e]$ depend, even for the same geometry, on the node numbering scheme, as shown in Figs. 8.2.10(a) and 8.2.10(b). For the same element, if the node numbering is changed, the element coefficients will change accordingly. For example, if we renumber the element nodes of the element in Fig. 8.2.10(a) to be those in Fig. 8.2.10(b), then $[K^e]$ for the element in Fig. 8.2.10(b) is obtained from (8.2.49) [which corresponds to the element numbering in Fig. 8.2.10(a)] by moving rows and columns $1 \to 3$, $3 \to 2$, and $2 \to 1$ (if the first row and column are moved after the third row and column, the last two

moves are automatic):

$$\frac{k_e}{2ab}\begin{bmatrix} b^2+a^2 & -b^2 & -a^2 \\ -b^2 & b^2 & 0 \\ -a^2 & 0 & a^2 \end{bmatrix} \to \frac{k_e}{2ab}\begin{bmatrix} -b^2 & -a^2 & b^2+a^2 \\ b^2 & 0 & -b^2 \\ 0 & a^2 & -a^2 \end{bmatrix} \to \frac{k_e}{2ab}\begin{bmatrix} b^2 & 0 & -b^2 \\ 0 & a^2 & -a^2 \\ -b^2 & -a^2 & b^2+a^2 \end{bmatrix}$$

In addition, all elements with the same geometry and node numbering, irrespective of their orientation (i.e., rigid body rotation about an axis perpendicular to the plane of the element), have the same coefficient matrix. Elements with the same coefficient matrix are listed in Fig. 8.2.11. For uniformity, we fix the sign convention and use counterclockwise numbering scheme for the element nodes.

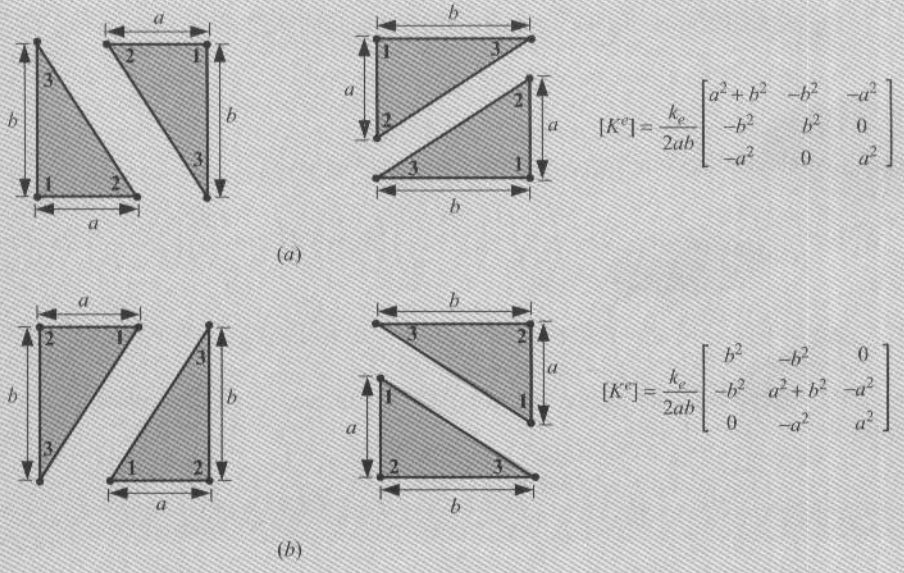

Figure 8.2.11 Coefficient matrices associated with Eq. (8.2.46) with $a_{11}^e = a_{22}^e = k_e$ for two different element node numbers of linear right-angle triangular elements.

Element Matrices of a Linear Rectangular Element

When the data a_{ij} $(i, j = 0, 1, 2)$ and f of the problem is not a function of x and y, we can use the interpolation functions in (8.2.32a), expressed in the local coordinates $(\bar{x}, \bar{y})$ that are mere translation of (x, y) (see Fig. 8.2.12), to compute the element coefficients $S_{ij}^{\alpha\beta}$ $(\alpha, \beta = 1, 2)$ of Eq. (8.2.39). For example, we have

$$S_{ij}^{00} = \int_{\Omega_e} \psi_i(x, y)\psi_j(x, y)\, dx\, dy = \int_0^a \int_0^b \psi_i \psi_j\, d\bar{x}\, d\bar{y}$$

where a and b are the lengths along the $\bar{x}$ and $\bar{y}$ axes of the element. Since the integration with respect to $\bar{x}$ and $\bar{y}$ can be carried out independent of each other, integration over a

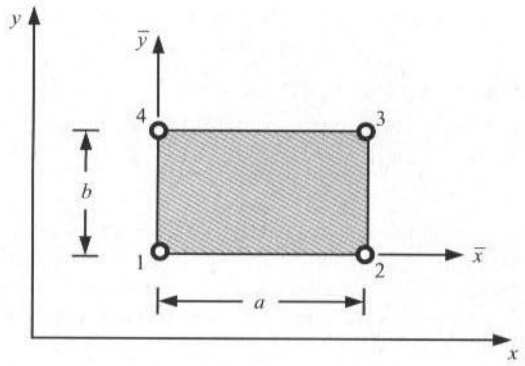

Figure 8.2.12 A rectangular element with the global and local coordinate systems.

rectangular element becomes a pair of line integrals. We have

$$S_{11}^{00} = \int_0^a \int_0^b \psi_1 \psi_1 \, d\bar{x} \, d\bar{y} = \int_0^a \int_0^b \left(1 - \frac{\bar{x}}{a}\right)\left(1 - \frac{\bar{y}}{b}\right)\left(1 - \frac{\bar{x}}{a}\right)\left(1 - \frac{\bar{y}}{b}\right) d\bar{x} \, d\bar{y}$$

$$= \int_0^a \left(1 - \frac{\bar{x}}{a}\right)^2 d\bar{x} \int_0^b \left(1 - \frac{\bar{y}}{b}\right)^2 d\bar{y} = \frac{a}{3}\frac{b}{3} = \frac{ab}{9}$$

Similarly, we can evaluate all the matrices $[S^{\alpha\beta}]$ with the aid of the following integral identities:

$$\int_0^a \left(1 - \frac{s}{a}\right) ds = \frac{a}{2}, \quad \int_0^a \frac{s}{a} \, ds = \frac{a}{2}$$

$$\int_0^a \left(1 - \frac{s}{a}\right)^2 ds = \frac{a}{3}, \quad \int_0^a \frac{s}{a}\left(1 - \frac{s}{a}\right) ds = \frac{a}{6}, \quad \int_0^a \left(\frac{s}{a}\right)^2 ds = \frac{a}{3} \tag{8.2.51}$$

In summary, the element matrices $[S^{\alpha\beta}]$ for a rectangular element are

$$[S^{11}] = \frac{b}{6a}\begin{bmatrix} 2 & -2 & -1 & 1 \\ -2 & 2 & 1 & -1 \\ -1 & 1 & 2 & -2 \\ 1 & -1 & -2 & 2 \end{bmatrix}, \quad [S^{12}] = \frac{1}{4}\begin{bmatrix} 1 & 1 & -1 & -1 \\ -1 & -1 & 1 & 1 \\ -1 & -1 & 1 & 1 \\ 1 & 1 & -1 & -1 \end{bmatrix}$$

$$[S^{22}] = \frac{a}{6b}\begin{bmatrix} 2 & 1 & -1 & -2 \\ 1 & 2 & -2 & -1 \\ -1 & -2 & 2 & 1 \\ -2 & -1 & 1 & 2 \end{bmatrix}, \quad [S^{00}] = \frac{ab}{36}\begin{bmatrix} 4 & 2 & 1 & 2 \\ 2 & 4 & 2 & 1 \\ 1 & 2 & 4 & 2 \\ 2 & 1 & 2 & 4 \end{bmatrix} \tag{8.2.52}$$

$$\{f\} = \frac{1}{4} f_e ab \{1 \quad 1 \quad 1 \quad 1\}^{\mathrm{T}}$$

Example 8.2.3

Here, we wish to determine the element coefficient matrix $[K^e]$ associated with the Poisson equation (8.2.46) over a linear rectangular element. We have

$$[K^e] = a_{11}^e [S^{11}] + a_{22}^e [S^{22}]$$

or

$$[K^e] = \frac{a_{11}^e b}{6a} \begin{bmatrix} 2 & -2 & -1 & 1 \\ -2 & 2 & 1 & -1 \\ -1 & 1 & 2 & -2 \\ 1 & -1 & -2 & 2 \end{bmatrix} + \frac{a_{22}^e a}{6b} \begin{bmatrix} 2 & 1 & -1 & -2 \\ 1 & 2 & -2 & -1 \\ -1 & -2 & 2 & 1 \\ -2 & -1 & 1 & 2 \end{bmatrix} \tag{8.2.53}$$

Note that the coefficient matrix is a function of both element aspect ratios a/b and b/a. Therefore, elements with very large aspect ratios should not be used as they will result in an ill-conditioned matrix (i.e., very large numbers are added to very small numbers), where either $[S^{11}]$ or $[S^{22}]$ will dominate the element matrix.

For $a_{11}^e = a_{22}^e = k_e$, the element coefficient matrix becomes

$$[K^e] = \frac{k_e}{6ab} \begin{bmatrix} 2(a^2+b^2) & a^2-2b^2 & -(a^2+b^2) & b^2-2a^2 \\ a^2-2b^2 & 2(a^2+b^2) & b^2-2a^2 & -(a^2+b^2) \\ -(a^2+b^2) & b^2-2a^2 & 2(a^2+b^2) & a^2-2b^2 \\ b^2-2a^2 & -(a^2+b^2) & a^2-2b^2 & 2(a^2+b^2) \end{bmatrix} \tag{8.2.54}$$

When the element aspect ratio is $a/b = 1$, the coefficient matrix in Eq. (8.2.54) becomes

$$[K^e] = \frac{k_e}{6} \begin{bmatrix} 4 & -1 & -2 & -1 \\ -1 & 4 & -1 & -2 \\ -2 & -1 & 4 & -1 \\ -1 & -2 & -1 & 4 \end{bmatrix} \tag{8.2.55}$$

Evaluation of Boundary Integrals

Here, we consider the evaluation of boundary integrals of the type [see Eq. (8.2.19*b*)]

$$Q_i^e = \oint_{\Gamma_e} q_n^e \psi_i^e(s)\, ds \tag{8.2.56}$$

where q_n^e is a known function of the distance s along the boundary Γ_e. It is not necessary to compute such integrals when a portion of Γ_e does not coincide with the boundary Γ of the total domain Ω [see Fig. 8.2.13(*a*)]. On portions of Γ_e that are in the interior of the domain Ω, q_n^e on side (i, j) of element Ω_e cancels with q_n^f on side (p, q) of element Ω_f when sides (i, j) of element Ω_e and (p, q) of element Ω_f are the same (i.e., at the interface of elements Ω_e and Ω_f). This can be viewed as the equilibrium of the internal "flux" [see Fig. 8.2.13(*b*)]. When Γ_e falls on the boundary of the domain Ω, q_n is either known as a function of s [see Fig. 8.2.13(*c*)] or to be determined in the postcomputation. The primary variable must be specified on the portion of the boundary where q_n is not specified.

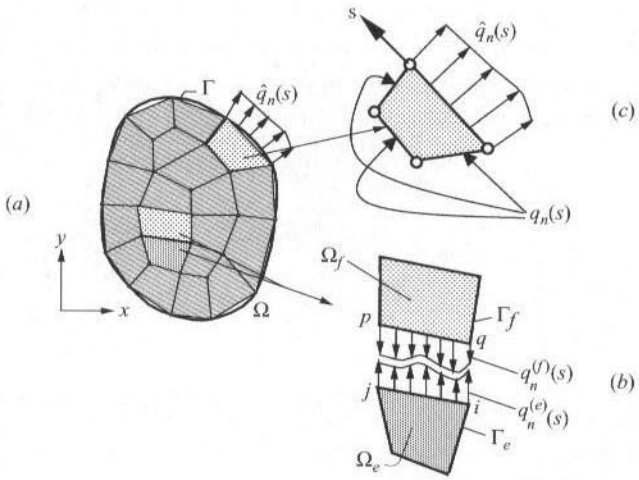

Figure 8.2.13 (*a*) Finite element discretization. (*b*) Equilibrium of fluxes at element interfaces. (*c*) Computation of forces on the boundary of the total domain.

The boundary Γ_e of a two-dimensional element consist of line segments, which can be viewed as one-dimensional elements. Thus, the evaluation of the boundary integrals on two-dimensional problems amounts to evaluating line integrals. It should not be surprising that when two-dimensional interpolation functions are evaluated on the boundary of an element, we obtain the corresponding one-dimensional interpolation functions.

For example, consider a linear triangular element shown in Fig. 8.2.14. The linear interpolation functions for this element are given by (8.2.25*b*). Now let us choose a coordinate system (s, t) with its origin at node 1 and the coordinate s parallel to the side connecting nodes 1 and 2. The two coordinate systems (x, y) and (s, t) are related as follows:

$$x = a_1 + b_1 s + c_1 t$$
$$y = a_2 + b_2 s + c_2 t$$

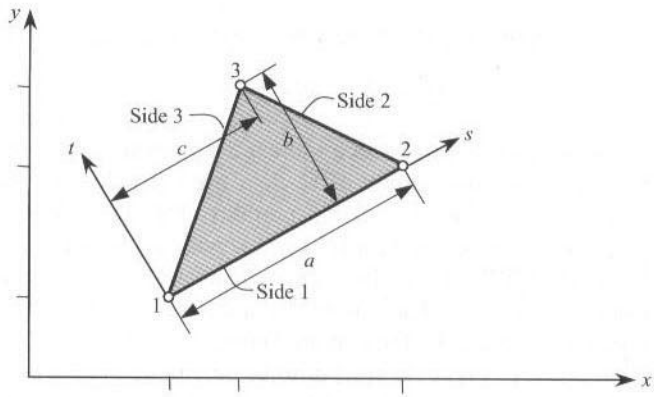

Figure 8.2.14 The linear triangular element in the global (x, y) and local (s, t) coordinate systems.

The constants a_1, b_1, c_1, a_2, b_2, and c_2 can be determined with the following conditions:

$$\begin{aligned} &\text{when } s=0,\ t=0, \quad x=x_1,\ y=y_1 \\ &\text{when } s=a,\ t=0, \quad x=x_2,\ y=y_2 \\ &\text{when } s=c,\ t=b, \quad x=x_3,\ y=y_3 \end{aligned}$$

We obtain

$$\begin{aligned} x(s,t) &= x_1 + (x_2 - x_1)\frac{s}{a} + \left[\left(\frac{c}{a} - 1\right)x_1 - \frac{c}{a}x_2 + x_3\right]\frac{t}{b} \\ y(s,t) &= y_1 + (y_2 - y_1)\frac{s}{a} + \left[\left(\frac{c}{a} - 1\right)y_1 - \frac{c}{a}y_2 + y_3\right]\frac{t}{b} \end{aligned} \tag{8.2.57}$$

Equations (8.2.57) allow us to express $\psi_i(x, y)$ as $\psi_i(s, t)$, which can be evaluated on the side connecting nodes 1 and 2 by setting $t = 0$ in $\psi_i(s, t)$:

$$\psi_i(s) \equiv \psi_i(s,0) = \psi_i(x(s,0), y(s,0))$$

$$x(s) = x_1 + (x_2 - x_1)\frac{s}{a}, \quad y(s) = y_1 + (y_2 - y_1)\frac{s}{a}$$

For instance, we have

$$\begin{aligned} \psi_1(s) &= \frac{1}{2A}\left\{\alpha_1 + \beta_1\left[\left(1 - \frac{s}{a}\right)x_1 + \frac{s}{a}x_2\right] + \gamma_1\left[\left(1 - \frac{s}{a}\right)y_1 + \frac{s}{a}y_2\right]\right\} \\ &= \frac{1}{2A}(\alpha_1 + \alpha_2 + \alpha_3)\left(1 - \frac{s}{a}\right) = 1 - \frac{s}{a} \end{aligned}$$

where the definitions of α_1, β_1, and γ_1 are used to rewrite the entire expression. Similarly, we have

$$\psi_2(s) = \frac{s}{a}, \quad \psi_3(s) = 0$$

where $a = h_{12}$ is the length of side 1–2. We note that $\psi_1(s)$ and $\psi_2(s)$ are precisely the linear, one-dimensional, interpolation functions associated with the line element connecting nodes 1 and 2.

Similarly, when $\psi_i(x, y)$ are evaluated on side 3–1 of the element, we obtain

$$\psi_1(s) = \frac{s}{h_{13}}, \quad \psi_2 = 0, \quad \psi_3(s) = 1 - \frac{s}{h_{13}}$$

where the s coordinate is taken along the side 3–1, with origin at node 3, and h_{13} is the length of side 1–3. Thus, evaluation of Q_i^e involves the use of appropriate one-dimensional interpolation functions and the known variation of q_n on the boundary.

In general, the integral (8.2.56) over the boundary of a linear triangular element can be expressed as

$$\begin{aligned} Q_i^e &= \int_{1-2} \psi_i(s) q_n(s)\, ds + \int_{2-3} \psi_i(s) q_n(s)\, ds + \int_{3-1} \psi_i(s) q_n(s)\, ds \\ &\equiv Q_{i1}^e + Q_{i2}^e + Q_{i3}^e \end{aligned} \tag{8.2.58a}$$

where $\int_{i-j}$ denotes integral over the line connecting node i to node j, the s coordinate is taken from node i to node j, with the origin at node i (see Fig. 8.2.15), and Q_{iJ}^e is defined

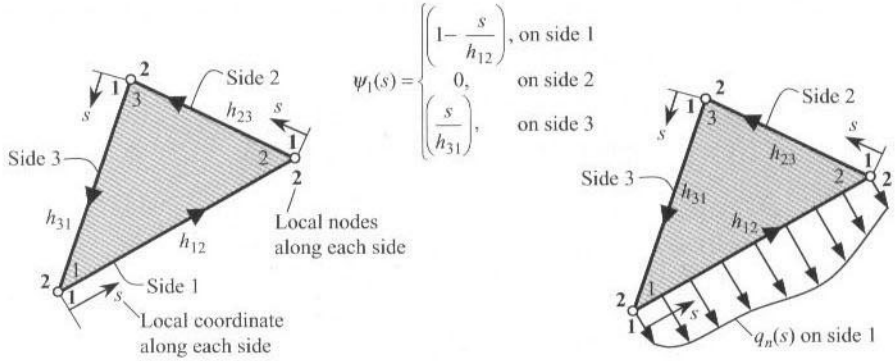

Figure 8.2.15 Computation of the boundary integral (8.2.56) over a linear triangular element.

to be the contribution of q_n on side J of element Ω_e to Q_i^e:

$$Q_{iJ}^e = \int_{\text{side } J} \psi_i q_n \, ds \tag{8.2.58b}$$

where i refers to the ith node of the element and J refers to the Jth side of the element. For example, we have

$$Q_1^e = \oint_{\Gamma_e} q_n \psi_1(s) \, ds = \int_{1-2} (q_n)_{1-2} \psi_1 \, ds + 0 + \int_{3-1} (q_n)_{3-1} \psi_1 \, ds$$

The contribution from side 2–3 is zero because ψ_1 is zero on side 2–3 of a triangular element. For a rectangular element, Q_1^e has four parts but only contributions from sides 1–2 and 4–1 are nonzero because ψ_1 is zero on sides 2–3 and 3–4.

Example 8.2.4

We wish to evaluate the boundary integral Q_i^e in (8.2.56) for the four cases of $q(s)$ and finite element meshes shown in Fig. 8.2.16. For each case we must use the $q(s)$ and the interpolation functions associated with the type of boundary element (i.e., linear or quadratic). On element sides on which q_n is not shown, assume that it is zero.

Case 1. $q(s) = q_0 =$ constant, linear element. Clearly, q_0 will contribute to the nodal values at element nodes 1 and 2. The contribution to node 3 is zero ($Q_3^e = 0$) as there is no specified flux on sides 2–3 and 3–1. We have

$$Q_1^e = \oint_{\Gamma_e} q_n(s)\psi_1(s) \, ds = \int_0^{h_{12}} q_0 (\psi_1)_{1-2} \, ds + \int_0^{h_{31}} (0)(\psi_1)_{3-1} \, ds = Q_{11}^e = \frac{1}{2} q_0 h_{12}$$

$$Q_2^e = \oint_{\Gamma_e} q_n(s)\psi_2(s) \, ds = \int_0^{h_{12}} q_0 (\psi_2)_{1-2} \, ds + \int_0^{h_{23}} (0)(\psi_2)_{2-3} \, ds = Q_{21}^e = \frac{1}{2} q_0 h_{12}$$

where

$$(\psi_1)_{1-2} = 1 - \frac{s}{h_{12}}, \quad (\psi_2)_{1-2} = \frac{s}{h_{12}}$$

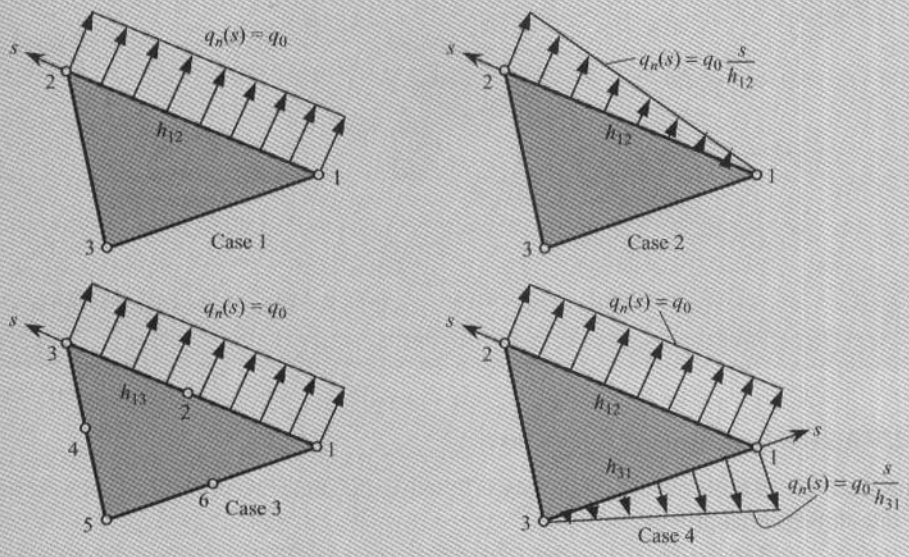

Figure 8.2.16 Evaluation of boundary integrals in the finite element analysis (Example 8.2.4).

Case 2. $q(s) = q_0 s / h_{12}$ (linear variation), linear element. The equations are the same as above except that the flux is linear. We have

$$Q_1^e = \oint_{\Gamma_e} q_n(s)\psi_1(s)\,ds = \int_0^{h_{12}} \left(q_0 \frac{s}{h_{12}}\right)(\psi_1)_{1-2}\,ds + \int_0^{h_{31}} (0)(\psi_1)_{3-1}\,ds = Q_{11}^e = \frac{1}{6} q_0 h_{12}$$

$$Q_2^e = \oint_{\Gamma_e} q_n(s)\psi_2(s)\,ds = \int_0^{h_{12}} \left(q_0 \frac{s}{h_{12}}\right)(\psi_2)_{1-2}\,ds + \int_0^{h_{23}} (0)(\psi_2)_{2-3}\,ds = Q_{21}^e = \frac{1}{3} q_0 h_{12}$$

Case 3. $q(s) = q_0 =$ constant, quadratic triangular element. In this case, quadratic interpolation functions must be used. We have ($Q_4^e = Q_5^e = Q_6^e = 0$)

$$Q_1^e = \oint_{\Gamma_e} q_n(s)\psi_1(s)\,ds = \int_0^{h_{13}} q_0(\psi_1)_{1-2-3}\,ds = Q_{11}^e = \frac{1}{6} q_0 h_{13}$$

$$Q_2^e = \oint_{\Gamma_e} q_n(s)\psi_2(s)\,ds = \int_0^{h_{13}} q_0(\psi_2)_{1-2-3}\,ds = Q_{21}^e = \frac{4}{6} q_0 h_{13}$$

$$Q_3^e = \oint_{\Gamma_e} q_n(s)\psi_3(s)\,ds = \int_0^{h_{13}} q_0(\psi_3)_{1-2-3}\,ds = Q_{31}^e = \frac{1}{6} q_0 h_{13}$$

where

$$(\psi_1)_{1-2-3} = \left(1 - \frac{s}{h_{13}}\right)\left(1 - \frac{2s}{h_{13}}\right), \quad (\psi_2)_{1-2-3} = 4\frac{s}{h_{13}}\left(1 - \frac{s}{h_{13}}\right)$$

$$(\psi_3)_{1-2-3} = -\frac{s}{h_{13}}\left(1 - \frac{2s}{h_{13}}\right)$$

Case 4. Two sides have nonzero $q(s)$, as shown in Fig. 8.2.16, on a linear element. In this case, all three nodes will have nonzero contributions. We have

$$Q_1^e = \oint_{\Gamma_e} q_n(s)\psi_1(s)\,ds = \int_0^{h_{12}} q_0(\psi_1)_{1-2}\,ds + \int_0^{h_{31}} \left(q_0 \frac{s}{h_{31}}\right)(\psi_1)_{3-1}\,ds$$

$$= Q_{11}^e + Q_{13}^e = q_0\left(\frac{h_{12}}{2} + \frac{h_{31}}{3}\right)$$

$$Q_2^e = \oint_{\Gamma_e} q_n(s)\psi_2(s)\,ds = \int_0^{h_{12}} q_0(\psi_2)_{1-2}\,ds + \int_0^{h_{31}} \left(q_0 \frac{s}{h_{31}}\right)(0)\,ds = Q_{21}^e = \frac{1}{2}q_0 h_{12}$$

$$Q_3^e = \oint_{\Gamma_e} q_n(s)\psi_3(s)\,ds = \int_0^{h_{12}} q_0(0)\,ds + \int_0^{h_{31}} \left(q_0 \frac{s}{h_{31}}\right)(\psi_3)_{3-1}\,ds = Q_{33}^e = \frac{1}{6}q_0 h_{31}$$

8.2.7 Assembly of Element Equations

The assembly of finite element equations is based on the same two principles that were used in one-dimensional problems:

1. Continuity of primary variables
2. "Equilibrium" (or "balance") of secondary variables

We illustrate the procedure by considering a finite element mesh consisting of a triangular element and a quadrilateral element [see Fig. 8.2.17(a)]. Let K_{ij}^1 $(i, j = 1, 2, 3)$ denote the coefficient matrix corresponding to the triangular element, and let K_{ij}^2 $(i, j = 1, \ldots, 4)$ denote the coefficient matrix corresponding to the quadrilateral element. From the finite element mesh shown in Fig. 8.2.17(a), we note the following correspondence (i.e., connectivity relations) between the global and element nodes:

$$[B] = \begin{bmatrix} 1 & 2 & 3 & \times \\ 2 & 4 & 5 & 3 \end{bmatrix} \tag{8.2.59}$$

where $\times$ indicates that there is no entry. The correspondence between the local and global nodal values is [see Fig. 8.2.17(a)]

$$u_1^1 = U_1, \quad u_2^1 = u_1^2 = U_2, \quad u_3^1 = u_4^2 = U_3, \quad u_2^2 = U_4, \quad u_3^2 = U_5 \tag{8.2.60}$$

which amounts to imposing the continuity of the primary variables at the nodes common to elements 1 and 2.

Note that the continuity of the primary variables at the interelement nodes guarantees the continuity of the primary variable along the entire interelement boundary. For the case in Fig. 8.2.17(a), the requirement $u_2^1 = u_1^2$ and $u_3^1 = u_4^2$ guarantees $u_h^1(s) = u_h^2(s)$ on the side connecting global nodes 2 and 3. This can be shown as follows. The solution $u_h^1(s)$ along the line connecting global nodes 2 and 3 is linear, and it is given by

$$u_h^1(s) = u_2^1\left(1 - \frac{s}{h}\right) + u_3^1 \frac{s}{h}$$

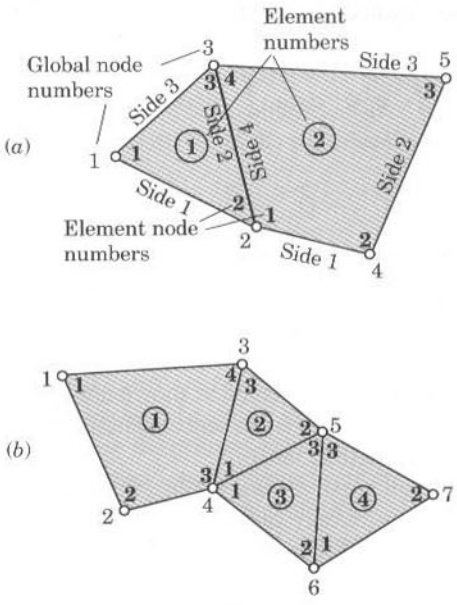

Global	⇒	Local (element)
K_{11}		K^1_{11}
K_{12}		K^1_{12}
K_{13}		K^1_{13}
K_{22}		$K^1_{22} + K^2_{11}$
K_{23}		$K^1_{23} + K^2_{14}$
K_{14}		0
K_{15}		0
K_{14}		K^1_{13}
K_{23}		K^1_{24}
K_{44}		$K^1_{33} + K^2_{11} + K^3_{11}$
K_{45}		$K^2_{12} + K^3_{13}$
K_{25}		0
K_{47}		0

Figure 8.2.17 Assembly of finite element coefficient matrices using the correspondence between global and element nodes (one unknown per node): (*a*) assembly of two elements; and (*b*) assembly of several elements. Single primary degree of freedom per node is assumed.

where s is the local coordinate with its origin at global node 2 and h is the length of the side 2–3 (or side 2). Similarly, the finite element solution along the same line but from element 2 is

$$u_h^2(s) = u_1^2\left(1 - \frac{s}{h}\right) + u_4^2\frac{s}{h}$$

Since $u_1^2 = u_2^1$ and $u_4^2 = u_3^1$, it follows that $u_h^1(s) = u_h^2(s)$ for every value of s along the interface of the two elements.

Next we use the balance of secondary variables. At the interface between the two elements, the flux from the two elements should be equal in magnitude and opposite in sign. For the two elements in Fig. 8.2.17(*a*), the interface is along the side connecting global nodes 2 and 3. Hence, the internal flux q_n^1 on side 2–3 of element 1 should balance the flux q_n^2 on side 4–1 of element 2 (recall the sign convention on q_n^e):

$$\left(q_n^1\right)_{2-3} = \left(q_n^2\right)_{4-1} \text{ or } \left(q_n^1\right)_{2-3} = \left(-q_n^2\right)_{1-4} \tag{8.2.61}$$

In the finite element method we impose the above relation in a weighted integral sense:

$$\int_{h_{23}^1} q_n^1 \psi_2^1 \, ds = -\int_{h_{14}^2} q_n^2 \psi_1^2 \, ds, \quad \int_{h_{23}^1} q_n^1 \psi_3^1 \, ds = -\int_{h_{14}^2} q_n^2 \psi_4^2 \, ds \tag{8.2.62a}$$

where h^e_{pq} denotes length of the side connecting node p to node q of element Ω_e. The above equations can be written in the form,

$$\int_{h^1_{23}} q^1_n \psi^1_2 \, ds + \int_{h^2_{14}} q^2_n \psi^2_1 \, ds = 0, \quad \int_{h^1_{23}} q^1_n \psi^1_3 \, ds + \int_{h^2_{14}} q^2_n \psi^2_4 \, ds = 0 \tag{8.2.62b}$$

or

$$Q^1_{22} + Q^2_{14} = 0, \quad Q^1_{32} + Q^2_{44} = 0 \tag{8.2.62c}$$

where Q^e_{iJ} denotes the part of Q^e_i that comes from side J of element e:

$$Q^e_{iJ} = \int_{\text{side } J} q^e_n \psi^e_i \, ds$$

The sides of triangular and quadrilateral elements are numbered as shown in Fig. 8.2.17(a). These balance relations must be imposed in assembling the element equations. We note that Q^e_{iJ} is only a portion of Q^e_i [see Eqs. (8.2.56) and (8.2.58b)].

The element equations of the two-element mesh shown in Fig. 8.2.17(a) are written first. For the model problem at hand, there is only one primary degree of freedom (NDF = 1) per node. For the triangular element, the element equations are of the form

$$\begin{aligned} K^1_{11}u^1_1 + K^1_{12}u^1_2 + K^1_{13}u^1_3 &= f^1_1 + Q^1_1 \\ K^1_{21}u^1_1 + K^1_{22}u^1_2 + K^1_{23}u^1_3 &= f^1_2 + Q^1_2 \\ K^1_{31}u^1_1 + K^1_{32}u^1_2 + K^1_{33}u^1_3 &= f^1_3 + Q^1_3 \end{aligned} \tag{8.2.63a}$$

For the quadrilateral element, the element equations are given by

$$\begin{aligned} K^2_{11}u^2_1 + K^2_{12}u^2_2 + K^2_{13}u^2_3 + K^2_{14}u^2_4 &= f^2_1 + Q^2_1 \\ K^2_{21}u^2_1 + K^2_{22}u^2_2 + K^2_{23}u^2_3 + K^2_{24}u^2_4 &= f^2_2 + Q^2_2 \\ K^2_{31}u^2_1 + K^2_{32}u^2_2 + K^2_{33}u^2_3 + K^2_{34}u^2_4 &= f^2_3 + Q^2_3 \\ K^2_{41}u^2_1 + K^2_{42}u^2_2 + K^2_{43}u^2_3 + K^2_{44}u^2_4 &= f^2_4 + Q^2_4 \end{aligned} \tag{8.2.63b}$$

In order to impose the balance of secondary variables in (8.2.62c), it is required that we add the second equation of element 1 to the first equation of element 2, and also add the third equation of element 1 to the fourth equation of element 2:

$$\begin{aligned} &\left(K^1_{21}u^1_1 + K^1_{22}u^1_2 + K^1_{23}u^1_3\right) + \left(K^2_{11}u^2_1 + K^2_{12}u^2_2 + K^2_{13}u^2_3 + K^2_{14}u^2_4\right) \\ &\quad = \left(f^1_2 + Q^1_2\right) + \left(f^2_1 + Q^2_1\right) \\ &\left(K^1_{31}u^1_1 + K^1_{32}u^1_2 + K^1_{33}u^1_3\right) + \left(K^2_{41}u^2_1 + K^2_{42}u^2_2 + K^2_{43}u^2_3 + K^2_{44}u^2_4\right) \\ &\quad = \left(f^1_3 + Q^1_3\right) + \left(f^2_4 + Q^2_4\right) \end{aligned}$$

Using the global-variable notation in (8.2.60), we can rewrite the above equations as [which amounts to imposing continuity of the primary variables in (8.2.60)]:

$$\begin{aligned} &K^1_{21}U_1 + \left(K^1_{22} + K^2_{11}\right)U_2 + \left(K^1_{23} + K^2_{14}\right)U_3 + K^2_{12}U_4 + K^2_{13}U_5 \\ &\quad = f^1_2 + f^2_1 + \left(Q^1_2 + Q^2_1\right) \end{aligned}$$

$$K_{31}^1 U_1 + \left(K_{32}^1 + K_{41}^2\right) U_2 + \left(K_{33}^1 + K_{44}^2\right) U_3 + K_{42}^2 U_4 + K_{43}^2 U_5$$
$$= f_3^1 + f_4^2 + \left(Q_3^1 + Q_4^2\right)$$

Now we can impose the conditions in (8.2.62*c*) by setting appropriate portions of the expressions in parenthesis on the right-hand side of the above equations to zero:

$$Q_2^1 + Q_1^2 = \left(Q_{21}^1 + Q_{22}^1 + Q_{23}^1\right) + \left(Q_{11}^2 + Q_{12}^2 + Q_{13}^2 + Q_{14}^2\right)$$
$$= Q_{21}^1 + Q_{23}^1 + \underline{\left(Q_{22}^1 + Q_{14}^2\right)} + Q_{11}^2 + Q_{12}^2 + Q_{13}^2$$
$$Q_3^1 + Q_4^2 = \left(Q_{31}^1 + Q_{32}^1 + Q_{33}^1\right) + \left(Q_{41}^2 + Q_{42}^2 + Q_{43}^2 + Q_{44}^2\right)$$
$$= Q_{31}^1 + Q_{33}^1 + \underline{\left(Q_{32}^1 + Q_{44}^2\right)} + Q_{41}^2 + Q_{42}^2 + Q_{43}^2$$

The underlined terms are zero by the balance requirement (8.2.62*c*). The remaining terms of each equation will be either known because q_n is known on the boundary or remain unknown because the primary variable is specified on the boundary.

In general, when several elements are connected, the assembly of the elements is carried out by putting element coefficients K_{ij}^e, f_i^e, and Q_i^e into proper locations of the global coefficient matrix and right-hand column vectors. This is done by means of the connectivity relations, i.e., correspondence of the local node number to the global node number. For example, if global node number 3 corresponds to node 3 of element 1 and node 4 of element 2, then we have

$$F_3 = F_3^1 + F_4^2 \equiv f_3^1 + f_4^2 + Q_3^1 + Q_4^2, \quad K_{33} = K_{33}^1 + K_{44}^2$$

If global node numbers 2 and 3 correspond, respectively, to nodes 2 and 3 of element 1 and nodes 1 and 4 of element 2, then global coefficients K_{22}, K_{23}, and K_{33} are given by

$$K_{22} = K_{22}^1 + K_{11}^2, \quad K_{23} = K_{23}^1 + K_{14}^2, \quad K_{33} = K_{33}^1 + K_{44}^2$$

Similarly, the source components of global nodes 2 and 3 are added:

$$F_2 = F_2^1 + F_1^2, \quad F_3 = F_3^1 + F_4^2$$

For the two-element mesh shown in Fig. 8.2.17(*a*), the assembled equations are given by

$$\begin{bmatrix} K_{11}^1 & K_{12}^1 & K_{13}^1 & 0 & 0 \\ K_{21}^1 & K_{22}^1 + K_{11}^2 & K_{23}^1 + K_{14}^2 & K_{12}^2 & K_{13}^2 \\ K_{31}^1 & K_{32}^1 + K_{41}^2 & K_{33}^1 + K_{44}^2 & K_{42}^2 & K_{43}^2 \\ 0 & K_{21}^2 & K_{24}^2 & K_{22}^2 & K_{23}^2 \\ 0 & K_{31}^2 & K_{34}^2 & K_{32}^2 & K_{33}^2 \end{bmatrix} \begin{Bmatrix} U_1 \\ U_2 \\ U_3 \\ U_4 \\ U_5 \end{Bmatrix} = \begin{Bmatrix} F_1^1 \\ F_2^1 + F_1^2 \\ F_3^1 + F_4^2 \\ F_2^2 \\ F_3^2 \end{Bmatrix} \tag{8.2.64}$$

The assembly procedure described above can be used to assemble elements of any shape and type. The procedure can be implemented in a computer, as described for one-dimensional problems, with the help of the array $[B]$ (program variable is NOD). For hand calculations, the readers are required to use the procedure described above. For example, consider the finite element mesh shown in Fig. 8.2.17(*b*). The location (4,4) of the global coefficient matrix contains $K_{33}^1 + K_{11}^2 + K_{11}^3$. The location 4 in the assembled column vector contains $F_3^1 + F_1^2 + F_1^3$. Locations (1,5), (1,6), (1,7), (2,5), (2,6), (2,7), (3,6), (3,7), and (4,7) of the

global matrix contain zeros because $K_{IJ} = 0$ when global nodes I and J do not correspond to nodes of the same element in the mesh.

This completes the first five steps in the finite element modeling of the model equation (8.2.1). The next two steps of the analysis, namely, the imposition of boundary conditions and solution of equations will remain the same as for one-dimensional problems. The postprocessing of the solution for two-dimensional problems is discussed next.

8.2.8 Postcomputations

The finite element solution at any point (x, y) in an element Ω_e is given by

$$u_h^e(x, y) = \sum_{j=1}^{n} u_j^e \psi_j^e(x, y) \tag{8.2.65}$$

and its derivatives are computed from (8.2.65) as

$$\frac{\partial u_h^e}{\partial x} = \sum_{j=1}^{n} u_j^e \frac{\partial \psi_j^e}{\partial x}, \qquad \frac{\partial u_h^e}{\partial y} = \sum_{j=1}^{n} u_j^e \frac{\partial \psi_j^e}{\partial y} \tag{8.2.66}$$

Equations (8.2.65) and (8.2.66) can be used to compute the solution and its derivatives at any point (x, y) in the element. It is useful to generate, by the interpolation of (8.2.65), information needed to plot contours of u_h^e and its gradient.

The derivatives of u_h^e will not be continuous at interelement boundaries because continuity of the derivatives is not imposed during the assembly procedure. The weak form of the equations suggests that the primary variable is u, which is to be carried as the nodal variable. If additional variables, such as higher-order derivatives of the dependent unknown, are carried as nodal variables in the interest of making them continuous across interelement boundaries, the degree of interpolation (or order of the element) increases. In addition, the continuity of higher-order derivatives that are not identified as the primary variables may violate the physical principles of the problem. For example, making $\partial u/\partial x$ continuous will violate the requirement that q_x $(= a_{11}\, \partial u/\partial x)$ be continuous at the interface of two dissimilar materials because a_{11} is different for the two materials at the interface.

For the linear triangular element, the derivatives are constants within each element:

$$\begin{gathered} \psi_j^e = \frac{1}{2A_e}(\alpha_j + \beta_j x + \gamma_j y), \qquad \frac{\partial \psi_j^e}{\partial x} = \frac{1}{2A_e}\beta_j, \qquad \frac{\partial \psi_j^e}{\partial y} = \frac{1}{2A_e}\gamma_j \\ \frac{\partial u_h^e}{\partial x} = \sum_{j=1}^{n} \frac{u_j^e \beta_j}{2A_e}, \qquad \frac{\partial u_h^e}{\partial y} = \sum_{j=1}^{n} \frac{u_j^e \gamma_j}{2A_e} \end{gathered} \tag{8.2.67}$$

For linear rectangular elements, $\partial U^e/\partial \bar{x}$ is linear in $\bar{y}$ and $\partial u_h^e/\partial \bar{y}$ is linear in $\bar{x}$ [see (8.2.32*b*)]:

$$\begin{gathered} \frac{\partial \psi_j^e}{\partial \bar{x}} = -\frac{1}{a}\left(1 - \frac{\bar{y} + \bar{y}_j}{b}\right), \qquad \frac{\partial \psi_j^e}{\partial \bar{y}} = -\frac{1}{b}\left(1 - \frac{\bar{x} + \bar{x}_j}{a}\right) \\ \frac{\partial u_h^e}{\partial \bar{x}} = \frac{1}{a}\sum_{j=1}^{n}(-1)^{j+2} u_j^e \left(1 - \frac{\bar{y} + \bar{y}_j}{b}\right), \qquad \frac{\partial u_h^e}{\partial \bar{y}} = \frac{1}{b}\sum_{j=1}^{n}(-1)^{j+2} u_j^e \left(1 - \frac{\bar{x} + \bar{x}_j}{a}\right) \end{gathered} \tag{8.2.68}$$

where $\bar{x}$ and $\bar{y}$ are the local coordinates [see Fig. 8.2.8(*a*)]. Although $\partial u_h^e/\partial \bar{x}$ and $\partial u_h^e/\partial \bar{y}$ are linear functions of y and x, respectively, in each element, they are discontinuous at interelement boundaries. Consequently, quantities computed using derivatives of the finite element solution u_h^e are discontinuous at interelement boundaries. For example, if we compute $q_x^e = a_{11}^e \partial u_h^e/\partial x$ at a node shared by three different elements, three different values of q_x^e are expected. The difference between the three values will diminish as the mesh is refined. Some commercial finite element software give a single value of q_x at the node by averaging the values obtained from various elements connected at the node.

8.2.9 Axisymmetric Problems

In studying problems involving cylindrical geometries, it is convenient to use the cylindrical coordinate system (r, θ, z) to formulate the problem. If the geometry, boundary conditions, and loading (or source) of the problem are independent of the angular coordinate θ, the problem solution will also be independent of θ. Consequently, a three-dimensional problem is reduced to a two-dimensional one in (r, z) coordinates (see Fig. 3.4.1). Here we consider a model axisymmetric problem, develop its weak form, and formulate the finite element model.

Model Equation

Consider the partial differential equation,

$$-\frac{1}{r}\frac{\partial}{\partial r}\left(r\hat{a}_{11}\frac{\partial u}{\partial r}\right) - \frac{\partial}{\partial z}\left(\hat{a}_{22}\frac{\partial u}{\partial z}\right) + \hat{a}_{00}u = \hat{f}(r, z) \tag{8.2.69}$$

where $\hat{a}_{00}$, $\hat{a}_{11}$, $\hat{a}_{22}$, and $\hat{f}$ are given functions of r and z. The equation arises in the study of heat transfer in cylindrical geometries, as well as in other fields of engineering and applied science. Our objective is to develop the finite element model of the equation based on the weak formulation of (8.2.69).

Weak Form

Following the three-step procedure, we write the weak form of (8.2.69):

$$\begin{aligned}
\text{(i)}\quad 0 &= \int_{\Omega_e} w\left[-\frac{1}{r}\frac{\partial}{\partial r}\left(r\hat{a}_{11}\frac{\partial u}{\partial r}\right) - \frac{\partial}{\partial z}\left(\hat{a}_{22}\frac{\partial u}{\partial z}\right) + \hat{a}_{00}u - \hat{f}\right] r\,dr\,dz \\
\text{(ii)}\quad 0 &= \int_{\Omega_e}\left(\frac{\partial w}{\partial r}\hat{a}_{11}\frac{\partial u}{\partial r} + \frac{\partial w}{\partial z}\hat{a}_{22}\frac{\partial u}{\partial z} + w\hat{a}_{00}u - w\hat{f}\right) r\,dr\,dz \\
&\quad - \oint_{\Gamma_e} w\left(\hat{a}_{11}\frac{\partial u}{\partial r}n_r + \hat{a}_{22}\frac{\partial u}{\partial z}n_z\right) ds \\
\text{(iii)}\quad 0 &= \int_{\Omega_e}\left(\hat{a}_{11}\frac{\partial w}{\partial r}\frac{\partial u}{\partial r} + \hat{a}_{22}\frac{\partial w}{\partial z}\frac{\partial u}{\partial z} + \hat{a}_{00}wu - w\hat{f}\right) r\,dr\,dz - \oint_{\Gamma_e} wq_n\,ds
\end{aligned} \tag{8.2.70}$$

where w is the weight function and q_n is the normal flux

$$q_n = \left(\hat{a}_{11} \frac{\partial u}{\partial r} n_r + \hat{a}_{22} \frac{\partial u}{\partial z} n_z \right) \tag{8.2.71}$$

Note that the weak form (8.2.70) does not differ significantly from that developed for model (8.2.1) when $a_{12} = a_{21} = 0$. The only difference is the presence of r in the integrand. Consequently, (8.2.70) can be obtained as a special case of (8.2.10) for $a_{00} = \hat{a}_{00} x$, $a_{11} = \hat{a}_{11} x$, $a_{22} = \hat{a}_{22} x$, and $f = \hat{f} x$; the coordinates r and z are treated like x and y, respectively.

Finite Element Model

Let us assume that $u(r, z)$ is approximated by the finite element interpolation u_h^e over the element Ω_e

$$u \approx u_h^e(r, z) = \sum_{j=1}^{n} u_j^e \psi_j^e(r, z) \tag{8.2.72}$$

The interpolation functions $\psi_j^e(r, z)$ are the same as those developed in (8.2.25*a*) and (8.2.32*a*) for linear triangular and rectangular elements, with $x = r$ and $y = z$. Substitution of (8.2.72) for u and ψ_i^e for w into the weak form gives the ith equation of the finite element model

$$\begin{aligned} 0 = \sum_{j=1}^{n} \left[\int_{\Omega_e} \left(\hat{a}_{11} \frac{\partial \psi_i^e}{\partial r} \frac{\partial \psi_j^e}{\partial r} + \hat{a}_{22} \frac{\partial \psi_i^e}{\partial z} \frac{\partial \psi_j^e}{\partial z} + \hat{a}_{00} \psi_i^e \psi_j^e \right) r \, dr \, dz \right] u_j^e \\ - \int_{\Omega_e} \psi_i^e \hat{f} \, r \, dr \, dz - \oint_{\Gamma_e} \psi_i^e q_n \, ds \end{aligned} \tag{8.2.73}$$

or

$$0 = \sum_{j=1}^{n} K_{ij}^e u_j^e - f_i^e - Q_i^e \tag{8.2.74a}$$

where

$$\begin{aligned} K_{ij}^e &= \int_{\Omega_e} \left(\hat{a}_{11} \frac{\partial \psi_i^e}{\partial r} \frac{\partial \psi_j^e}{\partial r} + \hat{a}_{22} \frac{\partial \psi_i^e}{\partial z} \frac{\partial \psi_j^e}{\partial z} + a_{00} \psi_i^e \psi_j^e \right) r \, dr \, dz \\ f_i^e &= \int_{\Omega_e} \psi_i^e \hat{f} \, r \, dr \, dz, \quad Q_i^e = \oint_{\Gamma_e} \psi_i^e q_n \, ds \end{aligned} \tag{8.2.74b}$$

The evaluation of the integrals in K_{ij}^e and f_i^e for polynomial forms of $\hat{a}_{ij}$ and $\hat{f}$ is possible. However, we evaluate them numerically using the numerical integration methods discussed in Chapter 7 for one-dimensional cases (see Section 7.1.5) and reviewed in Chapter 9 for two-dimensional problems. This completes the development of finite element model of an axisymmetric problem.

8.3 A NUMERICAL EXAMPLE

The model equation in (8.2.1) arises in many fields of engineering and applied sciences, and some examples are given in Table 8.1.1. The application of the finite element model developed in Sections 8.2.2–8.2.8 to problems governed by the Poisson equations is discussed here. This example is designed to illustrate selection of the computational domain, choice of elements and mesh, assembly of element equations, imposition of boundary conditions,

and postprocessing. The physical background of the problem is not discussed here but Table 8.1.1 provides the background.

Example 8.3.1

Consider a problem described by the Poisson equation

$$-\nabla^2 u = f_0 \quad \text{or} \quad -\left(\frac{\partial^2 u}{\partial x^2} + \frac{\partial^2 u}{\partial y^2}\right) = f_0 \quad \text{in } \Omega \tag{8.3.1}$$

in a square region [see Fig. 8.3.1(*a*)]

$$\Omega = \{(x, y) : -A < x < A,\ -A < y < A\}$$

where $u(x, y)$ is the dependent unknown and f_0 is the uniformly distributed source. We shall consider the following boundary conditions for the problem:

$$u = 0 \text{ on the entire boundary } \Gamma \tag{8.3.2}$$

We wish to use the finite element method to determine $u(x, y)$ everywhere in Ω.

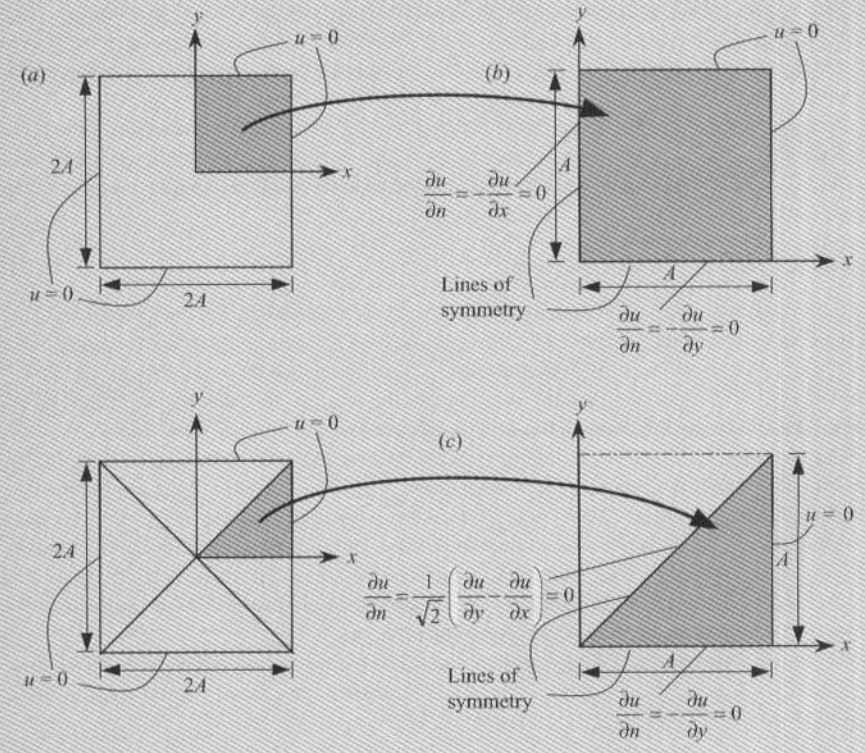

Figure 8.3.1 Finite element analysis of the Poisson equation in a square region: (*a*) Geometry of the actual domain with boundary conditions. (*b*) Computational domain based on biaxial symmetry. (*c*) Computational domain based on biaxial as well as diagonal symmetry.

Selection of the Computational Domain

When the given domain Ω exhibits solution symmetries, it is sufficient to solve the problem on a portion of Ω that provides the solution on the entire domain. A problem possesses symmetry of the solution about a line only when symmetry of the (*a*) geometry, (*b*) material properties, (*c*) source variation, and (*d*) boundary conditions exist about the line. Whenever a portion of the domain is modeled to exploit symmetries available in the problem, the lines of symmetries become a portion of the boundary of the computational domain. On lines of symmetry, the normal derivative of the solution (i.e., derivative of the solution with respect to the coordinate normal to the line of symmetry) is zero:

$$q_n = \frac{\partial u}{\partial n} = \frac{\partial u}{\partial x} n_x + \frac{\partial u}{\partial y} n_y = 0 \tag{8.3.2}$$

The problem at hand has the geometric symmetry about the $x = 0$ and $y = 0$ axes; since the coefficients describing the material behavior, a_{ij}, are either zero or unity, material symmetry about the $x = 0$ and $y = 0$ axes is automatically met. The symmetry of source variation is dictated by f. Since it is uniform, i.e., $f = f_0$, constant, the data is symmetric with respect to the $x = 0$ and $y = 0$ axes. Lastly, the boundary conditions are symmetric with respect to the $x = 0$ and $y = 0$ axes. Thus, the solution is symmetric about the $x = 0$ and $y = 0$ axes, and hence, a quadrant of the domain can be used as the computational domain [see Fig. 8.3.1(*b*)]. The solution is also symmetric about the diagonal lines, and an octant can be used as the computational domain [see Fig. 8.3.1(*c*)]. In the latter case, a mesh of only rectangular elements cannot be used.

While it is possible to mix triangular and rectangular elements to represent the computational domain as well as the solution, in much of this book we shall use only one type of element at a time. Two different finite element meshes for the triangular and rectangular computational domains are shown in Figs. 8.3.2 and 8.3.3, respectively.

Solution by Linear Triangular Elements

Due to the symmetry along the diagonal $x = y$, we model the triangular domain shown in Fig. 8.3.1(*c*). As a first choice we use a uniform mesh of four linear triangular elements, as shown in Fig. 8.3.2(*a*), to represent the domain (mesh T1), and then use the refined mesh (mesh T2) shown in Fig. 8.3.2(*b*) to compare the solutions. In the present case, there is no discretization error involved because the geometry is exactly represented.

The elements 1, 3, and 4 are identical in orientation as well as geometry. Element 2 is geometrically identical to element 1, except that it is oriented differently. If we number the local nodes of element 2 to match those of element 1, then all four elements have the same element matrices, and it is necessary to compute them only for element 1. When the element matrices are computed on a computer, such considerations are not taken into account. In solving the problem by hand, we use the similarity between a master element (element 1) and the other elements in the mesh to avoid unnecessary computations.

We consider element 1 as the typical element. The element is exactly the same as the one shown in Fig. 8.2.11(*b*). Hence, the element coefficient matrix and source vector are (the reader should independently verify this)

$$[K^1] = \frac{1}{2ab} \begin{bmatrix} b^2 & -b^2 & 0 \\ -b^2 & a^2 + b^2 & -a^2 \\ 0 & -a^2 & a^2 \end{bmatrix}, \quad \{f^1\} = \frac{f_0 ab}{6} \begin{Bmatrix} 1 \\ 1 \\ 1 \end{Bmatrix} \tag{8.3.4}$$

where in the present case $a = b = A/2 = 0.5$.

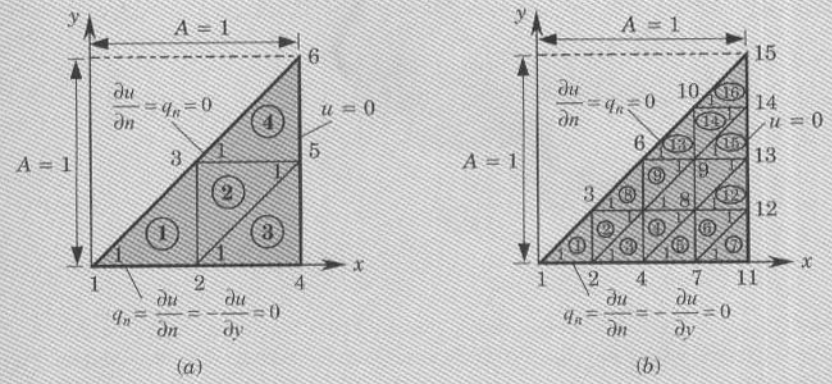

Figure 8.3.2 (*a*) Mesh T1 of triangular elements. (*b*) Mesh T2 of triangular elements.

The element matrix in (8.3.4) is valid for the Laplace operator $-\nabla^2$ on any right-angle triangle with sides a and b in which the right angle is at node 2, and the diagonal line of the triangle connects node 3 to node 1. Note that the off-diagonal coefficient associated with the nodes on the diagonal line is zero for a right-angled triangle.

In summary, for the mesh shown in Fig. 8.3.2(*a*), we have

$$[K^1]=[K^2]=[K^3]=[K^4], \quad \{f^1\}=\{f^2\}=\{f^3\}=\{f^4\}$$

with

$$[K^e]=\frac{1}{2}\begin{bmatrix} 1 & -1 & 0 \\ -1 & 2 & -1 \\ 0 & -1 & 1 \end{bmatrix}, \quad \{f^e\}=\frac{f_0}{24}\begin{Bmatrix} 1 \\ 1 \\ 1 \end{Bmatrix} \tag{8.3.5}$$

The assembled coefficient matrix for the finite element mesh is 6×6, because there are six global nodes with one unknown per node. The assembled matrix can be obtained directly by using the correspondence between the global nodes and the local nodes, expressed through the connectivity matrix,

$$[B]=\begin{bmatrix} 1 & 2 & 3 \\ 5 & 3 & 2 \\ 2 & 4 & 5 \\ 3 & 5 & 6 \end{bmatrix} \tag{8.3.6}$$

A few representative global coefficients are given below in terms of the element coefficients.

$$K_{11}=K_{11}^1=\frac{1}{2}, \quad K_{12}=K_{12}^1=-\frac{1}{2}, \quad K_{22}=K_{22}^1+K_{33}^2+K_{11}^3=\frac{2}{2}+\frac{1}{2}+\frac{1}{2}$$

$$K_{13}=K_{13}^1=0, \quad K_{14}=0, \quad K_{15}=0, \quad K_{16}=0, \quad K_{23}=K_{23}^1+K_{32}^2=-\frac{1}{2}-\frac{1}{2}$$

$$K_{33}=K_{33}^1+K_{22}^2+K_{11}^4=\frac{1}{2}+\frac{2}{2}+\frac{1}{2}, \quad F_1=F_1^1=Q_1^1+f_1^1 \tag{8.3.7}$$

$$F_2=\left(Q_2^1+Q_3^2+Q_1^3\right)+\left(f_2^1+f_3^2+f_1^3\right), \quad F_3=\left(Q_3^1+Q_2^2+Q_1^4\right)+\left(f_3^1+f_2^2+f_1^4\right)$$

$$F_4=F_2^3=Q_2^3+f_2^3, \quad F_5=\left(Q_1^2+Q_3^3+Q_2^4\right)+\left(f_1^2+f_3^3+f_2^4\right), \quad F_6=F_3^4=Q_3^4+f_3^4$$

The assembled system of equations associated with mesh T1 are

$$\frac{1}{2}\begin{bmatrix} 1 & -1 & 0 & 0 & 0 & 0 \\ -1 & 4 & -2 & -1 & 0 & 0 \\ 0 & -2 & 4 & 0 & -2 & 0 \\ 0 & -1 & 0 & 2 & -1 & 0 \\ 0 & 0 & -2 & -1 & 4 & -1 \\ 0 & 0 & 0 & 0 & -1 & 1 \end{bmatrix} \begin{Bmatrix} U_1 \\ U_2 \\ U_3 \\ U_4 \\ U_5 \\ U_6 \end{Bmatrix} = \frac{f_0}{24} \begin{Bmatrix} 1 \\ 3 \\ 3 \\ 1 \\ 3 \\ 1 \end{Bmatrix} + \begin{Bmatrix} Q_1^1 \\ Q_2^1 + Q_3^2 + Q_1^3 \\ Q_3^1 + Q_2^2 + Q_1^4 \\ Q_2^3 \\ Q_1^2 + Q_3^3 + Q_2^4 \\ Q_3^4 \end{Bmatrix} \tag{8.3.8}$$

Note that at nodes 4 and 6, both u and q_n are specified (a type of singularity in the specified data). However, we shall give priority to the primary variable over the secondary variable. Thus, we assume that

$$U_4 = U_5 = U_6 = 0 \tag{8.3.9}$$

and Q_4, Q_5, and Q_6, assumed to be unknown, are determined in the postcomputation. The specified secondary degrees of freedom are (all due to symmetry)

$$Q_1 = Q_1^1 = 0, \quad Q_2 = Q_2^1 + Q_3^2 + Q_1^3 = 0, \quad Q_3 = Q_3^1 + Q_2^2 + Q_1^4 = 0 \tag{8.3.10}$$

For example, consider the sum

$$\begin{aligned} Q_2^1 + Q_3^2 + Q_1^3 &= (Q_{21}^1 + Q_{22}^1) + (Q_{32}^2 + Q_{33}^2) + (Q_{11}^3 + Q_{13}^3) \\ &= Q_{21}^1 + (Q_{22}^1 + Q_{32}^2) + (Q_{33}^2 + Q_{13}^3) + Q_{11}^3 = 0 + 0 + 0 + 0 \end{aligned}$$

where Q_{21}^1 and Q_{11}^3 are zero because of $q_n = 0$ and $Q_{22}^1 + Q_{32}^2$ and $Q_{33}^2 + Q_{13}^3$ are zero because of the balance of fluxes between neighboring elements.

Since the only unknown primary variables for mesh T1 are U_1, U_2, and U_3, the condensed equations for the primary unknowns can be obtained by deleting rows and columns 4, 5, and 6 from the system (8.3.8). In retrospect, it would have been sufficient to write the finite element equations associated with the global nodes 1, 2, and 3:

$$\begin{aligned} K_{11}U_1 + K_{12}U_2 + K_{13}U_3 &= F_1 \\ K_{21}U_1 + K_{22}U_2 + K_{23}U_3 + K_{24}U_4 + K_{25}U_5 &= F_2 \\ K_{31}U_1 + K_{32}U_2 + K_{33}U_3 + K_{35}U_5 + K_{36}U_6 &= F_3 \end{aligned}$$

Noting that $U_4 = U_5 = U_6 = 0$, we can write the above equations in terms of the element coefficients:

$$\begin{bmatrix} K_{11}^1 & K_{12}^1 & K_{13}^1 \\ K_{21}^1 & K_{22}^1 + K_{33}^2 + K_{11}^3 & K_{23}^1 + K_{32}^2 \\ K_{31}^1 & K_{32}^1 + K_{23}^2 & K_{33}^1 + K_{22}^2 + K_{11}^4 \end{bmatrix} \begin{Bmatrix} U_1 \\ U_2 \\ U_3 \end{Bmatrix} = \begin{Bmatrix} f_1^1 \\ f_2^1 + f_3^2 + f_1^3 \\ f_3^1 + f_2^2 + f_1^4 \end{Bmatrix} \tag{8.3.11}$$

The unknown secondary variables Q_4, Q_5, and Q_6 can be computed from the element equations

$$\begin{Bmatrix} Q_4 \\ Q_5 \\ Q_6 \end{Bmatrix} = -\begin{Bmatrix} f_2^3 \\ f_1^2 + f_3^3 + f_2^4 \\ f_3^4 \end{Bmatrix} + \begin{bmatrix} 0 & K_{21}^3 & 0 \\ 0 & K_{13}^2 + K_{31}^3 & K_{12}^2 + K_{21}^4 \\ 0 & 0 & K_{31}^4 \end{bmatrix} \begin{Bmatrix} U_1 \\ U_2 \\ U_3 \end{Bmatrix} \tag{8.3.12}$$

For example, we have

$$\begin{aligned} Q_4 = Q_2^3 &= Q_{21}^3 + Q_{22}^3 + Q_{23}^3 \\ &= \int_{1-2} q_n^3 \psi_2^3 \, dx + \int_{2-3} q_n^3 \psi_2^3 \, dy + \int_{3-1} q_n^3 \psi_2^3 \, ds \end{aligned} \tag{8.3.13a}$$

where

$$\begin{aligned} (q_n^3)_{1-2} &= \left(\frac{\partial u}{\partial x} n_x + \frac{\partial u}{\partial y} n_y \right)_{1-2} = 0 \quad \left(n_x = 0, \quad \frac{\partial u}{\partial y} = 0 \right) \\ (q_n^3)_{2-3} &= \left(\frac{\partial u}{\partial x} n_x + \frac{\partial u}{\partial y} n_y \right)_{2-3} = \frac{\partial u}{\partial x} \quad (n_x = 1, \quad n_y = 0) \\ (\psi_2^3)_{2-3} &= 1 - \frac{y}{h_{23}}, \quad (\psi_2^3)_{3-1} = 0 \end{aligned} \tag{8.3.13b}$$

Thus, we have

$$Q_4 = Q_{22}^3 = \int_0^{h_{23}} \frac{\partial u}{\partial x} \left(1 - \frac{y}{h_{23}} \right) dy$$

where $\partial u / \partial x$ is calculated using $\partial u_h / \partial x$ from the finite element interpolation

$$\frac{\partial u_h}{\partial x} = \sum_{j=1}^{3} u_j^3 \frac{\beta_j^3}{2A_3}$$

We obtain ($h_{23} = a = 0.5$, $\beta_1^3 = -a = -0.5$, $2A_3 = a^2 = 0.25$, $U_4 = U_5 = 0$),

$$Q_4 = \frac{h_{23}}{4A_3} \sum_{j=1}^{3} u_j^3 \beta_j^3 = \frac{h_{23}}{4A_3} \left(\beta_1^3 U_2 + \beta_2^3 U_4 + \beta_3^3 U_5 \right) = -0.5 U_2 \tag{8.3.14}$$

Using the numerical values of the coefficients K_{ij}^e and f_i^e, (with $f_0 = 1$), we write the condensed equations for U_1, U_2, and U_3 as

$$\begin{bmatrix} 0.5 & -0.5 & 0.0 \\ -0.5 & 2.0 & -1.0 \\ 0.0 & -1.0 & 2.0 \end{bmatrix} \begin{Bmatrix} U_1 \\ U_2 \\ U_3 \end{Bmatrix} = \frac{1}{24} \begin{Bmatrix} 1 \\ 3 \\ 3 \end{Bmatrix} \tag{8.3.15}$$

Solving (8.3.15) for U_i ($i = 1, 2, 3$), we obtain

$$\begin{Bmatrix} U_1 \\ U_2 \\ U_3 \end{Bmatrix} = \frac{1}{24} \begin{bmatrix} 3 & 1 & 0.5 \\ 1 & 1 & 0.5 \\ 0.5 & 0.5 & 0.75 \end{bmatrix} \begin{Bmatrix} 1 \\ 3 \\ 3 \end{Bmatrix} = \frac{1}{24} \begin{Bmatrix} 7.5 \\ 5.5 \\ 4.25 \end{Bmatrix} = \begin{Bmatrix} 0.31250 \\ 0.22917 \\ 0.17708 \end{Bmatrix} \tag{8.3.16}$$

and, from (8.3.12), we have

$$\begin{Bmatrix} Q_{22}^3 \\ Q_{32}^3 + Q_{22}^4 \\ Q_{32}^4 \end{Bmatrix} = -\frac{1}{24}\begin{Bmatrix} 1 \\ 3 \\ 1 \end{Bmatrix} + \begin{bmatrix} 0 & -0.5 & 0 \\ 0 & 0 & -1 \\ 0 & 0 & 0 \end{bmatrix}\begin{Bmatrix} U_1 \\ U_2 \\ U_3 \end{Bmatrix} = \begin{Bmatrix} -0.197917 \\ -0.302083 \\ -0.041667 \end{Bmatrix} \tag{8.3.17}$$

By interpolation, Q_4 is equal to $-0.5U_2$, and it differs from Q_{22}^3 computed from equilibrium by the amount f_2^3 $(= \frac{1}{24})$.

Solution by Linear Rectangular Elements

We use a 2×2 (2 elements in the x direction and 2 elements in the y direction) uniform mesh (mesh R1) of four linear rectangular elements [see Fig. 8.3.3(*a*)] to discretize a quadrant of the domain. The 4×4 mesh (mesh R2) [see Fig. 8.3.3(*b*)] will be used for comparison. Once again, no discretization error is introduced in the present case.

Since all the elements in the mesh are identical, we need to compute the element coefficient matrices for only one element, say element 1. The element coefficient matrix is available from Example 8.2.3 with $a = b$. We have

$$[K^e] = \frac{1}{6}\begin{bmatrix} 4 & -1 & -2 & -1 \\ -1 & 4 & -1 & -2 \\ -2 & -1 & 4 & -1 \\ -1 & -2 & -1 & 4 \end{bmatrix}, \quad \{f^e\} = \frac{f_0 a^2}{4}\begin{Bmatrix} 1 \\ 1 \\ 1 \\ 1 \end{Bmatrix} \tag{8.3.18}$$

The coefficient matrix of the condensed equations for the primary unknowns in mesh R1 can be directly assembled. There are four unknowns (at nodes 1, 2, 4, and 5). The finite element equations associated with the four unknowns are (noting that $U_3 = U_6 = U_7 = U_8 = U_9 = 0$)

$$\begin{aligned} K_{11}U_1 + K_{12}U_2 + K_{14}U_4 + K_{15}U_5 &= F_1 \\ K_{21}U_1 + K_{22}U_2 + K_{24}U_4 + K_{25}U_5 &= F_2 \\ K_{41}U_1 + K_{42}U_2 + K_{44}U_4 + K_{45}U_5 &= F_4 \\ K_{51}U_1 + K_{52}U_2 + K_{54}U_4 + K_{55}U_5 &= F_5 \end{aligned} \tag{8.3.19a}$$

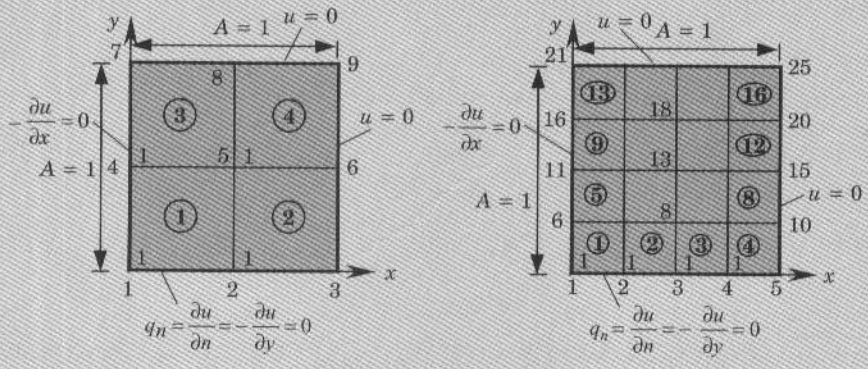

Figure 8.3.3 (*a*) Mesh R1 (2×2) of rectangular elements. (*b*) Mesh R2 (4×4) of rectangular elements.

where K_{IJ} and F_I are the global coefficients, which can be written in terms of the element coefficients as

$$\begin{aligned}
&K_{11}=K^1_{11}, \quad K_{12}=K^1_{12}, \quad K_{14}=K^1_{14}, \quad K_{15}=K^1_{13}\\
&K_{22}=K^1_{22}+K^2_{11}, \quad K_{24}=K^1_{24}, \quad K_{25}=K^1_{23}+K^2_{14}\\
&K_{44}=K^1_{44}+K^3_{11}, \quad K_{45}=K^1_{43}+K^3_{12}, \quad K_{55}=K^1_{33}+K^2_{44}+K^4_{11}+K^3_{22} \qquad (8.3.19b)\\
&F_1=f^1_1+Q^1_1, \quad F_2=f^1_2+f^2_1+Q^1_2+Q^2_1, \quad F_4=f^1_4+f^3_1+Q^1_4+Q^3_1\\
&F_5=f^1_3+f^2_4+f^4_1+f^3_2+Q^1_3+Q^2_4+Q^4_1+Q^3_2
\end{aligned}$$

The boundary conditions on the secondary variables are

$$Q^1_1=0, \quad Q^1_2+Q^2_1=0, \quad Q^1_4+Q^3_1=0 \qquad (8.3.20a)$$

and the balance of secondary variables at global node 5 requires

$$Q^1_3+Q^2_4+Q^3_2+Q^4_1=0 \qquad (8.3.20b)$$

Thus, the condensed equations for the primary unknowns are (for $f_0=1$ and $a=0.5$)

$$\frac{1}{6}\begin{bmatrix} 4 & -1 & -1 & -2\\ -1 & 8 & -2 & -2\\ -1 & -2 & 8 & -2\\ -2 & -2 & -2 & 16 \end{bmatrix}\begin{Bmatrix} U_1\\ U_2\\ U_4\\ U_5 \end{Bmatrix}=\frac{1}{16}\begin{Bmatrix} 1\\ 2\\ 2\\ 4 \end{Bmatrix} \qquad (8.3.21)$$

The solution of these equations is

$$U_1=0.31071, \quad U_2=0.24107, \quad U_4=0.24107, \quad U_5=0.19286 \qquad (8.3.22)$$

The secondary variables $Q_3=Q_7$, $Q_6=Q_8$, and Q_9 at nodes 3 (7), 6 (8), and 9, respectively (by symmetry), can be computed from the equations ($Q_3=Q^2_2$, $Q_6=Q^3_3+Q^4_2$, and $Q_9=Q^4_3$)

$$\begin{Bmatrix} Q_3\\ Q_6\\ Q_9 \end{Bmatrix}=-\begin{Bmatrix} f^2_2\\ f^2_3+f^4_2\\ f^4_3 \end{Bmatrix}+\begin{bmatrix} K_{31} & K_{32} & K_{34} & K_{35}\\ K_{61} & K_{62} & K_{64} & K_{65}\\ K_{91} & K_{92} & K_{94} & K_{95} \end{bmatrix}\begin{Bmatrix} U_1\\ U_2\\ U_4\\ U_5 \end{Bmatrix} \qquad (8.3.23a)$$

where

$$\begin{aligned}
&K_{31}=0, \quad K_{32}=K^2_{21}, \quad K_{34}=0, \quad K_{35}=K^2_{24}\\
&K_{61}=0, \quad K_{62}=K^2_{31}, \quad K_{64}=0, \quad K_{65}=K^2_{34}+K^4_{21} \qquad (8.3.23b)\\
&K_{91}=0, \quad K_{92}=0, \quad K_{94}=0, \quad K_{95}=K^4_{31}
\end{aligned}$$

Substituting the numerical values, we obtain

$$\begin{Bmatrix} Q_3\\ Q_6\\ Q_9 \end{Bmatrix}=-\frac{1}{16}\begin{Bmatrix} 1\\ 2\\ 1 \end{Bmatrix}+\frac{1}{6}\begin{bmatrix} 0 & -1 & 0 & -2\\ 0 & -2 & 0 & -2\\ 0 & 0 & 0 & -2 \end{bmatrix}\begin{Bmatrix} U_1\\ U_2\\ U_4\\ U_5 \end{Bmatrix}=-\begin{Bmatrix} 0.16697\\ 0.26964\\ 0.12679 \end{Bmatrix} \qquad (8.3.24)$$

Table 8.3.1 Comparison of the finite element solutions $u(0, y)$ with the series solution and the Ritz solution of (8.3.1).

	Triangular elem.		Rectangular elem.		Ritz solution	Series solution
y	Mesh T1	Mesh T2	Mesh R1	Mesh R2	(2.5.39)	(2.5.40)
0.00	0.3125	0.3013	0.3107	0.2984	0.3125	0.2947
0.25	0.2708†	0.2805	0.2759†	0.2824	0.2930	0.2789
0.50	0.2292	0.2292	0.2411	0.2322	0.2344	0.2293
0.75	0.1146†	0.1393	0.1205†	0.1414	0.1367	0.1397
1.00	0.0000	0.0000	0.0000	0.0000	0.0000	0.0000

†Interpolated values

The finite element solutions obtained by two different meshes of triangular elements and two different meshes of rectangular elements are compared in Table 8.3.1 with the 50-term series solution (at $x = 0$ for varying y) in (2.5.40) (set $k = 1$, $g_0 = f_0 = 1$) and the one-parameter Ritz solution in (2.5.39); see also Fig. 8.3.4. The finite element solution obtained by 16 triangular elements (in an octant) is the most accurate when compared to the series solution. The accuracy of the triangular element mesh is due to the large number of elements it has compared to the number of elements in the rectangular element mesh for the same size of the domain.

The solution u and components of flux (q_x, q_y) can be computed at any interior point of the domain. For a point (x, y) in element Ω_e, we have $(k = 1)$

$$u_h^e(x, y) = \sum_{j=1}^{n} u_j^e \psi_j^e(x, y) \tag{8.3.25a}$$

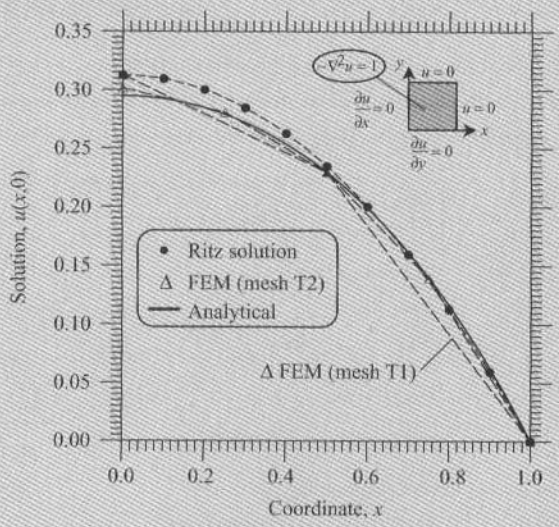

Figure 8.3.4 Comparison of the finite element solution with the two-parameter Ritz solution and the analytical (series) solution.

$$q_y^e(x,y) = -k\frac{\partial u_h^e}{\partial y} = -\sum_{i=1}^{n} u_i^e \frac{\partial \psi_i^e}{\partial y}, \quad q_x^e(x,y) = -k\frac{\partial u_h^e}{\partial x} = -\sum_{i=1}^{n} u_i^e \frac{\partial \psi_i^e}{\partial x} \tag{8.3.25b}$$

The negative sign in the definition of fluxes is dictated by the physics of the problem. Here we interpreted the problem at hand to be one of heat transfer. Note that for a linear triangular element, q_x and q_y are constants over an entire element, whereas q_x is linear in y and q_y is linear in x for a linear rectangular element. For example, consider element 1 of mesh T1 of triangular elements

$$\begin{aligned} q_x^1(x,y) &= -\frac{k}{2A_1}\sum_{i=1}^{3} u_i^1 \beta_i^1 = -2(U_2 - U_1) = 0.16667 \\ q_y^1(x,y) &= -\frac{k}{2A_1}\sum_{i=1}^{3} u_i^1 \gamma_i^1 = -2(U_3 - U_2) = 0.10417 \end{aligned} \tag{8.3.26a}$$

Clearly, the gradients (and hence the components of flux) are constant. For element 1 of mesh R1 rectangular element (four elements) we have

$$\begin{aligned} q_x^1(x,y) &= -k\sum_{i=1}^{4} u_i^1 \frac{\partial \psi_i^1}{\partial x} = 2U_1(1-2y) - 2U_2(1-2y) - 4yU_5 + 4yU_4 \\ q_x^1(0.25, 0.25) &= 0.11785 \end{aligned} \tag{8.3.26b}$$

$$\begin{aligned} q_y^1(x,y) &= -k\sum_{i=1}^{4} u_i^1 \frac{\partial \psi_i^1}{\partial y} = 2U_1(1-2x) - 2U_2(1-2x) - 4xU_5 + 4xU_4 \\ q_y^1(0.25, 0.25) &= 0.11785 \end{aligned}$$

Plots of q_x, obtained by mesh T1 (8 elements) and mesh T2 (16 elements) of linear triangular elements as a function of x (for $y = 0.0$) are shown in Fig. 8.3.5.

The computation of *isolines*, i.e., lines of constant u, for linear finite elements is straightforward. Suppose that we wish to find $u = u_0$ (constant) isoline. On a side of a linear triangle or rectangular element, the solution u varies according to the equation

$$u_h^e(s) = u_1^e + \frac{u_2^e - u_1^e}{h}s$$

where s is the local coordinate with its origin at node 1 of the side, (u_1^e, u_2^e) are the nodal values (see Fig. 8.3.6), and h is the length of the side. Then, if $u \equiv u_0$ lies on the line (i.e., $u_1^e < u_0 < u_2^e$ or $u_2^e < u_0 < u_1^e$), the point s_0 at which $U^e(s_0) = u_0$ is given by

$$s_0 = \frac{(u_0 - u_1^e)h}{(u_2^e - u_1^e)} \tag{8.3.27}$$

Similar equations apply for other sides of the element. Since the solution varies linearly between any two points of linear elements, the isoline is determined by joining two points on any two sides of the element for which (8.3.27) gives a positive value (and $s_0 < h$).

For quadratic elements, isolines are determined by finding three points s_i in the element at which $u_h^e(s_i) = u_0$ ($i = 1, 2$, and 3):

$$\frac{s_0}{h} = \frac{-b \pm \sqrt{b^2 - 4ac}}{2a} > 0 \tag{8.3.28a}$$

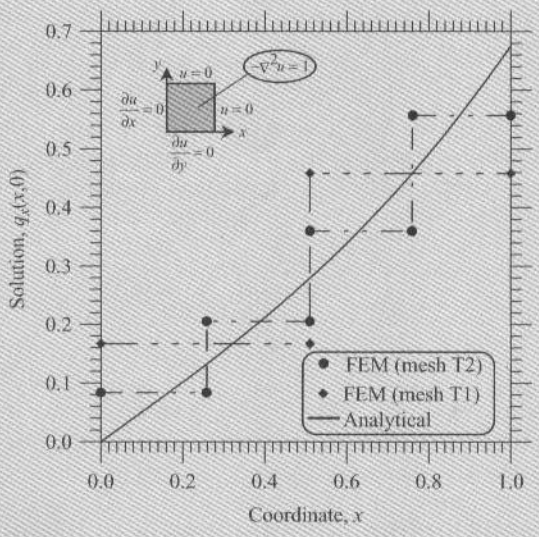

Figure 8.3.5 Comparison of the finite element solution with the analytical (series) solution of $q_x(x, 0)$.

where

$$c = u_1^e - u_0, \quad b = -3u_1^e + 4u_2^e - u_3^e, \quad a = 2\left(u_1^e - 2u_2^e + u_3^e\right) \tag{8.3.28b}$$

Equation (8.3.28*a*) is to be applied on any three lines in the element until three different values $h > s_0 > 0$ are found.

The problem considered here has several physical interpretations (see Table 8.1.1). The problem can be viewed as one of finding the temperature u in a unit square with uniform internal heat generation, where the sides $x = 0$ and $y = 0$ are insulated and the other two sides are subjected to zero temperature (see Section 8.5.1). Another interpretation of the equation is that it defines the torsion of a 2-inch-square cross-sectional cylindrical bar (see Section 8.5.3). In this case, u denotes the stress function Ψ, and the components of the gradient of the solution

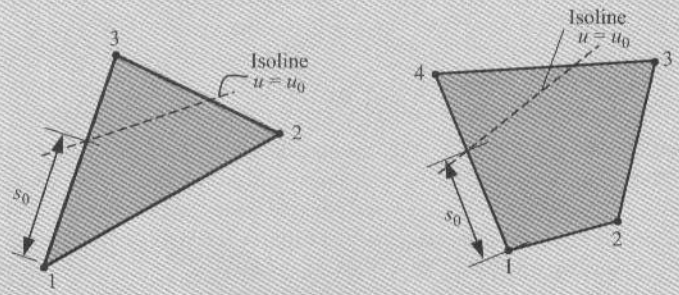

Figure 8.3.6 Isolines for linear triangular and quadrilateral elements.

are the stresses (which are of primary interest):

$$\sigma_{xz} = G\theta \frac{\partial \Psi}{\partial y}, \quad \sigma_{yz} = -G\theta \frac{\partial \Psi}{\partial x}$$

where G is the shear modulus and θ is the angle of twist per unit length of the bar.

A third interpretation of (8.3.1) is provided by groundwater (seepage) and potential flow problems. In this case, u denotes the piezometric head ϕ, stream function ψ, or velocity potential ϕ (see Section 8.5.2). The x and y components of the velocity for the groundwater flow are defined as

$$u_1 = -a_{11} \frac{\partial \phi}{\partial x}, \quad u_2 = -a_{22} \frac{\partial \phi}{\partial y}$$

where a_{11} and a_{22} are the permeabilities of the soil along the x and y directions, respectively. Examples of each of these field problems will be considered in Section 8.5.

8.4 SOME COMMENTS ON MESH GENERATION AND IMPOSITION OF BOUNDARY CONDITIONS

8.4.1 Discretization of a Domain

The representation of a given domain by a collection of finite elements requires engineering judgement on the part of the finite element practitioner. The number, type (e.g., linear or quadratic), shape (e.g., triangular or rectangular), and density (i.e., mesh refinement) of elements used in a given problem depend on a number of considerations. The first consideration is to discretize the domain as closely as possible with elements that are admissible. As we shall see later, we can use one set of elements for the approximation of a domain and another set for the solution. In discretizing a domain, consideration must be given to an accurate representation of the domain, point sources, distributed sources with discontinuities (i.e., sudden change in the intensity of the source), and material and geometric discontinuities, including a reentrant corner. The discretization should include, for example, nodes at point sources (so that the point source is accurately lumped at the node), reentrant corners, and element interfaces where abrupt changes in geometry and material properties occur.

A second consideration, which requires some engineering judgement, is to discretize the body or portions of the body into sufficiently small elements so that steep gradients of the solution are accurately calculated. The engineering judgement should come from both a qualitative understanding of the behavior of the solution and an estimate of the computational costs involved in the mesh refinement (i.e., reducing the size of the elements). For example, consider the inviscid flow around a cylinder in a channel. The flow entering the channel at the left goes around the cylinder and exits the channel at the right [see Fig. 8.4.1(a)]. Since the section at the cylinder is smaller than the inlet section, it is expected that the flow accelerates in the vicinity of the cylinder. On the other hand, the velocity field far from the cylinder (e.g., at the inlet) is essentially uniform. Such knowledge of the qualitative behavior of the flow allows us to employ a coarse mesh (i.e., elements that are relatively

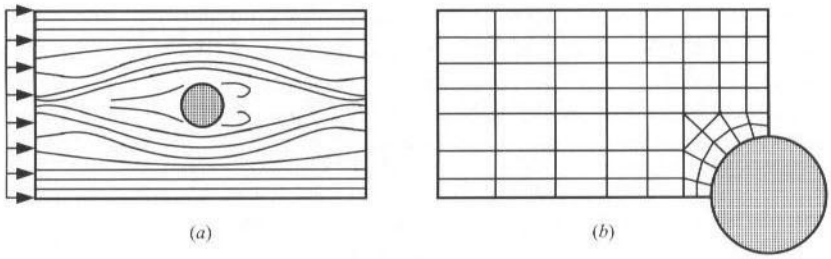

Figure 8.4.1 (*a*) Flow of an inviscid fluid around a cylinder (streamlines). (*b*) A typical mesh for a quadrant of the domain.

large in size) at sites sufficiently far from the cylinder, and a fine one at closer distances to the cylinder [see Fig. 8.4.1(*b*)]. Another reason for using a refined mesh near the cylinder is to accurately represent the curved boundary of the domain there. In general, a refined mesh is required in places where acute changes in geometry, boundary conditions, loading, material properties, or solution occur.

A mesh refinement should meet three conditions: (1) All the previous meshes should be contained in the current refined mesh; (2) every point in the body can be included within an arbitrarily small element at any stage of the mesh refinement; and (3) the same order of approximation for the solution should be retained through all stages of the refinement process. The last requirement eliminates comparison of two different approximations in two different meshes.

When a mesh is refined, care should be taken to avoid elements with very large aspect ratios (i.e., the ratio of one side of an element to the other) or small angles. Recall from the element matrices in Eqs. (8.2.48) and (8.2.53) that the coefficient matrices depend on the ratios of a to b and b to a, where a and b are the lengths of elements in the x and y directions, respectively. If the value of a/b or b/a is very large, the resulting coefficient matrices are ill-conditioned (i.e., numerically not invertible). Although the safe lower and upper limits on b/a are believed to be 0.1 and 10, respectively, the actual values are much more extreme and they depend on the nature of physical phenomenon being modeled. For example, in the inviscid flow problem discussed above, large aspect ratios are allowed at the entrance of the channel.

The words "coarse" and "fine" are relative. In any given problem, we begin with a finite element mesh that is believed to be adequate (based on experience and engineering judgement) to solve the problem at hand. Then, as a second choice, we select a mesh that consists of a larger number of elements (and includes the first one as a subset) to solve the problem once again. If there is a significant difference between the two solutions, we see the benefit of mesh refinement and further mesh refinement may be warranted. If the difference is negligibly small, further mesh refinements are not necessary. Such numerical experiments with mesh refinements are not always feasible in practice, mostly due to the computational costs involved.

In cases where computational cost is the prime concern, we must depend on our judgement concerning what is a reasonably good mesh, which is often dictated by the geometry and qualitative understanding of the variations of the solution and its gradient. Since most

practical problems are approximated in their engineering formulations, we should not be overly concerned with the numerical accuracy of the solution. A feel for the relative proportions and directions of various errors introduced into the analysis helps the finite element practitioner to make a decision on when to stop refining a mesh. In summary, engineering knowledge and experience with a given class of problems are essential to a suitable numerical study.

8.4.2 Generation of Finite Element Data

An important part of finite element modeling is the mesh generation, which involves numbering the nodes and elements, and the generation of nodal coordinates and the connectivity matrix. While the task of generating such data is not difficult, the type of the data has an effect on the computational efficiency as well as on accuracy. More specifically, the numbering of the nodes directly affects the bandwidth of the final assembled equations, which in turn increases the storage requirement and computational cost if equation solvers with the Gauss elimination procedure are used. The elements can be numbered arbitrarily because it has no effect on the half-bandwidth. In a general-purpose program with a preprocessor, options to minimize the bandwidth are included. The saving of computational cost due to a smaller bandwidth in the solution of equations can be substantial, especially in problems where a large number of nodes and degrees of freedom per node are involved. While element numbering does not affect the half-bandwidth, it may affect the computer time required to assemble the global coefficient matrix (usually, a very small percentage of the time required to solve the equations).

The accuracy of the finite element solution can also depend on the choice of the finite element mesh. For instance, if the mesh selected violates the symmetry present in the problem, the resulting solution will be less accurate than one obtained using a mesh that agrees with the physical symmetry present in the problem. Geometrically, a triangular element has fewer (or no) lines of symmetry when compared to a rectangular element, and therefore meshes of triangular elements should be used with care (e.g., select a mesh that does not contradict the mathematical symmetry present in the problem).

The effect of the finite element meshes shown in Fig. 8.4.2 on the solution of the Poisson equation in Example 8.3.1 is investigated. The finite element solutions obtained by the three meshes are compared with the series solution in Table 8.4.1. Clearly, the solution obtained using mesh 3 is less accurate. This is expected because mesh 3 is symmetric about the diagonal line connecting node 3 to node 7, whereas the mathematical symmetry is about the diagonal line connecting node 1 to node 9 (see Fig. 8.4.2). Mesh 1 is the most desirable of the three because it does not contradict the mathematical symmetry of the problem.

Next, the effect of mesh refinement with rectangular elements is investigated. Four different meshes of rectangular elements are shown in Fig. 8.4.3. Each of the meshes contains the previous mesh as a subset. The mesh shown in Fig. 8.4.3(c) is nonuniform; it is obtained by subdividing the first two rows and columns of elements of the mesh shown in Fig. 8.4.3(b). The finite element solutions obtained by these meshes are compared in Table 8.4.2. The numerical convergence of the finite element solution of the refined meshes to the series solution is apparent from the results presented.

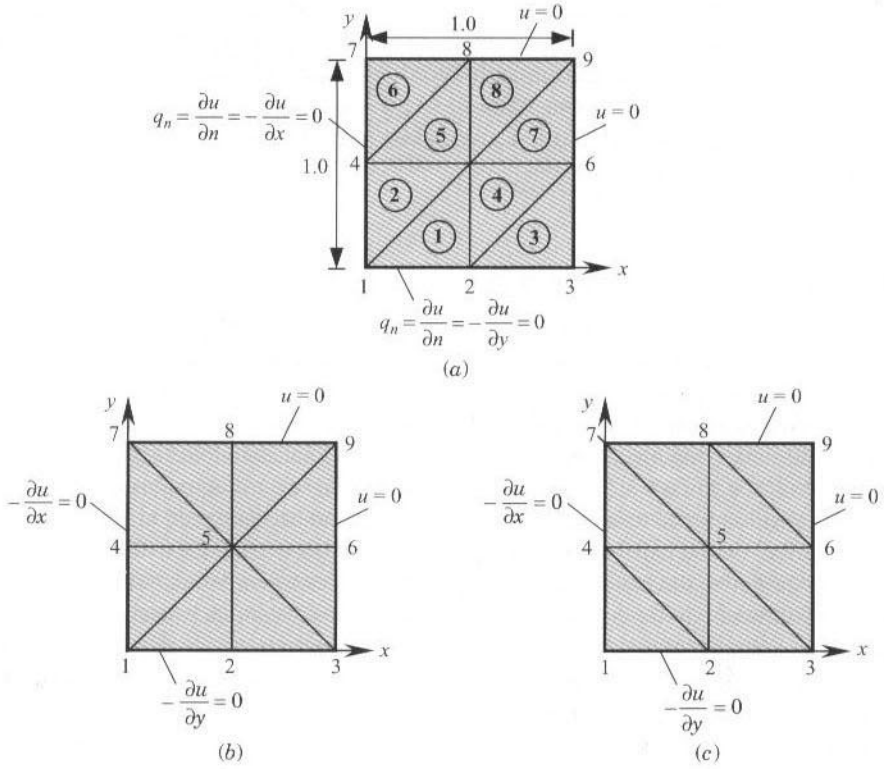

Figure 8.4.2 Various types of triangular-element meshes for the domain of Example 8.3.1: (*a*) mesh 1; (*b*) mesh 2; and (*c*) mesh 3.

8.4.3 Imposition of Boundary Conditions

In some problems of interest we encounter situations where at a point of the boundary both primary and secondary degrees of freedom are specified at the same point. Such points are called *singular points*. In this case we impose the boundary condition on the primary variable and let the secondary variable take its value (calculated in the postcomputation).

Table 8.4.1 Comparison of the finite element solutions obtained using various linear triangular-element meshes† with the series solution of the problem in Example 8.3.1.

	Finite element solution			
Node	Mesh 1	Mesh 2	Mesh 3	Series solution
1	0.31250	0.29167	0.25000	0.29469
2	0.22917	0.20833	0.20833	0.22934
3	0.22917	0.20833	0.20833	0.22934
4	0.17708	0.18750	0.16667	0.18114

†See Fig. 8.4.2 for the finite element meshes.

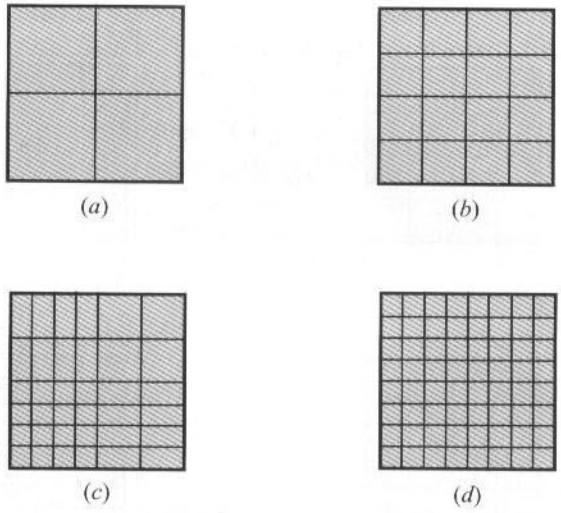

Figure 8.4.3 Mesh refinement; the meshes in (*a*), (*b*), and (*d*) are uniform; the mesh in (*c*) is nonuniform: (*a*) 2×2 mesh; (*b*) 4×4 mesh; (*c*) 6×6 mesh; and (*d*) 8×8 mesh.

This is because the boundary conditions on the primary variables are often maintained more strictly than those on the secondary variables. Of course, if the problem is such that the essential boundary conditions are a result of the natural boundary conditions, then we must impose the natural boundary conditions.

Another type of singularity we encounter in the solution of boundary value problems is the specification of two different values of a primary variable at the same point.

Table 8.4.2 Convergence of the finite element solution (with mesh refinement)† of the problem in Example 8.3.1.

Location		Finite element solution				
x	y	2×2	4×4	6×6	8×8	Series solution
0.000	0.0	0.31071	0.29839	0.29641	0.29560	0.29469
0.125	0.0	—	—	0.29248	0.29167	0.29077
0.250	0.0	—	0.28239	0.28055	0.27975	0.27888
0.375	0.0	—	—	0.26022	0.24943	0.25863
0.500	0.0	0.24107	0.23220	0.23081	0.23005	0.22934
0.625	0.0	—	—	—	0.19067	0.19009
0.750	0.0	—	0.14137	0.14064	0.14014	0.13973
0.875	0.0	—	—	—	0.07709	0.07687
0.125	0.125	—	—	0.28862	0.28781	0.28692
0.250	0.250	—	0.26752	0.26580	0.26498	0.26415
0.375	0.375	—	—	0.22960	0.22873	0.22799
0.500	0.50	0.19286	0.18381	0.18282	0.18179	0.18114
0.625	0.625	—	—	—	0.12813	0.12757
0.750	0.750	—	0.07506	0.07481	0.07332	0.07282
0.875	0.875	—	—	—	0.02561	0.02510

†See Fig. 8.4.3 for the finite element meshes.

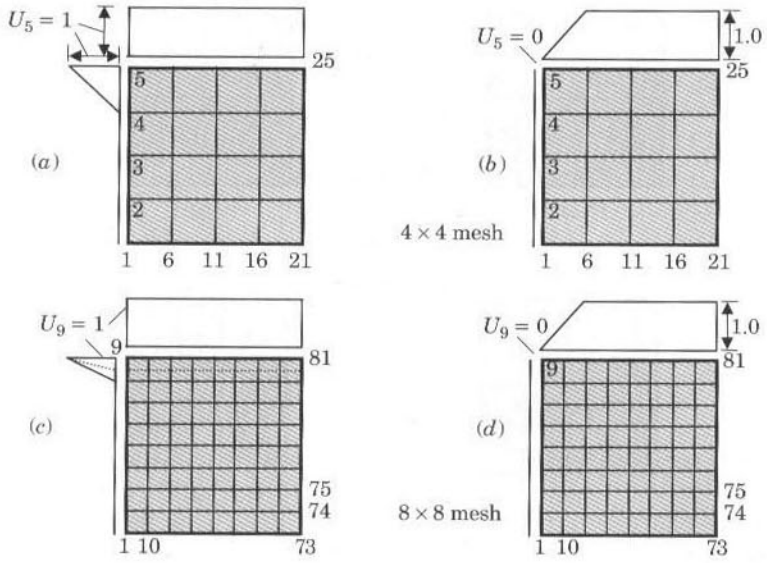

Figure 8.4.4 Effect of specifying two values of a primary variable at a node [node 5 in (*a*) and (*b*) and node 9 in (*c*) and (*d*)].

An example of such cases is provided by the problem in Fig. 8.4.4, where u is specified to be zero on the boundary defined by the line $x = 0$ and is specified to be unity on the boundary defined by the line $y = 1$. Consequently, at $x = 0$ and $y = 1$, u has two different values. The analyst must make a choice between the two values. In either case, the true boundary condition is replaced by an approximate condition. Often, the larger value is used to obtain a conservative design. The closeness of the approximate boundary condition to the true one depends on the size of the element containing the point (see Fig. 8.4.3). A mesh refinement in the vicinity of the singular point often yields an acceptable solution.

Additional comments on the choice of element geometry, meshes, and load-representation in finite element analysis are presented in Section 9.4.

8.5 APPLICATIONS

8.5.1 Conduction and Convection Heat Transfer

In Section 4.3, heat transfer (by conduction and convection) in one-dimensional (axial and radially symmetric) systems was considered. Here we consider heat transfer in two-dimensional plane and axisymmetric systems. The derivation of two-dimensional heat transfer equations in plane and axisymmetric geometries follows the same procedure as in one dimension but the heat transfer is in two directions. Details of such derivations can be found in textbooks on heat transfer [e.g., Holman (1986) and Özisik (1985)]. Here we record the governing equations for various cases, construct their finite element models, and present typical applications.

For heat conduction in plane or axisymmetric geometries, the finite element models developed in Sections 8.2 and 8.3 are immediately applicable with the following interpretation of the variables:

$$\begin{aligned} u &= T \equiv \text{temperature } (^\circ\text{C}) \\ q_n &\equiv \text{negative of heat flux } [\text{W}/(\text{m}^2 \cdot {}^\circ\text{C})] \\ a_{11}, a_{22} &\equiv \text{conductivities } [\text{W}/(\text{m} \cdot {}^\circ\text{C})] \text{ of an orthotropic medium} \\ &\quad \text{whose principal material axes coincide with the } (x, y) \text{ axes} \\ f &\equiv \text{internal heat generation } (\text{W}/\text{m}^3) \\ a_{00} &= 0 \end{aligned} \tag{8.5.1}$$

For convection heat transfer, i.e., when heat is transferred from one medium to the surrounding medium (often, a fluid) by convection, the finite element model developed earlier requires some modification. The reason for this modification is that in two-dimensional problems, the convective boundary is a curve as opposed to a point in one-dimensional problems. Therefore, the contribution of the convection (or Newton's type) boundary condition to the coefficient matrix and source vector are to be computed by evaluating boundary integrals involving the interpolation functions of elements with convection boundaries. The model to be presented allows the computation of the additional contributions to the coefficient matrix and source vector whenever the element has the convection boundary condition.

Plane Systems

The governing equation for steady-state heat transfer in plane systems is a special case of (8.2.1) and is given by

$$-\frac{\partial}{\partial x}\left(k_x \frac{\partial T}{\partial x}\right) - \frac{\partial}{\partial y}\left(k_y \frac{\partial T}{\partial y}\right) = f(x, y) \tag{8.5.2}$$

where T is the temperature (in °C), k_x and k_y are the thermal conductivities [in W/(m · °C)] along the x and y directions, respectively, and f is the internal heat generation per unit volume (in W/m^3). For a convection boundary, the natural boundary condition is a balance of energy transfer across the boundary due to conduction *and/or* convection (i.e., Newton's law of cooling):

$$k_x \frac{\partial T}{\partial x} n_x + k_y \frac{\partial T}{\partial y} n_y + \beta(T - T_\infty) = \hat{q}_n \tag{8.5.3}$$

where β is the convective conductance (or the convective heat transfer coefficient) [in W/(m^2 · °C)], T_∞ is the (ambient) temperature of the surrounding fluid medium, and $\hat{q}_n$ is the specified heat flux. The first term accounts for heat transfer by conduction, the second by convection, and the third accounts for the specified heat flux, if any. It is the presence of the term $\beta(T - T_\infty)$ that requires some modification of (8.2.10).

The weak form of (8.5.2) can be obtained from (8.2.8). The boundary integral should be modified to account for the convection heat transfer boundary condition in (8.5.3).

The coefficient of w, $k_x(\partial T/\partial x)n_x + k_y(\partial T/\partial y)n_y$, in the boundary integral is replaced with $q_n - \beta(T - T_\infty)$:

$$\begin{aligned} 0 &= \int_{\Omega_e} \left(k_x \frac{\partial w}{\partial x}\frac{\partial T}{\partial x} + k_y \frac{\partial w}{\partial y}\frac{\partial T}{\partial y} - wf \right) dx\, dy - \oint_{\Gamma_e} w \left(k_x \frac{\partial T}{\partial x} n_x + k_y \frac{\partial T}{\partial y} n_y \right) ds \\ &= \int_{\Omega_e} \left(k_x \frac{\partial w}{\partial x}\frac{\partial T}{\partial x} + k_y \frac{\partial w}{\partial y}\frac{\partial T}{\partial y} - wf \right) dx\, dy - \oint_{\Gamma_e} w\, [\hat{q}_n - \beta(T - T_\infty)]\, ds \\ &= B(w, T) - l(T) \end{aligned} \tag{8.5.4a}$$

where w is the test function and $B(\cdot, \cdot)$ and $l(\cdot)$ are the bilinear and linear forms, respectively,

$$\begin{aligned} B(w, T) &= \int_{\Omega_e} \left(k_x \frac{\partial w}{\partial x}\frac{\partial T}{\partial x} + k_y \frac{\partial w}{\partial y}\frac{\partial T}{\partial y} \right) dx\, dy + \oint_{\Gamma_e} \beta w T\, ds \\ l(T) &= \int_{\Omega_e} wf\, dx\, dy + \oint_{\Gamma_e} \beta w T_\infty\, ds + \oint_{\Gamma_e} w\hat{q}_n\, ds \end{aligned} \tag{8.5.4b}$$

The finite element model of (8.5.4a) and (8.5.4b) is obtained by substituting the finite element approximation of the form,

$$T = \sum_{j=1}^{n} T_j^e \psi_j^e(x, y) \tag{8.5.5}$$

for T and ψ_i^e for w into (8.5.4a):

$$\sum_{j=1}^{n} (K_{ij}^e + H_{ij}^e) T_j^e = F_i^e + P_i^e \tag{8.5.6a}$$

where

$$\begin{aligned} K_{ij}^e &= \int_{\Omega_e} \left(k_x \frac{\partial \psi_i^e}{\partial x}\frac{\partial \psi_j^e}{\partial x} + k_y \frac{\partial \psi_i^e}{\partial y}\frac{\partial \psi_j^e}{\partial y} \right) dx\, dy \\ F_i^e &= \int_{\Omega_e} f\psi_i^e\, dx\, dy + \oint_{\Gamma_e} \hat{q}_n^e \psi_i^e\, ds \equiv f_i^e + Q_i^e \\ H_{ij}^e &= \beta^e \oint_{\Gamma_e} \psi_i^e \psi_j^e\, ds, \quad P_i^e = \beta^e \oint_{\Gamma_e} \psi_i^e T_\infty\, ds \end{aligned} \tag{8.5.6b}$$

Note that by setting the heat transfer coefficient β to zero, we obtain the heat conduction model that accounts for no convection.

The additional coefficients H_{ij}^e and P_i^e due to the convection boundary conditions can be computed by evaluating boundary integrals. These coefficients must be computed only for those elements and boundaries that are subjected to a convection boundary condition. The computation of the coefficients for the linear triangular and rectangular elements is presented in the following paragraphs. The coefficients H_{ij}^e and P_i^e for a linear triangular

element are defined by

$$
\begin{aligned}
H_{ij}^e &= \beta_{12}^e \int_0^{h_{12}^e} \psi_i^e \psi_j^e \, ds + \beta_{23}^e \int_0^{h_{23}^e} \psi_i^e \psi_j^e \, ds + \beta_{31}^e \int_0^{h_{31}^e} \psi_i^e \psi_j^e \, ds \\
P_i^e &= \beta_{12}^e T_\infty^{12} \int_0^{h_{12}^e} \psi_i^e \, ds + \beta_{23}^e T_\infty^{23} \int_0^{h_{23}^e} \psi_i^e \, ds + \beta_{31}^e T_\infty^{31} \int_0^{h_{31}^e} \psi_i^e \, ds
\end{aligned}
\tag{8.5.7}
$$

where β_{ij}^e is the film coefficient (assumed to be constant) for the side connecting nodes i and j of element Ω_e, T_∞^{ij} is the ambient temperature on the side, and h_{ij}^e is the length of the side. For a rectangular element, expressions in (8.5.7) must be modified to account for four line integrals on four sides of the element.

Only those line integrals that have a convection boundary condition need to be evaluated. The boundary integrals are line integrals involving the interpolation functions. The local coordinate s is taken along the side, with its origin at the first node of the side (see Fig. 8.5.1). As noted earlier, the interpolation functions on any given side are the one-dimensional interpolation functions. Therefore, the evaluation of integrals is made easy. Indeed, the integrals

$$
\int_0^{h_{ij}^e} \psi_i^e \psi_j^e \, ds, \quad \int_0^{h_{ij}^e} \psi_i^e \, ds
$$

have been evaluated in Chapter 3 in connection with mass matrix coefficients and source vector coefficients for linear and quadratic elements. We summarize the results here.

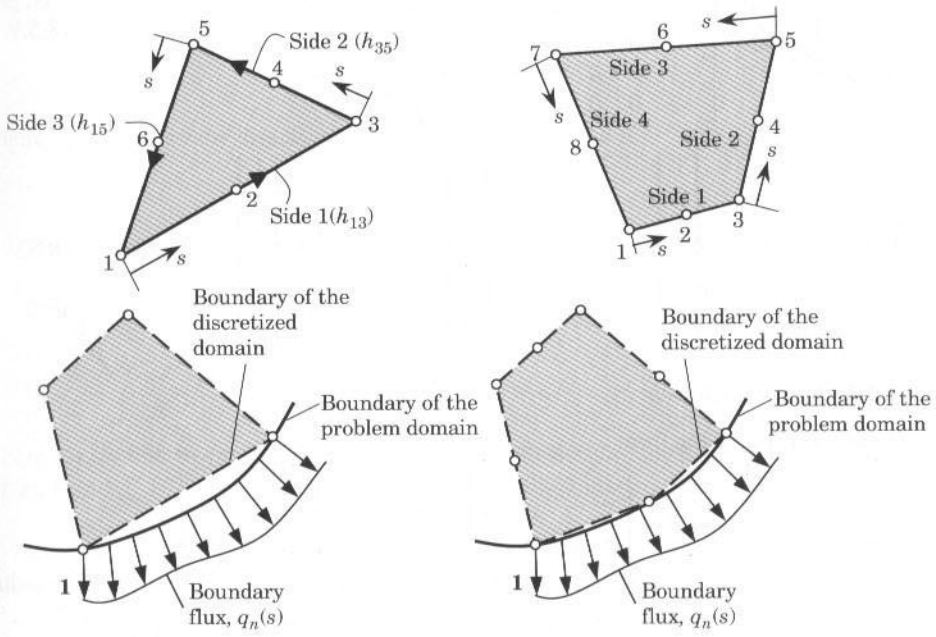

Figure 8.5.1 Triangular and quadrilateral elements, with node numbers and local coordinates for the evaluation of the boundary integrals. Also shown are the boundary approximation and flux representation using linear and quadratic elements.

Linear Triangular Element

The matrices $[H^e]$ and $\{P^e\}$ are given by

$$[H^e] = \frac{\beta_{12}^e h_{12}^e}{6}\begin{bmatrix}2 & 1 & 0\\ 1 & 2 & 0\\ 0 & 0 & 0\end{bmatrix} + \frac{\beta_{23}^e h_{23}^e}{6}\begin{bmatrix}0 & 0 & 0\\ 0 & 2 & 1\\ 0 & 1 & 2\end{bmatrix} + \frac{\beta_{31}^e h_{31}^e}{6}\begin{bmatrix}2 & 0 & 1\\ 0 & 0 & 0\\ 1 & 0 & 2\end{bmatrix} \tag{8.5.8a}$$

$$\{P^e\} = \frac{\beta_{12}^e T_\infty^{12} h_{12}^e}{2}\begin{Bmatrix}1\\ 1\\ 0\end{Bmatrix} + \frac{\beta_{23}^e T_\infty^{23} h_{23}^e}{2}\begin{Bmatrix}0\\ 1\\ 1\end{Bmatrix} + \frac{\beta_{31}^e T_\infty^{31} h_{31}^e}{2}\begin{Bmatrix}1\\ 0\\ 1\end{Bmatrix} \tag{8.5.8b}$$

Quadratic Triangular Element

$$[H^e] = \frac{\beta_{13}^e h_{13}^e}{30}\begin{bmatrix}4 & 2 & -1 & 0 & 0 & 0\\ 2 & 16 & 2 & 0 & 0 & 0\\ -1 & 2 & 4 & 0 & 0 & 0\\ 0 & 0 & 0 & 0 & 0 & 0\\ 0 & 0 & 0 & 0 & 0 & 0\\ 0 & 0 & 0 & 0 & 0 & 0\end{bmatrix} + \frac{\beta_{35}^e h_{35}^e}{30}\begin{bmatrix}0 & 0 & 0 & 0 & 0 & 0\\ 0 & 0 & 0 & 0 & 0 & 0\\ 0 & 0 & 4 & 2 & -1 & 0\\ 0 & 0 & 2 & 16 & 2 & 0\\ 0 & 0 & -1 & 2 & 4 & 0\\ 0 & 0 & 0 & 0 & 0 & 0\end{bmatrix}$$

$$+ \frac{\beta_{51} h_{51}^e}{30}\begin{bmatrix}4 & 0 & 0 & 0 & -1 & 2\\ 0 & 0 & 0 & 0 & 0 & 0\\ 0 & 0 & 0 & 0 & 0 & 0\\ 0 & 0 & 0 & 0 & 0 & 0\\ -1 & 0 & 0 & 0 & 4 & 2\\ 2 & 0 & 0 & 0 & 2 & 16\end{bmatrix} \tag{8.5.9a}$$

$$\{P^e\} = \frac{\beta_{13}^e T_\infty^{13} h_{13}^e}{6}\begin{Bmatrix}1\\ 4\\ 1\\ 0\\ 0\\ 0\end{Bmatrix} + \frac{\beta_{35}^e T_\infty^{35} h_{35}^e}{6}\begin{Bmatrix}0\\ 0\\ 1\\ 4\\ 1\\ 0\end{Bmatrix} + \frac{\beta_{51}^e T_\infty^{51} h_{51}^e}{6}\begin{Bmatrix}1\\ 0\\ 0\\ 0\\ 1\\ 4\end{Bmatrix} \tag{8.5.9b}$$

Linear Rectangular Element

The matrix $[H^e]$ is of the form

$$[H^e] = \frac{\beta_{12}^e h_{12}^e}{6}\begin{bmatrix}2 & 1 & 0 & 0\\ 1 & 2 & 0 & 0\\ 0 & 0 & 0 & 0\\ 0 & 0 & 0 & 0\end{bmatrix} + \frac{\beta_{23}^e h_{23}^e}{6}\begin{bmatrix}0 & 0 & 0 & 0\\ 0 & 2 & 1 & 0\\ 0 & 1 & 2 & 0\\ 0 & 0 & 0 & 0\end{bmatrix}$$

$$+ \frac{\beta_{34}^e h_{34}^e}{6}\begin{bmatrix}0 & 0 & 0 & 0\\ 0 & 0 & 0 & 0\\ 0 & 0 & 2 & 1\\ 0 & 0 & 1 & 2\end{bmatrix} + \frac{\beta_{41}^e h_{41}^e}{6}\begin{bmatrix}2 & 0 & 0 & 1\\ 0 & 0 & 0 & 0\\ 0 & 0 & 0 & 0\\ 1 & 0 & 0 & 2\end{bmatrix} \tag{8.5.10a}$$

and $\{P^e\}$ is given by

$$\{P^e\} = \frac{\beta_{12}^e T_\infty^{12} h_{12}^e}{2}\begin{Bmatrix}1\\1\\0\\0\end{Bmatrix} + \frac{\beta_{23}^e T_\infty^{23} h_{23}^e}{2}\begin{Bmatrix}0\\1\\1\\0\end{Bmatrix} + \frac{\beta_{34}^e T_\infty^{34} h_{34}^e}{2}\begin{Bmatrix}0\\0\\1\\1\end{Bmatrix} + \frac{\beta_{41}^e T_\infty^{41} h_{41}^e}{2}\begin{Bmatrix}1\\0\\0\\1\end{Bmatrix} \tag{8.5.10b}$$

Similar expressions hold for a quadratic rectangular element.

Axisymmetric Systems

For symmetric heat transfer about the z axis (i.e., independent of the circumferential coordinate), the governing equation is given by

$$-\left[\frac{1}{r}\frac{\partial}{\partial r}\left(rk_r\frac{\partial T}{\partial r}\right) + \frac{\partial}{\partial z}\left(k_z\frac{\partial T}{\partial z}\right)\right] = f(r,z) \tag{8.5.11}$$

where r is the radial coordinate and z is the axial coordinate. We define the flux vector (i.e., negative of heat flux) by

$$\mathbf{q} = \left(k_r\frac{\partial T}{\partial r}\hat{\mathbf{i}} + k_z\frac{\partial T}{\partial z}\hat{\mathbf{j}}\right)$$

and its normal component across the surface is

$$q_n = \left(k_r\frac{\partial T}{\partial r}n_r + k_z\frac{\partial T}{\partial z}n_z\right) \tag{8.5.12}$$

where n_r and n_z are the direction cosines of the unit normal $\hat{\mathbf{n}}$

$$\hat{\mathbf{n}} = n_r\hat{\mathbf{i}} + n_z\hat{\mathbf{j}}$$

The weak form of (8.5.11) is given by

$$\begin{aligned} 0 &= 2\pi\int_{\Omega_e} w\left\{-\left[\frac{1}{r}\frac{\partial}{\partial r}\left(k_r r\frac{\partial T}{\partial r}\right) + \frac{\partial}{\partial z}\left(k_z\frac{\partial T}{\partial z}\right)\right] - f\right\} r\,dr\,dz \\ &= 2\pi\int_{\Omega_e}\left(k_r\frac{\partial w}{\partial r}\frac{\partial T}{\partial r} + k_z\frac{\partial w}{\partial z}\frac{\partial T}{\partial z} - wf\right) r\,dr\,dz - 2\pi\oint_{\Gamma_e} wq_n\,ds \end{aligned} \tag{8.5.13a}$$

where 2π is due to the integration with respect to the circumferential coordinate over $(0, 2\pi)$, and q_n is given by (8.5.12). The convection boundary condition is of the form

$$q_n + \beta(T - T_\infty) = \hat{q}_n \tag{8.5.13b}$$

Substituting for $q_n = -\beta(T - T_\infty) + \hat{q}_n$ into (8.5.13a), we obtain

$$\begin{aligned} 0 = 2\pi\int_{\Omega_e}\left(k_r\frac{\partial w}{\partial r}\frac{\partial T}{\partial r} + k_z\frac{\partial w}{\partial z}\frac{\partial T}{\partial z} - wf\right) r\,dr\,dz \\ - 2\pi\oint_{\Gamma_e} w\left[-\beta(T - T_\infty) + \hat{q}_n\right] ds \end{aligned} \tag{8.5.14}$$

The finite element model of (8.5.11) with convective boundary condition (8.5.13*b*) is

$$[K^e + H^e]\{T^e\} = \{f^e\} + \{P^e\} + \{Q^e\} \tag{8.5.15a}$$

where

$$K_{ij}^e = 2\pi \int_{\Omega_e} \left(k_r \frac{\partial \psi_i^e}{\partial r} \frac{\partial \psi_j^e}{\partial r} + k_z \frac{\partial \psi_i^e}{\partial z} \frac{\partial \psi_j^e}{\partial z} \right) r \, dr \, dz$$

$$H_{ij}^e = 2\pi \oint_{\Gamma_e} \beta^e \psi_i^e \psi_j^e \, ds, \quad f_i^e = 2\pi \int_{\Omega_e} \psi_i^e f(r) \, r \, dr \, dz \tag{8.5.15b}$$

$$Q_i^e = 2\pi \oint_{\Gamma_e} \hat{q}_n \psi_i^e \, ds, \quad P_i^e = 2\pi \oint_{\Gamma_e} \beta^e T_\infty^e \psi_i^e \, ds$$

Evaluation of the integrals in $[K^e]$, $[H^e]$, $\{F^e\}$, and $\{P^e\}$ follows from the discussion of Section 8.2.6.

Clearly, the finite element models in (8.5.6*a*) and (8.5.15*a*) are valid for Newton's type (i.e., convective heat transfer) boundary conditions. Radiative heat transfer boundary conditions are nonlinear and therefore are not considered here. For problems with no convective boundary conditions, the convective contributions $[H^e]$ and $\{P^e\}$ to the element coefficients are omitted. In addition, the convective heat transfer contributions have to be included only for those elements whose sides fall on the problem boundary with convection heat transfer specified. For example, if side 2–3 of a linear triangular element Ω_e is on the boundary with convection boundary conditions, then the only contribution to $[H^e]$ and $\{P^e\}$ comes from the second integral of respective expressions in (8.5.7).

Example 8.5.1

Consider steady-state heat conduction in an isotropic rectangular region of dimensions $3a \times 2a$ [see Fig. 8.5.2(*a*)]. The origin of the x and y coordinates is taken at the lower left corner such that x is parallel to the side $3a$ and y is parallel to side $2a$. The boundaries $x = 0$ and $y = 0$ are insulated, the boundary $x = 3a$ is maintained at zero temperature, and the boundary $y = 2a$ is maintained at a temperature $T = T_0 \cos(\pi x/6a)$. We wish to determine the temperature distribution using the finite element method in the region and the heat required at boundary $x = 3a$ to maintain it at zero temperature.

To analyze the problem, first we note that the problem is governed by (8.5.2) with zero internal heat generation, $f = 0$, and no convection boundary conditions:

$$-k\nabla^2 T = 0 \tag{8.5.16}$$

Hence, the finite element model of the problem is given by

$$[K^e]\{T^e\} = \{Q^e\}$$

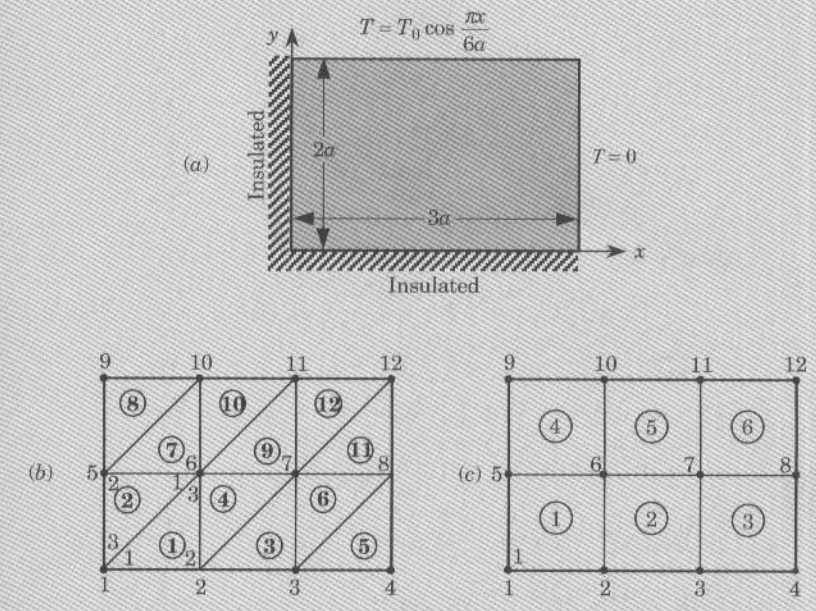

Figure 8.5.2 Finite element analysis of a heat conduction problem over a rectangular domain: (*a*) domain; (*b*) mesh of linear triangular elements; and (*c*) mesh of linear rectangular elements.

where T_i^e is the temperature at node i of element Ω_e, and

$$K_{ij}^e = \int_{\Omega_e} k \left(\frac{\partial \psi_i}{\partial x} \frac{\partial \psi_j}{\partial x} + \frac{\partial \psi_i}{\partial y} \frac{\partial \psi_j}{\partial y} \right) dx\, dy, \quad Q_i^e = \oint_{\Gamma_e} q_n \psi_i \, ds$$

Suppose that we use a 3×2 mesh (i.e., 3 subdivisions along the x axis and 2 subdivisions along the y axis) of linear triangular elements and then with a 3×2 mesh of linear rectangular elements, as shown in Fig. 3.5.2(*b*) and 3.5.2(*c*). Both meshes have the same number of global nodes (12) but differing numbers of elements.

Triangular Element Mesh (12 Elements)

The global node numbers, element numbers, and element node numbers used are shown in Fig. 8.5.2(*b*). Of course, the global node numbering and element numbering is arbitrary (does not have to follow any particular pattern), although the global node numbering dictates the size of the half bandwidth of the assembled equations, which in turn affects the computational time of Gauss elimination methods used in the solution of algebraic equations in a computer. The element node numbering scheme should be the one that is used in the development of element interpolation functions. In the present study a counterclockwise numbering system was adopted (see Figs. 8.2.4 and 8.2.8). By a suitable numbering of the element nodes, all similar elements can be made to have the same element coefficient matrix. Such considerations are important only when hand calculations are carried out.

For a typical element of the mesh of triangles in Fig. 8.5.2(*b*), the element coefficient matrix is given by [see Eqs. (8.3.4) and (8.3.5)],

$$[K^e] = \frac{k}{2}\begin{bmatrix} 1 & -1 & 0 \\ -1 & 2 & -1 \\ 0 & -1 & 1 \end{bmatrix} \tag{8.5.17}$$

where k is the conductivity of the medium. Note that the element matrix is independent of the size of the element, as long as the element is a right-angle triangle with its base equal to its height.

The assembly of the elements (in a computer) follows the logic discussed earlier. For example, we have

$$K_{11} = K_{11}^1 + K_{33}^2 = \frac{k}{2}(1+1), \quad K_{12} = K_{12}^1 = \frac{k}{2}(-1), \quad K_{13} = 0$$

$$K_{15} = K_{32}^2 = \frac{k}{2}(-1), \quad K_{16} = K_{13}^1 + K_{31}^2 = 0 + 0, \quad \text{etc.}$$

$$F_1 = Q_1^1 + Q_3^2, \quad F_6 = Q_3^1 + Q_1^2 + Q_2^4 + Q_2^7 + Q_1^9 + Q_3^{10}, \quad \text{etc.}$$

The boundary conditions require that (U_i denotes the temperature at global node i)

$$\begin{gathered} U_4 = U_8 = U_{12} = 0, \quad U_9 = T_0, \quad U_{10} = \frac{\sqrt{3}}{2}T_0, \quad U_{11} = \frac{T_0}{2} \\ F_1 = F_2 = F_3 = F_5 = 0 \quad \text{(zero heat flow due to insulated boundary)} \end{gathered} \tag{8.5.18}$$

and the balance of internal heat flow requires that

$$F_6 = F_7 = 0 \tag{8.5.19}$$

Thus, the unknown primary variables and secondary variables of the problem are:

$$\begin{gathered} U_1, \quad U_2, \quad U_3, \quad U_5, \quad U_6, \quad U_7 \\ F_4, \quad F_8, \quad F_9, \quad F_{10}, \quad F_{11}, \quad F_{12} \end{gathered}$$

We first write the six finite element equations for the six unknown primary variables. These equations come from rows 1, 2, 3, 5, 6, and 7 (corresponding to the same global nodes):

$$\begin{gathered} K_{11}U_1 + K_{12}U_2 + \cdots + K_{1(12)}U_{12} = F_1 = \left(Q_1^1 + Q_3^2\right) = 0 \\ K_{21}U_1 + K_{22}U_2 + \cdots + K_{2(12)}U_{12} = F_2 = \left(Q_2^1 + Q_1^3 + Q_3^4\right) = 0 \\ \vdots \\ K_{71}U_1 + K_{72}U_2 + \cdots + K_{7(12)}U_{12} = F_7 = \left(Q_3^3 + Q_1^4 + Q_2^6 + Q_2^9 + Q_1^{11} + Q_3^{12}\right) = 0 \end{gathered} \tag{8.5.20}$$

Using the boundary conditions and the values of K_{IJ}, we obtain

$$k\left(U_1 - \frac{1}{2}U_2 - \frac{1}{2}U_5\right) = 0$$

$$k\left(-\frac{1}{2}U_1 + 2U_2 - \frac{1}{2}U_3 - U_6\right) = 0$$

$$k\left(-\frac{1}{2}U_2 + 2U_3 - U_7\right) = 0$$

$$k\left(-\frac{1}{2}U_1 + 2U_5 - U_6 - \frac{1}{2}U_9\right) = 0 \quad (U_9 = T_0)$$

$$k(-U_2 - U_5 + 4U_6 - U_7 - U_{10}) = 0 \quad \left(U_{10} = \frac{\sqrt{3}}{2}T_0\right)$$

$$k(-U_3 - U_6 + 4U_7 - U_{11}) = 0 \quad \left(U_{11} = \frac{1}{2}T_0\right)$$

In matrix form we have

$$\frac{k}{2}\begin{bmatrix} 2 & -1 & 0 & -1 & 0 & 0 \\ -1 & 4 & -1 & 0 & -2 & 0 \\ 0 & -1 & 4 & 0 & 0 & -2 \\ -1 & 0 & 0 & 4 & -2 & 0 \\ 0 & -2 & 0 & -2 & 8 & -2 \\ 0 & 0 & -2 & 0 & -2 & 8 \end{bmatrix} \begin{Bmatrix} U_1 \\ U_2 \\ U_3 \\ U_5 \\ U_6 \\ U_7 \end{Bmatrix} = \frac{k}{2}\begin{Bmatrix} 0 \\ 0 \\ 0 \\ T_0 \\ \sqrt{3}T_0 \\ T_0 \end{Bmatrix} \tag{8.5.21}$$

The solution of these equations is (in °C)

$$\begin{aligned} U_1 &= 0.6362T_0, \quad U_2 = 0.5510T_0, \quad U_3 = 0.3181T_0 \\ U_5 &= 0.7214T_0, \quad U_6 = 0.6248T_0, \quad U_7 = 0.3607T_0 \end{aligned} \tag{8.5.22}$$

The exact solution of (8.5.16) for the boundary conditions shown in Fig. 8.5.2(*a*) is,

$$T(x, y) = T_0 \frac{\cosh(\pi y/6a)\cos(\pi x/6a)}{\cosh(\pi/3)} \tag{8.5.23}$$

Evaluating the exact solution at the nodes, we have (in °C)

$$\begin{aligned} T_1 &= 0.6249T_0, \quad T_2 = 0.5412T_0, \quad T_3 = 0.3124T_0 \\ T_5 &= 0.7125T_0, \quad T_6 = 0.6171T_0, \quad T_7 = 0.3563T_0 \end{aligned} \tag{8.5.24}$$

The heat at node 4, for example, can be computed from the fourth finite element equation

$$\begin{aligned} F_4 = Q_2^5 = {} & K_{41}U_1 + K_{42}U_2 + K_{43}U_3 + K_{44}U_4 + K_{45}U_5 \\ & + K_{46}U_6 + K_{47}U_7 + K_{48}U_8 + \cdots \end{aligned} \tag{8.5.25}$$

Noting that $K_{41} = K_{42} = K_{45} = \cdots = K_{4(12)} = 0$ and $U_4 = U_8 = 0$, we obtain

$$Q_2^5 = -\frac{1}{2}kU_3 = -0.1591kT_0 \text{ (in W)} \tag{8.5.26}$$

Rectangular Element Mesh (6 Elements)

For a 3×2 mesh of linear rectangular elements [see Fig. 8.5.2(*c*)], the element coefficient matrix is given by (8.2.55)

$$[K^e] = \frac{k}{6}\begin{bmatrix} 4 & -1 & -2 & -1 \\ -1 & 4 & -1 & -2 \\ -2 & -1 & 4 & -1 \\ -1 & -2 & -1 & 4 \end{bmatrix}, \quad \{f^e\} = \{0\} \tag{8.5.27}$$

The present mesh of rectangular elements is nodewise equivalent to the triangular element mesh considered in Fig. 8.5.2(*b*). Hence the boundary conditions in (8.5.18) and (8.5.19) are valid for the present case. The six finite element equations for the unknowns U_1, U_2, U_3, U_5, U_6, and U_7 again have the same form as those in (8.5.20), with

$$\begin{aligned} &K_{11} = K^1_{11}, \quad K_{12} = K^1_{12}, \quad K_{15} = K^1_{14} \\ &K_{16} = K^1_{13}, \quad K_{22} = K^1_{22} + K^2_{11}, \quad K_{23} = K^2_{12}, \quad K_{25} = K^1_{24} \\ &K_{26} = K^1_{23} + K^2_{14}, \quad K_{27} = K^2_{13}, \quad \text{etc.} \\ &F_1 = Q^1_1, \quad F_2 = Q^1_2 + Q^2_1, \quad F_3 = Q^2_2 + Q^3_1, \quad F_4 = Q^3_2, \quad \text{etc.} \end{aligned}$$

The equations for the unknown temperatures (i.e., condensed equations for the unknown primary variables) are

$$\frac{k}{6}\begin{bmatrix} 4 & -1 & 0 & -1 & -2 & 0 \\ -1 & 8 & -1 & -2 & -2 & -2 \\ 0 & -1 & 8 & 0 & -2 & -2 \\ -1 & -2 & 0 & 8 & -2 & 0 \\ -2 & -2 & -2 & -2 & 16 & -2 \\ 0 & -2 & -2 & 0 & -2 & 16 \end{bmatrix}\begin{Bmatrix} U_1 \\ U_2 \\ U_3 \\ U_5 \\ U_6 \\ U_7 \end{Bmatrix} = \frac{k}{6}\begin{Bmatrix} 0 \\ 0 \\ 0 \\ T_0 + \sqrt{3}T_0 \\ 2T_0 + \sqrt{3}T_0 + T_0 \\ \sqrt{3}T_0 + T_0 \end{Bmatrix} \tag{8.5.28}$$

Table 8.5.1 Comparison of the nodal temperatures $T(x, y)/T_0$, obtained using various finite element meshes† with the analytical solution (Example 8.5.1).

		Triangles		Rectangles		Analytical solution
x	y	3×2	6×4	3×2	6×4	
0.0	0.0	0.6362	0.6278	0.6128	0.6219	0.6249
0.5	0.0	—	0.6064	—	0.6007	0.6036
1.0	0.0	0.5510	0.5437	0.5307	0.5386	0.5412
1.5	0.0	—	0.4439	—	0.4398	0.4419
2.0	0.0	0.3181	0.3139	0.3064	0.3110	0.3124
2.5	0.0	—	0.1625	—	0.1610	0.1617
0.0	1.0	0.7214	0.7148	0.7030	0.7102	0.7125
0.5	1.0	—	0.6904	—	0.6860	0.6882
1.0	1.0	0.6248	0.6190	0.6088	0.6150	0.6171
1.5	1.0	—	0.5054	—	0.5022	0.5038
2.0	1.0	0.3607	0.3574	0.3515	0.3551	0.3563
2.5	1.0	—	0.1850	—	0.1838	0.1844

†See Fig. 8.5.2 for the geometry and meshes.

The solution of these equations is (in °C)

$$\begin{aligned} U_1 &= 0.6128T_0, \quad U_2 = 0.5307T_0, \quad U_3 = 0.3064T_0 \\ U_5 &= 0.7030T_0, \quad U_6 = 0.6088T_0, \quad U_7 = 0.3515T_0 \end{aligned} \tag{8.5.29}$$

The value of the heat at node 4 is given by

$$Q_2^3 = K_{43}U_3 + K_{47}U_7 = -\frac{k}{6}U_3 - \frac{2k}{6}U_7 = -0.1682kT_0 \text{ (in W)} \tag{8.5.30}$$

We note that the results obtained using the 3×2 mesh of rectangular elements is not as accurate as that obtained with the 3×2 mesh of triangular elements. This is due to the fact that there are only half as many elements in the former case when compared to the latter. Table 8.5.1 contains a comparison of the finite element solutions with the analytical solution (8.5.23) for two different meshes of linear triangular and rectangular elements.

Example 8.5.2

Consider heat transfer in a rectangular region of dimensions a by b, subjected to the boundary conditions shown in Fig. 8.5.3. We wish to write the finite element algebraic equations for the unknown nodal temperatures and heats. For illustrative purposes a 4×2 mesh of rectangular elements is chosen. We assume that the medium is orthotropic, with conductivities k_x and k_y in the x and y directions, respectively. No internal heat generation is assumed.

The heat transfer in the region is governed by the energy equation

$$-\frac{\partial}{\partial x}\left(k_x \frac{\partial T}{\partial x}\right) - \frac{\partial}{\partial y}\left(k_y \frac{\partial T}{\partial y}\right) = 0 \text{ in } \Omega$$

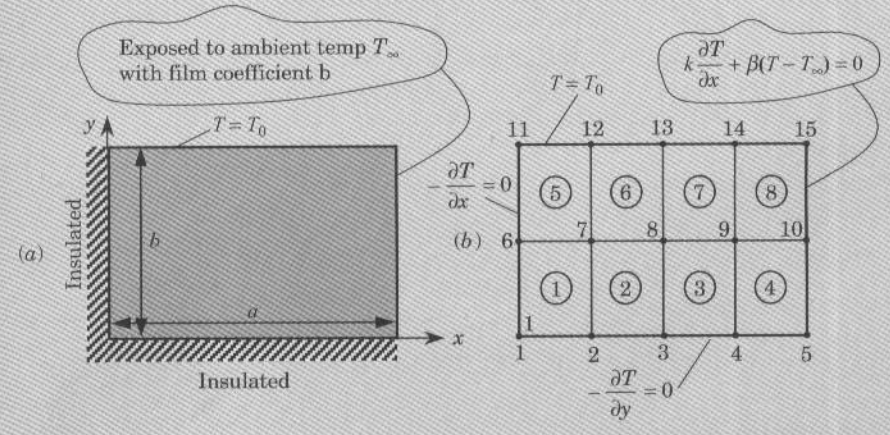

Figure 8.5.3 Domain and boundary conditions for convective heat transfer in a rectangular domain. A mesh of linear rectangular elements is also shown (Example 8.5.2).

The finite element model of the equation is given by

$$[K^e + H^e]\{T^e\} = \{Q^e\} + \{P^e\} \quad (\{f^e\} = \{0\}) \tag{8.5.31}$$

where T_i^e denotes the temperature at node i of element Ω_e, and

$$\begin{aligned} K_{ij}^e &= \int_{\Omega_e} \left(k_x \frac{\partial \psi_i}{\partial x}\frac{\partial \psi_j}{\partial x} + k_y \frac{\partial \psi_i}{\partial y}\frac{\partial \psi_j}{\partial y} \right) dx\, dy \\ H_{ij}^e &= \oint_{\Gamma_e} \beta^e \psi_i \psi_j \, ds \\ Q_i^e &= \oint_{\Gamma_e} q_n \psi_i \, ds, \quad P_i^e = \oint_{\Gamma_e} \beta^e T_\infty^e \psi_i \, ds \end{aligned} \tag{8.5.32}$$

We note that $[H^e]$ and $\{P^e\}$ must be calculated only for elements 4 and 8, which have convective boundaries.

The element matrices for the problem at hand are given by [see Eq. (8.2.53)]

$$[K^e] = \frac{k_x \mu}{6}\begin{bmatrix} 2 & -2 & -1 & 1 \\ -2 & 2 & 1 & -1 \\ -1 & 1 & 2 & -2 \\ 1 & -1 & -2 & 2 \end{bmatrix} + \frac{k_y}{6\mu}\begin{bmatrix} 2 & 1 & -1 & -2 \\ 1 & 2 & -2 & -1 \\ -1 & -2 & 2 & 1 \\ -2 & -1 & 1 & 2 \end{bmatrix} \quad (e = 1, 2, \ldots, 8)$$

$$[H^e] = \frac{\beta_{23}^e h_{23}^e}{6}\begin{bmatrix} 0 & 0 & 0 & 0 \\ 0 & 2 & 1 & 0 \\ 0 & 1 & 2 & 0 \\ 0 & 0 & 0 & 0 \end{bmatrix}, \quad \{P^e\} = \frac{\beta_{23}^e T_\infty^{23} h_{23}^e}{2}\begin{Bmatrix} 0 \\ 1 \\ 1 \\ 0 \end{Bmatrix} \quad (\text{for } e = 4, 8)$$

where μ is the aspect ratio

$$\mu = \frac{1}{2}b \Big/ \frac{1}{4}a = 2b/a$$

There are ten nodal temperatures that are to be determined, and heats at all nodes except nodes 1, 2, 3, 4 and 6 are to be computed. To illustrate the procedure, we write algebraic equations for only representative temperatures and heats.

Node 1 (for Temperatures)

$$K_{11}^1 U_1 + K_{12}^1 U_2 + K_{14}^1 U_6 + K_{13}^1 U_7 = Q_1^1 = 0$$

Node 2 (for Temperatures)

$$K_{21}^1 U_1 + \left(K_{22}^1 + K_{11}^2\right) U_2 + K_{12}^2 U_3 + K_{24}^1 U_6 + \left(K_{23}^1 + K_{14}^2\right) U_7 + K_{13}^2 U_8 = Q_2^1 + Q_1^2 = 0$$

Node 5 (for Temperatures)

$$K_{21}^4 U_4 + \left(K_{22}^4 + H_{22}^4\right) U_5 + K_{24}^4 U_9 + \left(K_{23}^4 + H_{23}^4\right) U_{10} = Q_2^4 + P_2^4 = P_2^4 \quad \text{(known)}$$

Node 10 (for Temperatures)

$$K_{31}^4 U_4 + (K_{32}^4 + H_{32}^4)U_5 + (K_{34}^4 + K_{21}^8)U_9 + (K_{33}^4 + H_{33}^4 + K_{22}^8 + H_{22}^8)U_{10} + K_{24}^8 U_{14} + (K_{23}^8 + H_{23}^8)U_{15} = (Q_3^4 + P_3^4) + (Q_2^8 + P_2^8) = P_3^4 + P_2^8 \text{ (known)}$$

Node 14 (for Heat Q_{14})

$$Q_{14} \equiv Q_3^7 + Q_4^8 = K_{31}^7 U_8 + (K_{32}^7 + K_{41}^8)U_9 + K_{42}^8 U_{10} + K_{34}^7 U_{13} + (K_{33}^7 + K_{44}^8)U_{14} + K_{43}^8 U_{15}$$

From the boundary conditions, we know temperatures at nodes 11 through 15 (i.e., U_{11}, $U_{12}, \ldots, U_{15}$ are known values). Substituting the values of K_{ij}^e, H_{ij}^e, and P_i^e, we obtain explicit form of the algebraic equations. For example, the algebraic equation corresponding to node 10 is

$$-\frac{1}{6}\left(k_x\mu + \frac{k_y}{\mu}\right)U_4 + \left[\frac{1}{6}\left(k_x\mu - \frac{2k_y}{\mu}\right) + \frac{1}{12}\beta b\right]U_5 + \frac{1}{6}\left[\left(-2k_x\mu + \frac{2k_y}{\mu}\right) + \left(-2k_x\mu + \frac{k_y}{\mu}\right)\right]U_9 + \frac{2}{3}\left[\left(k_x\mu + \frac{k_y}{\mu}\right) + \frac{\beta b}{2}\right]U_{10} + \frac{1}{6}\left(k_x\mu - \frac{2k_y}{\mu}\right)U_{14} + \frac{1}{6}\left[k_x\mu - \frac{2k_y}{\mu} + \frac{\beta b}{2}\right]U_{15} = \frac{1}{2}\beta b T_\infty$$

This completes the example.

Example 8.5.3

Consider heat transfer in a homogeneous, isotropic medium. The governing equation, in nondimensional form, is given by

$$-\nabla^2 u = f_0 \text{ in } \Omega$$

over the domain shown in Fig. 8.5.4.

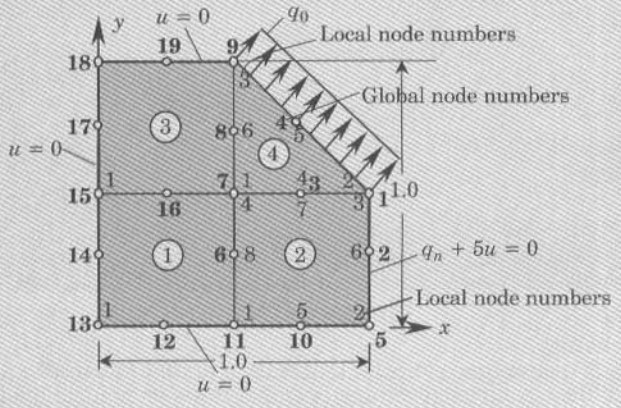

Figure 8.5.4 Domain with finite element mesh and boundary conditions for a heat transfer problem discussed in Example 8.5.3.

We wish to

(*a*) write the finite element equation associated with global node 1 in terms of element coefficients,

(*b*) compute the contribution of the flux q_0 to global nodes 1 and 4, and

(*c*) compute the contribution of the boundary condition $q_n + 5u = 0$ to the finite element equations.

(*a*) The finite element equation associated with global node 1 is

$$K_{11}U_1 + K_{12}U_2 + K_{13}U_3 + K_{14}U_4 + K_{16}U_6 + K_{17}U_7 + K_{18}U_8 = F_1$$

Writing the global coefficients in terms of the element coefficients, we obtain

$$\begin{aligned}&\left(K_{33}^{(2)} + K_{22}^{(4)} + H_{33}^{(2)} + H_{22}^{(4)}\right)U_1 + \left(K_{36}^{(2)} + H_{36}^{(2)}\right)U_2 + \left(K_{37}^{(2)} + K_{24}^{(4)}\right)U_3\\ &\quad + K_{25}^{(4)}U_4 + K_{38}^{(2)}U_6 + \left(K_{34}^{(2)} + K_{21}^{(4)}\right)U_7 + K_{26}^{(4)}U_8 = F_3^{(2)} + P_3^{(2)} + F_2^{(4)}\end{aligned}$$

Explicit form of H_{ij}^e ($P_i^e = 0$ because $u_\infty = 0$) will be given in Part (*c*).

(*b*) The contributions of uniform flux q_0 to global nodes 1, 4, and 9 are readily known from one-dimensional quadratic element [see Eq. (3.2.37*b*)]. It can be calculated as follows:

$$\begin{aligned}Q_2^4 &= \int_0^L q_0\psi_2^4(s)\,ds = q_0\int_0^L \left(1 - \frac{s}{L}\right)\left(1 - \frac{2s}{L}\right)ds\\ &= q_0\int_0^L \left(1 - 3\frac{s}{L} + \frac{2s^2}{L^2}\right)ds = q_0\left(L - 3\frac{L}{2} + \frac{2L}{3}\right) = \frac{q_0 L}{6} = Q_3^4\end{aligned}$$

where $L = 1/\sqrt{2} = 0.7071$. Similarly, contribution to global node 4 is

$$\begin{aligned}Q_5^4 &= \int_0^L q_0\psi_5^4(s)\,ds = q_0\int_0^L 4\frac{s}{L}\left(1 - \frac{s}{L}\right)ds\\ &= 4q_0\int_0^L \left(\frac{s}{L} - \frac{s^2}{L^2}\right)ds = 4q_0\left(\frac{L}{2} - \frac{L}{3}\right) = \frac{4q_0 L}{6}\end{aligned}$$

(*c*) The contribution of the boundary condition $q_n + 5u = 0$ to the finite element equation associated with node 1 is

$$\begin{aligned}Q_3^2 &= \int_0^{0.5} q_n\psi_3^{(2)}(s)\,ds = -5\int_0^{0.5}\left(u_2^{(2)}\psi_2^{(2)} + u_6^{(2)}\psi_6^{(2)} + u_3^{(2)}\psi_3^{(2)}\right)\psi_3^{(2)}\,ds\\ &= -5\left(\frac{0.5}{30}\right)(4\times U_1 + 2\times U_2 - 1\times U_5) = -\frac{1}{3}U_1 - \frac{1}{6}U_2\end{aligned}$$

8.5.2 Fluid Mechanics

Here, we consider the equations governing potential flows of an ideal fluid. An *ideal fluid* is one that has zero viscosity and is incompressible. A fluid is said to be *incompressible* if the volume change is zero, (i.e., ρ is constant)

$$\nabla \cdot \mathbf{v} = 0 \tag{8.5.33}$$

where $\mathbf{v}$ is the velocity vector. A fluid is termed *inviscid* if the viscosity is zero, $\mu = 0$. A flow with negligible angular velocity is called *irrotational* if

$$\nabla \times \mathbf{v} = 0 \tag{8.5.34}$$

The irrotational flow of an ideal fluid (i.e., $\rho =$ constant and $\mu = 0$) is called a *potential flow*.

For an ideal fluid, the continuity and the momentum equations can be written as [see Schlichting (1969)]

$$\nabla \cdot \mathbf{v} = 0 \tag{8.5.35a}$$

$$\frac{1}{2}\rho \nabla(\mathbf{v} \cdot \mathbf{v}) - \rho[\mathbf{v} \times (\nabla \times \mathbf{v})] = -\nabla \hat{P} \tag{8.5.35b}$$

where $\nabla \hat{P} = \nabla P - \mathbf{f}$. For irrotational flow the velocity field $\mathbf{v}$ satisfies (8.5.34). For two-dimensional irrotational flows, these equations have the form

$$\frac{\partial v_x}{\partial x} + \frac{\partial v_y}{\partial y} = 0 \tag{8.5.35c}$$

$$\frac{1}{2}\rho\left(v_x^2 + v_y^2\right) + \hat{P} = \text{constant} \tag{8.5.35d}$$

$$\frac{\partial v_x}{\partial y} - \frac{\partial v_y}{\partial x} = 0 \tag{8.5.35e}$$

These three equations are used to determine v_x, v_y, and $\hat{P}$.

The problem of determining v_x, v_y, and $\hat{P}$ is simplified by introducing a function $\psi(x, y)$ such that the continuity equation is identically satisfied:

$$v_x = \frac{\partial \psi}{\partial y}, \quad v_y = -\frac{\partial \psi}{\partial x} \tag{8.5.36}$$

Then the irrotational flow condition in terms of ψ takes the form,

$$\frac{\partial^2 \psi}{\partial y^2} + \frac{\partial^2 \psi}{\partial x^2} \equiv \nabla^2 \psi = 0 \tag{8.5.37}$$

Equation (8.5.37) is used to determine ψ; then velocities v_x and v_y are determined from (8.5.36) and $\hat{P}$ from (8.5.35*d*). The function ψ has the physical significance that lines of constant ψ are lines across which there is no flow, i.e., they are streamlines of the flow. Hence, $\psi(x, y)$ is called the *stream function*.

In the cylindrical coordinates, the continuity equation (8.5.35*a*) takes the form

$$\frac{\partial v_r}{\partial r} + \frac{1}{r}\frac{\partial v_\theta}{\partial \theta} = 0 \tag{8.5.38}$$

where v_r and v_θ are the radial and circumferential velocity components. The stream function $\psi(r, \theta)$ is defined as

$$v_r = \frac{1}{r}\frac{\partial \psi}{\partial \theta}, \quad v_\theta = -\frac{\partial \psi}{\partial r} \tag{8.5.39}$$

and (8.5.37) takes the form

$$\nabla^2\psi \equiv \frac{\partial^2\psi}{\partial r^2} + \frac{1}{r}\frac{\partial\psi}{\partial r} + \frac{1}{r^2}\frac{\partial^2\psi}{\partial\theta^2} = 0 \tag{8.5.40}$$

There exists an alternative formulation of the potential flow equations (8.5.35*a*) and (8.5.35*b*). We can introduce a function $\phi(x, y)$, called the *velocity potential*, such that the condition of irrotational flow, Eq. (8.5.35*e*) is identically satisfied:

$$v_x = -\frac{\partial\phi}{\partial x}, \quad v_y = -\frac{\partial\phi}{\partial y} \tag{8.5.41}$$

Then the continuity equation (8.5.35*c*) takes the form,

$$-\nabla^2\phi = 0 \tag{8.5.42}$$

Comparing (8.5.39) with (8.5.41), we note that

$$-\frac{\partial\phi}{\partial x} = \frac{\partial\psi}{\partial y}, \quad -\frac{\partial\phi}{\partial y} = -\frac{\partial\psi}{\partial x} \tag{8.5.43}$$

The velocity potential has the physical significance that lines of constant ϕ are lines along which there is no change in velocity. The equipotential lines and streamlines intersect at right angles.

Although both ψ and ϕ are governed by the Laplace equation, the boundary conditions on them are different in a flow problem, as should be evident by the definitions (8.5.39) and (8.5.41). In this section, we consider applications of the finite element method to potential flows, i.e., the solution of (8.5.36) and (8.5.43).

We consider two examples of fluid flow. The first one deals with a groundwater flow problem and the second with the flow around a cylindrical body. In discussing these problems, emphasis is placed on certain modeling aspects, data generation, and postprocessing of solutions. Evaluation of element matrices and assembly are amply illustrated in previous examples and will not be discussed as it takes substantial space to write the assembled equations even for the crude meshes used in these examples.

Example 8.5.4 (Groundwater Flow or Seepage)

The governing differential equation for a homogeneous (i.e., material properties do not vary with position) acquifer of unit depth, with flow in the xy plane, is given by

$$-\frac{\partial}{\partial x}\left(a_{11}\frac{\partial\phi}{\partial x}\right) - \frac{\partial}{\partial y}\left(a_{22}\frac{\partial\phi}{\partial y}\right) = f \text{ in } \Omega \tag{8.5.44}$$

where a_{11} and a_{22} are the coefficients of permeability (in $m^3/day/m^2$) along the x and y directions, respectively, ϕ is the piezometric head or velocity potential (in m), measured from a reference level (usually the bottom of the aquifer), and f is the rate of pumping (in $m^3/day/m^3$). We know from the previous discussions that the natural and essential boundary conditions associated with (8.5.44) are as follows:

Natural

$$a_{11}\frac{\partial\phi}{\partial x}n_x + a_{22}\frac{\partial\phi}{\partial y}n_y = \phi_n \quad \text{on } \Gamma_2 \tag{8.5.45}$$

Essential

$$\phi = \phi_0 \quad \text{on } \Gamma_1 \tag{8.5.46}$$

where Γ_1 and Γ_2 are the portions of the boundary Γ of Ω such that $\Gamma_1 + \Gamma_2 = \Gamma$.

Here we consider the following specific problem: Find the lines of constant potential ϕ (equipotential lines) in a 3000 m × 1500 m rectangular aquifer Ω (see Fig. 8.5.5) bounded on the long sides by an impermeable material (i.e., $\partial\phi/\partial n = 0$) and on the short sides by a constant head of 200 m ($\phi_0 = 200$ m). In the way of sources, suppose that a river is passing through the aquifer, infiltrating the aquifer at a rate of $q_0 = 0.24$ m^3/day/m, and that two pumps are located at (830, 1000) and (600, 1900), pumping at a rate of $Q_1 = 1200$ m^3/day and $Q_2 = 2400$ m^3/day, respectively.

A mesh of 64 triangular elements and 45 nodes is used to model the domain [see Fig. 8.5.6(*a*)]. The river forms the interelement boundary between elements (26, 28, 30, 32) and (33, 35, 37, 39). In the mesh selected, neither pump is located at a node. This is done intentionally for the purpose of illustrating the calculation of the generalized forces due to a point source within an element. If the pumps are located at a node, then the rate of pumping Q_0 is input as the specified secondary variable of the node. When a source (or sink) is located at a point other than a node, we must calculate its contribution to the nodes. Similarly, the source components due to the distributed line source (i.e., the river) should be computed.

First, consider the line source. We can view the river as a line source of constant intensity, $q_0 = 0.24$ m^3/day/m. Since the length of the river is equally divided by nodes 21 through 25 (into four parts), we can compute the contribution of the infiltration of the river at each of the nodes 21 through 25 by evaluating the integrals [see Fig. 8.5.6(*b*)]:

$$\text{node 25:} \quad \int_0^h (0.24)\psi_1^1 \, ds$$

$$\text{node 24:} \quad \int_0^h (0.24)\psi_2^1 \, ds + \int_0^h (0.24)\psi_1^2 \, ds$$

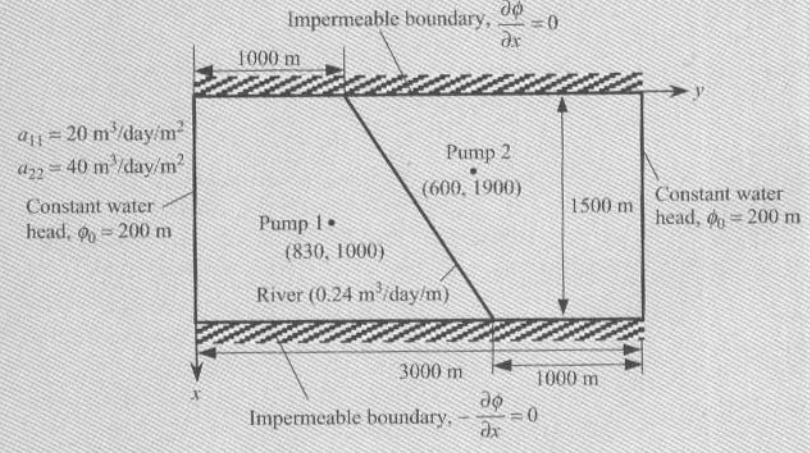

Figure 8.5.5 Geometry and boundary conditions for the groundwater flow problem of Example 8.5.4.

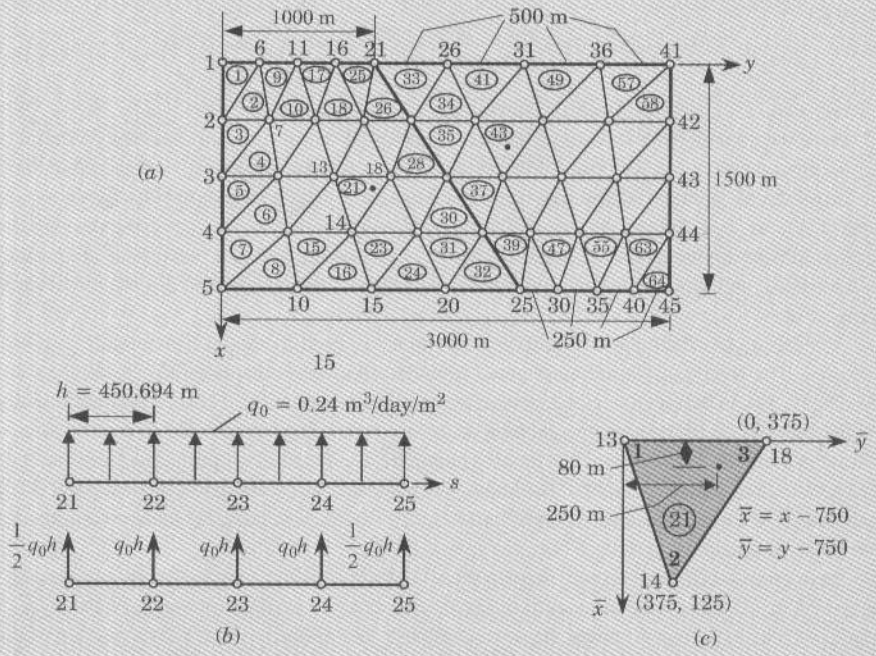

Figure 8.5.6 (*a*) Finite element mesh of triangular elements (45 nodes and 64 elements), (*b*) computation of global forces due to the infiltration of the river, and (*c*) computation of global forces for pump 1 located inside element 21 for the groundwater flow problem of Example 8.5.4.

$$\text{node 23:} \quad \int_0^h (0.24)\psi_2^2\, ds + \int_0^h (0.24)\psi_1^3\, ds$$

$$\text{node 22:} \quad \int_0^h (0.24)\psi_2^3\, ds + \int_0^h (0.24)\psi_1^4\, ds$$

$$\text{node 21:} \quad \int_0^h (0.24)\psi_2^4\, ds$$

For constant intensity q_0 and the linear interpolation functions $\psi_1^e(s) = 1 - s/h$ and $\psi_2^e(s) = s/h$, the contribution of these integrals is well known:

$$\int_0^h q_0 \psi_i^e\, ds = \frac{1}{2} q_0 h, \quad h = \frac{1}{4}[(1000)^2 + (1500)^2]^{\frac{1}{2}}, \quad q_0 = 0.24$$

Hence, we have

$$F_{21} = \frac{1}{2} q_0 h, \quad F_{22} = F_{23} = F_{24} = q_0 h, \quad F_{25} = q_0 h \frac{1}{2}$$

Next, we consider the contribution of the point sources. Since the point sources are located inside an element, we distribute the source to the nodes of the element by interpolation [see Fig. 8.5.6(*c*)]:

$$f_i^e = \int_{\Omega_e} Q_0 \delta(x - x_0, y - y_0) \psi_i^e(x, y)\, dx\, dy = Q_0 \psi_i^e(x_0, y_0)$$

For example, the source at pump 1 (located at $x_0 = 830$ m, $y_0 = 1000$ m) can be expressed as (pumping is considered to be a negative point source)

$$Q_1(x, y) = -1200\, \delta(x - 830, y - 1000) \quad \text{or} \quad Q_1(\bar{x}, \bar{y}) = -1200\, \delta(\bar{x} - 80, \bar{y} - 250)$$

where $\delta(\cdot)$ is the Dirac delta function [see Eq. (3.3.3)]. The interpolation functions ψ_i^e for element 21 are [in terms of the local coordinates $\bar{x}$ and $\bar{y}$; see Fig. 8.5.6(*c*)]

$$\psi_i(\bar{x}, \bar{y}) = \frac{1}{2A}(\alpha_i + \beta_i \bar{x} + \gamma_i \bar{y}), \quad (i = 1, 2, 3)$$

$$2A = (375)^2, \quad \alpha_1 = (375)^2, \quad \alpha_2 = 0, \quad \alpha_3 = 0$$

$$\beta_1 = -250, \quad \beta_2 = 375, \quad \beta_3 = -125, \quad \gamma_1 = -375, \quad \gamma_2 = 0, \quad \gamma_3 = 375$$

Therefore, we have

$$\psi_1(80, 250) = 0.1911, \quad \psi_2(80, 250) = 0.5956, \quad \psi_3(80, 250) = 0.2133$$

Similar computations can be done for pump 2 (see Problem 8.8).

In summary, primary variables and nonzero secondary variables are:

$$U_1 = U_2 = U_3 = U_4 = U_5 = U_{41} = U_{42} = U_{43} = U_{44} = U_{45} = 200.0$$

$$F_{21} = 54.0833, \quad F_{22} = F_{23} = F_{24} = 108.1666, \quad F_{25} = 54.0833$$

$$F_{13} = -229.33, \quad F_{14} = -256.0, \quad F_{18} = -714.67, \quad F_{27} = -411.429$$

$$F_{28} = -1440.0, \quad F_{32} = -548.571$$

The secondary variables at nodes 6–12, 15–17, 19, 20, 26, 29–31, and 33–40 are zero. This completes the data generation for the problem.

The assembled equations are solved after imposing the specified boundary conditions for the values of ϕ at the nodes. The equipotential lines can be determined using (8.3.27). The lines of constant ϕ are shown in Fig. 8.5.7(*a*).

The velocity components are determined in the postcomputation using the definition (8.5.41)

$$v_x = -\frac{\partial \phi}{\partial x}, \quad v_y = -\frac{\partial \phi}{\partial y}$$

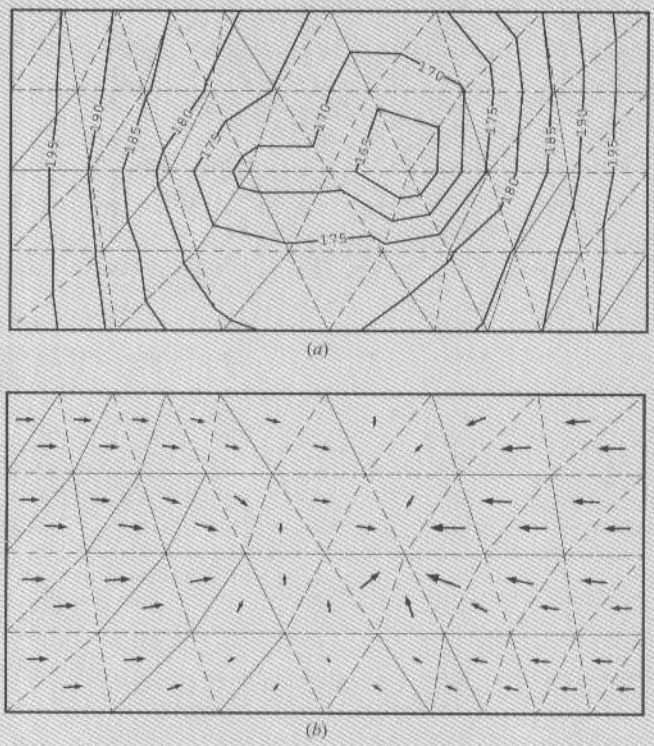

Figure 8.5.7 Plots of constant piezometric head and velocity vector for the groundwater flow: (*a*) lines of constant ϕ; and (*b*) plot of velocity vectors (Example 8.5.4).

and the velocity vector is given by

$$\mathbf{v} = v_x\hat{\mathbf{i}} + v_y\hat{\mathbf{j}}, \quad |\mathbf{v}| = \sqrt{v_x^2 + v_y^2}, \quad \theta = \tan^{-1}\frac{v_y}{v_x}$$

where θ is the angle, measured in counterclockwise direction, of the velocity vector form along the +ve x axis. The velocity vectors for the problem at hand are shown in Fig. 8.5.7(*b*). The greatest drawdown of water occurs at node 28, which has the largest portion of discharge from pump 2. This completes the discussion of the groundwater flow problem.

Next, we consider an example of irrotational flows of an ideal fluid (i.e., a nonviscous fluid). Examples of physical problems that can be approximated by such flows are provided by flow around bodies such as weirs, airfoils, buildings, and so on, and by flow of water through the earth and dams. Laplace equations (8.5.37) and (8.5.42) governing these flows are a special case of (8.2.1) and therefore, we can use the finite element equations developed earlier to model these problems.

Example 8.5.5 (Confined Flow around a Circular Cylinder)

The irrotational flow of an ideal fluid about a circular cylinder, placed with its axis perpendicular to the plane of the flow between two *long* horizontal walls (see Fig. 8.5.8) is to be analyzed using the finite element method. The equation governing the flow is given by

$$-\nabla^2 u = 0 \quad \text{in } \Omega$$

where u is either (a) the stream function or (b) the velocity potential. If u is the stream function ψ, the velocity components $\mathbf{v} = (v_x, v_y)$ of the flow field are given by

$$v_x = \frac{\partial \psi}{\partial y}, \quad v_y = -\frac{\partial \psi}{\partial x}$$

If u is the velocity potential, ϕ, the velocity components can be computed from

$$v_x = -\frac{\partial \phi}{\partial x}, \quad v_y = -\frac{\partial \phi}{\partial y}$$

In either case, the velocity field is not affected by a constant term in the solution u. We analyze the problem using both formulations. For both formulations, symmetry exists about the horizontal and vertical center lines, therefore, only a quadrant of the flow region is used as the computational domain. To determine the constant state of the solution, which does not affect the velocity field, we arbitrarily set the functions ψ and ϕ to zero (or a constant) on appropriate boundary lines.

Stream Function Formulation

The boundary conditions on the stream function ψ can be determined as follows. Streamlines have the property that flow perpendicular to a streamline is zero. Therefore, the fixed walls correspond to streamlines. Note that for inviscid flows, fluid does not stick to rigid walls. Due to the biaxial symmetry about the horizontal and vertical centerlines, only a quadrant (say, ABCDE in Fig. 8.5.9) of the domain need be used in the analysis. The fact that the velocity component perpendicular to the horizontal line of symmetry is equal to zero allows us to use that line as a streamline. Since the velocity field depends on the relative difference of two

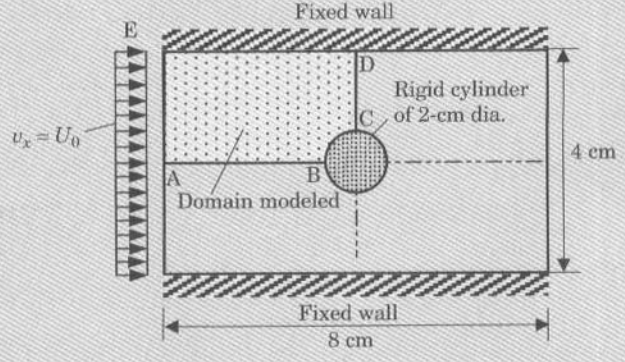

Figure 8.5.8 Domain and boundary conditions for the stream function and velocity potential formulations of irrotational flow about a cylinder (Example 8.5.5).

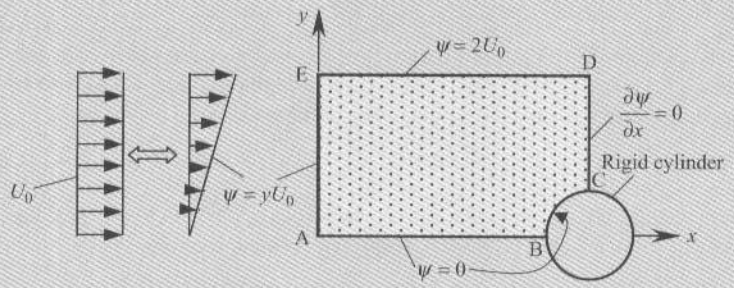

Figure 8.5.9 Computational domain and boundary conditions for the stream function formulation of inviscid flow around a cylinder (see Fig. 8.5.8).

streamlines, we take the value of the stream function that coincides with the horizontal axis of symmetry (i.e., on ABC) to be zero and then determine the value of ψ on the upper wall from the condition

$$\frac{\partial \psi}{\partial y} = U_0$$

where U_0 is the inlet horizontal velocity of the field. We determine the value of the stream function on the boundary $x = 0$ by integrating the above equation with respect to y

$$\int_0^y \frac{d\psi}{dy}\, dy = \int_0^y U_0\, dy + \psi_A = U_0 y + 0 \tag{8.5.47}$$

because $\psi_A = 0$ by the previous discussion. This gives the boundary condition on AE. Since the line ED is a streamline and its value at point E is $2U_0$, it follows that $\psi = 2U_0$ on line ED. Lastly, on CD we assume the vertical velocity is zero (i.e., $v_y = 0$); hence, $\partial\psi/\partial x = 0$ on CD. The boundary conditions are shown on the computational domain in Fig. 8.5.9.

In selecting a mesh, we should note that the velocity field is uniform (i.e., streamlines are horizontal) at the inlet and that it takes a parabolic profile at the exit (along CD). Therefore, the mesh at the inlet should be uniform, and the mesh close to the cylinder should be relatively more refined to be able to model the curved boundary and capture the rapid change in ψ. Two coarse finite element meshes are used to discuss the boundary conditions, and results for refined meshes will be discussed subsequently. Mesh T1 consists of 32 triangular elements and mesh Q1 consists of 16 quadrilateral elements. Both meshes contain 25 nodes (see Fig. 8.5.10). The mesh with solid lines in Fig. 8.5.10 corresponds to mesh Q1, and the mesh with solid and dashed lines in Fig. 8.5.10 correspond to mesh T1. It should be noted that the discretization error is not zero for this case.

The specified primary degrees of freedom (i.e., nodal values of ψ) for mesh T1 and mesh Q1 are:

$$\begin{gathered} U_1 = U_2 = \cdots = U_6 = U_{12} = U_{18} = U_{24} = U_{30} = U_{36} = U_{42} = 0.0 \\ U_7 = 1.333, \quad U_{13} = 0.667, \quad U_{19} = U_{25} = U_{31} = U_{37} = 2.0 \end{gathered} \tag{8.5.48}$$

There are no nonzero specified secondary variables; the secondary variables are specified to be zero at the nodes on line CD:

$$F_{38} = F_{39} = F_{40} = F_{41} = 0$$

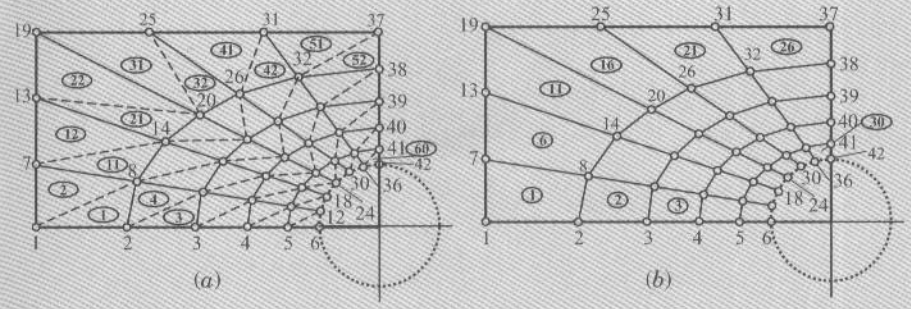

Figure 8.5.10 Meshes used for inviscid flow around a cylinder. (*a*) Mesh of linear triangles. (*b*) Mesh of linear quadrilaterals.

Although the secondary variable is specified to be zero at nodes 37 and 42, where the primary variable is also specified, we choose to impose the boundary conditions on the primary variable over the secondary variables.

Velocity Potential Formulation (PF)

The boundary conditions on the velocity potential ϕ can be derived as follows (see Fig. 8.5.11). The fact that $v_y = -\partial\phi/\partial y = 0$ (no penetration) on the upper wall as well as on the horizontal line of symmetry gives the boundary conditions there. Along AE the velocity $v_x = -\partial\phi/\partial x$ is specified to be U_0. On the surface of the cylinder the normal velocity, $v_n = -\partial\phi/\partial n$, is zero. Thus, all boundary conditions, so far, are of the flux type. On the boundary CD we must know either ϕ or $\partial\phi/\partial n = \partial\phi/\partial x$. It is clear that $-\partial\phi/\partial x = v_x$ is not known on CD. Therefore, we assume that ϕ is known, and we set it equal to $\phi_0 =$ constant. The constant ϕ_0 is arbitrary, and it does not contribute to the velocity field (because $-\partial\phi/\partial x = v_x$ and $-\partial\phi/\partial y = v_y$ are independent of the constant ϕ_0). It should be noted that determining the constant part in the solution for ϕ (i.e., eliminating the rigid body motion) requires knowledge of ϕ at one or more points of the mesh. We take $\phi = \phi_0 = 0$ on CD.

The mathematical boundary conditions of the problem must be translated into finite element data. The boundary conditions on the primary variables come from the boundary CD. We have

$$U_{37} = U_{38} = U_{39} = U_{40} = U_{41} = U_{42} = 0.0$$

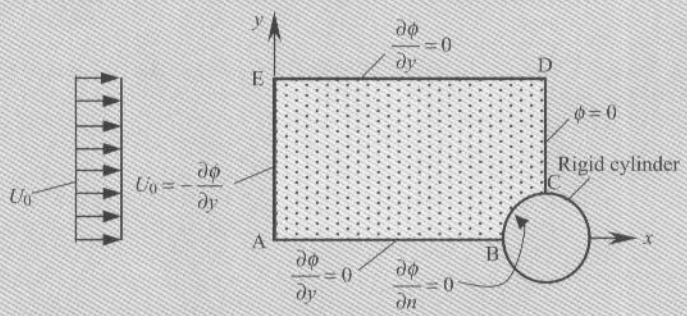

Figure 8.5.11 Computational domain and boundary conditions for the velocity potential formulation of inviscid flow around a cylinder (see Fig. 8.5.8).

The only nonzero boundary conditions on the secondary variables come from the boundary AE. There, we must evaluate the boundary integral

$$\int_{\Gamma_e} \frac{\partial \phi}{\partial n} \psi_i \, ds = U_0 \int_{AE} \psi_i(y) \, dy$$

for each node i on AE. We obtain ($h = 2/3 = 0.66667$)

$$Q_1 = U_0 \int_0^h \left(1 - \frac{\bar{y}}{h}\right) d\bar{y} = 0.33333 U_0$$

$$Q_7 = U_0 \int_0^h \frac{\bar{y}}{h} d\bar{y} + U_0 \int_0^h \left(1 - \frac{\bar{y}}{h}\right) d\bar{y} = 0.66667 U_0$$

$$Q_{13} = U_0 \int_0^h \frac{\bar{y}}{h} d\bar{y} + U_0 \int_0^h \left(1 - \frac{\bar{y}}{h}\right) d\bar{y} = 0.66667 U_0$$

$$Q_{19} = U_0 \int_0^h \frac{\bar{y}}{h} d\bar{y} = \frac{h U_0}{2} = 0.3333 U_0$$

Numerical Results

Table 8.5.2 contains the values of the stream function and its derivative $(\partial \psi / \partial y)(= v_x)$ at selected *points/elements* of the meshes. The finite element program **FEM2D** (see Chapter 13 for details) is used in the analysis. The stream function values obtained with mesh T1 and mesh Q1 are very close to each other. Recall that the derivative $\partial \psi / \partial y$ is constant in a linear triangular element, whereas it varies linearly with x in a linear rectangular element. Therefore, mesh T1 and mesh Q1 results will not be the same. The velocities included in Table 8.5.2 correspond to elements closest to the symmetry line (i.e., $y = 0$ line) and surface of the cylinder.

The tangential velocity v_t on the cylinder surface can be computed from the relation,

$$v_t(\theta) = v_x \sin\theta + v_y \cos\theta = \frac{\partial \psi}{\partial y} \sin\theta - \frac{\partial \psi}{\partial x} \cos\theta \tag{8.5.49}$$

Contour plots of streamlines, velocity potential, and horizontal velocity $v_x = \partial \psi / \partial y$ obtained with mesh Q1 are shown in Fig. 8.5.12. Note that there is a difference between the

Table 8.5.2 Finite element results from the stream function formulation of inviscid flow around a cylinder (Example 8.5.5).

		Stream function		Velocity $v_t = \partial \psi / \partial y$		Velocity $v_x = -\partial \phi / \partial x$	
x	y	Mesh T1	Mesh Q1	Mesh T1	Mesh Q1	Mesh T1	Mesh Q1
1.3183	0.7354	0.7092	0.7095	0.9643(1)†	0.9852(1)	0.9922(1)	0.9989(1)
2.2705	0.5444	0.4372	0.4379	0.8032(3)	0.9005(2)	0.9371(3)	0.9408(2)
2.8564	0.4268	0.1667	0.1650	0.3906(5)	0.6432(3)	0.7047(5)	0.7018(3)
1.4112	1.4459	1.4241	1.4270	0.0000(7)	0.2679(4)	0.2999(7)	0.3197(4)
2.4305	1.0457	0.8730	0.8823	0.4469(15)	0.8746(8)	0.6469(15)	0.8364(8)
3.0577	0.7995	0.3357	0.3384	1.636(24)	1.586(12)	1.873(24)	1.453(12)
2.6931	1.5388	1.3758	1.4010	2.544(32)	2.4551(16)	2.163(32)	2.075(16)
3.1937	1.2057	0.7706	0.7980				
3.5018	1.0007	0.2520	0.2658				
4.0000	1.5714	1.2395	1.2065				
4.0000	1.2619	0.6191	0.5796				
4.0000	1.0714	0.1817	0.1588				

†The numbers in parentheses denote element number; the derivatives of ψ and ϕ are evaluated at the center of this element.

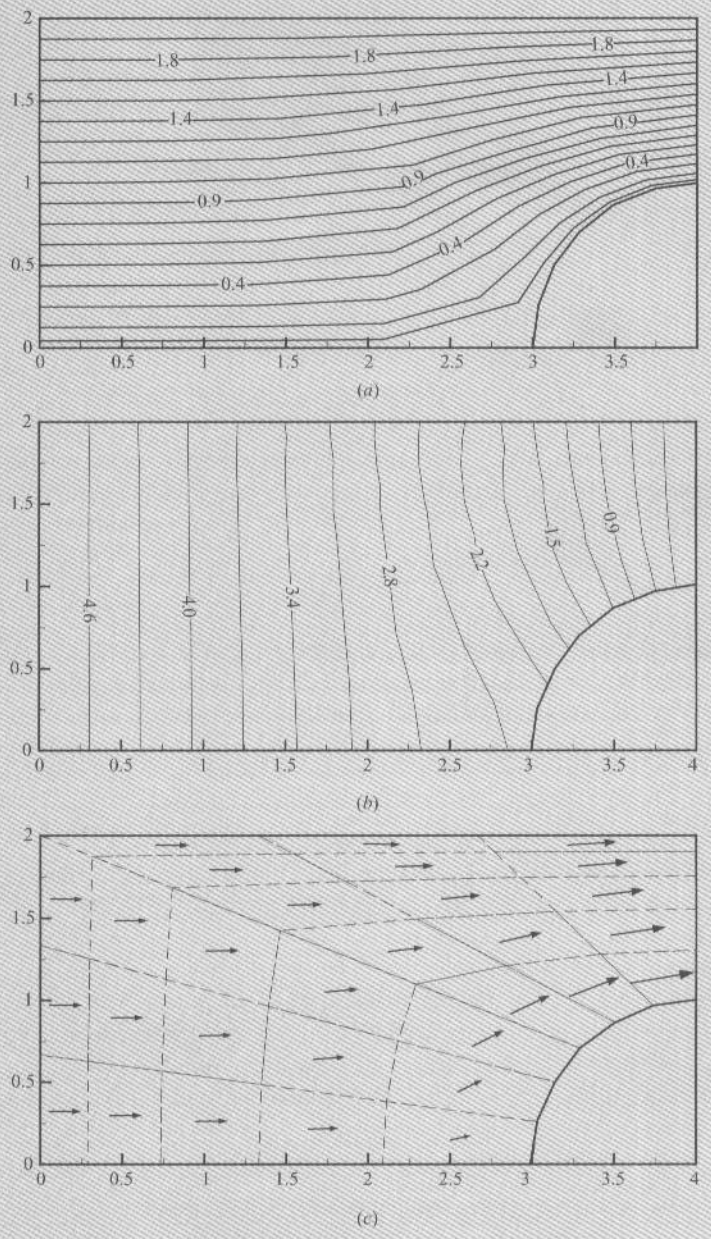

Figure 8.5.12 Contours of (*a*) stream function, (*b*) velocity potential, and (*c*) x component of velocity (with the velocity potential formulation), as obtained using mesh Q1.

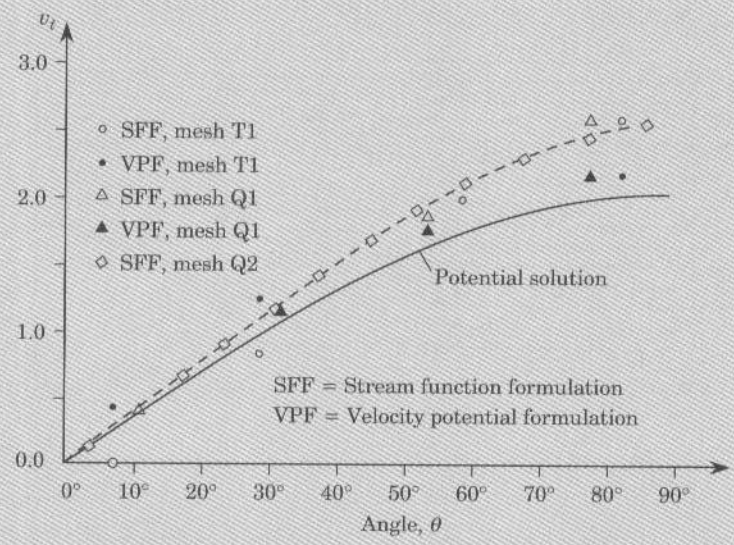

Figure 8.5.13 Variation of the tangential velocity along the cylinder surface: comparison of the finite element results with the potential theory solution (mesh Q2 contains 96 elements and 117 nodes).

velocities obtained with the two formulations (for either mesh). This is primarily due to the nature of the boundary value problems in the two formulations. In the stream function formulation, there are more boundary conditions on the primary variable than in the velocity potential formulation.

A plot of the variation of the tangential velocity with the angular distance along the cylinder surface is shown in Fig. 8.5.13 along with the analytical potential solution

$$v_t = U_0(1 + R^2/r^2)\sin\theta \tag{8.5.50a}$$

valid on the cylinder surface. The finite element solution of a refined mesh, mesh Q2, is also included in the figure. The angle θ, radial distance r, and tangential velocity v_t can be computed from the relations

$$\theta = \tan^{-1}\left(\frac{y}{4-x}\right), \quad r = \sqrt{(4-x)^2 + y^2}, \quad v_t = v_x \sin\theta + v_y \cos\theta \tag{8.5.50b}$$

The finite element solution is in general agreement with the potential solution of the problem. However, the finite element solution is not expected to agree closely because v_t is evaluated at a radial distance $r > R$, whereas the potential solution is evaluated at $r = R$ only.

This completes the section on fluid mechanics problems that are cast in terms of a single dependent unknown, such as the stream function or velocity potential. We return to fluid

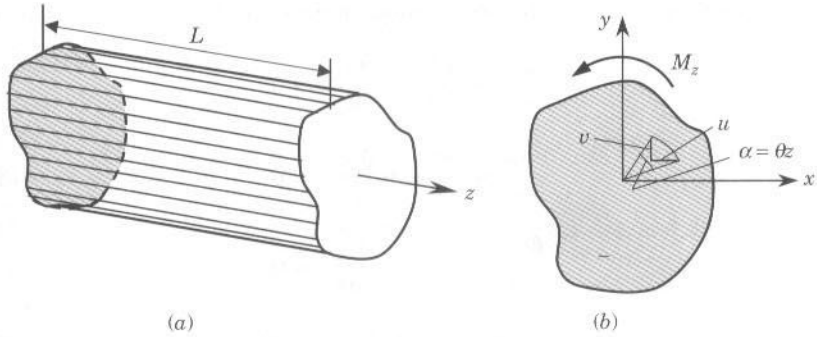

Figure 8.5.14 Torsion of cylindrical members: (*a*) a cylindrical member and (*b*) domain of analysis.

mechanics later in Chapter 10 to consider two-dimensional flows of viscous, incompressible fluids. The governing equations of such problems consist of several dependent variables and as many differential equations.

8.5.3 Solid Mechanics

In this section we consider two-dimensional boundary value problems of solid mechanics that are cast in terms of a single dependent unknown. These problems include torsion of cylindrical members and transverse deflection of membranes. This study is restricted to small deformations.

Torsion of Cylindrical Members

Consider a cylindrical bar (i.e., a long, uniform cross-sectional member), fixed at one end and twisted by a couple (i.e., torque) of magnitude M_z that is directed along the axis (z) of the bar, as shown in Fig. 8.5.14(*a*). We wish to determine the amount of twist and the associated stress field in the bar. To this end, we first derive the governing equations and then analyze the equation using the finite element method.

In general, a noncircular cross-sectional member subjected to torsional moment experiences warping at any section. We assume that all cross sections warp in the same way (which holds true for small twisting moments and deformation). This assumption allows us to assume that the displacements (u, v, w) along the coordinates (x, y, z) are of the form [see Fig. 8.5.14(*b*)]

$$u = -\theta z y, \quad v = \theta z x, \quad w = \theta \phi(x, y) \tag{8.5.51}$$

where $\phi(x, y)$ is a function to be determined and θ is the angle of twist per unit length of the bar.

The displacement field in (8.5.51) can be used to compute the strains, and stresses are computed using an assumed constitutive law. The stresses thus computed must satisfy the

three-dimensional equations of stress equilibrium in Eq. (2.3.52):

$$\begin{aligned}
\frac{\partial \sigma_{xx}}{\partial x} + \frac{\partial \sigma_{xy}}{\partial y} + \frac{\partial \sigma_{xz}}{\partial z} &= 0 \\
\frac{\partial \sigma_{xy}}{\partial x} + \frac{\partial \sigma_{yy}}{\partial y} + \frac{\partial \sigma_{yz}}{\partial z} &= 0 \\
\frac{\partial \sigma_{xz}}{\partial x} + \frac{\partial \sigma_{yz}}{\partial y} + \frac{\partial \sigma_{zz}}{\partial z} &= 0
\end{aligned} \tag{8.5.52}$$

and the stress boundary conditions on the lateral surface and at the end of the cylindrical bar. Calculation of strains and then stresses using the generalized Hooke's law gives the expressions,

$$\sigma_{xz} = G\theta\left(\frac{\partial \phi}{\partial x} - y\right), \quad \sigma_{yz} = G\theta\left(\frac{\partial \phi}{\partial y} + x\right) \tag{8.5.53}$$

and all other stresses are identically zero. Here G denotes the shear modulus of the material of the bar. Substitution of these stresses into (8.5.52) yields [the first two equations in (8.5.52) are identically satisfied and the third one leads to the following equation]:

$$\frac{\partial}{\partial x}\left(G\theta\frac{\partial \phi}{\partial x}\right) + \frac{\partial}{\partial y}\left(G\theta\frac{\partial \phi}{\partial y}\right) = 0 \tag{8.5.54}$$

throughout the cross section Ω of the cylinder. The boundary conditions on the lateral surfaces Γ require that $\sigma_{xz}n_x + \sigma_{yz}n_y = 0$:

$$\left(\frac{\partial \phi}{\partial x} - y\right)n_x + \left(\frac{\partial \phi}{\partial y} + x\right)n_y = 0 \Rightarrow \frac{\partial \phi}{\partial n} = yn_x - xn_y \tag{8.5.55}$$

Here (n_x, n_y) denote the direction cosines of the unit normal at a point on Γ.

In summary, the torsion of a cylindrical bar is governed by the equations (8.5.54) and (8.5.55). The function $\phi(x, y)$ is called the *torsion function* or *warping function*. Since the boundary condition in (8.5.55) is of the flux type, the function can be determined within an additive constant. The stresses in (8.5.53), however, are independent of this constant. The additive constant has the meaning of rigid body movement of the cylinder as a whole in the z-direction. For additional discussion of the topic the reader is referred to Timoshenko and Goodier (1970).

The Laplace equation (8.5.54) and the Neumann boundary condition (8.5.55) governing ϕ are not convenient in the analysis because of the nature and form of the boundary condition, especially for irregular cross-sectional members. The theory of analytic functions can be used to rewrite these equations in terms of the *stress function* $\Psi(x, y)$, which is related to the warping function $\phi(x, y)$ by the equations

$$\frac{\partial \Psi}{\partial x} = -\frac{\partial \phi}{\partial y} - x, \quad \frac{\partial \Psi}{\partial y} = \frac{\partial \phi}{\partial x} - y \tag{8.5.56}$$

Eliminating ϕ from (8.5.54) and (8.5.55) gives, respectively, the results

$$-\left(\frac{\partial^2 \Psi}{\partial x^2}+\frac{\partial^2 \Psi}{\partial y^2}\right)=2 \tag{8.5.57}$$

$$\frac{\partial \Psi}{\partial y} n_x-\frac{\partial \Psi}{\partial x} n_y=0 \tag{8.5.58}$$

The left side of (8.5.58) denotes the tangential derivative $d\Psi/ds$, and $d\Psi/ds=0$ implies that

$$\Psi=\text{constant} \quad \text{on } \Gamma$$

Since the constant part of Ψ does not contribute to the stress field

$$\sigma_{xz}=G\theta\frac{\partial \Psi}{\partial y}, \quad \sigma_{yz}=-G\theta\frac{\partial \Psi}{\partial x} \tag{8.5.59}$$

we can take $\Psi=0$ on the boundary.

In summary, the torsion problem can now be stated as one of determining the stress function Ψ such that

$$\begin{aligned} -\nabla^2 \Psi &= 2 \quad \text{in } \Omega \\ \Psi &= 0 \quad \text{on } \Gamma \end{aligned} \tag{8.5.60}$$

Once Ψ is determined, the stresses can be computed from (8.5.59) for a given angle of twist per unit length (θ) and shear modulus (G).

The finite element model of (8.5.60) follows immediately from that of Eq. (8.2.1):

$$[K^e]\{u^e\}=\{f^e\}+\{Q^e\} \tag{8.5.61a}$$

where u_i^e is the value of Ψ at the ith node of Ω_e and

$$\begin{aligned} K_{ij}^e &= \int_{\Omega_e}\left(\frac{\partial \psi_i}{\partial x}\frac{\partial \psi_j}{\partial x}+\frac{\partial \psi_i}{\partial y}\frac{\partial \psi_j}{\partial y}\right) dx\, dy \\ f_i^e &= \int_{\Omega_e} 2\psi_i\, dx\, dy \quad Q_i^e=\oint_{\Gamma_e}\frac{\partial \Psi}{\partial n}\psi_i\, ds \end{aligned} \tag{8.5.61b}$$

Example 8.5.6 (Torsion of a Square Cross-Sectional Bar)

Here we consider torsion of a square ($a \times a$) cross-section bar. Note that the problem is antisymmetric as far as the loading and stress distribution are concerned; however, the stress function, being a scalar function governed by the Poisson equation (8.5.60), is symmetric about the x and y axes as well as the diagonal lines. When using rectangular elements, one quadrant of the bar cross section can be used in the finite element analysis. The biaxial symmetry about the x and y axes requires imposition of the following boundary conditions on Ψ (see Example 8.3.1):

$$\frac{\partial \Psi}{\partial x}=0 \quad \text{on the line } x=0, \qquad \frac{\partial \Psi}{\partial y}=0 \quad \text{on the line } y=0$$

In addition, on the actual boundary we have the condition $\Psi=0$ on lines $x=a$ and $y=b=a$.

Table 8.5.3 Convergence of the finite element solutions for Ψ using linear and quadratic rectangular elements (four-node and nine-node elements) in Example 8.5.6.

		Linear elements			Quadratic elements†		
x	y	2×2	4×4	8×8	1×1	2×2	4×4
0.0000	0.0000	0.15536	0.14920	0.14780	0.14744	0.14730	0.14734
0.0625	0.0000	—	—	0.14583	—	—	0.14538
0.1250	0.0000	—	0.14120	0.13987	—	0.13941	0.13944
0.1875	0.0000	—	—	0.12972	—	—	0.12931
0.2500	0.0000	0.12054	0.11610	0.11502	0.11378	0.11463	0.11467
0.3125	0.0000	—	—	0.09534	—	—	0.09505
0.3750	0.0000	—	0.07069	0.07007	—	0.069873	0.06986
0.4375	0.0000	—	—	0.03854	—	—	0.03844
0.1250	0.2500	—	0.11031	0.10925	—	0.10887	0.10890
0.2500	0.2500	0.09643	0.09191	0.09090	0.09095	0.09056	0.09057
0.3750	0.2500	—	0.05729	0.05660	—	0.05626	0.05636

†The 4×4 mesh of nine-node quadratic elements gives a solution that coincides with the analytical solution to five significant decimal places.

The results of a convergence study are summarized in Tables 8.5.3 and 8.5.4. The analytical solution of the problem is given by [see (2.5.40)]

$$\Psi(x,y)=\frac{a^2}{4}-x^2-\frac{8a^2}{\pi^3}\sum_{n=0}^{\infty}\frac{(-1)^n}{(2n+1)^3}\frac{\cosh\, k_n y\cos\, k_n x}{\cosh(k_n b/2)} \tag{8.5.62a}$$

$$\sigma_{xz}=-\frac{8aG\theta}{\pi^2}\sum_{n=0}^{\infty}\frac{(-1)^n}{(2n+1)^2}\frac{\sinh\, k_n y\cos\, k_n x}{\cosh(k_n b/2)} \tag{8.5.62b}$$

$$\sigma_{yz}=G\theta\left[2x-\frac{8a}{\pi^2}\sum_{n=0}^{\infty}\frac{(-1)^n}{(2n+1)^2}\frac{\cosh\, k_n y\sin\, k_n x}{\cosh(k_n b/2)}\right] \tag{8.5.62c}$$

Table 8.5.4 Comparison of finite element solutions for the shear stress $\bar{\sigma}_{yz}(x,y)\,[=-\bar{\sigma}_{xz}(y,x)]$, computed using various meshes, with the analytical solution (Example 8.5.6).

		Mesh			Analytical
x	y	2×2	4×4	8×8	solution
0.03125	0.03125	—	—	0.0312	0.0312
0.09375	0.03125	—	—	0.0946	0.0946
0.15625	0.03125	—	—	0.1612	0.1611
0.21875	0.03125	—	—	0.2332	0.2331
0.28125	0.03125	—	—	0.03127	0.3124
0.34375	0.03125	—	—	0.4015	0.4011
0.40625	0.03125	—	—	0.5013	0.5008
0.46875	0.03125	—	—	0.6135	0.6128
0.06250	0.0625	—	0.06175	—	0.0618
0.1875	0.0625	—	0.1942	—	0.1939
0.3125	0.0625	—	0.3529	—	0.3516
0.4375	0.0625	—	0.5528	—	0.5504
0.1250	0.1250	0.1179	—	—	0.1193
0.3750	0.1250	0.4339	—	—	0.4272

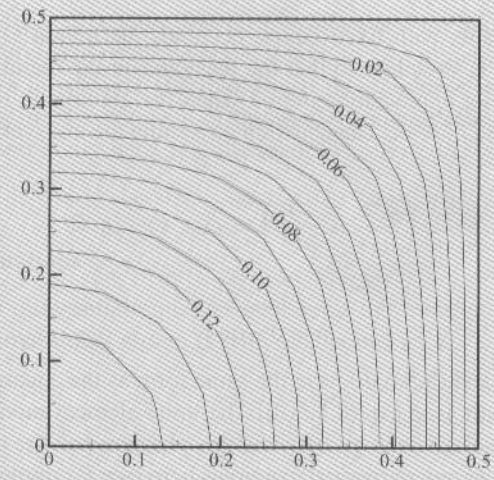

(*a*)

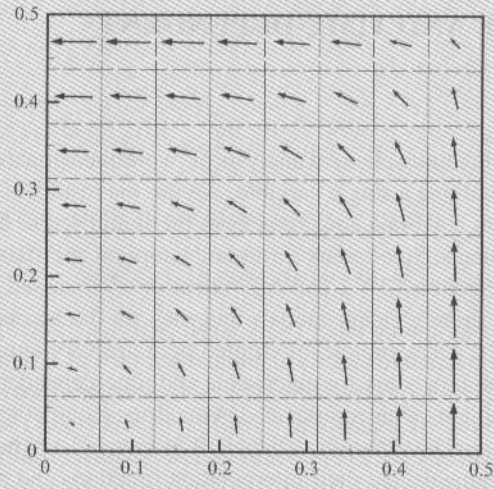

(*b*)

Figure 8.5.15 Contour plot of the stress function and vector plot of the shear stresses ($\mathbf{v} = \bar{\sigma}_{xz}\hat{\mathbf{i}} + \bar{\sigma}_{yz}\hat{\mathbf{j}}$) obtained using the 8×8 mesh of linear rectangular elements in a quadrant of square cross section in Example 8.5.6: (*a*) stress function and (*b*) $\mathbf{v}$.

where $k_n = (2n+1)\frac{\pi}{2}$. The problem is reanalyzed here for shear stresses σ_{xz} and σ_{yz} [see (8.5.59)]. The convergence of the finite element solutions for the stress function and stresses to the analytical solutions (8.5.62) is seen from the results presented in the tables. The contour lines of the surface $\Psi(x, y)$, and contour lines of

$$\bar{\sigma}_{xz} = \frac{\sigma_{xz}}{G\theta} = \frac{\partial \Psi}{\partial y}, \quad \bar{\sigma}_{yz} = \frac{\sigma_{yz}}{G\theta} = -\frac{\partial \Psi}{\partial x}$$

are shown in Fig. 8.5.15.

Transverse Deflections of Membranes

Suppose that a membrane, with fixed edges, occupies the region Ω in the (x, y) plane. Initially the membrane is stretched so that the tension a in the membrane is uniform and a is so large that it is not appreciably altered when the membrane is deflected by a distributed transverse force, $f(x, y)$. The equation governing the transverse deflection u of the membrane is given by

$$-a\left(\frac{\partial^2 u}{\partial x^2}+\frac{\partial^2 u}{\partial y^2}\right)=f(x, y) \quad \text{in } \Omega \tag{8.5.63a}$$

with

$$u=0 \quad \text{on } \Gamma \tag{8.5.63b}$$

Note that (8.5.63a) and (8.5.63b) have the same form as the equations used to describe torsion of cylindrical bars [see Eq. (8.5.60)]. The finite element model of the equation is obvious. In view of the close analogy between this problem and the torsion of cylindrical bars, we will not consider any numerical examples here (see Examples 8.3.1 and 8.5.6).

8.6 EIGENVALUE AND TIME-DEPENDENT PROBLEMS

8.6.1 Introduction

This section deals with the finite element analysis of two-dimensional eigenvalue and time-dependent problems involving a single variable. We use the results of Sections 2.4 and 6.2 to develop finite element algebraic equations from the semidiscrete finite element models of time-dependent problems. Since weak forms and temporal approximations were already discussed in detail in Sections 2.4.2 and 6.2, attention is focussed here on how to develop the semidiscrete finite element models and then on the associated eigenvalue and fully discretized models. The examples presented here are very simple because they are designed to illustrate the procedure for eigenvalue and time-dependent problems; solution of two-dimensional problems with complicated geometries require the use of isoparametric formulation and numerical integration. Chapter 9 is devoted to the discussion of various two-dimensional elements and their interpolation functions and numerical integration methods.

The finite element model development of eigenvalue and time-dependent problems involves, as described in Section 6.2, two main stages. The first stage, called *semidiscretization*, is to develop the weak form or weighted-residual form of the equations over an element and to seek spatial approximation of the dependent variables of the problem. The end result of this step is a set of ordinary differential equations in time among the nodal values of the dependent variables. For transient problems, the second stage consists of time approximations of the ordinary differential equations (i.e., numerical integration of the equations) by finite difference schemes. This step leads to a set of algebraic equations involving the nodal values at time t_{s+1} [$=(s+1)\Delta t$, where s is an integer and Δt is the time increment] in terms of known values from the previous time step(s). For eigenvalue problems, the second stage consists of seeking a solution of the form $u_j(t)=U_j e^{-\lambda t}$

for nodal values and determining the eigenvalues λ and eigenfunctions $U_j\psi_j(x, y)$ (no sum on j). The two-stage procedure was clearly illustrated for one-dimensional problems in Section 6.2. The procedure will be applied here to two-dimensional problems involving a single equation in a single variable. Since the emphasis in this section is on the time approximations, the development of the weak form and spatial finite element model will not be covered explicitly here, and the reader is referred to Sections 8.2 and 8.3 for details.

8.6.2 Parabolic Equations

Consider the partial differential equation governing the transient heat transfer and like problems in a two-dimensional region Ω with total boundary Γ,

$$c\frac{\partial u}{\partial t} - \frac{\partial}{\partial x}\left(a_{11}\frac{\partial u}{\partial x}\right) - \frac{\partial}{\partial y}\left(a_{22}\frac{\partial u}{\partial y}\right) + a_0 u = f(x, y, t) \tag{8.6.1}$$

with the boundary conditions

$$u = \hat{u} \text{ or } q_n = \hat{q}_n \quad \text{on } \Gamma \quad (t \geq 0) \tag{8.6.2a}$$

where

$$q_n = a_{11}\frac{\partial u}{\partial x}n_x + a_{22}\frac{\partial u}{\partial y}n_y \tag{8.6.2b}$$

The initial conditions (i.e., at $t = 0$) are of the form

$$u(x, y, 0) = u_0(x, y) \quad \text{in } \Omega \tag{8.6.3}$$

Here t denotes time, and c, a_{11}, a_{22}, a_0, $\hat{u}$, u_0, f, and $\hat{q}_n$ are given functions of position and/or time. Equation (8.6.1) is a modification of (8.2.1) in that it contains a time derivative term, which accounts for time variations of the physical process represented by (8.2.1).

The weak form of (8.6.1) and (8.6.2) over an element Ω_e is obtained by the standard procedure: Multiply (8.6.1) with the weight function $v(x, y)$ and integrate over the element, integrate by parts (spatially) those terms that involve higher-order derivatives using the gradient or divergence theorem, and replace the coefficient of the weight function in the boundary integral with the secondary variable [i.e., use (8.6.2*b*)]. We obtain

$$0 = \int_{\Omega_e}\left[v\left(c\frac{\partial u}{\partial t} + a_0 u - f\right) + a_{11}\frac{\partial v}{\partial x}\frac{\partial u}{\partial x} + a_{22}\frac{\partial v}{\partial y}\frac{\partial u}{\partial y}\right]dx\,dy - \oint_{\Gamma_e} q_n v\,ds \tag{8.6.4}$$

Note that the procedure to obtain the weak form for time-dependent problems is not much different from that used for steady-state problems in Section 8.2.3. The difference is that all terms of the equations may be functions of time. Also, no integration by parts with respect to time is used, and the weight function v is not a function of time.

The *semidiscrete* finite element model is obtained from (8.6.4) by substituting a finite element approximation for the dependent variable, u. In selecting the approximation

for u, once again we assume that the time dependence can be separated from the space variation,

$$u(x, y, t) \approx \sum_{j=1}^{n} u_j^e(t)\psi_j^e(x, y) \tag{8.6.5}$$

where u_j^e denotes the value of $u(x, y, t)$ at the spatial location (x_j, y_j) at time t. The ith differential equation (in time) of the finite element model is obtained by substituting $v = \psi_i^e(x, y)$ and replacing u by (8.6.5) in (8.6.4):

$$0 = \sum_{j=1}^{n} \left(M_{ij}^e \frac{du_j^e}{dt} + K_{ij}^e u_j^e \right) - f_i^e - Q_i^e \tag{8.6.6a}$$

or, in matrix form

$$[M^e]\{\dot{u}^e\} + [K^e]\{u^e\} = \{f^e\} + \{Q^e\} \tag{8.6.6b}$$

where a superposed dot on u denotes a derivative with time ($\dot{u} = \partial u/\partial t$), and

$$\begin{aligned} M_{ij}^e &= \int_{\Omega_e} c\psi_i^e \psi_j^e \, dx\, dy \\ K_{ij}^e &= \int_{\Omega_e} \left(a_{11} \frac{\partial \psi_i^e}{\partial x} \frac{\partial \psi_j^e}{\partial x} + a_{22} \frac{\partial \psi_i^e}{\partial y} \frac{\partial \psi_j^e}{\partial y} + a_0 \psi_i^e \psi_j^e \right) dx\, dy \\ f_i^e &= \int_{\Omega_e} f(x, y, t)\psi_i^e \, dx\, dy \end{aligned} \tag{8.6.6c}$$

This completes the semidiscretization step.

Eigenvalue Analysis

The problem of finding $u_j^e(t) = U_j e^{-\lambda t}$ such that (8.6.6) holds for homogeneous boundary and initial conditions and $f = 0$ is called an *eigenvalue problem*. Substituting for $u_j^e(t)$ into (8.6.6*b*), we obtain

$$(-\lambda[M^e] + [K^e])\{u^e\} = \{Q^e\} \tag{8.6.7}$$

Upon assembly of the element equations (8.6.7), the right column vector of the condensed equations is zero (because of the homogeneous boundary conditions), giving rise to the global eigenvalue problem

$$([K] - \lambda[M])\{U\} = \{0\} \tag{8.6.8}$$

The order of the matrix equations is $N \times N$, where N is the number of nodes at which the solution is not known. A nontrivial solution to (8.6.8) exists only if the determinant of the coefficient matrix is zero:

$$|[K] - \lambda[M]| = 0$$

which, when expanded, results in an Nth-degree polynomial in λ. The N roots λ_j ($j = 1, 2, \ldots, N$) of this polynomial give the first N eigenvalues of the discretized system (the continuous system, in general, has an infinite number of eigenvalues). There exist standard eigenvalue routines to solve (8.6.8), which give N eigenvalues and eigenvectors.

Transient Analysis

Note that the form of (8.6.6*b*) is the same as the parabolic equation discussed in Section 6.2 [see Eq. (6.2.21*a*)]. Whether a problem is one-dimensional, two-dimensional, or three-dimensional, the form of the semidiscrete finite element model is the same. Therefore, the time approximation schemes discussed in Section 6.2 for parabolic equations can be readily applied.

Using the α-family of approximation

$$\{u\}_{s+1} = \{u\}_s + \Delta t[(1-\alpha)\{\dot{u}\}_s + \alpha\{\dot{u}\}_{s+1}] \quad (0 \le \alpha \le 1) \tag{8.6.9}$$

we can transform the ordinary differential equations (8.6.6*b*) into a set of algebraic equations at time t_{s+1}:

$$[\hat{K}]_{s+1}\{u\}_{s+1} = \{\hat{F}\}_{s,s+1} \tag{8.6.10a}$$

where

$$[\hat{K}]_{s+1} = [M] + a_1[K]_{s+1}$$

$$\{\hat{F}\} = \Delta t(\alpha\{F\}_{s+1} + (1-\alpha)\{F\}_s) + ([M] - a_2[K]_s)\{u\}_s \tag{8.6.10b}$$

$$a_1 = \alpha\Delta t, \quad a_2 = (1-\alpha)\Delta t$$

Equation (8.6.10*a*), after assembly and imposition of boundary conditions, is solved at each time step for the nodal values u_j at time $t_{s+1} = (s+1)\Delta t$. At time $t = 0$ (i.e., $s = 0$), the right-hand side of (8.6.10*a*) is computed using the initial values $\{u\}_0$; the vector $\{F\}$, which is the sum of the source vector $\{f\}$ and internal flux vector $\{Q\}$, is always known for both times t_s and t_{s+1}, at all nodes at which the solution is unknown [because $f(x, t)$ is a *known* function of time and the sum of Q_j^e at these nodes is zero].

It should be recalled from Section 6.2 that, for different values of α, we obtain the following well-known time approximation schemes [see Eq. (6.2.20)]:

$$\alpha = \begin{cases} 0, & \text{the forward difference scheme (conditionally stable); } O(\Delta t) \\ \dfrac{1}{2}, & \text{the Crank–Nicolson scheme (unconditionally stable); } O(\Delta t)^2 \\ \dfrac{2}{3}, & \text{the Galerkin scheme (unconditionally stable); } O(\Delta t)^2 \\ 1, & \text{the backward difference scheme (unconditionally stable); } O(\Delta t) \end{cases}$$

For the forward difference scheme the stability requirement is

$$\Delta t < \Delta t_{\text{cri}} = \frac{2}{(1-2\alpha)\lambda_{\max}}, \quad \alpha < \frac{1}{2} \tag{8.6.11}$$

where $\lambda_{\max}$ is the largest eigenvalue of the finite element equations (8.6.8).

We consider examples of an eigenvalue problem and a time-dependent problem next.

Example 8.6.1 (Eigenvalue Analysis)

Consider the differential equation,

$$\frac{\partial u}{\partial t} - \left(\frac{\partial^2 u}{\partial x^2} + \frac{\partial^2 u}{\partial y^2}\right) = f \tag{8.6.12a}$$

in a unit square, subjected to the boundary conditions

$$\frac{\partial u}{\partial x}(0, y, t) = 0, \quad \frac{\partial u}{\partial y}(x, 0, t) = 0, \quad u(x, 1, t) = 0, \quad u(1, y, t) = 0 \tag{8.6.12b}$$

and initial conditions

$$u(x, y, 0) = 0 \tag{8.6.12c}$$

As a first choice we may choose a 1×1 mesh of two triangular elements. Alternatively, for the choice of triangles, we can use the diagonal symmetry and model the domain with one triangular element (see Fig. 8.3.1*c*). The element matrices for a right-angle triangle with $a = b$ are:

$$[K^e] = \frac{1}{2}\begin{bmatrix} 1 & -1 & 0 \\ -1 & 2 & -1 \\ 0 & -1 & 1 \end{bmatrix}, \quad [M^e] = \frac{a^2}{24}\begin{bmatrix} 2 & 1 & 1 \\ 1 & 2 & 1 \\ 1 & 1 & 2 \end{bmatrix}$$

The eigenvalue problem becomes ($a = 1.0$)

$$\left(-\frac{\lambda}{24}\begin{bmatrix} 2 & 1 & 1 \\ 1 & 2 & 1 \\ 1 & 1 & 2 \end{bmatrix} + \frac{1}{2}\begin{bmatrix} 1 & -1 & 0 \\ -1 & 2 & -1 \\ 0 & -1 & 1 \end{bmatrix}\right)\begin{Bmatrix} U_1 \\ U_2 \\ U_3 \end{Bmatrix} = \begin{Bmatrix} Q_1^1 \\ Q_2^1 \\ Q_3^1 \end{Bmatrix}$$

The boundary conditions require $U_2 = U_3 = 0$ and $Q_1^1 = 0$. Hence, we have

$$\left(-\frac{\lambda}{12} + \frac{1}{2}\right)U_1 = 0 \quad \text{or} \quad \lambda = 6$$

The eigenfunction becomes

$$U(x, y) = \psi_1(x, y) = 1 - x$$

which is defined over the octant of the domain. For a quadrant of the domain, by symmetry, the eigenfunction becomes $U(x, y) = (1 - x)(1 - y)$.

For a mesh of single rectangular element with $a = b$ (see Fig. 8.3.1*b*), we have

$$[K^e] = \frac{1}{6}\begin{bmatrix} 4 & -1 & -2 & -1 \\ -1 & 4 & -1 & 2 \\ -2 & -1 & 4 & -1 \\ -1 & -2 & -1 & 4 \end{bmatrix}, \quad [M^e] = \frac{a^2}{36}\begin{bmatrix} 4 & 2 & 1 & 2 \\ 2 & 4 & 2 & 1 \\ 1 & 2 & 4 & 2 \\ 2 & 1 & 2 & 4 \end{bmatrix}$$

and

$$\left(-\frac{\lambda}{36}\begin{bmatrix} 4 & 2 & 1 & 2 \\ 2 & 4 & 2 & 1 \\ 1 & 2 & 4 & 2 \\ 2 & 1 & 2 & 4 \end{bmatrix} + \frac{1}{6}\begin{bmatrix} 4 & -1 & -2 & -1 \\ -1 & 4 & -1 & 2 \\ -2 & -1 & 4 & -1 \\ -1 & -2 & -1 & 4 \end{bmatrix}\right)\begin{Bmatrix} U_1 \\ U_2 \\ U_3 \\ U_4 \end{Bmatrix} = \begin{Bmatrix} Q_1^1 \\ Q_2^1 \\ Q_3^1 \\ Q_4^1 \end{Bmatrix}$$

Table 8.6.1 Comparison of finite element solutions for eigenvalues, obtained using various meshes, with the analytical solution (Example 8.6.1).

	Triangles				Rectangles				Analytical
λ	1×1	2×2	4×4	8×8	1×1	2×2	4×4	8×8	solution[†]
$\lambda_1(\lambda_{11})$	6.000	5.415	5.068	4.969	6.000	5.193	4.999	4.951	4.935
$\lambda_2(\lambda_{13})$	—	32.000	27.250	25.340	—	34.290	27.370	25.330	24.674
$\lambda_3(\lambda_{31})$	—	38.200	28.920	25.730	—	34.290	27.370	25.330	24.674
$\lambda_4(\lambda_{33})$	—	76.390	58.220	48.080	—	63.380	49.740	45.710	44.413
$\lambda_4(\lambda_{15})$	—	—	85.350	69.780	—	—	84.570	69.260	64.152
$\lambda_5(\lambda_{51})$	—	—	86.790	69.830	—	—	84.570	69.260	64.152

[†]The analytical solution is $\lambda_{mn}=\frac{1}{4}\pi^2(m^2+n^2)$ $(m, n=1, 3, 5, \ldots)$.

Using the boundary conditions $U_2=U_3=U_4=0$ and $Q_1^1=0$, we obtain

$$\left(-\frac{\lambda}{36}\times4+\frac{4}{6}\right)U_1=0, \quad \text{or } \lambda=6$$

The eigenfunction over the quadrant of the domain is given by

$$U(x, y)=\psi_1(x, y)=(1-x)(1-y)$$

For this problem, the one-element mesh of triangles in an octant of the domain gives the same solution as the one-element mesh of rectangular elements in a quadrant of the domain.

Table 8.6.1 contains eigenvalues obtained with various meshes of triangular and rectangular elements, along with the analytical solution of the problem. It is clear that the convergence of the minimum eigenvalue obtained with the finite element method to the analytical value is rapid compared to the convergence of the higher eigenvalues, i.e., error in the higher eigenvalues is always larger than that in the minimum eigenvalue. Also, the minimum eigenvalue converges faster with mesh refinements.

Example 8.6.2 (Transient Analysis)

We wish to solve the transient heat conduction equation

$$\frac{\partial T}{\partial t}-\left(\frac{\partial^2 T}{\partial x^2}+\frac{\partial^2 T}{\partial y^2}\right)=1 \tag{8.6.13a}$$

subject to the boundary conditions (see Fig. 8.6.1*a*), for $t\geq0$,

$$\begin{aligned}&\frac{\partial T}{\partial x}(0, y, t)=0, \quad \frac{\partial T}{\partial y}(x, 0, t)=0\\ &T(1, y, t)=0, \quad T(x, 1, t)=0\end{aligned} \tag{8.6.13b}$$

and the initial conditions

$$T(x, y, 0)=0 \quad \text{for all } (x, y) \text{ in } \Omega \tag{8.6.13c}$$

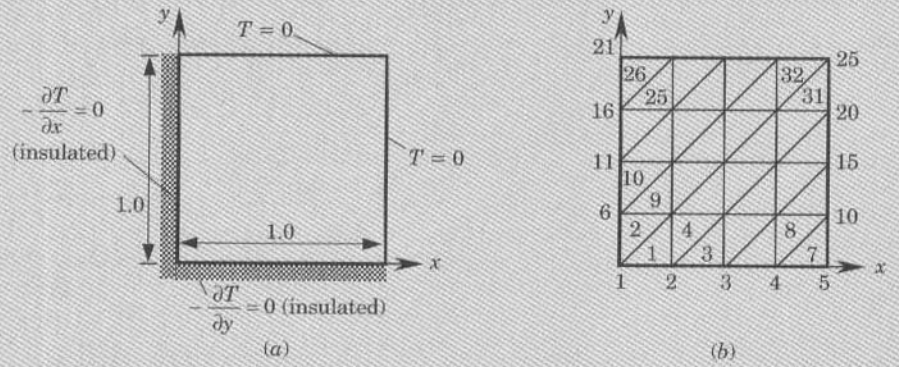

Figure 8.6.1 (*a*) Domain, boundary conditions and (*b*) finite element mesh for the transient heat conduction problem of Example 8.6.2.

We choose a 4×4 mesh of linear triangular elements (see Fig. 8.6.1*b*) to model the domain, and investigate the stability and accuracy of the Crank–Nicolson method (i.e., $\alpha = 0.5$) and the forward difference scheme ($\alpha = 0.0$) for the temporal approximation. Since the Crank–Nicolson method is unconditionally stable, we can choose any value of Δt. However, for large values of Δt the solution may not be accurate. The forward difference scheme is conditionally stable; it is stable if $\Delta t < \Delta t_{\text{cri}}$, where

$$\Delta t_{\text{cri}} = \frac{2}{\lambda_{\max}} = \frac{2}{386.4} = 0.00518$$

where the maximum eigenvalue of (8.6.13*a*) for the 4×4 mesh of triangles is 386.4.

The element equations are given by (8.6.6*b*), with $[M^e]$, $[K^e]$, and $\{f^e\}$ defined by (8.6.6*c*), wherein $c = 1$, $a_{11} = 1$, $a_{22} = 1$, $a_0 = 0$, and $f = 1$. The boundary conditions of the problem for the 4×4 mesh are given by

$$U_5 = U_{10} = U_{15} = U_{20} = U_{21} = U_{22} = U_{23} = U_{24} = U_{25} = 0.0$$

Beginning with the initial conditions $U_i = 0$ ($i = 1, 2, \ldots, 25$), we solve the assembled set of equations associated with (8.6.10).

The forward difference scheme would be unstable for $\Delta t > 0.00518$. To illustrate this point, the equations are solved using $\alpha = 0$, $\Delta t = 0.01$ and $\alpha = 0.5$, $\Delta t = 0.01$. The Crank–Nicolson method gives stable and accurate solution, while the forward difference scheme yields unstable solution (i.e., the solution error grows unboundedly with time), as can be seen from Fig. 8.6.2. For $\Delta t = 0.005$, the forward difference scheme yields stable solution.

The Crank–Nicolson method gives a stable and accurate solution for even $\Delta t = 0.05$. The temperature $T(x, 0, t)$ versus x for various values of time are shown in Fig. 8.6.3(*a*). The steady state is reached at time $t = 1.0$. The temperature $T(0, 0, t)$ versus time, predicted by the Crank–Nicolson method, is shown in Fig. 8.6.3(*b*), which indicates the evolution of the temperature from zero to the steady state. A comparison of the transient solution at $t = 1.0$ is given in Table 8.6.2 with the steady-state finite element, the finite difference, and the analytical solutions. Table 8.6.3 contains the finite element solutions for temperature predicted by 4×4 meshes of triangles and rectangles and various values of Δt and $\alpha = 0.5$.

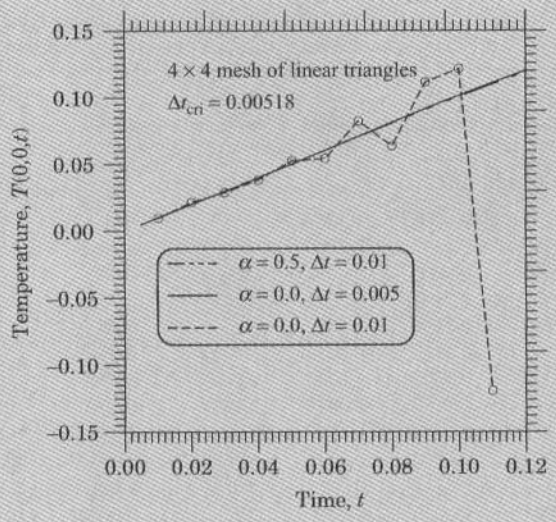

Figure 8.6.2 Stability of the transient solutions of the heat conduction problem in Example 8.6.2 analyzed using a 4 × 4 mesh of linear triangular elements and the Crank–Nicolson ($\alpha = 0.5$) and forward difference ($\alpha = 0.0$) time integration schemes.

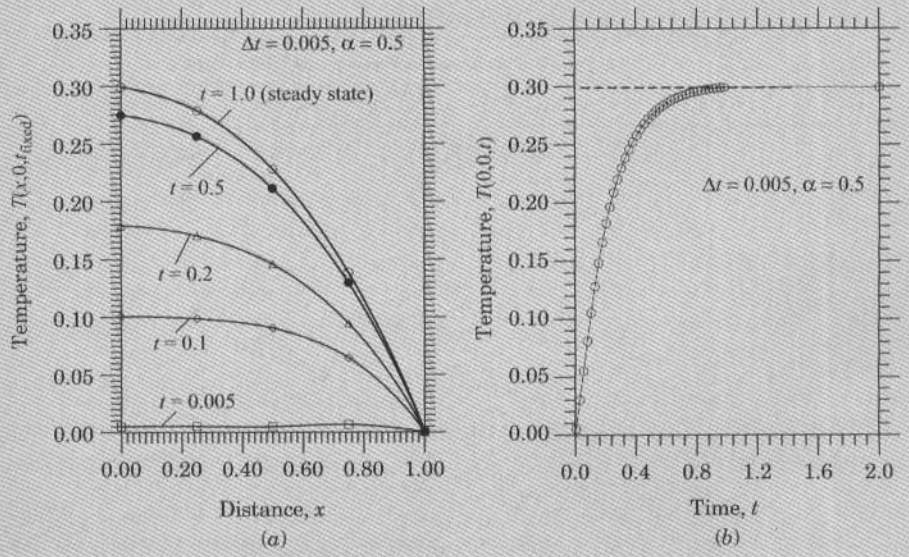

Figure 8.6.3 Variation of the temperature as a function of position x and time t for the transient heat conduction problem of Example 8.6.2 (4 × 4 mesh of linear triangles).

Table 8.6.2 Comparison of finite difference method (FDM) and finite element method (FEM) solutions with the exact solution of the heat conduction problem in Example 8.6.2.

Node	Exact (steady)	FDM (steady)	Error	FEM (steady)	Error	(FEM) at $t = 1.0^{\dagger}$
1	0.2947	0.2911	0.0036	0.3013	−0.0066	0.2993
2	0.2789	0.2755	0.0034	0.2805	−0.0016	0.2786
3	0.2293	0.2266	0.0027	0.2292	0.0001	0.2278
4	0.1397	0.1381	0.0016	0.1392	0.0005	0.1385
5	0.0000	0.0000	0.0000	0.0000	0.0000	0.0000
7	0.2642	0.2609	0.0033	0.2645	−0.0003	0.2628
8	0.2178	0.2151	0.0027	0.2172	0.0006	0.2159
9	0.1333	0.1317	0.0016	0.1327	0.0006	0.1320
10	0.0000	0.0000	0.0000	0.0000	0.0000	0.0000
13	0.1811	0.1787	0.0024	0.1801	0.0010	0.1791
14	0.1127	0.1110	0.0017	0.1117	0.0010	0.1111
15	0.0000	0.0000	0.0000	0.0000	0.0000	0.0000
19	0.0728	0.0711	0.0017	0.0715	0.0013	0.0712
20	0.0000	0.0000	0.0000	0.0000	0.0000	0.0000
25	0.0000	0.0000	0.0000	0.0000	0.0000	0.0000

†Obtained with the Crank–Nicolson scheme with $\Delta t = 0.005$

Table 8.6.3 Comparison of transient solutions of (8.6.13*a*) and (8.6.13*b*) obtained using meshes of triangular and rectangular elements.

Time t	Element†	Temperature along the line $y = 0$: $T(x, 0, t) \times 10$			
		$x = 0.0$	$x = 0.25$	$x = 0.5$	$x = 0.75$
0.1	T1	0.9758	0.9610	0.9063	0.7104
	R1	0.9684	0.9556	0.8956	0.6887
	T2	0.9928	0.9798	0.9168	0.6415
	R2	0.9841	0.9718	0.9020	0.6323
0.2	T1	1.8003	1.7238	1.4891	0.9321
	R1	1.7723	1.7216	1.4829	0.9367
	T2	1.7979	1.7060	1.4644	0.9462
	R2	1.7681	1.6990	1.4626	0.9469
0.3	T1	2.3130	2.1671	1.7961	1.1466
	R1	2.2747	2.1650	1.8084	1.1499
	T2	2.2829	2.1448	1.7943	1.1249
	R2	2.2479	2.1432	1.8018	1.1319
1.0	T1	2.9960	2.7871	2.2804	1.3843
	R1	2.9648	2.8053	2.3090	1.4059
	T2	2.9925	2.7862	2.2776	1.3849
	R2	2.9621	2.8037	2.3065	1.4053

†T1, triangular element mesh with $\Delta t = 0.1$; T2, triangular element mesh with $\Delta t = 0.05$; R1, rectangular element mesh with $\Delta t = 0.1$; R2, rectangular element mesh with $\Delta t = 0.05$. In all cases, $\alpha = 0.5$.

8.6.3 Hyperbolic Equations

The transverse motion of a membrane, for example, is governed by the partial differential equation of the form,

$$c\frac{\partial^2 u}{\partial t^2} - \frac{\partial}{\partial x}\left(a_{11}\frac{\partial u}{\partial x}\right) - \frac{\partial}{\partial y}\left(a_{22}\frac{\partial u}{\partial y}\right) + a_0 u = f(x, y, t) \tag{8.6.14a}$$

where $u(x, y, t)$ denotes the transverse deflection, c the material density of the membrane, a_{11} and a_{22} are the tensions in the x and y directions of the membrane, a_0 is the modulus of elastic foundation on which the membrane is stretched (often $a_0 = 0$, i.e., there is no foundation), and $f(x, y, t)$ is the transversely distributed force. Equation (8.6.14a) is known as the *wave equation* and is classified mathematically as an hyperbolic equation. The function u must be determined such that it satisfies (8.6.14a) in a region Ω and the following boundary and initial conditions:

$$u = \hat{u} \quad \text{on } \Gamma \quad \text{or} \quad q_n = \hat{q}_n \quad \text{on } \Gamma \quad (t \geq 0) \tag{8.6.14b}$$

$$u(x, y, 0) = u_0(x, y), \qquad \frac{\partial u}{\partial t}(x, y, 0) = v_0(x, y) \tag{8.6.14c}$$

where $\hat{u}$ and $\hat{q}_n$ are specified boundary values of u and q_n [see (8.6.2b)], and u_0 and v_0 are specified initial values of u and its time derivative, respectively.

The weak form of (8.6.14a) and (8.6.14b) over a typical element Ω_e is similar to that of (8.6.1) [see Eq. (8.6.4)], except that here we have the second time derivative of u:

$$0 = \int_{\Omega_e}\left[v\left(c\frac{\partial^2 u}{\partial t^2} + a_0 u - f\right) + a_{11}\frac{\partial v}{\partial x}\frac{\partial u}{\partial x} + a_{22}\frac{\partial v}{\partial y}\frac{\partial u}{\partial y}\right] dx\, dy - \oint_{\Gamma_e} q_n v\, ds \tag{8.6.15}$$

where $v = v(x, y)$ is the weight function.

The semidiscrete finite element model is obtained by substituting the finite element approximation (8.6.5) for u and $v = \psi_i$ into (8.6.15):

$$0 = \sum_{j=1}^{n}\left(M_{ij}^e \frac{d^2 u_j^e}{dt^2} + K_{ij}^e u_j^e\right) - f_i^e - Q_i^e \tag{8.6.16a}$$

or, in matrix form, we have

$$[M^e]\{\ddot{u}^e\} + [K^e]\{u^e\} = \{f^e\} + \{Q^e\} \tag{8.6.16b}$$

The coefficients M_{ij}^e, K_{ij}^e, and f_i^e are the same as those in (8.6.6c).

Eigenvalue Analysis

The problem of finding $u_j(t) = U_j e^{-i\omega t}$ ($i = \sqrt{-1}$) such that (8.6.16a) and (8.6.16b) hold for homogeneous boundary and initial conditions and $f = 0$ is called an eigenvalue problem associated with (8.6.14a). We obtain,

$$(-\omega^2[M^e] + [K^e])\{u^e\} = \{Q^e\} \tag{8.6.17}$$

The eigenvalues ω^2 and eigenfunctions $\sum_j^n U_j \psi_j(x, y)$ are determined from the assembled equations associated with (8.6.17), after imposing the homogeneous boundary conditions.

For a membrane problem, ω denotes the frequency of natural vibration. The number of eigenvalues of the discrete system (8.6.17) of the problem is equal to the number of unknown nodal values of U in the mesh.

Example 8.6.3 (Natural Vibration Analysis)

Consider the free vibrations of a homogeneous-material rectangular membrane of dimension a by b (in ft.), material density ρ (in slugs/ft.^{2}), and fixed on all its edges, i.e., $u = 0$ on Γ. Although the problem has symmetry about the center horizontal line and center vertical lines of the domain (see Fig. 8.6.4), use of any symmetry in the finite element analysis will eliminate the unsymmetric modes of vibration of the membrane. For example, if we consider a quadrant of the domain in the finite element analysis, the frequencies ω_{mn} $(m, n \neq 1, 3, 5, \ldots)$ and associated eigenfunctions will be missed in the results [i.e., we can only obtain ω_{mn} $(m, n = 1, 3, 5, \ldots)$]. By considering the full domain, the first N frequencies allowed by the mesh can be computed, where N is the number of unknown nodal values in the mesh.

If only the first eigenvalue ω_{11} is of interest or only symmetric frequencies are required, we can use a quadrant of the domain in the analysis. Indeed, results of Example 8.6.1 are applicable here, with $\lambda_{mn} = \omega_{mn}^2$. The results presented in Table 8.6.1 can be interpreted as the squares of the symmetric natural frequencies of a square $a = b = 2$ membrane with $\rho = 1$ and $a_{11} = a_{22} \equiv T = 1$. The exact natural frequencies of a rectangular membrane of dimension a by b, with tensions $a_{11} = a_{22} = T$ and density ρ are:

$$\omega_{mn} = \pi \sqrt{\frac{T}{\rho}} \sqrt{\frac{m^2}{a^2} + \frac{n^2}{b^2}} \quad (m, n = 1, 2, \ldots)$$

To obtain all the frequencies, the full domain must be modeled.

Table 8.6.4 contains the first nine frequencies of a rectangular membrane of 4 ft. by 2 ft., tension $T = 12.5$ lb/ft., and density $\rho = 2.5$ slugs/ft.^{2}, as computed using various meshes of linear triangular and rectangular elements in the total domain. The convergence of the finite element results to the analytical solution is clear. The accuracy of frequencies associated with the symmetric modes is the same when $(n/2) \times (n/2)$ mesh used in a quadrant as when $n \times n$ mesh is used the total domain. The mesh of linear rectangular element yields more accurate results compared with the mesh of linear triangular elements.

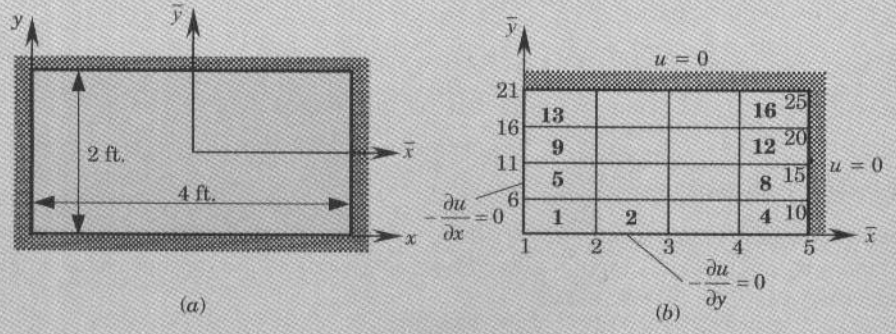

Figure 8.6.4 Analysis of a rectangular membrane: (*a*) actual geometry and (*b*) computational domain with finite element mesh of rectangular elements and boundary conditions (4×4 mesh of linear elements or 2×2 mesh of nine-node quadratic elements).

Table 8.6.4 Comparison of natural frequencies computed using various meshes of linear triangular and rectangular elements with the analytical solution of a rectangular membrane fixed on all its sides ($a_{11} = a_{22} = 12.5$, $\rho = T = 2.5$).

	Triangular (linear)			Rectangular (linear)			
ω_{mn}	2×2	4×4	8×8	2×2	4×4	8×8	Analytical
ω_{11}	5.0000	4.2266	4.0025	4.3303	4.0285	3.9522	3.9270
ω_{21}	—	5.9083	5.2068	—	5.2899	5.0478	4.9673
ω_{31}	—	8.2392	6.8788	—	7.2522	6.6020	6.3321
ω_{12}	—	8.3578	7.5271	—	7.9527	7.4200	7.2410
ω_{22}	—	10.0618	8.4565	—	8.6603	8.0571	7.8540
ω_{41}	—	12.1021	8.8856	—	9.9805	8.5145	7.8540
ω_{32}	—	13.2011	9.9280	—	12.7157	9.1117	8.7810
ω_{51}	—	14.6942	11.1193	—	13.1700	10.5797	9.4574
ω_{42}	—	15.8117	11.4425	—	14.0734	10.7280	9.9346

Transient Analysis

The hyperbolic equation (8.6.16*b*) can be reduced to a system of algebraic equations by approximating the second-order time derivative. As discussed in Section 6.2, the Newmark time integration schemes are the most commonly used ones in structural dynamics. Since Eq. (8.6.16*b*) is a special case (with $[C] = [0]$) of Eq. (6.2.28*a*), the results in Eqs. (6.2.38)–(6.2.40) hold with $[C] = [0]$. For ready reference, the main results are summarized here.

Newmark's Scheme

$$\begin{aligned} \{u\}_{s+1} &= \{u\}_s + \Delta t\{\dot{u}\}_s + \frac{(\Delta t)^2}{2}\{\ddot{u}\}_{s+\gamma} \\ \{\dot{u}\}_{s+1} &= \{\dot{u}\}_s + \Delta t\{\ddot{u}\}_{s+\alpha} \\ \{\ddot{u}\}_{s+\theta} &= (1-\theta)\{\ddot{u}\}_s + \theta\{\ddot{u}\}_{s+1} \end{aligned} \tag{8.6.18a}$$

where

$$\begin{aligned} &\alpha = \frac{1}{2},\ \gamma = \frac{1}{2}: && \text{constant-average acceleration method (stable scheme)} \\ &\alpha = \frac{1}{2},\ \gamma = \frac{1}{3}: && \text{linear acceleration method (conditionally stable)} \\ &\alpha = \frac{1}{2},\ \gamma = 0: && \text{central difference method (conditionally stable)} \end{aligned} \tag{8.6.18b}$$

Stability Criterion

$$\Delta t < \Delta t_{\text{cri}} = \left[\frac{1}{2}\omega_{\max}^2 (\alpha - \gamma)\right]^{-\frac{1}{2}}, \quad \alpha \geq \frac{1}{2}, \quad \gamma < \alpha \tag{8.6.19}$$

where $\omega^2_{\max}$ is the maximum eigenvalue of the corresponding discrete eigenvalue problem (8.6.17) (i.e., the same mesh and element type used in the transient analysis must be used in the eigenvalue analysis). Note that a more refined mesh will yield a higher maximum eigenvalue and a lower Δt_{cri}.

Time Marching Scheme

$$[\hat{K}^e]_{s+1}\{u^e\}_{s+1} = \{\hat{F}^e\}_{s,s+1} \tag{8.6.20a}$$

where (the superscript e is omitted for brevity in the following),

$$[\hat{K}]_{s+1} = [K]_{s+1} + a_3[M]_{s+1}$$

$$\{\hat{F}\}_{s,s+1} = \{F\}_{s+1} + [M]_{s+1}(a_3\{u\}_s + a_4\{\dot{u}\}_s + a_5\{\ddot{u}\}_s) \tag{8.6.20b}$$

$$a_3 = \frac{2}{\gamma(\Delta t)^2}, \quad a_4 = \Delta t a_3, \quad a_5 = \frac{1}{\gamma} - 1$$

Once $\{u\}_{s+1}$ is calculated from (8.6.20*a*), the velocities and accelerations at time $t_{s+1} = \Delta t(s+1)$ are calculated from

$$\begin{aligned} \{\ddot{u}\}_{s+1} &= a_3(\{u\}_{s+1} - \{u\}_s) - a_4\{\dot{u}\}_s - a_5\{\ddot{u}\}_s \\ \{\dot{u}\}_{s+1} &= \{\dot{u}\}_s + a_2\{\ddot{u}\}_s + a_1\{\ddot{u}\}_{s+1} \end{aligned} \tag{8.6.21}$$

$$a_1 = \alpha\Delta t, \quad a_2 = (1-\alpha)\Delta t$$

For the centered difference scheme ($\gamma = 0$), the alternative formulation of Problem 6.23 must be used.

Note that (8.6.20*a*) is valid for an element. Therefore, operations indicated in (8.6.20*b*) are carried out for an element, and $[\hat{K}^e]$ and $\{\hat{F}^e\}$ are assembled as in a static analysis. For the first time step, the initial conditions on u and $\partial u/\partial t$ are used to compute $\{u\}_0$ and $\{\dot{u}\}_0$ for each element of the entire mesh. The acceleration vector $\{\ddot{u}\}_0$ is computed from (8.6.16*b*) at $t = 0$:

$$\{\ddot{u}\}_0 = [M]^{-1}(\{F\}_0 - [K]\{u\}_0) \tag{8.6.22}$$

Often, it is assumed that $\{F\}_0 = \{0\}$. If the initial conditions are zero, $\{u\}_0 = \{0\}$, and the applied force is assumed to be zero at $t = 0$, we then take $\{\ddot{u}\}_0 = \{0\}$.

Example 8.6.4 (Transient Analysis)

Consider a homogeneous rectangular membrane of sides $a = 4$ ft. and $b = 2$ ft. fixed on all its four edges. Assume that the tension in the membrane is 12.5 lb/ft. (i.e., $a_{11} = a_{22} = 12.5$) and the density is $\rho = c = 2.5$ slugs/ft.^{2}. The initial deflection of the membrane is assumed to be

$$u_0(x, y) = 0.1(4x - x^2)(2y - y^2) \tag{8.6.23}$$

and the initial velocity is $v_0 = 0$. We wish to determine the deflection $u(x, y, t)$ of the membrane as a function of time using the finite element method. The analytical solution of this problem

is [see Kreyszig (1988), p. 684)],

$$u(x, y, t) = \frac{409.6}{\pi^6} \sum_{m,n=1,3,\ldots} \frac{1}{m^3 n^3} \cos \omega_{mn} t \sin \frac{m\pi x}{4} \sin \frac{n\pi y}{2} \tag{8.6.24a}$$

$$\omega_{mn} = \frac{\pi}{4} \sqrt{5(m^2 + 4n^2)} \tag{8.6.24b}$$

where the origin of the (x, y) coordinate system is located at the lower corner of the domain [see Fig. 8.6.4(*a*)].

In the finite element analysis, we can utilize the biaxial symmetry of the problem and model one quadrant of the domain [see Fig. 8.6.4(*b*)]. We set up a new coordinate system $(\bar{x}, \bar{y})$ for the computational domain. The initial displacement in the new coordinates is given by (8.6.23) with x and y replaced in terms of $\bar{x}$ and $\bar{y}$: $x = \bar{x} + 2$, $y = \bar{y} + 1$. The initial values of $\ddot{u}$ are calculated using (8.6.22) with $\{F\}_0 = \{0\}$ and $\{u\}_0$ as given in (8.6.23) by $u_0(x, y)$. At $\bar{x} = 2$ and $\bar{y} = 1$, all nodal values for the function u and its time derivatives are zero.

As for the critical time step, we calculate $\lambda_{\max}$ from the solution of (8.6.17) using the same mesh as that used for the transient analysis and then use (8.6.19) to compute Δt_{cri}. Of course, for $\alpha = \frac{1}{2}$ and $\gamma = \frac{1}{2}$, there is no restriction on the time step for a stable solution. For a 4×4 mesh of linear rectangular elements in a quadrant, the maximum eigenvalue is found to be $\lambda_{\max} = 1072.68$, which yields $\Delta t_{\text{cri}} = 0.1058$ for the linear acceleration scheme ($\alpha = 0.5$, $\gamma = \frac{1}{3}$).

Stability characteristics of the solutions computed using the constant-average acceleration ($\alpha = 0.5$, $\gamma = 0.5$) and linear acceleration ($\alpha = 0.5$, $\gamma = \frac{1}{3}$) schemes for $\Delta t = 0.25 > \Delta t_{\text{cri}}$ are shown in Fig. 8.6.5. Plots of the center deflection $u(0, 0, t)$ versus time t are shown in Fig. 8.6.6. The finite element solutions are in good agreement with the analytical solution (8.6.24*a*) and (8.6.24*b*).

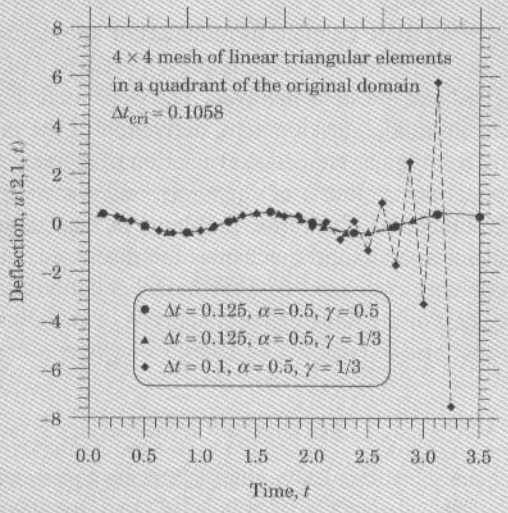

Figure 8.6.5 Stability characteristics of the constant-average acceleration and linear acceleration schemes (a 4×4 mesh of linear rectangular elements is used in a quadrant of the domain).

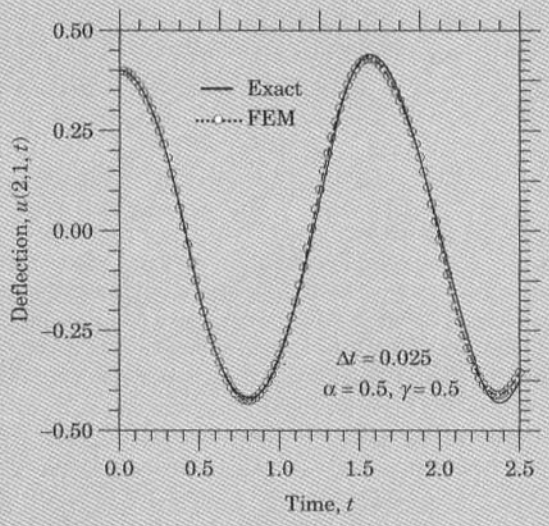

Figure 8.6.6 Comparison of the center deflection obtained using various meshes with the analytical solution of a rectangular membrane with initial deflection.

8.7 SUMMARY

A step by step procedure for finite element formulation of second-order equations in two dimensions with a single dependent variable is presented. The Poisson equation in two dimensions is used to illustrate the steps involved. The steps include: weak formulation of the equation, finite element model development, derivation of the interpolation functions for linear triangular and rectangular elements, evaluation of element matrices and vectors, assembly of element equations, solution of equations, and postcomputation of the gradient of the solution. A number of illustrative problems of heat transfer (conduction and convection), fluid mechanics, and solid mechanics are discussed. Finally, the eigenvalue and time-dependent problems associated with the model equation are also discussed. This chapter constitutes the heart of the finite element analysis of two-dimensional problems in Chapters 10–12.

PROBLEMS

Note: Most problems require some formulative effort (sketching a mesh when it is not given, calculations of element matrices and source vectors in some cases, assembling equations, identifying the boundary conditions in terms of the nodal variables, writing condensed equations, and so on). In some cases, a complete solution is required. When the problem size is large, essential steps of setting up the problem are required. Many of these problems will be solved by **FEM2D** in Chapter 13.

8.1 For a linear triangular element, show that

$$\sum_{i=1}^{3} \alpha_i^e = 2A_e, \quad \sum_{i=1}^{3} \beta_i^e = 0, \quad \sum_{i=1}^{3} \gamma_i^e = 0$$

$$\alpha_i^e + \beta_i^e \hat{x}^e + \gamma_i^e \hat{y}^e = \frac{2}{3} A_e \quad \text{for any } i$$

where

$$\hat{x}^e = \sum_{i=1}^{3} x_i^e, \quad \hat{y}^e = \sum_{i=1}^{3} y_i^e$$

and (x_i^e, y_i^e) are the coordinates of the ith node of the element ($i = 1, 2, 3$).

8.2 Consider the partial differential equation over a typical element Ω_e with boundary Γ_e

$$-\nabla^2 u + cu = 0 \quad \text{in } \Omega_e, \qquad \text{with} \quad \frac{\partial u}{\partial n} + \beta u = q_n \quad \text{on } \Gamma_e$$

Develop the weak form and finite element model of the equation over an element Ω_e.

8.3 Assuming that c and β are constant in Problem 8.2, write the element coefficient matrix and source vector for a linear (*a*) rectangular element and (*b*) triangular element.

8.4 Calculate the linear interpolation functions for the linear triangular and rectangular elements shown in Fig. P8.4. *Answer:* (*a*) $\psi_1 = (12.25 - 2.5x - 1.5y)/8.25$.

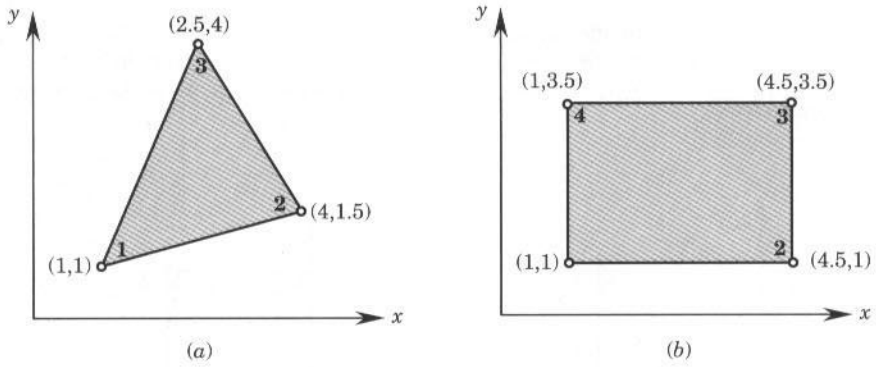

Figure P8.4

8.5 The nodal values of a triangular element in the finite element analysis of a field problem, $-\nabla^2 u = f_0$, are:

$$u_1 = 389.79, \quad u_2 = 337.19, \quad u_3 = 395.08$$

The interpolation functions of the element are given by

$$\psi_1 = \frac{1}{8.25}(12.25 - 2.5x - 1.5y), \quad \psi_2 = \frac{1}{8.25}(-1.5 + 3x - 1.5y)$$

$$\psi_3 = \frac{1}{8.25}(-2.5 - 0.5x + 3y)$$

(*a*) Find the component of the flux in the direction of the vector $4\hat{\mathbf{i}} + 3\hat{\mathbf{j}}$ at $x = 3$ and $y = 2$.

(*b*) A point source of magnitude Q_0 is located at point $(x_0, y_0) = (3, 2)$ inside the triangular element. Determine the contribution of the point source to the element source vector. Express your answer in terms of Q_0.

8.6 The nodal values of an element in the finite element analysis of a field problem $-\nabla^2 u = f_0$ are $u_1 = 389.79$, $u_2 = 337.19$, and $u_3 = 395.08$ (see Fig. P8.6). (*a*) Find the gradient of the solution, and (*b*) Determine where the 392 isoline intersects the boundary of the element in Fig. P8.6.

Answer: $\nabla u_h = 10.58\hat{\mathbf{e}}_1 - 105.2\hat{\mathbf{e}}_2$.

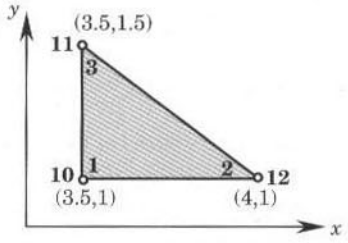

Figure P8.6

8.7 If the nodal values of the elements shown in Fig. P8.7 are $u_1 = 0.2645$, $u_2 = 0.2172$, and $u_3 = 0.1800$ for the triangular element and $u_1 = 0.2173$, $u_3 = 0.1870$, and $u_2 = u_4 = 0.2232$ for the rectangular element, compute u, $\partial u/\partial x$, and $\partial u/\partial y$ at the point $(x, y) = (0.375, 0.375)$.

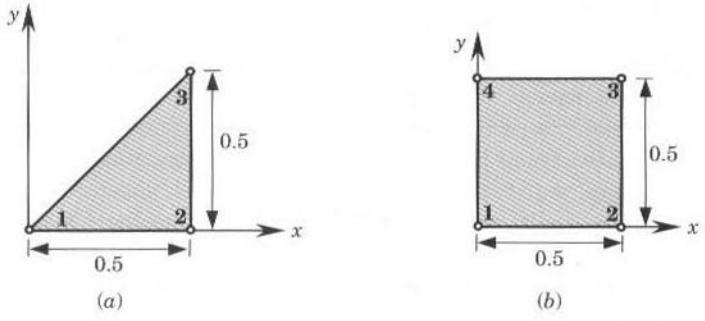

Figure P8.7

8.8 Compute the contribution of the pump 2 discharge to the nodes of element 43 in the groundwater flow problem of Example 8.5.4.

8.9 Find the coefficient matrix associated with the Laplace operator when the rectangular element in Fig. P8.9(*a*) is divided into two triangles by joining node 1 to node 3 [see Fig. P8.9(*b*)]. Compare the resulting matrix with that of the rectangular element in Eq. (8.2.54).

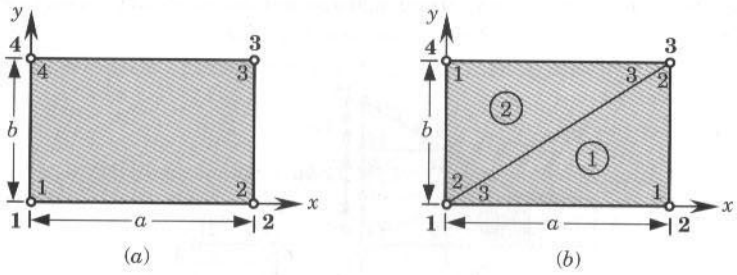

Figure P8.9

8.10 Compute the element matrices

$$S_{ij}^{01} = \int_0^a \int_0^b \psi_i \frac{d\psi_j}{dx}\, dx\, dy, \quad S_{ij}^{02} = \int_0^a \int_0^b \psi_i \frac{d\psi_j}{dy}\, dx\, dy$$

where $\psi_i(x, y)$ are the linear interpolation functions of a rectangular element with sides a and b.

8.11 Give the assembled coefficient matrix for the finite element meshes shown in Figs. P8.11(a) and P8.11(b). Assume one degree of freedom per node, and let $[K^e]$ denote the element coefficient matrix for the eth element. The answer should be in terms of element matrices K_{ij}^e.

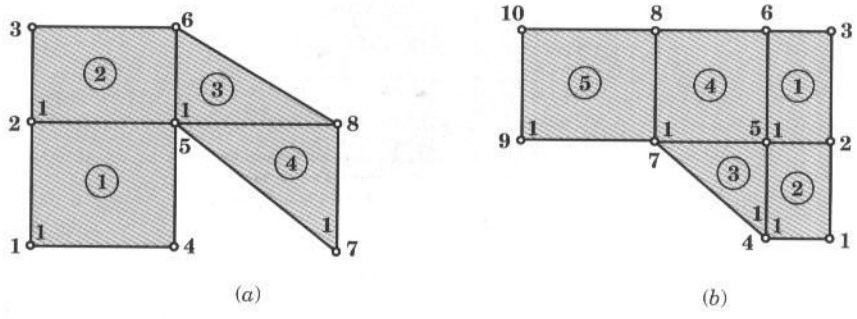

Figure P8.11

8.12 Repeat Problem 8.11 for the mesh shown in Fig. P8.12.

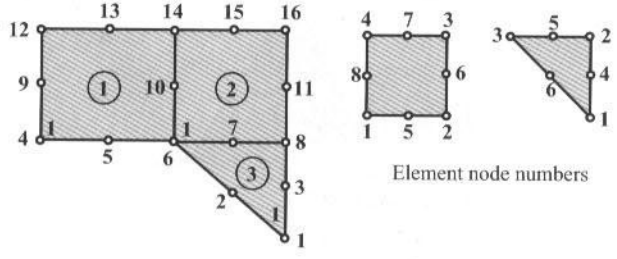

Figure P8.12

8.13 Compute the global source vector corresponding to the nonzero specified boundary flux for the finite element meshes of linear elements shown in Fig. P8.13.

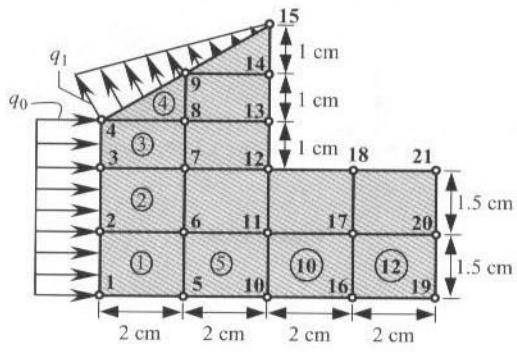

Figure P8.13

8.14 Repeat Problem 8.13 for the finite element mesh of quadratic elements shown in Fig. P8.14.

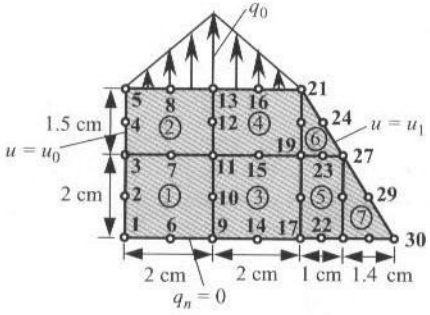

Figure P8.14

8.15 A line source of intensity q_0 is located across the triangular element shown in Fig. P8.15. Compute the element source vector.

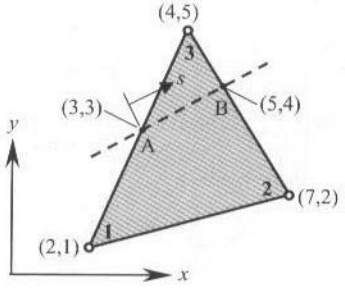

Figure P8.15

8.16 Repeat Problem 8.15 when the line source has varying source, $q(s) = q_0 s/L$, where s is the coordinate along the line source.

8.17 Consider the following partial differential equation governing the variable u:

$$c\frac{\partial u}{\partial t} - \frac{\partial}{\partial x}\left(a\frac{\partial u}{\partial x}\right) - \frac{\partial}{\partial y}\left(b\frac{\partial u}{\partial y}\right) - f_0 = 0$$

where c, a, b, and f_0 are constants. Assume an approximation of the form

$$u_h(x, y, t) = (1 - x)yu_1(t) + x(1 - y)u_2(t)$$

where u_1 and u_2 are nodal values of u at time t.

(*a*) Develop the fully discretized finite element model of the equation.

(*b*) Evaluate the element coefficient matrices and source vector for a square element of dimension 1 unit by 1 unit (so that the evaluation of the integrals is made easy).

Note: You should not be concerned with this nonconventional approximation of the dependent unknown but just use it as given to answer the question.

8.18 Solve the Laplace equation

$$-\left(\frac{\partial^2 u}{\partial x^2} + \frac{\partial^2 u}{\partial y^2}\right) = 0 \quad \text{in } \Omega$$

on a rectangle, when $u(0, y) = u(a, y) = u(x, 0) = 0$ and $u(x, b) = u_0(x)$. Use the symmetry and (*a*) a mesh of 2×2 triangular elements and (*b*) a mesh of 2×2 rectangular elements (see Fig. P8.18). Compare the finite element solution with the exact solution

$$u(x, y) = \sum_{n=1}^{\infty} A_n \sin\frac{n\pi x}{a} \sinh\frac{n\pi y}{b}$$

where

$$A_n = \frac{2}{a \sinh(n\pi b/a)} \int_0^a u_0(x) \sin\frac{n\pi x}{a} dx$$

Take $a = b = 1$, and $u_0(x) = \sin \pi x$ in the computations. For this case, the exact solution becomes

$$u(x, y) = \frac{\sin \pi x \sinh \pi y}{\sinh \pi}$$

Answer: For a 2×2 mesh of triangles, $U_4 = 0.23025$ and $U_5 = 0.16281$; for a 2×2 mesh of rectangles, $U_4 = 0.1520$ and $U_5 = 0.1075$.

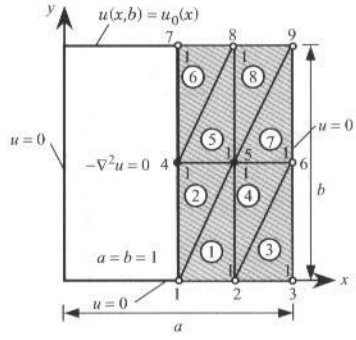

Figure P8.18

8.19 Solve Problem 8.18 when $u_0(x) = 1$. The analytical solution is given by

$$u(x, y) = \frac{4}{\pi} \sum_{n=0}^{\infty} \frac{\sin(2n+1)\pi x \sinh(2n+1)\pi y}{(2n+1)\sinh(2n+1)\pi}$$

Answer: (*a*) $U_4 = 0.2647$ and $U_5 = 0.2059$.

8.20 Solve Problem 8.18 when $u_0(x) = 4(x - x^2)$. *Answer:* (*a*) $U_4 = 0.2353$ and $U_5 = 0.1691$; (*b*) $U_4 = 0.1623$ and $U_5 = 0.1068$

8.21 Solve the Laplace equation for the unit square domain and boundary conditions given in Fig. P8.21. Use one rectangular element.

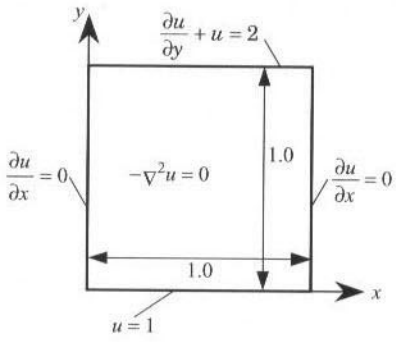

Figure P8.21

8.22 Use two triangular elements to solve the problem in Fig. P8.21. Use the mesh obtained by joining points (1,0) and (0,1).

8.23 Consider the steady-state heat transfer (or other phenomenon) in a square region shown in Fig. P8.23. The governing equation is given by

$$-\frac{\partial}{\partial x}\left(k\frac{\partial u}{\partial x}\right) - \frac{\partial}{\partial y}\left(k\frac{\partial u}{\partial y}\right) = f_0$$

The boundary conditions for the problem are:

$$u(0, y) = y^2, \quad u(x, 0) = x^2, \quad u(1, y) = 1 - y, \quad u(x, 1) = 1 - x$$

Assuming $k = 1$ and $f_0 = 2$, determine the unknown nodal value of u using the uniform 2×2 mesh of rectangular elements. *Answer:* $U_5 = 0.625$.

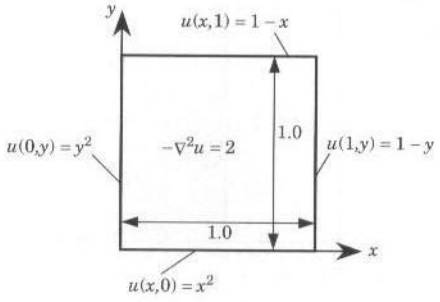

Figure P8.23

8.24 Solve Problem 8.23 using the mesh of a rectangle and two triangles, as shown in Fig. P8.24. *Answer:* $U_5 = 0.675$.

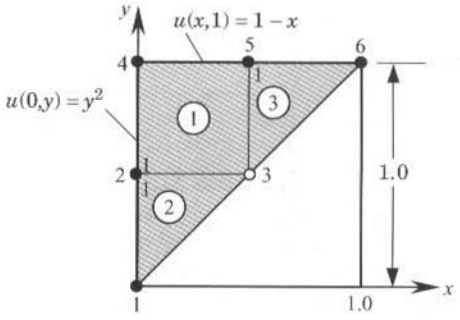

Figure P8.24

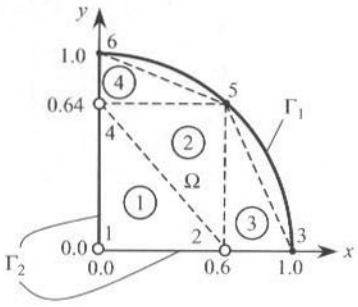

Figure P8.25

8.25 Solve the Poisson equation $-\nabla^2 u = 2$ in Ω, $u = 0$ on Γ_1, $\partial u/\partial n = 0$ on Γ_2, where Ω is the first quadrant bounded by the parabola $y = 1 - x^2$ and the coordinate axes (see Fig. P8.25), and Γ_1 and Γ_2 are the boundaries shown in Fig. P8.25.

8.26 Solve the axisymmetric field problem shown in Fig. P8.26 for the mesh shown there. Note that the problem has symmetry about any $z =$ constant line. Hence, the problem is essentially one dimensional. You are only required to determine the element matrix and source vector for element 1 and give the known boundary conditions on the primary and secondary variables.

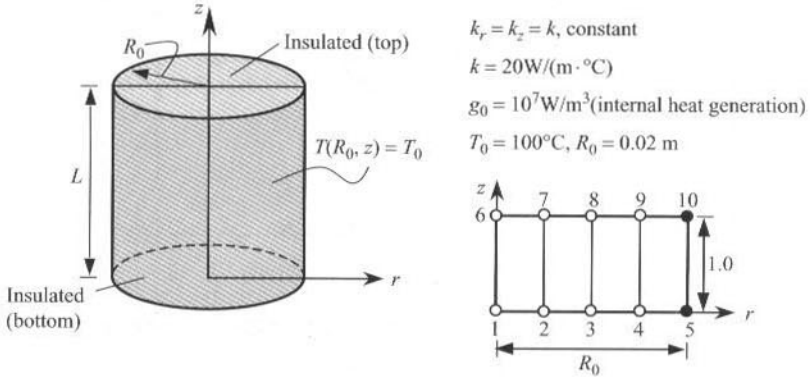

Figure P8.26

8.27 Formulate the axisymmetric field problem shown in Fig. P8.27 for the mesh shown. You are only required to give the known boundary conditions on the primary and secondary variables and compute the secondary variable at $r = R_0/2$ using equilibrium and the definition. Use the element at the left of the node.

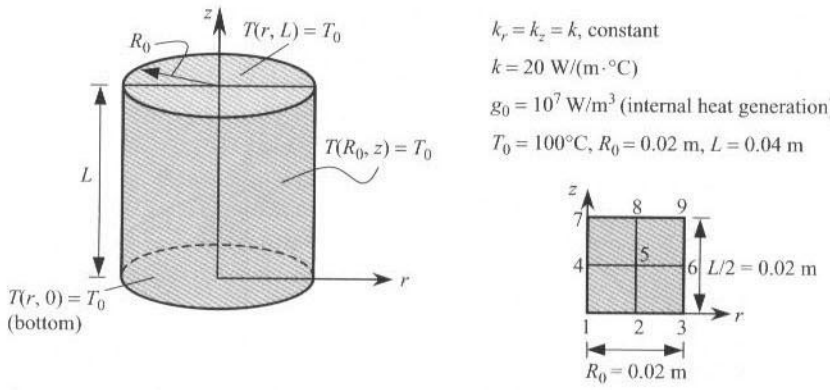

Figure P8.27

8.28 A series of heating cables have been placed in a conducting medium, as shown in Fig. P8.28. The medium has conductivities of $k_x = 10$ W/(cm · °C) and $k_y = 15$ W/(cm · °C), the upper surface is exposed to a temperature of −5°C, and the lower surface is bounded by an insulating medium. Assume that each cable is a point source of 250 W/cm. Take the convection coefficient between the medium and the upper surface to be $\beta = 5$ W/(cm² · K). Use a 8 × 8 mesh of linear rectangular (or triangular) elements in the computational domain (use any symmetry available in the problem), and formulate the problem (i.e., give element matrices for a typical element, give boundary conditions on primary and secondary variables, and compute convection boundary contributions).

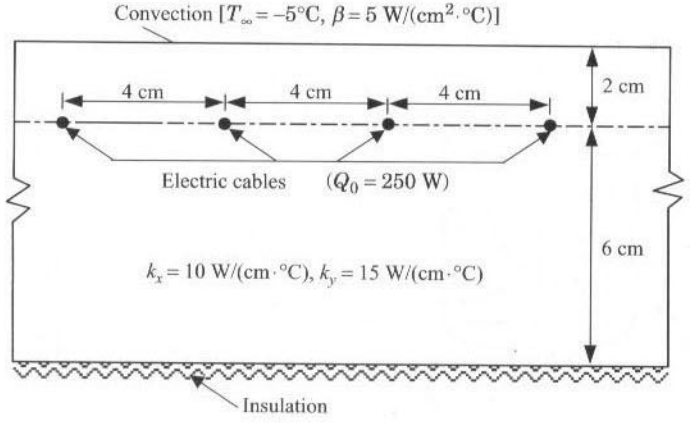

Figure P8.28

8.29 Formulate the finite element analysis information to determine the temperature distribution in the molded asbestos insulation shown in Fig. P8.29. Use the symmetry to identify a computational domain and give the specified boundary conditions at the nodes of the mesh. What is the connectivity of matrix for the mesh shown?

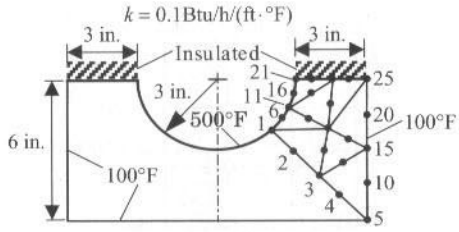

Figure P8.29

8.30 Consider steady-state heat conduction in a square region of side $2a$. Assume that the medium has conductivity of k (in W/(m·°C)) and uniform heat (energy) generation of g_0 (in W/m^3). For the boundary conditions and mesh shown in Fig. P8.30, write the finite element algebraic equations for nodes 1, 3, and 7.

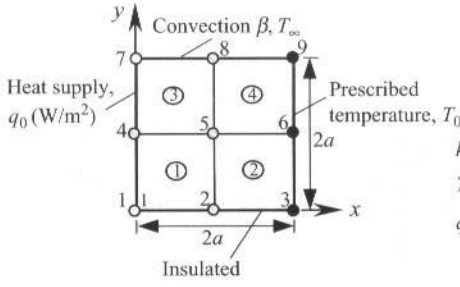

$k = 30$ W/(m·°C), $\beta = 60$ W/(m^2·°C)

$T_\infty = 0$°C, $T_0 = 100$°C, $a = 1$ cm

$q_0 = 2 \times 10^5$ W/m^2, $g_0 = 10^7$ W/m^3

Figure P8.30

8.31 For the convection heat transfer problem shown in Fig. P8.31, write the four finite element equations for the unknown temperatures. Assume that the thermal conductivity of the material is $k = 5$ W/(m·°C), the convection heat transfer coefficient on the left surface is $\beta = 28$ W/(m^2 · °C), and the internal heat generation is zero. Compute the heats at nodes 2, 4 and 9 using (*a*) element equations (i.e., equilibrium), and (*b*) definition in Eq. (8.2.19*b*) (use the temperature field of elements 1 and 2).

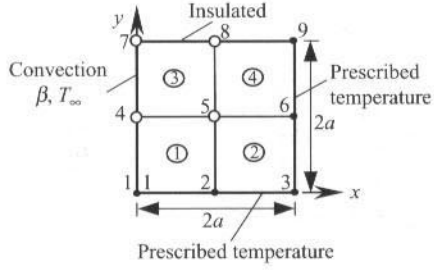

$k = 5$ W/(m·°C), $\beta = 28$ W/(m^2·°C)

$T_\infty = 0$°C, $T_3 = T_6 = T_9 = 40$°C,

$T_1 = T_2 = 10$°C, $a = 0.15$ m

Figure P8.31

8.32 Write the finite element equations for the unknown temperatures of the problem shown in Fig. P8.32.

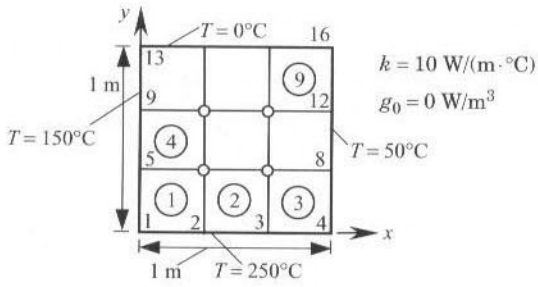

Figure P8.32

8.33 Write the finite element equations for the heats at nodes 1 and 13 of Problem 8.32. The answer should be in terms of the nodal temperatures $T_1, T_2, \ldots, T_{16}$.

8.34 Write the finite element equations associated with nodes 13, 16, and 19 for the problem shown in Fig. P8.34.

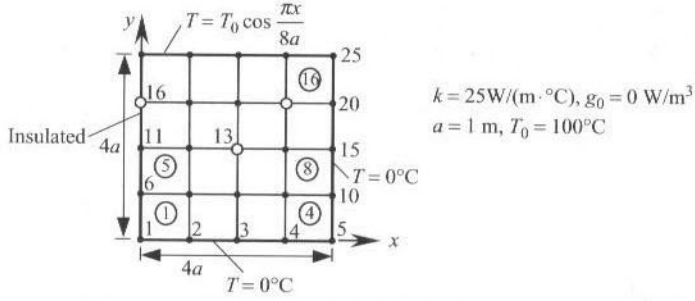

Figure P8.34

8.35 The fin shown in Fig. P8.35 has its base maintained at 300°C and exposed to convection on its remaining boundary. Write the finite element equations at nodes 7 and 10.

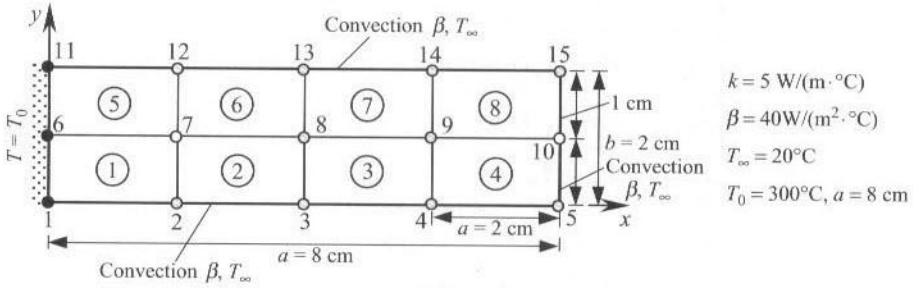

Figure P8.35

8.36 Compute the heat loss at nodes 10 and 13 of Problem 8.35.

8.37 Consider the problem of the flow of groundwater beneath a coffer dam. Solve the problem using the velocity potential formulation. The geometry and boundary conditions are shown in Fig. P8.37.

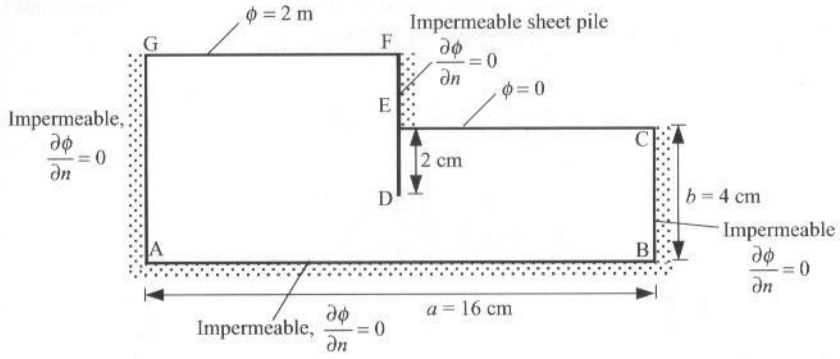

Figure P8.37

8.38 Formulate the groundwater flow problem of the domain shown in Fig. P8.38 for finite element analysis. The pump is located at $(x, y) = (787.5, 300)$ m.

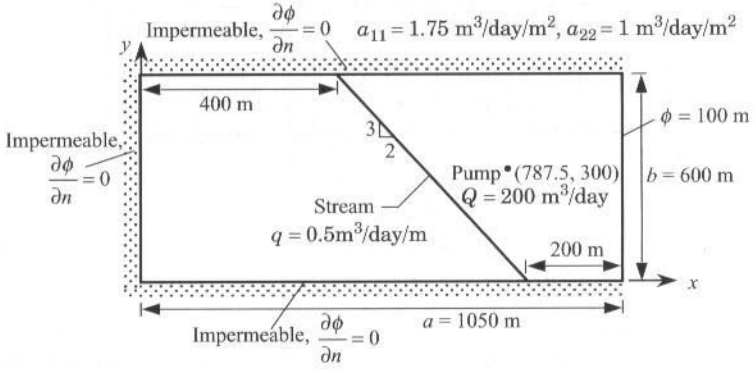

Figure P8.38

8.39 Repeat Problem 8.38 for the domain shown in Fig. P8.39.

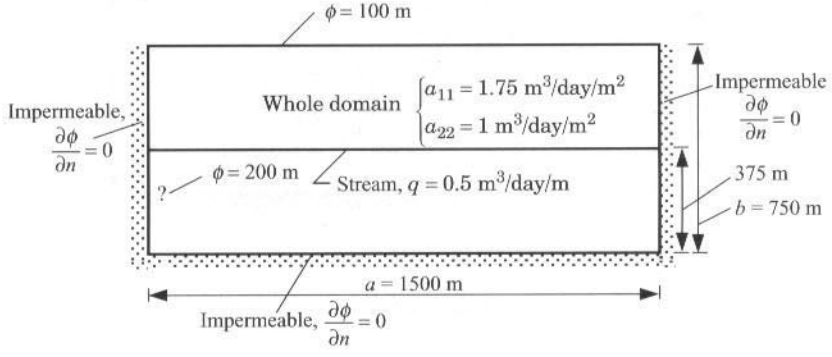

Figure P8.39

8.40 Consider the steady confined flow through the foundation soil of a dam (see Fig. P8.40). Assuming that the soil is isotropic ($k_x = k_y$), formulate the problem for finite element analysis (identify the specified primary and secondary variables and their contribution to the nodes). In particular, write the finite element equations at nodes 8 and 11. Write the finite element equations for the horizontal velocity component in 5th and 10th elements.

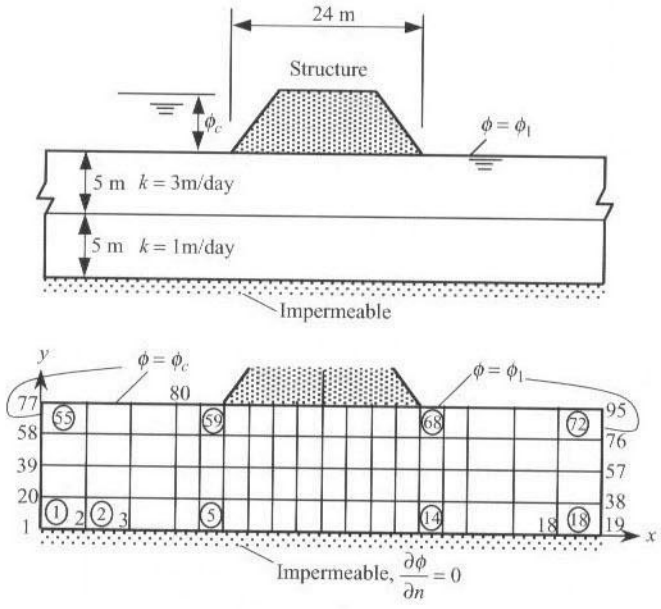

Figure P8.40

8.41 Formulate the problem of the flow about an elliptical cylinder using the (*a*) stream function and (*b*) velocity potential. The geometry and boundary conditions are shown in Fig. P8.41.

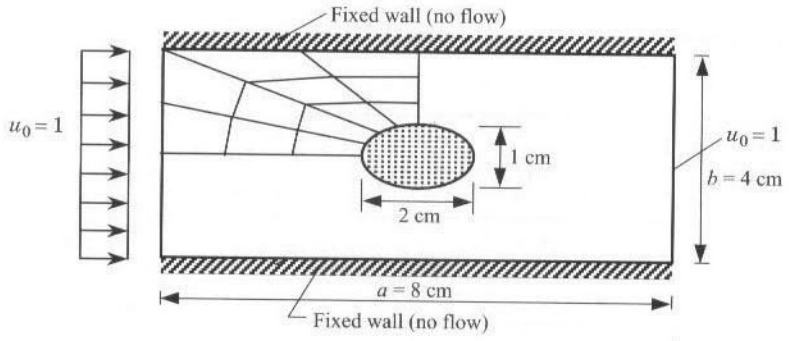

Figure P8.41

8.42 Repeat Problem 8.41 for the domain shown in Fig. P8.42.

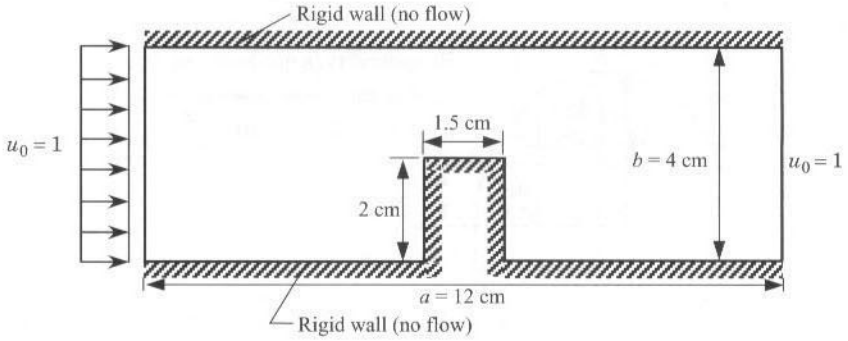

Figure P8.42

8.43 The Prandtl theory of torsion of a cylindrical member leads to

$$-\nabla^2 u = 2G\theta \quad \text{in } \Omega; \quad u = 0 \quad \text{on } \Gamma$$

where Ω is the cross section of the cylindrical member being twisted, Γ is the boundary of Ω, G is the shear modulus of the material of the member, θ is the angle of twist, and u is the stress function. Solve the equation for the case in which Ω is a circular section (see Fig. P8.43) using the mesh of linear triangular elements. Compare the finite element solution with the exact solution (valid for elliptical sections with axes a and b):

$$u = \frac{G\theta a^2 b^2}{a^2 + b^2}\left(1 - \frac{x^2}{a^2} - \frac{y^2}{b^2}\right)$$

Use $a = 1$, $b = 1$, and $f_0 = 2G\theta = 10$.

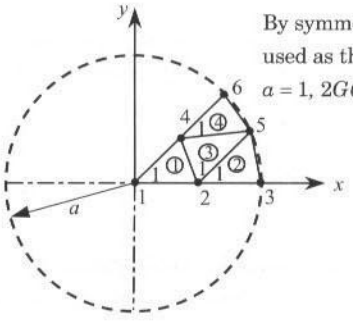

By symmetry, any sector can be used as the computational domain

$a = 1$, $2G\theta = 10$

Figure P8.43

8.44 Repeat Problem 8.43 for an elliptical section member (see Fig. P8.44). Use $a = 1$ and $b = 1.5$.

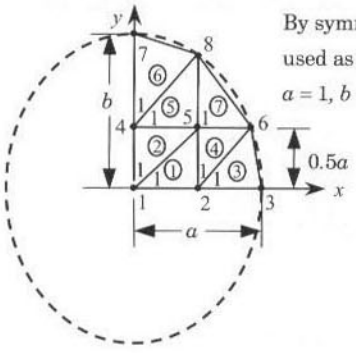

By symmetry, a quadrant can be used as the computational domain
$a = 1,\ b = 1.5,\ 2G\theta = 10$

Figure P8.44

8.45 Repeat Problem 8.43 for the case in which Ω is an equilateral triangle (see Fig. P8.45). The exact solution is given by

$$u = -G\theta\left[\frac{1}{2}(x^2 + y^2) - \frac{1}{2a}(x^3 - 3xy^2) - \frac{2}{27}a^2\right]$$

Take $a = 1$ and $f_0 = 2G\theta = 10$. Give the finite element equation for node 5.

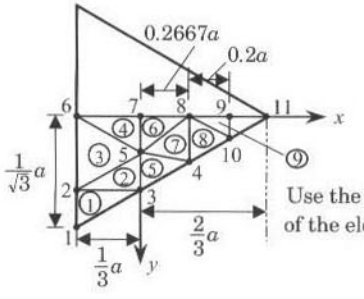

$y_5 = 0.5y_3,\ y_2 = y_3$
$x_8 = 0.2667a$
$x_9 = x_8 + 0.2a$
$x_{10} = x_8 + 0.4a$
Use the smallest node as the first node of the element to write the connectivity

Figure P8.45

8.46 Consider the torsion of a hollow square cross-sectional member. The stress function Ψ is required to satisfy the Poisson equation in (8.5.60) and the following boundary conditions:

$$\Psi = 0 \quad \text{on the outer boundary;} \quad \Psi = 2r^2 \quad \text{on the inner boundary}$$

where r is the ratio of the outside dimension to the inside dimension, $r = 6a/2a$. Formulate the problem for finite element analysis using the mesh shown in Fig. P8.46.

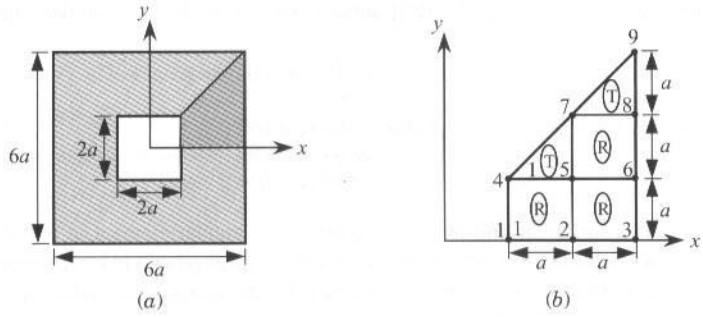

Figure P8.46

8.47 Repeat Problem 8.46 with the mesh of linear triangles [join nodes 1 and 5, 2 and 6, and 5 and 8 in Fig. P8.46(*b*)].

8.48 The membrane shown in Fig. P8.48 is subjected to uniformly distributed transverse load of intensity f_0 (in N/m^2). Write the condensed equations for the unknown displacements.

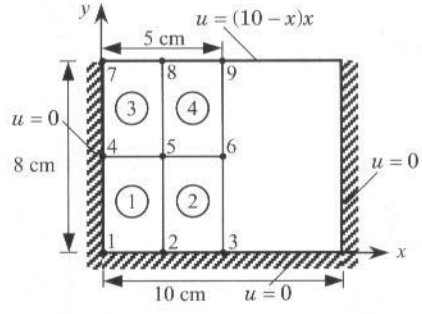

Figure P8.48

8.49 The circular membrane shown in Fig. P8.49 is subjected to uniformly distributed transverse load of intensity f_0 (in N/m^2). Write the condensed equations for the unknown displacements.

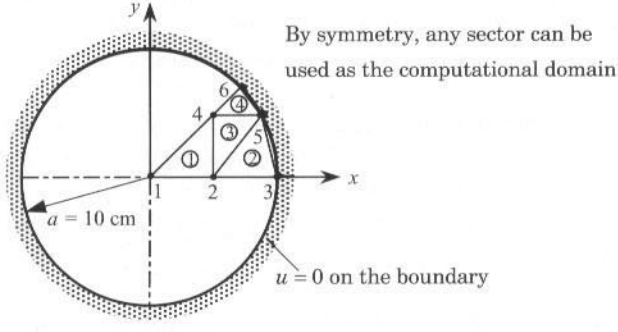

Figure P8.49

8.50 Determine the critical time step for the transient analysis (with $\alpha \leq \frac{1}{2}$) of the problem

$$\frac{\partial u}{\partial t} - \nabla^2 u = 1 \quad \text{in } \Omega; \quad u = 0 \quad \text{in } \Omega \text{ at } t = 0$$

by determining the maximum eigenvalue of the problem

$$-\nabla^2 u = \lambda u \quad \text{in } \Omega; \quad u = 0 \quad \text{on } \Gamma$$

The domain is a square of unit length. Use (*a*) one triangular element in the octant, (*b*) four linear elements in the octanta, and (*c*) a 2×2 mesh of linear rectangular elements in a quadrant (see Fig. P8.50). Determine the critical time step for the forward difference scheme. *Answer:* (*a*) $\lambda = 24$. (*b*) $\lambda_{max} = 305.549$.

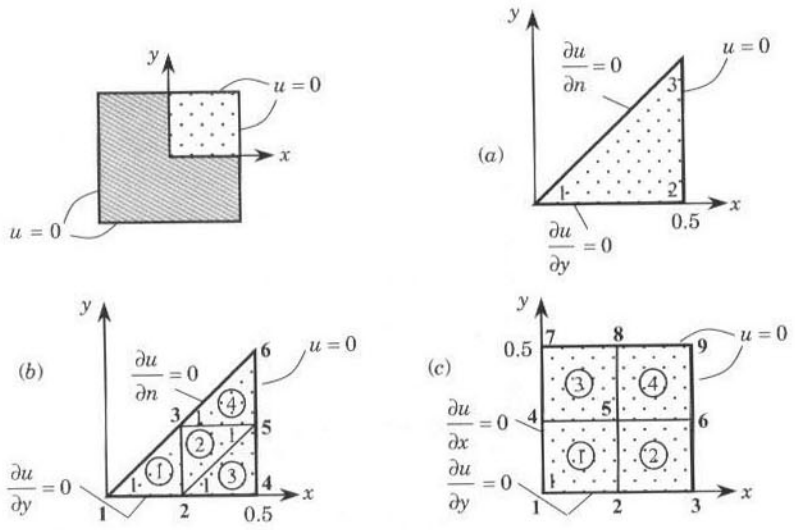

Figure P8.50

8.51 Set up the condensed equations for the transient problem in Problem 8.50 for the α-family of approximation. Use the mesh shown in Fig. P8.50(*b*).

8.52 Set up the condensed equations for the time-dependent analysis of the circular membrane in Problem 8.49.

8.53 Determine the fundamental natural frequency of the rectangular membrane in Problem 8.48.

8.54 Determine the critical time step based on the forward difference scheme for the time-dependent analysis of the circular membrane in Problem 8.49.

8.55 (*Central difference method*) Consider the following matrix differential equation in time:

$$[M]\{\ddot{U}\} + [C]\{\dot{U}\} + [K]\{U\} = \{F\}$$

where the superposed dot indicates differentiation with respect to time. Assume

$$\{\ddot{U}\}_n = \frac{1}{(\Delta t)^2}(\{U\}_{n-1} - 2\{U\}_n + \{U\}_{n+1}), \quad \{\dot{U}\}_n = \frac{1}{2(\Delta t)}(\{U\}_{n+1} - \{U\}_{n-1})$$

and derive the algebraic equations for the solution of $\{U\}_{n+1}$ in the form

$$[A]\{U\}_{n+1} = \{F\}_n - [B]\{U\}_n - [D]\{U\}_{n-1}$$

Define $[A]$, $[B]$, and $[D]$ in terms of $[M]$, $[C]$, and $[K]$.

8.56 Consider the first-order differential equation in time

$$a\frac{du}{dt} + bu = f$$

Using linear approximation, $u(t) = u_1\psi_1(t) + u_2\psi_2(t)$, $\psi_1 = 1 - t/\Delta t$, and $\psi_2 = t/\Delta t$, derive the associated algebraic equation and compare with that obtained using the α-family of approximation.

8.57 (*Space-time element*) Consider the differential equation

$$c\frac{\partial u}{\partial t} - \frac{\partial}{\partial x}\left(a\frac{\partial u}{\partial x}\right) = f \quad \text{for } 0 < x < L, \quad 0 \le t \le T$$

with

$$u(0,t) = u(L,t) = 0 \quad \text{for } 0 \le t \le T, \quad u(x,0) = u_0(x) \quad \text{for } 0 < x < L$$

where $c = c(x)$, $a = a(x)$, $f = f(x,t)$, and u_0 are given functions. Consider the rectangular domain defined by

$$\Omega = \{(x,t) : 0 < x < L, \quad 0 \le t \le T\}$$

A finite element discretization of Ω by rectangles is a time-space rectangular element (with y replaced by t). Give a finite element formulation of the equation over a time-space element, and discuss the *mathematical/practical* limitations of such a formulation. Compute the element matrices for a linear element.

8.58 (*Space-time finite element*) Consider the time-dependent problem

$$\frac{\partial^2 u}{\partial x^2} = c\frac{\partial u}{\partial t}, \quad \text{for } 0 < x < 1, \quad t > 0$$

$$u(0,t) = 0, \quad \frac{\partial u}{\partial x}(1,t) = 1, \quad u(x,0) = x$$

Use linear rectangular elements in the (x,t)-plane to model the problem. Note that the finite element model is given by $[K^e]\{u^e\} = \{Q^e\}$, where

$$K_{ij}^e = \int_0^{\Delta t}\int_{x_a}^{x_b}\left(\frac{\partial \psi_i^e}{\partial x}\frac{\partial \psi_j^e}{\partial x} + c\psi_i^e\frac{\partial \psi_j^e}{\partial t}\right)dx\,dt$$

$$Q_1^e = \left(-\int_0^{\Delta t}\frac{\partial u}{\partial x}\,dt\right)\Bigg|_{x=x_a}, \quad Q_2^e = \left(\int_0^{\Delta t}\frac{\partial u}{\partial x}\,dt\right)\Bigg|_{x=x_b}$$

8.59 The collocation time approximation methods are defined by the following relations:

$$\{\ddot{u}\}_{n+\alpha} = (1-\alpha)\{\ddot{u}\}_n + \alpha\{\ddot{u}\}_{n+1}$$

$$\{\dot{u}\}_{n+\alpha} = \{\dot{u}\}_n + \alpha\Delta t[(1-\gamma)\{\ddot{u}\}_n + \gamma\{\ddot{u}\}_{n+\alpha}]$$

$$\{u\}_{n+\alpha} = \{u\}_n + \alpha\Delta t\{\dot{u}\}_n + \frac{\alpha(\Delta t)^2}{2}[(1-2\beta)\{\ddot{u}\}_n + 2\beta\{\ddot{u}\}_{n+\alpha}]$$

The collocation scheme contains two of the well-known schemes: $\alpha = 1$ gives the Newmark's scheme; and $\beta = \frac{1}{6}$ and $\gamma = \frac{1}{2}$ gives the Wilson scheme. The collocation scheme is unconditionally stable, second-order accurate for the following values of the parameters:

$$\alpha \geq 1, \quad \gamma = \frac{1}{2}, \quad \frac{\alpha}{2(1+\alpha)} \geq \beta \geq \frac{2\alpha^2 - 1}{4(2\alpha^3 - 1)}$$

Formulate the algebraic equations associated with the matrix differential equation

$$[M]\{\ddot{u}\} + [C]\{\dot{u}\} + [K]\{u\} = \{F\}$$

using the collocation scheme.

8.60 Consider the following pair of coupled partial differential equations:

$$-\frac{\partial}{\partial x}\left(a\frac{\partial u}{\partial x}\right) - \frac{\partial}{\partial y}\left[b\left(\frac{\partial u}{\partial y} + \frac{\partial v}{\partial x}\right)\right] + \frac{\partial u}{\partial t} - f_x = 0 \tag{i}$$

$$-\frac{\partial}{\partial x}\left[b\left(\frac{\partial u}{\partial y} + \frac{\partial v}{\partial x}\right)\right] - \frac{\partial}{\partial y}\left(c\frac{\partial v}{\partial y}\right) + \frac{\partial v}{\partial t} - f_y = 0 \tag{ii}$$

where u and v are the dependent variables (unknown functions), a, b, and c are known functions of x and y, and f_x and f_y are known functions of position (x, y) and time t.

(*a*) Use the three-step procedure on each equation with a different weight function for each equation (say, w_1 and w_2) to develop the (semidiscrete) weak form.

(*b*) Assume finite element approximation of (u, v) in the following form

$$u(x, y) = \sum_{j=1}^{n} \psi_j(x, y) U_j(t), \quad v(x, y) = \sum_{j=1}^{n} \psi_j(x, y) V_j(t) \tag{iii}$$

and develop the (semidiscrete) finite element model in the form

$$\begin{aligned} 0 &= \sum_{j=1}^{n} M_{ij}^{11} \dot{U}_j + \sum_{j=1}^{n} K_{ij}^{11} U_j + \sum_{j=1}^{n} K_{ij}^{12} V_j - F_i^1 \\ 0 &= \sum_{j=1}^{n} M_{ij}^{22} \dot{V}_j + \sum_{j=1}^{n} K_{ij}^{21} U_j + \sum_{j=1}^{n} K_{ij}^{22} V_j - F_i^2 \end{aligned} \tag{iv}$$

You must define the algebraic form of the element coefficients K_{ij}^{11}, K_{ij}^{12}, F_i^1 etc.

(*c*) Give the fully discretized finite element model of the model (in the standard form; you are not required to derive it).

REFERENCES FOR ADDITIONAL READING

1. Eskinazi, S., *Principles of Fluid Mechanics*, Allyn and Bacon, Boston, MA, 1962.
2. Holman, J. P., *Heat Transfer*, 6th ed., McGraw-Hill, New York, 1986.
3. Kohler, W. and Pittr, J., "Calculation of Transient Temperature Fields with Finite Elements in Space and Time Dimensions," *International Journal for Numerical Methods in Engineering*, **8**, 625–631, 1974.
4. Kreyszig, E., *Advanced Engineering Mathematics*, 6th ed., John Wiley, New York, 1988.
5. Mikhlin, S. G., *Variational Methods in Mathematical Physics*, (translated from the Russian by T. Boddington), Pergamon Press, Oxford, UK, 1964.

6. Mikhlin, S. G., *The Numerical Performance of Variational Methods*, (translated from the Russian by R. S. Anderssen), Wolters-Noordhoff, The Netherlands, 1971.
7. Oden, J. T. and Reddy, J. N., *Variational Methods in Theoretical Mechanics*, 2nd ed., Springer-Verlag, Berlin, 1983.
8. Özisik, M. N., *Heat Transfer A Basic Approach*, McGraw-Hill, New York, 1985.
9. Reddy, J. N., *Applied Functional Analysis and Variational Methods in Engineering*, McGraw-Hill, New York, 1986; reprinted by Krieger, Melbourne, FL, 1991.
10. Reddy, J. N., *Energy Principles and Variational Methods in Applied Mechanics*, 2nd ed., John Wiley, New York, 2002.
11. Reddy, J. N. and Rasmussen, M. L., *Advanced Engineering Analysis*, John Wiley, New York, 1982; reprinted by Krieger, Melbourne, FL, 1990.
12. Rektorys, K., *Variational Methods in Mathematics, Science and Engineering*, D. Reidel Publishing Co., Boston, MA, 1980.
13. Schlichting, H., *Boundary-Layer Theory* (translated by J. Kestin), 7th ed., McGraw-Hill, New York, 1979.
14. Sobey, R. J., "Hermitian Space-Time Finite Elements for Estuarine Mass Transport," *International Journal for Numerical Methods in Fluids*, **2**, 277–297, 1982.
15. Timoshenko, S. P. and Goodier, J. N., *Theory of Elasticity*, 3rd ed., McGraw-Hill, New York, 1970.
16. Ugural, A. C. and Fenster, S. K., *Advanced Strength and Applied Elasticity*, 4th ed., Prentice Hall, Upper Saddle River, NJ, 2003.

Chapter 9

INTERPOLATION FUNCTIONS, NUMERICAL INTEGRATION, AND MODELING CONSIDERATIONS

9.1 INTRODUCTION

In the previous chapter we studied the finite element analysis of a model second-order equation and its analogues in the fields of heat transfer, fluid mechanics, and solid mechanics. As part of this study we developed the interpolation functions for the basic elements, namely, the linear triangular and rectangular elements. These elements, which were developed in connection with the finite element analysis of a second-order partial differential equation in a single variable, are useful in all finite element models that admit Lagrange interpolation of the primary variables of the weak formulation. Thus, if a library of interpolation functions is available, then we can select admissible functions for the model from the library.

The objective of this chapter is to develop a library of two-dimensional triangular and rectangular elements of the Lagrange family, i.e., elements over which only the function—not its derivatives—are interpolated. The Hermite cubic interpolation functions are also presented, without a derivation, for the sake of completeness and reference. Once we have elements of different shapes and order at our disposal, we can choose appropriate elements and associated interpolation functions for a given problem. The regularly shaped elements, called *master elements*, for which interpolation functions are developed here, can be used for numerical evaluation of integrals defined on irregular elements. Of course, this requires a transformation of the geometry from the actual element shape to an associated master element. Section 9.3 deals with the transformation and numerical integration.

9.2 ELEMENT LIBRARY

9.2.1 Triangular Elements

The linear (three-node) triangular element was developed in Section 8.2.5. Higher-order triangular elements (i.e., triangular elements with interpolation functions of higher degree) can be systematically developed with the help of the so-called *Pascal's triangle*, which

Pascal's triangle	Degree of the complete polynomial	Number of terms in the polynomial	Element with nodes
1	0	1	
$x \quad y$	1	3	
$x^2 \quad xy \quad y^2$	2	6	
$x^3 \quad x^2y \quad xy^2 \quad y^3$	3	10	
$x^4 \quad x^3y \quad x^2y^2 \quad xy^3 \quad y^4$	4	15	
$x^5 \quad x^4y \quad x^3y^2 \quad x^2y^3 \quad xy^4 \quad y^5$	5	21	(Figure not shown)

Figure 9.2.1 Topmost six rows of Pascal's triangle for the generation of the Lagrange family of triangular elements.

contains the terms of polynomials of various degrees in the two coordinates x and y, as shown in Fig. 9.2.1. Here x and y denote some local coordinates; they do not, in general, represent the global coordinates of the problem. We can view the position of the terms as the nodes of the triangle, with the constant term and the first and last terms of a given row being the vertices of the triangle. Of course, the shape of the triangle is arbitrary—not necessarily an equilateral triangle, as might appear from the position of the terms in Pascal's triangle. For example, a triangular element of order 2 (i.e., the degree of the polynomial is 2) contains six nodes, as can be seen from the third row of Pascal's triangle. The position of the six nodes in the triangle is at the three vertices and at the midpoints of the three sides. The polynomial involves six constants, which can be expressed in terms of the nodal values of the variable being interpolated:

$$u = \sum_{i=1}^{6} u_i \psi_i(x, y) \tag{9.2.1}$$

where ψ_i are the quadratic interpolation functions obtained following the same procedure as that used for the linear element in Section 8.2. In general, a pth-order triangular element has a number of n nodes

$$n = \frac{1}{2}(p+1)(p+2) \tag{9.2.2}$$

and a complete polynomial of pth degree is given by

$$u(x, y) = \sum_{i=1}^{n} a_i x^r y^s = \sum_{j=1}^{n} u_j \psi_j, \qquad r + s \leq p \tag{9.2.3}$$

The location of the entries in Pascal's triangle gives a symmetric location of nodal points in elements that will produce exactly the right number of nodes to define a Lagrange interpolation of any degree. It should be noted that the Lagrange family of triangular elements (of order greater than zero) should be used for second-order problems that require only the dependent variables (not their derivatives) of the problem to be continuous at interelement boundaries. It can be easily seen that the pth-degree polynomial associated with the pth-order Lagrange element, when evaluated on the boundary of the element, yields a pth-degree polynomial in the boundary coordinate. For example, the quadratic polynomial associated with the quadratic (six-node) triangular element shown in Fig. 9.2.2(a) is given by

$$u^e(x, y) = a_1 + a_2 x + a_3 y + a_4 xy + a_5 x^2 + a_6 y^2 \tag{9.2.4}$$

The derivatives of u^e are

$$\frac{\partial u^e}{\partial x} = a_2 + a_4 y + 2a_5 x, \qquad \frac{\partial u^e}{\partial y} = a_3 + a_4 x + 2a_6 y \tag{9.2.5}$$

The element shown in Fig. 9.2.2(a) is an arbitrary quadratic triangular element. By rotating and translating the (x, y) coordinate system, we obtain the (s, t) coordinate system [see Fig. 9.2.2(b)]. Since the transformation from the (x, y) system to the (s, t) system involves only rotation (which is linear) and translation, a kth-degree polynomial in the (x, y)

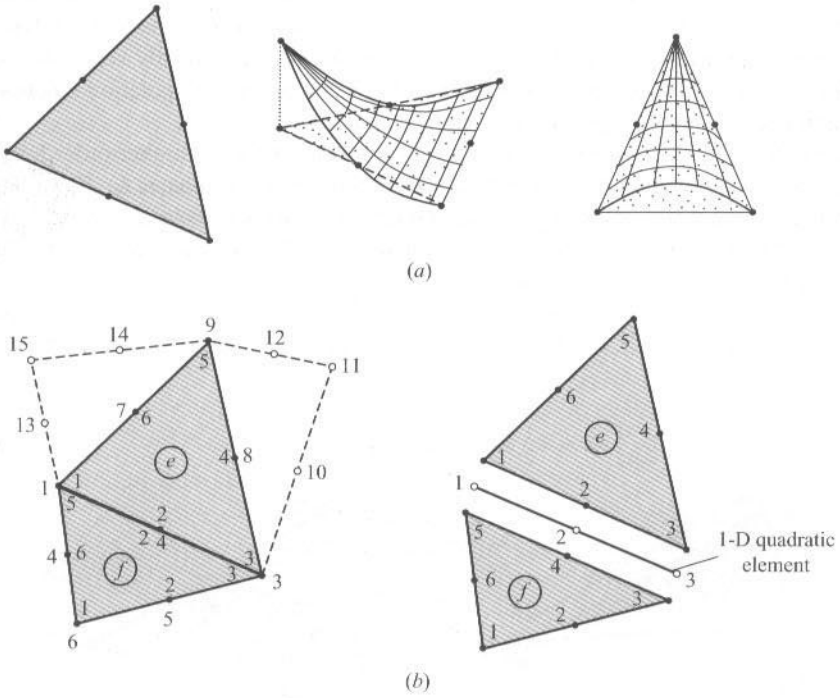

Figure 9.2.2 Variation of a function along the interelement boundaries of higher-order Lagrange elements: (a) a quadratic triangular element and (b) interelement continuity of a quadratic interpolation function.

coordinate system is still a kth-degree polynomial in the (s, t) system:

$$u^e(s,t) = \hat{a}_1 + \hat{a}_2 s + \hat{a}_3 t + \hat{a}_4 st + \hat{a}_5 s^2 + \hat{a}_6 t^2 \tag{9.2.6}$$

where $\hat{a}_i$ $(i = 1, 2, \ldots, 6)$ are constants that depend on a_i and the angle of rotation α. Now by setting $t = 0$, we get the restriction of u to side 1–2–3 of element Ω_e:

$$u^e(s,0) = \hat{a}_1 + \hat{a}_2 s + \hat{a}_5 s^2 \tag{9.2.7}$$

which is a quadratic polynomial in s. If a neighboring element Ω_f has its side 5–4–3 in common with side 1–2–3 of element Ω_e, then the function u on side 5–4–3 of element Ω_f is also a quadratic polynomial

$$u^f(s,0) = \hat{b}_1 + \hat{b}_2 s + \hat{b}_5 s^2 \tag{9.2.8}$$

Since the polynomials are uniquely defined by the same nodal values $U_1 = u_1^e = u_5^f$, $U_2 = u_2^e = u_4^f$, and $U_3 = u_3^e = u_3^f$, we have $u^e(s, 0) = u^f(s, 0)$ and hence the function u is uniquely defined on the interelement boundary of elements e and f.

The ideas discussed above can be easily extended to three dimensions, in which case Pascal's triangle takes the form of a Christmas tree and the elements are of a pyramid shape, called tetrahedral elements. We shall not elaborate on this any further because the scope of the present study is limited to two-dimensional elements only. A brief introduction to three-dimensional elements is presented in Chapter 14.

Recall from (8.2.21)–(8.2.25) that the procedure for deriving the interpolation functions involves the inversion of a $n \times n$ matrix, where n is the number of terms in the polynomial used to represent a function. When $n > 3$, this procedure is algebraically very tedious, and therefore we should devise an alternative way of developing the interpolation functions, as was discussed for one-dimensional elements in Chapter 3.

The alternative derivation of the interpolation functions for the higher-order Lagrange family of triangular elements is simplified by use of the *area* coordinates L_i. For triangular elements it is possible to construct three nondimensionalized coordinates L_i $(i = 1, 2, 3)$ that relate respectively to the sides directly opposite nodes 1, 2, and 3 such that (see Fig. 9.2.3)

$$L_i = \frac{A_i}{A} \qquad A = \sum_{i=1}^{3} A_i \tag{9.2.9}$$

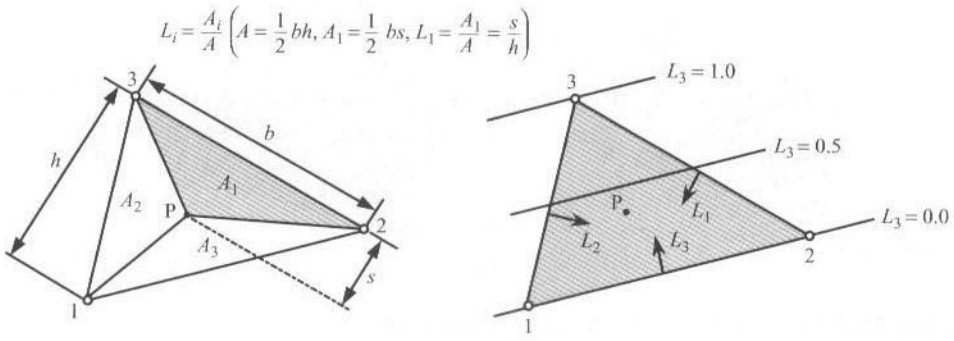

Figure 9.2.3 Definition of the natural coordinates of a triangular element.

where A_i is the area of the triangle formed by nodes j and k and an arbitrary point P in the element, and A is the total area of the element. For example, A_1 is the area of the shaded triangle, which is formed by nodes 2 and 3 and point P. The point P is at a perpendicular distance of s from the side connecting nodes 2 and 3. We have $A_1 = \frac{1}{2}bs$ and $A = \frac{1}{2}bh$. Hence,

$$L_1 = \frac{A_1}{A} = \frac{s}{h}$$

Clearly, L_1 is zero on side 2–3 (hence, zero at nodes 2 and 3) and has a value of unity at node 1. Thus, L_1 is the interpolation function associated with node 1. Similarly, L_2 and L_3 are the interpolation functions associated with nodes 2 and 3, respectively. In summary, we have

$$\psi_i = L_i \tag{9.2.10}$$

for a linear triangular element. We shall use L_i to construct interpolation functions for higher-order triangular elements.

Consider a higher-order element with k nodes (equally spaced) per side [see Fig. 9.2.4(*a*)]. Then the total number of nodes in the element is given by

$$n = \sum_{i=0}^{k-1}(k-i) = k + (k-1) + \cdots + 1 = \frac{1}{2}k(k+1) \tag{9.2.11}$$

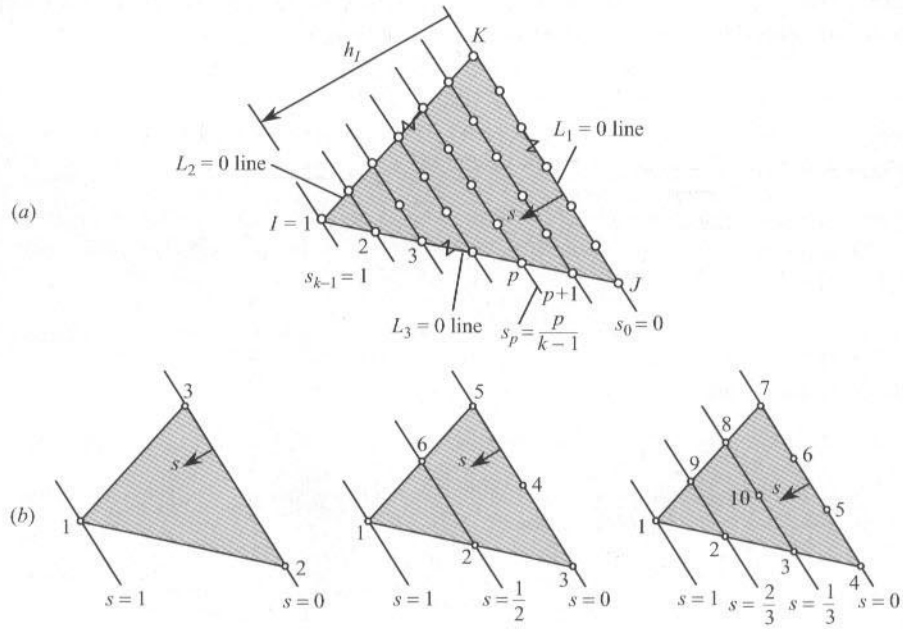

Figure 9.2.4 Construction of the element interpolation functions of the Lagrange triangular elements: (*a*) an arbitrary $(k-1)$th-order element; and (*b*) linear, quadratic, and cubic elements.

and the degree of the interpolation functions is equal to $k-1$. For example, for the quadratic element we have $k-1=2$ and $n=6$. Let the corner (i.e., vertex) nodes be denoted by I, J, and K, and let h_I be the perpendicular distance of the node I from the side connecting J and K. Then the distance s_p to the pth row parallel to side J–K (under the assumption that the nodes are equally spaced along the sides and the rows) is given in nondimensional form by

$$s_p = \frac{p}{k-1}, \qquad s_0 = 0, \qquad s_{k-1} = 1 \tag{9.2.12}$$

The interpolation function ψ_I should be zero at the nodes on the lines $L_I = 0, 1/(k-1), \ldots, p/(k-1)$ $(p = 0, 1, \ldots, k-2)$, and ψ_I should be equal to 1 at $L_I = s_{k-1}$. Thus, we have the necessary information for constructing the interpolation function ψ_I for vertex node I $(I = 1, 2, 3)$:

$$\psi_I = \frac{(L_I - s_0)(L_I - s_1)(L_I - s_2)\cdots(L_I - s_{k-2})}{(s_{k-1} - s_0)(s_{k-1} - s_1)\cdots(s_{k-1} - s_{k-2})} = \prod_{p=0}^{k-2} \frac{L_I - s_p}{s_{k-1} - s_p} \tag{9.2.13}$$

Similar expressions can be derived for nodes located at other than the vertices. In general, ψ_i for node i is given by

$$\psi_i = \prod_{j=1}^{k-1} \frac{f_j}{f_j^i} \tag{9.2.14}$$

where f_j are functions of L_1, L_2, and L_3, and f_j^i is the value of f_j at node i. The functions f_j are derived from the equations of $k-1$ lines that pass through all the nodes except node i. The procedure is illustrated below via an example.

Example 9.2.1

First, consider the triangular element that has two nodes per side (i.e., $k = 2$). This is the linear triangular element with the total number of nodes equal to three $(n = 3)$. For node 1 [see Fig. 9.2.4(*b*)], we have $k - 2 = 0$ and

$$s_0 = 0, \qquad s_1 = 1, \qquad \psi_1 = \frac{L_1 - s_0}{s_1 - s_0} = L_1 \tag{9.2.15a}$$

Similarly, for ψ_2 and ψ_3, we obtain

$$\psi_2 = L_2, \qquad \psi_3 = L_3 \tag{9.2.15b}$$

Next, consider the triangular element with three nodes per side $(k = 3)$. The total number of nodes is equal to six. For node 1, we have

$$s_0 = 0, \qquad s_1 = \frac{1}{2}, \qquad s_2 = 1$$

$$\psi_1 = \frac{L_1 - s_0}{s_2 - s_0}\frac{L_1 - s_1}{s_2 - s_1} = L_1(2L_1 - 1) \tag{9.2.16a}$$

The function ψ_2 [see Fig. 9.2.4(*b*)] should vanish at nodes 1, 3, 4, 5, and 6, and should be equal to 1 at node 2. Equivalently, ψ_2 should vanish along the lines connecting nodes 1 and 5, and 3 and 5. These two lines are given in terms of L_1 and L_2 (note that the subscripts of L refer to the nodes in the three-node triangular element) as $L_2=0$ and $L_1=0$. Hence, we have

$$\psi_2=\frac{L_2-s_0}{s_1-s_0}\frac{L_1-s_0}{s_1-s_0}=\frac{L_2-0}{\frac{1}{2}}\frac{L_1-0}{\frac{1}{2}}=4L_1L_2 \tag{9.2.16b}$$

Similarly,

$$\psi_3=L_2(2L_2-1),\qquad \psi_4=4L_2L_3,\qquad \psi_5=L_3(2L_3-1),\qquad \psi_6=4L_1L_3 \tag{9.2.16c}$$

As a last example, consider the cubic element (i.e., $k-1=3$). For ψ_1 we note that it must vanish along lines $L_1=0$, $L_1=\frac{1}{3}$, and $L_1=\frac{2}{3}$. Therefore, we have

$$\psi_1=\frac{L_1-0}{1-0}\frac{L_1-\frac{1}{3}}{1-\frac{1}{3}}\frac{L_1-\frac{2}{3}}{1-\frac{2}{3}}=\frac{1}{2}L_1(3L_1-1)(3L_1-2)$$

The function ψ_2 must vanish along lines $L_1=0$, $L_2=0$, and $L_1=1/3$ (and node 2 is at a distance of 2/3 along L_1 and a distance of 1/3 along L_2)

$$\psi_2=\frac{L_1-0}{\frac{2}{3}-0}\frac{L_2-0}{\frac{1}{3}-0}\frac{L_1-\frac{1}{3}}{\frac{2}{3}-\frac{1}{3}}=\frac{9}{2}L_2L_1(3L_1-1)$$

Similarly, we can derive other functions. Thus, we have

$$\begin{aligned}
\psi_1&=\frac{1}{2}L_1(3L_1-1)(3L_1-2), & \psi_2&=\frac{9}{2}L_2L_1(3L_1-1)\\
\psi_3&=\frac{9}{2}L_1L_2(3L_2-1), & \psi_4&=\frac{1}{2}L_2(3L_2-1)(3L_2-2)\\
\psi_5&=\frac{9}{2}L_2L_3(3L_2-1), & \psi_6&=\frac{9}{2}L_2L_3(3L_3-1)\\
\psi_7&=\frac{1}{2}L_3(3L_3-1)(3L_3-2), & \psi_8&=\frac{9}{2}L_3L_1(3L_3-1)\\
\psi_9&=\frac{9}{2}L_1L_3(3L_1-1), & \psi_{10}&=27L_1L_2L_3
\end{aligned} \tag{9.2.17}$$

It should be pointed out that the area coordinates L_i facilitate not only the construction of the interpolation functions for the higher-order elements but also the integration of functions of L_i over line paths and areas. The following exact integration formulas prove to be useful:

$$\int_a^b L_1^m L_2^n\,ds=\frac{m!n!}{(m+n+1)!}(b-a) \tag{9.2.18a}$$

$$\int\int_{\text{area}} L_1^m L_2^n L_3^p\,dA=\frac{m!n!p!}{(m+n+p+2)!}2A \tag{9.2.18b}$$

where m, n, and p are arbitrary (positive) integers, A is the area of the domain of integration, and $m!$ denotes the factorial of m $(0! = 1)$. Of course, we should transform the integrals from the x and y coordinates to L_i coordinates using the transformation,

$$x = \sum_{i=1}^{n} x_i L_i \qquad y = \sum_{i=1}^{n} y_i L_i \tag{9.2.19}$$

where (x_i, y_i) are the global coordinates of the ith node of the element.

9.2.2 Rectangular Elements

Analogous to the Lagrange family of triangular elements (see Fig. 9.2.1), the Lagrange family of rectangular elements can be developed from a rectangular array as shown in Fig. 9.2.5. Since a linear rectangular element has four corners (hence, four nodes), the polynomial should have the first four terms 1, x, y, and xy (which form a parallelogram in Pascal's triangle and a rectangle in the array given in Fig. 9.2.5). The coordinates (x, y) are usually taken to be the element (i.e., local) coordinates. In general, a pth-order Lagrange rectangular element has n nodes, with

$$n = (p+1)^2 \quad (p = 0, 1, \ldots)$$

and the associated polynomial contains the terms from the pth parallelogram or the pth rectangle in Fig. 9.2.5. When $p = 0$, it is understood (as in triangular elements) that the node is at the center of the element (i.e., the variable is a constant on the entire element). The Lagrange quadratic rectangular element has nine nodes, and the associated polynomial is given by

$$\begin{aligned} u(x, y) &= a_1 + a_2 x + a_3 y + a_4 xy + a_5 x^2 + a_6 y^2 \\ &\quad + a_7 x^2 y + a_8 x y^2 + a_9 x^2 y^2 \end{aligned} \tag{9.2.20a}$$

$$\frac{\partial u}{\partial x} = a_2 + a_4 y + 2a_5 x + 2a_7 xy + a_8 y^2 + 2a_9 x y^2$$

$$\frac{\partial u}{\partial y} = a_3 + a_4 x + 2a_6 y + a_7 x^2 + 2a_8 xy + 2a_9 x^2 y \tag{9.2.20b}$$

The polynomial contains the complete polynomial of the second degree plus the third-degree terms $x^2 y$ and xy^2 and also the $x^2 y^2$ term. Four of the nine nodes are placed at the four corners, four at the midpoints of the sides, and one at the center of the element. The polynomial is uniquely determined by specifying its values at each of the nine nodes. Moreover, along the sides of the element, the polynomial is quadratic (with three terms—as can be seen by setting $y = 0$) and is determined by its values at the three nodes on that side. If two rectangular elements share a side and the polynomial is required to have the same values from both elements at the three nodes of the elements, then u is uniquely defined along the entire side (shared by the two elements). Note that the normal derivatives of u approximated by the quadratic Lagrange polynomials is quadratic in the tangential direction and linear in the normal direction (i.e., $\partial u/\partial x$ is quadratic in y and linear in x, and $\partial u/\partial y$ is quadratic in x and linear in y). Plots of ψ_1, ψ_2, and ψ_5

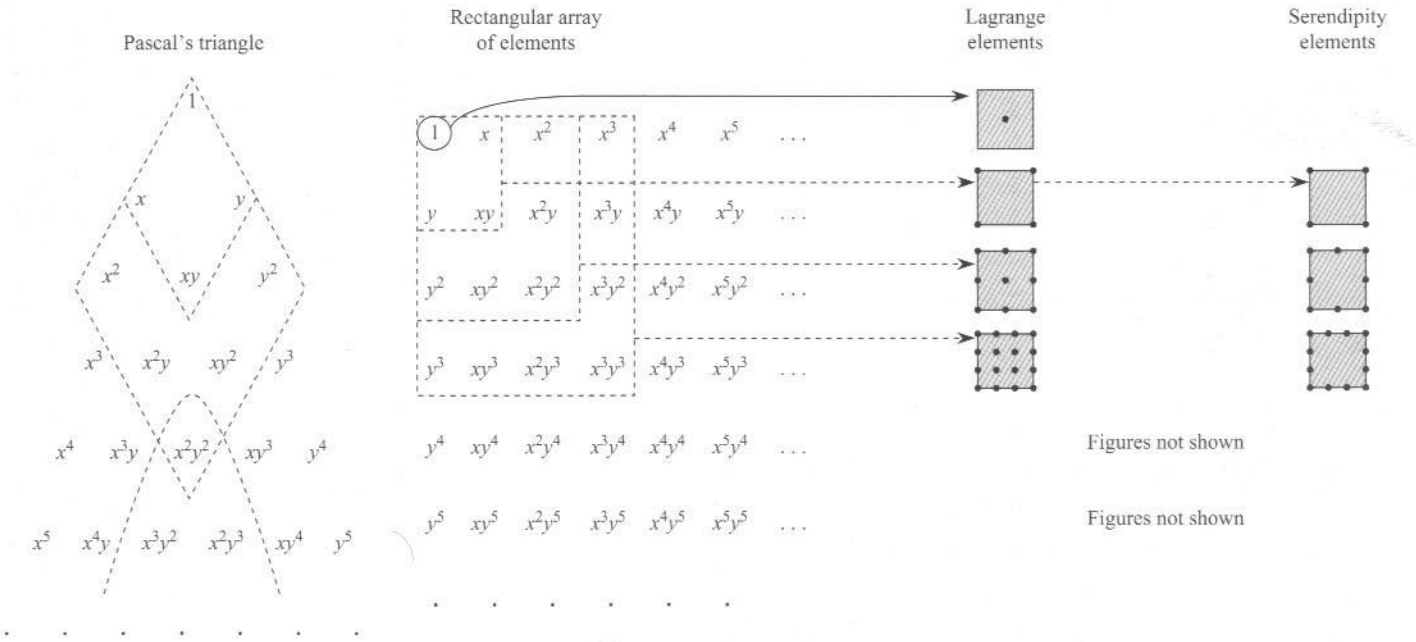

Figure 9.2.5 Lagrange and serendipity families of rectangular finite elements.

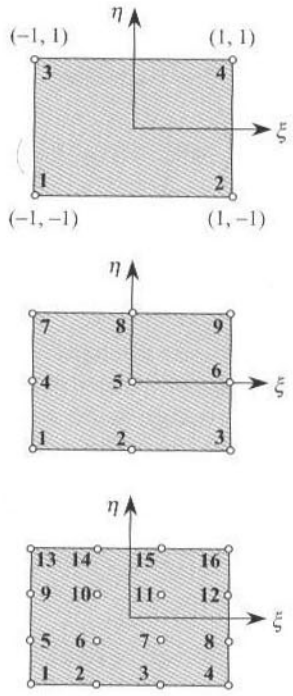

$$\psi_1 = \frac{1}{4}(1-\xi)(1-\eta)$$
$$\psi_2 = \frac{1}{4}(1+\xi)(1-\eta)$$
$$\psi_3 = \frac{1}{4}(1-\xi)(1+\eta)$$
$$\psi_4 = \frac{1}{4}(1+\xi)(1+\eta)$$

$$\psi_1 = \frac{1}{4}(\xi^2-\xi)(\eta^2-\eta), \quad \psi_2 = \frac{1}{2}(1-\xi^2)(\eta^2-\eta)$$
$$\psi_3 = \frac{1}{4}(\xi^2+\xi)(\eta^2-\eta), \quad \psi_4 = \frac{1}{2}(\xi^2-\xi)(1-\eta^2)$$
$$\psi_5 = (1-\xi^2)(1-\eta^2), \quad \psi_6 = \frac{1}{2}(\xi^2+\xi)(1-\eta^2)$$
$$\psi_7 = \frac{1}{4}(\xi^2-\xi)(\eta^2+\eta), \quad \psi_8 = \frac{1}{2}(1-\xi^2)(\eta^2+\eta)$$
$$\psi_9 = \frac{1}{4}(\xi^2+\xi)(\eta^2+\eta)$$

Use Eqs. (9.2.25)–(9.2.27) to develop the interpolation functions

Figure 9.2.6 Node numbers and interpolation functions for the rectangular elements of the Lagrange family.

(the node numbers correspond to those in Fig. 9.2.6) of the nine-node rectangular element are shown in Fig. 9.2.7.

The pth-order Lagrange rectangular element has the pth-degree polynomial

$$u(x, y) = \sum_{i=1}^{n} a_i x^j y^k \qquad (j + k \le p + 1;\ j, k \le p)$$
$$= \sum_{i=1}^{n} u_i \psi_i \tag{9.2.21}$$

and ψ_i are called the pth-order Lagrange interpolation functions.

The Lagrange interpolation functions associated with rectangular elements can be obtained from corresponding one-dimensional Lagrange interpolation functions by taking the tensor product of the x direction (one-dimensional) interpolation functions with the y direction (one-dimensional) interpolation functions. Let the x and y coordinates be taken along element sides with the origin of the coordinate system at the lower left corner of the rectangle. Then for an element with dimensions a and b along the x and y directions, respectively, the interpolation functions are given as follows:

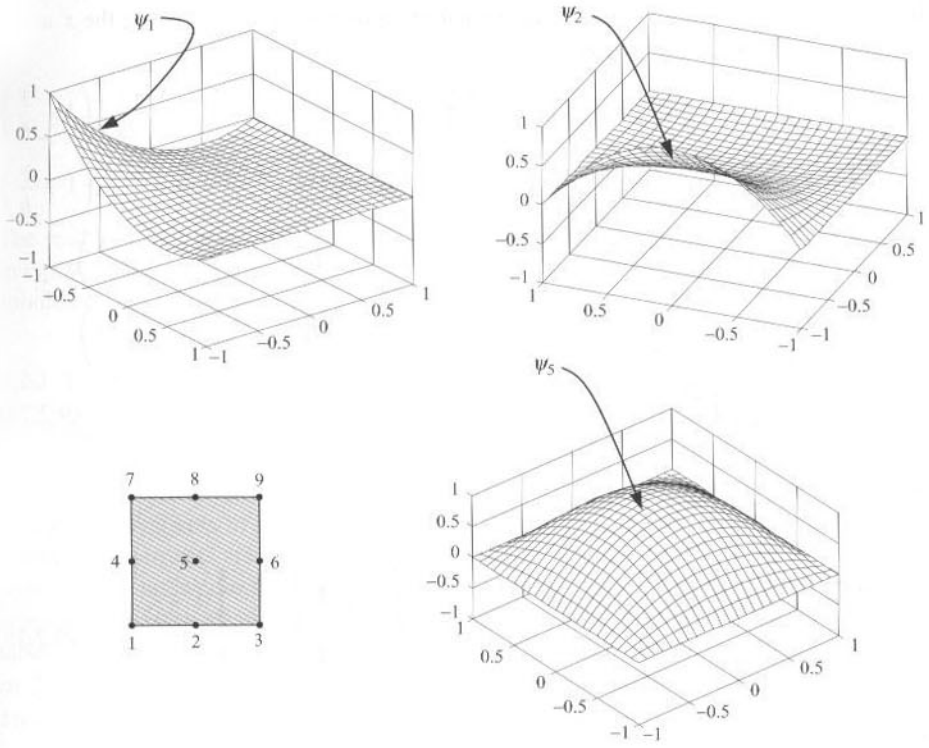

Figure 9.2.7 Geometric variation of the Lagrange interpolation functions at nodes 1, 2, and 5 (see Fig. 9.2.6) of the nine-node quadratic element.

Linear ($p = 1$)

$$\begin{bmatrix} \psi_1 & \psi_3 \\ \psi_2 & \psi_4 \end{bmatrix} = \begin{Bmatrix} 1 - \dfrac{x}{a} \\ \dfrac{x}{a} \end{Bmatrix} \begin{Bmatrix} 1 - \dfrac{y}{b} & \dfrac{y}{b} \end{Bmatrix}$$

$$= \begin{bmatrix} \left(1 - \dfrac{x}{a}\right)\left(1 - \dfrac{y}{b}\right) & \left(1 - \dfrac{x}{a}\right)\dfrac{y}{b} \\ \dfrac{x}{a}\left(1 - \dfrac{y}{b}\right) & \dfrac{x}{a}\dfrac{y}{b} \end{bmatrix} \tag{9.2.22}$$

Quadratic ($p = 2$)

$$\begin{bmatrix} \psi_1 & \psi_4 & \psi_7 \\ \psi_2 & \psi_5 & \psi_8 \\ \psi_3 & \psi_6 & \psi_9 \end{bmatrix} = \begin{Bmatrix} \dfrac{\left(x - \frac{1}{2}a\right)(x - a)}{\left(-\frac{1}{2}a\right)(-a)} \\ \dfrac{x(x - a)}{\frac{1}{2}a\left(\frac{1}{2}a - a\right)} \\ \dfrac{x\left(x - \frac{1}{2}a\right)}{a\left(\frac{1}{2}a\right)} \end{Bmatrix} \begin{Bmatrix} \dfrac{\left(y - \frac{1}{2}b\right)(y - b)}{\frac{1}{2}b^2} \\ \dfrac{y(y - b)}{-\frac{1}{4}b^2} \\ \dfrac{y(y - b/2)}{\frac{1}{2}b^2} \end{Bmatrix}^T \tag{9.2.23}$$

where the two vectors are the one-dimensional interpolation functions along the x and y directions, respectively. We obtain

$$\psi_1 = \left(1-\frac{2x}{a}\right)\left(1-\frac{x}{a}\right)\left(1-\frac{2y}{b}\right)\left(1-\frac{y}{b}\right), \qquad \psi_2 = \frac{4x}{a}\left(1-\frac{x}{a}\right)\left(1-\frac{2y}{b}\right)\left(1-\frac{y}{b}\right)$$

$$\psi_3 = \frac{x}{a}\left(\frac{2x}{a}-1\right)\left(1-\frac{2y}{b}\right)\left(1-\frac{y}{b}\right), \qquad \psi_4 = \left(1-\frac{2x}{a}\right)\left(1-\frac{x}{a}\right)\frac{4y}{b}\left(1-\frac{y}{b}\right)$$

$$\psi_5 = \frac{4x}{a}\left(1-\frac{x}{a}\right)\frac{4y}{b}\left(1-\frac{y}{b}\right), \qquad \psi_6 = \frac{x}{a}\left(\frac{2x}{a}-1\right)\frac{4y}{b}\left(1-\frac{y}{b}\right)$$

$$\psi_7 = \left(1-\frac{2x}{a}\right)\left(1-\frac{x}{a}\right)\frac{y}{b}\left(\frac{2y}{b}-1\right), \qquad \psi_8 = \frac{4x}{a}\left(1-\frac{x}{a}\right)\frac{y}{b}\left(\frac{2y}{b}-1\right)$$

$$\psi_9 = \frac{x}{a}\left(\frac{2x}{a}-1\right)\frac{y}{b}\left(\frac{2y}{b}-1\right) \tag{9.2.24}$$

pth Order

$$\begin{bmatrix} \psi_1 & \psi_{p+2} & \cdots & \psi_k \\ \psi_2 & & & \\ \vdots & \ddots & & \vdots \\ & & \ddots & \\ \psi_p & & & \\ \psi_{p+1} & \psi_{2p+2} & \cdots & \psi_n \end{bmatrix} = \begin{Bmatrix} f_1 \\ f_2 \\ \vdots \\ f_{p+1} \end{Bmatrix} \begin{Bmatrix} g_1 \\ g_2 \\ \vdots \\ g_{p+1} \end{Bmatrix}^T \tag{9.2.25}$$

$$k = (p+1)p+1, \qquad n = (p+1)^2$$

where $f_i(x)$ and $g_i(y)$ are the pth-order interpolants in x and y, respectively. For example, the polynomial

$$f_i(\xi) = \frac{(\xi-\xi_1)(\xi-\xi_2)\cdots(\xi-\xi_{i-1})(\xi-\xi_{i+1})\cdots(\xi-\xi_{p+1})}{(\xi_i-\xi_1)(\xi_i-\xi_2)\cdots(\xi_i-\xi_{i-1})(\xi_i-\xi_{i+1})\cdots(\xi_i-\xi_{p+1})} \tag{9.2.26}$$

(where ξ_i is the ξ coordinate of node i) is the pth-degree interpolation polynomial in ξ that vanishes at points $\xi_1, \xi_2, \ldots, \xi_{i-1}, \xi_{i+1}, \ldots, \xi_{p+1}$. We recall that (x, y) are the element coordinates.

It is convenient (for numerical integration purposes) to express the interpolation functions in (9.2.22)–(9.2.25) in terms of the natural coordinates ξ and η:

$$\xi = \frac{2(x-x_1)-a}{a}, \qquad \eta = \frac{2(y-y_1)-b}{b} \tag{9.2.27}$$

where x_1 and y_1 are the global coordinates of node 1 in the local x and y coordinates. For a coordinate system with origin fixed at node 1 and coordinates parallel to the sides of the element, we have $x_1 = y_1 = 0$. In this case, the quadratic interpolation functions in (9.2.24) can be written in terms of the natural coordinates ξ and η as

$$\psi_1 = \frac{1}{4}(\xi-\xi^2)(\eta-\eta^2), \qquad \psi_5 = (1-\xi^2)(1-\eta^2)$$

$$\psi_2 = -\frac{1}{2}(1-\xi^2)(\eta-\eta^2), \qquad \psi_6 = \frac{1}{2}(\xi+\xi^2)(1-\eta^2)$$

$$\psi_3 = -\frac{1}{4}(\xi + \xi^2)(\eta - \eta^2), \qquad \psi_7 = -\frac{1}{4}(\xi - \xi^2)(\eta + \eta^2) \tag{9.2.28}$$
$$\psi_4 = -\frac{1}{2}(\xi - \xi^2)(1 - \eta^2), \qquad \psi_8 = \frac{1}{2}(1 - \xi^2)(\eta + \eta^2)$$
$$\psi_9 = \frac{1}{4}(\xi + \xi^2)(\eta + \eta^2)$$

The reader should be cautioned that the subscripts of ψ_i refer to the node numbering used in Fig. 9.2.6. For any renumbering of the nodes, the subscripts of the interpolation functions should be changed accordingly.

9.2.3 The Serendipity Elements

Since the internal nodes of the higher-order elements of the Lagrange family do not contribute to the interelement connectivity, they can be condensed out at the element level so that the size of the element matrices is reduced. Alternatively, we can use the so-called serendipity elements to avoid the internal nodes present in the Lagrange elements. The serendipity elements are those rectangular elements which have no interior nodes. In other words, all the node points are on the boundary of the element. The interpolation functions for serendipity elements cannot be obtained using tensor products of one-dimensional interpolation functions. Instead, an alternative procedure that employs the interpolation properties in (8.2.33) is used. Here we illustrate how to construct the interpolation functions for the eight-node (quadratic) element using the natural coordinates (ξ, η).

The interpolation function for node 1 should take on a value of zero at nodes 2, 3, . . . , 8, and a value of unity at node 1. Equivalently, ψ_1 should vanish on the sides defined by the equations $1 - \xi = 0$, $1 - \eta = 0$, and $1 + \xi + \eta = 0$ (see Fig. 9.2.8). Therefore, ψ_1 is of the

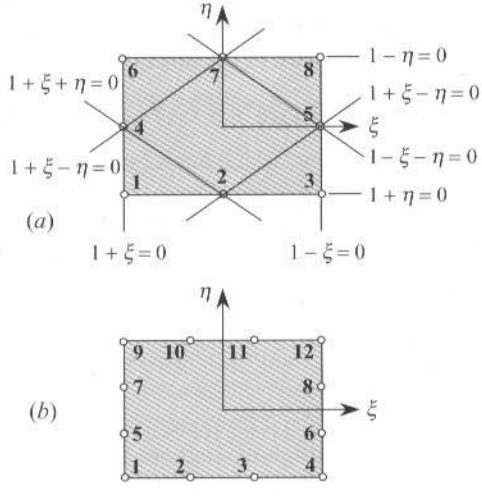

$$\psi_1 = -\frac{1}{4}(1 - \xi)(1 - \eta)(1 + \xi + \eta)$$
$$\psi_2 = \frac{1}{2}(1 - \xi^2)(1 - \eta)$$
$$\psi_3 = -\frac{1}{4}(1 + \xi)(1 - \eta)(1 - \xi + \eta)$$
$$\psi_4 = \frac{1}{2}(1 - \xi)(1 - \eta^2), \quad \psi_5 = \frac{1}{2}(1 + \xi)(1 - \eta^2)$$
$$\psi_6 = -\frac{1}{4}(1 - \xi)(1 + \eta)(1 + \xi - \eta)$$
$$\psi_7 = \frac{1}{2}(1 - \xi^2)(1 + \eta)$$
$$\psi_8 = -\frac{1}{4}(1 + \xi)(1 + \eta)(1 - \xi - \eta)$$

See Eq. (9.2.33) for the interpolation functions

Figure 9.2.8 Node numbers and interpolation functions associated with the serendipity family of elements.

form

$$\psi_1(\xi, \eta) = c(1-\xi)(1-\eta)(1+\xi+\eta) \tag{9.2.29a}$$

where c is a constant that should be determined so as to yield $\psi_1(-1,-1)=1$. We obtain $c=-\frac{1}{4}$, and therefore

$$\psi_1(\xi, \eta) = -\frac{1}{4}(1-\xi)(1-\eta)(1+\xi+\eta) \tag{9.2.29b}$$

We can construct other interpolation functions in a similar manner. We have

$$\begin{aligned}
\psi_1 &= -\frac{1}{4}(1-\xi)(1-\eta)(1+\xi+\eta), & \psi_2 &= \frac{1}{2}(1-\xi^2)(1-\eta) \\
\psi_3 &= \frac{1}{4}(1+\xi)(1-\eta)(-1+\xi-\eta), & \psi_4 &= \frac{1}{2}(1-\xi)(1-\eta^2) \\
\psi_5 &= \frac{1}{2}(1+\xi)(1-\eta^2), & \psi_6 &= \frac{1}{4}(1-\xi)(1+\eta)(-1-\xi+\eta) \\
\psi_7 &= \frac{1}{2}(1-\xi^2)(1+\eta), & \psi_8 &= \frac{1}{4}(1+\xi)(1+\eta)(-1+\xi+\eta)
\end{aligned} \tag{9.2.30}$$

Note that all the ψ_i for the eight-node element have the form

$$\psi_i = c_1 + c_2\xi + c_3\eta + c_4\xi\eta + c_5\xi^2 + c_6\eta^2 + c_7\xi^2\eta + c_8\xi\eta^2 \tag{9.2.31a}$$

The derivatives of ψ_i with respect to ξ and η are of the form,

$$\begin{aligned}
\frac{\partial \psi_i}{\partial \xi} &= c_2 + c_4\eta + 2c_5\xi + 2c_7\xi\eta + c_8\eta^2 \\
\frac{\partial \xi_i}{\partial \eta} &= c_3 + c_4\xi + 2c_6\eta + c_7\xi^2 + 2c_8\xi\eta
\end{aligned} \tag{9.2.31b}$$

Plots of ψ_1 and ψ_2 (the node numbers correspond to those in Fig. 9.2.8) for the eight-node serendipity element are shown in Fig. 9.2.9. It should be noted that ψ_2 of the nine-node element is zero at the element center, whereas ψ_2 of the eight-node element is nonzero there. The interpolation functions ψ_i for the twelve-node element are of the form

$$\psi_i = \text{terms of the form in (9.2.31}a\text{)} + c_9\xi^3 + c_{10}\eta^3 + c_{11}\xi^3\eta + c_{12}\xi\eta^3 \tag{9.2.32}$$

The interpolation functions for the cubic serendipity element, which has 12 nodes, are

$$\begin{aligned}
\psi_1 &= \frac{1}{32}(1-\xi)(1-\eta)[-10+9(\xi^2+\eta^2)], & \psi_2 &= \frac{9}{32}(1-\eta)(1-\xi^2)(1-3\xi) \\
\psi_3 &= \frac{9}{32}(1-\eta)(1-\xi^2)(1+3\xi), \\
\psi_4 &= \frac{1}{32}(1+\xi)(1-\eta)[-10+9(\xi^2+\eta^2)] \\
\psi_5 &= \frac{9}{32}(1-\xi)(1-\eta^2)(1-3\eta), & \psi_6 &= \frac{9}{32}(1+\xi)(1-\eta^2)(1-3\eta) \\
\psi_7 &= \frac{9}{32}(1-\xi)(1-\eta^2)(1+3\eta), & \psi_8 &= \frac{9}{32}(1+\xi)(1-\eta^2)(1+3\eta)
\end{aligned}$$

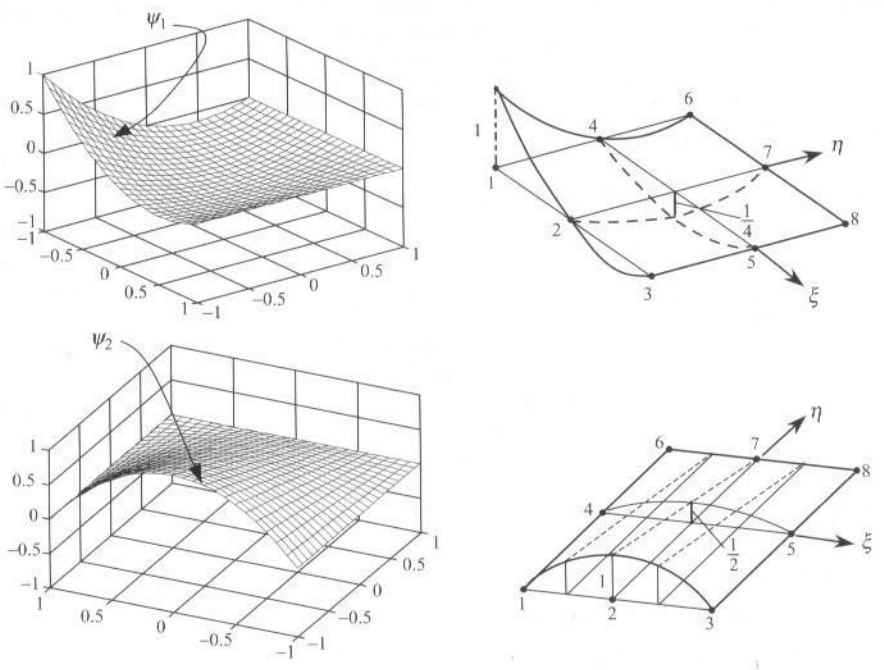

Figure 9.2.9 Graphical representation of the interpolation functions associated with nodes 1 and 2 of the eight-node serendipity element (see Fig. 9.2.8).

$$\psi_9 = \frac{1}{32}(1-\xi)(1+\eta)[-10+9(\xi^2+\eta^2)], \quad \psi_{10} = \frac{9}{32}(1+\eta)(1-\xi^2)(1-3\xi)$$
$$\psi_{11} = \frac{9}{32}(1+\eta)(1-\xi^2)(1+3\xi),$$
$$\psi_{12} = \frac{1}{32}(1+\xi)(1+\eta)[-10+9(\xi^2+\eta^2)] \tag{9.2.33}$$

9.2.4 Hermite Cubic Interpolation Functions

In the above discussion, we developed only the Lagrange interpolation functions for triangular and rectangular elements. The Hermite family of interpolation functions (which interpolate the function and its derivatives) were not discussed. We recall that such functions are required in the finite element formulation of fourth-order (or higher-order) differential equations (e.g., the Euler–Bernoulli beam theory of Chapter 4 and the classical or Kirchhoff plate theory of Chapter 12). For the sake of completeness, while not presenting the details of the derivation, the Hermite cubic interpolation functions for two rectangular elements are summarized in Table 9.2.1. The first one is based on the interpolation of $(u, \partial u/\partial x, \partial u/\partial y, \partial^2 u/\partial x \partial y)$ at each node, and the second one is based on the interpolation

Table 9.2.1 Interpolation functions for the linear and quadratic Lagrange rectangular elements, quadratic serendipity element, and Hermite cubic rectangular elements.[†]

Element type	Interpolation functions	Remarks
Lagrange element		
Linear	$\frac{1}{4}(1+\xi_0)(1+\eta_0)$	Node $i=1,\ldots,4$
Quadratic	$\psi_i = \frac{1}{4}\xi_0(1+\xi_0)\,\eta_0(1+\eta_0)$	Corner node i
	$\psi_i = \frac{1}{2}\eta_0(1+\eta_0)(1-\xi^2)$	Side node i, $\xi_i = 0$
	$\psi_i = \frac{1}{2}\xi_0(1+\xi_0)(1-\eta^2)$	Side node i, $\eta_i = 0$
	$\psi_i = (1-\xi^2)(1-\eta^2)$	Interior node i
Serendipity element		
Quadratic	$\psi_i = \frac{1}{4}(1+\xi_0)(1+\eta_0)(\xi_0+\eta_0-1)$	Corner node i
	$\psi_i = \frac{1}{2}(1-\xi^2)(1+\eta_0)$	Side node i, $\xi_i = 0$
	$\psi_i = \frac{1}{2}(1+\xi_0)(1-\eta^2)$	Side node i, $\eta_i = 0$
Hermite cubic element		
Nonconforming element	$[I = 4(i-1)+1,\ i=1,\ldots,4]$	
Variable u	$\varphi_I = \frac{1}{16}(\xi+\xi_i)^2(\xi_0-2)(\eta+\eta_i)^2(\eta_0-2)$	
Derivative $(\partial u/\partial x)$	$\varphi_{I+1} = -\frac{1}{16}\xi_i(\xi+\xi_i)^2(\xi_0-1)(\eta+\eta_i)^2(\eta_0-2)$	
Derivative $(\partial u/\partial y)$	$\varphi_{I+2} = -\frac{1}{16}(\xi+\xi_i)^2(\xi_0-2)\eta_i(\eta+\eta_i)^2(\eta_0-1)$	
Derivative $(\partial^2 u/\partial x\partial y)$	$\varphi_{I+3} = \frac{1}{16}\xi_i(\xi+\xi_i)^2(\xi_0-1)\eta_i(\eta+\eta_i)^2(\eta_0-1)$	
Conforming element	$[I = 3(i-1)+1,\ i=1,\ldots,4]$	
Variable u	$\varphi_I = \frac{1}{8}(\xi_0+1)(\eta_0+1)(2+\xi_0+\eta_0-\xi^2-\eta^2)$	
Derivative $(\partial u/\partial x)$	$\varphi_{I+1} = \frac{1}{8}\xi_i(\xi_0+1)^2(\xi_0-1)(\eta_0+1)$	
Derivative $(\partial u/\partial y)$	$\varphi_{I+2} = \frac{1}{8}\eta_i(\xi_0+1)(\eta_0+1)^2(\eta_0-1)$	
	$\xi = (x-x_c)/a,\ \eta = (y-y_c)/b,\ \xi_0 = \xi\xi_i,\ \eta_0 = \eta\eta_i$	

[†] See Fig. 9.2.10 for the coordinate system; (ξ_i, η_i) denote the natural coordinates of the ith node of the element; (x_c, y_c) are the global coordinates of the center of the element; and $2a$ and $2b$ are the sides of the rectangular element.

of $(u, \partial u/\partial x, \partial u/\partial y)$ at each node. The node numbering system in Table 9.2.1 refers to that used in Fig. 9.2.10.

9.3 NUMERICAL INTEGRATION

9.3.1 Preliminary Comments

An accurate representation of irregular domains (i.e., domains with curved boundaries) can be accomplished by the use of refined meshes and/or irregularly shaped curvilinear elements. For example, a nonrectangular region cannot be represented accurately using rectangular elements; however, it can be represented by quadrilateral elements. Since the interpolation functions are easily derivable for a rectangular element and it is easier to evaluate integrals over rectangular geometries, we transform the finite element integral statements defined over quadrilaterals to a rectangle. The transformation results in complicated expressions in terms of the coordinates used for the rectangular element. Therefore, numerical integration is used to evaluate such complicated expressions. Numerical integration schemes, such as the Gauss–Legendre numerical integration scheme, require the integral to be evaluated on a specific domain or with respect to a specific coordinate system. The Gauss–Legendre quadrature, for example, requires the integral to be expressed over a square region $\hat{\Omega}$ of

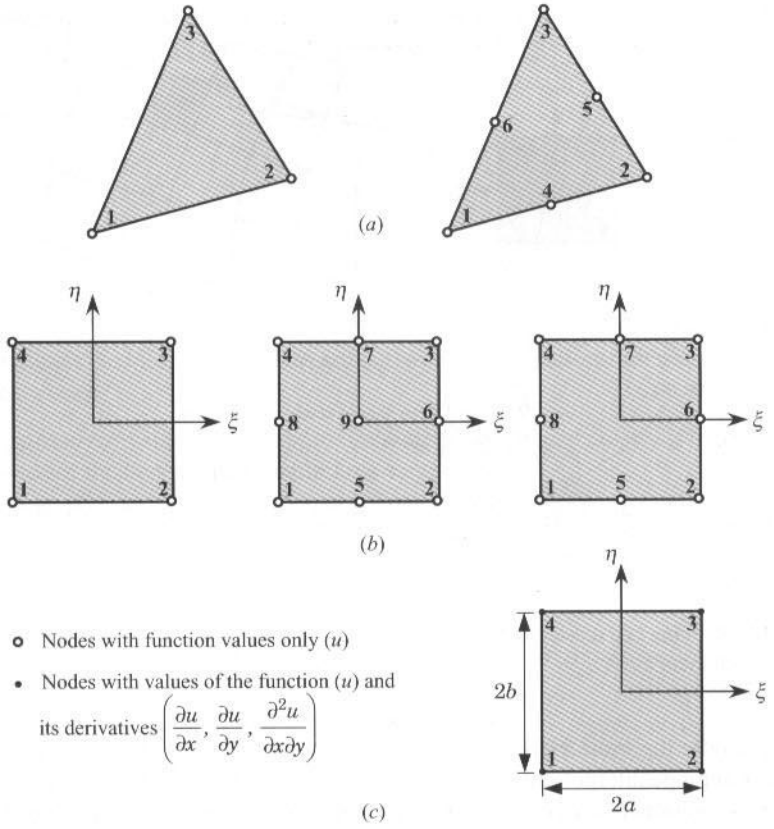

Figure 9.2.10 Triangular and rectangular elements with the standard node numbering system. (*a*) linear and quadratic triangular elements; (*b*) linear and quadratic Lagrange elements; and (*c*) Hermite cubic element.

dimension 2 by 2 and the coordinate system (ξ, η) to be such that $-1 \leq (\xi, \eta) \leq 1$. The transformation of the geometry and the variable coefficients of the differential equation from the problem coordinates (x, y) to the coordinates (ξ, η) results in algebraically complex expressions, and they preclude analytical (i.e., exact) evaluation of the integrals. Thus, the transformation of a given integral expression, defined over element Ω_e, to one on the domain $\hat{\Omega}$ facilitates the numerical integration. Each element of the finite element mesh is transformed to $\hat{\Omega}$ only for the purpose of numerically evaluating the integrals. The element $\hat{\Omega}$ is called a *master element*. For example, every quadrilateral element can be transformed to a square element with side 2 that facilitates the use of Gauss–Legendre quadrature to evaluate integrals defined over the quadrilateral element.

The transformation between Ω_e and $\hat{\Omega}$ [or equivalently, between (x, y) and (ξ, η)] is accomplished by a coordinate transformation of the form

$$x = \sum_{j=1}^{m} x_j^e \hat{\psi}_j^e(\xi, \eta) \qquad y = \sum_{j=1}^{m} y_j^e \hat{\psi}_j^e(\xi, \eta) \tag{9.3.1}$$

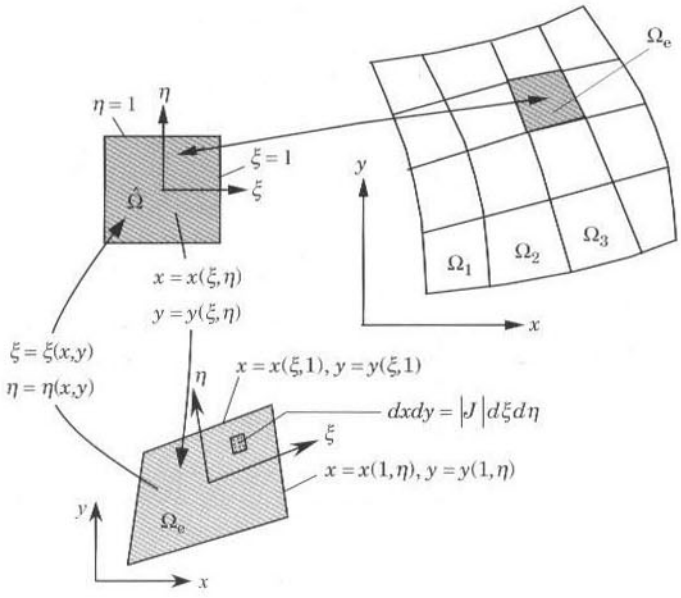

Figure 9.3.1 Mapping of a master rectangular element to an arbitrary quadrilateral element of a finite element mesh.

where $\hat{\psi}_j^e$ denote the finite element interpolation functions of the master element $\hat{\Omega}$. Although the Lagrange interpolation of the geometry is implied by Eq. (9.3.1), we can also use Hermite interpolation. Consider, as an example, the master element shown in Fig. 9.3.1. The coordinates in the master element are chosen to be the natural coordinates (ξ, η) such that $-1 \le (\xi, \eta) \le 1$. This choice is dictated by the limits of integration in the Gauss–Legendre quadrature rule, which is used to evaluate the integrals. For this case, the $\hat{\psi}_j^e$ denote the interpolation functions of the four-node rectangular element shown in Fig. 9.3.1 (i.e., $m = 4$). The transformation (9.3.1) maps a point (ξ, η) in the master element $\hat{\Omega}$ onto a point (x, y) in element Ω_e and vice versa if the Jacobian of the transformation is positive-definite. The transformation maps the line $\xi = 1$ in $\hat{\Omega}$ to the line defined parametrically by $x = x(1, \eta)$ and $y = y(1, \eta)$ in the (x, y) plane. For instance, consider the line $\xi = 1$ in the master element $\hat{\Omega}$. We have

$$
\begin{aligned}
x(1,\eta) &= \sum_{i=1}^{4} x_i \hat{\psi}_i(1,\eta) = x_1 \cdot 0 + \frac{1}{2}x_2(1-\eta) + \frac{1}{2}x_3(1+\eta) + x_4 \cdot 0 \\
&= \frac{1}{2}(x_2 + x_3) + \frac{1}{2}(x_3 - x_2)\eta \qquad (9.3.2) \\
y(1,\eta) &= \sum_{i=1}^{4} y_i \hat{\psi}_i(1,\eta) = \frac{1}{2}(y_2 + y_3) + \frac{1}{2}(y_3 - y_2)\eta
\end{aligned}
$$

Clearly, x and y are linear functions of η. Therefore, they define a straight line. Similarly, the lines $\xi = -1$ and $\eta = \pm 1$ are mapped into straight lines in the element Ω_e. In other words, the master element $\hat{\Omega}$ is transformed, under the linear transformation, into a quadrilateral element (i.e., a four-sided element whose sides are not parallel) in the (x, y) plane.

Conversely, every quadrilateral element of a mesh can be transformed to the same four-node square (master) element $\hat{\Omega}$ in the (ξ, η) plane (see Fig. 9.3.1).

In general, the dependent variable(s) of the problem are approximated by expressions of the form,

$$u(x, y) = \sum_{j=1}^{n} u_j^e \psi_j^e(x, y) \tag{9.3.3}$$

The interpolation functions ψ_j^e used for the approximation of the dependent variable are, in general, different from $\hat{\psi}_j^e$ used in the approximation of the geometry. Depending on the relative degree of approximations used for the geometry [see Eq. (9.3.1)] and the dependent variable(s) [see Eq. (9.3.3)], the finite element formulations are classified into three categories.

1. *Superparametric* $(m > n)$: The approximation used for the geometry is higher order than that used for the dependent variable.
2. *Isoparametric* $(m = n)$: Equal degree of approximation is used for both geometry and dependent variables.
3. *Subparametric* $(m < n)$: Higher-order approximation of the dependent variable is used. (9.3.4)

For example, in the finite element analysis of the Euler–Bernoulli beams, we used linear Lagrange interpolation of the geometry,

$$x = \sum_{j=1}^{2} x_j^e \hat{\psi}_j^e(\xi) = x_A + \frac{1}{2} h_e(1 + \xi) \tag{9.3.5}$$

whereas the Hermite cubic interpolation was used to approximate the transverse deflection. Such formulation falls into the subparametric category. Since the axial displacement is approximated by the linear Lagrange interpolation functions, it can be said that isoparametric formulation is used for the axial displacement. Superparametric formulations are rarely used. Also, the approximation of the geometry by Hermite family of interpolation functions is not common.

9.3.2 Coordinate Transformations

It should be noted that the transformation of a quadrilateral element of a mesh to the master element $\hat{\Omega}$ is solely for the purpose of numerically evaluating the integrals. *No transformation of the physical domain or elements is involved in the finite element analysis.* The resulting algebraic equations of the finite element formulation are always among the nodal values of the physical domain. Different elements of the finite element mesh can be generated from the same master element by assigning the global coordinates of the elements (see Fig. 9.3.1). Master elements of different order define different transformations and hence different collections of finite element meshes. For example, a cubic-order master rectangular element can be used to generate a mesh of cubic curvilinear quadrilateral elements. Thus, with the help of an appropriate master element, any arbitrary element of a mesh can be generated. However, the transformations of a master element should be such that there exist no spurious gaps between elements and no element overlaps occur. The elements in Figs. 9.2.6 and 9.2.8 can be used as master elements.

When a typical element of the finite element mesh is transformed to its master element for the purpose of numerically evaluating integrals, the integrand also must be expressed in terms of the coordinates (ξ, η) of the master element. For example, consider the element coefficients

$$K_{ij}^e = \int_{\Omega^e} \left[a(x, y) \frac{\partial \psi_i^e}{\partial x} \frac{\partial \psi_j^e}{\partial x} + b(x, y) \frac{\partial \psi_i^e}{\partial y} \frac{\partial \psi_j^e}{\partial y} + c(x, y) \psi_i^e \psi_j^e \right] dx\, dy \tag{9.3.6}$$

The integrand (i.e., the expression in the square brackets under the integral) is a function of the global coordinates x and y. We must rewrite it in terms of ξ and η using the transformation (9.3.1). Note that the integrand contains not only functions but also derivatives with respect to the global coordinates (x, y). Therefore, we must relate $\partial \psi_i^e / \partial x$ and $\partial \psi_i^e / \partial y$ to $\partial \psi_i^e / \partial \xi$ and $\partial \psi_i^e / \partial \eta$ using the transformation (9.3.1).

The functions $\psi_i^e(x, y)$ can be expressed in terms of the local coordinates ξ and η by means of Eq. (9.3.1). Hence, by the chain rule of partial differentiation, we have

$$\begin{aligned} \frac{\partial \psi_i^e}{\partial \xi} &= \frac{\partial \psi_i^e}{\partial x} \frac{\partial x}{\partial \xi} + \frac{\partial \psi_i^e}{\partial y} \frac{\partial y}{\partial \xi} \\ \frac{\partial \psi_i^e}{\partial \eta} &= \frac{\partial \psi_i^e}{\partial x} \frac{\partial x}{\partial \eta} + \frac{\partial \psi_i^e}{\partial y} \frac{\partial y}{\partial \eta} \end{aligned} \tag{9.3.7a}$$

or, in matrix notation

$$\begin{Bmatrix} \dfrac{\partial \psi_i^e}{\partial \xi} \\ \dfrac{\partial \psi_i^e}{\partial \eta} \end{Bmatrix} = \begin{bmatrix} \dfrac{\partial x}{\partial \xi} & \dfrac{\partial y}{\partial \xi} \\ \dfrac{\partial x}{\partial \eta} & \dfrac{\partial y}{\partial \eta} \end{bmatrix}^e \begin{Bmatrix} \dfrac{\partial \psi_i^e}{\partial x} \\ \dfrac{\partial \psi_i^e}{\partial y} \end{Bmatrix} \equiv [J] \begin{Bmatrix} \dfrac{\partial \psi_i^e}{\partial x} \\ \dfrac{\partial \psi_i^e}{\partial y} \end{Bmatrix} \tag{9.3.7b}$$

which gives the relation between the derivatives of ψ_i^e with respect to the global and local coordinates. The matrix $[J]$ is called the *Jacobian matrix* of the transformation (9.3.1):

$$[J] = \begin{bmatrix} \dfrac{\partial x}{\partial \xi} & \dfrac{\partial y}{\partial \xi} \\ \dfrac{\partial x}{\partial \eta} & \dfrac{\partial y}{\partial \eta} \end{bmatrix}^e \tag{9.3.8}$$

Note from the expression given for K_{ij}^e in Eq. (9.3.6) that we must relate $\partial \psi_i^e / \partial x$ and $\partial \psi_i^e / \partial y$ to $\partial \psi_i^e / \partial \xi$ and $\partial \psi_i^e / \partial \eta$, whereas Eq. (9.3.7) provides the inverse relations. Therefore, Eq. (9.3.7*b*) must be inverted

$$\begin{Bmatrix} \dfrac{\partial \psi_i^e}{\partial x} \\ \dfrac{\partial \psi_i^e}{\partial y} \end{Bmatrix} = [J]^{-1} \begin{Bmatrix} \dfrac{\partial \psi_i^e}{\partial \xi} \\ \dfrac{\partial \psi_i^e}{\partial \eta} \end{Bmatrix} \tag{9.3.9}$$

This requires that the Jacobian matrix $[J]$ be nonsingular.

Although it is possible to write the relationship (9.3.9) directly by means of the chain rule,

$$\begin{aligned} \frac{\partial \psi_i^e}{\partial x} &= \frac{\partial \psi_i^e}{\partial \xi} \frac{\partial \xi}{\partial x} + \frac{\partial \psi_i^e}{\partial \eta} \frac{\partial \eta}{\partial x} \\ \frac{\partial \psi_i^e}{\partial y} &= \frac{\partial \psi_i^e}{\partial \xi} \frac{\partial \xi}{\partial y} + \frac{\partial \psi_i^e}{\partial \eta} \frac{\partial \eta}{\partial y} \end{aligned} \tag{9.3.10}$$

it is not possible to evaluate $\partial\xi/\partial x$, $\partial\xi/\partial y$, $\partial\eta/\partial x$, and $\partial\eta/\partial y$ directly from the transformation equation (9.3.1). The transformation equation (9.3.1) allows direct evaluation of $\partial x/\partial\xi$, $\partial x/\partial\eta$, $\partial y/\partial\xi$, and $\partial y/\partial\eta$, and therefore $[J]$, as discussed next.

Using the transformation (9.3.1), we can write

$$\begin{aligned} \frac{\partial x}{\partial \xi} &= \sum_{j=1}^{m} x_j \frac{\partial \hat{\psi}_j^e}{\partial \xi}, \qquad \frac{\partial y}{\partial \xi} = \sum_{j=1}^{m} y_j \frac{\partial \hat{\psi}_j^e}{\partial \xi} \\ \frac{\partial x}{\partial \eta} &= \sum_{j=1}^{m} x_j \frac{\partial \hat{\psi}_j^e}{\partial \eta}, \qquad \frac{\partial y}{\partial \eta} = \sum_{j=1}^{m} y_j \frac{\partial \hat{\psi}_j^e}{\partial \eta} \end{aligned} \tag{9.3.11a}$$

and

$$\begin{aligned} [J] &= \begin{bmatrix} \dfrac{\partial x}{\partial \xi} & \dfrac{\partial y}{\partial \xi} \\ \dfrac{\partial x}{\partial \eta} & \dfrac{\partial y}{\partial \eta} \end{bmatrix} = \begin{bmatrix} \sum_{i=1}^{m} x_i \dfrac{\partial \hat{\psi}_i}{\partial \xi} & \sum_{i=1}^{m} y_i \dfrac{\partial \hat{\psi}_i}{\partial \xi} \\ \sum_{i=1}^{m} x_i \dfrac{\partial \hat{\psi}_i}{\partial \eta} & \sum_{i=1}^{m} y_i \dfrac{\partial \hat{\psi}_i}{\partial \eta} \end{bmatrix} \\ &= \begin{bmatrix} \dfrac{\partial \hat{\psi}_1}{\partial \xi} & \dfrac{\partial \hat{\psi}_2}{\partial \xi} & \cdots & \dfrac{\partial \hat{\psi}_m}{\partial \xi} \\ \dfrac{\partial \hat{\psi}_1}{\partial \eta} & \dfrac{\partial \hat{\psi}_2}{\partial \eta} & \cdots & \dfrac{\partial \hat{\psi}_m}{\partial \eta} \end{bmatrix} \begin{bmatrix} x_1 & y_1 \\ x_2 & y_2 \\ \vdots & \vdots \\ x_m & y_m \end{bmatrix} \end{aligned} \tag{9.3.11b}$$

Thus, given the global coordinates (x_j, y_j) of element nodes and the interpolation functions $\hat{\psi}_j^e$ used for geometry, the Jacobian matrix can be evaluated using Eq. (9.3.8). Note that $\hat{\psi}_j^e$ are different, in general, from ψ_j^e used in the approximation of the dependent variables.

In order to compute the global derivatives of ψ_i^e (i.e., derivatives of ψ_i^e with respect to x and y), Eq. (9.3.9) requires inversion of the Jacobian matrix. A necessary and sufficient condition for $[J]^{-1}$ to exist is that the determinant $|J|$, called the Jacobian J, be nonzero at every point (ξ, η) in $\hat{\Omega}$:

$$J \equiv \det[J] = \frac{\partial x}{\partial \xi}\frac{\partial y}{\partial \eta} - \frac{\partial x}{\partial \eta}\frac{\partial y}{\partial \xi} > 0 \tag{9.3.12}$$

From Eq. (9.3.12) it is clear that the functions $\xi = \xi(x, y)$ and $\eta = \eta(x, y)$ must be continuous, differentiable, and invertible. Moreover, the transformation should be algebraically simple so that the Jacobian matrix can be easily evaluated. Transformations of the form in Eq. (9.3.1) satisfy these requirements and the requirement that no spurious gaps between elements or overlapping of elements should occur. We consider an example to illustrate the invertibility requirements.

Example 9.3.1

Consider the three-element mesh of quadrilaterals shown in Fig. 9.3.2. The master element is the four-node square. Elements 1 and 2 have counterclockwise element node numbering consistent with the node numbering in the master element, and element 3 has node numbering

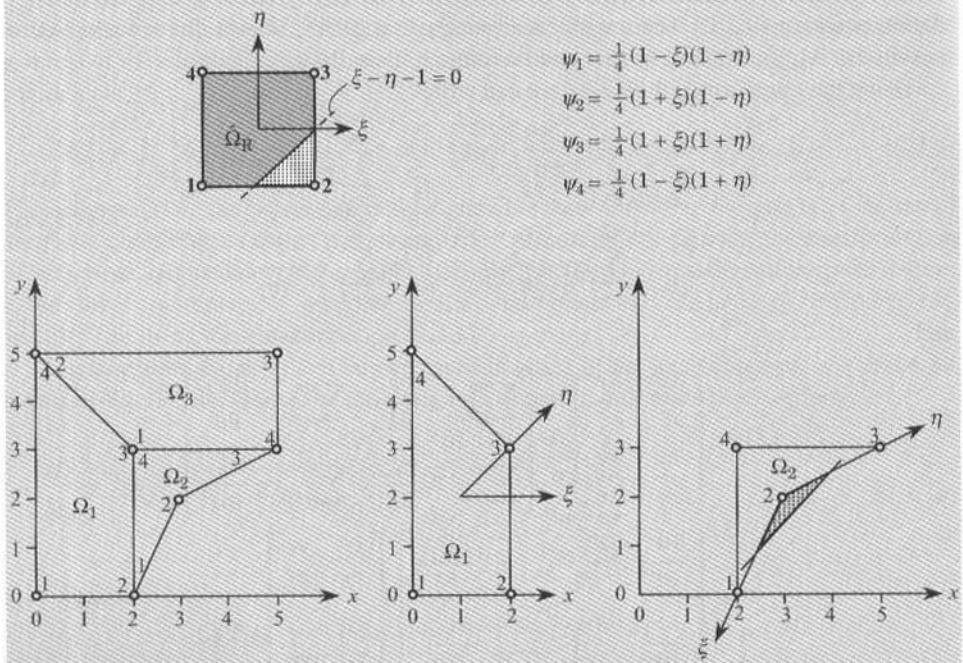

Figure 9.3.2 Examples of transformations of the master rectangular element $\hat{\Omega}_R$.

opposite to that of the master element. Elements 1 and 3 are *convex* domains in the sense that the line segment connecting any two arbitrary points of a convex domain lies entirely in the element. Clearly, element 2 is not convex because, for example, the line segment joining nodes 1 and 3 is not entirely inside the element. In the following paragraphs, we investigate the effect of node numbering and element convexity on the transformations from the master element to each of the three elements.

First, we compute the elements of the Jacobian matrix (the interpolation functions are given in Fig. 9.3.2)

$$\begin{aligned}
\frac{\partial x}{\partial \xi} &= \sum_{i=1}^{4} x_i \frac{\partial \hat{\psi}_i}{\partial \xi} = \frac{1}{4}[-x_1(1-\eta) + x_2(1-\eta) + x_3(1+\eta) - x_4(1+\eta)] \\
\frac{\partial x}{\partial \eta} &= \sum_{i=1}^{4} x_i \frac{\partial \hat{\psi}_i}{\partial \eta} = \frac{1}{4}[-x_1(1-\xi) - x_2(1+\xi) + x_3(1+\xi) + x_4(1+\xi)] \\
\frac{\partial y}{\partial \xi} &= \sum_{i=1}^{4} y_i \frac{\partial \hat{\psi}_i}{\partial \xi} = \frac{1}{4}[-y_1(1-\eta) + y_2(1-\eta) + y_3(1+\eta) - y_4(1+\eta)] \\
\frac{\partial y}{\partial \eta} &= \sum_{i=1}^{4} y_i \frac{\partial \hat{\psi}_i}{\partial \eta} = \frac{1}{4}[-y_1(1-\xi) - y_2(1+\xi) + y_3(1+\xi) + y_4(1+\xi)]
\end{aligned} \tag{9.3.13}$$

Next, we evaluate the Jacobian for each of the elements.

Element 1. We have $x_1 = x_4 = 0$, $x_2 = x_3 = 2$; $y_1 = y_2 = 0$, $y_3 = 3$, $y_4 = 5$. The transformation and Jacobian are given by

$$x = 2\hat{\psi}_2 + 2\hat{\psi}_3 = 1 + \xi, \qquad y = 3\hat{\psi}_3 + 5\hat{\psi}_4 = (1+\eta)\left(2 - \tfrac{1}{2}\xi\right) \tag{9.3.14a}$$

$$J = \det[J] = \begin{vmatrix} \dfrac{\partial x}{\partial \xi} & \dfrac{\partial y}{\partial \xi} \\ \dfrac{\partial x}{\partial \eta} & \dfrac{\partial y}{\partial \eta} \end{vmatrix} = \begin{vmatrix} 1 & -\dfrac{1}{2}(1+\eta) \\ 0 & 2 - \dfrac{1}{2}\xi \end{vmatrix} = \frac{1}{2}(4 - \xi) > 0 \tag{9.3.14b}$$

Clearly, the Jacobian is linear in ξ, and for all values of ξ in $-1 \le \xi \le 1$, it is positive. Therefore, the transformation (9.3.14*a*) is invertible:

$$1 + \xi = x, \quad 1 + \eta = \frac{2y}{5 - x}$$

Element 2. Here we have $x_1 = x_4 = 2$, $x_2 = 3$, $x_3 = 5$, $y_1 = 0$, $y_2 = 2$, and $y_3 = y_4 = 3$. The transformation and the Jacobian are given by

$$x = 3 + \xi + \frac{1}{2}\eta + \frac{1}{2}\xi\eta, \qquad y = 2 + \frac{1}{2}\xi + \eta - \frac{1}{2}\xi\eta \tag{9.3.15a}$$

$$J = \begin{vmatrix} \dfrac{\partial x}{\partial \xi} & \dfrac{\partial y}{\partial \xi} \\ \dfrac{\partial x}{\partial \eta} & \dfrac{\partial y}{\partial \eta} \end{vmatrix} = \begin{vmatrix} 1 + \dfrac{1}{2}\eta & \dfrac{1}{2}(1-\eta) \\ \dfrac{1}{2}(1+\xi) & 1 - \dfrac{1}{2}\xi \end{vmatrix} = \frac{3}{4}(1 + \eta - \xi) \tag{9.3.15b}$$

The Jacobian is *not* nonzero everywhere in the master element. It is zero along the line $\xi = 1 + \eta$, and it is negative in the shaded area of the master element (see Fig. 9.3.2). Moreover, this area is mapped into the shaded area outside element 2. Thus, elements with any interior angle greater than π should not be used in any finite element mesh.

Element 3. We have $x_1 = 2$, $x_2 = 0$, $x_3 = x_4 = 5$, $y_1 = y_4 = 3$, and $y_2 = y_3 = 5$. The transformation and the Jacobian become (note that the nodes are numbered clockwise)

$$x = 3 - \frac{1}{2}\xi + 2\eta + \frac{1}{2}\xi\eta, \qquad y = 4 + \xi \tag{9.3.16a}$$

$$J = \begin{vmatrix} \dfrac{\partial x}{\partial \xi} & \dfrac{\partial y}{\partial \xi} \\ \dfrac{\partial x}{\partial \eta} & \dfrac{\partial y}{\partial \eta} \end{vmatrix} = \begin{vmatrix} -\dfrac{1}{2}(1-\eta) & 1 \\ 2 + \dfrac{1}{2}\xi & 0 \end{vmatrix} = -\left(2 + \frac{1}{2}\xi\right) < 0 \tag{9.3.16b}$$

The negative Jacobian indicates that a right-hand coordinate system is mapped into a left-hand coordinate system. Such coordinate transformations should be avoided.

The above example illustrates, for the four-node master element, that nonconvex elements are not admissible in finite element meshes. In general, any interior angle θ (see Fig. 9.3.3) should not be too small or too large because the Jacobian $J = (|dr_1||dr_2| \sin\theta)/d\xi d\eta$ will be very small. Similar restrictions hold for higher-order master elements. Additional restrictions also exist for higher-order elements. For example, for higher-order triangular and rectangular elements, the placing of the side and interior nodes is restricted.

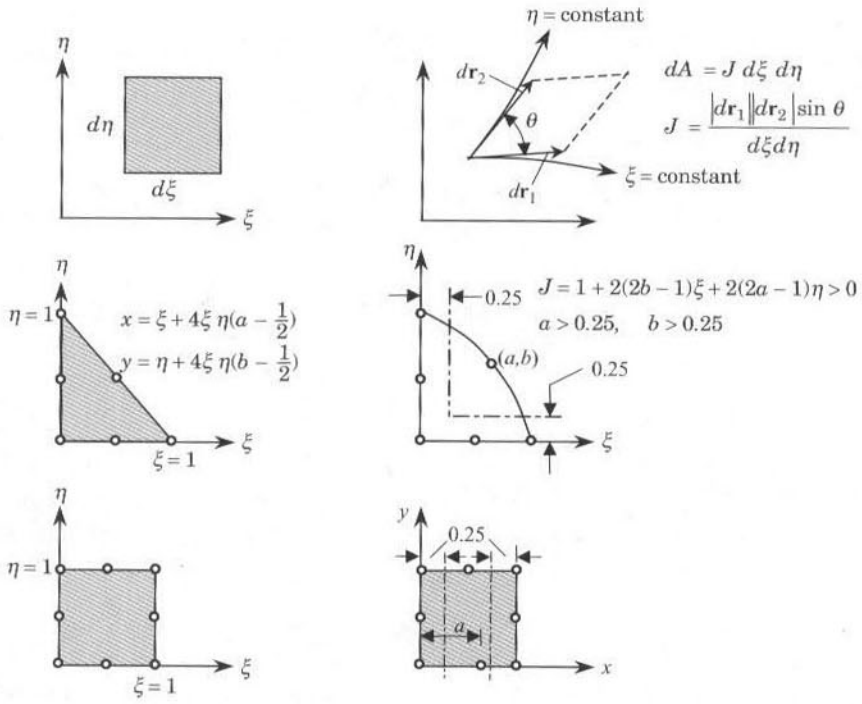

Figure 9.3.3 Some restrictions on element transformations.

For the eight-node rectangular element, it can be shown that the side nodes should be placed at a distance greater than or equal to a quarter of the length of the side from either corner node (see Fig. 9.3.3).

Returning to numerical evaluation of integrals, we have from Eq. (9.3.9),

$$\begin{Bmatrix} \dfrac{\partial \psi_i^e}{\partial x} \\ \dfrac{\partial \psi_i^e}{\partial y} \end{Bmatrix} = [J]^{-1} \begin{Bmatrix} \dfrac{\partial \psi_i^e}{\partial \xi} \\ \dfrac{\partial \psi_i^e}{\partial \eta} \end{Bmatrix} \equiv [J^*] \begin{Bmatrix} \dfrac{\partial \psi_i^e}{\partial \xi} \\ \dfrac{\partial \psi_i^e}{\partial \eta} \end{Bmatrix} \tag{9.3.17}$$

where J_{ij}^* is the element in position (i, j) of the inverse of the Jacobian matrix,

$$[J]^{-1} \equiv [J^*] = \begin{bmatrix} J_{11}^* & J_{12}^* \\ J_{21}^* & J_{22}^* \end{bmatrix} \tag{9.3.18}$$

The element area $dA = dx\, dy$ in element Ω_e is transformed to

$$dA \equiv dx\, dy = J d\xi\, d\eta \tag{9.3.19}$$

in the master element $\hat{\Omega}$.

Equations (9.3.9), (9.3.11), (9.3.18), and (9.3.19) provide the necessary relations to transform integral expressions on any element Ω_e to an associated master element $\hat{\Omega}$. For instance, consider the integral expression in Eq. (9.3.6) where $a = a(x, y)$, $b = b(x, y)$, and $c = c(x, y)$ are functions of x and y. Suppose that the mesh of finite elements is generated

by a master element $\hat{\Omega}$. Under the transformation (9.3.1), we can write

$$
\begin{aligned}
K_{ij}^e &= \int_{\Omega_e} \left(a \frac{\partial \psi_i}{\partial x} \frac{\partial \psi_j}{\partial x} + b \frac{\partial \psi_i}{\partial y} \frac{\partial \psi_j}{\partial y} + c \psi_i \psi_j \right) dx\, dy \\
&= \int_{\hat{\Omega}} \left[\hat{a} \left(J_{11}^* \frac{\partial \psi_i}{\partial \xi} + J_{12}^* \frac{\partial \psi_i}{\partial \eta} \right) \left(J_{11}^* \frac{\partial \psi_j}{\partial \xi} + J_{12}^* \frac{\partial \psi_j}{\partial \eta} \right) \right. \\
&\quad \left. + \hat{b} \left(J_{21}^* \frac{\partial \psi_i}{\partial \xi} + J_{22}^* \frac{\partial \psi_i}{\partial \eta} \right) \left(J_{21}^* \frac{\partial \psi_j}{\partial \xi} + J_{22}^* \frac{\partial \psi_j}{\partial \eta} \right) + \hat{c} \psi_i \psi_j \right] J d\xi\, d\eta \\
&\equiv \int_{\hat{\Omega}} F(\xi, \eta) d\xi\, d\eta
\end{aligned} \tag{9.3.20}
$$

where J_{ij}^* are the elements of the inverse of the Jacobian matrix in (9.3.18), and $\hat{a} = a(\xi, \eta)$, and so on. Equations (9.3.9), (9.3.11), and (9.3.18)–(9.3.20) are valid for master elements of both rectangular and triangular geometry. The master triangular and rectangular elements for linear and quadratic triangular and quadrilateral elements are shown in Fig. 9.3.4.

9.3.3 Integration over a Master Rectangular Element

Quadrature formulas for integrals defined over a rectangular master element $\hat{\Omega}_R$ (such as that shown in Fig. 9.3.4) can be derived from the one-dimensional quadrature formulae presented in Section 7.6.4. We have

$$
\begin{aligned}
\int_{\hat{\Omega}_R} F(\xi, \eta) d\xi d\eta &= \int_{-1}^{1} \left[\int_{-1}^{1} F(\xi, \eta) d\eta \right] d\xi \approx \int_{-1}^{1} \left[\sum_{J=1}^{N} F(\xi, \eta_J) W_J \right] d\xi \\
&\approx \sum_{I=1}^{M} \sum_{J=1}^{N} F(\xi_I, \eta_J) W_I W_J
\end{aligned} \tag{9.3.21}
$$

where M and N denote the number of quadrature points in the ξ and η directions, (ξ_I, η_J) denote the Gauss points, and W_I and W_J denote the corresponding Gauss weights (see Table 7.1.2). The selection of the number of Gauss points is based on the same formula as that given in Section 7.1.5: A polynomial of degree p is integrated exactly employing $N = \text{int}[\frac{1}{2}(p+1)]$, i.e., the smallest integer greater than $\frac{1}{2}(p+1)$. In most cases, the interpolation functions are of the same degree in both ξ and η, and therefore $M = N$. When the integrand is of different degree in ξ and η, the number of Gauss points is selected on the basis of the largest-degree polynomial. The minimum allowable quadrature rule is one that computes the mass of the element exactly when the density is constant.

Table 9.3.1 contains information on the selection of the integration order and the location of the Gauss points for linear, quadratic, and cubic elements. The maximum degree of the polynomial refers to the degree of the highest polynomial in ξ or η that is present in the integrands of the element matrices of the type in Eq. (9.3.20). Note that the polynomial degree of coefficients as well as J_{ij}^* and J should be accounted for in determining the total polynomial degree of the integrand. Of course, the coefficients a, b, and c, and J_{ij}^* in general may not be polynomials. In those cases, their functional variations must be approximated

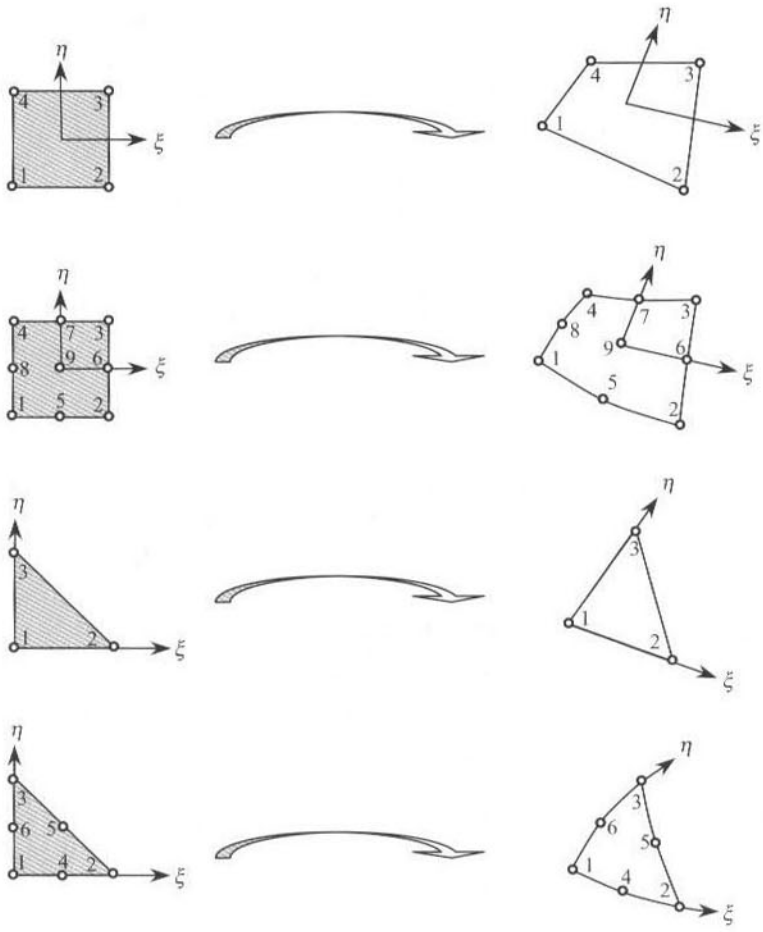

Figure 9.3.4 Linear and quadratic master finite elements and their typical counterparts in the problem coordinate system.

by a suitable polynomial (for example, by a binomial series) in order to determine the polynomial degree of the integrand.

The $N \times N$ Gauss point locations are given by the *tensor product* of one-dimensional Gauss points ξ_I :

$$\begin{Bmatrix} \xi_1 \\ \xi_2 \\ \vdots \\ \xi_N \end{Bmatrix} \{\xi_1, \xi_2, \ldots, \xi_N\} \equiv \begin{bmatrix} (\xi_1, \xi_1) & (\xi_1, \xi_2) & \ldots & (\xi_1, \xi_N) \\ (\xi_2, \xi_1) & \ddots & & \vdots \\ \vdots & & & \\ (\xi_N, \xi_1) & \ldots & & (\xi_N, \xi_N) \end{bmatrix} \tag{9.3.22}$$

The values of ξ_I $(I = 1, 2, \ldots, N)$ are presented in Table 9.3.1 (also, see Table 7.1.2).

The next two examples illustrate the evaluation of the Jacobian and element matrices on rectangular elements.

Table 9.3.1 Selection of the integration order and location of the Gauss points for linear, quadratic, and cubic quadrilateral elements (nodes not shown).

Element type	Maximum polynomial degree	Order of integration ($r \times r$)	Order of the residual	Location of integration points* in master element
Constant ($r = 1$)	0	1×1	$O(h^2)$	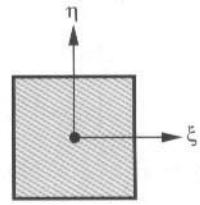
Linear ($r = 2$)	2	2×2	$O(h^4)$	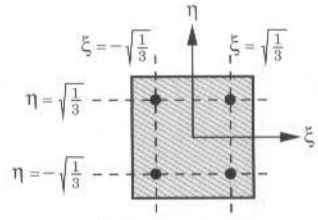
Quadratic ($r = 3$)	4	(3×3)	$O(h^6)$	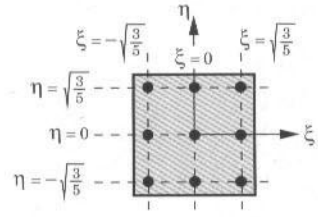
Cubic ($r = 4$)	6	(4×4)	$O(h^8)$	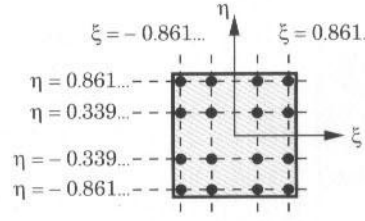

*See Table 6.1.2 for the integration points and weights for each coordinate direction.

Example 9.3.2

Consider the quadrilateral element Ω_i shown in Fig. 9.3.2. We wish to evaluate $\partial\psi_i/\partial x$ and $\partial\psi_i/\partial y$ at $(\xi, \eta) = (0, 0)$ and $(\frac{1}{2}, \frac{1}{2})$ using the isoparametric formulation (i.e., $\hat{\psi}_i = \psi_i$). From

Eq. (9.3.11*b*) we have

$$[J] = \begin{bmatrix} \dfrac{\partial x}{\partial \xi} & \dfrac{\partial y}{\partial \xi} \\ \dfrac{\partial x}{\partial \eta} & \dfrac{\partial y}{\partial \eta} \end{bmatrix} = \frac{1}{4}\begin{bmatrix} -(1-\eta) & 1-\eta & 1+\eta & -(1+\eta) \\ -(1-\xi) & -(1+\xi) & 1+\xi & 1-\xi \end{bmatrix} \begin{bmatrix} 0.0 & 0.0 \\ 2.0 & 0.0 \\ 2.0 & 3.0 \\ 0.0 & 5.0 \end{bmatrix}$$

$$= \begin{bmatrix} 1 & -\dfrac{1}{2}(1+\eta) \\ 0 & \dfrac{1}{2}(4-\xi) \end{bmatrix}$$

The inverse of the Jacobian matrix is given by

$$[J]^{-1} = \begin{bmatrix} 1 & \dfrac{1+\eta}{4-\xi} \\ 0 & \dfrac{2}{4-\xi} \end{bmatrix}, \quad J^*_{11} = 1, \quad J^*_{21} = 0, \quad J^*_{12} = \frac{1+\eta}{4-\xi}, \quad J^*_{22} = \frac{2}{4-\xi}$$

From (9.3.9), we have

$$\frac{\partial \psi_i}{\partial x} = \frac{\partial \psi_i}{\partial \xi} + \frac{1+\eta}{4-\xi}\frac{\partial \psi_i}{\partial \eta}, \quad \frac{\partial \psi_i}{\partial y} = \frac{2}{4-\xi}\frac{\partial \psi_i}{\partial \eta}$$

where

$$\psi_i = \frac{1}{4}(1+\xi\xi_i)(1+\eta\eta_i), \quad \frac{\partial \psi_i}{\partial \xi} = \frac{1}{4}\xi_i(1+\eta\eta_i), \quad \frac{\partial \psi_i}{\partial \eta} = \frac{1}{4}\eta_i(1+\xi\xi_i) \tag{9.3.23}$$

(ξ_i, η_i) being the coordinates of the ith node in the master element (see Fig. 9.3.2):

Node	ξ_i	η_i
1	−1	−1
2	1	−1
3	1	1
4	−1	1

Thus, we have

$$\frac{\partial \psi_i}{\partial x} = \frac{1}{4}\xi_i(1+\eta\eta_i) + \frac{1}{4}\left(\frac{1+\eta}{4-\xi}\right)\eta_i(1+\xi\xi_i)$$

$$\frac{\partial \psi_i}{\partial y} = \frac{1}{4}\frac{2}{(4-\xi)}\eta_i(1+\xi\xi_i)$$

In particular, at $(\xi, \eta) = (0, 0)$ the derivatives of ψ_i with respect to the global coordinates (x, y) are

$$\frac{\partial \psi_i}{\partial x} = \frac{1}{4}\xi_i + \frac{1}{16}\eta_i, \quad \frac{\partial \psi_i}{\partial y} = \frac{1}{8}\eta_i$$

and at $(\xi, \eta) = (0.5, 0.5)$ they are

$$\frac{\partial \psi_i}{\partial x} = \frac{1}{8}\xi_i(2+\eta_i) + \frac{3}{56}\eta_i(2+\xi_i), \quad \frac{\partial \psi_i}{\partial y} = \frac{1}{14}\eta_i(2+\xi_i)$$

Example 9.3.3

Consider the quadrilateral element in Fig. 9.3.5. We wish to compute the following element matrices using the Gauss–Legendre quadrature:

$$\begin{aligned} S_{ij}^{00} &= \int_\Omega \psi_i \psi_j \, dx\, dy, & S_{ij}^{11} &= \int_\Omega \frac{\partial \psi_i}{\partial x}\frac{\partial \psi_j}{\partial x} \, dx\, dy \\ S_{ij}^{22} &= \int_\Omega \frac{\partial \psi_i}{\partial y}\frac{\partial \psi_j}{\partial y} \, dx\, dy, & S_{ij}^{12} &= \int_\Omega \frac{\partial \psi_i}{\partial x}\frac{\partial \psi_j}{\partial y} \, dx\, dy \end{aligned} \tag{9.3.24}$$

The transformation equations are

$$x = 0\cdot\hat{\psi}_1 + 5\hat{\psi}_2 + 4\hat{\psi}_3 + 1\cdot\hat{\psi}_4 = \frac{1}{4}(10 + 8\xi - 2\xi\eta)$$

$$y = 0\cdot\hat{\psi}_1 - 1\cdot\hat{\psi}_2 + 5\hat{\psi}_3 + 4\hat{\psi}_4 = \frac{1}{4}(8 + 10\eta + 2\xi\eta)$$

the Jacobian matrix and its inverse are

$$[J] = \begin{bmatrix} \dfrac{\partial x}{\partial \xi} & \dfrac{\partial y}{\partial \xi} \\ \dfrac{\partial x}{\partial \eta} & \dfrac{\partial y}{\partial \eta} \end{bmatrix} = \frac{1}{4}\begin{bmatrix} 8-2\eta & 2\eta \\ -2\xi & 10+2\xi \end{bmatrix}, \quad J = \frac{1}{4}[(4-\eta)(5+\xi) + \xi\eta] = \frac{1}{4}(20 + 4\xi - 5\eta)$$

$$[J]^{-1} = \frac{1}{4J}\begin{bmatrix} 10+2\xi & -2\eta \\ 2\xi & 8-2\eta \end{bmatrix}, \quad J_{11}^* = \frac{10+2\xi}{20+4\xi-5\eta}, \quad J_{12}^* = -\frac{2\eta}{20+4\xi-5\eta}$$

$$J_{21}^* = \frac{2\xi}{20+4\xi-5\eta}, \quad J_{22}^* = \frac{8-2\eta}{20+4\xi-5\eta}$$

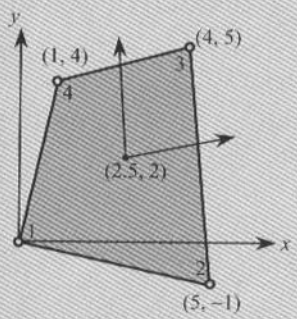

Figure 9.3.5 Geometry of the bilinear element used in Example 9.3.3.

The matrix $[J]$ transforms base vectors $\hat{\mathbf{e}}_x = (1, 0)$ and $\hat{\mathbf{e}}_y = (0, 1)$ in the xy system to the base vectors $\hat{\mathbf{e}}_\xi$ and $\hat{\mathbf{e}}_\eta$ in the $\xi\eta$ system

$$\frac{1}{4}\begin{bmatrix} 8-2\eta & 2\eta \\ -2\xi & 10+2\xi \end{bmatrix}\begin{Bmatrix} 1 \\ 0 \end{Bmatrix} = \frac{1}{4}\begin{Bmatrix} 8-2\eta \\ 2\eta \end{Bmatrix}, \quad \frac{1}{4}\begin{bmatrix} 8-2\eta & 2\eta \\ -2\xi & 10+2\xi \end{bmatrix}\begin{Bmatrix} 0 \\ 1 \end{Bmatrix} = \frac{1}{4}\begin{Bmatrix} -2\xi \\ 10+2\xi \end{Bmatrix}$$

or

$$\hat{\mathbf{e}}_\xi = \frac{1}{4}[(8-2\eta)\hat{\mathbf{e}}_x + 2\eta\hat{\mathbf{e}}_y], \quad \hat{\mathbf{e}}_\eta = \frac{1}{4}[-2\xi\hat{\mathbf{e}}_x + (10+2\xi)\hat{\mathbf{e}}_y]$$

Hence, the area element $dx\,dy$ in the xy system is related to the area element $d\xi\,d\eta$ in the $\xi\eta$ system by

$$dx\,dy = \frac{1}{16}\begin{vmatrix} 8-2\eta & -2\xi \\ 2\eta & 10+2\xi \end{vmatrix} d\xi\,d\eta = J\,d\xi\,d\eta \tag{9.3.25}$$

The coefficients S_{ij}^{00} and S_{ij}^{11}, for example, can be expressed in natural coordinates (for numerical evaluation) as

$$S_{ij}^{00} = \int_{\Omega_e} \psi_i\psi_j\,dx\,dy = \int_{-1}^{1}\int_{-1}^{1} \psi_i\psi_j J\,d\xi\,d\eta$$

$$S_{ij}^{11} = \int_{\Omega_e} \frac{\partial\psi_i}{\partial x}\frac{\partial\psi_j}{\partial x}\,dx\,dy$$

$$= \int_{-1}^{1}\int_{-1}^{1}\left(J_{11}^{*}\frac{\partial\psi_i}{\partial\xi} + J_{12}^{*}\frac{\partial\psi_i}{\partial\eta}\right)\left(J_{11}^{*}\frac{\partial\psi_j}{\partial\xi} + J_{12}^{*}\frac{\partial\psi_j}{\partial\eta}\right) J\,d\xi\,d\eta$$

where $\partial\psi_i/\partial\xi$ and $\partial\psi_i/\partial\eta$ are given by Eqs. (9.3.23). Note that the integrand of S_{ij}^{00} is a polynomial of the order $p = 3$ in each coordinate ξ and η. Hence, $N = M = [(p+1)/2] = 2$ will evaluate S_{ij} exactly. For example, consider the coefficient S_{11}^{00}

$$S_{11}^{00} = \int_{\Omega_e} \psi_1\psi_1\,dx\,dy = \int_{-1}^{1}\int_{-1}^{1} \psi_1\psi_1 J\,d\xi\,d\eta$$

$$= \frac{1}{64}\int_{-1}^{1}\int_{-1}^{1}(1-\xi)^2(1-\eta)^2(20+4\xi-5\eta)d\xi\,d\eta$$

$$= \frac{1}{64}\sum_{i,j=1}^{2}(1-\xi_i)^2(1-\eta_j)^2(20+4\xi_i-5\eta_j)$$

where (ξ_i, η_i) are the Gauss points

$$(\xi_1, \eta_2) = \left(-\frac{1}{\sqrt{3}}, \frac{1}{\sqrt{3}}\right), \quad (\xi_2, \eta_2) = \left(\frac{1}{\sqrt{3}}, \frac{1}{\sqrt{3}}\right)$$

$$(\xi_1, \eta_1) = \left(-\frac{1}{\sqrt{3}}, -\frac{1}{\sqrt{3}}\right), \quad (\xi_2, \eta_1) = \left(\frac{1}{\sqrt{3}}, -\frac{1}{\sqrt{3}}\right)$$

We have

$$S_{11}^{00} = \frac{1}{64}\left[\left(1+\frac{1}{\sqrt{3}}\right)^4\left(20-\frac{4}{\sqrt{3}}+\frac{5}{\sqrt{3}}\right)+\left(1+\frac{1}{\sqrt{3}}\right)^2\left(1-\frac{1}{\sqrt{3}}\right)^2\left(20-\frac{4}{\sqrt{3}}-\frac{5}{\sqrt{3}}\right)\right.$$
$$\left.+\left(1-\frac{1}{\sqrt{3}}\right)^2\left(1+\frac{1}{\sqrt{3}}\right)^2\left(20+\frac{4}{\sqrt{3}}+\frac{5}{\sqrt{3}}\right)+\left(1-\frac{1}{\sqrt{3}}\right)^4\left(20+\frac{4}{\sqrt{3}}-\frac{5}{\sqrt{3}}\right)\right]$$
$$= \frac{1}{64}\left[\frac{1120}{9}+\frac{160}{9}+\frac{32}{3\sqrt{3}}\left(-\frac{4}{\sqrt{3}}+\frac{5}{\sqrt{3}}\right)\right] = \frac{1312}{576} = 2.27778$$

Similarly, consider the coefficient S_{12}^{11}:

$$S_{12}^{11} = \int_{\Omega_e} \frac{\partial\psi_1}{\partial x}\frac{\partial\psi_2}{\partial x}\,dx\,dy$$
$$= \int_{-1}^{1}\int_{-1}^{1}\left(J_{11}^{*}\frac{\partial\psi_1}{\partial\xi}+J_{12}^{*}\frac{\partial\psi_1}{\partial\eta}\right)\left(J_{11}^{*}\frac{\partial\psi_2}{\partial\xi}+J_{12}^{*}\frac{\partial\psi_2}{\partial\eta}\right)J\,d\xi\,d\eta$$
$$= \frac{1}{64}\int_{-1}^{1}\int_{-1}^{1}[-(10+2\xi)(1-\eta)+2\eta(1-\xi)]\,[(10+2\xi)(1-\eta)+2\eta(1-\xi)]$$
$$\times\frac{1}{(20+4\xi-5\eta)}\,d\xi\,d\eta$$
$$= \frac{1}{64}\int_{-1}^{1}\int_{-1}^{1}\left[-(10+2\xi)^2(1-\eta)^2+4\eta^2(1-\xi)^2\right]\frac{1}{(20+4\xi-5\eta)}\,d\xi\,d\eta$$

which is a ratio of polynomials. Hence, we do not expect to evaluate the integral exactly. The integrand varies, approximately, as a quadratic polynomial in each ξ and η. Hence, we may use the two-point Gauss integration to evaluate the integral

$$S_{12}^{11} = \frac{1}{64}\int_{-1}^{1}\int_{-1}^{1}\left[-(10+2\xi)^2(1-\eta)^2+4\eta^2(1-\xi)^2\right]\frac{1}{(20+4\xi-5\eta)}\,d\xi\,d\eta$$
$$\approx \sum_{i,j=1}^{2}\left[-(10+2\xi_i)^2(1-\eta_j)^2+4\eta_j^2(1-\xi_i)^2\right]\frac{1}{64(20+4\xi_i-5\eta_j)}$$
$$= \left[-\left(10-\frac{2}{\sqrt{3}}\right)^2\left(1+\frac{1}{\sqrt{3}}\right)^2+\frac{4}{3}\left(1+\frac{1}{\sqrt{3}}\right)^2\right]\frac{1}{64\left(20+\frac{1}{\sqrt{3}}\right)}$$
$$+\left[-\left(10+\frac{2}{\sqrt{3}}\right)^2\left(1+\frac{1}{\sqrt{3}}\right)^2+\frac{4}{3}\left(1-\frac{1}{\sqrt{3}}\right)^2\right]\frac{1}{64\left(20+\frac{9}{\sqrt{3}}\right)}$$
$$+\left[-\left(10-\frac{2}{\sqrt{3}}\right)^2\left(1-\frac{1}{\sqrt{3}}\right)^2+\frac{4}{3}\left(1+\frac{1}{\sqrt{3}}\right)^2\right]\frac{1}{64\left(20-\frac{9}{\sqrt{3}}\right)}$$
$$+\left[-\left(10+\frac{2}{\sqrt{3}}\right)^2\left(1-\frac{1}{\sqrt{3}}\right)^2+\frac{4}{3}\left(1-\frac{1}{\sqrt{3}}\right)^2\right]\frac{1}{64\left(20-\frac{1}{\sqrt{3}}\right)} = -0.36892$$

A three-point integration gives $S_{11}^{00} = -0.36998$.

Evaluating the integrals in Eq. (9.3.24) using 2×2 quadrature rule, we obtain

$$[S^{00}] = \begin{bmatrix} 2.27778 & 1.25000 & 0.55556 & 1.00000 \\ 1.25000 & 2.72222 & 1.22222 & 0.55556 \\ 0.55556 & 1.22222 & 2.16667 & 0.97222 \\ 1.00000 & 0.55556 & 0.97222 & 1.72222 \end{bmatrix} \quad \text{(exact)}$$

$$[S^{11}] = \begin{bmatrix} 0.40995 & -0.36892 & -0.20479 & 0.16376 \\ -0.36892 & 0.34516 & 0.25014 & -0.22639 \\ -0.20479 & 0.25014 & 0.43155 & -0.47690 \\ 0.16376 & -0.22639 & -0.47690 & 0.53953 \end{bmatrix} \quad \text{(inexact)}$$

$$[S^{22}] = \begin{bmatrix} 0.26237 & 0.16389 & -0.13107 & -0.29520 \\ 0.16389 & 0.22090 & -0.23991 & -0.14489 \\ -0.13107 & -0.23991 & 0.27619 & 0.09478 \\ -0.29520 & -0.14489 & 0.09478 & 0.34530 \end{bmatrix} \quad \text{(inexact)}$$

$$[S^{12}] = \begin{bmatrix} 0.24731 & 0.25156 & -0.25297 & -0.24589 \\ -0.24844 & -0.25090 & 0.25172 & 0.24762 \\ -0.25297 & -0.24828 & 0.24671 & 0.25454 \\ 0.25411 & 0.24762 & -0.24546 & -0.25627 \end{bmatrix} \quad \text{(inexact)}$$

These matrices would have been exact if the element had its sides parallel to the coordinate system (i.e., for a rectangular element). The values are accurate enough to yield good solutions for most problems (depends on the problem).

To see the effect of skewed elements on the accuracy of the results, we revisit the problem in Example 8.3.1. We consider the nine-element mesh shown in the figure below and investigate the effect of skewness (measured in terms of the angle α) on the solution accuracy. The same number of Gauss points (2×2) as in the case of a regular mesh are used. The results are summarized below (compare with the results in Table 8.3.1). The results are not very sensitive to the mesh distortion.

$\alpha = 0°$	$\alpha = 15°$	$\alpha = 30°$	$\alpha = 45°$
0.3014	0.2972	0.3017	0.2972

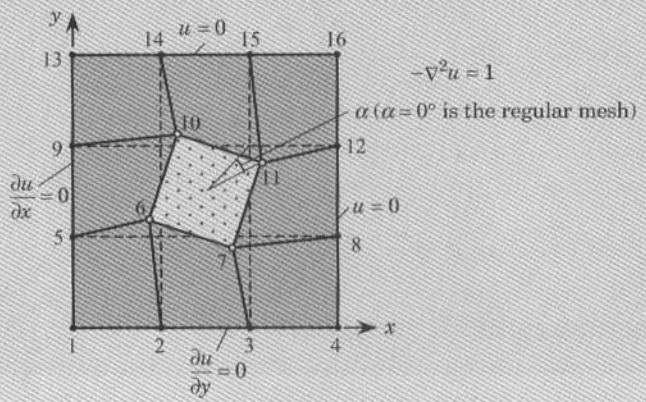

9.3.4 Integration over a Master Triangular Element

In the preceding section we discussed numerical integration on quadrilateral elements that can be used to represent very general geometries as well as field variables in a variety of problems. Here we discuss numerical integration on triangular elements. Since quadrilateral elements can be geometrically distorted, it is possible to distort a quadrilateral element to obtain a required triangular element by moving the position of the corner nodes to one of the neighboring nodes. In actual computation, this is achieved by assigning the same global node number to two corner nodes of the quadrilateral element. Thus, master triangular elements can be obtained in a natural way from associated master rectangular elements. Here we discuss the transformations from an arbitrary triangular element to an arbitrary triangular element.

We choose the unit right isosceles triangle [see Fig. 9.3.6(a)] as the master element. An arbitrary triangular element Ω_e can be generated from the master triangular element $\hat{\Omega}_T$ by transformation of the form (9.3.1). The coordinate lines $\xi = 0$ and $\eta = 0$ in $\hat{\Omega}_T$ correspond to the skew curvilinear coordinate lines 1–3 and 1–2 in Ω_e. For the three-node triangular element, the transformation (9.3.1) is taken to be

$$x = \sum_{i=1}^{3} x_i \hat{\psi}_i(\xi, \eta), \qquad y = \sum_{i=1}^{3} y_i \hat{\psi}_i(\xi, \eta) \tag{9.3.26}$$

where $\hat{\psi}_i(\xi, \eta)$ are the interpolation functions of the master three-node triangular element [see Fig. 9.3.6(b)],

$$\hat{\psi}_1 = 1 - \xi - \eta, \qquad \hat{\psi}_2 = \xi, \qquad \hat{\psi}_3 = \eta \tag{9.3.27}$$

The inverse transformation from element Ω_e to $\hat{\Omega}_T$ is given by inverting Eqs. (9.3.26):

$$\begin{aligned} \xi &= \frac{1}{2A}[(x - x_1)(y_3 - y_1) - (y - y_1)(x_3 - x_1)] \\ \eta &= \frac{1}{2A}[(x - x_1)(y_1 - y_2) + (y - y_1)(x_2 - x_1)] \end{aligned} \tag{9.3.28}$$

where A is the area of Ω_e.

With the help of (9.3.28), we can show that the interpolation functions in (8.2.25b) are equivalent to the $\hat{\psi}_i$ in Eqs. (9.3.27). Moreover, the area coordinates L_i in (9.2.9) are also equivalent to $\hat{\psi}_i$. The interpolation functions for the linear and higher-order triangular elements can be obtained from the area coordinates, as described in Section 9.2.

The Jacobian matrix for the linear triangular element is given by

$$[J]^{-1} = \begin{bmatrix} x_2 - x_1 & y_2 - y_1 \\ x_3 - x_1 & y_3 - y_1 \end{bmatrix} = \begin{bmatrix} \gamma_3 & -\beta_3 \\ -\gamma_2 & \beta_2 \end{bmatrix} \tag{9.3.29}$$

where β_i and γ_i are the constants defined in (8.2.24b). The inverse of the Jacobian matrix is given by

$$[J]^{-1} = \frac{1}{J}\begin{bmatrix} \beta_2 & \beta_3 \\ \gamma_2 & \gamma_3 \end{bmatrix}, \qquad J = \beta_2\gamma_3 - \gamma_2\beta_3 = 2A \tag{9.3.30}$$

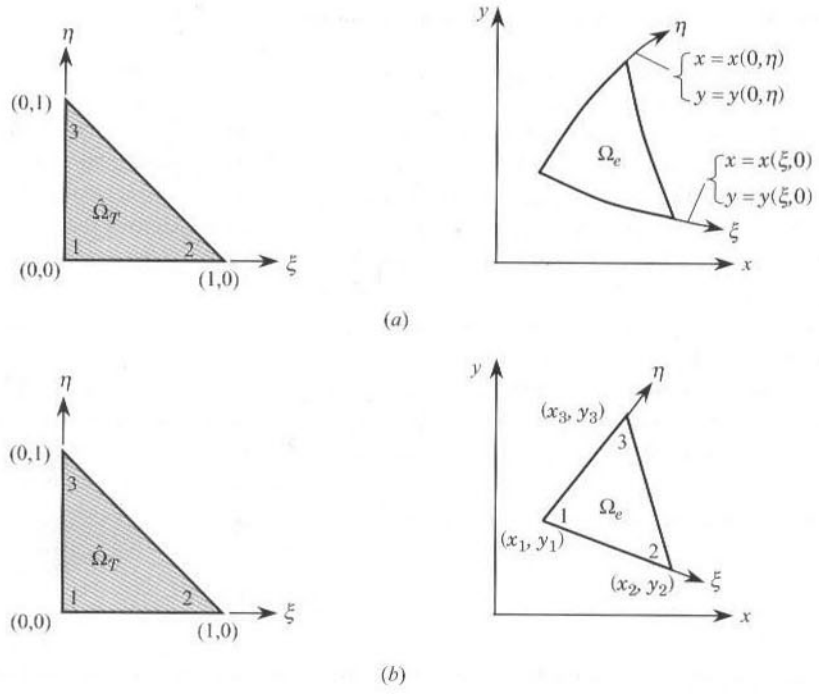

Figure 9.3.6 Triangular master finite element and its transformations: (*a*) general transformation; and (*b*) linear transformation of a master element to a triangular element.

The relations in (9.3.9) for isoparametric formulation with linear triangular elements have the explicit form,

$$\frac{\partial \psi_1}{\partial x} = -\frac{\beta_2+\beta_3}{2A} = \frac{\beta_1}{2A}, \qquad \frac{\partial \psi_1}{\partial y} = -\frac{\gamma_2+\gamma_3}{2A} = \frac{\gamma_1}{2A}$$
$$\frac{\partial \psi_2}{\partial x} = \frac{\beta_2}{2A}, \qquad \frac{\partial \psi_2}{\partial y} = \frac{\gamma_2}{2A}, \qquad \frac{\partial \psi_3}{\partial x} = \frac{\beta_3}{2A}, \qquad \frac{\partial \psi_3}{\partial y} = \frac{\gamma_3}{2A} \tag{9.3.31}$$

In a general case, the derivatives of ψ_i with respect to the global coordinates can be computed from Eqs.(9.3.9), which take the form

$$\frac{\partial \psi_i}{\partial x} = \frac{\partial \psi_i}{\partial L_1}\frac{\partial L_1}{\partial x} + \frac{\partial \psi_i}{\partial L_2}\frac{\partial L_2}{\partial x}$$
$$\frac{\partial \psi_i}{\partial y} = \frac{\partial \psi_i}{\partial L_1}\frac{\partial L_1}{\partial y} + \frac{\partial \psi_i}{\partial L_2}\frac{\partial L_2}{\partial y} \tag{9.3.32a}$$

or

$$\begin{Bmatrix} \dfrac{\partial \psi_i}{\partial x} \\ \dfrac{\partial \psi_i}{\partial y} \end{Bmatrix} = [J]^{-1} \begin{Bmatrix} \dfrac{\partial \psi_i}{\partial L_1} \\ \dfrac{\partial \psi_i}{\partial L_2} \end{Bmatrix}, \quad [J] = \begin{bmatrix} \dfrac{\partial x}{\partial L_1} & \dfrac{\partial y}{\partial L_1} \\ \dfrac{\partial x}{\partial L_2} & \dfrac{\partial y}{\partial L_2} \end{bmatrix} \tag{9.3.32b}$$

Note that only L_1 and L_2 are treated as linearly independent coordinates, because $L_3 = 1 - L_1 - L_2$.

After transformation, integrals on $\hat{\Omega}_T$ have the form

$$\int_{\hat{\Omega}_T} G(\xi, \eta) d\xi \, d\eta = \int_{\hat{\Omega}_T} \hat{G}(L_1, L_2, L_3) dL_1 \, dL_2 \tag{9.3.33}$$

which can be approximated by the quadrature formula

$$\int_{\hat{\Omega}_T} \hat{G}(L_1, L_2, L_3) dL_1 \, dL_2 \approx \frac{1}{2} \sum_{I=1}^{N} W_I \hat{G}(\mathrm{S}_I) \tag{9.3.34}$$

where W_I and S_I denote the weights and integration points of the quadrature rule. Table 9.3.2 contains the location of integration points and weights for one-, three-, and seven-point quadrature rules over triangular elements. For evaluation of integrals whose integrands are polynomials of degree higher than five (in any of the area coordinates), the reader should consult books on numerical integration [e.g., see Froberg (1969) and Carnahan, et al. (1969)].

Table 9.3.2 Quadrature points and weights for triangular elements.

Number of integration points	Degree of polynomial and order of the residual	Integration points and weights				Nodes	Geometric locations
		L_1	L_2	L_3	W		
1	1; $O(h^2)$	$\frac{1}{3}$	$\frac{1}{3}$	$\frac{1}{3}$	1	a	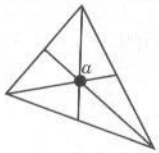
3	2; $O(h^3)$	$\frac{1}{2}$	0	$\frac{1}{2}$	$\frac{1}{3}$	a	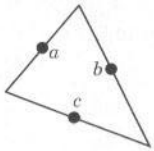
		$\frac{1}{2}$	$\frac{1}{2}$	0	$\frac{1}{3}$	b	
		0	$\frac{1}{2}$	$\frac{1}{2}$	$\frac{1}{3}$	c	
4	3; $O(h^4)$	$\frac{1}{3}$	$\frac{1}{3}$	$\frac{1}{3}$	$-\frac{27}{48}$	a	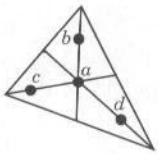
		0.6	0.2	0.2	$\frac{25}{48}$	b	
		0.2	0.6	0.2	$\frac{25}{48}$	c	
		0.2	0.2	0.6	$\frac{25}{48}$	d	
7	5; $O(h^6)$	$\frac{1}{3}$	$\frac{1}{3}$	$\frac{1}{3}$	0.225	a	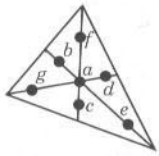
		α_1†	β_1	β_1		b	
		β_1	α_1	β_1	W_2	c	
		β_1	β_1	α_1		d	
		α_2	β_2	β_2		e	
		β_2	α_2	β_2	W_3	f	
		β_2	β_2	α_2		g	

† $\alpha_1 = 0.797\,426\,985\,353$, $\beta_1 = 0.101\,286\,507\,323$, $\alpha_2 = 0.059\,715\,871\,789$, $\beta_2 = 0.470\,142\,064\,105$, $W_2 = 0.125\,939\,180\,544$, $W_3 = 0.132\,394\,152\,788$.

Example 9.3.4

Consider the quadratic triangular element shown in Fig. 9.3.7. We wish to calculate $\partial\psi_1/\partial x$, $\partial\psi_1/\partial y$, $\partial\psi_4/\partial x$, and $\partial\psi_4/\partial y$ at the point $(x, y) = (2, 4)$ and evaluate the integral of the product $(\partial\psi_1/\partial x)(\partial\psi_4/\partial x)$.

Since the element has straight edges, its geometry is defined by the interpolation functions of the corner nodes (i.e., subparametric formulation can be used). Note that if the element is curvilinear, we cannot use three corner nodes only to describe the geometry exactly (hence, the isoparametric formulation must be used). For the element at hand, we have

$$x = \sum_{i=1}^{3} x_i L_i = 7L_2 + 2L_3 = 2 - 2L_1 + 5L_2$$

$$y = \sum_{i=1}^{3} y_i L_i = 2L_2 + 6L_3 = 6 - 6L_1 - 4L_2 \tag{9.3.35a}$$

$$[J] = \begin{bmatrix} -2 & -6 \\ 5 & -4 \end{bmatrix}, \qquad [J]^{-1} = \frac{1}{38}\begin{bmatrix} -4 & 6 \\ -5 & -2 \end{bmatrix}$$

$$\begin{Bmatrix} \dfrac{\partial\psi_1}{\partial x} \\ \dfrac{\partial\psi_1}{\partial y} \end{Bmatrix} = \frac{1}{38}\begin{bmatrix} -4 & 6 \\ -5 & -2 \end{bmatrix} \begin{Bmatrix} \dfrac{\partial\psi_1}{\partial L_1} \\ \dfrac{\partial\psi_1}{\partial L_2} \end{Bmatrix} = \begin{Bmatrix} -\dfrac{4(4L_1 - 1)}{38} \\ -\dfrac{5(4L_1 - 1)}{38} \end{Bmatrix}$$

$$\begin{Bmatrix} \dfrac{\partial\psi_4}{\partial x} \\ \dfrac{\partial\psi_4}{\partial y} \end{Bmatrix} = \frac{1}{38}\begin{bmatrix} -4 & 6 \\ -5 & -2 \end{bmatrix} \begin{Bmatrix} \dfrac{\partial\psi_4}{\partial L_1} \\ \dfrac{\partial\psi_4}{\partial L_2} \end{Bmatrix} = \frac{1}{38}\begin{Bmatrix} -16L_2 + 24L_1 \\ -20L_2 - 8L_1 \end{Bmatrix} \tag{9.3.35b}$$

where $\psi_1 = L_1(2L_1 - 1)$ and $\psi_4 = 4L_1L_2$ [see Eq. (9.2.16) and Fig. 9.2.4(*b*)], so that

$$\frac{\partial\psi_1}{\partial L_1} = L_1 - 1, \qquad \frac{\partial\psi_1}{\partial L_2} = 0, \qquad \frac{\partial\psi_4}{\partial L_1} = 4L_2, \qquad \frac{\partial\psi_4}{\partial L_2} = 4L_1$$

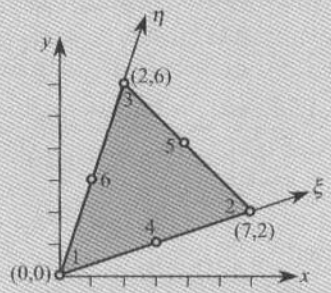

Figure 9.3.7 A quadratic triangular element in the global (x, y) and local coordinate systems (Example 9.3.4).

For the point (2, 4), the area coordinates can be calculated from Eqs. (9.3.35a):

$$2 = 7L_2 + 2L_3, \qquad 4 = 2L_2 + 6L_3$$

Once L_2 and L_3 are computed from the above relations, L_1 is found from the relation $L_1 = 1 - L_2 - L_3$. We have

$$L_1 = \frac{5}{19}, \qquad L_2 = \frac{2}{19}, \qquad L_3 = \frac{12}{19}$$

Evaluating $\partial\psi_4/\partial x$ and $\partial\psi_4/\partial y$ at the point (2, 4), we obtain

$$\begin{aligned}
\frac{\partial\psi_1}{\partial x} &= -\frac{2}{19}\left(\frac{20}{19} - 1\right) = -\frac{2}{361} \\
\frac{\partial\psi_1}{\partial y} &= -\frac{5}{38}\left(4 \times \frac{5}{19} - 1\right) = -\frac{5}{722} \\
\frac{\partial\psi_4}{\partial x} &= -\frac{16}{(19)^2} + \frac{60}{(19)^2} = \frac{44}{361} \\
\frac{\partial\psi_4}{\partial y} &= -\frac{20}{(19)^2} - \frac{20}{(19)^2} = -\frac{40}{361}
\end{aligned} \tag{9.3.36}$$

The integral of $(\partial\psi_1/\partial x)(\partial\psi_4/\partial x)$ over the quadratic element is ($J = 38$)

$$\int_{\Omega_T} \frac{\partial\psi_1}{\partial x}\frac{\partial\psi_4}{\partial x}\,dx\,dy = -\frac{4J}{361}\int_0^1 \int_0^{1-L_2} (4L_1 - 1)(6L_1 - 4L_2)\,dL_1\,dL_2$$

Since the integrand is quadratic in L_1 and bilinear in L_1 and L_2, we use the three-point quadrature (see Table 9.3.2) to evaluate the integral exactly [see Eq. (9.3.34)]:

$$\begin{aligned}
&-\frac{4J}{361}\int_0^1 \int_0^{1-L_2} (4L_1 - 1)(6L_1 - 4L_2)\,dL_1\,dL_2 \\
&\quad = -\frac{1}{2}\frac{4 \times 38}{361}\frac{1}{3}\left[\left(\frac{4}{2} - 1\right)\left(\frac{6}{2} - 0\right) + \left(\frac{4}{2} - 1\right)\left(\frac{6}{2} - \frac{4}{2}\right) + (0 - 1)\left(0 - \frac{4}{2}\right)\right] \\
&\quad = -\frac{8}{19}
\end{aligned} \tag{9.3.37}$$

The result can be verified using the exact integration formula in (9.2.18*b*):

$$\int_{\Omega_T} \frac{\partial\psi_1}{\partial x}\frac{\partial\psi_4}{\partial x}\,dx\,dy = \frac{4}{361}\left[6 \times \frac{1}{3!} - 4 \times \frac{1}{3!} - 24 \times \frac{2!}{4!} + 16 \times \frac{1}{4!}\right] 2A = -\frac{8}{19}$$

The area A of the triangle is equal to 19, and therefore we obtain the same result as above.

9.4 MODELING CONSIDERATIONS

9.4.1 Preliminary Comments

Numerical simulation of a physical processes requires (*a*) a mathematical model that describes the process and (*b*) a numerical method to analyze the mathematical model. In

the development of a mathematical model we often make a set of assumptions about the process (e.g., constitutive behavior, loads, and boundary conditions) to derive the mathematical relationships governing the system. The mathematical model, which is often in the form of differential equations, is used to gain an understanding of how the corresponding process works. If the relationships are simple, it is possible to obtain *exact* information on the quantities of interest. This is known as the *analytic* solution. However, most practical problems are too complicated to allow analytical solutions of the models. Hence, these mathematical models must be studied by numerical methods, such as the finite element method.

Finite element analysis is a numerical simulation of a physical process. Therefore, finite element modeling involves assumptions concerning the representation of the system and/or its behavior. Valid assumptions can be made only if we have a qualitative understanding of how the process or system works. A good knowledge of the basic principles governing the process and the finite element theory enable the development of a good numerical model of the actual process.

Here we discuss several aspects of development of finite element models. Guidelines concerning element geometries, mesh refinements, and load representations are given.

9.4.2 Element Geometries

Recall from Section 9.3 that the numerical evaluation of integrals over actual elements involves a coordinate transformation from the actual element to a master element. The transformation is acceptable if and only if every point in the actual element is mapped uniquely into a point in the master element, and vice versa. Such mappings are termed *one-to-one*. This requirement can be expressed as [see Eq. (9.3.12)]

$$J^e \equiv \det[J^e] > 0 \qquad \text{everywhere in the element } \Omega_e \tag{9.4.1}$$

where $[J^e]$ is the Jacobian matrix in Eq. (9.3.11*b*). Geometrically, the Jacobian J^e represents the ratio of an area element in the real element to the corresponding area element in the master element,

$$dA \equiv dx\, dy = J^e d\xi\, d\eta$$

If J^e is zero, then a nonzero area element in the real element is mapped into zero area in the master element, which is unacceptable. Also, if $J^e < 0$, a right-handed coordinate system is mapped into a left-handed coordinate system.

In general, the Jacobian is a function of ξ and η, implying that the real element is nonuniformly mapped into the master element, i.e., the element is distorted. Excessive distortion of elements is not good because a nonzero area element can be mapped into a zero or nearly zero area.

To ensure $J^e > 0$ and keep within the extreme limits of acceptable distortion, certain geometric shapes of real elements must be avoided. For example, the interior angle at each vertex of a triangular element should not be equal to either 0° or 180°. Indeed, in practice the angle should reasonably be larger than 0° and smaller than 180° to avoid numerical ill-conditioning of element matrices. Although the acceptable range depends on the problem, the range $15^\circ - 165^\circ$ can be used as a guide. Figure 9.4.1 shows elements with unacceptable vertex angles for straight-sided and curved-sided elements.

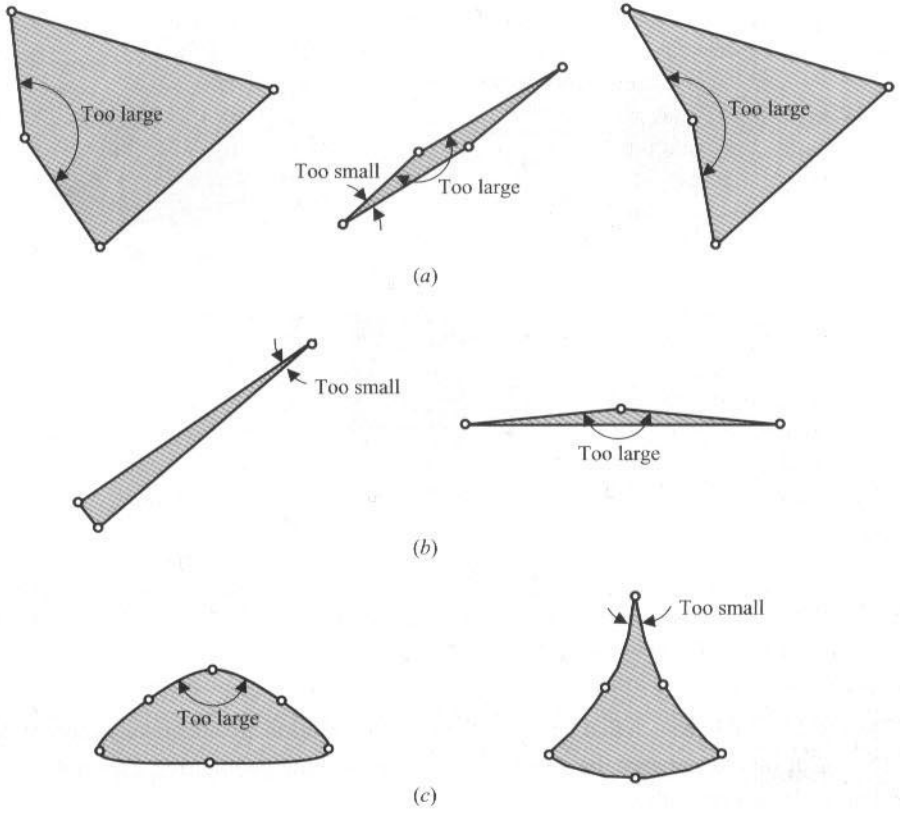

Figure 9.4.1 Finite elements with unacceptable vertex angles: (*a*) linear quadrilateral elements; (*b*) linear triangular elements; and (*c*) quadratic triangular elements. The angles marked are either too small compared with 0° or too large compared with 180°.

For higher-order Lagrange elements (also called the C^0 elements), the locations of the interior nodes contribute to the element distortion, and therefore they are constrained to lie within certain distance from the vertex nodes. For example, in the case of a quadratic element the midside node should be at a distance not less than one-fourth of the length of the side from the vertex nodes (see Fig. 9.4.2). When the midside node is located exactly at a distance of one fourth of the side length from a vertex, the element exhibits special properties (see Problem 9.19). Such elements, called *quarter-point elements*, are used in fracture mechanics problems to represent an inverse square-root singularity in the gradient of the solution at the nearest vertex node.

9.4.3 Mesh Generation

Generation of a finite element mesh for a given problem should follow the guidelines listed below:

1. The mesh should represent the geometry of the computational domain and load representation accurately.

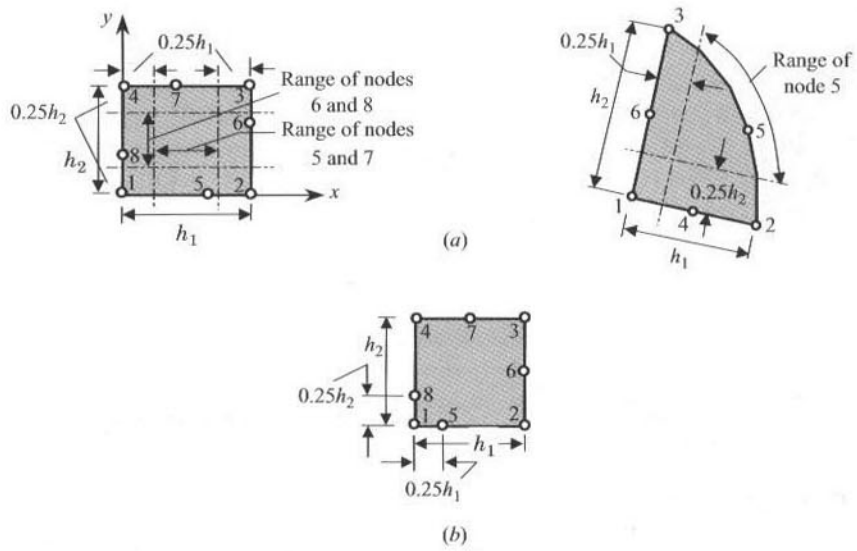

Figure 9.4.2 Range of acceptable locations of the midside nodes for quadratic elements: (*a*) eight-node quadratic element and six-node quadratic triangular element; and (*b*) the quarter-point quadrilateral element.

2. The mesh should be such that large gradients in the solution are adequately represented.
3. The mesh should not contain elements with unacceptable geometries, especially in regions of large gradients.

Within the above guidelines, the mesh used can be *coarse* (i.e., have few elements) or *refined* (i.e., have many elements), and may consist of one or more orders and types of elements (e.g., linear and quadratic, triangular and quadrilateral). A judicious choice of element order and type could save computational cost while giving accurate results. It should be noted that the choice of elements and mesh is problem-dependent. What works well for one problem may not work well for another problem. An analyst with physical insight into the process being simulated can make a better choice of elements and mesh for the problem at hand. We should start with a coarse mesh that meets the three requirements listed above, exploit symmetries available in the problem, and evaluate the results thus obtained in light of physical understanding and approximate analytical and/or experimental information. These results can be used to guide subsequent mesh refinements and analyses.

Generation of meshes of single element type is easy because elements of the same degree are compatible with each other (see Fig. 9.4.3). Mesh refinements involve several options. Refine the mesh by subdividing existing elements into two or more elements of the same type [see Fig. 9.4.4(*a*)]. This is called the *h-version mesh refinement*. Alternatively, existing elements can be replaced by elements of higher order [see Fig. 9.4.4(*b*)]. This type of refinement is called the *p-version mesh refinement*. The *h, p-version mesh refinement*, in which elements are subdivided into two or more elements in some places and replaced with higher-order elements in other places. Generally, local mesh refinements should be such that very small elements are not placed adjacent to very large ones (see Fig. 9.4.5).

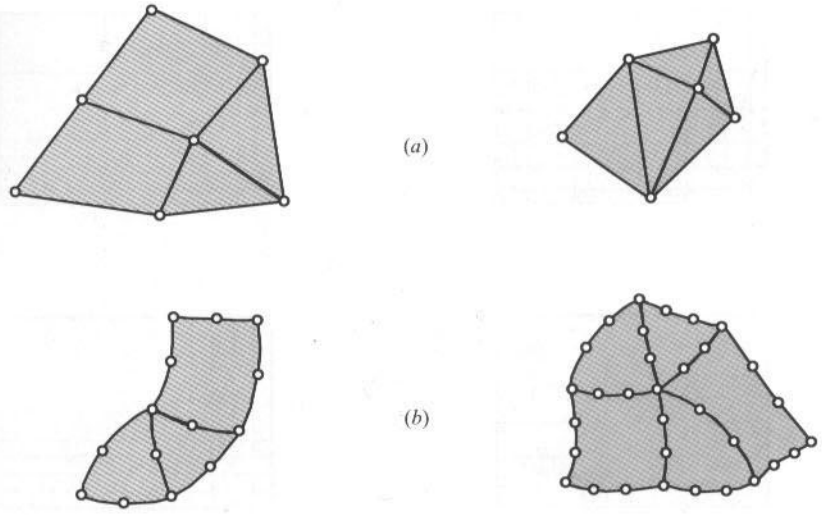

Figure 9.4.3 Connecting elements of the same order. The C^0 elements of the same order ensure the C^0 continuity along the element interfaces: (*a*) linear elements; and (*b*) quadratic and cubic elements.

Combining elements of different *kinds* naturally arises in solid and structural mechanics problems. For example, plate bending elements (2-D) can be connected to a beam element (1-D). If the plate element is based on the classical plate theory (see Chapter 12), the beam element should be one based on the Euler–Bernoulli beam theory so that they have the same degrees of freedom at the connecting node. When a plane elasticity element (see Chapter 11) is connected to a beam element, which are not compatible with the former

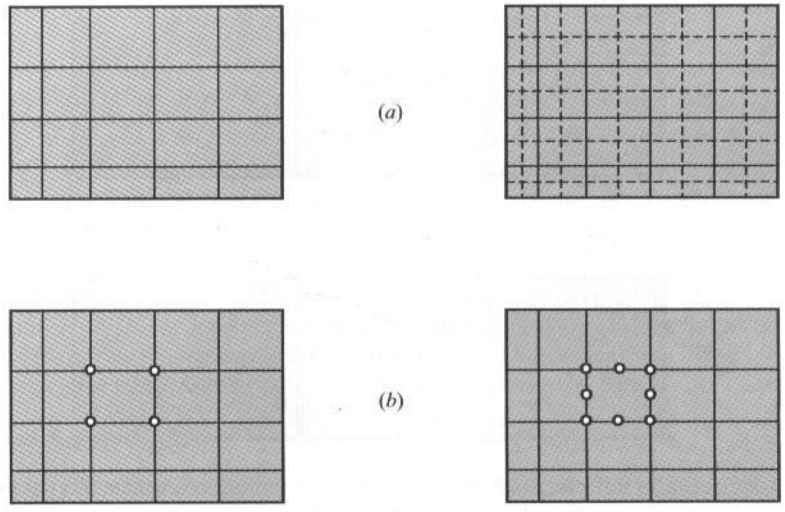

Figure 9.4.4 The (*a*) *h*-version and (*b*) *p*-version mesh refinements.

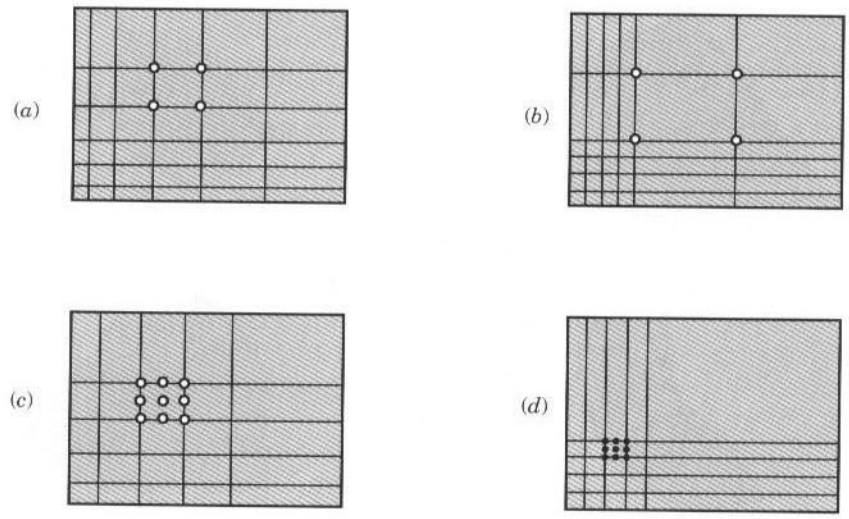

Figure 9.4.5 Finite element mesh refinements. Meshes shown in (*a*) and (*c*) are acceptable, and those shown in (*b*) and (*d*) are unacceptable.

in terms of the degrees of freedom at the nodes, we must construct a special element that makes the transition from the 2-D plane elasticity element to the 1-D beam element (see Problem 11.8). Such elements are called *transition elements*.

Combining elements of different order, say linear to quadratic elements, may be necessary to accomplish local mesh refinements. There are two ways to do this. One way is to use a transition element, which has different number of nodes on different sides [see Fig. 9.4.6(*a*)]. The other way is to impose a condition that constrains the midside node

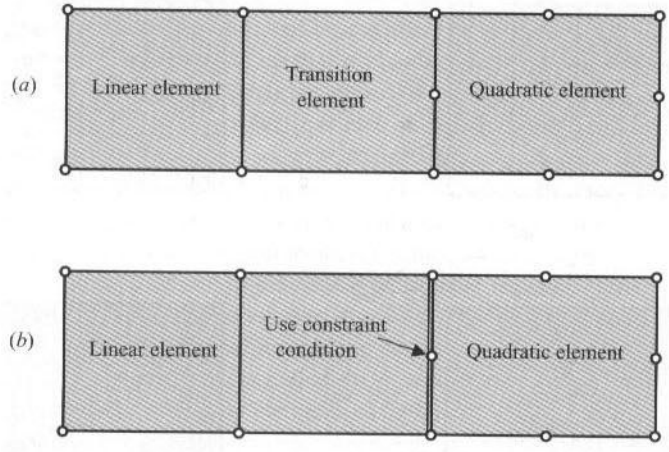

Figure 9.4.6 Combining different order elements: (*a*) use of a transition element that has three sides linear and one side quadratic; and (*b*) use of a linear constraint equation to connect a linear side to a quadratic side.

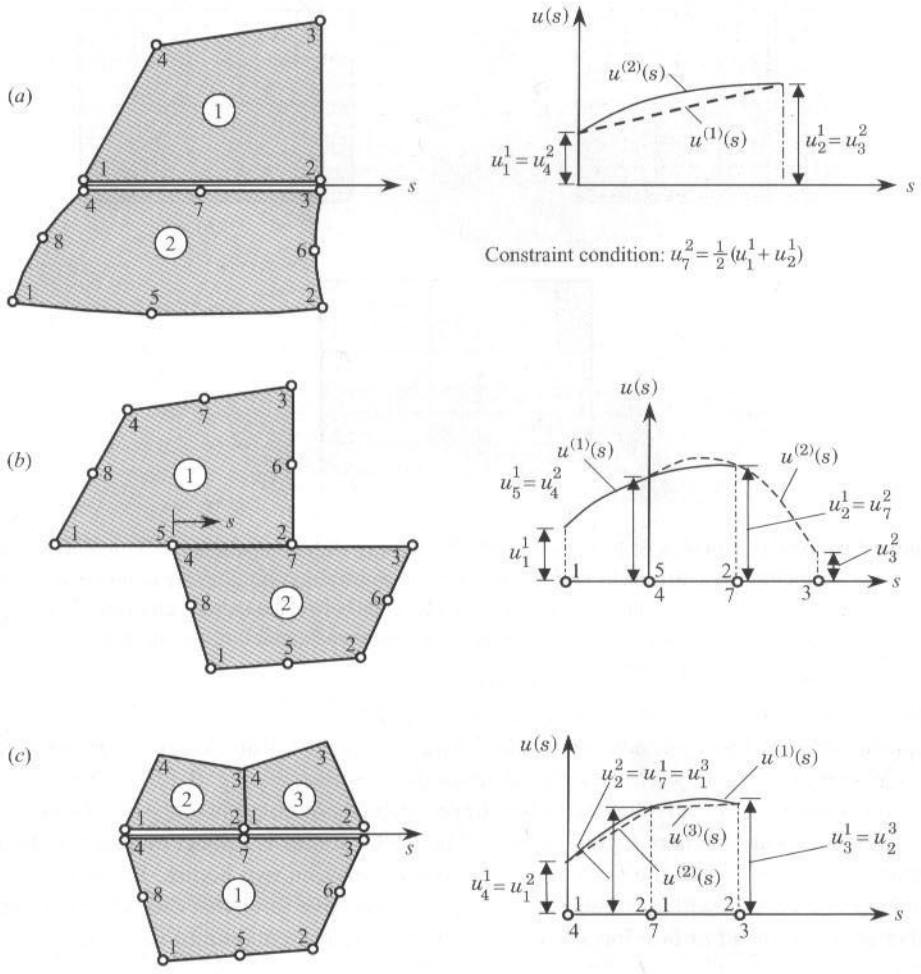

Figure 9.4.7 Various types of incompatible connections of finite elements. In all cases the interelement continuity of the function is violated along the connecting side.

to have the same value as that experienced at the node by the lower-order element [see Fig. 9.4.6(*b*)]. However, such combinations do not enforce interelement continuity of the solution along the entire interface. Figure 9.4.7 contains element connections that do not satisfy the C^0 continuity along the connecting sides. Use of transition elements and constraint conditions in local mesh refinements is a common practice. Figure 9.4.8 shows a few examples of such refinements.

9.4.4 Load Representation

Computation of the nodal contributions of a distributed boundary source was discussed in Chapter 8 [see Eq. (8.2.56)]. The accuracy of the result depends on the element and mesh used to represent the domain. For example, in heat transfer problems the boundary source

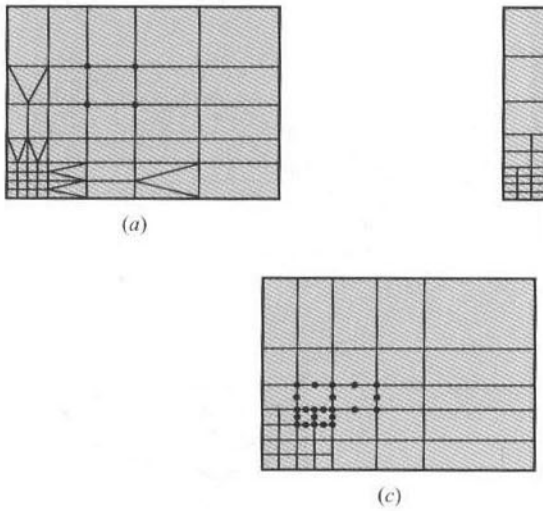

Figure 9.4.8 Some examples of local mesh refinements; (*a*) with compatible (C^0-continuous) elements; (*b*) with transition elements (or when constraint conditions are imposed) between linear elements; and (*c*) with transition elements between quadratic elements. In (*b*) and (*c*), the transition elements can be between linear and quadratic, and quadratic and cubic elements, respectively.

is the heat flux across (i.e., normal to) the boundary. Use of linear elements, for example, to represent the boundary will change the actual distribution (see Fig. 9.4.9). Of course, *h*-version or *p*-version mesh refinements will improve the representation of the boundary flux.

Another situation where representation of boundary forces is subject to different interpretations is found when the force is due to contact between two bodies. For example, a solid plate in contact with a circular disc generates a reactive force that can be represented either as a point load or as a locally distributed force. Representation of the contact force

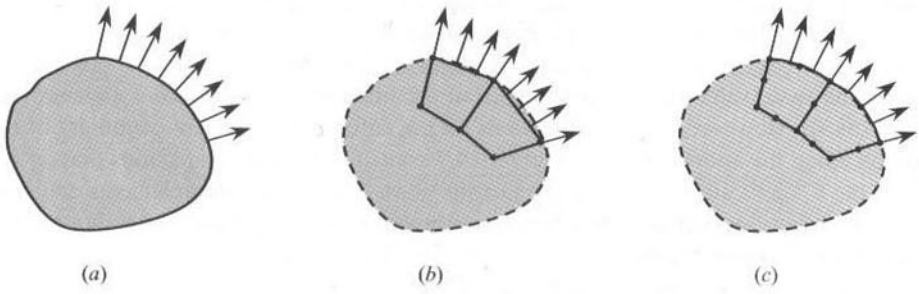

Figure 9.4.9 Approximation of the boundary fluxes in the finite element method; (*a*) actual geometry of the domain and distribution of flux; (*b*) approximation of the domain by linear finite elements and associated representation of the boundary flux; and (*c*) approximation of the domain by quadratic finite elements and associated representation of the boundary flux.

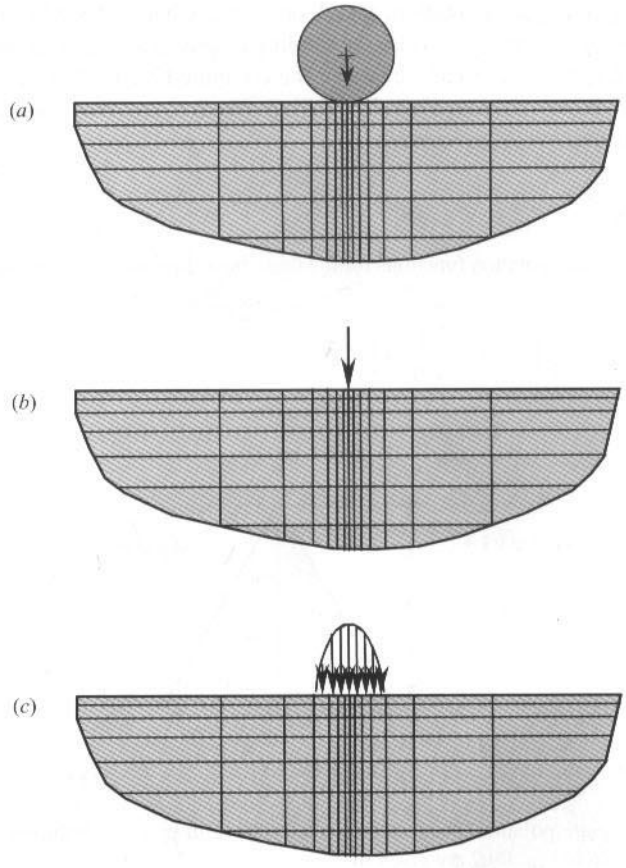

Figure 9.4.10 Representation of contact pressure developed between two bodies; (*a*) geometry of the bodies in contact; (*b*) representation of the contact pressure as a point load; and (*c*) representation of the contact pressure as a distributed surface load. In the latter case, often the surface area of the distributed force is unknown.

between deformable bodies as a point load is an approximation of the true distribution. A sine distribution might be more realistic representation of the actual force (see Fig. 9.4.10).

9.5 SUMMARY

In this chapter three major topics have been discussed: (1) Lagrange interpolation functions for triangular and rectangular elements; (2) numerical integration to evaluate integral expressions over triangular and rectangular elements; and (3) some modeling guidelines. Interpolation functions for linear, quadratic, and cubic triangular elements are developed using the area coordinates. Linear, quadratic, and cubic interpolation functions for Lagrange and serendipity family of rectangular elements are also developed. A systematic description of numerical evaluation of integral expressions involving interpolation functions and their derivatives with respect to global coordinates has been presented. This development is

suitable for computer implementation, as will be seen in Chapter 13. Modeling is an art that can be improved by experience and understanding of physical interactions involved in the process. It is necessary to critically evaluate the computed results before using them. The guidelines are given to encourage good modeling practice, and they should be followed to determine the actual "working" model.

PROBLEMS

9.1 Show that the interpolation functions for the three-node equilateral triangular element given in Fig. P9.1 are

$$\psi_1 = \frac{1}{2}\left(1 - \xi - \frac{1}{\sqrt{34}}\eta\right), \quad \psi_2 = \frac{1}{2}\left(1 + \xi - \frac{1}{\sqrt{34}}\eta\right), \quad \psi_3 = \frac{1}{\sqrt{34}}\eta$$

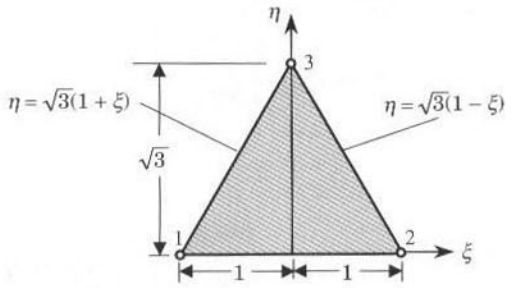

Figure P9.1

9.2 Show that the interpolation functions that involve the term $\xi^2 + \eta^2$ for the five-node rectangular element shown in Fig. P9.2 are given by

$$\psi_1 = 0.25(-\xi - \eta + \xi\eta) + 0.125(\xi^2 + \eta^2)$$
$$\psi_2 = 0.25(\xi - \eta - \xi\eta) + 0.125(\xi^2 + \eta^2)$$
$$\psi_3 = 0.25(\xi + \eta + \xi\eta) + 0.125(\xi^2 + \eta^2)$$
$$\psi_4 = 0.25(-\xi + \eta - \xi\eta) + 0.125(\xi^2 + \eta^2)$$
$$\psi_5 = 1 - 0.5(\xi^2 + \eta^2)$$

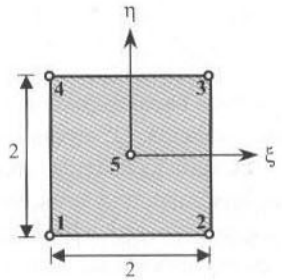

Figure P9.2

9.3 Calculate the interpolation functions $\psi_i(x, y)$ for the quadratic triangular element shown in Fig. P9.3. *Hint:* Use Eq. (9.2.16), where L_i are given by Eq. (9.2.9).

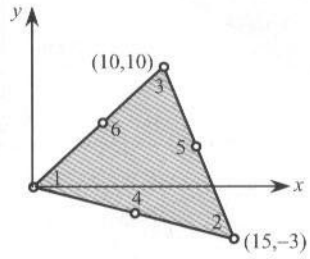

Figure P9.3

9.4 Determine the interpolation function ψ_{14} in terms of the area coordinates, L_i for the triangular element shown in Fig. P9.4.
Answer: $32L_1L_2L_3(4L_2 - 1)$.

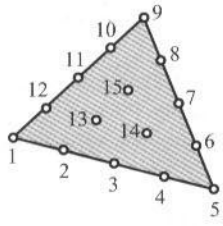

Figure P9.4

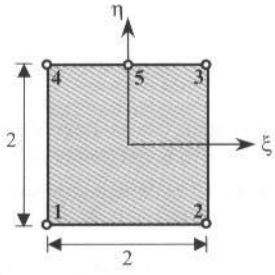

Figure P9.6

9.5 Derive the interpolation function of a corner node in a cubic serendipity element.

9.6 Consider the five-node element shown in Fig. P9.6. Using the basic linear and quadratic interpolations along the coordinate directions ξ and η, derive the interpolation functions for the element. Note that the element can be used as a transition element connecting four-node elements to eight- or nine-node elements.

9.7 (*Nodeless variables*) Consider the four-node rectangular element with interpolation of the form

$$u = \sum_{i=1}^{4} u_i \psi_i + \sum_{i=1}^{4} c_i \phi_i$$

where u_i are the nodal values and c_i are arbitrary constants. Determine the form of ψ_i and ϕ_i for the element.

9.8–9.10 Determine the Jacobian matrix and the transformation equations for the elements given in Fig. P9.8–P9.10.

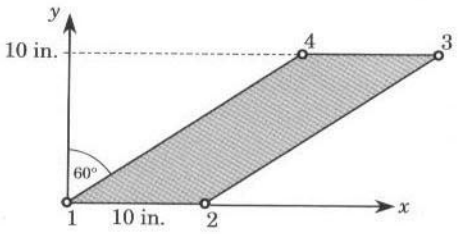

Figure P9.8

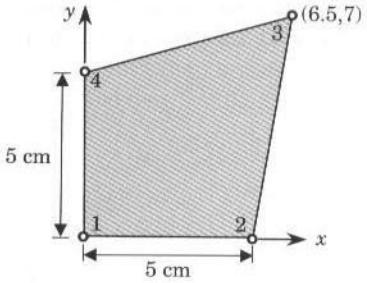

Figure P9.9

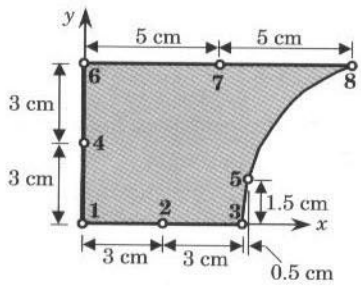

Figure P9.10

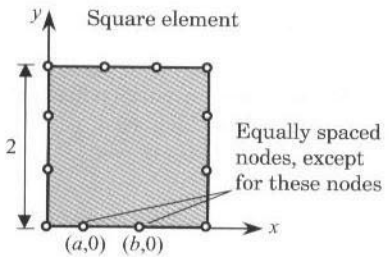

Figure P9.12

9.11 Using the Gauss–Legendre quadrature, determine the contribution of a constant distributed source to nodal points of the four-node finite element in Fig. P9.9.

9.12 For a 12-node serendipity (cubic) element, as illustrated in Fig. P9.12, show that the Jacobian $J = J_{11}$ is

$$\begin{aligned} J \; &= 0.4375 + 0.84375(b-a) + 0.5625\eta - 0.84375(b-a)\eta \\ &\quad + 1.125\xi - 0.5625(a+b)\xi - 1.125\eta\xi + 0.5625(a+b)\eta\xi \\ &\quad + 1.6875\xi^2 - 2.53125(b-a)\xi^2 - 1.6875\eta\xi^2 + 2.53125(b-a)\eta\xi^2 \end{aligned}$$

What can you conclude from the requirement $J > 0$?

9.13 Determine the Jacobian of the eight-node rectangular element of Fig. P9.13 in terms of the parameter a.

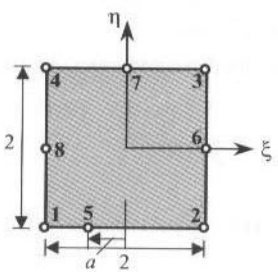

Figure P9.13

9.14 Determine the conditions on the location of node 3 of the quadrilateral element shown in Fig. P9.14. Show that the transformation equations are given by

$$x = \frac{1}{4}(1+\xi)\,[2(1-\eta) + a(1+\eta)]$$

$$y = \frac{1}{4}(1+\eta)\,[2(1-\xi) + b(1+\xi)]$$

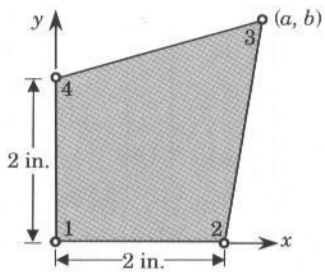

Figure P9.14

9.15 Determine the global derivatives of the interpolation functions for node 3 of the element shown in Fig. P9.9.

9.16 Let the transformation between the global coordinates (x, y) and local normalized coordinates (ξ, η) in a Lagrange element Ω_e be

$$x = \sum_{i=1}^{m} x_i \hat{\psi}_i(\xi, \eta), \qquad y = \sum_{i=1}^{m} y_i \hat{\psi}_i(\xi, \eta)$$

where (x_i, y_i) denote the global coordinates of the element nodes. The differential lengths in the two coordinates are related by

$$dx_e = \frac{\partial x_e}{\partial \xi} d\xi + \frac{\partial x_e}{\partial \eta} d\eta, \qquad dy_e = \frac{\partial y_e}{\partial \xi} \xi + \frac{\partial y_e}{\partial \eta} d\eta$$

or

$$\begin{Bmatrix} dx_e \\ dy_e \end{Bmatrix} = \begin{bmatrix} \dfrac{\partial x_e}{\partial \xi} & \dfrac{\partial x_e}{\partial \eta} \\ \dfrac{\partial y_e}{\partial \xi} & \dfrac{\partial y_e}{\partial \eta} \end{bmatrix} \begin{Bmatrix} d\xi \\ d\eta \end{Bmatrix} = [T] \begin{Bmatrix} d\xi \\ d\eta \end{Bmatrix}$$

In the finite element literature, the transpose of $[T]$ is called the Jacobian matrix, $[J]$. Show that the derivatives of the interpolation function $\psi_i^e(\xi, \eta)$ with respect to the global coordinates (x, y) are related to their derivatives with respect to the local coordinates (ξ, η) by

$$\begin{Bmatrix} \dfrac{\partial \psi_i^e}{\partial x} \\ \dfrac{\partial \psi_i^e}{\partial y} \end{Bmatrix} = [J]^{-1} \begin{Bmatrix} \dfrac{\partial \psi_i^e}{\partial \xi} \\ \dfrac{\partial \psi_i^e}{\partial \eta} \end{Bmatrix}$$

and

$$\begin{Bmatrix} \dfrac{\partial^2 \psi_i^e}{\partial x^2} \\ \dfrac{\partial^2 \psi_i^e}{\partial y^2} \\ \dfrac{\partial^2 \psi_i^e}{\partial x\, \partial y} \end{Bmatrix} = \begin{bmatrix} \left(\dfrac{\partial x_e}{\partial \xi}\right)^2 & \left(\dfrac{\partial y_e}{\partial \xi}\right)^2 & 2\dfrac{\partial x_e}{\partial \xi}\dfrac{\partial y_e}{\partial \xi} \\ \left(\dfrac{\partial x_e}{\partial \eta}\right)^2 & \left(\dfrac{\partial y_e}{\partial \eta}\right)^2 & 2\dfrac{\partial x_e}{\partial \eta}\dfrac{\partial y_e}{\partial \eta} \\ \dfrac{\partial x_e}{\partial \xi}\dfrac{\partial x_e}{\partial \eta} & \dfrac{\partial y_e}{\partial \xi}\dfrac{\partial y_e}{\partial \eta} & \dfrac{\partial x_e}{\partial \eta}\dfrac{\partial y_e}{\partial \xi} + \dfrac{\partial x_e}{\partial \xi}\dfrac{\partial y_e}{\partial \eta} \end{bmatrix}^{-1}$$
$$\times \left(\begin{Bmatrix} \dfrac{\partial^2 \psi_i^e}{\partial \xi^2} \\ \dfrac{\partial^2 \psi_i^e}{\partial \eta^2} \\ \dfrac{\partial^2 \psi_i^e}{\partial \xi\, \partial \eta} \end{Bmatrix} - \begin{bmatrix} \dfrac{\partial^2 x_e}{\partial \xi^2} & \dfrac{\partial^2 y_e}{\partial \xi^2} \\ \dfrac{\partial^2 x_e}{\partial \eta^2} & \dfrac{\partial^2 y_e}{\partial \eta^2} \\ \dfrac{\partial^2 x_e}{\partial \xi\, \partial \eta} & \dfrac{\partial^2 y_e}{\partial \xi\, \partial \eta} \end{bmatrix} \begin{Bmatrix} \dfrac{\partial \psi_i^e}{\partial x} \\ \dfrac{\partial \psi_i^e}{\partial y} \end{Bmatrix} \right)$$

9.17 (*Continuation of Problem 9.16*) Show that the Jacobian can be computed from the equation

$$[J] = \begin{Bmatrix} \dfrac{\partial \psi_1^e}{\partial \xi} & \dfrac{\partial \psi_2^e}{\partial \xi} & \cdots & \dfrac{\partial \psi_n^e}{\partial \xi} \\ \dfrac{\partial \psi_1^e}{\partial \eta} & \dfrac{\partial \psi_2^e}{\partial \eta} & \cdots & \dfrac{\partial \psi_n^e}{\partial \eta} \end{Bmatrix} \begin{bmatrix} x_1^e & y_1^e \\ x_2^e & y_2^e \\ \vdots & \vdots \\ x_n^e & y_n^e \end{bmatrix}$$

9.18 Find the Jacobian matrix for the nine-node quadrilateral element shown in Fig. P9.18. What is the determinant of the Jacobian matrix?

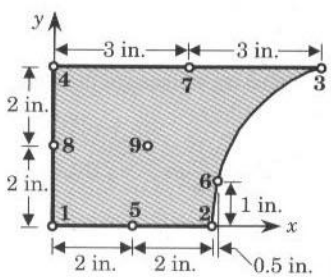

Figure P9.18

9.19 For the eight-node element shown in Fig. P9.19, show that the x coordinate along the side 1–2 is related to the ξ coordinate by the relation

$$x = -\frac{1}{2}\xi(1-\xi)x_1^e + \frac{1}{2}\xi(1+\xi)x_2^e + (1-\xi^2)x_5^e$$

and that the following relations hold:

$$\xi = 2\left(\frac{x}{a}\right)^{1/2} - 1, \qquad \frac{\partial x}{\partial \xi} = (xa)^{1/2}$$

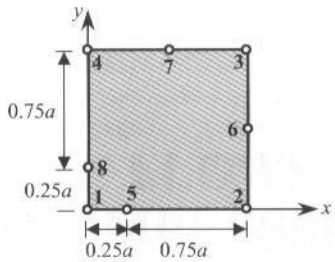

Figure P9.19

Also, show that

$$u_h(x,0) = -\left[2\left(\frac{x}{a}\right)^{1/2} - 1\right]\left[1 - \left(\frac{x}{a}\right)^{1/2}\right] u_1^e + \left[-1 + 2\left(\frac{x}{a}\right)^{1/2}\right]\left(\frac{x}{a}\right)^{1/2} u_2^e + 4\left[\left(\frac{x}{a}\right)^{1/2} - \frac{x}{a}\right] u_5^e$$

$$\left.\frac{\partial u_h}{\partial x}\right|_{(x,0)} = -\frac{1}{(xa)^{1/2}}\left\{\frac{1}{2}\left[3 - 4\left(\frac{x}{a}\right)^{1/2}\right] u_1^e + \frac{1}{2}\left[-1 + 4\left(\frac{x}{a}\right)^{1/2}\right] u_2^e + 2\left[1 - 2\left(\frac{x}{a}\right)^{1/2}\right] u_5^e\right\}$$

Thus, $\partial u_h/\partial x$ grows at a rate of $(xa)^{-1/2}$ as x approaches zero along the side 1–2. In other words, we have a $x^{-1/2}$ singularity at node 1. Such elements are used in fracture mechanics problems.

9.20 Using the tensor product of the one-dimensional Hermite cubic interpolation functions, obtain the Hermite cubic interpolation functions (16 of them) for the four-node rectangular element.

REFERENCES FOR ADDITIONAL READING

1. Burnett, D. S., *Finite Element Analysis from Concepts to Applications*, Addison-Wesley Publishing Company, Reading, MA, 1987.
2. Carnahan, B., Luther, H. A., and Wilkes, J. O., *Applied Numerical Methods*, John Wiley, New York, 1969.
3. Cowper, G. R., "Gaussian Quadrature Formulas for Triangles," *International Journal for Numerical Methods in Engineering*, **7**, 405–408, 1973.
4. Froberg, C. E., *Introduction to Numerical Analysis*, Addison-Wesley, Reading, MA, 1969.
5. Hammer, P. C., Marlowe, O. P., and Stroud, A. H., "Numerical Integration over Simplexes and Cones," *Mathematics Tables Aids Comp.*, National Research Council (Washington), **10**, 130–137, 1956.
6. Irons, B. M., "Quadrature Rules for Brick-Based Finite Elements," *International Journal for Numerical Methods in Engineering*, **3**, 293–294, 1971.
7. Loxan, A. N., Davids, N., and Levenson, A., "Table of the Zeros of the Legendre Polynomials of Order 1–16 and the Weight Coefficients for Gauss' Mechanical Quadrature Formula," *Bulletin of the American Mathematical Society*, **48**, 739–743, 1942.
8. Reddy, C. T. and Shippy, D. J., "Alternative Integration Formulae for Triangular Finite Elements," *International Journal for Numerical Methods in Engineering*, **17**, 133–139, 1981.
9. Silvester, P., "Newton–Cotes Quadrature Formulae for N-Dimensional Simplexes," *Proceedings of 2nd Canadian Congress of Applied Mechanics* (Waterloo, Ontario, Canada), 1969.
10. Stroud, A. H. and Secrest, D., *Gaussian Quadrature Formulas*, Prentice-Hall, Engelwood Cliffs, NJ, 1966.

Chapter 10

FLOWS OF VISCOUS INCOMPRESSIBLE FLUIDS

10.1 PRELIMINARY COMMENTS

In Chapter 8, we considered the finite element analysis of second-order partial differential equations in one dependent unknown. Such equations arise in two-dimensional heat transfer, torsion of a cylindrical members of arbitrary cross section, deflection of membranes in a plane, and inviscid flows in two dimensions. In this chapter, we consider flows of viscous incompressible fluids in two dimensions whose governing equations are described by a set of three *coupled* partial differential equations expressed in terms of three dependent variables, namely, two velocity components and pressure. The word "coupled" is used here to imply that the same dependent variables appear in more than one equation of the set, and no equation can be solved independently of the other(s) in the set.

A brief introduction to fluids was given in Sections 4.4 and 8.5.2. The finite element analysis of fluid flow problems that can be described as one-dimensional systems was discussed in Section 4.4. In Section 8.5.2, finite element models of two-dimensional flows of inviscid, incompressible fluids (i.e., potential flows) were considered. The potential flow problems were cast in terms of either the stream function or the velocity potential, and the governing equation in each case was shown to be the Laplace equation, $\nabla^2 u = 0$.

In this chapter we consider the finite element analysis of two-dimensional flows of viscous, incompressible fluids. We begin with a review of the pertinent equations governing low-speed, laminar flows of viscous incompressible fluids.

10.2 GOVERNING EQUATIONS

Consider the *slow* flow of a *viscous* and *incompressible fluid* in a closed domain Ω:

$$\text{Slow (inertial effects are negligible):} \quad \mathbf{v} \cdot \nabla \mathbf{v} \approx 0$$

$$\text{Viscous:} \quad \mu \neq 0$$

$$\text{Incompressible:} \quad \frac{D\rho}{Dt} = 0 \quad (\rho = \text{constant})$$

Assume that one of the dimensions, say, along the z direction (into the plane of the paper) of the domain is very long and there is no flow along that direction, and the velocity components in the other two directions (v_x and v_y) do not vary with the z direction. Under these conditions, the flow can be approximated by a two-dimensional model. The governing equations of such flows in rectangular Cartesian coordinates (x, y) are summarized below.

Conservation of Linear Momentum

$$\rho \frac{\partial v_x}{\partial t} - \frac{\partial \sigma_{xx}}{\partial x} - \frac{\partial \sigma_{xy}}{\partial y} - f_x = 0 \tag{10.2.1}$$

$$\rho \frac{\partial v_y}{\partial t} - \frac{\partial \sigma_{xy}}{\partial x} - \frac{\partial \sigma_{yy}}{\partial y} - f_y = 0 \tag{10.2.2}$$

Conservation of Mass (or Continuity Equation)

$$\frac{\partial v_x}{\partial x} + \frac{\partial v_y}{\partial y} = 0 \tag{10.2.3}$$

Constitutive Equations

$$\sigma_{xx} = \tau_{xx} - P, \quad \sigma_{xy} = \tau_{xy}, \quad \sigma_{yy} = \tau_{xy} - P \tag{10.2.4}$$

$$\tau_{xx} = 2\mu \frac{\partial v_x}{\partial x}, \quad \tau_{xy} = \mu \left(\frac{\partial v_x}{\partial y} + \frac{\partial v_y}{\partial x} \right), \quad \tau_{yy} = 2\mu \frac{\partial v_y}{\partial y} \tag{10.2.5}$$

Boundary Conditions. Specify one element of each of the following pairs at each point on the boundary Γ:

$$(v_x, t_x), \quad (v_y, t_y) \quad \text{for any } t > 0 \tag{10.2.6}$$

$$t_x = \sigma_{xx} n_x + \sigma_{xy} n_y, \quad t_y = \sigma_{xy} n_x + \sigma_{yy} n_y \tag{10.2.7}$$

Initial Conditions. Specify velocities at time $t = 0$ at each point in the domain Ω and on the boundary Γ:

$$v_x(x, y, 0) = v_x^0(x, y), \quad v_y(x, y, 0) = v_y^0(x, y) \tag{10.2.8}$$

Here (v_x, v_y) are the velocity components, $(\sigma_{xx}, \sigma_{yy}, \sigma_{xy})$ the Cartesian components of the total stress tensor $\boldsymbol{\sigma}$, P the pressure, $(\tau_{xx}, \tau_{xy}, \tau_{yy})$ the Cartesian components of the viscous stress tensor $\boldsymbol{\tau}$, μ the viscosity, f_x and f_y the components of body force vector, (t_x, t_y) the components of stress vector on the boundary, and (v_x^0, v_y^0) the specified initial values of the velocity components.

Using the constitutive relations (10.2.4) and (10.2.5), the momentum and continuity equations in a flow domain Ω can be expressed as

$$\rho\frac{\partial v_x}{\partial t} - \frac{\partial}{\partial x}\left(2\mu\frac{\partial v_x}{\partial x}\right) - \frac{\partial}{\partial y}\left[\mu\left(\frac{\partial v_x}{\partial y} + \frac{\partial v_y}{\partial x}\right)\right] + \frac{\partial P}{\partial x} - f_x = 0 \tag{10.2.9}$$

$$\rho\frac{\partial v_y}{\partial t} - \frac{\partial}{\partial x}\left[\mu\left(\frac{\partial v_x}{\partial y} + \frac{\partial v_y}{\partial x}\right)\right] - \frac{\partial}{\partial y}\left(2\mu\frac{\partial v_y}{\partial y}\right) + \frac{\partial P}{\partial y} - f_y = 0 \tag{10.2.10}$$

$$\frac{\partial v_x}{\partial x} + \frac{\partial v_y}{\partial y} = 0 \tag{10.2.11}$$

and the boundary stress components in (10.2.7) become

$$\begin{aligned} t_x &= \left(2\mu\frac{\partial v_x}{\partial x} - P\right)n_x + \mu\left(\frac{\partial v_x}{\partial y} + \frac{\partial v_y}{\partial x}\right)n_y \\ t_y &= \mu\left(\frac{\partial v_x}{\partial y} + \frac{\partial v_y}{\partial x}\right)n_x + \left(2\mu\frac{\partial v_y}{\partial y} - P\right)n_y \end{aligned} \quad \text{on } \Gamma \tag{10.2.12}$$

Thus, we have three partial differential equations (10.2.9)–(10.2.11) in three unknowns (v_x, v_y, P).

In the present study, we shall consider two different finite element models of Eqs. (10.2.9)–(10.2.11). The first one is a natural and direct formulation of Eqs. (10.2.9)–(10.2.11) in (v_x, v_y, P) and is known as the *velocity-pressure formulation* or *mixed formulation*. The second model is based on the interpretion that the continuity equation (10.2.11) is an additional relation among the velocity components (i.e., a constraint on v_x and v_y); the constraint is satisfied in a least-squares (i.e., approximate) sense. This particular method of including the constraint in the formulation is known as the penalty function method, and the formulation is termed the *penalty formulation*. It is informative to note that the velocity-pressure formulation is the same as the Lagrange multiplier formulation, and the Lagrange multiplier turns out to be the negative of the pressure.

10.3 VELOCITY-PRESSURE FORMULATION

10.3.1 Weak Formulation

The weak forms of Eqs. (10.2.9)–(10.2.11) over an element Ω_e can be obtained by the three-step procedure discussed in Chapter 8. We multiply the three equations, (10.2.1)–(10.2.3) wherein $(\sigma_{xx}, \sigma_{xy}, \sigma_{yy})$ are known in terms of (v_x, v_y, P) through Eqs. (10.2.4) and (10.2.5), with three different weight functions (w_1, w_2, w_3), integrate over the element, and integrate by parts (i.e., apply the Green–Gauss theorem) to obtain the following weak forms:

$$\begin{aligned} 0 &= \int_{\Omega_e} w_1\left[\rho\frac{\partial v_x}{\partial t} - \frac{\partial \sigma_{xx}}{\partial x} - \frac{\partial \sigma_{xy}}{\partial y} - f_x\right]dx\,dy \\ &= \int_{\Omega_e}\left[\rho w_1\frac{\partial v_x}{\partial t} + \frac{\partial w_1}{\partial x}\sigma_{xx} + \frac{\partial w_1}{\partial y}\sigma_{xy} - w_1 f_x\right]dx\,dy \\ &\quad + \oint_{\Gamma_e} w_1\left(\sigma_{xx}n_x + \sigma_{xy}n_y\right)ds \end{aligned} \tag{10.3.1}$$

$$0 = \int_{\Omega_e} w_2 \left[\rho \frac{\partial v_y}{\partial t} - \frac{\partial \sigma_{xy}}{\partial x} - \frac{\partial \sigma_{yy}}{\partial y} - f_y \right] dx\, dy$$

$$= \int_{\Omega_e} \left[\rho w_2 \frac{\partial v_y}{\partial t} + \frac{\partial w_2}{\partial x} \sigma_{xy} + \frac{\partial w_2}{\partial y} \sigma_{yy} - w_2 f_y \right] dx\, dy$$

$$+ \oint_{\Gamma_e} w_2 \left(\sigma_{xy} n_x + \sigma_{yy} n_y \right) ds \tag{10.3.2}$$

$$0 = \int_{\Omega_e} w_3 \left(\frac{\partial v_x}{\partial x} + \frac{\partial v_y}{\partial y} \right) dx\, dy \tag{10.3.3}$$

The weight functions (w_1, w_2, w_3) can be interpreted physically as follows: Since the first equation is the momentum equation and $f_x\, dxdy$ denotes the force, w_1 must be like the x component of velocity v_x so that the product $f_x w_1$ gives the power. Similarly, w_2 must be like the y component of velocity v_y. The third equation represents the volume change in an element of dimensions dx and dy. Therefore, w_3 must be like a force that causes the volume change. Volume changes occur under the action of hydrostatic pressure, hence, w_3 is like $-P$:

$$w_1 \sim u,\ w_2 \sim v, \text{ and } w_3 \sim -P \tag{10.3.4}$$

This interpretation is useful in developing the finite element model because w_1, for example, will be replaced by the ith interpolation function used in the approximation of v_x. Similarly, w_3 will be replaced by the ith interpolation function used in the approximation of P. When different interpolations are used for (v_x, v_y) and P, this interpretation becomes necessary. Expressing the equations in terms of (v_x, v_y, P), the weak forms (10.3.1)–(10.3.3) become

$$0 = \int_{\Omega_e} \left[\rho w_1 \frac{\partial v_x}{\partial t} + \frac{\partial w_1}{\partial x} \left(2\mu \frac{\partial v_x}{\partial x} - P \right) + \mu \frac{\partial w_1}{\partial y} \left(\frac{\partial v_x}{\partial y} + \frac{\partial v_y}{\partial x} \right) - w_1 f_x \right] dx\, dy$$

$$- \oint_{\Gamma_e} w_1 t_x\, ds \tag{10.3.5}$$

$$0 = \int_{\Omega_e} \left[\rho w_2 \frac{\partial v_y}{\partial t} + \mu \frac{\partial w_2}{\partial x} \left(\frac{\partial v_x}{\partial y} + \frac{\partial v_y}{\partial x} \right) + \frac{\partial w_2}{\partial y} \left(2\mu \frac{\partial v_y}{\partial y} - P \right) - w_2 f_y \right] dx\, dy$$

$$- \oint_{\Gamma_e} w_2 t_y\, ds \tag{10.3.6}$$

$$0 = - \int_{\Omega_e} w_3 \left(\frac{\partial v_x}{\partial x} + \frac{\partial v_y}{\partial y} \right) dx\, dy \tag{10.3.7}$$

Note that there is no boundary integral involving w_3 because no integration by parts is used. This implies that P is not a primary variable; it is a part of the secondary variables (t_x and t_y). This in turn requires that P not be made continuous across interelement boundaries. If P by itself is not specified in a problem (but t_x and t_y are specified), then P is arbitrarily set to a value at some node to determine the constant state of the pressure. Thus, P can be determined only within an arbitrary constant. The minus sign in the third statement is inserted because $P \sim -w_3$, which makes the resulting finite element model symmetric.

The problem described by weak forms (10.3.5)–(10.3.7) can be restated as a variational problem of finding (v_x, v_y, P) such that

$$\begin{aligned} B_t(\mathbf{w}, \mathbf{v}) + B_v(\mathbf{w}, \mathbf{v}) - \bar{B}_p(\mathbf{w}, P) &= l(\mathbf{w}) \\ -B_p(w_3, \mathbf{v}) &= 0 \end{aligned} \tag{10.3.8}$$

holds for all (w_1, w_2, w_3) and $t > 0$. Here, we have used the notation

$$\mathbf{w} = \begin{Bmatrix} w_1 \\ w_2 \end{Bmatrix}, \quad \mathbf{v} = \begin{Bmatrix} v_x \\ v_y \end{Bmatrix}, \quad \mathbf{f} = \begin{Bmatrix} f_x \\ f_y \end{Bmatrix}, \quad \mathbf{t} = \begin{Bmatrix} t_x \\ t_y \end{Bmatrix} \tag{10.3.9}$$

Since w_i are linearly independent of each other, the sum of the three equations in (10.3.5)–(10.3.7) is the same as the three individual equations. Thus, the bilinear forms $B_t(\mathbf{w}, \mathbf{v})$, $B_v(\mathbf{w}, \mathbf{v})$, $\bar{B}_p(\mathbf{w}, P)$, and $B_p(w_3, \mathbf{v})$, and the linear form $l(\mathbf{w})$ are defined by

$$\begin{aligned} B_t(\mathbf{w}, \mathbf{v}) &= \int_{\Omega_e} \rho \mathbf{w}^{\mathrm{T}} \dot{\mathbf{v}} \, d\mathbf{x} \\ B_v(\mathbf{w}, \mathbf{v}) &= \int_{\Omega_e} (\mathbf{D}\mathbf{w})^{\mathrm{T}} \mathbf{C} (\mathbf{D}\mathbf{v}) \, d\mathbf{x} \\ \bar{B}_p(\mathbf{w}, P) &= \int_{\Omega_e} \left(\mathbf{D}_1^{\mathrm{T}} \mathbf{w}\right)^{\mathrm{T}} P \, d\mathbf{x} \\ B_p(w_3, \mathbf{v}) &= \int_{\Omega_e} (w_3)^{\mathrm{T}} \left(\mathbf{D}_1^{\mathrm{T}} \mathbf{v}\right) d\mathbf{x} \\ l(\mathbf{w}) &= \int_{\Omega_e} \mathbf{w}^{\mathrm{T}} \mathbf{f} \, d\mathbf{x} + \oint_{\Gamma_e} \mathbf{w}^{\mathrm{T}} \mathbf{t} \, ds \end{aligned} \tag{10.3.10a}$$

where

$$\mathbf{D} = \begin{bmatrix} \dfrac{\partial}{\partial x} & 0 \\ 0 & \dfrac{\partial}{\partial y} \\ \dfrac{\partial}{\partial y} & \dfrac{\partial}{\partial x} \end{bmatrix}, \quad \mathbf{D}_1 = \begin{Bmatrix} \dfrac{\partial}{\partial x} \\ \dfrac{\partial}{\partial y} \end{Bmatrix}, \quad \mathbf{C} = \mu \begin{bmatrix} 2 & 0 & 0 \\ 0 & 2 & 0 \\ 0 & 0 & 1 \end{bmatrix} \tag{10.3.10b}$$

The transpose of a scalar (or 1×1 matrix) used in the Eq. (10.3.10a) may look a bit strange at the moment, but it is necessary to obtain the correct form of the finite element model, as will be seen shortly.

10.3.2 Finite Element Model

An examination of the weak form reveals that v_x and v_y are the primary variables that should be made continuous at interelement boundaries, while P is a nodal variable that need not be made continuous across the interelement boundaries. Therefore, the Lagrange family of finite elements can be used for (v_x, v_y, P). The weak form shows that the minimum continuity requirements on (v_x, v_y, P) are:

$$(v_x, v_y) \text{ linear in } x \text{ and } y, \quad P \text{ constant}$$

Thus, there are different continuity requirements on the interpolation of the velocity field and pressure. Let (the element label "e" on the variables is omitted)

$$v_x(x, y, t) = \sum_{j=1}^{n} v_x^j(t)\psi_j(x, y), \quad v_y(x, y, t) = \sum_{j=1}^{n} v_y^j(t)\psi_j(x, y) \tag{10.3.11a}$$

$$P(x, y, t) = \sum_{J=1}^{m} P_J(t)\phi_J(x, y) \tag{10.3.11b}$$

where ψ_j $(j = 1, 2, \ldots, n)$ and ϕ_J $(J = 1, 2, \ldots, m)$ are interpolation functions of different order. In view of the fact that pressure appears without a derivative while (v_x, v_y) appear with derivatives with respect to x and y, we often take $n = m + 1$. If the degree of the approximation functions is high, we may use the same degree of interpolation for P and (v_x, v_y).

Substituting (10.3.11a) and (10.3.11b) into Eqs. (10.3.5)–(10.3.7), we obtain the following finite element model:

$$\begin{bmatrix} 2[S^{11}]+[S^{22}] & [S^{21}] & -[S^{10}] \\ [S^{12}] & [S^{11}]+2[S^{22}] & -[S^{20}] \\ -[S^{10}]^T & -[S^{20}]^{\mathrm{T}} & [0] \end{bmatrix} \begin{Bmatrix} \{v_x\} \\ \{v_y\} \\ \{P\} \end{Bmatrix} + \begin{bmatrix} [M] & [0] & [0] \\ [0] & [M] & [0] \\ [0] & [0] & [0] \end{bmatrix} \begin{Bmatrix} \{\dot{v}_x\} \\ \{\dot{v}_y\} \\ \{\dot{P}\} \end{Bmatrix} = \begin{Bmatrix} \{F^1\} \\ \{F^2\} \\ \{0\} \end{Bmatrix} \tag{10.3.12}$$

The coefficient matrices shown in Eqs. (10.3.12) are defined by

$$\begin{aligned} M_{ij} &= \int_{\Omega_e} \rho\psi_i^e\psi_j^e \, dx\, dy \\ S_{ij}^{\alpha\beta} &= \int_{\Omega_e} \mu \frac{\partial\psi_i^e}{\partial x_\alpha}\frac{\partial\psi_j^e}{\partial x_\beta} \, dx\, dy\,; \quad \alpha, \beta = 1, 2 \\ S_{iJ}^{\alpha 0} &= \int_{\Omega_e} \mu \frac{\partial\psi_i^e}{\partial x_\alpha}\phi_J^e \, dx\, dy\,; \quad \alpha = 1, 2 \\ F^1 &= \int_{\Omega_e} \psi_i^e f_x \, dx\, dy + \oint_{\Gamma_e} \psi_i^e t_x \, ds \\ F^2 &= \int_{\Omega_e} \psi_i^e f_y \, dx\, dy + \oint_{\Gamma_e} \psi_i^e t_y \, ds \end{aligned} \tag{10.3.13}$$

We note that $[K^{33}] = [0]$ because the continuity equation does not contain P. Therefore, the assembled equations will also have zeros in diagonal elements corresponding to the nodal values of P (i.e., the system of equations is not positive-definite).

The vector form of the finite element model (10.3.12) can be obtained as follows: The finite element approximations (10.3.11a) and (10.3.11b) is expressed as

$$\begin{aligned} \mathbf{v} &= \begin{Bmatrix} v_x \\ v_y \end{Bmatrix} = \Psi\Delta, \quad \mathbf{w} = \begin{Bmatrix} w_1 \\ w_2 \end{Bmatrix} = \Psi\delta\Delta \\ P &= \Phi^{\mathrm{T}}\mathbf{P}, \quad w_3 = \Phi^{\mathrm{T}}\delta\mathbf{P} \end{aligned} \tag{10.3.14a}$$

where δ denotes the variational symbol, $\mathbf{w} = \delta\mathbf{v}$ denotes the virtual variation of $\mathbf{v}$, and δP_i is the virtual variation of P_i. Various symbols used in Eq. (10.3.14*a*) are defined as

$$\begin{aligned}
\Psi &= \begin{bmatrix} \psi_1 & 0 & \psi_2 & 0 & \cdots & \psi_n & 0 \\ 0 & \psi_1 & 0 & \psi_2 & \cdots & 0 & \psi_n \end{bmatrix} \\
\Delta &= \{v_x^1 \quad v_y^1 \quad v_x^2 \quad v_y^2 \quad \cdots \quad v_x^n \quad v_y^n\}^{\mathrm{T}} \\
\Phi &= \{\phi_1 \quad \phi_2 \quad \cdots \quad \phi_m\}^{\mathrm{T}}, \qquad \mathbf{P} = \{P_1 \quad P_2 \quad \cdots \quad P_m\}^{\mathrm{T}}
\end{aligned} \tag{10.3.14b}$$

Substituting (10.3.14*a*) into Eq. (10.3.8) and noting that δv_x^i and δv_y^i are arbitrary and linearly independent, we obtain

$$\mathbf{M}\dot{\Delta} + \mathbf{K}^{11}\Delta + \mathbf{K}^{12}\mathbf{P} = \mathbf{F}^1, \quad \mathbf{K}^{21}\Delta = \mathbf{0} \tag{10.3.15}$$

where

$$\begin{aligned}
\mathbf{M} &= \int_{\Omega_e} \rho\Psi^{\mathrm{T}}\Psi \, d\mathbf{x}, \quad \mathbf{K}^{11} = \int_{\Omega_e} \mathbf{B}_v^{\mathrm{T}}\mathbf{C}\mathbf{B}_v \, d\mathbf{x} \\
\mathbf{K}^{12} &= \int_{\Omega_e} \mathbf{B}_p^{\mathrm{T}}\Phi^{\mathrm{T}} \, d\mathbf{x}, \quad \mathbf{K}^{21} = \int_{\Omega_e} \Phi\mathbf{B}_p \, d\mathbf{x} \\
\mathbf{F}^1 &= \int_{\Omega_e} \Psi^{\mathrm{T}}\mathbf{f} \, d\mathbf{x} + \oint_{\Gamma_e} \Psi^{\mathrm{T}}\mathbf{t} \, ds \\
\mathbf{B}_v &= \mathbf{D}\Psi, \quad \mathbf{B}_p = \mathbf{D}_1^{\mathrm{T}}\Psi
\end{aligned} \tag{10.3.16}$$

Note that $\mathbf{M}$ and $\mathbf{K}^{11}$ are of the order $2n \times 2n$, $\mathbf{K}^{12}$ is of the order $2n \times m$, $\mathbf{K}^{21}$ is of the order $m \times 2n$, and $\mathbf{F}^1$ is of the order $2n \times 1$.

10.4 PENALTY FUNCTION FORMULATION

10.4.1 Preliminary Comments

The penalty function method was introduced in Section 4.6.4 in connection with algebraic constraint equations. It can also be used to reformulate a problem with differential constraints as one without constraints. Since the basic idea of the method was already introduced (see Example 4.6.2), we proceed directly to its application to the viscous flow problem at hand. The question we may ask is: Where is the constraint in the flow problem? There are no constraint conditions in the way the equations were presented. We have three equations (10.2.9)–(10.2.11) in three unknowns (v_x, v_y, P). Since the pressure P is uncoupled from the continuity equation (10.2.11) [which has the consequence of yielding a nonpositive-definite system of finite element equations (10.3.12)], we would like to eliminate it from the set of governing equations. The elimination of pressure leads to a constraint equation among the velocity components, as described next.

10.4.2 Formulation of the Flow Problem as a Constrained Problem

The equations governing flows of viscous incompressible fluids can be viewed as equivalent to minimizing a quadratic functional with a constraint. Here we present the formulation, in

the interest of simplicity, for the static case since the constraint condition does not involve time derivative terms. Then, we add the time derivative terms to study transient problems.

We begin with unconstrained problem described by the weak forms of the mixed model, namely, Eqs. (10.3.8) without the time-derivative terms

$$\begin{aligned} B_v(\mathbf{w}, \mathbf{v}) - \bar{B}_p(\mathbf{w}, P) &= l(\mathbf{w}) \\ -B_p(w_3, \mathbf{v}) &= 0 \end{aligned} \tag{10.4.1}$$

where $B_v(\cdot, \cdot)$, $\bar{B}_p(\cdot, \cdot)$, $B_p(\cdot, \cdot)$, and $l(\cdot)$ are defined in Eqs. (10.3.10*a*) and (10.3.10*b*). Now, suppose that the velocity field (v_x, v_y) is such that the continuity equation (10.2.3) is satisfied identically. Then the weight functions (w_1, w_2), being (virtual) variations of the velocity components, also satisfy the continuity equation

$$\frac{\partial w_1}{\partial x} + \frac{\partial w_2}{\partial y} = 0 \tag{10.4.2}$$

As a result, variational problem (10.4.1) now can be stated as follows: Among all (v_x, v_y) that satisfy the continuity equation (10.2.3), find the one that satisfies the variational problem

$$B_v(\mathbf{w}, \mathbf{v}) = l(\mathbf{w}) \tag{10.4.3}$$

for all admissible weight functions (w_1, w_2), i.e., the one that satisfies condition (10.4.2).

The variational problem in Eq. (10.4.3) is a constrained variational problem because the solution (v_x, v_y) is constrained to satisfy the continuity equation (10.2.3). We note that $B_v(\cdot, \cdot)$ is symmetric (because $\mathbf{C}$ is symmetric)

$$B_v(\mathbf{w}, \mathbf{v}) = B_v(\mathbf{v}, \mathbf{w}) \tag{10.4.4}$$

and it is linear in $\mathbf{w}$ as well as $\mathbf{v}$, while $l(\cdot)$ is linear in $\mathbf{w}$. Hence, the quadratic functional is given by the expression [see Eq. (2.4.19)]

$$I_v(\mathbf{v}) = \frac{1}{2} B_v(\mathbf{v}, \mathbf{v}) - l(\mathbf{v}) \tag{10.4.5}$$

Now we can state that the equations governing steady flows of viscous incompressible fluids are equivalent to

$$\begin{aligned} &\text{minimize } I_v(\mathbf{v}) \\ &\text{subjected to the constraint } G(\mathbf{v}) \equiv \frac{\partial v_x}{\partial x} + \frac{\partial v_y}{\partial y} = 0 \end{aligned} \tag{10.4.6}$$

The constrained problem (10.4.6) can be reformulated as an unconstrained problem using the Lagrange multiplier method or the penalty function method. These are discussed next.

10.4.3 Lagrange Multiplier Model

In the Lagrange multiplier method the constrained problem (10.4.6) is reformulated as one of finding the stationary points of the unconstrained functional

$$I_L(\mathbf{v}, \lambda) \equiv I_v(\mathbf{v}) + \int_{\Omega_e} \lambda G(\mathbf{v})\, dx dy \tag{10.4.7}$$

where $\lambda(x, y)$ is the *Lagrange multiplier*. The necessary condition for I_L to have a stationary value is that

$$\delta I_L = \delta_{v_x} I_L + \delta_{v_y} I_L + \delta_\lambda I_L = 0 \rightarrow \delta_{v_x} I_L = 0, \quad \delta_{v_y} I_L = 0, \quad \delta_\lambda I_L = 0 \tag{10.4.8}$$

where δ_{v_x}, δ_{v_y}, and δ_λ denote the partial variations (see Section 2.3) with respect to v_x, v_y, and λ, respectively. Calculating the first variations in (10.4.8), we obtain

$$0 = \int_{\Omega_e} \left[\frac{\partial \delta v_x}{\partial x} \left(2\mu \frac{\partial v_x}{\partial x} + \lambda \right) + \mu \frac{\partial \delta v_x}{\partial y} \left(\frac{\partial v_x}{\partial y} + \frac{\partial v_y}{\partial x} \right) \right] dx\, dy$$

$$- \int_{\Omega_e} \delta v_x f_x \, dx\, dy - \oint_{\Gamma_e} \delta v_x t_x \, ds \tag{10.4.9}$$

$$0 = \int_{\Omega_e} \left[\mu \frac{\partial \delta v_y}{\partial x} \left(\frac{\partial v_x}{\partial y} + \frac{\partial v_y}{\partial x} \right) + \frac{\partial \delta v_y}{\partial y} \left(2\mu \frac{\partial v_y}{\partial y} + \lambda \right) \right] dx\, dy$$

$$- \int_{\Omega_e} \delta v_y f_y \, dx\, dy - \oint_{\Gamma_e} \delta v_y t_y \, ds \tag{10.4.10}$$

$$0 = \int_{\Omega_e} \delta\lambda \left(\frac{\partial v_x}{\partial x} + \frac{\partial v_y}{\partial y} \right) dx\, dy \tag{10.4.11}$$

where

$$\begin{aligned} t_x &= \left(2\mu \frac{\partial v_x}{\partial x} + \lambda \right) n_x + \mu \left(\frac{\partial v_x}{\partial y} + \frac{\partial v_y}{\partial x} \right) n_y \\ t_y &= \mu \left(\frac{\partial v_x}{\partial y} + \frac{\partial v_y}{\partial x} \right) n_x + \left(2\mu \frac{\partial v_y}{\partial y} + \lambda \right) n_y \end{aligned} \tag{10.4.12}$$

or, in vector form

$$B_v(\mathbf{w}, \mathbf{v}) + \bar{B}_p(\mathbf{w}, \lambda) = l(\mathbf{w}), \quad B_p(\delta\lambda, \mathbf{v}) = 0 \tag{10.4.13}$$

and the bilinear forms are the same as those in Eqs. (10.3.10*a*) and (10.3.10*b*). A comparison of Eq. (10.4.13) with Eq. (10.3.8) [or comparison of Eqs. (10.3.5)–(10.3.7) with (10.4.9)–(10.4.11)] reveals that $\lambda = -P$. Hence, the Lagrange multiplier formulation is the same as the velocity-pressure formulation.

10.4.4 Penalty Model

In the penalty function method, the constrained problem (10.4.6) is reformulated as an unconstrained problem as follows: Minimize the modified functional

$$I_P(\mathbf{v}) \equiv I_v(\mathbf{v}) + \frac{\gamma_e}{2} \int_{\Omega_e} [G(\mathbf{v})]^2 d\mathbf{x} \tag{10.4.14}$$

where γ_e is called the *penalty parameter*. Note that the constraint is included in a least-squares sense into the functional. Seeking the minimum of the modified functional $I_P(\mathbf{v})$ is equivalent to seeking the minimum of both $I_v(\mathbf{v})$ and $G(\mathbf{v})$, the latter with respect to the weight γ_e. The larger the value of γ_e, the more exactly the constraint is satisfied. The necessary condition for the minimum of I_P is

$$\delta I_P = 0 \tag{10.4.15}$$

We have

$$0 = \int_{\Omega_e} \left[2\mu \frac{\partial \delta v_x}{\partial x} \frac{\partial v_x}{\partial x} + \mu \frac{\partial \delta v_x}{\partial y} \left(\frac{\partial v_x}{\partial y} + \frac{\partial v_y}{\partial x} \right) - \delta v_x f_x \right] dx\, dy$$
$$- \oint_{\Gamma_e} \delta v_x t_x \, ds + \int_{\Omega_e} \gamma_e \frac{\partial \delta v_x}{\partial x} \left(\frac{\partial v_x}{\partial x} + \frac{\partial v_y}{\partial y} \right) dx\, dy \tag{10.4.16}$$

$$0 = \int_{\Omega_e} \left[2\mu \frac{\partial \delta v_y}{\partial y} \frac{\partial v_y}{\partial y} + \mu \frac{\partial \delta v_y}{\partial x} \left(\frac{\partial v_x}{\partial y} + \frac{\partial v_y}{\partial x} \right) - \delta v_y f_y \right] dx\, dy$$
$$- \oint_{\Gamma_e} \delta v_y t_y \, ds + \int_{\Omega_e} \gamma_e \frac{\partial \delta v_y}{\partial y} \left(\frac{\partial v_x}{\partial x} + \frac{\partial v_y}{\partial y} \right) dx\, dy \tag{10.4.17}$$

or, in vector form,

$$B_p(\mathbf{w}, \mathbf{v}) = l(\mathbf{w}) \tag{10.4.18}$$

where ($w_1 = \delta v_x$ and $w_2 = \delta v_y$)

$$B_p(\mathbf{w}, \mathbf{v}) = B_v(\mathbf{w}, \mathbf{v}) + \int_{\Omega_e} \gamma_e \left(\mathbf{D}_1^{\mathrm{T}} \mathbf{w} \right)^{\mathrm{T}} \mathbf{D}_1^{\mathrm{T}} \mathbf{v} \, d\mathbf{x}$$
$$l(\mathbf{w}) = \int_{\Omega_e} \mathbf{w}^{\mathrm{T}} \mathbf{f} \, dx\, dy + \oint_{\Gamma_e} \mathbf{w}^{\mathrm{T}} \mathbf{t} \, ds \tag{10.4.19}$$

and $B_v(\cdot, \cdot)$ and $\mathbf{D}_1$ are defined in Eqs. (10.3.10*a*) and (10.3.10*b*). We note that the pressure does not appear explicitly in the weak forms (10.4.16) and (10.4.17), although it is a part of the boundary stresses [see Eq. (10.4.12), $\lambda = -P$].

A comparison of the weak forms in (10.4.16) and (10.4.17) with those in (10.4.9) and (10.4.10) show that

$$\lambda = \gamma_e \left(\frac{\partial v_x}{\partial x} + \frac{\partial v_y}{\partial y} \right) = -P \quad \text{or} \quad P = -\gamma_e \mathbf{D}_1^{\mathrm{T}} \mathbf{v} \tag{10.4.20}$$

where $\mathbf{v} = \mathbf{v}(\gamma_e)$ is the solution of Eqs. (10.4.16) and (10.4.17). Thus, an approximation for the pressure can be postcomputed using (10.4.20).

The time derivative terms can be added to equations (10.4.9)–(10.4.11) as well as to (10.4.16) and (10.4.17) without affecting the above discussion. For the penalty model, we have

$$0 = \int_{\Omega_e} \left[\rho \delta v_x \frac{\partial v_x}{\partial t} + 2\mu \frac{\partial \delta v_x}{\partial x} \frac{\partial v_x}{\partial x} + \mu \frac{\partial \delta v_x}{\partial y} \left(\frac{\partial v_x}{\partial y} + \frac{\partial v_y}{\partial x} \right) \right.$$
$$\left. + \gamma_e \frac{\partial \delta v_x}{\partial x} \left(\frac{\partial v_x}{\partial x} + \frac{\partial v_y}{\partial y} \right) \right] dx\, dy - \int_{\Omega_e} \delta v_x f_x \, dx\, dy - \oint_{\Gamma_e} \delta v_x t_x \, ds \tag{10.4.21}$$

$$0 = \int_{\Omega_e} \left[\rho \delta v_y \frac{\partial v_y}{\partial t} + 2\mu \frac{\partial \delta v_y}{\partial y} \frac{\partial v_y}{\partial y} + \mu \frac{\partial \delta v_y}{\partial x} \left(\frac{\partial v_x}{\partial y} + \frac{\partial v_y}{\partial x} \right) \right.$$
$$\left. + \gamma_e \frac{\partial \delta v_y}{\partial y} \left(\frac{\partial v_x}{\partial x} + \frac{\partial v_y}{\partial y} \right) \right] dx\, dy - \int_{\Omega_e} f_y \delta v_y \, dx\, dy - \oint_{\Gamma_e} \delta v_y t_y \, ds \tag{10.4.22}$$

or

$$B_t(\mathbf{w}, \mathbf{v}) + B_p(\mathbf{w}, \mathbf{v}) = l(\mathbf{w}) \tag{10.4.23}$$

where $B_t(\cdot, \cdot)$ is defined in Eq. (10.3.10a), and $B_p(\cdot, \cdot)$ and $l(\cdot)$ are defined in Eq. (10.4.19).

The penalty finite element model can be constructed using Eqs. (10.4.21) and (10.4.22) [or Eq. (10.4.23)] by substituting $\delta v_x = \psi_i$ and $\delta v_y = \psi_i$ and approximations (10.3.11a) for (v_x, v_y). We obtain

$$\begin{bmatrix} [M] & [0] \\ [0] & [M] \end{bmatrix} \begin{Bmatrix} \{\dot{v}_x\} \\ \{\dot{v}_y\} \end{Bmatrix} + \begin{bmatrix} [K^{11}] & [K^{12}] \\ [K^{21}] & [K^{22}] \end{bmatrix} \begin{Bmatrix} \{v_x\} \\ \{v_y\} \end{Bmatrix} = \begin{Bmatrix} \{F^1\} \\ \{F^2\} \end{Bmatrix} \tag{10.4.24}$$

where

$$\begin{aligned} [K^{11}] &= 2[S^{11}] + [S^{22}] + [\bar{S}^{11}], \quad [K^{12}] = [S^{21}] + [\bar{S}^{12}] \\ [K^{22}] &= [S^{11}] + 2[S^{22}] + [\bar{S}^{22}], \quad [K^{21}] = [S^{12}] + [\bar{S}^{21}] \end{aligned} \tag{10.4.25}$$

with the coefficients

$$\begin{aligned} M_{ij} &= \int_{\Omega_e} \rho \psi_i^e \psi_j^e \, dx \, dy \\ S_{ij}^{\alpha\beta} &= \int_{\Omega_e} \mu \frac{\partial \psi_i^e}{\partial x_\alpha} \frac{\partial \psi_j^e}{\partial x_\beta} \, dx \, dy \; ; \quad \alpha, \beta = 1, 2 \\ S_{ij}^{\alpha 0} &= \int_{\Omega_e} \mu \frac{\partial \psi_i^e}{\partial x_\alpha} \psi_j^e \, dx \, dy \; ; \quad \alpha = 1, 2 \\ \bar{S}_{ij}^{\alpha\beta} &= \int_{\Omega_e} \gamma_e \frac{\partial \psi_i^e}{\partial x_\alpha} \frac{\partial \psi_j^e}{\partial x_\beta} \, dx \, dy \; ; \quad \alpha, \beta = 1, 2 \\ \bar{S}_{ij}^{\alpha 0} &= \int_{\Omega_e} \gamma_e \frac{\partial \psi_i^e}{\partial x_\alpha} \psi_j^e \, dx \, dy \; ; \quad \alpha = 1, 2 \\ F^1 &= \int_{\Omega_e} \psi_i^e f_x \, dx \, dy + \oint_{\Gamma_e} \psi_i^e t_x \, ds \\ F^2 &= \int_{\Omega_e} \psi_i^e f_y \, dx \, dy + \oint_{\Gamma_e} \psi_i^e t_y \, ds \end{aligned} \tag{10.4.26}$$

In vector form, the finite element model is given by

$$\mathbf{M}\dot{\Delta} + (\mathbf{K}_v + \mathbf{K}_p)\,\Delta = \mathbf{F} \tag{10.4.27}$$

where ($\mathbf{M}$, $\mathbf{K}_v$, and $\mathbf{K}_p$ are of the order $2n \times 2n$, and $\mathbf{F}$ is of the order $2n \times 1$)

$$\begin{aligned} \mathbf{M} &= \int_{\Omega_e} \rho \boldsymbol{\Psi}^{\mathrm{T}} \boldsymbol{\Psi} \, d\mathbf{x}, \quad \mathbf{K}_v = \int_{\Omega_e} \mathbf{B}_v^{\mathrm{T}} \mathbf{C} \mathbf{B}_v \, d\mathbf{x} \\ \mathbf{K}_p &= \int_{\Omega_e} \gamma_e \mathbf{B}_p^{\mathrm{T}} \mathbf{B}_p \, d\mathbf{x}, \quad \mathbf{F} = \int_{\Omega_e} \boldsymbol{\Psi}^{\mathrm{T}} \mathbf{f} \, d\mathbf{x} + \oint_{\Gamma_e} \boldsymbol{\Psi}^{\mathrm{T}} \mathbf{t} \, ds \\ \mathbf{B}_v &= \mathbf{D}\boldsymbol{\Psi}, \qquad\qquad \mathbf{B}_p = \mathbf{D}_1^{\mathrm{T}} \boldsymbol{\Psi} \end{aligned} \tag{10.4.28}$$

10.4.5 Time Approximation

For the unsteady case, Eqs. (10.3.15) and (10.4.27) are further approximated using a time approximation scheme. Equations (10.3.15) and (10.4.27) are of the form [see (6.2.21*a*)]

$$\mathbf{M}\dot{\Delta} + \mathbf{K}\Delta = \mathbf{F} \tag{10.4.29}$$

where $\{\Delta\}$ denotes the vector of nodal velocities and pressure in the velocity-pressure formulation and only velocities in the penalty formulation. Using the α-family of approximation we reduce Eq. (10.4.27) (with $\mathbf{K} = \mathbf{K}_v + \mathbf{K}_p$) to [see Eqs. (6.2.21*a*)–(6.2.24*b*)],

$$\hat{\mathbf{K}}\Delta_{s+1} = \tilde{\mathbf{K}}\Delta_s + \hat{\mathbf{F}}_{s,s+1} \tag{10.4.30}$$

where

$$\hat{\mathbf{K}} = \mathbf{M} + a_1\mathbf{K}_{s+1}, \quad \tilde{\mathbf{K}}_s = \mathbf{M} - a_2\mathbf{K}_s \tag{10.4.31}$$

$$\hat{\mathbf{F}}_{s,s+1} = a_1\mathbf{F}_{s+1} + a_2\mathbf{F}_s, \quad a_1 = \alpha\Delta t, \quad a_2 = (1-\alpha)\Delta t \tag{10.4.32}$$

where $\mathbf{M}$ and $\mathbf{K}$ for the penalty model are defined in Eqs. (10.4.28).

10.5 COMPUTATIONAL ASPECTS

10.5.1 Properties of the Matrix Equations

Some of the properties of the matrix equations in (10.3.15) and (10.4.27) are listed below.

1. The matrix equations (10.3.15) and (10.4.27) represent discrete analogs of conservation of mass and momentum. An inspection of the structure of the individual matrices shows that $\mathbf{M}$ and $\mathbf{K}$ are symmetric.
2. A negative aspect of the mixed finite element model is the presence of zeroes on the matrix diagonals corresponding to the pressure variables [see Eq. (10.3.15)]. Direct equation-solving methods must use some type of pivoting strategy, while the use of iterative solvers is severely handicapped by poor convergence behavior.
3. The computer implementation of the mixed model is somewhat complicated by the fact that the element contains variable degrees of freedom, e.g., in the quadratic approximation of the velocity field and bilinear continuous approximation of the pressure, the element has three degrees of freedom (v_x, v_y, P) at the corner nodes and two degrees of freedom (v_x, v_y) at the interior and midside nodes. This complicates the calculation of element matrices as well as the assembly of element equations.
4. Equations (10.3.15) and (10.4.27) represent a set of ordinary differential equations in time. The fact that the pressure does not appear explicitly in the continuity equation makes the system time-singular in pressure and precludes the use of purely explicit time-integration methods.
5. The choice of the penalty parameter is largely dictated by the ratio of the magnitude of penalty terms to the viscous terms, the mesh, and the precision of the computer. Generally, a value of $\gamma = 10^4\mu$ to $10^{12}\mu$, where μ denotes the viscosity, gives good results. It is found that the pressure is more sensitive to the value of γ than the velocity field.

10.5.2 Choice of Elements

As is clear from the weak forms, both finite element models require only the C^0-continuous functions to approximate the field variables (i.e., velocities and pressure). Thus, any of the Lagrange and serendipity family of interpolation functions are admissible for the interpolation of the velocity field in mixed and penalty finite element models.

The choice of interpolation functions used for the pressure variable in the mixed finite element model is further constrained by the special role that pressure plays in incompressible flows. Recall that the pressure can be interpreted as a Lagrange multiplier that serves to enforce the incompressibility constraint on the velocity field. From Eq. (10.3.11*b*) it is seen that the approximation functions ϕ_J used for pressure is the weighting function for the continuity equation. In order to prevent an overconstrained system of discrete equations, the interpolation used for pressure must be at least one order lower than that used for the velocity field (i.e., unequal order interpolation). Furthermore, the pressure need not be made continuous across elements because the pressure variable does not constitute a primary variable of the weak form presented in Eqs. (10.3.5)–(10.3.7).

Commonly used elements for two-dimensional flows of viscous incompressible fluids are shown in Fig. 10.5.1. In the case of linear elements, pressure is treated as discontinuous between elements; otherwise, the whole domain will have the same pressure. Two different pressure approximations have been used when the velocities are approximated by quadratic Lagrange functions. The first is a continuous bilinear approximation in which the pressure is defined at the corner nodes of the element and is made continuous across element boundaries. The second pressure approximation involves a discontinuous (between elements) linear variation defined on the element by $\Phi = \{1 \;\; x \;\; y\}^{\mathrm{T}}$. Here the unknowns are not nodal point values of the pressure but correspond to the coefficients in $P = a \cdot 1 + b \cdot x + c \cdot y$.

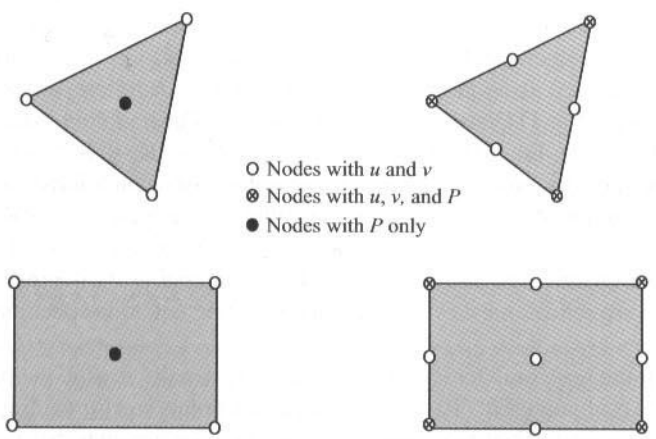

Figure 10.5.1 The triangular and quadrilateral elements used for the mixed and penalty finite element models.

When the eight-node quadratic element is used to represent the velocity field, a continuous, bilinear pressure approximation may be selected. When a discontinuous pressure variation is utilized with this element, the constant pressure representation over each element must be used. The quadratic quadrilateral elements shown in Fig. 10.5.1 are known to give reliable solutions for velocity and pressure fields. Other elements may yield acceptable solutions for the velocity field, but the pressure field is often in error.

10.5.3 Evaluation of Element Matrices in the Penalty Model

The numerical evaluation of the coefficient matrices appearing in equation (10.4.27) requires special consideration. This aspect is discussed here for the steady-state case. For the steady-state flows with constant material properties, Eq. (10.4.27) is of the form

$$(\mathbf{K}_v + \mathbf{K}_p)\Delta = \mathbf{F} \tag{10.5.1}$$

where $\mathbf{K}_v$ is the contribution from the viscous terms and $\mathbf{K}_p$ is the contribution from the penalty terms (and depends on γ), which comes from the incompressibility constraint. In theory, as we increase the value of γ, the conservation of mass is satisfied more exactly. However, in practice, for some large value of γ, the contribution from the viscous terms would be negligibly small compared to the penalty terms. Thus, if $\mathbf{K}_p$ is a nonsingular (i.e., invertible) matrix, the solution of Eq. (10.5.1) for a large value of γ is trivial, $\Delta = \mathbf{0}$. While the solution satisfies the continuity equation, it does not satisfy the momentum equations. In this case the discrete problem (10.5.1) is said to be overconstrained or "locked." If $\mathbf{K}_p$ is singular, then the sum $(\mathbf{K}_v + \mathbf{K}_p)$ is nonsingular (because $\mathbf{K}_v$ is nonsingular), and a nontrivial solution to the problem is obtained.

The numerical problem described above is eliminated by proper evaluation of the integrals in $\mathbf{K}_v$ and $\mathbf{K}_p$. It is found that if the coefficients of $\mathbf{K}_p$ (i.e., penalty matrix coefficients) are evaluated using a numerical integration rule where the order is one less than that required to integrate them exactly, the finite element equations (10.5.1) give acceptable solutions for the velocity field. This technique of underintegrating the penalty terms is known in the literature as *reduced integration*. For example, if a linear quadrilateral element is used to approximate the velocity field, the matrix coefficients $\mathbf{K}_v$ (as well as $\mathbf{M}$ for unsteady problems) are evaluated using the 2×2 Gauss–Legendre quadrature, and $\mathbf{K}_p$ is evaluated using the one-point (1×1) Gauss–Legendre quadrature. The one-point quadrature yields a singular $\mathbf{K}_p$. Therefore, Eq. (10.5.1) can be solved because $(\mathbf{K}_v + \mathbf{K}_p)$ is nonsingular and can be inverted (after assembly and imposition of boundary conditions) to obtain a good finite element solution of the original problem. When a quadratic quadrilateral element is used, the 3×3 Gauss–Legendre quadrature is used to evaluate $\mathbf{K}_v$ and $\mathbf{M}$, and the 2×2 Gauss–Legendre quadrature is used to evaluate $\mathbf{K}_p$. Of course, as the degree of interpolation goes up, or as very refined meshes are used, the resulting equations become less sensitive to locking.

Concerning the postcomputation of pressure in the penalty model, the pressure should be computed by evaluating Eq. (10.4.20) at integration points corresponding to the reduced Gauss rule. This is equivalent to using an interpolation for pressure that is one order less than the one used for the velocity field. The pressure computed using equation (10.4.20) at the reduced integration points is not always reliable and accurate. The pressures predicted

using the linear elements, especially for coarse meshes, are seldom acceptable. Quadratic elements are known to yield more reliable results.

10.5.4 Postcomputation of Stresses

The analysis of a flow problem generally includes calculation of not only the velocity field and pressure but also the computation of the stress field. A brief discussion of the stress calculation is presented next.

For a plane two-dimensional flow, the stress components $(\sigma_{xx}, \sigma_{yy}, \sigma_{xy})$ are given by

$$\sigma_{xx} = 2\mu \frac{\partial v_x}{\partial x} - P, \quad \sigma_{yy} = 2\mu \frac{\partial v_y}{\partial y} - P, \quad \sigma_{xy} = \mu \left(\frac{\partial v_x}{\partial y} + \frac{\partial v_y}{\partial x} \right) \tag{10.5.2}$$

where μ is the viscosity of the fluid. Substitution of the finite element approximations (10.3.11*a*) and (10.3.11*b*) for the velocity field and pressure into Eqs. (10.5.2) yields

$$\begin{aligned} \sigma_{xx} &= 2\mu \sum_{j=1}^{n} \frac{\partial \psi_j}{\partial x} v_x^j - P, \quad \sigma_{yy} = 2\mu \sum_{j=1}^{n} \frac{\partial \psi_j}{\partial y} v_y^j - P \\ \sigma_{xy} &= \mu \sum_{j=1}^{n} \left(\frac{\partial \psi_j}{\partial y} v_x^j + \frac{\partial \psi_j}{\partial x} v_y^j \right) \end{aligned} \tag{10.5.3}$$

where P is calculated from

$$P(x, y) = \sum_{J=1}^{m} \phi_J(x, y) P_J \tag{10.5.4}$$

for the mixed model and from

$$P_\gamma(x, y) = -\gamma \sum_{j=1}^{n} \left(\frac{\partial \psi_j}{\partial x} v_x^j + \frac{\partial \psi_j}{\partial y} v_y^j \right) \tag{10.5.5}$$

for the penalty model.

The spatial derivatives of the interpolation functions in Eqs. (10.5.3) and (10.5.5) must be evaluated using the reduced Gauss point rule. Thus, the stresses (as well as the pressure) are computed using the one-point Gauss rule for linear elements and with the 2×2 Gauss rule for the quadratic elements. The stresses computed at interior integration points can be extrapolated to the nodes by a simple linear extrapolation procedure, and they may be appropriately averaged between adjacent elements to produce a continuous stress field.

10.6 NUMERICAL EXAMPLES

A number of simple examples of two-dimensional Stokes flows of viscous incompressible fluids are presented in this section [see Reddy (2004)]. The examples presented herein were solved using the mixed and *reduced integration penalty* finite element models. The objective here is to evaluate the accuracy of the penalty and mixed finite element models by comparing with the available analytical results and to illustrate the effect of the penalty parameter on the accuracy of the solutions.

Example 10.6.1 (Viscous Fluid Squeezed between Parallel Plates)

Consider the slow flow of a viscous incompressible material squeezed between two long parallel plates [see Fig. 10.6.1(*a*)]. When the length of the plates is very large compared to both the width and the distance between the plates, we have a case of plane flow. Although this is a moving boundary problem, we wish to determine the velocity and pressure fields for a fixed distance between the plates, assuming that a state of plane flow exists.

Let v_0 be the velocity with which the two plates are moving toward each other (i.e., squeezing out the fluid), and let $2b$ and $2a$ denote, respectively, the distance between and the length of the plates [see Fig. 10.6.1(*a*)]. Due to the biaxial symmetry present in the problem, it suffices to model only a quadrant of the domain. As a first mesh, we use a 5×3 nonuniform mesh of nine-node quadratic elements in the mixed model, and a 10×6 mesh of the four-node linear elements and 5×3 mesh of nine-node quadratic elements in the penalty model [see Fig. 10.6.1(*b*)]. The nonuniform mesh, with smaller elements near the free surface (i.e., at $x = a$), is used to approximate accurately the singularity in the shear stress at the point $(a, b) = (6, 2)$. The mesh used for the penalty model has exactly the same number of nodes as the mesh used for the nine-node mesh of the mixed model.

The velocity boundary conditions are shown in Fig. 10.6.1(*b*). The velocity field at $x = 6$ (outflow boundary) is not known; if we do not impose any boundary conditions there, it amounts to requiring $t_x = t_y = 0$ in the integral sense. In the mixed finite element model, it is necessary to specify the pressure at least at one node. In the present case, the node at $(x, y) = (a, 0)$ is specified to have zero pressure. An approximate analytical solution to this two-dimensional problem is provided by Nadai (1963), and it is given by

$$v_x(x, y) = \frac{3V_0 x}{2b}\left(1 - \frac{y^2}{b^2}\right), \quad v_y(x, y) = -\frac{3V_0 y}{2b}\left(3 - \frac{y^2}{b^2}\right)$$
$$P(x, y) = \frac{3\mu V_0}{2b^3}(a^2 + y^2 - x^2) \tag{10.6.1}$$

The velocities $v_x(x, 0)$ obtained with the two finite element models compare well with the analytical solution, as shown in Table 10.6.1. The nine-node element gives very good results for both the penalty and mixed models. The influence of the penalty parameter on the accuracy of

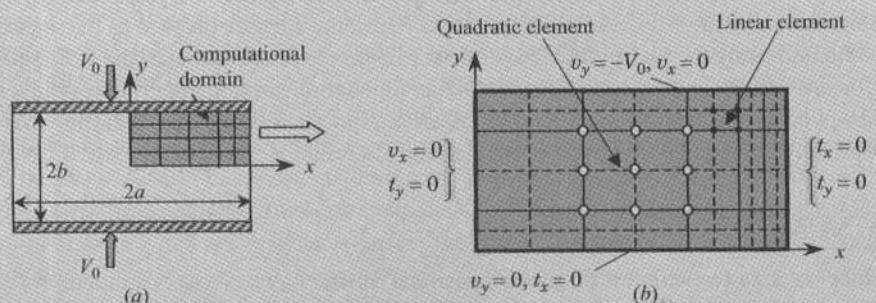

Figure 10.6.1 (*a*) Geometry, computational domain, and (*b*) the finite element mesh used for the analysis of the slow flow of viscous incompressible fluid between parallel plates.

Table 10.6.1 Comparison of finite element solution $v_x(x, 0)$ with the analytical solution for fluid squeezed between plates.

	$\gamma = 1.0$		$\gamma = 100$		$\gamma = 10^8$		Mixed model	
x	Four -node	Nine* -node	Four -node	Nine -node	Four -node	Nine -node	Nine -node	Series solution
1.00	0.0303	0.0310	0.6563	0.6513	0.7576	0.7505	0.7497	0.7500
2.00	0.0677	0.0691	1.3165	1.3062	1.5135	1.4992	1.5031	1.5000
3.00	0.1213	0.1233	1.9911	1.9769	2.2756	2.2557	2.2561	2.2500
4.00	0.2040	0.2061	2.6960	2.6730	3.0541	3.0238	3.0203	3.0000
4.50	0.2611	0.2631	3.0718	3.0463	3.4648	3.4307	3.4292	3.3750
5.00	0.3297	0.3310	3.4347	3.3956	3.8517	3.8029	3.8165	3.7500
5.25	0.3674	0.3684	3.6120	3.5732	4.0441	3.9944	3.9893	3.9375
5.50	0.4060	0.4064	3.7388	3.6874	4.1712	4.1085	4.1204	4.1250
5.75	0.4438	0.4443	3.8316	3.7924	4.2654	4.2160	4.2058	4.3125
6.00	0.4793	0.4797	3.8362	3.7862	4.2549	4.1937	4.2364	4.5000

*The 3×3 Gauss rule is used for nonpenalty terms, and the 2×2 Gauss rule for penalty terms is used for quadratic elements.

the solution is clear from the results. Whether the element is linear or quadratic, it is necessary to use a large value of the penalty parameter.

Figure 10.6.2 contains plots of the velocity $v_x(x, y)$ for $x = 4$ and $x = 6$, and Fig. 10.6.3 contains plots of pressure $P(x, y)$, for $y = y_0$, where y_0 is the y coordinate of the Gauss point nearest to the centerline or top plate. These results were obtained with two different meshes: 5×3 and 10×8. The pressure in the penalty model was computed using Eq. (10.5.5) with the 2×2 Gauss rule for the quadratic rectangular element and the one-point formula for the linear element, whereas in the mixed model (as well as the analytical solution) it is computed at the nodes. If the pressure in the penalty model were computed using the full quadrature

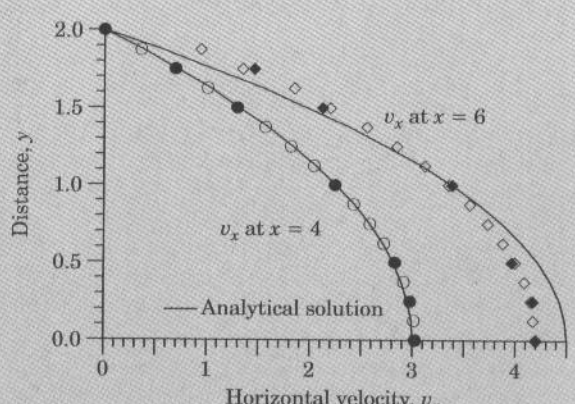

Figure 10.6.2 Velocity fields for fluid squeezed between parallel plates.

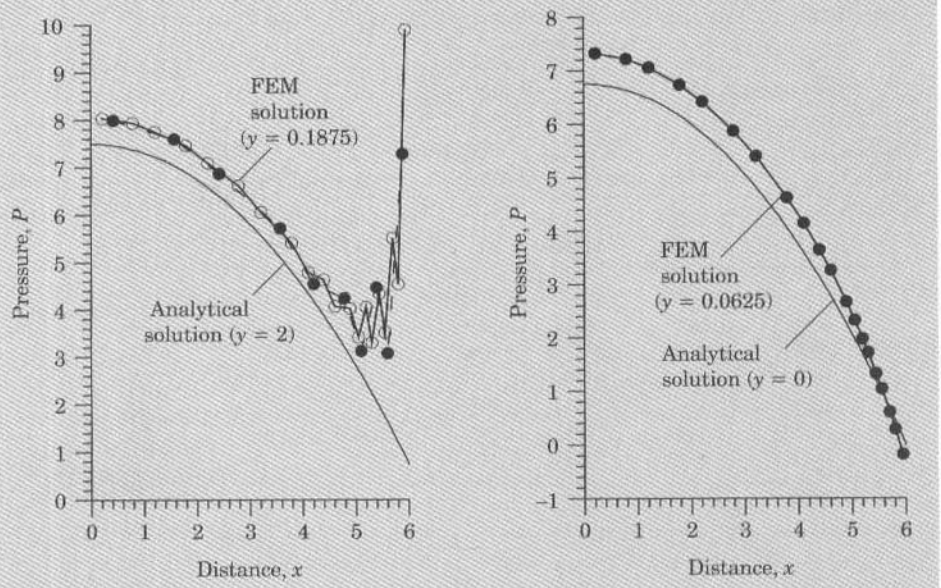

Figure 10.6.3 Pressures for fluid squeezed between parallel plates.

rule for rectangular elements, we would have obtained erroneous values. In general, the same integration rule as that used for the evaluation of the penalty terms in the coefficient matrix must be used to compute the pressure. The oscillations in pressure computed nearest to the top plate are due to the singularity in the boundary conditions at $(x, y) = (6, 2)$.

Example 10.6.2 (Flow of a Viscous Lubricant in a Slider Bearing)

The slider (or slipper) bearing consists of a short sliding pad moving at a velocity $u = V_0$ relative to a stationary pad inclined at a small angle with respect to the stationary pad, and the small gap between the two pads is filled with a lubricant [see Fig. 10.6.4(*a*)]. Since the ends of the bearing are generally open, the pressure there is atmospheric, P_0. If the upper pad is parallel to the base plate, the pressure everywhere in the gap must be atmospheric (because dP/dx is a constant for flow between parallel plates), and the bearing cannot support any transverse load. If the upper pad is inclined to the base pad, a pressure distribution, in general, a function of x and y, is set up in the gap. For large values of V_0, the pressure generated can be of sufficient magnitude to support heavy loads normal to the base pad.

When the width of the gap and the angle of inclination are small, we may assume that $v_y = 0$ and the pressure is not a function of y. Assuming a two-dimensional state of flow and a small angle of inclination, and neglecting the normal stress gradient (in comparison with the shear stress gradient), the equations governing the flow of the lubricant between the pads

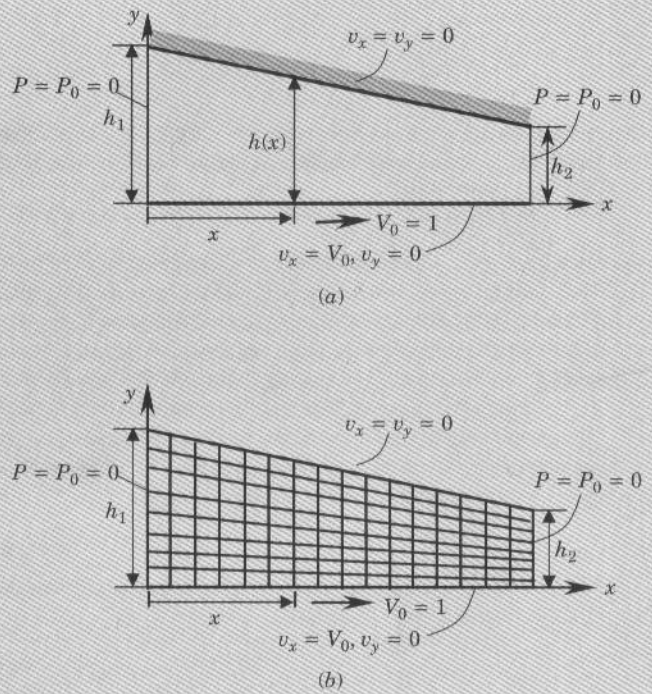

Figure 10.6.4 Schematic and the finite element mesh for slider bearing.

can be reduced to (see Schlichting, 1979)

$$\mu \frac{\partial^2 v_x}{\partial y^2} = \frac{dP}{dx}, \quad 0 < x < L \tag{10.6.2a}$$

where the pressure gradient is given by

$$\frac{dP}{dx} = \frac{6\mu V_0}{h^2}\left(1 - \frac{H}{h}\right), \quad H = \frac{2h_1 h_2}{h_1 + h_2} \tag{10.6.2b}$$

The solution of Eqs. (10.6.2*a*) and (10.6.2*b*), subject to the boundary conditions

$$v_x(0, 0) = V_0, \quad v_x(x, h) = 0 \tag{10.6.2c}$$

is

$$v_x(x, y) = \left(V_0 - \frac{h^2}{2\mu}\frac{dP}{dx}\frac{y}{h}\right)\left(1 - \frac{y}{h}\right) \tag{10.6.3a}$$

$$P(x) = \frac{6\mu V_0 L(h_1 - h)(h - h_2)}{h^2\left(h_1^2 - h_2^2\right)} \tag{10.6.3b}$$

$$\sigma_{xy}(x, y) = \mu \frac{\partial v_x}{\partial y} = \frac{dP}{dx}\left(y - \frac{h}{2}\right) - \mu \frac{V_0}{h} \tag{10.6.3c}$$

where

$$h(x) = h_1 + \frac{h_2 - h_1}{L} x \tag{10.6.4}$$

In the finite element analysis we do not make any assumptions concerning v_y and the pressure gradient, and solve the Stokes equations with the following choice of parameters:

$$h_1 = 2h_2 = 8 \times 10^{-4} \text{ ft.}, \quad L = 0.36 \text{ ft.}, \quad \mu = 8 \times 10^{-4} \text{ lb/ft.}^2, \quad V_0 = 30 \text{ ft.} \tag{10.6.5}$$

We use a mesh (mesh 1) of 18×8 linear quadrilateral elements to analyze the problem. The mesh and boundary conditions are shown in Fig. 10.6.4(*b*). The penalty parameter is chosen to be $\gamma = \mu \times 10^8$. Table 10.6.2 contains a comparison of the finite element solutions and analytical solutions for the velocity, pressure, and shear stress. Figure 10.6.5 contains plots of the horizontal velocity v_x at $x = 0$, 0.18, and 0.36 ft. Figure 10.6.6 contains plots of pressure and shear stress as a function of x at $y = 0$. The finite element solutions for the pressure and shear stress were computed at the center of the first row of elements along the moving block. The results are in good agreement with the analytical solutions (10.6.3*a*)–(10.6.3*c*), validating the assumptions made in the development of the analytical solution.

Table 10.6.2 Comparison of finite element solutions velocities with the analytical solutions for viscous fluid in a slider bearing.

	$v_x(0, y)$			$v_x(0.18, y)$			$v_x(0.36, y)$	
$\bar{y}$	FEM	Analy.	$\bar{y}$	FEM	Analy.	$\bar{y}$	FEM	Analy.
0.0	30.000	30.000	0.00	30.000	30.000	0.00	30.000	30.000
1.0	22.923	22.969	0.75	25.139	25.156	0.50	29.564	29.531
2.0	16.799	16.875	1.50	20.596	20.625	1.00	28.182	28.125
3.0	11.626	11.719	2.25	16.372	16.406	1.50	25.853	25.781
4.0	7.403	7.500	3.00	12.465	12.500	2.00	22.577	22.500
5.0	4.130	4.219	3.75	8.874	8.906	2.50	18.354	18.281
6.0	1.805	1.875	4.50	5.600	5.625	3.00	13.184	13.125
7.0	0.429	0.469	5.25	2.642	2.656	3.50	7.066	7.031
8.0	0.000	0.000	6.00	0.000	0.000	4.00	0.000	0.000

Analytical solution			FEM Solution			
x	$\bar{P}(x, 0)$	$-\sigma_{xy}(x, 0)$	$\bar{x}$	$\bar{y}$	$\bar{P}$	$-\sigma_{xy}$
0.01	7.50	59.99	0.1125	0.4922	8.46	56.61
0.03	22.46	59.89	0.3375	0.4766	25.46	56.60
0.05	37.29	59.67	0.5625	0.4609	42.31	56.47
0.07	51.89	59.30	0.7875	0.4453	58.76	56.17
0.09	66.12	58.77	1.0125	0.4297	74.69	55.69
0.27	129.60	38.40	2.5875	0.3203	134.40	41.77
0.29	118.57	32.71	2.8125	0.3047	125.60	36.93
0.31	99.58	25.70	3.0375	0.2891	107.60	30.76
0.33	70.30	17.04	3.2625	0.2734	77.39	22.89
0.35	27.61	6.31	3.4875	0.2578	30.80	12.82

$\bar{x} = 10x$, $\bar{y} = y \times 10^4$, $\bar{P} = P \times 10^{-2}$.

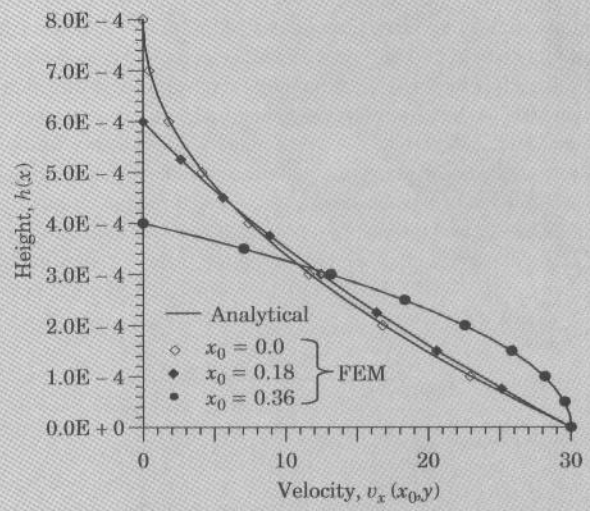

Figure 10.6.5 Velocity distributions for the slider bearing problem.

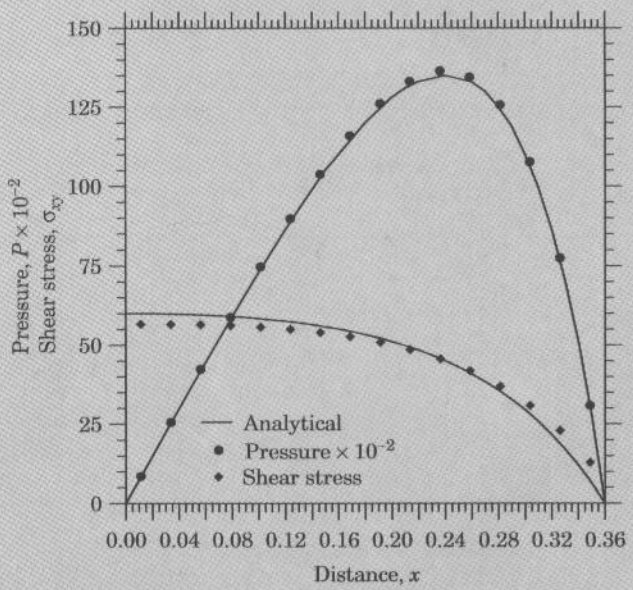

Figure 10.6.6 Pressure and shear stress distributions for the slider bearing problem.

Example 10.6.3 (Lid-Driven Cavity Flow)

Consider the laminar flow of a viscous, incompressible fluid in a square cavity bounded by three motionless walls and a lid moving at a constant velocity in its own plane (see Fig. 10.6.7). Singularities exist at each corner where the moving lid meets a fixed wall. This example is one that has been extensively studied by analytical, numerical, and experimental methods, and it is often used as a benchmark problem to test a new numerical method or formulation.

Assuming a unit square and a unit velocity of the top wall, we can discretize the flow region using a uniform 8×8 mesh of linear elements or 4×4 of nine-node quadratic elements. At the singular points, namely at the top corners of the lid, we assume that $v_x(x, 1) = v_0 = 1.0$. The linear solution for the horizontal velocity along the vertical centerline obtained with the two meshes is shown in Fig. 10.6.8, and the variation of pressure along the top wall (computed

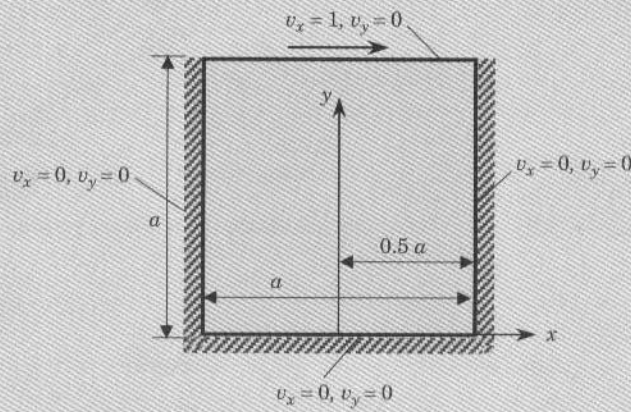

Figure 10.6.7 Boundary conditions for lid-driven cavity problem.

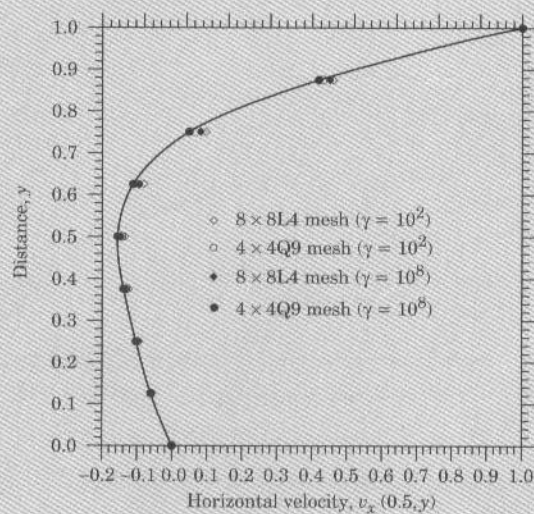

Figure 10.6.8 Plots of horizontal velocity $v_x(0.5, y)$ along the vertical centerline of the cavity.

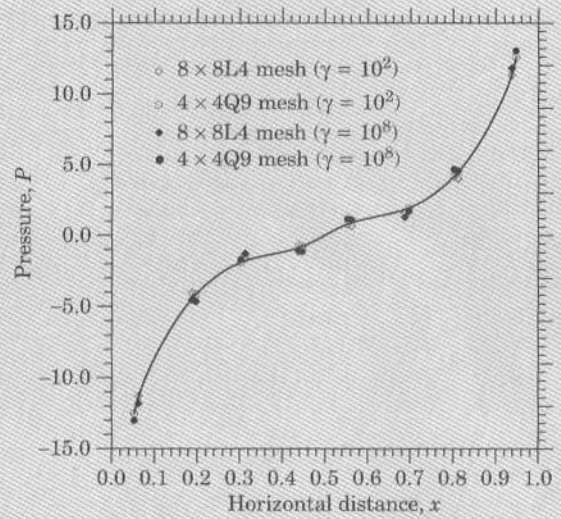

Figure 10.6.9 Plots of pressure $P(x, y_0)$ along the top wall of the cavity.

at the reduced Gauss points) is shown in Fig. 10.6.9. The numerical values of the velocity field are tabulated in Table 10.6.3. It is clear that the value of the penalty parameter between $\gamma = 10^2$ and 10^8 has a small effect on the accuracy of the solution. Figure 10.6.10 contains plots of center velocity $v_x(0.5, y)$ as a function of y for 8×8 and 16×20 meshes of bilinear elements.

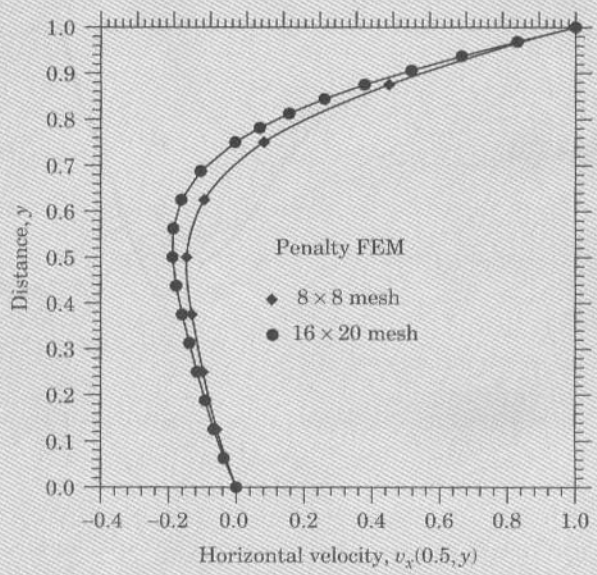

Figure 10.6.10 Velocity $v_x(0.5, y)$ versus y for 8×8 and 16×20 meshes of bilinear elements.

Table 10.6.3 Velocity $v_x(0.5, y)$ obtained with various values of the penalty parameter γ.

	Mesh: 8 × 8L4		Mesh: 4 × 4Q9	
y	$\gamma = 10^2$	$\gamma = 10^8$	$\gamma = 10^2$	$\gamma = 10^8$
0.125	−0.0557	−0.0579	−0.0589	−0.0615
0.250	−0.0938	−0.0988	−0.0984	−0.1039
0.375	−0.1250	−0.1317	−0.1320	−0.1394
0.500	−0.1354	−0.1471	−0.1442	−0.1563
0.625	−0.0818	−0.0950	−0.0983	−0.1118
0.750	0.0958	0.0805	0.0641	0.0481
0.875	0.4601	0.4501	0.4295	0.4186

Example 10.6.4 (Transient Analysis of Fluid Squeezed between Plates)

Consider the unsteady flow of a viscous fluid squeezed between two parallel plates [see Fig. 10.6.1(*a*)]. The flow is induced by the uniform motion of the plates toward each other. The boundary conditions of the model are the same as shown in Fig. 10.6.1(*b*). The initial boundary conditions are assumed to be zero.

We use the 6 × 4 mesh of nine-node quadratic elements, employed in Example 10.6.1, to model the problem. Figure 10.6.11 contains plots of the horizontal velocity $v_x(6, y)$ as a

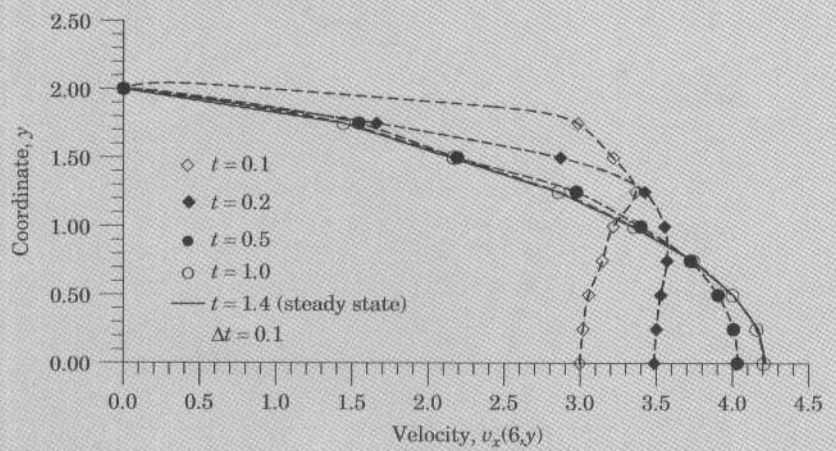

Figure 10.6.11 Velocity $v_x(6, y)$ versus y for various times (6 × 4 mesh of nine-node quadratic elements using penalty FEM).

function of y for various times and for two different time steps. The transient solution reaches a steady state around $t = 1.4$ (for a difference of 10^{-3} between the solutions at two consecutive time steps with $\Delta t = 0.1$).

Example 10.6.5 (Transient Analysis of the Lid-Driven Cavity)

Lastly, we study the motion of a viscous fluid inside a lid-driven cavity. We use 16×20Q4 nonuniform mesh (of four-node rectangular elements) in the domain. The element sizes in each coordinate direction are given by

$$\{\mathrm{DX}\} = \{0.0625,\ 0.0625,\ \ldots,\ 0.0625\}$$

$$\{\mathrm{DY}\} = \{0.0625, \ldots, 0.0625,\ 0.03125, \ldots,\ 0.03125\}$$

The Crank–Nicolson method ($\alpha = 0.5$) with two different time steps $\Delta t = 0.01$ and $\Delta t = 0.001$ are used. Table 10.6.4 contains the velocity field $v_x(0.5, y, t) \times 10$ for times $t = 0.01$, 0.05, and 0.1. The solution reaches the steady state ($\epsilon = 10^{-2}$) at time $t = 0.1$ when $\Delta t = 0.01$ is used. The evolution of the horizontal velocity component $v_x(0.5, y, t)$ is shown in Fig. 10.6.12 ($\Delta t = 0.01$).

Table 10.6.4 The horizontal velocity field $v_x(0.5, y, t) \times 10$ versus time t for the wall-driven cavity problem (16×20 Q4 mesh).

y	$t = 0.01$ $\Delta t = 0.01$	$t = 0.01$ $\Delta t = 0.001$	$t = 0.05$ $\Delta t = 0.01$	$t = 0.05$ $\Delta t = 0.001$	$t = 0.10$ $\Delta t = 0.01$	Steady state
0.0625	−0.1342	−0.1953	−0.3103	−0.3247	−0.3655	−0.3688
0.1250	−0.1936	−0.3140	−0.5624	−0.5841	−0.6558	−0.6631
0.1875	−0.2314	−0.3940	−0.7888	−0.8163	−0.9108	−0.9198
0.2500	−0.2691	−0.4651	−1.0122	−1.0435	−1.1499	−1.1593
0.3125	−0.3157	−0.5475	−1.2346	−1.2746	−1.3802	−1.3886
0.3750	−0.3759	−0.6536	−1.4790	−1.5053	−1.5967	−1.6028
0.4375	−0.4516	−0.7902	−1.6964	−1.7151	−1.7793	−1.7820
0.5000	−0.5435	−0.9605	−1.8536	−1.8643	−1.8906	−1.8895
0.5625	−0.6465	−1.1577	−1.8846	−1.8878	−1.8700	−1.8652
0.6250	−0.7474	−1.3479	−1.7011	−1.6946	−1.6336	−1.6250
0.6875	−0.8097	−1.4428	−1.1889	−1.1653	−1.0700	−1.0572
0.7500	−0.7536	−1.1523	−0.2093	−0.1693	−0.0520	−0.0382
0.7813	−0.6325	−0.7744	0.5100	0.5471	0.6713	0.6820
0.8125	−0.4077	−0.1695	1.4014	1.4197	1.5467	1.5526
0.8438	−0.0054	0.7336	2.4885	2.4716	2.5918	2.5965
0.8750	0.6329	1.9318	3.7259	3.6716	3.7646	3.7824
0.9063	1.7000	3.5232	5.1185	5.0707	5.1198	5.1616
0.9375	3.3334	5.3837	6.5139	6.5756	6.6082	6.6410
0.9688	5.9470	7.5970	7.9975	8.2488	8.3805	8.2838

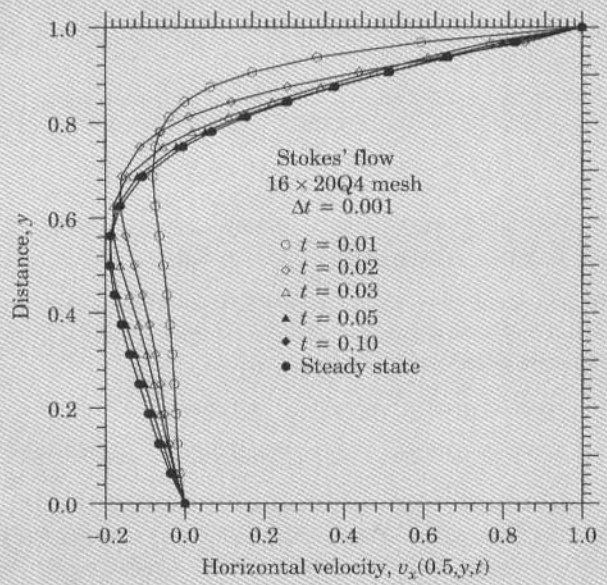

Figure 10.6.12 Evolution of the horizontal velocity $v_x(0.5, y, t)$ inside a wall-driven cavity.

10.7 SUMMARY

Finite element models of the equations governing two-dimensional flows of viscous, incompressible fluids are developed. Two different types of finite element models are presented: (1) the velocity-pressure finite element model, with (v_x, v_y, P) as the primary nodal degrees of freedom and (2) the penalty finite element model with (v_x, v_y) as the primary nodal degrees of freedom. In the penalty function method, the pressure is calculated from the velocity field in the postcomputation. The coefficient matrix in the penalty finite element model is evaluated using mixed integration: full integration for the viscous terms and reduced integration for the penalty terms (i.e., terms associated with the incompressibility or divergence-free condition on the velocity field). Both triangular and rectangular elements are discussed. In general, triangular elements do not yield accurate pressure fields. The linear and quadratic quadrilateral elements are more reliable for pressure as well as for velocity fields in the penalty finite element model.

A more complete treatment of finite element models of fluid flow can be found in the books by Gresho and Sani (1998), Reddy and Gartling (2001), and Reddy (2004). These books also contain extensive references to the literature on finite element analysis of fluid flow problems.

PROBLEMS

10.1 Consider Eqs. (10.2.1) and (10.2.2) in cylindrical coordinates (r, θ, z). For axisymmetric flows of viscous incompressible fluids (i.e., flow field is independent of θ coordinate), we have

$$\rho\frac{\partial u}{\partial t} = \frac{1}{r}\frac{\partial}{\partial r}(r\sigma_{rr}) - \frac{\sigma_{\theta\theta}}{r} + \frac{\partial \sigma_{rz}}{\partial z} + f_r \tag{1}$$

$$\rho\frac{\partial w}{\partial t} = \frac{1}{r}\frac{\partial}{\partial r}(r\sigma_{rz}) + \frac{\partial \sigma_{zz}}{\partial z} + f_z \tag{2}$$

$$\frac{1}{r}\frac{\partial}{\partial r}(ru) + \frac{\partial w}{\partial z} = 0 \tag{3}$$

where

$$\sigma_{rr} = -P + 2\mu\frac{\partial u}{\partial r}, \quad \sigma_{\theta\theta} = -P + 2\mu\frac{u}{r}, \quad \sigma_{zz} = -P + 2\mu\frac{\partial w}{\partial z}, \quad \sigma_{rz} = \mu\left(\frac{\partial u}{\partial z} + \frac{\partial w}{\partial r}\right) \tag{4}$$

Develop the semidiscrete finite element model of the equation by the pressure-velocity formulation.

10.2 Develop the semidiscrete finite element model of the equations in Problem 10.1 using the penalty function formulation.

10.3 Write the fully discretized finite element equations of the finite element models in Problems 10.1 and 10.2. Use the α-family of approximation.

10.4 The equations governing unsteady slow flow of viscous, incompressible fluids in the (x, y) plane can be expressed in terms of vorticity ζ and stream function ψ:

$$\rho\frac{\partial \zeta}{\partial t} - \mu\nabla^2\zeta = 0, \quad -2\zeta - \nabla^2\psi = 0$$

Develop the semidiscrete finite element model of the equations. Discuss the meaning of the secondary variables. Use α-family of approximation to reduce the ordinary differential equations to algebraic equations.

10.5–10.7 For the viscous flow problems given in Figs. P10.5–P10.7, give the specified primary and secondary degrees of freedom and their values.

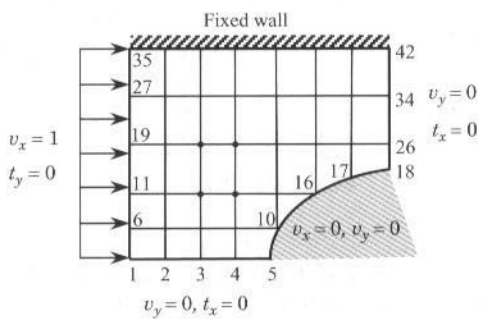

Figure P10.5

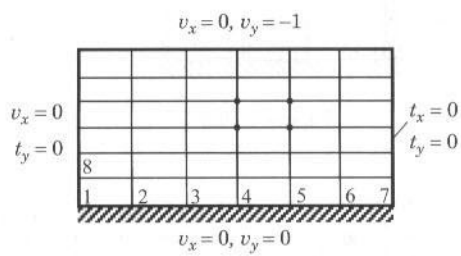

Figure P10.6

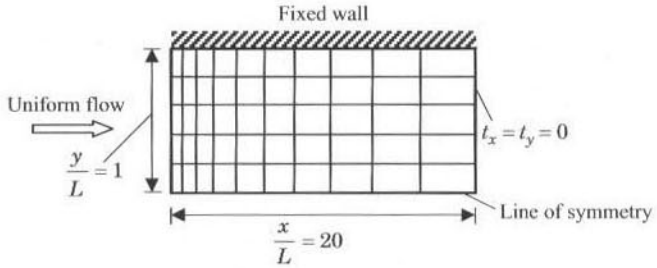

Figure P10.7

10.8. Consider the flow of a viscous incompressible fluid in a square cavity (Fig. P10.8). The flow is induced by the movement of the top wall (or lid) with a velocity $v_x = \sin \pi x$. For a 5 × 4 mesh of linear elements, give the primary and secondary degrees of freedom.

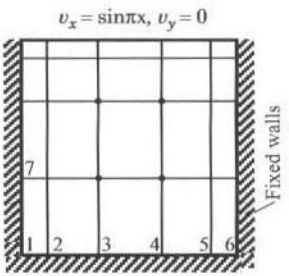

Figure P10.8

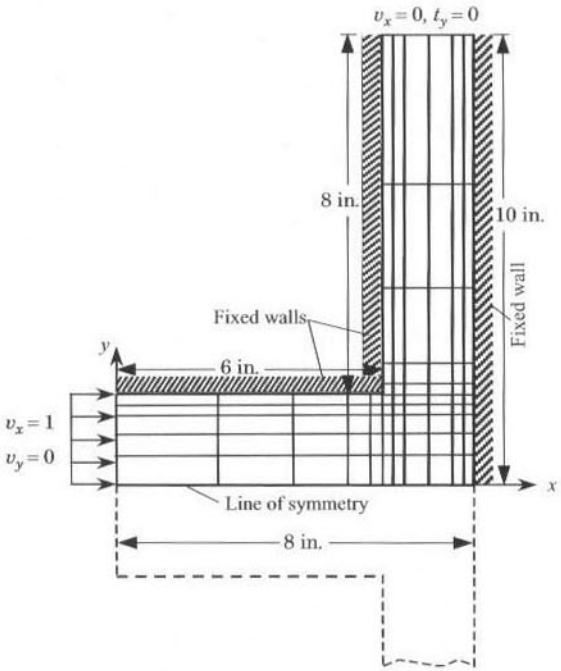

Figure P10.9

10.9. Consider the flow of a viscous incompressible fluid in a 90° plane tee. Using the symmetry and the mesh shown in Fig. P10.9. Write the specified primary and secondary variables for the computational domain.

10.10. Repeat Problem 10.9 for the geometry shown in Fig. P10.10.

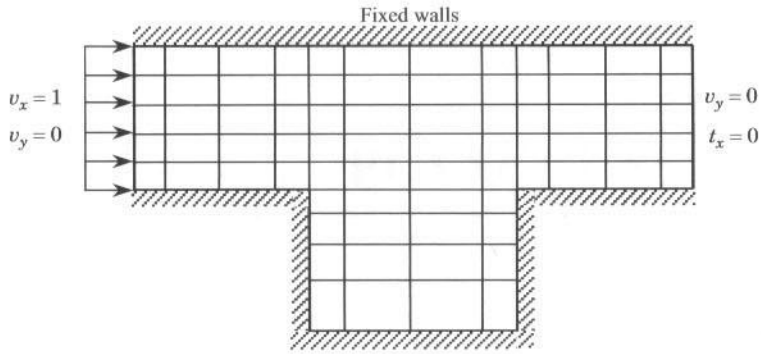

Figure P10.10

REFERENCES FOR ADDITIONAL READING

1. Bird, R. B., Stewart, W. E., and Lightfoot, E. N., *Transport Phenomena*, John Wiley, New York, 1960.
2. Gresho, P. M. and Sani, R. L., *Incompressible Flow and the Finite Element Method*, John Wiley, West Sussex, UK, 2000.
3. Nadai, A, *Theory of Flow and Fracture of Solids*, Vol. II, McGraw-Hill, New York, 1963.
4. Oden, J. T., "RIP Methods for Stokesian Flows," in Gallagher, R. H., Zienkiewicz, O. C., Oden, J. T., and Norrie, D. (eds.), *Finite Element Method in Flow Problems*, Vol. IV, John Wiley, London, UK, 1982.
5. Reddy, J. N., "On the Accuracy and Existence of Solutions to Primitive Variable Models of Viscous Incompressible Fluids," *International Journal Engineering Science,* **16**, 921–929, 1978.
6. Reddy, J. N., "On the Finite Element Method with Penalty for Incompressible Fluid Flow Problems," in Whiteman, J. R. (ed.), *The Mathematics of Finite Elements and Applications III*, Academic Press, New York, 1979.
7. Reddy, J. N., *Applied Functional Analysis and Variational Methods in Engineering*, McGraw-Hill, New York, 1986; reprinted by Krieger, Melbourne, FL, 1991.
8. Reddy, J. N., *An Introduction to Nonlinear Finite Element Analysis*, Oxford University Press, Oxford, UK, 2004.
9. Reddy, J. N. and Gartling, D. K., *The Finite Element Method in Heat Transfer and Fluid Dynamics*, 2nd ed., CRC Press, Boca Raton, FL, 2001.
10. Roache, P. J., *Fundamentals of Computational Fluid Dynamics*, 2nd ed., Hermosa, Albuquerque, NM, 1998.
11. Schlichting, H., *Boundary Layer Theory* (translated by J. Kestin), 7th ed., McGraw-Hill, New York, 1979.

Chapter 11
PLANE ELASTICITY

11.1 INTRODUCTION

Elasticity is the part of solid mechanics that deals with stress and deformation of solid continua. Linearized elasticity is concerned with small deformations (i.e., strains and displacements that are very small compared to unity) in linear elastic solids (i.e., obey Hooke's law). There is a class of problems in elasticity whose solutions (i.e., displacements and stresses) are not dependent on one of the coordinates because of their geometry, boundary conditions, and external applied loads. Such problems are called plane elasticity problems. The plane elasticity problems considered here are grouped into *plane strain* and *plane stress* problems. Both classes of problems are described by a set of two *coupled* partial differential equations expressed in terms of two dependent variables that represent the two components of the displacement vector. The governing equations of plane strain problems differ from those of the plane stress problems only in the coefficients of the differential equations.

The primary objective of this chapter is three-fold: (1) review the governing equations in the Cartesian rectangular coordinate system (x, y, z), (2) develop the weak forms, and (3) construct finite element model of the plane elasticity equations. The treatment of topics (2) and (3) proceeds along the same lines as the discussion in Chapter 10 on viscous incompressible fluids. In fact, the governing equations of the two fields are quite similar, as we shall see shortly. We utilize suitable approximation functions from the library of two-dimensional finite element interopolation functions already developed in Chapters 8 and 9 to derive finite element equations.

11.2 GOVERNING EQUATIONS

11.2.1 Plane Strain

Plane strain problems are characterized by the displacement field

$$u_x = u_x(x, y), \quad u_y = u_y(x, y), \quad u_z = 0 \tag{11.2.1}$$

where (u_x, u_y, u_z) denote the components of the displacement vector $\mathbf{u}$ in the (x, y, z) coordinate system. The displacement field (11.2.1) results in the following strain field:

$$\varepsilon_{xz} = \varepsilon_{yz} = \varepsilon_{zz} = 0$$
$$\varepsilon_{xx} = \frac{\partial u_x}{\partial x}, \quad 2\varepsilon_{xy} = \frac{\partial u_x}{\partial y} + \frac{\partial u_y}{\partial x}, \quad \varepsilon_{yy} = \frac{\partial u_y}{\partial y} \tag{11.2.2}$$

Clearly, the body is in a state of plane strain. For an orthotropic material, with principal material axes (x_1, x_2, x_3) coinciding with the (x, y, z) coordinates, the stress components are given by

$$\sigma_{xz} = \sigma_{yz} = 0, \quad \sigma_{zz} = E_3 \left(\frac{\nu_{13}}{E_1} \sigma_{xx} + \frac{\nu_{23}}{E_2} \sigma_{yy} \right) \tag{11.2.3a}$$

$$\begin{Bmatrix} \sigma_{xx} \\ \sigma_{yy} \\ \sigma_{xy} \end{Bmatrix} = \begin{bmatrix} \bar{c}_{11} & \bar{c}_{12} & 0 \\ \bar{c}_{12} & \bar{c}_{22} & 0 \\ 0 & 0 & \bar{c}_{66} \end{bmatrix} \begin{Bmatrix} \varepsilon_{xx} \\ \varepsilon_{yy} \\ 2\varepsilon_{xy} \end{Bmatrix} \tag{11.2.3b}$$

where $\bar{c}_{ij}$ are the elastic stiffnesses

$$\begin{aligned} \bar{c}_{11} &= \frac{E_1(1 - \nu_{12})}{(1 + \nu_{12})(1 - \nu_{12} - \nu_{21})} \\ \bar{c}_{22} &= \frac{E_2(1 - \nu_{21})}{(1 + \nu_{21})(1 - \nu_{12} - \nu_{21})} \\ \bar{c}_{12} &= \nu_{12}\bar{c}_{22}, \quad \bar{c}_{66} = G_{12} \end{aligned} \tag{11.2.4}$$

and E_1 and E_2 are principal (Young's) moduli in the x and y directions, respectively, G_{12} the shear modulus in the xy plane, and ν_{12} and ν_{21} the Poisson ratio (i.e., the negative of the ratio of the transverse strain in the y direction to the strain in the x direction when stress is applied in the x direction). The Poisson ratio ν_{21} can be computed from the reciprocal relation

$$\nu_{21} = \nu_{12} \frac{E_2}{E_1} \tag{11.2.5}$$

Additional engineering constants E_3, ν_{23}, and ν_{13} are required to compute σ_{zz}. For an isotropic material, we have

$$E_1 = E_2 = E_3 = E, \quad \nu_{12} = \nu_{21} = \nu_{13} = \nu_{23} = \nu, \quad G_{12} = G = \frac{E}{2(1 + \nu)} \tag{11.2.6}$$

The equations of motion of three-dimensional linear elasticity, $\sigma_{ij,j} + f_i = \rho \ddot{u}_i$ with the body force components $f_3 = f_z = 0$, $f_1 = f_x = f_x(x, y)$, and $f_2 = f_y = f_y(x, y)$, and ρ the density of the material, reduce to the following two plane strain equations of motion

$$\rho \frac{\partial^2 u_x}{\partial t^2} - \frac{\partial \sigma_{xx}}{\partial x} - \frac{\partial \sigma_{xy}}{\partial y} - f_x = 0 \tag{11.2.7}$$

$$\rho \frac{\partial^2 u_y}{\partial t^2} - \frac{\partial \sigma_{xy}}{\partial x} - \frac{\partial \sigma_{yy}}{\partial y} - f_y = 0 \tag{11.2.8}$$

An example of a plane strain problem is provided by the long cylindrical member under external loads that are independent of z, as shown in Fig. 11.2.1. For cross sections sufficiently far from the ends, it is clear that the displacement u_z is zero and that u_x and u_y are independent of z, i.e., a state of plane strain exists.

11.2.2 Plane Stress

A state of plane stress is defined as one in which the following stress field exists:

$$\begin{aligned} &\sigma_{xz} = \sigma_{yz} = \sigma_{zz} = 0 \\ &\sigma_{xx} = \sigma_{xx}(x, y), \quad \sigma_{xy} = \sigma_{xy}(x, y), \quad \sigma_{yy} = \sigma_{yy}(x, y) \end{aligned} \tag{11.2.9a}$$

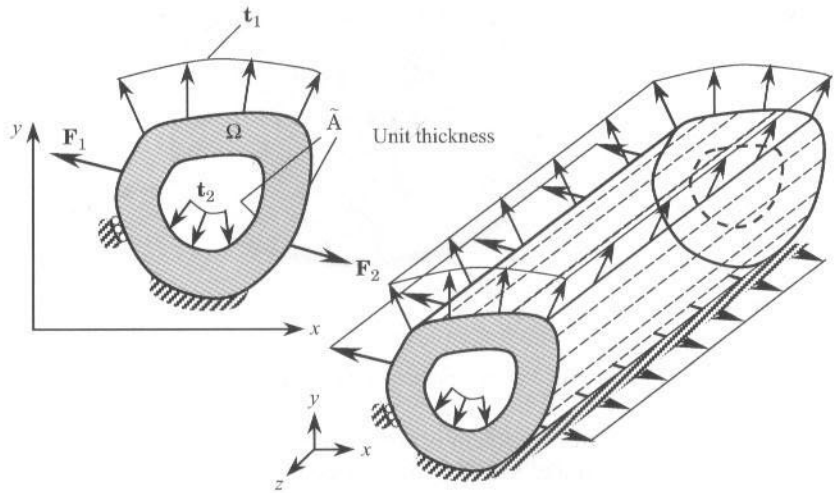

Figure 11.2.1 A hollow cylindrical member with internal and external applied loads.

The strain field associated with the stress field in (11.2.9a) is

$$\begin{Bmatrix} \varepsilon_{xx} \\ \varepsilon_{yy} \\ 2\varepsilon_{xy} \end{Bmatrix} = \begin{bmatrix} s_{11} & s_{12} & 0 \\ s_{12} & s_{22} & 0 \\ 0 & 0 & s_{66} \end{bmatrix} \begin{Bmatrix} \sigma_{xx} \\ \sigma_{yy} \\ \sigma_{xy} \end{Bmatrix} \tag{11.2.9b}$$

$$\varepsilon_{xz} = \varepsilon_{yz} = 0, \quad \varepsilon_{zz} = s_{13}\sigma_{xz} + s_{23}\sigma_{yz} \tag{11.2.9c}$$

where s_{ij} are the elastic compliances

$$\begin{aligned} s_{11} &= \frac{1}{E_1}, \quad s_{22} = \frac{1}{E_2}, \quad s_{33} = \frac{1}{E_3} \\ s_{12} &= -\nu_{21}s_{22} = -\nu_{12}s_{11}, \quad s_{66} = \frac{1}{G_{12}} \\ s_{13} &= -\nu_{31}s_{33} = -\nu_{13}s_{11}, \quad s_{23} = -\nu_{32}s_{33} = -\nu_{23}s_{22} \end{aligned} \tag{11.2.10}$$

The inverse of (11.2.9*b*) is given by

$$\begin{Bmatrix} \sigma_{xx} \\ \sigma_{yy} \\ \sigma_{xy} \end{Bmatrix} = \begin{bmatrix} \hat{c}_{11} & \hat{c}_{12} & 0 \\ \hat{c}_{12} & \hat{c}_{22} & 0 \\ 0 & 0 & \hat{c}_{66} \end{bmatrix} \begin{Bmatrix} \varepsilon_{xx} \\ \varepsilon_{yy} \\ 2\varepsilon_{xy} \end{Bmatrix} \tag{11.2.11}$$

where $\hat{c}_{ij}$ are the elastic stiffnesses

$$\begin{aligned} \hat{c}_{11} &= \frac{E_1}{(1-\nu_{12}\nu_{21})}, \quad \hat{c}_{22} = \frac{E_2}{(1-\nu_{12}\nu_{21})} \\ \hat{c}_{12} &= \nu_{12}\hat{c}_{22} = \nu_{21}\hat{c}_{11}, \quad \hat{c}_{66} = G_{12} \end{aligned} \tag{11.2.12}$$

The equations of motion of a plane stress problem are the same as those listed in Eqs. (11.2.7) and (11.2.8). Note that the equations of motion of plane stress and plane strain differ from each other only on account of the difference in the constitutive equations for the two cases.

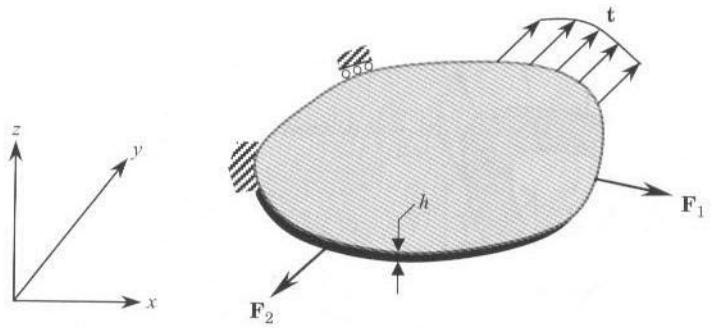

Figure 11.2.2 A thin plate in a state of plane stress.

An example of a plane stress problem is provided by a thin plate under external loads applied in the xy plane (or parallel to it) that are independent of z, as shown in Fig. 11.2.2. The top and bottom surfaces of the plate are assumed to be traction free, and the specified boundary forces are in the xy plane so that $f_z = 0$ and $u_z = 0$.

11.2.3 Summary of Equations

The governing equations for the two types of plane elasticity problems discussed above are summarized below, both in expanded form and vector form.

Equations of Motion

$$\begin{aligned} \frac{\partial \sigma_{xx}}{\partial x} + \frac{\partial \sigma_{xy}}{\partial y} + f_x &= \rho \frac{\partial^2 u_x}{\partial t^2} \\ \frac{\partial \sigma_{xy}}{\partial x} + \frac{\partial \sigma_{yy}}{\partial y} + f_y &= \rho \frac{\partial^2 u_y}{\partial t^2} \end{aligned} \tag{11.2.13a}$$

or

$$\mathbf{D}^* \boldsymbol{\sigma} + \mathbf{f} = \rho \ddot{\mathbf{u}} \tag{11.2.13b}$$

where f_x and f_y denote the components of the body force vector (measured per unit volume) along the x and y directions, respectively, ρ is the density of the material, and

$$\mathbf{D}^* = \begin{bmatrix} \partial/\partial x & 0 & \partial/\partial y \\ 0 & \partial/\partial y & \partial/\partial x \end{bmatrix}, \quad \boldsymbol{\sigma} = \begin{Bmatrix} \sigma_{xx} \\ \sigma_{yy} \\ \sigma_{xy} \end{Bmatrix}, \quad \mathbf{f} = \begin{Bmatrix} f_x \\ f_y \end{Bmatrix}, \quad \mathbf{u} = \begin{Bmatrix} u_x \\ u_y \end{Bmatrix} \tag{11.2.13c}$$

Strain-Displacement Relations

$$\varepsilon_{xx} = \frac{\partial u_x}{\partial x}, \quad \varepsilon_{yy} = \frac{\partial u_y}{\partial y}, \quad 2\varepsilon_{xy} = \frac{\partial u_x}{\partial y} + \frac{\partial u_y}{\partial x} \tag{11.2.14a}$$

or

$$\boldsymbol{\varepsilon} = \mathbf{D}\mathbf{u}, \quad \boldsymbol{\varepsilon} = \begin{Bmatrix} \varepsilon_{xx} \\ \varepsilon_{yy} \\ 2\varepsilon_{xy} \end{Bmatrix}, \quad \mathbf{D} = (\mathbf{D}^*)^{\mathrm{T}} \tag{11.2.14b}$$

Stress-Strain (or Constitutive) Relations

$$\begin{Bmatrix} \sigma_{xx} \\ \sigma_{yy} \\ \sigma_{xy} \end{Bmatrix} = \begin{bmatrix} c_{11} & c_{12} & 0 \\ c_{12} & c_{22} & 0 \\ 0 & 0 & c_{66} \end{bmatrix} \begin{Bmatrix} \varepsilon_{xx} \\ \varepsilon_{yy} \\ 2\varepsilon_{xy} \end{Bmatrix} \tag{11.2.15a}$$

or

$$\boldsymbol{\sigma} = \mathbf{C}\boldsymbol{\varepsilon}, \quad \mathbf{C} = \begin{bmatrix} c_{11} & c_{12} & 0 \\ c_{12} & c_{22} & 0 \\ 0 & 0 & c_{66} \end{bmatrix} \tag{11.2.15b}$$

where c_{ij} ($c_{ji} = c_{ij}$) are the elasticity (material) constants for an orthotropic medium with the material principal directions (x_1, x_2, x_3) coinciding with the coordinate axes (x, y, z) used to describe the problem. The c_{ij} can be expressed in terms of the engineering constants $(E_1, E_2, \nu_{12}, G_{12})$ for an orthotropic material by Eqs. (11.2.3*b*) for plane strain problems ($c_{ij} = \bar{c}_{ij}$) and by Eqs. (11.2.11) for plane stress problems ($c_{ij} = \hat{c}_{ij}$).

Boundary Conditions

Natural boundary conditions are

$$\left.\begin{aligned} t_x &\equiv \sigma_{xx} n_x + \sigma_{xy} n_y = \hat{t}_x \\ t_y &\equiv \sigma_{xy} n_x + \sigma_{yy} n_y = \hat{t}_y \end{aligned}\right\} \quad \text{on } \Gamma_\sigma \tag{11.2.16a}$$

or

$$\mathbf{t} \equiv \bar{\sigma}\mathbf{n} = \hat{\mathbf{t}} \text{ on } \Gamma_\sigma, \quad \mathbf{n} = \begin{Bmatrix} n_x \\ n_y \end{Bmatrix}, \ \bar{\sigma} = \begin{bmatrix} \sigma_{xx} & \sigma_{xy} \\ \sigma_{xy} & \sigma_{yy} \end{bmatrix} \tag{11.2.16b}$$

Essential boundary conditions are

$$u_x = \hat{u}_x, \quad u_y = \hat{u}_y \quad \text{on } \Gamma_u \tag{11.2.17a}$$

or

$$\mathbf{u} = \hat{\mathbf{u}} \quad \text{on } \Gamma_u \tag{11.2.17b}$$

where (n_x, n_y) denote the components (or direction cosines) of the unit normal vector on the boundary Γ; Γ_σ and Γ_u are (disjoint) portions of the boundary; $\hat{t}_x$ and $\hat{t}_y$ denote the components of the specified traction vector; and $\hat{u}_x$ and $\hat{u}_y$ are the components of specified displacement vector. Only one element of each pair, (u_x, t_x) and (u_y, t_y), may be specified at a boundary point.

Equations (11.2.7) and (11.2.8) can be expressed in terms of only the displacements u_x and u_y by substituting Eqs. (11.2.14) into Eqs. (11.2.15), and the result into Eqs. (11.2.13):

$$\begin{aligned} -\frac{\partial}{\partial x}\left(c_{11}\frac{\partial u_x}{\partial x} + c_{12}\frac{\partial u_y}{\partial y}\right) - \frac{\partial}{\partial y}\left[c_{66}\left(\frac{\partial u_x}{\partial y} + \frac{\partial u_y}{\partial x}\right)\right] &= f_x - \rho\frac{\partial^2 u_x}{\partial t^2} \\ -\frac{\partial}{\partial x}\left[c_{66}\left(\frac{\partial u_x}{\partial y} + \frac{\partial u_y}{\partial x}\right)\right] - \frac{\partial}{\partial y}\left(c_{12}\frac{\partial u_x}{\partial x} + c_{22}\frac{\partial u_y}{\partial y}\right) &= f_y - \rho\frac{\partial^2 u_y}{\partial t^2} \end{aligned} \tag{11.2.18a}$$

or

$$-\mathbf{D}^*\mathbf{C}\mathbf{D}\mathbf{u} = \mathbf{f} + \rho\ddot{\mathbf{u}} \tag{11.2.18b}$$

The boundary stress components (or tractions) can also be expressed in terms of the displacements:

$$\begin{aligned} t_x &= \left(c_{11}\frac{\partial u_x}{\partial x} + c_{12}\frac{\partial u_y}{\partial y}\right)n_x + c_{66}\left(\frac{\partial u_x}{\partial y} + \frac{\partial u_y}{\partial x}\right)n_y \\ t_y &= c_{66}\left(\frac{\partial u_x}{\partial y} + \frac{\partial u_y}{\partial x}\right)n_x + \left(c_{12}\frac{\partial u_x}{\partial x} + c_{22}\frac{\partial u_y}{\partial y}\right)n_y \end{aligned} \tag{11.2.19a}$$

or

$$\mathbf{t} = \bar{\mathbf{n}}\mathbf{C}\mathbf{D}\mathbf{u}, \quad \bar{\mathbf{n}} = \begin{bmatrix} n_x & 0 & n_y \\ 0 & n_y & n_x \end{bmatrix} \tag{11.2.19b}$$

This completes the review of the governing equations of a plane elastic body undergoing small deformations. Next, we discuss the finite element model development of the equations.

11.3 WEAK FORMULATIONS

11.3.1 Preliminary Comments

Here, we study two different ways of constructing the weak forms and associated finite element model of the plane elasticity equations (11.2.18*a*) and (11.2.19*a*). The first one uses the principle of virtual displacements (or the principle of minimum total potential energy), expressed in terms of matrices relating displacements to strains, strains to stresses, and the equations of motion. This approach is used in most finite element texts on solid mechanics. The second approach follows a procedure consistent with the previous sections and employs the weak formulation of Eqs. (11.2.18*a*) and (11.2.19*a*) to construct the finite element model. Of course, both methods give, mathematically, the *same* finite element model, but differ in their algebraic forms.

11.3.2 Principle of Virtual Displacements in Vector Form

Here, we use the (dynamic version of) the principle of virtual displacements [see Reddy (2002)] applied to a plane elastic finite element Ω_e with volume $V_e = h_e\Omega_e$ (see Fig. 11.3.1)

$$0 = \int_{V_e} (\sigma_{ij}\delta\varepsilon_{ij} + \rho\ddot{u}_i\delta u_i)dV - \int_{V_e} f_i\delta u_i\, dV - \oint_{s_e} \hat{t}_i\delta u_i\, ds \tag{11.3.1}$$

where s_e is the surface of the volume element V_e, h_e is the thickness of the element, δ denotes the variational operator, σ_{ij} and ε_{ij} are the components of stress and strain tensors, respectively, and f_i and $\hat{t}_i$ are the components of the body force and boundary stress vectors, respectively. The correspondence between the (x, y) components and (x_1, x_2) components is given by

$$\begin{aligned} &\sigma_{11} = \sigma_{xx},\ \sigma_{12} = \sigma_{xy},\ \sigma_{22} = \sigma_{yy},\ \varepsilon_{11} = \varepsilon_{xx},\ \varepsilon_{12} = \varepsilon_{xy},\ \varepsilon_{22} = \varepsilon_{yy} \\ &u_1 = u_x,\ u_2 = u_y,\ h_e f_1 = f_x,\ h_e f_2 = f_y,\ h_e t_1 = t_x,\ h_e t_2 = t_y \end{aligned} \tag{11.3.2}$$

The first term in Eq. (11.3.1) corresponds to the virtual strain energy stored in the body, the second term corresponds to the kinetic energy stored in the body, the third term represents the virtual work done by the body forces, and the fourth term represents the virtual work done by the surface tractions. We assume that all quantities are independent of the

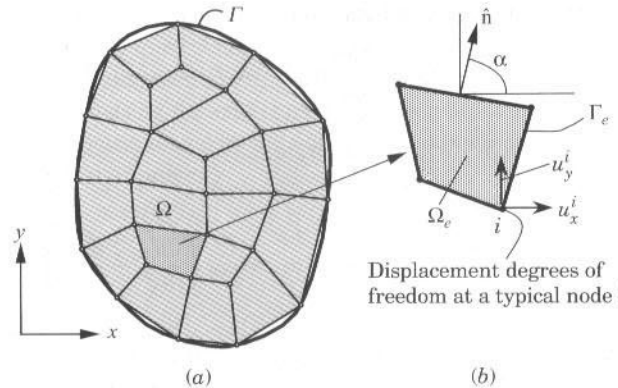

Figure 11.3.1 (*a*) Finite element discretization of a plane elastic domain and (*b*) a typical finite element.

thickness coordinate, z. Hence,

$$0 = \int_{\Omega_e} h_e[\sigma_{xx}\delta\varepsilon_{xx} + \sigma_{yy}\delta\varepsilon_{yy} + 2\sigma_{xy}\delta\varepsilon_{xy} + \rho(\ddot{u}_x\delta u_x + \ddot{u}_y\delta u_y)]\,dx\,dy$$
$$- \int_{\Omega_e} (f_x\delta u_x + f_y\delta u_y)\,dx\,dy - \oint_{\Gamma e} (t_x\delta u_x + t_y\delta u_y)\,ds \tag{11.3.3}$$

wherein, now, f_x and f_y are body forces per unit area and t_x and t_y are boundary forces per unit length. When the stresses are expressed in terms of strains through Eq. (11.2.15*a*) and strains in terms of displacements by Eq. (11.2.14*a*), Eq. (11.3.3) takes the form associated with minimizing the total potential energy, $\delta\Pi_e = 0$.

Equation (11.3.3) can be rewritten using the notation introduced in Eqs. (11.2.13)–(11.2.15) (note that $\delta\boldsymbol{\varepsilon} = \mathbf{D}\delta\mathbf{u}$ and $(\mathbf{AB})^{\mathrm{T}} = \mathbf{B}^{\mathrm{T}}\mathbf{A}^{\mathrm{T}}$)

$$0 = \int_{\Omega_e} h_e \left[(\mathbf{D}\delta\mathbf{u})^{\mathrm{T}}\,\mathbf{C}\,(\mathbf{D}\mathbf{u}) + \rho\mathbf{u}^{\mathrm{T}}\ddot{\mathbf{u}}\right] d\mathbf{x} - \int_{\Omega_e} (\delta\mathbf{u})^{\mathrm{T}}\mathbf{f}\,d\mathbf{x} - \oint_{\Gamma_e} (\delta\mathbf{u})^{\mathrm{T}}\mathbf{t}\,ds \tag{11.3.4}$$

11.3.3 Weak Form of the Governing Differential Equations

Here we present an alternative procedure to develop the weak form of the plane elasticity equations (11.2.18*a*) and (11.2.18*b*). The present approach, which has been used throughout the book thus far, does not require knowledge of the principles of virtual displacements or the total minimum potential energy but only needs the governing differential equations of the problem. We use the three-step procedure for each of the two differential equations: multiply the first equation with a weight function w_1 and integrate by parts to trade the differentiation equally between the weight function and the dependent variables (u_x, u_y). We have

$$0 = \int_{\Omega_e} h_e \left(\frac{\partial w_1}{\partial x}\sigma_{xx} + \frac{\partial w_1}{\partial y}\sigma_{xy} - w_1 f_x + \rho w_1 \ddot{u}_x\right) dx\,dy$$
$$- \oint_{\Gamma_e} h_e w_1(\sigma_{xx}n_x + \sigma_{xy}n_y)ds \tag{11.3.5}$$

Similarly, for the second equation, we have

$$0 = \int_{\Omega_e} h_e \left(\frac{\partial w_2}{\partial x}\sigma_{xy} + \frac{\partial w_2}{\partial y}\sigma_{yy} - w_2 f_y + \rho w_2 \ddot{u}_y \right) dx\, dy$$
$$- \oint_{\Gamma_e} h_e w_2 (\sigma_{xy} n_x + \sigma_{yy} n_y) ds \tag{11.3.6}$$

where

$$\sigma_{xx} = c_{11}\frac{\partial u_x}{\partial x} + c_{12}\frac{\partial u_y}{\partial y}, \quad \sigma_{xy} = c_{66}\left(\frac{\partial u_x}{\partial y} + \frac{\partial u_y}{\partial x}\right)$$
$$\sigma_{yy} = c_{12}\frac{\partial u_x}{\partial x} + c_{22}\frac{\partial u_y}{\partial y} \tag{11.3.7}$$

The last step of the development is to identify the primary and secondary variables of the formulation and rewrite the boundary integrals in terms of the secondary variables. Examination of the boundary integrals in Eqs. (11.3.5) and (11.3.6) reveals that the expressions in the parentheses constitute the secondary variables. By comparing these expressions with those in Eq. (11.2.16*a*), it follows that the boundary forces t_x and t_y are the secondary variables. The weight functions w_1 and w_2 are the first variations of u_x and u_y, respectively. Thus, the final weak forms are given by

$$0 = \int_{\Omega_e} h_e \left[\frac{\partial w_1}{\partial x}\left(c_{11}\frac{\partial u_x}{\partial x} + c_{12}\frac{\partial u_y}{\partial y}\right) + c_{66}\frac{\partial w_1}{\partial y}\left(\frac{\partial u_x}{\partial y} + \frac{\partial u_y}{\partial x}\right) + \rho w_1 \ddot{u}_x \right] dx\, dy$$
$$- \int_{\Omega_e} h_e w_1 f_x\, dx\, dy - \oint_{\Gamma_e} h_e w_1 t_x\, ds \tag{11.3.8a}$$

$$0 = \int_{\Omega_e} h_e \left[c_{66}\frac{\partial w_2}{\partial x}\left(\frac{\partial u_x}{\partial y} + \frac{\partial u_y}{\partial x}\right) + \frac{\partial w_2}{\partial y}\left(c_{12}\frac{\partial u_x}{\partial x} + c_{22}\frac{\partial u_y}{\partial y}\right) + \rho w_2 \ddot{u}_y \right] dx\, dy$$
$$- \int_{\Omega_e} h_e w_2 f_y\, dx\, dy - \oint_{\Gamma_e} h_e w_2 t_y\, ds \tag{11.3.8b}$$

This completes the development of the weak formulation of the plane elasticity equations in (11.2.18*a*). The alternative formulation in Eqs. (11.3.8*a*) and (11.3.8*b*) is exactly the same as that in Eq. (11.3.4); one is in vector form and the other is in explicit form. Therefore, the finite element models developed using the weak forms (11.3.4) and (11.3.8*a*) and (11.3.8*b*) would be the same.

11.4 FINITE ELEMENT MODEL

11.4.1 General Model

Here, we develop the finite element model of the plane elasticity equations using both the expanded forms (11.3.8*a*) and (11.3.8*b*) as well as the vector form (11.3.4) so that readers with different backgrounds can follow the development. An examination of the weak forms (11.3.8*a*) and (11.3.8*b*) reveals that: (*a*) u_x and u_y are the primary variables, which must be carried as the primary nodal degrees of freedom, and (*b*) only first derivatives of u_x and u_y with respect to x and y, respectively, appear. Therefore, u_x and u_y must be approximated by the Lagrange family of interpolation functions, and at least bilinear (i.e., linear both in x

and y) interpolation is required. The simplest elements that satisfy those requirements are the linear triangular and linear quadrilateral elements. Although u_x and u_y are independent of each other, they are the components of the displacement vector. Therefore, both components should be approximated using the same type and degree of interpolation.

Let u_x and u_y be approximated by the finite element interpolations (the element label e is omitted in the interest of brevity)

$$u_x \approx \sum_{j=1}^{n} u_x^j \psi_j(x, y), \quad u_y \approx \sum_{j=1}^{n} u_y^j \psi_j(x, y) \tag{11.4.1a}$$

or

$$\mathbf{u} = \begin{Bmatrix} u_x \\ u_y \end{Bmatrix} = \Psi \Delta, \quad \mathbf{w} = \delta \mathbf{u} = \begin{Bmatrix} w_1 = \delta u_x \\ w_2 = \delta u_y \end{Bmatrix} = \Psi \delta \Delta \tag{11.4.1b}$$

where

$$\begin{aligned} \Psi &= \begin{bmatrix} \psi_1 & 0 & \psi_2 & 0 & \dots & \psi_n & 0 \\ 0 & \psi_1 & 0 & \psi_2 & \dots & 0 & \psi_n \end{bmatrix} \\ \Delta &= \{ u_x^1 \quad u_y^1 \quad u_x^2 \quad u_y^2 \quad \dots \quad u_x^n \quad u_y^n \}^{\mathrm{T}} \end{aligned} \tag{11.4.2}$$

At the moment, we will not restrict ψ_j to any specific element so that the finite element formulation to be developed is valid for any admissible element. For example, if a linear triangular element ($n = 3$) is used, we have two (u_x^i, u_y^i) $(i = 1, 2, 3)$ degrees of freedom per node and a total of six nodal displacements per element [see Fig. 11.4.1(a)]. For a linear quadrilateral element, there are a total of eight nodal displacements per element [see Fig. 11.4.1(b)]. Since the first derivatives of ψ_i for a triangular element are elementwise constant, all the strains $(\varepsilon_{xx}, \varepsilon_{yy}, \varepsilon_{xy})$ computed for the linear triangular element are elementwise constant. Therefore, the linear triangular element for plane elasticity problems is known as the *constant-strain triangular* (CST) *element*. For a quadrilateral element the first derivatives of ψ_i are not constant: $\partial \psi_i^e / \partial \xi$ is linear in η and constant in ξ, and $\partial \psi_i^e / \partial \eta$ is linear in ξ and constant in η.

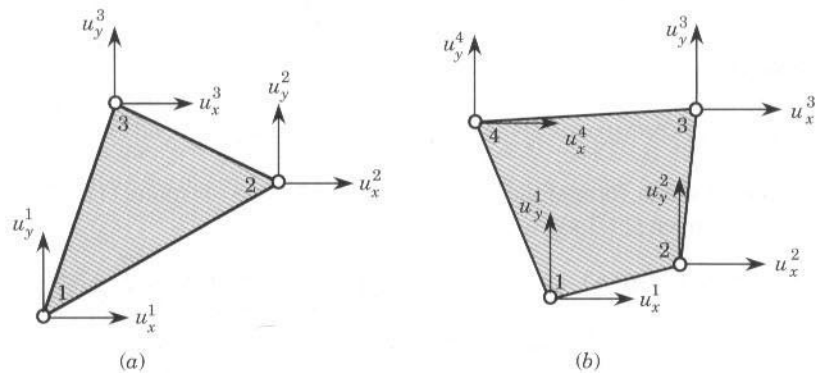

Figure 11.4.1 (a) Linear triangular element and (b) linear quadrilateral element for plane elasticity problems.

The strains are

$$\varepsilon = \mathbf{D}\mathbf{u} = \mathbf{D}\Psi\Delta \equiv \mathbf{B}\Delta, \quad \sigma = \mathbf{C}\mathbf{B}\Delta \tag{11.4.3}$$

where $\mathbf{D}$ is defined earlier in Eq. (11.2.14*b*) and $\mathbf{B}$ is a $3 \times 2n$ matrix

$$\mathbf{B} = \mathbf{D}\Psi = \begin{bmatrix} \dfrac{\partial \psi_1}{\partial x} & 0 & \dfrac{\partial \psi_2}{\partial x} & 0 & \cdots & \dfrac{\partial \psi_n}{\partial x} & 0 \\ 0 & \dfrac{\partial \psi_1}{\partial y} & 0 & \dfrac{\partial \psi_2}{\partial y} & \cdots & 0 & \dfrac{\partial \psi_n}{\partial y} \\ \dfrac{\partial \psi_1}{\partial y} & \dfrac{\partial \psi_1}{\partial x} & \dfrac{\partial \psi_2}{\partial y} & \dfrac{\partial \psi_2}{\partial x} & \cdots & \dfrac{\partial \psi_n}{\partial y} & \dfrac{\partial \psi_n}{\partial x} \end{bmatrix} \tag{11.4.4}$$

Substituting Eq. (11.4.1) for u_x and u_y, setting $w_1 = \psi_i$ and $w_2 = \psi_i$ [to obtain the ith algebraic equation associated with each of the weak statements in Eqs. (11.3.8*a*) and (11.3.8*b*)], and writing the resulting algebraic equations in matrix form, we obtain

$$\begin{bmatrix} [M] & [0] \\ [0] & [M] \end{bmatrix} \begin{Bmatrix} \{\ddot{u}_x\} \\ \{\ddot{u}_y\} \end{Bmatrix} + \begin{bmatrix} [K^{11}] & [K^{12}] \\ [K^{12}]^{\mathrm{T}} & [K^{22}] \end{bmatrix} \begin{Bmatrix} \{u_x\} \\ \{u_y\} \end{Bmatrix} = \begin{Bmatrix} \{F^1\} \\ \{F^2\} \end{Bmatrix} \tag{11.4.5}$$

where

$$\begin{aligned} M_{ij} &= \int_{\Omega_e} \rho h \psi_i \psi_j \, dx \, dy \\ K_{ij}^{11} &= \int_{\Omega_e} h \left(c_{11} \frac{\partial \psi_i}{\partial x} \frac{\partial \psi_j}{\partial x} + c_{66} \frac{\partial \psi_i}{\partial y} \frac{\partial \psi_j}{\partial y} \right) dx \, dy \\ K_{ij}^{12} &= K_{ji}^{21} = \int_{\Omega_e} h \left(c_{12} \frac{\partial \psi_i}{\partial x} \frac{\partial \psi_j}{\partial y} + c_{66} \frac{\partial \psi_i}{\partial y} \frac{\partial \psi_j}{\partial x} \right) dx \, dy \\ K_{ij}^{22} &= \int_{\Omega_e} h \left(c_{66} \frac{\partial \psi_i}{\partial x} \frac{\partial \psi_j}{\partial x} + c_{22} \frac{\partial \psi_i}{\partial y} \frac{\partial \psi_j}{\partial y} \right) dx \, dy \\ F_i^1 &= \int_{\Omega_e} h \psi_i f_x \, dx \, dy + \oint_{\Gamma_e} h \psi_i t_x \, ds, \quad F_i^2 = \int_{\Omega_e} h \psi_i f_y \, dx \, dy + \oint_{\Gamma_e} h \psi_i t_y \, ds \end{aligned} \tag{11.4.6}$$

The body forces f_x and f_y are measured per unit area where the coefficient matrix $[K^{12}]$, for example, corresponds to the coefficient of u_y (second variable) in the first equation, i.e., the first superscript corresponds to the equation number and the second one to the variable number.

To obtain the vector form of the finite element model, we substitute (11.4.1*b*) into the virtual work statement (11.3.4)

$$\begin{aligned} 0 &= \int_{\Omega_e} h(\delta\Delta)^{\mathrm{T}} \left(\mathbf{B}^{\mathrm{T}} \mathbf{C} \mathbf{B} \{\Delta\} + \rho \Psi^{\mathrm{T}} \Psi \ddot{\Delta} \right) d\mathbf{x} - \int_{\Omega_e} h(\delta\Delta)^{\mathrm{T}} \Psi^{\mathrm{T}} \mathbf{f} \, d\mathbf{x} - \oint_{\Gamma_e} h(\delta\Delta)^{\mathrm{T}} \Psi^{\mathrm{T}} \mathbf{t} \, ds \\ &= (\delta\Delta)^{\mathrm{T}} \left(\mathbf{K}^e \Delta^e + \mathbf{M}^e \ddot{\Delta}^e - \mathbf{F}^e - \mathbf{Q}^e \right) \end{aligned} \tag{11.4.7}$$

Since the above equation holds for any *arbitrary* variations $\delta\Delta$, it follows (from the fundamental lemma of variational calculus) that the coefficient of $\delta\Delta$ in the expression (11.4.7)

should be identical to zero, giving the result

$$\mathbf{M}^e \ddot{\Delta}^e + \mathbf{K}^e \Delta^e = \mathbf{F}^e + \mathbf{Q}^e \tag{11.4.8}$$

where

$$\mathbf{K}^e = \int_{\Omega_e} h_e \mathbf{B}^{\mathrm{T}} \mathbf{C} \mathbf{B}\, d\mathbf{x}, \quad \mathbf{M}^e = \int_{\Omega_e} \rho h_e \Psi^{\mathrm{T}} \Psi\, d\mathbf{x}$$
$$\mathbf{F}^e = \int_{\Omega_e} h_e \Psi^{\mathrm{T}} \mathbf{f}\, d\mathbf{x}, \quad \mathbf{Q}^e = \oint_{\Gamma_e} h_e \Psi^{\mathrm{T}} \mathbf{t}\, ds \tag{11.4.9}$$

The element mass matrix $\mathbf{M}^e$ and stiffness matrix $\mathbf{K}^e$ are of order $2n \times 2n$, and the element load vector $\mathbf{F}^e$ and the vector of internal forces $\mathbf{Q}^e$ are of order $2n \times 1$, where n is the number of nodes in a Lagrange finite element [see Eq. (11.4.1)].

11.4.2 Eigenvalue and Transient Problems

For natural vibration study of plane elastic bodies, we seek a periodic solution of the form

$$\{\Delta\} = \{\Delta_0\} e^{-i\omega t} \tag{11.4.10}$$

where ω is the frequency of natural vibration and $i = \sqrt{-1}$. Then Eq. (11.4.5) or (11.4.8) reduces to an eigenvalue problem

$$(-\omega^2 \mathbf{M}^e + \mathbf{K}^e)\Delta_0^e = \mathbf{Q}^e \tag{11.4.11}$$

For transient analysis, using the time-approximation method discussed in Section 6.2.4 (Newmark integration scheme), Eq. (11.4.5) or (11.4.8) can be reduced to the following system of algebraic equations:

$$\hat{\mathbf{K}}^e_{s+1} \Delta^e_{s+1} = \hat{\mathbf{F}}^e_{s,s+1} \tag{11.4.12a}$$

where

$$\hat{\mathbf{K}}^e_{s+1} = \mathbf{K}^e_{s+1} + a_3 \mathbf{M}^e_{s+1}$$
$$\hat{\mathbf{F}}^e_{s,s+1} = \bar{\mathbf{F}}^e_{s+1} + \mathbf{M}^e_{s+1} \left(a_3 \Delta^e_s + a_4 \dot{\Delta}^e_s + a_5 \ddot{\Delta}^e_s \right) \tag{11.4.12b}$$
$$a_3 = \frac{2}{\gamma (\Delta t)^2}, \quad a_4 = \Delta t a_3, \quad a_5 = \frac{1}{\gamma} - 1$$

where $\mathbf{K}^e$, $\mathbf{M}^e$, and $\bar{\mathbf{F}}^e$ $(= \mathbf{F}^e + \mathbf{Q}^e)$ are the vectors appearing in Eq. (11.4.9) and γ is the parameter in the Newmark scheme [see Eqs. (6.2.29)–(6.2.31)]. For $\gamma = 0$ (centered difference scheme), the alternative formulation of Problem 6.23 must be used. For additional details, the reader should consult Section 6.2.4.

11.5 EVALUATION OF INTEGRALS

For the linear triangular (i.e., CST) element, the ψ_i^e and its derivatives are given by

$$\psi_i^e = \frac{1}{2A_e} \left(\alpha_i^e + \beta_i^e x + \gamma_i^e y \right), \quad \frac{\partial \psi_i^e}{\partial x} = \frac{\beta_i^e}{2A_e}, \quad \frac{\partial \psi_i^e}{\partial y} = \frac{\gamma_i^e}{2A_e} \tag{11.5.1}$$

Since the derivatives of ψ_i^e are constant, we have

$$\mathbf{B}^e = \frac{1}{2A_e}\begin{bmatrix} \beta_1^e & 0 & \beta_2^e & 0 & \cdots & \beta_n^e & 0 \\ 0 & \gamma_1^e & 0 & \gamma_2^e & \cdots & 0 & \gamma_n^e \\ \gamma_1^e & \beta_1^e & \gamma_2^e & \beta_2^e & \cdots & \gamma_n^e & \beta_n^e \end{bmatrix} \quad (3 \times 2n) \tag{11.5.2}$$

where A_e is the area of the triangular element. Since $\mathbf{B}^e$ and $\mathbf{C}^e$ are independent of x and y, the element stiffness matrix in (11.4.9) for the CST element is given by

$$\mathbf{K}^e = h_e A_e (\mathbf{B}^e)^{\mathrm{T}} \mathbf{C}^e \mathbf{B}^e \quad (2n \times 2n) \tag{11.5.3}$$

For the case in which the body force components f_x and f_y are elementwise constant (say, equal to f_{x0}^e and f_{y0}^e, respectively), the load vector $\mathbf{F}^e$ has the form

$$\mathbf{F}^e = \int_{\Omega_e} h_e (\Psi^e)^{\mathrm{T}} \mathbf{f}_0^e \, d\mathbf{x} = \frac{A_e h_e}{3} \begin{Bmatrix} f_{x0}^e \\ f_{y0}^e \\ f_{x0}^e \\ f_{y0}^e \\ f_{x0}^e \\ f_{y0}^e \end{Bmatrix} \quad (6 \times 1) \tag{11.5.4}$$

For a general quadrilateral element, it is not easy to compute the coefficients of the stiffness matrix by hand. In such cases we use the numerical integration method discussed in Section 9.2. However, for a linear rectangular element of sides a and b, the element coefficient matrices in Eq. (8.2.52) can be used to obtain the stiffness matrix. For a linear quadrilateral element with constant body force components (f_{x0}, f_{y0}), the load vector is given by

$$\mathbf{F}^e = \frac{A_e h_e}{4} \begin{Bmatrix} f_{x0}^e \\ f_{y0}^e \\ f_{x0}^e \\ f_{y0}^e \\ \vdots \end{Bmatrix} \quad (8 \times 1) \tag{11.5.5}$$

The vector $\mathbf{Q}^e$ is computed only when the element Ω_e falls on the boundary of the domain on which tractions are specified (i.e., known). Computation of $\mathbf{Q}^e$ involves the evaluation of line integrals (for any type of element), as explained in Sec. 8.2.6; also, see Example 8.2.4. For plane elasticity problems, the surface tractions t_x and t_y take the place of q_n in the single-variable problems [see Eq. (8.2.56)]. However, it should be noted that t_x and t_y are the horizontal and vertical components (i.e., parallel to the coordinate lines x and y), respectively, of the traction vector $\mathbf{t}$, which, in general, is oriented at an angle to the boundary. In practice, it is convenient to express the surface traction $\mathbf{t}$ in the element coordinates. In that case, $\mathbf{Q}^e$ can be evaluated in the element coordinates and then transformed to the global coordinates for assembly. If $\mathbf{Q}^e$ denotes the element load vector referred to the element coordinates, then the corresponding load vector referred to the global coordinates is given by

$$\mathbf{F}^e = \mathbf{R}^{\mathrm{T}} \mathbf{Q}^e \tag{11.5.6a}$$

where $\mathbf{R}$ is the transformation matrix

$$\mathbf{R}^e = \begin{bmatrix} \cos\alpha & \sin\alpha & 0 & 0 & \\ -\sin\alpha & \cos\alpha & 0 & 0 & \\ 0 & 0 & \cos\alpha & \sin\alpha & \\ 0 & 0 & -\sin\alpha & \cos\alpha & \\ & & & & \ddots \end{bmatrix} \quad (2n \times 2n) \qquad (11.5.6b)$$

and α is the angle between the global x axis and the traction vector $\mathbf{t}$.

Example 11.5.1

As a specific example, first consider the structure shown in Fig. 11.5.1(*a*). Side 2–3 of element 7 is subjected to linearly varying normal force:

$$t_n \neq 0, \quad t_s = 0$$

where the subscripts n and s refer to normal and tangential directions, respectively. We have (for $e = 7$)

$$\mathbf{Q}^e = \oint_{\Gamma_e} h_e \Psi^{\mathrm{T}} \begin{Bmatrix} t_n \\ t_s \end{Bmatrix} ds = \int_{\Gamma^e_{12}} h_e \Psi^{\mathrm{T}} \begin{Bmatrix} t_n \\ t_s \end{Bmatrix} ds + \int_{\Gamma^e_{23}} h_e \Psi^{\mathrm{T}} \begin{Bmatrix} t_n \\ 0 \end{Bmatrix} ds + \int_{\Gamma^e_{31}} h_e \Psi^{\mathrm{T}} \begin{Bmatrix} t_n \\ t_s \end{Bmatrix} ds \qquad (11.5.7a)$$

The first and third integrals cannot be evaluated because we do not know t_n and t_s on these sides of the element. However, because of internal stress equilibrium, contributions of these integrals cancel with like contributions from the neighboring elements (elements 4 and 5) in the assembled force vector of the structure. Thus, we must compute only the integral over side

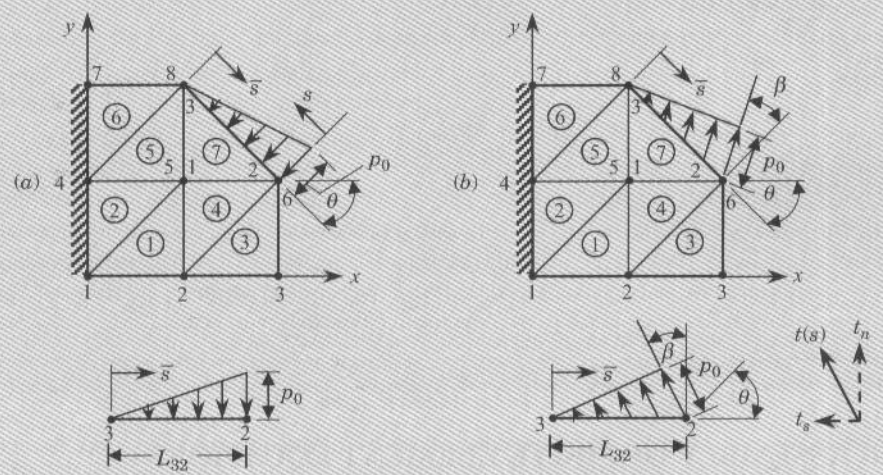

Figure 11.5.1 Plane elasticity problem with (*a*) traction normal to the boundary and (*b*) traction in an arbitrary direction.

2–3 of the element. We have (for $e = 7$)

$$\mathbf{Q}^{(7)}_{2-3} = \int_0^{L_{23}} h\Psi^{\mathrm{T}} \begin{Bmatrix} t_n \\ 0 \end{Bmatrix} ds, \quad t_n = -p_0 \left(1 - \frac{s}{L_{23}}\right) \tag{11.5.7b}$$

where the minus sign in front of p_0 is added to account for the direction of the applied traction, which is acting toward the body in the present case. The local coordinate system s used in the above expression is chosen along the side connecting node 2 to node 3, with its origin at node 2. We are not restricted to this choice. If we feel that it is convenient to choose the local coordinate system $\bar{s}$, which is taken along side 3–2, with its origin at node 3 of element 7, we can write

$$\mathbf{Q}^{(7)}_{3-2} = \int_0^{L_{32}} h\Psi^{\mathrm{T}} \begin{Bmatrix} t_n \\ 0 \end{Bmatrix} d\bar{s}, \quad t_n = -\frac{p_0 \bar{s}}{L_{32}} \tag{11.5.7c}$$

wherein now Ψ^e is expressed in terms of the local coordinate $\bar{s}$. We have ($L_{32} = L_{23}$)

$$\mathbf{Q}^{(7)}_{3-2} = \int_0^{L_{32}} h \begin{Bmatrix} 0 \\ 0 \\ \psi_2^7 t_n \\ 0 \\ \psi_3^7 t_n \\ 0 \end{Bmatrix} d\bar{s} = -\frac{L_{32} p_0 h}{6} \begin{Bmatrix} 0 \\ 0 \\ 2 \\ 0 \\ 1 \\ 0 \end{Bmatrix} \tag{11.5.8a}$$

The global components of this force vector are [set $\alpha = 90^\circ - \theta$ in Eq. (11.5.6*b*)]

$$\mathbf{Q}^{(7)}_{3-2} = -\frac{L_{32} p_0 h}{6} \begin{Bmatrix} 0 \\ 0 \\ 2\sin\theta \\ 2\cos\theta \\ \sin\theta \\ \cos\theta \end{Bmatrix} \tag{11.5.8b}$$

Next, consider the case in which the tractions are oriented at an angle β, as shown in Fig. 11.5.1(*b*). Then, we may resolve the applied traction into normal and tangential components

$$t_n = t(s)\cos\beta, \quad t_s = t(s)\sin\beta \tag{11.5.9}$$

and repeat the procedure described above.

The same procedure applies to linear quadrilateral elements. In general, the loads due to specified boundary stresses can be computed using an appropriate local coordinate system and one-dimensional interpolation functions. When higher-order elements are involved, the corresponding order of one-dimensional interpolation functions must be used.

11.6 ASSEMBLY OF FINITE ELEMENT EQUATIONS

The assembly procedure for problems with many degrees of freedom is the same as that used for a single degree of freedom problem (see Section 8.2), except that the procedure should be applied to both degrees of freedom at each node. For example, consider the plane

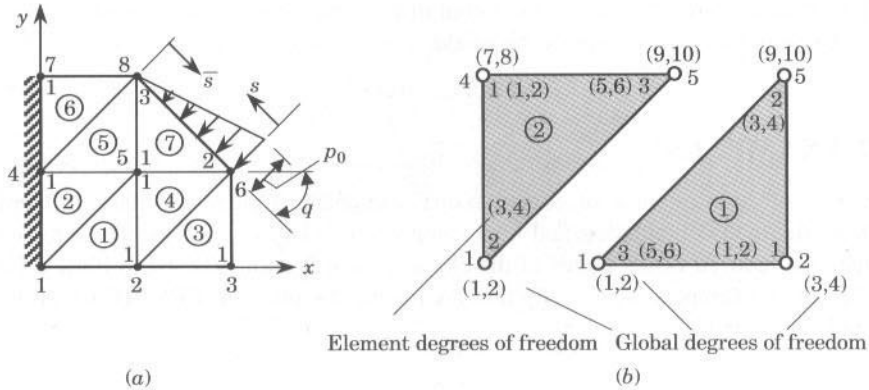

Figure 11.6.1 Plane elasticity problem with global degrees of freedom.

elastic structure and the finite element mesh used in Fig. 11.6.1(*a*). There are eight nodes in the mesh; hence, the total size of the assembled stiffness matrix will be 16×16, and the force vector will be 16×1. The first two rows and columns of the global stiffness matrix, for example, correspond to the global degrees (1, 2) of freedom at global node 1, which has contributions from nodes 2 and 3 of elements 1 and 2, respectively, as indicated in Fig. 11.6.1(*b*). Thus, the contributions to global coefficients K_{IJ} $(I, J = 1, 2)$ come from K^1_{ij} $(i, j = 3, 4)$ and K^2_{ij} $(i, j = 5, 6)$.

For instance, the global stiffness matrix coefficients K_{11}, K_{12}, K_{13}, K_{15}, K_{22}, K_{33}, and K_{34} are known in terms of the element coefficients as follows:

$$\begin{aligned} &K_{11} = K^1_{55} + K^2_{33}, \quad K_{22} = K^1_{66} + K^2_{44}, \quad K_{12} = K^1_{56} + K^2_{34}, \quad K_{13} = K^1_{51} \\ &K_{33} = K^1_{11} + K^3_{55} + K^4_{33}, \quad K_{34} = K^1_{12} + K^3_{56} + K^4_{34}, \quad K_{15} = 0 \end{aligned} \tag{11.6.1}$$

Note that K_{34}, for example, denotes the coupling stiffness coefficient between the third (u_x) and fourth (u_y) global displacement degrees of freedom, both of which are at global node 2. On the other hand, K_{13} denotes the coupling coefficient between the first displacement degree of freedom (u_x) at global node 1 and third global displacement degree (u_x) of freedom at global node 2. Similar arguments apply for the assembly of the force vector.

With regard to the specification of the displacements (the primary degrees of freedom) and forces (the secondary degrees of freedom) in a finite element mesh, we have the following four distinct possibilities:

Case 1: u_x and u_y are specified (and t_x and t_y are unknown)
Case 2: u_x and t_y are specified (and t_x and u_y are unknown)
Case 3: t_x and u_y are specified (and u_x and t_y are unknown)
Case 4: t_x and t_y are specified (and u_x and u_y are unknown)

In general, only one of the quantities of each of the pairs (u_x, t_x) and (u_y, t_y) is known at a nodal point in the mesh. As discussed in Chapter 9, we are required to make a decision as to which degree of freedom is known when singular points (i.e., points at which both displacement and force degrees of freedom are known or when two different values of the same degree of freedom are specified) are encountered.

For time-dependent problems, the initial displacement and velocity must be specified for each component of the displacement field:

$$\mathbf{u} = \mathbf{u}^0, \quad \dot{\mathbf{u}} = \mathbf{v}^0 \tag{11.6.2}$$

11.7 EXAMPLES

Next, we consider a couple of computational examples of plane elasticity problems to illustrate the load computation and imposition of boundary conditions. The stresses are evaluated at reduced Gauss points of the elements [see Section 10.5.4 and Barlow (1976, 1989)]. These examples are actually analyzed using the program **FEM2D,** which is discussed in Chapter 13.

Example 11.7.1

Consider a thin elastic plate subjected to a uniformly distributed edge load, as shown in Fig. 11.7.1. We wish to determine the static solution to the problem. First, we consider a two-element discretization of the plate by triangular elements and perform the required algebra to obtain the nodal displacements.

The assembly of element matrices for two *degree-of-freedom* (DOF) elements is described in Section 11.6. For the finite element mesh at hand, the correspondence between the global and local nodes and stiffness is given in Table 11.7.1. If two global nodes correspond to two (local) nodes of the same element, then the corresponding stiffness coefficient is nonzero; otherwise, it is zero.

The specified global degrees of freedom for the problem are

$$U_1 = U_2 = U_5 = U_6 = 0 \tag{11.7.1}$$

The known forces are

$$F_3 = F_3^1 = \frac{p_0 bh}{2}, \quad F_4 = F_4^1 = 0, \quad F_7 = F_5^1 + F_3^2 = \frac{p_0 bh}{2}, \quad F_8 = F_6^1 + F_4^2 = 0 \tag{11.7.2}$$

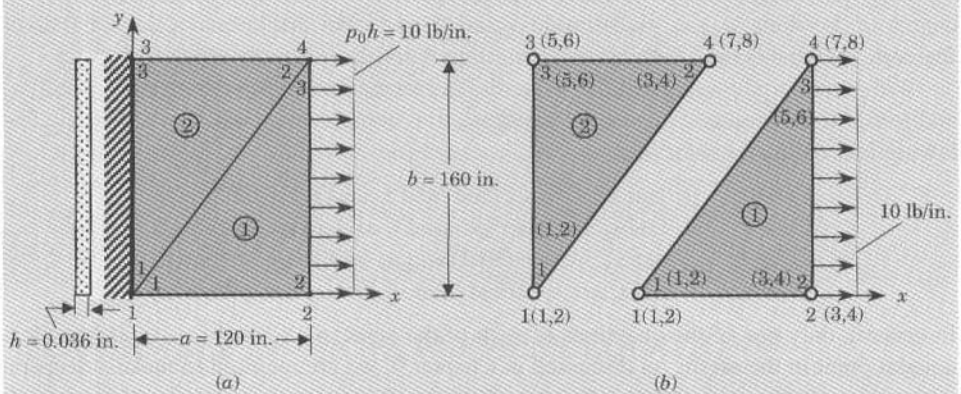

Figure 11.7.1 Geometry and finite element mesh of a plane elasticity problem by the CST elements.

Table 11.7.1 Correspondence between the global and element nodes of the mesh shown in Fig. 11.7.1.

Nodal corespondence		Stiffness correspondence	
Global Node (DOF)	Local Node (DOF)	Global	Local
1 (1, 2)	1 of element 1 (1, 2)	K_{11}	$K_{11}^1 + K_{11}^2$
		K_{22}	$K_{22}^1 + K_{22}^2$
	1 of element 2 (1, 2)	K_{12}	$K_{12}^1 + K_{12}^2$
2 (3, 4)	2 of element 1 (3, 4)	K_{33}	K_{33}^1
		K_{44}	K_{44}^1
		K_{34}	K_{34}^1
3 (5, 6)	3 of element 2 (5, 6)	K_{55}	K_{55}^2
		K_{66}	K_{66}^2
		K_{56}	K_{56}^2
4 (7, 8)	2 of element 2 (3, 4)	K_{77}	$K_{55}^1 + K_{33}^2$
		K_{88}	$K_{66}^1 + K_{44}^2$
	3 of element 1 (5, 6)	K_{78}	$K_{56}^1 + K_{34}^2$

The first two rows and columns and the last two rows and columns of the assembled $[K]$ can be deleted (since the specified boundary conditions are homogeneous) to obtain the following condensed equations

$$\begin{bmatrix} K_{33}^1 & K_{34}^1 & K_{35}^1 & K_{36}^1 \\ K_{43}^1 & K_{44}^1 & K_{45}^1 & K_{46}^1 \\ K_{53}^1 & K_{54}^1 & K_{55}^1 + K_{33}^2 & K_{56}^1 + K_{34}^2 \\ K_{63}^1 & K_{64}^1 & K_{65}^1 + K_{43}^2 & K_{66}^1 + K_{44}^2 \end{bmatrix} \begin{Bmatrix} U_3 \\ U_4 \\ U_7 \\ U_8 \end{Bmatrix} = \begin{Bmatrix} \dfrac{p_0 bh}{2} \\ 0 \\ \dfrac{p_0 bh}{2} \\ 0 \end{Bmatrix} \tag{11.7.3}$$

or (using $a = 120$ in., $b = 160$ in., $h = 0.036$ in., $\nu = 0.25$, $E = 30 \times 10^6$ psi, and $p_0 = 10$ lb/in.)

$$10^4 \begin{bmatrix} 93.0 & -36.0 & -16.2 & 14.4 \\ -36.0 & 72.0 & 21.6 & -43.2 \\ -16.2 & 21.6 & 93.0 & 0.0 \\ 14.4 & -43.2 & 0.0 & 72.0 \end{bmatrix} \begin{Bmatrix} U_3 \\ U_4 \\ U_7 \\ U_8 \end{Bmatrix} = \begin{Bmatrix} 800.0 \\ 0.0 \\ 800.0 \\ 0.0 \end{Bmatrix} \tag{11.7.4}$$

Inverting the matrix, we obtain

$$\begin{Bmatrix} U_3 \\ U_4 \\ U_7 \\ U_8 \end{Bmatrix} = \frac{10^{-6}}{3} \begin{bmatrix} 4.07 & 2.34 & 0.17 & 0.59 \\ 2.24 & 8.65 & -1.60 & 4.72 \\ 0.17 & -1.60 & 3.63 & -0.99 \\ 0.59 & 4.72 & -0.99 & 6.88 \end{bmatrix} \begin{Bmatrix} 800.0 \\ 0.0 \\ 800.0 \\ 0.0 \end{Bmatrix}$$

$$= 10^{-4} \begin{Bmatrix} 11.291 \\ 1.964 \\ 10.113 \\ -1.080 \end{Bmatrix} \text{ in} \tag{11.7.5}$$

Table 11.7.2 Finite element results for a thin plate (plane stress assumption) using various meshes of triangular and rectangular elements and material properties.[†]

Mesh	Material	U_3 ($\times 10^{-4}$)	U_4 ($\times 10^{-4}$)	U_7 ($\times 10^{-4}$)	U_8 ($\times 10^{-4}$)
1×1	Isotropic: $E = 30 \times 10^6$ psi $\nu = 0.25$ $G = E/[2(1+\nu)]$	11.291 10.853	1.964 2.326	10.113 10.853	−1.080 −2.326
1×1	Orthotropic: $E_1 = 31 \times 10^6$ psi $E_2 = 2.7 \times 10^6$ psi $G_{12} = 0.75 \times 10^6$ psi $\nu_{12} = 0.28$	10.767 10.728	1.666 2.675	10.651 10.728	−1.579 −2.675

[†]For each mesh, the first row corresponds to triangular elements and the second row to one rectangular element.

Table 11.7.2 contains the finite element solutions (deflections and stresses) for the displacements at the points (120, 0) and (120, 160) of isotropic and orthotropic plates for the meshes shown. The results were obtained using the computer code **FEM2D.** Note that the finite element solutions (e.g., displacements) obtained with two-element meshes do not yield symmetric results (i.e., $U_3 = U_7$ and $U_4 = -U_8$). This is because of the lack of symmetry of the meshes used. As the mesh is refined, even with unsymmetric meshes, the solution will become symmetric about $y = b/2$ line within a certain degree of accuracy.

Table 11.7.3 Deflections and stresses in an isotropic plate subjected to uniform edge load (Example 11.7.1).

	Mesh	$u_x(120, 0)$ ($\times 10^{-4}$)	$u_y(120, 0)$ ($\times 10^{-4}$)	σ_{xx}	σ_{yy}	σ_{xy}
Triangles	1×1	11.291	1.964	285.9 (80, 53.33)[†]	67.42 (40, 106.7)	10.80 (80, 53.33)
	2×2	11.372	2.175	294.1 (40, 26.67)	69.36 (20, 53.33)	23.20 (40, 26.67)
	4×4	11.284	2.126	306.2 (20, 13.33)	69.59 (10, 26.67)	35.93 (20, 13.33)
	16×16	11.179	2.014	372.5 (5, 3.33)	75.39 (2.5, 6.67)	58.90 (5, 3.33)
Rectangles	1×1	10.853	2.326	277.8 (60, 80)	25.84 (60, 80)	0.0 (60, 80)
	2×2	11.372	2.175	29418 (40, 26.67)	69.36 (20, 53.33)	23.20 (40, 26.67)
	4×4	11.150	2.009	288.1 (15, 20)	64.77 (45, 20)	27.73 (15, 20)
	16×16	11.166	1.992	339.5 (3.75, 5)	61.2 (3.75, 75)	53.14 (3.75, 5)

[†]Location of the stress.

Deflections and stresses obtained with various uniform meshes of triangular elements or rectangular elements are presented in Table 11.7.3. Mesh $m \times n$ means that m elements in the x direction and n elements in the y direction are used.

Example 11.7.2

Consider the cantilever beam ($E = 30 \times 10^6$ psi, $\nu = 0.25$, $a = 10$ in., $b = 2$ in., $h = 1$ in.) shown in Fig. 11.7.2(a). We wish to determine, using the elasticity equations, the maximum deflection and bending stress in the beam when it is subjected to a uniformly distributed shear stress $\tau_0 = 150$ psi. The boundary conditions of the problem are

$$u_x(a, y) = 0, \quad u_y(a, b/2) = 0, \quad t_y(a, y) = 0 \text{ except at } y = b/2$$
$$t_x = t_y = 0 \text{ at } y = 0, b \text{ for any } x, \quad t_x = 0, \quad t_y = -h\tau_0 \text{ at } x = 0 \text{ for any } y \qquad (11.7.6)$$

We shall solve the problem using the plane stress assumption. The elastic coefficients c_{ij} for the plane stress case are defined (assuming that steel is isotropic) as

$$c_{11} = c_{12} = \frac{E}{1-\nu^2}, \quad c_{12} = \frac{E\nu}{1-\nu^2}, \quad c_{66} = \frac{E}{2(1+\nu)} \ (= G) \qquad (11.7.7)$$

Three different, increasingly refined finite element meshes are shown in Fig. 11.7.2(b). The meshes shown are those consisting of linear rectangular elements. Equivalent triangular

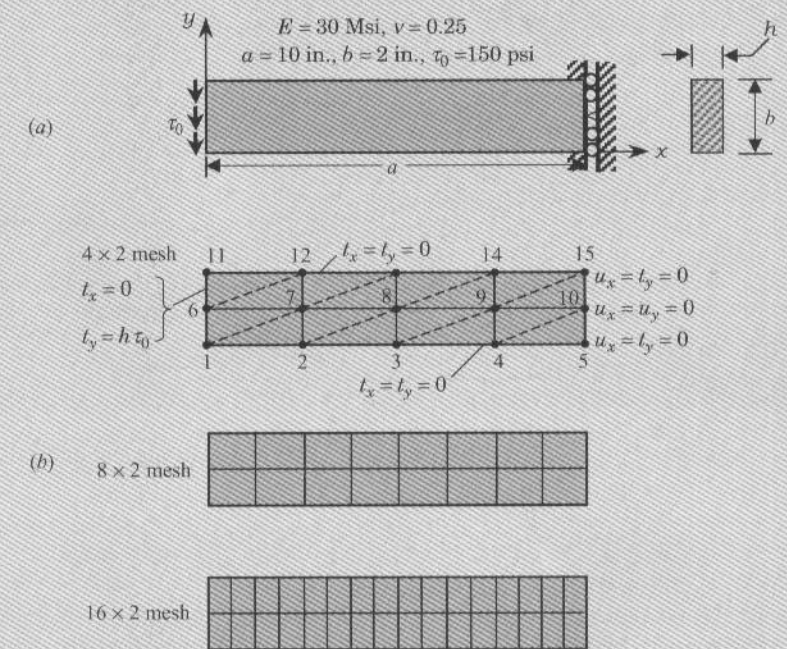

Figure 11.7.2 Finite element meshes for an end-loaded cantilever beam.

Table 11.7.4 Comparison of the finite element solution with the elasticity solution for a cantilever beam subjected to a uniform shear load at the free end (Example 11.7.2).

Number of nodes	Tip deflection, $-u_y \times 10^{-2}$			Normal stress, σ_{xx}		
	LT*	LR	QR	LT	LR	QR
15	0.1611	0.3134	0.5031	1209 (15)†	1196 (8.75, 1.5)‡	2196 (8.943, 1.577)
27	0.2662	0.4388	0.5129	2270 (31)	1793 (9.375, 1.5)	2439 (9.471, 1.577)
51	0.3166	0.4878	0.5137	2829 (63)	2056 (9.6875, 1.5)	226 (9.736, 1.577)
Elasticity§		0.5188 (0.0, 1.0)		2876 (9.583, 1.667)	2180 (9.6875, 1.5)	2528 (9.736, 1.577)

*LT = linear triangular elements; LR = linear rectangular elements; and QR = quadratic rectangular elements.
†Element number.
‡Quadrature points.
§From Reddy (1984), p. 53:

$$u_y(0,1) = -(PL^3/3EI)[1 + 3(1+\nu)/L^2], \quad \sigma_{xx} = Px(1-y)/I, \quad I = \frac{2}{3}$$

element meshes are obtained by joining node 1 to node 3 of each rectangular element, as indicated by the dotted lines. Equivalent meshes of nine-node quadratic Lagrange elements are obtained by considering a 2×2 mesh of linear Lagrange elements equivalent to a quadratic element.

For the finite element model, the boundary conditions on the primary and secondary variables, e.g., for the 15-node mesh, are given by

$$U_9 = U_{19} = U_{20} = U_{29} = 0.0$$

$$F_1^y = -\frac{(\tau_0 h)b}{4} = -75.0, \quad F_6^y = -150.0, \quad F_{11}^y = -75.0 \tag{11.7.8}$$

and all other forces are zero on the boundary.

Table 11.7.4 contains a comparison of the finite element solutions with the elasticity solutions for the tip deflection (i.e., deflection at the center node of the left end) and bending stress σ_{xx}, obtained using two-dimensional elasticity theory [see Reddy (1984)]. The linear triangular element mesh has the slowest convergence compared to the linear and quadratic rectangular elements.

The last example of this chapter deals with free vibration and transient analysis of the cantilever beam of Example 11.7.2.

Example 11.7.3

Consider the cantilever beam shown in Fig. 11.7.2(*a*). We wish to determine the natural frequencies and transient response using the plane elements. We use the finite element meshes of linear triangular and rectangular elements shown in Fig. 11.7.2(*b*) and their nodal equivalent meshes of quadratic elements to analyze the problem (mass density of steel is taken

Table 11.7.5 Comparison of first ten frequencies of the cantilever beam of Example 11.7.3 as computed using various meshes of linear and quadratic triangular and rectangular elements.

	Triangular elements				Rectangular elements			
	Linear element		Quadratic element		Linear element		Quadratic element	
ω	4×2	8×2	2×1	4×1	4×2	8×2	2×1	4×1
1	2,019.4	1,583.0	1,186.4	1,156.7	1,465.5	1,242.3	1,169.9	1,151.8
2	9,207.4	8,264.0	7,896.6	6,496.5	8,457.9	6,845.8	7,197.7	6,341.4
3	10,449.6	9,177.7	9,158.2	9,156.0	9,218.4	9,171.7	9,158.2	9,156.0
4	25,339.2	19,540.5	18,369.1	16,219.9	22,334.0	16,887.7	17,890.8	15,572.7
5	29,193.2	27,843.9	27,805.3	27,441.7	29,113.3	27,836.8	27,869.8	27,226.3
6	42,363.4	32,727.8	40,399.2	28,696.9	40,309.7	29,433.6	39,583.7	27,442.2
7	52,937.0	46,840.4	50,469.6	39,762.6	52,991.9	44,231.1	50,964.4	39,302.3
8	67,964.6	48,014.4	66,260.9	45,815.6	66,842.5	47,441.0	67,015.3	45,839.9
9	76,833.2	61,560.4	74,582.1	57,429.5	74,523.3	60,078.3	74,064.6	56,949.9
10	79,443.0	68,257.4	79,241.8	64,867.4	76,515.5	67,813.3	80,029.3	64,636.0

to be $\rho = 8.8255 \times 10^{-3}$ slugs/in.^{3}). Table 11.7.5 contains a comparison of first ten natural frequencies obtained with various meshes. The convergence of the natural frequencies with mesh refinement is clear.

For transient analysis, the time step Δt used in the linear acceleration scheme ($\alpha = 0.5$, $\gamma = 1/3$) is restricted by the stability requirement

$$\Delta t < \Delta t_{\text{cri}} = \sqrt{\frac{12}{\lambda_{\max}}} \tag{11.7.9}$$

For the 4×2 mesh of rectangular elements, for example, we have $\Delta t_{\text{cri}} = 1.617 \times 10^{-5}$. The load, $h\tau_0$ lb/in., is used with zero initial conditions. The load at the nodes of the free end are

$$\begin{aligned} &-75.0 \text{ lb}, \quad -150.0 \text{ lb}, \quad -75 \text{ lb} \quad \text{for linear element mesh} \\ &-50.0 \text{ lb}, \quad -200.0 \text{ lb}, \quad -50 \text{ lb} \quad \text{for quadratic element mesh} \end{aligned}$$

Figure 11.7.3 contains plots of the tip deflection $u_y(0, 0, t)$ versus time as predicted by the 4×2 mesh of linear rectangular elements and the two time approximation schemes: (1) $\alpha = \gamma = \frac{1}{2}$ and (2) $\alpha = \frac{1}{2}$, $\gamma = \frac{1}{3}$. The time step used in these computations is greater than the critical time step for the mesh, i.e., $\Delta t = 2.5 \times 10^{-4} > \Delta t_{\text{cri}}$. Therefore, the second scheme yields unstable transient response. Note that the solution predicted by the linear acceleration scheme is stable for the first several time steps, but it eventually becomes unstable. Figures 11.7.4 contains plots of the tip deflection as a function of time as predicted by various meshes of linear and quadratic rectangular elements. The notation $L4$ implies a mesh of four-node linear elements, and $Q9$ indicates a mesh of nine-node quadratic elements. Clearly, the solution gets refined as the mesh is refined. Obviously, mesh 4×2 $L4$ is too crude to predict the right wavelength of the time response.

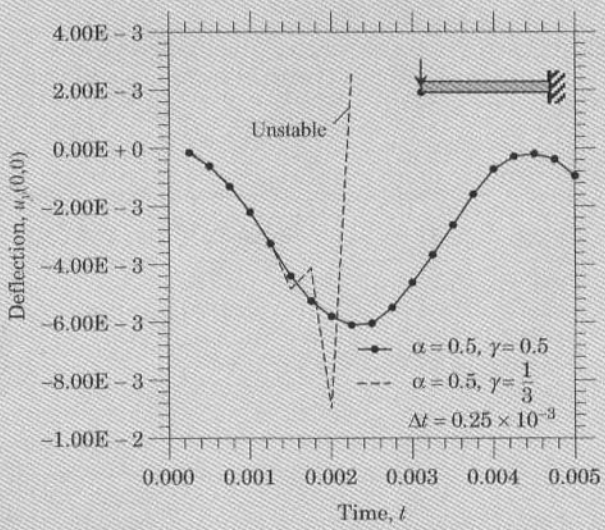

Figure 11.7.3 Stability of the finite element solutions predicted by two different time integration schemes (Example 11.7.3). The 4×2 mesh of linear rectangular elements is used.

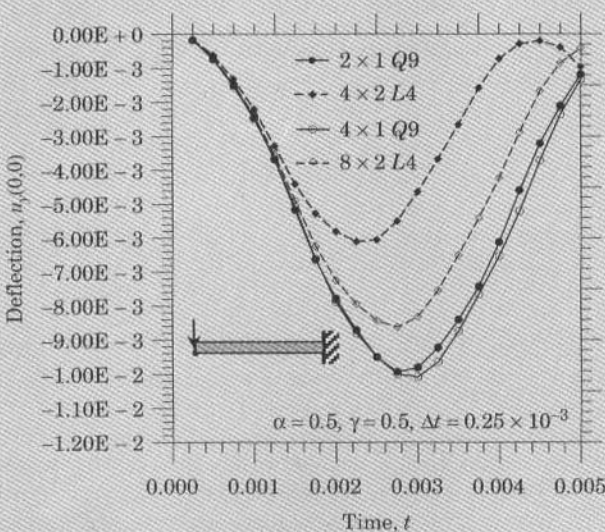

Figure 11.7.4 Tip deflection versus times, as predicted by various meshes of rectangular elements: L4, 4×2 mesh of linear elements; L8, 8×2 mesh of linear elements; Q2, 2×1 mesh of nine-node quadratic elements; and Q4, 4×1 mesh of nine-node quadratic elements.

11.8 SUMMARY

In this chapter equations of the plane elasticity (i.e., two-dimensional problems of elasticity) are introduced and their finite element models are formulated. The plane strain and plane stress problems, which differ only in the use of constitutive relations, are discussed. The governing equations are expressed in terms of the displacements, and their weak form and finite element model are developed in two alternative ways:

1. The vector/matrix formulation ($\mathbf{B}^T\mathbf{C}\mathbf{B}$) using the principle virtual displacements, which is most common in finite element books on solid and structural mechanics and
2. The weak-form formulation, which is used throughout the book.

Triangular and rectangular elements are developed. The eigenvalue and time-dependent problems of plane elasticity are also discussed. Several numerical examples are presented to illustrate the evaluation of element stiffness matrices and load vectors.

PROBLEMS

11.1–11.3 Compute the contribution of the boundary forces to the global force DOF in the plane elasticity problems given in Figs. P11.1–P11.3. Give nonzero forces for at least two global nodes. *Answer for Problem 11.1*: $F_7^x = \frac{17p_1+p_0}{72}$ and $F_{14}^x = \frac{5p_1+p_0}{12}$.

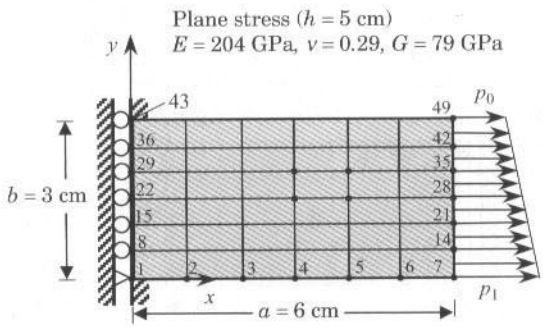

Figure P11.1

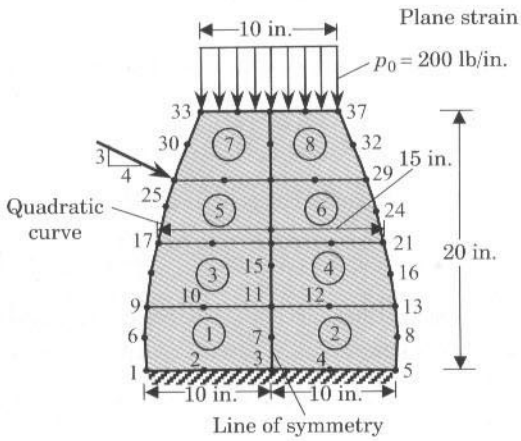

Figure P11.2

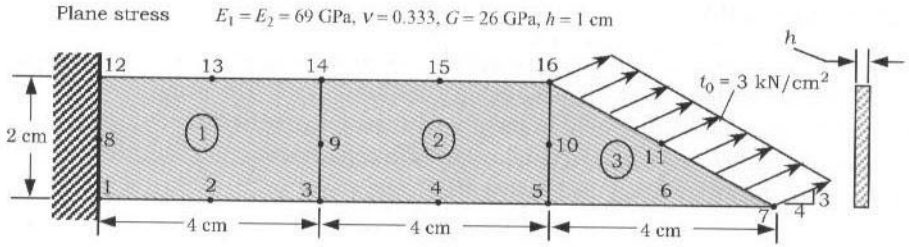

Figure P11.3

11.4–11.6 Give the connectivity matrices and the specified primary degrees of freedom for the plane elasticity problems given in Figs. P11.1–P11.3. Give only the first three rows of the connectivity matrix.

11.7 Consider the cantilevered beam of length 6 cm, height 2 cm, thickness 1 cm, and material properties $E = 3 \times 10^7$ N/cm^2 and $\nu = 0.3$, and subjected to a bending moment of 600 N-cm at the free end, (as shown in P11.7). Replace the moment by an equivalent distributed force at $x = 6$ cm, and model the domain by a nonuniform 10×4 mesh of linear rectangular elements. Identify the special displacements and global forces. *Answer:* $F_{11}^x = -187.5$ N and $F_{22}^x = -225$ N.

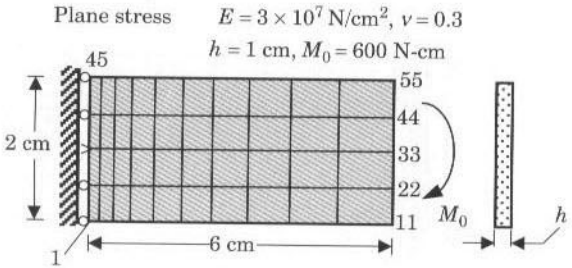

Figure P11.7

11.8 Consider the ("transition") element shown in Fig. P11.8. Define the generalized displacement vector of the element by

$$\{u\} = \{u_1, v_1, \Theta_1, u_2, v_2, u_3, v_3\}^T$$

and represent the displacement components u and v by

$$u = \psi_1 u_1 + \psi_2 u_2 + \psi_3 u_3 + \frac{b}{2}\eta\psi_1\theta_1, \quad v = \psi_1 v_1 + \psi_2 v_2 + \psi_3 v_3$$

where ψ_1 is the interpolation function for the beam, and ψ_2 and ψ_3 are the interpolation functions for nodes 2 and 3:

$$\psi_1 = \frac{1}{2}(1-\xi), \quad \psi_2 = \frac{1}{4}(1+\xi)(1-\eta), \quad \psi_3 = \frac{1}{4}(1+\xi)(1+\eta)$$

Derive the stiffness matrix for the element.

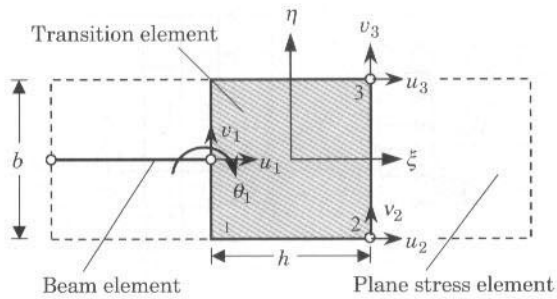

Figure P11.8

11.9 Consider a square, isotropic, elastic body of thickness h shown in Fig. P11.9. Suppose that the displacements are approximated by

$$u_x(x, y) = (1 - x)yu_x^1 + x(1 - y)u_x^2, \quad u_y(x, y) = 0$$

Assuming that the body is in a plane state of stress, derive the 2×2 stiffness matrix for the unit square

$$[K]\begin{Bmatrix} u_x^1 \\ u_x^2 \end{Bmatrix} = \begin{Bmatrix} F_1 \\ F_2 \end{Bmatrix}$$

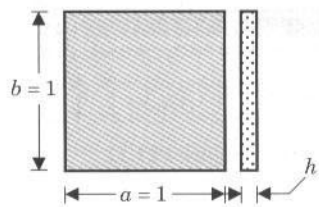

Figure P11.9

11.10–11.14. For the plane elasticity problems shown in Figs. P11.10–11.14, give the boundary DOF and compute the contribution of the specified forces to the nodes. *Answer for Problem 11.11:* $F_{37}^y = -37.5$ kN and $F_{38}^y = -75$ kN.

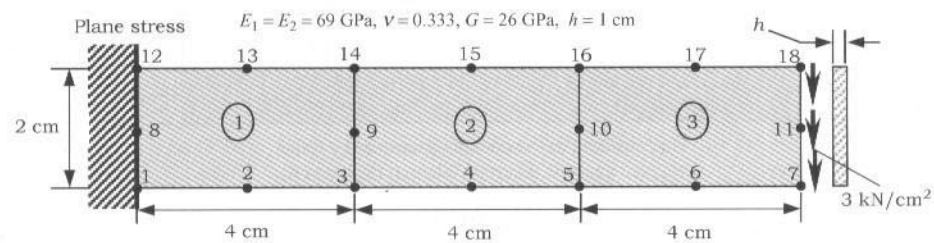

Figure P11.10

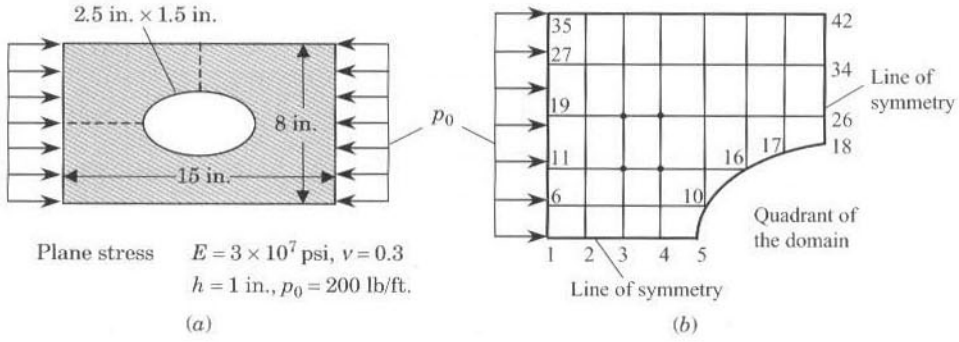

Figure P11.11

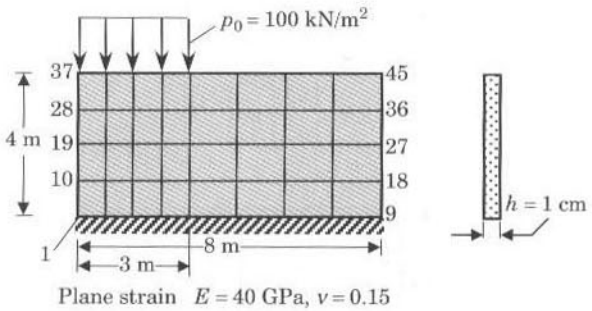

Figure P11.12

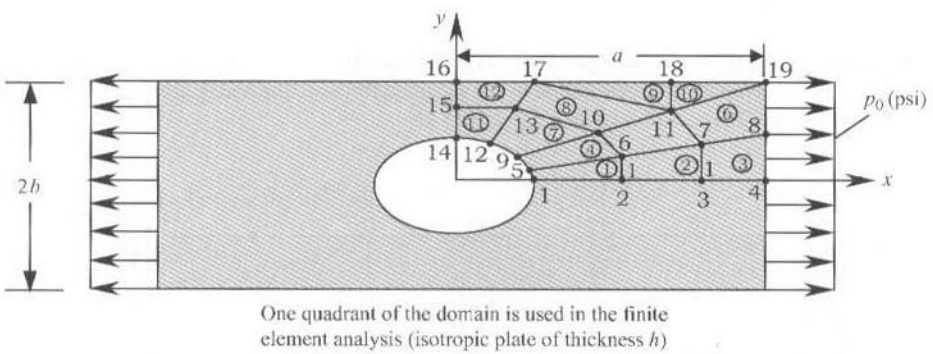

Figure P11.13

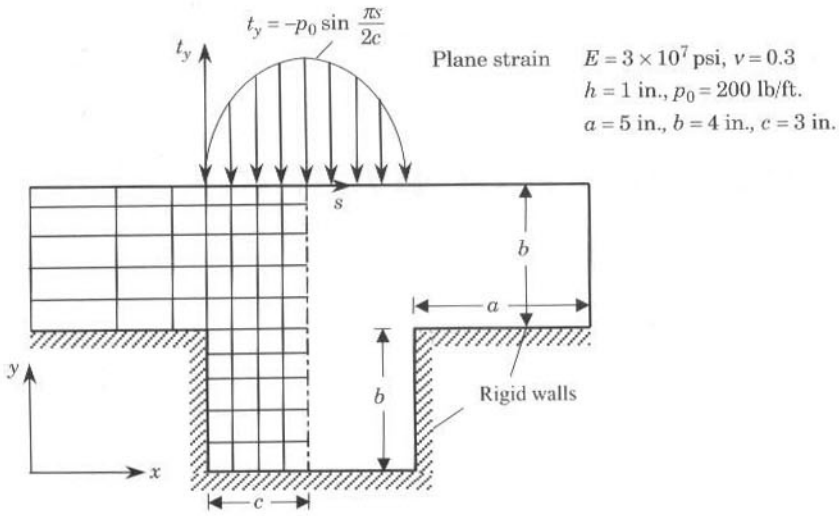

Figure P11.14

REFERENCES FOR ADDITIONAL READING

1. Barlow, J., "Optimal Stress Locations in Finite Element Models," *Int. Journal for Numerical Methods in Engineering*, **10**, 243–251, 1976.
2. Barlow, J., "More on Optimal Stress Points—Reduced Integration Element Distortions and Error Estimation," *Int. Journal for Numerical Methods in Engineering*, **28**, 1487–1504, 1989.
3. Budynas, R. G., *Advanced Strength and Applied Stress Analysis*, 2nd ed., McGraw-Hill, New York, 1999.
4. Reddy, J. N. and Rasmussen, M. L., *Advanced Engineering Analysis*, John Wiley, New York, 1982.
5. Reddy, J. N., *Energy and Variational Methods in Applied Mechanics*, (with an Introduction to the Finite Element Method), John Wiley, New York, 1984.
6. Reddy, J. N., *Energy Principles and Variational Methods in Applied Mechanics*, 2nd ed., John Wiley, New York, 2002.
7. Rektorys, K., *Variational Methods in Mathematics, Science and Engineering*, D. Reidel Publishing, Boston, MA, 1980.
8. Rektorys, K., *The Method of Discretization in Time*, D. Reidel Publishing, Boston, MA, 1982.
9. Shames, I. H., and Dym, C. L., *Energy and Finite Element Methods in Structural Mechanics*, Taylor and Francis, Philadelphia, PA, 1995.
10. Slaughter, W. S., *The Linearized Theory of Elasticity*, Birkhäuser, Boston, MA, 2002.
11. Timoshenko, S. P. and Goodier, J. N., *Theory of Elasticity*, 3rd ed., McGraw-Hill, New York, 1970.
12. Ugural, A. C. and Fenster, S. K., *Advanced Strength and Applied Elasticity*, Prentice Hall, Upper Saddle River, NJ, 1995.
13. Volterra, E. and Gaines, J. H., *Advanced Strength of Materials*, Prentice-Hall, Engelwood Cliffs, NJ, 1971.

Chapter 12

BENDING OF ELASTIC PLATES

12.1 INTRODUCTION

The term "plate" refers to solid bodies that are bounded by two parallel planes whose lateral dimensions are large compared with the separation between them (i.e., thickness of the plate), as shown in Fig. 12.1.1. In most cases, the thickness is no greater than one-tenth of the smallest in-plane dimension. Geometrically, plate problems are similar to the plane stress problems considered in Chapter 11 except that plates are also subjected to transverse loads (i.e., loads perpendicular to the plane of the plate) that cause bending about axes in the plane of the plate. In other words, a plate is a two-dimensional analog of a beam (see Chapter 5). Because of the smallness of the thickness dimension, it is often not necessary to model plates using three-dimensional elasticity theory. Simple two-dimensional theories that account for the kinematics of bending deformation of thin bodies subjected to transverse loads have been developed, and they are known as *plate theories*. An overview of plate theories can be found in Reddy (1999, 2002, 2004*a*).

Governing equations of displacement-based plate theories are derived using the principle of virtual displacements [see Reddy (1999, 2002)]. As we shall see shortly (and has already been shown in Chapter 11), the principle of virtual displacements directly yields the weak forms of the governing equations. The starting point in the development of the governing equations of a plate theory is to choose a displacement field. Typically, the displacement components are selected in the form of a linear combination of unknown functions and powers of the thickness coordinate z so that certain kinematics (i.e., geometry of deformation) of the plate are represented. For example, if $u_i(x, y, z, t)$ is the ith displacement component in the plate, it is expanded in the form

$$u_i(x, y, z, t) = \sum_{k=0}^{N} (z)^k u_i^{(k)}(x, y, t) \tag{12.1.1}$$

where $u_i^{(k)}$ are functions of (x, y) that are to be determined, (x, y) are the in-plane coordinates, z is the thickness coordinate, and t denotes time.

The principle of virtual displacements or Hamilton's principle [see Reddy (1999, 2002)] requires

$$0 = \int_{t_1}^{t_2} [\delta K - (\delta U + \delta V)]\, dt \tag{12.1.2}$$

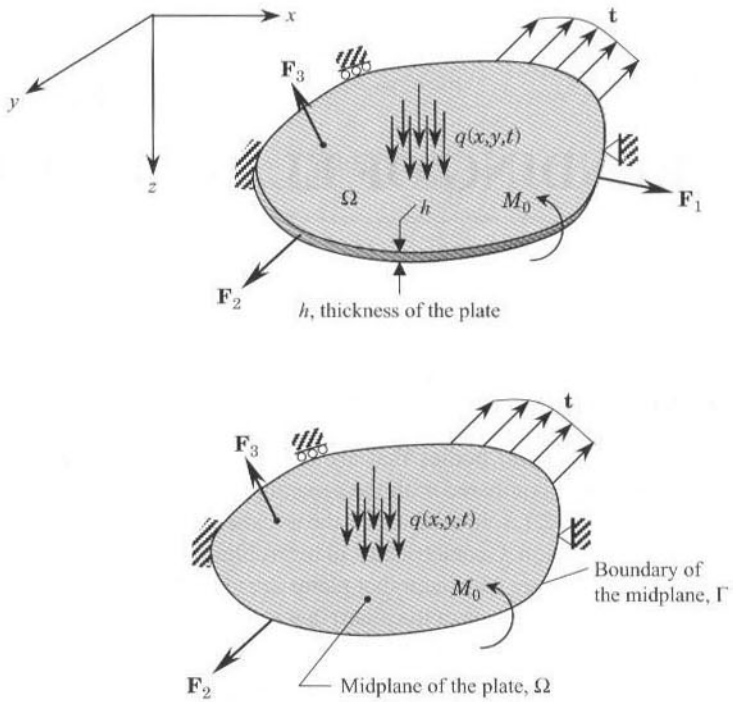

Figure 12.1.1 A plate structure subjected to external applied loads.

where $\delta U, \delta V$, and δK denote the virtual strain energy, virtual work done by external applied forces, and virtual kinetic energy, respectively (see Section 2.3.6). These quantities are expressed in terms of actual stresses and virtual strains, which depend on the assumed displacement functions, $u_i^{(k)}$, and their variations. For plate structures, the integration over the domain of the plate is represented as the (tensor) product of integration over the plane of the plate and integration over the thickness of the plate (volume integral = integral over the plane × integral over the thickness). This is possible because of the explicit nature of the assumed displacement field (12.1.1) in the thickness coordinate. Thus, we can write

$$\int_V (\cdot)\, dV = \int_{-\frac{h}{2}}^{\frac{h}{2}} \int_{\Omega_0} (\cdot)\, d\Omega\, dz \tag{12.1.3}$$

where h denotes the total thickness of the plate and Ω denotes the undeformed midplane of the plate, which is assumed to coincide with the xy plane. Since all undetermined variables are explicit functions of the thickness coordinate, integration over the plate thickness is carried out explicitly, reducing the problem to a two-dimensional one. Consequently, the governing equations associated with the assumed expansion in Eq. (12.1.1) consist of differential equations involving the dependent variables $u_i^{(k)}(x, y, t)$ and thickness-averaged stress resultants, $R_{ij}^{(m)}$:

$$R_{ij}^{(m)} = \int_{-\frac{h}{2}}^{\frac{h}{2}} (z)^m \sigma_{ij}\, dz \tag{12.1.4}$$

The resultants can be written in terms of $u_i^{(k)}$ with the help of the assumed constitutive equations (stress-strain relations) and strain-displacement relations. More complete development of this procedure can be found in the textbooks by Reddy (1999, 2002, 2004*a*).

The two most commonly used displacement-based plate theories are the *classical plate theory* (CPT) and *first-order shear deformation theory* (SDT). CPT is an extension of the Euler–Bernoulli beam theory (see Section 5.2) from one dimension to two dimensions and is also known as the *Kirchhoff plate theory*. SDT is an extension of the Timoshenko beam theory (see Section 5.3) and is often known as the *Hencky–Mindlin plate theory*. A review of these plate theories and other refined plate theories can be found in Reddy (1999, 2004*a*). In this study, we shall review the governing equations and develop the finite element models of only the CPT and SDT.

For a linear theory based on infinitesimal strains and orthotropic material properties, the in-plane displacements (u_x, u_y) are uncoupled from the transverse deflection $u_z = w$. The in-plane displacements (u_x, u_y) are governed by the plane elasticity equations discussed in Chapter 11. If there are no in-plane forces, the inplane displacements will be zero. Hence, we discuss only the equations governing the bending deformation and the associated finite element models.

12.2 CLASSICAL PLATE THEORY

12.2.1 Displacement Field

The CPT is based on the assumptions that a straight line perpendicular to the plane of the plate is (1) inextensible, (2) remains straight, and (3) rotates such that it remains perpendicular to the tangent to the deformed surface [see Fig. 12.2.1(*a*)]. These assumptions are equivalent to specifying

$$\varepsilon_{zz} = 0, \quad \varepsilon_{yz} = 0, \quad \varepsilon_{xz} = 0 \tag{12.2.1}$$

The following assumed displacement field satisfies the assumptions

$$\begin{aligned} u_1(x, y, z, t) &= u_x(x, y, t) - z\frac{\partial w}{\partial x} \\ u_2(x, y, z, t) &= u_y(x, y, t) - z\frac{\partial w}{\partial y} \\ u_3(x, y, z, t) &= u_z(x, y, t) \equiv w(x, y, t) \end{aligned} \tag{12.2.2}$$

where (u_1, u_2, u_3) denote the total displacements of the point (x, y, z) along the x, y, and z directions, respectively, and (u_x, u_y, u_z) represent displacements of a point on the midplane $(x, y, 0)$ at time t.

The linear bending strains (due to the displacement w only) in (12.2.2) are (virtual strains are also listed)

$$\begin{Bmatrix} \varepsilon_{xx} \\ \varepsilon_{yy} \\ 2\varepsilon_{xy} \end{Bmatrix} = -z \begin{Bmatrix} \dfrac{\partial^2 w}{\partial x^2} \\ \dfrac{\partial^2 w}{\partial y^2} \\ 2\dfrac{\partial^2 w}{\partial x \partial y} \end{Bmatrix}, \quad \begin{Bmatrix} \delta\varepsilon_{xx} \\ \delta\varepsilon_{yy} \\ 2\delta\varepsilon_{xy} \end{Bmatrix} = -z \begin{Bmatrix} \dfrac{\partial^2 \delta w}{\partial x^2} \\ \dfrac{\partial^2 \delta w}{\partial y^2} \\ 2\dfrac{\partial^2 \delta w}{\partial x \partial y} \end{Bmatrix} \tag{12.2.3}$$

and $\varepsilon_{xz} = 0$, $\varepsilon_{yz} = 0$, and $\varepsilon_{zz} = 0$.

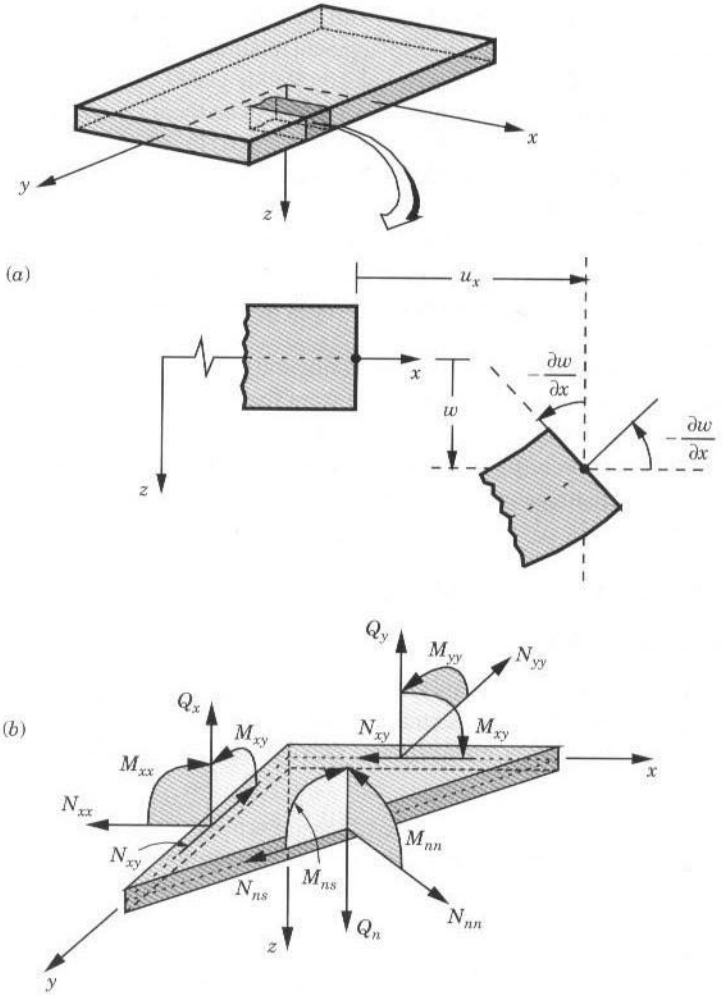

Figure 12.2.1 (*a*) Undeformed and deformed geometries of an edge in CPT. (*b*) Bending moments and shear forces on a plate element.

12.2.2 Virtual Work Statement

The principle of virtual displacements (12.1.2) applied to a plate finite element occupying a volume V_e and whose midplane is Ω_e takes the form [Reddy (1999, 2002)]

$$0 = \int_{V_e} \left[\rho z^2 \left(\frac{\partial \delta w}{\partial x} \frac{\partial^3 w}{\partial x \partial t^2} + \frac{\partial \delta w}{\partial y} \frac{\partial^3 w}{\partial y \partial t^2} \right) + \rho \delta w \frac{\partial^2 w}{\partial t^2} + \delta \varepsilon_{xx} \sigma_{xx} + \delta \varepsilon_{yy} \sigma_{yy} + 2 \delta \varepsilon_{xy} \sigma_{xy} \right] dV - \int_{\Omega_e} q \delta w \, dx \, dy - \oint_{\Gamma_e} \left(-M_{nn} \frac{\partial \delta w}{\partial n} + V_n \delta w \right) ds \tag{12.2.4}$$

The first three terms in (12.2.4) represent the virtual work done by the inertial forces in the three coordinate directions, while the remaining terms in the volume integral represent the virtual strain energy stored in the plate. The last two integrals, one defined on the midplane Ω_e and the other on the boundary Γ_e, denote the virtual work done by the transversely distributed load q, edge bending moment M_{nn} and shear force V_n [see Fig. 12.2.1(*b*)]. Since $V_e = \Omega_e \times (-\frac{h_e}{2}, \frac{h_e}{2})$ and the integrand is separable into functions of x and y alone and functions of z

$$F(x, y, z) = g(x, y) f(z) \tag{12.2.5}$$

we can carry out integration with respect to z (through thickness) explicitly.

Substitution of (12.2.3) for virtual displacements and strains into (12.2.4) and integrating with respect to z, we obtain

$$\begin{aligned} 0 = \int_{\Omega_e} \Bigg(& I_0 \delta w \frac{\partial^2 w}{\partial t^2} + I_2 \frac{\partial \delta w}{\partial x} \frac{\partial^3 w}{\partial x \partial t^2} + I_2 \frac{\partial \delta w}{\partial y} \frac{\partial^3 w}{\partial y \partial t^2} \\ & - M_{xx} \frac{\partial^2 \delta w}{\partial x^2} - M_{yy} \frac{\partial^2 \delta w}{\partial y^2} - 2 M_{xy} \frac{\partial^2 \delta w}{\partial x \partial y} - q \delta w \Bigg) dx\, dy \\ & - \oint_{\Gamma_e} \left(-M_{nn} \frac{\partial \delta w}{\partial n} + V_n \delta w \right) ds \end{aligned} \tag{12.2.6}$$

where $(M_{xx},\ M_{yy},\ M_{xy})$ are the bending moments [see Fig. 12.2.1(*b*)],

$$\begin{aligned} M_{xx} &= \int_{-h/2}^{h/2} \sigma_{xx} z\, dz = -\left(D_{11} \frac{\partial^2 w}{\partial x^2} + D_{12} \frac{\partial^2 w}{\partial y^2} \right) \\ M_{yy} &= \int_{-h/2}^{h/2} \sigma_{yy} z\, dz = -\left(D_{12} \frac{\partial^2 w}{\partial x^2} + D_{22} \frac{\partial^2 w}{\partial y^2} \right) \\ M_{xy} &= \int_{-h/2}^{h/2} \sigma_{xy} z\, dz = -2 D_{66} \frac{\partial^2 w}{\partial x \partial y} \end{aligned} \tag{12.2.7}$$

I_0 and I_2 are the mass moments of inertia (the rotatory inertia I_2 is neglected often)

$$I_0 = \int_{-h/2}^{h/2} \rho\, dz = \rho h, \quad I_2 = \int_{-h/2}^{h/2} \rho z^2\, dz = \frac{1}{12} \rho h^3 \tag{12.2.8a}$$

and D_{ij} are the plate material stiffnesses

$$\begin{aligned} D_{11} &= \frac{E_1 h^3}{12(1 - \nu_{12}\nu_{21})}, \quad D_{22} = \frac{E_2 h^3}{12(1 - \nu_{12}\nu_{21})} \\ D_{12} &= \frac{\nu_{12} E_2 h^3}{12(1 - \nu_{12}\nu_{21})}, \quad D_{66} = \frac{G_{12} h^3}{12} \end{aligned} \tag{12.2.8b}$$

where the plane-stress reduced constitutive equations (11.2.11) are used in arriving at the expressions (12.2.7); M_{nn} and M_{ns} denote the normal and twisting moments, respectively, on an edge with unit normal vector $\hat{\mathbf{n}}$, and V_n is the shear force. The moment M_{nn} and

shear force V_n on an edge with unit normal $\hat{\mathbf{n}}$ can be related to moments M_{xx}, M_{yy}, and M_{xy} on edges $x =$ constant and $y =$ constant by [see Reddy (2000)]

$$M_{nn} = M_{xx}n_x^2 + M_{yy}n_y^2 + 2M_{xy}n_x n_y, \quad V_n = \hat{Q}_n + \frac{\partial M_{ns}}{\partial s}$$

$$\hat{Q}_n = Q_x n_x + Q_y n_y + I_2\left(\frac{\partial^3 w}{\partial x \partial t^2}n_x + \frac{\partial^3 w}{\partial y \partial t^2}n_y\right) \tag{12.2.9a}$$

$$M_{ns} = (M_{yy} - M_{xx})n_x n_y + M_{xy}\left(n_x^2 - n_y^2\right)$$

$$Q_x = \frac{\partial M_{xx}}{\partial x} + \frac{\partial M_{xy}}{\partial y}, \quad Q_y = \frac{\partial M_{xy}}{\partial x} + \frac{\partial M_{yy}}{\partial y} \tag{12.2.9b}$$

where (n_x, n_y) are the direction cosines of the unit normal, $\hat{\mathbf{n}} = n_x\hat{\mathbf{i}} + n_y\hat{\mathbf{j}}$, on the boundary Γ_e.

Substituting (12.2.7) into (12.2.6) yields the following weak form of the problem:

$$\begin{aligned} 0 = \int_{\Omega_e}\Bigg[& I_0\delta w\frac{\partial^2 w}{\partial t^2} + I_2\frac{\partial \delta w}{\partial x}\frac{\partial^3 w}{\partial x \partial t^2} + I_2\frac{\partial \delta w}{\partial y}\frac{\partial^3 w}{\partial y \partial t^2} + 4D_{66}\frac{\partial^2 w}{\partial x \partial y}\frac{\partial^2 \delta w}{\partial x \partial y} \\ & + \left(D_{11}\frac{\partial^2 w}{\partial x^2} + D_{12}\frac{\partial^2 w}{\partial y^2}\right)\frac{\partial^2 \delta w}{\partial x^2} + \left(D_{12}\frac{\partial^2 w}{\partial x^2} + D_{22}\frac{\partial^2 w}{\partial y^2}\right)\frac{\partial^2 \delta w}{\partial y^2} \\ & - \delta w q\Bigg] dx\, dy - \oint_{\Gamma_e}\left(-M_{nn}\frac{\partial \delta w}{\partial n} + V_n\delta w\right) ds \end{aligned} \tag{12.2.10}$$

The differential equation [i.e., the Euler–Lagrange equation resulting from (12.2.10)] governing w is

$$\begin{aligned} & \frac{\partial^2}{\partial x^2}\left(D_{11}\frac{\partial^2 w}{\partial x^2} + D_{12}\frac{\partial^2 w}{\partial y^2}\right) + \frac{\partial^2}{\partial y^2}\left(D_{12}\frac{\partial^2 w}{\partial x^2} + D_{22}\frac{\partial^2 w}{\partial y^2}\right) \\ & \quad + 2\frac{\partial^2}{\partial x \partial y}\left(2D_{66}\frac{\partial^2 w}{\partial x \partial y}\right) = q - I_0\frac{\partial^2 w}{\partial t^2} + I_2\frac{\partial^2}{\partial t^2}\left(\frac{\partial^2 w}{\partial x^2} + \frac{\partial^2 w}{\partial y^2}\right) \end{aligned} \tag{12.2.11}$$

Note that the expressions in parentheses in the first three terms are the bending moments $-M_{xx}$, $-M_{yy}$, and $-M_{xy}$, respectively [see (12.2.7)]. The boundary conditions for the CPT are given below:

$$\begin{aligned} \text{clamped:} \quad & w = 0, \quad \frac{\partial w}{\partial n} = 0 \\ \text{simply supported:} \quad & w = 0, \quad M_{nn} = 0 \\ \text{free:} \quad & V_n = 0, \quad M_{nn} = 0 \end{aligned} \tag{12.2.12}$$

We do not need Eq. (12.2.11) but only the weak form (12.2.10) to develop the finite element model. Alternatively, we can construct the weak form of the governing equation (12.2.11) using the usual procedure. We obtain

$$\begin{aligned} 0 = \int_{\Omega_e}\Bigg[& \frac{\partial^2 v}{\partial x^2}\left(D_{11}\frac{\partial^2 w}{\partial x^2} + D_{12}\frac{\partial^2 w}{\partial y^2}\right) + \frac{\partial^2 v}{\partial y^2}\left(D_{12}\frac{\partial^2 w}{\partial x^2} + D_{22}\frac{\partial^2 w}{\partial y^2}\right) \\ & + 4D_{66}\frac{\partial^2 v}{\partial x \partial y}\frac{\partial^2 w}{\partial x \partial y} - vq + I_0 v\frac{\partial^2 w}{\partial t^2} + I_2\left(\frac{\partial v}{\partial x}\frac{\partial^3 w}{\partial x \partial t^2} + \frac{\partial v}{\partial y}\frac{\partial^3 w}{\partial y \partial t^2}\right)\Bigg] dx dy \end{aligned}$$

$$
\begin{aligned}
&-\oint_{\Gamma_e} v\left[\left(\frac{\partial M_{xx}}{\partial x}+\frac{\partial M_{xy}}{\partial y}\right)n_x+\left(\frac{\partial M_{xy}}{\partial x}+\frac{\partial M_{yy}}{\partial y}\right)n_y\right.\\
&\left.+I_2\left(\frac{\partial^3 w}{\partial x\partial t^2}n_x+\frac{\partial^3 w}{\partial y\partial t^2}n_y\right)\right]ds\\
&+\oint_{\Gamma_e}\left[\frac{\partial v}{\partial x}(M_{xx}n_x+M_{xy}n_y)+\frac{\partial v}{\partial y}(M_{xy}n_x+M_{yy}n_y)\right]ds
\end{aligned}
\tag{12.2.13}
$$

where v denotes the weight function, which can be interpreted as the first variation, $\delta w = v$. Next, we convert the derivatives of w with respect to the rectangular coordinates (x, y) to those with respect to the local (normal and tangential) coordinates (n, s). We use the identities

$$
\frac{\partial}{\partial x}=n_x\frac{\partial}{\partial n}-n_y\frac{\partial}{\partial s},\quad \frac{\partial}{\partial y}=n_x\frac{\partial}{\partial s}+n_y\frac{\partial}{\partial n}
\tag{12.2.14}
$$

and the definitions (12.2.9) to rewrite the boundary integrals of (12.2.13) as

$$
-\oint_{\Gamma_e} v\hat{Q}_n\,ds+\oint_{\Gamma_e}\left(\frac{\partial v}{\partial n}M_{nn}+\frac{\partial v}{\partial s}M_{ns}\right)ds
$$

The second term in the second integral is integrated by parts to yield the expression

$$
-\oint_{\Gamma_e}\left[v\left(\hat{Q}_n+\frac{\partial M_{ns}}{\partial s}\right)-\frac{\partial v}{\partial n}M_{nn}\right]ds
\tag{12.2.15}
$$

The expression in parenthesis $(\cdot)$ is denoted by V_n, and its specification is known as the *Kirchhoff free-edge condition*. We have made the assumption that $[vM_{ns}]_s = 0$, which holds only when the boundary is smooth. It is clear that the weak form in (12.2.13), with the boundary integrals replaced by (12.2.15), is the same as that in (12.2.10).

The weak form (12.2.10) can be expressed in vector form as ($\mathbf{w} = w$ and $\delta\mathbf{w} = \delta w$)

$$
\begin{aligned}
0=&\int_{\Omega_e}\left[I_0(\delta\mathbf{w})^{\mathrm{T}}\ddot{\mathbf{w}}+I_2(\mathbf{D}_1\delta\mathbf{w})^{\mathrm{T}}(\mathbf{D}_1\ddot{\mathbf{w}})+(\mathbf{D}_2\delta\mathbf{w})^{\mathrm{T}}\mathbf{C}(\mathbf{D}_2\mathbf{w})-(\delta\mathbf{w})^{\mathrm{T}}q\right]d\mathbf{x}\\
&-\oint_{\Gamma_e}\left[-(\delta\mathbf{w}_{,n})^{\mathrm{T}}M_{nn}+(\delta\mathbf{w})^{\mathrm{T}}V_n\right]ds
\end{aligned}
\tag{12.2.16}
$$

where $\mathbf{w}_{,n} = (\partial\mathbf{w}/\partial n)$ and

$$
\mathbf{D}_1=\begin{Bmatrix}\dfrac{\partial}{\partial x}\\[2ex] \dfrac{\partial}{\partial y}\end{Bmatrix},\quad
\mathbf{D}_2=\begin{Bmatrix}\dfrac{\partial^2}{\partial x^2}\\[2ex] \dfrac{\partial^2}{\partial y^2}\\[2ex] 2\dfrac{\partial^2}{\partial x\partial y}\end{Bmatrix},\quad
\mathbf{C}=\begin{bmatrix}D_{11} & D_{12} & 0\\ D_{12} & D_{22} & 0\\ 0 & 0 & D_{66}\end{bmatrix}
\tag{12.2.17}
$$

This completes the development of the CPT and its variational (or weak) form. Next, we develop the finite element model based on Eqs. (12.2.10) and (12.2.16).

12.2.3 Finite Element Model

An examination of the boundary terms in the weak form (12.2.10) suggests that the essential boundary conditions involve specifying the transverse deflection w and the normal derivative of w, which constitute the primary variables of the problem (like in the Euler–Bernoulli beam model). Hence, the finite element interpolation of w must be such that w and $\partial w/\partial n$ are continuous across the interelement boundaries in CPT elements. Note that $\partial/\partial n$ and $\partial/\partial s$ are related to the global derivatives $\partial/\partial x$ and $\partial/\partial y$ by the relations [the inverse of those in (12.2.14)]

$$\frac{\partial}{\partial n} = n_x \frac{\partial}{\partial x} + n_y \frac{\partial}{\partial y}, \quad \frac{\partial}{\partial s} = n_x \frac{\partial}{\partial y} - n_y \frac{\partial}{\partial x} \tag{12.2.18}$$

Thus, the primary variables at the nodes of a rectangular element with sides parallel to the x and y axes should be

$$w, \quad \frac{\partial w}{\partial x}, \quad \frac{\partial w}{\partial y}$$

Finite elements that require continuity of w and its first derivatives are called C^1 elements.

Towards developing the CPT finite element model, we assume that w is interpolated over a typical element Ω_e by expressions of the form

$$w(x, y, t) = \sum_{j=1}^{n} \Delta_j(t)\varphi_j(x, y) \tag{12.2.19a}$$

or

$$\mathbf{w} = \Phi^{\mathrm{T}}\Delta, \quad \Phi^{\mathrm{T}} = \{\varphi_1 \ \varphi_2 \ \cdots \ \varphi_n\} \tag{12.2.19b}$$

where Δ_j denote the nodal values of w and its derivatives, and $\varphi_j(x, y)$ are the Hermite interpolation functions (see Table 9.2.1). The nature of the interpolation functions φ_j will be discussed in the sequel. Substitution of (12.2.19a) for w and $\delta w = \varphi_i$ $(i = 1, 2, \ldots, n)$ into (12.2.10) gives the finite element model

$$[M^e]\{\ddot{\Delta}^e\} + [K^e]\{\Delta^e\} = \{F^e\} + \{Q^e\} \tag{12.2.20}$$

where

$$\begin{aligned}
M_{ij}^e &= \int_{\Omega_e} \left[I_0 \varphi_i \varphi_j + I_2 \left(\frac{\partial \varphi_i}{\partial x}\frac{\partial \varphi_j}{\partial x} + \frac{\partial \varphi_i}{\partial y}\frac{\partial \varphi_j}{\partial y} \right) \right] dx\, dy \\
K_{ij}^e &= \int_{\Omega_e} \left[D_{11} \frac{\partial^2 \varphi_i}{\partial x^2}\frac{\partial^2 \varphi_j}{\partial x^2} + D_{12} \left(\frac{\partial^2 \varphi_i}{\partial x^2}\frac{\partial^2 \varphi_j}{\partial y^2} + \frac{\partial^2 \varphi_i}{\partial y^2}\frac{\partial^2 \varphi_j}{\partial x^2} \right) \right. \\
&\quad \left. + D_{22} \frac{\partial^2 \varphi_i}{\partial y^2}\frac{\partial^2 \varphi_j}{\partial y^2} + 4D_{66} \frac{\partial^2 \varphi_i}{\partial x \partial y}\frac{\partial^2 \varphi_j}{\partial x \partial y} \right] dx\, dy \\
F_i^e &= \int_{\Omega_e} q\varphi_i \, dx\, dy, \quad Q_i^e = \oint_{\Gamma_e} \left(-M_{nn}\frac{\partial \varphi_i}{\partial n} + V_n \varphi_i \right) ds
\end{aligned} \tag{12.2.21}$$

The vector form of the finite element model is obtained by substituting (12.2.19b) into Eq. (12.2.16) and setting the coefficient of $\delta\Delta^{\mathrm{T}}$ to zero:

$$\mathbf{M}^e \ddot{\Delta}^e + \mathbf{K}^e \Delta^e = \mathbf{F}^e + \mathbf{Q}^e \tag{12.2.22}$$

where [see Eq. (12.2.17) for the definitions of $\mathbf{D}_1$, $\mathbf{D}_2$, and $\mathbf{C}$]

$$\mathbf{M}^e = \int_{\Omega_e} \left(I_0 \Phi \Phi^{\mathrm{T}} + I_2 \mathbf{B}_1^{\mathrm{T}} \mathbf{B}_1 \right) d\mathbf{x}$$

$$\mathbf{K}^e = \int_{\Omega_e} \mathbf{B}_2^{\mathrm{T}} \mathbf{C} \mathbf{B}_2 \, d\mathbf{x}, \quad \mathbf{F}^e = \int_{\Omega_e} \Phi q \, d\mathbf{x}$$

$$\mathbf{Q}^e = \oint_{\Gamma_e} \left(-\Phi_{,n} M_n + \Phi V_n \right) ds$$

$$\mathbf{B}_1 = \mathbf{D}_1 \Phi^{\mathrm{T}} = \begin{bmatrix} \dfrac{\partial \varphi_1}{\partial x} & \dfrac{\partial \varphi_2}{\partial x} & \cdots & \dfrac{\partial \varphi_n}{\partial x} \\ \dfrac{\partial \varphi_1}{\partial y} & \dfrac{\partial \varphi_2}{\partial y} & \cdots & \dfrac{\partial \varphi_n}{\partial y} \end{bmatrix}_{(2 \times n)} \tag{12.2.23}$$

$$\mathbf{B}_2 = \mathbf{D}_2 \Phi^{\mathrm{T}} = \begin{bmatrix} \dfrac{\partial^2 \varphi_1}{\partial x^2} & \dfrac{\partial^2 \varphi_2}{\partial x^2} & \cdots & \dfrac{\partial^2 \varphi_n}{\partial x^2} \\ \dfrac{\partial^2 \varphi_1}{\partial y^2} & \dfrac{\partial^2 \varphi_2}{\partial y^2} & \cdots & \dfrac{\partial^2 \varphi_n}{\partial y^2} \\ 2\dfrac{\partial^2 \varphi_1}{\partial x \partial y} & 2\dfrac{\partial^2 \varphi_2}{\partial x \partial y} & \cdots & 2\dfrac{\partial^2 \varphi_n}{\partial x \partial y} \end{bmatrix}_{(3 \times n)}$$

12.2.4 Plate Bending Elements

A number of C^1 rectangular and triangular plate bending elements with $(w, \partial w/\partial x, \partial w/\partial y)$ or with $(w, \partial w/\partial x, \partial w/\partial y, \partial^2 w/\partial x \partial y)$ as the degrees of freedom at each node exist in the literature. A rectangular element with four nodes, with $(w, \partial w/\partial x, \partial w/\partial y)$ at each node, requires the 12-term $(n = 12)$ polynomial approximation of w

$$\begin{aligned} w = {} & a_1 + a_2 x + a_3 y + a_4 xy + a_5 x^2 + a_6 y^2 + a_7 x^2 y \\ & + a_8 x y^2 + a_9 x^3 + a_{10} y^3 + a_{11} x^3 y + a_{12} x y^3 \end{aligned} \tag{12.2.24}$$

The polynomial is *not* a complete fourth-order polynomial; it is a complete third-order polynomial. For a three-node triangular element with $(w, \partial w/\partial x, \partial w/\partial y)$ at each node, the following nine-term $(n = 9)$ polynomial is selected

$$w = a_1 + a_2 x + a_3 y + a_4 xy + a_5 x^2 + a_6 y^2 + a_7 (x^2 y + x y^2) + a_8 x^3 + a_9 y^3 \tag{12.2.25}$$

This is an incomplete third-order polynomial because $x^2 y$ and $y^2 x$ do not vary independently.

Some comments are in order on the interelement continuity of w and $\partial w/\partial n$ for the four-node rectangular element $(n = 12)$ and three-node triangular element $(n = 9)$. We note from (12.2.24) that w varies as a cubic along any line $x =$ constant or $y =$ constant. Along a given side, there are two nodes and two values (w and its normal derivative) per node to define the cubic variation uniquely. Hence, w is uniquely defined along the element boundary and is continuous along interelement boundaries. The normal derivative, say, $\partial w/\partial x$ on a line $x =$ constant, also varies as a cubic function of y along the side. Since only two values of $\partial w/\partial x$ are available on the side, the cubic variation cannot be uniquely defined and the normal slope continuity is not satisfied. In addition, $\partial^2 w/\partial x \partial y$ is not single-valued at the corner points of the element. Elements that violate any of the continuity conditions are known as

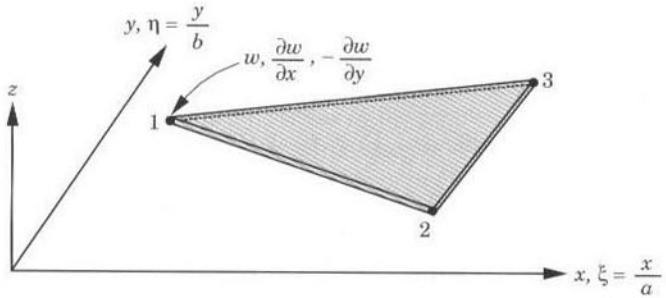

Figure 12.2.2 A nonconforming triangular element with three degrees of freedom (w, $\partial w/\partial x$, $\partial w/\partial y$) per node.

nonconforming elements. Thus, the four-node rectangular element with w represented by (12.2.24) is a nonconforming element. Despite this deficiency, the element is known to give good results. A similar discussion leads to the conclusion that the three-node triangular element is nonconforming. In addition, the triangular element is found to have convergence problems and singular behavior for certain meshes.

Triangular Elements

An effective nonconforming triangular element (the BCIZ triangle) was developed by Bazeley, Cheung, Irons, and Zienkiewicz (1965), and it consists of three degrees of freedom $(w, -\partial w/\partial y, \partial w/\partial x)$ at the three vertex nodes (see Fig. 12.2.2). The interpolation functions for the triangular element can be expressed in terms of the area coordinates as

$$\begin{Bmatrix} \varphi_1 \\ \varphi_2 \\ \varphi_3 \\ \varphi_4 \\ \varphi_5 \\ \varphi_6 \\ \varphi_7 \\ \varphi_8 \\ \varphi_9 \end{Bmatrix} = \begin{Bmatrix} L_1 + L_1^2 L_2 + L_1^2 L_3 - L_1 L_2^2 - L_1 L_3^2 \\ x_{31}(L_3 L_1^2 - 0.5 L_{123}) - x_{12}(L_1^2 L_2 + 0.5 L_{123}) \\ y_{31}(L_3 L_1^2 + 0.5 L_{123}) - y_{12}(L_1^2 L_2 + 0.5 L_{123}) \\ L_2 + L_2^2 L_3 + L_2^2 L_1 - L_2 L_3^2 - L_2 L_1^2 \\ x_{12}(L_1 L_2^2 - 0.5 L_{123}) - x_{23}(L_2^2 L_3 + 0.5 L_{123}) \\ y_{12}(L_1 L_2^2 + 0.5 L_{123}) - y_{23}(L_2^2 L_3 + 0.5 L_{123}) \\ L_3 + L_3^2 L_1 + L_3^2 L_2 - L_3 L_1^2 - L_3 L_2^2 \\ x_{23}(L_2 L_3^2 - 0.5 L_{123}) - x_{31}(L_3^2 L_1 + 0.5 L_{123}) \\ y_{23}(L_2 L_3^2 + 0.5 L_{123}) - y_{31}(L_3^2 L_1 + 0.5 L_{123}) \end{Bmatrix} \tag{12.2.26}$$

where $L_{123} = L_1 L_2 L_3$, $x_{ij} = x_i - x_j$, and $y_{ij} = y_i - y_j$, (x_i, y_i) being the global coordinates of the ith node.

A conforming triangular element due to Clough and Tocher (1965) is an assemblage of three triangles as shown in Fig. 12.2.3 [Clough and Felippa (1968) developed a quadrilateral element by dividing it into four triangles and each triangle divided into three subtriangles]. The normal slope continuity is enforced at the midside nodes between the subtriangles. In the ith subtriangle, the transverse deflection is represented by the polynomial

$$w^i(x, y) = a_1^i + a_2^i \xi + a_3^i \eta + a_4^i \xi^2 + a_5^i \xi\eta + a_6^i \eta^2 + a_7^i \xi^3 + a_8^i \xi\eta^2 + a_9^i \eta\xi^2 + a_{10}^i \eta^3 \tag{12.2.27}$$

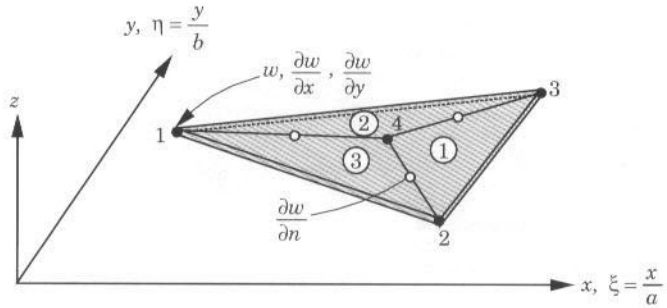

Figure 12.2.3 A conforming triangular element with three degrees of freedom.

where $(i = 1, 2, 3)$ and (ξ, η) are the local coordinates, as shown in the Fig. 12.2.3. The thirty coefficients are reduced to nine, three $(w, \partial w/\partial x, \partial w/\partial y)$ at each vertex of the triangle, by equating the variables from the vertices of each subtriangle at the common points and normal slope between the midside points of the subtriangles.

Rectangular Elements

A nonconforming rectangular element with 12 degrees of freedom [see Eq. (12.2.24)] with w, $\partial w/\partial x$, and $\partial w/\partial y$ as the nodal variables [see Fig. 12.2.4(a)] is based on the work of Melosh (1963) and Zienkiewicz and Cheung (1964). The normal slope varies cubically along an edge whereas there are only two values of $\partial w/\partial n$ available on the edge. Therefore, the cubic polynomial for the normal derivative of w is not the same on the edge common to two elements. The interpolation functions for this element can be expressed compactly as

$$\begin{aligned} &\varphi_i^e = g_{i1} \ (i = 1, 4, 7, 10); \quad \varphi_i^e = g_{i2} \ (i = 2, 5, 8, 11) \\ &\varphi_i^e = g_{i3} \ (i = 3, 6, 9, 12) \end{aligned} \tag{12.2.28a}$$

where

$$\begin{aligned} g_{i1} &= \frac{1}{8}(1 + \xi_0)(1 + \eta_0)(2 + \xi_0 + \eta_0 - \xi^2 - \eta^2) \\ g_{i2} &= \frac{1}{8}\xi_i(\xi_0 - 1)(1 + \eta_0)(1 + \xi_0)^2 \\ g_{i3} &= \frac{1}{8}\eta_i(\eta_0 - 1)(1 + \xi_0)(1 + \eta_0)^2 \\ \xi &= (x - x_c)/a, \ \eta = (y - y_c)/b, \ \xi_0 = \xi\xi_i, \ \eta_0 = \eta\eta_i \end{aligned} \tag{12.2.28b}$$

$2a$ and $2b$ are the sides of the rectangle, and (x_c, y_c) are the global coordinates of the center of the rectangle. We denote this element as the CPT(N) element.

A conforming rectangular element with w, $\partial w/\partial x$, $\partial w/\partial y$, and $\partial^2 w/\partial x \partial y$ as the nodal variables (a total of 16 degrees of freedom) was developed by Bogner, Fox, and Schmidt (1965). The interpolation functions (obtained from the tensor products of the one-dimensional Hermite cubic polynomials) for this element [see Fig. 12.2.4(b) and Table 9.2.1]

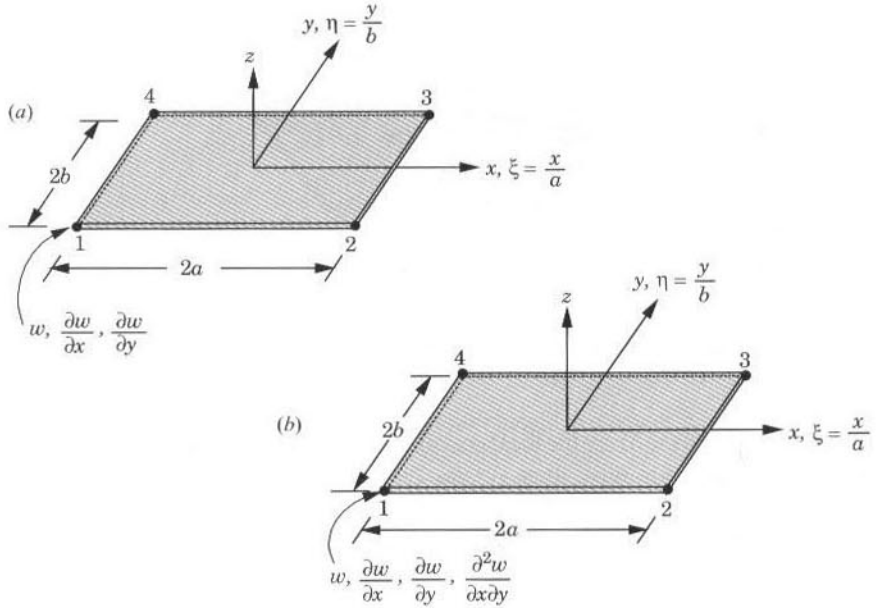

Figure 12.2.4 (*a*) A nonconforming rectangular element with three degrees of freedom (w, $\partial w/\partial x$, $\partial w/\partial y$) per node. (*b*) A conforming rectangular element with four degrees of freedom (w, $\partial w/\partial x$, $\partial w/\partial y$, $\partial^2 w/\partial x \partial y$) per node.

are

$$\begin{aligned} \varphi_i^e &= g_{i1} \ (i = 1, 5, 9, 13); \qquad \varphi_i^e = g_{i2} \ (i = 2, 6, 10, 14) \\ \varphi_i^e &= g_{i3} \ (i = 3, 7, 11, 15); \qquad \varphi_i^e = g_{i4} \ (i = 4, 8, 12, 16) \end{aligned} \tag{12.2.29a}$$

where

$$\begin{aligned} g_{i1} &= \frac{1}{16}(\xi + \xi_i)^2(\xi_0 - 2)(\eta + \eta_i)^2(\eta_0 - 2) \\ g_{i2} &= \frac{1}{16}\xi_i(\xi + \xi_i)^2(1 - \xi_0)(\eta + \eta_i)^2(\eta_0 - 2) \\ g_{i3} &= \frac{1}{16}\eta_i(\xi + \xi_i)^2(\xi_0 - 2)(\eta + \eta_i)^2(1 - \eta_0) \\ g_{i4} &= \frac{1}{16}\xi_i\eta_i(\xi + \xi_i)^2(1 - \xi_0)(\eta + \eta_i)^2(1 - \eta_0) \end{aligned} \tag{12.2.29b}$$

This element is denoted as CPT(C).

12.3 SHEAR DEFORMATION PLATE THEORY

12.3.1 Displacement Field

In the SDT, we relax the normality assumption of CPT, i.e., transverse normals may rotate without remaining normal to the midplane (see Fig. 12.3.1). SDT is based on the

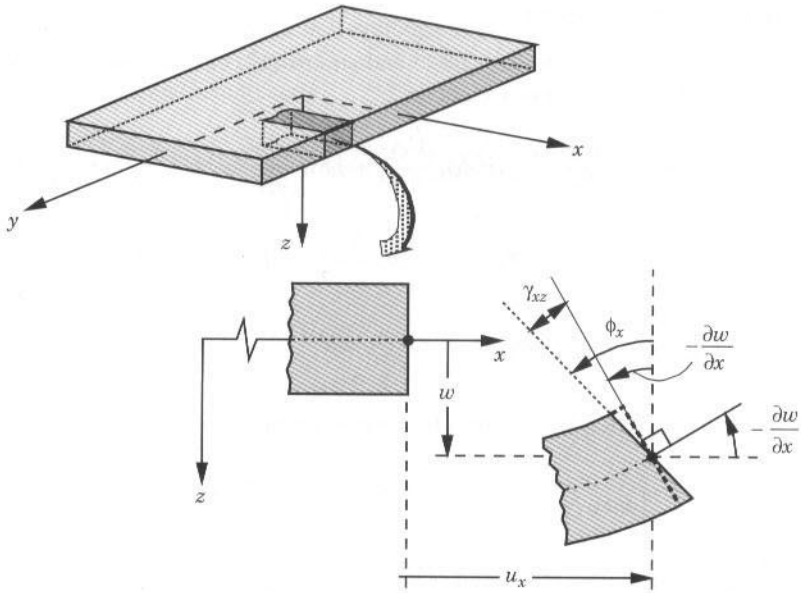

Figure 12.3.1 Undeformed and deformed geometries of an edge in SDT.

displacement field

$$\begin{aligned} u_1(x, y, z, t) &= u_x(x, y, t) + z\phi_x(x, y, t) \\ u_2(x, y, z, t) &= u_y(x, y, t) + z\phi_y(x, y, t) \\ u_3(x, y, z, t) &= u_z(x, y, t) \equiv w(x, y, t) \end{aligned} \tag{12.3.1}$$

where $(u_x,\ u_y,\ u_z = w)$ are the displacements of a point on the midplane in the (x, y, z) coordinate directions, and ϕ_x and ϕ_y are rotations of the transverse normal about the y and $-x$ axes, respectively. Since $(u_x,\ u_y)$ are uncoupled from $(w,\ \phi_x,\ \phi_y)$, we develop the equations governing $(w,\ \phi_x,\ \phi_y)$.

The bending strains associated with (12.3.1) are

$$\left\{\begin{array}{c} \varepsilon_{xx} \\ \varepsilon_{yy} \\ 2\varepsilon_{xy} \\ 2\varepsilon_{xz} \\ 2\varepsilon_{yz} \end{array}\right\} = \left\{\begin{array}{c} z\dfrac{\partial \phi_x}{\partial x} \\ z\dfrac{\partial \phi_y}{\partial y} \\ z\left(\dfrac{\partial \phi_x}{\partial y} + \dfrac{\partial \phi_y}{\partial x}\right) \\ \phi_x + \dfrac{\partial w}{\partial x} \\ \phi_y + \dfrac{\partial w}{\partial y} \end{array}\right\}, \quad \left\{\begin{array}{c} \delta\varepsilon_{xx} \\ \delta\varepsilon_{yy} \\ 2\delta\varepsilon_{xy} \\ 2\delta\varepsilon_{xz} \\ 2\delta\varepsilon_{yz} \end{array}\right\} = \left\{\begin{array}{c} z\dfrac{\partial \delta\phi_x}{\partial x} \\ z\dfrac{\partial \delta\phi_y}{\partial y} \\ z\left(\dfrac{\partial \delta\phi_x}{\partial y} + \dfrac{\partial \delta\phi_y}{\partial x}\right) \\ \delta\phi_x + \dfrac{\partial \delta w}{\partial x} \\ \delta\phi_y + \dfrac{\partial \delta w}{\partial y} \end{array}\right\} \tag{12.3.2}$$

Note that the transverse shear strains are nonzero and $\varepsilon_{zz} = 0$.

12.3.2 Virtual Work Statement

Substituting the displacement field (12.3.1) and strains (12.3.2) into the statement of the principle of virtual displacements, we obtain

$$0 = \int_{V_e} \left(\rho z^2 \delta\phi_x \frac{\partial^2 \phi_x}{\partial t^2} + \rho z^2 \delta\phi_y \frac{\partial^2 \phi_y}{\partial t^2} + \rho \delta w \frac{\partial^2 w}{\partial t^2} + \delta\varepsilon_{xx}\sigma_{xx} + \delta\varepsilon_{yy}\sigma_{yy} \right.$$
$$\left. + 2\delta\varepsilon_{xy}\sigma_{xy} + 2\delta\varepsilon_{xz}\sigma_{xz} + 2\delta\varepsilon_{yz}\sigma_{yz} \right) dV - \int_{\Omega_e} \delta w q \, dx \, dy$$
$$- \oint_{\Gamma_e} (\delta\phi_n M_{nn} + \delta\phi_s M_{ns} + \delta w \, Q_n) \, ds$$

Carrying out the integration with respect to z, we arrive at

$$0 = \int_{\Omega_e} \left[I_0 \delta w \frac{\partial^2 w}{\partial t^2} + I_2 \left(\delta\phi_x \frac{\partial^2 \phi_x}{\partial t^2} + \delta\phi_y \frac{\partial^2 \phi_y}{\partial t^2} \right) \right.$$
$$+ M_{xx} \frac{\partial \delta\phi_x}{\partial x} + M_{yy} \frac{\partial \delta\phi_y}{\partial y} + M_{xy} \left(\frac{\partial \delta\phi_x}{\partial y} + \frac{\partial \delta\phi_y}{\partial x} \right)$$
$$\left. + Q_x \left(\delta\phi_x + \frac{\partial \delta w}{\partial x} \right) + Q_y \left(\delta\phi_y + \frac{\partial \delta w}{\partial y} \right) - \delta w \, q \right] dx \, dy$$
$$- \oint_{\Gamma_e} (\delta\phi_n M_{nn} + \delta\phi_s M_{ns} + \delta w \, Q_n) \, ds \tag{12.3.3}$$

where M_{nn}, M_{ns}, and Q_n are defined in Eq. (12.2.9a) with

$$Q_x = K_s \int_{-h/2}^{h/2} \sigma_{xz} \, dz = K_s A_{55} \left(\phi_x + \frac{\partial w}{\partial x} \right)$$
$$Q_y = K_s \int_{-h/2}^{h/2} \sigma_{yz} \, dz = K_s A_{44} \left(\phi_y + \frac{\partial w}{\partial y} \right) \tag{12.3.4}$$

$$M_{xx} = D_{11} \frac{\partial \phi_x}{\partial x} + D_{12} \frac{\partial \phi_y}{\partial y}, \quad M_{yy} = D_{12} \frac{\partial \phi_x}{\partial x} + D_{22} \frac{\partial \phi_y}{\partial y}$$
$$M_{xy} = D_{66} \left(\frac{\partial \phi_x}{\partial y} + \frac{\partial \phi_y}{\partial x} \right) \tag{12.3.5}$$

$$Q_n = Q_x n_x + Q_y n_y, \quad \phi_n = \phi_x n_x + \phi_y n_y, \quad \phi_s = \phi_y n_x - \phi_x n_y$$
$$A_{44} = G_{23} h, \quad A_{55} = G_{13} h \tag{12.3.6}$$

Here K_s denotes the shear correction coefficient. This coefficient is introduced to account for the discrepancy between the distribution of transverse shear stresses in SDT and the actual distribution (see Section 5.3 on the Timoshenko beam element).

The virtual work statement (12.3.3) contains three weak forms for the three displacements $(w,\ \phi_x,\ \phi_y)$. They are identified by collecting the terms involving δw, $\delta\phi_x$, and $\delta\phi_y$ seperately and equating them to zero:

$$0 = \int_{\Omega_e} \left(I_0 \delta w \frac{\partial^2 w}{\partial t^2} + Q_x \frac{\partial \delta w}{\partial x} + Q_y \frac{\partial \delta w}{\partial y} - q\delta w \right) dx\, dy - \oint_{\Gamma_e} \delta w\, Q_n\, ds \tag{12.3.7a}$$

$$0 = \int_{\Omega_e} \left(I_2 \delta\phi_x \frac{\partial^2 \phi_x}{\partial t^2} + M_{xx} \frac{\partial \delta\phi_x}{\partial x} + M_{xy} \frac{\partial \delta\phi_x}{\partial y} + Q_x \delta\phi_x \right) dx\, dy$$
$$- \oint_{\Gamma_e} \delta\phi_x \left(M_{nn} n_x - M_{ns} n_y \right) ds \tag{12.3.7b}$$

$$0 = \int_{\Omega_e} \left(I_2 \delta\phi_y \frac{\partial^2 \phi_y}{\partial t^2} + M_{xy} \frac{\partial \delta\phi_y}{\partial x} + M_{yy} \frac{\partial \delta\phi_y}{\partial y} + Q_y \delta\phi_y \right) dx\, dy$$
$$- \oint_{\Gamma_e} \delta\phi_y \left(M_{nn} n_y + M_{ns} n_x \right) ds \tag{12.3.7c}$$

The governing differential equations of SDT are [obtained from the weak forms (12.3.7*a*)–(12.3.7*c*)]

$$\frac{\partial Q_x}{\partial x} + \frac{\partial Q_y}{\partial y} + q = I_0 \frac{\partial^2 w}{\partial t^2} \tag{12.3.8a}$$

$$\frac{\partial M_{xx}}{\partial x} + \frac{\partial M_{xy}}{\partial y} - Q_x = I_2 \frac{\partial^2 \phi_x}{\partial t^2} \tag{12.3.8b}$$

$$\frac{\partial M_{xy}}{\partial x} + \frac{\partial M_{yy}}{\partial y} - Q_y = I_2 \frac{\partial^2 \phi_y}{\partial t^2} \tag{12.3.8c}$$

The boundary conditions for the CPT are given below.

$$\begin{aligned} \text{clamped:} \quad & w = 0, \quad \phi_n = 0 \\ \text{simply supported:} \quad & w = 0, \quad M_{nn} = 0 \\ \text{free:} \quad & Q_n = 0, \quad M_{nn} = 0 \end{aligned} \tag{12.3.9}$$

The three-step procedure can be used to develop the weak forms of (12.3.8*a*)–(12.3.8*c*), which will be equivalent to those listed in (12.3.7*a*)–(12.3.7*c*). To see the equivalence, the following identities must be used:

$$\begin{aligned} M_{nn} n_x - M_{ns} n_y &= M_{xx} n_x + M_{xy} n_y \equiv \hat{M}_{nn} \\ M_{nn} n_y + M_{ns} n_x &= M_{xy} n_x + M_{yy} n_y \equiv \hat{M}_{ns} \\ \phi_x = \phi_n n_x - \phi_s n_y, \quad & \phi_y = \phi_n n_y + \phi_s n_x \end{aligned} \tag{12.3.10}$$

The vector form of the virtual work statement (12.3.3) [after replacing the stress resultants Q_x, Q_y, M_{xx}, M_{xy}, and M_{yy} in terms of the generalized displacements (w, ϕ_x, ϕ_y)

using Eqs. (12.3.4) and (12.3.5)] is given by

$$0 = \int_{\Omega_e} \left[I_0(\delta \mathbf{w})^{\mathrm{T}} \ddot{\mathbf{w}} + I_2 \delta \Phi^{\mathrm{T}} \ddot{\Phi} + (\delta \Phi + \mathbf{D}_1 \delta \mathbf{w})^{\mathrm{T}} \mathbf{A} (\Phi + \mathbf{D}_1 \mathbf{w}) + (\mathbf{D} \delta \Phi)^{\mathrm{T}} \mathbf{C} (\mathbf{D} \Phi) - \mathbf{w}^{\mathrm{T}} q \right] d\mathbf{x} - \oint_{\Gamma_e} \left(\delta \Phi_n^{\mathrm{T}} \mathbf{M}_n + \mathbf{w}^{\mathrm{T}} Q_n \right) ds \tag{12.3.11}$$

where

$$\Phi = \begin{Bmatrix} \phi_x \\ \phi_y \end{Bmatrix}, \quad \Phi_n = \begin{Bmatrix} \phi_n \\ \phi_s \end{Bmatrix}, \quad \mathbf{M}_n = \begin{Bmatrix} M_n \\ M_s \end{Bmatrix}, \quad \mathbf{D}_1 = \begin{Bmatrix} \dfrac{\partial}{\partial x} \\ \dfrac{\partial}{\partial y} \end{Bmatrix} \tag{12.3.12a}$$

$$\mathbf{D} = \begin{bmatrix} \dfrac{\partial}{\partial x} & 0 \\ 0 & \dfrac{\partial}{\partial y} \\ \dfrac{\partial}{\partial y} & \dfrac{\partial}{\partial x} \end{bmatrix}, \quad \mathbf{A} = \begin{bmatrix} A_{55} & 0 \\ 0 & A_{44} \end{bmatrix}, \quad \mathbf{C} = \begin{bmatrix} D_{11} & D_{12} & 0 \\ D_{12} & D_{22} & 0 \\ 0 & 0 & D_{66} \end{bmatrix} \tag{12.3.12b}$$

12.3.3 Finite Element Model

We note from the boundary integrals in (12.3.7*a*)–(12.3.7*c*) that the primary variables of the theory are (w, ϕ_x, ϕ_y) and the secondary variables are (Q_n, M_{nn}, M_{ns}) (or a linear combination of Q_x, Q_y, M_{xx}, M_{yy}, and M_{xy}). Therefore, the Lagrange interpolation of w, ϕ_x and ϕ_y is admissible for SDT.

We assume finite element interpolation of w, ϕ_x, and ϕ_y in the form

$$\begin{aligned} w(x, y, t) &= \sum_{j=1}^{n} w_j(t) \psi_j^1(x, y) \\ \phi_x(x, y, t) = \sum_{j=1}^{m} S_j^x(t) \psi_j^2(x, y), \quad \phi_y(x, y, t) &= \sum_{j=1}^{m} S_j^y(t) \psi_j^2(x, y) \end{aligned} \tag{12.3.13}$$

or

$$w(x, y, t) = (\Psi^1)^{\mathrm{T}} \mathbf{W}, \quad \Phi = \begin{Bmatrix} \phi_x \\ \phi_y \end{Bmatrix} = \Psi^2 \mathbf{S} \tag{12.3.14}$$

where

$$\begin{aligned} (\Psi^1)^{\mathrm{T}} &= \{ \psi_1^1 \ \psi_2^1 \ \cdots \ \psi_n^1 \}, \quad \Psi^2 = \begin{bmatrix} \psi_1^2 & 0 & \psi_2^2 & \cdots & \psi_n^2 & 0 \\ 0 & \psi_1^2 & 0 & \psi_2^2 & \cdots & \psi_n^2 \end{bmatrix} \\ \mathbf{S}^{\mathrm{T}} &= \{ S_1^x \ S_1^y \ S_2^x \ S_2^y \ \cdots \ S_m^x \ S_m^y \}, \quad \mathbf{W}^{\mathrm{T}} = \{ w_1 \ w_2 \ w_3 \ \cdots \ w_n \} \end{aligned} \tag{12.3.15}$$

and ψ_j^1 and ψ_j^2 are interpolation functions used for w and (ϕ_x, ϕ_y), respectively. In general, ψ_j^1 and ψ_j^2 are polynomials of different degree. However, in the present study, we take $\psi_j^1 = \psi_j^2 \equiv \psi_j$. This choice, as discussed for the Timoshenko beam element, requires the use of reduced integration for the evaluation of stiffness coefficients associated with the transverse shear strains.

Substituting (12.3.13) into (12.3.7*a*)–(12.3.7*c*), we obtain the finite element model in expanded form

$$\begin{bmatrix} [M^{11}] & [0] & [0] \\ & [M^{22}] & [0] \\ \text{symmetric} & & [M^{33}] \end{bmatrix} \begin{Bmatrix} \{\ddot{w}\} \\ \{\ddot{S}^x\} \\ \{\ddot{S}^y\} \end{Bmatrix} + \begin{bmatrix} [K^{11}] & [K^{12}] & [K^{13}] \\ & [K^{22}] & [K^{23}] \\ \text{symmetric} & & [K^{33}] \end{bmatrix} \begin{Bmatrix} \{w\} \\ \{S^x\} \\ \{S^y\} \end{Bmatrix} = \begin{Bmatrix} \{F^1\} \\ \{F^2\} \\ \{F^3\} \end{Bmatrix} \tag{12.3.16}$$

where

$$\begin{aligned}
M_{ij}^{11} &= I_0 M_{ij}, \quad M_{ij}^{22} = M_{ij}^{33} = I_2 M_{ij}, \quad M_{ij} = \int_{\Omega_e} \psi_i \psi_j \, dx \, dy \\
K_{ij}^{11} &= \int_{\Omega_e} \left(A_{55} \frac{\partial \psi_i}{\partial x} \frac{\partial \psi_j}{\partial x} + A_{44} \frac{\partial \psi_i}{\partial y} \frac{\partial \psi_j}{\partial y} \right) dx \, dy \\
K_{ij}^{12} &= \int_{\Omega_e} A_{55} \frac{\partial \psi_i}{\partial x} \psi_j \, dx \, dy \\
K_{ij}^{13} &= \int_{\Omega_e} A_{44} \frac{\partial \psi_i}{\partial y} \psi_j \, dx \, dy \\
K_{ij}^{22} &= \int_{\Omega_e} \left(D_{11} \frac{\partial \psi_i}{\partial x} \frac{\partial \psi_j}{\partial x} + D_{66} \frac{\partial \psi_i}{\partial y} \frac{\partial \psi_j}{\partial y} + A_{55} \psi_i \psi_j \right) dx \, dy \\
K_{ij}^{23} &= \int_{\Omega_e} \left(D_{12} \frac{\partial \psi_i}{\partial x} \frac{\partial \psi_j}{\partial y} + D_{66} \frac{\partial \psi_i}{\partial y} \frac{\partial \psi_j}{\partial x} \right) dx \, dy \\
K_{ij}^{33} &= \int_{\Omega_e} \left(D_{66} \frac{\partial \psi_i}{\partial x} \frac{\partial \psi_j}{\partial x} + D_{22} \frac{\partial \psi_i}{\partial y} \frac{\partial \psi_j}{\partial y} + A_{44} \psi_i \psi_j \right) dx \, dy \\
F_i^1 &= \int_{\Omega_e} q \psi_i \, dx \, dy + \oint_{\Gamma_e} Q_n \psi_i \, ds \\
F_i^2 &= \oint_{\Gamma_e} \hat{M}_{nn} \psi_i \, ds, \quad F_i^3 = \oint_{\Gamma_e} \hat{M}_{ns} \psi_i \, ds
\end{aligned} \tag{12.3.17}$$

The vector of the finite element model is obtained by substituting (12.3.14) into (12.3.11):

$$\begin{bmatrix} \mathbf{M}^{11} & \mathbf{0} \\ \mathbf{0} & \mathbf{M}^{22} \end{bmatrix} \begin{Bmatrix} \ddot{\mathbf{W}} \\ \ddot{\mathbf{S}} \end{Bmatrix} + \begin{bmatrix} \mathbf{K}^{11} & \mathbf{K}^{12} \\ \mathbf{K}^{21} & \mathbf{K}^{22} \end{bmatrix} \begin{Bmatrix} \mathbf{W} \\ \mathbf{S} \end{Bmatrix} = \begin{Bmatrix} \mathbf{F}^1 \\ \mathbf{F}^2 \end{Bmatrix} \tag{12.3.18}$$

where [see Eqs. (12.3.12*a*) and (12.3.12*b*) for the definitions of $\mathbf{D}$, $\mathbf{D}_1$, etc.]

$$\begin{aligned}
\mathbf{M}^{11} &= \int_{\Omega_e} I_0 \Psi^1 (\Psi^1)^{\mathrm{T}} \, d\mathbf{x}, \quad \mathbf{M}^{22} = \int_{\Omega_e} I_2 (\Psi^2)^{\mathrm{T}} (\Psi^2) \, d\mathbf{x} \\
\mathbf{K}^{11} &= \int_{\Omega_e} \mathbf{B}_1^{\mathrm{T}} \mathbf{A} \mathbf{B}_1 \, d\mathbf{x}, \qquad \mathbf{K}^{12} = \int_{\Omega_e} \mathbf{B}_1^{\mathrm{T}} \mathbf{A} \Psi^2 \, d\mathbf{x} = (\mathbf{K}^{21})^{\mathrm{T}} \\
\mathbf{K}^{22} &= \int_{\Omega_e} [(\Psi^2)^{\mathrm{T}} \mathbf{A} \Psi^2 + \mathbf{B}^{\mathrm{T}} \mathbf{C} \mathbf{B}] d\mathbf{x}
\end{aligned} \tag{12.3.19}$$

$$\mathbf{F}^1 = \int_{\Omega_e} \Psi^1 q \, d\mathbf{x} + \oint_{\Gamma_e} \Psi^1 Q_n \, ds, \qquad \mathbf{F}^2 = \oint_{\Gamma_e} (\Psi^2)^{\mathrm{T}} \mathbf{M}_{nn} \, ds$$

$$\mathbf{B}_1 = \mathbf{D}_1 (\Psi^1)^{\mathrm{T}} = \begin{bmatrix} \psi^1_{1,x} & \psi^1_{2,x} & \cdots & \psi^1_{n,x} \\ \psi^1_{1,y} & \psi^1_{2,y} & \cdots & \psi^1_{n,y} \end{bmatrix}_{(2\times n)}$$

$$\mathbf{B} = \mathbf{D}\Psi^2 = \begin{bmatrix} \psi^2_{1,x} & 0 & \psi^2_{2,x} & 0 & \cdots & \psi^2_{m,x} & 0 \\ 0 & \psi^2_{1,y} & 0 & \psi^2_{2,y} & \cdots & 0 & \psi^2_{m,y} \\ \psi^2_{1,y} & \psi^2_{1,x} & \psi^2_{2,y} & \psi^2_{2,x} & \cdots & \psi^2_{m,y} & \psi^2_{m,x} \end{bmatrix}_{(3\times 2m)}$$

The element equations (12.3.16) and (12.3.18) both can be written in compact form as

$$\mathbf{M}\ddot{\boldsymbol{\Delta}} + \mathbf{K}\boldsymbol{\Delta} = \mathbf{F} \tag{12.3.20}$$

where $\boldsymbol{\Delta} = \{\mathbf{W}\ \mathbf{S}\}^{\mathrm{T}}$. The element stiffness matrix $\mathbf{K}$ and mass matrix $\mathbf{M}$ in (12.3.20) are of order $(n + 2m) \times (n + 2m)$, where n is the number of nodes per the Lagrange element used for w and m is the number of nodes per the Lagrange element used for ϕ_x and ϕ_y. The individual matrices in (12.3.18) have the following dimensions: $\mathbf{M}^{11}$ is $n \times n$; $\mathbf{M}^{22}$ is $2m \times 2m$; $\mathbf{K}^{11}$ is $n \times n$; $\mathbf{K}^{12}$ is $n \times 2m$; $\mathbf{K}^{22}$ is $2m \times 2m$; $\mathbf{F}^1$ is $n \times 1$; and $\mathbf{F}^2$ is $2m \times 1$. When equal interpolation is used, $\psi^1_i = \psi^2_i$, the four-node quadrilateral element has a total of 12 degrees of freedom and the nine-node quadrilateral element has 27 degrees of freedom (see Fig. 12.3.2).

12.3.4 Shear Locking and Reduced Integration

The transverse shear strains (i.e., terms involving A_{44} and A_{55}) in the element equations of SDT present computational difficulties when the side-to-thickness ratio, a/h, of the plate

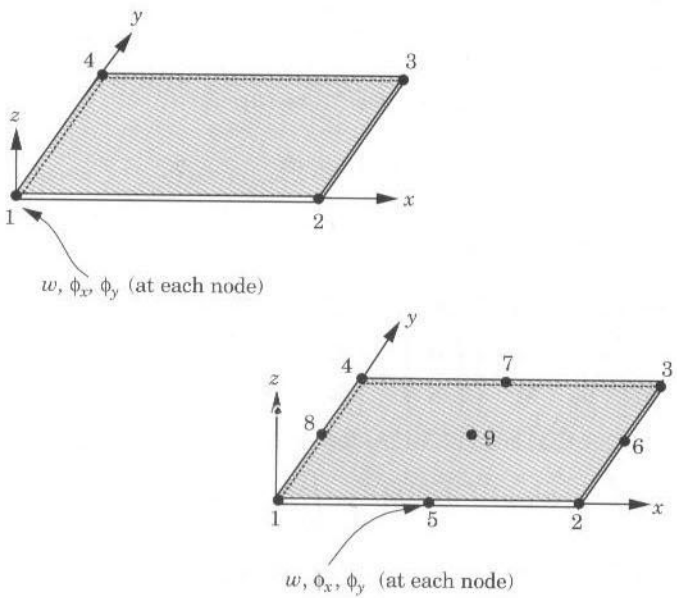

Figure 12.3.2 Linear and quadratic rectangular elements for SDT with three degrees of freedom (w, ϕ_x, ϕ_y) per node.

is large (i.e., when the plate becomes thin, say $a/h \geq 50$). For thin plates, the transverse shear strains $2\varepsilon_{xz} = \gamma_{xz} = \phi_x + \partial w/\partial x$ and $2\varepsilon_{yz} = \gamma_{yz} = \phi_y + \partial w/\partial y$ are negligible, and consequently the element stiffness matrix becomes stiff and yields erroneous results for the generalized displacements (w_i, S_i^x, S_i^y). This phenomenon is known as *shear locking*, and it can be interpreted as being caused by the inclusion of the following constraints into the variational form [see Reddy (1980) and Averill and Reddy (1990)]:

$$\phi_x + \frac{\partial w}{\partial x} = 0, \quad \phi_y + \frac{\partial w}{\partial y} = 0 \tag{12.3.21}$$

The energy due to transverse shear strains in the total potential energy of SDT is given by

$$\frac{1}{2}\int_{\Omega_e} \left[A_{44}\left(\phi_y + \frac{\partial w}{\partial y}\right)^2 + A_{55}\left(\phi_x + \frac{\partial w}{\partial x}\right)^2 \right] dx\, dy \tag{12.3.22}$$

The locking observed in the displacement finite element model of SDT is the result of the fact that the discrete form of (12.3.21) is not satisfied when the plate is very thin. Of course, when the plate is thick, the relations (12.3.21) do not have to be satisfied, and the locking does not occur (at least, it is not severe enough to give completely wrong results). However, for thin plates, the constraints (12.3.21) are valid but not satisfied in the numerical model, and we therefore face the same problem as in the Timoshenko beam finite element. Therefore, we use the same remedy as before: reduced integration to evaluate stiffness coefficients involving the transverse shear terms [see Zienkiewicz, et al. (1971) and Hughes, et al. (1977)]. For example, when a four-node rectangular element is used, the one-point Gauss rule should be used to evaluate the shear energy terms (i.e., terms involving A_{44} and A_{55}) while the two-point Gauss rule should be used for all other terms. When an eight- or nine-node rectangular element is used, the two- and three-point Gauss rules should be used to evaluate the shear and bending terms, respectively. For the triangular elements, we use one- and three-point integrations for transverse shear stiffnesses in the linear and quadratic elements, respectively. However, in the present study, we shall not consider triangular plate bending elements.

12.4 EIGENVALUE AND TIME-DEPENDENT PROBLEMS

The differential equations in (12.2.20) and (12.3.20) can be reduced to various special cases depending on the type of analysis. In both cases, the finite element equations have the same vector form, namely (12.3.20), facilitating the discussion of the eigenvalue and transient analysis for both CPT and SDT.

Static Analysis

For static analysis, we set the inertia term $\{\ddot{\Delta}\}$ equal to zero and solve the problem

$$\mathbf{K}^e \boldsymbol{\Delta}^e = \mathbf{F}^e \tag{12.4.1}$$

Natural Vibration

For natural vibration problems, we replace the inertia term by

$$\ddot{\boldsymbol{\Delta}}^e = -\omega^2 \boldsymbol{\Delta}_0^e \quad (\text{or } \boldsymbol{\Delta}^e = \boldsymbol{\Delta}_0^e e^{-i\omega t}) \tag{12.4.2}$$

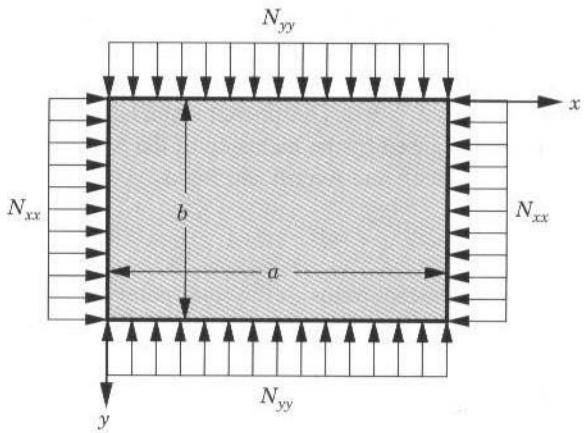

Figure 12.4.1 Biaxial compression of a rectangular plate.

Then Eq. (12.3.20) takes the form of an eigenvalue problem:

$$(\mathbf{K}^e - \omega^2 \mathbf{M}^e)\Delta_0^e = \mathbf{0} \tag{12.4.3}$$

Buckling Analysis

For buckling analysis (i.e., to determine the value of the in-plane compressive forces at which the plate buckles; also see Fig. 12.4.1), we replace the mass matrix in (12.4.3) with the stability matrix $\mathbf{G}$ and ω^2 with the buckling load λ. This expression comes from the in-plane force due to the nonlinear inplane strains (underlined);

$$\varepsilon_{xx} = \underline{\frac{1}{2}\left(\frac{\partial w}{\partial x}\right)^2} - z\frac{\partial^2 w}{\partial x^2}, \quad \varepsilon_{yy} = \underline{\frac{1}{2}\left(\frac{\partial w}{\partial y}\right)^2} - z\frac{\partial^2 w}{\partial y^2}$$
$$2\varepsilon_{xy} = \underline{\frac{\partial w}{\partial x}\frac{\partial w}{\partial y}} - 2z\frac{\partial^2 w}{\partial x \partial y} \tag{12.4.4}$$

For CPT, $\mathbf{G}$ is given by

$$G_{ij} = \int_{\Omega_e} \left[\bar{N}_{xx}\frac{\partial \varphi_i}{\partial x}\frac{\partial \varphi_j}{\partial x} + \bar{N}_{yy}\frac{\partial \varphi_i}{\partial y}\frac{\partial \varphi_j}{\partial y} + \bar{N}_{xy}\left(\frac{\partial \varphi_i}{\partial x}\frac{\partial \varphi_j}{\partial y} + \frac{\partial \varphi_i}{\partial y}\frac{\partial \varphi_j}{\partial x}\right)\right] dx\, dy \tag{12.4.5}$$

where $\bar{N}_{xx}$, $\bar{N}_{yy}$, and $\bar{N}_{xy}$ are the applied in-plane force resultants. The eigenvalue λ represents the ratio of the actual buckling load to the applied in-plane forces:

$$\lambda = \frac{N_{xx}}{\bar{N}_{xx}} = \frac{N_{yy}}{\bar{N}_{yy}} = \frac{N_{xy}}{\bar{N}_{xy}} \tag{12.4.6}$$

For SDT, only $\mathbf{M}^{11}$ [see Eq. (12.3.18)] is replaced by $\mathbf{G}$, where

$$G_{ij} = \int_{\Omega_e} \left[\bar{N}_{xx}\frac{\partial \psi_i}{\partial x}\frac{\partial \psi_j}{\partial x} + \bar{N}_{yy}\frac{\partial \psi_i}{\partial y}\frac{\partial \psi_j}{\partial y} + \bar{N}_{xy}\left(\frac{\partial \psi_i}{\partial x}\frac{\partial \psi_j}{\partial y} + \frac{\partial \psi_i}{\partial y}\frac{\partial \psi_j}{\partial x}\right)\right] dx\, dy \tag{12.4.7}$$

and $\mathbf{M}^{22}$ is set equal to zero. Hence, the stability matrix is non-positive-definite, requiring special eigenvalue solvers for SDT.

Transient Analysis

To solve a time-dependent problem, we must approximate the time derivatives in (12.2.20) or (12.3.20) to obtain algebraic equations relating solution Δ_{s+1} at time $t + \Delta t$ to solution Δ_s at time t, where Δt is the time step. In the Newmark integration scheme (see Section 6.2.4), the vectors Δ_{s+1} and $\dot{\Delta}_{s+1}$ at time $t = (s+1)\Delta t$ are approximated by the expressions

$$\begin{aligned} \dot{\boldsymbol{\Delta}}_{s+1} &= \dot{\boldsymbol{\Delta}}_s + a_1 \ddot{\boldsymbol{\Delta}}_s + a_2 \ddot{\boldsymbol{\Delta}}_{s+1} \\ \boldsymbol{\Delta}_{s+1} &= \boldsymbol{\Delta}_s + \dot{\boldsymbol{\Delta}}_s \Delta t + \frac{1}{2}\left[(1-\gamma)\ddot{\boldsymbol{\Delta}}_s + \gamma \ddot{\boldsymbol{\Delta}}_{s+1}\right](\Delta t)^2 \end{aligned} \tag{12.4.8}$$

where $a_1 = (1-\alpha)\Delta t$ and $a_2 = \alpha \Delta t$, (α and γ are parameters that control the accuracy and stability of the scheme), and the subscript s indicates that the vectors are evaluated at the sth time step (i.e., at time $t = s\Delta t$).

Rearranging (12.3.20) and (12.4.8), we obtain

$$\hat{\mathbf{K}}_{s+1} \boldsymbol{\Delta}_{s+1} = \hat{\mathbf{F}}_{s,s+1} \tag{12.4.9a}$$

where

$$\begin{aligned} \hat{\mathbf{K}}_{s+1} &= \mathbf{K}_{s+1} + a_3 \mathbf{M}_{s+1} \\ \hat{\mathbf{F}}_{s,s+1} &= \mathbf{F}_{s+1} + \mathbf{M}_{s+1}(a_3 \boldsymbol{\Delta}_s + a_4 \dot{\boldsymbol{\Delta}}_s + a_5 \ddot{\boldsymbol{\Delta}}_s) \\ a_3 &= \frac{2}{\gamma(\Delta t)^2}, \quad a_4 = a_3 \Delta t, \quad a_5 = \frac{1}{\gamma} - 1 \end{aligned} \tag{12.4.9b}$$

Once the solution $\boldsymbol{\Delta}_{s+1}$ at time $t_{s+1} = (s+1)\Delta t$ is known, the velocity and acceleration at t_{s+1} are computed from

$$\begin{aligned} \ddot{\boldsymbol{\Delta}}_{s+1} &= a_3(\boldsymbol{\Delta}_{s+1} - \boldsymbol{\Delta}_s) - a_4 \dot{\boldsymbol{\Delta}}_s - a_5 \ddot{\boldsymbol{\Delta}}_s, \\ \dot{\boldsymbol{\Delta}}_{s+1} &= \dot{\boldsymbol{\Delta}}_s + a_1 \ddot{\boldsymbol{\Delta}}_s + a_2 \ddot{\boldsymbol{\Delta}}_{s+1} \end{aligned} \tag{12.4.10}$$

12.5 EXAMPLES

Here we consider several numerical examples of rectangular plates with different boundary conditions. We will use the conforming CPT(C) and nonconforming CPT(N) rectangular elements and the linear and quadratic SDT elements to present numerical results. Various types of boundary conditions on an edge of a plate element are given in Eqs. (12.2.12) and (12.3.9) for CPT and SDT, respectively. When the edge is parallel to the x (or y) axis, the normal and tangential components of a variable become the y and x (or x and y) components, respectively, of the variable. For CPT, ϕ_n and ϕ_s of SDT must be replaced with $-\partial w/\partial n$ and $-\partial w/\partial s$, respectively. In all cases, the stresses are computed at the reduced Gauss points.

The first example deals with the bending of a simply supported plate using CPT and SDT. The effect of reduced integration on the deflections and stresses of a simply supported plate as computed using the SDT plate element is investigated.

Example 12.5.1

Consider a simply supported, isotropic ($\nu = 0.25$), square plate subjected to a uniformly distributed transverse load of intensity q_0. We shall solve the problem using CPT and SDT plate bending elements. Owing to the biaxial symmetry, we need to model only a quadrant of the plate. The essential (i.e., geometric) boundary conditions at simply supported edges ($x = \frac{1}{2}a$ and $y = \frac{1}{2}a$), for SDT, are (see Fig. 12.5.1)

$$\begin{aligned} w = 0, \quad \phi_y = 0 \quad \text{at} \quad x = a/2 \\ w = 0, \quad \phi_x = 0 \quad \text{at} \quad y = a/2 \end{aligned} \tag{12.5.1}$$

The essential boundary conditions along the symmetry lines ($x = 0$ and $y = 0$) are

$$\phi_x(0, y) = \phi_y(x, 0) = 0 \tag{12.5.2}$$

The natural (i.e., force) boundary conditions, which enter the finite element equations through the forces $\{F\}$, are

$$\begin{aligned} Q_n = 0 \quad &\text{along} \quad x = 0 \quad \text{and} \quad y = 0 \\ M_{xx} = 0 \quad &\text{along} \quad y = 0 \quad \text{and} \quad x = a/2 \\ M_{yy} = 0 \quad &\text{along} \quad x = 0 \quad \text{and} \quad y = a/2 \end{aligned} \tag{12.5.3}$$

The essential boundary conditions for a quadrant, when using the CPT element, are shown in Fig. 12.5.1.

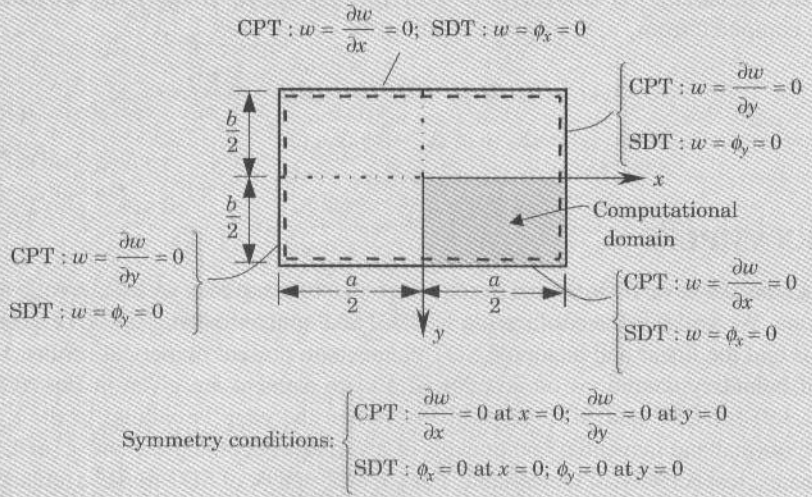

Figure 12.5.1 Geometry and coordinate system used for a rectangular plate. Boundary and symmetry conditions in CPT and SDT for simply supported plates.

For a linear (four-node) rectangular element of SDT, the contribution of a uniformly distributed load q_0 is given by

$$f_i = \int_0^{h_x} \int_0^{h_y} q_0 \psi_i \, dx \, dy = \frac{1}{4} h_x h_y q_0 \tag{12.5.4}$$

where h_x and h_y are the plane-form dimensions of the element. This contribution goes to the first, fourth, seventh, and tenth nodal degrees of freedom of the element (corresponding to w). For CPT, the nodal forces due to the uniform transverse load of intensity q_0 are computed using the definition

$$f_i = \int_{\Omega_e} q_0 \varphi_i \, dx \, dy \tag{12.5.5}$$

The effect of reduced integration, thickness, and mesh on the center deflection and normal stress σ_{xx} is investigated, and the results are presented in Table 12.5.1. The displacement and stress are nondimensionalized as

$$\bar{w} = \frac{w(0,0) E h^3 \times 10^2}{q_0 a^4}, \quad \bar{\sigma}_{xx} = \left(\frac{h}{a}\right)^2 \frac{1}{q_0} \sigma_{xx} \left(A, A, \pm \frac{1}{2} h\right) \tag{12.5.6}$$

where A is the Gauss-point location with respect to the (x, y) system located at the center of the plate (see Fig. 12.5.1), Q4 denotes the four-node rectangular element, and Q9

Table 12.5.1 The effect of reduced integration, thickness, and mesh refinement on the center deflections and stresses† of a simply supported, isotropic ($\nu = 0.25$), square plate under a uniform transverse load of intensity q_0 (Example 12.5.1).

		1×1 Linear		2×2 Linear		4×4 Linear		2×2 Quadratic		Exact‡	
a/h	Integ.	$\bar{w}$	$\bar{\sigma}_x$	$\bar{w}$	$\bar{\sigma}_x$	$\bar{w}$	$\bar{\sigma}_x$	$\bar{w}$	$\bar{\sigma}_x$	$\bar{w}$	$\bar{\sigma}_x$
10	F	0.964	0.018	2.474	0.119	3.883	0.216	4.770	0.290	4.791	0.276
	M	3.950	0.095	4.712	0.235	4.773	0.266	4.799	0.272		
20	F	0.270	0.005	0.957	0.048	2.363	0.138	4.570	0.268	4.625	0.276
	M	3.669	0.095	4.524	0.235	4.603	0.266	4.633	0.272		
40	F	0.070	0.001	0.279	0.014	0.944	0.056	4.505	0.270	4.584	0.276
	M	3.599	0.095	4.375	0.235	4.560	0.266	4.592	0.271		
50	F	0.005	0.000	0.182	0.009	0.652	0.039	4.496	0.267	4.579	0.276
	M	3.590	0.095	4.472	0.235	4.555	0.266	4.587	0.271		
100	F	0.011	0.000	0.047	0.002	0.182	0.011	4.482	0.266	4.572	0.276
	M	3.579	0.095	4.465	0.235	4.548	0.266	4.580	0.272		
CPT(N)		5.643	0.260	4.857	0.274	4.643	0.276	—	—	4.570	0.276
CPT(C)		4.638	0.262	4.574	0.272	4.570	0.275	—	—	4.570	0.276

†$\bar{w} = w E h^3 \times 10^2 / q_0 a^4, \bar{\sigma}_x = \sigma_x(A, A, \pm h) h^2 / q_0 a^2, A = \frac{1}{4} a$ (1×1 linear), $\frac{1}{8} a$ (2×2 linear), $\frac{1}{16} a$ (4×4 linear), $0.05283a$ (2×2 quadratic).

‡ From Reddy (2002).

the nine-node rectangular element. The Gauss point locations for various meshes are given below.

$2 \times 2Q4$	$4 \times 4Q4$	$2 \times 2Q9$
$0.125a$	$0.0625a$	$0.05283a$

In Table 12.5.1, F denotes full integration for all terms, and M denotes mixed integration: full integration for bending terms and reduced integration for the shear terms. The following observations can be made from the results of Table 12.5.1:

1. The nine-node element gives virtually the same results for full (3×3 Gauss rule) and mixed (3×3 and 2×2 Gauss rules for bending and shear terms, respectively) integrations. However, the results obtained using the mixed integration are closest to the exact solution.
2. Full integration gives less accurate results than mixed integration, and the error increases with an increase in side-to-thickness ratio (a/h). This implies that mixed integration is essential for thin plates, especially when modeled by lower-order elements.
3. Full integration results in smaller errors for quadratic elements and refined meshes than for linear elements and/or coarser meshes.
4. The conforming plate finite element CPT(C) gives more accurate results when compared with the nonconforming plate element CPT(N).

The next example deals with a clamped square plate under a distributed transverse load. The mixed integration rule is used in the evaluation of stiffness coefficients of the SDT model.

Example 12.5.2

Consider an isotropic ($\nu = 0.3$) square plate under a uniform load of intensity q_0. We shall consider clamped boundary conditions (see Fig. 12.5.2). Note that, for the case of the conforming displacement model based on CPT, we must also specify the boundary conditions on the cross-derivative $\partial^2 w/\partial x \partial y$. Once again, we exploit the biaxial symmetry and model only a quadrant of the plate.

The center deflection $\bar{w} = w(0, 0)D \times 10^2/q_0 a^4$ [where $D = Eh^3/12(1 - \nu^2)$] and center normal stress $\bar{\sigma}_x = \sigma_x(A, A) \times 10/q_0$ as obtained using uniform meshes of the two types of elements, CPT(N) and CPT(C), are presented in Table 12.5.2. In both models, the values of A used are given in the following table.

Element type		Location A			
Mesh for CPT & SDT(L)		1×1	2×2	4×4	8×8
Mesh for SDT(Q)			1×1	2×2	4×4
CPT model		$0.05635a$	$0.02817a$	$0.01409a$	$0.03125a$
SDT model	linear	$0.25a$	$0.125a$	$0.0625a$	$0.03125a$
	quadratic	—	$0.1057a$	$0.0528a$	$0.02642a$

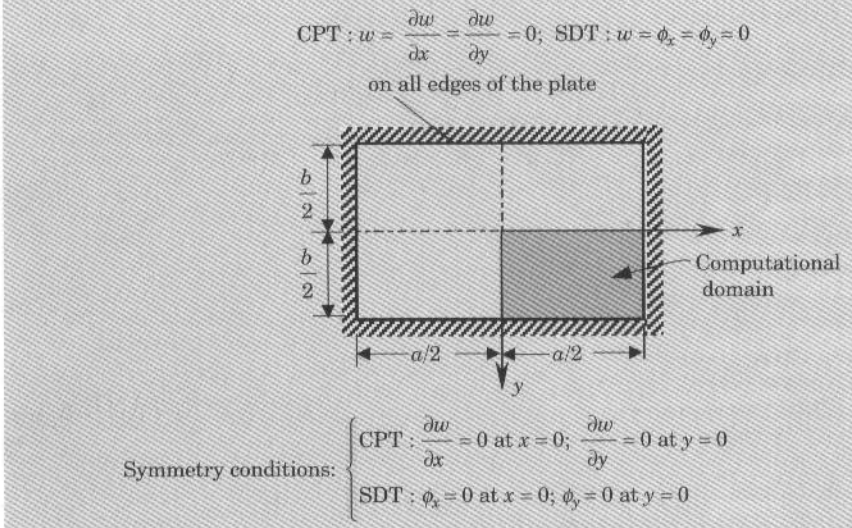

Figure 12.5.2 Boundary and symmetry conditions in CPT and SDT for clamped rectangular plates.

The distance is measured from the center of the plate. The mesh SDT(L) refers to four-node linear elements and SDT(Q) refers to the nine-node quadratic elements used in the SDT model. Clearly, both finite element models exhibit good convergence characteristics. The difference between the CPT and SDT is attributed to the inclusion of transverse shear strains in SDT.

Table 12.5.2 Comparison of the center deflection and normal stress of a clamped square plate under a uniformly distributed load as obtained using various finite element meshes.

Mesh	Displacement model (CPT)	Displacement model (SDT; $a/h = 10$)	
		Linear	Quadratic
	Center deflection $\bar{w}$		
1×1	0.1943	0.0357	—
2×2	0.1265	0.1459	0.1757
4×4	0.1266	0.1495	0.1586
Analytical	0.1266		
	Center stress $\bar{\sigma}_{xx}$		
1×1	2.443	0.000	—
2×2	1.415	1.142	1.321
4×4	1.381	1.333	1.345

The next example deals with a simply supported orthotropic plate under a uniformly distributed transverse load.

Example 12.5.3

Here we consider an orthotropic square plate with the following material (graphite-epoxy) properties ($\nu_{21} = \nu_{12}E_2/E_1$; Mpsi $= 10^6$ psi):

$$E_1 = 31.8 \text{ Mpsi}, \quad E_2 = 1.02 \text{ Mpsi}, \quad \nu_{12} = 0.31, \quad G_{12} = G_{23} = G_{13} = 0.96 \text{ Mpsi} \tag{12.5.7}$$

The nondimensionalized center deflection $\bar{w}$ and normal stress $\bar{\sigma}_{xx}$ obtained using the conforming CPT(C) element and the SDT element are compared in Table 12.5.3.

Table 12.5.3 Comparison of the center deflection [$\bar{w} = w \times 10^3(H/q_0a^4)$] and normal stress [$\bar{\sigma}_{xx} = \sigma_{xx} \times 10(h^2/q_0a^2)$] of a graphite-epoxy, simply supported square plate under a uniform transverse load (Example 12.5.3).

Mesh	Displacement model (CPT)	Displacement model (SDT; $a/h = 10$) Linear	Quadratic
	Center deflection $\bar{w}$		
2×2	0.9220	1.2545	1.2715
4×4	0.9224	1.2186	1.2147
8×8	0.9224	1.2152	1.2147
Exact[†]	0.9225	1.215	
	Center stress $\bar{\sigma}_{xx}$		
2×2	7.678	6.277	7.192
4×4	7.616	7.256	7.399
8×8	7.600	7.449	7.478
Exact[†]	7.595	7.512	

[†]From Reddy (2002); $H = D_{12} + 2D_{66}$.

The next example deals with natural vibration of the plate of Example 12.5.1.

Example 12.5.4

Consider the simply supported, isotropic, square plate of Example 12.5.1. We wish to determine the natural frequencies of the plate. Once again, a quadrant of the plate is used as the computational domain to obtain the first few symmetric natural frequencies. To obtain all the frequencies (i.e., symmetric as well as antisymmetric), we must use the full plate model. The geometric boundary conditions used are shown in Fig. 12.5.1.

The natural frequencies of the simply supported plate, obtained using various meshes of CPT and SDT elements, are presented in Table 12.5.4. It is clear that CPT overpredicts the natural frequencies for the side-to-thickness ratio of $a/h = 10$ (i.e., thick plate) when compared to SDT. The difference is attributed to the inclusion of transverse shear strains, γ_{xz} and γ_{yz}, in SDT. In other words, the normality assumption (or neglecting transverse shear strains) in CPT amounts to overestimating the stiffness of the plate.

Table 12.5.4 The first three symmetric vibrational frequencies $(\bar{\omega} \times 10^{-2})^1$ of an isotropic, simply supported square plate obtained using CPT and SDT $(a/h = 10)$.

Theory	Mesh	$\bar{\omega}_{11}$	$\bar{\omega}_{13}$	$\bar{\omega}_{33}$
	1×1 Q4	0.0746	—	—
	2×2 Q4	0.0608	0.4473	0.4810
	4×4 Q4	0.0579	0.2913	0.4654
SDT	1×1 Q9	0.0575	0.4030	0.5476
	3×2 Q9	0.0570	0.2651	0.4342
	Exact	0.0569	0.2552	0.4217
CPT(N)	1×1	0.0535	0.3118	0.3565
CPT(C)	1×1	0.0597	0.2912	0.3360
CPT(N)	2×2	0.0567	0.2762	0.4406
CPT(C)	2×2	0.0584	0.4842	0.4842
CPT(N)	4×4	0.0579	0.2792	0.4665
CPT(C)	4×4	0.0584	0.2821	0.4900
	Exact	0.0584	0.2829	0.4943

$^1\bar{\omega} = \omega(\rho/E)^{1/2}a^2/h$.

The final example deals with the transient response of an isotropic plate subjected to a sudden uniform patch loading at the center of the plate (an idealization of impact load).

Example 12.5.5

Consider an isotropic ($\nu = 0.3$, $\rho = 1.0$), simply supported, rectangular plate ($a/b = \sqrt{2}$, $h/b = 0.2$) under a suddenly applied, uniformly distributed load on a square ($c/b = 0.4$) area at the center (see Fig. 12.5.3):

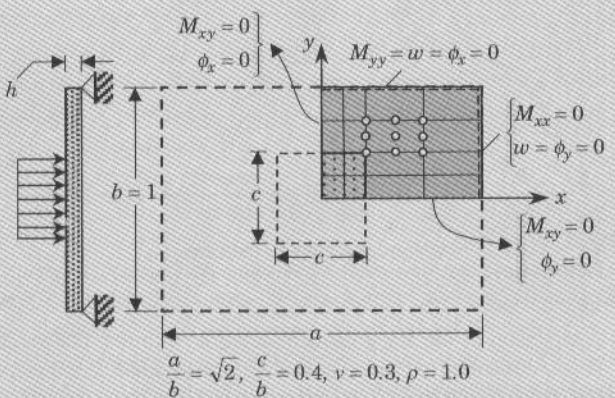

Figure 12.5.3 Domain, boundary conditions, and finite element mesh for the bending of a rectangular plate under a suddenly applied pulse loading at the central square area.

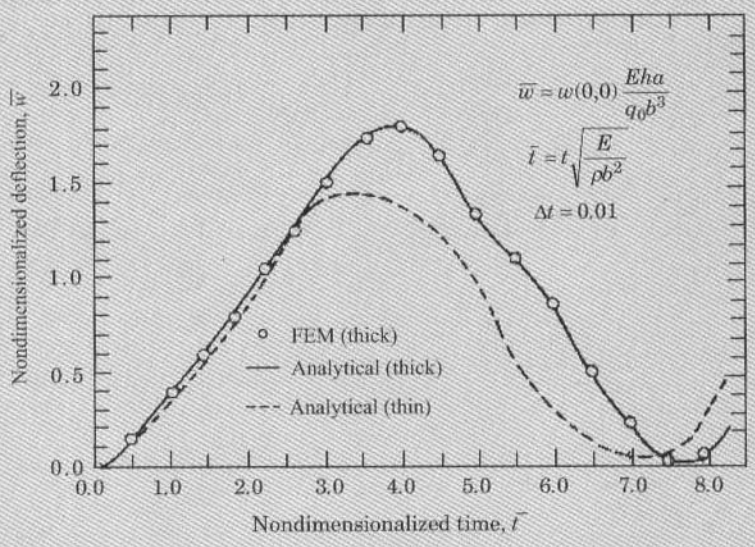

(*a*)

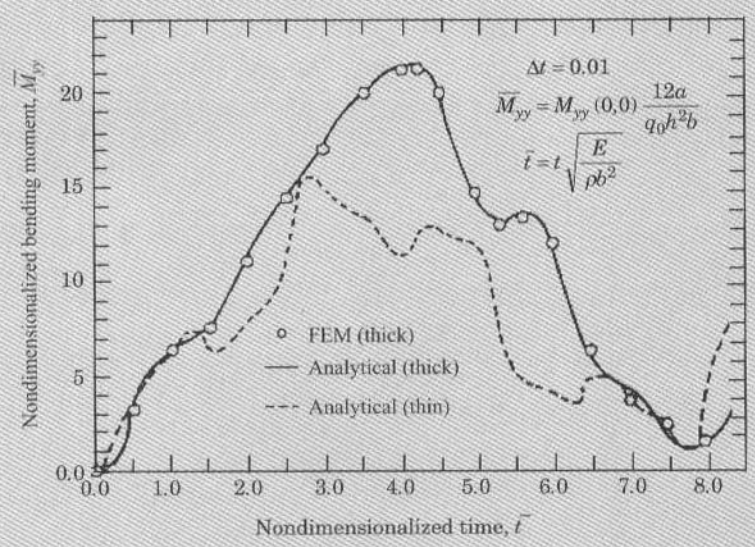

(*b*)

Figure 12.5.4 Comparison of the finite element solution with the analytical solution for a simply supported rectangular isotropic plate under a suddenly applied pulse loading at the central square area. (*a*) Deflection $\bar{w}$ versus time t. (*b*) Center bending moment $\bar{M}_{yy}$ versus time t.

$$a/b=\sqrt{2}, \quad \Delta t = 0.01$$

$$q(x, y, t)=q_0(x, y)H(t) \quad \text{where} \quad q_0(x, y) = \begin{cases} 1 & \text{for} \quad 0 < x, y \leq 0.2 \\ 0 & \text{for} \quad x, y > 0.2 \end{cases} \tag{12.5.8}$$

and $H(t)$ is the Heaviside unit step function. The geometry and boundary conditions are shown in Fig. 12.5.3. A nonuniform mesh of 4×4 nine-node shear deformation elements is used in a quadrant of the plate.

The center deflection and bending moments of the present linear analysis are compared with the analytical thick- and thin-plate solutions of Reismann and Lee (1969) in Fig. 12.5.4. We note significant difference between the solutions of the two theories. The present finite element solutions for the center deflection and bending moment are in excellent agreement with the thick-plate solution of Reismann and Lee (1969). Since the bending moment in the finite element method is calculated at the Gauss points, it is not expected to match exactly with the analytical solution at the center of the plate.

12.6 SUMMARY

Finite element models of the CPT and SDT have been developed in this chapter. C^1 continuity of the transverse deflection w (i.e., the deflection and its derivatives are continuous between elements) is required in CPT, whereas C^0 continuity (i.e., only the variables are continuous between elements) of the generalized displacements (w, ϕ_x, ϕ_y) is required in SDT. Triangular and rectangular elements with C^1 continuity have been discussed. Two four-node rectangular elements, one with $(w, \partial w/\partial x, \partial w/\partial y)$ and another with $(w, \partial w/\partial x, \partial w/\partial y, \partial^2 w/\partial x \partial y)$ as degrees of freedom, have been presented for CPT. The first one is a nonconforming element that does not satisfy continuity of the normal derivative along element sides, and the second is a conforming element. Linear and quadratic rectangular elements of SDT have been developed. They require selective evaluation of the stiffness coefficients. The bending stiffness coefficients are evaluated using full integration, and the transverse shear stiffness coefficients are evaluated using reduced integration to avoid the shear locking that occurs when these elements are used to model thin plates. Finite element equations of vibration, stability, and static and dynamic responses have been developed and numerical results are presented.

PROBLEMS

12.1 Investigate the displacement and slope compatibility of the nonconforming rectangular element CPT(N). *Hint:* Use the edge connecting nodes 1 and 2 and check if the displacement w and slopes $\partial w/\partial x$ and $\partial w/\partial y$ are continuous.

12.2–12.10 For the plate bending problems (CPT and SDT) given in Figs. P12.2–P12.10, give the specified primary and secondary degrees of freedom and their values for the meshes shown. The dashed lines in the figures indicate simply supported boundary conditions. You are required to give values of the loads for at least a couple of representative loads.

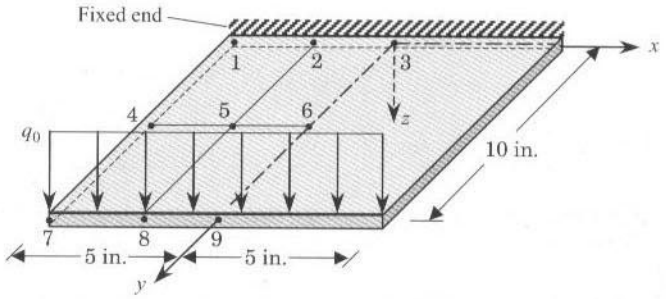

Figure P12.2

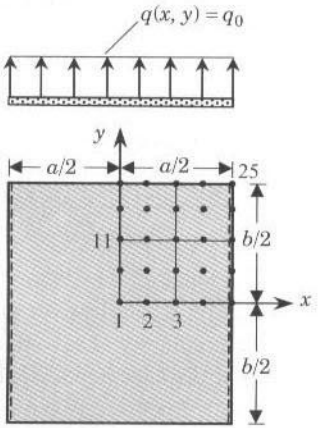

Simply supported at $x = \pm a/2$
and under uniform load
Use 2×2 mesh for CPT(C)

Figure P12.3

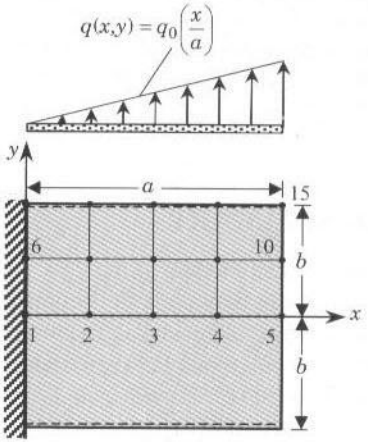

Simply supported at $y = \pm b/2$
and under linearly varying load

Figure P12.4

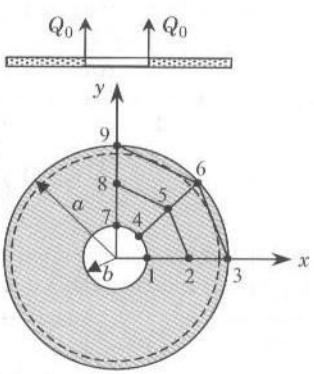

Simply supported at $r = a$
and under line load at $r = b$

Figure P12.5

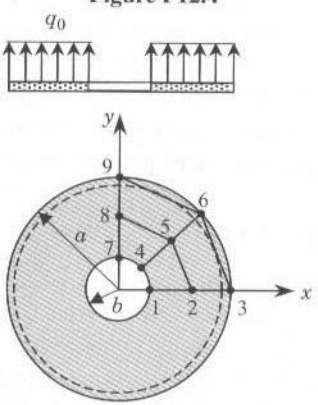

Simply supported at $r = a$
and under uniform load

Figure P12.6

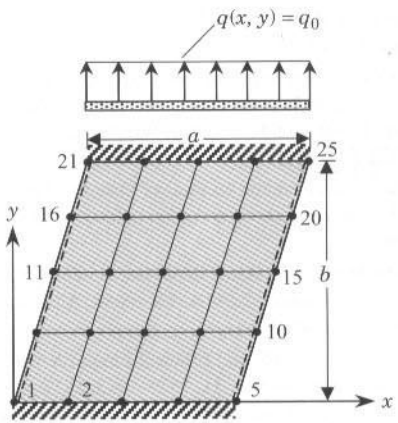

Simply supported along the slant edge and under uniform load

Figure P12.7

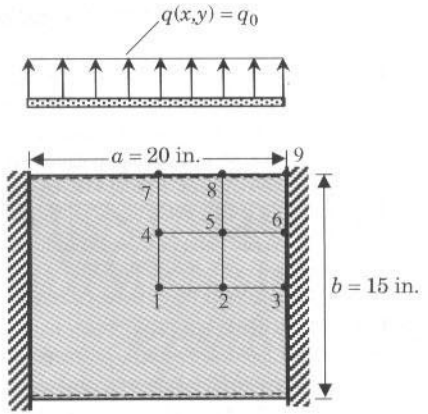

$E_1 = 30 \times 10^6$ psi, $E_2 = 0.75 \times 10^6$ psi
$\nu_{12} = 0.25$, $G_{12} = 0.375 \times 10^6$ psi
$h = 2$ in., $q_0 = 100$ lb/in.

Figure P12.8

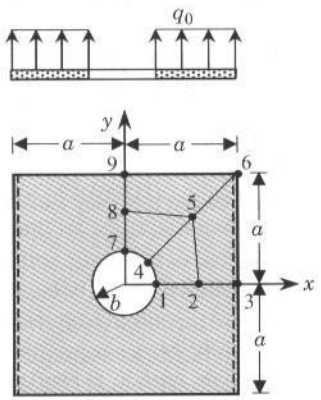

Simply supported at $y = \pm a/2$ and under uniform load

Figure P12.9

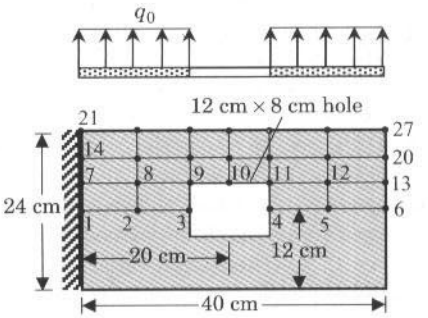

Under uniform load
$E = 200$ GPa, $\nu = 0.3$
$h = 1$ cm, $q_0 = 60$ kN/m^2

Figure P12.10

REFERENCES FOR ADDITIONAL READING

1. Averill, R. C. and Reddy, J. N., "On the Behavior of Plate Elements Based on the First-Order Shear Deformation Theory," *Engineering Computations*, **7**(1), 57–74, 1990.
2. Bathe, K. J. and Dvorkin, E. N., "A Four-Node Plate Bending Element Based on Mindlin/Reissner Plate Theory and a Mixed Interpolation," *International Journal for Numerical Methods in Engineering*, **21**, 367–383, 1985.
3. Bazeley, G. P., Cheung, Y. K., Irons, B. M., and Zienkiewicz, O. C., "Triangular Elements in Plate Bending—Conforming and Non-Conforming Solutions," *Proceedings of the First Conference on Matrix Methods in*

Structural Mechanics, AFFDL-TR-66-80, Air Force Institute of Technology, Wright–Patterson Air Force Base, Ohio, 547–576, 1965.

4. Belytschko, T., Tsay, C. S., and Liu, W. K., "Stabilization Matrix for the Bilinear Mindlin Plate Element," *Computer Methods in Applied Mechanics and Engineering,* **29**, 313–327, 1981.
5. Bogner, F. K., Fox, R. L., and Schmidt, Jr. L. A., "The Generation of Inter-Element-Compatible Stiffness and Mass Matrices by the Use of Interpolation Formulas," *Proceedings of the First Conference on Matrix Methods in Structural Mechanics,* AFFDL-TR-66-80, Air Force Institute of Technology, Wright–Patterson Air Force Base, Ohio, 397–443, 1965.
6. Clough, R. W. and Felippa, C. A.,"A Refined Quadrilateral Element for Analysis of Plate Bending," *Proceedings of the Second Conference on Matrix Methods in Structural Mechanics,* Air Force Institute of Technology, Wright–Patterson Air Force Base, Ohio, 399–440, 1968.
7. Clough, R. W. and Tocher, J. L., "Finite Element Stiffness Matrices for Analysis of Plate Bending," *Proceedings of the First Conference on Matrix Methods in Structural Mechanics,* AFFDL-TR-66-80, Air Force Institute of Technology, Wright–Patterson Air Force Base, Ohio, 515–545, 1965.
8. Hughes, T. J. R., Taylor, R. L., and Kanoknukulchai, W., "A Simple and Efficient Finite Element for Plate Bending," *International Journal for Numerical Methods in Engineering,* **11**, 1529–1543, 1977.
9. Hughes, T. J. R., Cohen, M., and Haroun, M., "Reduced and Selective Integration Techniques in the Finite Element Analysis of Plates," *Nuclear Engineering and Design,* **46**, 203–222, 1978.
10. Melosh, R. J., "Basis of Derivation of Matrices for the Direct Stiffness Method," *AIAA Journal,* **1**, 1631–1637, 1963.
11. Reddy, J. N., "A Penalty Plate-Bending Element for the Analysis of Laminated Anisotropic Composite Plates," *International Journal for Numerical Methods in Engineering,* **15**(8), 1187–1206, 1980.
12. Reddy, J. N., "On the Solutions to Forced Motions of Rectangular Composite Plates," *Journal of Applied Mechanics*, **49**, 403–408, 1982.
13. Reddy, J. N., *Theory and Analysis of Elastic Plates*, Taylor and Francis, Philadelphia, PA, 1999.
14. Reddy, J. N., *Energy Principles and Variational Methods in Applied Mechanics*, 2nd ed., John Wiley, New York, 2002.
15. Reddy, J. N., *Mechanics of Laminates Composite Plates and Shells: Theory and Analysis*, CRC Press, 2nd ed., Boca Raton, FL, 2004*a*.
16. Reddy, J. N., *An Introduction to Nonlinear Finite Element Analysis*, Oxford University Press, Oxford, UK, 2004*b*.
17. Reismann, H. and Lee, Y., "Forced Motions of Rectangular Plates," in *Developments in Theoretical and Applied Mechanics*, Vol. 4, Frederick, D. (ed.), Pergamon Press, New York, pp. 3–18, 1969.
18. Tsay, C. S. and Reddy, J. N., "Bending, Stability, and Free Vibration of Thin Orthotropic Plates by Simplified Mixed Finite Elements," *Journal of Sound and Vibration*, **59**, 307–311, 1978.
19. Zienkiewicz, O. C. and Cheung, Y. K., "The Finite Element Method for Analysis of Elastic Isotropic and Orthotropic Slabs," *Proceeding of the Institute of Civil Engineers*, London, **28**, 471–488, 1964.
20. Zienkiewicz, O. C., Taylor, R. L., and Too, J. M., "Reduced Integration Technique in General Analysis of Plates and Shells," *International Journal for Numerical Methods in Engineering,* **3**, 275–290, 1971.

Chapter 13

COMPUTER IMPLEMENTATION OF TWO-DIMENSIONAL PROBLEMS

13.1 INTRODUCTION

In Chapter 7, we discussed some basic ideas concerning the development of a typical finite element program, and the use of **FEM1D** in the solution of one-dimensional problems was illustrated via many example problems. Specific details of various logical units of a finite element program for one-dimensional problems were given. Most of the ideas presented there are also valid for two-dimensional problems. The imposition of the boundary conditions and the solution of the equations remain the same as in one-dimensional problems. Here we focus attention on the computer implementation of two-dimensional elements. The use of a model program **FEM2D** is discussed. The program **FEM2D** contains linear and quadratic triangular and rectangular elements, and it can be used for the solution of heat conduction and convection problems, laminar flows of viscous incompressible fluids using the penalty function formulation, plane elasticity problems, and plate-bending problems using classical and shear deformation theories. A flow chart of **FEM2D** is given in Fig. 13.1.1.

In two dimensions, the element calculations are more involved than in one dimension, owing to the following considerations:

1. Various geometric shapes of elements
2. Single as well as multivariable problems
3. Integrations performed over areas as opposed to along lines (for one-dimensional elements)
4. Mixed-order integrations used in certain formulations (shear-deformable plates and penalty function formulations of viscous incompressible fluids)

A brief description of the function of each subroutine from program **FEM2D** is given below.

BOUNDARY: Subroutine to impose specified (essential, natural, and mixed) boundary conditions on the primary and secondary variables.

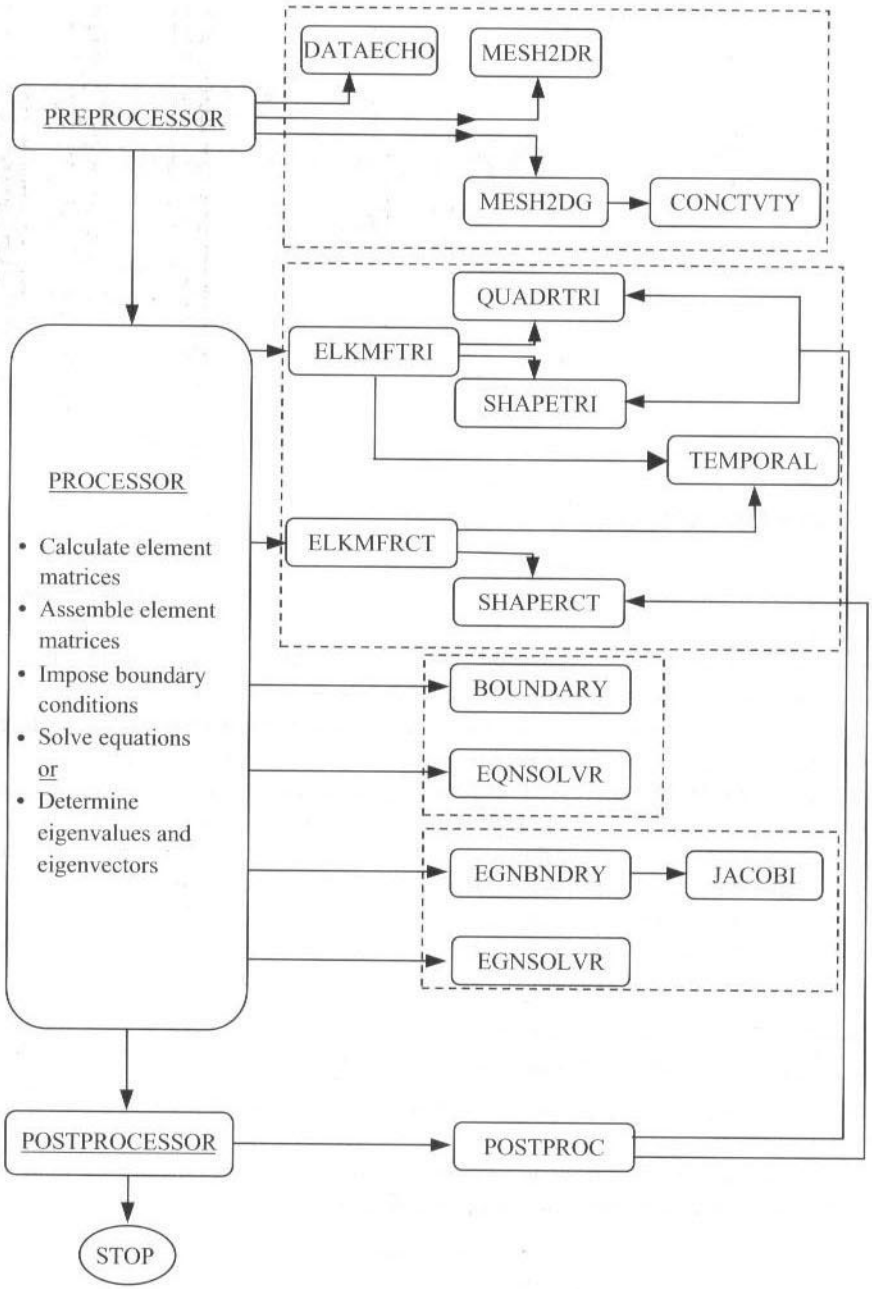

Figure 13.1.1 Flow chart of the computer program **FEM2D**.

CONCTVTY: Subroutine called from the mesh generator **MESH2DG**.

DATAECHO: Subroutine to echo the input data to the program (to facilitate the user to check the input data).

EGNBNDRY: Subroutine to impose specified homogeneous (essential and mixed) boundary conditions on the primary variables when an eigenvalue problem is solved.

EGNSOLVR: Subroutine to determine eigenvalues and eigenvectors.

ELKMFRCT: Subroutine to compute the element matrices $[K]$, $[M]$, and $\{F\}$ for various field problems when rectangular elements are used.

ELKMFTRI: Subroutine to compute the element matrices $[K]$, $[M]$, and $\{F\}$ for various field problems when triangular elements are used.

EQNSOLVR: Subroutine to solve a banded, symmetric system of algebraic equations using the Gauss elimination method.

INVERSE: Subroutine to invert a 3×3 matrix explicitly.

JACOBI: Subroutine called inside **EGNSOLVR**.

MESH2DG: Subroutine to generate mesh for nonrectangular domains.

MESH2DR: Subroutine to generate mesh for rectangular domains only.

POSTPROC: Subroutine to postcompute the solution, gradient of solution, and stresses for various field problems.

QUADRTRI: Subroutine to generate the quadrature points and weights for triangular elements.

SHAPERCT: Subroutine to compute the shape (interpolation) functions for linear and quadratic (eight- and nine-node) rectangular elements.

SHAPETRI: Subroutine to compute the shape (interpolation) functions for linear and quadratic triangular elements.

TEMPORAL: Subroutine to compute the equivalent coefficient matrices and column vectors for parabolic and hyperbolic equations when time-dependent analysis is carried (matrices of fully discretized system).

13.2 PREPROCESSOR

In the preprocessor unit, the program **MESH2DR** is used to generate triangular- and rectangular-element meshes of rectangular domains. The subroutine requires minimal input but is not general enough to generate finite element meshes of arbitrary domains. The subroutine **MESH2DG** is more general and can be used to generate meshes for nonrectangular domains. Of course, we can use any other mesh generation program in place of **MESH2DR** or **MESH2DG**. The subroutines **MESH2DR** and **MESH2DG** generate the connectivity matrix (array NOD) and the global coordinates of the nodes (array GLXY). When the mesh generators cannot be used, the mesh information should be read in.

13.3 ELEMENT COMPUTATIONS (PROCESSOR)

The two-dimensional problems of interest in this book require the evaluation of element matrices that involve products of interpolation functions and their derivatives with respect

to the global coordinates. Since the integrals are evaluated numerically, the integrands must be evaluated at the quadrature points and summed over the number of integration points. Thus, evaluation of the interpolation functions and their derivatives must be carried out inside the do-loops.

Element calculations for linear and quadratic triangular (**ELKMFTRI**) and quadrilateral (**ELKMFRCT**) elements can be carried out according to the concepts presented in Chapters 8 and 9. The principal steps involved are as follows.

1. Development of a subroutine for the evaluation of the interpolation functions and their derivatives with respect to the global coordinates [see Eqs. (9.3.7)–(9.3.11)].
2. Numerical integration of the coefficients of the element matrices using numerical quadrature formulas [see Eqs. (9.3.21) and (9.3.34)].
3. Setting up of the element matrices required for the class of problems being solved (e.g., static, transient, and eigenvalue problems).

We begin with the notation used for shape functions and their derivatives with respect to the natural (local) coordinates (ξ, η) and global coordinates (x, y) for rectangular elements. The variable names adopted are very transparent, and thus it is easy to see how the theoretical developments are translated into Fortran statements. We use the following notation:

XI(I)	Natural coordinate ξ_I of element node I
ETA(I)	Natural coordinate η_I of element node I
ELXY(I, 1)	Global coordinate x of element node I
ELXY(I, 2)	Global coordinate y of element node I
GLXY(I, 1)	Global coordinate x of the Ith node of the mesh
GLXY(I, 2)	Global coordinate y of the Ith node of the mesh
SF(I)	Interpolation function ψ_I of the Ith node of an element
DSF(1, I)	Derivative of SF(I) with respect to ξ: DSF(1, I) $= \partial\psi_I/\partial\xi$
DSF(2, I)	Derivative of SF(I) with respect to η: DSF(2, I) $= \partial\psi_I/\partial\eta$
GDSF(1, I)	Derivative of SF(I) with respect to x: GDSF(1, I) $= \partial\psi_I/\partial x$
GDSF(2, I)	Derivative of SF(I) with respect to y: GDSF(2, I) $= \partial\psi_I/\partial y$
DET	Determinant J of the Jacobian matrix $[J]$
CONST	Product of Jacobian J with the weights corresponding to the Gauss integration point (ξ_{NI}, η_{NJ}) = DET * GAUSWT(NI, NGP) * GAUSWT(NJ, NGP)

The subroutines **SHAPETRI** and **SHAPERCT** (called in a do-loop based on the number of quadrature points) contain the expressions of the interpolation functions and their derivatives for various-order triangular (TRI) and rectangular (RCT) elements, respectively. The derivatives of the interpolation functions with respect to global coordinates [see Eq. (9.3.9)] are also computed in these subroutines. The Fortran statements to carry out the operations in Eqs. (9.3.7)–(9.3.11) is summarized in Box 13.3.1.

Once the arrays SF and GDSF are available in do-loops on a number of Gauss points in each coordinate direction, it is easy to evaluate the matrix coefficients using the Gauss

Box 13.3.1 Fortran statements for the calculation of the Jacobian matrix and local and global derivatives of shape functions.

Given the interpolation functions (SF) and their derivatives with respect to the natural coordinates (array DSF), the Jacobian matrix (GJ), its determinant (DET) and inverse (matrix GJINV), and global derivative of the shape functions (array GDSF) can be computed as follows:

```
      DO 40 I = 1, 2
      DO 40 J = 1, 2
      GJ(I, J) = 0.0
      DO 40 K = 1, NPE
40    GJ(I, J) = GJ(I, J) + DSF(I, K)*ELXY(K, J)

      DET = GJ(1, 1)*GJ(2, 2) − GJ(1, 2)*GJ(2, 1)
      GJINV(1, 1) = GJ(2, 2)/DET
      GJINV(2, 2) = GJ(1, 1)/DET
      GJINV(1, 2) = −GJ(1, 2)/DET
      GJINV(2, 1) = −GJ(2, 1)/DET

      DO 50 I = 1, 2
      DO 50 J = 1,NPE
      GDSF(I, J) = 0.0
      DO 50 K = 1, 2
50    GDSF(I, J) = GDSF(I, J) + GJINV(I, K)*DSF(K, J)
```

quadrature formula (9.3.21). For example, $S_{ij}^{\alpha\beta}$ of Eq. (8.2.39)

$$S_{ij}^{\alpha\beta} = \int_{\Omega^e} \frac{\partial \psi_i}{\partial x_\alpha} \frac{\partial \psi_j}{\partial x_\beta} \, dx \, dy \tag{13.3.1}$$

where $x_1 = x$ and $x_2 = y$, can be translated into Fortran statement by

$$\begin{aligned}
\text{S00(I, J)} &= \text{S00(I, J)} + \text{SF(I)} * \text{SF(J)} * \text{CONST} \\
\text{S11(I, J)} &= \text{S11(I, J)} + \text{GDSF(1, I)} * \text{GDSF(1, J)} * \text{CONST} \\
\text{S12(I, J)} &= \text{S12(I, J)} + \text{GDSF(1, I)} * \text{GDSF(2, J)} * \text{CONST} \\
\text{S22(I, J)} &= \text{S22(I, J)} + \text{GDSF(2, I)} * \text{GDSF(2, J)} * \text{CONST}
\end{aligned} \tag{13.3.2}$$

The summed values of S00(I, J), S11(I, J), and so on, over the number of Gauss points yields the numerical values of the integral coefficients in (13.3.1). The Fortran statements listed in Box 13.3.2 summarize the discussion.

To set up the element coefficient matrices of a given problem, we make use of the element matrices defined above. As an example, consider the problem described by the Poisson equation in Eq. (8.2.1). The element coefficient matrix and the column vectors for the problem are given by Eqs. (8.2.19*b*). The element matrix K_{ij} [denoted ELK(I, J)] can be expressed in terms of S_{ji}^{00}, S_{ij}^{11}, ... by

$$\begin{aligned}
\text{ELK(I, J)} = {} & \text{A00} * \text{S00(I, J)} + \text{A11} * \text{S11(I, J)} + \text{A12} * \text{S12(I, J)} \\
& + \text{A21} * \text{S12(J, I)} + \text{A22} * \text{S22(I, J)}
\end{aligned}$$

Box 13.3.2 Fortran statements to compute matrix coefficients $S_{ij}^{\alpha\beta}$.

```
NPE = Number of nodes per elements
IPDF = Number of integration points (i.e., Gauss points)

   DIMENSION GAUSPT(5, 5), GAUSWT(5, 5), SF(9), GDSF(2, 9),
1    ELXY(9, 2), S00(9, 9), S11(9, 9), S12(9, 9), S22(9, 9)

   DATA GAUSPT/5*0.0D0, −0.57735027D0, 0.57735027D0, 3*0.0D0,
2  −0.77459667D0, 0.0D0, 0.77459667D0, 2*0.0D0, −0.86113631D0,
3  −0.33998104D0, 0.33998104D0, 0.86113631D0, 0.0D0, −0.90617984D0,
4  −0.53846931D0, 0.0D0, 0.53846931D0, 0.90617984D0/

   DATA GAUSWT/2.0Do, 4*0.0D0, 2*1.0D0, 3*0.0D0, 0.55555555D0,
2  0.88888888D0, 0.55555555D0, 2*0.0D0, 0.34785485D0,
3  2*0.65214515D0, 0.34785485D0, 0.0D0, 0.23692688D0,
4  0.47862867D0, 0.56888888D0, 0.47862867D0, 0.23692688D0/

Initialize the arrays

      DO 120 I = 1, NPE
      DO 120 J = 1, NPE
            S00(I, J) = 0.0
            S11(I, J) = 0.0
            S12(I, J) = 0.0
            S21(I, J) = 0.0
            S22(I, J) = 0.0
120  CONTINUE

DO-loops on numerical (Gauss) integration begin here:

      DO 200 NI = 1, IPDF
      DO 200 NJ = 1, IPDF
      XI = GAUSPT(NI, IPDF)
      ETA = GAUSPT(NJ, IPDF)

Subroutine SHAPERCT (SHAPE functions for ReCTangular
elements) is called to compute arrays SF and GDSF:

      CALL SHPRCT (NPE,XI,ETA,ELXY,DET,SF,GDSF)
      CNST = DET*GAUSWT(NI,IPDF)*GAUSWT(NJ,IPDF)

Compute S_ij^αβ of Eq. (13.3.1):

      DO 180 I = 1, NPE
        DO 180 J = 1, NPE
            S00(I, J) = S00(I, J) + SF(I)*SF(J)*CNST
            S11(I, J) = S11(I, J) + GDSF(1, I)*GDSF(1, J)*CNST
            S12(I, J) = S12(I, J) + GDSF(1, I)*GDSF(2, J)*CNST
            S21(I, J) = S21(I, J) + GDSF(2, I)*GDSF(1, J)*CNST
            S22(I, J) = S22(I, J) + GDSF(2, I)*GDSF(2, J)*CNST
180    CONTINUE
200  CONTINUE
```

where $a_{00} = \text{A00}$, $a_{11} = \text{A11}$, $a_{12} = \text{A12}$, $a_{21} = \text{A21}$, and $a_{22} = \text{A22}$ are the constant coefficients of the differential equation (8.2.1).

In multivariable problems, the element matrices are themselves defined in terms of submatrices, as was the case for plane fluid flow, elasticity, and plate bending. In such cases, the nodal degrees of freedom should be renumbered to reduce the half-bandwidth of the assembled coefficient matrix. For example, consider the element equations (10.4.24) associated with the penalty formulation of two-dimensional viscous flow problems, which have a close resemblance to the finite element model of the plane elasticity problem; see Eq. (11.4.5). The element nodal variables Δ_i are given (say, for a linear rectangular element) by

$$\begin{Bmatrix} \Delta_1 \\ \Delta_2 \\ \Delta_3 \\ \vdots \\ \Delta_8 \end{Bmatrix} = \begin{Bmatrix} v_x^1 \\ v_x^2 \\ v_x^3 \\ v_x^4 \\ v_y^1 \\ v_y^2 \\ v_y^3 \\ v_y^4 \end{Bmatrix} \tag{13.3.3}$$

Thus, at any node, the difference between the label number of the first degree of freedom and that of the second degree of freedom is 4 (in a general case, the difference is n, where n is the number of nodes per element). This difference contributes to an increase in the half-bandwidth of the assembled coefficient matrix and hence in computational cost when Gauss elimination methods are used to solve the equations. To remedy this situation, we reorder the element nodal degrees of freedom as follows:

$$\begin{Bmatrix} \Delta_1 \\ \Delta_2 \\ \Delta_3 \\ \Delta_4 \\ \vdots \\ \Delta_{2n-1} \\ \Delta_{2n} \end{Bmatrix} = \begin{Bmatrix} v_x^1 \\ v_y^1 \\ v_x^2 \\ v_y^2 \\ \vdots \\ v_x^n \\ v_y^n \end{Bmatrix} \tag{13.3.4}$$

In reordering the nodal degrees of freedom, we must retain the symmetry, if one is present, of the system of algebraic equations. This is accomplished by renumbering the equations in the same way as the nodal degrees of freedom. To illustrate how this can be done, we consider the matrix equation

$$\begin{bmatrix} [S^{11}] & [S^{12}] \\ [S^{21}] & [S^{22}] \end{bmatrix} \begin{Bmatrix} \{u\} \\ \{v\} \end{Bmatrix} = \begin{Bmatrix} \{F^1\} \\ \{F^2\} \end{Bmatrix} \tag{13.3.5a}$$

which is a set of four equations in four unknowns. In expanded form, we have

$$\begin{aligned} S_{11}^{11}u_1 + S_{12}^{11}u_2 + S_{11}^{12}v_1 + S_{12}^{12}v_2 &= F_1^1 \\ S_{21}^{11}u_1 + S_{22}^{11}u_2 + S_{21}^{12}v_1 + S_{22}^{12}v_2 &= F_2^1 \\ S_{11}^{21}u_1 + S_{12}^{21}u_2 + S_{11}^{22}v_1 + S_{12}^{22}v_2 &= F_1^2 \\ S_{21}^{21}u_1 + S_{22}^{21}u_2 + S_{21}^{22}v_1 + S_{22}^{22}v_2 &= F_2^2 \end{aligned} \tag{13.3.5b}$$

Box 13.3.3 Fortran statements to rearrange the degrees of freedom to reduce the bandwidth of the coefficient matrix.

```
Rearrangement of element equations for problems with multiple degrees
of freedom per node (Illustrated using plane elasticity model, NDF = 2).

  NDF = Number of degrees of freeedom per node
  NPE = Number of nodes per element
  CMAT(I, J) = Matrix of elastic coefficients
  ELK(I, J) = Element stiffness matrix coefficients
```

```
Dimension the arrays: ELK(NN, NN) and CMAT(3, 3), where
  NN = NPE*NDF

Computation of coefficients ELK11(I, J), ELK12(I, J), ELK21(I, J), and
ELK22(I, J) of Eqs. (11.4.5) and (11.4.6) using numerical integration.

Initialize arrays ELK11(I, J), ELK12(I, J), ELK21(I, J) and ELK22(I, J).
Initialization loops are not included here. The following statements
go inside the Gauss–Legendre quadrature loops; see Box 13.3.2 for
evaluation of S_ij^αβ:

    DO 140 I = 1, NPE
    DO 120 J = 1, NPE
    ELK11(I, J) = ELK11(I, J) + CMAT(1, 1)*S11(I, J) + CMAT(3, 3)*S22(I, J)
    ELK12(I, J) = ELK12(I, J) + CMAT(1, 2)*S12(I, J) + CMAT(3, 3)*S21(I, J)
    ELK21(I, J) = ELK21(I, J) + CMAT(1, 2)*S21(I, J) + CMAT(3, 3)*S12(I, J)
    ELK22(I, J) = ELK22(I, J) + CMAT(3, 3)*S11(I, J) + CMAT(2, 2)*S22(I, J)
120 CONTINUE
140 CONTINUE

Rearrange the coefficients

    II = 1
    DO 180 I = 1, NN
      JJ = 1
      DO 160 J = 1, NN
        ELK(II, JJ) = ELK11(I, J)
        ELK(II, JJ+1) = ELK12(I, J)
        ELK(II+1, JJ) = ELK21(I, J)
        ELK(II+1, JJ+1) = ELK22(I, J)
160 JJ = NDF*J+1
180 II = NDF*I+1
```

Here (u_i, v_i) are the degrees of freedom at element node i. Now letting

$$\Delta_1 = u_1, \quad \Delta_2 = v_1, \quad \Delta_3 = u_2, \quad \Delta_4 = v_2 \tag{13.3.6}$$

(i.e., the third nodal variable is renamed as the second, and vice versa) and rearranging (13.3.5a) (i.e., the third equation becomes the second equation, and vice versa), we obtain

$$\begin{aligned}
S_{11}^{11}\Delta_1 + S_{11}^{12}\Delta_2 + S_{12}^{11}\Delta_3 + S_{12}^{12}\Delta_4 &= F_1^1 \\
S_{11}^{21}\Delta_1 + S_{11}^{22}\Delta_2 + S_{12}^{21}\Delta_3 + S_{12}^{22}\Delta_4 &= F_1^2 \\
S_{21}^{11}\Delta_1 + S_{21}^{12}\Delta_2 + S_{22}^{11}\Delta_3 + S_{22}^{12}\Delta_4 &= F_2^1 \\
S_{21}^{21}\Delta_1 + S_{21}^{22}\Delta_2 + S_{22}^{21}\Delta_3 + S_{22}^{22}\Delta_4 &= F_2^2
\end{aligned} \tag{13.3.7a}$$

or, in matrix form,

$$\mathbf{S}\Delta = \mathbf{F} \tag{13.3.7b}$$

where

$$\begin{gathered}
S_{ij} = S_{\alpha\beta}^{11}, \quad S_{i,j+1} = S_{\alpha\beta}^{12}, \quad S_{i+1,j} = S_{\alpha\beta}^{21}, \quad S_{i+1,j+1} = S_{\alpha\beta}^{22} \\
F_i = F_\alpha^1, \quad F_{i+1} = F_\alpha^2 \\
i = 2\alpha - 1, \quad j = 2\beta - 1, \quad \alpha, \beta = 1, 2
\end{gathered} \tag{13.3.7c}$$

The above discussion applies to any number of degrees of freedom per node (NDF). Computer implementation of the rearrangement of nodal degees of freedom and the associated equations [see Eqs.(13.3.7c)] is straightforward, and the Fortran statements of the procedure are given in Box 13.3.3.

The Fortran statements provided in Boxes 13.3.1 through 13.3.3 should help the reader see the ease with which finite element models can be implemented in a computer. No attempt is made here to discuss equation solver and eigenvalue solver. These are considered to be extraneous to the method. The Fortran source code of **FEM2D** gives a more complete idea as to how various computational steps of finite element analysis are carried out. The program can be modified to include one's own finite element formulation. In the next section, we illustrate the capabilities and limitations of the educational program **FEM2D**.

13.4 APPLICATIONS OF THE COMPUTER PROGRAM FEM2D

13.4.1 Introduction

The computer program **FEM2D** is developed to solve the following four types of problems:

Case 1. Single-variable problems, including convective-type boundary conditions for heat transfer problems

$$c_t\left(\frac{\partial u}{\partial t} + \frac{\partial^2 u}{\partial t^2}\right) - \frac{\partial}{\partial x}\left(a_x\frac{\partial u}{\partial x}\right) - \frac{\partial}{\partial y}\left(a_y\frac{\partial u}{\partial y}\right) + a_0 u = f \tag{13.4.1a}$$

with

$$c_t = c_0 + c_x x + c_y y, \quad a_x = a_{10} + a_{1x} x + a_{1y} y$$
$$a_y = a_{20} + a_{2x} x + a_{2y} y, \quad f_0 = f_0 + f_x x + f_y y \tag{13.4.1b}$$
$$a_0 = \text{constant}$$

Case 2. Viscous incompressible fluid flows using the penalty function formulation of Chapter 10 [Eqs. (10.2.9) and (10.2.10) with P replaced by (10.4.20)]

Case 3. The plane elasticity problems of Chapter 11 [Eq. (11.2.18a)]

Case 4. Plate bending problems using classical plate theory [Eq. (12.2.11)] and shear deformation plate theory [Eqs. (12.3.8a)–(12.3.8c)] of Chapter 12; only rectangular elements are included

The first category of problems is quite general and includes, as special cases, many other field problems of engineering and science. As a special case, axisymmetric problems can also be analyzed. The last three categories are specialized to linear (i.e., Stokes) viscous incompressible fluid flow, linear elasticity, and linear plate bending, respectively.

The type of gradient of the solution computed (in subroutine **POSTPROC**) for single-variable problems (Case 1) differs for different physical problems. For heat transfer problems, we wish to compute the x and y components of heat flux

$$q_x = -a_x \frac{\partial u}{\partial x}, \quad q_y = -a_y \frac{\partial u}{\partial y} \tag{13.4.2}$$

The same definition applies to the calculation of the velocity components in the velocity potential formulation of inviscid fluid flows [i.e., q_x and q_y of Eq. (13.4.2) are the velocity components v_x and v_y, respectively]. In the stream function formulation, the velocity components (v_x, v_y) are defined by

$$v_x = a_y \frac{\partial u}{\partial y}, \quad v_y = -a_x \frac{\partial u}{\partial x} \tag{13.4.3}$$

The (total) stresses for multivariable problems are computed using the constitutive equations, with the strains (or strain rates for fluid flow problems) computed at the reduced Gauss points using the strain-displacement relations.

For heat transfer problems (i.e., ITYPE = 0), the variable ICONV is used to indicate the presence (ICONV = 1) or absence (ICONV = 0) of convective boundaries. When convective boundaries are involved (i.e., ICONV = 1), the elements whose boundaries coincide with such a boundary will have additional contributions to their coefficient matrices [see Eqs. (8.5.6)–(8.5.10)]. The array IBN is used to store elements that have convective boundaries, and the array INOD is used to store the pairs of element local nodes (of elements in array IBN) that are on the convective boundary (to specify the side of the element on the convective boundary). If an element has more than one of its sides on the convective boundary, it should be repeated as many times as the number of sides on the convective boundary.

A complete list of the input variables of the program **FEM2D** is included in Table 13.4.1, which contains an explanation of the key variables for the six classes (ITYPE = 0, 1, 2, . . . , 5) of problems.

Table 13.4.1 Description of the input variables to the program **FEM2D**.

• Data Card 1

TITLE Title of the problem being solved (80 characters)

• Data Card 2

ITYPE Problem type
- ITYPE = 0 Single variable problems
- ITYPE = 1 Viscous incompressible flow problems
- ITYPE = 2 Plane elasticity problems
- ITYPE = 3 Plate bending problems by FSDT
- ITYPE = 4 Plate bending problems by CPT(N)
- ITYPE = 5 Plate bending problems by CPT(C)

IGRAD Indicator for computing the gradient of the solution or stresses in the postprocessor
- IGRAD = 0 No postprocessing is required
- IGRAD > 0 Postprocessing is required

When ITYPE = 0 and IGRAD = 1, the gradient is computed as in Eq. (13.4.2); for ITYPE = 0 and IGRAD > 1 the gradient is computed by Eq. (13.4.3)

ITEM Indicator for dynamic analysis
- ITEM = 0 Static analysis is required
- ITEM > 0 Either eigenvalue or transient analysis is required:
  - ITEM = 1 Parabolic equation
  - ITEM = 2 Hyperbolic equation

NEIGN Indicator for eigenvalue analysis
- NEIGN = 0 Static or transient analysis
- NEIGN > 0 Eigenvalue analysis:
  - NEIGN = 1 Vibration analysis
  - NEIGN > 1 Stability of plates

Skip card 3 if NEIGN = 0.

• Data Card 3

NVALU Number of eigenvalues to be printed

NVCTR Indicator for printing eigenvectors:
- NVCTR = 0 Do not print eigenvectors
- NVCTR > 0 Print eigenvectors

• Data Card 4

IELTYP Element type used in the analysis
- IELTYP = 0 Triangular elements
- IELTYP > 0 Quadrilateral elements

NPE Nodes per element
- NPE = 3 Linear triangle (IELTYP = 0)
- NPE = 4 Linear quadrilateral (IELTYP > 0)
- NPE = 6 Quadratic triangle (IELTYP = 0)
- NPE = 8 or 9 Quadratic quadrilateral (IELTYP > 0)

MESH Indicator for mesh generation by the program
- MESH = 0 Mesh is not generated by the program
- MESH = 1 Mesh is generated by the program for rectangular domains by **MESH2DR**
- MESH >1 Mesh is generated by the program for nonrectangular domains by **MESH2DG**

NPRNT Indicator for printing certain output
- NPRNT = 0 Not print array NOD, element matrices or global matrices
- NPRNT = 1 Print array NOD and element 1 matrices ELK and ELF

(**Table 13.4.1** continued)

NPRNT = 2 Print array NOD and assembled matrices GLK and GLF
NPRNT > 2 Combination of NPRNT = 1 and 2

Skip card 5 if MESH = 1.

• **Data Card 5**

NEM	Number of elements in the mesh when the user inputs the mesh or the mesh is generated by **MESH2DG**
NNM	Number of nodes in the mesh when the user inputs the mesh or the mesh is generated by **MESH2DG**

Skip cards 6 and 7 if MESH $\neq$ 0; otherwise, read card 6 in a loop on the number of elements (N = 1, NEM) and card 7 in loops on I and J.

• **Data Card 6**

NOD(N, I)	Connectivity for the Nth element (I=1, NPE)

• **Data Card 7**

GLXY(I, J)	Global x and y coordinates of the Ith global node in the mesh (J = 1, x coordinate; J = 2, y coordinate) Loops on I and J are: [(J = 1, 2), I = 1, NNM]; the NNM pairs of (x, y) coordinates are read sequentially

Cards 8–11 are read in **MESH2DG**. Skip them unless MESH > 1.

• **Data Card 8**

NRECL	Number of line records to be read in the mesh

• **Data Card 9**

Read the following variables NRECL times:

NOD1	First global node number of the line segment
NODL	Last global node number of the line segment
NODINC	Node increment on the line
X1	The global x coordinate of the NOD1
Y1	The global y coordinate of the NOD1
XL	The global x coordinate of NODL
YL	The global y coordinate of NODL
RATIO	The ratio of the first element length to the last element length

• **Data Card 10**

NRECEL	Number of rows of elements to be read in the mesh

• **Data Card 11**

Read the following variables NRECEL times:

NEL1	First element number of the row
NELL	Last element number of the row
IELINC	Increment of element number in the row
NODINC	Increment of the global node number in the row
NPE	Number of nodes in each element
NODE(I)	Connectivity array of the first element in the row (I=1, NPE)

Skip cards 12–14 if MESH $\neq$ 1.

• **Data Card 12**

NX	Number of elements in the x direction
NY	Number of elements in the y direction

• **Data Card 13**

X0	The x coordinate of global node 1
DX(I)	The x dimension of the Ith element (I = 1, NX)

(**Table 13.4.1** continued)

- **Data Card 14**

Y0	The y coordinate of gobal node 1
DY(I)	The y dimension of the Ith element (I = 1, NY)

- **Data Card 15**

NSPV	The number of specified primary variables

Skip card 16 if NSPV = 0

- **Data Card 16**

ISPV(I, J)	Node number and local degree of freedom (DOF) number of the Ith specified primary variable ISPV(I, 1) = Node number ISPV(I, 2) = Local DOF number The do-loops on I and J are: [(J = 1, 2), I = 1, NSPV]

Skip card 17 if NSPV = 0 or NEIGN $\neq$ 0.

- **Data Card 17**

VSPV(I)	Specified value of the Ith primary variable (I = 1, NSPV)

Skip card 18 if NEIGN $\neq$ 0.

- **Data Card 18**

NSSV	Number of (nonzero) specified secondary variables

Skip card 19 if NSSV = 0 or NEIGN $\neq$ 0.

- **Data Card 19**

ISSV(I, J)	Node number and local DOF number of the Ith specified secondary variable ISSV(I, 1) = Node number ISSV(I, 2) = Local DOF number The loops on I and J are: ((J = 1, 2), I = 1, NSSV)

Skip card 20 if NSSV = 0 or NEIGN $\neq$ 0.

- **Data Card 20**

VSSV(I)	Specified value of the Ith secondary variable (I = 1, NSSV)

Data Cards 21–27 are for the single variable problems (ITYPE = 0).

- **Data Card 21**

A10	Coefficients of the differential equation
A1X	
A1Y	a11 = A10 + A1X*X + A1Y*Y

- **Data Card 22**

A20	Coefficients of the differential equation
A2X	
A2Y	a22 = A20 + A2X*X + A2Y*Y

- **Data Card 23**

A00	Coefficient of the differential equation

- **Data Card 24**

ICONV	Indicator for convection boundary conditions ICONV = 0 No convection boundary conditions ICONV > 0 Convection boundary conditions present

- **Data Card 25**

NBE	Number elements with convection

- **Data Card 26**

The following cards are read for each I, I = 1, NBE:

IBN(I)	Ith element number with convection
BETA(I)	Film coefficient for convection on Ith element
TINF(I)	Ambient temperature of the Ith element

(**Table 13.4.1** continued)

- **Data Card 27**

INOD(I, J)	Local node numbers of the side with convection (J = 1, 2; for quadratic elements, give end nodes) Loops on I and J are: [(J = 1, 2), I = 1, NBE]

Data Card 28 is for viscous fluid flows (ITYPE = 1) only.

- **Data Card 28**

VISCSITY	Viscosity of the fluid
PENALTY	Value of the penalty parameter

Data Cards 29 and 30 are for plane elasticity problems (ITYPE = 2) only.

- **Data Card 29**

LNSTRS	Flag for plane stress or plane strain problems LNSTRS = 0 Plane strain elastic problems LNSTRS > 0 Plane stress elastic problems

- **Data Card 30**

E1	Young's moduli along the global x axis
E2	Young's moduli along the global y axis
ANU12	Poisson's ratio in the xy plane
G12	Shear modulus in the xy plane
THKNS	Thickness of the plane elastic body analyzed

Data Card 31 is for plate bending problems (ITYPE = 3 to 5) only.

- **Data Card 31**

E1	Young's moduli along the global x axis
E2	Young's moduli along the global y axis
ANU12	Poisson's ratio in the xy plane
G12	Shear modulus in the xy plane
G13	Shear modulus in the xz plane
G23	Shear modulus in the yz plane
THKNS	Thickness of the plate analyzed

*** Remaining data cards are for all problem types. ***

Skip card 32 if NEIGN $\neq$ 0.

- **Data Card 32**

F0	Coefficients to define the source term
FX	
FY	f(x, y) = F0 + FX*x + FY*y

*** Cards 33–37 are for transient analysis (ITEM $\neq$ 0) only. ***

Skip card 33 if ITEM = 0.

- **Data Card 33**

C0	Coefficients defining the temporal parts of the
CX	differential equations, as defined below:
CY	

CT = C0 + CX*X + CY*Y when ITYPE = 0 or 1
CT = (C0 + CX*X + CY*Y)*THKNS when ITYPE = 2
I0 = C0*THKNS, I2 = C0*(THKNS**3)/12
and CX and CY are not used (when NEIGH $\leq$ 1 and ITYPE = 3 to 5)
C0, CX, and CY denote the buckling parameters when ITYPE = 3 and NEIGN > 1

Skip card 34 if ITEM = 0 or NEIGN $\neq$ 0.

(**Table 13.4.1** continued)

• **Data Card 34**

NTIME	Number of time steps for the transient solution
NSTP	Time step number at which the source is removed
INTVL	Time step interval at which to print the solution
INTIAL	Indicator for nature of initial conditions
	INTIAL = 0 Zero initial conditions are used
	INTIAL > 0 Nonzero initial conditions are used

Skip card 35 if ITEM = 0 or NEIGN $\neq$ 0.

• **Data Card 35**

DT	Time step used for the transient solution
ALFA	Parameter in the alfa-family of time approximation used for parabolic equations:
	ALFA = 0 The forward difference scheme (C.S.)†
	ALFA = 0.5 The Crank–Nicolson scheme (stable)
	ALFA = 2/3 The Galerkin scheme (stable)
	ALFA = 1 The backward difference scheme (stable)
	†C.S. = conditionally stable; for all schemes with ALFA < 0.5, the time step DT is restricted to DT < 2/[MAXEGN*(1-2*ALFA)], where MAXEGN is the maximum eigenvalue of the discrete problem
GAMA	Parameter in the Newmark time integration scheme used for hyperbolic equations:
	GAMA = 0.5 Constant-average acceleration (stable)
	GAMA = 1/3 Linear acceleration scheme (C.S.)
	GAMA = 0.0 The central difference scheme (C.S.)
	ALFA = 0.5 for all schemes; For schemes for which ALFA $\leq$ 0.5 and GAMA < ALFA, DT is restricted to: DT < 2/SQRT[MAXEGN*(ALFA-GAMA)], MAXEGN being the maximum eigenvalue of the discrete system
EPSLN	A small parameter to check if the solution has reached a steady state

Skip card 36 if ITEM or INTIAL = 0, or NEIGN $\neq$ 0.

• **Data Card 36**

GLU(I)	Vector of initial value of the primary variables (I = 1, NEQ), where NEQ = Number of nodal values in the mesh

Skip card 37 if ITEM $\leq$ 1, NEIGN $\neq$ 0, or INTIAL = 0.

• **Data Card 37**

GLV(I)	Vector of the initial values of the first derivative of the primary variables (velocity) (I = 1, NEQ)

13.4.2 Description of Mesh Generators

A major limitation of the program **FEM2D** lies in the mesh generation [i.e., the computation of arrays NOD(I, J) and GLXY(I, J) for arbitrary domains]. For such problems, the user is required to input the mesh information, which can be a tedious job if many elements are used. Of course, the program can be modified to accept other mesh generation subroutines. Here we discuss the input data to the two mesh generators, namely, **MESH2DR** and **MESH2DG**.

First, let us consider **MESH2DR**. The program is restricted to rectangular domains with sides parallel to the global x and y axes. The subroutine requires the following input data:

NX	Number of elements in the x direction
NY	Number of elements in the y direction
(X_0, Y_0)	Global coordinates of global node 1, which is located at the lower left corner of the domain (see Fig. 13.4.1)
DX(I)	The array of element lengths along the x direction
DY(I)	The array of element lengths along the y direction

The node and element numbering schemes for triangular and rectangular element meshes generated by **MESH2DR** are shown in Fig. 13.4.1.

Next, we consider **MESH2DG**, which is relatively more general than **MESH2DR**. The program, based on the straight line generation logic used by Akay, Willhite, and Didandeh (1987), requires the user to sketch a desired mesh with certain regularity of node and element numbering. It exploits the regularity to generate the mesh. The program **MESH2DG** requires the following input (except for NEM and NNM, all other variables are read from the subroutine):

NEM	Number of total elements in the mesh
NNM	Number of total nodes in the mesh
NRECL	Number of line-segment records

For each line segment, read the following variables:

NOD1	First node number on the line segment
NODL	Last node number on the line segment
NODINC	Increment between two consecutive nodes on the line
(X1, Y1)	Global coordinates of the first node, NOD1 on the line
(XN, YN)	Global coordinates of the last node, NODL on the line
RATIO	Ratio of the first element length to the last element length

Similar information on the elements is read as follows:

NRECEL	Number of rows of elements

For each row of elements, read the following variables:

NEL1	First element number in the row
NELL	Last element number in the row
NODINC	Increment between respective nodes of consecutive elements in the row
NPE	Number of nodes per element
NODE(I) (I = 1, NPE)	Nodal connectivity for element NEL1

The type of data being read in **MESH2DG** should give some indication of the restrictions of the program. The node and element numbering should be regular along the lines and rows being read. Figures 13.4.2(a)–13.4.2(d) show typical examples of meshes of linear and quadratic triangular and quadrilateral elements. For each of these meshes, the input data required for **MESH2DG** is listed in Boxes 13.4.1 and 13.4.2.

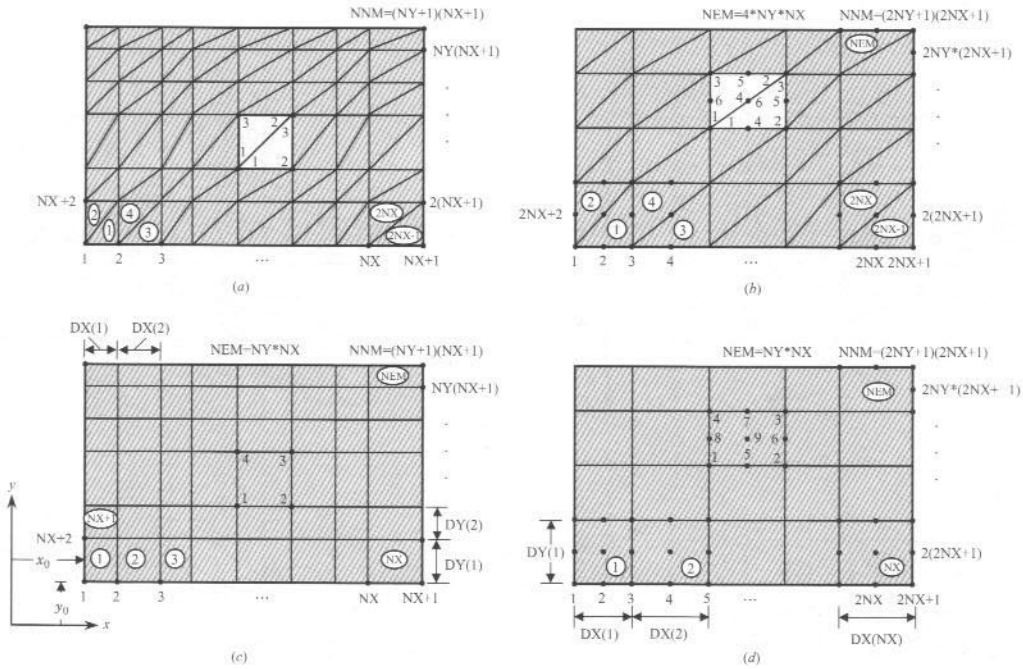

Figure 13.4.1 Element numbering and global and element node numbering system used in subroutine **MESH2DR** for the generation of meshes for rectangular domains. (*a*) Mesh of linear triangles. (*b*) Mesh of quadratic triangles. (*c*) Mesh of linear rectangles. (*d*) Mesh of quadratic (nine-node) rectangles.

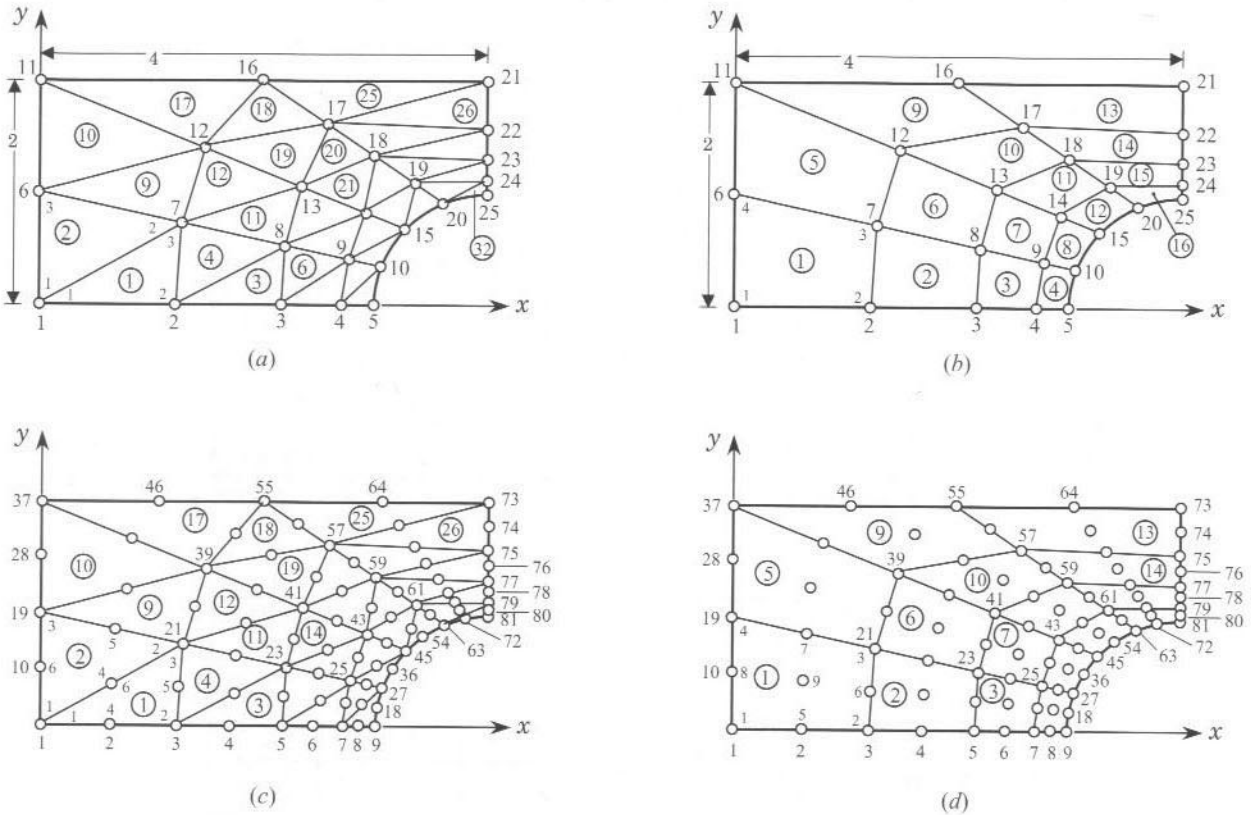

Figure 13.4.2 Typical examples of mesh generation in irregular domains using subroutine **MESH2DG**. (*a*) Mesh of linear triangles. (*b*) Mesh of linear quadrilaterals. (*c*) Mesh of quadratic triangles. (*d*) Mesh of quadratic (nine-node) quadrilateral elements.

Box 13.4.1 The input data to program **FEM2D** to generate the finite element meshes shown in Figs. 13.4.2(*a*) and 13.4.2(*b*).

```
(a) Mesh of linear triangles [see Figure 13.4.2(a)]
  32  25                                                  NEM, NNM
   5                                                      NRECL
   1   5  1  0.0   0.0  3.0      0.0      6.0             NOD1, NODL, NODINC,
   6  10  1  0.0   1.0  3.07612  0.38268  6.0             X1, Y1, XL, YL, RATIO
  11  15  1  0.0   2.0  3.29289  0.7071   6.0             for each of the five
  16  20  1  2.0   2.0  3.61732  0.92388  6.0             line segments
  21  25  1  4.0   2.0  4.0      1.0      6.0

   8                                                      NRECEL
   1   7    2    1    3      1  2   7                    NEL1, NELL, IELINC,
   2   8    2    1    3      1  7   6                    NODINC, NPE, NOD(I,J)
   9  15    2    1    3      6  7  12                    for each of the
  10  16    2    1    3      6 12  11                    eight rows of
  17  23    2    1    3     11 12  16                    elements
  18  24    2    1    3     12 17  16
  25  31    2    1    3     16 17  21
  26  32    2    1    3     17 22  21

(b) Mesh of linear quadrilaterals [see Figure 13.4.2(b)]

  16  25                                                  NEM, NNM

   5                                                      NRECL
   1   5  1  0.0   0.0  3.0      0.0      6.0             NOD1,NODL,NODINC,
   6  10  1  0.0   1.0  3.07612  0.38268  6.0             etc.
  11  15  1  0.0   2.0  3.29289  0.7071   6.0
  16  20  1  2.0   2.0  3.61732  0.92388  6.0
  21  25  1  4.0   2.0  4.0      1.0      6.0

   4                                                      NRECEL
   1   4    1    1    4      1  2   7   6                NEL1,NELL,IELINC,
   5   8    1    1    4      6  7  12  11                etc.
   9  12    1    1    4     11 12  17  16
  13  16    1    1    4     16 17  22  21
```

Box 13.4.2 The input data to program **FEM2D** to generate the finite element meshes shown in Figs. 13.4.2(*c*) and 13.4.2(*d*).

```
(c) Mesh of quadratic triangles [see Fig. 13.4.2(c)]

  32  81                                                  NEM, NNM

   9                                                      NRECL
   1   9  1  0.0  0.0  3.0      0.0      6.0  |
  10  18  1  0.0  0.5  3.01921  0.19509  6.0  |
  19  27  1  0.0  1.0  3.07612  0.38268  6.0  |
  28  36  1  0.0  1.5  3.16853  0.55557  6.0  | NOD1,NODL,NODINC,
  37  45  1  0.0  2.0  3.29289  0.7071   6.0  | X1,Y1,XL,YL,RATIO
  46  54  1  1.0  2.0  3.44443  0.83147  6.0  | for each line segment
  55  63  1  2.0  2.0  3.61732  0.92388  6.0  |
  64  72  1  3.0  2.0  3.80491  0.98078  6.0  |
  73  81  1  4.0  2.0  4.0      1.0      6.0  |
```

(**Box 13.4.2** is continued from the previous page)

```
   8                                                          NRECEL
   1    7  2  2  6     1  3 21  2 12 11          |
   2    8  2  2  6     1 21 19 11 20 10          |
   9   15  2  2  6    19 21 39 20 30 29          |
  10   16  2  2  6    19 39 37 29 38 28          | NEL1,NELL,IELINC,NODINC,
  17   23  2  2  6    37 39 55 38 47 46          | NPE,NOD(I,J)
  18   24  2  2  6    39 57 55 48 56 47          |
  25   31  2  2  6    55 57 73 56 65 64          |
  26   32  2  2  6    57 75 73 66 74 65          |

(d) Mesh of quadratic (nine-node) quadrilaterals [see Fig. 13.4.2(d)]:

  16  81                                                      NEM, NNM

   9                                                         NRECL
   1    9  1  0.0  0.0  3.0      0.0      6.0   |
  10   18  1  0.0  0.5  3.01921  0.19509  6.0   |
  19   27  1  0.0  1.0  3.07612  0.38268  6.0   |
  28   36  1  0.0  1.5  3.16853  0.55557  6.0   | NOD1,NODL,NODINC,
  37   45  1  0.0  2.0  3.29289  0.7071   6.0   | X1,Y1,XL,YL,RATIO
  46   54  1  1.0  2.0  3.44443  0.83147  6.0   | for each line segment
  55   63  1  2.0  2.0  3.61732  0.92388  6.0   |
  64   72  1  3.0  2.0  3.80491  0.98078  6.0   |
  73   81  1  4.0  2.0  4.0      1.0      6.0   |

   4                                                         NRECEL
   1    4  1  2  9     1  3 21 19  2 12 20 10 11
   5    8  1  2  9    19 21 39 37 20 30 38 28 29  NEL1,NELL,IELINC,NODINC,
   9   12  1  2  9    37 39 57 55 38 48 56 46 47  NPE,NOD(I,J)
  13   16  1  2  9    55 57 75 73 56 66 74 64 65
```

13.4.3 Applications (Illustrative Examples)

In this section, the input data to **FEM2D** for several example problems are discussed. The example problems are selected from those discussed in Chapters 8–12. For a description of the variables used in the input data, see Table 13.4.1.

Example 13.4.1 (Poisson's Equation)

We consider the Poisson equation

$$-\nabla^2 u = 1 \text{ in } \Omega, \quad u = 0 \text{ on } \Gamma$$

where Ω is a square of two units and Γ denotes the boundary of Ω. Due to the biaxial symmetry, we can use a quadrant of the domain to solve the problem using the finite element method. We represent the computational domain by two different meshes (1) mesh of linear triangles [Fig. 13.4.3(*a*)], and (2) mesh of linear rectangles [Fig. 13.4.3(*b*)].

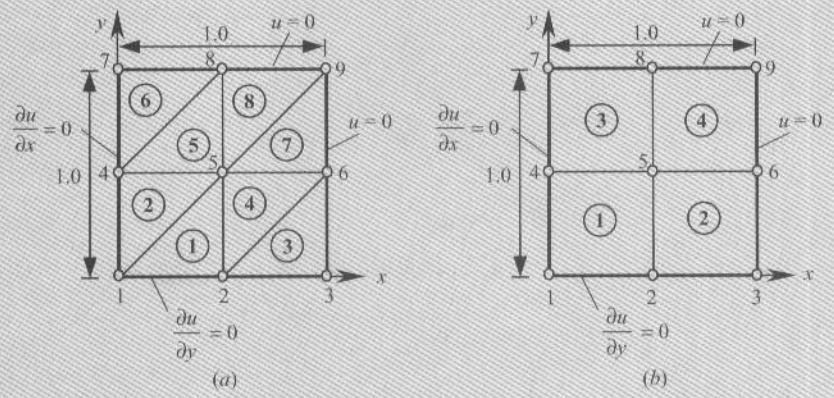

Figure 13.4.3 Finite element meshes of (*a*) linear triangles and (*b*) linear rectangles.

Triangular elements. We use the 2×2 mesh shown in Fig. 13.4.3(*a*). We have

$$\text{ITYPE} = 0, \quad \text{IGRAD} = 1, \quad \text{ITEM} = 0, \quad \text{NEIGN} = 0$$
$$\text{IELTYP} = 0, \quad \text{NPE} = 3, \quad \text{MESH} = 1, \quad \text{NPRNT} = 0$$

Note that we chose to generate the mesh using the subroutine **MESH2DR**. Therefore, we must specify the number of subdivisions and their lengths along each direction:

$$\text{NX} = 2, \quad \text{NY} = 2, \quad \text{X0} = 0.0, \quad \text{Y0} = 0.0$$
$$\text{DX(1)} = 0.5, \quad \text{DX(2)} = 0.5, \quad \text{DY(1)} = 0.5, \quad \text{DY(2)} = 0.5$$

The number of specified primary variables (NSPV), the node numbers and the specified local degree of freedom (ISPV), and their specified values (VSPV) for the problem are: NSPV = 5, ISPV(I, J) = (3, 1; 6, 1; 7, 1; 8, 1; 9, 1), and VSPV(I) = (0.0, 0.0, 0.0, 0.0, 0.0). There are no specified secondary variables, NSSV = 0.

The coefficients a_x and a_y of the differential equation (13.4.1*a*) are unity, $a_0 = 0$, the source term f is unity, and there is no convection:

$$\text{A10} = 1.0, \quad \text{A1X} = 0.0, \quad \text{A1Y} = 0.0, \quad \text{A20} = 1.0, \quad \text{A2X} = 0.0$$
$$\text{A2Y} = 0.0, \quad \text{A00} = 0.0, \quad \text{ICONV} = 0, \quad \text{FO} = 1.0, \quad \text{FX} = 0.0, \quad \text{FY} = 0.0$$

Rectangular elements. For the 2×2 (four-element) mesh of rectangular elements [see Fig. 13.4.3(*b*)], the data input to the program differ only in the specification of the element type and the number of nodes per element: IELTYP = 1 and NPE = 4.

The input data to **FEM2D** for these two meshes are presented in Box 13.4.3, and the corresponding (edited) output in Box 13.4.4. The numerical results of this problem were discussed in Example 8.3.1.

Box 13.4.3 The input data to program **FEM2D** for the Poisson equation of Example 13.4.1.

```
Example 13.4.1: Solution of the Poisson equation (mesh of triangles)
  0   1   0   0                                   ITYPE,IGRAD,ITEM,NEIGN
  0   3   1   0                                   IELTYP,NPE,MESH,NPRNT
  2   2                                           NX,NY
  0.0  0.5  0.5                                   X0,DX(I)
  0.0  0.5  0.5                                   Y0,DY(I)
  5                                               NSPV
  3 1    6 1    7 1    8 1    9 1                 ISPV(I,J)
  0.0    0.0    0.0    0.0    0.0                 VSPV(I)
  0                                               NSSV
  1.0  0.0  0.0                                   A10, A1X, A1Y
  1.0  0.0  0.0                                   A20, A2X, A2Y
  0.0                                             A00
  0                                               ICONV
  1.0  0.0  0.0                                   F0,  FX,  FY

Example 13.4.1: Solution of the Poisson equation (mesh of rectangles)
  0   1   0   0                                   ITYPE,IGRAD,ITEM,NEIGN
  1   4   1   0                                   IELTYP,NPE,MESH,NPRNT
  2   2                                           NX,NY
  0.0  0.5  0.5                                   X0,DX(I)
  0.0  0.5  0.5                                   Y0,DY(I)
  5                                               NSPV
  3 1    6 1    7 1    8 1    9 1                 ISPV(I,J)
  0.0    0.0    0.0    0.0    0.0                 VSPV(I)
  0                                               NSSV
  1.0  0.0  0.0                                   A10, A1X, A1Y
  1.0  0.0  0.0                                   A20, A2X, A2Y
  0.0                                             A00
  0                                               ICONV
  1.0  0.0  0.0                                   F0,  FX,  FY
```

Box 13.4.4 The output from program **FEM2D** for the Poisson equation of Example 13.4.1.

```
Example 13.4.1: Solution of the Poisson equation on a square domain

          OUTPUT  from  program  FEM2DV2.5  by J. N. REDDY

              ANALYSIS  OF  A  POISSON/LAPLACE  EQUATION

   COEFFICIENTS OF THE DIFFERENTIAL EQUATION

      Coefficient, A10 ..........................=  0.1000E+01
      Coefficient, A1X ..........................=  0.0000E+00
      Coefficient, A1Y ..........................=  0.0000E+00
      Coefficient, A20 ..........................=  0.1000E+01
      Coefficient, A2X ..........................=  0.0000E+00
      Coefficient, A2Y ..........................=  0.0000E+00
      Coefficient, A00 ..........................=  0.0000E+00
```

(**Box 13.4.4** is continued from the previous page)

```
CONTINUOUS SOURCE COEFFICIENTS:

   Coefficient, F0  .........................=  0.1000E+01
   Coefficient, FX  .........................=  0.0000E+00
   Coefficient, FY  .........................=  0.0000E+00

   ******* A STEADY-STATE PROBLEM is analyzed *******
   *** A mesh of   TRIANGLES    is chosen by user ***

FINITE ELEMENT MESH INFORMATION:

   Element type: 0 = Triangle; >0 = Quad.)..=   0
   Number of nodes per element, NPE ........=   3
   No. of primary deg. of freedom/node, NDF =   1
   Number of elements in the mesh, NEM .....=   8
   Number of nodes in the mesh, NNM ........=   9
   Number of equations to be solved, NEQ ...=   9
   Half bandwidth of the matrix GLK, NHBW ..=   5
   Mesh subdivisions, NX and NY ............=   2   2

   No. of specified PRIMARY variables, NSPV =   5
```

Node	x-coord.	y-coord.	Speci. primary & secondary variables (0, unspecified; >0, specified) Primary DOF	Secondary DOF
1	0.0000E+00	0.0000E+00	0	0
2	0.5000E+00	0.0000E+00	0	0
3	0.1000E+01	0.0000E+00	1	0
4	0.0000E+00	0.5000E+00	0	0
5	0.5000E+00	0.5000E+00	0	0
6	0.1000E+01	0.5000E+00	1	0
7	0.0000E+00	0.1000E+01	1	0
8	0.5000E+00	0.1000E+01	1	0
9	0.1000E+01	0.1000E+01	1	0

```
NUMERICAL INTEGRATION DATA:

    Full integration polynomial degree, IPDF  = 3
    Number of full integration points,  NIPF  = 4
    Reduced integration polynomial deg.,IPDR  = 1
    No. of reduced integration points,  NIPR  = 1
    Integ. poly. deg. for stress comp., ISTR  = 1
    No. of integ. pts. for stress comp.,NSTR  = 1
```

(**Box 13.4.4** is continued from the previous page)

```
SOLUTION:

 Node   x-coord.      y-coord.     Primary DOF

   1   0.00000E+00  0.00000E+00  0.31250E+00
   2   0.50000E+00  0.00000E+00  0.22917E+00
   3   0.10000E+01  0.00000E+00  0.00000E+00
   4   0.00000E+00  0.50000E+00  0.22917E+00
   5   0.50000E+00  0.50000E+00  0.17708E+00
   6   0.10000E+01  0.50000E+00  0.00000E+00
   7   0.00000E+00  0.10000E+01  0.00000E+00
   8   0.50000E+00  0.10000E+01  0.00000E+00
   9   0.10000E+01  0.10000E+01  0.00000E+00

The orientation of gradient vector is measured from the positive x-axis

   x-coord.    y-coord. -a11(du/dx) -a22(du/dy) Flux Mgntd Orientation

0.3333E+00 0.1667E+00 0.1667E+00 0.1042E+00  0.1965E+00   32.01
0.1667E+00 0.3333E+00 0.1042E+00 0.1667E+00  0.1965E+00   57.99
0.8333E+00 0.1667E+00 0.4583E+00 0.0000E+00  0.4583E+00    0.00
0.6667E+00 0.3333E+00 0.3542E+00 0.1042E+00  0.3692E+00   16.39
0.3333E+00 0.6667E+00 0.1042E+00 0.3542E+00  0.3692E+00   73.61
0.1667E+00 0.8333E+00 0.0000E+00 0.4583E+00  0.4583E+00   90.00
0.8333E+00 0.6667E+00 0.3542E+00 0.0000E+00  0.3542E+00    0.00
0.6667E+00 0.8333E+00 0.0000E+00 0.3542E+00  0.3542E+00   90.00
```

Example 13.4.2 (Convective Heat Transfer)

Consider a square region of 1 m × 1 m. The left side of the region (i.e., $x = 0$) is maintained at 100°C, while the boundary $y = 1$ m is maintained at 500°C. The boundaries $x = 1$ m and $y = 0$ are exposed to an ambient temperature of 100°C, and the film coefficient $\beta = 10$ W/(m^2 · °C). There is no internal heat generation ($f = 0$). The conductivity is taken to be $k_x = k_y = 12.5$ W/(m · °C).

The input variables associated with convective boundary conditions are

ICONV = 1, NBE = 16 (for an 8 × 8 mesh of linear rectangular elements)

[IBN(I), BETA(I), TINF(I)] = [1, 10.0, 100.0; 2, 10.0, 100.0, . . .]

[INOD(I, J)] = [1, 2; 1, 2; . . .]

A10 = 12.5, A1X = 0.0, A1Y = 0.0, A20 = 12.5,

A2X = 0.0, A2Y = 0.0, A00 = 0.0

Box 13.4.5 contains the input data for the 8×8 mesh of linear rectangular elements. The output for this problem is not included here, but the results are included in the form of figures. Plots of temperature variations and heat flow

$$q_x = -k_x \frac{\partial T}{\partial x}, \quad q_y = -k_y \frac{\partial T}{\partial y}$$

along the boundaries are shown in Fig 13.4.4 and 13.4.5, respectively. Note that q_x is linear in x and constant in y, and q_y is linear in y and constant in x (for constant k_x and k_y). A nonuniform mesh with smaller elements in the high-gradient region gives more accurate results:

$$\{\text{DY(I)}\} = \{\text{DX(I)}\} = (0.25,\ 0.125,\ 0.125,\ 0.125,\ 0.125,\ 0.125,\ 0.0625,\ 0.0625)$$

Box 13.4.5 The input data to program **FEM2D** for the convective heat transfer problem of Example 13.4.2.

```
Example 13.4.2: Convective heat transfer in a square region
0   1   0    0                                  ITYPE,IGRAD,ITEM,NEIGN
1   4   1    0                                   IELTYP,NPE,MESH,NPRNT
8   8                                                            NX,NY
0.0  0.125  0.125  0.125  0.125  0.125  0.125
     0.125  0.125                                              X0,DX(I)
0.0  0.125  0.125  0.125  0.125  0.125  0.125
     0.125  0.125                                              Y0,DY(I)

17                                                               NSPV
 1 1   10 1   19 1   28 1   37 1   46 1   55 1   64 1   73 1
74 1   75 1   76 1   77 1   78 1   79 1   80 1   81 1    ISPV(I,J)
100.0  100.0  100.0  100.0  100.0  100.0  100.0  100.0  500.0
500.0  500.0  500.0  500.0  500.0  500.0  500.0  500.0   VSPV(I)
0                                                                NSSV

12.5   0.0   0.0                                        A10, A1X, A1Y
12.5   0.0   0.0                                        A20, A2X, A2Y
 0.0                                                             A00

 1                                                             ICONV
16                                                  NBE; IBN, BETA, TINF
 1 10.0  100.0   2 10.0  100.0   3 10.0  100.0   4 10.0  100.0
 5 10.0  100.0   6 10.0  100.0   7 10.0  100.0   8 10.0  100.0
 8 10.0  100.0  16 10.0  100.0  24 10.0  100.0  32 10.0  100.0
40 10.0  100.0  48 10.0  100.0  56 10.0  100.0  64 10.0  100.0
 1 2  1 2   1 2   1 2   1 2  1 2   1 2   1 2   2 3  2 3
 2 3  2 3   2 3   2 3   2 3  2 3                          INOD(I,J)

 0.0   0.0   0.0                                          F0, FX, FY
```

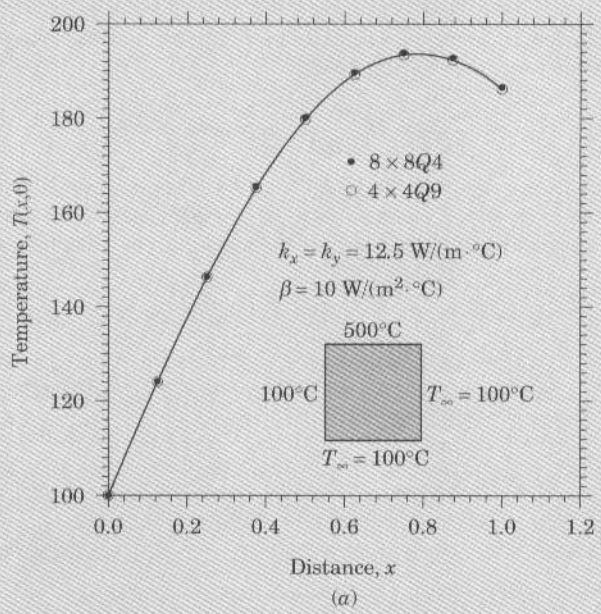

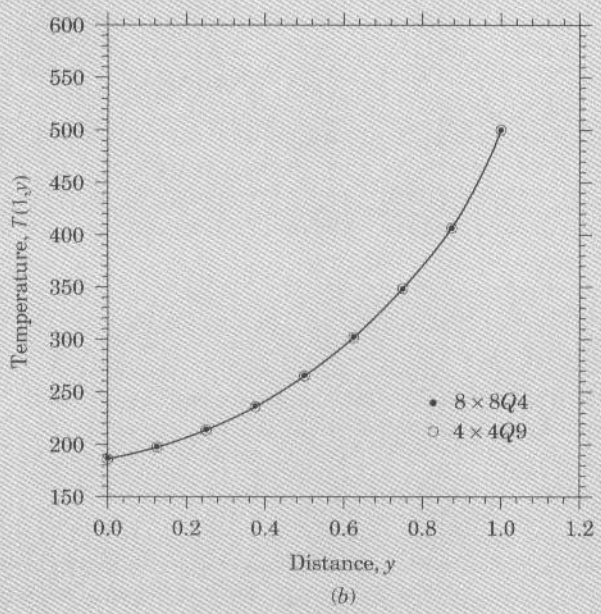

Figure 13.4.4 Temperature variations along the boundaries (*a*) $y = 0$ and (*b*) $x = 1$ for the convective heat transfer problem of Example 13.4.2: 4Q9, 4×4 mesh of nine-node quadrilateral elements; 8Q4, 8×8 mesh of four-node quadrilateral elements.

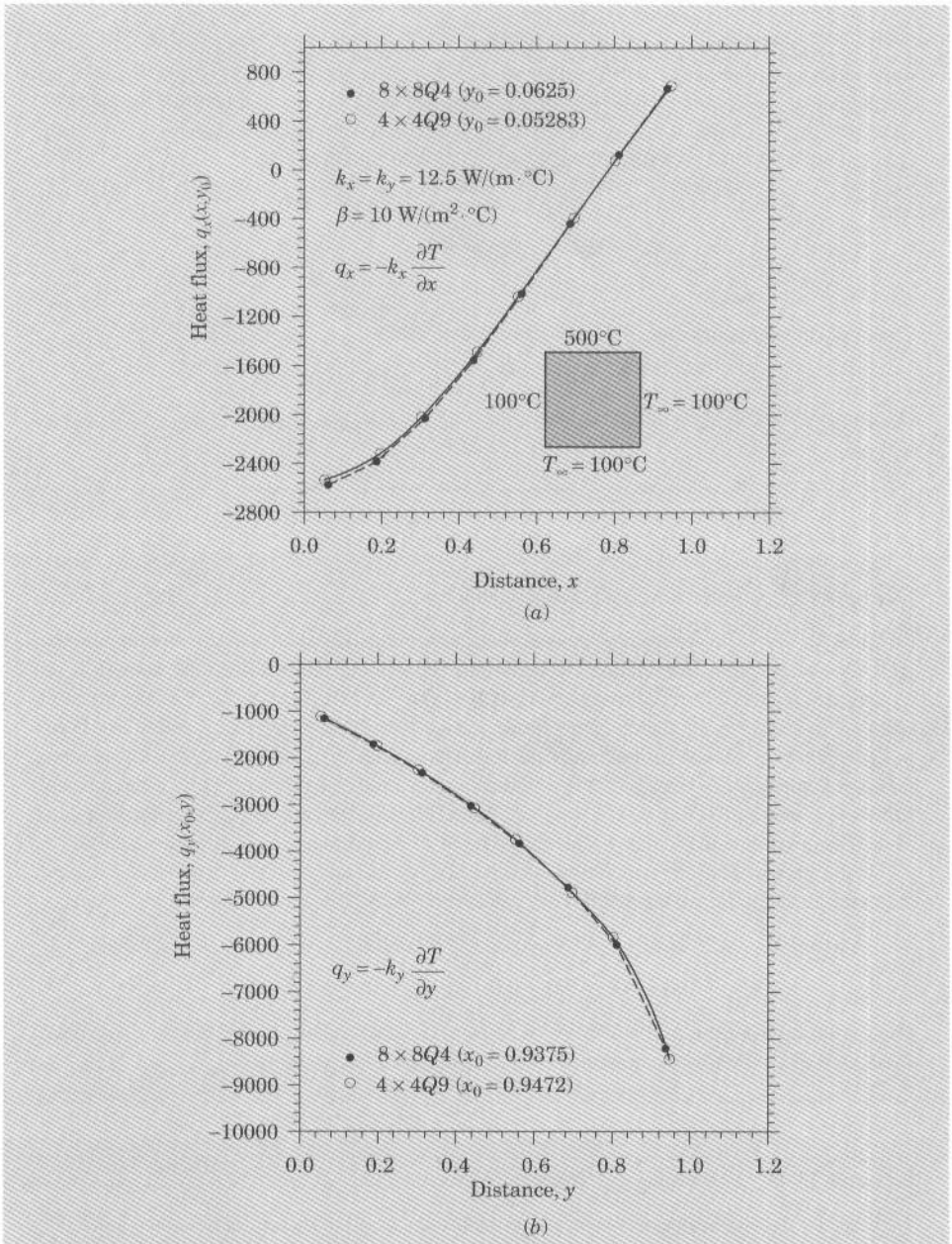

Figure 13.4.5 Variations of the heat flow along the (*a*) vertical ($x_0 = 0.9472$ and $x_0 = 0.9375$) and (*b*) horizontal ($y_0 = 0.05283$ and $y_0 = 0.0625$) boundaries (at the Gauss points nearest to the boundaries). See Fig. 13.4.4 for the explanation of the notation 4Q9 and 8Q4.

The program can also be used to analyze axisymmetric problems. For example, consider a finite cylinder of radius $R_0 = 1$ m and length $L = 1$ m. The bottom and top of the cylinder are maintained at $T_0 = 100°C$, while the surface is exposed to an ambient temperature $T_\infty = 100°C$ ($\beta = 10 W/(m^2 \cdot °C)$. For this case, the governing differential equation is given by (8.5.11). The coefficients A10, A1X, A1Y, A20, A2X, A2Y, and A00 for **FEM2D** are

$$\text{A10} = 0.0, \quad \text{A1X} = 2\pi k_r, \quad \text{A1Y} = 0.0$$
$$\text{A20} = 0.0, \quad \text{A2X} = 2\pi k_z, \quad \text{A2Y} = 0.0$$
$$\text{A00} = 0.0$$

The uniform heat generation f_0 (if not zero) is entered as

$$\text{F0} = 0.0, \quad \text{FX} = 2\pi f_0, \quad \text{FY} = 0.0$$

For a mesh of $m \times n$ mesh of linear elements, the number of elements with convective boundary will be n.

Example 13.4.3 (Flow around a Circular Cylinder)

Consider the flow of an inviscid fluid around a cylinder. We shall use the stream function and velocity potential formulations to determine the velocity fields. Since the domain is not rectangular, we should use subroutine **MESH2DG** (i.e., set MESH = 2). We consider the mesh of 25 nodes and 32 triangular elements shown in Fig. 13.4.2. We have ITYPE = 0; IGRAD = 1 in the velocity potential formulation and IGRAD = 2 in the stream function formulation; ITEM = 0 and NEIGN = 0; IELTYP = 0 for triangles and IELTYP = 1 for quadrilaterals; and MESH = 2 and NPRNT = 0. The input for **MESH2DG** is given in Box 13.4.1 for triangular as well as quadrilateral elements. The partial input of the problem is given in Box 13.4.6.

In the stream function formulation, we have NSPV = 13 and NSSV = 0; and in the velocity potential formulation, we have NSPV = 5 and NSSV = 3. The coefficients are

$$\text{A10} = 1.0, \quad \text{A20} = 1.0, \quad \text{A1X} = 0.0, \quad \text{A1Y} = 0.0, \quad \text{A2X} = 0.0, \quad \text{A2Y} = 0.0$$
$$\text{A00} = 0.0, \quad \text{F0} = 0.0, \quad \text{FX} = 0.0, \quad \text{FY} = 0.0$$

The partial input of the problem is given in Box 13.4.6 (see Box 13.4.1 for the mesh data). A detailed discussion of the numerical results is presented in Example 8.5.5.

Example 13.4.4 (Eigenvalue and Transient Analysis)

We consider the eigenvalue and transient problems discussed in Examples 8.6.1 and 8.6.2. The governing differential equation is [see Eqs. (8.6.12*a*)–(8.6.12*c*)]

$$\frac{\partial u}{\partial t} - \left(\frac{\partial^2 u}{\partial x^2} + \frac{\partial^2 u}{\partial y^2} \right) = 1$$
$$\frac{\partial u}{\partial x}(0, y, t) = 0, \quad \frac{\partial u}{\partial y}(x, 0, t) = 0, \quad u(x, 1, t) = 0, \quad u(1, y, t) = 0$$
$$u(x, y, 0) = 0$$

Box 13.4.6 The input data to program **FEM2D** for the flow of an inviscid fluid around a cylinder.

```
Example 13.4.3(a): Flow around a circular cylinder (VEL.POTENTIAL)
  0   1   0   0                                    ITYPE,IGRAD,ITEM,NEIGN
  0   3   2   0                                    IEL, NPE, MESH, NPRNT

 *** See TABLE 13.4.1(a) for the MESH2DG input ***

  5                                                NSPV
 21 1  22 1  23 1  24 1  25 1                      ISPV(I,J)
  0.0   0.0   0.0   0.0   0.0                      VSPV(I)
  3                                                NSSV
  1 1   6 1  11 1                                  ISSV(I,J)
  0.5   1.0   0.5                                  VSSV(I)
  1.0  0.0  0.0                                    A10, A1X, A1Y
  1.0  0.0  0.0                                    A20, A2X, A2Y
  0.0                                              A00
  0                                                ICONV
  0.0  0.0  0.0                                    F0, FX, FY

Example 13.4.3(b): Flow around a circular cylinder(STRM FUNCN)
  0   2   0   0                                    ITYPE,IGRAD,ITEM,NEIGN
  0   3   2   0                                    IELTYP,NPE,MESH,NPRNT

  *** See TABLE 13.4.1(a) for the MESH2DG input ***

 13                                                NSPV
  1 1   2 1   3 1   4 1   5 1   10 1   15 1   20 1   25 1
  6 1  11 1  16 1  21 1                            ISPV(I,J)
  0.0   0.0   0.0   0.0   0.0    0.0    0.0    0.0    0.0
  1.0   2.0   2.0   2.0                            VSPV(I)
  0                                                NSSV

*** Remaining data is the same as in Example 13.4.3(a) above ***
```

For eigenvalue analysis, we set ITEM = 1 and NEIGN = 1; for the transient analysis, we set ITEM = 1 (parabolic equation) and NEIGN = 0. In addition, we must input the following parameters:

Eigenvalue Analysis

NVALU (number of eigenvalues to be printed) and NVCTR (if eigenvectors to be printed).

Transient Analysis

$$\text{NTIME} = 20,\quad \text{NSTP} = 21,\ (> \text{NTIME}),\quad \text{INTVL} = 1$$

$$\text{INTIAL} = 0,\quad \text{DT} = 0.05,\quad \text{ALFA} = 0.5,\quad \text{GAMA} = 0.5 \text{ (not used)}$$

$$\text{C0} = 1.0,\quad \text{CX} = 0.0,\quad \text{CY} = 0.0$$

The parameter NSTP allows removal of the source (i.e., f) at a given time step. For example, if NSTP = 5, then at the fifth time step and at each subsequent time step f will be set equal to zero. In the present case, the source $f = 1$ is kept at all times; hence, we must choose NSTP to be greater than NTIME (say NSTP = 21).

The input files and partial output for the eigenvalue and transient analyses are presented in Boxes 13.4.7 and 13.4.8, respectively. For a discussion of the numerical results of these two problems, see Examples 8.6.1 and 8.6.2.

The problems in Examples 8.6.3 and 8.6.4 can be analyzed using **FEM2D**, with minor changes to the input data given in Boxes 13.4.7 and 13.4.8. The input data for the two problems of Examples 8.6.3 and 8.6.4 is included in Box 13.4.9.

Box 13.4.7 The input data and partial output of program **FEM2D** for the eigenvalue analysis of a parabolic equation (Example 13.4.4).

```
Example 13.4.4:  EIGENVALUE ANALYSIS of a parabolic equation
   0   0   1    1                              ITYPE,IGRAD,ITEM,NEIGN
  16   0                                       NVALU, NVCTR
   1   4   1    0                              IELTYP,NPE,MESH,NPRNT
   4   4                                       NX, NY
   0.0  0.25  0.25  0.25  0.25                  X0,DX(I)
   0.0  0.25  0.25  0.25  0.25                  Y0,DY(I)
   9                                           NSPV
   5 1   10 1   15 1     20 1   21 1
  22 1   23 1   24 1     25 1                  ISPV
  1.0    0.0    0.0                           A10, A1X, A1Y
  1.0     0.0    0.0                          A20, A2X, A2Y
  0.0                                         A00
  0                                           ICONV
  1.0   0.0   0.0                            C0, CX, CY
    S O L U T I O N (from FEM2D):
       Number of Jacobi iterations ..... NROT = 371
       E I G E N V A L U E  (1) = 0.343256E+03
       E I G E N V A L U E  (2) = 0.253701E+03
       E I G E N V A L U E  (3) = 0.253701E+03
       E I G E N V A L U E  (4) = 0.196500E+03
       E I G E N V A L U E  (5) = 0.196500E+03
       E I G E N V A L U E  (6) = 0.174127E+03
       E I G E N V A L U E  (7) = 0.174127E+03
       E I G E N V A L U E  (8) = 0.164145E+03
       E I G E N V A L U E  (9) = 0.106945E+03
       E I G E N V A L U E (10) = 0.106945E+03
       E I G E N V A L U E (11) = 0.845720E+02
       E I G E N V A L U E (12) = 0.845720E+02
       E I G E N V A L U E (13) = 0.497442E+02
       E I G E N V A L U E (14) = 0.273714E+02
       E I G E N V A L U E (15) = 0.273714E+02
       E I G E N V A L U E (16) = 0.499854E+01
```

Box 13.4.8 The input data and partial output of program **FEM2D** for the transient analysis of a parabolic equation (Example 13.4.4).

```
Example 13.4.4: TRANSIENT ANALYSIS of a parabolic equation
   0   0   1   0                                  ITYPE,IGRAD,ITEM,NEIGN
   1   4   1   0                                  IELTYP,NPE,MESH,NPRNT
   4   4                                          NX,NY
   0.0  0.25   0.25   0.25   0.25                 X0,DX(I)
   0.0  0.25   0.25   0.25   0.25                 Y0,DY(I)
   9                                              NSPV
    5 1  10 1  15 1  20 1  21 1  22 1
   23 1  24 1  25 1                               ISPV
   0.0 0.0 0.0 0.0 0.0 0.0 0.0 0.0 0.0            VSPV
   0                                              NSSV
   1.0  0.0  0.0                                  A10, A1X, A1Y
   1.0  0.0  0.0                                  A20, A2X, A2Y
   0.0                                            A00
   0                                              ICONV
   1.0  0.0  0.0                                  F0, FX, FY
   1.0  0.0  0.0                                  C0, CX, CY
   20    21    1    0                            NTIME,NSTP,INTVL,INTIAL
   0.05  0.5  0.5  1.0E-3                         DT,ALFA,GAMA,EPSLN


  Edited output from FEM2D

    *TIME* = 0.50000E-01          Time Step Number = 1
    S O L U T I O N :

    Node    x-coord.          y-coord.          Primary DOF

      1   0.00000E+00       0.00000E+00       0.49867E-01
      2   0.25000E+00       0.00000E+00       0.49718E-01
      3   0.50000E+00       0.00000E+00       0.48620E-01
      4   0.75000E+00       0.00000E+00       0.41808E-01

    *TIME*= 0.10000E+01           Time Step Number = 20
    S O L U T I O N :

    Node    x-coord.          y-coord.          Primary DOF

      1   0.00000E+00       0.00000E+00       0.29621E+00
      2   0.25000E+00       0.00000E+00       0.28037E+00
      3   0.50000E+00       0.00000E+00       0.23065E+00
      4   0.75000E+00       0.00000E+00       0.14053E+00
```

Box 13.4.9 The input data and partial output of program **FEM2D** for vibration and transient analysis of the rectangular membrane of Examples 8.6.3 and 8.6.4.

```
Example 13.4.4: Natural vibration of a rectangular membrane
   0   0   2   1                          ITYPE,IGRAD,ITEM,NEIGN
  10   0                                  NVALU, NVCTR
   1   4   1   0                          IELTYP,NPE,MESH,NPRNT
   4   4                                  NX,NY
   0.0  1.0  1.0  1.0  1.0                X0,DX(I)
   0.0  0.5  0.5  0.5  0.5                Y0,DY(I)
  16                                      NSPV
   1 1   2 1   3 1   4 1   5 1   6 1   10 1   11 1
  15 1  16 1  20 1  21 1  22 1  23 1   24 1   25 1
  12.5  0.0  0.0                         A10, A1X, A1Y
  12.5  0.0  0.0                         A20, A2X, A2Y
   0.0                                   A00
   0                                     ICONV
   2.5  0.0  0.0                         C0, CX, CY

Example 13.4.4: Transient analysis of a rectangular membrane
   0   0   2   0                          ITYPE,IGRAD,ITEM,NEIGN
   1   4   1   0                          IELTYP,NPE,MESH,NPRNT
   4   4                                  NX,NY
   0.0  0.5    0.5    0.5    0.5         X0,DX(I) (a quadrant)
   0.0  0.25   0.25   0.25   0.25        Y0,DY(I)  (is used)
   9                                      NSPV
   5 1  10 1  15 1  20 1  21 1  22 1  23 1  24 1  25 1  ISPV
   0.0   0.0   0.0   0.0   0.0   0.0   0.0   0.0   0.0  VSPV
   0                                     NSSV
   12.5  0.0  0.0                        A10, A1X, A1Y
   12.5  0.0  0.0                        A20, A2X, A2Y
    0.0                                  A00
   0                                     ICONV
    0.0  0.0  0.0                        F0, FX, FY
    2.5  0.0  0.0                        C0, CX, CY
   20    21    1    1                   NTIME,NSTP,INTVL,INTIAL
   0.025 0.5  0.5  1.0E-3                DT,ALFA,GAMA,EPSLN
   0.400   0.375    0.300    0.175     0.0
   0.375   0.35156  0.28125  0.16406   0.0
   0.300   0.28125  0.225    0.13125   0.0
   0.175   0.16406  0.13125  0.076563  0.0
   0.0     0.0      0.0      0.0       0.0  Ini. cond., GLU(I)
   0.0     0.0      0.0      0.0       0.0
   0.0     0.0      0.0      0.0       0.0
   0.0     0.0      0.0      0.0       0.0
   0.0     0.0      0.0      0.0       0.0
   0.0     0.0      0.0      0.0       0.0
   0.0     0.0      0.0      0.0       0.0  Ini. cond., GLV(I)
```

Example 13.4.5 (Fluid Squeezed between Parallel Plates)

We set up the data for a 12×8 uniform mesh of linear rectangular elements and the equivalent 6×4 mesh of nine-node elements. Most of the data is exactly the same for both meshes. We have

$$\text{ITYPE} = 1, \quad \text{IGRAD} = 1, \quad \text{ITEM} = 0 \text{ (for static analysis)}$$
$$\text{ITEM} = 1 \text{ (for transient analysis)}, \quad \text{NEIGN} = 0$$
$$\text{NX} = 6, \quad \text{NY} = 4, \quad \text{NSPV} = 47$$
$$\text{AMU}(= \mu) = 1.0, \quad \text{PENLTY}(= \gamma) = 10^8$$

Box 13.4.10 contains the complete input data for the 6×4 mesh of nine-node elements for the transient case. For additional details, see Examples 10.6.1 and 10.6.4.

Box 13.4.10 The input data to program **FEM2D** for the transient analysis of fluid squeezed between plates (Example 13.4.5).

```
Example 13.4.5: TRANSIENT ANALYSIS of fluid squeezed between plates
   1   1   1   0                                        ITYPE,IGRAD,ITEM,NEIGN
   2   9   1   0                                        IEL, NPE, MESH, NPRNT
   6   4                                                NX, NY
   0.0  1.0  1.0  1.0  1.0  1.0  1.0                    X0, DX(I)
   0.0  0.5  0.5  0.5  0.5                              Y0, DY(I)
   47                                                   NSPV
    1 1    1 2    2 2    3 2    4 2    5 2    6 2    7 2    8 2    9 2
   10 2   11 2   12 2   13 2   14 1   27 1   40 1   53 1   66 1   79 1
   92 1  105 1  105 2  106 1  106 2  107 1  107 2  108 1  108 2  109 1
  109 2  110 1  110 2  111 1  111 2  112 1  112 2  113 1  113 2  114 1
  114 2  115 1  115 2  116 1  116 2  117 1  117 2  ISPV(I,J)
    0.0    0.0    0.0    0.0    0.0    0.0    0.0    0.0    0.0    0.0
    0.0    0.0    0.0    0.0    0.0    0.0    0.0    0.0    0.0    0.0
    0.0    0.0   -1.0    0.0   -1.0    0.0   -1.0    0.0   -1.0    0.0
   -1.0    0.0   -1.0    0.0   -1.0    0.0   -1.0    0.0   -1.0    0.0
   -1.0    0.0   -1.0    0.0   -1.0    0.0   -1.0  VSPV(I)
   0                                                    NSSV
   1.0    1.0E8                                         AMU,PENLTY
   0.0    0.0    0.0                                    F0, FX, FY
   1.0    0.0    0.0                                    C0, CX, CY
   20     50     1     0                                NTIME,NSTP,INTVL,INTIAL
   0.1    0.5    0.25  1.0D-3                           DT, ALFA, GAMA, EPSLN
```

The next example deals with plane elasticity problem of Examples 11.7.2 and 11.7.3.

Example 13.4.6 (Elasticity Problem)

This is a plane elasticity problem with plane stress assumption (i.e., LNSTRS = 1). Here we consider both triangular and rectangular element meshes (see Fig. 13.4.6); **MESH2DR** can be used to generate the meshes (i.e., MESH = 1). For the 8 × 2 mesh of linear elements, we have the following input parameters:

$$\text{ITYPE} = 2, \quad \text{IGRAD} = 1 \quad (\text{or} > 0), \quad \text{ITEM} = 0$$

for static analysis and ITEM = 2 for dynamic analysis. There are four specified primary variables and three nonzero specified forces for the mesh:

$$\text{NSSV} = 4, \quad \text{ISVP(I, J)} = (9, 1; 18, 1; 18, 2; 27, 1)$$

$$\text{VSPV(I)} = (0.0,\ 0.0,\ 0.0,\ 0.0)$$

$$\text{NSSV} = 3, \quad \text{ISSV(I, J)} = (1, 2; 10, 2; 19, 2), \quad \text{VSSV(I)} = (-75.0, -150.0, -75.0)$$

For the 4 × 1 mesh of nine-node quadratic elements, the data remains the same as above, except for the values of the specified forces (−50.0, −200.0, −50.0).

Box 13.4.11 contains the data sets for natural vibration and transient analysis for the 4 × 1 mesh of nine-node quadratic elements. The data for the static case follows easily from the transient case. The results were discussed in Examples 11.7.2 and 11.7.3.

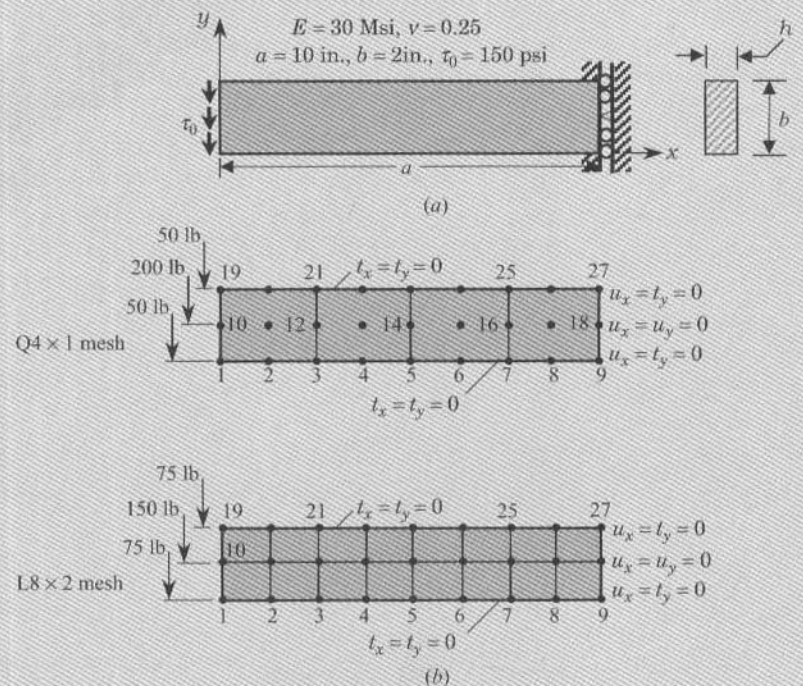

Figure 13.4.6 Bending of a cantilever plate using the elasticity equations: (*a*) geometry and loading; and (*b*) meshes of four-node linear elements (8 × 2) and nine-node quadratic elements (4 × 1).

Box 13.4.11 The input data to program **FEM2D** for natural vibration and transient analysis of a cantilever plate (Example 13.4.6).

```
Example 13.4.6: Natural vibration of a beam by plane elasticity
   2   0   2   1                                   ITYPE,IGRAD,ITEM,NEIGN
   10  0                                           NVALU,NVCTR
   2   9   1   0                                   IELTYP,NPE,MESH,NPRNT
   4   1                                           NX, NY
   0.0  2.5   2.5   2.5    2.5                     X0, DX(I)
   0.0  2.0                                       Y0, DY(I)
   4                                               NSPV
   9 1   18 1   18 2   27  1                       ISPV
   1                                               LNSTRS
   30.0E06  30.0E06  0.25  12.0E06  1.0           E1,E2,ANU12,G12,THKNS
   8.8255E-03  0.0   0.0                           C0, CX, CY

Example 13.4.6: Transient analysis of a beam by plane elasticity
   2   1   2   0                                   ITYPE,IGRAD,ITEM,NEIGN
   2   9   1   0                                   IELTYP,NPE,MESH,NPRNT
   4   1                                           NX, NY
   0.0  2.5   2.5   2.5   2.5                     X0,DX(I)
   0.0  2.0                                       Y0,DY(I)
   4                                               NSPV
   9 1  18 1   18 2   27 1                        ISPV
   0.0  0.0    0.0    0.0                         VSPV
   3                                               NSSV
   1  2  10  2  19 2                              ISSV
  -50.0 -200.0  -50.0                             VSSV
   1                                               LNSTRS
   30.0E06  30.0E06  0.25   12.0E06  1.0          E1,E2,ANU12,G12,THKNS
   0.0    0.0   0.0                               F0, FX, FY
   8.8255E-03  0.0  0.0                           C0, CX, CY
   20   21   1    0                               NTIME,NSTP,INTVL,INTIAL
   0.25E-03     0.5  0.5  1.0E-3                   DT,ALFA,GAMA,EPSLN
```

The next two examples are concerned with plate bending problems (see Chapter 12).

Example 13.4.7 (Bending of a Plate)

Consider bending of a square plate under uniformly distributed load. The 1×1 mesh of Hermite elements and 4×4 mesh of nine-node elements are used to model the square plate. Only rectangular elements are allowed:

Classical Plate Theory (CPT) (ITYPE = 4 or 5)

ITYPE = 5 (conforming element), IGRAD = 1

Shear Deformation Theory (SDT)

$$\text{ITYPE} = 3, \quad \text{IGRAD} = 1$$

The classical plate model has three degrees of freedom per node when the nonconforming element is used (i.e., ITYPE = 4), and four degrees of freedom per node for the conforming element (i.e., ITYPE = 5). This must be taken into consideration in specifying boundary conditions. For additional details, see Example 12.5.1.

The input data for static analysis of a simply supported, square, isotropic plate using CPT(C) and SDT models is presented in Box 13.4.12. A quadrant of the plate is used as the computational domain. For the nonconforming element, the data is the same as that used for the shear deformation model, except that ITYPE = 4. For free vibration (NEIGN = 1) and stability analysis (NEIGN = 2), most of the data remain the same. For transient analysis, the time step used for unconditionally stable schemes is arbitrary, but should be small enough to give a complete and accurate response curve.

Box 13.4.12 The input data to program **FEM2D** for (static) bending analysis of a simply supported, square, isotropic plate (see Fig. 12.5.1).

```
Example 13.4.7: Bending of a simply-supported plate (SDT)
   3   1   0   0                          ITYPE,IGRAD,ITEM,NEIGN
   1   4   1   0                          IEL, NPE, MESH, NPRNT
   4   4                                  NX, NY
   0.0  1.25   1.25   1.25  1.25          X0, DX(I)
   0.0  1.25   1.25   1.25  1.25          Y0, DY(I)
   27                                     NSPV
    1 2    1 3    2 3    3 3    4 3     5 1    5 3    6 2   10 1
   10 3   11 2   15 1   15 3   16 2    20 1   20 3   21 1   21 2
   22 1   22 2   23 1   23 2   24 1    24 2   25 1   25 2   25 3
   0.0    0.0    0.0    0.0    0.0     0.0    0.0    0.0    0.0
   0.0    0.0    0.0    0.0    0.0     0.0    0.0    0.0    0.0
   0.0    0.0    0.0    0.0    0.0     0.0    0.0    0.0    0.0
   0                                     NSSV
   1.0E7 1.0E7 0.25 0.4E7 0.4E7 0.4E7 1.0  E1,E2,ANU12,G12, etc.
   1.0   0.0   0.0                       F0, FX, FY

 Example 13.4.7: Bending of a simply-supported plate [CPT(C)]
   5   1   0   0                          ITYPE,IGRAD,ITEM,NEIGN
   1   4   1   0                          IEL, NPE, MESH, NPRNT
   1   1                                  NX, NY
   0.0  5.0                               X0, DX(I)
   0.0  5.0                               Y0, DY(I)
   12                                     NSPV
   1  2   1  3   2  1   2  3   3  1   3  2   4  1   4  2
   4  3   1  4   2  4   3  4              ISPV(I,J)

   0.0    0.0    0.0    0.0    0.0    0.0    0.0    0.0
   0.0    0.0    0.0    0.0           VSPV(I)

   0                                     NSSV
   1.0E7  1.0E7  0.25  0.4E7  0.4E7  0.4E7 1.0 E1,E2,ANU12,G12,etc.
   1.0    0.0    0.0                     F0,FX, FY
```

Example 13.4.8 (Transient Response of a Clamped Circular Plate)

Consider a clamped circular plate of radius $R = 100$ in., thickness $h = 20$ in., modulus $E = 100$ psi, Poisson's ratio $\nu = 0.3$, and density $\rho = 10$ slug/in.^{3}, and subjected to a suddenly applied pressure load of intensity $q_0 = 1$ psi. We analyze the problem by modeling one quadrant (using the symmetry) of the plate by five nine-node elements (see Fig. 13.4.7) and $\Delta t = 2.5$ s. The input data to **FEM2D** is presented in Box 13.4.13. Plots of the center deflection and stress versus time are shown in Fig. 13.4.8.

Box 13.4.13 The input data to program **FEM2D** for transient analysis of a clamped, circular, isotropic plate under uniform load.

```
Example 13.4.8: Transient analysis of a circular plate (SDT)
   3    1    2    0                                   ITYPE,IGRAD,ITEM,NEIGN
   2    9    0    0                                   IEL, NPE, MESH, NPRNT
   5   29                                             NEM, NNM
   1    5    7    9    2    6    8    4    3         NOD(1,I), I=1,NPE
   5   15   17    7   10   16   12    6   11         NOD(2,I), I=1,NPE
   9    7   17   19    8   12   18   14   13         NOD(3,I), I=1,NPE
  15   25   27   17   20   26   22   16   21         NOD(4,I), I=1,NPE
  19   17   27   29   18   22   28   24   23         NOD(5,I), I=1,NPE
  0.0000  0.0000   16.5000   0.0000                  11.6673  11.6673
  0.0000  16.5     33.0      0.0                     30.488   12.6286
  23.3345 23.3345  12.6286   30.488                  0.0      33.0
  49.5    0.0      45.732    18.9428                 35.0     35.0
  18.9428 45.732   0.0       49.5                    66.0     0.0
  60.976  25.2571  46.669    46.669                  25.2571  60.976
  0.0     66.0     83.0      0.0                     76.682   31.7627
  58.6898 58.6898  31.7627   76.682                  0.0      83.0
  100.0   0.0      92.388    38.2683                 70.7107  70.7107
  38.2683 92.388   0.0       100.0                   GLXY(I,J)
   27                                                NSPV
    1 2     1 3      2 3      4 2      5 3          9 2     10 3     14 2     15 3
   19 2    20 3     24 2     25 1     25 2          25 3    26 1     26 2     26 3
   27 1    27 2     27 3     28 1     28 2          28 3    29 1     29 2     29 3
   0.0     0.0      0.0      0.0      0.0           0.0     0.0      0.0      0.0
   0.0     0.0      0.0      0.0      0.0           0.0     0.0      0.0      0.0
   0.0     0.0      0.0      0.0      0.0           0.0     0.0      0.0      0.0
   0                                                NSSV
  1.0E2 1.0E2  0.3 0.3845E2 0.3845E2 0.3845E2 20.0 E1,E2, etc.
   1.0   0.0    0.0                                FO, FX, FY
  10.0   0.0    0.0                                CO, CX, CY
   200   201     10    0                           NTIME,NSTP,INTVL,INTIAL
   2.5   0.5    0.5   1.0E-03                      DT, ALFA, GAMA, EPSLN
```

13.5 SUMMARY

A description of finite element computer program **FEM2D** and its application to problems discussed in Chapters 8–12 have been presented. The program can be used to analyze two-dimensional field problems and problems of plane elasticity, two-dimensional flows of viscous incompressible fluids, and plate bending. It allows static, eigenvalue, and time-dependent analyses. Linear and quadratic, and triangular and rectangular elements can be used. The program **FEM2D** is a true reflection of the theory presented in Chapters 8–12, and it can be extended to analyze other field problems with appropriate modifications.

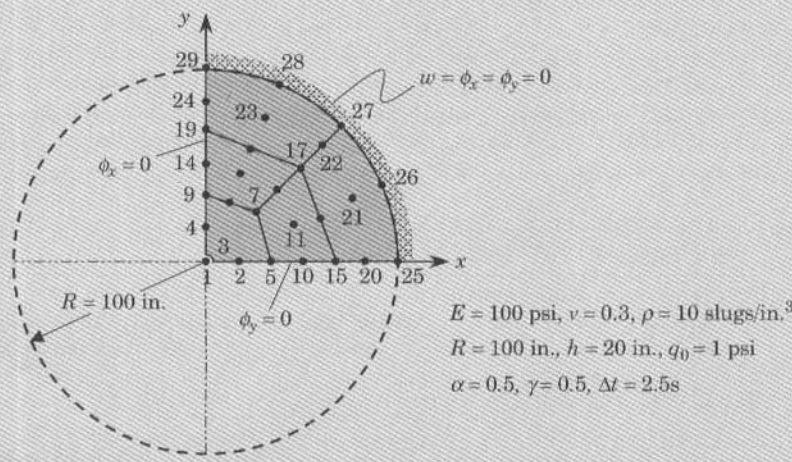

Figure 13.5.7 The geometry, boundary conditions, and finite element mesh of the clamped circulate plate of Example 13.4.8.

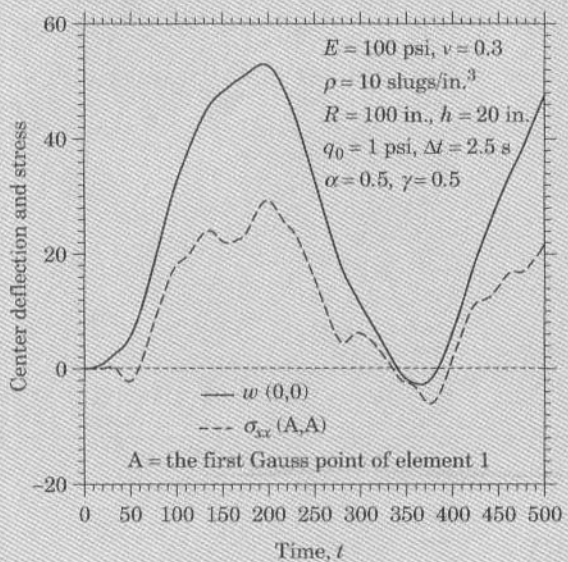

Figure 13.5.8 Center deflection and stress versus time for the clamped circular plate of Example 13.4.8.

PROBLEMS

Note that most of the problems may be analyzed using **FEM2D**. The results obtained from the program should be evaluated for their accuracy in the light of analytical solutions for qualitative understanding of the solutions of the problems. New problems can be generated from those given here by changing the problem data, mesh, type of element, etc. For time-dependent problems, the time step (whose order of magnitude is given by the critical time step) and number of time steps should be chosen such that the solution pattern is established or a steady state is reached. When specific material properties are not given, use values such that the solution can be interpreted as the nondimensional solution of the problem.

General Field Problems (Chapter 8)

13.1 Investigate the convergence of solutions to Problem 8.18 using 2×2, 4×4, and 8×8 meshes of linear triangular elements, and compare the results (in graphical or tabular form) with the analytical solution.

13.2 Repeat Problem 13.1 with rectangular elements.

13.3 Repeat Problem 13.1 for the case $u_0(x) = 1$ (see Problem 8.19 for the analytical solution).

13.4 Repeat Problem 13.3 with rectangular elements.

13.5 Investigate the convergence of the solution to Problem 8.23 using 2×2, 4×4, and 8×8 meshes of linear triangular elements and equivalent meshes of quadratic triangular elements. *Answer:* For a 4×4 mesh of quadratic triangles, the values of $u(x, 0.125)$ at nodes 11 through 17 are 0.1145, 0.1977, 0.2829, 0.3787, 0.4880, 0.6111, and 0.7436.

13.6 Repeat Problem 13.5 using rectangular elements. *Answer:* For a 4×4 mesh of quadratic rectangles, the values of $u(x, 0.125)$ at nodes 11 through 17 are 0.1165, 0.1982, 0.2834, 0.3789, 0.4884, 0.6114, and 0.7449.

13.7 Analyze the axisymmetric problem in Problem 8.26 using 4×1 and 8×1 linear rectangular elements, and compare the solution with the exact solution. *Answer:* For a 8×1 mesh the values at $r = 0$, 0.005, 0.01, 0.015 and 0.02 are: $U_1 = 150.53$, $U_3 = 147.05$, $U_5 = 137.59$, and $U_7 = 121.91$. The exact values are $T_1 = 150.0$, $T_2 = 146.875$, $T_3 = 137.50$, and $T_4 = 121.875$.

13.8 Analyze the axisymmetric problem in Problem 8.27 using 4×4 and 8×8 meshes of linear rectangular elements.

13.9 Analyze Problem 8.18 for eigenvalues (take $c = 1.0$), using a 4×4 uniform mesh of triangular elements. Calculate the critical time step for a parabolic equation. *Answer:* $\Delta t_{\text{cri}} = 2.172 \times 10^{-3}$.

13.10 Analyze Problem 8.18 using a 4×4 mesh of triangles for transient response. Assume zero initial conditions. Use $\alpha = 0.5$ and $\Delta t = 0.001$. Investigate the stability of the solution when $\alpha = 0.0$ and $\Delta t = 0.0025$. The number of time steps should be such that the solution reaches its peak value or a steady state.

13.11 Analyze Problem 8.23 for transient response (take $c = 1.0$) using a 4×4 mesh of linear rectangular elements and a 2×2 mesh of nine-node quadratic rectangular elements. Assume zero initial conditions. Investigate the stability and accuracy of the Crank–Nicolson scheme ($\alpha = 0.5$) and the forward difference scheme ($\alpha = 0$).

13.12 Repeat Problem 13.11 for the axisymmetric problem in Fig. P8.27. Assume zero initial conditions.

Heat Transfer (Chapter 8)

13.13 Analyze the heat transfer problem in Problem 8.28 using an 8×16 mesh of linear triangular elements and an equivalent mesh of linear rectangular elements.

13.14 Analyze the heat transfer problem in Fig. P8.29.

13.15 Analyze Problem 8.30 for nodal temperatures and heat flow across the boundaries. Use the following data: $k = 30$ W/(m · °C), $\beta = 60$ W/(m^2 · °C), $T_\infty = 0$°C, $T_0 = 100$°C, $q_0 = 2 \times 10^5$ W/m^2, $g_0 = 10^7$ W/m^3, and $a = 1$ cm.

13.16 Repeat Problem 13.15 with an equivalent mesh of triangular elements.

13.17 Analyze Problem 8.35 for nodal temperature and heat flows across the boundary. Take $k = 5$ W/(m · °C).

13.18 Consider heat transfer in a rectangular domain with a central heated circular cylinder (see Fig. P13.18 for the geometry). Analyze the problem using the mesh of linear quadrilateral elements shown in Fig. 13.4.2(b).

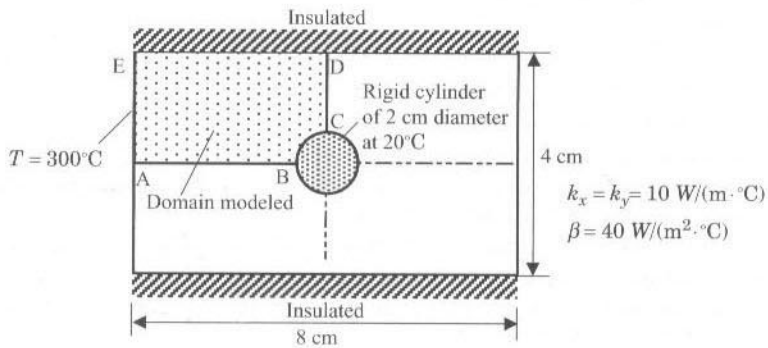

Figure P13.18

13.19 Analyze the heat transfer problem in Fig. P8.31 with (a) 2×2 and (b) 4×4 meshes of linear rectangular elements.

13.20 Repeat Problem 13.19 with triangular elements.

13.21 Analyze the problem in Fig. P8.32 with (a) 3×3, and (b) 6×6 meshes of linear rectangular elements. Take $k = 10$ W/(m · °C).

13.22 Repeat Problem 13.21 with linear triangular elements.

13.23 Analyze the heat transfer problem in Fig. P8.34 with a 4×4 mesh of linear rectangular elements and an equivalent mesh of quadratic (nine-node) elements. Take $a = 1$ cm, $T_0 = 100$°C, and $k = 3$ W/(m · °C).

13.24 Analyze the problem in Fig. P8.35 for transient response using (a) $\alpha = 0$ and (b) $\alpha = 0.5$. Use $c = \rho$, $c_p = 1.0$.

13.25 Analyze the axisymmetric problem in Fig. P8.26 using the Crank–Nicolson method. Use an 8×1 mesh of linear rectangular elements. Use $c = \rho c_p = 3.6 \times 10^6$ J/(m^3 · K).

Groundwater and Inviscid Flows (Chapter 8)

13.26 Analyze the groundwater flow in Problem 8.38 using the mesh of linear quadrilateral elements in Fig. 8.3.8 (remove the diagonal lines to obtain the mesh of quadrilateral elements).

13.27 Repeat Problem 13.26 with the mesh of linear triangular elements shown in Fig. 8.3.8.

13.28 Analyze Problem 8.39 with an 8×4 mesh of (*a*) linear triangular elements and (*b*) linear quadrilateral elements.

13.29 Repeat Problem 8.39 with a 4×2 mesh of (*a*) quadratic triangular elements and (*b*) quadratic (nine-node) quadrilateral elements.

13.30 Analyze Problem 8.37 using linear rectangular elements and an equivalent mesh of quadratic rectangular elements. Use an 8×6 mesh in the first rectangle and an 8×4 mesh in the second. The meshes should be refined in the horizontal direction to have smaller elements around the sheet pile.

13.31 Analyze the flow around a cylinder of elliptical cross section (see Fig. P8.41). Use the symmetry and an appropriate mesh of linear triangular elements. Use the stream function approach.

13.32 Repeat Problem 13.31 using the velocity potential formulation.

Membrane and Torsion Problems (Chapter 8)

13.33 Analyze the torsion of a member of circular cross section (see Fig. P8.43) for the state of shear stress distribution. Investigate the accuracy with mesh refinements (by subdividing the mesh in Fig. P8.43 with horizontal and vertical lines).

13.34 Analyze the torsion problem in Fig. P8.45.

13.35 Analyze the hollow-cross-section torsion problem in Fig. P8.46 using a mesh of (*a*) linear triangular elements in an octant and (*b*) linear rectangular elements in a quadrant. The meshes should be nodewise equivalent.

13.36 Analyze the rectangular membrane problem in Fig. P8.48 with 4×4 and 8×8 meshes of linear rectangular elements in the computational domain. Take $a_{11} = a_{22} = 1$ and $f_0 = 1$.

13.37 Repeat Problem 13.36 with equivalent meshes of quadratic elements.

13.38 Determine the eigenvalues of the rectangular membrane in Fig. P8.48 using a 4×4 mesh of linear rectangular elements in the half-domain. Use $c = 1.0$.

13.39 Determine the eigenvalues of the circular membrane problem in Fig. P8.49 with a mesh of four quadratic triangular elements. Use $c = 1.0$.

13.40 Determine the transient response of the problem in Fig. P8.49 (see Problem 13.39). Assume zero initial conditions, $c = 1$ and $f_0 = 1$. Use $\alpha = \gamma = 0.5$ and $\Delta t = 0.05$, and plot the center deflection versus time t for $t = 0$ to $t = 2.4$.

Viscous Incompressible Fluids (Chapter 10)

13.41 Analyze the viscous flow problem in Problem 10.8 using an 8×8 mesh of linear rectangular elements. Plot the horizontal velocity $u(0.5, y)$ versus y, and the pressure along the top surface of the cavity. Investigate the effect of the penalty parameter on the solution (see Fig. P10.8).

13.42 Repeat Problem 13.41 with nine-node quadratic elements.

13.43 Analyze the slider bearing problem of Example 10.6.2 to investigate the effect of the penalty parameter on the velocity and pressure fields. Use an 8×8 mesh of linear rectangular elements.

13.44 Repeat Problem 13.43 with nine-node quadratic elements.

13.45 Analyze the problem of a viscous incompressible fluid being squeezed through a 4:1 contraction, as shown in Fig. P13.45. Take $L_1 = 10$, $L = 6$, $R_1 = 4$, and $R_2 = 1$, and linear quadrilateral elements. The inlet velocity $v_x(y)$ is the fully developed solution of the flow between parallel plates. Plot the velocity $v_x(x, y)$ and pressure along the horizontal centerline.

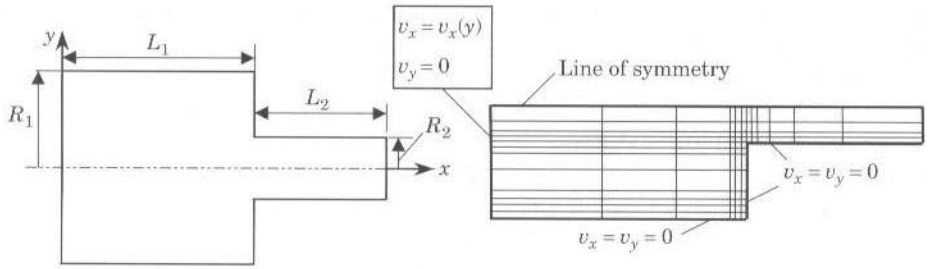

Figure P13.45

13.46 Analyze the cavity problem in Problem 13.41 for its transient solution. Use $\rho = 1.0$, zero initial conditions, penalty parameter $\gamma = 10^8$, time parameter $\alpha = 0.5$, and a time step of $\Delta t = 0.005$ to capture the evolution of $v_x(0.5, y)$ with time.

13.47 Analyze the slider bearing problem of Example 10.6.2 for its transient solution. Use $p = 20$, zero initial conditions, $\gamma = 10^8$, $\alpha = 0.5$, and a time step of 10^{-4}.

Plane Elasticity (Chapter 11)

13.48 Analyze the plane elasticity problem in Fig. P11.7 using 10×4 mesh of linear rectangular elements. Evaluate the results (i.e., displacements and stresses) qualitatively. Use the plane stress assumption.

13.49 Repeat Problem 13.48 using triangular elements.

13.50–13.59 Analyze the plane elasticity problems shown in Figs. P11.1–11.3 and P10.10–P10.16 using suitable meshes of triangular or rectangular elements (the instructor should specify the element type and mesh).

13.60 Analyze the plane elasticity problem in Fig. P11.7 for natural frequencies. Use a density of $\rho = 0.0088$ kg/cm^3.

13.61 Repeat Problem 13.60 with triangular elements.

13.62 Analyze the plane elasticity problem in Fig. P11.7 for the transient response. Use $\alpha = \frac{1}{2}$, $\gamma = \frac{1}{2}$, and $\Delta t = 10^{-5}$. Assume zero initial conditions.

13.63–13.66 Analyze Problems 13.50–13.53 for transient response. Use $\alpha = \frac{1}{2}$, $\gamma = \frac{1}{2}$, and $\Delta t \approx \Delta t_{\text{cri}}$.

Plate Bending (Chapter 12)

13.67 Analyze the plate problem in Fig. P12.2 using (*a*) 2×4 and (*b*) 4×8 meshes of CPT(N) elements in the half-plate, and compare the maximum deflections and stresses. Use $E = 10^7$ psi, $\nu = 0.25$, $h = 0.25$ in., and $q_0 = 10$ lb/in.^{2}

13.68 Repeat Problem 13.67 with a CPT(C) element.

13.69 Repeat Problem 13.67 with an 4×8 mesh of linear plate elements and a 2×4 mesh of nine-node quadratic plate elements based on the first-order plate theory.

13.70–13.72 Analyze the plate bending problems shown in Figs. P12.3, P12.4 and P12.8 with the CPT (C) elements. Use the meshes shown in the figures, and take $E = 10^7$ psi, $\nu = 0.25$, $h = 0.25$ in., and $q_0 = 10$ lb/in.^{2}

13.73–13.75 Repeat Problems 13.70–13.72 using SDT and meshes shown in Figs. P12.3, P12.4, and P12.8.

13.76 Analyze the annular plate in Fig. P12.5 using a four element mesh of CPT(C) elements. Use $E = 10^7$ psi, $\nu = 0.25$, $a = 10$ in., $b = 5$ in., $h = 0.25$ in., and $Q_0 = 1$ lb/in.

13.77 Repeat Problem 13.76 with four-node SDT elements.

13.78 Analyze the plate problem in Fig. P12.2 for its transient response. Use a mesh of 2×4 CPT(N) elements and $E = 10^7$ psi, $\nu = 0.25$, $\rho = 1$ lb/in.^{3}, $h = 0.25$ in., $q_0 = 10$ lb/in., $\Delta t = 0.05$, and $\alpha = \gamma = 0.5$.

13.79 Repeat Problem 13.78 using 2×4 mesh of four-node SDT elements.

13.80 Determine the transient response of the annular plate in Fig. P12.5 using four SDT elements, $\Delta t = 0.05$, $\rho = 1.0$, and $\alpha = \gamma = 0.5$. Plot the deflection at node 1 as a function of time for at least two periods.

REFERENCES FOR ADDITIONAL READING

Fluid Mechanics

1. Bird, R. B., Stewart, W. E., and Lightfoot, E. N., *Transport Phenomena,* John Wiley, New York, 1960.
2. Gresho, P. M. and Sani, R. L., *Incompressible Flow and the Finite Element Method,* John Wiley, West Sussex, UK, 2000.
3. Schlichting, H., *Boundary-Layer Theory* (translated by Kestin, J.), 7th ed., McGraw-Hill, New York, 1979.
4. Verruijt, A., *Theory of Groundwater Flow,* Gordon and Breach, New York, 1970.
5. White, F. M., *Fluid Mechanics,* 4th ed., McGraw-Hill, New York, 1999.

Heat Transfer

6. Carslaw, H. S. and Jaeger, J. C., *Conduction of Heat in Solids,* Oxford University Press, Oxford, 1959.
7. Holloman, J. P., *Heat Transfer,* 7th ed., McGraw-Hill, New York, 1990.
8. Kreith, F. and Bohn, M. S., *Principles of Heat Transfer,* 5th ed., West Publishing Co., St. Paul, MN 1993.
9. Myers, G. E., *Analytical Methods in Conduction Heat Transfer,* McGraw-Hill, New York, 1972.
10. Özisik, M. N., *Heat Conduction,* 2nd ed., John Wiley, New York, 1993.

Elasticity

11. Budynas, R. G., *Advanced Strength and Applied Stress Analysis,* 2nd ed., McGraw-Hill, New York, 1999.
12. Harris, C. M. and Crede, C. E., *Shock and Vibration Handbook,* vol. 1, McGraw-Hill, New York, 1961.
13. Slaughter, W. S., *The Linearized Theory of Elasticity,* Birkhäuser, Boston, MA, 2002.
14. Ugrual, A. C. and Fenster, S. K., *Advanced Strength and Applied Elasticity,* Prentice-Hall, Upper Saddle River, NJ, 1995.
15. Volterra, E. and Gaines, J. H., *Advanced Strength of Materials,* Prentice-Hall, Englewood Cliffs, NJ, 1971.

Plates

16. Reddy, J. N., *Theory and Analysis of Elastic Plates,* Taylor and Francis, Philadelphia, PA, 1999.
17. Reddy, J. N., *Energy Principles and Variational Methods in Applied Mechanics,* 2nd ed., John Wiley, New York, 2002.

18. Reddy, J. N., *Mechanics of Laminates Composite Plates and Shells: Theory and Analysis*, 2nd ed., CRC Press, Boca Raton, FL, 2004.

19. Szilard, R., *Theories and Applications of Plate Analysis*, John Wiley, New York, 2004.

20. Timoshenko, S. and Woinowsky-Krieger, S., *Theory of Plates and Shells*, 2nd ed., McGraw-Hill, New York, 1959.

Computer Implementation

21. Akay, H. U., Willhite, P. G., and Didandeh, H., "UCODE2, Version 87.1," Computational Fluid Dynamics Laboratory, Department of Mechanical Engineering, Indiana Uuiversity-Purdue University at Indianapolis (IUPUI), Indianapolis, 1987.

22. Bathe, K. J., *Finite Element Procedures,* Prentice Hall, Englewood Cliffs, NJ, 1996.

23. Burnett, D. S., *Finite Element Analysis,* Addison-Wesley, Reading, MA, 1987.

24. Chandrupatla, T. R. and Belegundu, A. D., *Introduction to Finite Elements in Engineering,* 3rd ed., Prentice Hall, Upper Saddle River, NJ, 2002.

25. Zienkiewicz, O. C. and Taylor, R. L., *The Finite Element Method,* 4th ed., vol. 1 *Basic Formulation and Linear Problems*, McGraw-Hill, London, UK, 1989.

Chapter 14
PRELUDE TO ADVANCED TOPICS

14.1 INTRODUCTION

The introduction to the finite element method presented in the preceding chapters is sufficient to provide the essential background for the development of finite element models and the associated computer programs for most linear boundary, initial, and eigenvalue problems in one and two dimensions. The background should also help one to intelligently use commercially available finite element software. However, there are many additional ideas that deserve some attention. In this chapter, we discuss some immediate extensions of the material presented in Chapters 8 through 12. These include alternative finite element models, finite element models of three-dimensional problems, finite element analysis of nonlinear problems, and errors in finite element analysis. The discussions presented here are brief and they are only meant to give some idea of the applicability of the finite element method to these advanced topics. The reader interested in a detailed treatment of any of these topics should consult the books listed at the end of the chapter.

14.2 ALTERNATIVE FINITE ELEMENT MODELS

14.2.1 Introductory Comments

The finite element models presented in Chapters 3 through 12 were based on *weak formulations* of governing differential equations. These models can be termed the *Ritz finite element models* or *weak-form finite element models*. The phrase "Galerkin finite element models" is used in the literature often to mean the weak-form (Ritz) models. A truly Galerkin finite element model is based on weighted integral statements and not on weak forms. This distinction is made here to differentiate between Galerkin's method and the Ritz method. In most cases, especially when the governing differential equations contain derivatives of even order, weak forms (which always include the natural boundary conditions) can be developed using the three-step procedure. In some cases, the governing equations may be recast in an alternative form that facilitates the use of lower-order (C^0) interpolations. In this section, we discuss a couple of such formulations and demonstrate the use of the weighted residual methods of Section 2.5.5 to develop alternative finite element models. More specifically, we shall study the following formulations:

1. Weighted residual formulations
2. Mixed formulations

While specific sets of equations are chosen to illustrate the basic ideas behind the two formulations, the ideas are applicable to other field equations and to two- and three-dimensional problems.

14.2.2 Weighted Residual Finite Element Models

In a weak formulation, integration by parts is used to introduce the secondary variables (i.e., natural boundary conditions) into the integral form. On the other hand, weighted residual methods are based on a weighted integral statement of a given differential equation and no integration by parts is employed. They are the natural and only choice for first-order equations, which do not admit a weak formulation. For second- and higher-order equations, we have a choice between the weak formulation and the weighted residual formulation to construct finite element models that will be different from each other. We begin with the description of weighted residual finite element models of a first-order differential equation in one dimension.

First-Order Equation in One Dimension

Consider the first-order equation

$$a\frac{du}{dx} + cu = f \quad \text{for} \quad 0 < x < L \tag{14.2.1}$$

where a, c, and f are given functions of x. An example of a situation in which the above equation arises is given by Newton's law of cooling of a body with temperature u in an environment at temperature u_0:

$$\frac{du}{dx} + k(u - u_0) = 0$$

which is the same as (14.2.1) with $c = k$, $a = 1$, and $f = ku_0$.

When u is approximated by an n-parameter approximation

$$u(x) \approx u_h^e(x) = \sum_{j=1}^{n} u_j^e \psi_j^e(x) \tag{14.2.2}$$

we need n algebraic equations to solve for the parameters u_j^e. The n equations are provided by n different (i.e., linearly independent) choices of the weight function w in the weighted residual statement

$$0 = \int_{x_a}^{x_b} w R_e \, dx, \quad R_e = \left(a\frac{du_h^e}{dx} + cu_h^e - f \right) \tag{14.2.3}$$

where R_e is the error, called the *residual*, in the approximation of the differential equation. Different choices of w dictate different methods.

Since the equation under consideration is first-order, there is no advantage in transferring the derivative to the weight function w. Note that there are no "flux" terms in (14.2.3). An examination of the weighted integral statement (14.2.3) shows that the minimum differentiability on the approximation functions ψ_j is the same as in the original differential

equation. In the present case, ψ_j should be once-differentiable with respect to x. Consequently, the Lagrange family of interpolation functions (i.e., C^0 approximations) are admissible.

The only requirements on the weight function w are that it (a) be integrable in the sense that (14.2.3) can be evaluated and (b) belong to a linearly independent set $\{w_i\}_{i=1}^n$ so that the resulting algebraic equations are solvable. The ith algebraic equation is obtained by replacing w in (14.2.3) with w_i. Different choices for the set $\{w_i\}$ have been suggested, and the resulting models bear the names of the original scientists who suggested them. The best-known choices for w_i are given below.

1. Petrov–Galerkin method: $w_i = \phi_i$ and $\phi_i \neq \psi_i$
2. Bubnov–Galerkin method: $w_i = \psi_i$
3. Collocation method: $w_i = \delta(x - x_i)$, the Dirac delta function (14.2.4)
4. Subdomain method: $w_i = \delta_{ij}$ (i.e., $w_i = 1$ in the ith subdomain)
5. Least-squares method: $w_i = A(\psi_i)$, where A is the operator in the differential equation $Au = f$

Although the least-squares method is listed as a member of weighted residual methods, it is based on the idea of minimizing the error (R_e) introduced in the approximation of an equation. The finite element models of (14.2.1), based on various methods, are discussed next.

The Petrov–Galerkin Model. Substitute (14.2.3) for u and $w = \phi_i$ into (14.2.2) to obtain

$$0 = \sum_{j=1}^{n} K_{ij} u_j - f_i \quad \text{or} \quad [K^e]\{u^e\} = \{f^e\} \tag{14.2.5a}$$

where

$$K_{ij}^e = \int_{x_a}^{x_b} \left(a\phi_i^e \frac{d\psi_j^e}{dx} + c\phi_i^e \psi_j^e \right) dx, \quad f_i^e = \int_{x_a}^{x_b} \phi_i^e f \, dx \tag{14.2.5b}$$

The Bubnov–Galerkin Model. Here we substitute $w = \psi_i^e$ into (14.2.3) to obtain the finite element model

$$[K^e]\{u^e\} = \{f^e\} \tag{14.2.6a}$$

where

$$K_{ij}^e = \int_{x_a}^{x_b} \left(a\psi_i^e \frac{d\psi_j^e}{dx} + c\psi_i^e \psi_j^e \right) dx, \quad f_i^e = \int_{x_a}^{x_b} \psi_i^e f \, dx \tag{14.2.6b}$$

Collocation Model. In this case, we take $w = \delta(x - x_i)$, the Dirac delta function. The collocation points x_i can be chosen arbitrarily, usually as the quadrature points in $\Omega_e = [x_a, x_b]$. We have

$$K_{ij}^e = a(x_i) \frac{d\psi_j^e}{dx}(x_i) + c(x_i)\psi_j^e(x_i), \quad f_i^e = f(x_i) \tag{14.2.7}$$

Subdomain Model. In this model the element domain Ω_e is subdivided further into n subdomains. The weight function for the ith subdomain Ω_i^e is unity over the subdomain

and zero outside it

$$w(x) = \begin{cases} 1 & \text{for} \quad x \in \Omega_i^e \\ 0 & \text{for} \quad x \notin \Omega_i^e \end{cases} \tag{14.2.8}$$

We obtain

$$K_{ij}^e = \int_{\Omega_i^e} \left(a \frac{d\psi_j^e}{dx} + c\psi_j^e \right) dx, \quad f_i^e = \int_{\Omega_i^e} f \, dx \tag{14.2.9}$$

Least-Squares Model. The weight function in this case is $w \equiv A(\psi_i) = a(d\psi_i^e/dx) + c\psi_i^e$. Consequently, we have

$$K_{ij}^e = \int_{x_a}^{x_b} \left(a \frac{d\psi_i^e}{dx} + c\psi_i^e \right) \left(a \frac{d\psi_j^e}{dx} + c\psi_j^e \right) dx \tag{14.2.10a}$$

$$f_i^e = \int_{x_a}^{x_b} \left(a \frac{d\psi_i^e}{dx} + c\psi_i^e \right) f \, dx \tag{14.2.10b}$$

Note that only the least-squares method gives a symmetric coefficient matrix. This is a strong point (in addition to the fact that it actually minimizes the error R_e) of the least-squares method over other methods.

Example 14.2.1

Here, we solve Eq. (14.2.1) with the boundary condition $u(0) = 1$ and data $a = 1$, $c = 2$, $f = 1$, and $L = 1$. We shall use two linear elements in the domain.

For the Bubnov–Galerkin model, we have

$$[K^e] = \frac{1}{2}\begin{bmatrix} -1 & 1 \\ -1 & 1 \end{bmatrix} + \frac{h_e}{3}\begin{bmatrix} 2 & 1 \\ 1 & 2 \end{bmatrix}, \quad \{f^e\} = \frac{h_e}{2}\begin{Bmatrix} 1 \\ 1 \end{Bmatrix} \tag{14.2.11}$$

The assembled equations (here, assembly is required only to reduce the number of equations to the number of unknowns) are given by

$$\left(\frac{1}{2}\begin{bmatrix} -1 & 1 & 0 \\ -1 & 0 & 1 \\ 0 & -1 & 1 \end{bmatrix} + \frac{1}{6}\begin{bmatrix} 2 & 1 & 0 \\ 1 & 4 & 1 \\ 0 & 1 & 2 \end{bmatrix} \right) \begin{Bmatrix} U_1 \\ U_2 \\ U_3 \end{Bmatrix} = \frac{1}{4}\begin{Bmatrix} 1 \\ 2 \\ 1 \end{Bmatrix} \tag{14.2.12}$$

Using the boundary condition, $U_1 = 1$, we obtain the following condensed equations:

$$\frac{1}{6}\begin{bmatrix} 4 & 4 \\ -2 & 5 \end{bmatrix} \begin{Bmatrix} U_2 \\ U_3 \end{Bmatrix} = \frac{1}{6}\begin{Bmatrix} 5 \\ 1.5 \end{Bmatrix} \tag{14.2.13}$$

The solution is $U_2 = 0.6786$ and $U_3 = 0.5714$. The exact solution of the problem is

$$u(x) = u(0)e^{-(c/a)x} - \frac{f}{c}(1 - e^{-(c/a)x}) = e^{-2x} - \frac{1}{2}(1 - e^{-2x}) \tag{14.2.14}$$

The exact values of u at $x = \frac{1}{2}$ and 1 are 0.6389 and 0.5677, respectively.

For the collocation model, we choose $x_1 = \frac{1}{3}h_e$ and $x_2 = \frac{2}{3}h_e$, and obtain

$$[K^e] = \frac{1}{h_e}\begin{bmatrix} -1 & 1 \\ -1 & 1 \end{bmatrix} + \frac{2}{3}\begin{bmatrix} 2 & 1 \\ 1 & 2 \end{bmatrix}, \quad \{f^e\} = \begin{Bmatrix} 1 \\ 1 \end{Bmatrix} \tag{14.2.15}$$

Table 14.2.1 Comparison of the numerical solution of (14.2.1) with the exact solution (Example 14.2.1).

Nodal values	Bubnov–Galerkin	Collocation	Subdomain	Least-squares	Exact
$u(0.5)$	0.6786	0.6786	0.6053	0.6793	0.6839
$u(1.0)$	0.5714	0.5714	0.4737	0.5094	0.5677

Clearly, the element equations obtained using the collocation points $x_1 = \frac{1}{3}h_e$ and $x_2 = \frac{2}{3}h_e$ are the same as those obtained in the Bubnov–Galerkin method (actually a multiple of $\frac{1}{2}h_e$). Hence, we obtain the same solution as in the Bubnov–Galerkin method.

In the case of the subdomain model, we use $\Omega_1^e = (0, \frac{1}{2}h_e)$ and $\Omega_2^e = (\frac{1}{2}h_e, h_e)$. For this choice, we obtain

$$[K^e] = \frac{1}{2}\begin{bmatrix} -1 & 1 \\ -1 & 1 \end{bmatrix} + \frac{h_e}{4}\begin{bmatrix} 3 & 1 \\ 1 & 3 \end{bmatrix}, \quad \{f^e\} = \frac{3h_e}{8}\begin{Bmatrix} 1 \\ 1 \end{Bmatrix} \tag{14.2.16}$$

The assembled equations become

$$\frac{1}{8}\begin{bmatrix} -1 & 5 & 0 \\ -3 & 6 & 5 \\ 0 & -3 & 7 \end{bmatrix}\begin{Bmatrix} U_1 \\ U_2 \\ U_3 \end{Bmatrix} = \frac{3}{16}\begin{Bmatrix} 1 \\ 2 \\ 1 \end{Bmatrix} \tag{14.2.17}$$

The solution, from the last two equations, is $U_2 = 0.6053$ and $U_3 = 0.4737$.

Last, we consider the least-squares model. We have

$$[K^e] = \frac{1}{h_e}\begin{bmatrix} 1 & -1 \\ -1 & 1 \end{bmatrix} + \frac{4h_e}{6}\begin{bmatrix} 2 & 1 \\ 1 & 2 \end{bmatrix} + \begin{bmatrix} -2 & 0 \\ 0 & 2 \end{bmatrix} \tag{14.2.18a}$$

$$\{f^e\} = \begin{Bmatrix} -1 \\ 1 \end{Bmatrix} + h_e\begin{Bmatrix} 1 \\ 1 \end{Bmatrix} \tag{14.2.18b}$$

The assembled equations are

$$\frac{1}{3}\begin{bmatrix} -2.5 & -0.5 & 0.0 \\ -0.5 & 7.0 & -0.5 \\ 0.0 & -0.5 & 9.5 \end{bmatrix}\begin{Bmatrix} U_1 \\ U_2 \\ U_3 \end{Bmatrix} = \begin{Bmatrix} -0.5 \\ 1.0 \\ 1.5 \end{Bmatrix} \tag{14.2.19}$$

The solution of these equations is

$$U_2 = 0.6793, \quad U_3 = 0.5094$$

Table 14.2.1 gives a summary of the solutions obtained using various models. Since the exact solution is exponential or hyperbolic, it is obvious that the meshes and degree of interpolation used are very crude. The accuracy of the finite element solutions can be improved by higher degree polynomials.

Second-Order Equations in One Dimension

Use of weighted residual finite element models in the solution of second- and higher-order equations is more involved. There are two possible ways to construct the weighted residual forms of higher-order equations: (1) Use the higher-order equations but use C^k-continuous functions, where $k \geq m$, m being the order of the highest derivative in the differential

equation; and (2) rewrite the higher-order equations as a set of first-order equations and use C^0-continuous functions. The latter requires a consistent set of approximations for the new variables introduced in rewriting the higher-order equations as a first-order set. Here we consider the first method and leave the second as an exercise to the reader (see Problem 14.1).

Consider the model second-order equation

$$-\frac{d}{dx}\left(a\frac{du}{dx}\right) = f \tag{14.2.20}$$

For the weak formulation of this equation, the approximation functions ψ_i^e must be such that u is continuous across interelement boundaries. The weak form includes the natural boundary conditions associated with the equation, and therefore interpolation of only u (but not its derivatives) is required.

In the weighted residual formulation of Eq. (14.2.20), we use the weighted integral form of the differential equation without weakening the differentiability on u. Therefore, the continuity conditions on the interpolation functions used in the weighted residual methods are dictated by the order of the differential equation. For example, the second-order differential equation (14.2.20) requires the approximation functions to be twice-differentiable with respect to x. In addition, the approximate solution must satisfy the end conditions on the primary and secondary variables (identified with the help of the weak formulation) of the problem. This amounts to, for second-order equations, using approximation functions that make the primary and secondary variables continuous between elements (i.e., interelement nodes). For the second-order equations under consideration, the natural boundary condition involves specifying the secondary variable $a(du/dx)$ at the element boundaries. Therefore, the interpolation functions must be selected such that u and $a(du/dx)$ are continuous across an interface between elements. This in turn, implies that, if a is continuous, du/dx is continuous throughout the domain $\Omega = (0, L)$. Hence, a C^1 approximation (i.e., Hermite interpolation) of u is required.

Because u and du/dx are required to be continuous across an interface between elements, and a typical element (in one dimension) has two such interfaces, the polynomial approximation of u must involve four parameters, i.e., it must be a cubic polynomial. Thus, the finite element is a line element with two nodes and two degrees of freedom, u and du/dx, at each node. The element is different from the Lagrange cubic element, which has four nodes with one degree of freedom per node. The Lagrange interpolation functions (of any order) do not satisfy the continuity of du/dx across element interfaces and therefore do not belong to $C^1(0, L)$. The two-node element with continuous u and du/dx at element interfaces is the Hermite cubic element developed in Section 5.2 for the Euler–Bernoulli beam element. We have

$$u_h^e(x) = \sum_{j=1}^{4} u_j^e \phi_j^e(x) \tag{14.2.21}$$

where u_1^e and u_3^e are the nodal values of u_h^e, u_2^e and u_4^e are the nodal values of du_h^e/dx at the two nodes, and ϕ_j^e are the Hermite cubic interpolation functions in (5.2.12). We consider various weighted residual finite element models of (14.2.20).

The weighted residual form of (14.2.20) over an element $\Omega_e = (x_a, x_b)$ is

$$0 = \int_{x_a}^{x_b} w R_e \, dx, \quad R_e = \left[-\frac{d}{dx}\left(a\frac{du_h^e}{dx}\right) - f\right] \tag{14.2.22}$$

Substituting ψ_i^e for the weight function w and (14.2.21) for u, we obtain

$$0 = \sum_{j=1}^{4} K_{ij}^e u_j^e - f_i^e, \quad \text{or} \quad [K^e]\{u^e\} = \{f^e\} \tag{14.2.23a}$$

where

$$K_{ij}^e = \int_{x_a}^{x_b} \left[-\psi_i^e \frac{d}{dx}\left(a \frac{d\phi_j^e}{dx} \right) \right] dx, \quad f_i^e = \int_{x_a}^{x_b} \psi_i^e f \, dx \tag{14.2.23b}$$

Equation (14.2.23*a*) is the Petrov–Galerkin model of (14.2.20) when $\phi_i^e \neq \psi_i^e$.

For different choices of ψ_i^e in (14.2.23*b*), we obtain different finite element models. These are presented below.

The Bubnov–Galerkin Model. For $\psi_i^e = \phi_i^e$, (14.2.23*b*) becomes

$$K_{ij}^e = \int_{x_a}^{x_b} \left[-\phi_i^e \frac{d}{dx}\left(a \frac{d\phi_j^e}{dx} \right) \right] dx, \quad f_i^e = \int_{x_a}^{x_b} \phi_i^e f \, dx \tag{14.2.24}$$

Least-Squares Model. For $\psi_i^e = A(\phi_i^e) \equiv -(d/dx)(a d\phi_i^e/dx)$, we have

$$K_{ij}^e = \int_{x_a}^{x_b} \frac{d}{dx}\left(a \frac{d\phi_i^e}{dx} \right) \frac{d}{dx}\left(a \frac{d\phi_j^e}{dx} \right) dx, \quad f_i^e = -\int_{x_a}^{x_b} \frac{d}{dx}\left(a \frac{d\phi_i^e}{dx} \right) f \, dx \tag{14.2.25}$$

Collocation Model. For $\psi_i^e = \delta(x - x_i)$, (14.2.23*b*) takes the form

$$K_{ij}^e = -\left\{ \frac{d}{dx}\left[a(x) \frac{d\phi_j^e}{dx}(x) \right] \right\}_{x=x_i}, \quad f_i^e = f(x_i) \tag{14.2.26}$$

where x_i are the collocation points.

While the Bubnov–Galerkin and least-squares models have the same form as the Ritz model, i.e., they are defined by integral expressions, the collocation model does not. In the latter, we simply evaluate the coefficient matrices and column vector at the collocation points, instead of evaluating the integral expressions. The number of collocation points should be equal to the number of unknowns after imposition of the boundary conditions of the problem. For second-order equations, we have two boundary conditions and $2(N+1)$ nodal degrees of freedom for an N-element model. Hence, a total of $2N$ collocation points, two per element, are needed. Also, note that the coefficient matrix in (14.2.26) is of order 2×4 ($i = 1, 2$), and there is no overlap of element matrices because there is no summation of equations over the number of elements. However, the continuity conditions on nodal variables are imposed in all the other models.

Example 14.2.2

Consider the boundary value problem

$$-\frac{d}{dx}\left[(1+x)\frac{du}{dx} \right] = 0 \quad \text{for} \quad 0 < x < 1 \tag{14.2.27a}$$

$$u(0) = 0, \quad \left[(1+x)\frac{du}{dx} \right]_{x=1} = 1 \tag{14.2.27b}$$

The exact solution of this problem is

$$u = \ln(1 + x) \tag{14.2.28}$$

We wish to solve the problem using various weighted residual finite element models.

Consider a two-element discretization of the problem. There are three nodes and six degrees of freedom. The known degrees of freedom for the weighted residual models are

$$U_1 = 0, \quad U_6 = 0.5 \tag{14.2.29}$$

whereas, in the four-element Ritz model (i.e., the weak-form finite element model) with linear elements, they are

$$U_1 = 0, \quad Q_5 = 1.0 \tag{14.2.30}$$

For the collocation model, the two-point Gauss–Legendre quadrature points are used as the collocation points. The two- and four-element finite element solutions obtained from three weighted residual finite element models, all using the Hermite cubic polynomials, are compared with the exact solution and the solution of the weak-form finite element model in Table 14.2.2. All the models give accurate results.

Table 14.2.2 Comparison of weighted residual finite element solutions[†] with the exact solution of the problem in (14.2.27*a*) and (14.2.27*b*).

x		Exact	Collocation	Bubnov–Galerkin	Least-squares	Ritz
0.00	u	0.00000	0.00000	0.00000	0.00000	0.00000
	u'	1.00000	0.99390	0.99604	0.99902	0.99612
	u'	1.00000	0.99967	0.99930	0.99993	0.99930
0.25	u	0.22314	—	—	—	—
	u	0.22314	0.22326	0.22313	0.22315	0.22313
	u'	0.80000	—	—	—	—
	u'	0.80000	0.80028	0.80004	0.79997	0.80004
0.50	u	0.40547	0.40487	0.40537	0.40554	0.40538
	u	0.40547	0.40562	0.40546	0.40547	0.40546
	u'	0.66667	0.66299	0.66707	0.66645	0.66728
	u'	0.66667	0.66646	0.66673	0.66665	0.66674
0.75	u	0.55962	—	—	—	—
	u	0.55962	0.55975	0.55961	0.55962	0.55961
	u'	0.57143	—	—	—	—
	u'	0.57143	0.57123	0.57146	0.57142	0.57148
1.00	u	0.69315	0.69202	0.69309	0.69324	0.69315
	u	0.69315	0.69325	0.69314	0.69315	0.69315
	u'	0.50000	0.50000	0.50000	0.50000	0.50102
	u'	0.50000	0.50000	0.50000	0.50000	0.50010

[†]The first and third rows for each value of x corresponds to two elements and the second and fourth rows to four elements.

Second-Order Equations in Two Dimensions

Here we describe the Bubnov–Galerkin, least-squares, and collocation finite element models of a second-order equation in two dimensions. We consider the Poisson equation ($Au = f$)

$$-\frac{\partial}{\partial x}\left(a_{11}\frac{\partial u}{\partial x}\right)-\frac{\partial}{\partial y}\left(a_{22}\frac{\partial u}{\partial y}\right)=f \quad \text{in} \quad \Omega \tag{14.2.31}$$

In the weighted residual finite element model, we seek an approximate solution u_h^e of u in Ω_e in the form

$$u_h^e(x, y)=\sum_{j=1}^{16} u_j^e \phi_j^e(x, y) \tag{14.2.32}$$

where $\phi_j^e(x, y)$ are the conforming Hermite interpolation functions of the four-node rectangular element (see Table 9.2.1); u_1^e, u_5^e, u_9^e, and u_{13}^e are the nodal values of u_h^e at the four nodes of the element; u_2^e, u_6^e, u_{10}^e, and u_{14}^e are the nodal values of $\partial u_h^e/\partial x$ at the four nodes; and so on.

The weighted residual statement of (14.2.31) over an element is given by

$$0=\int_{\Omega_e} w\left[-\frac{\partial}{\partial x}\left(a_{11}\frac{\partial u}{\partial x}\right)-\frac{\partial}{\partial y}\left(a_{22}\frac{\partial u}{\partial y}\right)-f\right] dx\, dy \tag{14.2.33}$$

Substituting $w = \psi_i^e$ and replacing u by (14.2.32), we obtain the usual form of the element equations

$$[K^e]\{u^e\}=\{f^e\} \tag{14.2.34}$$

The specific forms of $[K^e]$ and $\{f^e\}$ are defined below for various models.

The Bubnov–Galerkin Model. For $w = \psi_i^e$, the coefficient matrix $[K^e]$ and column vector $\{f^e\}$ are defined by

$$K_{ij}^e=-\int_{\Omega_e} \psi_i^e\left[\frac{\partial}{\partial x}\left(a_{11}\frac{\partial \psi_j^e}{\partial x}\right)+\frac{\partial}{\partial y}\left(a_{22}\frac{\partial \psi_j^e}{\partial y}\right)\right] dx\, dy \tag{14.2.35a}$$

$$f_i^e=\int_{\Omega_e} \psi_i^e f\, dx\, dy \tag{14.2.35b}$$

The Least-Squares Model. For $w = A(\psi_i^e)$, where A is the differential operator in (14.2.31), the coefficients of $[K^e]$ and $\{f^e\}$ are defined by

$$\begin{aligned} K_{ij}^e=&\int_{\Omega_e}\left[\frac{\partial}{\partial x}\left(a_{11}\frac{\partial \psi_i^e}{\partial x}\right)+\frac{\partial}{\partial y}\left(a_{22}\frac{\partial \psi_i^e}{\partial y}\right)\right] \\ &\times\left[\frac{\partial}{\partial x}\left(a_{11}\frac{\partial \psi_j^e}{\partial x}\right)+\frac{\partial}{\partial y}\left(a_{22}\frac{\partial \psi_j^e}{\partial y}\right)\right] dx\, dy \end{aligned} \tag{14.2.36a}$$

$$f_i^e=-\int_{\Omega_e}\left[\frac{\partial}{\partial x}\left(a_{11}\frac{\partial \psi_i^e}{\partial x}\right)+\frac{\partial}{\partial y}\left(a_{22}\frac{\partial \psi_i^e}{\partial y}\right)\right] f\, dx\, dy \tag{14.2.36b}$$

The Collocation Model. In this model, we select four collocation points per element and satisfy (14.2.31) exactly at those four points of each element. For the best results, the

Gauss–Legendre quadrature points are selected. We have

$$K_{ij}^e = \left[-\frac{\partial}{\partial x}\left(a_{11}\frac{\partial \psi_j^e}{\partial x} \right) - \frac{\partial}{\partial y}\left(a_{22}\frac{\partial \psi_j^e}{\partial y} \right) \right]\Bigg|_{(x,y)=(x_i,y_i)} \tag{14.2.37a}$$

$$f_i^e = f(x_i, y_i) \tag{14.2.37b}$$

for $i = 1, 2, 3, 4$ and $j = 1, 2, \ldots, 16$. Note that the coefficient matrix is rectangular (4×16) and that each coefficient of the global matrix and column vector has a contribution from no more than one element. After imposing the boundary conditions of the problem, the number of linearly independent equations (which is equal to four times the number of elements in the finite element mesh) will be equal to the number of unknown nodal degrees of freedom.

Example 14.2.3

Consider the Dirichlet problem for the Poisson equation

$$\begin{aligned} -\nabla^2 u &= 2 \quad \text{in} \quad \Omega \\ u &= 0 \quad \text{on} \quad \Gamma \end{aligned} \tag{14.2.38}$$

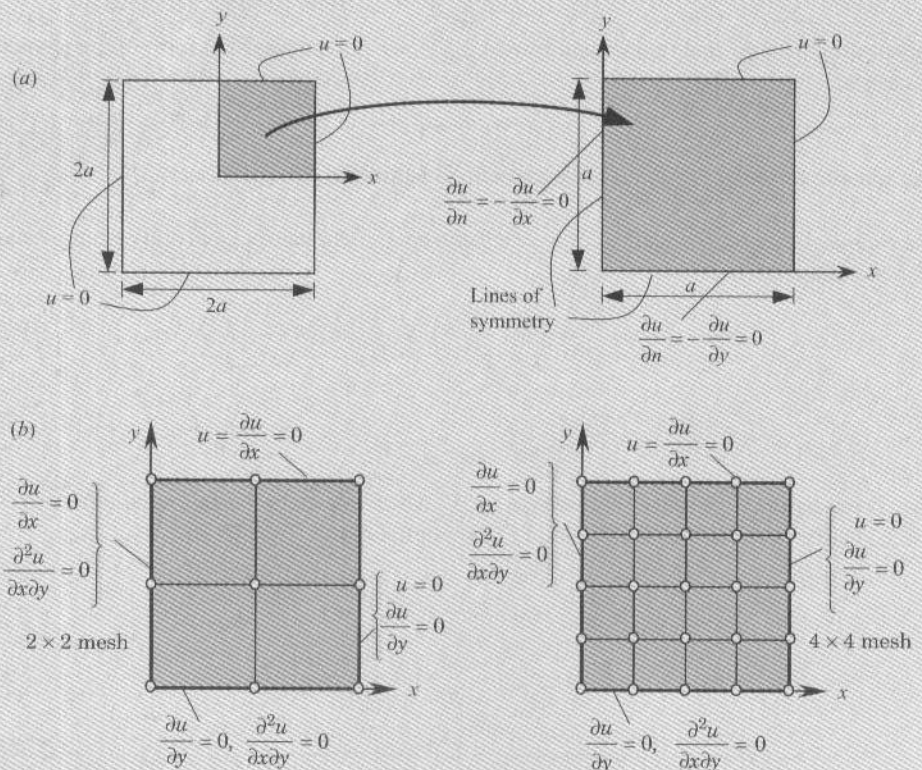

Figure 14.2.1 (*a*) Domain, boundary conditions and (*b*) finite element meshes of the problem in Example 14.2.3.

where Ω is a square region [see Fig. 14.2.1(a)]. The exact solution of this problem is given by (8.5.62a). Exploiting the biaxial symmetry, we model only a quadrant, say the region bounded by the positive axes.

Two different uniform meshes, shown in Fig. 14.2.1(b), of Hermite rectangular elements are used to solve the problem, employing various finite element models. Since the element has u, $\partial u/\partial x$, $\partial u/\partial y$, and $\partial^2 u/\partial x \partial y$ as nodal degrees of freedom, we must impose all known boundary values of these quantities. For the problem at hand, we impose the following boundary conditions: $u = 0$ on the lines $x = 1$ and $y = 1$, $\partial u/\partial x = 0$ on the line $x = 0$, and $\partial u/\partial y = 0$ on the line $y = 0$. The boundary conditions for the weighted residual models are indicated in Fig. 14.2.1(b). For the 2×2 mesh, the number of known boundary conditions is 20, whereas the number of total nodal variables is 36. Thus, for the collocation model, we have 16 unknowns and 16 equations, 4 from each element. Similarly, for the 4×4 mesh, we have 36 boundary conditions, among 100 nodal variables, requiring 64 collocation equations, which are provided by the 16 elements.

The finite element solutions obtained from the three finite element models for the two meshes are compared with the exact solution (8.5.62a) in Table 14.2.3. The collocation finite element solution is relatively more accurate than the other two solutions. The numerical convergence of all three models is apparent from the results.

Table 14.2.3 Comparison of the various finite element solutions[1] with the exact solution of the Dirichlet problem for the Poisson equation (14.2.38) (Example 14.2.3).

		$u(x, y)$				$\partial u/\partial x$			
x	y	Exact	Bubnov–Galerkin	Least-squares	Collocation	Exact	Bubnov–Galerkin	Least-squares	Collocation
0.0	0.0	0.5894	0.5890	0.5890	0.5893	0.0000	0.0000	0.0000	0.0000
			0.5894	0.5894	0.5894				
0.25	0.0	0.5578	0.5577	0.5577	0.5578	0.2554	0.2557	0.2557	0.2557
0.50	0.0	0.4587	0.4584	0.4585	0.4586	0.5455	0.5444	0.5454	0.5455
			0.4587	0.4589	0.4587		0.5454	0.5454	0.5456
0.75	0.0	0.2795	0.2794	0.2795	0.2795	0.9027	0.9018	0.9018	0.9019
1.00	0.00	0.0000	0.0000	0.0000	0.0000	1.3349	1.3463	1.3491	1.3507
							1.3504	1.3506	1.3506
0.25	0.25	0.5283	0.5283	0.5283	0.5283	0.2383	0.2368	0.2386	0.2386
0.50	0.25	0.4356	0.4356	0.4356	0.4356	0.5117	0.5116	0.5116	0.5117
0.75	0.25	0.2667	0.2666	0.2667	0.2667	0.8551	0.8542	0.8543	0.8544
1.00	0.25	0.0000	0.0000	0.0000	0.0000	1.2819	1.2971	1.2974	1.2975
0.50	0.50	0.3623	0.3619	0.3620	0.3623	0.4079	0.4074	0.4069	0.4072
			0.3623	0.3623	0.3623		0.4079	0.4078	0.4078
0.75	0.50	0.2255	0.2254	0.2255	0.2255	0.7042	0.7032	0.7031	0.7034
1.00	0.50	0.0000	0.0000	0.0000	0.0000	1.1102	1.1158	1.1182	1.1227
							1.12448	1.1252	1.12552
0.75	0.75	0.1456	0.1456	0.1456	0.1456	0.4242	0.4236	0.4231	0.4232

[1]The first line in each case corresponds to the solution obtained using a 2×2 mesh and the second to a 4×4 mesh. The Ritz finite element solution coincides with the Galerkin solution for the same choice of the Hermite interpolation.

14.2.3 Mixed Formulations

Higher-order differential equations place higher-order continuity on the approximation functions, as witnessed in the case of Euler–Bernoulli beam theory (Chapter 5) and the classical plate theory in Chapter 12. When the governing differential equations are second- or higher-order, it is possible to rewrite them as a set of lower-order differential equations and then develop their finite element models by using either their weak forms or weighted residual statements. Such alternative formulations are often considered primarily in the interest of using C^0 finite element approximations. Rewriting of higher-order differential equations as a set of lower-order equations requires introduction of additional variables, which are often physical quantities. The variables appearing in the original differential equations and the additional variables introduced in rewriting as a set of lower-order equations have quite different meaning. In fact, they are like primary and secondary variables of the original higher-order equation. Formulations that independently approximate both primary and secondary variables (of the traditional formulation) are termed *mixed* or *hybrid formulations*. The mixed formulations in turn can be based on weak forms or weighted residual methods. We shall illustrate these ideas with the help of the equations governing the Euler–Bernoulli beam theory.

Model Equation

The equation governing the bending of beams according to the Euler–Bernoulli beam theory is given by [Eq. (5.2.1) with $c_f = 0$]

$$\frac{d^2}{dx^2}\left(EI\frac{d^2w}{dx^2}\right) - q = 0 \tag{14.2.39}$$

where w is the transverse deflection, q the distributed transverse load, and EI the bending stiffness. As we have seen in Chapter 5, the weak-form finite element model of this fourth-order equation requires Hermite cubic interpolation of w that includes w and dw/dx as the nodal variables (i.e., a C^1 element). On the other hand, a weighted integral finite element model of (14.2.39) requires an approximation of w that includes w, dw/dx, $EI\,d^2w/dx^2$, and $(d/dx)(EI\,d^2w/dx^2)$ as the nodal degrees of freedom (i.e., seventh-degree Hermite polynomial and C^3 element). To reduce the differentiability requirements on w in the weak form and include the bending moment (or stress) as a nodal degree of freedom, Eq. (14.2.39) can be decomposed into a pair of lower-order equations:

$$-\frac{d^2M}{dx^2} - q = 0, \quad -\frac{d^2w}{dx^2} - \frac{M}{EI} = 0 \quad (EI > 0) \tag{14.2.40}$$

The assumption $EI \neq 0$ always holds in practice because neither the modulus of elasticity nor the moment of inertia is zero. We can develop either a weak-form finite element model or a weighted integral finite element model of the pair of equations in (14.2.40). These two models are discussed next. It is also possible to further reduce the order of the equations, say, to four first-order equations and then use the weighted residual method. Such a mixed formulation would include the deflection, rotation, bending moment, and shear force and will result in C^0 approximation of all unknowns. We will not discuss the details here.

Weak-Form Mixed Finite Element Model

The weak forms of the two equations in (14.2.40) are

$$0 = \int_{x_a}^{x_b} \left(\frac{dv_1}{dx}\frac{dM}{dx} - v_1 q \right) dx - v_1(x_a)\bar{Q}_1 - v_1(x_b)\bar{Q}_2, \tag{14.2.41a}$$

$$0 = \int_{x_a}^{x_b} \left(\frac{dv_2}{dx}\frac{dw}{dx} - v_2 \frac{M}{EI} \right) dx - v_2(x_a)\Theta_1 + v_2(x_b)\Theta_2, \tag{14.2.41b}$$

where (v_1, v_2) are the weight functions that have the interpretation of virtual deflection δw and virtual moment δM, respectively, and

$$\begin{aligned} \bar{Q}_1 &= -\left(\frac{dM}{dx}\right)_{x=x_a}, \quad \bar{Q}_2 = \left(\frac{dM}{dx}\right)_{x=x_b} \\ \Theta_1 &= \left(-\frac{dw}{dx}\right)_{x=x_a}, \quad \Theta_2 = \left(-\frac{dw}{dx}\right)_{x=x_b} \end{aligned} \tag{14.2.42}$$

The weak forms (14.2.41a) and (14.2.41b) suggest that both w and M may be approximated using the Lagrange interpolation. Suppose that w and M are approximated as (see Fig. 14.2.2)

$$w(x) \approx \sum_{i=1}^{m} w_i \phi_i(x), \quad M(x) \approx \sum_{i=1}^{n} M_i \psi_i(x) \tag{14.2.43}$$

where (ϕ_i, ψ_i) are the Lagrange interpolation functions of different degree used for w and M, respectively. Substituting Eq. (14.2.43) for w and M, and $v_1 = \phi_i$ and $v_2 = \psi_i$ into Eqs. (14.2.41a) and (14.2.41b), we obtain

$$\begin{bmatrix} \mathbf{0} & \mathbf{K}^e \\ (\mathbf{K}^e)^{\mathrm{T}} & -\mathbf{G}^e \end{bmatrix} \begin{Bmatrix} \mathbf{w}^e \\ \mathbf{M}^e \end{Bmatrix} = \begin{Bmatrix} \mathbf{F}^e + \bar{\mathbf{Q}}^e \\ \bar{\Theta}^e \end{Bmatrix} \tag{14.2.44}$$

where

$$\begin{aligned} K_{ij}^e &= \int_{x_a}^{x_b} \frac{d\phi_i}{dx}\frac{d\psi_j}{dx} dx, \quad G_{ij} = \frac{1}{EI}\int_{x_a}^{x_b} \psi_i \psi_j \, dx \\ F_i^e &= \int_{x_a}^{x_b} q\phi_i \, dx, \quad \bar{\Theta}_i^e = (-1)^{i+1}\Theta_i^e \end{aligned} \tag{14.2.45}$$

This completes the development of the weak-form mixed model.

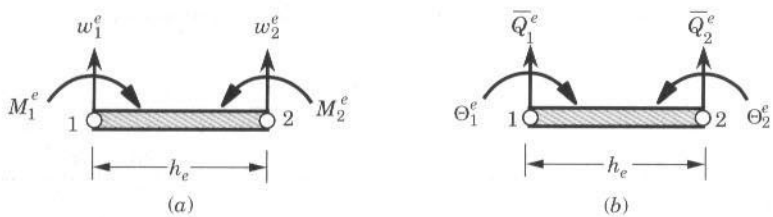

Figure 14.2.2 (a) Generalized displacements and (b) generalized forces for the mixed finite element formulation of the fourth-order equation (14.2.39) [or the weak-form model of (14.2.40)].

The pair of matrix equations (14.2.44) in terms of the nodal values of the displacements and moments can be reduced to a single matrix equation in terms of the generalized displacements $\mathbf{w}^e$ and Θ^e (i.e., converting a mixed model to a displacement model). In the interest of brevity, we omit the element label "e" in the quantities. Solving the second equation in (14.2.44) for $\mathbf{M}$, we obtain

$$\mathbf{M} = \mathbf{G}^{-1}[\mathbf{K}^{\mathrm{T}}\mathbf{w} - \bar{\Theta}] \tag{14.2.46a}$$

Substituting the result into the first equation in (14.2.44), we obtain

$$\mathbf{K}\mathbf{G}^{-1}\mathbf{K}^{\mathrm{T}}\mathbf{w} - \mathbf{K}\mathbf{G}^{-1}\bar{\Theta} = \mathbf{F} + \bar{\mathbf{Q}} \tag{14.2.46b}$$

Now we can write Eqs. (14.2.46a) and (14.2.46b) in a single matrix equation as

$$\begin{bmatrix} \mathbf{K}_w & -\mathbf{K}_\theta \\ -\mathbf{K}_\theta^{\mathrm{T}} & \mathbf{G}^{-1} \end{bmatrix} \begin{Bmatrix} \mathbf{w} \\ \Theta \end{Bmatrix} = \begin{Bmatrix} \mathbf{F} + \bar{\mathbf{Q}} \\ -\mathbf{M} \end{Bmatrix} \tag{14.2.47a}$$

where

$$\mathbf{K}_w = \mathbf{K}\mathbf{G}^{-1}\mathbf{K}^{\mathrm{T}}, \quad \mathbf{K}_\theta = \mathbf{K}\mathbf{G}^{-1} \tag{14.2.47b}$$

It is interesting to note that for the choice of linear interpolation of both w and M, the element stiffness matrix in (14.2.47a) can be shown to be the same as that in Eq. (5.2.18) (see Problem 14.5).

Weighted Residual Mixed Finite Element Model

The weighted residual mixed finite element model of the pair in Eq. (14.2.40) requires higher-order approximations of both w and M because they must satisfy both essential and natural boundary conditions. This leads to a complicated set of finite element equations. Here we present the main ideas behind the development of the model.

The weighted residual statements of the pair of equations is

$$0 = \int_{x_a}^{x_b} v_1 \left(-\frac{d^2 w_0}{dx^2} - \frac{M}{EI} \right) dx \tag{14.2.48a}$$

$$0 = \int_{x_a}^{x_b} v_2 \left(-\frac{d^2 M}{dx^2} - q \right) dx \tag{14.2.48b}$$

where (v_1, v_2) are the weight functions. A close examination of the above statements indicate that $v_1 \sim M$ and $v_2 \sim w$. Suppose that w and M are approximated as

$$w(x) \approx \sum_{i=1}^{4} \Delta_i \varphi_i^{(1)}(x), \quad M(x) \approx \sum_{i=1}^{4} \Lambda_i \varphi_i^{(2)}(x) \tag{14.2.49}$$

For the Galerkin finite element model, we take $v_1 \sim \varphi_i^{(2)}$ and $v_2 \sim \varphi_i^{(1)}$ and obtain the finite element model

$$\begin{bmatrix} \mathbf{0} & \mathbf{K}^{12} \\ \mathbf{K}^{21} & \mathbf{K}^{22} \end{bmatrix} \begin{Bmatrix} \Delta^e \\ \Lambda^e \end{Bmatrix} = \begin{Bmatrix} \mathbf{F}^e \\ \mathbf{0} \end{Bmatrix} \tag{14.2.50a}$$

where

$$K_{ij}^{12} = \int_{x_a}^{x_b} \varphi_i^{(1)} \frac{d^2\varphi_j^{(2)}}{dx^2} dx, \quad F_i^e = -\int_{x_a}^{x_b} q\varphi_i^{(1)}\, dx,$$
$$K_{ij}^{21} = \int_{x_a}^{x_b} \varphi_i^{(2)} \frac{d^2\varphi_j^{(1)}}{dx^2}\, dx, \quad K_{ij}^{22} = \int_{x_a}^{x_b} \varphi_i^{(2)} \frac{d^2\varphi_j^{(2)}}{dx^2}\, dx \tag{14.2.50b}$$

The coefficient matrix in Eq. (14.2.50*a*) is *not* symmetric.

The least-squares finite element model is based on the variational statement

$$0 = \delta \int_{x_a}^{x_b} \left[\left(\frac{d^2w}{dx^2} + \frac{M}{EI} \right)^2 + \left(\frac{d^2M}{dx^2} + q \right)^2 \right] dx$$
$$= 2 \int_{x_a}^{x_b} \left[\left(\frac{d^2w}{dx^2} + \frac{M}{EI} \right) \left(\frac{d^2\delta w}{dx^2} + \frac{\delta M}{EI} \right) + \left(\frac{d^2M}{dx^2} + q \right) \frac{d^2\delta M}{dx^2} \right] dx$$

or

$$0 = \int_{x_a}^{x_b} \frac{d^2\delta w}{dx^2} \left(\frac{d^2w}{dx^2} + \frac{M}{EI} \right) dx \tag{14.2.51a}$$

$$0 = \int_{x_a}^{x_b} \left[\delta M \left(\frac{d^2w}{dx^2} + \frac{M}{EI} \right) + EI \frac{d^2\delta M}{dx^2} \left(\frac{d^2M}{dx^2} + q \right) \right] dx \tag{14.2.51b}$$

Substituting the approximations in (14.2.49) into Eqs. (14.1.51*a*) and (14.2.51*b*), we obtain

$$\begin{bmatrix} \mathbf{A}^e & \mathbf{B}^e \\ (\mathbf{B}^e)^{\mathrm{T}} & \mathbf{D}^e \end{bmatrix} \begin{Bmatrix} \boldsymbol{\Lambda}^e \\ \boldsymbol{\Delta}^e \end{Bmatrix} = \begin{Bmatrix} \mathbf{F}^e \\ \mathbf{0} \end{Bmatrix} \tag{14.2.52a}$$

where

$$A_{ij}^e = \int_{x_a}^{x_b} \left(EI \frac{d^2\varphi_i^{(2)}}{dx^2} \frac{d^2\varphi_j^{(2)}}{dx^2} + \varphi_i^{(2)} \varphi_j^{(2)} \right) dx, \quad F_i^e = -\int_{x_a}^{x_b} \frac{d^2\varphi_i^{(2)}}{dx^2} q\, dx$$
$$B_{ij}^e = \int_{x_a}^{x_b} \varphi_i^{(2)} \frac{d^2\varphi_j^{(1)}}{dx^2}\, dx, \quad D_{ij}^e = \int_{x_a}^{x_b} \frac{d^2\varphi_i^{(1)}}{dx^2} \frac{d^2\varphi_j^{(1)}}{dx^2}\, dx \tag{14.2.52b}$$

14.3 THREE-DIMENSIONAL PROBLEMS

Most of the basic ideas covered in Chapter 8 for two-dimensional problems can be extended to three-dimensional problems. For the sake of completeness, here we discuss finite element formulations of (1) the Poisson equation governing three-dimensional heat transfer, (2) three-dimensional elasticity equations, and (3) equations governing three-dimensional flows of viscous incompressible fluids. In addition, some of the commonly used three-dimensional finite elements will be presented. To keep the size as well as the scope of the book to reasonable limits, only essential steps are presented and only one numerical example is included.

14.3.1 Heat Transfer

Consider the Poisson equation

$$-\frac{\partial}{\partial x}\left(k_x\frac{\partial T}{\partial x}\right)-\frac{\partial}{\partial y}\left(k_y\frac{\partial T}{\partial y}\right)-\frac{\partial}{\partial z}\left(k_z\frac{\partial T}{\partial z}\right)=g \quad \text{in} \quad \Omega \tag{14.3.1}$$

subjected to boundary conditions of the form

$$T=\hat{T} \quad \text{on} \quad \Gamma_1, \quad k_x\frac{\partial T}{\partial x}n_x+k_y\frac{\partial T}{\partial y}n_y+k_z\frac{\partial T}{\partial z}n_z+\beta(T-T_\infty)=\hat{q} \quad \text{on} \quad \Gamma_2 \tag{14.3.2}$$

where k_x, k_y, and k_z are conductivities of an orthotropic solid in the three coordinate directions, g is the internal heat generation per unit volume in a three-dimensional domain Ω, and $\hat{T}$ and $\hat{q}$ are specified functions of position on the portions Γ_1 and Γ_2, respectively, of the surface Γ of the domain (see Fig. 14.3.1); β is the convection coefficient and T_∞ is the ambient temperature.

The weak form of (14.3.1) over an element Ω_e is given by

$$\begin{aligned}0&=\int_{\Omega_e} w\left[-\frac{\partial}{\partial x}\left(k_x\frac{\partial T}{\partial x}\right)-\frac{\partial}{\partial y}\left(k_y\frac{\partial T}{\partial y}\right)-\frac{\partial}{\partial z}\left(k_z\frac{\partial T}{\partial z}\right)-g\right]d\mathbf{x}\\&=\int_{\Omega_e}\left[k_x\frac{\partial w}{\partial x}\frac{\partial T}{\partial x}+k_y\frac{\partial w}{\partial y}\frac{\partial T}{\partial y}+k_z\frac{\partial w}{\partial z}\frac{\partial T}{\partial z}-wg\right]d\mathbf{x}\\&\quad+\oint_{\Gamma^e}\beta wT\,ds-\oint_{\Gamma^e} w\,(q_n+\beta T_\infty)\,ds\end{aligned} \tag{14.3.3}$$

where w is the weight function.

Assume a finite element interpolation of the form

$$T=\sum_{j=1}^{n} T_j^e\psi_j^e(x,y,z) \tag{14.3.4}$$

over the element Ω_e (see Fig. 14.3.1). Substituting $w=\psi_i^e$ and (14.3.4) into (14.3.3), we obtain the finite element model

$$\mathbf{K}^e\mathbf{T}^e=\mathbf{f}^e+\mathbf{Q}^e \tag{14.3.5a}$$

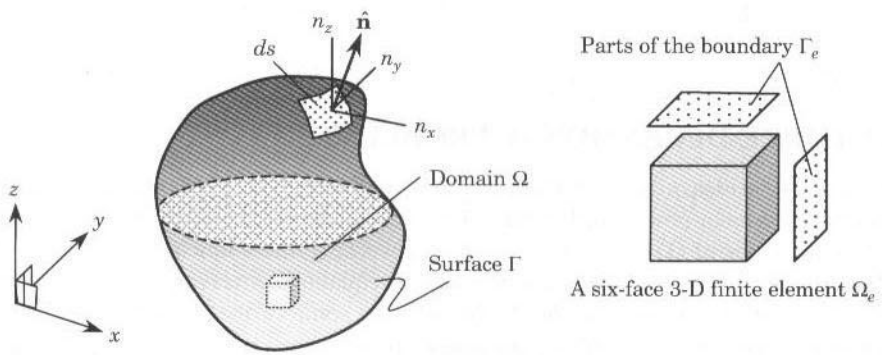

Figure 14.3.1 A three-dimensional domain Ω, its boundary Γ with unit normal $\hat{\mathbf{n}}$, and a typical three-dimensional finite element.

where

$$K_{ij}^e = \int_{\Omega_e} \left(k_x \frac{\partial \psi_i^e}{\partial x}\frac{\partial \psi_j^e}{\partial x} + k_y \frac{\partial \psi_i^e}{\partial y}\frac{\partial \psi_j^e}{\partial y} + k_z \frac{\partial \psi_i^e}{\partial z}\frac{\partial \psi_j^e}{\partial z} \right) d\mathbf{x} + \oint_{\Gamma^e} \beta \psi_i^e \psi_j^e \, ds$$

$$f_i^e = \int_{\Omega_e} g\psi_i^e \, d\mathbf{x}, \quad Q_i^e = \oint_{\Gamma^e} (q_n + \beta T_\infty)\psi_i^e \, ds \tag{14.3.5b}$$

Note that the boundary Γ_e of a three-dimensional element is a collection of two-dimensional elements. The numerical integration of volume and surface integrals is carried out in the same way as described in Chapter 9.

14.3.2 Flows of Viscous Incompressible Fluids

Here we develop the penalty finite element model of the Stokes equations governing three-dimensional flows of incompressible fluids. The governing equations consist of three momentum equations and a continuity equation

$$\begin{aligned}
2\mu\frac{\partial^2 v_x}{\partial x^2} + \mu\frac{\partial}{\partial y}\left(\frac{\partial v_x}{\partial y} + \frac{\partial v_y}{\partial x}\right) + \mu\frac{\partial}{\partial z}\left(\frac{\partial v_x}{\partial z} + \frac{\partial v_z}{\partial x}\right) - \frac{\partial P}{\partial x} + f_x = 0 \\
2\mu\frac{\partial^2 v_y}{\partial y^2} + \mu\frac{\partial}{\partial x}\left(\frac{\partial v_x}{\partial y} + \frac{\partial v_y}{\partial x}\right) + \mu\frac{\partial}{\partial z}\left(\frac{\partial v_y}{\partial z} + \frac{\partial v_z}{\partial y}\right) - \frac{\partial P}{\partial y} + f_y = 0 \\
2\mu\frac{\partial^2 v_z}{\partial z^2} + \mu\frac{\partial}{\partial x}\left(\frac{\partial v_x}{\partial z} + \frac{\partial v_z}{\partial x}\right) + \mu\frac{\partial}{\partial y}\left(\frac{\partial v_y}{\partial z} + \frac{\partial v_z}{\partial y}\right) - \frac{\partial P}{\partial z} + f_z = 0 \\
\frac{\partial v_x}{\partial x} + \frac{\partial v_y}{\partial y} + \frac{\partial v_z}{\partial z} = 0
\end{aligned} \tag{14.3.6}$$

In developing the penalty finite element model, we replace the pressure P in the momentum equations with

$$P = -\gamma\left(\frac{\partial v_x}{\partial x} + \frac{\partial v_y}{\partial y} + \frac{\partial v_z}{\partial z}\right) = 0 \tag{14.3.7}$$

and omit the continuity equation. The variational problem of the resulting equations can be cast in vector form as [see Eqs. (10.4.18) and (10.4.19)]

$$B_p(\mathbf{w}, \mathbf{v}) = l(\mathbf{w}) \tag{14.3.8}$$

where the bilinear forms $B_v(\mathbf{w}, \mathbf{v})$ and $\bar{B}_p(\mathbf{w}, P)$ and the linear form $l(\mathbf{w})$ are defined as in Eqs. (10.3.10*a*) and (10.4.19)

$$\mathbf{w} = \begin{Bmatrix} w_1 \\ w_2 \\ w_3 \end{Bmatrix}, \quad \mathbf{v} = \begin{Bmatrix} v_x \\ v_y \\ v_z \end{Bmatrix}, \quad \mathbf{f} = \begin{Bmatrix} f_x \\ f_y \\ f_z \end{Bmatrix}, \quad \mathbf{t} = \begin{Bmatrix} t_x \\ t_y \\ t_z \end{Bmatrix} \tag{14.3.9}$$

$$\begin{aligned}
B_p(\mathbf{w}, \mathbf{v}) &= \int_{\Omega_e} (\mathbf{D}\mathbf{w})^{\mathrm{T}} \mathbf{C} (\mathbf{D}\mathbf{v}) \, d\mathbf{x} + \int_{\Omega_e} \gamma_e \left(\mathbf{D}_1^{\mathrm{T}}\mathbf{w}\right)^{\mathrm{T}} \mathbf{D}_1^{\mathrm{T}}\mathbf{v} \, d\mathbf{x} \\
l(\mathbf{w}) &= \int_{\Omega_e} \mathbf{w}^{\mathrm{T}}\mathbf{f} \, dx \, dy + \oint_{\Gamma_e} \mathbf{w}^{\mathrm{T}}\mathbf{t} \, ds
\end{aligned} \tag{14.3.10}$$

$$\mathbf{D}=\begin{bmatrix} \dfrac{\partial}{\partial x} & 0 & 0 \\ 0 & \dfrac{\partial}{\partial y} & 0 \\ 0 & 0 & \dfrac{\partial}{\partial z} \\ \dfrac{\partial}{\partial y} & \dfrac{\partial}{\partial x} & 0 \\ \dfrac{\partial}{\partial z} & 0 & \dfrac{\partial}{\partial x} \\ 0 & \dfrac{\partial}{\partial z} & \dfrac{\partial}{\partial y} \end{bmatrix}, \quad \mathbf{D}_1=\begin{Bmatrix} \dfrac{\partial}{\partial x} \\ \dfrac{\partial}{\partial y} \\ \dfrac{\partial}{\partial z} \end{Bmatrix}, \quad \mathbf{C}=\mu\begin{bmatrix} 2 & 0 & 0 & 0 & 0 & 0 \\ 0 & 2 & 0 & 0 & 0 & 0 \\ 0 & 0 & 2 & 0 & 0 & 0 \\ 0 & 0 & 0 & 1 & 0 & 0 \\ 0 & 0 & 0 & 0 & 1 & 0 \\ 0 & 0 & 0 & 0 & 0 & 1 \end{bmatrix} \tag{14.3.11}$$

We assume finite element approximation of the form

$$\mathbf{v}=\begin{Bmatrix} v_x \\ v_y \\ v_z \end{Bmatrix}=\Psi\Delta, \quad \mathbf{w}=\begin{Bmatrix} w_1 \\ w_2 \\ w_3 \end{Bmatrix}=\Psi\delta\Delta \tag{14.3.12}$$

where

$$\Psi=\begin{bmatrix} \psi_1 & 0 & 0 & \psi_2 & 0 & 0 & \dots & \psi_n & 0 & 0 \\ 0 & \psi_1 & 0 & 0 & \psi_2 & 0 & 0 & \dots & \psi_n & 0 \\ 0 & 0 & \psi_1 & 0 & 0 & \psi_2 & 0 & 0 & \dots & \psi_n \end{bmatrix} \quad (3\times 3n)$$
$$\Delta=\begin{Bmatrix} v_x^1 & v_y^1 & v_z^1 & v_x^2 & v_y^2 & v_z^2 & \dots & v_x^n & v_y^n & v_z^n \end{Bmatrix}^{\mathrm{T}} \quad (3n\times 1) \tag{14.3.13}$$

Substituting (14.3.12) into the variational statement (14.3.8), we obtain the following finite element equation:

$$(\mathbf{K}_v+\mathbf{K}_p)\Delta=\mathbf{F} \tag{14.3.14}$$

where $\mathbf{K}_v$ is the contribution of the viscous terms (i.e., terms containing the viscosity μ), $\mathbf{K}_p$ is the contribution of the penalty terms (i.e., terms containing the penalty parameter γ), and $\mathbf{K}_v$ and $\mathbf{K}_p$ are of the order $3n\times 3n$; and $\mathbf{F}$ is the contribution of the body forces (f_x, f_y, f_z) as well as the boundary stresses (t_x, t_y, t_z), and $\mathbf{F}$ is of the order $3n\times 1$

$$\begin{aligned} \mathbf{K}_v &= \int_{\Omega_e} \mathbf{B}_v^{\mathrm{T}}\mathbf{C}\mathbf{B}_v\, d\mathbf{x}, \quad \mathbf{K}_p=\int_{\Omega_e}\gamma_e\mathbf{B}_p^{\mathrm{T}}\mathbf{B}_p\, d\mathbf{x} \\ \mathbf{F} &= \int_{\Omega_e}\Psi^{\mathrm{T}}\mathbf{f}\, d\mathbf{x}+\oint_{\Gamma_e}\Psi^{\mathrm{T}}\mathbf{t}\, ds \\ \mathbf{B}_v &= \mathbf{D}\Psi, \quad \mathbf{B}_p=\mathbf{D}_1^{\mathrm{T}}\Psi \end{aligned} \tag{14.3.15}$$

This completes the finite element model development.

14.3.3 Elasticity

Here, we develop the finite element models of three-dimensional elasticity problems [see Eqs. (2.3.48)–(2.3.53)]. First, we write the governing equations (2.3.51)–(2.3.53) in vector form.

Strain-Displacement Relations

$$\varepsilon_{xx} = \frac{\partial u_x}{\partial x}, \quad \varepsilon_{yy} = \frac{\partial u_y}{\partial y}, \quad \varepsilon_{zz} = \frac{\partial u_z}{\partial z}$$

$$2\varepsilon_{xy} = \frac{\partial u_x}{\partial y} + \frac{\partial u_y}{\partial x}, \quad 2\varepsilon_{xz} = \frac{\partial u_x}{\partial z} + \frac{\partial u_z}{\partial x}, \quad 2\varepsilon_{yz} = \frac{\partial u_y}{\partial z} + \frac{\partial u_z}{\partial y} \tag{14.3.16a}$$

or

$$\boldsymbol{\varepsilon} = \mathbf{D}\mathbf{u}, \quad \boldsymbol{\varepsilon} = \begin{Bmatrix} \varepsilon_{xx} \\ \varepsilon_{yy} \\ \varepsilon_{zz} \\ 2\varepsilon_{xz} \\ 2\varepsilon_{yz} \\ 2\varepsilon_{xy} \end{Bmatrix}, \quad \mathbf{D}^{\mathrm{T}} = \begin{bmatrix} \partial/\partial x & 0 & 0 & \partial/\partial z & 0 & \partial/\partial y \\ 0 & \partial/\partial y & 0 & 0 & \partial/\partial z & \partial/\partial x \\ 0 & 0 & \partial/\partial z & \partial/\partial x & \partial/\partial y & 0 \end{bmatrix} \tag{14.3.16b}$$

Equations of Motion

$$\begin{aligned} \frac{\partial \sigma_{xx}}{\partial x} + \frac{\partial \sigma_{xy}}{\partial y} + \frac{\partial \sigma_{xz}}{\partial z} + f_x &= \rho \frac{\partial u_x}{\partial t^2} \\ \frac{\partial \sigma_{xy}}{\partial x} + \frac{\partial \sigma_{yy}}{\partial y} + \frac{\partial \sigma_{yz}}{\partial z} + f_y &= \rho \frac{\partial u_y}{\partial t^2} \\ \frac{\partial \sigma_{xz}}{\partial x} + \frac{\partial \sigma_{yz}}{\partial y} + \frac{\partial \sigma_{zz}}{\partial z} + f_z &= \rho \frac{\partial u_z}{\partial t^2} \end{aligned} \tag{14.3.17a}$$

or

$$\mathbf{D}^{\mathrm{T}}\boldsymbol{\sigma} + \mathbf{f} = \rho\ddot{\mathbf{u}} \tag{14.3.17b}$$

where f_x, f_y, and f_z denote the components of the body force vector (measured per unit volume) along the x, y, and z directions, respectively, ρ is the density of the material, and

$$\boldsymbol{\sigma} = \begin{Bmatrix} \sigma_{xx} \\ \sigma_{yy} \\ \sigma_{zz} \\ \sigma_{xy} \\ \sigma_{xz} \\ \sigma_{yz} \end{Bmatrix}, \quad \mathbf{f} = \begin{Bmatrix} f_x \\ f_y \\ f_z \end{Bmatrix}, \quad \mathbf{u} = \begin{Bmatrix} u_x \\ u_y \\ u_z \end{Bmatrix} \tag{14.3.17c}$$

Stress-Strain (or *Constitutive*) *Relations*

$$\begin{Bmatrix} \sigma_{xx} \\ \sigma_{yy} \\ \sigma_{zz} \\ \sigma_{xz} \\ \sigma_{yz} \\ \sigma_{xy} \end{Bmatrix} = \begin{bmatrix} c_{11} & c_{12} & c_{13} & 0 & 0 & 0 \\ c_{12} & c_{22} & c_{23} & 0 & 0 & 0 \\ c_{13} & c_{23} & c_{33} & 0 & 0 & 0 \\ 0 & 0 & 0 & c_{44} & 0 & 0 \\ 0 & 0 & 0 & 0 & c_{55} & 0 \\ 0 & 0 & 0 & 0 & 0 & c_{66} \end{bmatrix} \begin{Bmatrix} \varepsilon_{xx} \\ \varepsilon_{yy} \\ \varepsilon_{zz} \\ 2\varepsilon_{xz} \\ 2\varepsilon_{yz} \\ 2\varepsilon_{xy} \end{Bmatrix} \quad \text{or} \quad \boldsymbol{\sigma} = \mathbf{C}\boldsymbol{\varepsilon} \tag{14.3.18}$$

where c_{ij} ($c_{ji} = c_{ij}$) are the elasticity (material) constants for an orthotropic medium with the material principal directions (x_1, x_2, x_3) coinciding with the coordinate axes (x, y, z) used to describe the problem. The c_{ij} can be expressed in terms of the engineering constants $(E_1, E_2, E_3, \nu_{12}, \nu_{13}, \nu_{23}, G_{12}, G_{13}, G_{23})$ for an orthotropic material by Eqs. (2.3.48*b*).

Boundary Conditions

$$\text{Natural} \quad \left.\begin{aligned} t_x &\equiv \sigma_{xx} n_x + \sigma_{xy} n_y + \sigma_{xz} n_z = \hat{t}_x \\ t_y &\equiv \sigma_{xy} n_x + \sigma_{yy} n_y + \sigma_{yz} n_z = \hat{t}_y \\ t_z &\equiv \sigma_{xz} n_x + \sigma_{yz} n_y + \sigma_{zz} n_z = \hat{t}_z \end{aligned}\right\} \quad \text{on } \Gamma_\sigma \tag{14.3.19}$$

$$\text{Essential} \quad \mathbf{u} = \hat{\mathbf{u}} \quad \text{on } \Gamma_u \tag{14.3.20}$$

The principle of virtual displacements for the three-dimensional elasticity problem can be expressed in vector form as in (11.3.4)

$$0 = \int_{\Omega_e} \left[(\mathbf{D}\delta\mathbf{u})^{\mathrm{T}} \mathbf{C} (\mathbf{D}\mathbf{u}) + \rho \mathbf{u}^{\mathrm{T}} \ddot{\mathbf{u}} \right] d\mathbf{x} - \int_{\Omega_e} (\delta\mathbf{u})^{\mathrm{T}} \mathbf{f}\, d\mathbf{x} - \oint_{\Gamma_e} (\delta\mathbf{u})^{\mathrm{T}} \mathbf{t}\, ds \tag{14.3.21}$$

The finite element approximation is assumed to be in the form

$$\mathbf{u} = \begin{Bmatrix} u_x \\ u_y \\ u_z \end{Bmatrix} = \Psi \Delta, \quad \mathbf{w} = \delta\mathbf{u} = \begin{Bmatrix} w_1 = \delta u_x \\ w_2 = \delta u_y \\ w_3 = \delta u_z \end{Bmatrix} = \Psi \delta\Delta \tag{14.3.22}$$

where

$$\begin{aligned} \Psi &= \begin{bmatrix} \psi_1 & 0 & 0 & \psi_2 & 0 & 0 & \dots & \psi_n & 0 & 0 \\ 0 & \psi_1 & 0 & 0 & \psi_2 & 0 & 0 & \dots & \psi_n & 0 \\ 0 & 0 & \psi_1 & 0 & 0 & \psi_2 & 0 & \dots & 0 & \psi_n \end{bmatrix} \\ \Delta &= \begin{Bmatrix} u_x^1 & u_y^1 & u_z^1 & u_x^2 & u_y^2 & u_z^2 & \dots & u_x^n & u_y^n & u_z^n \end{Bmatrix}^{\mathrm{T}} \end{aligned} \tag{14.3.23}$$

Substituting Eq. (14.3.22) into the statement of the principle of virtual work (14.3.21), we arrive at the finite element model of a three-dimensional elastic body

$$\mathbf{M}^e \ddot{\Delta}^e + \mathbf{K}^e \Delta^e = \mathbf{F}^e + \mathbf{Q}^e \tag{14.3.24}$$

where

$$\begin{aligned} \mathbf{K}^e &= \int_{\Omega_e} \mathbf{B}^{\mathrm{T}} \mathbf{C} \mathbf{B}\, d\mathbf{x}, \quad \mathbf{M}^e = \int_{\Omega_e} \rho \Psi^{\mathrm{T}} \Psi^e\, d\mathbf{x} \\ \mathbf{F}^e &= \int_{\Omega_e} \Psi^{\mathrm{T}} \mathbf{f}\, d\mathbf{x}, \quad \mathbf{Q}^e = \oint_{\Gamma_e} \Psi^{\mathrm{T}} \mathbf{t}\, ds \end{aligned} \tag{14.3.25}$$

The element mass matrix $\mathbf{M}^e$ and stiffness matrix $\mathbf{K}^e$ are of order $3n \times 3n$ and the element load vector $\mathbf{F}^e$ and the vector of internal forces $\mathbf{Q}^e$ is of order $3n \times 1$, where n is the number of nodes in a finite element.

Computer implementation of three classes of problems described in this section is straightforward, and we can modify the computer program **FEM2D** to implement the finite

element models in (14.3.5*a*), (14.3.14), and (14.3.24). The main change is in the subroutine **SHAPE3D** in which the interpolation functions and their global derivatives are evaluated. In the next section, interpolation functions for a number of commonly used three-dimensional finite elements are presented. We note that in going from two dimensions to three dimensions, we increase the number of geometries (i.e., shapes) that can be used to define finite element interpolation functions.

14.3.4 Three-Dimensional Finite Elements

The element matrices in (14.3.5*b*), (14.3.15), and (14.3.25) require the use of C^0 (i.e., the Lagrange) family of interpolation functions. The interpolation functions can be derived as described in Chapters 8 and 9 for two-dimensional elements, and they have the same interpolation properties as those of two-dimensional elements

$$\sum_{i=1}^{n} \psi_i^e(x, y, z) = 1, \quad \psi_i^e(x_j, y_j, z_j) = \delta_{ij} \tag{14.3.26}$$

For example, consider the linear elements shown in the first column of Fig. 14.3.2. The polynomials used to develop the interpolation functions for these elements are of the form

$$\begin{aligned}
u(x, y, z) &= a_0 + a_1 x + a_2 y + a_3 z && \text{(four-node tetrahedral element)} \\
u(x, y, z) &= a_0 + a_1 x + a_2 y + a_3 z + a_4 xz + a_5 yz && \text{(six-node prism element)} \\
u(x, y, z) &= a_0 + a_1 x + a_2 y + a_3 z + a_4 yz + a_5 xz && \text{(eight-node brick or} \\
&\quad + a_6 xy + a_7 xyz && \text{hexahedral element)}
\end{aligned} \tag{14.3.27}$$

In evaluating the element matrices numerically, the geometry of the elements can be described by the transformation equations

$$x = \sum_{i=1}^{m} x_i \hat{\psi}_i(\xi, \eta, \zeta), \quad y = \sum_{i=1}^{m} y_i \hat{\psi}_i(\xi, \eta, \zeta), \quad z = \sum_{i=1}^{m} z_i \hat{\psi}_i(\xi, \eta, \zeta) \tag{14.3.28}$$

Under these transformations, the master tetrahedral and prism elements transform to the arbitrary tetrahedral, prism, and hexahedral elements shown in Fig. 14.3.2. The definition of the Jacobian matrix and the numerical quadrature rules described in Chapter 9 can easily be extended to the three-dimensional case. For example, Eqs. (9.3.8) and (9.3.9) take the form

$$[J] = \begin{bmatrix} \dfrac{\partial x}{\partial \xi} & \dfrac{\partial y}{\partial \xi} & \dfrac{\partial z}{\partial \xi} \\ \dfrac{\partial x}{\partial \eta} & \dfrac{\partial y}{\partial \eta} & \dfrac{\partial z}{\partial \eta} \\ \dfrac{\partial x}{\partial \zeta} & \dfrac{\partial y}{\partial \zeta} & \dfrac{\partial z}{\partial \zeta} \end{bmatrix} = \begin{bmatrix} \dfrac{\partial \hat{\psi}_1}{\partial \xi} & \dfrac{\partial \hat{\psi}_2}{\partial \xi} & \cdots & \dfrac{\partial \hat{\psi}_m}{\partial \xi} \\ \dfrac{\partial \hat{\psi}_1}{\partial \eta} & \dfrac{\partial \hat{\psi}_2}{\partial \eta} & \cdots & \dfrac{\partial \hat{\psi}_m}{\partial \eta} \\ \dfrac{\partial \hat{\psi}_1}{\partial \zeta} & \dfrac{\partial \hat{\psi}_2}{\partial \zeta} & \cdots & \dfrac{\partial \hat{\psi}_m}{\partial \zeta} \end{bmatrix} \begin{bmatrix} x_1 & y_1 & z_1 \\ x_2 & y_2 & z_2 \\ \vdots & \vdots & \vdots \\ x_m & y_m & z_m \end{bmatrix} \tag{14.3.29}$$

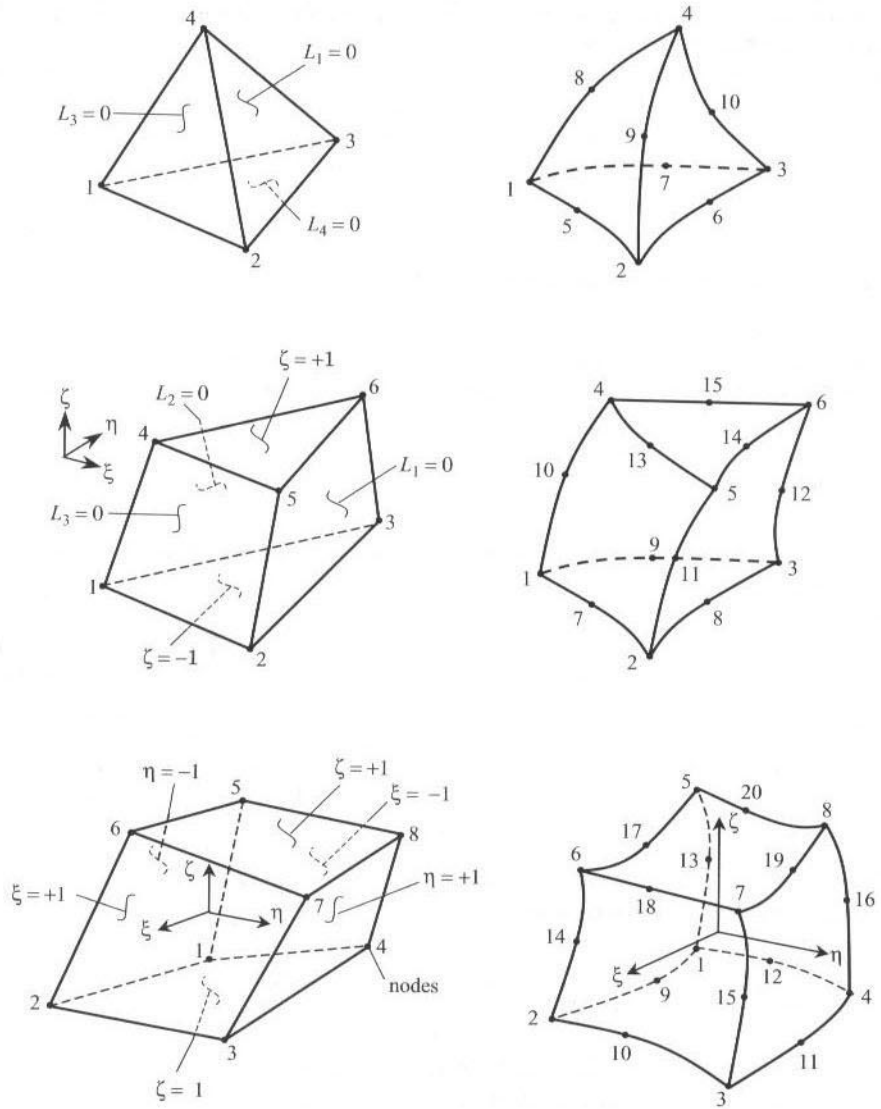

Figure 14.3.2 Linear and quadratic tetrahedral, prism, and brick elements (whose surfaces are two-dimensional triangular or quadrilateral elements).

$$\begin{Bmatrix} \dfrac{\partial \psi_i^e}{\partial x} \\ \dfrac{\partial \psi_i^e}{\partial y} \\ \dfrac{\partial \psi_i^e}{\partial z} \end{Bmatrix} = [J]^{-1} \begin{Bmatrix} \dfrac{\partial \psi_i^e}{\partial \xi} \\ \dfrac{\partial \psi_i^e}{\partial \eta} \\ \dfrac{\partial \psi_i^e}{\partial \zeta} \end{Bmatrix} \tag{14.3.30}$$

Interpolation functions for some standard elements are recorded in Eqs. (14.3.31)–(14.3.35) [see Reddy and Gartling (2001)].

Linear and Quadratic Hexhedral (Brick) Elements

$$\{\Psi^e\} = \frac{1}{8}\begin{Bmatrix} (1-\xi)(1-\eta)(1-\zeta) \\ (1+\xi)(1-\eta)(1-\zeta) \\ (1+\xi)(1+\eta)(1-\zeta) \\ (1-\xi)(1+\eta)(1-\zeta) \\ (1-\xi)(1-\eta)(1+\zeta) \\ (1+\xi)(1-\eta)(1+\zeta) \\ (1+\xi)(1+\eta)(1+\zeta) \\ (1-\xi)(1+\eta)(1+\zeta) \end{Bmatrix} \tag{14.3.31}$$

$$\{\Psi^e\} = \frac{1}{8}\begin{Bmatrix} (1-\xi)(1-\eta)(1-\zeta)(-\xi-\eta-\zeta-2) \\ (1+\xi)(1-\eta)(1-\zeta)(\xi-\eta-\zeta-2) \\ (1+\xi)(1+\eta)(1-\zeta)(\xi+\eta-\zeta-2) \\ (1-\xi)(1+\eta)(1-\zeta)(-\xi+\eta-\zeta-2) \\ (1-\xi)(1-\eta)(1+\zeta)(-\xi-\eta+\zeta-2) \\ (1+\xi)(1-\eta)(1+\zeta)(\xi-\eta+\zeta-2) \\ (1+\xi)(1+\eta)(1+\zeta)(\xi+\eta+\zeta-2) \\ (1-\xi)(1+\eta)(1+\zeta)(-\xi+\eta+\zeta-2) \\ 2(1-\xi^2)(1-\eta)(1-\zeta) \\ 2(1+\xi)(1-\eta^2)(1-\zeta) \\ 2(1-\xi^2)(1+\eta)(1-\zeta) \\ 2(1-\xi)(1-\eta^2)(1-\zeta) \\ 2(1-\xi)(1-\eta)(1-\zeta^2) \\ 2(1+\xi)(1-\eta)(1-\zeta^2) \\ 2(1+\xi)(1+\eta)(1-\zeta^2) \\ 2(1-\xi)(1+\eta)(1-\zeta^2) \\ 2(1-\xi^2)(1-\eta)(1+\zeta) \\ 2(1+\xi)(1-\eta^2)(1+\zeta) \\ 2(1-\xi^2)(1+\eta)(1+\zeta) \\ 2(1-\xi)(1-\eta^2)(1+\zeta) \end{Bmatrix} \tag{14.3.32}$$

Linear and Quadratic Prism Elements

$$\{\Psi^e\} = \frac{1}{2}\begin{Bmatrix} L_1(1-\zeta) \\ L_2(1-\zeta) \\ L_3(1-\zeta) \\ L_1(1+\zeta) \\ L_2(1+\zeta) \\ L_3(1+\zeta) \end{Bmatrix} \tag{14.3.33}$$

$$\{\Psi^e\} = \frac{1}{2}\begin{Bmatrix} L_1[(2L_1-1)(1-\zeta)-(1-\zeta^2)] \\ L_2[(2L_2-1)(1-\zeta)-(1-\zeta^2)] \\ L_3[(2L_3-1)(1-\zeta)-(1-\zeta^2)] \\ L_1[(2L_1-1)(1+\zeta)-(1-\zeta^2)] \\ L_2[(2L_2-1)(1+\zeta)-(1-\zeta^2)] \\ L_3[(2L_3-1)(1+\zeta)-(1-\zeta^2)] \\ 4L_1L_2(1-\zeta) \\ 4L_2L_3(1-\zeta) \\ 4L_3L_1(1-\zeta) \\ 2L_1(1-\zeta^2) \\ 2L_2(1-\zeta^2) \\ 2L_3(1-\zeta^2) \\ 4L_1L_2(1+\zeta) \\ 4L_2L_3(1+\zeta) \\ 4L_3L_1(1+\zeta) \end{Bmatrix} \tag{14.3.34}$$

Linear and Quadratic Tetrahedral Elements

$$\{\Psi^e\} = \begin{Bmatrix} L_1 \\ L_2 \\ L_3 \\ L_4 \end{Bmatrix}, \quad \{\Psi^e\} = \begin{Bmatrix} L_1(2L_1-1) \\ L_2(2L_2-1) \\ L_3(2L_3-1) \\ L_4(2L_4-1) \\ 4L_1L_2 \\ 4L_2L_3 \\ 4L_3L_1 \\ 4L_1L_4 \\ 4L_2L_4 \\ 4L_3L_4 \end{Bmatrix} \tag{14.3.35}$$

The volume coordinates, L_i, are used to describe the interpolation functions for linear and quadratic elements, where $L_1 + L_2 + L_3 + L_4 = 1$.

14.3.5 A Numerical Example

Here, we consider an example of heat conduction in a three-dimensional solid. The problem is analyzed using program **FEM3D**, which is an extension of **FEM2D**. The program **FEM3D** is not discussed here.

Example 14.3.1

Consider an isotropic slab of dimensions $1 \times 1 \times 10$ m. The left face is maintained at a temperature of 100°C while the bottom, top and the right faces are maintained at 0°C, as shown in Fig. 14.3.3(*a*). The front and back faces are assumed to be insulated. There is no internal heat generation. Since only temperature boundary conditions are involved, the solution will be independent of the conductivity of the medium. Using the symmetry, a quadrant of the domain is modeled using a $4 \times 2 \times 2$ mesh of eight-node brick elements [see Fig.14.3.3(*b*)].

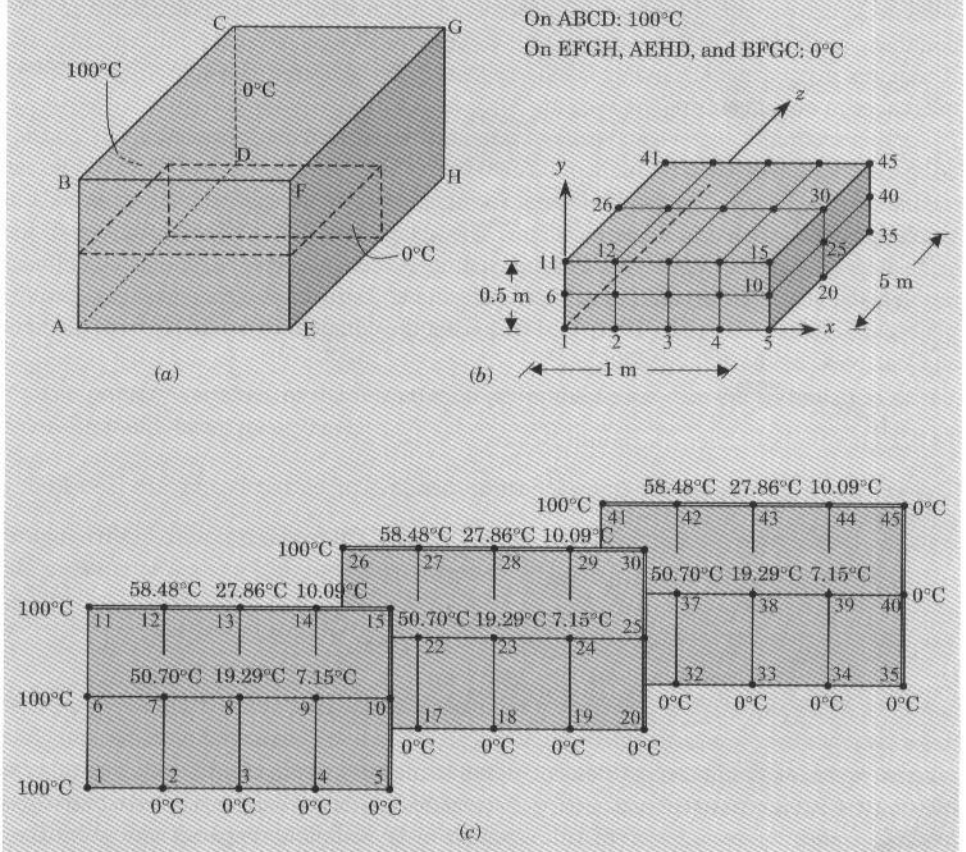

Figure 14.3.3 Heat conduction in an isotropic slab. (*a*) Geometry and boundary conditions. (*b*) Computational domain. (*c*) Predicted temperature field.

The resulting temperature field is depicted in Fig. 14.3.3(*c*). As we might expect, the three-dimensional solution is the same as the two-dimensional (in the xy plane) solution because the two-dimensional problem is equivalent to assuming that the slab is infinitely long in the z direction. Thus, all planes parallel to the plane $z = 0$ have the same temperature distribution. The three-dimensional solution would have been different from the two-dimensional one if we had specified, for example, the temperature on the front and back faces (AEFB and DHGC).

14.4 NONLINEAR PROBLEMS

14.4.1 General Comments

Many engineering problems are described by nonlinear differential equations. Under certain simplifying assumptions, these problems can be described by linear differential equations. While a small percentage (about 10 percent) of practical engineering problems require nonlinear analysis, it is not a trivial task to determine when to use nonlinear analysis. It requires a good understanding of the system being analyzed and the allowed design tolerances in manufacturing the system.

In this section, we give some taste of nonlinear finite element formulations by considering the one-dimensional problem of beam bending and two-dimensional flows of viscous incompressible fluids. The finite element formulation of nonlinear problems preceeds in much the same way as for linear problems. The main difference lies in the solution of the finite element algebraic equations. For more complete details and applications to nonlinear problems in heat transfer, fluid dynamics, and solid and structural mechanics (e.g., beams, plates, and shells), the reader is advised to consult the companion nonlinear finite element analysis book by the author (2004).

14.4.2 Bending of Euler–Bernoulli Beams

The equations governing the large-deflection bending of elastic beams are [see Reddy (2004)]

$$-\frac{d}{dx}\left\{EA\left[\frac{du}{dx}+\frac{1}{2}\left(\frac{dw}{dx}\right)^2\right]\right\}-f=0 \tag{14.4.1}$$

$$\frac{d^2}{dx^2}\left(EI\frac{d^2w}{dx^2}\right)-\frac{d}{dx}\left\{EA\frac{dw}{dx}\left[\frac{du}{dx}+\frac{1}{2}\left(\frac{dw}{dx}\right)^2\right]\right\}-q=0 \tag{14.4.2}$$

where u is the longitudinal displacement, w is the transverse deflection, E is the modulus of elasticity, A is the cross-sectional area, f is the axial distributed load, and q is the transverse loading. Under the assumption that the slope dw/dx is small compared with unity [i.e., $(dw/dx)(du/dx) \approx 0$, $(dw/dx)^2 \approx 0$], Eqs. (14.4.1) and (14.4.2) become uncoupled and reduce to the bar equation (3.2.1) and beam equation (14.2.39), respectively. However, when the slope dw/dx is not too small, we must solve the coupled set of nonlinear equations (14.4.1) and (14.4.2).

These weak forms of (14.4.1) and (14.4.2) over an element (x_a, x_b) are

$$0=\int_{x_a}^{x_b}\left\{EA\frac{dv_1}{dx}\left[\frac{du}{dx}+\frac{1}{2}\left(\frac{dw}{dx}\right)^2\right]-v_1 f\right\}dx-Q_1^e v_1(x_a)-Q_4^e v_1(x_b) \quad (14.4.3a)$$

where v_1 is the weight function ($v_1 \sim \delta u$) and

$$Q_1^e=-\left\{EA\left[\frac{du}{dx}+\frac{1}{2}\left(\frac{dw}{dx}\right)^2\right]\right\}\Bigg|_{x_a}, \quad Q_4^e=\left\{EA\left[\frac{du}{dx}+\frac{1}{2}\left(\frac{dw}{dx}\right)^2\right]\right\}\Bigg|_{x_b} \quad (14.4.3b)$$

Similarly,

$$\begin{aligned}0=&\int_{x_a}^{x_b}\left\{EI\frac{d^2v_2}{dx^2}\frac{d^2w}{dx^2}+EA\frac{dv_2}{dx}\frac{dw}{dx}\left[\frac{du}{dx}+\frac{1}{2}\left(\frac{dw}{dx}\right)^2\right]-v_2 q\right\}dx\\&-Q_2^e v_2(x_a)-Q_3^e\left(-\frac{dv_2}{dx}\right)\Bigg|_{x_a}-Q_5^e v_2(x_b)-Q_6^e\left(-\frac{dv_2}{dx}\right)\Bigg|_{x_b} \quad (14.4.4a)\end{aligned}$$

where v_2 is the weight function ($v_2 \sim \delta w$), and

$$\begin{aligned}Q_2^e&=\left\{\frac{d}{dx}\left(EI\frac{d^2w}{dx^2}\right)-EA\frac{dw}{dx}\left[\frac{du}{dx}+\frac{1}{2}\left(\frac{dw}{dx}\right)^2\right]\right\}\Bigg|_{x_a}\\Q_5^e&=-\left\{\frac{d}{dx}\left(EI\frac{d^2w}{dx^2}\right)-EA\frac{dw}{dx}\left[\frac{du}{dx}+\frac{1}{2}\left(\frac{dw}{dx}\right)^2\right]\right\}\Bigg|_{x_b} \quad (14.4.4b)\\Q_3^e&=\left(EI\frac{d^2w}{dx^2}\right)\Bigg|_{x_a}, \quad Q_6^e=-\left(EI\frac{d^2w}{dx}\right)\Bigg|_{x_b}\end{aligned}$$

The primary variables of the formulation (as in the frame element formulation of the Euler–Bernoulli beam theory) are

$$u, \quad w, \quad \theta \equiv -\frac{dw}{dx}$$

From the discussions presented in Chapters 3 and 5, it is clear that we must use a Lagrange interpolation of u and a Hermite interpolation of w:

$$u=\sum_{j=1}^{n} u_j\psi_i(x), \quad w=\sum_{j=1}^{4}\Delta_j\phi_j(x) \quad (14.4.5)$$

where ψ_j are the Lagrange interpolation functions of degree $n-1$ and ϕ_j are the Hermite cubic interpolation functions. For $n=2$ (i.e., linear approximation of u), the elements used for u and w contain the same number of nodes, which is convenient in the computer implementation of the model (see Fig. 14.4.1).

Substituting the approximations (14.4.5) for u and w, and $v_1=\psi_i$ and $v_2=\phi_i$, into (14.4.3a) and (14.4.4a), we obtain the finite element model

$$\begin{bmatrix}\mathbf{K}^{11} & \mathbf{K}^{12}\\ \mathbf{K}^{21} & \mathbf{K}^{22}\end{bmatrix}\begin{Bmatrix}\mathbf{u}\\ \Delta\end{Bmatrix}=\begin{Bmatrix}\mathbf{F}^1\\ \mathbf{F}^2\end{Bmatrix} \quad (14.4.6a)$$

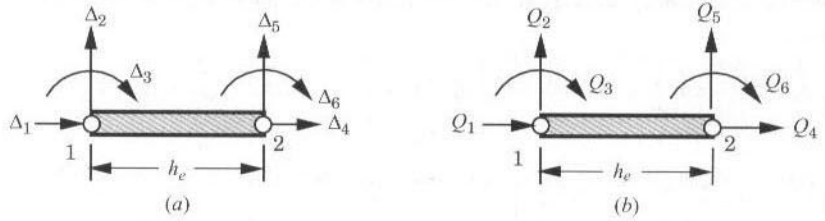

Figure 14.4.1 Nonlinear Euler–Bernoulli beam element based on linear interpolation of the axial displacement u and Hermite cubic interpolation of the transverse deflection w.

where

$$
\begin{aligned}
K_{ij}^{11} &= \int_{x_a}^{x_b} EA \frac{d\psi_i}{dx}\frac{d\psi_j}{dx}\,dx, \quad K_{ij}^{12} = \int_{x_a}^{x_b} \frac{1}{2} EA \frac{dw}{dx}\frac{d\psi_i}{dx}\frac{d\phi_j}{dx}\,dx \\
K_{ij}^{22} &= \int_{x_a}^{x_b} EI \frac{d^2\phi_i}{dx^2}\frac{d^2\phi_j}{dx^2}\,dx + \int_{x_a}^{x_b} \frac{1}{2} EA \left(\frac{dw}{dx}\right)^2 \frac{d\phi_i}{dx}\frac{d\phi_j}{dx}\,dx \\
K_{ji}^{21} &= \int_{x_a}^{x_b} EA \frac{dw}{dx}\frac{d\phi_j}{dx}\frac{d\psi_i}{dx}\,dx, \quad F_i^1 = \int_{x_a}^{x_b} \psi_i f\,dx + Q_{3i-2} \\
F_i^2 &= \int_{x_a}^{x_b} \phi_i q\,dx + Q_{i+1} \qquad \begin{cases} I = 1 & \text{if } i = 1 \text{ or } 2 \\ I = 2 & \text{if } i = 3 \text{ or } 4 \end{cases}
\end{aligned}
\tag{14.4.6b}
$$

This completes the finite element model of the nonlinear bending of beams.

14.4.3 The Navier–Stokes Equations in Two Dimensions

When the inertial effects are larger than the viscous effects, Eqs. (10.2.9) and (10.2.10) must be modified to include the convective terms, i.e., the following Navier–Stokes equations must be solved:

$$
\begin{aligned}
&\rho\left(v_x\frac{\partial v_x}{\partial x} + v_y\frac{\partial v_x}{\partial y}\right) - \mu\left[2\frac{\partial^2 v_x}{\partial x^2} + \frac{\partial}{\partial y}\left(\frac{\partial v_x}{\partial y} + \frac{\partial v_y}{\partial x}\right)\right] + \frac{\partial P}{\partial x} = f_x \\
&\rho\left(v_x\frac{\partial v_y}{\partial x} + v_y\frac{\partial v_y}{\partial y}\right) - \mu\left[\frac{\partial}{\partial x}\left(\frac{\partial v_x}{\partial y} + \frac{\partial v_y}{\partial x}\right) + 2\frac{\partial^2 v_y}{\partial y^2}\right] + \frac{\partial P}{\partial y} = f_y \\
&\frac{\partial v_x}{\partial x} + \frac{\partial v_y}{\partial y} = 0
\end{aligned}
\tag{14.4.7}
$$

where ρ is the density of the fluid and all the other symbols have the same meaning as in Chapter 10.

Here, we present the penalty finite element model of the Navier–Stokes equations (14.4.7) over an element, i.e., replace the pressure P by

$$
P = -\gamma\left(\frac{\partial v_x}{\partial x} + \frac{\partial v_y}{\partial y}\right) \tag{14.4.8}
$$

and omit the continuity equation. The weak form is given by (see Section 10.3 for details)

$$\begin{aligned}
&\int_{\Omega_e} \left\{ w_1 \rho \left(v_x \frac{\partial v_x}{\partial x} + v_y \frac{\partial v_x}{\partial y} \right) + [\ldots] \right\} d\mathbf{x} - \int_{\Omega_e} w_1 f_x \, d\mathbf{x} - \oint_{\Gamma_e} w_1 t_x \, ds = 0 \\
&\int_{\Omega_e} \left\{ w_2 \rho \left(v_x \frac{\partial v_y}{\partial x} + v_y \frac{\partial v_y}{\partial y} \right) + [\ldots] \right\} d\mathbf{x} - \int_{\Omega_e} w_2 f_y \, d\mathbf{x} - \oint_{\Gamma_e} w_2 t_y \, ds = 0
\end{aligned} \tag{14.4.9}$$

where [...] denotes the expressions (omitting the time-derivative terms) in the square brackets of Eqs. (10.4.21) and (10.4.22) (also, note that $w_1 = \delta v_x$ and $w_2 = \delta v_y$). The finite element model of these equations is given by

$$(\mathbf{K}_c + \mathbf{K}_v + \mathbf{K}_p)\boldsymbol{\Delta} = \mathbf{F} \tag{14.4.10a}$$

where $\mathbf{K}_v$, $\mathbf{K}_p$, and $\mathbf{F}$ are defined in Eq. (10.4.28) [also, see Eq. (10.3.10*b*)] and $\mathbf{K}_c$ is the contribution of the nonlinear (convective) terms to the coefficient matrix

$$\mathbf{K}_c = \int_{\Omega_e} \rho(\Psi \bar{\mathbf{v}}^{\mathrm{T}} \mathbf{D}_1)^{\mathrm{T}} \Psi \, d\mathbf{x}, \quad \bar{\mathbf{v}} = \Psi \bar{\boldsymbol{\Delta}} \tag{14.4.10b}$$

and $\bar{\Delta}$ is the solution vector known from the previous iteration.

14.4.4 Solution Methods for Nonlinear Algebraic Equations

Note that the element coefficient matrices in Eqs. (14.4.6*a*) and (14.4.10*a*) are nonlinear and unsymmetric. In the case of beams, the element stiffness matrix is a function of the unknown transverse deflection, whereas in the case of fluid flow, the coefficient matrix is a function of unknown velocity components. The assembled nonlinear equations must be solved, after imposing boundary conditions, by a suitable method. Here, we describe two iterative methods in which we seek an approximate solution to the nonlinear algebraic equations by linearization. The iterative methods are outlined using a nonlinear matrix equation of the form

$$\mathbf{K}(\boldsymbol{\Delta})\boldsymbol{\Delta} = \mathbf{F} \tag{14.4.11}$$

where $\boldsymbol{\Delta}$ is the vector of unknown nodal values; the dependence of $\mathbf{K}$ on $\boldsymbol{\Delta}$ is clearly indicated.

The *direct iteration method,* also known as the *Picard method,* is based on the scheme

$$\mathbf{K}(\boldsymbol{\Delta}^r)\boldsymbol{\Delta}^{r+1} = \mathbf{F} \tag{14.4.12}$$

where $\boldsymbol{\Delta}^r$ denotes the solution at the rth iteration. Thus, in the direct iteration method, the coefficients K_{ij} (and hence $K_{ij}^{\alpha\beta}$) are evaluated using the solution $\boldsymbol{\Delta}^r$ from the previous iteration, and the solution at the $(r+1)$th iteration is obtained by solving (14.4.12):

$$\boldsymbol{\Delta}^{r+1} = (\mathbf{K}(\boldsymbol{\Delta}^r))^{-1}\mathbf{F} \tag{14.4.13}$$

At the beginning of the iteration (i.e., $r = 0$), we assume a solution $\boldsymbol{\Delta}^0$ based on our qualitative understanding of the solution behavior. For example, $\boldsymbol{\Delta}^0 = \mathbf{0}$ for large-deflection bending would reduce the nonlinear stiffness matrix to a linear one, and (14.4.13) would

yield the linear solution of the problem at the end of the first iteration, $\boldsymbol{\Delta}^1$. The iteration is continued [i.e., (14.4.13) is solved in each iteration] until the difference between $\boldsymbol{\Delta}^r$ and $\boldsymbol{\Delta}^{r+1}$ reduces to a preselected error tolerance. The *error criterion* is of the form (other criteria may also be used)

$$\frac{|\boldsymbol{\Delta}^{r+1} - \boldsymbol{\Delta}^r|}{|\boldsymbol{\Delta}^{r+1}|} < \epsilon \quad (\text{say}, 10^{-3}) \tag{14.4.14}$$

where $|\cdot|$ denotes the Euclidean norm (root-mean-square value) of N nodal values, where N is the total number of primary unknowns (i.e., generalized displacements) in the finite element mesh.

The other iterative method is the *Newton–Raphson method,* which is based on the Taylor series expansion of the algebraic equations (14.4.11) about the known solution $\boldsymbol{\Delta}^r$. To describe the method, we rewrite (14.4.11) in the form

$$\mathbf{R} \equiv \mathbf{K}\boldsymbol{\Delta} - \mathbf{F} = \mathbf{0} \tag{14.4.15}$$

where $\mathbf{R}$ denotes the residual due to the linearization of $\mathbf{K}$. Expanding $\mathbf{R}$ about $\boldsymbol{\Delta}^r$, we obtain

$$\mathbf{0} = \mathbf{R} = \mathbf{R}^r + \left(\frac{\partial \mathbf{R}}{\partial \boldsymbol{\Delta}}\right)_r (\boldsymbol{\Delta}^{r+1} - \boldsymbol{\Delta}^r) + \frac{1}{2!}\left(\frac{\partial^2 \mathbf{R}}{\partial \boldsymbol{\Delta}^2}\right)_r (\boldsymbol{\Delta}^{r+1} - \boldsymbol{\Delta}^r)^2 + \cdots \tag{14.4.16a}$$

or

$$\mathbf{0} \approx \mathbf{R}^r + \mathbf{K}_T^r \, \delta\boldsymbol{\Delta} + O(\delta\boldsymbol{\Delta})^2 \tag{14.4.16b}$$

where $\delta\boldsymbol{\Delta}$ denotes the increment in $\boldsymbol{\Delta}$ and $\mathbf{K}_T$ is the *tangent (stiffness) matrix*

$$\begin{aligned} \mathbf{K}_T^r &\equiv \frac{\partial \mathbf{R}}{\partial \boldsymbol{\Delta}} \quad \text{evaluated at} \quad \boldsymbol{\Delta} = \boldsymbol{\Delta}^r \\ \delta\boldsymbol{\Delta} &= \boldsymbol{\Delta}^{r+1} - \boldsymbol{\Delta}^r \quad \text{(incremental solution)} \end{aligned} \tag{14.4.17}$$

For structural problems with variational principles, it can be shown that $\mathbf{K}_T$ is symmetric even if $\mathbf{K}$ is not. From (14.4.16*b*), we have

$$\delta\boldsymbol{\Delta} = -(\mathbf{K}_T)^{-1}\mathbf{R}^r = (\mathbf{K}_T(\boldsymbol{\Delta}^r))^{-1}(\mathbf{F} - \mathbf{K}(\boldsymbol{\Delta}^r)\boldsymbol{\Delta}^r) \tag{14.4.18a}$$

and the total solution at the $(r+1)$th iteration is given by

$$\boldsymbol{\Delta}^{r+1} = \boldsymbol{\Delta}^r + \delta\boldsymbol{\Delta} \tag{14.4.18b}$$

The iteration in (14.4.18*a*) is continued until the convergence criteria in (14.4.14) is satisfied or the residual $\mathbf{R}$ [measured in the same way as the solution error in (14.4.14)] is less than a certain preselected value. For additional details on iterative methods, consult the references at the end of the chapter [e.g., Reddy (2004) and Reddy and Gartling (2001)].

14.4.5 Numerical Examples

In this section we present some representative numerical examples of nonlinear bending of beams and fluid flow. A more complete discussion of the nonlinear formulations presented in Sections 14.4.2 and 14.4.3 as well as examples presented here can be found in Reddy (2004).

Example 14.4.1

Consider a straight beam made of steel ($E = 30 \times 10^6$ psi), of length $L = 100$ in., width B, and height H, and subjected to uniformly distributed load of intensity q_0 lb/in. The beam is assumed to be fixed at both ends. Noting the symmetry of the solution about $x = L/2$, one-half of the domain is used as the computational domain. The geometric boundary conditions for the computational domain of the problem are

$$u(0) = w(0) = \left.\frac{dw}{dx}\right|_{x=0} = u\left(\frac{L}{2}\right) = \left.\frac{dw}{dx}\right|_{x=\frac{L}{2}} = 0 \tag{14.4.19}$$

The load increments of $\Delta q_0 = 1.0$ lb/in., a tolerance of $\epsilon = 10^{-3}$, and maximum allowable iterations of 25 (per load step) are used in the analysis. The initial solution vector is chosen to be the zero vector. The exact solution to the linear problem is

$$u(x) = 0, \quad w(x) = \frac{q_0 L^4}{24D}\left(\frac{x}{L} - 2\frac{x^3}{L^3} + \frac{x^4}{L^4}\right) \tag{14.4.20}$$

and the maximum deflections occurs at $L/2$. For $q_0 = 1$ lb/in., $L = 100$ in., $B \times H = 1$ in. $\times$ 1 in., and $E = 30 \times 10^6$ psi, they are given by ($D = EH^3/12$, $H = 1$)

$$w\left(\frac{L}{2}\right) = \frac{q_0 L^4}{384D} = 0.1042 \text{ in.} \tag{14.4.21}$$

Table 14.4.1 contains the results of the nonlinear analysis of the clamped-clamped beam; the results were obtained with both the direct and Newton–Raphson iteration methods. The two-point Gauss rule for the linear terms and one-point Gauss rule for nonlinear terms is used to eliminate the so-called membrane locking (Reddy, 2004). Figure 14.4.2 shows the load-deflection curve for the beam.

Table 14.4.1 Finite element results for the deflections of a clamped-clamped beam under uniform load.

	Direct iteration		Newton–Raphson iteration	
Load q_0	4 elements	8 elements	4 elements	8 elements
1.0	0.1033 (3)*	0.1034 (3)	0.1034 (3)	0.1034 (3)
2.0	0.2022 (4)	0.2023 (4)	0.2022 (3)	0.2023 (3)
3.0	0.2938 (4)	0.2939 (4)	0.2939 (3)	0.2939 (3)
4.0	0.3773 (5)	0.3774 (5)	0.3773 (3)	0.3774 (3)
5.0	0.4529 (5)	0.4531 (5)	0.4528 (3)	0.4530 (3)
6.0	0.5213 (6)	0.5215 (6)	0.5214 (3)	0.5216 (3)
7.0	0.5840 (7)	0.5842 (7)	0.5839 (3)	0.5841 (3)
8.0	0.6412 (8)	0.6412 (8)	0.6413 (3)	0.6414 (3)
9.0	0.6945 (9)	0.6944 (9)	0.6943 (3)	0.6943 (3)
10.0	0.7433 (10)	0.7431 (10)	0.7435 (3)	0.7433 (3)

* Number of iterations taken to converge.

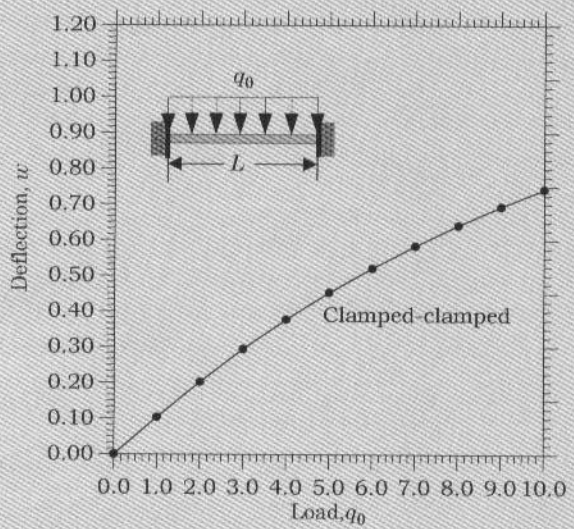

Figure 14.4.2 Load versus deflection curves for a clamped beam.

Example 14.4.2

Here, we consider the lid-driven cavity problem of Example 10.6.3 for nonlinear analysis (i.e., solve Navier–Stokes equations). For the problem at hand, the Reynolds number, $Re = \rho v_0 a/\mu$, can be varied by varying the density while keeping the viscosity constant. Thus, we take ($v_0 = 1$ and $a = 1$) $\mu = 1$ so that $Re = \rho$. The problem is solved using uniform 8×8 mesh of linear elements as well as 4×4 mesh of nine-node quadratic elements, and the results are presented in Table 14.4.2 for $Re = 100$, 500, and 700 ($\gamma = 10^8$ and $\epsilon = 10^{-2}$). The converged nonlinear solution of the preceding Reynolds number, is used as the initial guess in the first iteration of the next Reynolds number. In general, for very high Reynolds numbers, underrelaxation must be used to accelerate the convergence by using the weighted average of velocities from two

Table 14.4.2 Velocity $v_x(0.5, y)$ obtained with linear and quadratic elements and for various values of the Reynolds number.

y	8×8L			4×4Q9		
$Re \rightarrow$	100(5)	500(8)	700(9)	100(5)	500(8)	700(10)*
0.125	−0.0498	−0.0242	−0.0140	−0.0554	−0.0141	−0.0106
0.250	−0.0870	−0.0503	−0.0345	−0.0968	−0.0540	−0.0089
0.375	−0.1164	−0.0733	−0.0564	−0.1313	−0.1143	−0.0672
0.500	−0.1231	−0.0700	−0.0586	−0.1414	−0.1252	−0.1181
0.625	−0.0635	0.0027	0.0039	−0.0814	−0.0455	−0.0831
0.750	0.0649	0.0389	0.0354	0.0486	0.1045	0.0808
0.875	0.3750	0.1761	0.1241	0.3629	0.2113	0.1628

* Number in parentheses denotes the number of iterations taken for convergence.

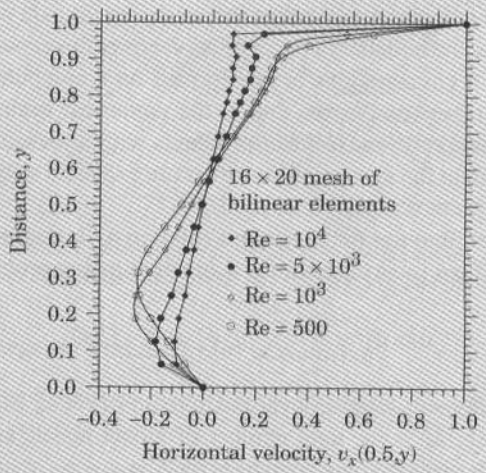

Figure 14.4.3 Velocity $v_x(0.5, y)$ versus y for various Reynolds numbers.

consecutive iterations

$$\tilde{\mathbf{v}}^r = \beta \mathbf{v}^{(r)} + (1 - \beta)\mathbf{v}^{(r-1)} \tag{14.4.22}$$

to compute the coefficient matrix. Here β is known as the acceleration parameter. Figure 14.4.3 contains plots of the horizontal velocity obtained with 16×20 mesh for $Re = 500, 10^3, 5 \times 10^3, 10^4$ (the increment of Re is taken to be 500 and $\beta = 0.5$).

14.5 ERRORS IN FINITE ELEMENT ANALYSIS

14.5.1 Types of Errors

The errors introduced into the finite element solution of a given differential equation can be attributed to three basic sources:

1. *Domain approximation error,* which is due to the approximation of the domain.
2. *Quadrature and finite arithmetic errors,* which are due to the numerical evaluation of integrals and the numerical computation on a computer.
3. *Approximation error,* which is due to the approximation of the solution:

$$u \approx u_h \equiv \sum_{I=1}^{N} U_I \Phi_I \tag{14.5.1}$$

where U_I denotes the value of u at global node I and Φ_I denotes the global interpolation function associated with global node I (see Fig. 3.2.9).

In the one-dimensional problems, the domains considered have been straight lines. Therefore, no approximation of the domain has been necessary. In two-dimensional problems involving nonrectangular domains, domain (or boundary) approximation errors are introduced into the finite element solutions. In general, these can be interpreted as errors in

the specification of the data of the problem because we are now solving the given differential equation on a modified domain. As we refine the mesh, the domain is more accurately represented, and, therefore, the boundary approximation errors are expected to approach zero.

When finite element computations are performed on a computer, round-off errors in the computation of numbers and errors due to the numerical evaluation of integrals are introduced into the solution. In most linear problems with a reasonably small number of total degrees of freedom in the system, these errors are expected to be small (or zero when only a certain decimal point accuracy is desired).

The error introduced into the finite element solution u_h^e because of the approximation of the dependent variable u in an element Ω_e is inherent to any problem

$$u \approx u_h = \sum_{e=1}^{N} \sum_{i=1}^{n} u_i^e \psi_i^e = \sum_{I=1}^{M} U_I \Phi_I \tag{14.5.2}$$

where u_h is the finite element solution over the domain ($u_h = u_h^e$ in Ω_e), N is the number of elements in the mesh, M is the total number of global nodes, and n is the number of nodes in an element. We wish to know how the error $E = u - u_h$, measured in a meaningful way, behaves as the number of elements in the mesh is increased. It can be shown that the approximation error is zero for the single second-order and fourth-order equations with elementwise-constant coefficients.

14.5.2 Measures of Errors

There are several ways in which we can measure the "difference" (or distance) between any two functions u and u_h. The *pointwise error* is the difference of u and u_h at each point of the domain. We can also define the difference of u and u_h to be the maximum of all absolute values of the differences of u and u_h in the domain $\Omega = (a, b)$:

$$\| u - u_h \|_\infty \equiv \max_{a \le x \le b} |u(x) - u_h(x)| \tag{14.5.3}$$

This measure of difference is called the *supmetric*. Note that the supmetric is a real number, whereas the pointwise error is a function and does not qualify as a distance or *norm* in a strict mathematical sense. The norm of a function is a nonnegative real number.

More generally used measures (or norms) of the difference of two functions are the *energy norm* and the L_2 *norm* (pronounced "L-two norm"). For any square-integrable functions u and u_h defined on the domain $\Omega = (a, b)$, the two norms are defined by

$$\text{energy norm} \qquad \| u - u_h \|_m = \left(\int_a^b \sum_{i=0}^{m} \left| \frac{d^i u}{dx^i} - \frac{d^i u_h}{dx^i} \right|^2 dx \right)^{1/2} \tag{14.5.4}$$

$$L_2 \text{ norm} \qquad \| u - u_h \|_0 = \left(\int_a^b |u - u_h|^2 \, dx \right)^{1/2} \tag{14.5.5}$$

where $2m$ is the order of the differential equation being solved. The term "energy norm" is used to indicate that this norm contains the same-order derivatives as the quadratic functional (which, for most solid mechanics problems, denotes the energy) associated with the equation. Various measures of the distance between two functions are illustrated in Fig. 14.5.1. These definitions can easily be modified for two-dimensional domains.

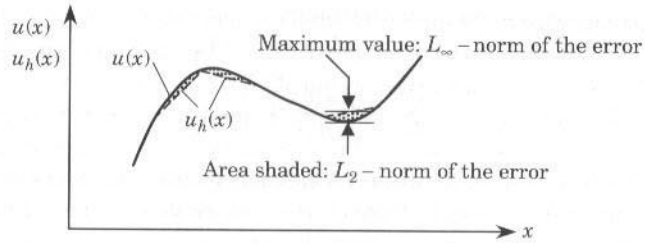

Figure 14.5.1 Different measures of the error $E = u - u_h$ between the exact solution u and the finite element solution u_h. The maximum norm and the L_2 norms are illustrated.

14.5.3 Convergence and Accuracy of Solutions

The finite element solution u_h in (14.5.1) is said to *converge in the energy norm* to the true solution u if

$$\| u - u_h \|_m \leq ch^p \quad \text{for} \quad p > 0 \tag{14.5.6}$$

where c is a constant independent of u and u_h, and h is the characteristic length of an element. The constant p is called the *rate of convergence*. Note that the convergence depends on h as well as on p; p depends on the order of the derivative of u in the weak form and the degree of the polynomials used to approximate u [see (14.5.15) below]. Therefore, the error in the approximation can be reduced either by reducing the size of the elements or increasing the degree of approximation. Convergence of the finite element solutions with mesh refinements (i.e., more of the same kind of elements are used) is termed *h-convergence*. Convergence with increasing degree of polynomials is called *p-convergence*.

Returning to the question of estimating the approximation error, we consider a $2m$th-order differential equation in one dimension ($m = 1$, second-order equations; $m = 2$, fourth-order equations):

$$\sum_{i=1}^{m} (-1)^i \frac{d^i}{dx^i}\left(a_i \frac{d^i u}{dx^i}\right) = f \quad \text{for} \quad 0 < x < L \tag{14.5.7}$$

where the coefficients $a_i(x)$ are assumed to be positive. Suppose that the essential boundary conditions of the problem are

$$u(0) = u(L) = 0 \quad (m = 1, 2) \tag{14.5.8}$$

$$\left(\frac{du}{dx}\right)\bigg|_{x=0} = \left(\frac{du}{dx}\right)\bigg|_{x=L} = 0 \quad (m = 2) \tag{14.5.9}$$

The variational formulation of (14.5.7) and (14.5.9) is given by

$$0 = \int_0^L \left(\sum_{i=1}^{m} a_i \frac{d^i v}{dx^i}\frac{d^i u}{dx^i} - vf\right) dx \tag{14.5.10}$$

The quadratic functional corresponding to the variational form is

$$I(u) = \int_0^L \frac{1}{2}\left[\sum_{i=1}^{m} a_i \left(\frac{d^i u}{dx^i}\right)^2\right] dx - \int_0^L uf\, dx \tag{14.5.11}$$

Now consider a finite element discretization of the domain by N elements of equal length h. If u_h denotes the finite element solution in (14.5.1), we have, from (14.5.11),

$$I(u_h) = \int_0^L \frac{1}{2}\left[\sum_{i=1}^{m} a_i \left(\frac{d^i u_h}{dx^i}\right)^2\right] dx - \int_0^L u_h f \, dx \tag{14.5.12}$$

In the following paragraphs, we show that the energy I associated with the finite element solution approaches the true energy from above, and we then give an error estimate. We confine our discussion, for the sake of simplicity, to the second-order equation ($m = 1$).

From (14.5.11) and (14.5.12), and

$$f = -\frac{d}{dx}\left(a_1 \frac{du}{dx}\right)$$

we have

$$\begin{aligned}
I(u_h) - I(u) &= \int_0^L \frac{1}{2}\left[a_1\left(\frac{du_h}{dx}\right)^2 - a_1\left(\frac{du}{dx}\right)^2 + 2f(u - u_h)\right] dx \\
&= \int_0^L \left[\frac{a_1}{2}\left(\frac{du_h}{dx}\right)^2 - \frac{a_1}{2}\left(\frac{du}{dx}\right)^2 - \frac{d}{dx}\left(a_1 \frac{du}{dx}\right)(u - u_h)\right] dx \\
&= \int_0^L \left\{\frac{a_1}{2}\left[\left(\frac{du_h}{dx}\right)^2 - \left(\frac{du}{dx}\right)^2\right] + a_1 \frac{du}{dx}\frac{d}{dx}(u - u_h)\right\} dx \\
&= \int_0^L \frac{a_1}{2}\left[\left(\frac{du_h}{dx}\right)^2 + \left(\frac{du}{dx}\right)^2 - 2\frac{du}{dx}\frac{du_h}{dx}\right] dx \\
&= \int_0^L \frac{a_1}{2}\left(\frac{du_h}{dx} - \frac{du}{dx}\right)^2 dx \geq 0
\end{aligned} \tag{14.5.13}$$

Thus,

$$I(u_h) \geq I(u) \tag{14.5.14}$$

The equality holds only for $u = u_h$. Equation (14.5.14) implies that the convergence of the energy of the finite element solution to the true energy is from above. Since the relation in (14.5.14) holds for any u_h, the inequality also indicates that the true solution u minimizes the energy. A similar relation can be established for the fourth-order equation ($m = 2$).

Now suppose that the finite element interpolation functions Φ_I ($I = 1, 2, \ldots, M$) are complete polynomials of degree k. Then the error in the energy norm can be shown to satisfy the inequality [see Reddy (1991), p. 401]

$$\| e \|_m \equiv \| u - u_h \|_m \leq c h^p, \quad p = k + 1 - m > 0 \tag{14.5.15}$$

where c is a constant. This estimate implies that the error goes to zero as the pth power of h as h is decreased (or the number of elements is increased). In other words, the logarithm of the error in the energy norm versus the logarithm of h is a straight line whose slope is $k + 1 - m$. The greater the degree of the interpolation functions, the more rapid the rate of convergence. Note also that the error in the energy goes to zero at the rate of $k + 1 - m$;

the error in the L_2 norm will decrease even more rapidly, namely, at the rate of $k+1$, i.e., derivatives converge more slowly than the solution itself.

Error estimates of the type in (14.5.15) are very useful because they give an idea of the accuracy of the approximate solution, whether or not we know the true solution. While the estimate gives an idea of how rapidly the finite element solution converges to the true solution, it does not tell us when to stop refining the mesh. This decision rests with the analysts, because only they know what a reasonable tolerance is for the problems they are solving.

As an example of estimating the error in the approximation, i.e., (14.5.15), consider the linear (two-node) element for a second-order equation ($m=1$). We have for an element

$$u_h = u_1(1-s) + u_2 s \tag{14.5.16}$$

where $s = \bar{x}/h$ and $\bar{x}$ is the local coordinate. Since u_2 can be viewed as a function of u_1 via (14.5.16), we can expand u_2 in a Taylor series around node 1 to obtain

$$u_2 = u_1 + u_1' + \frac{1}{2}u_1'' + \cdots \tag{14.5.17}$$

where $u' \equiv du/ds$. Substituting this into (14.5.16), we obtain

$$u_h = u_1 + u_1' s + \frac{1}{2}u_1'' s + \cdots \tag{14.5.18}$$

Expanding the true solution in a Taylor series about node 1, we obtain

$$u = u_1 + u_1' s + \frac{1}{2}u_1'' s^2 + \cdots \tag{14.5.19}$$

Therefore, we have, from (14.5.18) and (14.5.19),

$$|u_h - u| \le \frac{1}{2}(s - s^2) \max_{0 \le s \le 1} \left| \frac{d^2 u_1}{ds^2} \right| = \frac{1}{2}(s - s^2)h^2 \max_{0 \le \bar{x} \le h} \left| \frac{d^2 u}{d\bar{x}^2} \right| \tag{14.5.20}$$

$$\left| \frac{d}{\bar{x}}(u_h - u) \right| \le \frac{1}{2}h \max_{0 \le \bar{x} \le h} \left| \frac{d^2 u_1}{d\bar{x}^2} \right| \tag{14.5.21}$$

These lead to

$$\| u - u_h \|_0 \le c_1 h^2, \qquad \| u - u_h \|_1 \le c_2 h \tag{14.5.22}$$

where the constants c_1 and c_2 depend only on the length L of the domain. The reader may wish to perform a similar error analysis for the fourth-order equation (14.2.39).

Example 14.5.1

Here we consider a computational example to verify the error estimates in (14.5.22). Consider the differential equation

$$-\frac{d^2 u}{dx^2} = 2 \quad \text{for} \quad 0 < x < 1 \tag{14.5.23}$$

with

$$u(0) = u(1) = 0$$

The exact solution is

$$u(x) = x(1-x) \tag{14.5.24}$$

while the finite element solutions are, for $N=2$,

$$u_h = \begin{cases} h^2(x/h) & \text{for } 0 \le x \le h \\ h^2(2-x/h) & \text{for } h \le x \le 2h \end{cases}$$

for $N=3$,

$$u_h = \begin{cases} 2h^2(x/h) & \text{for } 0 \le x \le h \\ 2h^2(2-x/h) + 2h^2(x/h-1) & \text{for } h \le x \le 2h \\ 2h^2(3-x/h) & \text{for } 2h \le x \le 3h \end{cases} \tag{14.5.25}$$

and, for $N=4$,

$$u_h = \begin{cases} 3h^2(x/h) & \text{for } 0 \le x \le h \\ 3h^2(2-x/h) + 4h^2(x/h-1) & \text{for } h \le x \le 2h \\ 4h^2(3-x/h) + 3h^2(x/h-2) & \text{for } 2h \le x \le 3h \\ 3h^2(4-x/h) & \text{for } 3h \le x \le 4h \end{cases}$$

For the two-element case ($h=0.5$), the errors are given by

$$\begin{aligned} \| u - u_h \|_0^2 &= \int_0^h (x - x^2 - hx)^2 \, dx + \int_h^{2h} (x - x^2 - 2h^2 + xh)^2 \, dx \\ &= 0.002083 \end{aligned} \tag{14.5.26}$$

$$\begin{aligned} \left\| \frac{du}{dx} - \frac{du_h}{dx} \right\|_0^2 &= \int_0^h (1 - 2x - h)^2 \, dx + \int_h^{2h} (1 - 2x + h)^2 \, dx \\ &= 0.08333 \end{aligned}$$

Similar calculations can be performed for $N=3$ and $N=4$. Table 14.5.1 gives the errors for N=2, 3, and 4.

Plots of $\log \| e \|_0$ and $\log \| e \|_1$ versus $\log h$ show that (see Fig. 14.5.2)

$$\log \| e \|_0 = 2 \log h + \log c_1, \quad \log \| e \|_1 = \log h + \log c_2 \tag{14.5.27}$$

In other words, the rate of convergence of the finite element solution is 2 in the L_2 norm and 1 in the energy norm, verifying the estimates in (14.5.22).

Table 14.5.1 The L_2 error and error in the energy norm of the solution to (14.5.23) (Example 14.5.1).

h	$\log_{10} h$	$\| e \|_0$	$\log_{10} \| e \|_0$	$\| e \|_1$	$\log_{10} \| e \|_1$
$\frac{1}{2}$	−0.301	0.04564	−1.341	0.2887	−0.5396
$\frac{1}{3}$	−0.477	0.02028	−1.693	0.1925	−0.7157
$\frac{1}{4}$	−0.601	0.01141	−1.943	0.1443	−0.8406

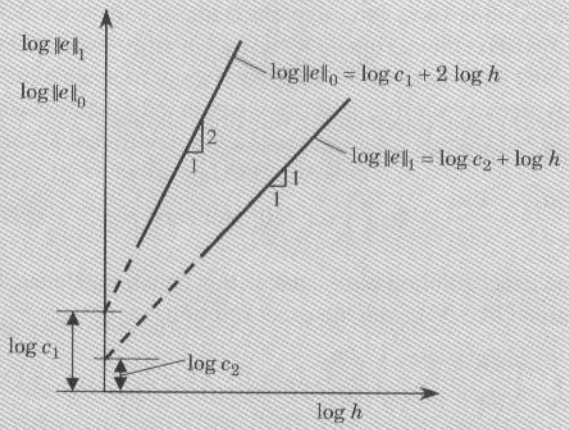

Figure 14.5.2 Plots of the L_2 and energy norms of errors versus the mesh size. The log–log plots give the rates of convergence in the respective norms. The rates of convergence are given by the slopes of the lines (the plots shown are for linear elements).

Much of the discussion presented in this section can be carried over to curved elements and two-dimensional elements. When the former, i.e., elements with nonstraight sides, are involved, the error estimate also depends on the Jacobian of the transformation. Because of the introductory nature of the present study, these topics are not discussed here. Interested readers can consult Wait and Mitchell (1985), Oden and Reddy (1982), Strang and Fix (1973), and Reddy (1991).

As noted earlier, in the case of both second- and fourth-order equations in a single unknown and with constant coefficients a and b, the finite element solutions of the equations

$$-\frac{d}{dx}\left(a\frac{du}{dx}\right) = f(x) \tag{14.5.28}$$

$$-\frac{d^2}{dx^2}\left(b\frac{d^2u}{dx^2}\right) = f(x) \tag{14.5.29}$$

coincide with the exact solutions at the nodes. The proof is presented below for the second-order equation.

Consider the equation

$$-a\frac{d^2u}{dx^2} = f \quad \text{for } 0 < x < L \tag{14.5.30}$$

with

$$u(0) = 0, \quad u(L) = 0 \tag{14.5.31}$$

The global finite element solution is given by ($U_1 = U_N = 0$)

$$u_h = \sum_{I=2}^{N-1} U_I \Phi_I \tag{14.5.32}$$

where Φ_I are the linear global interpolation functions shown in Fig. 3.2.9. From the definition of the variational problem, we have

$$\int_0^L \left(\frac{du}{dx} - \frac{du_h}{dx} - \Phi_I \hat{f} \right) dx = 0 \quad \text{for each } I = 2, \ldots, N-1 \tag{14.5.33}$$

where $\hat{f} = f/a$. The exact solution also satisfies this equation. Hence, by subtracting the finite element equation (14.5.33) from the exact solution, we obtain

$$\int_0^L \left(\frac{du}{dx} - \frac{du_h}{dx} \right) \frac{d\Phi_I}{dx} dx = 0 \quad (I = 2, \ldots, N-1)$$

Since we have $\Phi_I = 0$ for $x \le (I+1)h$ and $x \ge (I-1)h$, and $d\Phi_I/dx = 1/h$ for $(I-1)h \le x \le Ih$ and $d\Phi_I/dx = -1/h$ for $Ih \le x \le (I+1)h$, it follows that

$$\int_{(I-1)h}^{Ih} \left(\frac{du}{dx} - \frac{du_h}{dx} \right) \frac{1}{h} dx + \int_{Ih}^{(I+1)h} \left(\frac{du}{dx} - \frac{du_h}{dx} \right) \left(-\frac{1}{h} \right) dx = 0 \tag{14.5.34}$$

for $I = 2, 3, \ldots, N-1$. Denoting $\epsilon(x) = u(x) - u_h(x)$, we have

$$\frac{1}{h}(\epsilon_I - \epsilon_{I-1}) + \left(-\frac{1}{h} \right)(\epsilon_{I+1} - \epsilon_I) = 0$$

or

$$\frac{1}{h}(-\epsilon_{I-1} + 2\epsilon_I - \epsilon_{I+1}) = 0 \quad (I = 2, 3, \ldots, N-1) \tag{14.5.35}$$

where $\epsilon_I = \epsilon(Ih)$ (i.e., the value of ϵ at $x = Ih$). Since $\epsilon_0 = \epsilon_N = 0$ (because both u and u_h satisfy the essential boundary conditions), it follows from the above homogeneous equations that the solution is trivial: $\epsilon_1 = \epsilon_2 = \cdots = \epsilon_{N-1} = 0$. This implies that the finite element solution coincides with the exact solution at the nodes.

14.6 SUMMARY

Three advanced topics have been discussed in this chapter: (1) weighted residual and mixed finite element formulations of differential equations; (2) finite element models of three-dimensional problems; and (3) finite element models of nonlinear equations. The weighted residual models discussed include the Petrov–Galerkin model, Bubnov–Galerkin model, collocation model, subdomain model, and least-squares model. First- and second-order differential equations have been considered. Three-dimensional finite element models of heat transfer, flows of viscous incompressible fluids, and elasticity have been also presented. A library of interpolation functions of some commonly used three-dimensional finite elements have been presented. Nonlinear finite element models of the Euler–Bernoulli beam theory and the Navier–Stokes equations governing two-dimensional viscous incompressible flows have been developed. Two iterative schemes, Picard and Newton–Raphson, for solving nonlinear algebraic equations have been discussed. Finally, various types of errors in the finite element approximation of differential equations have been discussed and different

measures of the error have been defined. It has been shown that the finite element solutions of differential equations with constant coefficients are exact at the nodes. This result does not hold for coupled second-order differential equations with constant coefficients.

The alternate finite element models presented in Section 14.2 can also be extended to nonlinear problems. For example, mixed least-squares finite element models of plates and shells as well as the Navier–Stokes equations have been already reported. The reader may consult the references listed at the end of the chapter.

PROBLEMS

14.1 Consider the second-order equation

$$-\frac{d}{dx}\left(a\frac{du}{dx}\right)=f \tag{1}$$

and rewrite it as a pair of first-order equations,

$$-\frac{du}{dx}+\frac{P}{a}=0, \quad -\frac{dP}{dx}-f=0 \tag{2}$$

Construct the weighted residual finite element model of the equations, and specialize it to the Galerkin model. Assume interpolation in the form

$$u=\sum_{j=1}^{m} u_j\psi_j(x), \quad P=\sum_{j=1}^{n} P_j\phi_j(x) \tag{3}$$

and use the equations in (2) in the right order that yields symmetric element equations:

$$\begin{bmatrix} [K^{11}] & [K^{12}] \\ [K^{12}]^T & [K^{22}] \end{bmatrix} \begin{Bmatrix} \{u\} \\ \{P\} \end{Bmatrix} = \begin{Bmatrix} \{F^1\} \\ \{F^2\} \end{Bmatrix} \tag{4}$$

The model can also be called a mixed model because (u, P) are of different kinds.

14.2 Evaluate the coefficient matrices $[K^{\alpha\beta}]$ in Problem 14.1 for $a=$ constant and column vectors $\{F^\alpha\}$ for $f=$ constant. Assume that $\psi_i=\phi_i$ are the linear interpolation functions. Eliminate $\{P\}$ from the two sets of equations (4) to obtain an equation of the form

$$[K]\{u\}=\{F\}$$

Compare the coefficient matrix $[K]$ and vector $\{F\}$ with those obtained with the weak form finite element model of (1). What conclusions can you draw?

14.3 Develop the least-squares finite element model of (2) in Problem 14.1, and compute element coefficient matrices and vectors when $\psi_i=\phi_i$ are the linear interpolation functions.

14.4 Solve the problem in Example 14.3.1 using three elements of the least-squares model developed in Problem 14.3. Compare the results with the exact solution and those of the weak form finite element model.

14.5 Show that the mixed finite element model of the Euler–Bernoulli beam theory, Eq. (14.2.47a), is the same as that used in Eq. (5.2.18) for the linear interpolation of w and M.

14.6 Consider the pair of equations

$$\nabla u-\mathbf{q}/k=0, \quad \nabla\cdot\mathbf{q}+f=0 \quad \text{in} \quad \Omega$$

where u and $\mathbf{q}$ are the dependent variables, and k and f are given functions of position (x, y) in a two-dimensional domain Ω. Derive the finite element formulation of the equations in the form

$$\begin{bmatrix} [K^{11}] & [K^{12}] & [K^{13}] \\ & [K^{22}] & [K^{23}] \\ \text{symm.} & & [K^{33}] \end{bmatrix} \begin{Bmatrix} \{u\} \\ \{q^1\} \\ \{q^2\} \end{Bmatrix} = \begin{Bmatrix} \{F^1\} \\ \{F^2\} \\ \{F^3\} \end{Bmatrix}$$

Caution: Do not eliminate the variable u from the given equations.

14.7 Compute the element coefficient matrices $[K^{\alpha\beta}]$ and vectors $\{F^\alpha\}$ of Problem 14.6 using linear triangular elements for all variables. Assume that k is a constant.

14.8 Repeat Problem 14.7 with linear rectangular elements.

14.9 Consider the following form of the governing equations of the classical plate theory:

$$-\left(\frac{\partial^2 M_{xx}}{\partial x^2} - 4D_{66}\frac{\partial^4 w}{\partial x^2 \partial y^2} + \frac{\partial^2 M_{yy}}{\partial y^2}\right) = q \tag{a}$$

$$\frac{\partial^2 w}{\partial x^2} = -\left(\bar{D}_{22} M_{xx} + \bar{D}_{12} M_{yy}\right),$$

$$\frac{\partial^2 w}{\partial y^2} = -\left(\bar{D}_{12} M_{xx} + \bar{D}_{11} M_{yy}\right) \tag{b}$$

where M_{xx} and M_{yy} are the bending moments, w is the transverse deflection, q is the distributed load, ν is the Poisson ratio, and

$$\bar{D}_{ij} = \frac{D_{ij}}{D_0}, \quad D_0 = D_{11} D_{22} - D_{12}^2$$

(a) Give the weak form of the equations, and (b) assume approximation of the form

$$w = \sum_{i=1}^{4} w_i \psi_i^1, \quad M_{xx} = \sum_{i=1}^{2} M_{xi} \psi_i^2, \quad M_{yy} = \sum_{i=1}^{2} M_{yi} \psi_j^3$$

to develop the (mixed) finite element model in the form

$$\begin{bmatrix} [K^{11}] & [K^{12}] & [K^{13}] \\ & [K^{22}] & [K^{23}] \\ \text{symm.} & & [K^{33}] \end{bmatrix} \begin{Bmatrix} \{w\} \\ \{M_x\} \\ \{M_y\} \end{Bmatrix} = \begin{Bmatrix} \{F^1\} \\ \{F^2\} \\ \{F^3\} \end{Bmatrix}$$

Comment on the choice of the functions ψ_i^α for $\alpha = 1, 2, 3$.

14.10 Use the interpolation

$$w = \sum_{i=1}^{4} w_i \psi_i^1, \quad M_{xx} = \sum_{i=1}^{2} M_{xi} \psi_i^2, \quad M_{yy} = \sum_{i=1}^{2} M_{yi} \psi_j^3$$

with

$$\psi_1^1 = \left(1 - \frac{x}{a}\right)\left(1 - \frac{y}{b}\right), \quad \psi_2^1 = \frac{x}{a}\left(1 - \frac{y}{b}\right), \quad \psi_3^1 = \frac{x}{a}\frac{y}{b}, \quad \psi_4^1 = \left(1 - \frac{x}{a}\right)\frac{y}{b}$$

$$\psi_1^2 = 1 - \frac{x}{a}, \quad \phi_2^2 = \frac{x}{a}, \quad \psi_1^3 = 1 - \frac{y}{b}, \quad \psi_2^3 = \frac{y}{b}$$

for a rectangular element with sides a and b to evaluate the matrices $[K^{\alpha\beta}](\alpha, \beta = 1, 2, 3)$ in Problem 14.9.

14.11 Repeat Problem 14.10 for the case in which $\phi_i^1 = \phi_i^2 = \psi_i$.

14.12 Evaluate the element matrices in (14.4.6*b*) by assuming that the nonlinear parts in the element coefficients are elementwise constant.

14.13 Give the finite element formulation of the following nonlinear equation over an element (x_a, x_b):

$$-\frac{d}{dx}\left(u\frac{du}{dx}\right)+1=0 \quad \text{for} \quad 0<x<1$$

$$\left(\frac{du}{dx}\right)\Big|_{x=0}=0, \quad u(1)=\sqrt{2}$$

14.14 Compute the tangent coefficient matrix for the nonlinear problems in Problem 14.13. What restriction(s) should be placed on the initial guess vector?

14.15 Compute the tangent stiffness matrix $\mathbf{K}_T$ in (14.4.17) for the Euler–Bernoulli beam element in (14.4.6*a*).

14.16 Develop the nonlinear finite element model of the Timoshenko beam theory. Equations (14.4.1) and (14.4.2) are valid for this case, with the following changes. In place of (d^2/dx^2) $(EI\,d^2w/dx^2)$ use $-(d/dx)(EI\,d\Psi/dx)+GAk(dw/dx+\Psi)$ and add the following additional equation for w:

$$-\frac{d}{dx}\left[GAk\left(\frac{dw}{dx}+\Psi\right)\right]=q$$

See Section 5.3 for additional details.

14.17 Compute the tangent stiffness matrix for the Timoshenko beam element in Problem 14.16.

14.18 (*Natural convection flow between heated vertical plates*) Consider the flow of a viscous incompressible fluid in the presence of a temperature gradient between two stationary long vertical plates. Assuming zero pressure gradient between the plates, we can write $v_x = v_x(y)$, $v_y = 0$, $T = T(y)$, and

$$0=\rho\beta g(T-T_m)+\mu\frac{d^2v_x}{dy^2}, \quad 0=k\frac{d^2T}{dy^2}+\mu\left(\frac{dv_x}{dy}\right)^2$$

where $T_m = \frac{1}{2}(T_0 + T_1)$ is the mean temperature of the two plates, g the gravitational acceleration, ρ the density, β the coefficient of thermal expansion, μ the viscosity, and k the thermal conductivity of the fluid. Give a finite element formulation of the equations and discuss the solution strategy for the computational scheme.

14.19 Derive the interpolation functions ψ_1, ψ_5, and ψ_8 for the eight-node prism element using the alternative procedure described in Section 8.2 for rectangular elements.

14.20 Evaluate the source vector components f_i^e and coefficients K_{ij}^e over a master prism element when f is a constant, f_0, and $k_x = k_y = k_z = k$, a constant in (14.3.5*b*).

REFERENCES FOR ADDITIONAL READING

1. Bathe, K. J., *Finite Element Procedures,* Prentice-Hall, Englewood Cliffs, NJ, 1996.
2. Bell, B. C. and Surana, K. S., "A Space-Time Coupled p-Version Least-Squares Finite Element Formulation for Unsteady Fluid Dynamics Problems," *International Journal for Numerical Methods in Engineerinng,* **37**, 3545–3569, 1994.

3. Belytschko, T., Liu, W. K., and Moran, B., *Nonlinear Finite Elements for Continua and Structures,* John Wiley, Chichester, UK, 2000.
4. Bochev, P. B. and Gunzburger, M. D., "Finite Element Methods of Least-Squares Type," *SIAM Review,* **40**, 789–837, 1998.
5. Brezzi, F. and Fortin, M., *Mixed and Hybrid Finite Element Methods,* Springer-Verlag, Berlin (1991).
6. Crisfield, M. A., *Non-Linear Finite Element Analysis of Solids and Structures, Vol. 1: Essentials,* John Wiley, Chichester, UK, 1991.
7. Crisfield, M. A., *Non-Linear Finite Element Analysis of Solids and Structures, Vol. 2: Advanced Topics,* John Wiley, Chichester, UK, 1997.
8. Gresho, P. M. and Sani, R. L., *Incompressible Flow and the Finite Element Method,* John Wiley, West Sussex, UK, 2000.
9. Hinton, E. (ed.) *NAFEMS Introduction to Nonlinear Finite Element Analysis,* NAFEMS, Glasgow, UK, 1992.
10. Irons, B. and Ahmad, S., "Quadrature Rules for Brick-Based Finite Elements," *International Journal for Numerical Methods in Engineering,* **3**, 293–294, 1971.
11. Jiang, B. N., "The Least-Squares Finite Element Method for Elasticity. Part II: Bending of Thin Plates," *International Journal for Numerical Methods in Engineering,* **54**, 1459–1475, 2002.
12. Oden, J. T., *Finite Elements of Nonlinear Continua,* McGraw-Hill, New York, 1972.
13. Oden, J. T. and Reddy, J. N., *An Introduction to the Mathematical Theory of Finite Elements,* Wiley-Interscience, New York, 1982.
14. Owen, D. R. J. and Hinton, E., *Finite Elements in Plasticity: Theory and Practice,* Pineridge Press, Swansea, UK, 1991.
15. Pontaza, J. P. and Reddy, J. N., "Spectral/*hp* Least-Squares Finite Element Formulation for the Navier–Stokes Equations," *Journal of Computional Physics,* **190**(2), 523–549, 2003.
16. Pontaza, J. P. and Reddy, J. N., "Mixed Plate Bending Elements Based on Least-Squares Formulation," *International Journal for Numerical Methods in Engineering,* **60**, 891–922, 2004.
17. Pontaza, J. P. and Reddy, J. N., "Hierarchical Least-Squares Shear Deformable Shell Elements," *Computer Methods in Applied Mechanics and Engineering,* to appear.
18. Pontaza, J. P. and Reddy, J. N., "Space-Time Coupled Spectral/*hp* Least-Squares Finite Element Formulation for the Incompressible Navier-Stokes Equations," *Journal of Computional Physics,* **197**(2), 418–459, 2004.
19. Putcha, N. S. and Reddy, J. N., "A Mixed Shear Flexible Finite Element for the Analysis of Laminated Plates," *Computer Methods in Applied Mechanics and Engineering,* **44**, 213–227, 1984.
20. Reddy, J. N., *Applied Functional Analysis and Variational Methods in Engineering,* McGraw-Hill, New York, 1986; Krieger, Melbourne, FL, 1991.
21. Reddy, J. N., *Energy Principles and Variational Methods in Applied Mechanics,* 2nd ed., John Wiley, New York, 2002.
22. Reddy, J. N., *An Introduction to Nonlinear Finite Element Analysis,* Oxford University Press, Oxford, UK, 2004.
23. Reddy, J. N., "Penalty-Finite-Element Analysis of 3-D Navier–Stokes Equations," *Computer Methods in Applied Mechanics and Engineering,* **35**, 87–106, 1982.
24. Reddy, J. N. and Gartling, D. K., *The Finite Element Method in Heat Transfer and Fluid Dynamics,* 2nd ed., CRC Press, Boca Raton, FL, 2001.
25. Reddy, J. N. and Sandidge, D., "Mixed Finite Element Models for Laminated Composite Plates," *Journal of Engineering for Industry,* **109**, 39–45, 1987.
26. Reddy, J. N. and Tsay, C. S., "Mixed Rectangular Finite Elements for Plate Bending," *Proceedings of the Oklahoma Academy of Science,* **47**, 144–148, 1977.
27. Reddy, J. N. and Tsay, C. S., "Stability and Vibration of Thin Rectangular Plates by Simplified Mixed Finite Elements," *Journal of Sound & Vibration,* **55**(2), 289–302, 1977.
28. Reddy, M. P. and Reddy, J. N., "Finite-Element Analysis of Flows of Non-Newtonian Fluids in Three-Dimensional Enclosures," *International Journal of Non-Linear Mechanics,* **27**, 9–26, 1992.

29. Pian, T. H. H. and Tong, P., "Basis of Finite Element Methods for Solid Continua," *International Journal of Numerical Methods in Engineering*, **1**, 3–28, 1969.

30. Strang, G. and Fix, G. J., *An Analysis of the Finite Element Method*, Prentice-Hall, Englewood Cliffs, NJ, 1973.

31. Tong, P., "New Displacement Hybrid Finite Element Methods for Solid Continua," *International Journal of Numerical Methods in Engineering*, **2**, 73–85, 1970.

32. Wait, R. and Mitchell, A. R., *Finite Element Analysis and Applications*, John Wiley, New York, 1985.

33. Wang, C. M., Reddy, J. N., and Lee, K. H., *Shear Deformable Beams and Plates. Relationships with Classical Solutions*, Elsevier, Oxford, UK, 2000.

34. Winterscheidt, D. and Surana, K. S., "p-Version Least-Squares Finite Element Formulation for Two-Dimensional Incompressible Fluid Flow," *International Journal for Numerical Methods in Fluids*, **18**, 43–69, 1994.

35. Zienkiewicz, O. C. and Taylor, R. L., *The Finite Element Method*, 4th ed., *Vol. 1: Basic Formulation and Linear Problems*, McGraw-Hill, London, UK, 1989.

36. Zienkiewicz, O. C. and Taylor, R. L., *The Finite Element Method*, 4th ed., *Vol. 2: Solid and Fluid Mechanics, Dynamics and Non-linearity*, McGraw-Hill, London, UK, 1989.